

Tailings and Mine Waste '09

Proceeding of the Thirteenth International Conference on Tailings and Mine Waste, 1-4 November 2009, Banff, Alberta, Canada

Tailings and Mine Waste '09

Edited by

David Segó, Moh'd Alostaz & Nicholas Beier

University of Alberta, Geotechnical Center and
Oil Sands Tailing Research Facility (UofA)

Copyright ©

All rights reserved. No part of this publication or the information contained herein may be reproduced, stored in a retrieval system or transmitted in any form or by any means, electronic, mechanical, by photocopying, recording or otherwise, without written prior permission from the publisher.

Although all care is taken to ensure the integrity and quality of this publication and the information herein, no responsibility is assumed by the publishers nor the author for any damage to property or persons as a result of operation or use of this publication and/or the information contained herein.

Published by: University of Alberta, Dept. of Civil & Environmental Engineering

ISBN 978-1-55195-255-0

Printed in Canada

Table of Contents

Preface	xii
Sponsorship	xiii

KEYNOTE PRESENTATION

A geotechnical perspective on oil sands tailings <i>J. Sobkowicz & N.R. Morgenstern</i>	xvii
--	------

Tailings & Mines Waste Management I – Session I

Mining market cycles and tailings dam incidents <i>M. Davies & T. Martin</i>	3
Uranium mill tailings impoundment closure: a retrospective <i>C. Strachan, G. Smith & J. Caldwell</i>	15
Best available technology design for a uranium tailings storage facility <i>M. Davis, C. Strachan, M. Abshire, D. Overton & T. Wright</i>	21
The Cannon Mine Tailings Impoundment: A Case History <i>J. Caldwell, I. Hutchison & R. Frechette</i>	33
Optimization of removal of overburden material for an open pit gold mine <i>J.S. Andrews, D.D. Overton & N. Legere</i>	41
A new design approach for thickened tailings slopes <i>D.G. Ritchie, A. Li & B. Fisseh</i>	53
Revisit to old South African slimes dams & where we are today <i>J. Caldwell & G. McPhail</i>	65
Cyanide and mercury contamination of surface sediments in three desert wash systems, Nelson, NV <i>D.B. Sims</i>	75
Development of material and compaction requirements for a mixed clay/sand tailings impoundment liner <i>M. Malusis, M. Davis, D. Overton, D. Castelbaum & T. Wright</i>	89
Closure system for waste sites using structured membranes and synthetic grass composite <i>M. R. Ayers & J.L. Urrutia</i>	101
Permeability, puncture, and shear strength testing of composite liner systems under high normal loads <i>C. Athanassopoulos, A. Kohlman, J. Kaul & J. Boschuk</i>	105

Hidden opportunities to improve tailings systems without capital <i>R. Hale & A. Jones</i>	119
Geotextile filtration performance with coal refuse under standard and reduced compaction energies <i>J.D. Quaranta, R. Tolikonda & S. Bell</i>	127
On-line remote tailings dam health condition monitoring system based on fiber optic seepage sensors <i>C. Wang, Y. Ning, T. Liu & Z. Zhou</i>	141
Influence of microstructure on self-weight settling of laterite ore slurries <i>S. Azam & J.D. Scott</i>	149
Laboratory versus field swcc data for mine tailings and mine waste covers <i>D.J. Williams</i>	159
Strategies for dealing with fine fluid tailings and suspended fines: some international perspectives <i>J.E.S. Boswell</i>	171
 Remediation – Session 2	
Framework conception for the remediation of the Culmützsch uranium tailings pond at Wismut (Germany) with respect to contaminant release <i>U. Bernekow, T. Metschies & M. Paul</i>	185
Activated aluminum tailings using mine waste to clean up mine sites <i>E. Mullenmeister & E. Stine</i>	199
Wetlands treatment of mine drainage at Antamina mine, Peru <i>H. Plewes, C. Strachotta, M. McBrien & L. Rey</i>	211
Laboratory through full-scale studies on the removal of nickel by zero-valent iron <i>T. Wildeman, A. Pinto & L.L.O. Fregadolli</i>	221
The use of waste rock inclusions in tailings impoundments to improve geotechnical and environmental performance <i>M. James & M. Aubertin</i>	233
Phased cleanup approach to arsenic contamination at Saginaw Hill mining district, Tucson, Arizona <i>C.G. LaBerge & R.J. Rudy</i>	247
Spatial distribution of soil physical properties in the tailings of Schneckenstein (Germany) <i>T. Naamoun, N. Kallel & B. Merkel</i>	257
Enhanced dewatering of fine tailings using electrokinetics <i>A. Fourie</i>	269
Project case study – composite soil cover for sulphide tailings at mine site in northeastern Ontario, Canada <i>R. Bygness & B. Herlin</i>	281
Oxic and anoxic tailings slurry aging studies at the Hope Bay project, Nunavut <i>K. Murphey, C. Bucknam, T. Wildeman, K. Sexsmith, L. Barazzuol & J. Chapman</i>	293

Electrokinetic dewatering of gypsum containing tailings <i>J.Q. Shang, A.R. Fernando & E.K. Lam</i>	303
North ZPL dam – case history of a foundation failure and subsequent remediation and foundation strengthening of an embankment constructed on soft lacustrine clays <i>B. Russell, I. Bruce, S. West & R Little</i>	315
Environmental desulphurization and geochemical behaviour of hemo-ilmenite mine products <i>V. Derycke, M Benzaazoua, B. Bussière, M. Kongolo, R. MJermillod-Blondin & P. Nadeau</i>	331
Chemical compound forms and release of lead in uranium tailings of Schneckenstein (Germany) <i>T. Naamoun, J. Kallel & B. Merkel</i>	347
Thiosalt in mining waste: reaction kinetics modeling <i>J. MirandaTrevino, K. Hawboldt, C. Bottaro & F. Khan</i>	355
Lessons learned from 30 years of mined land reclamation <i>H.T. Williams</i>	369
 Oil Sands Tailings I – Session 3	
Reduction of oil sands fine tailings <i>B. Ozum & J.D. Scott</i>	383
The development of centrifugal separation technology for tailings treatment <i>P. Mundy & B. Madsen</i>	397
Tailings research at Shell’s Muskeg River mine tailings testing facility <i>M. Matthews & S. Masala</i>	405
Paste pumping and deposition field trials and concepts on Syncrude’s dewatered mft (centrifuge cake) <i>I. Ahmed, M. Labelle, R. Brown & R. Lahie</i>	417
Vertical “wick” drains and accelerated dewatering of fine tailings in oil sands <i>P.S. Wells & J. Caldwell</i>	429
Dynamic simulation of tailings management options <i>N. Beier, D. Segó & N. Morgenstern</i>	441
Zoned strength model for oilsands upstream tailings beaches <i>S. Martens, T. Lappin & T. Eaton</i>	451
In pit dyke construction planning <i>D. Treacy, L. Bowie, T. Eaton, R. Fauquier & J. Horton</i>	463
Fluorescence characterization of oil sands naphthenic acids <i>A.M. Ewanchuk, M. Alostaz, A.C. Ulrich & D.C. Segó</i>	475
Capacity for sorption of naphthenic acids from oil sands process-affected water to soils from Athabasca oil sands region <i>L.D. Brown, M. Alostaz & A. Ulrich</i>	487
Potential use of carbonaceous materials for the treatment of process-affected water <i>C.C. Small, Z. Hashisho & A.C. Ulrich</i>	499
Geochemical interactions between process-affected water and native soils in Fort McMurray <i>A.A. Holden, A.C. Ulrich & R.B. Donahue</i>	513

Fate and transport of process-affected water in out-of-pit tailings ponds in the oil sands industry in Canada <i>A. Holden, L. Perez, J. Martin, C. Mendoza, D. Segó, A. Ulrich, T. Tompkins, J.F. Barker, S. Haque, K. Mayer, H. Sutherland, M. Bowron, K. Biggar & R. Donahue</i>	527
Heightened oil sands extraction by pressure cycles <i>P.K.A. Hong & H. Cha</i>	541
Anvil points oil shale tailings management Rifle, Colorado <i>R. Rudy, C. LaBerge & J. McClurg</i>	551
Treatment of produced water by pressure-assisted ozonation and sand filtration <i>P.K.A. Hong, Z. Cha, C-J. Cheng & C-F. Lin</i>	561
Determination of particle size distribution of oil sand solids using laser diffraction method <i>R. Mahood, J. Norgaard, T. Eaton, B. Liu and M. Nixon</i>	571
Breakthrough results in oilsands projects <i>A. Siddiqi</i>	579
 <i>Tailings & Mines Waste Management II – Session 4</i>	
A new, dynamic, internet- based mine site water and solute management tool <i>J.R. Kunkel & V. Lishnevsky</i>	589
Use of the hydrogeosphere code to simulate water flow and contaminants transport through mining wastes disposed in a symmetric open pit within fractured rock <i>F.B. Abdelghani, R. Simon, M. Aubertin, J. Molson & R. Therrien</i>	601
Water balance management approach to mine closure at the Royal Mountain King mine, Copperopolis, CA <i>A. Whitman, I. Hutchinson, J. Juliani & S. Bortz</i>	613
Subaqueous disposal of sulphide tailings – reclamation of the sherridon orphan mine site, Manitoba, Canada <i>D. Ramsey & J. Martin</i>	627
Modelling techniques for evaluating net percolation through soil covers for solid and hazardous waste – a comparative case study <i>B.S. Dobchuk, M.A. O’Kane, R.E. Shurniak, G.P. Newman & S.L. Barbour</i>	639
Techniques for creating mining landforms with natural appearance <i>G. McKenna</i>	651
Community perceptions and Consultation for Tailings Disposal Facilities in the developing world <i>M. Thorpe & R. Oboro-O’fferie</i>	661
Mining market cycles and tailings dam incidents <i>D. van Zyl</i>	671
Structured geomembrane liners in mining base and closure systems <i>C. West</i>	677
Innovative approach to closure of a mixed wastes process water pond <i>A. Whitman, T. Hadj-Hamou & J. Juliani</i>	681

Optimization of tailings pond design for effective effluent quality management 693
S. Daughney, T. Plikas, J. Zhang, L. Gunnewiek, T. Miller, A. Laagcé & D. Yaschyshyn

Application of quantitative micro-mineralogy to tailings and mining waste 703
K. Olson Hoal, J.G. Stammer, K.S. Smith, K. Walton-Day, C.C. Russell

Fulcrum: an innovation in hydrologic data management 711
C.M.S. Butt & R. Martel

Tailings & Mines Waste Management III – Session 5

Large-strain 1D, 2D, and 3D consolidation modeling of mine tailings 729
M.D. Fredlund, M. Donaldson & G.G. Gitirana

Innovative expansion of a centerline constructed tailings storage facility - settlement modeling 739
G. Gjerapic, K.F. Morrison, J.M. Johnson, B. Doughty & D. Znidarcic

Generic predictions of drying time in surface deposited thickened tailings in a “wet” climate 749
P. Simms, A. Dunmola & B. Fisseha

Storm-water management at mine sites using sedimentation ponds 759
J.P. Clark

Nanisivik mine tailings disposal an example of a mining best practice 771
J. Cassie, G. Claypool & B. Carreau

Oil Sands Tailings II – Session 6

High pore pressures within embankment constructed of lean oil sands 785
J.T.C. Seto, K.W. Biggar, G.W. Ferris & T. Eaton

Cross flow filtration of oil sand total tailings 799
C. Zhang, M. Alostaz, N. Beier & D. Segó

Geotechnical characteristics of laboratory in-line thickened oil sands tailings 813
S. Jeeravipoolvarn, J.D. Scott & R.J. Chalaturnyk

Thickened tailings (paste) technology and its applicability in oil sand tailings management 829
S. Yuan & R. Lahaie

Natural dewatering strategies for oil sands fine tailings 845
N. Beier, M. Alostaz & D. Segó

Applications in the oil sands industry for Particlear® Silica Microgel 859
R.H. Moffett

Screening study of oil sand tailings technologies and practices 871
R. Nelson & D. Devenny

Economic screening of tailings options for oil sands plants 881
D. Devenny & R. Nelson

A robotic system to characterize soft tailings deposits 889
M.G. Lipsett & S.C. Dwyer

Preface

The purpose of the **Tailings and Mine Waste Management 2009** is to provide an exchange of information between people responsible for managing tailings and mine wastes, researchers and providers of management services who have experience with the mining industry. The presentations and conference proceedings will provide an update to the advances since Tailings and Mine Waste 2008 held in Vail, Colorado and will highlight the extensive research and experience from projects presently underway.

A special thanks and recognition is extended to Dr. John Nelson for his vision in establishing the Tailings and Mine Waste Conference in 1994 at Colorado State University in Fort Collins. The conferences were held yearly between 1994 and 2004, then after a three year hiatus Tailings and Mine Waste was restarted in 2008 at Vail Colorado. Tailings and Mine Waste, 2009 is the 13th conference and it is being held in Banff, Alberta. Tailings and Mine Waste 2010 will return to Colorado and then Tailings and Mine Waste 2011 is being planned for Vancouver, BC.

Management of Tailings and Mine Wastes is beset with technical challenges and is an area of increasing public interest. The large volume of mature fine tailings (MFT) associated with Alberta's Oil Sands Industry requiring safe containment and the vigilant management of capping waters represent the most visible of these challenges in Alberta. Ongoing environmental concerns with Acid Mine Drainage from waste rock piles and tailings facilities associated with base metal mining also challenge the industry and regulators.

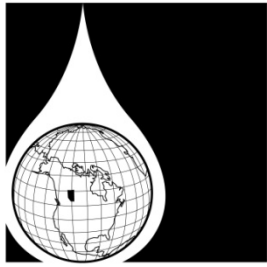
I want to personally thank the Oil Sands Tailings Research Facility (OSTRF) and Dr. N.R. Morgenstern for their encouragement and support for this conference. Organizing this event would not have been possible without the dedication of Dr. Moh'd Alostaz, Nicholas Beier and Sally Petaske who assisted with various aspects of the conference organization.

The success of this conference is only possible due to the breadth of the presentations and the quality of the manuscripts contained in the Proceedings. I want to thank all our professional colleagues who willingly took the time and expended the effort to share their experiences and insight with us. To all the authors, thank you for contributing your technical knowledge and for your efforts in submitting your manuscripts, especially in these extremely busy days when time is our most precious commodity.

The Proceedings contain information representing hundreds of years of collective experience. I hope each of you find insight and answers that will assist you in a better understanding of tailings and mine waste management.

David C. Seago/Chair, Organizing Committee

Thank you to the following sponsors for their support in making the 13th International Conference on Tailings and Mine Waste a success:



OSTRF
Oil Sands Tailings Research Facility



The *UofA*
Geotechnical Centre



Alfa Laval Inc.



Canadian Natural



Keynote Speaker

A GEOTECHNICAL PERSPECTIVE ON OIL SANDS TAILINGS

John C. Sobkowicz, Ph.D., P.Eng.

Thurber Engineering Ltd., Calgary, Alberta, Canada

Norbert R. Morgenstern, Ph.D., P.Eng.

University of Alberta, Edmonton, Alberta, Canada

ABSTRACT: This paper provides a geotechnical perspective and some thoughts on the production, treatment, transport and storage of oil sands tailings, and in particular the capture of fines in a “dedicated disposal area” (DDA), as prescribed in the recently released ERCB Directive 074. Concepts include: available technology for dewatering tailings; the impact of tailings characteristics on methods of transport; necessary characteristics for discharge, capping and reclamation; the relationship between solids content and various geotechnical parameters; simple geotechnical (classification) tests to aid in predicting tailings behaviour; and practical aspects of reliably achieving a uniform, non-segregated tailings deposit.

INTRODUCTION

Of current intense interest in the oil sands industry is the transformation of tailings materials into products that can be stored in a closure landscape in a reliable, geotechnically safe manner, which meets the requirements of closure obligations. These tailings products include:

- Fines resulting from the unintentional segregation of tailings (particularly whole tailings, typically producing MFT in an external or in-pit tailings pond).
- Fines and fines/sand mixtures resulting from the intentional classification of tailings (e.g., by cyclones). These fines may be stored in ponds, but more commonly are treated further in thickeners and/or by various other chemical, mechanical, electrical or environmental methods, and/or by mixing with other materials (such as overburden clays).

To meet long-term storage objectives, it is necessary to remove water from the tailings, which increases their solids content, density, strength and deformation modulus. This can be achieved using a variety of tailings treatment methods, in a number of stages, to meet various short-term (operational) and long-term (permanent storage and closure) objectives.

A large amount of work has been undertaken by various research organizations and oil sand mine operators, to characterize oil sands tailings materials – particularly to determine segregation potential, methods of preventing segregation during transport and placement, and techniques for efficiently removing water (e.g., various types of thickening). With the advent of ERCB Directive 074, this work has intensified as operators seek to develop practical storage solutions for the fines component of the tailings.

This paper discusses oil sands tailings treatment technologies and provides a geotechnical perspective on the many issues associated with tailings, from their production in the extraction plant to their eventual storage as part of the reclaimed landscape. The design of tailings retention structures is not considered in any detail.

BACKGROUND

Tailings Challenges

Oil sands tailings consist of a mixture of sand, fines and water in varying proportions. However, there are some unique aspects of oil sands tailings that challenge operators in their handling, transport, treatment and disposal:

- Oil sands tailings contain a residual amount of un-extracted bitumen, in the order of a few percent by total mass. While small in relative quantity, the bitumen is viscous and very sticky, which significantly impacts the characteristics and behaviour of the tailings, and introduces operational complexities.
- Development of in-pit tailings storage space can take 5 or more years, during which time the tailings must be stored in a relatively large, external, above-ground facility.
- The mine pits are 100 m or more deep. The overburden, consisting of glacial clay and Cretaceous clay shale deposits, can be a few meters to a few tens of meters thick, underlain by the Cretaceous McMurray formation, which contains the bitumen-saturated sand. The ore is 40 m to 80 m thick, and can contain interbedded clay shale and siltstone. The former is often not amenable to selective mining at the face and is thus the source of much of the fines in the tailings stream.

- To develop in-pit storage for tailings, mining must proceed to the base of ore, and a sufficiently large footprint must be opened up within the mine, not only to accommodate the tailings but also any in-pit dykes required for containment. Due to poor foundation conditions, these in-pit dykes can have very flat slopes and thus they place a high demand on providing available footprint at the base of the mine, before construction commences.
- When tailings disposal does move in-pit, the storage areas are deep and often laterally constrained, which can result in the accumulation of very thick deposits in a short period of time.
- Due to the abundance of ore grade deposits, many of the mine leases are highly constrained in available surface area on which to dispose of waste. Overburden dumps, tailings ponds, DDAs, thin lift dewatering areas, and other waste disposal facilities all compete for limited out-of-pit and in-pit space.
- Unlike many mines in areas closer to the equator, the potential for evaporative drying of the tailings is low, and much below demand.
- The industry is constrained during operation to zero discharge of process-affected water. Therefore tailings management is intimately related to the site-wide water balance and the provision of reclaim water to the extraction plant.

Tailings Characteristics of Interest

The main tailings characteristics of interest to the industry are:

- Basic tailings properties.
- Segregation potential and processes (after production, during transport, and during discharge / placement).
- Ease of pumping and tendency for internal wear of pumps and pipes.

- Flow behaviour after discharge.
- Rate of dewatering (during and after placement; includes various settlement behaviour mechanisms).
- Strength at placement and rate of strength gain after placement.
- Rate of consolidation and potential for future surface settlement.

All of these issues have been studied at various research institutes and operating mines. Excellent background information on progress to date can be found in the following references:

- Basic properties of oil sands CT are given in Caughill et. al. (1993) and Qiu & Seago (2001), and of TT in Jeeravipoolvam et. al. (2008a).
- A good general reference on oil sands tailings is Morgenstern & Scott (2000).
- The impact of clay mineralogy and water chemistry is found in Mikula et. al. (2008) and Jeeravipoolvam et. al. (2008a).
- Information on the compressibility and hydraulic conductivity of fine oil sands tailings is found in Pollock (1988), Suthaker & Scott (1996), Scott et.al. (2008), and Jeeravipoolvam et. al. (2008b).
- Consolidation of high fines CT is discussed in Liu et. al. (1994).
- A consideration of the pumping of oil sands tailings is given in Cooke (2008).
- Some of the issues associated with treatment and placement of tailings at an operating mine are discussed in Fair (2008).
- Issues around capping and reclamation of oil sands (and other) tailings is given in Jakubick et. al. (2003).

COMMUNICATING TAILINGS PROPERTIES

Basic Properties of Tailings

Oil sand tailings researchers and practitioners have for many years used a ternary plot of sand, fines and water content to characterize oil sands tailings and illustrate its properties. The use of this plot is discussed in Scott (2005) and illustrated on Figure 1.

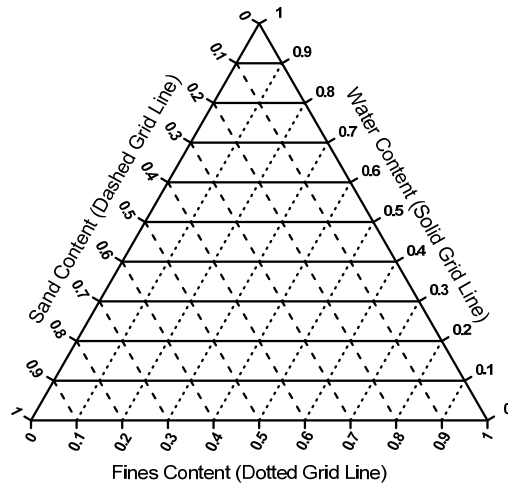


Figure 1 - Layout of Ternary Diagram for Tailings Components

The fines content adopted in the oil sands industry is $< 44 \mu\text{m}$ (and consequently the sand is described as being $> 44 \mu\text{m}$). The vertical apex of the ternary plot represents 100% water, the lower left corner represents 100% sand, and the lower right corner represents 100% fines (all by total mass). Grid lines for each component are drawn parallel to the side opposite its respective corner, as shown on Figure 1.

Defining the mass of sand, fines, water and bitumen in a sample as s , f , w , and b respectively, and $T=s+f+w+b$, then the sand content $S=s/T$, the fines content $F=f/T$, the water content $W=w/T$, and the bitumen content $B=b/T$. The solids content, $SO=(s+f+b)/T$ is then just $1-W$, and can be read off the right axis on Figure 1.

Other quantities can also be shown on the ternary plot, as required. For example, Figure 2 shows lines of constant F^* and FFW, defined as:

$$F^* = \text{geotechnical fines content} = f/(f+s)$$

$$FFW = f/(f+w)$$

The ternary plot is often shown with these “alternate” axes, (but they are not, in fact, the primary axes of the plot).

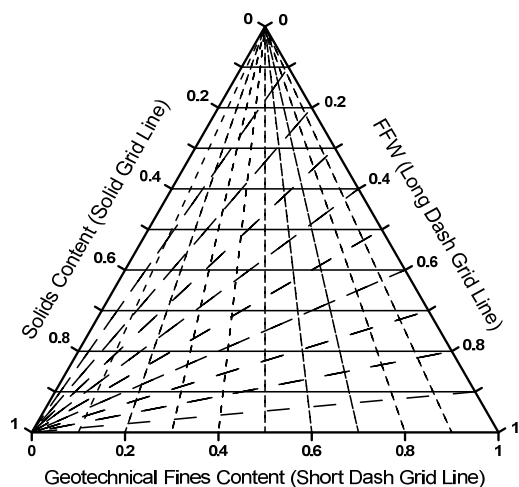


Figure 2 - Alternate Axes for Ternary Diagram

Contours of other geotechnical parameters, such as geotechnical water content (W^*) or void ratio (e), may also be plotted on the ternary diagram, as shown on Figure 3. to

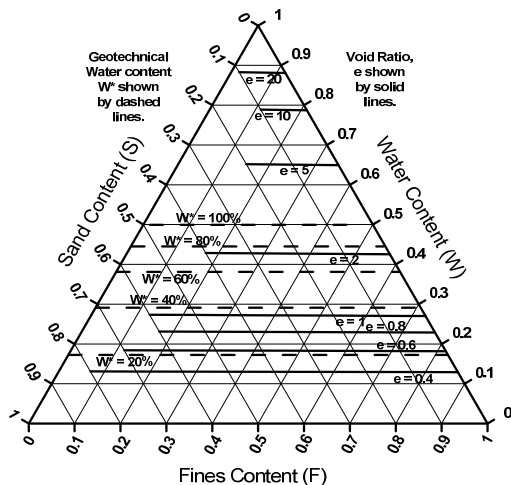


Figure 3 - Void Ratio and Geotechnical Water Content

Since, for saturated materials, these are both measurements of the relative amount of water and solids in the material, the contours are either parallel to (for W^*), or nearly parallel (for e), constant values of W . In a similar manner, contours could be developed for wet or dry density on the ternary plot.

Expected Tailings Behaviour

Scott (2005) used the ternary plot to illustrate areas with different geotechnical behaviour of the tailings, as shown on Figure 4.

The boundaries on Figure 4 defined by Scott are:

- Sedimentation (A) vs Consolidation (B),
- Segregating (C) vs Non-segregating (D) mixtures (untreated tailings),
- Pumpable (E) vs Non-pumpable (F),
- Liquid (G) vs Solid (H),
- Saturated (J) vs Unsaturated (K) soil, and
- Fines-dominated matrix (L) vs Sand-dominated matrix (M).

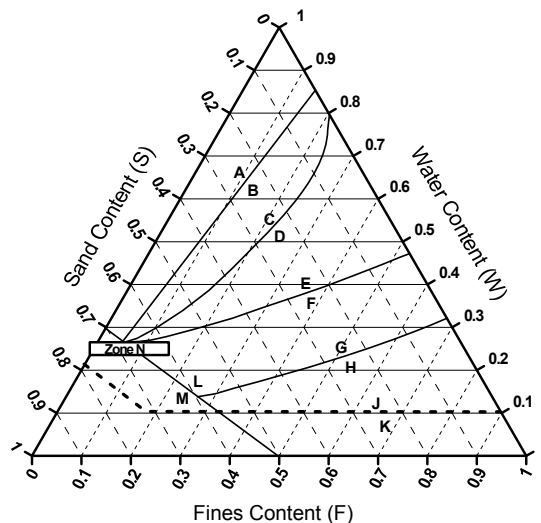


Figure 4 - Zones of Different Geotechnical Behaviour (after Scott, 2005)

The boundaries shown on Figure 4 are not accurate for the tailings from any particular oil sands mine, i.e., these boundaries will vary significantly, depending on the fines

mineralogy, clay activity, water chemistry, bitumen extraction method, tailings treatment method, etc. This plot should thus be regarded as giving only a very general indication of tailings behaviour, and should only be used for illustrative purposes. Site-specific correlations must in all cases be developed for any particular lease and mining/extraction/tailings treatment method. Further discussion is provided later in this paper regarding the theoretical basis/derivation of these behavioural boundaries.

It is interesting to note that portions of the boundaries A/B and G/H, and to a lesser extent C/D, are roughly parallel to constant values of FFW of 0.15, 0.68 and 0.3 respectively, (this is one of the reasons the alternate plot axes shown on Figure 2 are in popular use). This suggests that, at least for mixtures with a fines-dominated matrix, it is the relative amount of fines and water (irrespective of the sand content) that determines sedimentation vs consolidation behaviour, liquid vs solid behaviour, and to some extent, segregating vs non-segregating behaviour, in the tailings.

One type of tailings behaviour that Scott did not include on Figure 4 is the liquefaction potential of sand tailings. Sobkowicz & Handford (1990) presented data showing the steady state line for Syncrude tailings passing through a void ratio of about 0.9 to 1.0 at an effective minor principal stress of 1 kPa, and of about 0.8 to 0.9 at an effective minor principal stress of 100 kPa, (depending upon fines content). This equates to a solids content of between 73%-75% for the former case and 75%-77% for the latter case, which can be adopted as a useful screening number on the ternary diagram. This liquefaction boundary has been added to Figure 4 as Zone N. Sand tailings plotting on or above Zone N

are potentially liquefiable; those plotting below Zone N are not.

While a very useful plot, one of the weaknesses of the ternary diagram is that it does not explicitly show clay content, which in some cases dominates geotechnical behaviour of tailings (more so than fines content).

TAILINGS PRODUCTS AND TREATMENT METHODS

Tailings Production / Variability

Oil sand from the mine is commonly processed in the following manner:

- The ore is crushed in-pit, to break it up into less than 100 – 200 mm size. At some mines, the crushed siltstone pieces are screened out of the ore feed.
- The crushed ore is mixed with hot water and pumped as a slurry to the extraction plant. Transit time in the pipeline provides some conditioning of the ore.
- The slurried ore is discharged into a Primary Separation Vessel (PSV), in which most of the bitumen is separated from the solids and water. An important aspect of the separation process is the addition of a dispersant (such as NaOH) to the slurry.
- Other secondary separation cells are used to collect bitumen that is not captured in the PSV.
- The underflow from the PSV is a mixture of sand, silt, water and a minor amount of un-recovered bitumen, which is released as tailings.
- The tailings may be discharged directly to a storage facility (referred to as a “whole tailings stream”) or may be processed in a variety of ways (e.g., through a cyclone separator and/or thickener). Details of

various tailings processing and treatment methods are given in Section 4.3.

Oil sands tailings are produced at a high rate – 12,000 to 15,000 t/hr per train. An upgrading plant producing ~200,000 barrels of synthetic crude oil daily would normally run 2 trains from the mine through the extraction plant.

Some properties of the tailings, such as solids, fines, and bitumen contents, can vary over a wide range, depending on variations in the ore from the mine, and on various operating and upset conditions within the extraction plant. Oil sands tailings are not, by any stretch of the imagination, a consistent product. There is thus a significant difference between oil sands and most other tailings, such as those encountered in the metal mining industry.

Objectives in Treating Tailings

While it may seem obvious, one of the main objectives in handling / treating the oil sands tailings is to remove water, so that the tailings eventually achieves a semi-solid state, with modest strength and limited compressibility.

The number of stages used to dewater the tailings, and the timing thereof, depends on several factors:

- The dewatering efficiency of any particular treatment technology.
- Requirements to achieve a robust mixture that will not segregate.
- Optimizing water content for pumping or other transport to a disposal area.
- Tailings discharge / placement issues (e.g. making a uniform, non-segregated deposit; cold weather; quick reclaimability, etc.).
- Achieving storage end objectives for strength and compressibility.
- Managing the water balance.

- Achieving cost and tailings operations efficiencies.

The optimal treatment strategy may involve several stages of dewatering, using a number of different technologies. These are discussed further in the following subsection.

Tailings Treatment – A Tailings Technology Road Map

A variety of technologies are available for dewatering and otherwise treating tailings. These are illustrated on the “Tailings Technology Road Map” (Diagram 1) and described below.

The following materials are associated with whole tailings, which are represented along the right hand side of the flow chart in Diagram 1. Reference should also be made to Figure 5a, which shows the composition of these tailings products on a ternary diagram.

- Whole Tailings (WT) are produced from the extraction plant (without any post-extraction processing). The solids content of this stream can be quite variable, as a result of dealing with various problems in the extraction plant, but usually is not much higher than 55%. The fines content can also vary considerably, depending on the amount of fines in the ore.
- The method for discharging tailings developed in the early years of oil sands mining was to pump it to an external or in-pit pond, where it was used for “cell construction” (i.e., construction of a sand dyke, in cells) or was discharged sub-aerially onto a beach. This method of tailings storage (or modifications thereof) is still in common use today. The sand in the dyke cells is densified by a combination of compaction (by dozers) and under-drainage. The sand discharged

onto the beach segregates to some extent, and forms beach angles of 1% to 2% above water, and 2% to 4% below water.

- The Beached Tailings (BT) is further subdivided into “BAW”, referring to tailings beached sub-aerially, and “BBW”, referring to tailings beached sub-aqueously. The former (BAW) is denser than the latter (BBW), due to its somewhat coarser PSD and downward drainage into the underlying, above-water beach. As a result, the BBW is more susceptible to liquefaction (compare Figures 4 and 5a).
- Beaching of a whole tailings line is an efficient way of capturing some of the fines in the ore. BT typically has a fines content up to about 15% (or geotechnical fines content, F^* , up to about 20%). The cell and beach deposits can account for capture of 50% to 60% of the total fines delivered in the ore from the mine (including fines both in the oil sands and in the interbedded silt and clay shale layers).
- The fines (+ water) that segregate from the cell sand and beach sand run into the pond and initially form a dilute suspension of ~10% solids content. This is referred to in the industry as TFT.
- Within a few years, the coarser silt size has settled out of suspension and the remaining combination of clay and silt still in suspension has increased in solids content to about 30% to 35%. This is a quasi-stable state that is referred to as MFT. This material is typically >95% fines and from 30% to 50% clay content. Over a much longer period of time, the MFT will continue to settle; solids contents in very old MFT deposits have been measured as high as 45%, although sometimes the sand content is also higher.
- There is an additional, smaller volume tailings stream referred to as FTT, which

represents sand recovered from the secondary extraction cycle. Where the tailings come from a Solvent Recovery Unit, they are also referred to as TSRU.

The materials described above, derived from a non-classified tailings stream, could experience the following fates:

- The sand (and captured fines) may be permanently stored in dykes and beaches, or it may be farmed for other uses, such as construction of chimney and filter drains in overburden dykes, or chemically treated and re-combined with MFT to form CT. It is also used to cap other waste deposits – to improve trafficability and to construct a closure landscape.
- The MFT may be permanently stored at the bottom of end-of-pit lakes or may be recovered (by dredging and pumping) and treated in a number of ways to form a variety of cappable tailings products, as shown in the middle portion of Diagram 1.
- As an alternative to placement in a tailings dyke/ pond, the whole tailings line could be chemically treated and/or filtered to form a non-segregating, higher solids content material that could be deposited in a permanent storage area. These tailings treatment technologies are currently only at the research stage.

Tailings products represented along the left-hand side of Diagram 1 are subjected to purposeful classification, typically by hydro-cyclones (although other methods are possible). The types of materials that could be produced are discussed below. Reference should also be made to Figure 5b, which shows the composition of these tailings products on a ternary diagram.

- Cyclone underflow tailings (CUT) are usually stripped of some fines and water, and are not too dissimilar, although somewhat more variable, in composition than CT.
- Cyclone overflow tailings (COT) are a higher fines content stream than the CUT. They have an SFR of $<$ or ~ 1 (dependent on cyclone design) and are often run through a secondary flotation cell to remove most of the residual bitumen (left over from the PSV). This stream is normally targeted for further treatment, as described below.
- Thickened tailings (TT) is COT that has been processed in a clarifier/thickener or by in-line thickening, to remove some water. Thickening processes can increase the solids content to about 50%. However, in practice the solids content of the thickener underflow is quite variable, due to the fact that the thickener also acts as a water clarifier and heat recovery unit for the extraction plant, and those functions often take precedence over tailings thickening objectives.
- Consolidated Tailings (CT) is a combination of CUT¹ and MFT, which has been chemically treated to create a mixture that does not segregate. At present, the operators that are producing CT are using gypsum as an additive, although other chemical treatment is possible (e.g., lime, CO₂, or acid). This material is targeted at a SFR of 3 to 5, with the expectation that after it is deposited, it will begin to develop some effective stress relatively quickly, and will act more as a granular material under vertical loading.
- Non-Segregated Tailings (NST) is similar to CT, except that it is a combination of TT and CUT.

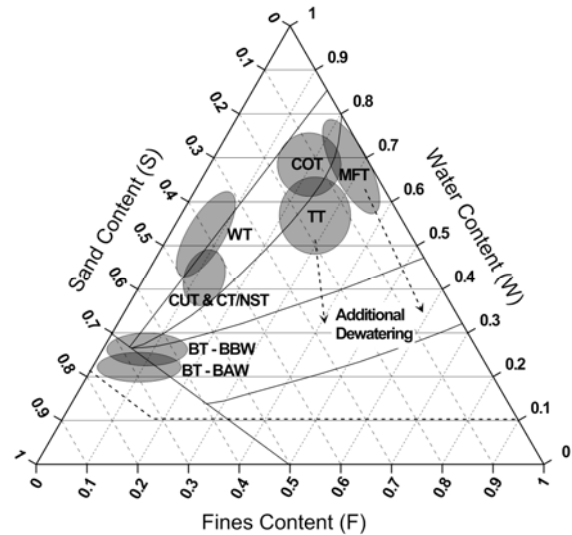


Figure 5b - Comparison of Classified and Whole Tailings Products
 It is clear from Figure 5b that all of these materials have low to moderate solids contents, and plot well above the “liquid-solid” boundary. Additional stages of dewatering are required to render these tailings suitable for long-term storage. The treatment paths and ultimate storage fates are described below:

- The CUT can be further dewatered using methods such as filtration and gravity drainage (i.e., deposition, drainage, and “farming”). The ultimate fate of this material is similar to BT – it can be combined with MFT or TT to form CT/NST, it can be used in the construction of dykes and dumps, and it can be used to cap other tailings deposits.
- One variation of CUT is the sand “stacker”, where the cyclones are located on a mobile unit and the CUT is deposited directly into its ultimate storage location (e.g., in a dyke).
- COT could be permanently stored at the bottom of an end-of-pit pond, although for several reasons this is not current practice. It has been stored in temporary ponds. It may be possible to remove and re-process this COT by dredging, although to do so,

¹ Some early work was done as well on creating CT from WT and MFT.

significant dilution of the material would likely be required.

- Most commonly, COT is thickened (to about 50% solids content) and then the resulting TT is either a) combined with sand to produce NST, or b) subject to further dewatering steps.
- Additional dewatering processes include chemical treatment (such as in-line flocculation), mechanical treatment (such as centrifuging), and electrical treatment (electrophoresis). The first two are both actively being researched by oil sands operators, and the expectation is that the solids contents of these fine streams could be increased to about 60% to 70% using these methods. The third method (electrophoresis) has been proposed but not investigated in a serious manner.
- In regards to the previous bullet, a possible next step is to deposit the flocculated or centrifuged tailings in thick lifts in a containment cell, relying on consolidation to reach target strengths (throughout the deposit) within a short time (1 to a few years). This is an area of active research, but the capability to reach the desired targets is uncertain, for which reason this path has been shown dashed in Diagram 1. However, if this approach was to prove effective over a slightly longer time frame (say 5 to 10 years), and was also attractive from a cost perspective, it raises the question of whether or not the time criteria in Directive 074 is un-necessarily restrictive.

As will be evident from later discussion, additional dewatering will very likely be required to render the fines streams suitable for long-term storage in the currently required time frame. Some methods of accomplishing this last stage of dewatering are:

- One approach is to mix the ~65% solids content (SFR 0 to 1) fines stream with

overburden, and co-dispose of the mixture in a dump. This has been researched in the past, and seen some limited application, but mostly with a lower solids content fines stream. Additional research on combining materials such as centrifuge cake with overburden may give a more satisfactory end product.

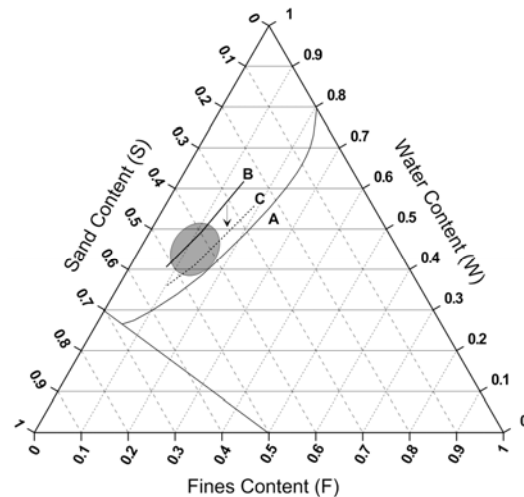


Figure 6 - CT - A Robust Recipe?

- Environmental assists, such as drying and freeze/ thaw, are quite capable of achieving sufficient dewatering to develop reasonable strengths within a tailings deposit. They are particularly effective when combined with suitable discharge methods, such as thin-lift deposition or “mud farming”. At present they are, in the authors’ opinion, the only final dewatering stage that has a high probability of success in the time frame outlined in the Directive 074, and thus should be considered essential to the overall process.
- Another environmental method of dewatering that has been suggested but not seriously researched is biological treatment of the thickened fines stream.

One last treatment option on the tailings technology road map is to combine very high-density thickened tailings (i.e., “paste”)

with aggressively dewatered sand to produce a mixture that would meet long-term storage objectives with no (or minimal) additional dewatering. The terms “Super CT” and “Enhanced NST” have been coined for this type of product.

Examples of Tailings Treatment Issues

Two examples illustrating some of the issues associated with tailings treatment are given below.

The first example involves the challenges of producing a robust CT. The shaded area on Figure 6 represents a possible range of compositions for CT. Line A shows the segregation boundary for untreated tailings; Line B shows the same for a CT that has been dosed with gypsum.

The increase in fines content and the gypsum treatment has improved the segregation boundary with respect to the CT composition. However, there are two issues related to this process that are important to understand:

- While the average recipe for the CT gives a non-segregating product, there is still some proportion of the total volume made that could segregate. Clearly, the less this volume, the more robust the CT recipe.
- The segregation boundary is sensitive to the amount of shear to which the tailings is subjected. If a large amount of shear occurs, either during transport or during discharge, the boundary could move downwards (say, for illustrative purposes, to Line C), meaning that a larger proportion of the CT could segregate. This underscores the importance of controlling shear rate during transport and

discharge, an issue that the oil sands industry has yet to fully address.

A second example is related to the pumping of tailings. The shaded area on Figure 7 is a typical TT product that could be produced from a high rate thickener. Its solids content is about 50%, with a SFR of 0.8 to 1.

In the long term, a target solids content for this material might be ~80%. It is clear from Figure 7 that this represents a large increase in solids content (i.e., a large decrease in W). In the process, the TT will undergo a significant change in its rheological properties.

A TT product as defined on Figure 7 will, apparently, have a sufficiently high solids content to be non-segregating. This will of course depend on the amount of shear introduced during the pumping and pipeline transportation phase, which could lower Boundary C sufficiently to allow some segregation in the pipe. The nature of the material during transport (i.e., whether or not some segregation occurs) will have an important impact on the design of the pumping system and on desired flow velocities.

Also shown on Figure 7 is Scott’s “pumping/no pumping” boundary (Line D), which corresponds to a yield stress of about 80 - 100 Pa. There are in fact several pumping boundaries, depending on the pump type, pump and line operating pressures, pipe diameter and length, etc., and their locations will vary depending on tailings mineralogy and chemistry.

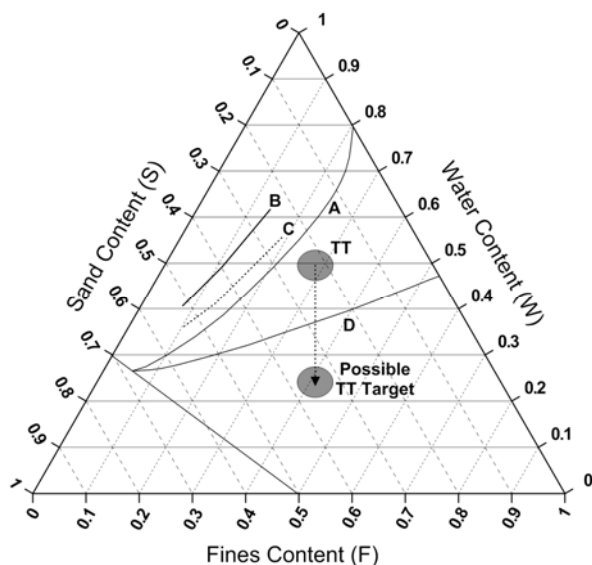


Figure 7 - Dewatering and Pumping TT

At lower solids contents and strengths, (nominally < 50 to 100 Pa and above Line D on Figure 7), the pump of choice is centrifugal. A centrifugal pump could handle the underflow from a conventional high rate thickener with no further treatment of the tailings.

However, one could adopt the philosophy of dewatering the tailings as much as possible at this stage by using a paste thickener. The resulting thickener underflow would plot below Line D on Figure 7, perhaps with $SO \sim 70-75\%$ and with a yield strength of $100 - 300$ Pa. In this case, a positive displacement (PD) pump would likely be required.

To date, oil sand operators have elected not to use PD pumps due to scale-up issues from existing equipment and an anticipated high maintenance. This situation may change, as there are cases where PD pumping would obviously be helpful (e.g., for short runs from a centrifuge to a deposition area), and experience gained with PD pumping might embolden operators to use them as a more

integrated component of their tailings transport system.

How does one decide how much dewatering is right at the thickening stage? This is essentially a cost decision. As noted by Boger (2002), the design of a tailings disposal system should start at the end point (for oil sand tailings, the DDA) and work upstream to the thickening stage. For the pumping stage, the design optimizes "...the pumping and pipeline conditions needed for...transport whilst ensuring the tailings reach the disposal site with the rheological properties necessary for the chosen disposal method....".

In other words, several stages of dewatering will be required for TT – an initial stage which raises the solids content enough to achieve efficient pumping, and then one or several stages after reaching the DDA, to efficiently place the tailings and at some point, to reach strength and compressibility target values. One of the issues to address during this design process is the tradeoff between early dewatering in a thickener, coupled with positive displacement pumping or “at the edge” centrifugal pumping, versus less dewatering at the thickening stage combined with centrifugal pumping, (and additional stages of dewatering near or at the disposal site).

TAILINGS DISPOSAL END TARGETS

The tailings stored in a DDA should meet several important end objectives:

- It should develop strength at a rate sufficient to allow timely capping, and meet reclamation and closure requirements.
- It should develop a low compressibility so as to minimize settlement and not disrupt the closure landscape.

Both of these mechanisms require consolidation and an increase in effective stress within the tailings deposit, which depends on both compressibility and permeability characteristics.

The ERCB Directive 074 defines its end targets as:

- A minimum undrained shear strength of 5 kPa for material deposited in the previous year.
- A deposit ready for reclamation within five years after active deposition has ceased, with a trafficable surface layer that has a minimum undrained strength of 10 kPa.

An historical perspective on the development of the ERCB Directive 074, and the rationale for the selection of the numbers listed above, is found in Houlihan & Mian (2008).

It is of interest to ask the question: “What solids content is necessary to achieve these strengths and how quickly will the tailings reach this state?” These questions will be addressed in the following two sections of this paper.

However, as a separate point, the authors are of the opinion that the minimum undrained strength criterion of 5 kPa is too restrictive, given the number of technical options being considered to meet the objectives of the Directive. It is not applicable to tailings materials that behave like a granular soil (e.g., BT or CT). For those materials that behave as a cohesive soil, the criterion precludes capping strategies proven elsewhere. The authors believe that the 5 kPa criterion should be replaced by a detailed consideration of the following:

- What are the anticipated properties of the tailings?

- How will they be capped?
- What will be the schedule for capping?
- What are the time-strength trajectory and the associated subsidence of the tailings deposit, and how is this addressed in the reclamation plan?
- How will the tailings be reclaimed to meet closure plan productivity requirements?
- What will be the anticipated schedule for doing so?

This set of questions will allow government regulators to manage reclamation of the DDAs and at the same time not preclude any viable tailings management strategies.

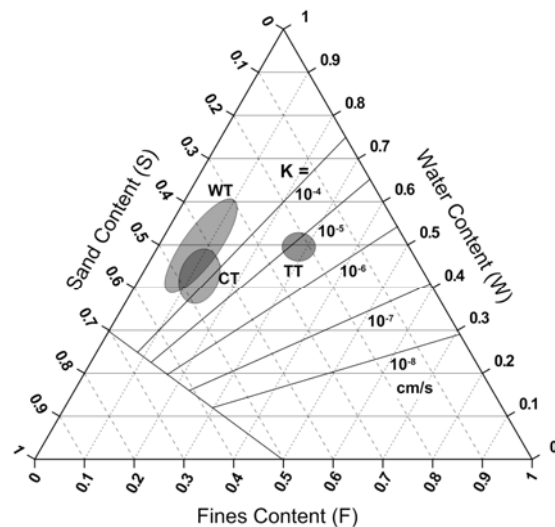


Figure 8 - Hydraulic Conductivity (cm/s) of (Untreated) Fines/Sand Mixtures

TAILINGS HYDRAULIC CONDUCTIVITY, COMPRESSIBILITY AND CONSOLIDATION

Hydraulic Conductivity

Suthaker & Scott (1996) showed that the hydraulic conductivity of MFT, or of mixtures of MFT and sand ($SFR = 2$ to 4), is dependent on the fines void ratio, e_F , and that there is approximately a power law relationship between the two, of the form:

$$K = A * e_F^B$$

(with $A = 6.16 * 10^{-9}$ and $B = 4.468$).

This relationship was valid down to a fines void ratio of about 0.6. Suthaker & Scott found a similar relationship between K and e_F for various types² of CT (or NST), with slightly different values of A and B . The results were demonstrated up to a fines void ratio of 8.

Liu et. al. (1994; for NST with a SFR = 3 to 5) and Scott et. al. (2008; for COT with a SFR ~ 1) found a similar relationship between K and e_F , (again, obtaining somewhat different values of A and B ; Scott more so than Liu).

For a fully saturated material, the fines void ratio is:

$$e_F = G_F * W / F$$

It is a relatively simple matter to demonstrate that contours of constant e_F on the ternary diagram are parallel to lines of constant FFW (see Figure 2). All contours of constant e_F pass through the point $S=1$ and have values of:

$$FFW = G_F / (e_F + G_F)$$

Scott & Suthaker's research indicates that the relationship between K and e_F applies down to a fines void ratio of ~0.6, which is equivalent to a FFW value of ~0.8. The authors suggest that this relationship may not be valid once the tailings material starts to develop a solid structure/fabric, and that for practical purposes the relationship between K

² That is, using various kinds of chemical additives – sulfuric acid, quick lime, fly ash and gypsum.

and e_F should be limited to values of $e_F > \sim 1.1$ (or $FFW < \sim 0.7$).

Contours of constant hydraulic conductivity should thus also parallel lines of constant FFW. For example, Figure 8 shows contours of constant K for untreated mixtures of fines, sand and water, using the relationship developed by Suthaker & Scott (1996), (respecting the $FFW < \sim 0.7$ criterion). Note that as tailings products transition to a solid, with $e_F < 1.1$, K will continue to decrease below the values shown on Figure 8, but will not necessarily be a function of e_F .

Also shown on Figure 8 are some “as produced”, typical compositions for WT, CT and TT. This figure illustrates that the hydraulic conductivity of “as produced” tailings products is relatively high (about 10^{-3} cm/s for WT, 10^{-4} cm/s for CT, and 10^{-5} cm/s for TT³), but that with dewatering, the hydraulic conductivity would decrease significantly.

Compressibility

Scott et. al. (2008) also show some compressibility data for the COT that they tested, which would be applicable to one value of SFR (=1). Their results are shown in Figure 9 (note: this figure shows e on the vertical axis; to convert to e_F , multiply by $1+SFR$, i.e., in this case, by 2).

³ Note that the hydraulic conductivities shown on Figure 8 are for un-treated tailings; gypsum treatment to produce CT or with flocculants to produce TT will affect K , possibly lowering its value by $\frac{1}{2}$ to 1 order of magnitude for CT and possibly increasing its value for flocculated TT.

Rate of Consolidation

As discussed in Section 4.3, the rate of consolidation in thick deposits of CT or TT is an issue of intense interest in the industry.

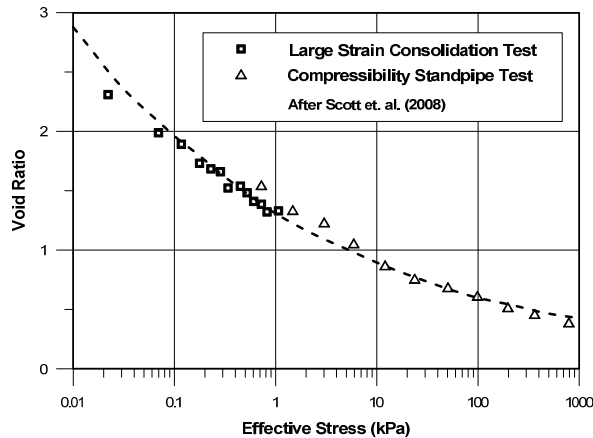


Figure 9 - Compressibility of Cyclone Overflow Tailings

The question of whether or not these deposits will consolidate quickly, to develop the strength required for capping and for the establishment of a closure landscape, in the time frame contemplated by recent regulations, is an important one. The resolution of this issue will determine the lease area required for disposal of tailings fines and the need for supplementary dewatering methods (such as drying or freeze/thaw), both of which have major cost implications.

To properly model the rate of consolidation of fine tailings, one needs to invoke large strain consolidation theory. However, some idea of this rate may be obtained by examining the variation of c_v with void ratio or solids content, as might be calculated (for example) from the data reported by Scott et. al. (2008). In this case, both K and m_v decrease by 4 to 5 orders of magnitude with a decrease in fines void ratio from 6 to 1. Since:

$$c_v = K / (m_v * \gamma_w)$$

The large variations in K and m_v mostly cancel out, and the resulting value of c_v in Scott's COT varies only between about $2 \times 10^{-3} \text{ cm}^2/\text{s}$ and $6 \times 10^{-3} \text{ cm}^2/\text{s}$. Liu et. al. (1994) found a similar, small variation in c_v with effective stress or SFR. This suggests that the rate of consolidation for a particular tailings product would vary by only a small amount over a wide range of void ratios or solids contents, increasing by ~3 to 5 times with increasing effective stress / solids content.

To properly model this situation, one would need to develop a model that includes successive yearly placement of fines tails and that uses finite strain theory to predict solids content at various depths with time. A good understanding of the relationship between solids content, permeability, compressibility and strength would also be needed.

However, one can obtain a general indication of consolidation rates using small strain theory, recognizing that the problem involves a moving top boundary and that the fine tailings in the DDA is consolidating during the time when the DDA is being filled. The theory for this case is given in Gibson (1958).

For example, consider the case of a DDA accumulating 5 m of fine tailings a year for a period of 8 years, producing a deposit about 40 m deep. Using the previously quoted values of c_v , one calculates that at the end of the 8 years, when the DDA is full, the average degree of consolidation is from 5% (for $c_v = 2 \times 10^{-3}$) to 13% (for $c_v = 6 \times 10^{-3}$). An additional 40 to 60+ years is required to reach an 80% average degree of consolidation. For a deposit accumulating 21 m of fine tailings over 7 years (3 m of tailings per year), the average degree of consolidation when the DDA is full is from 13% to 30% (for the same values of c_v) and from 25 to 40 years is needed to reach 80% consolidation.

Note that this calculation only applies once the fine tailings start consolidating. If the fine tailings are still in a hindered settlement mode when they are deposited into the DDA, then some additional time would be required to initiate consolidation, and after that point of time, the full excess pore pressures would need to be dissipated. For the quoted values of c_v , this is about 30 to 50 years for a 20 m deep deposit, and 50 to 80+ years for a 40 m deep deposit.

Settlement versus Consolidation

It is important to distinguish between the process of settlement or hindered settlement and the process of consolidation. The former occurs for a number of years after deposition and applies essentially to suspensions of fines in water, which behave like a liquid. This is the state in which MFT exists in the tailings ponds. The latter is initiated after sufficient dewatering has occurred to form a more solid soil structure, and is associated with the development of effective stress in the soil skeleton. In the context of Directive 074, an area worthy of additional practical research is the development of methods to enhance the rate of settlement in the fine tailings.

STRENGTH OF TAILINGS MATERIALS

Strength Variation

The strength of a tailings material varies with its grain size distribution, clay content, clay mineralogy, water chemistry and solids content. At low solids contents, the tailings acts as a slurry (i.e., as a “liquid”) with a very low yield stress under shear. As the solids content increases, the yield stress at first increases slowly, and then at some point, increases very quickly, after which the

tailings acts more as a solid. This is portrayed in Figure 10.

Where do various oil sands tailings materials plot on this graph? There appears to be limited published data on this subject. Mihiretu et. al. (2008) show some data for MFT at 30% solids content, which has a yield stress of 4 to 5 Pa, and of thickener underflow fines at 35% solids content (and pH of 12) which has a yield stress of 5 to 6 Pa, but these tests were run at solids contents well below that at which a significant yield stress developed.

Figure 4 suggests that the transition from “liquid” to “solid” behaviour should occur somewhere around 70% solids content for MFT and other high fines oil sands tailings, around 80% for TT and other SFR ~ 1 tailings, and around 85% for CT (note that these numbers are just indicators and will vary from lease to lease and with type of tailings, as discussed previously). A possible relationship between shear yield stress and solids content is shown for MFT and TT on Figure 10. These curves are meant for illustrative purposes and are not based on real data, (see discussion at the end of this section for derivation). Further work is required to define these curves for various oil sands tailings products, which would provide important input into the design of pumping systems for transporting tailings to a disposal area.

Strength from Atterberg Limits

Another way to estimate the undrained strength of tailings is to use the geotechnical test referred to as an “Atterberg Limit”. Of most interest is the liquid limit (W_L), which is the geotechnical water content (W^*) of the soil at the liquid/solid boundary, as defined by a specific test method (ASTM Standard Test D4318-05). This method identifies the

point when the undrained strength of the sample is in the range of 1.5 to 2.5 kPa (beyond the upper end of the tests shown on Figure 10).

The liquid limit is a function of a number of variables, the main ones being clay type and mineralogy (or “activity”), and pore water chemistry (pH, salinity, other dissolved ions, etc.). Jeeravipoolvarn et. al. (2008) show that for oil sand tailings, W_L is also a function of bitumen content.

For materials with a clay-dominated matrix, W_L is a linear function of clay content, C^* (Polidori, 2007). For any tailings product, if we know W_L for the fines portion of the material, then we can also calculate W_L for any mixture of fines and sand, assuming that the proportion of clay to fines remains relatively constant and that the ratio of bitumen to clay is also relatively constant⁴.

$$W_L = k_1 \times C^* = k_1 \times k_2 \times F^*$$

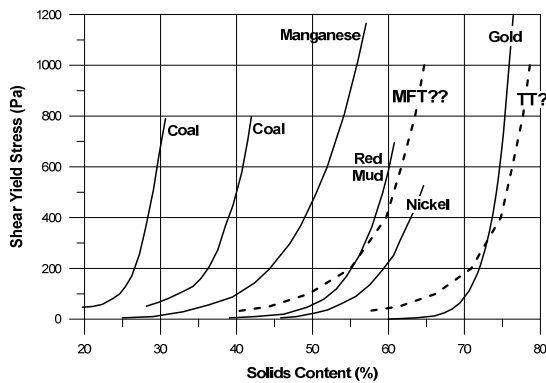


Figure 10- Variation of Yield Stress with Solids Content for various Tailings Products (modified after Boger, 2002)

Where: k_1, k_2 are constants ($k_2 = c/f$)

⁴ These assumptions may not apply to all products – for example, TT from the plant may have a different clay content or water chemistry compared to MFT from a pond, and thus the solid-liquid boundary may be different for the two materials (i.e., discontinuous if plotted together on a ternary diagram).

If these assumptions hold, then the liquid/solid boundary should be parallel to a line of constant FFW, and W_L along this boundary can be calculated using the above equation. For example, on Figure 4, Scott (2005) shows the solid/liquid boundary at $FFW = 0.68$. This intersects the $S=0$ line at a water content, W of 0.32, or a geotechnical water content, W^* of 0.47. The solid/liquid boundary shown on Figure 4 is thus equivalent to a material with a liquid limit (of the fines portion, $F^* \sim 1$) of 47%.

Others have reported Atterberg Limits for various tailings products as follows:

- Devenny (1993) reported W_L of fine tailings ranging from 60% to 70%.
- Suthaker & Scott (1996) report W_L of fine tailings between 40% and 60%. This material had $F^* = 97\%$ and $k_2 = 0.47$.
- Jeeravipoolvarn et. al. (2008a) report the W_L of the $< 45 \mu m$ TT fines as 57%, and the W_L of a fine tailings with $F^* = 94\%$ as 52%.
- Additional Atterberg Limit data is given in Jeeravipoolvarn et. al. (2008b) – a 2008 Syncrude COT ($k_2 = 0.52$) with $W_L = 42\%$; 1982 Syncrude MFT samples ($F^* \sim 100\%$; no k_2 given) with W_L from 42% to 55%; 2005 ILTT East Pilot Pond samples ($k_2 \sim 0.5$) with W_L from 40% to 65% (most samples); and 2005 ILTT West Pilot Pond samples ($k_2 \sim 0.5$) with W_L from 60% to 85% (most samples). The higher W_L in the latter samples was attributed to possibly higher bitumen content or different ore type (i.e., it wasn't really determined).

In summary, it seems that the fines portion of the oil sands tailings products typically has $k_2 \sim 0.5$ and W_L ranging from 40% to 70%, with some higher values if the material contains more clay content, more active clay

minerals, or more than “normal” (1-2%) bitumen content.

Figure 11 shows the approximate liquid/solid boundaries for oil sands tailings, given that the assumptions stated earlier apply. Line A is the boundary associated with a tailings material whose fines (i.e., at $F^* \sim 1$) have a $W_L = 70\%$. Likewise, Line B – W_L of fines = 60%; Line C – W_L of fines = 50%;

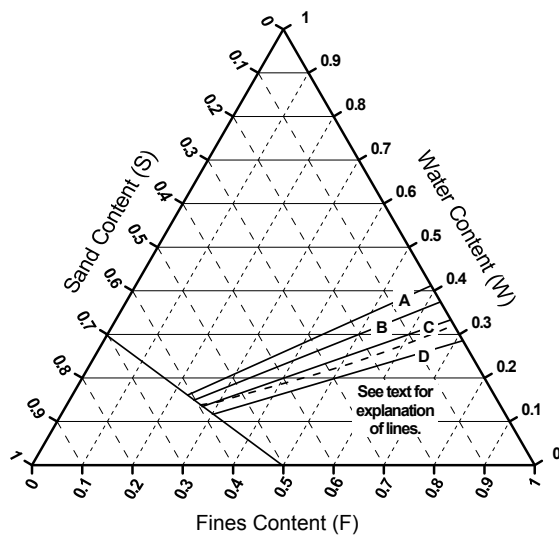


Figure 11 - Solid / Liquid Boundary - Range of Locations for Oil Sands Tailings

Line D – W_L of fines = 40%. Since tailings materials will have somewhat variable Atterberg limits, the reader should anticipate that the boundary separating “liquid” from “solid” will be a transitional one, spanning a range of solids contents of from 5% to 10%.

Figure 11 indicates that to reach the liquid/solid boundary and develop a very modest undrained strength (~ 2 kPa), various tailings products might have to exceed a larger range of target solids contents than stated previously – for MFT, from 58% to 72%; for TT, from 70% to 85% (depending on SFR); and for CT, from 80% to 85% (again, depending on SFR; at the higher solids content, the CT would behave more as a material with a sand-dominated matrix). To

meet the ERCB Tailings Directive 074 strength values discussed earlier, the target solids contents for these tailings products may have to be even higher than the values quoted above (discussed further below).

It should be clear from this discussion that it would be very helpful to determine the liquid limit and clay content of various tailings products, to gain insight into the solids contents required for disposal. To date, very few Atterberg Limit tests have been performed on oil sands tailings (except by some researchers).

This type of (geotechnical) testing will be essential for on-going monitoring and control of operations. Variations in the ore or in the extraction process can cause changes in the tailings clay content, clay mineralogy, bitumen content and/or water chemistry, which could impact the target solids content for each tailings product. These variations need to be tracked during operations to optimize tailings characteristics for pumping and discharge, and to ensure that DDA objectives are met.

In this regard, Rajani & Morgenstern (1991) and Lee (2004) have published some useful correlations for the slump test. In the former case, the correlation for slump versus yield stress (in a Bingham fluid) could be used to indicate acceptability of tailings products as placed in a DDA. In the latter case, the correlation is for slump versus liquid limit. This could be combined with the measurement of bulk density (and thus geotechnical water content), and used to predict the required additional dewatering of a tailings product to achieve a target undrained strength.

Strength versus Solids Content

Further work should be undertaken to determine (or perhaps just to publish?) the shear yield stress for “liquid” tailings materials and the undrained strength of “solid” tailings materials. Portrayal of this information, as contours of yield stress or undrained strength, would be beneficial.

As an example of what might be achieved, a general relationship between LI and c_u is used to illustrate how strength might be portrayed on the ternary diagram. The relationship is taken after Atkinson & Bransby (1978) and Terzaghi, Peck and Mesri (1996), shown in Figure 12.

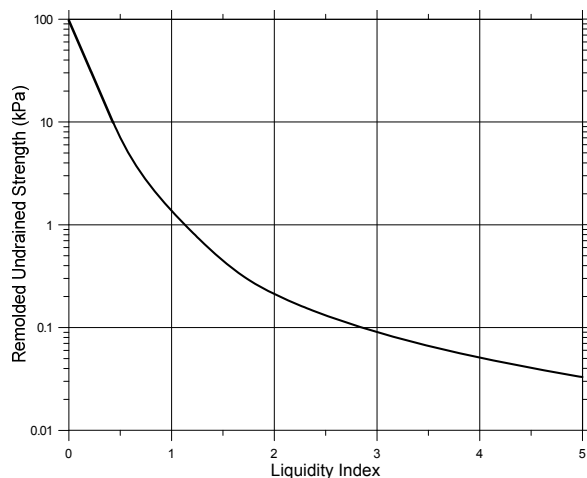


Figure 12 - Remolded Undrained Strength of Clays
(after Atkinson & Bransby, 1978; and Terzaghi, Peck & Mesri, 1996)

Contours of c_u are shown for oil sands tailings on the ternary plot in Figure 13. These assume that:

- The relationship in Figure 12 applies.
- The values of k_2 and bitumen content are relatively constant ($k_2 \sim 0.5$; $B \sim 1-2\%$).
- Lines of constant LI are parallel to lines of constant FFW (follows on previous point).
- The fines in the oil sands tailings (i.e., at $F^* = 1$) have $W_L = 52\%$, $W_P = 27\%$, $PI = 25\%$, and $k_2 = 0.5$ (similar

solid/liquid boundary as Line C on Figure 11).

In Figure 13, the contours of c_u are shown with a dashed line for $F^* < 0.4$, as the relationship between W_L and C^* starts to deviate from linear for $C^* < 0.2$. The c_u contours in Figure 13 were used to derive the MFT and TT curves shown in Figure 10. The location of these strength contours would shift for tailings materials with different Atterberg Limits.

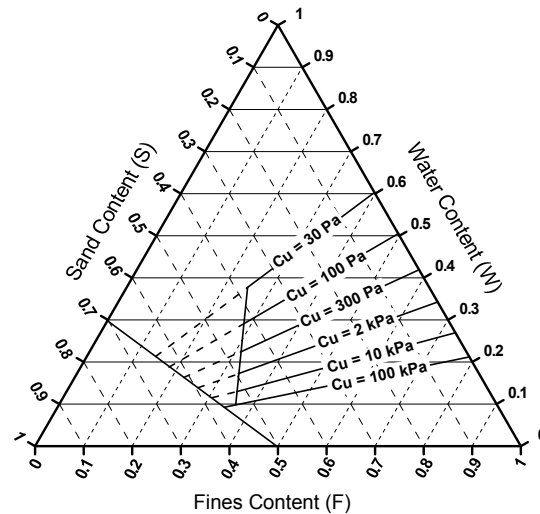


Figure 13 - Possible Distribution of Oil Sands Tailings Undrained Strength (See Text for Details)

Revised tailings end product target solids contents are shown on Figure 14, which take into account the information given on Figures 11 to 13, discussed in this and the preceding sub-section. Note that these targets are only applicable for the strength correlations shown on Figure 13; they will vary, depending on the actual strength characteristics of the tailings products at any specific mine site.

MEASURING GRAIN SIZE

There is insufficient room in this paper to discuss this subject properly. The only point that will be made is that an understanding of the true grain size distribution of real tailings products, in an operating environment, are

critical when applying geotechnical thinking to tailings behaviour.

Jeeravipoolvam et. al., (2008a).

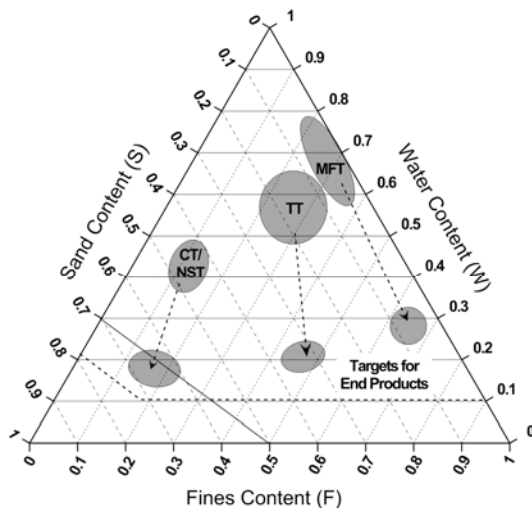


Figure 14 - Possible Targets for Tailings End Products

Of particular interest to geotechnical engineers is the determination of clay content, which in some cases dominates the behaviour of the tailings. Geotechnical correlations of other parameters to clay content are based on its measurement in a hydrometer test. This can give very different results than other fines PSD test methods in common use in the oil sands industry.

Several issues that need to be addressed are:

- Differences caused by sample preparation techniques, (e.g., to dry or not, to “grind” or not, whether or not to disperse, etc.).
- Differences due to grain size testing methods (sieve/hydrometer, laser diffraction, methylene blue, etc.).
- Preservation of sample properties during the test, (e.g., clay particle size or charge, or pore water chemistry).

There is a good discussion of this topic in

FINAL LANDSCAPE

Developing sufficient tailings strength and stiffness to meet regulatory requirements in a DDA is one objective, but not the only one. In fact, the primary objective is to allow timely reclamation and development of closure landscapes. Jakubick et. al. (2003) state these objectives as follows:

- Is the bearing capacity of the tailings surface sufficient for machinery and material to advance a cover?
- How large is the rate and amount of settlement of the tailings surface induced by the load of the cover (or the load of the long term landscape)?
- For the final reclamation surface, is there (1) a medium for re-vegetation of the surface, (2) control of erosion, (3) isolation of surface flow (from contacting the tailings), and (4) reduced infiltration?

There are many geotechnical issues involved in answering these questions; the reader is referred to the above paper for further discussion.

Of relevance to this discussion is the concept that, to meet these objectives, one must also achieve final solids content and strength targets that are quite stringent and beyond the capabilities of positive displacement pumping. Hence, the final stage of tailings dewatering will have to occur either right at the DDA or after placement in the DDA. This is why environmental methods (such as drying or freeze/thaw), downward drainage, and consolidation in the DDA are an essential part of any dewatering strategy. Little experience is available upon which to optimize the effectiveness of these methods.

CONCLUSIONS

It has been the intent of this paper to demonstrate that knowledge of the geotechnical properties of various tailings materials can enhance our understanding of a) the anticipated behaviour of those materials, and b) the target solids contents needed to meet various criteria during their production, transport, discharge and storage. Specific points are:

- 1 The Tailings Technology Road Map (Diagram 1) illustrates current technologies for treating/dewatering oil sands tailings and assists in considering the evolution on modified or new technologies.
- 2 Ternary plots of (f,w,s) are very useful for showing tailings properties and the anticipated geotechnical behaviour of oil sands tailings. A certain amount of acuity and visualization skills are required to fully understand these plots, but the benefits are more than worth the learning time.
- 3 For tailings with a fines-dominated matrix, behaviour boundaries, lines of constant permeability, and lines of constant undrained strength all approximately parallel lines of constant FFW on the ternary diagram.
- 4 The primary objective of treating tailings is to remove water, to enhance strength and stiffness. For various operational and practical reasons, this is likely to be accomplished in stages, with the final stage occurring near the DDA or after disposal in the DDA.
- 5 Environmental assists to dewatering, such as drying and freeze/thaw, combined with consolidation (and possibly downward drainage) are essential mechanisms in reaching final dewatering objectives. Attention should be given to optimizing the effectiveness of these methods in the design of the DDAs.
- 6 Robust recipes for CT require solids contents that are all (or mostly) below the relevant segregation boundary.
- 7 Consideration should be given to the impact of shear on the location of the segregation boundary. Methods of discharging tailings under low shear conditions have yet to be fully addressed by the oil sands industry.
- 8 Design of tailings pumping systems need to consider the required rheological properties of the tailings when it arrives at the DDA. There will always be a tradeoff between early, cost-effective dewatering and proven pumping systems operating at lower solids contents.
- 9 Both permeability and compressibility decrease by 4 to 5 orders of magnitude from the “as produced” tailings to tailings “in the DDA”. However, the rate of consolidation is governed by the ratio between permeability and compressibility, which is much less variable.
- 10 There is little good, published information on the strength of oil sand tailings. A simple geotechnical test (“Atterberg Limit”) can be run which, for small cost, provides much insight into the relationship between solids content and tailings strength. This test has been almost ignored, or at the least highly under-utilized, by industry.
- 11 Various issues regarding measurement of the grain size of tailings products needs to be resolved, so that industry, university and other research participants can communicate accurately about tailings properties, and so that maximum benefit can be obtained from existing geotechnical knowledge and correlations.

ACKNOWLEDGEMENTS

Discussions with colleague Jeremy Boswell are gratefully acknowledged. Ted Lord and Bob Saunders both reviewed and provided valuable comments on an early version of this paper, which was much appreciated. However, any errors or omissions contained in this paper are the sole responsibility of the authors.

DEFINITIONS

The following symbols have been used in this paper:

- s - Mass of sand ($> 44 \mu\text{m}$)
- f - Mass of fines ($< 44 \mu\text{m}$)
- c - Mass of clay ($< 2 \mu\text{m}$)
- w - Mass of water
- b - Mass of bitumen
- k_2 - c / f
- T - Total mass ($s+f+w+b$)
- S - Sand content (s / T)
- F - Fines content (f / T)
- W - Water content (w / T)
- B - Bitumen content (b / T)
- SO - Solids content ($[(b+f+s) / T] = (1 - W)$)
- F* - Geotechnical fines content ($f / [f+s]$)
- C* - Geotechnical clay content ($c / [f+s]$)
- FFW - Ratio of fines to (fines+water) $f / (f+w)$
- SFR - Sand to fines ratio (s / f)
- W* - Geotechnical water content ($w / [f+s]$)
- e - Void ratio (V_W / V_{SO}) (for Sat.=1)
- e_F - Fines void ratio (V_W / V_F)
- K - Hydraulic Conductivity
- W_L - Liquid Limit
- W_P - Plastic Limit
- PI - Plasticity Index ($W_L - W_P$)
- LI - Liquidity index = $(W^* - W_P) / PI$
- G_F - Specific gravity of the fines
- c_v - Coefficient of consolidation
- m_v - Coefficient of volume change
- γ_w - Density of water (9.81 kN/m³)

c_u - Undrained strength

ACRONYMS

The following acronyms have been used in this paper:

- BT - Beached Tailings
- BAW - Tailings beached sub-aerially
- BBW - Tailings beached sub-aqueously
- CT - “Consolidated” Tailings
- CUT - Cyclone Underflow Tailings
- COT - Cyclone Overflow Tailings
- DDA - Dedicated Disposal Area
- FTT - Froth Treatment Tailings
- MFT - Mature Fine Tailings
- NST - Non-segregated Tailings
- PSD - Particle Size Distribution
- PSV - Primary Separation Vessel
- TSRU - Tailings from Solvent Recovery Unit
- TFT - Thin Fine Tailings
- TT - Thickened Tailings
- WT - Whole Tailings (from extraction plant)

REFERENCES

- Atkinson, J.H., and Bransby, P.L. (1978) “The Mechanics of Soils – An Introduction to Critical State Soil Mechanics”, McGraw Hill, p. 339.
- Boger, D. (2002) “Rheological Concepts”, in “Paste and Thickened Tailings: A Guide”, edited by Jewell, Fourie and Lord, published by the University of Western Australia, pp. 23-34.
- Caughill, D.L., Morgenstern, N.R., and Scott, J.D. (1993) “Geotechnics of nonsegregating oil sand tailings”. Canadian Geotechnical Journal, N30, pp. 801-811.

Cooke, R. (2008) "Design Considerations for Paste and Thickened Tailings Pipeline Systems". First International Oil Sands Tailings Conference, OSTRF/CONRAD, Edmonton, (not in Proceedings; copy of Powerpoint presentation).

Devenny, D. (1993) "The role of consolidation in the solidification of fine fluid tails". In Oil Sands – Our Petroleum Future Conference, April 1993, Edmonton. Paper F13.

Fair, A. (2008) "The Past, Present and Future of Tailings at Syncrude". First International Oil Sands Tailings Conference, OSTRF/CONRAD, Edmonton, (not in Proceedings; copy of Powerpoint presentation on OSTRF web site).

Gibson, R.E. (1958) "The Progress of Consolidation in a Clay Layer Increasing in Thickness with Time". *Geotechnique*, V8, pp. 171 – 182.

Houlihan, R. and Mian, H. (2008) "Past, Present, Future Tailings Regulatory Perspective". First International Oil Sands Tailings Conference, OSTRF/CONRAD, Edmonton, (paper not included in Proceedings; copy distributed separately).

Jakubick, A. T., McKenna, G., and Robertson, A.M. (2003) "Stabilization of Tailings Deposits: International Experience". Proceedings of Mining and the Environment III, Sudbury, Ontario, May 2003.

Jeeravipoolvam, S., Scott, J.D., Donahue, R. and Ozum, B. (2008a) "Characterization of Oil Sands Thickened Tailings". First International Oil Sands Tailings Conference, OSTRF/ CONRAD, Edmonton, pp. 132-142.

Jeeravipoolvarn, S., Scott, J.D., Chalaturnyk, R.J., Shaw, W., and Wang, N. (2008b)

"Sedimentation and Consolidation of In-Line Thickened Fine Tailings". First International Oil Sands Tailings Conference, OSTRF/CONRAD, Edmonton, pp. 209-223.

Lee, L.T. (2004) "Predicting Geotechnical Parameters for Dredged Materials using the Slump Test Method and Index Property Correlations". DOER Technical Notes Collection (ERDC TN-DOER-D-X), U.S Army Engineer Research and Development Center, Vicksburg, Mississippi.

Liu, Y., Caughill, D., Scott, J.D., and Burns, R. (1994) "Consolidation of Suncor nonsegregating tailings". Proceedings of the 47th Canadian Geotechnical Conference, Halifax, N.S., pp. 504-513.

Mikula, R.J., Munoz, V.A., Omotoso, O.E., and Kasperski, K.L. (2008) "The Chemistry of Oil Sands Tailings: Production to Treatment". First International Oil Sands Tailings Conference, OSTRF/CONRAD, Edmonton, pp. 23-33.

Mihiretu, Y., Chalaturnyk, R., and Scott, J.D. (2008) "Tailings Segregation Fundamentals from Flow Behaviour Perspective". First International Oil Sands Tailings Conference, OSTRF/CONRAD, Edmonton, pp. 112 - 120.

Morgenstern, N.R. and Scott, J.D. (2000) "Geotechnics of Fine Tailings Management". *Geoenvironment 2000*, ASCE, pp. 1663-1673.

Polidori, Ennio (2007) "Relationship between the Atterberg Limits and Clay Content". *Soils and Foundations*, V47, N5, pp. 887-896.

Pollock, G.W. (1988) "Large strain consolidation of oil sand tailings sludge". M.Sc. thesis, Department of Civil Engineering, University of Alberta.

Qiu, Yunxin and Segoo, D.C. (2001) "Laboratory Properties of Mine Tailings". Canadian Geotechnical Journal, N38, pp. 183-190.

Rajani, B. and Morgenstern, N.R. (1991) "On the yield strength of geotechnical materials from the slump test". Canadian Geotechnical Journal, V18, pp. 457-462.

Scott, J.D. (2005) "Revisiting the Ternary Diagram for Tailings Characterization and Management". Geotechnical News, December 2005, pp. 43-46.

Scott, J.D., Jeeravipoolvarn, S., and Chalaturnyk, R.J. (2008) "Tests for Wide Range of Compressibility and Hydraulic

Conductivity of Flocculated Tails". Proceedings of the 61st Canadian Geotechnical Conference, Edmonton, Alberta, pp. 738-745.

Sobkowicz, J.C. and Handford, G.T. (1990) "The Application of State-of-the Art Liquefaction Concepts at Syncrude Canada Ltd." Presented at the 43rd Canadian Geotechnical Conference, October 1990, Quebec City, (paper distributed at conference; PDF copy available from authors).

Suthaker, N.N. and Scott, J.D. (1996) "Measurement of Hydraulic Conductivity in Oil Sand Tailings Slurries". Canadian Geotechnical Journal, N33, pp. 642-653.

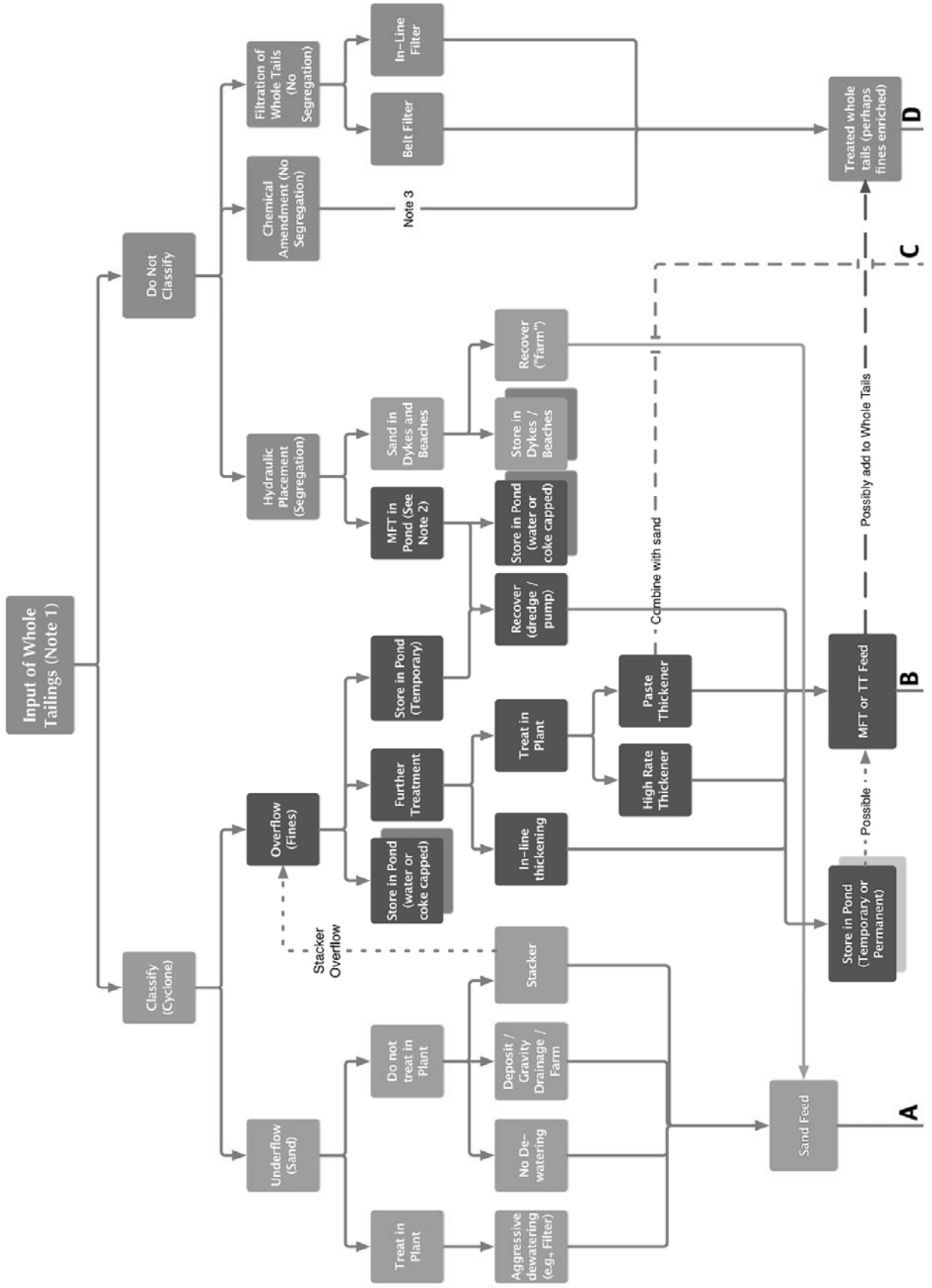
Terzaghi, Peck and Mesri (1996) "Soil Mechanics in Engineering Practice". John Wiley & Sons, p. 184.

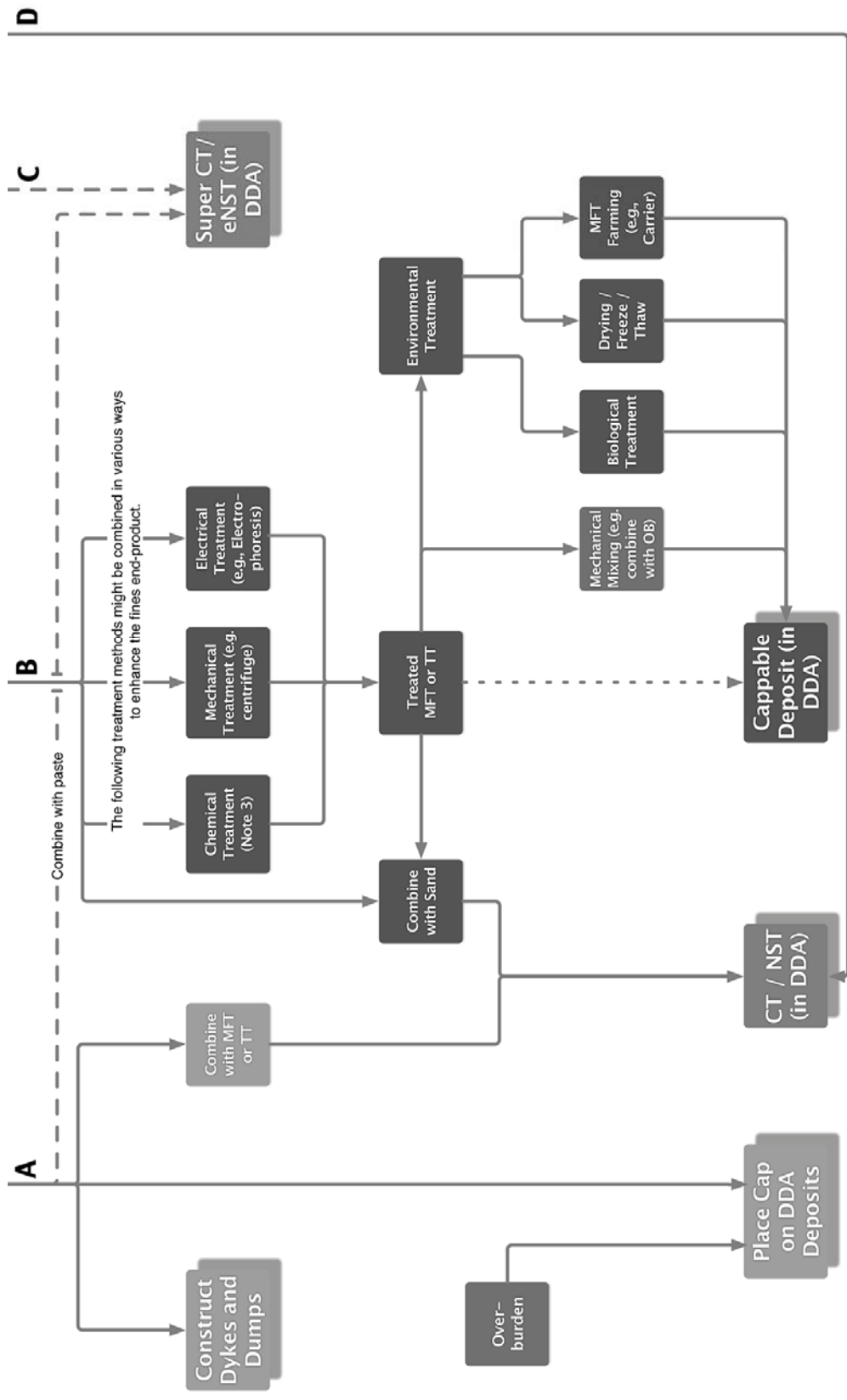
Diagram 1 - Reclaiming Oil Sands Tailings - A Technology Roadmap

by

J.C. Sobkowicz and N.R. Morgenstern

20090903





To navigate flow chart, proceed down or laterally along paths, (with the exception of dotted lines). At a path intersection, any lateral or downward direction is possible. Dashed line styles are independent paths.

Proceeding of the Thirteenth International Conference on Tailings and Mine Waste, 1-4 November 2009, Banff, Alberta, Canada

Tailings and Mine Waste '09

Edited by

David Segó, Moh'd Alostaz & Nicholas Beier

University of Alberta, Geotechnical Center and
Oil Sands Tailing Research Facility (UofA)

Copyright ©

All rights reserved. No part of this publication or the information contained herein may be reproduced, stored in a retrieval system or transmitted in any form or by any means, electronic, mechanical, by photocopying, recording or otherwise, without written prior permission from the publisher.

Although all care is taken to ensure the integrity and quality of this publication and the information herein, no responsibility is assumed by the publishers nor the author for any damage to property or persons as a result of operation or use of this publication and/or the information contained herein.

Published by: University of Alberta, Dept. of Civil & Environmental Engineering

ISBN 978-1-55195-255-0

Printed in Canada

Tailings and Mine Waste Management I

MINING MARKET CYCLES AND TAILINGS DAM INCIDENTS

Michael Davies

AMEC Earth & Environmental

Todd Martin

AMEC Earth & Environmental, Vancouver, British Columbia

ABSTRACT: Tailings dam incidents, namely physical failures and major operational upsets, have been described in literature for over 30 years. These accounts typically address the contributing physical attributes and/or design/operational deficiencies that led in whole, or in part, to the recorded incident. One aspect of tailings dam stewardship not typically noted let alone evaluated in terms of contribution to incidents of record are the prevailing economic conditions during a key period of dam design, construction and/or operation. An evaluation of the temporal trends in tailings dam incidents relative to the cyclical nature of the economic realities of the mining industry is examined. Although clearly no perfect correlation exists, there appears some validity to the hypothesis that the frequency of tailings dam incidents can be expected to increase some relatively short period after a cyclical “boom” in the mining industry.

INTRODUCTION

The Mining Industry is driven by cyclical global economic conditions. The demand for the commodities produced by the industry, though certainly having trends that for individual metal and non-metal commodities can differ from overall global industry trends, is an excellent barometer of global economic health. The end to the most recent high in the economic cycle hit the commodity prices for most mined materials severely. Though there have been exceptions such as gold, most commodities are, in mid 2009, trading at levels at or below the beginning of the most recent boom. This most recent boom cycle started gathering some modest signs of life in 2003 through 2005 but took off in early 2006

to what eventually became many unprecedented highs in commodity prices.

Though this most recent 2006-2008 boom was exceptional in terms of its height and the rapid and severe nature of its contraction, it is far from the first such cycle the mining industry has seen. Using data from indicator commodities such as copper and gold, a comparison of tailings dam incidents with mining cycles over the past few cycles (up to about 30 years) is explored. Both the nature and frequency of tailings dam incidents is noted in the comparison. Incident records are from both published and less available sources. From the comparisons made, trends appear that should reinforce high prioritization within the Mining Industry for enhanced tailings dam stewardship in the near

future. The paper includes some anecdotes from projects completed in this most recent boom to illustrate some of the reasons why the trends noted may exist. Further, the paper will provide some thoughts on how to prevent this trend reappearing during the inevitable next cycle in the Mining Industry.

TAILINGS DAM INCIDENT RECORDS

Though no single comprehensive public database of mine tailings dam incidents exists, there are numerous sources of information including:

- USCOLD (1994)
- UNEP (1996)
- U.S. EPA (1997)
- Vick (1997)
- Davies et al. (2000)
- WISE (wise-uranium.org).

In addition, through incident review assignments and other similar sources the authors have been able to augment the published information with approximately 20 additional incidents beyond the published accounts. In total, from December 1968 through to August 2009, there were 143 tailings dam incidents that were available to evaluate in terms of their trends. These 143 events occurred over the nearly 42 years of record used in the database.

Figure 1 presents a summary of the incidents from all available sources over the nearly 42 years. Figure 1 depicts the total number of “incidents” (defined as physical failure of some or all of a given tailings dam and/or a significant operational issue leading to disruption of the associated mining operation for a period of greater than one month) and plots these incidents on a per two year basis. The data used to develop Figure 1 are considered more thorough post approximately

1992 as since that time, it is more difficult to have incidents that go unreported. The two year basis was selected to provide a better sampling of the information and due to how it “worked” with trends presented later in this paper. In each case, the date provided is the end of the given two year period for which the data is provided. For the last data point, which is August 2009, the period of record is only 20 months versus 24 for all other periods noted.

From Figure 1, which makes no attempt to regionalize or discretize the data by failure mode for the purposes of this paper, “peaks and valleys” in the temporal distribution of failure events certainly appear to exist with several cycles of increased incident frequency apparent, raising the question as to the drivers behind these cycles.

MINING MARKET CONDITIONS

The global mining market constitutes a diverse number of commodities mined and marketed across all regions of the world. The historic global market conditions and trends for each of these commodities are individually complex and worthy of extensive evaluation in their own right (which they do, and will continue to receive). Perhaps the most predictable aspect of these conditions is their unpredictability. For example, while there are no shortage of supposedly prescient “experts” now assuring the industry they had the dramatic Q3-Q4 2008 fall in mined commodity prices “fully predicted and accounted for”, the reality is this most recent decline was seemingly just as surprising to an industry that has experienced these cycles many times before as all the other declines have been over the decades. To quote George Bernard Shaw, “We learn from history that we learn nothing from history.”

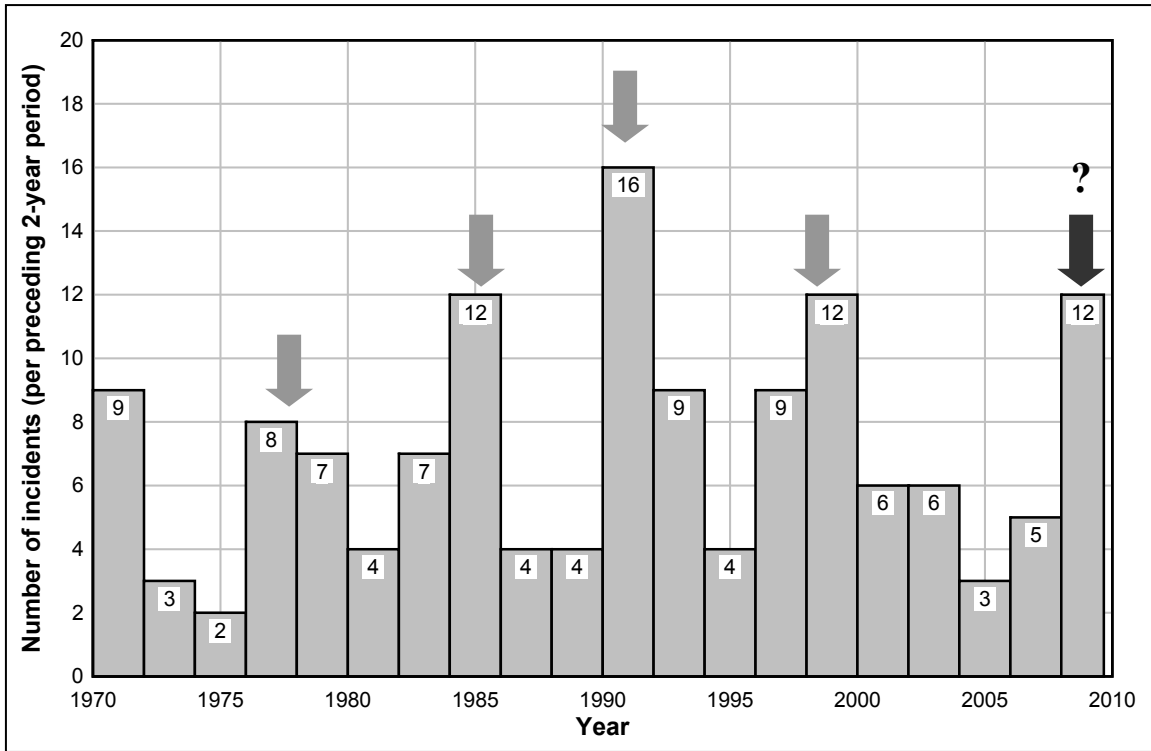


Figure 1. Tailings Dam Failure Incidents – 1968 to 2009

While the 2005-2008 rally in most mined commodity prices may have been unprecedented in terms of the market capitalization values reached by mining companies, and the commodity prices realized, in many ways it was simply just another cycle in a cyclical industry that very much mirrors the global economic situation.

To mirror the industry, copper is an excellent bellwether commodity. In many ways, it is the engine that powers the mining industry and its “health” dictates global mining (and overall economic) conditions like no other commodity. Figure 2 shows the price of copper, in period pricing, from January 1968 to present. In addition to copper, and to have another comparative commodity for evaluative purposes, gold was selected as an additional commodity of interest for this paper. Though in terms of commodity tonnage gold is far from the second most prevalent mined material, there

are an abundance of gold mines and gold mine tailings dams that have contributed a significant portion of the tailings dam incident record; in fact providing more dam failures than any other single commodity. Figure 2 therefore also provides the historic gold price from January 1968 to present, and it is apparent that the cycles in both copper and gold prices are largely similar. As such, for the purposes of this paper, copper price is taken as a proxy for mining commodity cycles.

An alternative means of plotting commodity price is in terms of the inflation-adjusted value. This in effect “normalizes” the commodity price over time, and, as illustrated in Figure 3 for copper, provides a means of amplifying the price cycles. The inflation-adjusted copper price plotted in Figure 3 is based on an average annual inflation rate (for the United States) of 4.1% from 1946 through 2008.

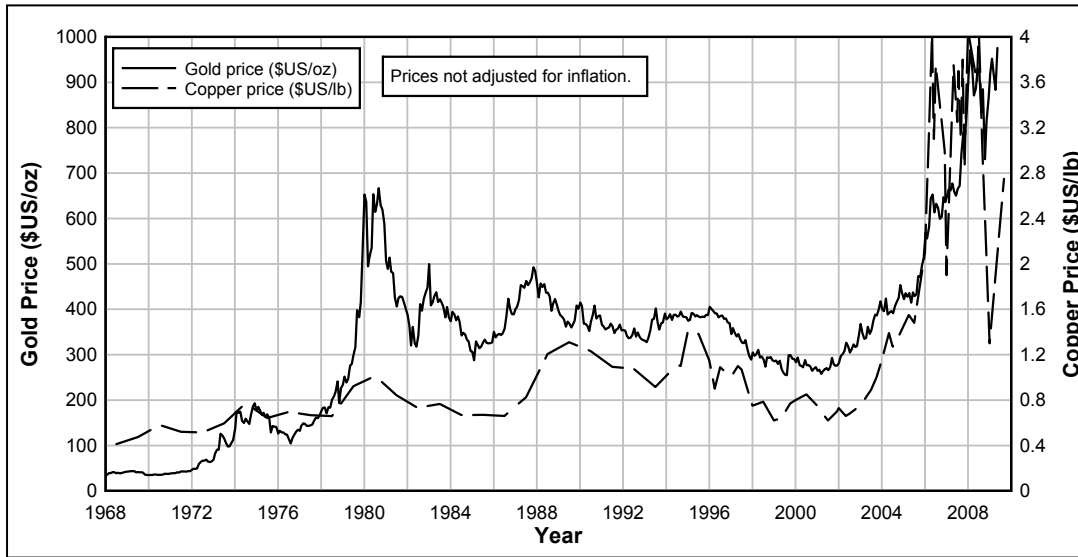


Figure 2 Copper & Gold Price – 1968 to 2009

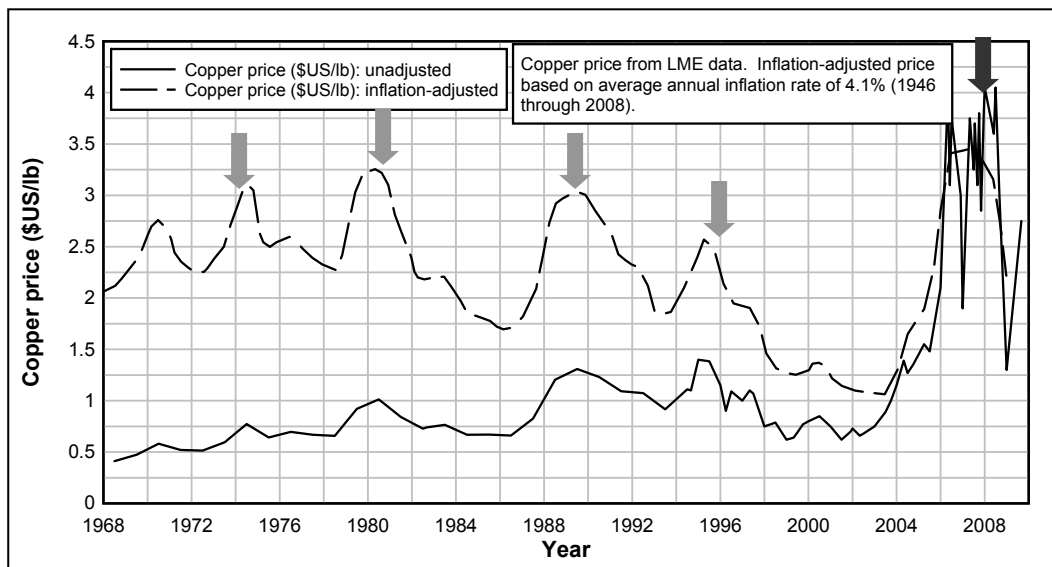


Figure 3. Copper Price (inflation-adjusted) - 1968 to 2009

TAILINGS DAM INCIDENTS AND MINING ECONOMIC CYCLES

Whenever data involving two or more variables is compared, the questions of relevancy and causation must be raised, for correlation alone cannot in isolation infer a causal relationship. There is no question in the thesis of this paper there are lots of “darts” that can be thrown at any

relationship derived between commodity prices for copper and gold and tailings dam incidents, given the many variables contributing to the latter. As an example of one such objection, commodity prices are a reflection on overall economic activity and when more mines are operating, the likelihood of incidents will be higher even if the rate of incident per operating mine remains the same. Another legitimate

objection would the reliability of the incidents database, given the increased likelihood of such incidents being reported, and documented, in recent years than would have been the case decades ago. However, the concept that there may be a relationship of some manner between the booms in the mining cycle and the damage to the overall mining industry created by tailings dam incidents seemed worthy of examination.

In evaluating the tailings dam incident database, a database that includes 143 incidents, a few trends were apparent:

- over the nearly 42 years of record, the 143 incidents leads to an average rate of incidents of about 6 to 7 per any average two year period.
- there were very distinct variations to any average trend with a range of between 2 and 16 incidents per any two year period (starting January 1968 and every two years afterwards)
- there were sub-trends or two-year windows outside of ones starting in January that included one two-year period (September 1980 to August 1982, inclusive) with 17 incidents.

From Figure 1, five periods of peak incident frequency (the starting date for a higher than average period of tailings dam incidents) can be identified. The fifth period includes the present which is not a complete record. It may be that the present time constitutes a lead up period versus a peak depending upon whether the trends of the previous four peaks sustain through to 2010-2011 as will be discussed later herein.

Table 1 provides a summary of the two-year periods from 1968 to present where higher than average tailings dam incidents were recorded.

Table 1 – Tailings Dam Incidents – Periods of Higher than Average Occurrence

Start of Two Year Period of Increased Tailings Dam Incidents	Peak of Copper Price	Peak of Gold Price
January 1976	January 1974	January 1974
January 1984	September 1980	September 1980
March 1990	June 1989	December 1987
February 1998	September 1995	January 1996
Q1-Q2 2009 (?)	February 2008	February 2008

Table 2 provides a summary of the peaks of the gold and copper prices over the past 42 years. Ironically, there have essentially been five peaks in each of these, in comparison to the peak periods in tailings dam incidents noted in Table 1.

Table 2 – Periods of Peak Copper and Gold Prices Compared to Periods of Peak Tailings Dam Incidents

Start of Two-Year Period	Number of Tailings Dam Incidents
January 1976	8
January 1984	12
March 1990	16
February 1998	12
Early to Mid 2009 (?)	>12

Using the first four peak periods, the time lag between the peak of the copper price and the start of the next two-year period of

increased frequency of tailings dam incidents was:

- 24 months
- 39 months
- 9 months
- 28 months

The average lag from peak of copper price to period of increased frequency of tailings dam incidents from these four event windows is 25 months. For the gold price peak data, the corresponding time lags from peak price to increased incidence frequency for the first four incidents peaks were:

- 24 months
- 39 months
- 27 months
- 25 months

The average lag in the gold peak price to start of increased incidence period was 29 months.

For the most recent boom there is insufficient information to know if a peak in incidents has occurred or there is a ramping up of activity towards one.

From the available information, there appears to be a lag of between 2 and 2.5 years from the end of a mining boom to the start of a two-year period of increased frequency of tailings dam incidents. This is illustrated in Figure 4, which plots both the tailings dam incidents (per two year period), and the inflation-adjusted copper price. While the time lag between the peak in the adjusted copper price and the peak of the tailings dam incidents varies for each cycle, it is very clear that each commodity price cycle peak, as represented by the copper price, can be correlated to a subsequent peak in the number of tailings dam incidents.

Looking at the data in some more depth, the two-year incident window could not be improved upon much though the number may be a range of between 18 and 36 months post peak price versus a set period as implied by the simplistic average used above. It is undoubtedly the case that the lag is driven by many factors, including for example the duration of the upswing in terms of commodity prices, as a longer such period would likely result in more projects being developed.

ANECDOTES FROM THE RECENT BOOM

There is a common discussion question amongst long-term designers of tailings dams during mining booms – who is doing all that extra work? The reputable design houses and their senior resources are typically fully-occupied during average economic conditions and can quickly become stretched during peak periods. When a prolonged peak of an unprecedented nature occurs as did recently between 2005 and 2008, it is difficult indeed to imagine where all that additional capacity came into the industry in terms of design, operating and regulatory experience.

The complexity of a tailings dam, in comparison to many engineered structures including conventional water retention dams, cannot be overstated. These structures are never at steady-state conditions during operations and are often constructed over decades where the initial portion of the dam may include design criteria and construction practices long out of date.

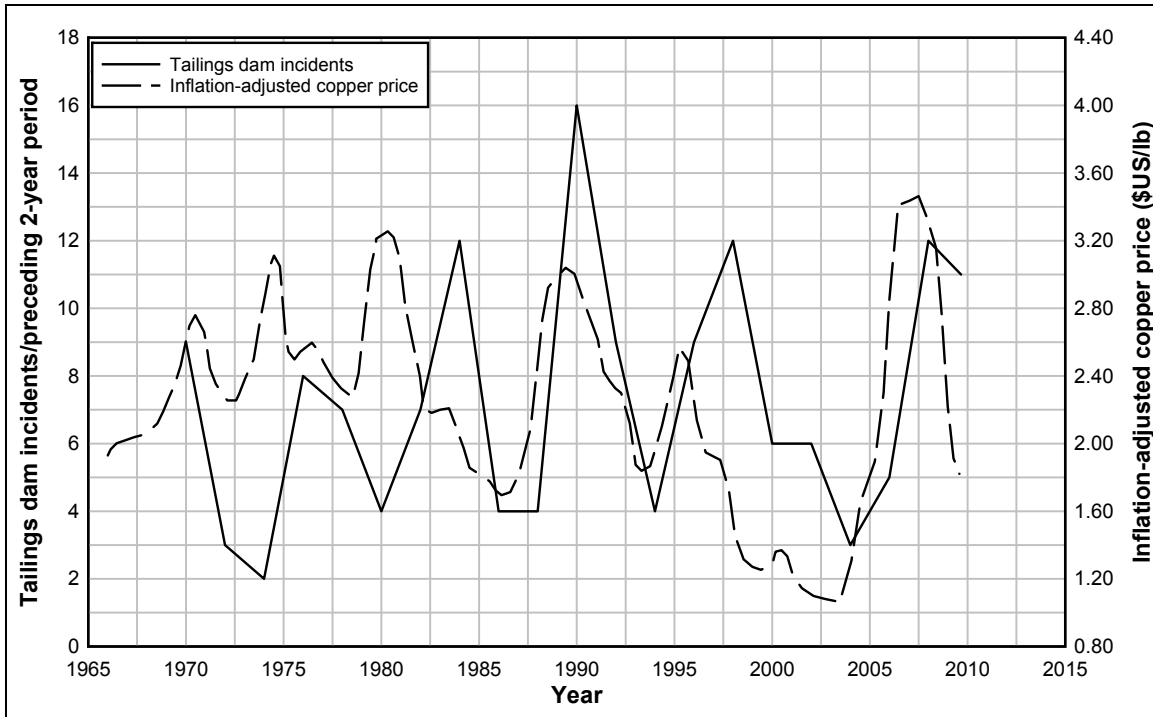


Figure 4. Adjusted copper price and tailings dam incidents

However, what really does occur during boom times that could represent the causal link between the trends noted in this paper? One window into a portion of the reasoning is offered through a few select anecdotes from the recent boom.

1. Following the OMS Manual?

At one mine, the Operating, Maintenance and Surveillance (OMS) Manual for the tailings area included a stipulation that the tailings dam and impoundment be visually inspected daily or whenever “*was convenient*” (the latter portion was handwritten, word for word, in the OMS manual). Apparently the daily requirement for this dam and impoundment, which was more than five km from the main operations, was onerous so a somewhat lesser frequency was adopted. When the long overdue viewing did take place it was discovered that the tailings line had cracked

at a valve on the crest of the dam, eroding a significant portion of the earthfill and allowing tailings to find their way into a stream bed for about two km downstream. During the incident review, it was determined that the “job” of the daily (or “convenient”) was formerly done by someone who had left the mine for another opportunity and they were awaiting some new hire to fill the position but were having problems getting someone. That problem had gone on for 14 months – clearly the period between inspections as well – so instead of daily, “convenient” turned out to be about every 400 days. The owners of the mine were “impressed” with how much damage a cracked line could do when left alone for about 400 days.

2. Interesting Design

At one mine, space was at a premium. There simply was very little room for all of the infrastructure and the desired tailings

impoundment directly adjacent to the mill. However, an enterprising designer came up with a solution by simply (seemingly) ignoring upstream failure modes. The rock shell was impressive and steep getting to more than 40 m in height at about 1.5H:1V. The dam was being constructed in an upstream manner with tailings and supernatant “supporting” the rock shell (this was the part the designer did not seem to include in their assessment). When the tailings in the impoundment simply could not take the loading of the rock shell any longer, and it is incredible failure did not occur prior to the rockfill reaching 40 m in height above the tailings, it failed into the tailings beach effectively shutting the mine down for a prolonged period of repair. A post-incident review confirmed no consideration of the upstream support requirement of the beach to the rock shell had ever been considered by the designers who, by their own admission, had “only started” designing tailings dams.

3. Drainage, Drainage, Drainage!

A review of a proposed tailings dam included a very insightful view to an interesting approach to dam design. Beached hydraulic tailings tend to create quite a high level of anisotropy in terms of their hydraulic conductivities (the horizontal value tends to be many times the vertical value – typically in the order of two orders of magnitude greater). As such, basal drains can have some impact for the first number of metres of a tailings impoundment but at some point, the influence of basal drains on the beached tailings becomes quite negligible. This was apparently lost on the design for this particular facility that was to be up to 150 m in height behind a fully drained and competent rock shell. There were no fewer than 300 separate drains in the basin design, totalling more than 20 km in length,

consisting of very expensive and totally unnecessary pipe that some supplier was very anxious to provide to the mine.

Not all design errors lead to failures – some are simply huge added expenses based upon nothing more than a lack of experience.

4. We Have a Permit!

The current regulatory climate around the world can only be termed “challenging” by those who work in the mining industry. There are a series of permits required with nearly every one offering a unique opportunity to create a design problem by getting caught up with the myopic drive to obtain the permit – fast, and at any cost. Getting a new tailings facility permitted can be one of the greatest of those challenges. However, meeting that challenge via a design for a facility that is either economically, technically, and/or operationally infeasible, but that expedites the granting of a permit, is not the answer.

On one particular project, the use of paste tailings technology was nominated as the panacea for the project. Some small bench scale laboratory testing showed that if the paste was thick enough (low water content) and had sufficient cement and other agents added, a 30 mm high pile could be repeatedly created at about a 10% slope. From this, it was extrapolated that such a result could be recreated at full field scale! Moreover, no bleed water emanated from the uniform hardening slope so no dam of any sort (starter or otherwise) would ever be required. Designs and extensive documentation with stunning three-dimensional pictures were developed showing uniform 10% slopes up to 50 metres in height without any need for anything more than the 5% by weight cement addition plus many other useful additives. No other works, particularly

earthworks, would be required. The regulators were enthusiastic over the concept and a permit was obtained “much quicker than we thought” for the no dam, no seepage and no worries uniform sloped tailings pile. Mission accomplished!

However, in the course of a subsequent review, once having convinced the owner that there may be a flaw, a somewhat larger scale trial was commissioned whereby it was shown that the laboratory slope could not be maintained over a few metres, let alone 500 metre long beaches. It was also eye-opening for the owner to see the calculation of how much money per tonne these tailings needed in terms of the paste additives (including the cement). However, the worst news (at that time it seemed) was the need for earthworks, which would mean a totally different impact situation and essentially restart the permitting process. While no other facility had ever been designed or constructed in any form similar to the conceptualized facility, none of the owner, the regulator, or the designer let that lack of precedent impede the single-minded task of getting this project its permit by writing promissory notes that physical reality, and project economics, could not honour.

REASONS FOR THE TRENDS?

Taking the trends in peak incident events relative to periods of commodity price peaks as valid indicators of a causal relationship, and then using the above and many, many similar anecdotes from the recent and previous booms, perhaps some “whys?” begin to emerge. The authors suggest the following are only a handful from a wide assortment of “whys?” but ones that would seemingly be avoidable with some better judgment from the key parties involved. In other words, it should

not be inevitable that more tailings dam failure incidents are recorded just because there is commensurately more activity brought about by more robust commodity prices.

Some potential reasons for the trends that have been readily observable from the past few boom cycles include:

- Permit haste:
 - use of fashionable but project-inappropriate tailings technologies
 - unprecedented design/operation to satisfy non-realistic regulatory or third party stakeholders preference
 - defaulting to flooding for potential ARD despite dam safety risks
 - acceptance of sites that are pleasing to regulators but not to geotechnical reality
 - over-taxed regulatory capacity.
- Fast tracking of investigation, design and construction to take advantage of the price cycle
- Inadequate appreciation of capital and operating costs associated with designs based more on rapid permit procurement than technical and economic realities
- Rapid cost escalation during project construction due to boom times, necessitating cost cutting
- Inexperienced (but overconfident) designers
- Experienced (but overly-subscribed) designers
- Lack of independent, third party review
- Rapid turnover of key mine management and operating personnel as new opportunities abound during the boom times
- Disconnect between design expectations and operational realities

- Development of long-known deposits that have been left undeveloped for good reasons
- Pressures to cut costs for once mines constructed on the basis of rising commodity prices are forced to operate with the reality of lower commodity prices
- “Cookie cutter” designs having attributes well and good in, for example, South Africa, but being used for a project in a high rainfall, high seismic environment.

The list above is *far* from exhaustive. However, there is not a single item in that list that would qualify as a justification for the postulated relationship between commodity price booms and tailings dam incidents, and as such merely points to a lack of discipline in sticking with well-established design and stewardship practices. A lack of discipline brought about by the need to make hay while that economic sun shines, even when it leads to another case history in the growing catalogue of tailings dam incidents, is understandable but is not acceptable.

SUMMARY THOUGHTS

The evaluation of tailings dam incidents versus the price of commonly mined commodities is admittedly not a scientific endeavour, *per se*, and certainly was not given extensive rigor in terms of statistical evaluation, assessment of other underlying causes in the data trends, etc. However, there appears to be some correlation between a mining boom cycle and an increased number of tailings dam incidents approximately 24 to 36 months after the end of the boom, in the manner of a hangover after a good party. Another way to look at it, as most booms are several

years in length, the increased number of incidents appears to occur within four or five years of there being more market capital and, commensurately, more project construction following ore definition, engineering, permitting and construction. The lag appears somewhat more quickly than a typical timeframe to get a mine from concept to operation but there are perhaps many projects just waiting the improved financial condition to finally be constructed, or restarted etc. The correlation may also imply that facilities that are constructed or restarted during a boom are seemingly more susceptible to having failure incident early on in their initial or restarted operating period.

Is there really a correlation between tailings dam incidents and mining cycle booms? If the trends suggested by the data over the booms of the period since 1968 provide some guide to the future, the implications to the mining industry in 2009, on the heels of an extraordinary boom, are clear and perhaps daunting. The recent boom that ended so abruptly in 2008 was unprecedented in terms of copper price. The apparent building up of tailings dam incidents of the past year or so may only be background level activity to a peak in incidents coming in the next 12 to 30 months.

Such a pessimistic viewpoint is perhaps an unlikely version of the future that unfolds. There are very sound guidance documents, corporate standards and increased awareness in design houses to avoid the failures of past periods. Major mining companies in particular have for over a decade now been implanting increasingly stringent controls, and applying consistently improved stewardship practices (e.g. the Mining Association of Canada guidelines) pertaining to tailings management facilities.

At the same time, some of the anecdotes offered in this paper lead one to a perhaps tempered optimism and a more of a “wait and see” approach. What is clear, the exercise of evaluating the incident database in a few years time will be very illustrative in light of the trends suggested by the data presented in this paper. Perhaps the trends of the past 40ish years will not be repeated; for the mining industry this is most certainly the desired outcome.

REFERENCES

- Agricola, G., 1556. *De Re Metallica*. 1st Edition.
- Davies, M.P., 2001. Impounded mine tailings: What are the failures telling us? Distinguished Lecturer Series. CIM Bulletin. July, p. 53-59.
- Davies, M.P. and Martin, T.E., 2000. Upstream Constructed Tailings Dams — A Review of the Basics. Proceedings, Tailings and Mine Waste '00. A.A. Balkema Publishers, Rotterdam, p.3-15.
- Davies, M.P., Dawson, B.B. and Chin, B.G., 1998. Static liquefaction slump of mine tailings — A case history. Proceeding, 51st Canadian Geotechnical Conference.
- Davies, M.P., Martin, T.E., and Lighthall, P.C., 2000. Tailing Dam Stability: Essential Ingredients for Success. Chapter 40. Slope stability in surface mining. *Edited by Hustrulic McCarter and Van Zyl*. Society for Mining, Metallurgy and Exploration Inc., p. 365-377.
- Dunne, B., 1997. Managing Design and Construction of Tailings Dams. Proceedings of the International Workshop on Managing the Risks of Tailing Disposal. ICME-UNEP, p. 77-88.
- International Council On Metals and The Environment (Icme) and United Nations Environment Programme (UNEP), 1997. Proceedings of the International Workshop on Managing the Risks of Tailings Disposal.
- International Council On Metals and The Environment (Icme) and United Nations Environment Programme (UNEP), 1998. Case studies in Tailings Management.
- MARTIN, T.E. and DAVIES, M.P., 2000. Trends in the stewardship of tailings dams. Proceedings, Tailings and Mine Waste '00. A.A. Balkema Publishers, Rotterdam, p. 393- 407.
- Morgenstern, N.R., 1998. Geotechnics and Mine Waste Management — An Update. Proceedings, ICME/UNEP Workshop on Risk Assessment and Contingency Planning in the Management of Mine Tailings, p. 172-175.
- Siwik, R., 1997. Tailings Management: Roles and Responsibilities. Proceedings of the International Workshop on Managing the Risks of Tailings Disposal, ICME-UNEP, Stockholm, p.143-158.
- United Nations Environment Programme, 1996. Environmental and Safety Incidents Concerning Tailings Dams at Mines: Results of a Survey for the Years 1980-1996. *Industry and Environment*, 129 p.
- U.S. Environmental Protection Agency, 1997. Damage Cases and Environmental Releases from Mines and Mineral Processing Sites. Office of Solid Waste, 231 p.
- USCOLD, 1994. Tailings Dam Incidents. A report prepared by the USCOLD Committee on Tailings Dams.

Vick, S.G., 1997. Tailings dam failures: Effects and consequences. Presented at the

Canadian Institute of Mining and Metallurgy Annual General Meeting.

URANIUM MILL TAILINGS IMPOUNDMENT CLOSURE: A RETROSPECTIVE

Clint Strachan

MWH Americans Inc, Fort Collins, Colorado, USA

Greg Smith

Geo-Smith Engineering, LLC, Grand Junction, Colorado, USA

Jack Caldwell

Robertson GeoConsultants, Vancouver, BC, Canada

ABSTRACT: Nearly twenty years ago the authors wrote papers comparing the technical approaches implemented to close inactive uranium mill tailings piles across the United States. We noted significant differences in the technical approach adopted for Title I (DOE) piles and Title II (private mining company) piles. In this paper, we review the differences and discuss the practical implications of those design differences, by looking at how the different reclaimed piles have performed in the ten to twenty years since closure and reclamation. We show that both approaches resulted in successful reclamation, but that neither approach resulted in a totally maintenance-free systems. We review advances in the science and technology of tailings pile reclamation since the time when the majority of uranium mill tailings piles were reclaimed and discuss how, if at all, these advances would have affected our design decisions at that time.

INTRODUCTION

In the 1980s remediation of uranium mill tailings impoundments (tailings piles) was undertaken in earnest. The U.S. Department of Energy (DOE) was given the task of remediating and closing twenty-four inactive uranium mill tailings sites in terms of the Uranium Mill Tailings Remedial Action (UMTRA) Project. This one-billion-dollar project was undertaken to address the so-called Title I piles from which the federal government had received uranium for use in the Manhattan Project. The Title II uranium

mill tailings piles were those owned by private mining companies that provided uranium to the nuclear power industry. They had to be closed by the private companies that had operated the mines.

Closure of the Title I piles was undertaken under the direction of the DOE from Albuquerque by a group of consultants including Jacobs Engineering, R. F. Weston, Sargent Hauskins & Beckwith, and MK Ferguson. Review of the work done by those consultants was primarily by the U.S. Nuclear Regulatory Commission (NRC) in

Washington DC. Two of the authors worked for these consultants on the UMTRA Project during the later 1980s.

Closure of the Title II sites was undertaken by a variety of consulting companies that worked for energy or mining companies that held title to these sites. Review of their work was undertaken primarily by the NRC in Denver, Colorado, and later by the NRC in Washington DC, after closure of NRC's Denver office. Review work in states such as Texas and Wyoming was undertaken by state regulatory agencies that had an agreement with NRC to administer the Title II program (agreement states). One of the authors worked for a consulting company in Colorado that prepared many of the Title II closure designs and oversaw closure construction work.

Thus we compile this paper almost twenty years after the major phase of design and closure construction in order to take a retrospective look at the differences of opinion and practice that prevailed then and to reassess our engineering and technology in the light of the performance of those closed piles in the years that have passed.

REGULATIONS

The regulations governing both the Title I and the Title II programs were the same: performance criteria from Appendix A of 10 CFR 40, as summarized below:

- Stabilize the sites for 1,000 years to the extent reasonably achievable, and at any rate for 200 years.
- Not rely on active maintenance.
- Reduce the radon flux from the pile to less than 20 picocuries per square meter per second.

The performance criteria from Appendix A of 10 CFR 40 also included technical approaches we implemented at both Title I and Title II sites:

- Performance for 1,000 years: use only natural materials that have proven long-term stability and integrity. Design for extreme events such as the maximum probable precipitation and the maximum credible earthquake.
- Minimize active maintenance: reduce the potential for erosion of critical areas or growth of unplanned vegetation. Provide for the establishment of climax vegetation in appropriate soil layers.
- Control dispersal of the tailings: construct covers that will not erode by using either riprap or rock mulch on cover surfaces, or vegetative covers on cover surfaces with very gentle slopes and suitable precipitation.
- Limit the flux of radon gas from the piles: provide radon barriers of natural materials (generally low-permeability clays, if available).
- Protect groundwater resources: achieve groundwater protection standards by active remediation, application of supplemental standards, or natural flushing. Limit infiltration via low-permeability (low saturated hydraulic conductivity) covers and/or the presence of vegetation that promotes evapotranspiration.

These regulations were interpreted in different ways by those involved in the programs (Caldwell & Shepherd, 1988). The resulting closed piles looked and were indeed very different. Let us proceed to a few examples.

TITLE I vs TITLE II TECHNICAL APPROACHES

Title I sites reflected the standard of practice for the early uranium recovery industry in the US. Many of the tailings piles were relatively small and constructed without significant siting or planning. The details of Title I closed sites varied considerably. This is to be expected for a program that took nearly a decade to complete and where the pile locations ranged from Oregon to Pennsylvania, and from Texas to South Dakota.

At ten sites, the tailings were picked up and relocated to new sites that were considered to be more geomorphically stable than each original site.

At most of the sites, however, the following details were adopted:

- Sideslopes were generally inclined at no more than five horizontal to one vertical.
- A thick, low-permeability clay layer formed the cover, functioning as both a radon barrier and an infiltration barrier.
- Sands and gravels were used as bedding and filter between the clay and the overlying erosion-resistant rip-rap of durable pebbles and cobbles.

Conversely the Title II sites represented a later stage in the uranium recovery industry, with some piles constructed under NRC regulations for embankments and liners that were promulgated in the late 1970s. The mills were typically larger, with some piles selected based on siting studies. At the Title II sites, no piles have been moved to date. However, the Atlas pile near Moab Utah (which was operated under the Title II

program) is being relocated under the Title I program.

The Title II piles ranged in location from Washington to Texas. At sites where clay was available, the clay was used for radon and infiltration barriers. At sites where clay was not available, other available materials (such as sands and gravels) were used. These sites required significantly thicker covers to provide the required radon attenuation, and utilized an evapotranspirative cover design to minimize infiltration through the cover. Cover surfaces utilized alluvial deposits or quarried rock for erosion protection for piles in arid areas. Where there was sufficient precipitation to provide full vegetative coverage (such as in Texas) erosion protection of cover surfaces was provided by vegetation. The top and sideslopes were graded to be as flat as practical, with maximum slopes of five to one.

The question that will be discussed in the remainder of this paper is: how have these very different approaches fared in the past twenty years?

TITLE I SURVEILLANCE AND MAINTENANCE

Even as the UMTRA Project was in progress, DOE established a Surveillance and Maintenance program (Caldwell et al., 1989). Ultimately the program was made permanent by transfer of activities to the DOE Grand Junction, Colorado office. We thank those still involved in that program for the information they have provided us in compiling this paper.

During the periods of peak construction of UMTRA pile covers, there was disagreement about the shortcomings of rip-rap on cover surfaces and its transition to filter sand, and clay. This transition zone could become an

ideal environment for vegetative growth. Concerns were voiced saying that vegetation would compromise these covers. One of us, who was in Albuquerque at the time, recalls the many efforts a colleague, Charles Reith, made to change the practice of using rock. He pleaded, he argued, he presented facts, and he took on us engineers, every last one. He mostly failed to change the prevailing culture in favor of rock (Reith & Caldwell, 1990). This culture was deeply engrained in the mind and practice of the engineers from the UMTRA consultants, the DOE, and indeed at the NRC.

We recall one meeting with the NRC in Washington at which we discussed vegetative covers in favor of rock covers. The NRC, who had the last word, reminded us that control of erosion of the cover and control of dissemination of the tailings took precedent over hypothetical concerns about aesthetics and groundwater---for at that time the groundwater protection part of the UMTRA Project was but a distant future issue.

The groundwater program eventually became a reality and the vegetation-supporting voices proved prescient. Jody Waugh has done a superb job documenting the conditions at many of the UMTRA sites (Waugh, 2004). As he reports: "Surface layers of rock reduce evaporation, increase soil water storage, and, consequently create habitat for deep-rooted plants."

The first site at which this was noted was Shiprock in the deserts of northern New Mexico, where vegetation flourished with its roots in the filter sand with abundant moisture. Vegetation has developed on other UMTRA sites including those in Burrell, Pennsylvania and Lakeview, Oregon. The impact of vegetative growth has been the effects of root growth into the cover, to subsequently increase the permeability of the clay layer making up the infiltration barrier.

The potential impact of this on groundwater is not documented.

A significant observation during monitoring of Title I disposal cell covers is that the local ecology has a huge effect on performance. Since all UMTRA covers use earthen materials, pedogenic processes have altered the initially constructed designs. This occurs in many ways, but for example, natural windborne sand and silt is deposited in the rock cover component (rock covers act as wonderful dust traps in the arid southwest), which in turn creates a seed bed for plant establishment.

Rock covers also reduce evaporation of precipitation thereby increasing infiltration and providing moisture for the plant seeding and growth. Radon barriers were typically constructed with clay, and unless the clay was processed in a pug mill to completely break down the inherent soil structure and moisture condition, preexisting preferential flow paths existed in the compacted radon barrier.

Freeze/thaw and wet/dry cycling have cracked the barriers as well, as have construction influences. These flow paths are subsequently followed by plant roots that further exacerbate the size of the flow path. It appears that nature is transforming the initially designed compacted clay barriers back to conditions that reflect surrounding native conditions. This phenomenon is a natural development of soil structure, transitioning (over decades) from the massive soil structure created by moisture conditioning and compaction of the radon barrier to a blocky or granular soil structure that is more permeable.

What all this leads to is a considerably more porous barrier with a significantly higher permeability. A higher permeability is not necessarily a problem. Excessive infiltration will only occur if excessive moisture is

present, but not utilized by plants and sent into the atmosphere via evapotranspiration. Moisture utilization by plants is especially the case in arid and semiarid climates.

Increased, out-of-compliance, radon releases have not yet been observed, partly due to the conservatism used in the radon emanation calculations. NRC required monitoring at the Lakeview, Oregon disposal site after the increase in the saturated hydraulic conductivity was recorded, and zero radon release was observed.

Observations have shown the covered tailings piles are still operating within design specifications and reducing radon releases to well below flux standards, although the saturated hydraulic conductivity of some covers has increased following construction. This may present future groundwater problems. There was never a design specification for a maximum permeability of the pile covers, only a goal of 10^{-7} cm/sec (i.e. lab testing), without field verification.

Thus, it can be said that generally all UMTRA reclaimed tailings piles are still compliant with the initial design and performance standards (with possible exception of the Lakeview site erosion protection riprap).

TITLE II SURVEILLANCE AND MAINTENANCE

The Title II program has benefited from the lessons learned from the performance of earlier-reclaimed tailings piles (both Title I and Title II). The most recently constructed and designed Title II sites have included evapotranspirative cover designs, biointrusion barriers, and accommodation for climatic variations (such as freezing and thawing). The Moab pile (described below) represents the current cover system design based on

observation of the performance of earlier Title I and II tailings piles.

THE MOAB PILE

The most recent UMTRA pile cover for the Moab site is described in the Remedial Action plan approved in 2008 (DOE, 2008). The tailings are to be relocated from the flood plain of the Colorado River. Much of the cell will be below grade in an excavation into the low-permeability Mancos Formation Shale at the site. The cover on the top of the cell is a modified version of those we used at many sites in the 1980s. The sides of the cell will be comprised of clean fill dikes.

The cover on the top of the pile consists of the following layers (from top down):

- Erosion Barrier: 0.5-ft of rock or rock mulch
- Frost Protection Layer: 3-ft alluvial and eolian soil and weathered Mancos shale
- Infiltration and Biointrusion Barrier: 0.5 ft sandy gravel
- Radon Barrier: 4 ft weathered Mancos shale

DISCUSSION

Twenty years ago, those of us in the Title I program could not agree with those in the Title II program on designs of reclaimed tailings piles, although we were designing to the same performance standards. The passage of the years and field observations of the performance of the cells we designed and observed through construction and post-closure monitoring has shown that comparison of those designs with actual performance has had a more important influence on current cover designs.

We did not, and we submit could not have, at that time have designed and constructed the thicker covers that have been formulated to address and possibly reconcile our differences. Some of us from UMTRA went on to work on the Weldon Springs site in Missouri. We even wrote a book about that resulting cell and the covers we continued to argue about (Caldwell & Reith, 1993).

At the time the costs of the UMTRA Project were approaching \$1 billion, which in the 1980's was one of the most expensive federal programs in history. There was no appetite or tolerance for ideas that might increase costs even more.

Admittedly, there is vegetation in many of our covers in areas where we did not anticipate vegetation. Admittedly, the potential influx through the infiltration barrier is greater than was initially estimated. But there have been no observations to indicate that the covers are eroding, are susceptible to erosion, or that intrusion to or dispersal of the tailings is likely now or through the design life. We suspect that in 1,000 years, the covers will be well-vegetated as the climax vegetation flourishes in a rocky soil that has been slightly eroded in certain areas and covered with windblown sand in other areas.

REFERENCES

Caldwell, J.A. and Shepherd, T.A. (1988) "Pile Stabilization and Groundwater Protection at Title I and Title II Uranium Mill Tailings Sites." Available on the web at <http://www.infomine.com/publications/docs/Caldwell1988c.pdf>

Caldwell, Kylo, Matthews, and D'Antonio (1989) "DOE Disposal Cell Design and Surveillance and Maintenance Programs." Available on the web at: <http://www.infomine.com/publications/docs/Caldwell1989a.pdf>

Caldwell, J.A. and Reith, C.C. (1993) "Principles and Practices of Waste Encapsulation." Lewis Publishers.

DOE (2008) "Final Remedial Action Plan and Site Design for Stabilization of Moab Title I Uranium Mill Tailings Site at the Crescent Junction, Utah, Disposal Site." U.S. Department of Energy Available on the web at http://www.gjem.energy.gov/moab/document/s/Crescent_Junction/RAS_RAP_July2008/RAS_RAPJuly2008.pdf

Reith, C. C., and Caldwell, J.A. (1990) "Vegetative Covers for Uranium Mill Tailings." Available on the web at <http://www.infomine.com/publications/docs/Reith1990.pdf>

W. Jody Waugh (undated) "Design, Performance, and Sustainability of Engineered Covers for Uranium Mill Tailings." Available on the web at: <http://www.cistems.fsu.edu/PDF/waugh.pdf>

W. Jody Waugh (2004) "Sustainability of Conventional and Alternative Landfill Covers." <http://www.rtdf.org/PUBLIC/phyto/minutes/031004/pdf/waugh-ses4.pdf>

BEST AVAILABLE TECHNOLOGY DESIGN FOR A URANIUM TAILINGS STORAGE FACILITY

Melanie Davis and Clint Strachan

WH Americas, Ft Collins, Colorado

Mark Abshire

Tetra Tech, Ft Collins, Colorado

Daniel Overton

Engineering Analytics, Ft Collins, Colorado

Toby Wright

Uranium One USA, Ft Collins, Colorado

ABSTRACT: This paper presents a best available technology (BAT) design and regulatory requirements for a proposed tailings storage facility to manage tailings for a uranium mill in an arid region of the western United States. The general design of the tailings storage facility consists of a single 30-acre (12-ha) cell with capacity for 4 to 8 years of storage, depending on ore production rates. Tailings are proposed to be placed into the cell using conventional slurry discharge methods.

The site is regulated by under the Agreement State Program with the Nuclear Regulatory Commission. To meet best available technology design, the design must meet a BAT design basis established with the agreement state. The components of the BAT designed liner system listed from the bottom to the top, are: 1) minimum 12-inch compacted clay liner, serving as the base layer, with a maximum permeability of 1×10^{-7} cm/sec; 2) secondary 60-mil HDPE geomembrane, overlaying the clay liner to form a composite liner; 3) HDPE geonet and 3-inch diameter HDPE perforated pipe for the leak detection system (LDS); 4) primary 60 mil HDPE geomembrane; 5) cushioning layer consisting of two 10 ounce nonwoven geotextiles; 6) leachate collection system (LCS) consisting of 4-inch to 8-inch diameter HDPE perforated pipe in gravel bedding; 7) minimum of 18 inch-thick layer of drainage gravel; and 8) minimum of 6-inch thick sand filter layer to separate tailings from the drainage layer. The best available technology performance monitoring and operating criteria include a maximum head on the primary HDPE geomembrane of 3 feet and a daily leak detection flow rate below the action leakage rate.

INTRODUCTION

A proposed tailings storage facility (TSF) currently is being designed to manage tailings

to be discharged as a slurry from a uranium mill in an arid region of the western United States. The current design consists of construction of a single 30-acre tailings cell.

The plan view of the proposed tailings cell is shown in Fig. 1. This paper presents a best available technology (BAT) design for the current proposed design of the TSF.

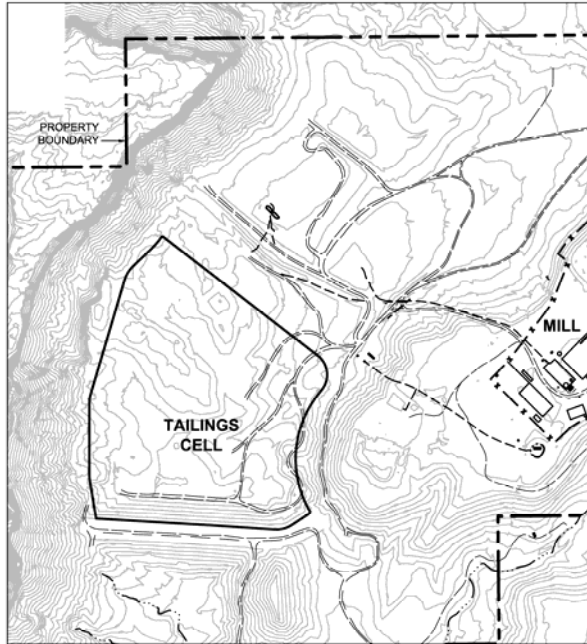


Figure 1. Plan View of Proposed Tailings Cell.

The agreement state rules require the use of a liner system beneath the tailings that “is designed, constructed, and installed to prevent any migration of wastes out of the impoundment to the adjacent subsurface soil, ground water, or surface water at any time during the active life (including the closure period) of the impoundment”. This performance criterion is met by the design of a multilayered liner system with two geomembranes consisting of high-density polyethylene (HDPE). This liner system design is consistent with BAT for liner systems. The liner system includes a leachate collection system (above the upper HDPE geomembrane) and a leak detection system (between the HDPE geomembranes).

Tailings fluid collected in the leachate collection system would be (1) recycled to the process circuit, (2) discharged to evaporation

ponds, or (3) retained within the TSF to submerge portions of the tailings during operation. The leak detection design provides for monitoring of fluids between the HDPE geomembranes and for removal of fluids (if detected) to remove the driving head across the lower HDPE geomembrane. This liner system significantly reduces the probability of leachate reaching underlying groundwater.

HDPE was selected for the geomembranes to provide superior liner durability and low permeability. The proposed components of the liner system listed from the bottom to the top, are shown in Figure 2 and described below:

- prepared subgrade;
- minimum 12-inch compacted clay liner with a maximum field permeability of 1×10^{-7} cm/s, serving as the base layer;
- secondary 60-mil HDPE geomembrane, overlaying the clay liner to form a composite liner;
- HDPE geonet and 3-inch diameter HDPE perforated pipe for the leak detection system (LDS);
- primary 60 mil HDPE geomembrane
- cushioning layer consisting of two 10 ounce nonwoven geotextile(s);
- leachate collection system (LCS) consisting of 4-inch to 8-inch diameter HDPE perforated pipe in gravel bedding;
- minimum of 18 inch-thick layer of drainage gravel; and
- minimum of 6-inch thick sand filter layer to separate tailings from the drainage layer.

The LCS would only be placed on the floors of the cells. Due to the steepness of the side slopes (2.5H:1V), side slope leachate accumulation is expected to be relatively low, thus the LCS would not be required on the

side slopes of the cells. The liner system design for the sideslopes of the tailings cell is shown in Figure 3.

The components of the liner system and the design of the LCS and LDS are described in more detail in the BAT Liner Design section. The following section discusses the regulatory requirements for the design.

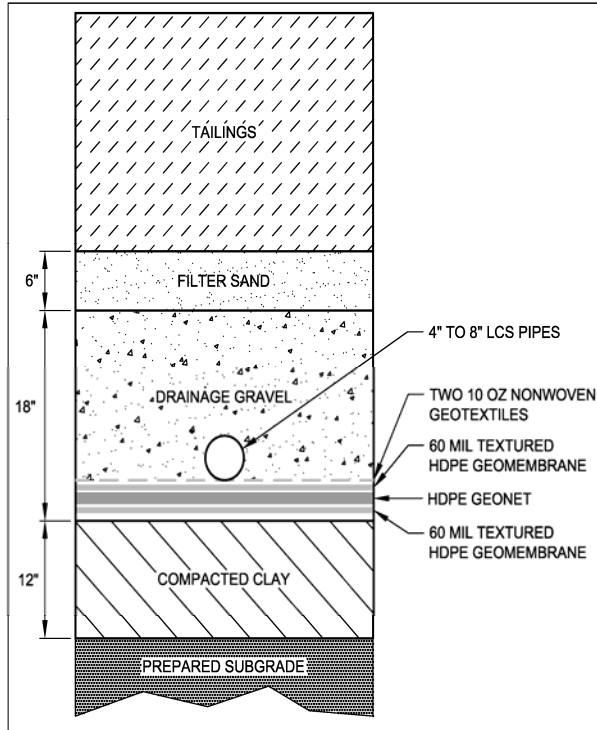


Figure 2. Liner System for Floors of Tailings Cell

REGULATORY REQUIREMENTS

The agreement state allows two design approaches for the TSF. One is a BAT design that meets their BAT design basis, which meets protective requirements by definition. Alternatively, if a design other than BAT is proposed, the state requires that design performance is demonstrated via modeling and other calculations to show that a design will meet state regulatory protection criteria.

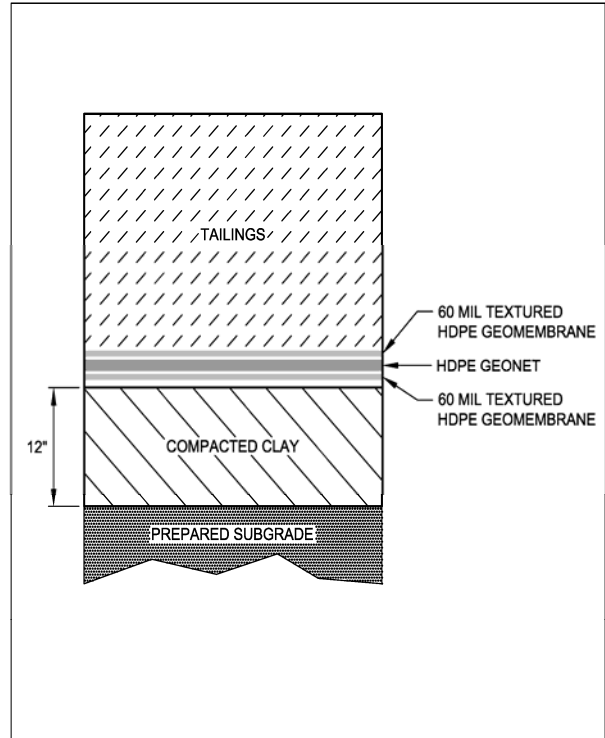


Figure 3. Liner System for Side Slopes of Tailings Cell

For the performance based design approach, infiltration and contaminant transport modeling would be developed to predict the performance of the design. For either the BAT or performance based engineering designs the primary points of performance monitoring for the liner system would be the

LDS while the primary points of compliance would consist of groundwater monitoring wells. The performance based design approach was not chosen by the owner for design of the TSF.

The owner chose to follow the BAT design approach for the TSF design. The owner is required to meet or exceed the design and operational guidelines agreed upon with the agreement state to meet the requirements for BAT design. The BAT design and operational guidelines are summarized below:

- design is applicable for slurried tailings;
- 3-inch corrugated advanced drainage system HDPE pipe leachate collection system installed within a sand filter bed and placed above the primary HDPE geomembrane liner;
- operational requirement of a maximum 3-foot head on the primary HDPE geomembrane liner to limit the head on the liner and minimize potential leakage through the primary liner;
- 60-mil HDPE primary geomembrane liner with maximum allowable design leakage rate (ALR) of 200 gallons per acre of disposal cell area per day;
- HDPE leak detection collection sumps for leak detection liquid collection;
- geonet leak detection layer with a transmissivity greater than the ALR to encourage flow to the LDS collection sumps;
- design requirement of 12 inches or less of fluid head on the lower liner;
- 60-mil HDPE secondary liner anchored with anchor trenches and placed in direct contact with the underlying clay liner;
- minimum of 12-inch thick compacted clay liner with a maximum permeability of 1×10^{-7} centimeters per second;
- native soil/bedrock layer prepared for the clay liner;
- 3H:1V side slopes;
- head monitoring of the LCS and flow rate monitoring of the LDS to be used as the primary points of performance monitoring, and as an early warning system to demonstrate protection of groundwater quality;
- BAT performance would be met if 1)

total head values in the LCS remain less than 3-feet above the lowest point on the primary HDPE membrane, and 2) daily LDS flow rates are below the 200 gallon/acre/day ALR value.

The intent of the BAT design guidelines above can be met with the current design. Design features that differ from the design guidelines are the LCS piping, the steepness of the cell side slopes, and the ALR as follows:

LCS Piping The current LCS piping design includes 4-inch to 8-inch diameter SDR 15.5 HDPE pipe. The 3-inch corrugated pipe listed in the design guidelines was determined to have insufficient load bearing capacity.

Side Slopes The maximum side slopes for the cell are designed as 2.5H:1V except for the upstream face of the existing dam, which is designed to remain unchanged. The side slopes were steepened to provide more storage capacity and to reduce construction fill volumes, and are stable for operational and pseudostatic conditions.

ALR A calculated ALR of 130 gallon/acre/day was used for the design. Based on the above engineering design and operational guidelines, any discharge from the lower HDPE liner to the foundation would be deemed a de-minimus discharge.

BAT LINER DESIGN

The components of the liner system and the design of the LCS and LDS are described in the following sections.

Cell Grading

The TSF will be constructed within a natural drainage feature (Fig. 1). The existing topography within the drainage feature provides excellent drainage characteristics for the collection of leakage and leachate. The TSF grading was designed to optimize the use of the existing topography, which will minimize both the materials needed and the time required to construct the cell.

Compacted Clay Liner

The composite liner system design for the TSF contains a low-permeability compacted clay liner over which the geosynthetic components are deployed. Initially this soil layer was proposed to consist of 12 inches of compacted clay. The design was modified to use a clay/sand mixture, which would result in several improved engineering characteristics relative to using clay alone and maximize utilization of the limited quantity of on-site clay and abundant sand materials. The selected clay/sand mixture would be used to construct a minimum 12-inch thick soil liner subject to the following specifications: (1) maximum particle size of 1 inch; (2) minimum of 30 percent passing the No. 200 sieve; (3) minimum plasticity index of 10; and (4) maximum field hydraulic conductivity of 1×10^{-7} cm/s when compacted within an acceptable zone of dry unit weight and moisture content. The clay/sand mixture would consist of a blended mixture containing 55 ± 5 percent (by weight) on site clay and 45 ± 5 percent on-site sand. The clay and sand borrow areas are located within the proposed TSF cell and proposed future expansion area.

Secondary HDPE Liner

A 60-mil HDPE geomembrane is designed to be installed above the clay liner to provide a composite liner below the LDS for the TSF.

The geomembrane is designed to be textured on both sides to provide additional stability and to facilitate construction on 2.5H:1V side slopes.

Leak Detection System (LDS)

The LDS is designed to intercept leachate that may pass through potential defects that develop in the primary liner. The LDS consists of a geonet drain, overlying the secondary composite liner of HDPE geomembrane and compacted clay. The geonet drain is intercepted by 3-inch diameter perforated HDPE pipe where necessary to collect solution from the geonet drain. The plan view of the LDS is shown in Figure 4.

The LDS for the TSF is designed to be subdivided into four subareas by utilizing site grading and small berms. The separation berms would be constructed as small (approximately 1 foot high) ridges on top of the compacted clay liner, and would be overlain with the full thickness of drainage system. Any leakage from a subarea would report to a separate chamber within the LDS sump system. Should the ALR be exceeded in any sump, the subarea contributing to the flow could be identified for repair or abandonment.

An HDPE geonet is designed to be used for leak detection through the primary HDPE geomembrane. The geonet would require a minimum transmissivity of 3.3×10^{-3} m²/s based on LDS capacity calculations performed as part of the design. The leak detection system is designed to handle flow significantly greater than the established ALR of 130 gallons/acre/day.

The ALR was calculated using methods presented in Giroud et al. (1997) and U.S. EPA (1992) for estimating leakage through the primary liner for a properly installed and functioning liner system. Assuming a small

hole diameter of 0.079 in (2 mm), a total head of 18 inches, and a hole density of 1 hole per acre results in an ALR of 130 gal/day/acre.

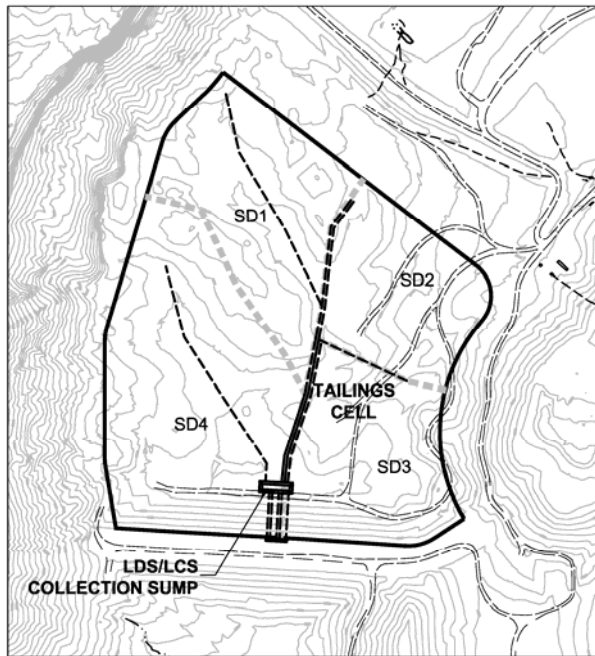


Figure 4. Plan View of Leak Detection System

The ALR of 130 gal/day/acre can be converted to a Sump Action Leakage Rate (SALR) by taking the product of the ALR and the area contributing to the sump. There are a total of four chambers in the LDS sump, one for each subarea as shown in Figure. 4.

The main collectors of the LDS are designed to carry leakage fluid to separate sump chambers. Each sump would be constructed as a dual LDS/LCS sump with separate collection areas for the leak detection discharge (lower sump) and the leachate collection discharge (upper sump) as shown in Figure. 5. The LDS sump would be divided into 4 separate chambers to collect leakage from the 4 individual LDS drainage areas. Within the composite sump, there are four 12-inch diameter access pipes for pump installation and instrumentation within the leak detection sump and one 12-inch diameter access pipe for pump installation and

instrumentation within the leachate collection sump, for a total of five pump installation pipes for the composite sump. The instrumentation access pipes would be used for installation of water level monitoring equipment.

Leakage through the primary geomembrane liner would be conveyed by the LDS consisting of geonet and perforated piping. The maximum steady state rate of leachate migration through a single defect in the primary liner that the geonet can accommodate without being filled with leachate at the point of the defect was calculated using the method presented by Giroud et al. (1997).

As the flow path within a unit width of geonet increases, the anticipated leakage flow rate would also increase, until the geonet is overwhelmed. To prevent the geonet from reaching its flow capacity, the geonet is intercepted at intervals by a perforated leak detection pipe. The LDS pipe would carry flow at a minimum slope of 1 percent to the sump. The LDS pipe capacity was calculated using Manning's equation, assuming a 3-inch diameter HDPE pipe, with a roughness coefficient of 0.01, and a minimum pipe slope of 0.01 ft/ft.

All factors of safety are adequate to ensure that the anticipated ALRs reporting to each sump area are within the capacity of the LDS components. In addition, fluid head within the LDS would be contained within the geonet and LDS pipe, and therefore the anticipated ALRs would result in fluid head on the secondary liner well below the regulatory requirement of one foot.

Average head on the secondary liner was calculated using methods presented by Giroud et al. (1997), and as a function of capacity of the geonet. Both procedures indicate the fluid head is contained within the

geonet itself, which is specified as having a minimum thickness of 300 mil (7.6 mm). This depth of fluid is well below the

compliance requirement of 12 inches or less of fluid head on the lower liner.

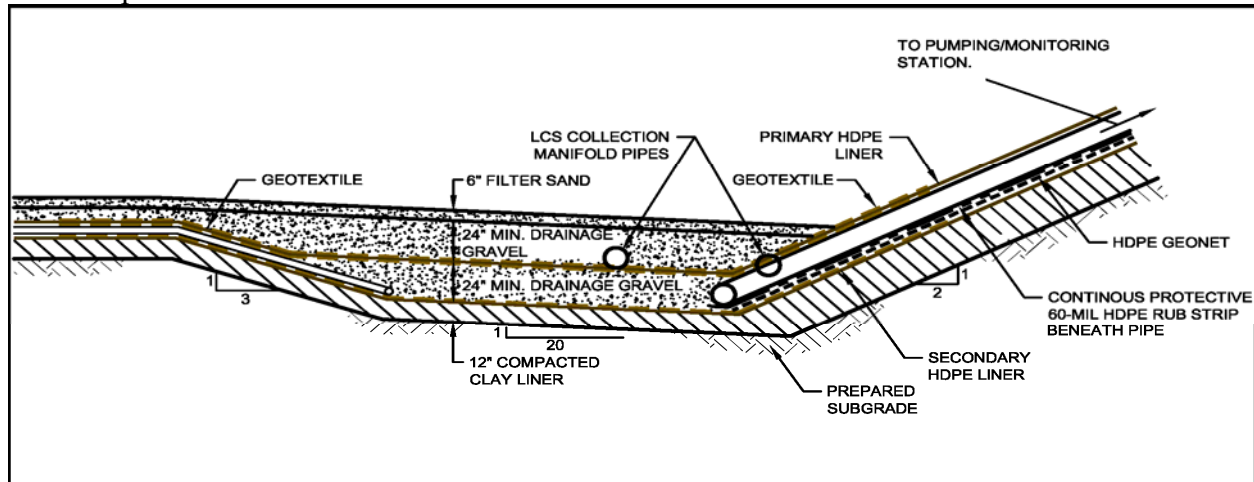


Figure 5. Cross Section of Sump for Leak Detection System

The design of the leak detection system allows for leaks to report to the sump within approximately 5 hours. This time frame is considered adequate in order to detect leakage in a timely fashion

TSF since there is not a gravel layer on the sideslopes in these areas. A cushioning layer is also not required for the anchor trenches since the on-site sands would be used for the backfill of the anchor trenches.

Primary HDPE Geomembrane Liner

The primary liner above the LDS is designed to be a 60-mil HDPE geomembrane. The geomembrane is designed to be textured on both sides to provide additional stability and to facilitate construction on 2.5H:1V side slopes.

Leachate Collection System (LCS)

An LCS was designed in order to limit the amount of head on the primary liner and to decrease the time required to dewater the tailings. The LCS consists of 4-inch to 8-inch diameter perforated HDPE pipe encased in 18 inches of drainage gravel. Six inches of filter sand would be placed over the gravel to prevent piping of tailings into the drainage gravel.

Cushioning Layer for Primary HDPE Geomembrane Liner

Cushioning calculations were performed for the primary liner to determine the geotextile thicknesses required to cushion the primary liner from the overlying 18-inch gravel layer. Two 10-ounce per square yard nonwoven geotextiles are recommended to allow for the option of future expansion (estimated using 110 feet of tailings and cover). A cushioning layer is not required for the side slopes of the

The drainage gravel serves the following functions: (1) providing a continuous drainage layer at the base of the tailings to prevent build-up of head on the primary liner; (2) adding drainage capacity to LCS; (3) preventing intrusion of tailings into the 0.25-inch slots in the perforated drainage pipe; (4) guarding the HDPE liner against penetration of stones or other objects; and

(5) protecting the HDPE liner against damage from construction equipment. The drainage gravel is designed to be subangular and have a maximum particle size (D_{100}) of 1 inch, in order to protect the integrity of the primary HDPE liner. The minimum particle size of less than 2% passing No. 10 sieve is designed to meet filter criteria with the pipe perforations of 0.25 inches, according to guidance given in the National Engineering Handbook, Part 633, Chapter 26 “Gradation Design of Sand and Gravel Filters” (USDA, 1994).

The sand filter is designed to prevent migration of tailings material into the pore spaces of the drainage gravel. As the tailings are discharged, tailings would segregate with the coarser fraction settling out close to the discharge point, with the finer fraction settling out at more distant locations. A gradation envelope for filter sand meeting filter criteria with both the fine tailings and the drainage gravel was developed using criteria presented in USDA (1994).

The LCS would be placed on the floor of the cells. Due to the steepness of the side slopes (2.5H:1V), leachate accumulation on the side slopes would be relatively low, and therefore the LCS would not need to extend up the side slopes of the cells. The minimum spacing between pipes has been designed to limit the head on the primary liner to 18 inches or less (thickness of the gravel drain). This is less than the operational BAT requirement of a maximum head on the primary liner of 3 feet. The size of the pipe has been designed to carry all of the predicted leachate at half the pipe capacity. Additional pipe capacity and flow through the drainage gravel add redundancy in the LCS design. The main leachate collectors would carry leachate to the LCS sump. The plan view of the LCS is shown in Fig. 6. The cross section of the leachate collection sump is shown in Fig. 7. The LCS sump would include a 12-inch

access pipe for a submersible pump and leachate level monitoring equipment.

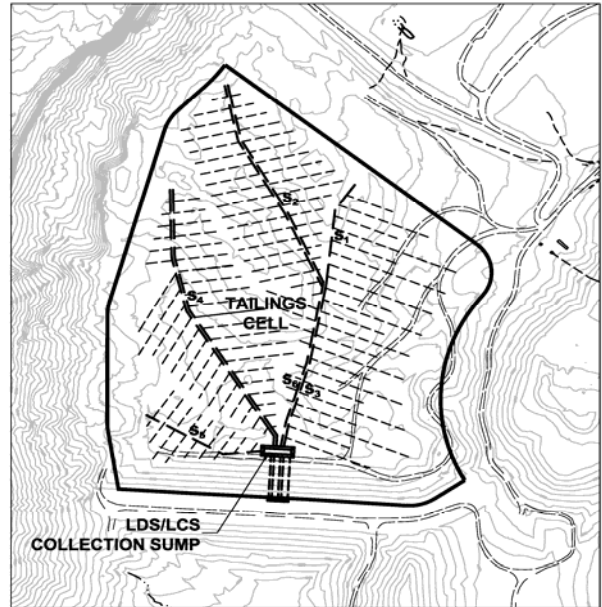


Figure 6. Plan View of Leachate Collection System

The maximum drainage distance to a collection pipe along the base of the cell(s) is limited to 80 feet or less. The gravel drain around the pipes would also provide substantial conveyance capacity to supplement that in the pipes.

Liner Anchorage

Liner anchorage for all of the tops of slopes for the TSF would be provided by anchor trenches. The most critical slope and loading condition was used for anchor trench design. The minimum perimeter trench depth was calculated as 24 inches.

Based on liner uplift calculations, the liner system would be capable of withstanding the tension forces exerted by the design wind velocity without tearing, pulling apart. The anchor trenches as designed would withstand the tension forces that would be generated by the wind uplift.

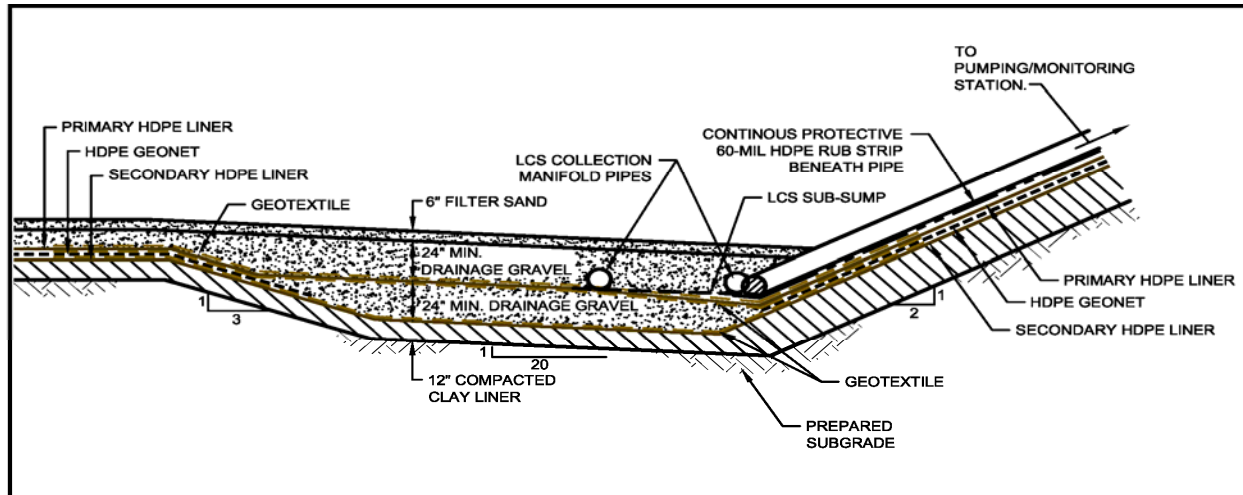


Figure 7. Cross Section of Sump for Leachate Collection System

MONITORING REQUIREMENTS

As noted, the design guidelines above were agreed to by the owner to meet BAT requirements. The liner system and collection sumps were designed to follow the intent of these design guidelines. A multilayered liner system with a LCS, LDS, and compacted clay liner would be used for containment and collection of the mill tailings solution in the TSF.

BAT monitoring requirements for the site during operation would include monitoring of the LCS and LDS of the TSF. The primary points of BAT performance monitoring include the water level of the LCS and flow rates in the LDS. These BAT monitoring points are discussed further below.

BAT Monitoring Requirements for LCS

The BAT operational head requirement for the LCS is a maximum of 3 feet on the primary HDPE geomembrane. As discussed above, the LCS has been designed for a maximum head of 18 inches. BAT monitoring for the LCS during operations

would include measurements of the water pressure on the lowest point of the primary liner of the TSF. A pressure transducer would be installed in the LCS access pipe to continuously monitor the water pressure in the LCS sump. This data would be used to calculate the maximum head on the primary HDPE geomembrane. This measurement would be made and documented on a daily basis.

BAT Monitoring Requirements for LDS

Daily LDS flow rates must be less than the calculated action leakage rate (ALR) for BAT monitoring during operations. The calculated ALR is 130 gal/acre/day. The ALR of 130 gal/acre/day can be converted to a Sump Action Leakage Rate (SALR) by taking the product of the ALR and the area contributing to the sump. There are a total of four sump chambers for LDS cells SD1 through SD4

The LDS sumps would be equipped with a submersible pump, flow meter, and pressure transducer. The pump would be equipped with a pressure-sensing transducer and would automatically activate when the water level in

the sump reaches half the maximum allowable level of 12 inches corresponding to 6 inches above the lowest level on the secondary liner. The water level information would be collected by an electronic data collector. The LDS would be monitored daily and if any water is present, the SALR would be calculated from the water level and total flow over time readings. The SALR values would be compared with the maximum SALR values.

Contingency Plan for BAT Monitoring

If the SALR is exceeded for any sump, notification would be required immediately and actions taken which include further notifications and preparation of a written report. The contents of the report may include the following information:

- a description of the event including the probable cause and the manufacturer and model number, if applicable, of equipment that failed or malfunctioned;
- the exact location of the event;
- date and time or time period of the event;
- the estimated time period that noncompliance is expected to continue if it has not been corrected;
- corrective actions taken or planned and results of evaluations or assessments; and
- if applicable, an estimation of quantity of material discharged or an estimation of the quantity of material released outside containment structures.

Measures required to immediately correct a problem would be discussed with the appropriate representatives of the agreement

state, implemented upon approval, and documented.

Upon approval from the agreement state, a series of steps would be taken to reduce the rate of discharge from the LDS. If the change in rate of discharge from the LDS is reasonably abrupt, it may indicate a new contact with a liner puncture. In areas of initial tailings placement the liner would be examined for damage. This may include excavating through recently placed tailings, where practical, to try to expose the area of the liner where the leak is likely to be located. If a damaged section of liner is located, the liner can be repaired and tested. During this process, the location of tailings placement can be changed or the tailings placement would be suspended within the suspect area. If the contributing punctures in the primary liner cannot be located, all ponded tailings solution would be pumped from the suspect area to an adjacent cell or to the most distant practical location within the cell. If the rate of discharge to the leak detection subsequently declines to acceptable levels, restrictions would be placed on the moisture content of tailings that can be placed within the area of the cell where the leak was suspected to have occurred. Only reduced moisture tailings would be permitted to be placed in the section of the cell contributing to the sump where the allowable leak detection rate was exceeded. No ponding of solution would be permitted within the section of the cell contributing to the leak detection sump.

If steps taken to reduce the discharge from the LDS are unsuccessful in reducing flow rates below ALRs for the sumps, then further action could be taken and may include one of the following:

- isolation of the point of failure and retrofit construction;

- cell closure should retrofit construction be infeasible; and
- contaminant transport modeling to demonstrate that groundwater quality would be protected despite the liner performance failure.

CONCLUSIONS

The design of the TSF was conducted to meet project requirements, conform to site conditions, and meet BAT design guidelines as defined by the agreement state. The design of the facility is currently awaiting final regulatory review and approval.

REFERENCES

Giroud, J.P, B.A. Gross, R. Bonaparte, and J.A. McKelvey, 1997. "Leachate Flow in Leakage Collection Layers Due to Defects in Geomembrane Liners", Geosynthetics International, Vol. 4, No. 3-4, pp. 215-292.

U.S. Environmental Protection Agency (EPA), 1992. Action Leakage Rates for Leak Detection Systems. Supplemental Background Document for the Final Double Liners and Leak Detection Systems Rule for Hazardous Waste Landfills, Waste Piles, and Surface Impoundments. EPA/530-R-92-004. NTIS Publication PB92-128214. Office of Solid Waste, Washington, D.C. January.

United States Department of Agriculture (USDA), 1994. *National Engineering Handbook, Part 633*, Chapter 26, Gradation Design of Sand and Gravel Filters.

THE CANNON MINE TAILINGS IMPOUNDMENT: A CASE HISTORY

Jack Caldwell,

Robertson GeoConsultants, Vancouver, BC

Ian Hutchison

Strategic Engineering and Science, Irvine, CA

Rick Frechette

Knight Piesold, Tucson, AZ

ABSTRACT: This is a case history. This is the story (history) of the design, construction, operation, and closure of the Cannon Mine Tailings Impoundment in Wenatchee, Washington. The Cannon Mine was a gold mine that opened in the early 1980s just to the southwest of Wenatchee, WA. The tailings impoundment included an initial 100-m high rock-fill embankment, diversion channels, and hydraulically discharged tailings. With time the embankment was increased to 140-m high. The impoundment was operated successfully for the life of the mine, and when mining stopped, the impoundment was reclaimed. Today the reclaimed site is fully integrated into the surroundings and an example of mining that can be successfully undertaken close to urban areas.

INTRODUCTION

The Cannon Mine, Wenatchee, WA was a joint venture project between Asamera Minerals (U.S.) Inc. and Breakwater Resources. The impoundment was constructed in the early 1980s, operated for a decade, and then reclaimed. This is the story of the impoundment from the perspective of the authors who designed the impoundment, were on site for most of its construction, and ultimately were involved in the reclamation of the impoundment.

THE IMPOUNDMENT SITE

The tailings impoundment site is to the southwest of the mine which is southwest of Wenatchee, Washington. The site was selected after a formal site selection study that included consideration of: health & safety (the potential for constructing a safe facility); economic (capital, operating, and reclamation cost); environmental impact (area of the impoundment and length of tailings delivery pipeline); socio-economic

consideration (current land use); and public attitude (visibility and perceived public concerns.)

The selected site was close to the mill, significantly impacted by prior silica mining, screened by the surrounding hills, and characterized by suitable bedrock. Significant disadvantages of the site included the need to pump tailings against a head of up to 200 m and its location upgradient of houses in the town of Wenatchee, WA.

The bedrock at the impoundment site was primarily Wenatchee rocks including interbedded sandstones and siltstones varying in thickness from 10 mm to six meters. Bedrock was covered by a variable thickness of soil that was stripped prior to construction of the embankment. On the crest of the hills adjacent to the site were thick deposits of Columbia River Basalt that was quarried to construct the rockfill shells of the embankment. Pleistocene windblown clayey, silty sand was obtained at a borrow site also close to the impoundment and this material was used in the core of the embankment.

THE EMBANKMENT

Initially the impoundment embankment was designed to rise to a height of approximately 100m. The cross section includes a low permeability core, drains, and rock-fill outer shells. A grout curtain was installed beneath the core. (Figures of the layout of the impoundment, and the details of the embankment are in the references and are not repeated here.)

The core and the primary drains are founded on the bedrock that underlies the entire site. The upstream and downstream toes are

founded on the materials that filled the gully at the base of the valley.

An inclined core was adopted in order to provide for staged construction of the embankment and to enhance performance during operation.

The filters and drains are three-meters wide. This width was chosen to facilitate placement and as a conservative seepage control feature. The filter material is a fine to coarse sand. The gradation was chosen so that the sand retains even a slurry of the core material; thus the filter was able to prevent piping of soil due to normal seepage through the core and to hold back any material dislodged into potential cracks in the core.

The downstream and upstream shells are of compacted, decomposed basalt. The downstream slope is two horizontal to one vertical. The average angle of friction of the basalt is about 37° , hence the factor of safety of the downstream slope is at least 1.5.

The upstream slope is 2.5 horizontal to one vertical. This slope was set on the basis of stability analyses which included consideration of excess pore pressure in the core and blanket (i.e., $u=0.3$ and the angle of friction being about twenty-five degrees.

In the course of operation, the embankment was raised three times to an ultimate height of 140 m. All raises were by the centerline method. The raises continued with the same zonation as established in the initial construction.

The final raise serves as the flood detention berm to this day. In the final raise no filter zone was necessary. The core and downstream slope in the final raise were steepened relative to the initial embankment geometry and subsequent raises.

Temporary CMP pipe spillways installed through the dam were replaced with a permanent open-cut channel spillway on the south abutment.

CONSTRUCTION

About 2.3 million cubic meters of soil and rock were placed in about nine months in 1984 and 1985 to form the embankment.

But first, we had to strip and excavate about 650,000 cubic meters of topsoil and colluvium; this was achieved with six CAT 623 scrapers in four months of two 10-hour shifts per day. Overburden removal started at the top of the left abutment. Materials were moved with a bulldozer. The colluvium was pushed down the slope to form a bench. Once the bench was wide enough to traverse, scrapers picked up the colluvium and deposited in waste piles downstream of the embankment. The abutment in the shell area was cleared of soil and loose rock. The specifications called for “machine cleaning”.

Foundation excavation was done before the winter snow. As a result of inadequate overburden removal and degradation of the rocks during the winter, further foundation cleaning was done during fill placement the following year. An area three meters ahead of the fill was cleaned with a backhoe or a slope board. Generally the rock thus exposed was competent and substantially free of loose pieces that could be removed by hand.

The specifications called for hand-cleaning of the core area. Shovels and air hoses were used to clean the foundation bedrock over the core area. Where the rock in the core area was loose, excessively fractured, or very rough because of friable sandstone or

shattered siltstone, mortar or shotcrete was applied.

Numerous benches and distinct changes of profile were encountered up the abutment. The edges of the benches were trimmed so that the following requirement was generally met: the angle between two straight edges about 300 mm apart should be no more than 20°.

The upstream and downstream toes are founded on the materials that filled the gully at the base of the valley. This fill was excavated and removed beneath the greater part of the embankment core as it was found to be deep (up to 15 m) and of soft, compressible clays and silt. Such excavation was, however, difficult and expensive. It was easy to establish that a better approach at the toe was to construct a toe dike or berm on the in situ gully fill.

A grout curtain was installed beneath the core. It consisted of two lines of holes about three meters apart. On average, tertiary boreholes were required for satisfactory closure (limited grout take) and sometimes quaternary holes were required. The average hole spacing was about one meter and the hole depth increases from 12 m at the crest to a maximum depth of about 50 m beneath the highest part of the embankment.

Placement and quality control of the embankment materials other than the shell basalt was straightforward and in accordance with standard practice. The basalt however, being a rockfill, called for special attention: specifications called for a minimum of four passes of the specified roller and a density no less than 98 percent of ASTM D698. Test pads of the basalt were placed and the effects of compaction were monitored. In particular, considerable work was done to establish correlation between variations in the gradation and quality of the basalt, the

lift thickness, the number of passes of the compactor, and the resulting settlement and density of the fill. These data were subsequently used to monitor and control basalt placement.

The core of the embankment is compacted clayey, silty loess. It was compacted in 150-mm layers to at least 98 percent ASTM D698 at a moisture content between two percent dry of optimum to one percent wet of optimum; this was done to avoid the generation of excess pore pressure. A zone of core materials at one to three percent wet of optimum and at least 600-mm thick was placed against the abutments in order to enhance contact by molding the soil into the irregular surface of the rock.

OPERATION

Deposition of tailings began in mid-July 1985. Tailings were pumped to the impoundment as a slurry and discharged from spigots along and some way upstream from the crest. Deposition was generally managed to form thin layers of tailings each of which was sun-dried to the extent possible. And so over the years the impoundment was filled. Just one point of interest: the design water balance which was generally achieved. No flood bedeviled the impoundment and no discharge of excess water occurred.

RECLAMATION

By 2004, the impoundment had been closed and reclaimed. It was by then the topic of symposia and Powerpoint presentations easily accessed via Google on the internet. One such presentation (Rothberg et al.) tells us that the impoundment covers 14 hectares, has a 104-m high embankment with a 335-m

long crest and contains between four and five million tonnes of tailings.

This same presentation tells us that the impoundment retains its high hazard designation as more than one-hundred homes are at risk.

The cover is also described. It reportedly consists of—from the bottom up:

- Geotextile support layer
- 750 mm well-graded sand and gravel
- 300 mm of topsoil
- Vegetation.

The 4.6-m wide open-cut spillway serves as the permanent emergency overflow structure for post-closure. The 300-m long channel is unlined but is founded in competent Wenatchee Formation sedimentary rock of the south abutment. The final 6.5-meters of embankment height along with the spillway serve as a flood detention and routing facility that can completely store the small to moderate storm events and safely route extreme flood events up to and including the 72-hour probable maximum flood (PMF) with a 20-year snowpack melt.

Operational seepage and groundwater interflow beneath the dam was estimated at a cumulative nominal flow rate of 1.3 to 1.6 liters per second at site closure. Most of the flow component, based on chemistry signatures, is from natural groundwater sources. To mitigate the presence of some mineralization byproducts generated by reactive components in the tailings particles and from mobilization of the associated pore fluids, passive treatment cells were installed at the dam toe area. Constituents characteristically found in the seepage include sodium, chloride, elevated pH, TDS and trace metals.

These passive treatment cells, collectively referred to as the wetland treatment system,

function in a truly passive manner and discharge the treated seepage back into Dry Gulch just below the embankment. Three ponds, each nominally 0.2 hectare in size, were constructed to treat the seepage flow from the tailings facility and operate in series. The first two cells incorporate both aerobic and anaerobic capabilities based on the direction of inflow to the cell (either from above or below). The third cell is a simple aerobic cell, or polishing pond. The wetland cells, nominally 2 meters in total depth, were populated primarily with cattails and bulrushes. The wetland treatment system was completed and commissioned in September 1996.

We are told that by 2001 county and state-held bonds were released and that in 2003 the impoundment (or at least those who undertook its closure) was/were the recipient(s) of the Washington Department of Natural Resources "Recognition for Reclamation Award."

PERSONNEL & PERSONAL

In that this paper is a case history, we include as follows some history about the people who worked on the initial phases of the construction of the embankment. Many more than we could write about here contributed. Those mentioned below are noted because of the technical contributions they made.

The authors of this paper worked for Steffen Robertson and Kirsten during the seminal phases of design and construction of the Cannon Mine Tailings Impoundment. We thank our many colleagues from SRK past and present who helped and contributed to its success.

Gary Bates was the Asamera project manager. It is he who kept us under control

and focused on success. He spent countless hours with us pouring over engineering reports as we tried to explain our concepts to those who were writing the project Environmental Impact Statement. We wanted more in the EIS; they want the essence and less. Gary always found the right balance and the EIS was a success. His personal, hands-on, day-to-day involvement with the details for the impoundment design and construction were the key to its success.

John Toften was Asamera's chief mining engineer in day-to-day charge of embankment construction. He was a large German mining engineer. The first day I met him, I presented to him the SRK budget for site characterizations. John looked me in the eye and said: "Jack, here we are miners. We are used to going into the ground and then deciding how to proceed and adjust. You cannot spend all this money drilling. Rather you come to site for a year and do the engineering as we move the soil and rock for you." And that is just what I did. For nearly two years I was on site every day observing, testing, and designing as we went. It was John who forced me to and worked with me as I implemented the Observational Method in geotechnical engineering. To him as a miner it was a normal way to proceed. To me it was an honored approach in geotechnical engineering that I was forced to implement in practice in real time application.

Syd Hillis was the design peer reviewer. He highlighted how a good peer reviewer operates. He would spend the day looking at the rocks, feeling the soil, counting the passes, and examining the results we produced in a small on-site soils laboratory. Then we would review the day's findings. He always came up with profound insight and practical solutions and details. He knew every detail, asked penetrating questions until we were all satisfied with the answers.

He brought his vast experience at earth days world-wide to our table and never let us do less than the best.

Don Moore was Asamera's process engineer. He and our Adrian Smith dealt with the chemical and geochemical issues. We reference one of their papers on the topic. They too focused on testing, facts, and practical approaches. They worked in concert with the geotechnical engineers and thus we succeeded. .

We do not know the many others who must have come after us as we moved on to other places and interests. They operated the impoundment and ultimately reclaimed it. To them our credits and plea: tell us more.

CONCLUSIONS

When we were designing and building the Cannon Mine Tailings Impoundment, we thought of the work as routine. And time has proven that for there are now many more, much larger and higher impoundments world-wide.

Yet, to-date, the embankment is still one of the highest in Washington State, and has stood the test of some time.

We are honored to have been given the chance to work on this project, which we submit is a testament to the fact that mines can be developed, operated, and closed in close proximity to urban centers.

REFERENCES

Breitenbach, A. "Rockfill for Mines." At http://www.infomine.com/publications/docs/E-Book_Rockfill_for_Mines.pdf

Caldwell, J., Sluder, T., Crews, T. "Engineering Geology and Soils Engineering in the Development of the Cannon Mine Tailings Impoundment" <http://www.infomine.com/publications/docs/Caldwell1986b.pdf>

Caldwell, J., Thatcher, J., Kiel, J. "Environmental Geotechnical Considerations in the Design of the Cannon Mine Tailings Impoundment." <http://www.infomine.com/publications/docs/Caldwell.pdf>

Caldwell, J., Hillis, S., Hutchinson, I. "The Design of the Cannon Mine Tailings Impoundment." <http://www.infomine.com/publications/docs/Caldwell1985d.pdf>

Caldwell, J., Moore, D., Hutchison, I., Sluder, T. "Design and construction outlined of the Cannon mine tailings impoundment." Mining Engineering August 1986. At SME OneMine. <http://www.onemine.org>

Caldwell, J., Moore, D., Smith, A. "Impoundment for Cyanided Tailings—Case History of the Cannon Mine Project." <http://www.infomine.com/publications/docs/Caldwell1984a.pdf>

Caldwell, J., Hillis, S., Crews, T. "Construction of the Embankment for the Cannon Mine Tailings Impoundment." <http://www.infomine.com/publications/docs/Caldwell1985a.pdf>

Cannon Mine Asamera Minerals (US) Inc and Breakwater Resources Ltd. Website at http://www.geocities.com/cannon_mine/

Pincock Allen & Holt, 2000. Permit Termination Request & Summary Technical Data Review, Cannon Mine Project, Wenatchee, Washington.

Steffen Robertson & Kirsten, 1994. Cannon Mine Tailings Impoundment Reclamation Plan, April 1994.

Rothberg Tamburini Winsor “Cannon Mine Tailings Closure” UNR Mining Life-Cycle

Center Tailings Closure Workshop. Elko Nevada. June 8-9, 2004 at http://www.unr.edu/mines/mlc/conf_workshops/tailings/Elko_8.pdf

OPTIMIZATION OF REMOVAL OF OVERBURDEN MATERIAL FOR AN OPEN PIT GOLD MINE

Jason S. Andrews and Daniel D. Overton

Engineering Analytics, Inc., Fort Collins, Colorado, United States

Nicholas Legere

Mine Geologist

ABSTRACT: An open pit gold mine located north-west of Yuma, AZ has historically experienced excessive slope failures along the north pit walls in the conglomerate overburden (waste rock) material that overlies the ore bearing gneiss. However, the stability of the south, west, and east walls has been acceptable. This paper presents an overview of slope stability modeling using anisotropic material properties and slope monitoring that has been conducted to optimize mining operations and reduce the number and size of failures of the north pit wall slopes.

The Mine has taken a proactive approach to slope stability monitoring and has developed a system of measurements and visual observation along the crests of the high walls in an effort to provide assurances for safety and to minimize loss of production. Additional slope stability analyses were performed to model the proposed slopes of the East Rainbow Pit. Past slope stability analyses were completed by modeling the pit material as a homogenous mass. Review of the geologic mapping completed by the Mine indicated that the slope failures were potentially controlled by the faulting and bedding planes, which could not be adequately modeled as a homogenous material. In order to analyze the effects of the faulting and bedding planes, slope stability analyses were completed using anisotropic properties to model the mapped faulting and bedding. The results of the modeling were consistent with the observed failures in the pit and allow for further optimization of the pit wall slopes by allowing the south, west, and east pit walls to be excavated at a steeper angle than the north pit wall thus reducing the amount of waste rock that will have to be removed to reach the ore body.

INTRODUCTION

The stability and optimization of the pit wall slopes are an important part of the mine economic analysis as they impact the amount of waste material/rock that must be removed to access the ore body. The amount of waste material that must be

removed will impact the profitability of a mine during operations and impact the closure actions that must be completed after mining.

The open pit gold mine which is located north-west of Yuma, AZ commenced stripping of the East Rainbow pit in August

2007. Mining of the pit required the removal of 25 million tons of overburden material. A slope failure occurred in the north pit wall on May 11, 2008. Historically, the north walls of the pits at the open pit gold mine have had a high rate of failure, and these failures have resulted in increased mining costs. Engineering Analytics performed additional slope stability analyses for the large scale slope failure of the north pit wall within the East Rainbow Pit.

Structural controls along with bedding orientation and low shear strength have been identified as conditions that contribute to failures in the overburden material at the Mine. However, prior to redevelopment of the Rainbow Pit the highwalls have been predominantly composed of gneissic bedrock and thus the thickness of the conglomerate has been relatively thin. Thus, the mine had no operational history of the performance of the conglomerate material in a thick section of overburden.

FAILURE OF THE NORTH PIT WALL

The Mine reported that a crack started developing north of the north excavation face within the East Rainbow Pit on approximately April 10, 2008, and propagated to the west. This crack was observed to extend from the east corner of the north excavation face in a westerly direction for approximately 1400 feet. The crack started at the north-east corner of the north excavation face and followed an arcuate surface expression with a maximum distance of approximately 120 feet back from the crest of the north pit wall.

Mine personnel constructed four extensometers across the tension cracks to monitor the slope movement. The extensometers consisted of two posts and two sections of pipe that were allowed to slip over each other. Mine personnel conducted readings of the difference between the outer pipe and a marking made on the inner pipe. Mine personnel also set targets for surveying the top of the north pit wall and the location of these targets was surveyed by mine personnel to determine the rate of movement.

The Mine personnel reported the north pit wall experienced a slope failure during the early morning of May 11, 2008, a photograph of that failure is shown in Figure 1. Prior to the May 2008 slope failure no movement of the slope was measured by the Mine personnel using either the extensometers or the survey targets. Engineering Analytics visited the Mine site to observe the failure and the on-going monitoring that was being performed by the Mine. The failure extended from the north-east corner of the pit westerly approximately 500 feet. The failure extended back approximately 60 feet from the crest of the pit wall. Mine personnel estimated that at least 400,000 tons of material was displaced by the failure.

Accelerated movement was not observed prior to the actual failure, and the failure occurred in less than one hour. The failure is a large Debris Slide type of failure as categorized on Figure 2.1 of "Landslides: Analysis and Control" (TRB 1978). The dominant movement of these types of slides is described as: "*Movement frequently is structurally controlled by surfaces of*

weakness, such as faults, joints, bedding planes, and variations in shear strength between layers of bedded deposits, or by the contact between firm bedrock and overlying detritus.”



Figure 1. Photograph of the May 11, 2008 Slope Failure of the North Pit Wall

The failure had a near vertical head scarp that was approximately 30 feet in height. The failed mass visually appeared to be a slough towards the bottom of the excavation, and did not show signs of rotational failure in the bottom of the pit. No water was observed in the area of the failed material. The failure continued to progress toward the west resulting in displacement of approximately 100,000 additional tons of material by June of 2008. Engineering Analytics observed the failure in May 2008 and again in November 2008. A photograph of the progression of the slope failure is shown in Figure 2. The geometry of the failure appeared to be impacted by the dip of the bedding in the conglomerate and by south dipping high angle faults that run in a north-west to south-east direction through the pit and north wall face. Slope failures at the Mine have predominantly occurred along the north wall of the pits.

The May 2008 failure covered approximately 5,000 ounces of gold ore. This ore will be recovered in the next mining phases but results in lost revenue until the next phase of the pit is advanced.



Figure 2. Photograph of the Progression of the May 2008 Slope Failure, Observed November 2008

GEOLOGIC CONDITIONS

The failure occurred in the overburden, which is regionally described as the Bear Canyon Conglomerate (BCC). Information on the BCC, as exposed in the East Rainbow Pit, is compiled from pit mapping performed by John Ochs, consultant geologist for the Mine; with other regional details based on descriptions provided in “The Conglomerate of Bear Canyon (Miocene), Chocolate Mountains, Southeastern California” (Hughes, 1997). The locations of the faults mapped within the East Rainbow Pit are presented in Figure 3.

The BCC (Figures 3 and 4), labeled as Tcg1 and Tcg2, consists of moderately to well indurated claystone, siltstone, sandstone and conglomerate. According to Hughes (1997), the BCC “is a very poorly sorted, moderately cemented, heterolithic cobble conglomerate deposited in proximal and medial fan environments. The unit unconformably overlies Tertiary volcanic

rocks and older crystalline rocks.” It is interpreted to represent sequential debris flows (with occasional stream channels) into a periodically lacustrine/marine depositional basin. In the immediate area of the East Rainbow Pit, this package has a thickness of roughly 200 feet, with an average bedding attitude of N45E, 20 degrees SE. The

majority of the BCC consists of the larger size fractions, silty sandstone to pebble/cobble conglomerate, and displays graded bedding occasionally topping off with substantial thicknesses of claystone, up to 3 feet thick.

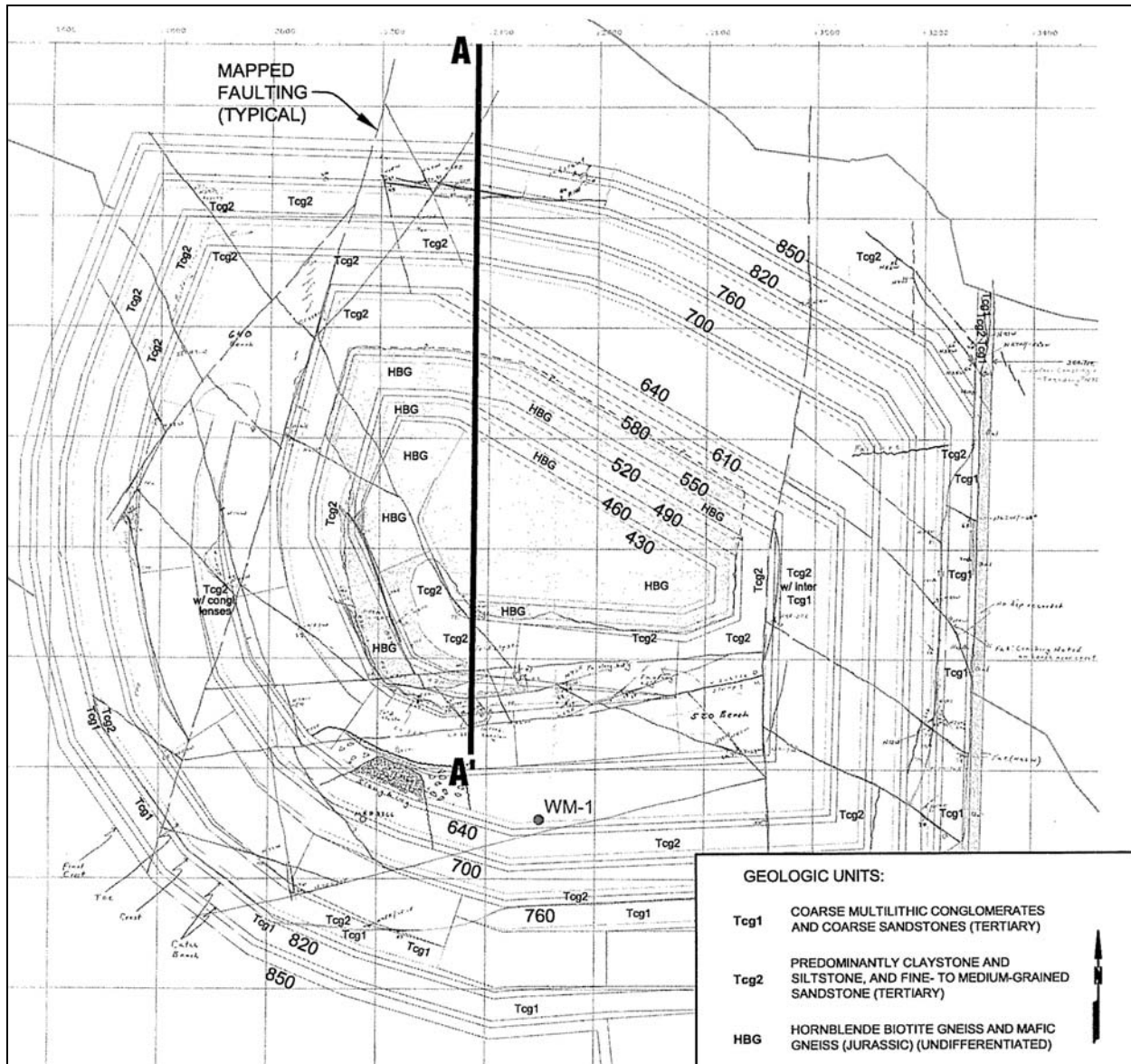


Figure 3. Geologic Mapping of the Faults and Cross-Section Location

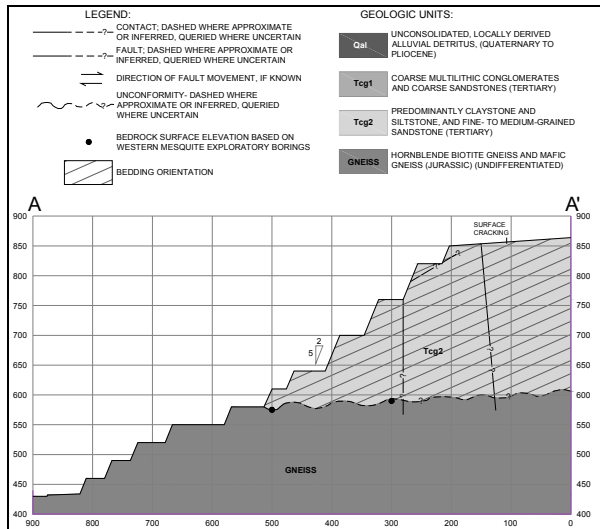


Figure 4. Representative Geologic Cross-Section

The Mine is contained within the San Andreas fault system. The Singer Fault, a parallel offset of the San Andreas, is the largest fault mapped at the Mine. There are two prominent fault trends that influence slope stability in the East Rainbow Pit vicinity. These are subvertical strike-slip faults that trend N45W and N10E. North-west trending faults are offset by the north-east trending faults. Southeastward movement along a normal-bedding fault, typically constrained to the claystone layers, has been identified in the BCC.

STRENGTH PARAMETERS AND SEISMIC COEFFICIENTS

Engineering Analytics was provided with historic geotechnical/mining reports addressing the stability of the pit walls. These reports contained the results of geotechnical strength testing, which were applied in the slope stability analyses. Past strength testing of samples collected at the mine site consisted of uniaxial compression

tests, Brazilian disk tension tests, density measurements, triaxial shear tests, and direct shear tests. The shear strength properties used in the past slope stability analyses were selected based on laboratory test results, review of previous investigations, observed performance in the existing pits, and typical values of similar materials. Shepherd Miller performed a stability analysis of the proposed pit in 1999 (SMI, 1999) and the cohesion values used for the conglomerate material were taken as half of the geotechnical laboratory test results to account for the bias of testing un-fractured samples. *“The strength properties for the HBG and MG were estimated from the rock mass descriptions from the two geotechnical core holes, the results of previous testing on intact core by Call and Nicholas, Inc. (1986) and the procedure for estimating strengths of jointed rock masses proposed by Hoek (1983). These shear strengths are consistent with the observation of numerous failures in the existing pits breaking back to a residual slope angles of 36 to 38 degrees.”* (SMI, 1999) The strength properties used in the past slope stability analyses are summarized in Table 1. The past shear strength testing focused on testing of the entire rock and soil mass and testing was not performed to determine the strength of the fault gouge and bedding that are encountered within in the walls of the pit.

Triaxial testing along with other geotechnical testing was completed on the collected samples. The samples selected for testing were air dry at the time of testing. This required the samples to be remolded prior to testing to replicate their in-situ conditions.

Table 1 Summary of Shear Strength and Material Properties Used for Slope Stability Analyses

Material Type	Unit Weight (pcf)	Peak Strength		Residual Strength	
		friction angle (degrees)	cohesion (psf)	friction angle (degrees)	cohesion (psf)
Conglomerate	125	29	4575	29	0
Hornblende Biotite Gneiss	160	37	0	37	0
Fault Gouge	150	32	0	32	0
Mafic Gneiss	160	37	0	37	0

Each sample was remolded to within 10 percent of its measured in-situ dry density, and to a water content of 17 percent based on the average water content of the triaxial samples tested in the SMI (1999) report. The samples were sheared in a staged consolidated un-drained triaxial test. A summary of the geotechnical laboratory testing results of the samples tested in triaxial tests is presented in Table 2.

SLOPE STABILITY ANALYSES

The geologic mapping along with the current and proposed pit design were provided to Engineering Analytics by the Mine and were used to develop geologic cross-sections used in the slope stability analyses. The locations of the cross-sections were selected based on past pit slope failures, the final proposed pit profile, and conversations with mine personnel. The apparent strike and dip of the identified faults and bedding were calculated and applied to the geologic cross sections. Based upon the cross-sections and observed failures within the pit, it was determined that bedding planes and faulting had a large effect on the pit wall stability. Therefore, stability analyses were performed by taking into account the reduced strength of the

bedding planes and faulting that was mapped in the pit walls. The past slope stability analyses that were reviewed analyzed the slope as a homogeneous material, thus not taking into account the effects of the highly fractured nature of the overburden material. Anisotropic strength parameters were applied to the soil and bedrock to model these conditions. Slope stability analyses were conducted using the Slope/W 2007 software from Geo-Slope International, Ltd.

The use of anisotropic strength parameters allow the user to define reduced (or increased) strength parameters within the analyzed cross-section at angles of known faulting and bedding without reducing the strength of the entire soil or rock mass. When a slice within the slip surface intercepts a specified fault or bedding plane, the frictional angle and cohesion at the base of that slice is reduced by a specified amount. By only reducing the strength parameters associated with the bedding planes and the faulting, steeper slopes of the pit walls can be maintained in areas not dominated by the faulting and bedding planes.

Table 2 Summary of Geotechnical Laboratory Testing Results

Sample Type and ID	Dry Density (pcf)	Atterberg Limits LL/PL/PI (%)	USCS Classification	Triaxial Test Results (Effective Stress)	
				Friction Angle (degrees)	Cohesion (psf)
Bucket of Clay	128.4	63/24/39	CH	3.9	2042
Bucket of Fault Gouge	122.3	89/63/26	MH	23.8	3245
Boring WM-1 Core at 277.5 ft	121.5	59/21/38	CH	9.3	1648
Boring WM-1 Core at 368 ft	114.3	105/36/69	CH	18.4	2989

Back-Calculation of Strength Parameters from Existing Slope Failure

Based on the Engineering Analytics site visits, the Shepherd Miller report (1999), the mapped geology, and the geotechnical laboratory results presented above, the slope stability at the location of cross-section A-A' (Figure 5) was analyzed using anisotropic properties to estimate the strength parameters of the faulting and bedding planes at the time of the May 2008 slope failure. Geologic mapping developed by the mine personnel was used to help develop the geologic cross-section (Figure 5) for slope of the north pit wall at the time of the May 2008 slope failure.

Engineering Analytics obtained topographic CAD files of the pit configuration from the Mine, which contained the pit slope at the time of the May 2008 failure. The pit slope along the north pit wall was 43 degrees. The cross-section shown in Figure 5 was analyzed using a friction angle of 29 degrees, cohesion of 4,575 psf, and a unit weight of 125 pcf for the conglomerate overburden (waste rock) material based on the SMI (1999) test data. The resulting friction angle and cohesion were varied within the bedding planes and faulting until a factor of safety of less than 1.0 was

achieved. A factor of safety of 1.0 is the minimum factor of safety at which a slope will remain stable. A tension crack was allowed to form at the slope crest and applied in the analyses. The tension crack used in the back-calculation was located approximately 100 feet from the crest of the slope. The location of the tension crack in the slope stability analysis of the failed slope was consistent with the location of the head scarp observed in the field.

The strength parameters were determined for the bedding planes and faulting in the conglomerate and the faulting planes in the gneiss by back calculation. A friction angle of 3.9 degrees was applied to the anisotropic strength function used for determining the strength of the bedding and faulting. A cohesion value of 2974 psf for the bedding planes and faulting was then back-calculated to achieve a factor of safety of 1.00 as shown in Figure 5. The strength parameters obtained from the slope stability analyses were verified with the additional triaxial testing of the fault gouge material. The results of the triaxial testing on material from the fault gouge and clay seams (Table 2) resulted in friction angles ranging from 3.9 degrees to 23.8 degrees. The reduced strength parameters were applied to the base of the failure surface slices that

were within plus or minus two degrees of the apparent dip of the mapped bedding planes and/or fractures or faults within the soil or rock.

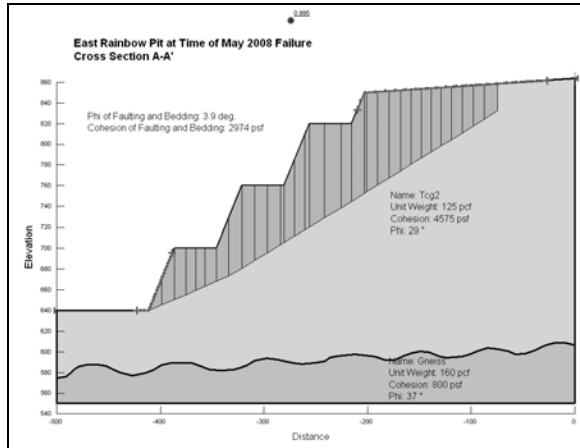


Figure 5. Back-Calculation of Strength Parameters

Strength Parameters and Seismic Coefficients

The slope stability analyses for the future slopes within the East Rainbow Pit used a friction angle of 29 degrees and a cohesion value of 4,575 psf for the conglomerate overburden and a friction angle of

37 degrees and a cohesion value of 800 psf for the gneiss. These values were obtained from the Shepherd Miller (1999) and Call and Nicholas, Inc. (1986) reports. The anisotropic analysis described in the previous section was also applied to the conglomerate and gneiss for the proposed mining slopes. For the purposes of the analyses, it was assumed that the faults mapped in the conglomerate extended down into the gneiss. The anisotropic parameters were applied in the gneiss along the fault locations at all of the cross-sections analyzed. However, the anisotropic properties for the bedding planes were only applied to the conglomerate material as the gneiss material is not bedded. The strength properties used in the analyses are summarized in Table 3. Slope/W (Geoslope, 2007) allows the user to apply a reduction or increase to the friction angle and/or the cohesion. For purposes of the analyses a reduction was applied to both the friction angle (ϕ) and a reduction/increase to the cohesion (c) for the bedding and faulting.

Table 3 Summary of Strength Parameters used for Analyses

Material Type	Unit Weight (pcf)	Peak Strength		Residual Strength	
		Friction Angle (degrees)	Cohesion (psf)	Friction Angle (degrees)	Cohesion (psf)
Waste Rock	125 ⁽¹⁾	29 ⁽¹⁾	0 ⁽¹⁾	29 ⁽¹⁾	0 ⁽¹⁾
Conglomerate	125 ⁽²⁾	29 ⁽²⁾	4,575 ⁽²⁾	29 ⁽²⁾	0 ⁽²⁾
Gneiss	160 ⁽²⁾	37 ⁽²⁾	800 ⁽³⁾	37 ⁽²⁾	0 ⁽²⁾
Faulting/Bedding	*	3.9 ⁽⁴⁾	2974 ⁽⁵⁾	3.9 ⁽⁴⁾	0 ⁽⁶⁾

* - The unit weight of the faulting and bedding is taken to be the same value as the surrounding soil/rock matrix.

1. Waste rock is generated from conglomerate overburden. The conglomerate friction angle was used, however the cohesion was assumed to be zero based on remolding of material.
2. SMI, 1999
3. Call and Nicholas, 1986. Based on plotting the Mohr circles for the mean value minus one standard deviation of the uniaxial compression tests and the Brazilian disk test results.
4. Based on the triaxial test results presented herein.
5. Based on the back-calculation presented herein.
6. Assumed residual value resulting from large deformation.

The seismic parameters used for the pseudostatic analyses were determined using EZ-Frisk, version 7.32 (Risk Engineering Inc., 2009). The peak ground acceleration for the operational life of the East Rainbow Pit and the long term stability of the east pit wall along Highway 78 were both analyzed. An earthquake with a 90-percent probability of non-exceedance in five years was chosen as the design earthquake for the operational period of the Pit. The horizontal pseudostatic coefficient associated with design earthquakes is commonly obtained by reducing the peak horizontal acceleration by 1/3 (Ploessel and Slosson, 1974). Table 4 summarizes the results of the seismic analyses.

Stability Analyses of Pit Slopes During Mining Operations

The mining plan for the East Rainbow Pit was divided into four phases. Each phase results in a larger pit either by deepening the bottom of the pit and/or expanding the crest of the pit. The May 2008 slope failure occurred on the north wall during Phase I of

mining. The result from the slope stability analyses of cross-section A-A during the Phase I mining was used to calibrate the strength parameters used for the bedding and fault gouge material. The results of the back-calculation of the strength parameters of the faults and bedding planes, discussed above, were used to analyze the stability of the other slopes in the pit.

The slopes were analyzed by applying anisotropic strength parameters to the faulting and bedding planes. The strike and dip of the faults and bedding planes were obtained from the geologic mapping completed by the Mine geologist as discussed in the Geology Section of this paper. A reduction in material strength was specified in the slope stability software (Geo Slope, 2007) at any portion of the slip plane that crossed the slope at an angle that fell within plus or minus two degrees of the apparent dip of a mapped fault or bedding plane. This resulted in a greater reduction in the factor of safety for slopes with more faulting in the direction of potential slope failure.

Table 4 Summary of Seismic Analyses Results

Scenario	Probability of Not Being Exceeded	Peak Ground Acceleration	2/3 of Peak Ground Acceleration Used for Pseudostatic Analyses
Operational Period of the East Rainbow Pit	90% in 5 years	0.08g	0.05g
Long Term Stability Involving Highway 78	90% in 50 years	0.20g	0.13g

The north (A-A), north-east (B-B), east (C-C) and south (D-D) pit slopes were analyzed for slope stability during Phases I, II and IV of the mining cycle of the pit. Phase I of mining occurred during the May 2008 slope failure. Phase II involved reducing the north slope from 43 degrees to 40 degrees after the May 2008 failure. Phase IV is the proposed final pit slope configuration. The slopes

from the Phase III development extended toward the west and were not analyzed as part of the scope of this paper. The slopes were analyzed using a tension crack along the crest. All of the cross-sections analyzed used the same strength values for the materials encountered in the pit, only the number of faults and apparent dip of the faults and bedding was changed in each

cross-section based on the geologic mapping. All of the cross-sections analyzed were based on the final proposed pit configuration for that phase of mining. The results for these analyses are summarized in Table 5. The effect of the faulting and bedding plane orientation on the stability of the slope allows for some slopes within the pit to be mined at a steeper angle and still maintain an adequate factor of safety.

CURRENT SLOPE BEHAVIOR

Optimizing the stability of the East Rainbow highwalls is crucial because mine revenue depends largely on the removal of the Rainbow deposit. There are four Rainbow mining phases; Rainbow I is completed, Rainbow II is in production and staged for completion September 2010, and Rainbow III will be completed August 2009. Rainbow IV will be mined from October 2009 through the fourth quarter of 2011.

Results from this investigation indicated that the north wall for the Rainbow pit phases

was too steep. The north highwall was initially set at 43 degrees above water table, 37 below, and was redesigned to 40 above and 37 below. The redesign was implemented after the completion of Phase I and resulted in approximately two million tons of additional waste to be removed from the north wall of the Rainbow Phase II.

Pit design alterations made as a result of the Rainbow I slope failure have thus far proved successful. There have been no new signs of activity along the north wall of the East Rainbow Pit. Mine engineers anticipate that the highwall slope changes contained in the Rainbow Phase II redesign should alleviate some of the geologic conditions that are favorable for debris slide type failures. There have been some ‘bench scale’ failures, but these failures have not been debris-slide failures, and have been contained on the slope benches. The crest of the north wall is inspected at least once a week for new tension crack development. Pit mapping continues to provide structural data that highlights potential problem areas.

Table 5 Summary of Stability Analyses Results of Pit Slopes During Mining Operations

Analysis Scenario	Factor of Safety	
	Static	Pseudostatic ($K_h=0.05g$)
Phase I		
Section A-A', North Pit Wall (43° conglomerate/30° gneiss) ¹	1.02	0.94
Section B-B', North-East Pit Wall (40° conglomerate/30° gneiss) ¹	1.54	1.41
Phase II		
Section A-A', North Pit Wall (40° conglomerate/30° gneiss) ¹	1.21	1.19
Phase IV		
Section A-A', North Pit Wall (40° conglomerate/30° gneiss) ¹	1.24	1.15
Section B-B', North-East Pit Wall (40° conglomerate/34° gneiss) ¹	1.26	1.16
Section C-C', East Pit Wall (43° conglomerate/40° gneiss) ¹	1.24	1.14
Section D-D', South Pit Wall (40° conglomerate/40° gneiss) ¹ Through the Waste Dump	1.50	1.35

1 – The angle listed is the angle of the current or proposed pit slope angle within each geologic unit.

Current Slope Monitoring Activities

The current monitoring plan includes the use of extensometers and observations of the high walls. The extensometers are connected to a light and siren system to alert the workers areas of excessive slope movement.

Mine personnel constructed five monitoring devices that were similar to “string potentiometers” across the top of the north face of the East Rainbow Pit. One end of the potentiometer was fixed to the ground near the top of the excavation or failed face, and a wire was run approximately 100 feet back to a switch. The tension was adjusted in the system such that if movement of the fixed end near the top of the slope exceeded one inch, then a switch would be triggered that would activate a warning siren and flashing light. Mine personnel currently conduct measurements of the difference between the rod attached to the wire and the pipe that housed the switch.

CONCLUSIONS AND LIMITATIONS

The use of anisotropic material properties in the slope stability analyses allowed the pit slopes to be optimized. As presented in Table 5, the east wall of the pit is able to be mined at a steeper angle (43 degrees) while maintaining a consistent factor of safety against slope failure with the north pit slope that is being mined at 40 degrees. The ability of the Mine to develop the east slope of the pit at a steeper angle than the other slopes allows the Mine to recover more ore. The east pit wall has minimum pit crest setback from the highway along the east side of the Mine property. Therefore, the crest of

the pit cannot be moved to the east without impacting the highway. The haul road is located on the south pit wall, therefore the slope of the southern wall was not increased as a result of the analyses.

Past analyses at the site relied on homogenous material properties within the pit material. The use of homogenous material properties results in all the slopes of the pit being cut at the same slope. This approach may result in an overly conservative slope in some cases and a less than desirable factor of safety in other cases. Both of these outcomes are not desirable and will result in higher production costs either from the unnecessary removal waste material or excessive slope failures.

The use of anisotropic material properties requires a good understanding of the geology of the material that is to be removed and additional testing of the strength parameters of the weak zones in the material profile. The results of the analyses indicate the need for detailed geologic mapping of the faults and bedding to refine the results of the slope stability analyses. Too often slope stability is thought of as a onetime analysis to be completed at the start of mining to determine acceptable pit slopes. The slope failure presented in this paper was dominated by faulting and bedding. The understanding of the dip and strike of the bedding and faulting can change as the mining progress through the pit. Therefore, the stability of the slopes should be reanalyzed as the actual geology in the pit is exposed. A proactive approach to slope stability will result in fewer pit failures, potential reduction in waste rock removal, and increased production.

REFERENCES

Call and Nicholas, Inc. 1986. *Mesquite Mine Pit Slope Design*. Dated January 1986.

GEO-SLOPE, 2007. *SLOPE/W Slope Stability Analysis Program – Version 7.11*. GEO-SLOPE International, Ltd., Calgary, Alberta, Canada.

Hughes, K.M., 1997, The Conglomerate of Bear Canyon (Miocene), Chocolate Mountains, Southeastern Calif. Published in Tertiary Stratigraphy of Highly Extended Terranes, California, Arizona, and Nevada.

Transportation Research Board, 1978. Landslides Analysis and Control, Special

Report 176 National Academy of Sciences, Washington, D.C.

Ploessel, M.R. and Slosson, J.E., 1974. *Repeatable High Ground Acceleration from Earthquakes*, California Geology, September issue.

Risk Engineering, Inc 2009. EZ-Frisk 7.32 Build 001. Boulder, Colorado, USA

Shepherd Miller, Incorporated. 1999. Geotechnical Stability Evaluation of the Rainbow Pit Extension Newmont's Mesquite Mine. Dated September 17, 1999.

A NEW DESIGN APPROACH FOR THICKENED TAILINGS SLOPES

D. G. Ritchie, A. Li & B. Fisseh

Golder Associates Ltd., Mississauga, Ontario, Canada

ABSTRACT: The trends in tailings management are to eliminate ponds on top of the tailings and to thicken tailings to increase the surface slope, conserve fresh water and simplify water management. Thickened tailings, with a consistency of a high density, non-segregating slurry or a paste can be transported by pipeline and deposited with a surface slope using relatively small containment dams at the toe. The deposited tailings slope can have significant bearing on project economics as steeper slopes often mean smaller dams. However, justification of the adopted design slope is an aspect that is highly scrutinized by stakeholders due to the potential for failures. Well documented methods exist to infer stability using cone penetration tests, for example, but it is difficult to infer stability before an actual deposit of tailings exists. The challenge lies in predicting the in situ properties of the deposited tailings before they are deposited.

This paper discusses an approach to predict the factor of safety against failure based on the predicted in situ void ratio (state) profile for various depositional slopes in both the short-term (i.e. during operations) and long-term (i.e. post-closure). Thin-layer deposition and drying are necessary to ensure the stability of these slopes, with consolidation adding further improvement. The approach is based on soil mechanics fundamentals and engineering judgment and allows evaluation of the sensitivity to operational variations (e.g. the rate of rise), climate and tailings characteristics.

INTRODUCTION

The growing trends in tailings management are to eliminate ponded water on top of tailings and to thicken tailings to conserve water and minimize the amount of water that has to be managed. There are various degrees of thickening ranging from a high density, non-segregating slurry, to a paste and even filtered tailings that can be used depending on the project drivers.

Thickened tailings, with a consistency of a high density, non-segregating slurry or a

paste can be deposited with a surface slope in thin layers using relatively small containment dams at the toe. Deposition in thin layers with adequate time for strength gain between lifts is required. But, by reducing the pond on top of tailings the consequences (risk) of a potential failure, whether triggered by dynamic (earthquake) or static (rapid rate of rise) forces are mitigated. Nonetheless, the perception of partial containment draws scrutiny from stakeholders. Failures and non-compliance can have serious adverse environmental

and social impacts that result in losses in production, reputation and investor confidence and a high cost of clean-up and remediation.

The challenge lies in predicting the in situ properties of the deposited tailings before the operation commences. Empirical relationships cannot be developed simply due to insufficient field data and limited case studies. Conventional slope stability approaches are not sufficient because they do not address the stability of tailings slopes at large strains.

The design problem therefore is to determine a stack (slope) geometry that will be stable under static and seismic conditions in both short and long term conditions. There is an economic driver to eliminate or minimize engineering and closure rehabilitation works to demonstrate long-term physical stability. The slopes that will be stable depends to a large extent on the properties of the paste or thickened tailings, the placement method and rate, and climate. The initial void ratio of a deposited thin layer before burial by the next lift is a key consideration.

Liquefaction and Tailings Slope Stability

The perceived risk with sloping tailings deposits is related to liquefaction. The basic problem in soil liquefaction is pore water pressures which are generated in soils during loading (which may be static or seismic loads). Positive pore pressures are generated in loose materials and these pore pressures reduce the strength of the soil. If the driving shear stresses are greater than this reduced strength, then large movements of the material occur, commonly known as flow liquefaction slides. In dense soils shear displacements that occur after the shaking lead to dilation and negative pore pressures, resulting in a strength increase and generally satisfactory behaviour. Cyclic mobility, with deformations only during the earthquake

shaking, results when the static shear stress is less than the shear strength of the liquefied tailings.

For existing facilities, in situ testing to determine the state of tailings is best carried out with the cone penetration test with pore pressure measurement (CPTu). Plewes et al. (1992) describe a CPT based screening procedure for evaluating liquefaction of materials such as tailings. (The distinction between tailings and clean sands is important, especially since much of the research on the CPT and liquefaction behaviour has been carried out for clean sands.) The approach is more fully developed by Jefferies & Been (2006) where critical state parameters are used to eliminate the need for corrections or adjustments for silty tailings.

The key point in the above discussion is that it is well documented that there are reliable and consistent approaches to determine in situ state of tailings materials based on the CPT and critical state testing.

Critical State Framework

The effect of density on soil behaviour is well captured by critical state soil mechanics (Schofield & Wroth 1968). The critical state line (CSL) is simply the void ratio at which shearing takes place continuously without volume change. This is to all intents and purposes the same as the steady state line first identified by Castro (1969) and the critical void ratio of Casagrande (1936). Figure 1 illustrates the basic concepts. A void ratio – effective stress plot such as Figure 1 is called a state diagram as it describes the “state” of a soil (just like pressure, volume and temperature describe the state of a gas). Soils above the CSL are “looser” than critical, while those below are “denser” than critical. State or density is quantified by the parameter ψ which measures the distance

from the CSL (Been & Jefferies 1985). Many current soil constitutive models use ψ as the state variable which most influences the soil behaviour (Jefferies 1993; Jefferies & Been 2006).

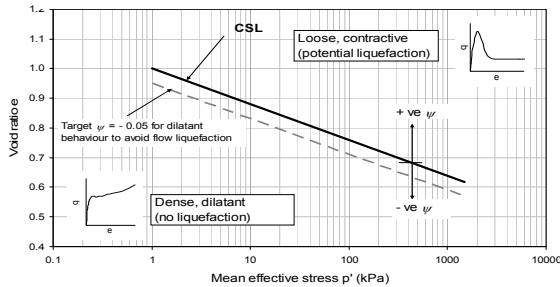
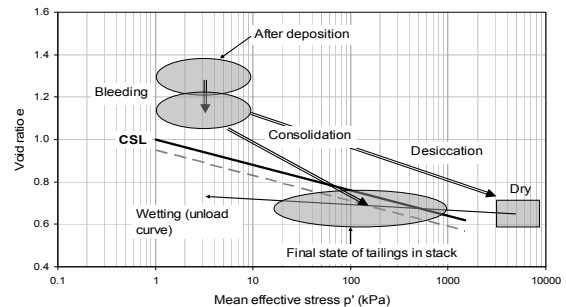


Figure 1. State diagram for cohesionless soils

Without going in to the detail of observed soil behaviour as a function of the state parameter, ψ which can be found in Jefferies & Been (2006), a good rule of thumb is that a soil needs to be denser than about $\psi = -0.08$ for liquefaction to be a non-issue in clean sands. For siltier, more compressible, materials such as most paste or thickened tailings this value can be increased, and it is shown as a broken line at $\psi = -0.05$ on Figure 1. Tailings denser materials than $\psi = -0.05$ tend to dilate on shearing and therefore flow slides and catastrophic failures are unlikely.

Paste or thickened tailings are designed to be pumped and deposited with minimal water loss after deposition. Therefore, by definition, deposited tailings are at or above the critical or steady state at the time of deposition. After deposition there might be some bleeding of excess water from the paste, desiccation by surface drying and consolidation under loading by deposition of additional tailings layers. The effect of these processes on the state of the deposited tailings is illustrated on Figure 2 which is a state diagram exactly like Figure 1 for a hypothetical tailings. After deposition in layers of about 0.5m the material will be at a void ratio of about 1.3 and a mean stress of

less than 10 kPa, illustrated by the shaded oval on Figure 2. Bleeding of water may reduce the void ratio somewhat. However, the state will then change, illustrated by two paths on Figure 2. One path shows desiccation where matric suctions give a the relatively high mean effective stress and void ratios close to the shrinkage limit, followed by wetting as more material is deposited over the desiccated layers. This path is as might occur in a dry, hot climate. However, for high production rate operations or those in wetter climates a second path involving simple loading by additional deposition without desiccation is more likely. Whichever path is followed, the bottom line is that the mechanics of consolidation of paste tailings is such that the final state of the material is typically going to be close to the critical state line, and at least above the $\psi = -0.05$ state for which dilation is likely to prevent flow



slides.

Figure 2. State Change After Deposition

Accepting that for high production or wet climate operations, paste or thickened tailings, without additional improvement, will be at states close to critical, it is almost inevitable that pore pressures will be generated during strong seismic loading and that the tailings will liquefy. No amount of cyclic testing and analysis is likely to prove otherwise, with any degree of certainty. This substantially simplifies the engineering problem for paste or thickened tailings and means that static and

cyclic liquefaction are dealt with similarly. It is the residual undrained strength after liquefaction that matters, and this residual strength should be used in stability analyses. The design of tailings slopes considering liquefaction and residual strength was presented in Been & Ritchie (2008) and Li et al. (2009).

Residual Strength of Tailings

Considering the residual strength is similar to the approach proposed by Poulos, Castro & France (1985) but must not be confused with that approach. Poulos et al asserted that the steady state line provides the assured (minimum) residual undrained shear strength but this appeared to be at odds with case histories, documented first by Seed (1987) and subsequently by others such as Stark & Mesri (1992) and Olson & Stark (2002). The residual strength that has been observed in the field is not the steady (or critical state) strength, because the constant volume condition assumed by Poulos et al does not hold at the field scale due to shear localization (Jefferies & Been 2006).

Figure 3 illustrates the difference between approaches, where the residual undrained strength from case histories is plotted against a cone penetration resistance. (In this case the cone penetration resistance is a surrogate for material density or state, as that is what can be measured in the field). Also shown on Figure 3 is the critical state strength, assuming undrained shearing, corresponding to the given penetration resistance. For very loose materials there is a good correspondence between the case histories and the critical state, but for slightly more dense materials the critical state strength increases rapidly, a trend not observed in the case histories.

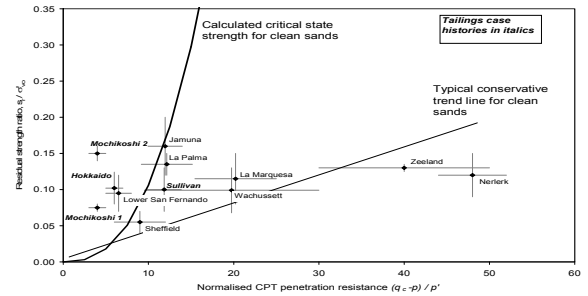


Figure 3. Residual strength from liquefaction case histories and critical state strength (Been & Ritchie 2008)

The mechanics of residual strength is explored in some detail in Jefferies & Been (2006), where a critical state constitutive model, NorSand, is used to determine undrained behaviour of loose sands.

Figure 4 provides a design curve of residual strength as a function of tailings state provided that the appropriate curve is developed for the tailings material in question. This requires a program of laboratory testing consisting of index and classification tests, undrained and drained triaxial tests to determine the critical state line (about 10 are required) and additional drained triaxial tests to determine stress-dilatancy parameters (about 5 are required).

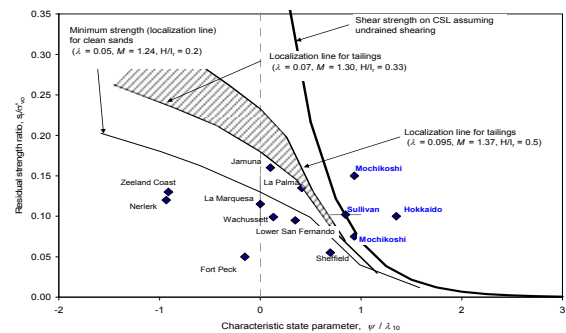


Figure 4. Residual strength as a function of *in situ* state parameter (Been & Ritchie 2008)

The residual strength of the liquefied sands shown on Figure 4 can be described by Equation 1 proposed by Jefferies & Been (2006):

$$\frac{s_r}{\sigma'_m} = \frac{M}{2} \exp\left(-\frac{\psi}{\lambda}\right) \quad (1)$$

where s_r is the residual strength, M is the critical friction ratio and λ the critical state line slope.

The predicted values from Equation 1 agree reasonably well with mobilized shear strength from the case history data for positive values of ψ (Jefferies & Been 2006).

The Design Challenge

However, to establish a design, it is also necessary to know the in situ state of tailings which cannot be determined in the laboratory. The only reliable method to determine in situ state is to measure it in the field for the actual operational conditions and tailings material. Clearly this can only be done once the tailings disposal facility is operational. Design predictions therefore have to be made based on experience with previous, similar, tailings deposits. Currently, this database for paste tailings is relatively sparse, but growth of the database could be greatly enhanced if consistent and uniform procedures were used to measure in situ state, and if operators shared or published such information freely.

The design problem for paste or thickened tailings slopes can now be condensed to two key questions:

- What is the in situ state of the tailings?
- What is the residual post liquefaction strength of tailings?

The first question is needed to answer the second as strength depends on the in situ state. The answers allow the designer to evaluate stability of an existing slope or selecting a design slope.

AN INTEGRATED DESIGN APPROACH

The key objective of a tailings deposition plan is to ensure that the tailings are deposited such that they are stable in both the short and long-term conditions. The deposited void ratio is considered the main indicator for achieving stability. Li et al. (2009) presented a tool to establish design slopes for sloping thickened tailings deposits and carry out sensitivity analyses for different operational conditions, such as the rate of rise, and tailings consolidation characteristics. Assuming that laboratory testing has been carried out to determine the residual strength curve on Figure 4 for a particular tailings, the challenge for design is to predict the in situ state, or the value of ψ / λ , so that the appropriate residual strength can be estimated. A key assumption required is the initial void ratio attained before burial of a layer by subsequent tailings (Li et al. 2009).

The current paper follows the same method but expands the discussion on the initial void ratio. This integrated approach is suitable for optimizing tailings deposition strategies. Non-segregating tailings and thin layer deposition are required.

Provided suitable engineering judgment is exercised the integrated method is considered reasonably conservative. An attractive feature of the method is that deviations from the design assumptions should be evident soon after deposition commences. This early indication of a

departure from the design assumptions allows the operator to time to implement mitigation measures before problems arise.

The method involves:

1. Laboratory testing – to establish the initial void ratio, consolidation characteristics and critical state line;
2. Consolidation modeling – to establish void ratio and the state parameter profiles;
3. Stability evaluation – for infinite slope / wedge failures using the residual strengths determined using Equation 1. (The residual strength varies with depth).

Operational Parameters

The primary operating parameters that dictate the size and slopes on a tailings deposit are the ore tonnage and production rate. For a given tailings basin, a higher production rate implies a faster rate of rise. The tailings discharge elevation will progressively rise as the basin fills, with a corresponding increase in the tailings surface area. The ability to place thin layers and achieve the required drying should become easier as the tailings surface rises and the available surface area increases, provided the tailings can be spread evenly. Multiple spigot panels spread around the facility are a way to increase flexibility. Operator controls on the attained density of the tailings are limited but include the lift thickness and discharge energy/velocity which are related to the number of operating spigots. At the design stage the variability in the operating data must be considered.

Operating parameters that can vary through the life of the mine that must be considered at the design stage include:

- ore type and throughput;
- thickened tailings yield stress – which affects deposition slope and flow distance;
- discharge slurry density – the quantity of water in the discharges tailings affects drying; and
- tailings gradation and hydraulic characteristics – which may vary by ore type.

The Influence of Climate

Drying of each freshly deposited lift is a key factor. The void ratio attained before burial relates to how much water can drain into the previous (underlying) layer or get removed by evaporation.

The key climate factors include temperature, precipitation, solar radiation, relative humidity, and wind speed. Average values are important but the range and seasonal variability should be understood. In particular the distribution of precipitation is important. Both the number of days with rain and duration of the events are factors that influence drying.

One or more weather stations located close to the tailings facility are recommended depending on the how important the variables are to the predicted results.

For a given climatic condition and rate of rise, laboratory drying tests, precedent data or soil-atmosphere boundary modelling can be used to establish the required number of the days for drying before placement of another tailings layer for tailings deposition for a given slope. During the early years of an operation, in-

situ testing and tailings characterization can be carried out to confirm the initial void ratio of the tailings before the tailings are buried due to deposition. Therefore, the operation can be optimized to achieve the requirements.

CASE EXAMPLES

Two large high-production copper operations have been selected for illustration of the method. Both involve down-valley sloping

tailings contained at the toe by rockfill dams. The tailings level rises throughout the facility operation.

Table 1 presents a comparison of the tailings characteristics, slurry density in the pipeline (degree of thickening) and deposited condition inferred through settling tests. The tailings have similar maximum and d_{60} sizes and are well graded (Figure 5) but Tailings 2 has slightly high coefficient of uniformity and a higher air-entry value as shown on Figure 6.

Table 1. Material Characteristics

	Project 1	Project 2
Gradation and particle density		
D ₁₀ size	0.003 mm	0.002 mm
D ₆₀ size	0.075 mm	0.08 mm
Coefficient of Uniformity	27	4
Clay sized fraction (%)	9	9
Specific gravity of particles (Gs)	3.0	2.8
Hydraulic Properties		
Air-entry value (kPa)	10 kPa	50 kPa
Saturated hydraulic conductivity	2.1×10^{-5} cm/s	5.0×10^{-5} cm/s
Drained column settling test results		
Water content (mass water / mass solids)	27.6%	24.6 % (assumed)
Void ratio after bleeding and settlement	0.85	0.83 (assumed)

Table 2 provides a comparison of the projects. Each involves very large tailings volumes and rates of rise in the order of several to tens of metres per year depending

on the period. The average rate of rise, the key input parameter in the Li et al. (2009) method, varies between 6 m and 15 m for the cases examined

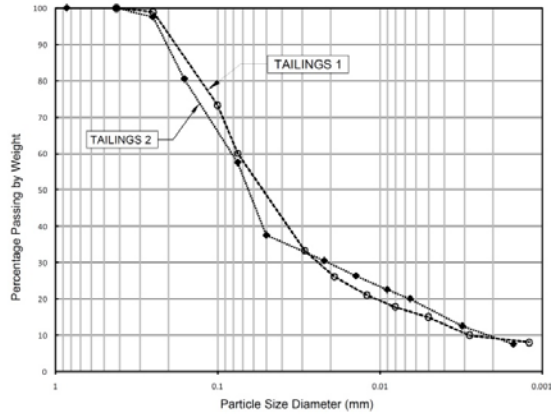


Figure 5. Tailings gradations

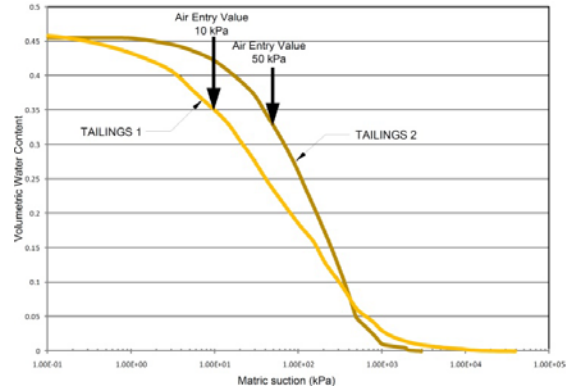


Figure 6. Soil-water characteristics

Table 2. Consolidation and stability analyses

Case	Tailings consistency in pipeline			Initial void ratio	Rate of rise (m/year)	Design slope for minimum FOS=1	Total height (m)	Time (yrs)
	Slurry density	Void ratio	Moisture content					
Project 1	69% solids	1.22	43.5%	0.74	8.3	5.0%	230	End of mine life (28 years)
				0.80	8.3	1.5%	230	End of mine life (28 years)
				0.74	6.0	8.0%	230	10 years post-closure
				0.80	15.0	0.9%	230	Mid life (15 years)
Project 2	65% solids	1.12	40.0%	0.74	7.5	2.5%	113	Mid life (15 years)
				0.74	4.0	6.0%	113	End of mine life (28 years)

Notes: Slurry density = solids mass / total mass
 Moisture content = mass of water / mass of solids

Initial Void Ratio Predictions

The initial void ratio of each tailings fresh tailings layer depends on many factors including the climatic condition, rate of rise, deposition methods and layer thickness. Despite the value achieved, thin layer deposition is essential.

Figure 7 shows a drained column test which is useful for estimating the deposited void ratio upon discharge on a subaerial beach. Alternatively a reasonably undisturbed sample could be taken from a flume test or other deposition trial.

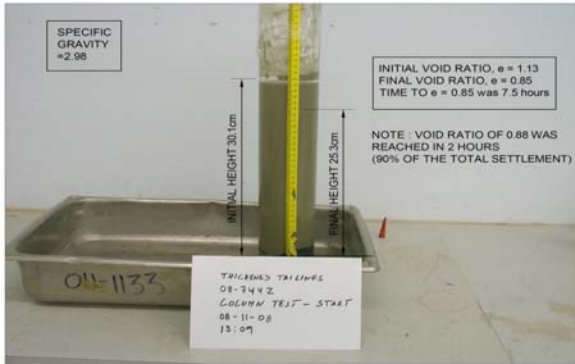


Figure 7. Drained settling test Design Slope Predictions

A limit equilibrium method for an infinite failure mechanism can be adopted considering the length of the tailings slope in analyzing the stability of the tailings stack. Since the residual strength of the tailings is a function of state that varies with depth the factor of safety profile will also change with depth and time. The factor of safety profile can be calculated for the infinite slope using the method by Li et al. (2009).

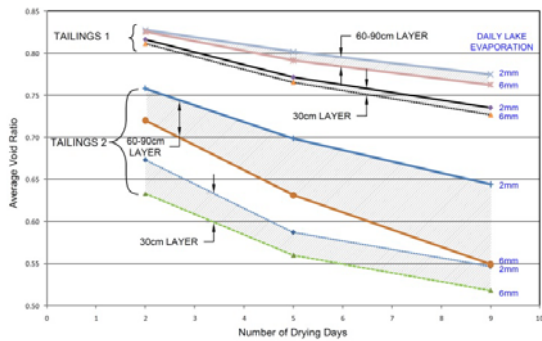


Figure 8. Comparison of initial void ratio vs. drying time

Figure 9 shows void ratio profiles calculated for the end of deposition and at 100% consolidation assuming a constant rate of rise and upward (one-way) drainage which introduces a degree of conservatism into the calculations. The state parameter and strength ratio variations with depth are also shown on Figure 9.

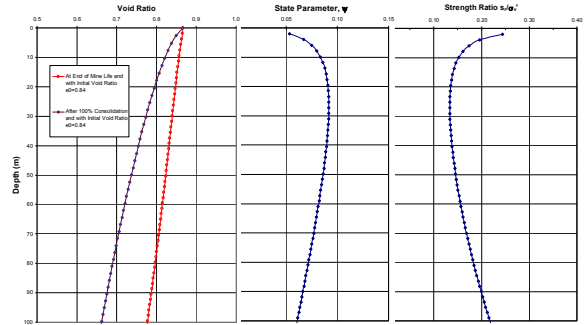


Figure 9. Typical void ratio, state parameter and strength ratio

Sensitivity studies can be carried out for different depositional slope angle and different operation conditions. Figure 10 shows results of a parametric evaluation to demonstrate the importance of the initial void ratio. Two deposition conditions are shown:

- Deposition Condition 1: Through thin layer deposition and desiccation, the initial conditions of the freshly deposited tailings should achieve an initial void ratio of 0.76 before the tailings is buried by next layer of the deposition to ensure the factor of safety is greater than 1.0 for a 5% slope at the end of mine life (solid squares on Figure 10).

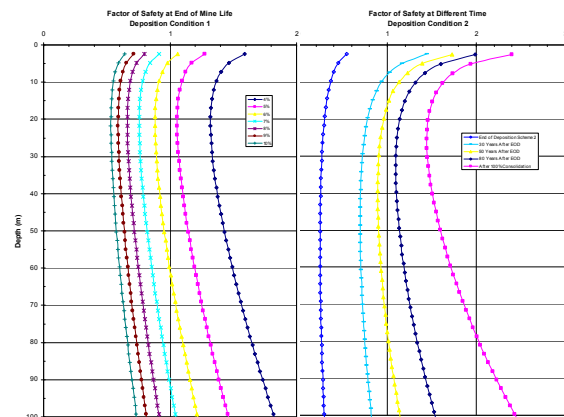


Figure 10. Calculated factor of safety sensitivity

- Deposition Condition 2. This represents the tailings deposition only achieves an initial void ratio of 0.84 and the calculated factor of safety for the 5% slope is lower than 1 during deposition. However, it increases to greater than 1.0 about 80 years after the deposition due to consolidation.

Comparison of the Two Examples

Table 2 compares the initial void ratio, rate of rise and consolidation parameters for the two tailings examples and the implication on the design slope adopted. The design slope is taken as the steepest slope with at minimum factor of safety of 1.0. The data for Project 1 data shows the effect of time. For example, with an initial void ratio of 0.74 a design slope of 5 % has a factor of safety of 1.0 at the end of mine life. Due to consolidation, at 10 years post-closure an 8 % slope would have a factor of safety of 1.0.

The results of the comparative study are presented together on Figure 11 which shows steeper design slopes are possible for lower initial void ratio ratios or tailings with a higher consolidation coefficient.

The findings on Figure 11 clearly indicate where the focus should be for the designer. The ore and tailings production schedule and rate are normally governed by the economics of mining and milling. In some cases tailings disposal costs may play a significant role in developing the mine plan. More likely, it is simply the duty of the tailings designer to determine the optimal tailings disposal cost and risk profile - the primary tool being the tailings deposition plan. By optimizing cycling of the discharge locations (spigots) and lift thickness, the drying can be enhanced such that the initial void ratio is minimized allowing the steepest safe slopes. Other possibilities include the use of chemical admixtures to increase drainage or energy at the surface of the tailings to increase the

density (or lower the initial void ratio) of the deposited tailings.

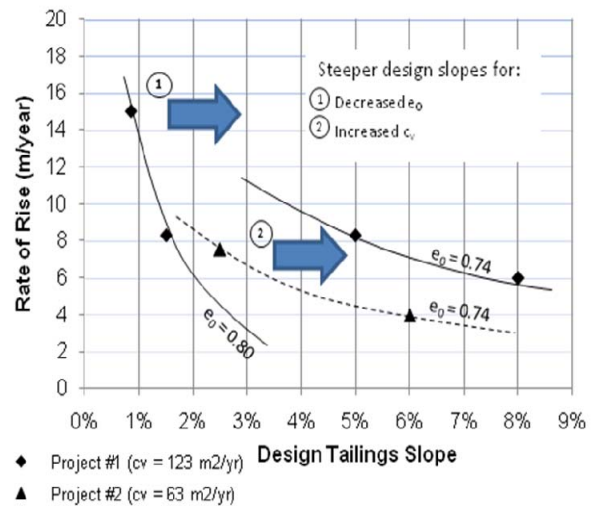


Figure 11. Design slope vs. rate of rise

SUMMARY

An integrated tailings management planning tool has been presented for design of large (high production rate) non-segregating (thickened) tailings slopes. The method provides a justification for maximizing deposited tailings slopes at the design stage while still providing a margin of safety against flow slides due to liquefaction. Deformations during strong earthquake shaking (cyclic mobility) may still occur. The key factors that affect the design slope are the rate of rise and influence of climatic drying, which is in turn related to the tailings characteristics and deposition plan. Non-segregating tailings deposited in thin layers are necessary. Along with engineering judgement, the method is suitable for both wet and dry climates.

REFERENCES

- Been, K. & Jefferies, M.G. 1985. A state parameter for sands. *Géotechnique* 35(2): 99-112.
- Been, K. & Ritchie, D.G. 2008. Designing Mine Tailings Disposal for Liquefaction. *Proceedings of the 4th International Conference on Mining & Industrial Waste Management, 11-12 March 2008*. South Africa.
- Cassagrande, A. 1936. Characteristics of cohesionless soils affecting the stability of earth fills. *Journal of Boston Society of Geotechnical Engineers* 23: 257-276.
- Castro, G. 1969. Liquefaction of sands. Ph.D. Thesis. (*Harvard Soil Mechanics Series 81*). Harvard University: Cambridge, Mass.
- Fisseha, B., Bryon, R. & Simms, P. 2008. Unsaturated flow and evaporation in multilayer deposits of gold paste tailings. *61st Canadian Geotechnical Conference*: 818-823. Edmonton, Alberta, Canada.
- Jefferies, M.G. 1993. NorSand: A simple critical state model for sand. *Géotechnique* 43: 91-103.
- Jefferies, M.G. & Been, K. 2006. *Soil liquefaction, a critical state approach*. Taylor and Francis, London UK.
- Li, A., Ritchie, D., Been K. & Welch, D. 2009. Paste 2009 - *Proceedings of the 12th International Seminar on Paste and Thickened Tailings, 21-24 April, 2009*. Vina Del Mar, Chile. Editors: R. Jewell, A. Fourie, S. Barrera & J. Wiertz.
- Olson, S.M. & Stark, T.D. 2002. Liquefied strength ratio from liquefaction flow failure case histories. *Canadian Geotechnical Journal* 39: 629-647.
- Plewes H.D., Davies M.P., & Jefferies M.G. (1992). *CPT based screening procedure for evaluating liquefaction susceptibility*. *Proc 45th Canadian Geotechnical Conference*, Toronto.
- Poulos, S.J., Castro, G. & France, J.W. 1985. Liquefaction evaluation procedure. *Journal of Geotechnical Engineering Division ASCE* 111 (GT6): 772-792.
- SVFLUX 2006. SVOoffice 2006™ *Geotechnical Modeling Software Suite*, Version J. 62.20, SoilVision Systems Ltd., Saskatoon, SK, Canada.
- Seed, H.B. 1987. Design problems in soil liquefaction. *Journal of Geotechnical Engineering, ASCE* 113 (GT8): 827-845.
- Stark, T.D. & Mesri, G.M. 1992. Undrained shear strength of liquefied sands for stability analyses. *Journal of Geotechnical Engineering ASCE* 118 (GT11): 1727-1747.

REVISIT TO OLD SOUTH AFRICAN SLIMES DAMS & WHERE WE ARE TODAY

Jack Caldwell

Robertson GeoConsultants, Vancouver BC

Gordon McPhail

Metago Environmental Engineers (Australia) Pty Ltd, Perth

ABSTRACT: In the 1970's the authors designed and built slimes dams, now called variously tailings impoundments or tailings storage facilities, in South Africa. We have also designed and overseen construction of tailings impoundments in North American and Australia. In this paper, we look back at the design and construction of some of those old slimes dams and the new tailings facilities we are involved with. We use this historical review to focus on the changing perspectives of the impact of water on the design, operation, and closure of tailings facilities. We describe the technical approaches that guided our design to highlight how in the 1960s drains were introduced by Professor Jennings to deal with the water that bedevilled every slimes dam. We describe how design approaches evolved to better deal with the water and the extent to which these have been successful. Hence we proceed to reflect on how the past has brought us to the present when there are multiple opportunities to avoid the issues of the past, design impoundments for closure, incorporate the essentials of sustainable development, save precious water, and create tailings storage structures that are more stable.

THE BAFOKENG SLIMES DAM IMPOUNDMENT SITE

Our careers as geotechnical engineers designing tailings impoundments begun with the failure of the Bafokeng slimes dam at the Impala Platinum mine in the Bushveld of South Africa in the early 1970s. The side of the slimes dam gave way; the tailings and water in the pool on top of the dam flowed out; thirteen people in a nearby shaft were killed as the slimes rushed down the shaft; the slimes flowed nearly 50 miles downstream to fill the local water reservoir.

First Professor Jennings got us involved in collecting data to evaluate the failure. Oskar Steffen got us involved in designing a new slimes dam to replace the one that failed.

Many technical papers have been written explaining the reasons for the failure. Most people disagree with each other why the dam failed. Some say there was piping of water through the coarse tailings sandwiched between layers of fine tailings. Some say it was static liquefaction of overstressed sandy tailings.

As designers of the new impoundment we had to have a theory of failure in order to design a new slimes dam that precluded repeat of the failure of the old. Without striving to add to the debate over the causes of failure, we still adhere to this simple cause as propounded to us by those who were working on the dam the day it failed: The mine, like all mines in the area, was perpetually short of water, so they stored as much water as possible on the top of the impoundment.

The day of the failure, the pool was very close to and some say lapping up against the outer dike thrown up to make a place for the discharge pipes and the next lift of tailings discharge. Then it rained. The bulldozer driver was sent to shore up a vulnerable-looking part of the outer dike. Who knows: maybe he vibrated the wet tailings and they liquefied; maybe he dug too deep or too inexpertly with his bucket as he struggled in the rain to do something unfamiliar and he just took away the freeboard; maybe some profound geotechnical occurrence happened deep in the tailings. Regardless, the water and liquid tailings flowed out, flowed far, and killed miners.

We walked around and climbed around that failure zone measuring the thickness of the layers of fine tailings and coarse tailings. We measured the size of the breach and estimated the volume that flowed out. We took samples all the way down the debris flow trail. The lawyers fought and the words flourished. But we noticed a funny thing: nowhere in the area was there a platinum slimes dam over about 30 m high. One operator said to us: "At that height, they just don't work good any more. They are more trouble than they are worth—so build a new one".

And we noticed that there were no drains in the old ones that failed: the entire outer zone exposed by the failure was wet—or at least

very moist in the soil classification system we knew and used.

OTHER PLATINUM SLIMES DAM

Before we proceed to describe the new slimes dam we designed to replace the one that failed, let us record some observations at a few other platinum slimes dams we worked on. We honestly cannot recall their names or who owned them, so we simply refer to them as Dam A and Dam B.

The owners of Dam A called us in one day and told us he was worried about the stability of his slimes dam: it was approaching 30-m height and there were reports from the operators of cracks near the crest. We went to site, installed piezometers, and urged the mine to keep the pool of water far back from the crest. One late Friday, we received the first piezometer readings. It was obvious they were too high for safety, so we put a late call through and made an appointment to be on site the next Monday. Recall how difficult it was to get a telephone call through on a Friday afternoon in South Africa in those days---we had done our best.

On Monday morning we arrived on site early. Too early for our appointment with the mine, so we took a quick drive around to the slimes dam. To our horror, as we turned the corner all we could see was a classic slope failure. The slope had failed on Sunday evening. Lucky the pool was far back and only the dry tailings had slide out on the weak, black clay that is so universal a feature of the area and the foundation of most of the dams in the area. We knew that its peak shear strength is about ten degrees—just perfect for a basal failure when the tailings are about 30-m high and wet. The dam was abandoned and not used again to our knowledge.

Dam B happened to be close to a weekend cottage we used regularly. We were

entertaining a visiting American tailings engineer and had arranged to take him over the weekend to see this closest local platinum slimes dam before returning to Johannesburg where he was scheduled to give a talk to the Society of Civil Engineers. Sunday afternoon I drove the American to see the slimes dam. I had on route told him of Dam A and how the black clay was prone to foundation and basal failure. To my horror and amazement, as we rounded the corner of the dam, we saw a huge earthmoving operation in progress. Apparently some tailings supervisor and his buddy, having heard of Dam A, had decided to keep themselves and their buddies busy that weekend excavating all the black clay at the toe of Dam B and to replace the clay with rock from the mine's waste rock dump. There before our eyes was a 1,000-ft long trench where the foundation clay had been removed along the toe of the slimes dam's outer slope.

Replacing the weak clay with strong rock is a good idea; removing what little toe support the clay offered is an extremely bad idea. I finally located my engineering contact playing cricket; I dragged him under protest off the field; and drove him to the dam to countermand the supervisor's ill-considered actions. The dam was still in operation last I checked. But I still wonder if the Bafokeng failure was not just a basal or foundation sliding event; the clays at all three sites are identical.

THE NEW BAFOKENG DAM

We clambered into the back of a backie, or pick-up truck in North American terminology. And we set off to drive the eleven miles of the perimeter of the area designated back in the office for the new Bafokeng slimes dam. There really was nothing to see: the ground rose slightly to the

north east, but was otherwise without topographic expression.

The same black clay covered it all. I am told the clay is the result of weathering of the underlying norite in which the platinum occurs. Some say it has taken since the beginning of the Cambrian for the 1-m thick layer of clay to develop. Its Plasticity Index (PI) is well over 80, so in the winter it dries and shrinks and large tension crack develop almost to the bottom of the layer. With summer, the rains come. The clays wet up and swell; the cracks close and the surface heaves. Put a pipe or the foundation for a fence post in the clay, and two or three years later the clay turn-over will have pushed the pipe and footing to the surface.

It was a simple matter to establish the low strength of the clay. It was all residual: in effective stresses we used zero cohesion and ten degrees friction. It was an equally simple matter to calculate the factor of safety of a sand embankment on this clay. We had Dam A to validate our calculations. It was easy to show that at a height of 30 m with any appreciable water table, such a slope is not stable.

The problem with the new site, however, was that at a maximum height of 30 m, we could use only a small part of the site. The difference in elevation across the site was almost 30 m. We had to do something different while sticking to the tried and trusted.

The solution lay in two tricks:

- A series of 30-m high impoundments along the downgradient perimeter of the site, essentially forming a berm for the inner, or main part of the dam.
- Lots and lots of drains to control the phreatic line or water table in the slimes.

In those days, the start of a new slimes dam was a simple earth dike pushed up to about 1 to 2 m high. From this the tailings were discharged. This usually meant the tailings had to go uphill---which of course they preferred not to do. They hung around the starter dike and the fines settled out in layers to form low permeability layers of weak material. Trouble is those low permeability layers settled out on top of any drains placed at ground level and promptly blinded them.

Our solution was joked about and we were teased---but the approach worked. This is what we did: place a series of outlet pipes in trenches going from well inside the new dam to the exterior perimeter; lay a gravel drain on the ground; proceed with initial slimes deposition, which of course pretty much blinded the initial gravel layer. But we persisted thus: continue to deposit the slimes until a sufficient beach had built up and the fines were pushed by natural flow back into the dam and were no longer settling near the outer dike. At that point go in and lay another gravel drain and connect it to the underlying drains with a series of what we called chimney drains.

This detail did the trick. We installed piezometers, the old fashioned open standpipe type, and found no significant water table or phreatic line. Occasionally the outlet pipes would gum up with a biological precipitate which was readily removed with a high pressure water hose. To our knowledge the systems are still operating.

KIMBERLITE TAILINGS DAM FAILURE

Construction of the new Bafokeng impoundment was underway, and we were sent to Kimberly to consult on a new slimes dam for the Big Hole or thereabouts. For as long as anybody could recall, the slimes had

been discharge from a single point and allowed to flow wherever it wished. And this it did; it had flowed miles over the gently sloping ground. Because it showed no intention of stopping, understandably, many years before some enterprising slimes-man had pushed up a long one to two meter high dike along the perimeter to catch the stuff.

But even that was now in danger of being overtopped. The mine had decided they needed a new slimes dam. The obvious place was on top of the old one; preferably near the discharge point where in theory the slimes should have been coarser. But this is a diamond tailings—it is not coarse in any part of the gradation curve. The sun had, however, beaten down for years and years and dried out the tailings, forming a reasonable foundation.

We designed something with drains and pool control and all the bright new ideas we were flush with from the Transvaal. But the miners would have none of these new-found ideas from the liberal north. *No Drains—We Will Control The Water* was their mantra. It took only one lunch at the Kimberly Club to persuade us to acquiesce.

The dam was built and operated for a few years. But the inevitable occurred: the miners lost control of the pool which came too close to the edge and it all failed. No real environmental harm and the materials running out of the breach simply continued on down and over the old tailings deposited for decades in an uncontrolled way. The replacement dam included drains.

This case history along with the story of the Bafokeng dams reinforced the need to provide drains, control seepage within the tailings outer slopes and limit the quantity of water on the top of the impoundments. None of these lessons learnt fully entered the system and some years later, after we had

both left South Africa, the slimes dam at Merriespruit failed for much the same reasons as had caused the failure of the dams we described here. .

Other tailings dams have continued to fail world-wide with alarming regularity for the same reasons as those early South African dam failures.

MT TOLMAN, GREENS CREEK, AND CANNON MINE

One of us moved to the United States. There we faced demands for far higher tailings impoundments in far less hospitable climates than in South Africa. The first dam we designed was for a proposed molybdenum mine called Mount Tollman in northeast Washington State. The mine never got off the ground and our design was never built. Yet for this tailings facility we designed and had approved by the regulators a 300-m high embankment, the lower 100 m of which would have been rockfill and the upper 200 m of which would have been tailings cyclone underflow placed and compacted into paddocks.

Then to Alaska and Greens Creek on Admiralty Island just off the coast of Juneau. Here is perpetual rain. We could find no way to control the excess water. The obvious solution was to dewater the tailings, add a little cement, and place as a dry pile. This is still being done today.

Finally to Wenatchee, Washington where we designed and spent two years on site overseeing construction of the Cannon Mine tailings impoundment. We write of this facility in a separate paper in these proceedings, but for the purposes of this paper, note that we chose a compacted rockfill berm with low permeability core and adjacent filters. All the details you would

expect for a facility directly above the town and built on foundation bedrock much the same as those at the Teton dam that had failed some years before as a result of uncontrolled seepage and hence piping through the friable sandstones of the foundations.

By now we had grown so conservative about water control and tailings encapsulation that we got the job of managing engineering design of the closure works for the uranium piles of the Uranium Mill Tailings Remedial Action Project. We have written extensively about the engineering details of that project and in this conference take a look back at how these piles have performed in the nearly twenty years since their construction. In a word: well, proving one can reclaim tailings piles that have no pond and little water, although the costs are high.

AUSTRALIAN PRACTICE

One of us went to Australia where we soon learnt that there is a dearth of water. Almost every mine is under severe constraints to limit water losses. Thus we became interested in high density thickened tailings deposition.

Tailings is considered to be 'high density' when the percentage solids in the tailings slurry is increased to 65% to 75% solids. The tailings density is increased by either passing the tailings through a bank of cyclones and/or a thickener. In both cases the underflow, from either the cyclones or new thickener is pumped to the tailings storage facility (TSF), the Australian term for a slimes dam, as thickened tailings and the over flow is returned to the plant or thickener.

The overflow is usually rich in chemicals (acid, cyanide, etc.) and may contain small quantities of dissolved metals which can be recovered if the overflow is re-circulated

through the processing plant. The increased recovery of process water (from the cyclone or thickener overflows) will effect a saving in the quantity of chemicals required for processing, thereby giving additional ‘chemical credits’ for the plant. Tailings underflow can be re-conditioned to the design moisture content for pumping using centrifugal pumps, i.e., positive displacement pumps are not required for pumping of high density tailings.

High density tailings deposition has a number of significant benefits over conventional tailings deposition. These are listed below and described in more detail in the ensuing sections.

- Lower ongoing operating costs,
- Reduced water losses and seepage,
- Improved slope stability
- Reagent savings,
- Improved environmental performance,
- Reduced closure costs

Here follows a discussion of each of these factors.

Lower On-going Operating Costs

Ongoing operating costs for above-ground high density facilities are reduced as civil works are limited to ongoing topsoil stripping and covering/rehabilitation of the completed areas of the TSF, limited embankment construction, construction of water management facilities (if required) and extension of the tailings delivery pipework.

The most common method of operating high density facilities is using a single “central” discharge point that is systematically raised. Originally this method was referred to as Central Thickened Discharge or CTD although whether the discharge is indeed central depends on whether the ground is flat.

The deposited tailings form a cone around the single “central” discharge. But this method of tailings deposition has a number of drawbacks:

- It is volumetrically inefficient especially on sloping ground.
- It requires burial of the discharge pipe within the tailings and if this pipe holes there are significant erosion issues.
- It requires access to the discharge point and this access is continually rising requiring on-going capital expenditure.
- It is not possible to effect progressive rehabilitation as the tailings surface is always rising.

A practical alternative to the single “central” discharge method is the advancing cone method.

The advancing cone method of high density tailings operation entails the progressive advancement of a delivery pipeline upwards, horizontally, or downwards as tailings is deposited.

Figure 1 shows a plan and section of a typical advancing cone. Figure 2 shows a typical method of pipeline advancement and Figure 3 shows alternative methods of developing adjacent advancing cones.

The advancing cone method has significant advantages over a single “central” discharge in that:

- Volumetric storage is significantly better. The pipe can be directed to create curved embankments and/or progressively raised as long as the angle of raising is less or equal to the beach angle.
- The delivery pipeline is not buried and always accessible.

- It is practical to effect progressive rehabilitation behind the discharge point.

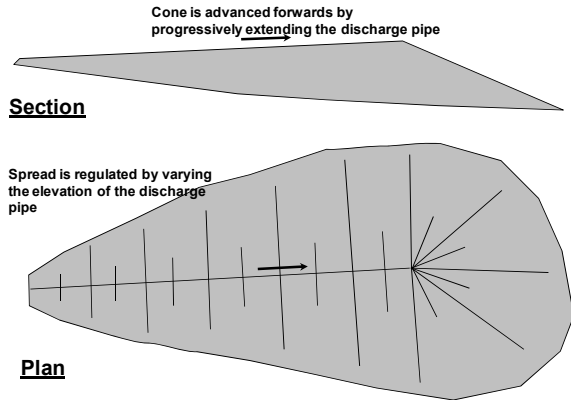


Figure 1. Plan and Section of a Typical Advancing Cone

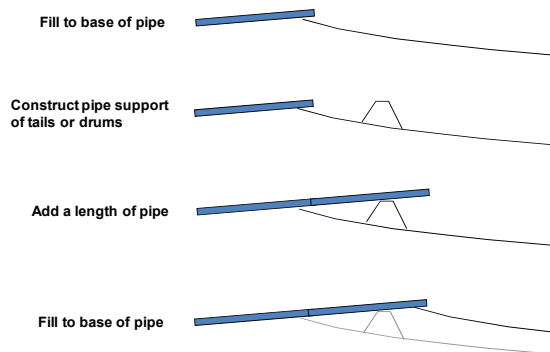


Figure 2. Typical Method of Pipeline Advancement

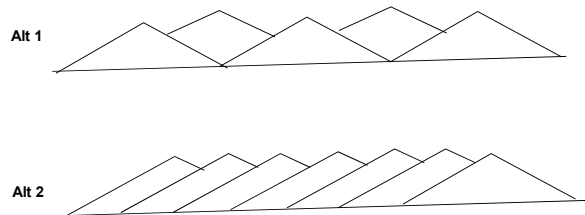


Figure 3. Alternative Methods of Developing Adjacent Advancing Cones

Reduced Water Losses

By pumping the slurry at high density the excess of water over the initial interstitial water of the newly settled slurry is reduced – the water has simply been kept in the plant water circuit instead of being sent to the TSF. This means lower volumes of supernatant water, smaller pond areas and lower evaporation area.

Water losses through seepage are reduced as with lower pond volumes comes lower driving heads over lower areas. Above the small ponds on the exposed beaches seepage is the difference between

Improved Slope Stability

Low seepage rates translate into low phreatic surfaces and shallow beaching angles translate into exceedingly flat slopes. Provided the density of the slurry is selected such that the material is able to consolidate to a void ratio below the critical state line there are unlikely to be any slope stability issues. Moreover, since the method of placement of the tailings relies on progressive advancement of the pipe over deposited tailings and no heavy equipment access for wall building or packing of the tailings, the allowable rate of rise can be taken to 15m/a without difficulty or risk of instability.

Only in limited circumstances, such as when impounding the high density tailings behind a confining embankment, is it necessary to provide any filter drains. Generally, in the arid climates of Australia, seepage and drainage requirements are not required.

Like all tailings facilities these issues need to be checked as a matter of design but we have not experienced problems in this regard in Australia so far.

Reagent Savings

As a result of collecting process water directly from the overflow from either the cyclones or the thickener all excess process water is recovered and re-circulated within the plant. This recirculated water is likely to contain chemicals and reagents required during the processing of the ore, and indeed some dissolved metal, so that recirculating the water maintains concentrations of often costly reagents and valuable metals within the plant circuit. Retention of reagents translates into lower reagent top up and therefore cost.

Improved Environmental Performance

High Density tailings disposal has a number of benefits over conventional tailings deposition. These include the following:

- Staged site clearance, minimising exposed areas (for above ground deposition).
- Reduced water requirements.
- Smaller carbon footprint due to minimal earthworks requirements during construction and ongoing development and operation of the facility.
- A water-shedding final geometry which is preferable for closure of the facility.
- An aesthetically pleasing final geometry that should blend into the surrounding environment more readily than a conventional facility.

Reduced Decommissioning Costs

Decommissioning costs are likely to be significantly lower than for a conventional TSF as the final geometry lends itself to ongoing rehabilitation. The high density facility is water-shedding thereby negating the need for the design and construction of surface water runoff management facilities.

Expected final slopes of between 1:30 and 1:50 (V:H) increase the ease of construction during decommissioning and reduce the long term erosion potential .

Successful Documented Application

TSF2 at Barrick Osborne Mine in Queensland is a good example of the effectiveness of high density thickened discharge. This facility is based on advancing-cone deposition and entailed conversion of a conventional TSF to high density in 2003. This facility is now fully operational and heading for decommissioning in 2010 when mining operations are due to stop.

A number of papers have been presented on the Barrick Osborne tailings facility^{1,2,3}.

That said, while we have succeeded at some sites we acknowledge that the high density approach is not for everyone. But it is the tailings management method of the future.

CANADA

Water continues to be an issue at some tailings impoundments. A quick reference to the web and you will find much information about the Alberta oil sands which are deposited as fluid streams into impoundments created by constructing large earth dikes. The tailings are still essentially a fluid (as is described in another paper in this conference that one of us has co-authored.)

The Alberta Energy Resources Conservation Board (ERCB) last year published new regulations demanding that the industry dewater the tailings to the point that they have a shear strength of at least 5 kPa. This number they picked up from an old technical paper that claims you can drive a truck on tailings of that strength. While we doubt it, we recognize that this was a genuine attempt

to force the industry to get as much water out of the tailings as possible before depositing them. Ignoring the ERCB's confusion between trafficability and flowability, we recognize that the idea behind dewatered tailings was presumably that such tailings were not susceptible to flow down the Athabasca River as did those of Bafokeng.

Industry and academia have pointed out the many flaws with this approach to regulating placement of dewatered tailings as a way to limit their susceptibility to long-term geomorphic instability. And the ERCB is backtracking into the part of the new regulations which says to the industry "tell us what you can and will do."

There are ways to dewater oil sands tailings: additives to make CT; flocculation; and wick drains are but some. Only time will tell which is best. But we must ask in all innocence why the fuss? If the dikes are strong and society is prepared to maintain them, let the natural processes of consolidation take place. A geomorphically-induced breach in a dike impounding dewatered tailings will have much the same consequences in an untended situation as one entraining un-dewatered tailings.

It may be aesthetically nice to think of the tailings as dewatered, but that is an ephemeral and transient benefit. If you do not do it as the tailings are deposited, then we suggest in practice you are stuck with maintaining the integrity of the encapsulating embankments in perpetuity.

If the ERCB really wants to protect the Athabasca River, maybe they should take a leaf out of the UMTRA regulations and write:

Design, build, operate, and close oil sands tailings impoundments so that they do not breach and the contents do not flow out for at least 1,000 years to the

extent reasonably achievable, and at any rate for 200 years.

Actually this or similar is the only regulation you need for any tailings impoundment. You may increase or decrease the periods. But at the end of the day that is the only reasonable regulation to force tailings design engineers to include drains, dewatering, and fluid solidification into their designs.

VAIL, COLORADO 2008

Thus we acknowledge the many changes in tailings disposal practices in the past few decade. These changes were on full display at last year's conference in this series. Here are some of the profound changes we noted in the many fine papers from that conference held in Vail, Colorado in blinding snow.

- Liners for impoundments are now accepted as good practice; no longer do we hear how liners are unnecessary components forced on the mining industry.
- Covers are now routinely four feet and thicker; gone are the days when the proud brag was a one-foot thick cover.
- Side slopes of three to one and even five to one are considered reasonable; no longer do we hear that the angle of repose is stable enough.
- Water is a component of interest and value; no longer a side issues and a nuisance.
- Regulations including CERCLA and RCRA are mentioned in passing and implemented routinely; no longer are there tirades against unwise regulators.
- Stochastic methods are used and the young recognize that extreme events do occur.

These we consider to be good changes. Although they have resulted in significant increases in the cost of tailings and mine waste management.

THE FUTURE

Factors that in future will contribute to even greater costs of tailings include:

- The new U.S. Environmental Protection Agency undertaking to make sure mines have sufficient funding to close and cleanup their mines.
- The need to dewater tailings prior to closure (an Alberta imperative for the oil sands industry)
- Legal fights to put tailings in lakes and the oceans when environmentalists would prefer upland piles (another Alaskan story.)
- Every increasing demand for less water consumption and import.
- Higher embankments for large tailings disposal facilities in harsher climates.
- And ultimately recognizing that you can, even if you would rather not, close the facility to be stable in the very-long-term.

CLOSURE

We will continue to mine for the simple reason that we must. Whether we need the materials for SUVs or windmills, we must get the materials from mines. We simply cannot see how the world's ever-increasing population can be supplied by recycle alone, desirable as the aim may be. And as long as

we mine, that long we will produce tailing and be faced with difficult decisions about costs, technology, and the balance of operational common sense versus the imperative to leave behind a topographic form that is geomorphically stable in the landscape we have altered.

The stories we tell in this paper reflect but a few years of mining but they have been years in which great changes have occurred in the practice of tailings disposal. Now we must continue, but ultimately leave it to new generations to deal with the new demands of the fast changing world of climate change, water shortages, and more people communicating via the web and twitter, and nationalism that inhibits mining even in formerly remote locations.

REFERENCES

McPhail, GI, Noble, A. Papageorgiou, G and Wilkinson, D (2004) *Development and Implementation of Thickened Tailings* , Proc Seventh International Seminar on Paste and Thickened Tailings, Cape Town, South Africa, May 2004

McPhail, GI, Brent, C (2007) *Osborne High Density Discharge – An Update from 2004* Proc Tenth International Seminar on Paste and Thickened Tailings , Perth, Australia, March 2007.

Brent, C and Dobb, M (2006), *Case Study: Realising the benefits at Osborne Mine from Converting a Conventional Tailings System to a Thickened Tailings System*, Proc MineTailings 2006, Brisbane, Australia, Feb 2006.

CYANIDE AND MERCURY CONTAMINATION OF SURFACE SEDIMENTS IN THREE DESERT WASH SYSTEMS, NELSON, NV

Douglas B. Sims

School of Earth Sciences and Geography, Centre for Earth and Environmental Science Research; Kingston University, Surrey UK; U.S.

ABSTRACT: The Carnation, Eagle and Techatticup wash systems in Nelson, Nevada were investigated to determine if Hg and CN^- from mining processes in sediments are migrating from historical mine tailings in dry ephemeral wash systems as a result of overland flow and transport. The subject sites are at an elevation ranging between 2500 and 2700 ft and are 4 and 6 miles upgradient from Lake Mohave, some 647 feet above sea level. Total Hg and CN^- were evaluated to determine if anthropogenic inputs from historical mining operations were being transported as trapped contaminants in sediments. Mercury and CN^- were chosen because Hg is low in ores and CN^- was completely input to the system from mining activities. It was found that both Hg and CN^- were transported down gradient to a distance of at least 6000 feet below source materials eroding into the wash systems.

INTRODUCTION

Mining activities, past and present, in Nelson, NV have created the potential for geogenic metals and metalloids to mobilize beyond small localized areas and into the surrounding environment (Fig. 1). Redistribution of mine tailings can transport sorbed metals, metalloids, and other anthropogenic contaminants present in surface sediments. Understanding trace element storage and mobilization in surficial sediments are key areas of inquiry in furthering the understanding of the potential for pollution and the resulting ecological and human health impacts from abandoned mines. This research examines the storage and transport of some trace elements in sediments to determine their redistribution by transport with surface sediments.

A number of studies have investigated release of mining contaminants to sediments and the distribution of these contaminants to the surrounding environment; however, these studies have focused on sites located in areas where precipitation was greater than arid conditions (Ge et al., 2005; Coulthard and Macklin, 2003; Sims and Francis, 2008; Sims, in press; Sims and Bottenberg, 2008; Mackenzie and Pulford, 2002). Coulthard and Macklin (2003) investigated mine sites where they were able to predict the movement of contaminated sediments in relation to the source areas. They showed the possible extent of contamination and found what Coulthard and Macklin (2003) refer to as secondary "hot spots." In these sediment hot spots sources of contamination can be found that occur some distance from the original

source. These hot spots can impact other areas that were not historically contaminated because of variable climactic conditions such as more intense storm events that resulted in flooding. The mass transport and deposition of hot spot material in surface waters can create new areas with contaminated soils (Ge et al., 2005; Coulthard and Macklin, 2003; Mackenzie and Pulford, 2002).

Anthropogenic inputs and their related effects on geogenic metals have been the focus of several studies using enrichment ratios (Sutherland, 2000; Zhang and Shan, 2008; Chow, 1970; Page and Ganje, 1970; Khalid et al., 1981; Motto et al., 1970; Liu et al., Frignana and Bellucci, 2004). It was shown that anthropogenic processes can release trace elements that would not otherwise be available. Sutherland (2000) studied the anthropogenic enhanced movement of Pb, Zn, and Cu and found that in an environment with high automobile emissions, Pb was more mobile at 7.2-10cm depth than in top soil.

ENVIRONMENTAL SETTING

Geological Setting

Ore bodies of gold and silver in the Nelson, NV area occur in fissured quartz monzonite dikes (Hansen, 1962; Bell and Smith, 1980). These dike structures dip nearly vertical and can be up to a mile in length on the surface (Hansen, 1962; Longwell, et al., 1965). Quartz monzonite dikes at the north end of the area cut through a series of lavas, breccias, tuffs, and andesite and rhyolite structures that strike north and dip twenty to sixty degrees eastward (Bell and Smith, 1980; Longwell, et al., 1965). Economic mineral deposits of gold and silver can be found in epithermal fissures located in the margins of the Nelson Quartz Monzonite and surrounding volcanic and foliated rocks of

Precambrian age (Hansen, 1962; Longwell, et al., 1965).

Hydrological Setting of Nelson, Nevada

Precipitation in Southern Nevada averages 7.6 cm per year (Greene, 1975). Summer rains usually occur during major conventional storms whereas winter rains are more commonly known to produce less than 1cm of precipitation per event (Greene, 1975). Approximately 35% to 40% of the measurable precipitation occurs in 1cm or greater events from a single summer thunderstorm (BOR, 1995). The nearest permanent water source to the town of Nelson, NV is Lake Mojave, located approximately 6 miles east of the town (Figure 1). Lake Mojave is an artificial lake that was created as a result of the completion of Davis Dam in 1953 (BOR, 1995). The Colorado River was a lifeline to the town of Nelson, NV, with the use of the river steamboats and vessels that brought supplies to the town and to mining camps located in the canyons adjacent to the river (Greene, 1975).

These wash systems (Carnation, Eagle and Techatticup) are large with no major confluences with other wash systems until approximately 800 m up gradient from Lake Mohave. There is only one major mining and milling site, the Techatticup Mine, within the wash and it is situated 4 miles up gradient from Lake Mohave. This wash was selected for its lack of multiple mining and milling sites other than the Techatticup Mine. Investigating this wash makes possible the evaluation of the impact that a large mining and milling operation can have on a wider environment because only one mine is located along the system that has the potential to erode contaminant tailings into the system. Furthermore, this wash does not have any large tributary systems that feed contaminated

sediments from sources other than from the Techatticup Mine.

The nature of the geologic setting is that it tends to prevent the movement of groundwater because of its synclinal structure (Bell and Smith, 1980). Groundwater can only flow west to east along geological orientation of ridges and mountains, and, because the area is composed of small valleys and mountains, the principal groundwater system has little or no influence on the area of investigation. There are numerous perched aquifers associated with the desert washes that capture water from precipitation events and contain water just beneath the surface (Longwell, et al., 1965). However, these perched aquifers are high in dissolved solids and therefore have limited use as a water resource for consumption. These perched aquifers are commonly found along washes where bedrock outcroppings occur, interrupting the flow continuum of the soil water after a storm event (Longwell, et al., 1965).

Soil Composition in Nelson, Nevada

Soils have fine aeolian silt deposits at the surface to a depth of approximately 15-25 cm. Wind-blown materials are covered by stage-2 desert pavement on alluvium fan deposits with exposed soils on the sides of small hills (Bell and Smith, 1980; Longwell et al., 1965). Below the wind-blown deposits are layers of alluvial gravels and cobbles with cemented layers ranging from a few inches to several feet in thickness. There are areas with exposed bedrock in deeply cut dry washes that formed with east to west trends at a constant 3-5 % downward slope towards Lake Mojave. Soils located in the project area have pH ranging between 9.1 and 9.4 SU, contain 1 to 2 % calcium-carbonate deposits, and < 1 % organic carbon from the lack of precipitation (Longwell et al., 1965).

Tailing dumps are comprised of a silty-fine grain soil <1.0 mm. Sediments within the wash are a sandy-gravel with fine particles ranging between 2 mm and 4 mm mixed with larger gravels and cobbles. Throughout the wash system pockets of the silty-fine grained tailings are found in wash bends and meanders. In the tailing dumps it is evident that stormwater transport processes are eroding tailings into the wash system and conveying sediments down gradient. Surface sediments have <0.1 % moisture and therefore soluble metals and elements are much less important than transport of particulate or adsorbed contaminants in this area.

METHODS AND MATERIALS

Sampling Methodology

The goal of sampling was to identify if pulses of elemental Hg and CN⁻ containing sediments are transported down gradient by stormwater runoff. To accomplish this goal, twelve samples were collected in a staggered pattern down gradient along a 6180 m transect of the Techatticup Wash. Field procedures involved the collection of nine (9) sediment samples at three equally spaced locations in a linear fashion across the wash at each sampling location, except for background samples. Samples were taken from the two banks and the center of the wash at each sampling location, at a 0-5 cm maximum depth. The exact size and shape of the sampling area were adjusted to meet site-specific conditions. Background samples were collected at 60 m (-60), 120 m (-120) and 180 m (-180) above where tailings were observed to be eroding into the wash. The beginning of the wash sampling was at the point where tailings were eroding into the wash, or the source area. Composite samples were collected at the source, 50 m, 100 m, 200 m, 400 m, 1000 m, 2000 m, 4000 m, and

6000 m below the source area (Figure 2). Sampling was careered out according to standard field procedures out line by Sims and Francis (2008) and Sims (*in press*).

Variations in the location of sampling points can affect the results for this study, for example, sampling in the field will be affected by stream bed, elevation, and location of sampling within the wash systems as the results can be affected by the size of a wash system. Stream bed material can also affect sampling if an area is composed mostly of bed rock rather than sediments. Elevation can also affect sample results because a particular sampling point might not be a good candidate for sampling because the wash has downcut the area, leaving the sampling location considerably higher than the stream bed. In this situation the designated sample area was relocated from the linear sampling line of the three samples to an area where sediments within the wash could be collected. Wash size will affect the deposit contaminated with sediments is more probable in an area where the wash broadens and flood waters slower as a result.

Sample Analysis

Samples were analyzed per USEPA method 3050B preparation procedures for total metals (As, Cu, Cr, Pb, Ag, Cd, Se and Ba) followed by analysis with an Inductively Coupled Plasma-Optical Emission Spectrometer (ICP-OES) per USEPA method 6010B. Mercury was analyzed according to USEPA method 7471, cold vapor atomic adsorption (CVAA). Analysis for CN⁻ was performed by colorimetric techniques per USEPA method 9010. Laboratory procedures were per USEPA procedures and outlined in Sims and Francis (2008) and Sims (*in press*).

Background

Background concentrations for Hg and CN⁻ were determined by collecting three samples above the source of tailing eroding into the wash (Tables 1, 2 and 3). Background levels for the target contaminants of concern (COCs) were analyzed for each location and averaged between the three samples so that a standard number can be used when discussing samples collected below the source of tailings that have eroded into the wash.

Table 1: Background levels of COCs in the Carnation Wash, Nelson, Nevada in meters (mg kg⁻¹)

COC	-60	-120	-180	averaged	detection limits
Hg	<0.01	<0.01	<0.01	<0.01	0.01
CN ⁻	<0.01	<0.01	<0.01	<0.01	0.01

Table 2: Background levels of COCs in the Eagle Wash, Nelson, Nevada in meters (mg kg⁻¹)

COC	-60	-120	-180	averaged	detection limits
Hg	<0.01	<0.01	<0.01	<0.01	0.01
CN ⁻	<0.01	<0.01	<0.01	<0.01	0.01

Table 3: Background levels of COCs in the Techatticup Wash Nelson, Nevada in meters (mg kg⁻¹)

COC	-60	-120	-180	averaged	detection limits
Hg	<0.01	<0.01	<0.01	<0.01	0.01
CN ⁻	<0.01	<0.01	<0.01	<0.01	0.01

Target elements and compounds indicate low concentrations present in wash sediments designated as background or, non-mine impacted sediments. Mercury and CN⁻ were not detected in background samples as expected because they are both anthropogenic inputs to the wash systems. Silver was also not detected in background samples and is most likely the result of background

sediments originating from weathered volcanic materials and not metal bearing ores that were sought after by the mining operations.

RESULTS

Hg and CN⁻ in Wash Sediments

Table 4 shows that Hg and CN⁻ concentrations in the three chosen washes, Carnation, Eagle and Techatticup, were unevenly distributed in surface sediments. Data from the three washes illustrate their own uniqueness within each wash with dissimilar patterns in the sediments across all three wash systems. Contaminant trends for individual washes are similar, however, within a limited distance from the source material. Results will be discussed here according to concentrations and hot spots within individual wash system and compared among the three individual washes.

Trends in the sediments of the Carnation, Eagle and Techatticup washes indicate an initial pulse of contaminated materials for source areas eroding into the wash at the mine sites (Table 4; Fig. 2). Carnation, Eagle and Techatticup wash sediments exhibited similar increases in CN⁻ over a distance of 200 m from source materials with the highest concentration in CN⁻ between the source and 200 m at 1.35 mg kg⁻¹ in the Carnation Wash sediment, whereas, the Eagle and Techatticup washes CN⁻ levels at 200 m were measured at 0.874 and 0.952 mg kg⁻¹, respectively.

Cyanide in Sediments

The Carnation Wash exhibits the highest CN⁻ concentrations in sediments nearest the source where CN⁻ containing sediments are eroded into the wash system and transported down gradient. Samples collected at the source, 100 m, 200 m and 4000 m were higher than

the mean CN⁻ concentration (1.23 mg kg⁻¹ CN⁻), whereas, at 50 m, 400 m, 1000 m, CN⁻ was within 1 standard deviation of the mean (0.51 mg kg⁻¹ CN⁻). At 200 m CN⁻ exhibited a decrease in concentration trend through 2000 m from the source and only 1800 m from the area of highest concentration, other than source materials, at 200 m.

The Carnation Wash sediments maintained the highest level of CN⁻ in sediment compared to measurements in sediments of the Eagle and the Techatticup wash systems, with concentrations decreasing from 1.35 mg kg⁻¹ to 1.15 mg kg⁻¹ at 400 m, 1.15 mg kg⁻¹ at 1000 m and 0.25 mg kg⁻¹ at 2000 m from source materials. CN⁻ in the Carnation Wash was near the mean concentration between sampling locations near the source area and at 2000 m. Cyanide was detected at 1.54 mg kg⁻¹ at 4000 m with a decrease to 0.88 mg kg⁻¹ at 6000 m (Fig. 2). This increase in CN⁻ at 4000 m is most likely the result of a hot spot where sediments containing elevated CN⁻ were deposited during a storm event and the wash channel probably scouring occurred at another location.

Sediments in the Eagle and Techatticup washes also exhibited a decrease in CN⁻ similar to the Carnation Wash sediments; however, concentration of CN⁻ containing sediments in these two wash systems were lower than in the Carnation wash. Eagle wash samples, collected at the source, 100 m, and 200 m, were higher than the mean CN⁻ concentration (0.71 mg kg⁻¹ CN⁻), whereas, at 50 m, 400 m, 1000 m, CN⁻ concentrations were within 1 standard deviation (0.36 mg kg⁻¹ CN⁻) of the mean. Techatticup wash samples, collected at the source, 50 m, 100 m, and 200 m, were higher than the mean CN⁻ concentration (0.89 mg kg⁻¹ CN⁻), whereas at 400 m, 1000 m, 2000 m and 4000 m, CN⁻ concentrations were within 1 standard deviation (0.82 mg kg⁻¹ CN⁻) of the mean.

Table 4: Concentrations (mg kg⁻¹) of CN⁻ and Hg across 3 wash systems. *Background is an average of three sample locations (-60, -120 and -180 feet) upgradient from source material. Background not used in statistical calculations.

Location (Meters)	Wash Systems							
	Carnation		Eagle	Techartticutip	Carnation		Eagle	Techartticutip
	CN ⁻	CN ⁻	CN ⁻	Hg	Hg	Hg	Hg	
Background	<0.01	<0.01	<0.01	<0.01	<0.01	<0.01	<0.01	
Source	2.14	4.15	2.72	1.31	0.854	1.49		
50	1.18	0.565	1.18	0.341	0.45	0.35		
100	1.35	0.571	1.36	0.363	0.318	0.36		
100 D	1.28	0.845	1.28	0.384	0.300	0.84		
200	1.35	0.874	0.952	0.402	0.790	0.46		
400	1.15	0.612	0.346	0.385	0.781	0.74		
1000	1.08	0.513	0.152	0.375	0.610	0.3		
2000	0.250	0.143	0.148	0.185	0.480	0.23		
4000	1.54	0.118	0.754	0.211	0.851	0.53		
6000	0.880	0.081	<0.01	0.085	0.612	<0.01		
STDV	0.51	0.36	0.82	0.34	0.21	0.42		
Mean	1.23	0.71	0.89	0.49	0.59	0.53		
Max	2.14	1.099	2.72	0.942	0.854	1.49		
Min	0.25	0.052	0.0	0.0	0.30	0.0		

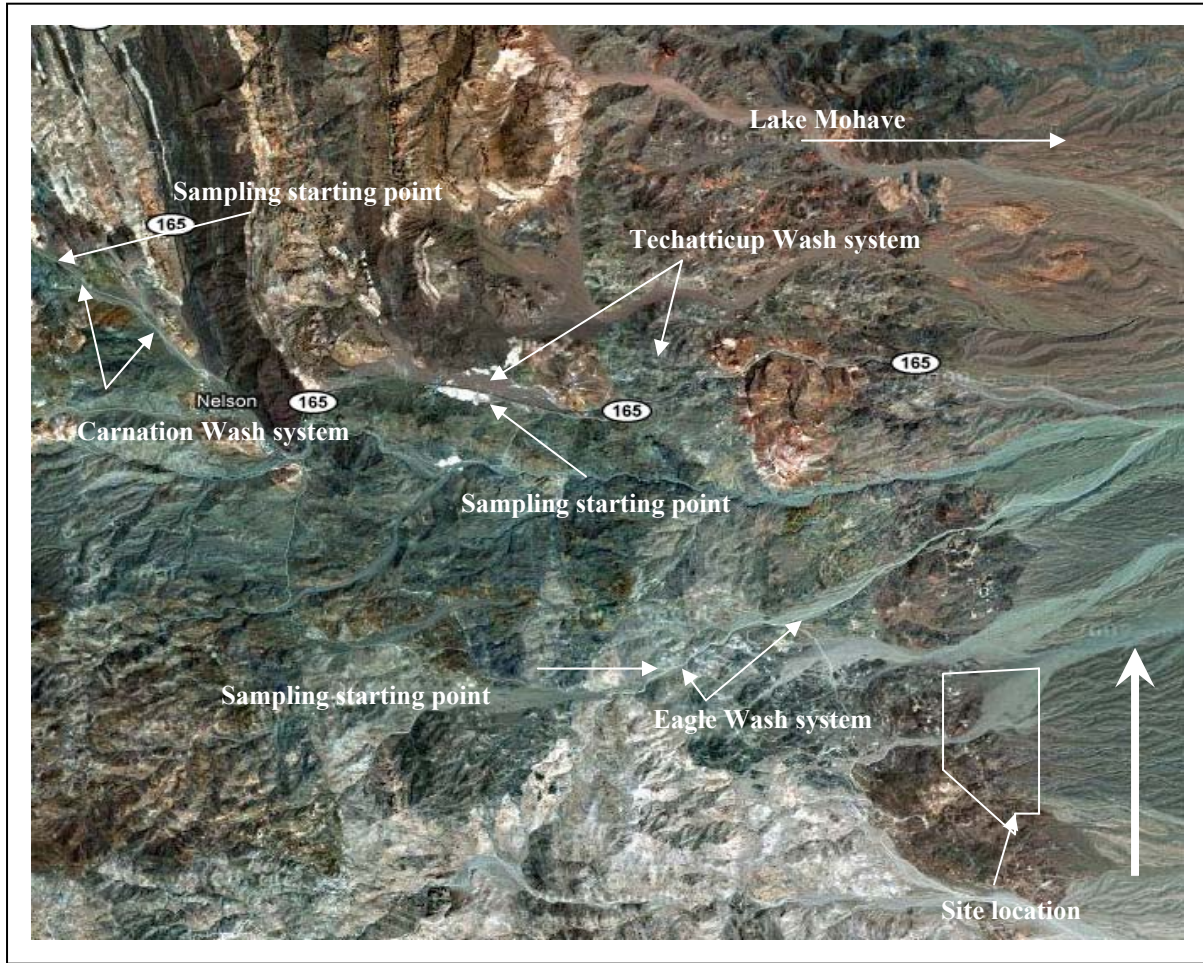


Figure 1 Carnation, Eagle and Techatticup wash system, Nelson Nevada

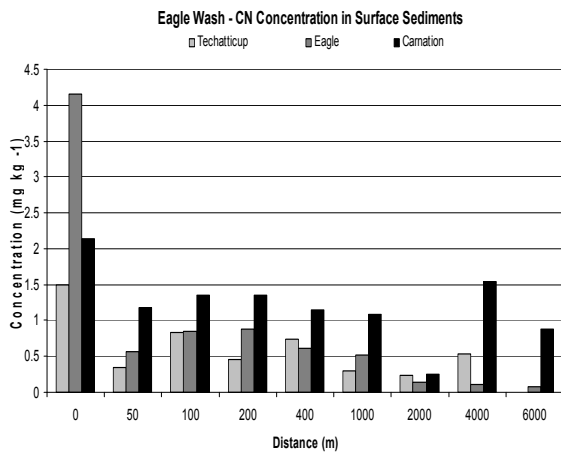


Figure 2: CN⁻ concentration in surface sediments

The Techatticup Wash contained the second highest concentration of CN⁻, with the Eagle Wash containing the least amount of CN⁻ of the three wash systems investigated. Concentrations of CN⁻ in sediments in the Eagle and Techatticup wash systems exhibited an increase in concentration, after the initial pulse, at 0.565 mg kg⁻¹ in Eagle wash sediments and 1.18 mg kg⁻¹ in Techatticup wash sediments, increasing to 0.874 mg kg⁻¹ and 0.954 mg kg⁻¹ at 200 m, respectively, from the source materials. In both wash system CN⁻ was lower than mean concentrations in the Eagle and Techatticup wash systems, at 0.71 mg kg⁻¹ and 0.89 mg kg⁻¹, respectively. Both washes exhibited a

decrease in CN^- containing sediments between 200 m and 2000 m, with concentrations decreasing to less than the mean concentration in both wash systems (Fig. 2).

However, the Eagle wash continued to decrease in CN^- concentrations in sediments up to 6500 m from source materials. Eagle Wash CN^- decreased to almost 9 times lower than the mean concentration of CN^- in sediments, whereas the Techatticup Wash sediments increased to $0.754 \text{ mg kg}^{-1} \text{ CN}^-$, closer to the mean concentration of CN^- 0.89 mg kg^{-1} in wash sediments. Interestingly, CN^- concentration in the Techatticup Wash sediments decreased to $<0.01 \text{ mg kg}^{-1}$ by 6000 m from the source materials. It is possible that the $<0.01 \text{ mg kg}^{-1}$ is the result of the sample location and therefore, represents an anomaly at a single location where sediments were not deposited during flow, or sediments were re-deposited to another area as a result of a high energy flow and scour in a narrow portion of the wash.

This increase in CN^- concentrations at 4000 m and decrease at 6000 m is most likely the result of sampling a hot spot at 4000 m and a location at 6000 m that was not impacted by contaminated sediments during a flash flood, called a “dead zone”. Later, flood action results in the isolation of the contaminated tailings deposit. High energy storm-water flow that scours sediments deposits them at locations where no sediments accrue for any length of time, creating the dead zone of no contaminated sediment at that location. A dead zone does not indicate that tailings are not present in the wash system, but rather, it is possible that tailings were transported farther down gradient and redeposited as a result of the flooding.

Concentrations of CN^- in the wash systems exhibited an initial pulse and one secondary pulse between 50 m and 2000 m beyond the

source area. However, the Carnation Wash exhibited a sizable third pulse of CN^- at 4000 and 6000 m with 1.54 and $0.880 \text{ mg kg}^{-1} \text{ CN}^-$, respectively. Both the Eagle and the Techatticup washes showed minor increases in CN^- at 4000 m and the Eagle Wash showed a second, extremely minor, increase at 6500 m beyond the source areas. Both the Eagle and the Techatticup CN^- concentrations in sediments were below the mean concentrations at 6000 and 6500 m with the Carnation Wash final pulse exceeding the mean concentration of CN^- in sediment by 40%.

Mercury in Sediments

The Carnation, Eagle and Techatticup washes showed initial pulses of Hg contaminated materials from source areas eroding into the wash at each mine site (Table 4; Fig. 3). There were no distinctive patterns of concentrations among the Carnation, Eagle or Techatticup wash sediments; however, there was a pattern of Hg spiking at the source locations where sediments were eroding into the wash systems. There were two pulses of Hg shown by the data; first pulse was at 100 m and the second pulse was at 4000 m beyond source materials. This pulsing illustrates that Hg is migrating down slope through storm events with the transportation of Hg containing sediments.

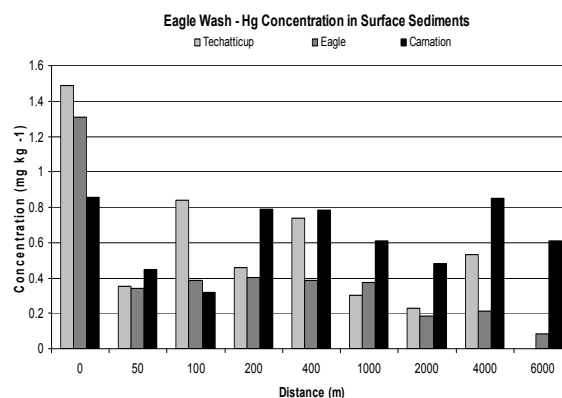


Figure 3: Hg concentrations in surface sediments

Mercury concentrations were greatest in the Carnation Wash with the Techatticup Wash containing the second highest, and the Eagle Wash with the least amount of Hg in this study. Sediments in the Carnation Wash were highest at $0.854 \text{ mg kg}^{-1} \text{ Hg}$ at the source, 1.45 times higher in concentration of Hg than the mean throughout the wash system. The trend in the Carnation Wash indicated a steady decrease in Hg between the initial pulse near the source area and 100 m down gradient at $0.318 \text{ mg kg}^{-1} \text{ Hg}$. At 200 m, Hg increased to 0.79 mg kg^{-1} and decreased to $0.48 \text{ mg kg}^{-1} \text{ Hg}$ at 2000 m from the source area (Fig. 3). Again however, Hg increased to $0.851 \text{ mg kg}^{-1} \text{ Hg}$ by 4000 m and decreased to $0.612 \text{ mg kg}^{-1} \text{ Hg}$ by 6000 m beyond the source area. The trend for Hg in the Carnation Wash indicates three distinct pulses of Hg laden sediments with a mean Hg concentration of 0.59 mg kg^{-1} . The Carnation wash samples collected at the source were higher than the mean Hg concentration ($0.49 \text{ mg kg}^{-1} \text{ Hg}$); whereas, at 50 m, 100 m, 200 m, 400 m, 1000 m, 2000 m, and 4000 m, Hg concentrations were within 1 standard deviation ($0.034 \text{ mg kg}^{-1} \text{ Hg}$) of the mean.

The Eagle Wash exhibited an initial pulse of Hg laden sediment at the source that was 1.31 mg kg^{-1} with a consistent concentration level to 1000 m beyond the source area (Fig. 3). Between the source area and 1000 m down gradient, Hg ranged from 0.341 mg kg^{-1} to 0.402 mg kg^{-1} decreasing in concentration to 0.185 mg kg^{-1} at 2000 m. At 4000 m Hg increased slightly to 0.211 mg kg^{-1} but decreased to 0.085 mg kg^{-1} by 6500 m beyond the source area. The increase and decrease of Hg in the wash is likely the result of hot spots; however, when compared to CN^- in the wash sediments, CN^- exhibited one initial pulse, then decreased in concentration to almost 9 times below the mean for CN^- in the sediments. Furthermore, Hg detected in the Carnation

Wash exhibited a similar distribution pattern with an initial pulse of Hg and two distinct pulses along the 6000 m sampling line. In the Eagle Wash, samples collected at the source, 50 m, 200 m, 400 m, and 1000 m were higher than the mean Hg concentration ($0.59 \text{ mg kg}^{-1} \text{ Hg}$) whereas at 50 m, 100 m, and 2000 m, Hg was within 1 standard deviation ($0.21 \text{ mg kg}^{-1} \text{ Hg}$) of the mean.

Trends found in the Techatticup Wash indicated a similar distribution of Hg in sediments as found in the Carnation and Eagle washes with an initial pulse at the source as expected at 1.49 mg kg^{-1} (Fig. 3). At 50 m beyond the source area, Hg in sediments was 0.35 mg kg^{-1} and increased to $0.84 \text{ mg kg}^{-1} \text{ Hg}$ by 100 m. Hg began to decrease in concentration by 200 m and continued to decrease to 0.23 mg kg^{-1} at 200 m beyond the source area. Concentrations of Hg were found to increase at 4000 m to 0.53 mg kg^{-1} and decreased to $<0.10 \text{ mg kg}^{-1}$ by 6000 m beyond the source area. This was most likely the result of a dead zone along the sampled wash where at 6000 m no Hg was found in sediments. In the Techatticup wash samples collected at the source, 100 m, 400 m and 4000 m were higher than the mean Hg concentration ($0.53 \text{ mg kg}^{-1} \text{ Hg}$) whereas at 50 m, 200 m, 1000 m, and 2000 m Hg concentrations were within 1 standard deviation ($0.42 \text{ mg kg}^{-1} \text{ Hg}$) of the mean.

In general, Hg exhibited multiple spikes along the Techatticup wash, whereas CN^- exhibited an initial spike with one major spike spanning between 50 m and 2000 m beyond the source area. Neither CN^- nor Hg were found to mimic similar patterns across the washes. When comparing CN^- to Hg, however, similar spiking of CN^- and Hg in sediments in all three wash systems was indicated with CN^- and Hg greatest at the source areas, followed by CN^- having one

major spike and Hg having two spikes down gradient from the source area (Fig. 2 and 3).

Hg and CN⁻ in sediment at Wash Convergence

Where the Carnation, Eagle and Techatticup washes converge, Hg and CN⁻ concentration follow inconsistent distributions in surface sediments (Table 5). However, Hg and CN⁻ concentrations were present in all 10 samples collected with the north side of the sampling grid producing higher concentration of both constituents than the south side of the wash. This pattern indicates that mine tailings are following a path of deposition along the northern side of the wash rather than the southern side in recent flood events as a result of erosion. The location of Hg and CN⁻ does not show that the northern side is more apt to receive Hg and CN⁻ but rather, recent flooding was not at a level conducive to more even distribution of contaminants across the wash.

In the wash convergence sampling event, the locations 3, 4, 5, 8, 9 and 10 were higher than the mean CN⁻ concentration (0.49 mg kg⁻¹ CN⁻), whereas at locations 1, 2, 6, and 7, CN⁻ was within 2 standard deviations (0.37 mg kg⁻¹ CN⁻) of the mean. Hg analysis indicated a similar distribution where locations 3, 4, 5, 8, 9 and 10 were higher than the mean Hg concentration (0.21 mg kg⁻¹ Hg), at location 2, Hg was within 2 standard deviations (0.14 mg kg⁻¹ Hg) of the mean, and locations 1, 6 and 7 were within 1 standard deviation (0.14 mg kg⁻¹ Hg). It appears that sediments containing Hg and CN⁻ were deposited on the northern side of the grid with little or no deposition on the southern side of the grid in the wash

Table 5: Carnation, Eagle and Techatticup wash Convergence (mg kg⁻¹)

Sample Location (meter)	CN ⁻	Hg
1	0.074	0.073
2	0.052	<0.01
3	0.676	0.231
4	0.842	0.285
5	0.881	0.412
6	0.068	0.101
7	0.058	0.089
8	0.621	0.315
9	0.791	0.257
10	0.824	0.368
STDV	0.37	0.14
Mean	0.49	0.21
Max	0.881	0.412
Min	0.052	<0.01

DISCUSSION

Concentrations of CN⁻ and Hg were similar to those reported in surface sediments as found in literature (Coulthard and Macklin, 2003; Mackenzie and Pulford, 2002; Lewis, 1977; Gammon, 1970; Pagenkopf et al., 1974; Ashley and Lottermoser, 1999; Macklin, et al., 2001). Macklin, et al. (2001) reported that Hg in sediments tends to follow an independent distribution to other metals with no correlation with CN⁻ or other metals in surface sediments where moisture is present. In areas where precipitation is high and organic mater is abundant, Hg was found to bound to the organic matter and at least in part, altered to methyl-mercury, a more mobile and more toxic speciation (Coulthard and Macklin, 2003; Macklin, et al., 2001).

This research focused on an area that receives very low precipitation and has virtually no organic matter in the sediments

for Hg association. Without soil moisture or organic matter, Hg migration is entirely dependent on the movement of trapped elemental Hg in sediments. Furthermore, according to researchers, CN^- follows similar transport patterns as Hg because CN^- requires soil moisture to mobilize under normal conditions (USEPA, Region 8, 1995). Without adequate soil moisture CN^- migration is entirely dependent on the movement of trapped CN^- in sediments rather than in a soluble phase.

The project area for this research receives less than 7.6 cm of precipitation per year, has <0.1 % organic matter and <0.1 % soil moisture in surface sediment (0-5 cm) and, therefore, the traditional forms of transport such as associations with organic matter and moisture are not significant. It is clear that the transport of CN^- and Hg in this area is directly related to sediment-enrobed contaminants rather than contaminants associated with organic matter and aqueous species transport. Transport in the wash sediments as a result of flooding can produce both hot spots and dead zones based on the structure of the wash and nature of the flow during the infrequent flood events associated with this region.

Focusing on total metals in soils in an area where there is little soil moisture requires an acid digestion analytical procedure so that all species can be quantified (Lottermoser, 2007). Desorption of metals and their transport through soils as aqueous species requires the presence of soil moisture with a $\text{pH} < 4.0$ (Ashley and Lottermoser, 1999; Ashley et al., 2004). In this environment, with the lack soil moisture most of the year acid digestion was utilized instead of a weak acid to desorb and quantify better the concentrations of metals sorbed to soil particles with greater potential for transport with sediment rather than as dissolved species in water (USEPA, Region 8, 1995).

Metals and metalloids desorption from sediments is influenced by factors such as physical and chemical characteristics like sediment size fraction, geologic composition, and the presence of cations such as Al, Fe, and Mn as found by Horowitz (1986). Size fraction is known to affect sediment binding capacity for metals and metalloids at high concentrations (Horowitz and Stephens, 2008; Correia and Costa, 2000).

CONCLUSIONS

Finding show that anthropogenic inputs of CN^- and Hg are being transported down gradient in surface sediments. It is evident in Table that CN^- is moving with sediment flow and as a result of the solubility of CN^- salts and can be trapped CN^- compounds. Figures 2 illustrates that CN^- has entered the wash in a pulse that peaks along the system and tapers off toward the end of the sample however, CN^- does show a second pulse in the Carnation Wash around the 4000 m to 6000 m sampling suggesting a possible influx of CN^- containing sediments from a previous storm event.

Figure 3 shows a similar distribution pattern in the washes samples for Hg as shown by CN^- data. However, Hg pulses into the wash systems with a mean concentration between the three wash systems of 0.53 mg kg^{-1} . Hg concentration trends were steady in the Carnation, Eagle and Techatticup wash sediments indicating that Hg is possibly being transported as elemental Hg trapped in the sediment rather than as complexes or ions of Hg. Furthermore, Hg being in the elemental form is most likely the mode of transport because the environmental conditions in the Nelson, Nevada area are not favorable to formation of Hg complexes with organic matter. However, it is possible for Hg to volatilize out of the soils in the form

of Hg vapor as there is little organic matter available or other processes for Hg to become bound.

SELECTED REFERENCES

Bell J and E Smith, 1980. Geological Maps of Henderson Quadrangle, Nevada, map 67. Nevada Bureau of mines and Geology, UNR.

BOR. 1995. Preliminary assessments – Henderson Lead Site, Clark County, Nevada-EPA ID No NV5141190608-Draft. Boulder City, Nevada.

Coulthard, TJ, MG Macklin, 2003. Modeling long-term contamination in river systems from historical metal mining. *Geology*, Vol. 31, issue. 5:451-454.

Frignana, M and LG Bellucci, 2004. Heavy metals in marine coastal sediments: Assessing source, flux, history and trends. *Ann Chim*, Vol 94:479-486.

Ge, Y, D MacDonald, S Sauvé and W Hendershot, 2005. Modeling of Cd and Pb speciation in soil solutions by WinHumicV and NICA-Donnan model. *Environmental Modeling & Software*, vol. 20, issue 3:353-359.

Greene, J. M, 1975. Life in Nelson Township, Eldorado Canyon, and Boulder City, Nevada: 1860-1960. Masters Thesis from the History Department, UNLV.

Hansen, SM, 1962. The Geology of the Eldorado Mining District, Clark County, Nevada. A dissertation in the Geology Department, University of Missouri.

Khalid BY, BM Salih, and MW Issac, 1981. Lead contamination of soils in Baghdad City, Iraq. *Bull. Environmental*

Contamination and Toxicology, Vol. 27:634-638.

Liu C, JA Jay, TE Ford, 2001. Evaluation of environmental effects on metal transport from capped contaminated sediments under conditions of submarine groundwater discharge. *Environmental Science and Technology*, Vol. 35:4549-4555.

Longwell, CR, EH Pampeyan, Ben Bowyer and R.J. Roberts, 1965. *Geology and Minerals Deposits of Clark County, Nevada*. Printed by A. Carlisle, Reno, NV.

Mackenzie, A B and ID Pulford, 2002. Investigation of contaminant metal dispersal from a disused mine site at Tyndrum, Scotland, using concentration gradients and stable Pb isotope ratios. *Applied Geochemistry*, Vol. 17, issue 8: 1093-1103.

Motto, HL, RH Daines, DM Chilko and CK Motto, 1970. Lead in the soils and Plants: Its relationship to traffic volume and proximity to highways. *Environmental Science and Technology*, Vol. 4:231-237.

Sims, DB, in press. Contaminant mobilization as a result of anthropogenic influences in the Techatticup wash, Nelson, Nevada (USA). *Soil and Sediment Contamination: An International Journal* Vol. 19:3.

Sims, DB and BC Bottenberg, 2008. Arsenic and Lead Contamination in Wash Sediments at Historic Three Kids Mine-Henderson, Nevada. *Journal of the Arizona-Nevada Academy of Science*, Vol. 40:1.

Sims DB and T Francis. 2008. Mercury and cyanide used as indicators of sediment transport in ephemeral washes at the Techatticup Mine and mill site, Nelson, Nevada (USA). *International J. of Soil, Sediment and Water*, 1(2) article 4.

Sutherland, RA, 2000. Depth Variation in Copper, Lead, and Zinc Concentrations and Mass Enrichment Ratios in Soils of an Urban Watershed. *Journal of Environmental Quality*, Vol. 29:1414-1422.

Zhang, H and B Shan, 2008. Historical records of heavy metals accumulation in sediments and the relationship with agricultural intensification in the Yangtze-Huaihe region, China. *Science of the Total Environment*, Vol. 399:113-120.

DEVELOPMENT OF MATERIAL AND COMPACTION REQUIREMENTS FOR A MIXED CLAY/SAND TAILINGS IMPOUNDMENT LINER

Michael Malusis

Bucknell University, Lewisburg, PA

Melanie Davis

MWH Americas, Ft Collins, CO

Daniel Overton

Engineering Analytics, Ft Collins, CO

David Castelbaum

Tetra Tech, Ft Collins, CO

Toby Wright

Uranium One USA, Ft Collins, CO

ABSTRACT: A laboratory study was performed to support the design of a compacted clay liner (CCL) for a proposed tailings storage facility in an arid region of the western United States. The objectives of the study were: (1) to evaluate the index, compaction, and hydraulic properties of blended mixtures of two on-site borrow soils (i.e., fine sand and high plasticity clay) for potential use as CCL material; and (2) to develop material and compaction requirements for a CCL mixture to achieve a field hydraulic conductivity (k_F) $\leq 10^{-9}$ m/s upon construction. Three candidate mixtures (40%, 50%, and 60% borrow clay by dry wt.) were characterized and subjected to laboratory compaction and hydraulic conductivity (k_L) testing to establish appropriate design mixture proportions and an acceptable compaction zone (ACZ) based on the line-of-optimums method. Measured plasticity index (PI) values for the mixtures (PI = 16 to 24) all meet the minimum PI required for the CCL (PI ≥ 10) and are considerably lower than the PI of the borrow clay alone (PI = 36 to 49). Thus, the mixtures are more suitable than the borrow clay for limiting shrinkage potential upon drying. Test results also indicate that: (1) the compaction behaviour of all three mixtures can be represented adequately by a common line of optimums; and (2) all test specimens exhibited $k_L \leq 10^{-9}$ m/s. Based on these results, a mixture containing 55 \pm 5% of the on-site borrow clay is recommended for the CCL. The proposed ACZ for the design CCL mixture encompasses only those test specimens that exhibited $k_L \leq 2 \times 10^{-10}$ m/s in order to accommodate potential differences between k_L and k_F due to scale effects. A robust field testing program is recommended to verify that the material and compaction requirements have been achieved and that $k_F \leq 10^{-9}$ m/s for the constructed CCL.

INTRODUCTION

A tailings storage facility (TSF) is being designed to manage tailings from a proposed uranium mill in an arid region of the western United States. The final TSF is expected to consist of dual 16-ha (40-acre) cells designed to accept tailings deposited using conventional slurry discharge methods. However, construction of the TSF is expected to be performed in stages, with a 12-ha (30-acre) tailings cell being constructed in the first stage. The layout of this tailings cell is shown in Fig. 1. This paper deals with the design approach used to establish proposed material and compaction specifications for the compacted clay liner (CCL) portion of the liner system for the tailings cell.

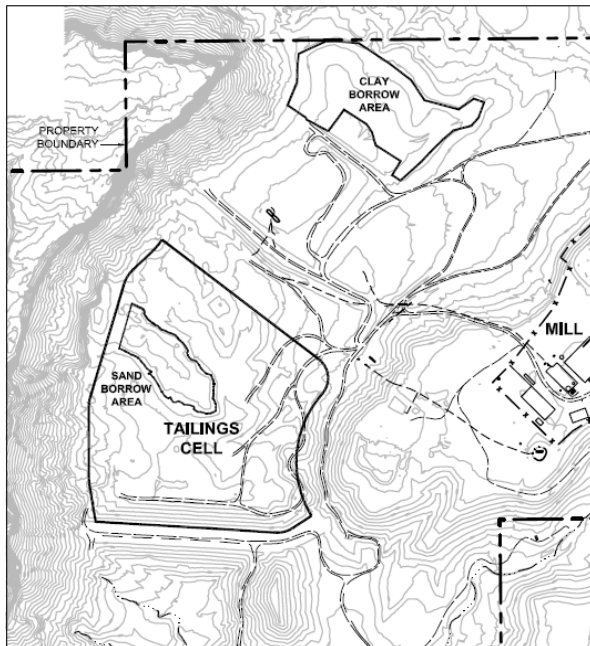


Figure 1. Plan view of proposed tailings cell and on-site borrow areas.

Liner Requirements

State regulations require the use of a liner system under the tailings that is designed and constructed to prevent migration of wastes out of the TSF during the active life

(including the closure period) of the facility. A multilayered liner system is proposed for the TSF in order to meet this performance requirement. The proposed liner system includes a minimum 305-mm (12-inch) CCL overlain by two 1.5-mm (60-mil) HDPE geomembranes that are separated by a leak detection system. A geotextile cushion layer, leachate collection layer, and sand filter/separation layer also are included above the primary geomembrane.

The CCL also is subject to the following index and hydraulic property requirements: (1) a maximum particle size of 25.4 mm (1 inch); (2) a minimum of 30 percent fines (i.e., passing the 0.075-mm sieve), (3) a minimum plasticity index (PI) of 10, and (4) a maximum field hydraulic conductivity (k_F) of 10^{-9} m/s. No specific restrictions have been established for the Unified Soil Classification System (USCS; ASTM D2487) soil types that may be used for the CCL, and no maximum allowable PI has been specified for the CCL material. However, field data from Benson et al. (1999) show that many CCLs exhibiting $k_F \leq 10^{-9}$ m/s have been constructed using soils that classify as low plasticity clay (i.e., USCS CL) and exhibit a PI of 30 or less. In addition, Daniel and Wu (1993) suggest that clayey sand (i.e., USCS SC) may be the most appropriate soil type for barriers at arid sites, since these soils can provide low hydraulic conductivity as well as low shrinkage potential upon drying. Daniel and Wu (1993) further recommend that engineered clay/sand mixtures be considered for soil barriers at arid sites when natural clayey sand is not available.

On-Site Soils for Liner Construction

The project site shown in Figure 1 occupies a broad valley flanked by a high, narrow sandstone mesa along the west side and a low bluff along the east side. The

depositional environment is primarily aeolian, with isolated to extensive surficial deposits underlain by weathered to unweathered Entrada Sandstone. The surficial deposits typically consist of fine, poorly-graded sand with silt (i.e., USCS SM and SP-SM).

The site is essentially devoid of borrow material exhibiting the required properties for CCL material as described above, with the exception of an existing stockpile of imported clay located in the northern portion of the site (see Figure 1). The clay was imported during previous construction in the 1980s from an off-site source located northwest of the site. Although properties of the stockpiled clay were not available at the time of this study, results of prior tests on clay samples collected from the off-site source area indicate that the off-site clay is highly plastic (i.e., USCS CH), with PI values typically ranging between 30 and 85 and fines contents between 70 and 90%. These prior test results suggested that the on-site clay likely would exhibit the required material properties for the CCL. However, while use of the on-site clay stockpile for CCL construction is desirable from a cost standpoint, the clay stockpile volume (i.e., ~38,000 m³) is less than the estimated total volume needed for construction of the tailings cell CCL (i.e., ~50,000 m³). Also, given the high PI values and fines contents measured in the off-site clay, the potential for desiccation cracking that could compromise the hydraulic performance of a CCL constructed entirely of this clay is a major concern.

Based on the above, the purpose of this study was to evaluate the potential for engineering an appropriate CCL material of sufficient volume by mixing the on-site borrow clay with the on-site borrow sand. The overall design objective was to establish an acceptable range of mixture proportions

and compaction properties, not only to meet the aforementioned material and hydraulic requirements for the CCL but also to reduce the potential for degradation of CCL hydraulic conductivity due to desiccation cracking. With regard to this latter issue, the specific design goal was to create a material that would classify as CL or SC and exhibit $PI \leq 30$. A candidate borrow area of on-site sand within the tailings cell footprint (~40,000 m³; see Figure 1) was identified for this study based on prior site characterization data. The remaining sections of this paper describe the testing program conducted to characterize the borrow materials and candidate design mixtures, the results of laboratory compaction and hydraulic conductivity tests on the candidate mixtures, and the resulting recommendations for construction of the CCL.

BORROW AREA CHARACTERIZATION

A field investigation of the two on-site borrow sources shown in Figure 1 was performed to collect samples of the clay and sand materials for visual-manual identification (ASTM D2488) and laboratory characterization. Each borrow area was subdivided into eight zones such that each zone represented approximately 5,000 m³ of borrow material. A test pit was excavated within each zone, and the excavated materials were logged and transported to the laboratory for evaluation of natural water content (ASTM D2216), Atterberg limits (ASTM D4318), grain-size distribution (ASTM D422), and specific gravity (ASTM D854). The water content, grain size, and Atterberg limits tests were performed at a frequency of one test per 5,000 m³ of borrow, in accordance with EPA-recommended testing frequencies for waste containment facilities (Daniel and Koerner 1993). In addition, samples of the on-site

clay were subject to X-ray diffraction analyses to characterize the mineralogy of the clay.

The results of the index tests described above are summarized in Table 1 for each of the eight zones of borrow sand (i.e., S1 through S8) and borrow clay (i.e., C1 through C8). The results show that the borrow sand classifies as silty sand (USCS SM) in all cases. Approximately 76 to 87% of the particles are within the sand range, whereas the remaining fraction is primarily fines. Little or no gravel was present in the test pit samples. The grain size distribution plots for the sand samples, shown in Fig. 2a, indicate that the sand is uniform and contains predominantly fine sand particles (i.e., 0.425 mm to 0.075 mm).

The borrow clay classifies as high-plasticity (fat) clay (USCS CH), with PI values between 36 and 49. The fines contents range between 75 and 89%, and the clay contents (i.e., particle sizes ≤ 0.002 mm) range between 31 and 44% (see Table 1 and Figure 2b). The X-ray diffraction results show that the borrow clay contains >70% of highly active clay minerals, namely montmorillonite and mixed-layer illite/smectite. Thus, the results confirm that the characteristics of the borrow clay, while excellent for achieving low hydraulic conductivity, could render the CCL susceptible to desiccation damage.

Table 1. Index test results for samples of borrow sand and borrow clay.¹

Borrow Area	Sample ID	G_s	w_n (%)	LL/PL/PI	Particle Sizes (%)				USCS Type
					Gravel	Sand	Fines	Clay ²	
Sand	S1	---	3.1	NP	0	83.4	16.6	4.1	SM
	S2	2.64	3.5	NP	0	79.2	20.8	6.7	SM
	S3	---	2.2	NP	0.2	86.3	13.5	4.8	SM
	S4	---	2.7	NP	0	84.6	15.4	4.0	SM
	S5	2.64	5.7	NP	0	86.4	13.6	6.6	SM
	S6	---	2.6	NP	0.6	76.7	22.7	8.0	SM
	S7	---	2.7	NP	2.9	76.6	20.5	8.1	SM
	S8	---	4.5	NP	0	86.4	13.6	7.1	SM
Clay	C1	---	22.9	76/26/49	0	12.9	87.1	43.5	CH
	C2	---	23.0	61/24/37	0	18.9	81.1	36.4	CH
	C3	2.76	18.6	62/24/38	0	17.1	82.9	37.2	CH
	C4	---	14.8	65/26/39	0	19.8	80.2	31.9	CH
	C5	---	21.0	68/26/42	0	15.1	84.9	36.9	CH
	C6	2.75	22.2	75/28/47	0	11.4	88.6	36.2	CH
	C7	---	17.4	56/20/36	0	17.8	82.2	32.1	CH
	C8	---	14.6	62/26/36	0	24.3	75.7	31.3	CH

¹ G_s = Specific gravity (ASTM D854); w_n = natural water content (ASTM D2216); LL/PL/PI = liquid limit/plastic limit/plasticity index (ASTM D4318); USCS = Unified Soil Classification System (ASTM D2487); NP = non-plastic.

² Clay fraction consists of particles with diameter ≤ 0.002 mm.

TESTING PROGRAM

Mixture Preparation and Characterization

Based on the results in Table 1, three mixtures of the borrow sand and borrow clay were developed as candidate materials for the CCL. The mixtures were prepared using composite borrow clay (CBC) from test pit samples C2, C3, C5, and C7 and composite borrow sand (CBS) from test pit samples S1, S3, S4, and S5. The proportions (by dry wt.) of the three mixtures were as follows: (1) 40% CBC/60% CBS; (2) 50% CBC/50% CBS; and (3) 60% CBC/40% CBS.

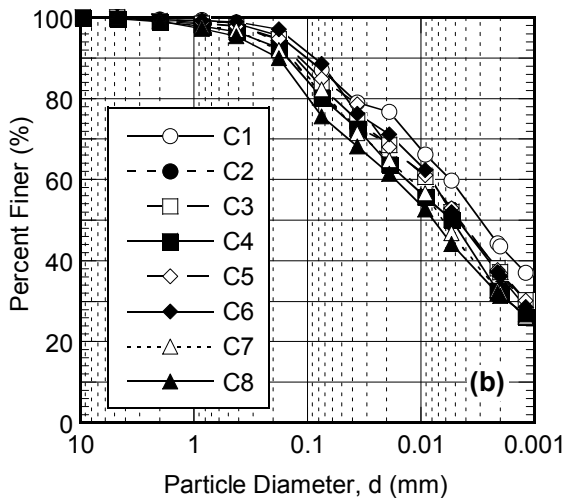
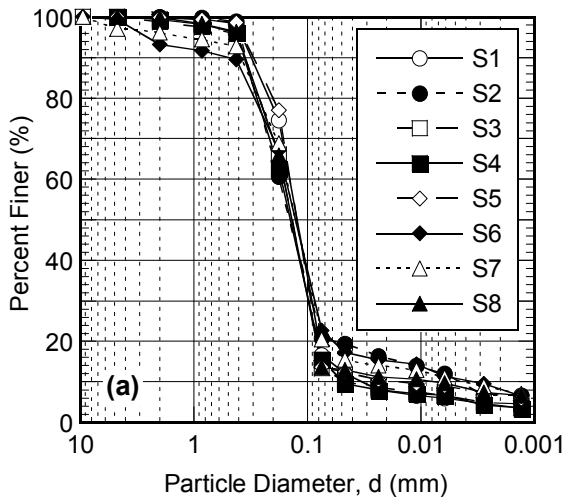


Figure 2. Measured grain-size distributions for (a) borrow sand and (b) borrow clay.

The composite borrow soils (CBS and CBC) and the three design mixtures (40% CBC, 50% CBC, and 60% CBC) were tested for grain-size distribution and Atterberg limits. The results of these tests are summarized in Table 2 along with the corresponding USCS classifications for each material, and the measured grain-size distributions are illustrated in Fig. 3. The results show that the three design mixtures all meet the material requirements for the CCL (i.e., $PI \geq 10$ and fines content $\geq 30\%$) but exhibit reduced plasticity and contain more sand relative to the pure borrow clay. Values of PI less than 30 were obtained for all three design mixtures, with the lowest PI value (i.e., $PI = 16$) obtained for the mixture containing 40% CBC and the highest value (i.e., $PI = 24$) obtained for the mixture containing 60% CBC. The mixture containing 40% CBC classifies as clayey sand (USCS SC), while the mixtures containing 50% CBC and 60% CBC classify as lean clays (USCS CL). Thus, the design mixtures exhibit the index properties established as the design goal for reducing the desiccation potential of the CCL.

Table 2. Index properties of composite borrow soils and candidate design mixtures.

Sample ID	Fines Content (%)	LL/PI	USCS Soil Type
CBS	83.9	NP	SM
CBC	19.6	75/49	CH
40% CBC/60% CBS	43.9	33/16	SC
50% CBC/50% CBS	50.7	35/18	CL
60% CBC/40% CBS	61.2	42/24	CL

CBS = composite borrow sand, CBC = composite borrow clay, LL = liquid limit, PI = plasticity index, NP = non-plastic.

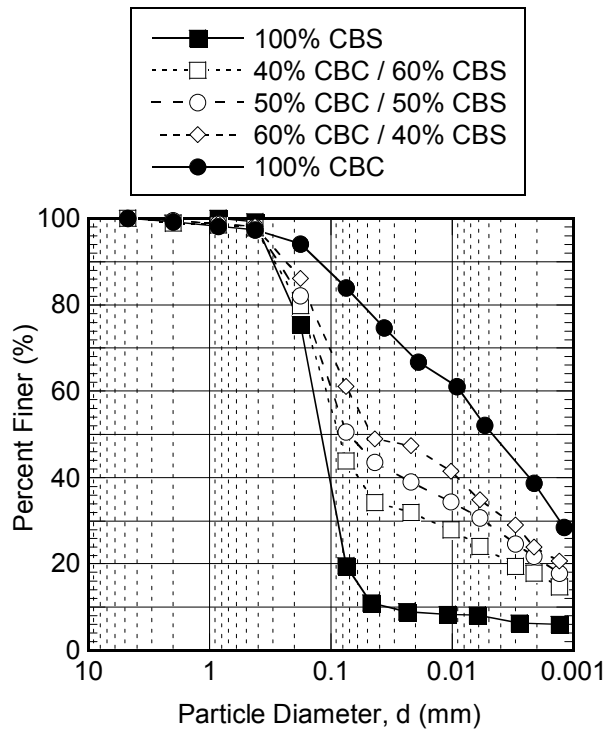


Figure 3. Measured grain-size distributions for the composite borrow soils (CBS and CBC) and candidate design mixtures.

Compaction wet of the line of optimums has been shown to be effective for constructing CCLs that exhibit $k_F \leq 10^{-9}$ m/s and generally are free of macroscopic defects (e.g., interclod voids or cracks) that tend to cause scale dependence of hydraulic conductivity (Benson and Daniel 1990, Benson and Boutwell 1992, Benson et al. 1999). Benson et al. (1999) state that a key to achieving $k_F \leq 10^{-9}$ m/s is to ensure $P_o > 70$ to 80%, where P_o is the percentage of field measured moisture content-dry unit weight ($w-\gamma_d$) points that lie on or wet of the line of optimums.

The line-of-optimums method involves compaction testing of the CCL material at three different compaction energies to establish the line of optimums, or the line connecting the optimum $w-\gamma_d$ points for the three compaction curves. Once the line of optimums is established, laboratory hydraulic

conductivity (k_L) tests are conducted on specimens compacted at water contents typically ranging from slightly dry to wet of the line of optimums. The ACZ then is developed as the zone of γ_d and w encompassing those values of k_L that are less than or equal to a maximum allowable k_L value. The ACZ may be further restricted to exclude certain combinations of γ_d and w that are considered undesirable on the basis of other factors, such as shear strength, shrink/swell potential, and constructability (see Daniel and Benson 1990).

The three compaction energies employed in this study were modified Proctor energy (2,700 kN-m/m³; see ASTM D1557), standard Proctor energy (600 kN-m/m³; see ASTM D644), and “reduced” Proctor energy (360 kN-m/m³). All compaction curves were developed using a minimum of five points, with no two adjacent data points separated by more than three percentage points on the water content axis.

Flexible-wall k_L tests were conducted on selected specimens obtained from the compaction tests for each mixture. All specimens chosen for k_L testing were compacted near or wet of the line of optimums for the given mixture. The tests were performed in accordance with Method C (falling headwater-rising tailwater) of ASTM D5084, with an average effective stress of 34.5 kPa and a hydraulic gradient ≤ 30 . The standard water used for backpressure saturation and permeation was tap water, and all specimens were backpressure saturated until a B-value of 0.95 or greater was measured. Termination criteria for flow balance and steadiness as defined in ASTM D5084 were met in all cases.

RESULTS AND DISCUSSION

Compaction Tests

Compaction tests at standard Proctor energy were conducted on all three of the clay/sand mixtures. In addition, compaction tests at modified and reduced Proctor energies were conducted on the mixtures containing 50% CBC and 60% CBC. The results of these tests are summarized in Table 3 and illustrated in Figure 4. The compaction curves in Figure 4 were fitted to the data systematically using least-squares, third-order polynomial regression as described by Howell et al. (1997). The values of maximum dry unit weight ($\gamma_{d,max}$) and optimum moisture content (w_{opt}) in Table 3 were obtained using the best-fit, third-order equations. Values of degree of saturation, S , were computed using a weighted average G_s of 2.7 based on the individual G_s values in Table 1.

The compaction test results are consistent with expected behavior for compacted soils, i.e., for a given mixture, $\gamma_{d,max}$ increases and w_{opt} decreases with increasing compaction energy. The data also show that decreasing the CBC content yields higher $\gamma_{d,max}$ and lower w_{opt} for a given compaction energy. However, values of degree of saturation at optimum (i.e., S_{opt}) are reasonably similar for all mixtures and compaction energies (S_{opt} between 81.8% and 88.3%; see Table 3). Past researchers have observed that the line of optimums for a compacted clay soil tends to lie parallel to lines of constant S and typically corresponds to a contour of $S \sim 85\%$ (e.g., Boutwell and Hedges 1989, Benson et al. 1994, Benson et al. 1999). The mixture containing 40% CBC was eliminated from further consideration based on the k_L test results, as explained in greater detail below. The average S_{opt} value for all of the

compaction tests conducted on mixtures containing 50% CBC and 60% CBC is 84.9%. Thus, the contour corresponding to $S = 85\%$ was established as the design line of optimums in this study (see Figure 4).

Hydraulic Conductivity (k_L) Tests

The compaction test specimens selected for k_L testing are denoted by the closed symbols in Figure 4. All but two of the k_L test specimens were compacted at or wet of the design line of optimums defined by $S = 85\%$. The final values of k_L for each of these specimens after ASTM D5084 termination criteria had been reached are provided along with the corresponding compaction properties in Table 3.

The results in Table 3 show that all of the test specimens exhibited a final $k_L \leq 10^{-9}$ m/s, regardless of mixture proportions or compaction energy. However, the k_L value for the standard Proctor test specimen containing 40% CBC was only slightly lower than 10^{-9} m/s (i.e., 8.5×10^{-10} m/s), whereas k_L values for the standard Proctor test specimens containing 50% CBC and 60% CBC were $\leq 3.8 \times 10^{-10}$ m/s in all cases. Thus, the 40% CBC mixture was eliminated from further consideration, and the design mixture proportions for the CCL were selected as $55 \pm 5\%$ borrow clay.

Values of k_L for mixtures containing 50% CBC and 60% CBC are plotted in Figure 5a as a function of compaction moisture content relative to the optimum moisture content (i.e., $w - w_{opt}$) for each compaction energy. Although all of the k_L values for these two mixtures are $\leq 10^{-9}$ m/s, the results in Figure 5a show a trend of decreasing k_L as the compaction moisture content transitions from the dry side to the wet side of optimum.

Table 3. Compaction and hydraulic conductivity test results for candidate design mixtures.

CBC Content (%)	Compaction Energy	Compacted Specimens				w _{opt} (%)	γ _{d,max} (kN/m ³)	S _{opt} (%)
		w (%)	□ _d (kN/m ³)	S (%)	K _L (m/s)			
40	Standard	14.9	16.4	65.7		17.8	16.7	81.8
		16.9	16.6	76.8				
		19.0	16.7	87.5	8.5x10 ⁻¹⁰			
		20.4	16.4	90.0				
		23.1	15.8	92.0				
50	Modified	10.4	17.4	54.2		13.8	18.4	84.0
		12.6	18.0	72.8				
		13.6	18.4	83.9	2.6x10 ⁻¹⁰			
		16.0	18.0	91.6				
		18.1	17.4	93.4	5.6x10 ⁻¹¹			
	Standard	14.4	16.0	59.5		19.1	16.3	82.1
		16.8	16.2	71.4				
		18.3	16.3	78.7	3.8x10 ⁻¹⁰			
		21.2	16.2	90.0				
		23.1	15.9	93.6	6.0x10 ⁻¹¹			
		25.1	15.3	93.3				
	Reduced	18.5	14.8	63.5		23.6	15.4	88.3
		20.6	15.1	73.5				
		22.3	15.3	83.1				
		23.8	15.3	88.7	1.1x10 ⁻¹⁰			
26.6		14.9	92.0					
60	Modified	11.4	17.8	62.7		14.0	18.3	84.0
		12.8	18.3	76.8				
		15.2	18.2	90.2	5.8x10 ⁻¹¹			
		17.5	17.6	94.4				
		19.6	17.1	97.2	7.2x10 ⁻¹¹			
	Standard	16.9	15.5	64.9		20.7	16.0	85.1
		19.2	15.9	77.6				
		21.2	16.0	88.0	1.9x10 ⁻¹⁰			
		22.9	15.7	90.7				
		24.6	15.4	92.1	7.4x10 ⁻¹¹			
	Reduced	19.5	14.6	64.6		24.7	14.9	85.8
		21.8	14.7	73.6				
		23.3	14.8	79.8				
		25.6	14.9	88.7	7.5x10 ⁻¹¹			
		27.1	14.5	89.3				

CBC = composite borrow clay; w = compaction moisture content; □_d = dry unit weight; S = compacted degree of saturation; k_L = laboratory hydraulic conductivity; w_{opt} = optimum moisture content; □_{d,max} = maximum dry unit weight; S_{opt} = degree of saturation at optimum.

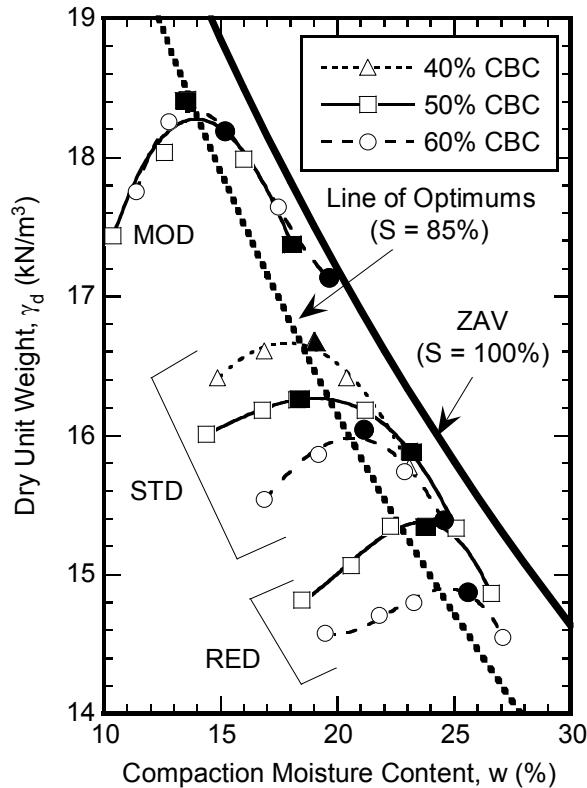


Figure 4. Compaction test results for candidate design mixtures using modified (MOD), standard (STD) and reduced (RED) compaction energies (ZAV = Zero Air Voids). Closed symbols represent k_L test specimens.

Values of k_L for specimens with $w > w_{opt}$ are $< 2 \times 10^{-10}$ m/s in all cases, regardless of compactive effort. Similarly, all specimens compacted wet of the design line of optimums (i.e., $S = 85\%$) exhibit $k_L < 2 \times 10^{-10}$ m/s as shown in Figure 5b. Thus, the $S = 85\%$ contour is a reasonable approximation of the line of optimums for mixtures containing $55 \pm 5\%$ borrow clay.

Acceptable Compaction Zone (ACZ)

A common approach for defining an ACZ is to set the maximum allowable k_L at the regulatory limit (i.e., 10^{-9} m/s in this case). Since $k_L \leq 10^{-9}$ m/s was achieved for all test specimens containing 50% CBC and 60% CBC, the ACZ for a design mixture

containing $55 \pm 5\%$ borrow clay could encompass all of the combinations of w and γ_d represented by these specimens. However, the regulatory limit is based on larger-scale k_F values typically measured via *in situ* methods (see Daniel 1989) or lab tests on large-diameter (e.g., 300-mm) specimens prepared from recovered block samples (see Trast and Benson 1995). The potential for deviations between smaller-scale k_L values and larger-scale k_F values measured on constructed CCLs has been well documented (e.g., see Day and Daniel 1985, Benson and Boutwell 1992, Benson et al. 1994).

Benson et al. (1999) indicate that k_F and k_L values typically are comparable for liners constructed primarily wet of the line of optimums (i.e., $P_o > 80\%$, where P_o is as defined previously). However, differences between k_F and k_L may still be significant from a regulatory compliance standpoint, even if $P_o > 80\%$ is achieved for the CCL. Benson et al. (1999) present k_F and k_L data for 85 different CCLs (i.e., 8 in-service liners and 77 test pads) constructed across North America. The k_F values were measured using sealed double-ring infiltrometer (SDRI) tests, lysimeters, dual stage borehole (DSB) tests, or flexible-wall tests on 300-mm-diameter specimens prepared from recovered block samples. Values of k_F for the CCLs exhibiting $P_o > 80\%$ (i.e., 44 total points of k_F versus k_L) are plotted against the corresponding k_L values in Figure 6. The results indicate that $k_F > k_L$ for many of these CCLs, illustrating the risk associated with setting the maximum k_L at the regulatory limit. A more conservative approach for defining an ACZ is to set a maximum allowable k_L that accommodates potential differences between k_L and k_F due to scale effects. For example, a vast majority of the data ($\sim 89\%$) in Fig. 6 plot below the line corresponding to $k_F/k_L = 5$.

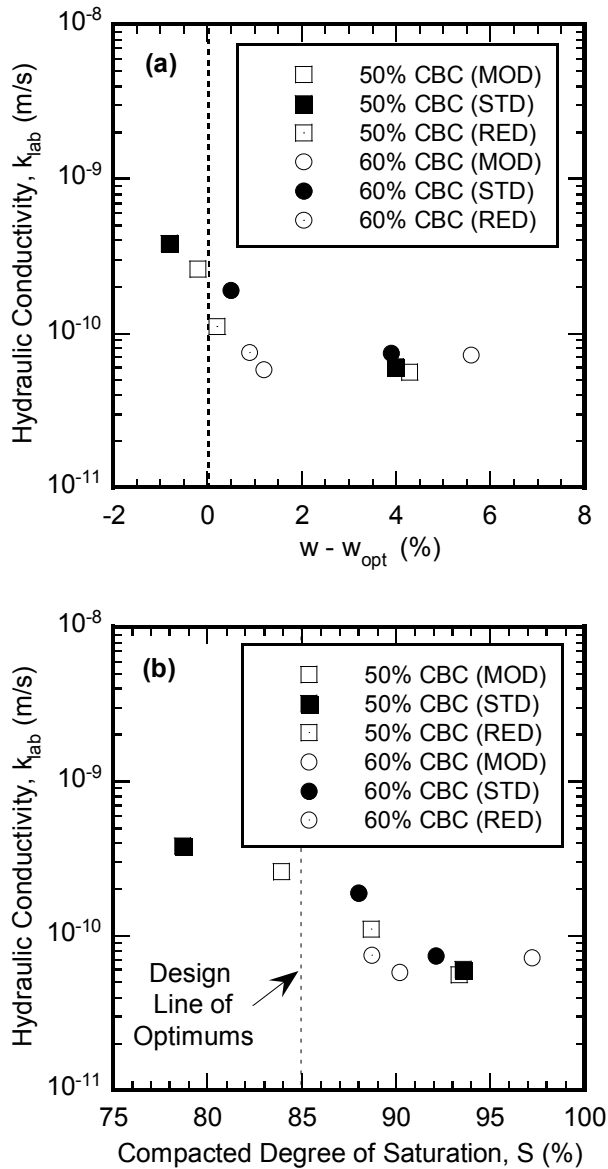


Figure 5. Hydraulic conductivity (k_L) as a function of (a) moisture content relative to optimum, and (b) degree of saturation.

Thus, these data suggest that a maximum allowable k_L of 2×10^{-10} m/s provides a reasonable level of confidence that $k_F \leq 10^{-9}$ m/s will be achieved for a well-built CCL.

The proposed ACZ for the design mixture (i.e., $55 \pm 5\%$ borrow clay) is illustrated in Figure 7. The ACZ is bounded by the design line of optimums ($S = 85\%$) and, thus,

should accommodate as much as a five-fold increase in k_F relative to k_L (see Figure 5). As shown in Figure 7, all combinations of w and γ_d reflected by the test specimens exhibiting $k_L > 2 \times 10^{-10}$ m/s are excluded from the ACZ. In addition, the ACZ includes only values of compaction moisture content w between 14% and 25%. The upper range of w has been established to ensure adequate workability and shear strength.

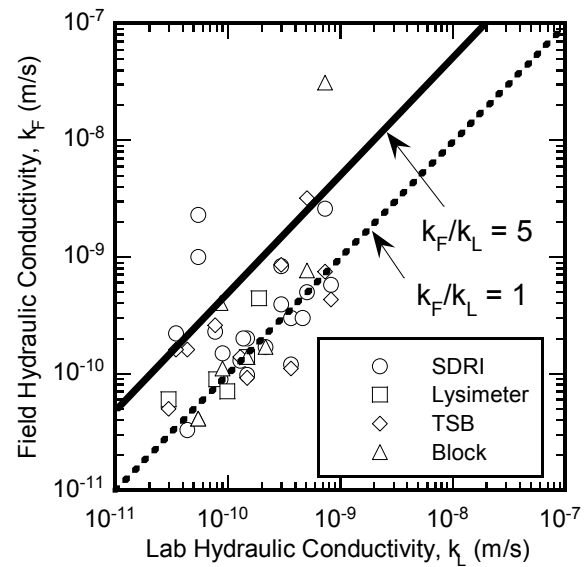


Figure 6. Field hydraulic conductivity plotted against lab hydraulic conductivity (75-mm undisturbed specimens) for CCLs compacted primarily wet of the line of optimums (i.e., $P_o > 80\%$) (data from Benson et al. 1999).

Finally, the ACZ is limited to a minimum γ_d of 15.3 kN/m^3 , which is the lowest γ_d for which $k_L \leq 2 \times 10^{-10}$ m/s was demonstrated for specimens with $w < 25\%$. This minimum γ_d corresponds to $\sim 95\%$ relative compaction (based on standard Proctor energy) for the mixture containing 60% borrow clay. These restrictions result in a reasonably conservative ACZ that still provides the earthwork contractor with a sufficiently broad range of allowable compaction properties.

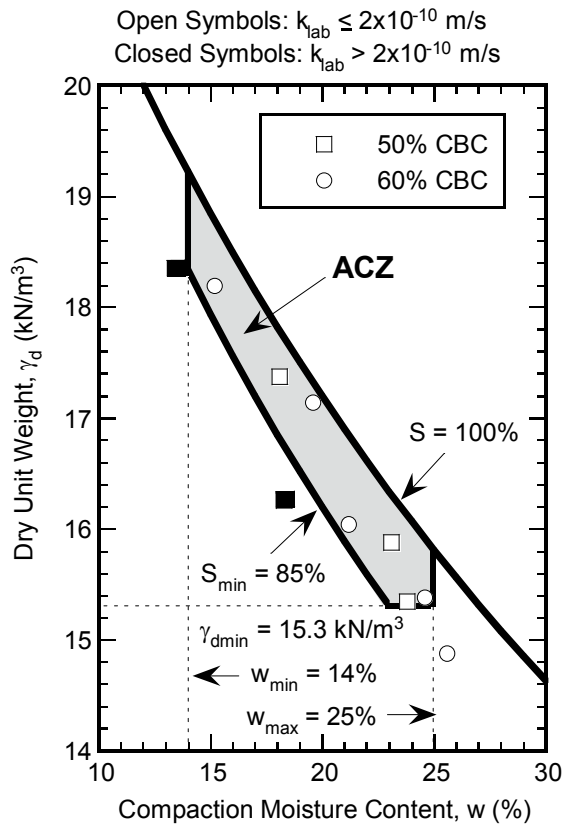


Figure 7. Acceptable compaction zone (ACZ) for tailings cell CCL based on design mixture containing 55±5% borrow clay.

CONCLUSIONS

This paper presents a unique case study involving application of the line of optimums approach for design of a mixed clay/sand CCL. The test results illustrate that the clay/sand mixtures within the range of proportions tested can be represented adequately by a single line of optimums corresponding to 85% saturation. The relative insensitivity of optimum saturation S_{opt} to differences in compaction energy and slight changes in soil texture is consistent with general observations made in previous work and allows for establishment of a single acceptable compaction zone (ACZ) for a design mixture containing 55±5% borrow clay. The ACZ recommended for

the design CCL mixture allows for as much as a five-fold increase in field hydraulic conductivity k_F relative to laboratory hydraulic conductivity k_L .

Although this paper is focused on the design basis used to establish appropriate mixture proportions and compaction requirements for the mixed clay/sand CCL, several key construction issues still must be addressed to ensure that the CCL is constructed properly and exhibits acceptable k_F . Most notably, the mixing process used to prepare the CCL mixture in the field must be sufficient to achieve uniform and thorough mixing of the borrow clay and borrow sand. Proper moisture conditioning and adequate hydration of the clay also are critical aspects for successful construction of this CCL. Robust field testing is recommended as part of either a test pad program or slow-start phase of CCL construction to demonstrate the efficacy of the material preparation and placement methods for achieving the required k_F .

REFERENCES

- Benson, C.H. and Daniel, D.E. (1990). Influence of clods on hydraulic conductivity of compacted clay. *J. Geotech. Engrg.*, ASCE, 116(8), 1231–1248.
- Benson, C.H., Daniel, D.E., and Boutwell, G.P. (1999). Field performance of compacted clay liners. *J. Geotech. and Geoenviron. Engrg.*, ASCE, 125(5), 390-403.
- Benson, C.H. and Boutwell, G.P. (1992). Compaction control and scale-dependent hydraulic conductivity of clay liners. *Proc., 15th Annual Madison Waste Conf.*, University of Wisconsin, Madison, WI, 62-83.

- Benson, C.H., Hardianto, F., and Motan, E. (1994). Representative specimen size for hydraulic conductivity assessment of compacted soil liners. *Hydraulic conductivity and waste contaminant transport in soils, ASTM STP 1142*, D. Daniel and S. Trautwein, eds., ASTM, West Conshohocken, PA, 3-29.
- Boutwell, G.P. and Hedges, S. (1989). Evaluation of water-retention liners by multivariate statistics. *Proc., 12th ICSMFE*, Balkema, Rotterdam, The Netherlands, 815–818.
- Daniel, D.E. (1989). In situ hydraulic conductivity tests for compacted clay liners. *J. Geotech. Engrg.*, ASCE, 115(9), 1205-1227.
- Daniel, D.E. and Benson, C.H. (1990). Water content-density criteria for compacted soil liners. *J. Geotech. Engrg.*, ASCE, 116(12), 1811-1830.
- Daniel, D.E. and Koerner, R.M. (1993). *Technical Guidance Document: Quality Control and Quality Assurance for Waste Containment Facilities*. EPA/600/R-93/182, U.S. Environmental Protection Agency, Cincinnati, OH, 305 p.
- Daniel, D.E. and Wu, Y. (1993). Compacted clay liners and covers for arid sites. *J. Geotech. Engrg.*, ASCE, 119(2), 223-237.
- Day, S. and Daniel, D.E. (1985). Hydraulic conductivity of two prototype clay liners. *J. Geotech. Engrg.*, ASCE, 111(8), 957-970.
- Howell, J.L., Shackelford, C.D., Amer, N.H., and Stern, R.T. (1997). Compaction of sand-processed clay soil mixtures. *Geotech. Testing J.*, ASTM, 20(4), 443-458.
- Majeski, M.J. and Shackelford, C.D. (1997). Evaluating alternative water content-dry unit weight criteria for compacted clay liners. *Engineering Geology and the Environment*, P.G. Marinos, G.C. Koukis, G.C. Tsiambaos, and G.C. Stournaras, eds., A.A. Balkema, Rotterdam, 1989-1995.
- Trast, J. and Benson, C.H. (1995). Estimating field hydraulic conductivity at various effective stresses. *J. Geotech. Engrg.*, ASCE, 121(10), 736-740.

CLOSURE SYSTEM FOR WASTE SITES USING STRUCTURED MEMBRANES AND SYNTHETIC GRASS COMPOSITE

Mr. Michael R. Ayers, PE and Mr. Jose L. Urrutia, PE

Closure Turf City; Duluth, GA USA

ABSTRACT: As a response to numerous failures of environmental closures at waste sites, engineers have looked at new approaches in establishing a more stable and environmentally sound solution. One potential solution has been the implementation of exposed geomembrane systems. This has had limited success, and has presented many new problems. The Closure Turf approach however, has shown great improvement and incorporates an exposed geomembrane system along with a combination of synthetic turf and a highly transmissive structured geomembrane. The Closure Turf system provides for a more stable and rapid installation, reduced gas emissions, a reduction of dirt usage, and lower suspended solids in the surface water. The system also eliminates the need for on-going maintenance as required by a vegetative closure, such as re-seeding, fertilizing, irrigation and mowing. The draining system of the approach allows installation of the cover on very steep slopes and does not require the use of extensive anchoring system to resist wind uplift as required in previous exposed synthetic systems.

INTRODUCTION

Exposed geomembranes cover systems (EGCS) have been used for construction of closures at landfill sites in the United States. The EGCS represents a new direction in landfill cover system designs and construction because the EGCS does not include the overlying soil and drainage layer component of a typical final cover system. Therefore, the EGCS can be installed at significantly less cost than the typical final caps at landfills, and other types of waste depositories. Such covers with just the exposed membrane have negative aesthetics. Additionally, the approach requires numerous anchors and very closely spaced

trenches to resist wind uplift on the exposed membrane.

The waste disposal industry continues to search for improved cover systems which are effective and economical and which meet the various local, state and US federal environmental laws, rules and guidelines for these systems. This new approach using synthetic turf and structured geomembranes for final landfill covers provides a pleasant visual appearance, and a drainage system that can handle severe wind and intense rain events. This makes it possible for applications on very steep slopes which typically occur at landfills and disposal piles. This approach also provides anchoring ballast that resists significant uplift forces

cause by hurricane force wind loads and achieves this without the use of anchor trenches. Other difference between this approach and the prior art of the EGCS is

the ability of the composite material to provide a high angle of internal friction to allow for the placement on steep slopes.

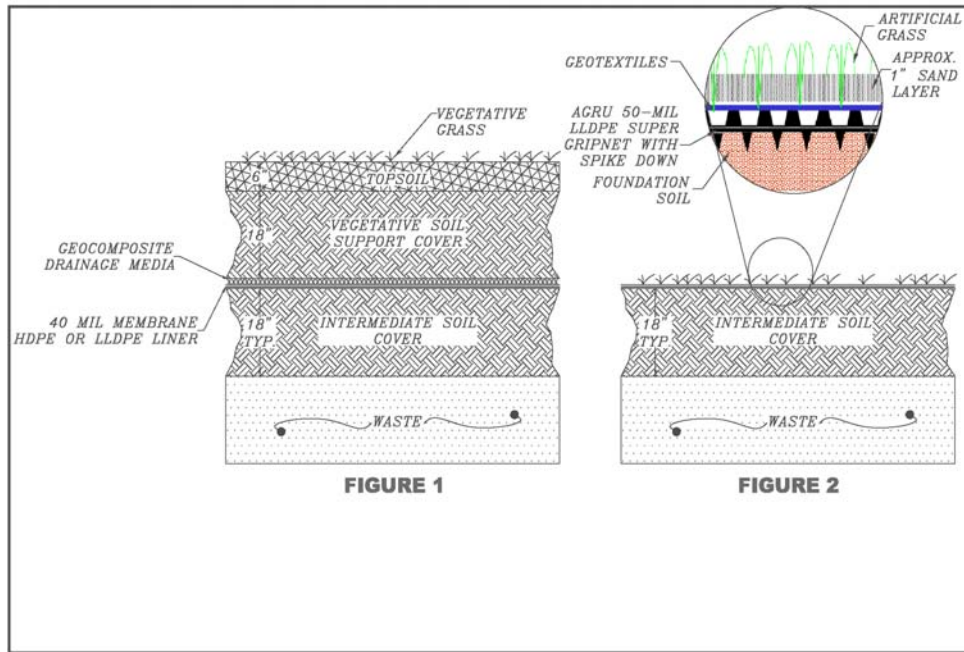


Figure 1. Standard vs. Synthetic Grass – Structured Geomembrane Composite

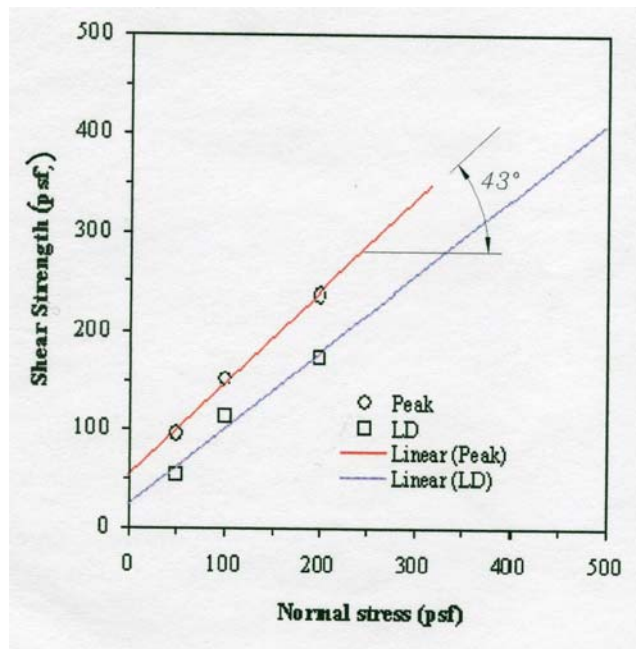


Figure 2.

The internal friction angle and ballast design provides for a highly stable system without expensive and intrusive surface anchor trenches. The system provides the required hydraulic transmissivity for the drainage Component as indicated in laboratory evaluations.

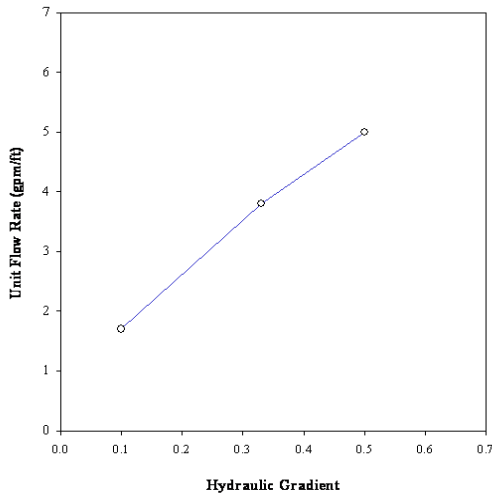


Figure 3.

APPLICATION

The composite material of this approach allows owners and operators to realize significant cost savings by constructing a cover system with the synthetic grass that does not require the vegetative support and topsoil layer of the typical final cover system. This synthetic grass/impermeable layer is particularly applicable to sites where the design life of the cover system is relatively short (i.e., 10 to 20 years), when future removal of the cover may be required (e.g., for landfill reclamation), when the landfill slopes are too steep to allow for the placement of soil on top of the liner, when cover soil can not be purchased, when the landfill may be expanded vertically at a later date or simply to allow the construction of rapid closures to control emissions and odors.

The cover system of this approach is designed from the bottom up with a lower impermeable layer placed over the soil intermediate cover comprising (1) a drain liner geomembrane or textured geomembrane liner and a geonet drainage media, or alternatively a drain liner with studs incorporated in the HD polyethylene sheet that acts as drainage (AGRU US Patent No. 5.258.217) (2) the synthetic turf that is engineered with polyethylene fibers with a length of 2 to 2.5 inches tufted into two fabrics consisting of needle punch non-woven polyester and woven polypropylene geotextiles and (3) a sand layer approximately 0.5 to 1.0 inch that is placed as infill, producing a weight of 10 pounds per square foot, to ballast the material and protect the system against wind uplift. With this approach an anchoring system typically associated with exposed geomembrane covers will not be required. The sand will provide additional protection of the geotextiles against UV light

The polyethylene yarns durability against UV light lends itself well to the closure cover on environmental projects. On landfills and mine piles, sliding of the cover along steep sideslopes is of primary concern, particularly after major storm events. The permeable turf percolates at different rates, such as approximately a rate of 180-gallons/sq ft/hr (0.2 cm/sec) or faster. During a rain event, the rainfall will penetrate quickly through the sand infill and drain directly in the geocomposite drainage system below. This allows minimizing erosion and maintaining stability of the sand infill. The infill is also held in place by the unique honeycomb structure of the synthetic grass that traps the sand to anchor and ballast the synthetic grass turf to the surface it covers

The selection of the chemical composition of the synthetic grass/impermeable membrane is a critical element of the design. The polymer should resist exposure to sunlight, which generates heat and contains ultraviolet radiation. The polymer yarns should not become brittle when subjected to low temperatures. The polyethylene grass filaments should have an extended operational life of at least 40 years. The selection of the synthetic grass color and texture should be aesthetically pleasing for the given geographic region.

PERFORMANCE ADVANTAGES

There are many advantages to the cover system of this approach, such as:

- ❑ There is an absence of soil cover, which will reduce construction costs depending on the availability of soil at the site.
- ❑ Aesthetics
- ❑ May reduce need for lower soil component.
- ❑ Reduces annual operation and maintenance requirement while providing superior and reliable/consistent aesthetics.
- ❑ Reduces the post closure maintenance costs of the cover.
- ❑ Systems works as a BMP dramatically reducing post-closure costs
- ❑ Can withstand hurricane-force winds as high as 120mph.

- ❑ Reduces the need for expensive riprap channels and drainage benches, with no substantial erosion or siltation problems, even during severe weather.
- ❑ Allows for steeper waste pile slopes, because there will not be soil stability problems either thru earthquakes or gas pressure build-up.
- ❑ Reduces infiltration thru the cap. Surface water is rapidly drained off and is not restricted by the hydraulic conductivity of the cover drainage system. As a result, the hydraulic head on the impermeable layer and subsequent infiltration into the waste are minimized. HELP infiltration models show that this type of cover will have less infiltration than current covers allowed by federal regulations.
- ❑ Clean water off cover, less treatment cost Less sediment build up
- ❑ Less post-closure liability exposure for municipalities should owner fail.

CONCLUSION

Closure Turf is the new generation of closure for landfills and mines where infiltration of liquids, surface run off and erosion control will cause problems at a later date. The economic benefits and with that lack of physical responsibility in the post closure scenario are invaluable to the clients be they private or public. Closure Turf provides superior and long lasting aesthetics while improving the way the problems in the past have been addressed

PERMEABILITY, PUNCTURE, AND SHEAR STRENGTH TESTING OF COMPOSITE LINER SYSTEMS UNDER HIGH NORMAL LOADS

Chris Athanassopoulos

CETCO, Hoffman Estates, Illinois, USA

Alyssa Kohlman

PE, Golden, Colorado, USA

Michael Henderson

Tetra Tech, Golden, Colorado, USA

Joseph Kaul

Kaul Corporation, Lakewood, Colorado, USA

John Boschuk

JLP Laboratories, Canonsburg, Pennsylvania, USA

INTRODUCTION

Geosynthetics, including geomembranes and geosynthetic clay liners (GCLs), are seeing increased usage in mining applications, such as tailings impoundments and heap leach pads. These applications can involve extreme conditions such as aggressive chemical environments and enormous compressive loads. Heap leach heights can reach 180 meters (600 feet), corresponding to normal loads of up to 3450 kPa (500 psi) on the leach pad liner system. Such loads exceed the limits of most standard laboratory testing devices, making it difficult to properly evaluate the behavior of geosynthetic materials in these applications. To address this limitation, CETCO and Tetra Tech performed the following laboratory evaluations of geomembrane and GCL performance under high normal loads:

Puncture

Heap leach pad fills are typically constructed by placing a layer of angular, large-diameter drainage rock (overliner) over the leach pad liner. Under load, geomembranes are vulnerable to damage from these large stones. There is evidence that liners at various facilities, including hazardous waste landfills, municipal landfills, surface impoundments, and mining heap leach facilities can experience leakage, and thus multiple liners, backup systems and monitoring systems are routinely included. Considering the recent price increases in precious and commodity metals, there may now be a stronger incentive to limit geomembrane punctures and pregnant leach solution (PLS) loss through liner systems in mining applications. Higher metals prices are also driving mining companies to design facilities that may be

closer to populated or environmentally sensitive areas. As a result, there is a trend toward improving the containment capabilities of lining systems installed in mines. A high-load shop press was fabricated to test the puncture resistance of different geomembranes, both with and without underlying GCLs, in contact with drainage rock under normal loads ranging from 1290 kPa (188 psi) to 5172 kPa (750 psi). These loads correspond to approximate ore heights of 45 to 183 meters (150 to 600 feet), with a factor of safety of 1.5. In addition to normal load, other variables examined included geomembrane type and thickness, GCL type, loading rate, and loading duration.

Permeability

Copper heap leaching requires the use of low-pH sulfuric acid solutions. Past research and experience have shown that GCL hydraulic performance can be negatively impacted by low pH or high ionic strength solutions (Jo et al., 2001). However, research has also shown that the effects of aggressive solutions on a GCL's hydraulic performance lessen at higher normal loads (Daniel, 2000 and Thiel and Criley, 2005). A high-load, rigid wall permeameter was constructed to test the long-term compatibility/permeability of GCL samples in contact with an acidic copper pregnant leach solution (PLS). The GCL samples were subjected to a hydraulic head of 1.4 meters (4.6 feet), and normal loads ranging from 34.5 to 3447 kPa (5 to 500 psi), to simulate the typical operational stages of a copper heap leach facility.

Shear Strength

Direct shear testing of geosynthetics is typically limited to loads less than 690 kPa (100 psi), representing 36 m (120 ft) of ore, which falls short of the maximum loads expected in many heap leach pads. To address this data gap, a series of interface shear tests

was performed between a needlepunch-reinforced GCL and different textured geomembranes, at normal loads ranging from 517 to 2758 kPa (75 to 400 psi).

LABORATORY TESTING DETAILS

Puncture Testing

A description of the high-load puncture testing system is provided in Athanassopoulos et al. (2008). A high-load shop press capable of exerting loads up to 667 kN (150,000 lbs) was fabricated for this study. This maximum load, distributed over a 0.093-m² (1-ft²) sample area, corresponds to possible pressures as high as 7184 kPa (1042 psi). A maximum test pressure of 5172 kPa (750 psi) was selected for this study, as it corresponds to 183 m (600 feet) of ore, with a factor of safety of 1.5.

Table 1 provides a summary of the different types of liner components (geomembranes, GCLs, and geotextiles) used in this study. The liner components were placed inside a custom-fabricated HDPE test cylinder with an inside diameter of 344 mm (13.54 in) and a wall thickness of 72 mm (2.85 in). A layer of standard commercial mortar sand was placed in the cylinder first and tamped in place to serve as the bedding layer. Where specified, a GCL was then placed over the sand layer, followed by the geomembrane. To be representative of field conditions, the GCL samples were slightly moistened with tap water to increase the bentonite moisture content from 35% (typical as-manufactured value for Bentomat) to a test moisture content of approximately 50%. As shown in USEPA (1996), even GCLs placed on dry subgrade soils see an increase in moisture content within several weeks of installation. Moistening the GCL provides conservative puncture testing conditions, since hydrated bentonite would be expected to provide less

cushioning. A 230-mm (9-in) thick layer of 50-mm (2-in) minus crushed stone was then placed over the geomembrane. One test incorporated a heavy (540 g/m², or 16 oz/yd²) nonwoven geotextile between the geomembrane and the drainage aggregate, to evaluate the geotextile's role as a protective cushion. The final layer was a thick steel loading plate, intended to uniformly distribute the applied load across the sample area. The loading plate was equipped with two dial gauges (left and right) accurate to 0.025 mm (0.001 inch) to monitor vertical displacement over time.

After each liner cross-section was stacked within the test column, the entire assembly was placed on the high-load shop press, and loaded gradually in increments of approximately 200 kPa (30 psi) every 15 to 20 minutes, until the specified test pressure was reached. The gradual increase in applied load was intended to allow some bedding down of the stone and to partially simulate the increase in load that would occur on site. Selected tests were repeated at a faster loading rate of 479 kPa (69 psi) every

10 minutes, to assess the possible effect of loading rate on geomembrane straining.

Once the full load was applied, load and dial gage readings were taken every 20 minutes for the first ten hours, and every 12 hours thereafter.

To be consistent with common past practice in the mining industry, a puncture test duration of 48 hours was used for all tests, with the exception of one, which was loaded for two weeks. Dial gauge readings over time showed that vertical displacements stabilized within 0.05 to 0.1 mm after approximately 48 hrs of loading (Figure 1), indicating that the selected puncture test duration is appropriate.

After loading, the geomembrane samples were removed and visually examined over a light table for signs of puncturing. In addition to punctures, other signs of distress, including yielding in the geomembrane (defined as permanent indentations in the geomembrane which do not recover after removal of the pressure) were also recorded.

Table 1. Materials Tested

Material Designation	Description	Manufacturer
<u>Geomembranes</u>		
60-mil LLDPE-S	1.5-mm smooth LLDPE	Polyflex
80-mil LLDPE-S	2.0-mm smooth LLDPE	Polyflex
60-mil HDPE-S	1.5-mm smooth LLDPE	Polyflex
60-mil LLDPE-T1	1.5-mm textured (co-extruded) LLDPE	Polyflex
60-mil LLDPE-T2	1.5-mm textured (embossed) LLDPE	Agru America
<u>Geosynthetic Clay Liners</u>		
Bentomat ST	3.6 kg/m ² bentonite, needlepunched between woven and nonwoven geotextiles	CETCO
Bentomat STM	2.4 kg/m ² bentonite, needlepunched between woven and nonwoven geotextiles	CETCO
Bentomat DN	3.6 kg/m ² bentonite, needlepunched between two nonwoven geotextiles	CETCO
<u>Geotextiles</u>		
GEOTEX 1701	540 g/m ² nonwoven geotextile	Propex

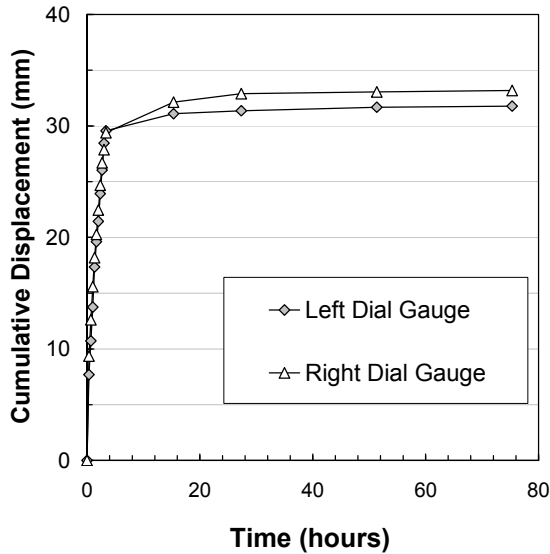


Figure 1. Geomembrane Deformation Readings

A method similar to the one recommended by the UK Environment Agency (2006) was used to quantify the extent of geomembrane deformation for comparison purposes.

The five areas of greatest deformation (taking into account both depth and steepness of the sides) were identified and selected for more detailed strain measurements. Indentations within 25 mm (1 in) of the sheet edge were not selected, due to possible edge effects. Two perpendicular axes, intersecting at the deepest point, were marked on each indentation (Figure 2). Vertical deformation was measured along the two perpendicular axes using digital calipers and a dial gauge (commonly used for asperity height measurements of geomembrane texturing, per GRI-GM-17). Starting at one edge of the indentation and working along each of the axes, the vertical deformation was measured at 2.5-mm horizontal intervals until the opposite edge of the indentation was reached. The edge of the indentation was defined as a point where two consecutive readings had a vertical height difference less than or equal to 0.05 mm. The measuring procedure was repeated along the second axis, and then for the remaining indentations, until all ten axes

on each geomembrane sample were measured.

From these measurements, incremental strains (across each discrete 2.5-mm interval) and average strains (across the entire indentation) along the two axes of each indentation were calculated using the method recommended by the UK Environment Agency, (2006):

$$\varepsilon_{inc} = \frac{\sqrt{x^2 + \Delta y^2} - x}{x} \quad (1)$$

$$\varepsilon_{average} = \frac{\sum \varepsilon_{inc}}{n} \quad (2)$$

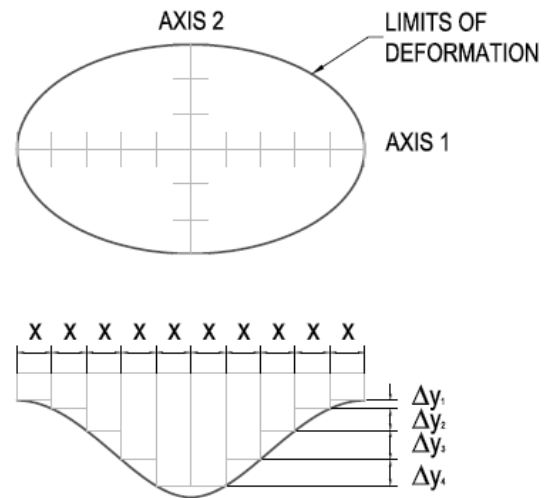


Figure 2. Geomembrane Deformation Measurement Method

Permeability/Compatibility Testing

Copper heap leaching requires the use of low-pH sulfuric acid solutions. To evaluate the long-term compatibility a GCL in contact with an acidic pregnant leach solution (PLS) under high loads, a rigid wall permeameter was constructed for this study. The permeameter was fabricated of stainless steel

to withstand both the high pressures and the harsh permeant chemistry. The permeameter was placed on a shop press capable of exerting loads up to 45 kN (10,000 lbs). This load, distributed over a 100-mm diameter circular sample (0.0081-m² sample area), corresponds to a maximum possible pressure as high as 5172 kPa (750 psi). Effective stresses ranging from 34.5 to 3166 kPa (5 to 459 psi) were selected for the GCL permeability testing program, corresponding to 1.8 to 183 m (6 to 600 feet) of ore, with a PLS head of 1.4 m (4.6 feet).

Permeability/compatibility tests were performed on an intact GCL sample and a sample of GCL that had been pierced by a large stone during one of the high-load puncture tests (Test No. 4). Using digital calipers, the area of the hole was estimated at approximately 1 cm². The punctured GCL sample was tested to evaluate sodium bentonite's potential for self-healing under heap leach liner conditions.

The acidic copper PLS was collected from an active copper leach pad in the southwestern U.S. The results of a chemical analysis on the copper PLS are summarized in Table 2.

Table 2. Copper PLS Chemistry

pH	1.8
Electrical Conductivity	37000 µmhos/cm
Aluminum	5044 ppm
Calcium	262 ppm
Copper	802 ppm
Iron	1788 ppm
Magnesium	498 ppm
Zinc	198 ppm

The GCL permeability/compatibility tests were performed in accordance with a modified version of ASTM D6766, the

Standard Test Method for Evaluation of Hydraulic Properties of Geosynthetic Clay Liners Permeated with Potentially Incompatible Liquids. The as-manufactured moisture content of the GCLs tested is approximately 35%, with additional moisture absorption from subgrade soils likely soon after installation. Accordingly, the GCL samples in this study were initially moistened with a small volume of tap water, to attain a starting moisture content of 50%, and then fully hydrated with the copper PLS for 48 hours. After hydrating with PLS, a hydraulic head of 13.8 kPa (2 psi) was applied to drive PLS flow through the GCL. Permeability testing was performed at effective stresses ranging from 34.5 to 3166 kPa (5 to 459 psi), to simulate the range of typical operational stages of a copper heap leach facility. Testing continued until specific termination criteria (steady-state flow and chemical equilibrium) were established between the effluent and influent. Flow and water quality measurements were collected periodically to monitor termination criteria throughout the testing period.

Interface Shear Strength Testing

Considering the potentially high normal loads involved in some mining applications, there have been concerns expressed over the interface shear strength between geosynthetic liner components. Past shear testing of geosynthetics has typically been limited to loads less than 690 kPa (100 psi), which falls short of the loads expected in a tall heap leach pad. To address this data gap, a series of interface shear tests was performed between different textured geomembranes and needlepunch-reinforced GCLs, at normal stresses ranging from 517 to 2758 kPa (75 to 400 psi). In order to improve friction between geomembranes and adjacent soils or geosynthetics, geomembranes are often manufactured with surface texturing. The two most common geomembrane texturing

processes are co-extruded texturing and embossed texturing. In this study, the shear performance of both types of textured geomembranes were evaluated against Bentomat DN, a high-peel strength, needlepunch-reinforced GCL consisting of 3.6 kg/m² of bentonite between two nonwoven geotextiles.

The geomembrane/GCL interface shear testing was performed in accordance with a modified version of ASTM D6243, the Standard Test Method for Determining the Internal and Interface Shear Resistance of Geosynthetic Clay Liner by the Direct Shear Method. Instead of the standard 300-mm by 300-mm (12-in by 12-in) shear box, testing was performed in a smaller 150-mm by 150-mm (6-in by 6-in) box, to allow application of higher normal stresses. Past testing by Olsta and Swan (2001) has demonstrated good correlation between these two shear box sizes.

RESULTS

Puncture Testing

The results of the high-load puncture testing program are summarized in Table 3. An inspection of the post-test geomembrane samples revealed significant yielding (i.e., permanent set deformations), with almost all of the samples subjected to stresses greater than 2586 kPa (375 psi) experiencing over 300 permanent deformations per m² (>30 per ft²). Two of the geomembrane samples tested at the highest normal stress, 5172 kPa (750 psi), were also punctured, with holes ranging from 1.5 to 7.5 mm in diameter. Table 3 includes both “typical” geomembrane strains (an average of the overall strains from the five deepest indentations) and “peak” geomembrane strains (the overall strain associated with the deepest indentation on each geomembrane). For simplicity,

incremental strains (local strains between two adjacent points on a single indentation) are not shown. In some of the deeper indentations and punctures, incremental strains in excess of 100% were calculated.

Effect of GCL. The calculated geomembrane strains in Table 3 show that the tests involving a GCL layer beneath the geomembrane (Test Nos. 1, 5, 7, 9, 13, 15) tended to show lower typical strains than geomembranes tested alone under the same conditions. The reduction in geomembrane strain afforded by an underlying GCL is also shown in Figure 3, which presents a plot of typical geomembrane strains with respect to normal stress for all tests involving 1.5-mm LLDPE geomembranes. Additionally, tests involving 2-mm LLDPE and 1.5-mm HDPE geomembrane samples showed significant improvement (greater than 50% reduction in strain) when a GCL was placed under the geomembrane. However, Table 3 also shows that peak strains and maximum deformation depths were much more variable, and likely depend more on the random orientation of the crushed rock particles in direct contact with the geomembrane than the subgrade beneath the geomembrane. Punctures and deformations due to sharp rock edges or points that happen to be in direct contact with the geomembrane could not be fully mitigated by the GCL (or, as discussed below, by a cushioning geotextile) due to the small contact areas and high stresses involved.

Effect of GCL Weight. Geomembrane strain measurements show that the GCL bentonite mass (either 2.4 or 3.6 kg/m²) does appear to impact the extent of geomembrane straining, with the heavier-weight GCL allowing slightly lower strains. To be conservative, the lighter-weight GCL (Bentomat STM, commonly used in mining applications) was used in the remaining tests involving GCLs.

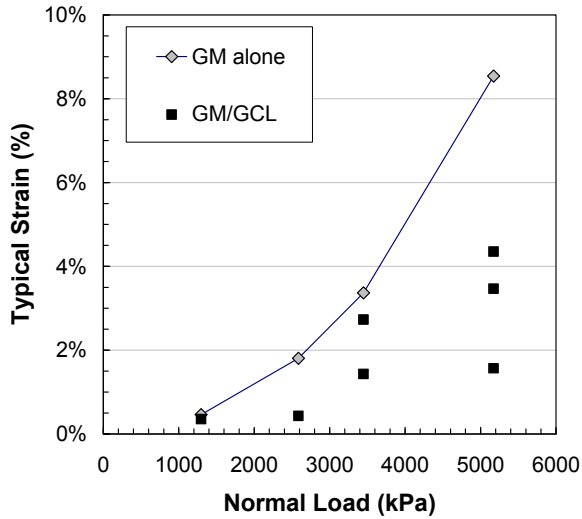


Figure 3. Geomembrane Strain vs. Normal Stress

Effect of Geomembrane Type. Table 3 also shows that the type of geomembrane plays a role in puncture performance. The peak and typical indentation depths and strains in the 1.5-mm HDPE geomembranes (Tests No. 15 and 16) were consistently less than those seen in the same thickness LLDPE geomembranes subjected to the same test conditions (Test 9, 10, and 11). This difference is not surprising, considering the different microstructures of HDPE and LLDPE. Although HDPE's semi-crystalline structure gives it greater strength and chemical resistance than LLDPE, this structure also makes HDPE more susceptible to stress cracking, and subject to failure at lower strains than LLDPE (Peggs et al., 2005).

Effect of Geomembrane Thickness. The strain values in Table 3 suggest that geomembrane thickness does not appear to influence the extent of straining. Peak and typical strains measured in 1.5-mm LLDPE and 2.0-mm LLDPE geomembrane samples tested under the same test conditions were almost identical. This finding is consistent with Brachman and Gudina (2008), who observed that geomembrane strain was not significantly affected by geomembrane

thickness, possibly due to the small geomembrane stiffness relative to the subgrade.

Effect of Test Duration. All of the puncture tests were run for 48 hours, with the exception of Test No. 4. Test No. 4 involved the same liner cross-section and test conditions as Test No. 3, except the test duration was extended to 2 weeks. A cursory comparison of Test No. 3 and 4 results might conclude that test duration plays a large role in geomembrane strain and puncture performance. However, it is important to note that the Test No. 4 results were skewed by a large (7.5-mm) hole in the geomembrane. Inspection of the post-test sample showed that a sharp 50-mm rock was driven through both the geomembrane and the underlying GCL. The puncture appears to have occurred instantaneously and was not related to the increased test duration. If the deformation associated with this large puncture is not included in the strain calculations, Test No. 4 would have a peak strain of 10% and a typical strain of 3.6%, much closer to the Test No. 3 values. This finding, together with the fact that vertical displacements in all tests stabilized within 48 hrs of loading (see example in Figure 1), suggest that test duration is not as critical a test variable as normal load, rock size, shape, and random orientation of the crushed rock on top of the geomembrane.

Effect of Loading Rate. Test Nos. 10 and 11 involved the same liner cross-section and test conditions, with the exception of loading rate. Test No. 10 was loaded at a faster rate than any other test (478 kPa, or 69 psi increments every 20 minutes), whereas Test No. 11 was loaded at less than half this rate, 192 kPa (27 psi) every 20 minutes, comparable to the remaining tests.

TABLE 3. SUMMARY OF GEOMEMBRANE PUNCTURE TESTING RESULTS

	Liner Cross-section	Normal Stress (kPa)	Holes (dia.)	Max. Depth (mm)	Average Depth (mm)	Peak Strain (%)	Typical Strain (%)
1	60-mil LLDPE-S (alone)	5172	2 and 2 mm	5.6	4.0	25.7%	8.5%
2	60-mil LLDPE-S over Bentomat ST	5172	--	4.5	3.2	3.0%	1.6%
3	60-mil LLDPE-S over Bentomat STM	5172	--	4.4	3.8	6.4%	3.5%
4	60-mil LLDPE-S over Bentomat STM ⁽¹⁾	5172	1.5 and 7.5 mm	8.6	4.9	12.5%	4.4%
5	60-mil LLDPE-S (alone)	2586	--	4.0	2.3	3.3%	1.8%
6	60-mil LLDPE-S over Bentomat STM	2586	--	2.3	1.4	0.6%	0.4%
7	60-mil LLDPE-S (alone)	1297	--	1.9	0.9	0.7%	0.5%
8	60-mil LLDPE-S over Bentomat STM	1297	--	3.3	2.6	0.5%	0.4%
9	60-mil LLDPE-S (alone)	3448	--	5.0	3.8	6.4%	3.4%
10	60-mil LLDPE-S over Bentomat STM ⁽²⁾	3448	--	4.7	3.5	4.6%	2.7%
11	60-mil LLDPE-S over Bentomat STM	3448	--	3.7	3.1	3.4%	1.4%
12	60-mil LLDPE-S under 540 g/m ² geotextile	3448	--	4.1	2.2	9.0%	1.8%
13	80-mil LLDPE-S (alone)	3448	--	4.9	3.2	6.2%	3.4%
14	80-mil LLDPE-S over Bentomat STM	3448	--	2.7	2.1	3.4%	1.1%
15	60-mil HDPE-S (alone)	3448	--	4.2	2.9	4.6%	2.6%
16	60-mil HDPE-S over Bentomat STM	3448	--	2.9	2.2	1.8%	1.1%

All tests performed with a mortar sand subgrade and a 50-mm (2-inch) minus crushed rock overliner.

⁽¹⁾ Two-week test duration.

⁽²⁾ Load applied at a faster rate (479 kPa every 10 minutes).

Deformation depths and strains were greater in the geomembrane sample that was loaded faster, likely because stress relaxation was minimized. As discussed by Peggs et al. (2005), because of stress relaxation, slower applied strains will result in lower geomembrane stresses. Peggs et al. also showed that stress relaxation will increase as temperature increases. Together, these factors suggest that in a heap leach liner,

where loads are applied over months or years, and elevated in-situ temperatures are common, stresses will not likely build to the same extent as in geomembrane samples tested in the laboratory. For this reason, laboratory testing could be considered to provide conservative results in terms of geomembrane strain behavior.

Effect of Geotextile. Test No. 12, which included a heavy nonwoven geotextile over the geomembrane, showed a reduction in typical strains. However, the peak strain in this sample – corresponding to one deep indentation over a small contact area, indicative of a sharp rock driven into the geomembrane – was very high (9%). This shows that, similar to the tests involving GCLs, geomembrane protective measures may have limited benefit against rocks randomly aligned with a sharp edge or point perpendicular to, and in direct contact with, the geomembrane. This finding speaks to the uncertainty involved in geomembrane puncture protection systems in the field; if sharp rock particles happen to be aligned in a certain way, the geomembrane can be punctured even with standard protective measures in place.

This finding further shows that a low-permeability soil or GCL beneath the geomembrane is warranted, not only for the nominal puncture protection offered, but also to limit PLS leakage through the holes that may develop in the geomembrane.

Allowable Strain. None of the geomembranes tested would meet the total strain requirement of 0.25% required by German regulators (Seeger and Muller, 1996). However, this is the most stringent requirement known, intended to not only avoid short-term puncturing, but to also avoid stress cracking of the geomembrane over time. In their critique of the European puncture requirements, Peggs et al. (2005), pointed out that the 0.25% strain criterion was based on durability testing of HDPE pipes in the early 1980s. In these tests, stress was maintained constant (i.e., no stress relaxation) and the pipes were not intimately confined between two confining layers like a geomembrane in a liner system would be. Additionally, the tests did not address newer HDPE formulations with stress crack

resistance, nor did they address other geomembrane types, like LLDPE, which are not subject to stress cracking. Due to these factors, Peggs et al. concluded that the European criteria were too restrictive. They proposed the following alternate allowable strains for geomembranes strained slowly between confining layers: 6-8% for smooth LLDPE and 10-12% for smooth HDPE. Almost every test in this study met these criteria, except for two tests at the highest normal stress (Test No. 1 and 4, at 5172 kPa), and surprisingly, the deepest indentation in the LLDPE geomembrane that was tested with a protective geotextile (Test No. 12, at 3448 kPa). This last finding speaks to the role played by variability in overliner rock position/alignment in affecting geomembrane puncture performance.

This variability in rock position, together with the high stresses involved, suggest that random puncturing of the geomembrane can take place in a heap leach liner setting, even if protective measures are in place. However, since heap fills typically operate over shorter periods of time (5 to 10 years) compared to solid waste landfills (more than 30 years), and are commonly built in less environmentally sensitive areas, maintenance of a completely defect-free geomembrane over the long-term may not be a critical design priority. In this case, rather than limiting strains to prevent long-term cracking, perhaps a most realistic strain criterion for geomembranes in heap leach liners is to tolerate elongation of the geomembrane past the yield point, but to prevent short-term puncturing of the geomembrane. This concept has been termed Level III protection (Narejo, 1995).

Overliner Puncture Behavior. During the tests with normal stresses greater than 3447 kPa (500 psi), significant fracturing of the drain rock was observed. Fracturing was so

extensive that there was an accumulation of fines on top of the geomembrane, and in many cases these fines had been cemented together by the high stress. The reduction in particle size and introduction of fines on top of the liner are both expected to result in less geomembrane damage; although this finding is non-conservative, it is believed to be representative of conditions in the field. Another implication of the overliner particle size reduction is that it could likely result in a less permeable overliner in the field.

Permeability Testing

Table 4 and Figure 4 present the results of the high-load compatibility/permeability tests performed on both intact and punctured GCL samples. At low effective stress, the permeability of the intact GCL sample in contact with the copper PLS was approximately 1×10^{-6} cm/sec, showing the impact of the harsh PLS on the bentonite clay. As effective stress was increased to simulate increasingly higher ore heights on the liner system, the permeability decreased significantly, reaching a value of approximately 5×10^{-11} cm/sec at 1440 kPa (200 psi) effective stress. A least-squares linear regression of the results showed the permeability of an intact GCL in contact with this copper PLS can be expressed as:

$$\ln K (cm/s) = -10.414 - 0.0091 \sigma' (kPa) \quad (3)$$

The punctured GCL sample also showed a high permeability ($> 10^{-7}$ cm/sec) at effective stresses up to 510 kPa (75 psi), evidence of preferential flow through the 1-cm² hole at the center of the sample. However, as effective stress increased further, sodium bentonite exuded into the open hole, forming a thin layer (~1 mm, compared to 3 mm in the remaining sample), partially sealing the hole. This self-sealing behavior appears to have brought the overall permeability of the punctured sample down

to 5×10^{-8} cm/sec at 3165 kPa (459 psi) effective stress. This result demonstrates that even if a sharp rock in the overliner penetrates the geomembrane and GCL, bentonite's ability to swell (even the reduced swell in the presence of an acidic solution) may be able to effectively seal the puncture opening, limiting overall leakage through the liner system. Without the underlying GCL, the same size hole in a geomembrane could allow hundreds of liters per hectare per day of PLS leakage.

Table 4. GCL Permeability Results

Effective Stress (kPa)	Intact GCL (cm/sec)	GCL w/ 1-cm ² hole (cm/sec)
35	--	6.8E-6
234	2.1E-6	1.7E-6
510	9.8E-7	1.1E-6
821	7.9E-9	1.8E-7
1131	2.1E-9	1.0E-7
1441	4.9E-11	8.4E-8
3165	--	4.9E-8

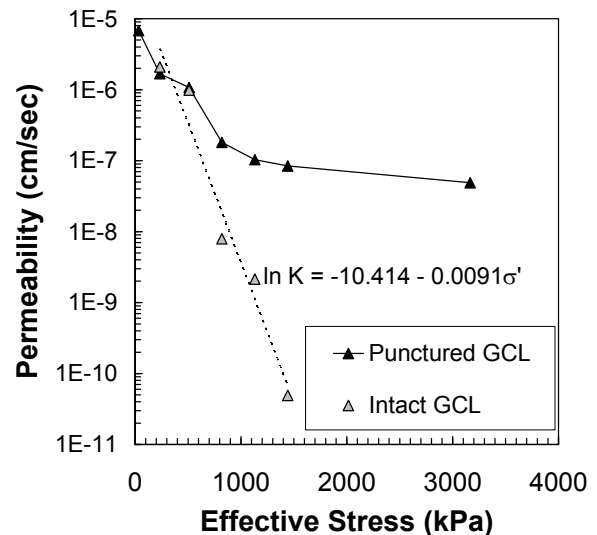


Figure 4. GCL Permeability With Copper PLS

Interface Shear Strength Testing

As shown in Figure 5, interface testing between Bentomat DN and an LLDPE

geomembrane with embossed texturing found a peak secant friction angle of 20 degrees and a large-displacement secant friction angle of 7 degrees, for normal loads up to 2758 kPa (400 psi). Testing between Bentomat DN and an LLDPE geomembrane with co-extruded texturing found a peak secant friction angle of 19 degrees and a large-displacement secant friction angle of 6 degrees. These angles are much higher than those expected for unreinforced, hydrated bentonite (less than 4 degrees at these loads), indicating that the GCL's internal reinforcement had not ruptured during testing. Inspection of the post-test samples verified that, with only one exception, the reinforcement in all of the GCL samples had remained intact, and that sliding had only occurred between the geomembrane and the GCL. The GCL sample tested against the co-extruded textured geomembrane at 2759 kPa (400 psi) experienced partial internal failure.

To minimize the potential for internal failure/rupture of the GCL (and residual conditions representative of unreinforced hydrated bentonite), a GCL with high peel strength (>900 N/m by ASTM D6496) is recommended for heap leach liner applications where extremely high loads are expected.

Past direct shear tests performed by Breitenbach and Swan (1999) under high fill loads showed that geomembrane interfaces with underlying and overlying soils gain strength with time, due to (1) high-load deformation, or dimpling, of the geomembrane, increasing the interface contact area; and (2) reduction in excess soil porewater pressures over time. They estimated a 5-degree increase in friction angle due to these factors. Since the high-load shear tests performed in this study did not include overliner and underliner soils, it is plausible that the actual peak shear

strengths in the field will be higher than those reported in Figure 5.

DISCUSSION

The findings of the high-load puncture and high-load permeability testing presented above were used to revisit the leakage calculations presented in Athanassopoulos et al. (2008), and based on Giroud's equations (1997). The evaluation compared the expected hydraulic performance and metal recovery of two potential liner options at a hypothetical copper heap leach site: (1) a 1.5-mm HDPE geomembrane overlying a GCL; and (2) a 1.5-mm HDPE geomembrane overlying a 0.3-m thick layer of compacted soil with a permeability of 1×10^{-6} cm/sec. The analysis assumed circular geomembrane punctures with a diameter of 2 mm, a puncture frequency of 10 per m^2 (based on the punctures per ft^2 found during testing at the highest loads) for both the GCL and compacted soil options, and a conservative GCL permeability of 5×10^{-8} cm/sec (corresponding to the measured permeability of the punctured GCL sample in contact with copper PLS under high loads).

Using these assumptions, the calculations show that a geomembrane/GCL composite liner would be expected to allow less than one-tenth as much leakage as a geomembrane/0.3-m thick compacted soil composite. By multiplying the leakage rates with 800 ppm of copper (from Table 2), a copper price of \$4.40 per kilogram (as of July 2009), and an estimated recovery of 80%, copper recovery rates for each liner option can be calculated and compared. The example calculations show that because of the large disparity in leakage rates between the two liner options, the improved recovery rate afforded by adding a GCL below the geomembrane could potentially translate to

millions of dollars per year of added revenue. This far exceeds the cost of the initial investment in the GCL for the heap leach pad liner system.

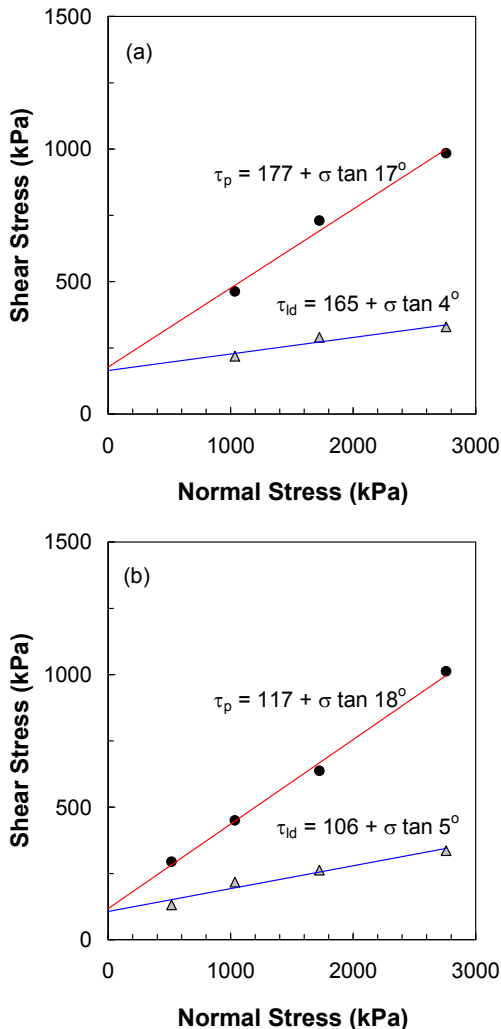


Figure 5. Geomembrane/GCL Shear Strength Envelopes: (a) geomembrane with co-extruded texturing; (b) geomembrane with embossed texturing

SUMMARY AND CONCLUSIONS

The results of high-load puncture testing showed that geomembranes alone are expected to experience more puncture damage (puncturing and/or strain deformation past yield) than a geomembrane with an underlying GCL or a geomembrane covered by a protective geotextile cushion.

The protection offered by a GCL is comparable to that of a 540 g/m² nonwoven cushioning geotextile placed above the geomembrane. The GCL's benefit, in terms of reducing biaxial strains in the geomembrane, appears to be greater at higher normal stresses.

Although protective measures (either GCL below or cushioning geotextile above the geomembrane) show reduced typical strain values, these measures may not be enough to protect the geomembrane from puncture in all cases, especially where sharp crushed rock particles happen to be aligned with a sharp point or edge in direct contact with the geomembrane.

Increased stress relaxation (due to slower loading rates and higher in-situ temperatures) in the field suggests that laboratory testing may provide conservative results in terms of geomembrane strain behavior.

High-load permeability testing of a GCL in contact with an acidic, high-ionic strength copper PLS shows a decrease in hydraulic conductivity with increasing confining stress. Additionally, a GCL sample with a 1-cm² puncture showed the ability to self-heal under high normal loads and maintain a low permeability (<10⁻⁷ cm/sec), even while in contact with the PLS.

High-load direct shear testing of geomembrane/GCL liner components showed peak secant friction angles of 19 to 20 degrees and large displacement secant friction angles of 6 to 7 degrees at 2758 kPa (400 psi) normal stress. To minimize the potential for internal failure/rupture of the GCL (and residual conditions representative of unreinforced hydrated bentonite), a GCL with high peel strength (>900 N/m by ASTM D6496) is recommended for heap

leach liner applications where extremely high normal stresses are expected.

A feasibility study of two lining alternatives for an example copper heap leach pad estimated that a geomembrane/GCL composite liner would be expected to allow only one-tenth as much leakage as a geomembrane/compacted soil composite. The resulting improvement in PLS capture is expected to result in a significant increase in copper recovery and increased revenue (potentially millions of dollars per year).

ACKNOWLEDGMENTS

The authors appreciate the valuable contributions of Mr. Ryan Ludwin of JLT Laboratories, in Canonsburg, Pennsylvania, who performed the high-load puncture and permeability testing, and Dr. Zehong Yuan, of SGI Testing in Norcross, Georgia, who performed the high-load direct shear testing. The authors also thank Mr. Clark West of Agru America, for providing the embossed textured geomembrane samples and for partnering with us on the high-load shear testing effort.

REFERENCES

Athanassopoulos, C., Kohlman, A., Henderson, M., and J. Kaul. 2008. Evaluation Of Geomembrane Puncture Potential And Hydraulic Performance In Mining Applications. *Tailings and Mine Waste*, 2008.

Brachman, R.W.I, and Gudina, S. 2008. Gravel contacts and Geomembrane Strains for a GM/CCL composite liner. *Geotextiles and Geomembranes*, 26:448-459.

Breitenbach, A.J. and Swan, R.H. 1999. Influence of High Load Deformations on

Geomembrane Liner Interface Strengths. *Geosynthetics '99*, vol. 1, pp. 517-529.

Daniel, D. 2000. Hydraulic Durability of Geosynthetic Clay Liners. GRI-14, Conference on Hot Topics in Geosynthetics.

Giroud, J.P. 1997. Equations for Calculating the Rate of Liquid Migration Through Composite Liners Due to Geomembrane Defects. *Geosynthetics International*, 4 (3-4): 335-348.

Jo, H.Y., Katsumi, K., Benson, C.H., and T. Edil. 2001. Hydraulic Conductivity and Swelling of Nonprehydrated GCLs Permeated with Single-Species Salt Solutions. *Journal of Geotechnical and Geoenvironmental Engineering, ASCE*. 127 (7): 557-567.

Narejo, D. 1995. Three Levels of Geomembrane Puncture Protection. *Geosynthetics International*, 2(4): 765-769.

Olst, J., and Swan, R. 2001. Internal Shear Strength Of A Geosynthetic Clay Liner At High Normal Loads. *Tailings and Mine Waste*, 2001.

Peggs, I. D., Schmucker, B., and Carey, P. 2005. Assessment of Maximum Allowable Strains in Polyethylene and Polypropylene Geomembranes. *Geofrontiers 2005, Waste Containment and Remediation*, Geo-Institute, ASCE.

Seeger, S., and Muller, W. 1996. Requirements and Testing of Protective Layer Systems for Geomembranes. *Geotextiles and Geomembranes*, 14:365-376.

Thiel, R. and Criley, K. 2005. Hydraulic Conductivity of a GCL Under Various High Effective Confining Stresses for Three Different Leachates. *Geofrontiers 2005, Waste Containment and Remediation*, Geo-Institute, ASCE.

UK Environmental Agency. 2006. A Methodology for Cylinder Testing of Protectors for Geomembranes on Landfill Sites.

USEPA. 1996. Report of 1995 Workshop on Geosynthetic Clay Liners, EPA/600/R-96/149. USEPA, ORD, Cincinnati, OH.

HIDDEN OPPORTUNITIES TO IMPROVE TAILINGS SYSTEMS WITHOUT CAPITAL

Ryan Hale and Andy Jones

Stoud Consulting 2009, Marblehead, MA, USA

ABSTRACT: Asset systems required for successful tailings management always face significant pressure to increase performance, whatever the stage of the economic cycle. On the upswing, businesses need to commission new assets and generate value to support capital growth plans. At the top of the cycle OEMs cannot meet demand, requiring additional performance from existing assets to continue meeting growth plans. On the downswing and in the trough, unit costs are critical and efficient asset usage becomes essential.

To complicate matters further, actual rates hardly ever meet design expectations—either because we do not achieve those implied in the system design, or if the operating requirements have exceeded original design expectations since start-up. Chronic underperformance requires mechanical assets, planning and operating processes to deliver significant year-on-year improvement.

Businesses typically respond to the requirement to increase an asset's performance by spending money. In every case, however, massive opportunity exists hidden beneath the surface of common belief. Generating capital-free improvement of between 10-30% (and in some cases over 145%) with the existing assets, workforce, and technology is possible in a matter of weeks.

Mechanical slurry transfer systems (e.g., siphons, pumps, dredges), tailings operations or maintenance processes (e.g., cell building, maintenance outages), and asset utilization (e.g., dozers, haulers, side booms) all contain hidden opportunity to improve. This paper includes recent examples from Alberta Oil Sands tailings and mine waste operations that highlight why hidden opportunity exists, how to expose it and how to realize it. The talk will briefly cover the thinking processes, analytical tools, and accountability structures that generate measurable results in 1-6 months.

INTRODUCTION

Between 2007-2009, an established operation in Alberta's Oil Sands faced a series of emerging risks relating to its tailings pond containment and construction. These risks had large financial implications to both

current production levels and future capital investment requirements.

In each of these were representative of risks many other businesses both in Alberta and in other industries face. These risks fall into two categories: immediate or emergent. Examples

of immediate risks in the tailings environment are rapidly declining water cap or rapidly rising elevation vs. freeboard. Emerging risks include beach and cell construction falling behind plan.

Regardless of their risk, businesses face a choice whether to improve performance from existing systems, or invest in additional equipment and labor. Many businesses choose the latter because they cannot see additional opportunities to improve their existing systems.

The first step in driving improvement is identifying all the opportunities, by measuring the gap between current performance and a standard. When business leaders do not see a gap they have confidence in closing, or any gap at all, they typically feel there is no choice but to invest.

Typical opportunity analysis methods measure current performance against budget, plan, or benchmark (internal or external). While this type of variance analysis is useful for understanding adherence to plan or performance relative to peers, a vast quantity of improvement opportunity will remain invisible. Budgets and targets are negotiated figures that are often divorced from the underlying forces that govern a system's performance.

Zero Based Analysis is a technique that measures the gaps between current performance and the theoretical best, as determined by the first principles governing the system's performance. In all cases, the magnitude of opportunities determined using Zero Based Analysis exceed those measured using traditional variance measures. Often people's assumptions, negative experiences, and "legacy information" cause them to believe that opportunities quantify using Zero Based Analysis are purely theoretical and could never be realized.

This article will explore examples of real-world opportunities identified using zero based analysis, and then rapidly realized using straightforward problem solving techniques to improve the existing systems. After providing a practical overview of how to apply these techniques, we will explore the implications of improvements of this magnitude to the region and the industry.

ANALYSIS METHODOLOGY

The first step in conducting a Zero Based Analysis (ZBA) is to select a representative time period. A 12-month period or a significant length of run since a major system change (e.g., maintenance outage or overhaul) is sufficient. The main point is to value opportunities using past performance data such that an estimate of the future value (when the problems are solved) is realistic.

After determining the time period for historical data, the next steps are to select the system's key performance metric and to construct a theoretical best performance level from first principles. For example, a hydrotransport system for moving slurry can be measured in kilotonnes per day of dry material, and the theoretical best performance is a function of a small number of variables: slurry flow rate, density, and run time. For a controlled beaching operation, the critical variables are mass flow rate of solids, retention rate in the beach zone, and run time. These variables must be set at their design or ideal values to determine the true theoretical best, not a budget, benchmark, previous best, or planned value. This is the critical step in applying ZBA and can be overlooked easily. Practice and self-awareness of assumptions and constraints are fundamental to applying ZBA without leaving any hidden opportunity. Most people simply cannot see these opportunities because of their own

assumptions and constraints about what improvements are possible.

After collecting historical data from operations and engineering logs, losses in the following categories can be quantified and expressed in the units of the key performance metric as defined above:

- Planned downtime
- Unplanned downtime
- Standby or idle time
- Turndown rate or slow running hours
- Off-spec production hours

Any difference between the theoretical best, known losses, and the actual output is the error or unknown loss. This data is visually represented in a waterfall or bridge diagram. The examples included here show the opportunities identified for a slurry transport pipeline (Figure 1) and a controlled beaching operation (Figure 2).

In cases where the calculated error is large or there are known deficiencies in the historical data set, supplementing the analysis with information obtained through field observations will improve the accuracy and relevance of the analysis. Extending the example above, operators can keep an hourly log of the reasons for changes in flow rate and density. Collecting this data over a series of shifts creates a snapshot of current system performance, which the ZBA team can put in context with historical data.

The quantitative analysis technique is very straightforward. The essential components, therefore, in order to identify hidden opportunities for improvement from existing systems are the mindsets to challenge assumptions around what is possible and to view problems as opportunities rather than barriers.

REALIZING OPPORTUNITIES

Once a team has identified and prioritized the top improvement opportunities, the next phase of work is to solve problems and then implement solutions in order to realize the measurable results. Many problem-solving methods are available; choosing the right one for each situation and applying it effectively are the main factors that determine the rate of improvement.

The two examples below illustrate how straightforward solutions to problems with high levels of perceived complexity can yield results at a surprisingly fast rate.

Controlled Beaching

As mentioned above, very few critical variables determine the rate of advance in a controlled beaching operation. In one particular operation, a long-held perception that feed quality reduced build rate was not supported by available data (Figure 3). This concern consumed a large amount of engineering resource (analyzing process data) and developed a legacy among operations staff and managers. While determining alternative means of collecting feed quality data, the team developed hourly logging and other tools to isolate the critical variables mentioned above. Having these simple logs in place raised the accountability for shift foremen and crews to maximize hours “turned in” to the cell and hence output (Figure 4).

Slurry Hydrotransport

After design, construction, and commissioning, the slurry transport system had underperformed since startup. Pressure mounted on the operations, maintenance, and engineering staff accountable for the system’s performance with each day that passed that

the system failed to meet plan. Many people in the organization gave up on the original system, and were busy designing and testing additional assets to bring online that would supplement the siphon-fed stream.

By performing a Zero Based Analysis, the facts revealed that “density below spec” was largest opportunity on the siphon-fed stream, followed by unplanned downtime for blown pump packings/sleeves. While this information itself was not new, the relative magnitude of the specific opportunities was compelling, and the team approached the low-density problem with the mindset that resolving it offered them the shortest path to putting the system’s performance back on track. This is another example of how certain mindsets can prevent organizations from improving even when the facts suggest that it is possible.

The team then applied a rigorous problem solving method called Variable Analysis to understand what factors reduced intake density from siphon. By systematically verifying the variables that had the highest likelihood of contributing the problem, the team discovered that intake weights (to reduce buoyancy of plastic intake pipes) were not installed per engineering drawings during construction. During an upcoming scheduled outage, the plates were installed the density immediately stabilized in the target range (Figure 5).

Energized by their breakthrough, the team applied the same Variable Analysis method to the largest pump downtime problem. Bench inspection of the pump seal assemblies showed a dimensional mismatch causing premature packing failure.

In both cases, the variable analysis method

provided rigor to verify values that were previously assumed to be in spec.

The end result of these changes was an immediate gain in throughput (Figure 6). Realizing additional opportunities using similar methods became the ongoing work of the leadership team in that asset area.

CONCLUSIONS

In the authors’ experience, results like these are available in every system and every asset because the largest opportunities are hidden from view by constraints and assumptions. These examples suggest that over 200% improvement is available in tailings systems for containment construction and material transfer, of which 100% improvement can be realized in a matter of months.

This suggests that existing mining systems already operating in Alberta could support at least an additional 1,500 million Tonnes per day¹.

Alternatively, the region could reduce capital spending by 50% for the same production level, for a savings of \$6 billion per year, based on estimates of more than \$12 billion per year for equipment and machinery in Alberta’s mineral industries.

Although these figures might seem impossibly large and would need to be explored using more specific analysis to debottleneck integrated production sites, the magnitude of potential improvement within existing systems should capture the attention of Alberta’s industry leaders and prompt them to question what hidden opportunities exist within their current assets.

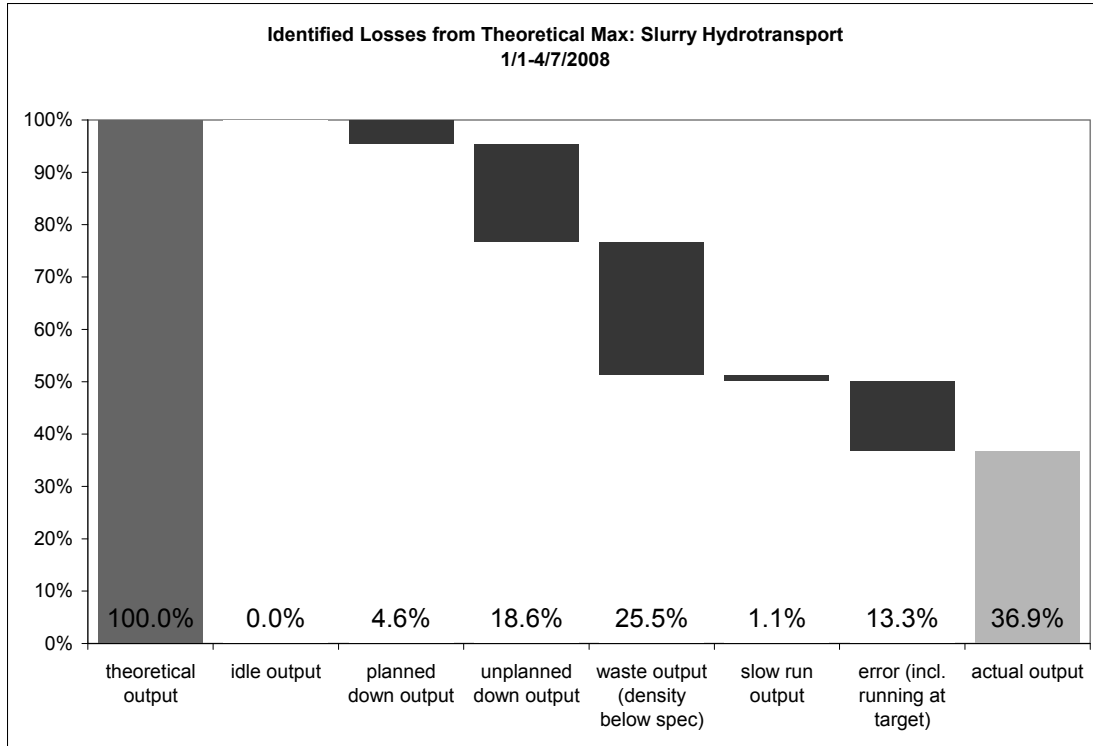


Figure 1. Waterfall diagram shows six standard categories of output loss

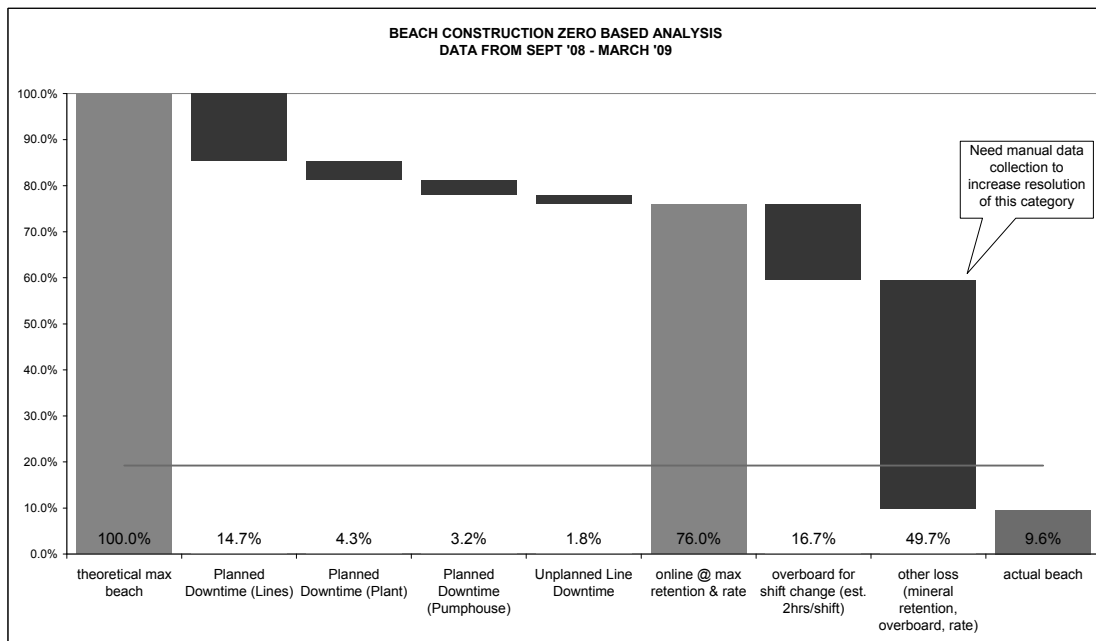


Figure 2. Waterfall diagram illustrates large opportunities when comparing actual performance to theoretical best

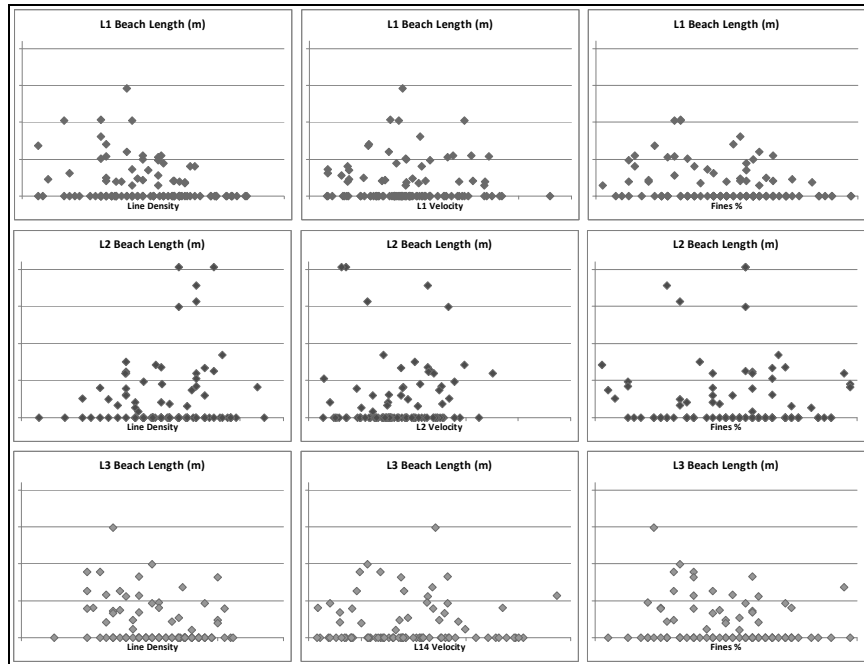


Figure 3. Weak correlations between feed quality and beach advance indicate another process variable has greater leverage on system performance. Chasing for more detailed or representative data of a perceived problem was a distraction from generating improvement by maximizing run hours in the beaching zone.

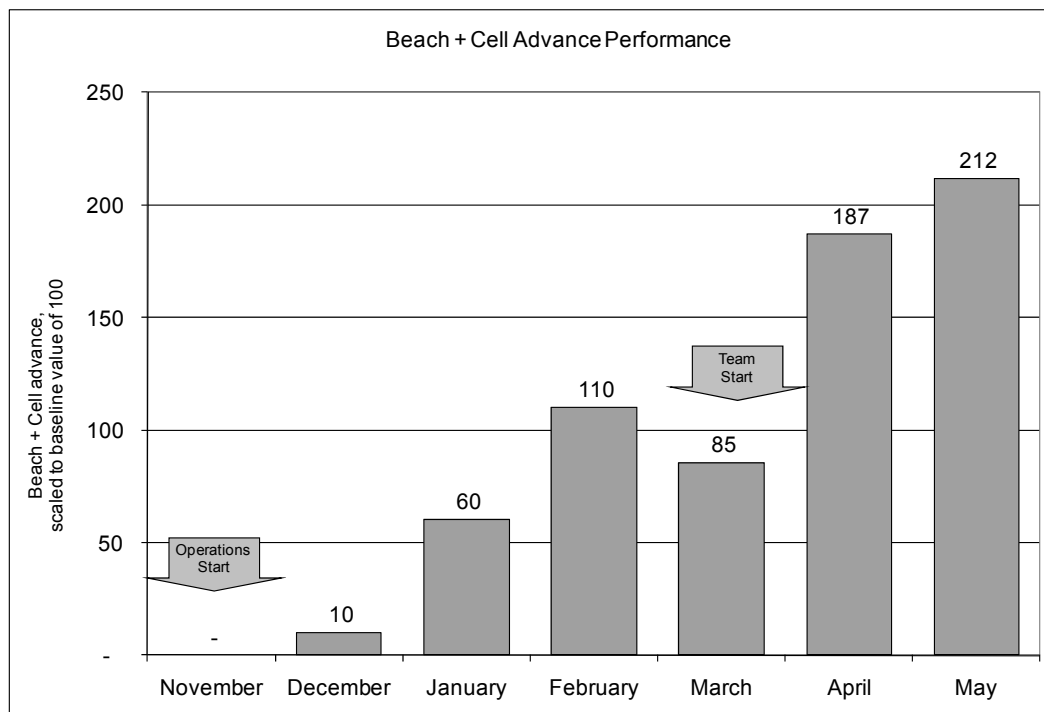


Figure 4. Weekly beach advanced with greater crew accountability--feed parameters unchanged.

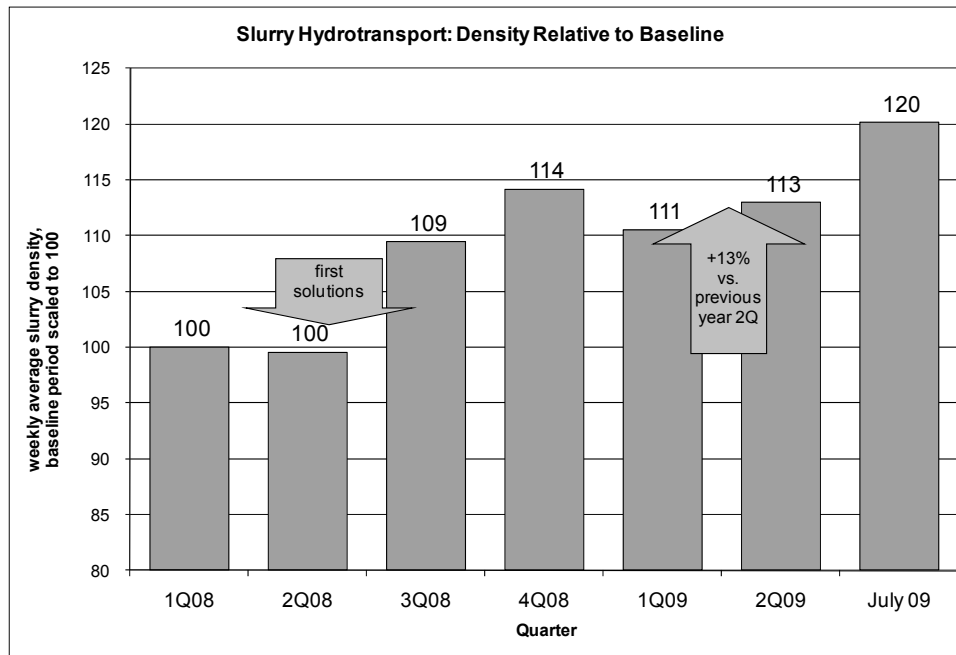


Figure 5. Step change in slurry density seen after correcting a problem that was present since commissioning

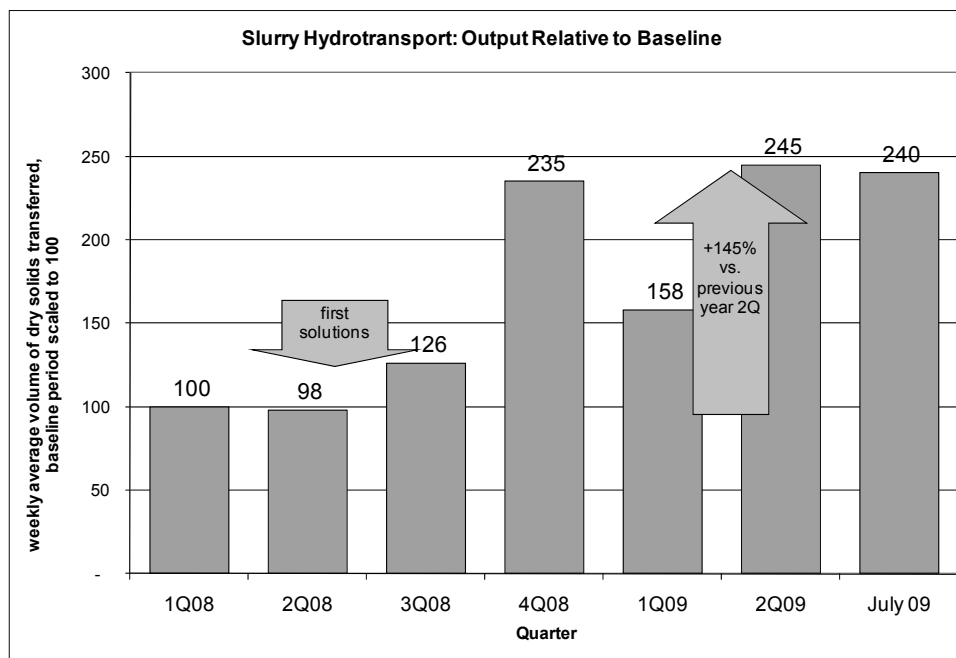


Figure 6. More than doubling the output of a chronically underperforming system benefits both the finances and the morale of the business

ⁱ Author's calculation from 2011 projections in *Investing in our Future: Responding to the Rapid Growth of Oil Sands Development*, 29 December 2006, p. 39.

GEOTEXTILE FILTRATION PERFORMANCE WITH COAL REFUSE UNDER STANDARD AND REDUCED COMPACTION ENERGIES

J.D. Quaranta and R Tolikonda

Department of Civil and Environmental Engineering, West Virginia University, Morgantown, West Virginia, USA

S. Bell

Bennett Department of Chemistry, West Virginia University, Morgantown, West Virginia, USA

ABSTRACT: Following the October 11, 2000 breakthrough and release of coal slurry from the Martin County Coal Corporation impoundment near Inez, Kentucky, the United States Congress requested the National Research Council (NRC) to study the accident with the objectives of reducing the potential for similar future accidents. The NRC completed their study (NRC, 2002) which identified numerous areas of concern and recommendations. This project addresses the National Research Council's findings to promote best available practices with regard to the design of impoundments. A research project was initiated to investigate the performance of non-woven geotextile filter fabrics when used in contact with coarse and fine coal refuse for impoundment filtration systems.

The conclusions of this work tend to indicate that the geotextile fabrics having an AOS of 0.212 mm or 0.15 mm did not have an appreciable effect in reducing the hydraulic conductivity of the CCR and Blended refuse for the percentage of fines tested in the permeability cells. The fine particles introduced by the 80/20 Blended sample did not effectively mobilize coal fines at various compaction energies or sample densities due to particle packing within the sample. The fine particle increase in the CCR samples was independent of compaction energy and the percent increase in fines resulted from effective compaction effort and occurred on a reduced fraction of refuse as the refuse larger than the #4 sieve size was removed from testing per ASTM requirements. There appeared to be no impact of geotextile clogging under these tests, however the laboratory scale testing may not reflect field conditions.

INTRODUCTION

West Virginia, with its mountainous terrain and historical coal mining production, has the largest number of pre- and post-law high hazard coal slurry impoundment facilities in the United States. These sites have been used

as impounding structures for coal slurry, process black water, and coarse refuse disposal. These structures are regulated by the US Department of Labor - Mine Safety and Health Administration (MSHA) and by the West Virginia Department of Environmental Protection (DEP).

Following the breakthrough and release of coal slurry from the Martin County Coal Corporation impoundment near Inez, Kentucky on October 11, 2000 the United States Congress requested the National Research Council (NRC) to examine ways to reduce these types of accidents. The NRC completed their study titled “Coal Waste Impoundments” which identified numerous areas of concern and the committee presented recommendations for improving the design, operation, and safety of coal slurry impoundments (NRC, 2002). In 2003 the Coal Impoundment Project began as a program of the National Technology Transfer Center (NTTC) at Wheeling Jesuit University (WJU). This research project supports the Coal Impoundment Project goals by conducting research into findings cited by the NRC study. Previous projects by the Coal Impoundment Project have included: studies into electronic real-time instrumentation and early-warning systems, development of guidance publications for performing table-top reviews of Emergency Action Plans, and supporting community outreach studies.

PURPOSE & OBJECTIVES

The purpose of this research was limited to investigating correlations between geotextile filter performance from coarse and fine coal refuse materials under different compaction densities. The objectives were to perform hydraulic conductivity tests on coal refuse specimens having different compaction densities and evaluate the filtration performance of non-woven geotextiles. Laboratory testing addressed the measurement of hydraulic conductivity of the permeant through Coarse Coal Refuse (CCR) and a blended refuse of 80% CCR and 20% Fine Coal Refuse (FCR). Grain size distribution profiles of exhumed geotextiles and refuse from tested permeameters were obtained to identify distributions of coal fines

within the column and geotextile filter performance.

MATERIALS & METHODS

Coarse & Fine Coal Refuse

The materials selected for this research consisted of both fine and coarse coal refuse produced from underground mining in Boone County, West Virginia, USA. The samples of coarse coal refuse (CCR) were obtained from randomly placed end-dump piles and the fine coal refuse (FCR) was obtained from the preparation plant prior to pumping to the coal refuse impoundment at the mine.

The first sample set consisted of a coarse coal refuse and the second sample set was a blended refuse (80% coarse / 20% fines). Experimentation equipment was based on ASTM D-5856 Standard Test Method for Measurement of Hydraulic Conductivity of Porous Material Using a Rigid-Wall, Compaction-Mold Permeameter.

A listing of the ASTM geotechnical material physical and engineering property tests performed on the coarse and fine coal refuse samples are presented in Table 1.

Table 1. ASTM Tests Performed

Test Name	ASTM
Moisture Content	D-2216
Sieve / Hydrometer	D-422
Specific Gravity of soils	D-854
Standard Proctor	D-698
Hydraulic Conductivity	D-5856

Selection of the maximum size of the coarse coal refuse particles followed ASTM requirements; where the maximum particle size tested ranged from ¾” (20mm) to No. 4 sieve (4mm). Inclusion of other fine particles

was carried out using a blend ratio discussed further on in the paper.

Moisture Content

The range of moisture content values of the coarse coal refuse samples varied from 3.5 percent to 5 percent. Slight variations in the moisture content were noted because the field collection of samples was performed on rainy days.

Specific Gravity

The range of specific gravity values for CCR samples used in this study was 2.4 to 2.6. These were consistent with values published by the US Mine Safety and Health Administration, MSHA (2007), which notes the range of specific gravity of coarse coal refuse as 1.8 to 2.3. Gonzalez et al. (1987) specifies the specific gravity value of 2.4 to 2.6 for the coal waste samples. The specific gravity values for the FCR used in this study ranged from 1.7 to 1.9. MSHA (2007) provides the typical range of specific gravity for FCR samples from 1.4 to 2.0.

Blended (Coarse and Fine) Coal Refuse

Coal fines were to be added in an appropriate amount to promote clogging of the geotextile. To accomplish this, an 80 percent coarse refuse to a 20 percent fine refuse ratio was selected and prepared following the method presented by Windisch (1996). Windisch (1996) discussed the procedure which was simple, rapid and efficient to blend different aggregates. This method used a mathematical function for the combination process in which grain-size distributions of known materials are the sets of known constants represented as

vectors A_i in terms of fractions passing given sieves:

$$[A_i] = [a_{i1}, a_{i2}, \dots, a_{in}], \quad i = 1 \text{ to } m$$

Where

a_{ij} = percentage of material i finer than sieve size j , $j = 1$ to n ,

m = number of materials to be combined, and

n = number of sieve sizes.

X is the proportion to which the m different material is combined. X is represented in vector form as:

$$[X] = [x_1, x_2, \dots, x_m]$$

x_1 will be the proportion of material 1 to be combined and x_2 will be the proportion of material 2 to be combined. The resulting combination gradation curve is given by the equation:

$$c_j = \sum_{i=1}^m a_{ij} x_i$$

The C vector is represented as $[C] = [c_1, c_2, \dots, c_n]$. To get the desired gradation of the combined analysis, the target curve is set to a known constant elements which are represented as vector D .

$$[D] = [d_1, d_2, \dots, d_n]$$

Where d_j = desired percentage of material finer than sieve size j . To get the desired gradation, the combined curve C should be close to target curve D ; therefore the difference between curves C and D are minimal, which is defined by convenient error function z on basis of squares of errors.

$$z = \sum_{j=1}^n (c_j - d_j)^2$$

Table 2. Blending of coarse and fine coal refuse (80% coarse, 20% fines)

mm	0.074	0.25	0.297	0.595	2	4.75
a ₁	5.81	11.08	16.26	27.83	61.89	99.55
a ₂	15.61	46.3	52.51	67.12	93.86	100
C ₁	4.648	8.864	13.008	22.264	49.512	79.64
C ₂	3.122	9.26	10.502	13.424	18.772	20
C	7.77	18.124	23.51	35.688	68.284	99.64

Table 2 presents the grain size distribution of blended refuse. Where a₁, a₂ are the percent of materials passing for coarse and fine coal refuse respectively. C₁ is the 80 percent blend for coarse refuse and C₂ is the 20 percent for fine refuse and C is the gradation of the combined refuse. There was a minimal difference in the calculated gradation and the actual gradation because of the percent of fines present in the coarse refuse and due to the pulverizing effort.

Particle Size Distribution

The grain size distribution of both the coarse and fine coal refuse is important because it

will affect the clogging potential within the refuse matrix and the fine particle intrusion into the geotextile filter. Particle size distribution has been shown to assist with estimating the hydraulic conductivity and also in designing the filter system to prevent piping in the water retaining structures. MSHA (2007) indicates the typical classification of coarse coal refuse as silty, clayey sand with gravel to clayey, silty gravel with sand. Generally fine coal refuse has fines content between 30 and 80 percent.

Due to settling of finer particles, the grain size distribution of fine coal refuse exhibits a wide range (MSHA). The grain size distribution of the specimens was evaluated

at the beginning and end of each permeability test. This was performed to evaluate potential material property changes; such as an increase in fine particle percentages resulting from the compaction process with varying energy efforts, as well as the potential of fine particle movement within the specimen matrix in the direction of seepage flow.

Hydrometer tests were performed for the refuse samples passing the No. 200 sieve. Fine coal refuse was prepared by first oven drying the coal slurry and then pulverizing to produce fines. The grain size distribution of the fine coal refuse fraction varied because of changes in the pulverizing effort. However, the effort for pulverizing the fine coal refuse was sought to be performed similarly for each test.

The graphs of the Grain Size Distribution for the coarse and blended refuse samples are illustrated in Figures 1.

Compaction and Density Tests

The Standard Proctor Test (ASTM D698) was used to determine the maximum dry density of the coarse coal refuse and the blended refuse specimens. The US Mine Safety and Health Administration require compaction efforts ranging 95% of the

Standard Proctor for placement of CCR at High Hazard Impoundment facilities.

The Standard Proctor Compaction test requires the soil matrix to be compacted into 3 layers with 25 blows of the drop hammer per layer. In order to promote and increase

geotextile fabric clogging potential reduced compaction efforts on the coal refuse samples were performed. The actual compaction energies used are presented in Table 3. Combined specific gravity values were used for calculating the density of the combined refuse.

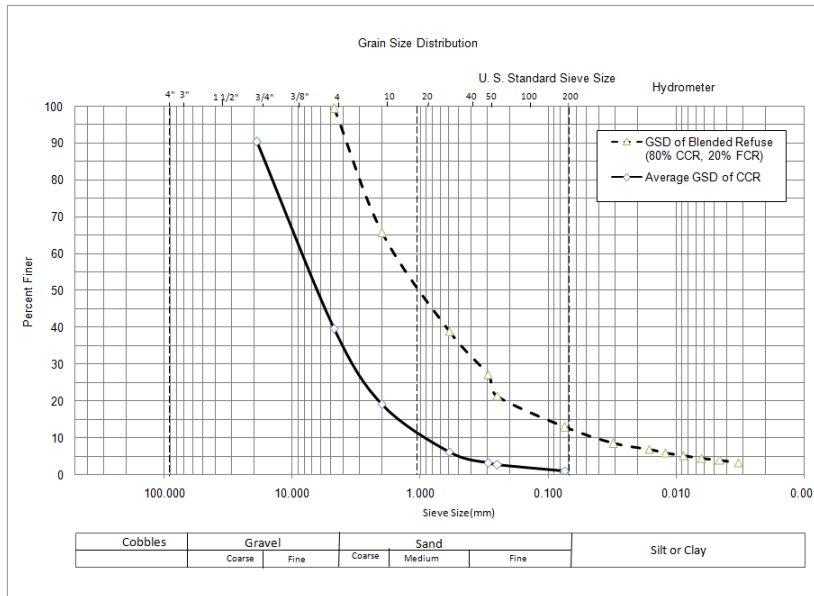


Figure 1. Grain Size Distribution of CCR and Blended Refuse

Table 3. Laboratory Compaction Energies

Configuration of Permeameter Compaction	Compaction Energy kJ/m ³ (ft-lb/ft ³)
Standard Proctor (ASTM D698)	592.5 (12375)
25 Blows/layer, 3 layers	636.21 (13288)
4 Blows/layer, 2 layers	67.84 (1417)
8 Blows/layer, 2 layers	135.73(2835)
12 Blows/layer, 2 layers	203.58 (4252)
15 Blows/layer, 1 layer	127.26 (2658)
15 Blows/layer, 3 layers	381.73 (7973)

Non-Woven Geotextiles

The non-woven geotextile fabrics used for this research are listed below:

Apparent Opening Size NW6 NW16 601
 (AOS) US Std. Sieve 70 100 70
 AOS (mm) 0.212 0.15 0.212

The fabric samples were provided by the GSE Lining Technology Inc. and the Propex Corporation.

Permeability test and Methodology

ASTM D-5856 *Standard Test Method for Measurement of Hydraulic Conductivity of Porous Material Using a Rigid-Wall, Compaction-Mold Permeameter* was used in order to evaluate the clogging potential of the geotextile fabric. This test was used rather than the gradient ratio test (ASTM D5101). The ASTM D-5856 was considered to best reflect the condition of geotextile and refuse interface contact promoting clogging. The coal refuse materials were compacted to specified densities by varying the water content and compaction energy in the permeability cell. The compaction effort was determined from the actual cell volume values for each test specimen. These values compensate for the porous stone and geotextile layers configured at the bottom of the mold. Duplicate and triplicate sampling was performed. Proctor graphs of the CCR and Blended refuse specimens are illustrated in Figures 2 and 3.

Selected geotextile fabrics were placed between the bottom porous stone and the compacted sample. Two filter papers were used; one was placed at the top of the compacted sample between specimen and the top porous stone and the other filter paper was placed between geotextile and the bottom porous stone. The setup of the permeability cell followed ASTM protocol with no deviations. The permeant water was de-aired water and the samples were allowed to saturate. After the saturation, the experiment was conducted until the completion of at least one reservoir volume.

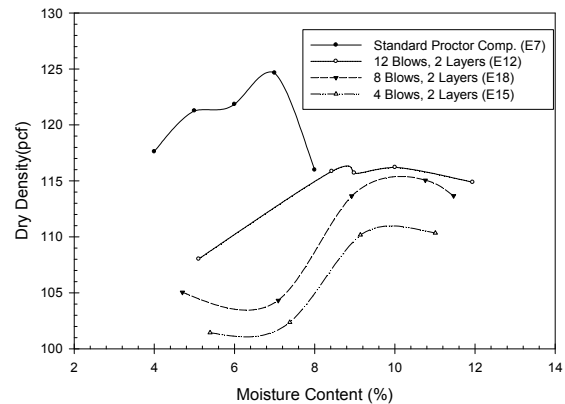


Figure 2. Proctor curves for CCR w/Variou Compaction Energies

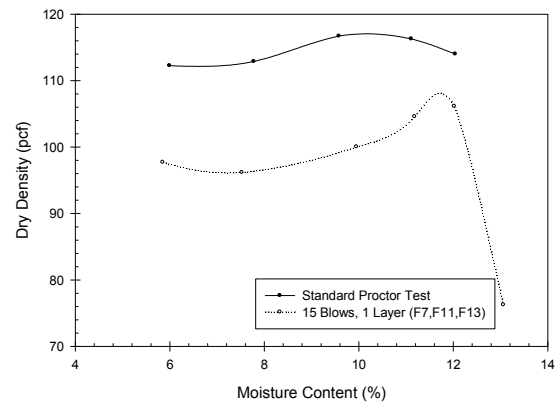


Figure 3. Proctor Curves for Blended Refuse

The seepage gradients used ranged from 5 to 7 for CCR permeability specimens E7, E12, E15, and E18. The corresponding blended refuse gradients ranged 15 to 33. The blended refuse samples were run at increased gradient to promote the hydraulic conductivity reduction.

RESULTS

Hydraulic Conductivity

The hydraulic conductivity experimental parameters and results are summarized in Tables 4 and 5 for the CCR and blended

refuse; and graphs of the hydraulic conductivity are shown in Figures 4 to 6.

The results of the hydraulic conductivity for the CCR samples (E7, E12,E15, E18) identify a close range of values from 1.94 e-6 m/s to 3.69e-7 m/s. The data does not clearly show a reduction in hydraulic conductivity to indicate geotextile clogging by the CCR. The seepage gradients were held steady at 5 and 7 for the duration of the tests. A total of between 430 ml to 13650 ml of permeant water was flushed through the samples.

The hydraulic conductivity data of the optimum compaction sample (E7) did not differ from the reduced compaction samples (E12,E15,E18). This may tend to indicate that the CCR hydraulic conductivity was not sensitive to compaction energy ranging from optimum of 636 kJ/m³ to 67 kJ/m³.

The graphed results for the hydraulic conductivity of the blended 80%CCR and 20%FCR samples are illustrated in Figure 5 and 6. This data tends to indicate more influence of the FCR and compaction energy on the hydraulic conductivity. The average hydraulic conductivity value for each of the sample F4, F7, F11 and F13 specimens identifies a clear order of magnitude difference between compaction efforts. The increase in compactive energy relates to a higher packing of the fine coal fraction. The hydraulic conductivity ranges from 3.13 e-6 m/s to 6.42 e-7 m/s at a compaction energy of 127 kJ/m³.

The hydraulic conductivity trends for all four samples do not clearly show a reduction to indicate geotextile clogging for the permeant volumes and test gradients.

Table 4. CCR Experimental Parameters and Results

	E7	E12	E15	E18
Dry Density, kN/m ³ (pcf)	19.66 (125.14)	18.78 (119.5)	16.07 (102.36)	16.38 (104.32)
Compaction Energy, kJ/m ³ (ft-lb/ft ³)	636.21 (13288)	203.58 (4252)	67.84 (1417)	135.73 (2835)
Number of Blows/Layer	25 Blows, 3 Layers	12 Blows, 2layers	4 Blows, 2 layers	8 Blows, 2 layers
Geotextile	NW-601	NW 6	NW 6	NW 6
AOS (mm)	0.212	0.212	0.212	0.212
Gradient	5	5	5	7.14
Test Duration (hours)	8	14.87	13.77	15.08
Average k (m/sec)	3.69 e-7	1.94 e-6	6.73 e -6	4.39 e -6
Standard Deviation for k	7.96 e-8	5.87 e-7	1.66 e -6	5.48 e -7
Void Ratio, e	0.26	0.32	0.54	0.51
Porosity, n	0.21	0.24	.35	0.34
Cumulative Permeant Volume (ml)	430	3650	13310	13650
Pore volume, pV (ml)	180.35	205.43	307.15	296.2

Table 5. Blended Refuse Experimental Parameters and Results

	F4	F7	F11	F13
Dry Density, kN/m ³ (pcf)	16.08 (102.38)	15.40 (98.09)	14.84 (94.49)	15.68 (99.87)
Compaction Energy, kJ/m ³ (ft-lb/ft ³)	381.73 (7973)	127.26 (2658)	127.26 (2658)	127.26 (2658)
Number of Blows/Layer	15 Blows 3 Layers	15 Blow 1 Layer	15 Blow 1 Layer	15 Blow 1 Layer
Geotextile	NW 6	NW 6	NW 16	No Fabric
AOS (mm)	0.212	0.212	0.150	---
Gradient	32.5	15	15	15
Test Duration (hours)	195.67	6.28	8.25	11.93
Average k (m/sec)	1.74 e-8	3.13 e-6	5.65 e-7	6.42 e-7
Standard Deviation for k	4.14 e-9	1.37 e-6	1.71 e-7	4.87 e-7
Void Ratio, e	0.40	0.46	0.52	0.44
Porosity, n	0.29	0.32	0.34	0.30
Cumulative Permeant Volume (ml)	3147	8887	2113	2857
Pore volume, pV (ml)	250	276.42	298.18	265.54

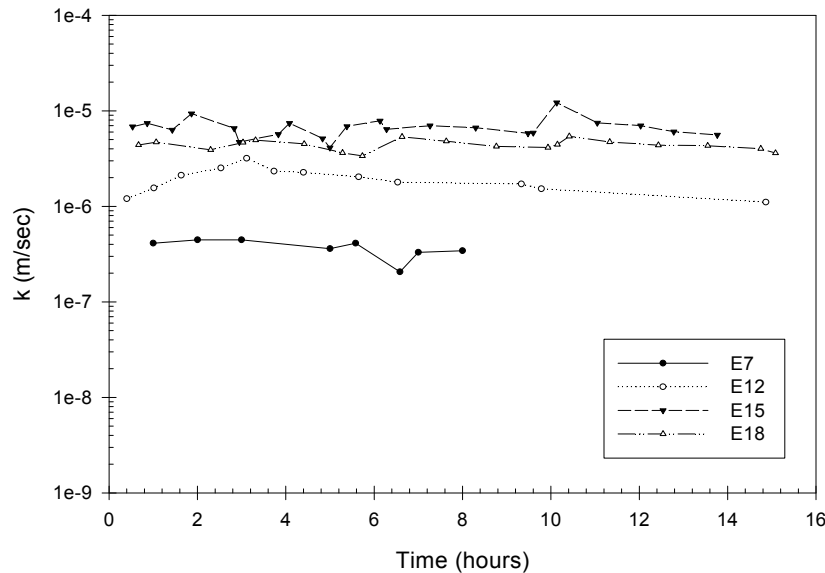


Figure 4. CCR Hydraulic Conductivity

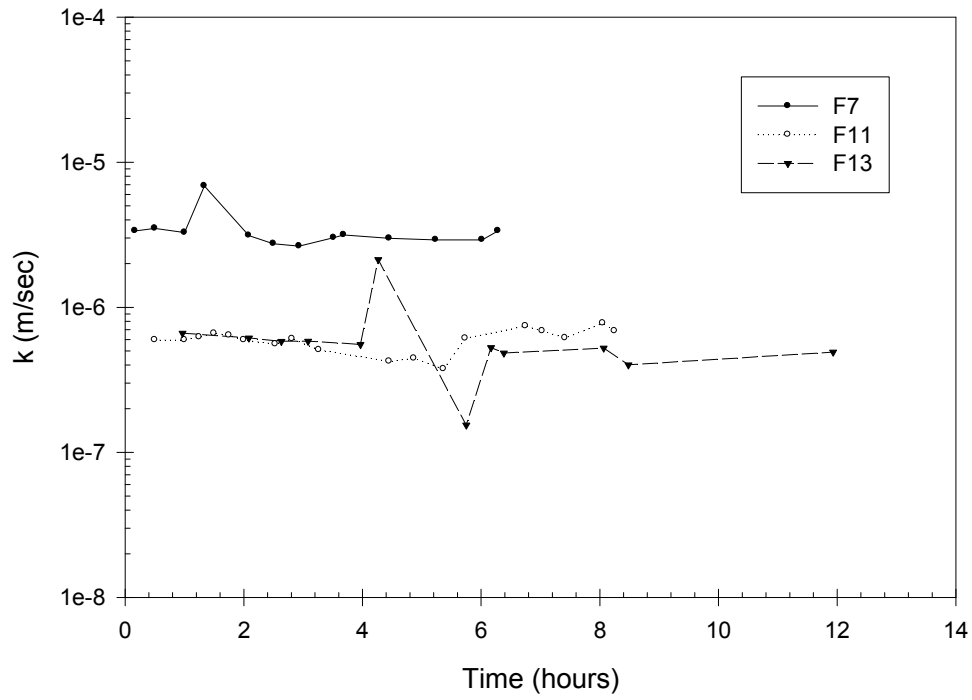


Figure 5. Blended Refuse Hydraulic Conductivity for F7, F11, F13

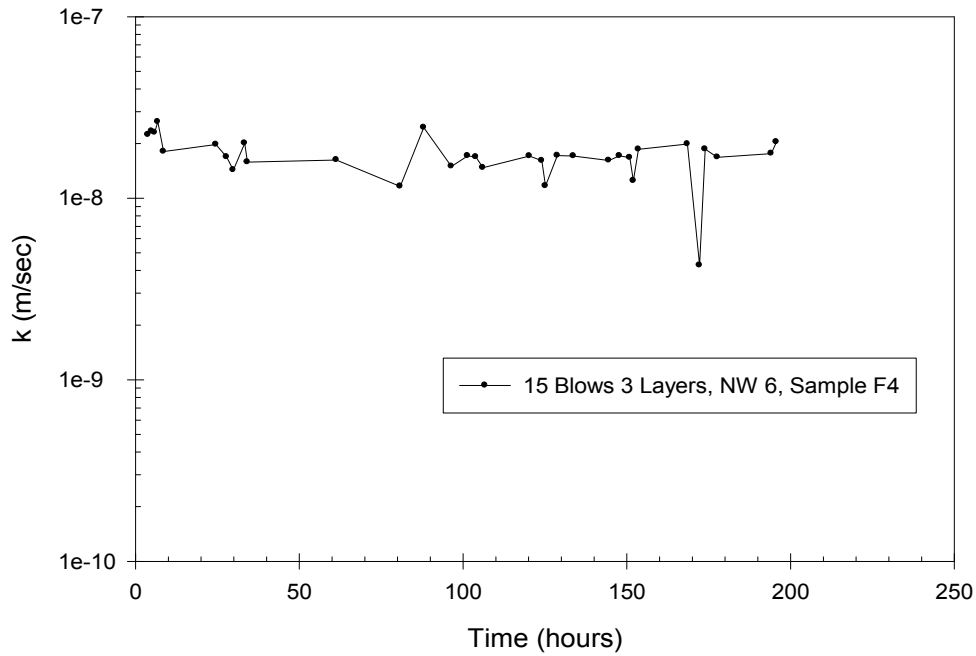


Figure 6. Blended Refuse Hydraulic Conductivity for F4

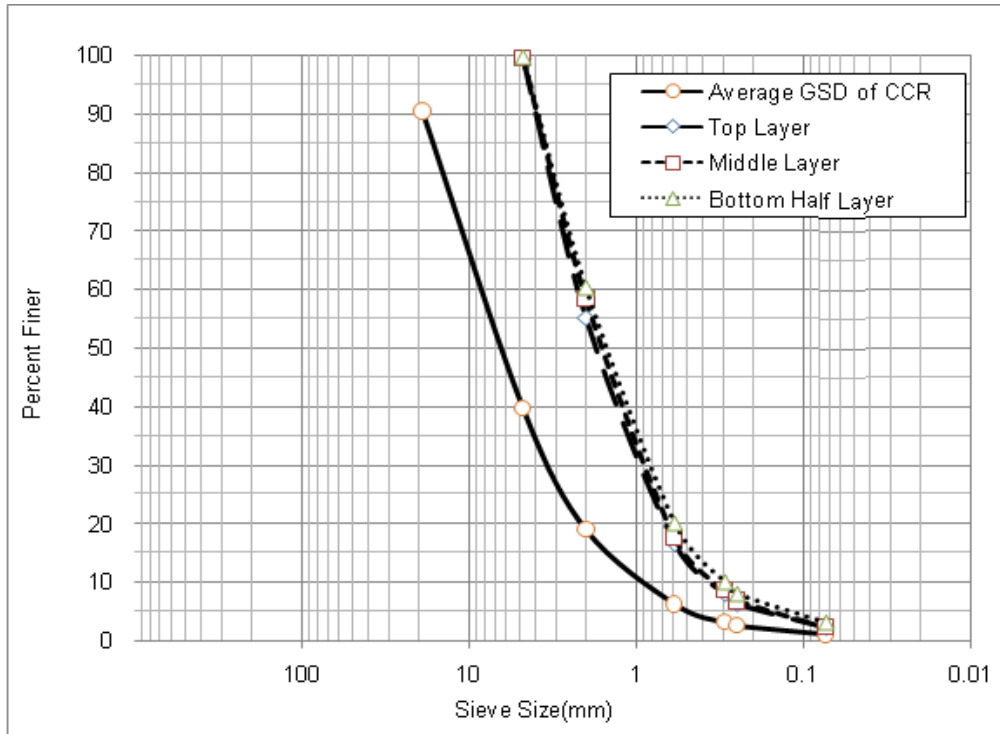


Figure 7. Average Grain Size Distribution by Layers for CCR Hydraulic Conductivity Samples

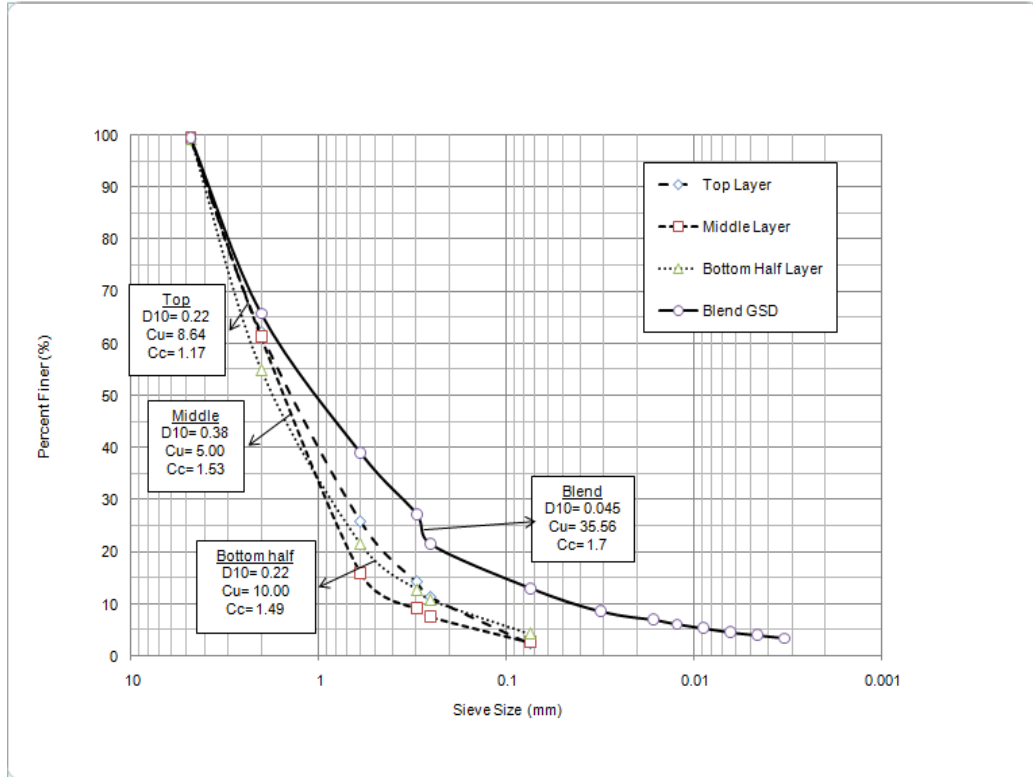


Figure 8. Sample F4 Grain Size Distribution by Layers

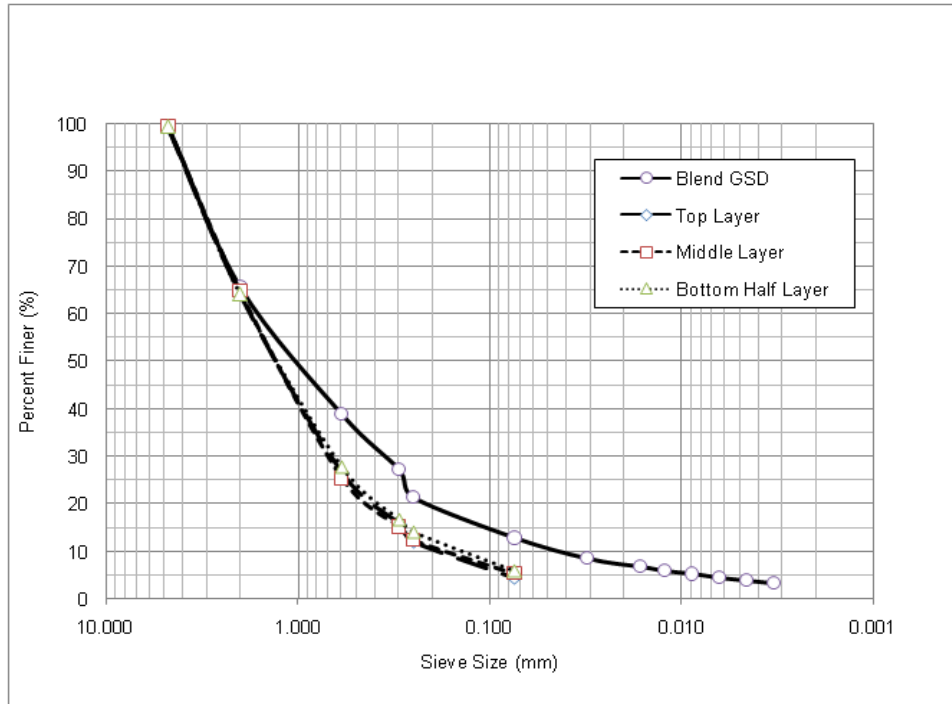


Figure 9. Average Grain Size Distribution by Layers for Blended Refuse Hydraulic Conductivity

Table 6. Post Grain Size Distribution Results for Permeability Cells

Specimen	Compaction Plan	D ₁₀ * Final	C _u * Final	C _c * Final	<i>i</i>	<i>k</i> (m/s)	AOS
CCR							
E-7	Stad. Proctor	0.29	9.58	1.36	5	3.69 e -7	NW601, 0.212
E-12	12Blowx2Lyr	0.35	5.71	1.16	5	1.94 e-6	NW6 , 0.212
E-15	4 Blowx2lyr	0.3	6.67	1.18	5	6.73 e-6	NW6, 0.212
E-18	8 Blowx2Lyr	0.29	6.21	1.08	7.1	4.39 e-6	NW6, 0.212
Blended 80% CCR / 20% FCR							
F-4	15 Blowx3Lyr	0.22	10	1.49	32.5	1.74 e-8	NW6, 0.212
F-7	15 Blow x1Lyr	0.13	13.08	1.91	15	3.13 e-6	NW6, 0.212
F-11	15 Blow x1Lyr	0.11	15.45	2.55	15	5.65 e-7	NW16, 0.150
F-13	15 Blow x1yr	0.13	13.08	1.91	15	6.42 e-7	No Fabric

* For CCR: D₁₀ Initial= 1.2, C_u Initial= 6.25, C_c Initial= 1.38
 For Blended Refuse: D₁₀ Initial= 0.045, C_u Initial=35.56, C_c Initial= 1.7

Grain Size Distribution Analysis

The grain size distributions of the CCR and Blended refuse samples obtained after the permeability testing were evaluated by sectioning the samples into thirds. The graph in Figure 7 shows the average CCR particle distribution increasing in fines percentage by a uniform reduction in particle diameter from compaction. The change is approximately 76 % for D60 and is 80% for D10 particles. This percent change is consistent for compaction energies ranging from 67 kJ/m³ to 636 kJ/m³. In Figure 8 the fine distribution of distribution for the Blended F4 specimen indicates an opposite trend where the particles less than 2 mm (#10 sieve) appear to have packed together and were not easily separated after compaction. The sieve analysis incorporated aggressive shaking and pulverizing, however the fine refuse appeared to pack together tightly and did not appear to be crushed by the compaction effort. The 20% increase in fine refuse did not appear to produce fine particle mobilization to reduce the hydraulic conductivity of the refuse/geotextile system.

CONCLUSIONS

The conclusions of this work tend to indicate that the geotextile fabrics having an AOS of 0.212 mm or 0.15 mm did not have an appreciable effect in reducing the hydraulic conductivity of the CCR and Blended refuse for the percentage of fines tested in the permeability cells. It appeared that the fine particle increase in the CCR samples was independent of compaction energy and that the percent increase in fines resulted from effective compaction effort and occurred on a reduced fraction of refuse as the refuse larger than the #4 sieve size was removed from testing per ASTM

requirements. Actual field particle size reductions would expect to be less. The fine particles introduced by the 80/20 Blended sample did not effectively mobilize coal fines at various compaction energies or sample densities due to particle packing within the sample. There appeared to be no impact of geotextile clogging under these tests. However, the laboratory scale testing may not reflect field conditions.

ACKNOWLEDGEMENTS

This project was made possible through funding from the Coal Impoundment Project at the National Technology Transfer Center (NTTC) at Wheeling Jesuit University through a grant from the US Mine Safety and Health Administration (MSHA). The authors wish to thank Mr. J. Davitt McAteer, Program Director for support in completing this work. The author's further thank the MSHA Pittsburgh Safety and Health Technology Center, Mine Waste and Geotechnical Engineering Division for their involvement and support of this work. The authors wish to acknowledge the management and field personnel from the Eastern Associated Coal - Patriot Coal Division for their in-kind support of this research. The authors express their gratitude to Matt Dudley, Jeremi Stawovy, and Eric Baker for supporting the laboratory efforts.

REFERENCES

ASTM Designation D-5856, 2005. Standard Test Method for Measurement of Hydraulic Conductivity of Porous Material Using a Rigid-Wall, Compaction-Mold Permeameter. Annual Book of ASTM Standards, *American Society of Testing Material*, Easton, MD.

ASTM Designation D-5101, 1999. Standard Test Method for Measuring the Soil-Geotextile System Clogging Potential by the Gradient Ratio. Annual Book of ASTM Standards, *American Society of Testing Material*, Easton, MD, D35-03.

MSHA. 2007. Engineering And Design Manual: Coal Refuse Disposal Facilities Advance Draft For Industry Review And Comment. U.S. Department of Labor, 937 pp.

NRC [National Research Council]. 2002. Coal Waste Impoundments: Risks, Responses, and Alternatives. Washington, DC: National Academy Press, 230 pp.

J.D. Quaranta, B. Gutta, B. Stout, D. McAteer, and P. Ziemkiewicz, "Improving the Safety of Coal Slurry Impoundments in West Virginia," Tailings 2004, Vail CO.

J. Gonzalez Cañibano and D. Leininger (1987), "The Characteristics and use of Coal Wastes," *Reclamation, Treatment, and Utilization of Coal Mining Wastes*, edited by A.K.M. Rainbow Elsevier Science Publishers B.V., Amsterdam, 1987.

Windisch, É. J., "Grain-size Distribution of Mixed Aggregates." *Geotechnical Testing Journal*, GTJODJ, Vol. 19, No. 2, June 1996, pp. 227-231.

ON-LINE REMOTE TAILINGS DAM HEALTH CONDITION MONITORING SYSTEM BASED ON FIBER OPTIC SEEPAGE SENSORS

Chang Wang

Key Laboratory of Optical Fiber Sensing Technologies in Shandong, Jinan, Shandong, China

Yanong Ning

Intelligent Sensor Systems Limited, Rockley Manor, Rockley, Marlborough, Wiltshire, UK

Tongyu Liu, Zhong Zhou

Shandong Micro-Sensor Photonics Limited, 19 Keyuan Road, Jinan, Shandong, China

ABSTRACT: This paper reports an on-line remote monitoring system employing optical fiber seepage sensors to monitor the position of phreatic surface within the embankment of tailings dam. The phreatic surface is monitored at real time along a number of cross sections of the tailings dam as required in the key portions of the tailing dam embankment. All data collected are sent to a control room and automatically logged in a pre-design format. The sensors can be deployed at any position in tailings dam embankment over a few kilometers away from the control room. Since there is no electric active component within the sensor probes and the optic fiber leads, the sensor system is immune to EMI such as lightning and storm. This system offers convenient and reliable means for long term, real-time phreatic surface and ground water management of tailings dam and exhibits significant application potential.

INTRODUCTION

Tailings storage facilities typically represent the most significant environmental liability associated with mining industries. The ongoing persistent occurrence of tailings dam incidents and failures have both environmental and economic impacts to local community. The results of those failures also are hazardous to biota and humans in many ways.

In the mining industry, tailings dam failures not only cause heavy losses of people's lives

and properties, but also have big impact to the local environment, which then directly or indirectly affects the safety of human life and wildlife for the years to come. According to statistics, between 2005 and 2007, there had been 17 major tailings dam failure accidents in China, causing 41 mortalities and 29 injuries. On September 8th, 2008, a big tailings dam accident at Xiangfen, Shanxi province, China, has claimed more than 260 people lives ^[1]. The damage caused by these failures in the form of human casualties, destruction of property, pollution of the environment and economic loss to the mining

industry was enormous. It is vital that the responsibility of long term safety management of mine waste needs to be addressed by mining industry and local authorities.

In order to reduce the risk of tailings dam failure accidents and protect people life and property, it is important to enhance the supervision and management of tailings dam facilities and monitor the current health conditions of the tailings dam. In order to constantly monitor the health condition of tailings dam, a number of parameters need to be measured and recorded, such as the movement or displacement of the embankment, the water level in the dam and the phreatic surface etc. The traditional method for a tailings dam monitoring relies on trained staffs to carry out routine survey using conventional instruments at the scene. The method is often affected by the weather condition and human errors. As the measurement data only reflect the status of the tailings dam at the time when the measurement is taken, it can not reflect the variation of tailings dam's conditions throughout the production process. Furthermore, due to the constraints of the technologies and measuring instruments, not all of technical parameters are monitored in a timely manner, for example the tailings dam phreatic line changes during the time between two measurement intervals. In addition, the manual observation and recording cannot display the dynamic variation of the tailings dam conditions and trends over time to make timely prediction and forecasting. Especially, for the monitoring of phreatic line that directly related to the stability of the embankment of a tailings dam to effectively provide important early warning information of the tailings dam-break disasters. Therefore, to introduce and promote real-time, continuous monitoring technology and

products for monitoring the health conditions of tailings dams is essential.

Optical fiber sensing technology is a multi-disciplinary technology which has been developed from 1970's along with the advancement of optical fiber communications technologies. New products and their applications have been increasing in recent years, at present more than 2000 types of optical fiber sensors have already introduced. These sensors have been widely employed for measurement of temperature, pressure, strain, vibration, ultrasound, methane gas and etc [2]. Optic fiber sensors have many unique merits compared to conventional electrical sensors, among their merits, the immunity to electromagnetic interference (EMI) and capability of making remote, real time measurement without requiring the local power suppliers. These features enable these sensors especially suitable to be deployed at the locations where the strong EMI is present, such as in the field where no facilities can be used to prevent the sensors from thundering and lighting attacks.

Laser Institute of Shandong Academy of Science and Chinese Academy of Safety Science carried out a joint R&D project to develop an optic fiber sensing system for real time tailings dam monitoring. The operation of the field experiment at a number of tailings dams shown that the system not only provide the re-mote, real time measurement data, but also withstand a long period of thunder and lighting whether.

TAILINGS DAM MONITORING SCHEME

In tailings dam health monitoring, one of the most important parameters is the phreatic line or seepage line that is formed due to the existence of a large quantity of tailings slurry

precipitation tail water. In normal operational condition, the constant discharge of tailings from the top of the dam, the pulp continuously downward infiltration of water and the substantial rainfall in flood season will form a large seepage field within the tailings dam's embankment. There are a number of factors that could affect the phreatic line of a tailings dam. For example, in normal operation, the tailings deposition is non-uniform, the depositing position needs to be changed regularly, the embankment of a dam keeps increasing, the source of ore and ore-dressing processes may be changed over the entire service. All of these make the seepage field of a tailings dam become very complex. Since the phreatic line is directly related to the tailings dam stability and safety, the phreatic line is also called as the “safety guard line” of a tailings dam. Therefore, to monitor the location of phreatic line and its variation during the operation is one of important aspects for monitoring tailing dam safety [3]. The key feature used to determine the location of the phreatic line within the dam embankment is to find out where the pore water pressure is zero, as shown in Figure 1, by measuring the pore water pressure across the embankment, the phreatic line can be determined.

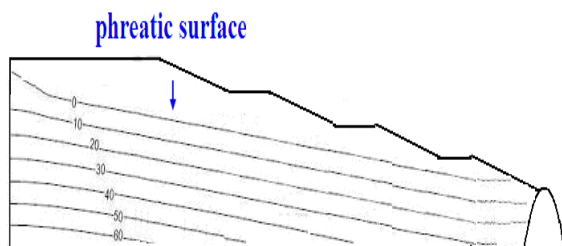


Figure 1. Distribution of pore water pressure within a tailings dam (unit: kPa)

To monitor a tailings dam embankment, the narrowest cross-section or the cross-sections where significant risk to the downstream areas may be imposed are normally selected for deploying the sensor probes. For each cross section, at least four monitoring points

are required. The selection of the probe position and its depth from the top of the embankment is dependent on the dam design information, such as the gradient variation of the pore water pressure along the downstream slope of dam. Documents such as "Tailings Dam Safety Technical Regulation" (AQ2006-2005) can be used as a guideline to calculate the location of phreatic line for each cross section [4]. In analyzing the dam stability against sliding, the design specifications of the phreatic line should be worked out in accordance with the provisions of the normal operation of infiltration routes and flood conditions. This phreatic line will determine the locations and the depth of the probes within the dam embankment.

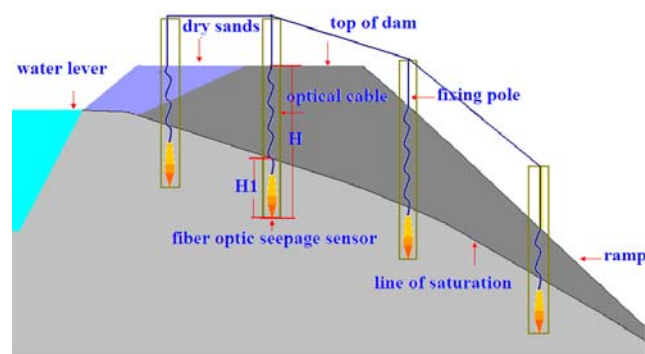


Figure 2. Fiber optic sensors for monitoring the phreatic line.

Figure 2 shows the arrangement of a number of measurement points at one of cross section of the dam embankment. In each borehole, an optical fiber phreatic sensor is installed. By measuring the hydraulic pressure, the water level within the borehole can be calculated, then the phreatic line can be worked out using the information of the probe depth and the water level.

The fiber-optic phreatic sensor consists of an optical fiber Bragg grating (FBG) with one end being fixed at a flexible diaphragm and the other end fixed to the sensor body. The elastic diaphragm is deformed by external

water pressure, which results in strain change in the FBG element and subsequently the FBG wavelength change. By detecting FBG wavelength variation, the water pressure applied to the sensor can be determined. The structure of the fiber-optic phreatic sensor and photograph of the sensor are shown in Figure 3. The sensor calibration results are shown in Figure 4, where the x-coordinate is wavelength (Unit: nm) and the y-coordinate

is pressure (Unit: MPa). To correct the measurement variation due to ambient temperature changes, a FBG based temperature sensor is also imbedded in each probe. The temperature information for each monitoring point can also be monitored and recorded, which is helpful in study the seasonal variation of the tailings dam.

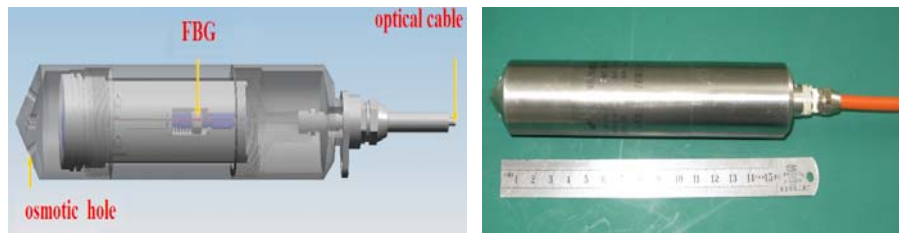


Figure 3. Structure and photograph image of the fiber-optic phreatic sensor.

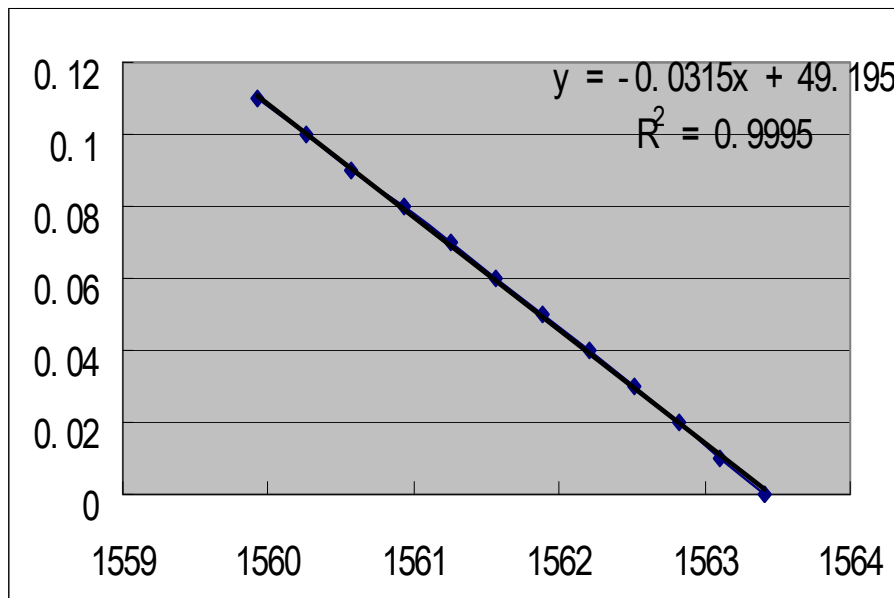


Figure 4. Sensor calibration curve (10m range).

It can be seen from figure 4, the sensor exhibits very good linearity. For water depth change over 10 m range, the sensor has 3.158 nm wavelength variation. Hence for

wavelength detection accuracy of 1 pm, this corresponds to 3.2 mm of depth accuracy. For a smaller range sensor 0-2 m, 0.5 mm of water level accuracy have been achieved.

DEMODULATION

Figure 5.a shows a schematic diagram of a demonstration project used at an iron ore tailing dam near Beijing, China. In this system, a high-precision multi-channel fiber Bragg grating demodulator was installed in the dam control room. Eight phreatic sensors

were connected to the sensor demodulator via a multi-core optical fiber cable to monitor two tailings dam cross-sections (4 sensors for each cross-section). The installation of sensors and fiber optic cable are shown in figure 5.b. The selected locations and installation depths of each sensor probe are shown in Figure 6.

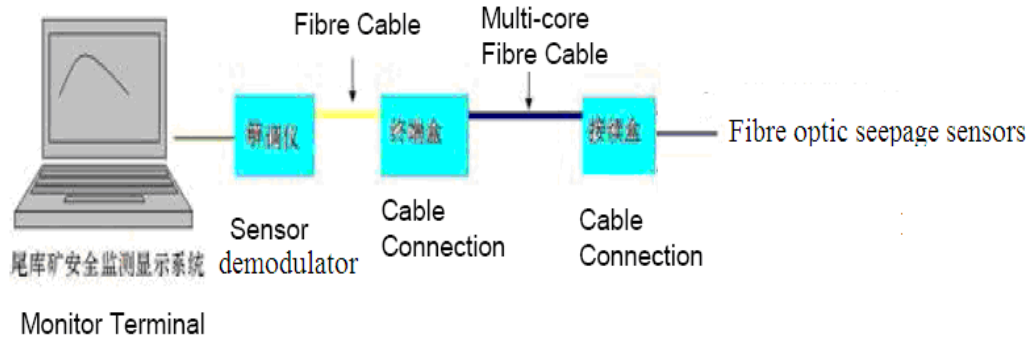


Figure 5. a) Schematic diagram of monitoring system; 5.b) installation and protection of the sensors and fiber optic cable.

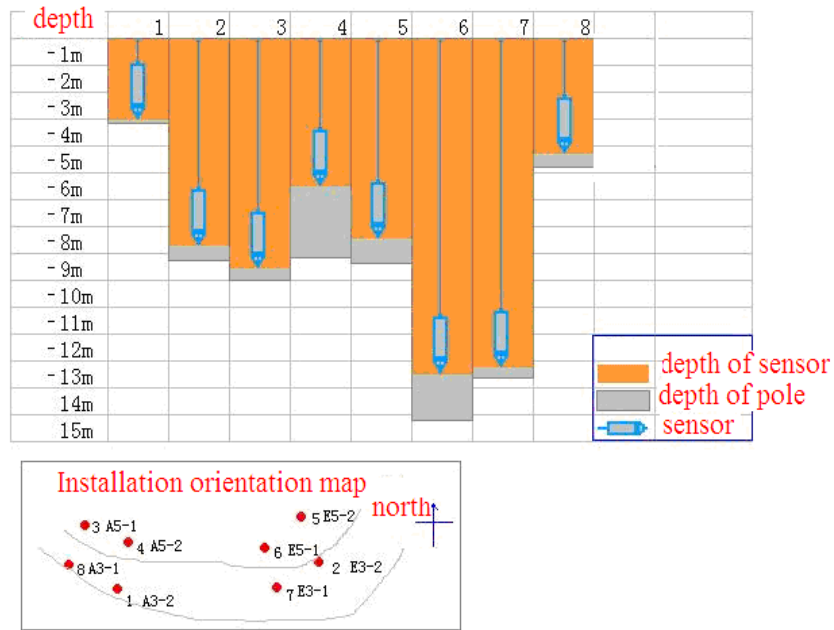


Figure 6. Locations and depths of each sensor probe

TEST RESULTS AND DISCUSSION

After the completion of the installation, a user friendly graphic interface developed for this project can be used to show the probe positions, as shown in Figure 6. The recorded data are logged according to the pre-determined format. For each probe, the alarm water level can be set through the use of the alarm setting menu. When the water level reaches or above the alarm level, the red spot will flag the alarm signal, sending out the warning message. The status of each probe is shown the interface, while the measured data can be checked using the data query menu. The data log report by a day, a week or a month are automatically generated and restored. These historical data reports can be traced by selecting the report menu. Figure 7 shows the user interface of the monitoring system.

With the use this monitoring system, the real-time monitoring of the phreatic line variation

can be easily achieved. In order to compare the fiber optic sensor system results and those obtained from conventional electrical system, a number of electronic piezometric probes were also employed in the project. Unfortunately, during the summer rain season, the piezometer based electrical system was damaged by lightning storm, whilst optic fiber phreatic sensor system was not affected by lightning. Fiber optic sensors demonstrated unparalleled advantage over conventional electric sensing device when used under extreme weather conditions. At present, further work are on going to interrogate more monitoring parameters in to the tailings dam monitoring system. This includes the optic fiber displacement sensors for monitoring the displacement of the dam embankment, the optic fiber water level sensors for monitoring the water level variation in the dam and the CCTV monitoring system for visual inspections.

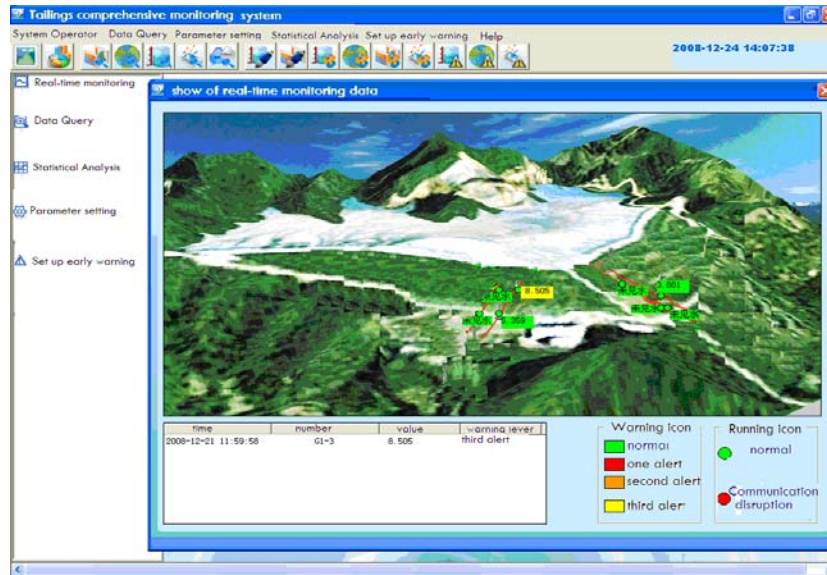


Figure. 7 monitoring system software interfaces

CONCLUSIONS

The demonstration of using advanced fiber-optic sensing technologies to monitor the operational condition of a tailings dam is reported. The fiber optic phreatic sensor system used not only provides on-line real time measurement, but also equipped with early warning features which can be set according to the conditions of each tailings dam. Because of the use of optic fiber cable to connect the sensor probe to the demodulator, it becomes much easier to deploy the sensor probes over a long distance (up to many kilometers) and cover a large area under the extreme weather conditions such as lightning. Next phase of the R&D work are focusing on extension to more critical parameters using fiber optic sensor technologies and evaluate long-term performance, which will be reported later.

ACKNOWLEDGEMENT:

The authors are grateful for Dr Yunhai Wang, and his team at China academy of safety

Science for their funding support and assistance in the user interface.

REFERENCES:

State Administration of Work Safety Supervision and Management I Division, the National Accident Analysis of non-coal mines during the first half 2007, <http://www.Chinasafety.gov.cn/feimeizhengzhi/feimeizhengzhi.htm>

R Wills. Application of Optical Fiber Sensors [C]. Proceedings of the SPIE, 2000, 4074:24-31.

Zhang Xinkai, Wang Sheng, Xiang Quisheng. Metal non-metal mine tailings and analysis of the safety status, Safety Science and Technology of China, 2006(2)

Sun Huashan, Steady progress in the activities of special rectification tailings. Labor Protection, 2007(12):10~13

INFLUENCE OF MICROSTRUCTURE ON SELF-WEIGHT SETTLING OF LATERITE ORE SLURRIES

Shahid Azam

University of Regina, Regina, Saskatchewan, Canada

J. Don Scott

University of Alberta, Edmonton, Alberta, Canada

ABSTRACT

Complex solid-liquid interactions govern the self-weight settling behavior of dilute laterite slurries. Resulting from ore mineralogy and process water chemistry, these interactions are exhibited in the initial slurry microstructure. Based on laboratory investigations, this paper aims at understanding the self-weight settling process in laterite slurries. The ore slurries exhibited variable microstructures ranging from a dense uniform aggregation to a loose particulate cardhouse. The initial hydraulic conductivity varied from 10^{-1} cm/sec to 10^{-4} cm/sec with a corresponding change in the final settling volume from 66% to 17%. The directly proportional rate and amount of settling empirically correlated with the slurry morphology.

INTRODUCTION

The disposal of mine waste tailings generally involves the physical understanding of the self-weight settling process (Morgenstern and Scott, 1995). In the presence of charged solids (clay and non-clay minerals) and ion-rich liquid (alkaline or acidic), the influence of complex physicochemical interactions can be significant. This is particularly true for applications such as thickening where the low initial solids content of the slurries helps maximize interactions at the solid-liquid interfaces thereby resulting in a distinct microstructure (Azam et al., 2007). Theoretically, a three-dimensional network is developed at the onset of the settling process. Such a mesh prevents free particle fall or

segregation and rapidly settles under gravity as a single unit while allowing upward water flow. This regime of *hindered sedimentation* refers to slurry dewatering without measurable effective stresses (Torfs et al., 1996). Overtime, the solid grains come closer and start transmitting effective stress. Under *self-weight consolidation*, slurry dewatering primarily occurs due to pore water expulsion (Terzaghi et al., 1996). The initial morphology is known to govern the rate and amount of settling in many sedimentary soils, for example, clay slurries (Pane and Schiffman, 1997). Comparable data is required for residual laterite slurries.

Laterites are the key source of economic metals. According to Golightly (1981), these

residual soils contain an estimated 80% of known nickel (Ni) reserves on land with sizeable amounts of cobalt (Co). The in situ profiles of laterites exhibit extensive mineral variability due to a variable rate and amount of weathering that, in turn, depends on parent geology and the prevalent climate. The metals are usually extracted from the retrieved ores by the sulphuric acid pressure leaching method. Washing the crushed ore with locally available water and simultaneously passing it through a series of sieves yields a fine-grained slurry. Although the composition of the wash water is different in the various mining operations, the slurry solids generally have a maximum grain size of 0.85 mm (corresponding to ASTM Sieve No. 20) and comprise 15% of the total mass of the material (Azam et al., 2005). To optimize operational throughput and acid and steam consumption during the hydrometallurgical extraction process, slurry settling in the various inline thickeners must be swift and large. With depleting high-grade ores, there is an exigent need to evaluate various low-grade and blended materials for cost-effective ore beneficiation.

The main objective of this paper was to understand the influence of microstructure (derived from physicochemical interactions) on the self-weight settling behaviour of laterite ore slurries. To capture the influence of ore geology and the slurry preparation environment, laterite samples were obtained from mining operations in different parts of the globe. The Metallurgical Technologies Division of Dynatec Corporation, Canada, provided the following samples: A, limonite (Cuba); B, limonite-saprolite blend (Philippines); C, limonite-saprolite blend (Australia); and D, saprolite (Indonesia). Based on laboratory characterization, the slurry composition including solids mineralogy and water chemistry was determined. Next, the slurry microstructure was captured at the onset of the self-weight

settling process at a solids content of 15%. Finally, self-weight settling tests were conducted and the results were studied in conjunction with solid-liquid interactions and slurry morphology.

SOLID MINERALOGY

Mineralogy was investigated by X-ray diffraction (XRD) analysis using a Phillips diffractometer (Model Pw 1710) that had a Cu broad focus tube at 40 kV and 40 mA alongside a monochromatic incident ray. To obtain a complete mineralogy, materials finer than 0.85 mm were obtained by manually pulverizing the oven-dried samples. Randomly oriented specimens were prepared in rectangular metal holders, 20 mm x 10 mm size. The specimen surfaces were pressed against a rough glass to maximize randomness in packing. Samples were scanned from a 4° through 90° angle (2θ) at a speed of 1° 2θ /min. To determine mineral species, the diffraction patterns were matched with the standard patterns prepared by the Joint Committee of Powder Diffraction Data Service (JCPDS). Semi-quantitative mineral estimates were made by the Reference Intensity Ratio method (Moore and Reynolds, 1997).

Figure 1 highlights the main constituent minerals on the X-ray diffraction patterns of these laterite ores. All samples contained goethite (α -FeO.OH) that was derived from the conversion of olivine (Eliopoulos and Economou-Eliopoulos, 2000). This mineral alteration or *laterization* is attributed to an equatorial climate that ensured intense and prolonged chemical weathering (Brady, 1990). The same process also involved leaching of silica and accumulation of Fe/Al oxides resulting in gibbsite ($\text{Al}(\text{OH})_3$) in sample A (Pickering, 1962). Dehydration or *desiccation* of sesquioxides yielded well-crystalline maghemite (Fe_2O_3) and hematite

(α -Fe₂O₃) in samples A, B, and C (Sherman et al., 1953). However, some of the silica and iron oxides were not completely converted and occurred in amorphous form in samples B, C, and D. These samples indicated chrysotile peaks at 14° and 28° angle (2 θ). A member of the 1:1 kaolinite-serpentine group, this clay mineral is associated with oxidation of the olivine-rich parent rock called peridotite. This *serpentinization* involved SiO₂ transformation and an increase in exchangeable Mg²⁺ in the soil (Dixon and Schulze, 2002). The shoulders between 5° and 10° angle (2 θ) in samples C and D were identified as chloritic intergrades. This hybrid 2:1–2:2 phyllosilicate mineral is believed to have evolved from the *depotassification* (progressive weathering involving K⁺ removal) of deeply buried mica that usually contains 9% potassium (Brady, 1990). The sharp and higher peak around 7° angle (2 θ) in sample C indicated a more active chloritic intergrade.

Table 1 summarizes the mineralogical composition of the investigated laterite ores. Despite the semi-quantitative nature of XRD analyses, the data depicted herein correlated well with the measured specific gravity of 3.0 ± 0.1 (Azam et al., 2005). The variability in mineral quantities among different laterite ores is attributed to local climate, lithology and topography (Golightly, 1981). Samples A and B respectively contained 80% and 50% sesquioxides (goethite, gibbsite) along with 20% and 40% iron oxides (hematite, maghemite). Conversely, samples C and D were primarily composed of clay minerals (50% and 45%, respectively) including chrysotile and chloritic intergrade and sizeable amounts of amorphous materials (15% and 40%, respectively) and iron oxides (30% and 15%, respectively). Overall, the investigated laterites can be categorized as oxide-rich (samples A and B) and clay-rich (samples C and D).

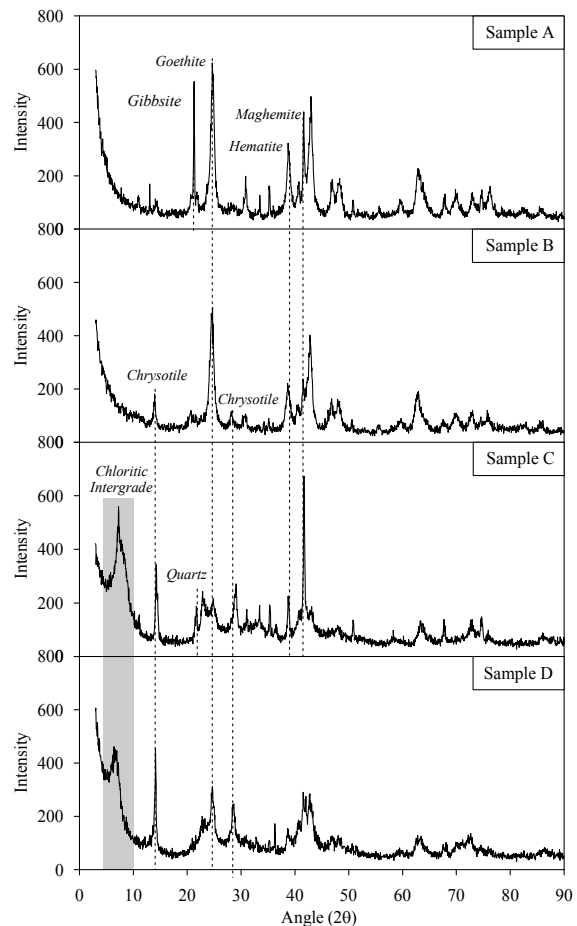


Figure 1: XRD patterns of the investigated samples

Table 1: Summary of solids mineralogy

Mineral (%)*	A	B	C	D
Goethite	60	50	10	15
Gibbsite	20	---	---	---
Hematite	10	20	10	---
Maghemite	10	20	10	---
Quartz	---	---	5	---
Chrysotile	---	10	10	10
Chloritic Intergrade	---	---	40	35
Silica & Iron oxide	---	---	15	40

* Accuracy is $\pm 5\%$

WATER COMPOSITION

An Accumant 50 instrument was used to measure pH and electrical conductivity (*EC*) as per ASTM procedures: D4972-01 and D1125-95(2005), respectively. Concentrations of Na⁺, K⁺, Ca²⁺, Mg²⁺ and SO₄²⁻ were determined by the Inductively Coupled Plasma method in a Thermal Jarrell Ash IRIS Advantage. The Automated Ferricyanide Method using Colorimetric Centripetal Analyzer (COBAS FARA II) determined Cl⁻. Similarly, NO₃⁻ and HCO₃⁻ were determined according to ASTM D4327-97 using a Dionex DX-500. Ion summation was recorded as total dissolved solids (*TDS*).

Table 2 summarizes the pore water chemistry of the laterite ore slurries. The pH was slightly basic and below the zero point of charge (*ZPC*) that ranges between 7.0 and 8.5 for laterites with mixed mineralogy (Golightly, 1981). The measured *EC* of slurry waters varied significantly and corroborated with soil composition (Sposito, 1989). Sample A was similar to silts ($50 \leq EC \leq 300$) whereas the other materials were identical to clays ($100 \leq EC \leq 10,000$). The high *EC* of sample C is attributed to the presence of salts in the slurry (Rhoades et al., 1990). The calculated *TDS* were generally in agreement with the measured *EC*.

The dissolved ions given in Table 2 exhibited electrical neutrality with differences between positive and negative charges always less than 5% (calculations not given in this paper). Salt forming ions such as Na⁺, K⁺, Ca²⁺, Mg²⁺, Cl⁻ and SO₄²⁻ were the main constituents in all of the pore waters. This indicated that readily available local waters affected by the background seawater concentration were used for slurry preparation in different countries.

Table 2: Summary of pore water composition

Property	A	B	C	D
pH	7.1	7.2	7.5	7.3
<i>EC</i> (μS/cm)	156	744	1250	442
<i>TDS</i> (mg/L)	86	564	8584	3857
Na ⁺	21	17.0	2530	1020
K ⁺	1.1	1.1	40	4
Ca ²⁺	3.5	19.5	134	21
Mg ²⁺	2.8	87	381	241
Cl ⁻	20.5	28.4	4070	1670
NO ₃ ⁻	1.9	1.3	34.3	21
HCO ₃ ⁻	15	24	94	30
SO ₄ ²⁻	20.2	386	1300	850

SLURRY MICROSTRUCTURE

The microscope (JSM-6301FXV) performed scanning electron microscopy (SEM). The cryogenically prepared samples ensured an intact fabric and minimal grain re-adjustment (Lilly and Sargent, 1990). The slurry was sucked in a 5 mm straw and immediately immersed in nitrogen slush at -208°C. The straw was clipped and peeled off after instantaneous freezing. The SEM chamber was flushed with argon to remove water vapour and vacuum cleaned with a rotary pump. Samples were placed in the chamber, sublimated at -40°C, and examined at 2.5 kV till complete ice removal. An ablation depth of approximately 10 μm, that evaded possible fabric collapse, was obtained in about 45 min. Samples were gold sputtered in the cryogenic system at -155°C to minimize ionization and transferred back to the chamber for visual examination. The vacuum pressure and scanning and recording speeds were 8 x 10⁻⁸ kPa, 450 frame/sec and 40 sec/frame, respectively. The 5 kV incident beam was kept at a vertical distance of 30 mm during photomicrograph capture. Slurry fabric was captured through photomicrographs at

representative locations using two magnifications: x500 indicating typical representative locations and x2000 denoting detailed features of selected areas.

Figure 2 gives the SEM photomicrographs of the investigated samples. Bright edges in some of the photomicrographs denote surface charging due to ionization. Overall, the figure confirms the XRD results by illustrating that the clay matrix is primarily composed of needle-shaped goethite, which is finer than 2 μm (Mitchell and Soga, 2005).

In general two types of microstructures were observed in the investigated slurries, namely: aggregated (samples A and B) and cardhouse (samples C and D). Flocculation was the primary mechanism in the aggregated samples. The oxide-rich samples predominantly constituted positively charged particles that had limited interaction with almost inert pore waters.

Aggregation in such colloid-water-electrolyte systems is attributed to the polar nature of goethite, maghemite, and hematite. These minerals acted as micromagnets and resulted in mutually conjoined agglomerated colonies. The phenomenon of positively charged particle accumulation is confirmed by sample B. The micrographs show negatively charged chrysotile clay platelets (arranged in a face-to-face association) on which the goethite particles are aligned similar to iron filings on a magnet.

Cardhouse clay microstructure was observed for clay-rich laterites (samples C and D). These samples contained clay minerals and siliceous materials with high water adsorbing capabilities (Briceno & Osseo-Asare, 1995).

Dispersion of clay particles is attributed to the presence of exchangeable Na^+ in a

slightly basic medium. Cross-linking between face-to-face arrangements was mainly due to partial coating of clay platelets with sesquioxides and amorphous materials amounting to 25% (samples C) and 55% (sample D). The slow freezing rate due to sample insulation by nitrogen at $-208\text{ }^\circ\text{C}$ and the high amount of water and salts in these samples possibly contributed to forming crystalline ice thereby influencing the cardhouse fabric development (Mikula, 1988). The high multivalent ion concentration in the pore water of sample C resulted in a five-fold decrease in void spacing when compared with sample D.

SEM analyses were used for qualitative fabric assessment. The observed 0.0002 mL (5 mm diameter and 0.01 mm depth) material represented 0.000001% of the original 20 L sample. Some large particles were eliminated as samples fractured along the weakest planes. The fabrics may have endured shrinkage due to pore and interlayer water removal during sublimation (Tovey and Wong, 1973) as well as localized underlying collapse due to breakage of the weak cross bonding by vacuum pressure during ablation (Erol et al., 1976). Still, the observed microstructure explained the distinct features of the investigated slurries. Abiding by the sample preparation method resulted in identical artefacts thereby allowing an empirical comparison of laterites.

SELF-WEIGHT SETTLING

Self-weight settling tests were conducted by pouring slurry samples in 850 mm (inside diameter) graduated jars up to a height of 850 mm. The resulting height-diameter ratio of 1.0 at test start was found to have no significant wall effects (Azam et al., 2007).

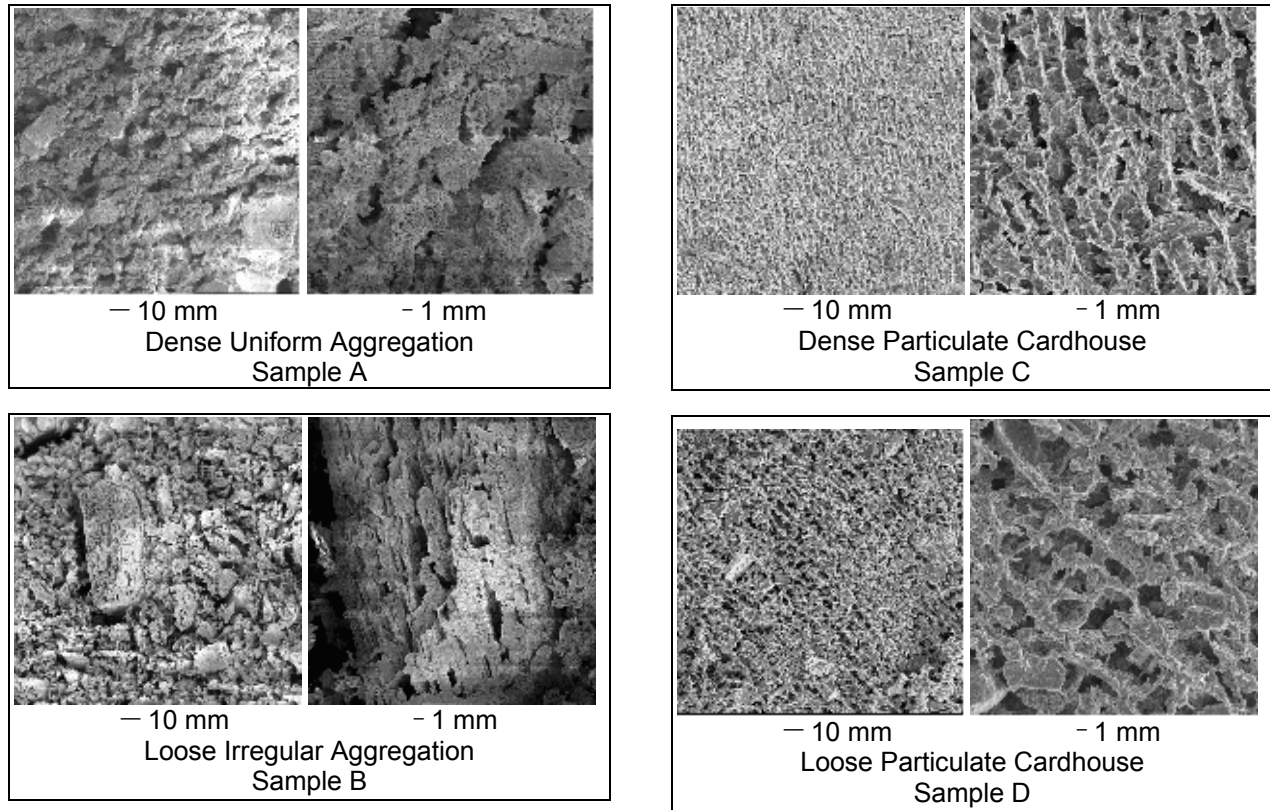


Figure 2: Micrographs of the investigated samples

The initial solids content was kept at 15% to mimic process conditions and obtain non-segregating slurries. The solid-liquid interface movement was recorded using a camcorder connected to a computer that digitally stored the captured movie. After the completion of the self-weight settling test, the digital movie files were viewed to plot the interface height versus elapsed time. Using the settling velocity (V_s) of the grains from slope of the initial straight-line portion of the settling curve and the unit weights of soil solids (γ_s) and water (γ_w), the initial hydraulic conductivity (k_i) was determined from the following equation (Pane and Schiffman, 1997):

$$k_i = V_s \left[\frac{\gamma_w (1 + e_i)}{\gamma_s - \gamma_w} \right] \quad (1)$$

Figure 3 gives the results of the self-weight settling tests in the form of interface height versus time on a semi-logarithmic scale. The self-weight settling curves of laterite ore slurries were characterized by three regimes of change in interface height: hindered sedimentation, transition, and self-weight consolidation. Table 3 gives the completion time of each settling stage for the investigated laterite ore slurries. The time to complete each of the settling phase progressively increased from sample A through to sample D. The data suggests two subgroups highlighting rapid settling for samples A and B and slow settling for samples C and D.

The physicochemical forces were able to carry part of the slurry weight during the initial settling stages. This prevented free particle fall and created a three

dimensional particulate network settling as one unit. Mitchell and Soga (2005) suggested a modified effective stress principle for soils involving significant physicochemical interactions such as dispersed clay systems. For the investigated laterite ore slurries, effective stress was observed to initiate during consolidation as marked by miniature surface features such as craters and humps. In addition, tiny longitudinal flow channels were also observed in the settled slurries indicating that the hydraulic conductivity during consolidation is governed by water flow through paths of least resistance (Suthaker and Scott, 1996).

Table 3: Completion time of settling stages

End Time (min)	A	B	C	D
Sedimentation	5	15	120	210
Transition	7	75	1440	2160
Consolidation	240	300	3240	3600

The observed data correlated well with the slurry microstructure. Aggregated fabric was found to be associated with rapid and significant settling whereas cardhouse morphology pertained to slow and low settling. In particular, the upward water flow during hindered sedimentation took place through the void space between the aggregates in samples A and B and through the voids between the clay particles in samples C and D.

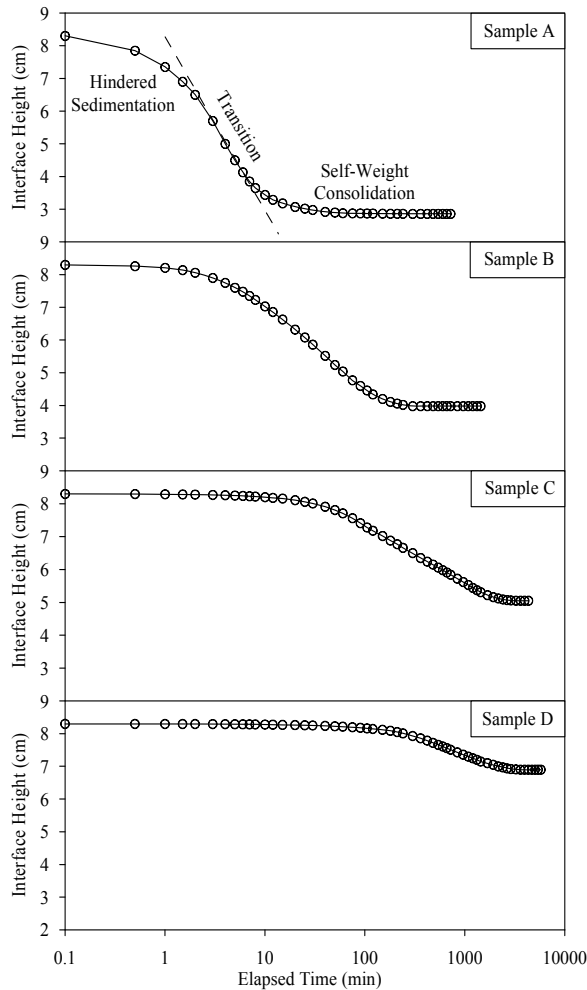


Figure 3: Self-weight settling test results

Figure 4 plots the interface height for the first four hours of the self-weight settling tests on a linear time scale. All samples had no induction time and indicated the commencement of transition by exhibiting an upward departure from the initial straight-line portion of the settling curves. Using the settling velocity during hindered sedimentation obtained from this figure, the initial hydraulic conductivity was calculated from equation 1. The initial hydraulic conductivity was about 10^{-1} cm/sec for sample A and consistently decreased by one order of magnitude for the remaining samples eventually recording about 10^{-4} cm/sec for sample D. Given identical initial test conditions ($17 < e < 18$), this three orders of magnitude variation clearly illustrated the influence of distinct physicochemical interactions between the solid and the liquid phases of various laterite ore slurries. Similar phenomena have been observed to affect the initial hydraulic conductivity of various other types of soils reported in the literature. For example,

10^{-3} cm/sec at $e = 17$ for Speswhite kaolinite (Pane and Schiffman, 1997); 10^{-4} cm/sec at $e = 8$ for oil sand fine tailings (Suthaker and Scott, 1996); and 10^{-5} cm/sec at $e = 15$ for phosphatic clays (Pane and Schiffman, 1997). For the investigated laterite ore slurries, the initial hydraulic conductivity was influenced by pore tortuosity (particularly samples C and D) in addition to void ratio. The upward water flow during hindered sedimentation mainly occurred through the soil microstructure (depicted in Figure 2) as flow channels appeared later during self-weight consolidation.

Samples A and B possessed good settling characteristics whereas samples C and D exhibited poor settling behavior. Physicochemical interactions in the former samples were low and the downward movement of the soil particles through near neutral waters was predominantly mechanical in nature. This is because both samples were composed of at least 90% of heavy iron oxides and sesquioxides and the pore water electrolytes were either negligible (sample A) or enough to neutralize the marginal unsatisfied surface charges on the 10% clays (sample B). Conversely, physicochemical interactions in samples C and D were high as both of these samples contained at least 45% of clay mineral. The highly alkaline pore water could significantly shrink the lateral spacing in sample C but the high Na^+ concentration ensured dispersion in both samples C and D. The cross-linking between the parallel clay platelets were not broken down to cause the collapse of the cardhouse fabric in both of these samples.

Table 4 summarizes the self-weight settling test results for the investigated laterite ore slurries. As mentioned earlier, the k_i varied by three orders of magnitude. The k_i values for oxide-rich laterites were 10^{-1} cm/sec to 10^{-2} cm/sec whereas those for clay-rich

laterite were 10^{-3} cm/sec to 10^{-4} cm/sec and close to other clayey sediments. Finally, the settling potential (SP) was found to be directly proportional to the k_i for the investigated slurries.

SUMMARY AND CONCLUSIONS

Economic metal extraction involving inline thickeners requires a clear understanding of the self-weight settling behavior of laterite ore slurries.

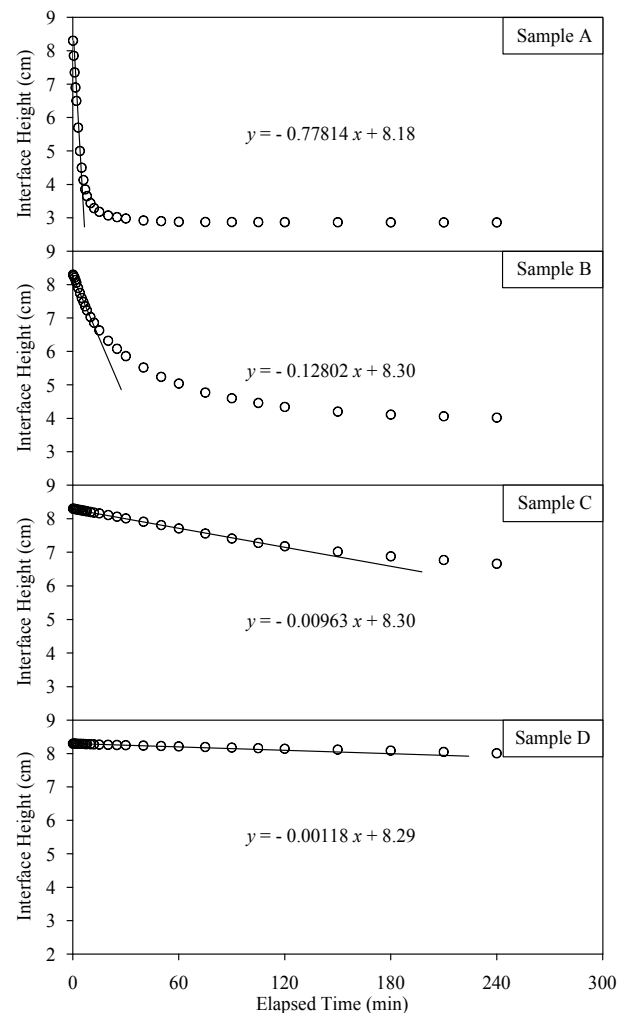


Figure 4: Determination of hydraulic conductivity

Four samples from different parts of the globe were characterized. The data revealed two types of materials. The oxide-rich

laterites in almost inert pore water exhibited an aggregated morphology and settled rapidly and significantly. Conversely, the clay-rich laterites in alkaline pore waters possessing high Na⁺ ion concentration showed a cardhouse microstructure and settled slowly and poorly. The initial hydraulic conductivity varied from 10⁻¹ cm/sec to 10⁻⁴ cm/sec with a corresponding change in the final settling volume from 66% to 17%. The rate and amount of settling empirically correlated with the slurry morphology.

Table 4: Summary of self-weight settling tests

Parameter	A	B	C	D
$k_i \times 10^{-4}$ (cm/s)	1200	190	15	1.8
SP (%)*	65.5	52.1	39.2	16.9

* SP (%) = 100 (change in height/initial height)

ACKNOWLEDGEMENTS

The authors would like to acknowledge the material support provided by Dynatec Inc., Canada. Thanks to the University of Alberta and the University of Regina for providing laboratory space and computing facilities.

REFERENCES

Azam S, Chalaturnyk R, Scott JD (2005) Geotechnical characterization and sedimentation behavior of laterite slurries. *Geotechnical Testing Journal*. 28(6):523-533.

Azam S, Scott JD, Jeeravipoolvarn S (2007) When does a slurry become a soil? *Geotechnical News*. 25(3):44-46.

Brady NC (1990) *The Nature and Properties of Soils*. 10th ed., Macmillan, New York.

Briceno A, Osseo-Asare K (1995) Particulates in hydrometallurgy: Part I. Characterization of laterite acid leach residues. *Metallurgical & Materials Transactions B*. 26:1123-1131.

Dixon JB, Schulze DG (2002) *Soil Mineralogy with Environmental Applications*. Soil Science Society of America, Madison, WI.

Eliopoulos DG, Economou-Eliopoulos M (2000) Geochemical and mineralogical characteristics of Fe-Ni- and bauxitic-laterite deposits of Greece. *Ore Geology Reviews*. 16(1-2):41-58.

Erol O, Lohnes RA, Demirel T (1976) Preparation of clay-type, moisture containing samples for scanning electron microscopy. *Proceedings, Workshop on Techniques for Particulate Matter Studies in SEM*, IIT Research Institute, Chicago, IL. 769-776.

Golightly JP (1981) Nilckeliferous laterite deposits. *Economic Geology*. 75: 710-735.

Lilly MR, Sargent JA (1990) Cryogenic scanning electron microscopy research application in arctic and polar regions. *Proceedings, 9th International Conference of Offshore Mechanics and Arctic Engineering*. Houston, TX. 4:51-60.

Mikula RJ (1988) Chemical characterization of an oil/water emulsion interface via electron microscope observation of a frozen hydrated sample. *Journal of Colloid and Interface Science*. 121:273-277.

Mitchell JK, Soga K (2005) *Fundamentals of Soil Behavior*. 3rd ed. Wiley, NY.

Moore DM, Reynolds Jr. RC (1997) X-Ray Diffraction and the Identification and Analysis of Clay Minerals, 2nd ed., Oxford, NY.

Morgenstern NR, Scott JD (1995) Geotechnics of fine tailings management. Proceedings, Specialty Conference on Geotechnical Practice in Waste Disposal. New Orleans, LA. 2:1663-1683.

Pane V, Schiffman RL (1997) The permeability of clay suspensions. *Geotechnique* 47(2):273-288.

Pickering RL (1962) Some leaching experiments on three quartz-free silicate rocks and their contribution to the understanding of laterization. *Economic Geology*. 57:1185-1206.

Rhoades JD, Shouse PJ, Alves WJ, Manteghi NA, Lesch SM (1990) Determining soil salinity from soil electrical conductivity using different models and estimates. *Soil Science Society of America Journal*. 54:46-54.

Sherman GD, Kanehiro Y, Matsu Saka Y (1953) Role of dehydration in the development of laterite crust. *Pacific Science*. 7:438-446.

Sposito G (1989) *The Chemistry of Soils*. Oxford, NY.

Suthaker NN, Scott JD (1996) Measurement of hydraulic conductivity in oil sand tailings slurries. *Canadian Geotechnical Journal*. 33:642-653.

Terzaghi K, Peck RB, Mesri G (1996) *Soil Mechanics in Engineering Practice*. 3rd ed., Wiley, NY.

Torfs H, Mitchener H, Huysentruyt H, Toorman E (1996) Settling and consolidation of mud/sand mixtures. *Coastal Engineering*. 29(1-2):27-45.

Tovey NK, Wong KY (1973) The preparation of soils and other geological materials for the SEM. Proceeding, International Symposium on Soil Structure, Gothenburg, Sweden. 1:59-67.

LABORATORY VERSUS FIELD SWCC DATA FOR MINE TAILINGS AND MINE WASTE COVERS

D.J. Williams

The University of Queensland, Brisbane, Australia

ABSTRACT: Soil Water Characteristic Curves (SWCCs) are typically determined in the laboratory by performing drying tests on samples in a Tempe cell. In some cases, re-wetting is also carried out. The advantage of using drying tests is that they are carried out from the saturated state at a given sample test density, so that there is some chance of obtaining repeatable results. However, re-wetting is carried out from the arbitrary end-point of a drying test, giving a unique re-wetting curve. SWCC data may also be collected directly in the laboratory and in the field. Depending on the stress history, structure and any cementation of samples under laboratory or field conditions, their SWCC data may be very different from the SWCC data collected after sample preparation and saturation for laboratory Tempe cell drying testing. The paper presents laboratory and field SWCC data for hypersaline mine tailings and for mine waste covers, which highlight the strong influence that stress history, structure, cementation, disturbance and saturation can have on the data.

INTRODUCTION

The paper describes laboratory and field SWCC data for hypersaline mine tailings, and for mine waste covers at Queensland Energy Resources Limited (QERL) in Queensland, Kidston Gold Mine in Queensland and Cadia Hill Gold Mine in New South Wales, Australia. The hypersaline mine tailings SWCC data display the effects of cementation on ageing.

For QERL, the performance of an instrumented thick mono-layer cover constructed from in situ overconsolidation and weakly cemented materials is described. The focus of the Kidston and Cadia case studies is the performance of instrumented store/release covers. The field instrumentation comprises TDR moisture and matric suction sensors installed in the covers, in addition to a local weather station measuring rainfall, air temperature, relative humidity, solar radiation, and wind speed and wind direction.

EFFECT OF CEMENTATION ON AGEING OF HYPERSALINE MINE TAILINGS

Description of hypersaline mine tailings and testing

Hypersaline mine tailings arise from the use of hypersaline process water and/or high salinity in the ore being processed. Due to the shortage of fresh water supplies, the use of hypersaline process water has become commonplace in the semi-arid to arid Goldfields region surrounding Kalgoorlie in Western Australia. The hypersaline water is sourced from deep ground waters, which are up to 250,000 ppm salt (up to seven times as salty as sea water). The tailings become even more hypersaline as they desiccate in their dry climatic environment.

Hypersaline tailings have been studied by Williams & Stolberg (2006) and Stolberg & Williams (2006), in the field and in a large-scale laboratory column experiment, respectively.

The field studies included regular direct sampling of the sandy silt-sized tailings profile at Mt Keith Nickel Operations over a 3-year period for the measurement of gravimetric moisture content, total suction and electrical conductivity, from which plots of moisture content versus suction were developed.

The deposition, desiccation, subsequent flooding and re-desiccation of Mt Keith tailings slurry was simulated in a 300 mm diameter by 2 m high laboratory column test with volumetric water content and matric suction measured down its axis.

Test results

Figures 1 and 2 show field SWCC data for the hypersaline Mt Keith tailings in the form of gravimetric moisture content versus osmotic and matric suctions, respectively. The osmotic suctions were obtained from the measured electrical conductivities of the sampled tailings, based on the USDA (1954) correlation between electrical conductivity and osmotic suction. The matric suctions were obtained by subtracting the correlated osmotic suctions from the total suctions measured using a psychrometer.

Figure 3 shows a comparison between the field SWCC data, the laboratory-determined re-drying and re-wetting SWCC, and the laboratory column test drying and re-drying SWCC data for the Mt Keith tailings, expressed in terms of gravimetric moisture content versus matric suction.

Figure 4 compares the estimated average field and average laboratory-based hydraulic conductivity functions calculated using the method of Fredlund et al. (1994) from the respective average drying SWCCs and the saturated hydraulic conductivity of the Mt Keith tailings of 6×10^{-8} m/s obtained using a laboratory falling head permeameter.

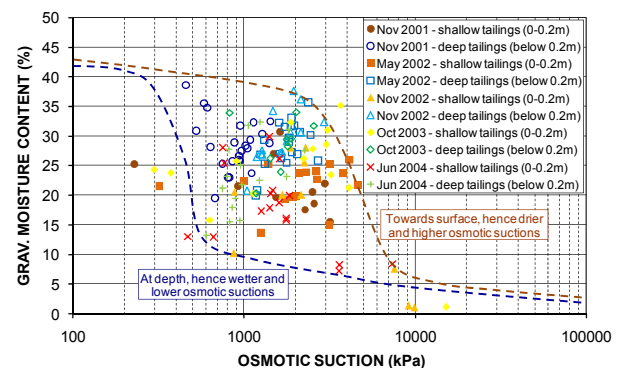


Figure 1. Field gravimetric moisture content versus osmotic suction for hypersaline Mt Keith tailings.

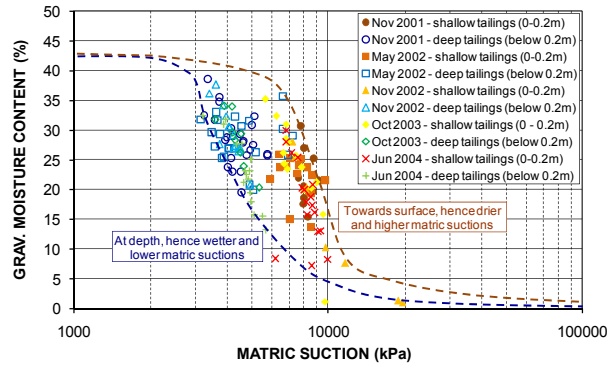


Figure 2. Field gravimetric moisture content versus matric suction for hypersaline Mt Keith tailings.

Discussion of test results

Figure 1 shows a wide spread in correlated osmotic suctions for the hypersaline Mt Keith tailings, ranging from about 200 to 15,000 kPa. There is some trend for the drier shallow tailings (to 0.2 m depth) to have a higher osmotic suction than the deeper tailings, due to the greater concentration of salts towards the surface of the tailings on desiccation.

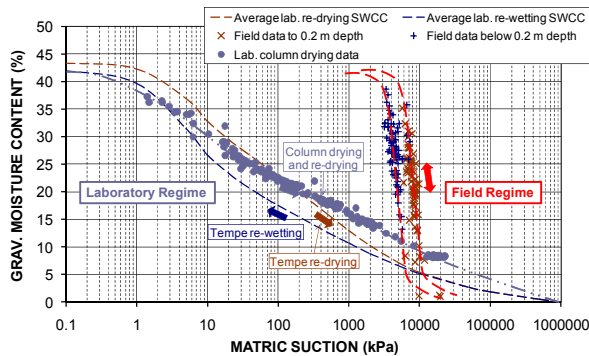


Figure 3. Comparison between field SWCC data, laboratory-determined re-drying and re-wetting SWCC, and laboratory column test drying and re-drying SWCC data for hypersaline Mt Keith tailings.

Figure 2 shows a relatively narrower spread in calculated matric suctions for the Mt Keith tailings, ranging from about 3,000 to

20,000 kPa, with the matric suctions generally dominating over osmotic suctions.

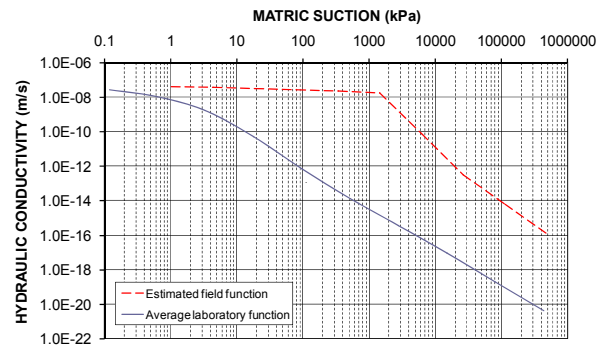


Figure 4. Estimated average field and average laboratory hydraulic conductivity functions for hypersaline Mt Keith tailings.

There is a strong trend for the drier shallow tailings (to 0.2 m depth) to have higher matric suction than the deeper tailings, due to increasing desiccation towards the surface of the tailings.

Figure 3 highlights the disparity between the field and laboratory unsaturated behaviour of hypersaline Mt Keith tailings. The apparent cementation of the tailings on desiccation in the field is destroyed by re-slurrying prior to laboratory Tempe cell testing, resulting in SWCCs almost identical to that obtained on the settling and desiccation of slurried tailings in the large-scale laboratory column test. Further, the effects of desiccation in the laboratory column are destroyed by re-flooding the tailings, resulting in re-drying data almost coincident with the initial drying data.

Figure 4 highlights the effect of unsaturated behaviour under field conditions on the calculated hydraulic conductivity function for desiccated, and hence cemented, hypersaline Mt Keith tailings. The implication is that at a given matric suction, the Mt Keith tailings under field conditions will have a far higher

unsaturated hydraulic conductivity than that implied by the laboratory test results (about three orders of magnitude higher over the typical range of matric suction determined under field conditions).

QERL'S THICK MONO-LAYER COVER

Climatic setting

QERL is located in a hot humid summer climate. The site experiences a long-term average annual rainfall of about 880 mm, spread throughout the year, with higher rainfall during the summer months of December to February (Australian Bureau of Meteorology). The average annual number of rainfall days is about 66. Average annual pan evaporation is about 1,600 mm, while annual average actual evapotranspiration is about 800 mm (91% of rainfall, according to the Australian Bureau of Meteorology). The average annual daily temperature ranges from 18 to 28°C. Over the last 5 years, annual rainfall has averaged only about 400 mm.

Testing of cover materials

The QERL site is underlain by overconsolidated Quaternary alluvium and Tertiary age weakly cemented weathered shale, which were selected for use in a 6 m thick mono-layer cover over spent oil shale. Testing of the alluvium and weathered rock included gravimetric moisture content (mass of water/mass of solids, expressed as a %), total suction, field density and electrical conductivity determinations on borehole samples, and laboratory drying SWCC and saturated hydraulic conductivity testing (Williams et al., 2006a). Total suctions were obtained using a psychrometer, osmotic suctions were obtained from the measured

electrical conductivity values, and matric suctions were obtained by subtracting the osmotic suctions from the total suctions.

Figures 5 and 6 show the measured gravimetric moisture content and estimated degree of saturation profiles with depth, respectively.

Figure 7 shows the gravimetric moisture content versus matric suction data, which includes measured drying data and the estimated SWCC for the in situ overburden and weathered rock, field data for the same material re-handled to form a cover, and laboratory drying SWCCs. The moisture data are plotted in terms of gravimetric moisture content, rather than the more conventional volumetric water content measured in the laboratory Tempe cell, since all of the field moisture data were measured gravimetrically.

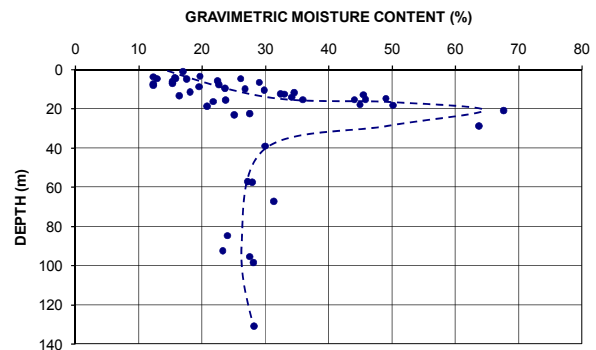


Figure 5. Gravimetric moisture content depth profiles for overburden and weathered rock.

Table 1 gives average saturated hydraulic conductivities for the in situ overburden and weathered rock and the same material used as a cover, as determined by laboratory falling head permeameter or field CSIRO disc permeameter testing.

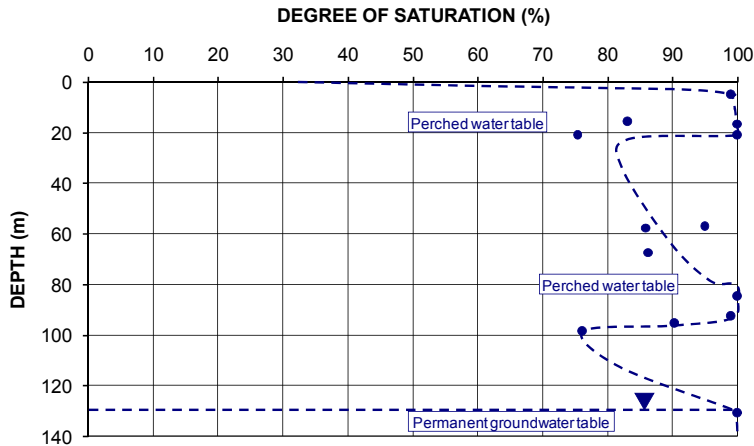


Figure 6. Degree of saturation depth profile for QERL overburden and weathered rock.

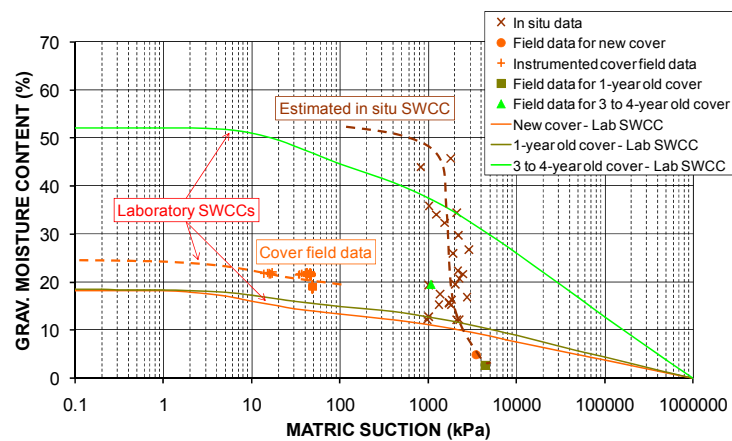


Figure 7. Comparison of field and laboratory SWCC data for overburden and weathered rock.

Table 1. Comparison of average saturated hydraulic conductivities of in situ and disturbed overburden and weathered rock.

Description (test)	Test dry density		Saturated hydraulic Conductivity	
	t/m ³		m/s	
In situ material (lab.) Cover:	1.470		8.3 x 10 ⁻¹¹	
New (lab.)	1.522		5.5 x 10 ⁻⁸	
1-year old (lab.)	1.611		8.7 x 10 ⁻⁸	
3 to 4-year old (lab.)	1.137 *		1.2 x 10 ⁻⁷	
New (field)	1.534		4.2 x 10 ⁻⁷	
1-year old (field)	1.611		3.3 x 10 ⁻⁷	
3 to 4-year old (field)	1.137 *		1.9 x 10 ⁻⁵	

* Low due to ripping to promote revegetation.

Discussion of test results

Figure 5 shows high gravimetric moisture contents at about 20 m depth, corresponding to the boundary between a saturated gravel layer and an underlying clay layer. Figure 6 shows full saturation at 15 to 20 m depth, at about 80 m depth and below about 130 m depth, indicating perched water tables at about 15 to 20 m and 80 m depth, above the permanent groundwater table at about 130 m depth.

Figure 7 demonstrates the dramatic effect of laboratory disturbance of the overconsolidated alluvium and weakly cemented weathered shale on their “stiff” in situ unsaturated behaviour. Matric suctions maintain high values in situ, generally in excess of 1,000 kPa, even at high gravimetric moisture contents, while laboratory sample preparation and saturation destroy these high suctions. A very new cover of the same material recorded intermediate matric suctions at typical field moisture contents, while ageing effects restored the high in situ matric suctions for older covers.

Table 1 highlights the dramatic effect of disturbance on the saturated hydraulic conductivity of the overconsolidated alluvium and weathered rock. The saturated hydraulic conductivities rose from a very low average value of 8.3×10^{-10} m/s (3 mm/year) in situ to a much higher average value of 3.4×10^{-7} m/s (over 10 m/year) when placed as a cover, rising further to about 1.9×10^{-5} m/s on ripping to facilitate revegetation of the cover.

KIDSTON’S STORE/RELEASE COVER

Climatic setting

Kidston Gold Mine is located in a dry sub-tropical climate. The site experiences a

long-term average annual rainfall of about 700 mm, which falls mainly in intense storms over the 3-month summer from about December to February or March (Australian Bureau of Meteorology). The high intensity of the storms results in high runoff coefficients to the ephemeral streams. The average annual number of rainfall days is about 45. Average annual pan evaporation is about 2,100 mm, while annual average actual evapotranspiration is about 600 mm (86% of rainfall, according to the Australian Bureau of Meteorology). The average annual daily temperature ranges from 18 to 30°C. Over the last 10 years, annual rainfall has averaged only about 550 mm.

Cover details

Kidston employed store/release covers (Williams et al., 1997) on the flat tops of their potentially acid generating waste rock dumps. The store/release covers comprised a 0.5 m thick compacted clayey sealing layer (comprising clayey mine overburden) overlain by a minimum 1.5 m thick, loose, rocky soil mulch layer (comprising more coarse mine overburden), which was left mounded, and was vegetated with native shrubs, eucalypts and grasses. The purpose of the sealing layer was to hold-up rainfall infiltration into the mulch, to be removed through evapotranspiration. The store/release cover was instrumented with volumetric water content and matric suction sensors, which have been monitored for over 10 years (Williams et al., 2006b).

Selected field SWCC data

The volumetric water contents and matric suctions monitored from 2000 to 2002 at selected depths within Kidston’s store/release cover are combined in Figure 8. Figure 9 shows the volumetric water contents and

matric suctions over 6-monthly intervals from 2000 to 2002 at 0.35 m depth.

Figure 10 compares the field and laboratory-determined SWCCs. In Figure 10, the laboratory SWCC for compacted clay corresponds to the field curve at 1.77 m depth and the laboratory SWCC for rocky soil mulch corresponds to the other field curves.

Discussion of test result

Figure 8 shows that the seasonal drying and wetting cycles to which Kidston's store/release cover is subjected results in a cycling of the moisture state of the store/release cover. In addition, the upper part of the cover remains generally drier and hence

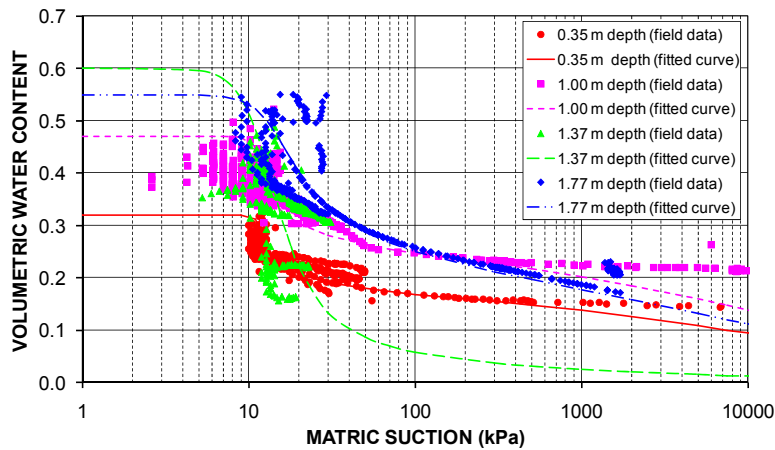


Figure 8. Combined volumetric water content and matric suction field data at selected depths within Kidston's store/release cover from 2000 to 2002.

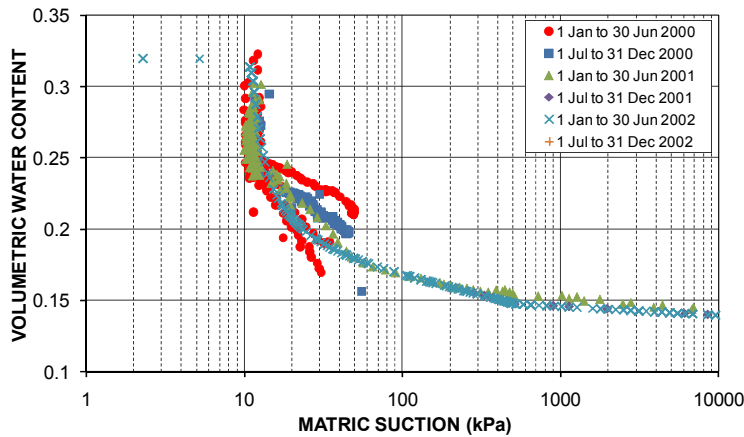


Figure 9. 6-monthly volumetric water content and matric suction field data at 0.35 m depth within Kidston's store/release cover from 2000 to 2002.

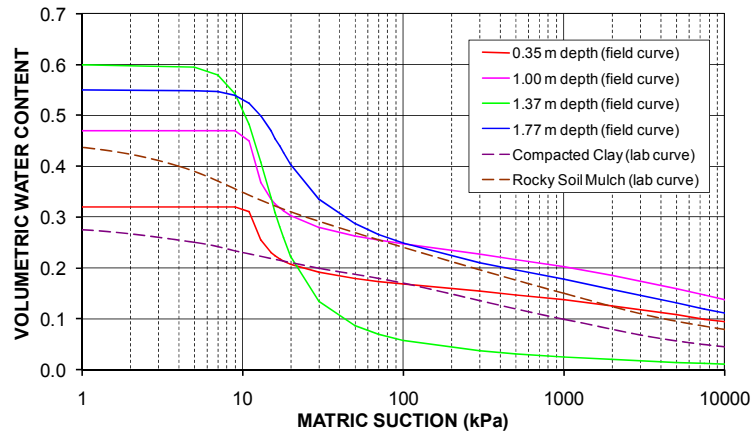


Figure 10. Comparison between field and laboratory-determined SWCCs for Kidston's store/release cover materials.

at higher matric suction than the lower parts of the cover, which generally trend increasingly wet with depth. The high, near-saturated (low matric suction) volumetric water contents at all depths indicate that all sensors were located in loose, rocky soil mulch cover material, rather than the underlying compacted sealing layer.

Figure 9 highlights that at 0.35 m depth, during the early life of the cover the unsaturated behaviour of the material is somewhat unstable, being affected by seasonal climatic conditions and physical changes to the cover. However, after a few years of seasonal drying and wetting cycles it stabilises and tracks a constant SWCC. It is apparent from Figure 4 that this is also generally the case at other depths within the cover.

Figure 10 shows that the laboratory-determined SWCCs provide poor estimates of the unsaturated behaviour of the materials in the field. In particular, the laboratory SWCC for the compacted clay is a very poor estimate of the field response of the sealing layer in the field and the laboratory SWCC for the rocky soil mulch is only a rough average of the responses of the rocky soil mulch in the field. Therefore, the design of a store/release

cover based on laboratory-determined SWCCs would provide a poor estimate of field behaviour.

CADIA'S STORE/RELEASE COVER

Climatic setting

Cadia Hill Gold Mine is located in a temperate climate. The site experiences a long-term average annual rainfall of about 886 mm, spread throughout the year, with somewhat higher rainfall during winter (Australian Bureau of Meteorology). The average annual number of rainfall days is about 94. Average annual pan evaporation is about 1,500 mm, while annual average actual evapotranspiration is about 580 mm (65% of rainfall, according to the Australian Bureau of Meteorology). The average annual daily temperature ranges from 6 to 20°C. Over the last 3 years, annual rainfall has averaged only about 770 mm.

Cover details

Cadia trialled store/release covers on the flat top of a 15 m high trial waste rock dump covering 0.7 ha. The cover trials made use of natural clays and waste materials, and were

aimed at demonstrating the suitability of waste materials for this purpose in the absence of sufficient natural clays. Three alternative covers were trialled, each employing different nominal 0.5 m thick sealing layers; which were each overlain by a minimum 1.5 m of loose rocky soil mulch comprising a mixture of benign trafficked waste rock (nominally passing 100 mm) and tailings harvested from the tailings storage facility, in a nominal 5:1 dry mass ratio. The three sealing layers comprised: (i) compacted natural clays, (ii) a compacted 5:1 mixture of trafficked waste rock and harvested tailings (TWR/Dry tailings) and, (iii) trafficked waste rock pushed into tailings slurry (TWR/Wet tailings). The store/release trial covers were instrumented with volumetric water content and matric suction sensors, which have been monitored for over 2 years (Rohde, 2009).

Initial moisture state of trial covers

Figures 11 and 12 show, respectively, the initial volumetric water content and matric suction profiles with depth through the three trial covers.

Discussion of test results

Figure 11 shows that the rocky soil mulch moisture profiles above the compacted clay and TWR/Wet tailings sealing layers are similar, while that above the compacted TWR/Dry tailings sealing layer is highly variable. This is likely the result of poor mixing of the tailings into the trafficked waste rock. Figure 12 also highlights the drier as-placed state of the compacted clay seal, despite efforts to moisture condition the clay prior to compaction, and the expected very much wetter as-placed state of the TWR/Wet tailings seal. Figure 12 shows similar matric suction profiles for the rocky soil mulch in all trials, while the compacted clay seal is much drier than the other two seals.

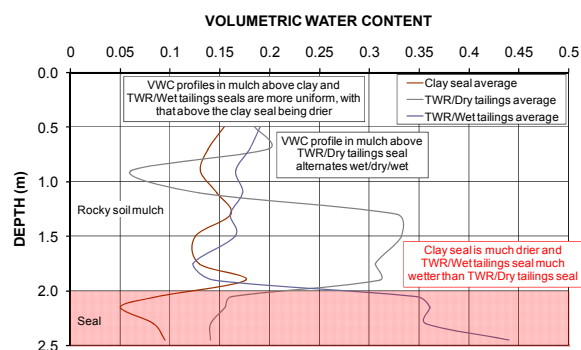


Figure 11. Initial volumetric water content profiles with depth through Cadia trial covers.

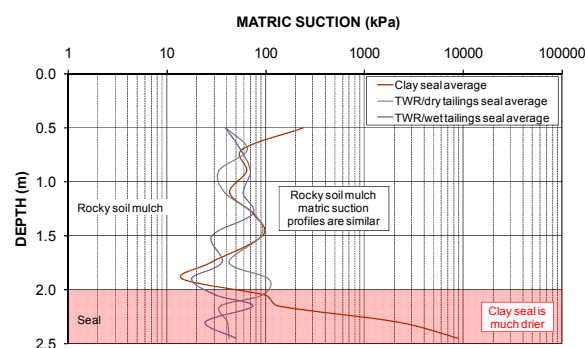


Figure 12. Initial matric suction profiles with depth through Cadia trial covers.

CONCLUSIONS

The paper clearly demonstrates the potential discrepancies between the unsaturated behaviours of hypersaline mine tailings and mine waste cover materials under in situ, laboratory test and re-constructed field conditions. Any structure and cementation that the materials may possess in situ is largely destroyed by sampling disturbance, sample preparation and saturation prior to laboratory SWCC testing.

At QERL, the destruction of in situ overconsolidation and weak cementation on re-handling is demonstrated by the much “stiffer” field SWCC compared with the laboratory drying SWCC. A very new cover of the same material recorded intermediate

matric suctions at typical field moisture contents, while ageing effects restored the high in situ matric suctions for older covers.

The affect of ageing of the Kidston store/release cover materials is demonstrated by somewhat unstable initial unsaturated behaviour, which stabilises after a few years of seasonal drying and wetting cycles. The field SWCC response is not well estimated by laboratory drying SWCC test results. The store/release trial covers at Cadia display a lack of uniformity and variable relative density, resulting in highly variable field SWCC data that are very different from laboratory Tempe cell data obtained for the same materials.

The implications of these findings for the design of soil covers over mine wastes under unsaturated conditions are that laboratory drying SWCC data, generally obtained using reconstituted samples from a saturated state, will destroy the effects of any structure and cementation that exist in situ, and therefore may not be at all representative of in situ conditions. Material uniformity and construction control can also have a very large influence on field SWCC data.

ACKNOWLEDGEMENTS

The test results reported in the paper are the result of research and consulting carried out or supervised by The University of Queensland. The assistance provided by University staff and industry collaborators at Mt Keith, QERL, Kidston and Cadia is gratefully acknowledged.

REFERENCES

Fredlund, D.G., Xing, A. & Huang, S. 1994. Predicting the permeability function for unsaturated soils using the soil water characteristic curve. *Canadian Geotechnical Journal*, 31, 533-546.

Rohde, T.K. (2009) Development of innovative landform and closure designs for potentially contaminating surface waste rock dumps. PhD Thesis, The University of Queensland, Brisbane, Australia.

Stolberg, D.J & Williams, D.J. 2006. Large-scale column testing of hypersaline tailings. *Proc. of Fifth Int. Cong. on Environmental Geotechnics, Cardiff, Wales, 26-30 June 2006*, II, 976-983. Thomas Telford.

USDA. 1954. *Agricultural Handbook No. 60, Diagnosis and Improvement of Saline and Alkali Soils*. L.A. Richards (ed.). United States Dept of Agriculture.

Williams, D.J., Wilson, G.W. & Currey, N.A. 1997. A cover system for a potentially acid forming waste rock dump in a dry climate. *Proc. of Fourth Int. Conf. on Tailings and Mine Waste '97, Fort Collins, Colorado, USA, 13-17 January 1997*, 231-235. Rotterdam: Balkema.

Williams, D.J., Rohde, T.K, Stolberg, D.J. & Pope, G. 2006a Alternative design and instrumentation of covers over potentially acid forming mine wastes. *Proc. of Fifth Int. Cong. on Environmental Geotechnics, Cardiff, Wales, 26-30 June 2006*, II, 1007-1014. Thomas Telford.

Williams, D.J., Stolberg, D.J. & Currey, N.A. 2006b. Long-term performance of a “store/release” cover over potentially acid forming waste rock in a semi-arid climate. *Proc. of Fourth Int. Conf. on Unsaturated Soils, Carefree, Arizona, 2-6 April 2006*, 1, 756-776. ASCE, Geo Institute.

Williams, D.J. & Stolberg, D.J. 2006. Field performance of capillary break covers over hypersaline tailings in an arid climate. *Proc. of Fourth Int. Conf. on Unsaturated Soils, Carefree, Arizona, 2-6 April 2006*, 1, 777-788. ASCE, Geo Institute.

STRATEGIES FOR DEALING WITH FINE FLUID TAILINGS AND SUSPENDED FINES: SOME INTERNATIONAL PERSPECTIVES

J.E.S. Boswell

Thurber Engineering Ltd., Calgary, Alberta, Canada

ABSTRACT: Recent developments in Canada have highlighted the critical need to manage fine fluid tailings so as to enable the sustainable closure of tailings facilities in the long term.

Drawn from international experience as a contractor and consultant over the past 25 years, the author presents examples of successful methods of dealing with the challenges presented by tailings fines associated with the mining and processing of diamond kimberlites (up to 30% minus 2 micron), Merensky and UG2 reef platinum, gold, uranium, coal ash, phosphogypsum and other minerals.

The concomitant requirements of Big Picture Thinking perspective, as well as attention to detail are highlighted through methodologies which have been successfully applied to a variety of tailings facilities worldwide.

INTRODUCTION

Advances over the last century in the extraction of minerals have led to the generation of growing quantities of increasingly finer tailings materials. While this has resulted in improved extraction rates and enabled the development of hitherto unpayable ore reserves, it has also generated substantial challenges in the disposal of mine tailings and the sustainable closure of tailings facilities.

- How to satisfactorily dispose of large volumes (typically millions of tons per month) of fine material (finer than 44 micron).

Recent changes to the law in Canada, typified by the publication on 3 February 2009 by the Energy Resources Conservation Board (ERCB) of the Directive 074 Tailings Performance Criteria and Requirements for Oil Sands Mining Schemes, placed substantially new requirements on all Oil Sands operators particularly in regard to consolidation, trafficability and reclamation of tailings. The challenges now faced by the Oil Sands industry include:

- How to deal with legacy tailings (fine material generated over the past years which has been accumulating in tailings ponds).

- Accelerating the consolidation of fine tailings.
- Achieving a trafficable sustainable landform on the final surface of closed tailings facilities.

These challenges have now become public, environmental and political issues, having moved centre stage into the international arena.

It is not enough to simply apply conventional geotechnical engineering to the problem currently at hand. There exist good models for tailings operators and mine owners to take the initiative and communicate proactively with the public and environmental stakeholder groups. This approach takes a step back, and considers the problem from a vantage point of Big Picture Thinking. Boswell et al (2000) at a previous Fort Collins conference reported on communication with the public about tailings projects. Although this aspect is not the focus of this paper, public and environmental aspects should be borne in mind by the geotechnical engineer, in seeking sustainable solutions for tailings.

This paper explores some of the practical lessons learned from tailings disposal in arid or semi-arid environments, in which reliance is placed on sun-drying and desiccation processes for the consolidation of tailings, aided and supplemented by tailings conditioning and deposition techniques which have made optimal use of the environment.

LITERATURE AND BACKGROUND

In applying the original theory of consolidation first advanced by Karl Terzaghi (1943) to the consolidation and behavior of thin layers of soil and tailings, and hydraulic fill structures, subsequent generations of geotechnical engineers have focused on such aspects as:

- Thin homogeneous clay layers (Gibson et al, 1967).
- Perspectives on and classification of hydraulic fill (Morgenstern et al 1988)
- Hydraulic fill structures: consolidation behavior and properties. (Schiffmann, et al (1988).
- Engineering properties of tailings (Vick, 1990)
- Master profile concept for tailings beaches (Blight, 1994)
- Successful application to subaqueous deposition (Blight et al, 1995)
- Theoretical formulas for sub-aerial deposition (Qiu and Segó, 1998)
- Solar evaporation (Blight et al, 2000)
- Prediction of desiccation rates (Fell et al, 2005)
- Physical, mechanical and chemical conditioning methods for assisting the tailings consolidation process (Segó et al, 2008).

This is quite clearly not a complete list. There now exist literally dozens of excellent and relevant papers and books on the subject of consolidation of tailings.

Much of the foregoing has developed the theoretical basis for the consolidation of soil and tailings, but has stopped short of practical application to the consolidation of tailings in thin lifts.

Although some researchers have examined the theory of consolidation in thin layers in detail, what is still needed is a theoretical method of calculating the optimal lift thickness in cases where environmental processes are primarily responsible for drainage, desiccation and consolidation.

When compared to mechanical, chemical and other forms of accelerated consolidation, the advantage of environmental processes of consolidation is of course that of low cost

(bearing in mind that tailings disposal is by nature a form of waste management, and waste management in turn is generally regarded as a grudge purchase by society).

While much published literature exists in regard to tailings management in general, and specialist topics in particular such as thickening, pumping, and beaching, very little has been published on so-called “thin lift” placement and on proven remedies for dealing with fluid fine tailings and suspended fines.

Conventional soil compaction practice has drawn attention to the importance of compaction lift thickness – usually to optimize compactive effort, improve soil shear strength, reduce permeability to ensure homogeneous and consistent results, and to reduce cost. The aim in compaction is usually to reduce air voids most efficiently. Recent efforts have focused on maximizing lift thickness in order to achieve economy of effort or in order to accommodate larger material size or larger compaction equipment.

Consolidation of soil on the other hand requires a reduction of void ratio, and in the case of tailings is usually associated with driving out interstitial moisture. This process may be far more gradual and is a function of load, drainage and environmental influences. The finer the material, the longer the consolidation process requires. In addition, the longer the drainage path, the more time required for consolidation.

This brief literature survey and some personal communication (Blight, Sobkowicz, 2009) has shown that little published literature exists which could guide tailings disposal practice in regard to the selection of optimal lift thickness.

Instead, from experience, it has been found that practical and operational considerations

have influenced the selection of lift thickness, rather than solely geotechnical constraints.

THE OBSERVATIONAL METHOD AND EMPIRICAL AND OPERATIONAL LEARNING APPLIED TO TAILINGS

The observational method was proposed by Karl Terzaghi, and discussed in a well known paper by Ralph B. Peck (1969), in an effort to reduce the costs during construction incurred by designing earth structures based on the most unfavorable assumptions, i.e., geological conditions, soil engineering properties, etc. Instead, the design is done based on the most probable conditions rather than the most unfavorable. The gaps in the available information are filled by observations: geotechnical instrumentation measurements, e.g., inclinometers and piezometers; and geotechnical site investigation.

The author has used aspects of the observational method in developing an understanding of the behavior of tailings, and remedies that have been successfully applied in full scale field operation. The observational method is useful in cases where the design can be modified during construction. This is particularly applicable to tailings operations.

The paragraphs below itemize a number of key observations by the author, drawn from the operational practice of tailings management in South Africa, Botswana, Chile, the USA and Canada.

THE DEPOSITION & CONSOLIDATION OF TAILINGS IN THIN LIFTS

The deposition of tailings in thin lifts holds potential for the acceleration of the consolidation process. The conditioning of

the tailings prior to discharge and the method of deposition are in turn able to significantly improve this process, accelerating the consolidation process, improving shear strength, maintaining permeability and achieving trafficability.

In addition, the deposition process is not complete without a careful consideration of the associated implications of deposition. These include:

- The effect on structures and processes from tailings fines which are decanted along with the supernatant.
- Erosion of beach profiles and failure of the beaching process.
- Re-suspension and re-entrainment of previously deposited fine material.
- Slug flow without segregation.
- Deposition of coarser material upon entry into deeper supernatant, typically in a lagoon, usually corresponding with reduced beach flow velocities.
- In arid areas, large losses of inventory water through evaporation and seepage, requiring increased raw water consumption.

In pursuing sustainable tailings practice which will enhance and ensure consolidation, a clear distinction should be made between:

- rate of rise, and
- lift thickness.

The maximum allowable rate of rise is governed by a number of factors, not amplified in this paper, including:

- geotechnical stability
- consolidation
- trafficability
- climate
- drainage and engineering

Lift thickness however, is determined from practical considerations. It is all too easy to rely on complete containment structures and mechanically placed impoundment dykes, without giving sufficient attention to the fact that increasingly deeper lift thicknesses will lead to the retarded consolidation of impounded tailings.

One of the happy benefits of the upstream construction of tailings dams is that if the deposit is geotechnically stable, it also has a good chance of being reasonably consolidated throughout the deposit. Downstream constructed tailings dams seldom deliver such benefits automatically, as the requirement for containment is inherent to their design.

An analogy exists between fine tailings and the evolution of the geo-environmental design of landfills: It is as insufficient to design a completely dry tomb landfill, isolated from the environment in which contained material remains unameliorated in the environment, as it is to design landfills which progressively leak hazardous leachate into the environment. The mandate for the engineer is to return the products of human activity back into the environment in methods and quantities which allow for gradual environmental re-absorption. So too, contained tailings should become increasingly consolidated and not present a risk for subsequent generations to have to deal with. This is inherent to the concept of sustainable development.

Attention should also be drawn to the fact that a lift may not be singly deposited, but may consist of successive (even) thinner layers within a single lift. As the name implies, the lift usually corresponds to an event whereby the tailings discharge, deposition pipe-work or beaching mechanism is “lifted” by manual or mechanical means. Successful thin lift disposal usually relies to a greater or lesser extent on the autogenous and self-healing properties of a well managed beach ring dyke. In practice the beached deposition of

subsequent layers is overlapping and spatially varied, generating substantial contrasts in vertical and horizontal permeability, up to three or four orders of magnitude.

The question arises as to the optimal thickness of lift, and how this should be determined. In the case of a beach profile, the lift thickness gradually reduces with distance along the beach.

In the author's experience, the following factors should be considered in selecting or specifying lift thickness:

FACTORS TO CONSIDER IN THE SELECTION OF LIFT THICKNESS

Particle Size Distribution (PSD) and particle characteristics

In general, the finer the material, the thinner the lift should be. Consolidation rate and drainage time is substantially dependent on the PSD.

Drying time

Evaporative drying, freeze-thaw or other desiccative processes are also a function of many environmental factors including:

- Atmospheric humidity
- Wind
- Salt concentration in the pore fluid

Cycle time (between successive deposition events)

There is a practical optimum between thicker lifts raised less frequently, and thinner lifts raised more often.

Drainage

The benefits of deposition onto a well drained drainage layer should not be overlooked. This has the effect of accelerating the

consolidation up to four times, compared to a saturated or completely non-draining foundation. In addition, in cold climates, the drainage could potentially continue throughout the year, and not be hindered by the vagaries of ground freezing and reduced sun-drying.

Solar radiation

Arid or semi-arid climates are clearly better suited to solar radiation. For most mining areas in South Africa, annual evaporation exceeds annual precipitation at least threefold. Fort McMurray, Alberta also has a climatic water deficit, but not as much as the typically South African, Australian, south-western USA or Chilean climates. In the typical Canadian winter there is not much potential for sun-drying, for extended periods. A distinction should be made between actual sun-drying and evaporative drying in a low relative humidity environment. While usually more limited in extent, evaporative drying can also take place off a frozen surface in circumstances of low relative humidity.

End requirement (trafficability, access)

In South Africa gold tailings paddock "wall building" traditionally took place in 150 to 200 mm lifts. ("Wall building" in the South African tailings context refers to the process of incremental raising of the outer shell of an upstream tailings deposit, and should not be confused with dyke construction or starter embankment construction). When applied to substantially finer diamond tailings however, it was found that thinner lifts were more effective, often deposited in multiple layers. Platinum and copper tailings being coarser, allowed a progression to lifts as thick as 500 to 1000 mm at a time, and allowed access onto beaches for wheeled front end loaders to assist with compartment building and spigot and delivery pipeline raising. The high particle SG of chrome content (over 4) in

UG2 platinum tailings allowed for even more rapid consolidation of outer beaches and accelerated trafficability. Pozzolanic action (cementitious hardening) contributed substantial shear strength gain in fly ash disposal. In the case of phosphogypsum tailings from the fertilizer manufacturing industry, substantial chemical hardening took place and enabled successive lifts to be placed almost daily.

Beach geometry (width, length, slope)

There can be no greater benefit for a successful beaching operation than that of sufficient length of beach. This can of course be negated by insufficient beach width (which would serve to constrain the flow and thus accelerate beach flowrates).

Most subaerial beaches appear to develop an average slope of between 0.5% and 2%. Blight (1994). The coarse end of the spectrum tends to be somewhat steeper than 2%, aided by cycloning or spigotting.

The addition of flocculant and the use of paste and other technologies serve to potentially increase these gradients.

Slurry water content

Tailings deposition is almost always improved with increasing solids content. Conventional practice is to adopt a water-to-solids content of at least 1:1 by mass (avoiding more dilute slurries). This enables conventional pumping using centrifugal pumps to still be possible, while limiting the amount of water held in inventory in the tailings circuit. Paste and other technologies have improved these ratios substantially, with attendant improvements in tailings depositional performance.

Slurry delivery flowrate

The challenge for tailings deposition in thin lifts (by beaching), especially for large discharge volumes is to achieve slow velocity planar flow from a large diameter delivery main.

This can be achieved by:

- Ensuring that the delivery flow velocity is as low as possible.
- Use of splitter chambers or mixing manifolds.
- Dividing the flow up into multiple smaller delivery lines.
- Spigotting or cycloning onto the tailings beach.
- Discharge into a “day wall” as in the gold tailings industry, where the tailings slurry is encouraged to flow around the perimeter of the tailings dam in a carefully shaped and controlled launder which allows beached deposition. Thus a day wall can be up to 50 metres wide. The finer material is decanted off the end of the day wall run (anywhere from 50 to 500 metres in beach length), and allowed to beach into the “night paddock”. Reference to “day” and “night” refers to the time of day when tailings is usually discharged into specific areas so designated.

Upstream construction (“wall-building”)

Trafficable access for the incremental raising of the outer shell of an upstream deposit requires a certain shear strength gain in the outer shell of the deposit. The geometry and layout of the slurry delivery system is used in part to determine optimal lift thickness (optimizing economy of effort and trafficability).

Robustness of design

Tailings disposal has often been described as more of an art than a science. This is true for paddock “wall building” and selection of lift thickness. The facility must be robust. Tailings deposition schemes need to be robust, and not prone to washouts, blockages and other failures. The best schemes are able to accommodate some variation in flowrate, slurry consistency and tailings characteristics. Table 1 (appended to this paper) indicates some empirical guidance for the selection of lift thickness based on the author’s experience. Clearly it is not a simple exercise to arrive at the optimal lift thickness. Some of the key variables which would influence the decision are listed, including:

- Governing material in the Particle Size Distribution (PSD)
- Nature of drainage
- Foundation shear strength
- Tailings slurry concentration (in terms of % solids of total, by mass)
- Typical annual rate of rise (in metres per year)
- Typical deposition rate (in tonnes per month per Hectare)
- Typical lift thickness (in millimeters, as placed, and before consolidation)

PRINCIPLES FOR MANAGING FINES AND TAILINGS SUPERNATANT

Avoid the accumulation of legacy problems

Easier said than done, but nevertheless critical.

Reduce slurry water content

The benefits of using less water in the slurry include:

- Reduced water inventory

- Lower pumping velocities (and in certain optimal conditions also reducing pressures, wear and costs)
- Smaller pipelines required and less pumps
- Reduced risk of segregation and blockages
- Reduced shear thinning of slurries
- Lower tailings placement velocities

Avoid flushing

A well designed slurry delivery system should avoid the requirements of water or air injection or flushing.

Reduce variation in feed

Although feed variation cannot be eliminated completely, the tailings facility will benefit from an approach which seeks to consider tailings delivery as a manufactured product output rather than a necessary evil.

Remove supernatant from tailings disposal areas as soon as possible

Both practical experience and research confirm that the storage of large volumes of supernatant on tailings disposal areas holds substantial risks.

Many catastrophic failures, especially of upstream constructed tailings dams could have been avoided completely by adherence to this single rule.

Less obvious interruption to a disposal process can also occur without catastrophic failure.

Catalan et al (2002) describe how wind-wave-induced resuspension of tailings under water cover could compromise suspended solids discharge criteria, increase the sulphide oxidation and reduce dissolved oxygen concentrations in pyrite tailings disposal.

Other researchers (Yanful and Mian) have published further work on this topic.

Avoid co-disposal of tailings with effluent or dilute slurries

Many mining operations generate a variety of waste water solutions or dilute suspensions.

These are commonly disposed of on tailings beaches. Not only do these waste products introduce increased layering and attendant effects on hydraulic fill structures, but they sometimes also precipitate artificial changes to the operational management of tailings, supernatant and return water.

Table 1: Empirical Chart for preliminary selection of Lift Thickness						
Criterion	Unit of measure	Quality of Criterion				
		excellent	good	moderate	poor	very poor
Governing material in PSD	description	Coarse sand	Sand	Silt	Fine silt	clay
Nature of drainage	description	fully underdrained	blanket drains	toe and elevated	toe drain only	no drainage
Foundation shear strength	description	very strong	strong	moderate	weak	very weak
Slurry concentration	% solids of total by mass	70	60	50	30	20
Typical rate of rise	metres per year	10	5	2.4	1.2	0.6
Typical deposition rate	tonnes per month per Hectare	10000	4000	2000	1000	500
Typical lift thickness	millimetres before drying	1000	500	200	100	50

Develop long beach profiles

A long beach may offer the following benefits:

- Removal of free standing supernatant pool to a remote location from outer impoundment slopes

- lowering phreatic surfaces
- aiding consolidation and
- improving impoundment stability
- robustness in dealing with variation in slurry feed delivery

Aim at planar flow over beaches

The achievement of planar flow over a beach maximizes the potential for desiccation by drainage and evaporation, and minimizes the effects of channel flow.

In addition, the effect of quasi-dilatant shear within beach flow in thin lifts is to allow a matrix to form in the beach, holding the solid particles back and allowing the pore fluid to drain off directly.

Use thin lifts

- The finer the material, the thinner the lift needs to be.
- Thin lifts do not automatically imply thin layers, as indicated previously.

Be careful of so-called “emergency tailings dams”.

One of the underlying flaws in the Merriespruit tailings facility immediately prior to the failure in 1994 was the overreliance on a tailings compartment that was supposedly closed and only to be used in “emergencies”. Frequent difficulties with tailings delivery pumps and return water capacity meant that a compartment not in daily use or undergoing regular surveillance accumulated significant risks which later events were to prove in tragic circumstances; ref Wagener et al (2007) and (www.tailings.info 2009).

STRATEGIES FOR REDUCING SLURRY WATER CONTENT

In keeping with the Big Picture Thinking perspective described earlier in this paper, it should not be forgotten that other disciplines and expertise can be focused with alacrity on substantially reducing the water that is pumped to a tailings facility. The following actions have been found to be useful:

- Pinpoint and eliminate all potential sources of dilution and water addition.
- Optimize thickener operation.
- Carefully optimize and refine the design and operation of slurry pumping systems.
- Eliminate artificial reasons for slurry dilution and variation.

FURTHER TECHNOLOGY OPTIONS FOR DEALING WITH FINE FLUID TAILINGS

Further progress can be made in the continuum towards effective management of fine fluid tailings and fine material suspended in supernatant, by considering the following technology options:

- Blending of tailings streams.
- Water reduction strategies.
- Recirculation of supernatant.
- Lime dosing.
- Thickening.
- Spigotting.
- Beaching.
- Supernatant pool location.
- Decant tower and penstock outfall design.
- Return water dam design.
- Silt traps.
- Tailings remining and redeposition.
- Test paddocks.
- Contracting out of tailings services.

CONCLUSION

Fine fluid tailings challenges do not resolve themselves. Left to their own devices, they have a habit of mushrooming into far more serious and long standing problems.

The “get rich quick” schemes of narrow technology options which are not integrated

as whole solutions have in the past invariably led to frustrations, delays, failures and cost balloons.

There is no silver bullet to dealing with fluid fine tailings. Instead, it is the “1000 tiny cuts of the Samurai warrior’s sword” that will ultimately prevail. A Big Picture Thinking perspective while paying painstaking attention to detail will reward the tailings manager with walk away solutions in the long term.

Tailings facilities are remarkably forgiving and robust. The temptation to adopt short term measures can be accommodated for a while, but will ultimately lead to legacy problems far more complex in nature and ultimately, failure.

The bitterness of poor quality is remembered long after the sweet taste of low cost is forgotten.

ACKNOWLEDGEMENTS

The advice and comment received from my colleagues Dr John Sobkowicz and Prof. Geoff Blight is gratefully acknowledged. Any errors or omissions contained in the paper are however my sole responsibility.

REFERENCES

Blight (1987) “The Concept of the Master Profile for Tailings Beaches”. Proceedings International Conference on Mining and Industrial Waste Management 1987.

Blight, G.E., Boswell, J.E.S., and Zenon, A. (1995). “Underwater Construction of an Embankment to Extend the Life of a Tailings Impoundment”. Proceedings of I.C.E.,

Geotechnical Engineering, Vol.113, London, U.K.

Blight, G.E. and Lufu L. (2000). “Principles of Tailings Dewatering by Solar Evaporation”. 7th International Conference on Tailings and Mine Waste 2000 at Fort Collins, Colorado. January 2000.

Boswell, J.E.S., De Waal, D. and Hattings, N. (2000). “Communication with the Public about Tailings Projects”. 7th International Conference on Tailings and Mine Waste 2000 at Fort Collins, Colorado. January 2000.

Catalan et al (2002). “Sediment-Trap Measurement of Suspended Mine Tailings in Shallow Water Cover”. ASCE Journal of Environmental Engineering, Vol. 128, No. 1, January 2002, pp. 19-30.

Fell R., MacGregor P., Stapledon D. and Bell G. (2005) “Geotechnical Engineering of Dams”. AA Balkema, p 786.

Gibson R.E., England G.L. and Hussey M.J.L. (1967). “The Theory of One-Dimensional Consolidation of Saturated Clays. I. Finite Non-Linear Consolidation of Thin Homogeneous Layers” Geotechnique 17, pp 261-273

Peck, R.B (1969). “Advantages and Limitations of the Observational Method in Applied Soil Mechanics”. Geotechnique 19, No. 1, pp. 171–187.

Qiu Y and Sego D.C. (1998) “Design of Sub-aerial Tailings Deposition in Arid Regions”. Proceedings 51st Canadian Geotechnical Conference, Edmonton, Alberta. Pp. 615-622.

Schiffmann, R.L., Vick, S.G. and Gibson R.E. (1988). “Behavior and Properties of Hydraulic Fills” Hydraulic Fill Structures ASCE Specialty Conference August 1988, Fort Collins, Colorado, USA. pp166-202.

Sego, D.C. (editor) (2008). First International Oil Sands Tailings Conference, Edmonton, Alberta, December 2008. 290 pages.

Terzaghi, K (1943). “Theoretical Soil Mechanics”. John Wiley and Sons, pp. 330-338.

Vick, S.G. (1990) “Planning, Design and Analysis of Tailings Dams” BiTech Publishers, pp 42 – 68.

Wagener, F v M, et al (1997) The Disaster at Merriespruit and its Consequences. Proceedings Second International Conference on Mining and Industrial Waste Management, Johannesburg June 1997.

Wikipedia (2009). “The Observational Method”. Online summary April 2009. [http://en.wikipedia.org/wiki/Observational_method_\(geotechnics\)](http://en.wikipedia.org/wiki/Observational_method_(geotechnics)).

Remediation

FRAMEWORK CONCEPTION FOR THE REMEDICATION OF THE CULMITZSCH URANIUM TAILINGS POND AT WISMUT (GERMANY) WITH RESPECT TO CONTAMINANT RELEASE

U. Barnekow, T. Metschies & M. Paul

WISMUT GmbH, Division Development / Optimization / Monitoring, Chemnitz, Germany

ABSTRACT: As part of its mine closure program Wismut GmbH is remediating the Culmitzsch Uranium tailings pond covering 2.4 km² and containing a volume of 85 Mill m³ of tailings. From 1967 till 1991 the former Soviet-German Wismut company disposed both tailings from acid leaching and from soda-alkaline leaching of uranium ores into two partial ponds (A and B) creating up to 72 m thick tailings layers. Several villages are located in the immediate vicinity of the tailings pond. Contaminant leakage from the tailings enters the surrounding aquifers and the receiving streams. Dry remediation in situ started with first securing measures in 1991 and will last till 2020. It consists of the following basic remediation steps: seepage catchment, expelling supernatant water and treatment of contaminated water before being discharged into the receiving streams, interim covering of tailings surfaces, recontouring of dams and ponds and final covering including vegetation and construction of a runoff diversion system including runoff retention ponds. The paper presents the framework conception for the entire remediation of the Culmitzsch tailings pond. The framework conception is based on results of geotechnical stability calculations, tailings consolidation modelling, hydrologic modelling of the day-to-day water balance of the final cover as well as hydrologic and hydraulic modelling of the runoff from the tailings pond cover via ditches to the receiving streams. In addition the framework conception takes into account the results of a compartment model representing the tailings and the surrounding aquifer layers for calculation of contaminant release and transport. The compartment model allows for implementing the results of both a simple geochemical approach and a detailed geochemical modelling of the individual tailings zones which are then used as source term for contaminant transport modelling in the aquifer and to the receiving streams. Finally the paper presents the combined effects of ongoing remediation and contaminant release on the remediation design, planning and progress.

INTRODUCTION

From 1947 till 1991 the Soviet-German Wismut company produced a total of 216,000 t of Uranium with about 110.000 t produced in the Seelingstädt mill from 1960 till 1990. According to the Wismut Act dated

October 31, 1990 a total of € 6.6 billion were committed to the remediation of the uranium mining liabilities in south-eastern Germany. The state-owned Wismut GmbH became responsible for remediation of the uranium mining and milling sites. As part of its mine closure program Wismut GmbH is

remediating the Culmitsch Uranium tailings pond covering 2.4 km² and containing a volume of 85 Mill m³ of tailings. Both tailings from acid leaching and from soda-alkaline leaching of uranium ores were disposed into separate partial ponds, from 1960 till 1967 into the Trünzig tailings pond (partial ponds A and B) and from 1967 till 1991 into the Culmitsch tailings pond (A and B). The Culmitsch tailings pond and the Trünzig tailings pond located in the vicinity south of Culmitsch tailings pond were erected in former Uranium open pits.

The framework conception encloses the baseline of remediation and is based on results of geotechnical stability calculations, tailings consolidation modelling, hydrologic modelling of the day-to-day water balance of the final cover as well as hydrologic and hydraulic modelling of the runoff from the tailings pond cover via ditches to the receiving streams. In addition the framework conception takes into account a compartment model representing the tailings and the surrounding aquifer layers for calculation of contaminant release and transport.

SITE CHARACTERISATION

The Culmitsch uranium open pit was mined out from 1957 till 1967. Two layers of grey mudstone or siltstone respectively were mined as uranium rich strata. The ore layers were part of nearly horizontally bedded sedimentary rock layers of Permian age situated in a half-graben. The up to max. 70 m thick Permian rocks are underlain by Ordovician shales folded in the Variscian orogenesis. The Permian sedimentary rocks consist from bottom to top of a base conglomerate, mudstone, siltstone and sandstone layers (in particular the “Culmitsch sandstone”) overlain by a thin layer of weathered dolomite residues, a

weathered mudstone and a sandstone layer of lower triassic age.

Due to open pit mining overburden materials were relocated onto the waste rock dumps called Lokhalde, Waldhalde, Jashalde, Südwesthalde and “Innenkippe”, the waste rock dumps located inside the open pit. Three waste rock dams were erected from 1963 till 1966 enclosing two partial ponds. The dams include the north dam, the south and southeast dam and the separating dam. The separating dam has a vertical sealing wall in the dam centre. Fig.1 shows a three-dimensional structural model of the site including the open pit surface, dams and waste rock dumps before tailings disposal.

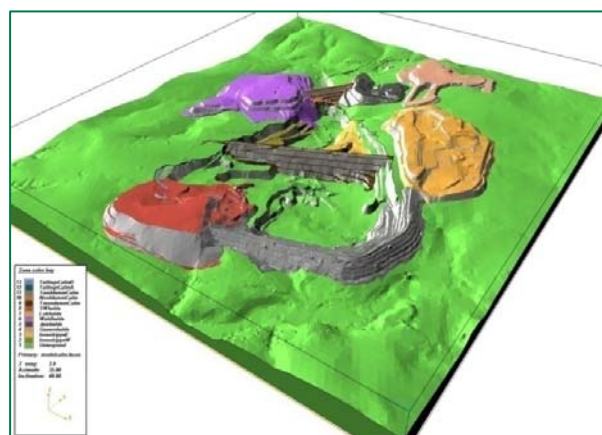


Figure 1: 3D structural model of Culmitsch open pit and dams (view from SE).

Tailings disposal lasted from 1967 till 1990. Tailings from acid leaching were discharged into pond A (in the foreground) applying the centreline method along the southern tailings beaches. Tailings from soda-alkaline leaching were disposed from the northern perimeter into pond B. According to the historic discharge regime sandy tailings beaches settled near the discharge spots while fine tailings settled more distant below water table.

The hydraulic regime in the permeable surrounding geological layers, in particular in the main aquifer layer Culmitzsch sandstone, is closely connected with the hydraulic conditions in the permeable sandy tailings. This led to significant contaminant seepage during and after the operation phase. Large areas in the ponds were covered by thick layers of pulpy or weak fine tailings characterized by low trafficability and large settlements over many years.

Fig. 2 shows an aerial view on the Culmitzsch tailings pond from SW in 1993. The South Dam and the Südwesthalde waste dump are in the foreground. Tailings data are listed in Table 1.



Figure 2: Culmitzsch tailings pond A and B: Aerial view from SW to NE.

Table 1: Tailings data

	unit	Pond A	Pond B
Surface area	ha	159	84
Tailings vol.	Mio m ³	61	24
Solid mass	Mio t	64	27
Max. thickness	m	72	63
Unat in solids	t	4800	2200
Ra-226 in solids	10 ¹⁴ Bq	7.9	2.4
Unat in pore water	mg/l	0.3 ... 3.9	1.0 ... 20
Ra-226 in pore water	mBq/l	...5000	...2300

DRY REMEDIATION IN SITU

Dry remediation in situ started with first securing measures against acute risks in 1991

and will last till 2020. Measures against acute risks comprised of:

- Installation of fences to prevent access.
- Interim covering of sandy tailings beaches to reduce radon exhalation, direct radiation and radioactively contaminated dusting.
- Geotechnical investigations on dam stability and dam stabilization measures
- (Re-)construction of catchment systems to collect the entire seepage and runoff from the tailings ponds and construction of the water treatment plant at the mill site (treatment of U and Ra)
- Installation of a monitoring system to track the impacts of the tailings ponds before, during and after remediation

The remediation has to ensure the safe long-term storage of the tailings reducing the additional equivalent dose to the population from all pathways to less than 1 mSv/year. Requirements for waste water discharge into the receiving streams were set by the authorities of Thuringia.

By 1995 the preferred option for remediation of the Culmitzsch tailings ponds was derived to be the dry remediation in situ including dewatering of tailings by technical means. This preferred option for remediation was agreed by the authorities and encloses the following fundamental remedial steps:

- Expelling of pond water, dewatering of permeable (sandy) tailings, collection of seepage and runoff including water treatment before being discharged into the receiving streams
- Interim covering of remaining air-exposed (fine) tailings surfaces to create a trafficable working platform for further remedial works
- Reshaping of dams to grant sufficient seismic dam stability to the long term and re-contouring of the pond surfaces with

respect to the functionality and erosion stability of the final cover and landscaping aspects

- Final covering including construction of water diversion systems, access roads and vegetation with respect to (restricted) re-use of the covered surface.
- Construction of a runoff diversion system including runoff retention ponds downstream of the tailings pond.
- After having expelled the major part of the supernatant water out of the ponds a new water treatment plant was erected in 2000/01 next to the Culmitzsch tailings pond

FRAMEWORK CONCEPTION

Objectives

The framework conception for remediation of the Culmitzsch tailings pond shall provide and follow-up the actual framework design planning of the overall remediation of the Culmitzsch tailings pond. It is prepared and revised annually by Wismut. The works enclose the coordination and elaboration of scientific studies and engineering design and planning works in numerous professional fields prepared either by Wismut or by external companies. In the following the framework conception including baseline studies, conceptual designs and detailed designs for re-contouring and final covering of the Culmitzsch tailings pond are presented in more detail. Based on the framework conception construction lots are defined and the follow-up of remedial works is planned allowing for a coordinated remediation progress of the different individual construction steps to be realized at different locations on the tailings pond at the same time.

Framework Conception for Re-contouring

The framework conception for the overall re-contouring of the Culmitzsch tailings pond was based on the evaluation of the technical, economical and environmental benefit following the German regulation (VOAS 1984) with respect to guaranteeing geotechnical stability of the entire re-contoured tailings pond including the dams; minimizing the volumes of soils and radioactively contaminated materials to be removed and creating a landscape and vegetation adapted to the surrounding landscape. The conceptual re-contouring design included the following basic work steps:

- 1 Development of a 3D-model of the tailings pond's structure and modeling of spatial distribution of tailings properties of interest
- 2 Modelling of time-dependent tailings consolidation including the design of measures to speed up tailings consolidation
- 3 Design of dam reshaping and reshaping/relocation of waste dumps with respect to geotechnical stability to the long term and/or for radiological/environmental reasons
- 4 Fixing outlet points, positions and gradients of trenches for diverting runoff and modeling of the optimum surface contour needing the minimum fill volume to build the re-contoured surface.
- 5 Hydrologic modelling of the runoff of the entire catchment area and hydraulic modelling of the flood levels and flooded areas along the receiving creeks.

The first framework conception was prepared by Wismut in May 2004 (Barnekow et. al. 2005) and submitted to the mining authority for review. In the beginning of 2006 we received from the mining authority the respective declaration of acceptance of the

framework conception for the overall re-contouring of the Culmitzsch tailings pond.

Fig. 3 shows the actual status of the re-contouring works of the Culmitzsch tailings pond (view from east to west). Only the central fine tailings zone of pond A (left pond on Fig. 3) still has to be interim covered. It shall be completed by 2012. Reshaping of the south/southeast dam (left hand side of Fig. 3) will start with preparatory measures in 2010. Pond water of pond B (right pond on Fig. 3) was expelled by 2002. The interim cover was placed on the entire pond B by 2006. The north dam was reshaped in 2007/8 (right hand side of Fig. 3). The respective excavated waste rock materials were relocated on the northern tailings beaches in pond B (right hand side of the pond B on Fig. 3). Since 2008 the northern part of the waste rock dump Waldhalde (see waste dump in the background on the right hand side of Fig. 3) is being relocated onto the fine tailings zone of pond B (central part of the right pond on Fig. 3). Recontouring is monitored by a radiological, environmental and a geotechnical monitoring system. The geotechnical monitoring includes among others pore pressure gauges, monitoring wells and regular geodetic surveys.

The north dam was reshaped by flattening inside the dam to a general slope inclination of $v : h = \text{ca. } 1 : 3.6$. The south and southeast dam is planned to be reshaped by combining a dam buttress with cutting the dam crests. In order to grant seismic stability with respect to the maximum credible earthquake (acc. to German regulation DIN 19700) the upper tailings layer located nearby the dam crest has to be relocated completely. The underlying fine tailings have to be consolidated by surcharge loading placing an embankment fill combined with the use of deep vertical wick drains. The upper fine tailings layer must be replaced by waste rock material.



Figure 3: Remediation status in 2008: Pond A (see left); Pond B (see right).

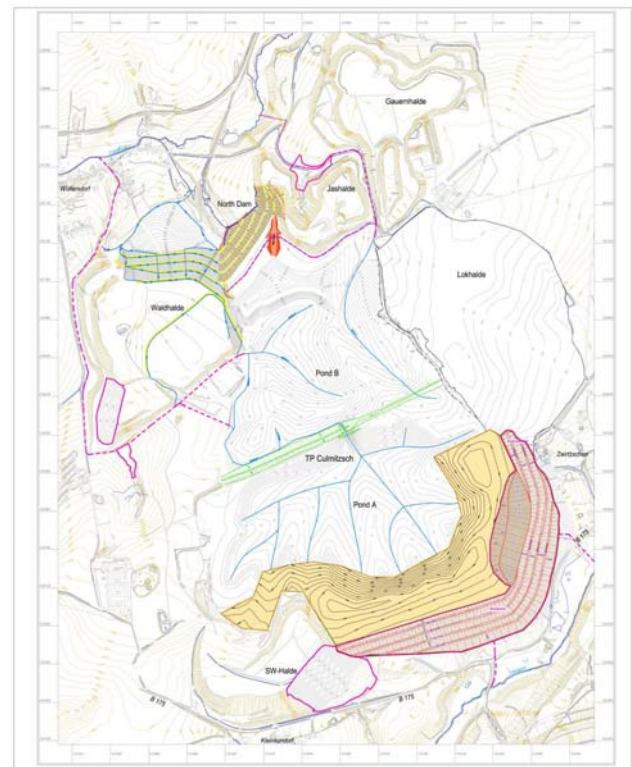


Figure 4. Surface contour of the re-contoured TP (design status: 2009).

The framework conceptual design for the re-contouring of the entire Culmitzsch tailings pond is presented with Fig. 4. The surface contour of the pond areas was optimized based on modeling of the time-dependent tailings consolidation with respect to the

designed re-contoured surface and the time dependent loading of the tailings surfaces during (future) re-contouring works. Fig. 5 shows the spatial distribution of the predicted total primary settlement. Settlement calculations resulted in an estimated total settlement volume of 4.9 Mill m³. Total settlements of 4 m to 7 m were predicted in the area of thick fine slimes (see fig. 5). To handle this problem the fine tailings consolidation is to be speeded up using deep vertical wick drains in certain areas, i.e. vertical wick drains stitched 15...25 m deep in up to ca. 60 m thick fine tailings in the central part of pond B. These works were carried out in the fine tailings zone of pond B from 2008 till 2009.

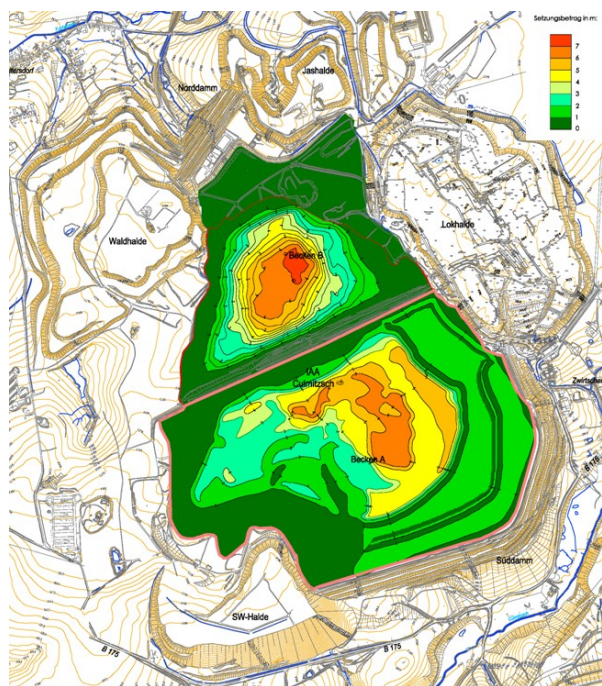


Figure 5. Predicted total settlement due to interim cover, re-contouring & final covering.

Certain slopes of the surrounding waste dumps are to be reshaped to achieve sufficient geotechnical stability to the long term. In addition some parts of waste rock dumps should be removed for radiological/environmental reasons. Fig. 4 shows the waste dump slopes to be relocated

and reshaped. The Lokhalde waste dump east of the tailings ponds will be completely relocated. By beginning of 2009 a total remaining volume of 19.5 Mill m³ will be needed for the remediation by re-contouring and final covering. According to the framework conception about 22 Mill m³ of mixed-grained waste dump materials will be planned to be available on site for the remaining remediation.

Framework conception for final covering

In order to evaluate the functionality of different final cover types several test fields including numerous cover designs were constructed at a nearby test field site. The water balance for each final cover design type was simulated applying the HELP and HYDRUS codes. Geotechnical calculations were carried out to prove the stability of the cover against sliding on steep dam slopes, erosion, suffosion, and effects of differential settlement.

The effect of the final cover and of the overall remediation on the release and transport of contaminants from the tailings pond (source) to the receiving streams is presented in detail below.

Resulting from the evaluations presented below the preferred cover design depends on the underlying tailings types. On sandy tailings beach zones the preferred cover should be a two-layer-cover consisting of a ca. 1.5...2 m thick storage layer above a compacted sealing layer. On fine tailings zones the functionality of the final cover shall be granted by a minimum 2.5 m thick layer consisting of mixed-grained waste dump material. The final cover is to reduce the percolation rate only on permeable tailings beaches. Further more the final cover shall provide sufficient plant available water during growing seasons. Afforestation is planned for the final cover on tailings beaches

in order to assist for controlling the percolation rate.

Based on a detailed ecological survey of the entire site the landscape planning and (re)vegetation is designed and realised with respect to balancing ecological intervention measures and compensatory measures as well as public interests. All construction works are continuously accompanied by an ecological monitoring. Fig. 6 presents the landscaping and vegetation plan for the long term status (after establishment of vegetation).

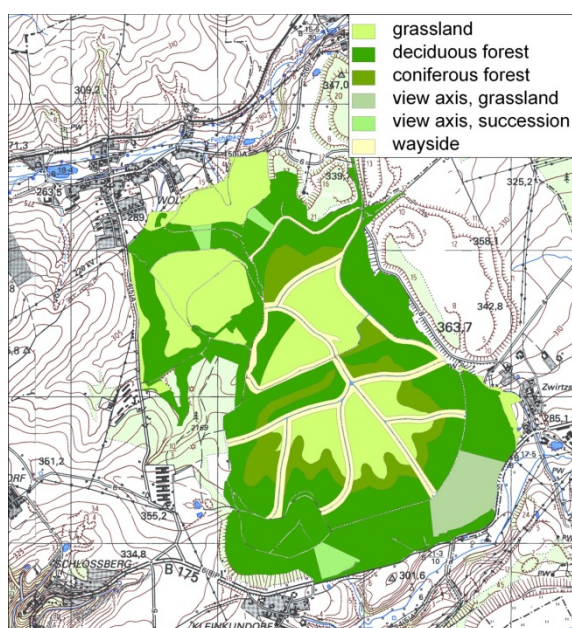


Figure 6. Landscaping and vegetation plan for Culmitzsch TP and surrounding dumps

Based on the interim results of the annually revised framework conceptions for re-contouring, final covering and landscape/vegetation design hydrologic modeling was carried out for designing the catchment areas comparing the runoff of 2-years to 100-years repeating flood events for the operational phase in 1990 (no runoff to the receiving streams) and after final covering implementing two different vegetation scenarios: initial grassland (sowed for initial erosion protection) and fully

established vegetation (long term status). Based on the results a decision was made to plan for two runoff retention ponds shown on Fig. 4 west and north of the Culmitzsch tailings pond avoiding any increase in flow rates and flood levels along the receiving creeks compared to the situation in 1990. In addition all trenches for diverting surface runoff were dimensioned with respect to the 100 years flood event. The framework conception implements a conceptual design of the tailings pond re-contouring that reconstructs the pre-mining catchment areas. The surface runoff is diverted via trenches from the southern pond A via the separating dam to pond B. The major part of the runoff from both ponds is diverted via the western border of pond B. A minor part of the runoff is collected on the eastern part of pond B and diverted in an additional trench to the north of pond B. The northern creek “Fuchsbach” will receive the runoff from the major part of both ponds A and B.

CONTAMINANT RELEASE AND TRANSPORT

For the planning and licensing of the necessary remediation work modelling tools are used to predict the development of the seepage water quantity and quality influencing the surrounding aquifers and surface waters. The main concern of the licensing authorities is focused on the salt load, the discharge of uranium and heavy metals from the tailings ponds entering the surrounding aquifers and receiving streams.

Characterization of hydrological and geochemical conditions

The tailings from an acidic processing were usually neutralised and pumped into pond A while the tailings from the alkaline processing were disposed in pond B. Therefore, the geochemical characteristics of the two partial

ponds differ considerably. The tailings in pond B are characterized by a high content of carbonates ensuring that there is no potential acidification of the material even in long term. However, the uranium contents in pore waters are considerably higher than in pond A due to the fact that under the present conditions of high hydrocarbonate contents in the solution uranium remains more mobile. On the other hand, the material in the pond A still has pyrite concentrations in the range of 2 to 5 mass% while the neutralization potential is limited resulting in an acidification potential under oxidizing conditions.

The tailings material was disposed resulting in a material classification depending on the distance from the discharge spots with more or less regular distribution of the discharge spots during the operational phase. With regard to the grain size distribution the tailings can be divided depending on their hydraulic and geochemical characteristics into 3 main zones: (1) a sandy zone, (2) a zone of fine slime tailings and (3) a transition zone. The transition zone is characterized by an interlayering of sandy and fine grained tailings layers. The seepage of meteoric water through the tailings is dominated by the sandy tailings with higher hydraulic conductivities. The hydraulic conductivity of fine slime tailings is some orders of magnitude lower than in the sandy part.

In addition the consolidation of the fine slime tailings leads not only to a release of contaminated pore water but also to a further reduction of the hydraulic conductivity to values smaller than 10^{-9} m/s. Consequently the seepage through these tailings materials will be limited by the hydraulic properties of consolidated slimes in the long-term.

The transition zones combine the properties of the fine-slime and sandy tailing zones. The transition zone with the interlayering of sandy

and slimy layers is dominated by horizontal flow feeding the sandy part. Due to the interbedded slime lenses the vertical water flow is retarded. Consolidation processes are also relevant for the slimy parts of the transition zone influencing contaminant release and the vertical hydraulic conductivity.

The tailings from the uranium milling activities were discharged into former open pits without any sealing at the bottom. Together with the Ordovician fractured aquifer at the bottom the Culmitsch sandstone is a regionally developed aquifer. Because tailings material is deposited in close contact with these aquifers and the high gradients resulting from elevated technological water levels contaminated pore water seeped into the surrounding aquifers. This was documented by geochemical monitoring of the groundwater in the vicinity of the tailings pond.

An east west directed phreatic divide exists between the 2 tailings ponds of the Culmitsch site. Seepage water from the pond A flows in southern direction and discharges in a meadow into the Culmitsch/Pöltzbach creek. The seepage water from the pond B and partly from pond A flows into northern direction to the Fuchsbach Creek which has a similar water discharge as the Culmitsch/Pöltzbach creek.

The seepage water has high loads of sulphate and total hardness. Technical measures are implemented to reduce the seepage by pumping from boreholes and drainage elements. The collected water is processed in a water treatment plant using a lime precipitation technology. The treated water is discharged into the Culmitsch/Pöltzbach creek. The Culmitsch/Pöltzbach creek has a catchment area of about 15 km² and, therefore, a limited discharge rate (MQ=162 l/s). This discharge is about double the

discharge of the collected seepage and surface waters from the site which is released after treatment into the Culmitsch/Pöltschbach creek.

Apart from the geotechnical stabilisation the remediation of the tailings ponds should also ensure the reduction of infiltration and oxygen diffusion into the tailings body by implementing an appropriate cover system. This will influence the long-term release of contaminants especially from the sandy tailings.

Modelling approach

For the optimisation of the cover design by balancing the environmental effects and costs prediction of the long-term contaminant release various technical solutions are to be evaluated. A model describing the conditions within the tailings ponds and their interaction with the adjacent aquifers and receiving creeks had to be prepared (Kahnt et. al 2007). This model had to integrate the available knowledge of the hydraulic, geochemical and geotechnical conditions of the site. In the past a vast amount of detailed analysis of individual aspects of the tailings pond remediation were prepared. Among them various detailed models addressed individual hydraulic, geotechnical or geochemical problems of parts of a single impoundment or the surrounding aquifers. However, to judge on the effectiveness of single remediation measures their influence on the whole catchment area has to be evaluated by integrating this knowledge into an overall site model. This model therefore also includes the two partial ponds of the Trünzig site which are situated south of the Culmitsch site and influence the same aquifers and surface waters. The ponds of the Trünzig site are described in the same way in the model as it was done for the Culmitsch site.

Because of unsatisfactory experience gained by implementing detailed geochemical and

hydrological models of the tailings impoundments and the surrounding aquifers a simple and flexible approach was followed for the development of the site model which reflects the relevant processes in a simple and traceable way. Basis is a box-model-concept with compartments representing parts of the relevant units such as tailings impoundments, aquifers and surface waters. The compartments of the model are not only boxes. They have an internal substructure to reflect the different types of materials and the different processes that have to be described. The compartments are described by effective geometric, hydraulic and geochemical parameters which take into account the wide range of measurement results of the natural system. This approach allows a better judgement on uncertainties which exist in the description of such a complex hydraulic and geochemical system than in a very detailed model.

Technological conditions are included in the model such as water treatment, enhancement of dewatering by introduction of wick drains in the fine slime zone and covering. This especially includes the influences of the technical measures onto the hydraulic and geochemical conditions in the different parts of the system. For example the reshaping and covering of the tailings forces the consolidation of the slimy parts of the tailings and changes the water conductivity but also the infiltration and oxygen diffusion.

Model Discretisation

Surface water compartments are represented by mixing cells which receive water from the groundwater compartments, upstream surface water compartments and if relevant from technical water inflows, such as water treatment plant discharge.

The aquifer affected by tailings seepage is divided into compartments depending on the hydraulic conductivity of the main

hydrogeological strata, tectonic features, the boundary of the tailings impoundments and the course of receiving waters.

The compartments representing the tailings material are divided into sub-compartments according to the three main material zones. This zonation was derived from measurements of the grain size distribution and CPT-measurements on the tailings impoundments. Each of the two Culmitzsch partial ponds A and B were divided into four compartments which include the sub-compartments for modelling of the fine-slime, sandy and transition zone materials with their different hydraulic geotechnical and geochemical behaviour. The internal structure of the tailings compartments is shown in Fig. 7.

Waste rock dumps from the uranium mining close to the tailings pond also influencing the long-term contaminant release have to be taken into account, too. Therefore, the waste rock dumps are included as additional sources in the model. Conceptually the model consists of two layers. The first one describes the sources such as the tailings and the waste rock dumps and the second the aquifers (Fig. 8).

A simple hydraulic model is used to define the water balance within the modelled system including the quantity of water flow between the compartments.

In addition to the infiltration of rainwater a significant interaction between the ponds of supernatant water and the deposited tailings materials occurs. As long as the technological water is on top of the tailings it influences the infiltration into the material, especially into the sandy and transition zone, and as a result the leaching of contaminants from the

impoundments continues. Prior to remediation the supernatant water is removed.

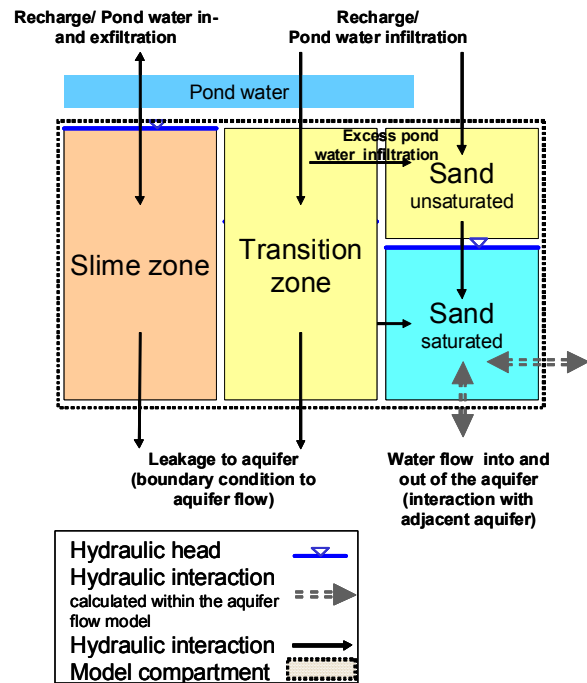
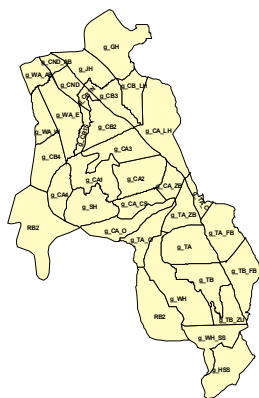


Figure 7: Scheme of the internal structure of a single tailings compartment.

The model is based on Darcy's law with average hydraulic heads for each compartment as well as conductance values. Adjacent compartments are connected to each other. In the hydraulic model the sandy zone of the tailings compartments is directly connected to the underlying groundwater compartment. The seepage from fine slime and transition zone also depends on the level of the groundwater and is included as additional boundary conditions (Fig. 8). The hydraulic conditions in the transition and fine slime zone are calculated separately.

The hydraulic model was calibrated based on the historic measurement data of water tables as well as seepage and discharge rates.

Groundwater - layer



Object - layer



Figure 8: Illustration of the compartments in the groundwater and the object layer.

Geochemical approach

The geochemical environment within the tailings pond is highly complex. In particular, it appears that the geochemical trends observed are in part artefacts of the ore beneficiation methodology used over time, rather than being only due to geochemical processes. This and the fact that the ponds A and B have significantly different geochemical conditions complicate or at least add to the uncertainties of any detailed geochemical modelling significantly, as it is not possible to calibrate the model to past and existing conditions based on geochemical considerations alone.

The geochemical conditions of the source is described separately for the sand, transition and fine slime zone. For the sand and transition zone it has to be taken into account that an unsaturated upper and the saturated lower part exist, which have different geochemical behaviour because of the availability of oxygen. Changing water tables due to remediation activities lead to a time dependent movement of the boundary between the saturated and unsaturated zone. This requires to account for changes in the mass balance of each part due to the change of water table in the model.

The geochemical conditions of the tailings material were determined by different

sampling campaigns where the composition of the solid and liquid phase have been analyzed. The respective results are the basis for the definition of the contaminant source term of the ponds. The parameters were derived by statistical analysis and plausibility tests using PHREEQC. For the simple approach of the site model two basic concepts of contaminant release were defined. Either the release is solubility controlled or adsorption (K_d) controlled. According to the solubility control model, dissolved concentrations are governed through dissolution or precipitation of mineral phases. In the K_d controlled model the adsorption-desorption ratio is governed by the dissolved concentrations. In both cases, as an initial condition the total mass of each contaminant is applied to the mixing cell based on the current observed dissolved and solids concentration in the slimes. For both cases the observed conditions are seen as initial condition to define the ratio between the contaminants in the solid and the fluid phase. It was determined by geochemical modelling that the dissolved concentrations of SO_4 , Ca and Mg are controlled by mineral dissolution. Therefore for these species only solubility control is considered. Chloride is treated as tracer without any additional source in the solid phase.

In the unsaturated zone mass budgets are calculated for pyrite oxidation and the connected neutralization reactions. As long as sufficient neutralization potential is available there are no changes of the pH. In case of changing pH-value the parameters for the solubility or the adsorption coefficient are changed. Two pH-states are considered in the model: a neutral pH and a low pH. Using the analysis results from the sampling campaigns the coefficients for the two pH approaches were determined.

Besides the simplified description of the geochemical conditions inside the tailings

impoundments, the results of detailed external geochemical models for the different tailings impoundments have been integrated. The use of either the simplified model for the interior of the tailings or the results of the external model could be chosen.

Modell implementation

The compartment model is implemented using the GoldSim decision support tool. GoldSim is a simulation software solution for dynamic modelling of complex systems in business, engineering and science. It offers a range of elements with predefined properties such as reservoirs, mixing cells or function elements which fulfil user defined mathematical operations. These elements were connected to set up the hydraulic and the geochemical model and to offer the necessary interfaces to import the results from the external models. Models implemented in GoldSim are flexible concerning further adaptations of parameters and even in the integration of relevant additional processes.

GoldSim allows to generate a so called player file from an existing model which can be run with a freely available GoldSim player. This gives the opportunity to provide this model to regulators and their consultants to support the process of granting necessary approvals for the remediation activities.

The general purpose of the implemented site model is the evaluation of different technical

measures with regard to the reduction of the environmental impacts. Therefore the system is modelled over a time period of up to 100 years. To ensure the toughness of the model, in front of the prognosis, a history matching was performed. This included to follow the changes of the hydraulic and geochemical characteristics of the system from the mid sixties till today. The approach was confirmed by comparison of the modelled results with averaged observations for the different compartments.

Modelling results

Based on the modelling of the history it was demonstrated, that the model is able to represent the time dependent average values of contaminant releases measured in the past and at present in the surface creeks, the average concentrations in the drainage systems and in groundwater. Additionally the development of the water table heights calculated for the boxes correspond to average values of observations in the respective area. Figure 9 shows as an example the prediction of loads released in the Culmitzsch creek downstream of the tailings impoundments. Using the different geochemical approaches and by variation of the model parameters within the measured data range various model runs could be executed. The results of these runs can in a quick and transparent way reproduce the range of model uncertainties.

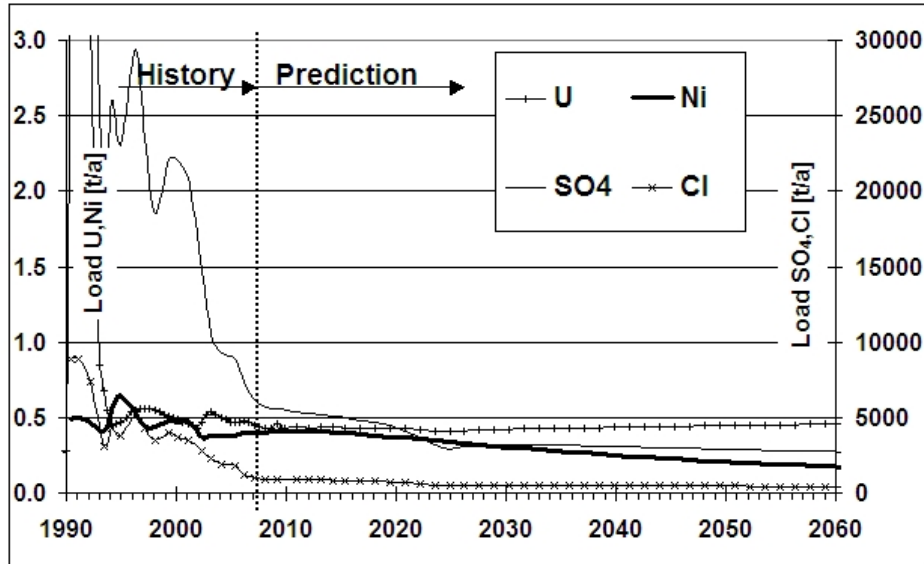


Figure 10. Prediction of loads in the Culmützsch creek downstream of the tailings site.

The approach demonstrated, that a complex site with a variety of contaminant sources can be represented by a compartment model approach integrating the results of different detail models and knowledge about the site.

CONCLUSIONS AND OUTLOOK

The remediation of large tailings ponds is a complex task. The framework conception for remediation of the Culmützsch tailings pond ensures a coordinated remediation progress of the different individual construction steps to be realised at different locations on the tailings pond at the same time.

It serves as a basis to involve stakeholders and permitting authorities. The framework conception is used as the regularly revised base document for the coordination of numerous closely interconnected permitting procedures according to mining law, water law, radiation protection law, environmental protection law, planning approvals, etc.

The design of the recontoured pond surfaces and minimization of relocation volumes needed depends on the time-dependent tailings consolidation due to surcharge loading with time. Resulting from consolidation modelling deep vertical wick drains were applied to speed up the tailings consolidation to achieve ca. 90% consolidation at the end of the final covering in 2020.

Due to the complex geotechnical, hydraulic and geochemical conditions no ready-to-use modelling tools exist. Therefore a simple and flexible compartment model approach taking into account the results of detailed models is applied successfully to predict the contaminant release to the long term as a basis for the decision on the preferred remediation option. The results are used for further detailed planning. The model approach could be easily amended taking into account the experiences made during ongoing remediation.

ACKNOWLEDGEMENTS

We would like to thank our colleagues involved in the preparation of the framework conception and the site modeling Dr. R. Kahnt, Mr. J. Priester, Mr. G. Merkel and Mr. B. Rassmann

REFERENCES

Barnekow, U., Neudert, A. & Hoepfner, U. 2005. Re-contouring and Final Covering of Trünzig and Culmützsch tailings ponds at Wismut. *Recent development in uranium exploration and environmental issues* IAEA TECDOC-1463. Vienna, Austria, September 2005.

Kahnt, R. & Metschies, T. 2007. Modelling of Contaminant Release from a Uranium Mine Tailings site. *Proc. of the 11th Int. Conf. on Environmental Remediation and Radioactive Waste Management ICEM2007*. Bruges (Belgium), 2-6 September 2007.

VOAS 1984. *Verordnung zur Gewährleistung von Atomsicherheit und Strahlenschutz und Durchführungsbestimmung zur VOAS*. (Engl.: Ordinance on Guarantee of Nuclear Safety and Radiation Protection and Implementing Regulation of this Ordinance, GDR 1984)

ACTIVATED ALUMINUM TAILINGS USING MINE WASTE TO CLEAN UP MINE SITES

Eugene Mullenmeister and Ernest Stine

Shaw Environmental & Infrastructure, Inc.

ABSTRACT: Activated aluminum tailings (AAT) is a product derived from red mud created when extracting aluminum from bauxite ore. It is an emerging technology that is effective in removing heavy metals, soluble cyanide, as well as iron, aluminum, manganese and silicate from water. It does not remove most Group IA (e.g., Na, K...) and IIA (e.g., Mg, Ca...) cations, Group VIIA (e.g., F, Cl...) anions or sulfate. It can be used as a pretreatment to remove metals that may foul RO membranes, post treatment to remove many metals from the reverse osmosis (RO) or evaporator reject stream and for metals removal for the in-situ treatment of tailings ponds and mine pits. It can also be used in pellet or powder form in large basins, tanks, in a conventional WWT plant or by spraying slurry into the pit or ponds. Activated aluminum tailings has proven effective in the treatment of metals in acid rock drainage and tailings impoundment leachate. In many cases, the adsorbed metals become more tightly bound into the activated tailings over time. Analyses of the TCLP, SPLP and CAL-WET procedures result show that spent solid AAT loaded with metals is an inert, non-hazardous solid, which requires no special handling.

INTRODUCTION

Activated aluminum tailings are derived from red mud created when extracting aluminum from bauxite ore. It has been demonstrated to be effective in removing heavy metals, soluble cyanide, as well as iron, aluminum, manganese and silicate from water (McConchie, 2002), (Genc-Fuhrman, et al., 2004a, 2004b), (Genc-Fuhrman, et al., 2005). It does not remove most Group IA and IIA cations, Group VIIA anions or sulfate. Activated aluminum tailings, consists mostly of a mixture of iron and aluminum oxide and carbonate minerals. The likely mechanism that binds the metals is chemisorption onto the iron in the AAT followed by more permanent incorporation of the heavy metals by migration into the AAT mineral matrix.

Activated aluminum tailings can be used as a pretreatment to remove metals that may foul RO membranes (e.g., Fe, Al, Si, and Mn), post treatment to remove many metals from the RO or evaporator reject stream and for metals removal for the in-situ treatment of soil sediment and impounded water. It can be applied in pellet or powder form in large basins, tanks, in a conventional WWT plant or by spraying slurry into the pit or ponds. Spent AAT reagent when dried is a non-hazardous solid as demonstrated by results using the California waste extraction test (CAL-WET) and Toxicity Characteristic Leaching Procedure (TCLP).

This paper describes bench-scale testing to simulate two types of applications. The first application simulates spraying slurries of

AAT over a pond or pit water and allowing the fine particulate to remove metals of concern as the solid settles to the bottom of the pond or pit. The particle size distribution of the AAT powder is such that some of it settles rapidly through the water column and the remaining solids may take a day or more to settle. This differential settling allows for effective metals removal throughout the water column. The other application simulates mixing AAT into soil to form zones of large-scale metal sequestration areas. Additional pilot-scale work is underway demonstrating the ability to inject slurries into the subsurface. The AAT pilot-scale and follow-up studies will be topic of future papers.

In this paper the results of bench-scale screening tests using AAT to remove metals from water at three different sites are presented. These tests were conducted on water from the McLaughlin Mine, the Jamestown Mine and a confidential chemical manufacturing facility.

MCLAUGHLIN MINE

Two sets of studies were conducted on water from the McLaughlin Mine. The first set was performed in 2006 and the second set was performed in 2008 and are ongoing at the time of this writing. The 2006 studies were proof-of-principle isotherm studies. The 2008 studies were expanded to not only include isotherms but larger column studies to substantiate that metals of concern will be effectively removed without rebound by the addition of AAT slurries to the top of the water columns. These studies were also designed to substantiate that metals would be removed from the complete water column not particular depths within the column. The McLaughlin Mine is a closed gold mine located in the Coast Range Province of Northern California. It is a zero discharge

facility. All water produced at the McLaughlin Mine is contained on site and has been throughout the entire life of the facility.

2006 Bench Tests

The first set of bench scale treatability studies were batch tests, conducted on McLaughlin Mine Site waters. The treatability studies included:

- Screening tests for the use of AAT products to remove heavy metals from three different water sources,
- Investigating the use of AAT as pretreatment for RO to decrease the rate of fouling of the RO membrane, and
- Hazardous material determination of metals loaded AAT using the CAL-Wet procedure.

Screening of the Effectiveness of AAT to Treat Three McLaughlin Mine Water Sources

Screening isotherm tests were performed on water from three different water sources at the McLaughlin Mine. Batch tests using reagents blends containing mostly AAT in powder form were added to aqueous samples from the site. AAT reagent blends were added to the waters at dose rates of 1 and 2 g/L. The final pH ranged from about 7 to nearly 10. Results are presented in Table 1, which shows that after treatment the concentration of most heavy metals, iron and aluminum decreased to less than drinking water standards. The treatments did not remove Group IA/IIA cations (sodium, potassium, calcium, magnesium, etc.), halides, or sulfate.

Table 1. Batch Test Results, McLaughlin Mine 2006 Three Individual Water Sources

Parameter	Sample Water #1		Sample Water #2		Sample Water #3	
	Untreated	Treated	Untreated	Treated	Untreated	Treated
	mg/L	mg/L	mg/L	mg/L	mg/L	mg/L
pH (s.u.)	4.08	8.52	7.1	9.94	6.35	8.54
Aluminum	21.12	ND (0.35)	ND (0.035)	ND (0.035)	ND (0.35)	ND (0.35)
Arsenic	0.015	ND (0.010)	0.019	0.0023	0.78	ND (0.01)
Barium	0.014	0.031	0.016	0.0254	0.022	0.0387
Copper	0.1	ND (0.035)	ND (0.035)	ND (0.035)	ND (0.035)	ND (0.035)
Iron	3.4	ND(0.100)	0.24	0.0018	143.5	ND (0.100)
Lead	ND (0.010)	ND (0.010)	0.011	0.0019	ND (0.010)	ND (0.01)
Magnesium	188.3	216.7	81.75	92.93	193.6	196.2
Manganese	26.61	26.17	0.98	ND (0.025)	4.52	0.71
Mercury	0.0004	ND(0.0002)	0.0003	ND (0.0002)	0.0002	ND (0.0002)
Nickel	10.4	9.3	0.17	0.03	8.823	0.45
Sulfur	532.3	647.1	505.7	481	588.9	532.8
Zinc	1.54	0.056	0.003	ND (0.01)	0.1	ND (0.002)
Antimony	ND (0.01)	ND (0.01)	0.1711	0.1348	ND (0.01)	0.1348
Calcium	287.6	352.7	363.4	367.4	185.8	62.96
Cobalt	0.9019	0.7153	0.0609	0.0333	0.2713	0.0117
Molybdenum	ND (0.010)	ND (0.010)	0.01	ND (0.010)	ND (0.010)	ND (0.010)
Phosphorous	0.17	0.1922	0.32	0.254	ND (0.030)	0.254
Potassium	15.79	14.33	36.24	30.2	18.46	30.2
Sodium	131.1	185.3	570.9	587.5	327.6	587.5
Thallium	0.01362	0.01	0.0105	ND (0.01)	ND (0.01)	ND (0.01)

Notes: mg/L – milligrams per liter

s.u. – standard units

ND – non detect

Pretreatment of Water to Improve RO Performance

Studies were conducted to determine the effectiveness of the addition of AAT for removal of soluble metals (e.g., Fe, Al, Si, and Mn) that are expected to foul RO systems. A composite water sample using water from multiple sources was prepared for these tests. The composition of the composite sample is shown in Table 2.

The tested waters contain significant levels of dissolved iron. Tests were conducted using AAT pellets and AAT pellets with caustic addition at a dose rate of 1 and 2 g/L. The test results show that heavy metals, iron and aluminum were removed at a dose rate of 2 mg/L. In particular manganese removal was improved when caustic was added. See Table 2.

Removing these metals should improve the performance of RO membranes by limiting fouling issues. This could allow higher recovery rates (i.e., higher percentage of permeate with less rejected water) which lowers capital costs for the RO system. As will be shown below in the CAL-Wet tests, “spent” AAT reagent is non-hazardous and will actually continue to remove metals from pits or ponds after it is added to the water body. This leads to an advantage of treatment with AAT. The metals are adsorbed on the “spent” AAT solid can be disposed in on-site pits or ponds with no detrimental effect. After disposal, the “spent” AAT will continue to remove metals such as arsenate.

Table 2. Composite Water, McLaughlin Mine (2006) AAT Treatment Results

Parameter	Sample								
	Composite	AAT Pellets @ 1 g/L - 4 hr Contact	AAT Pellets @ 2 g/L - 4 hr Contact	AAT Pellets @ 1 g/L - 2 day Contact	AAT Pellets @ 2 g/L - 2 day Contact	AAT @ 1g/L, NaOH to pH 9	AAT @ 2g/L, NaOH to pH 9	NaOH to pH 9, AAT @ 1 g/L	NaOH to pH 9, AAT @ 2 g/L
	mg/L	mg/L	mg/L	mg/L	mg/L	mg/L	mg/L	mg/L	mg/L
Silver	0.077 J	<0.022	<0.022	<0.022	<0.022	<0.035	<0.035	<0.035	<0.035
Aluminum	0.1235	<0.055	<0.055	<0.055	<0.055	<0.055	<0.055	<0.055	<0.055
Arsenic	0.4866	<0.011	<0.011	<0.011	<0.011	<0.011	<0.011	<0.011	<0.011
Barium	0.0175	0.017	0.020	0.030	0.037	0.0137	0.0112	0.0089	0.0106
Calcium	314.2	365	394	400	407	380.7	343.2	324.8	337.3
Cobalt	0.8504	0.818	0.751	0.586	0.378	<0.025	<0.025	<0.025	<0.025
Iron	311	48.5	21.9	<0.150	<0.150	<0.150	<0.150	<0.150	<0.150
Potassium	15.2	16.7	17.3	17.5	16.9	17.2	18.36	17.6	18.04
Magnesium	1882	Not Anal.	Not Anal.	Not Anal.	Not Anal.	1322	1363	1258	1336
Manganese	29.93	30.6	29.6	30.4	27.2	0.6002	3.449	1.029	4.104
Sodium	178.3	206	225	220	225	426	430.3	419.5	435.6
Nickel	7.722	7.31	6.68	5.84	4.05	0.0215	0.0792	0.059	0.0632
Phosphorus	0.0386	<0.025	<0.025	<0.025	<0.025	<0.025	<0.025	<0.025	<0.025
Sulfur	2627	Not Anal.	Not Anal.	Not Anal.	Not Anal.	2403	2354	2228	2382
Vanadium	0.0348	<0.025	<0.025	<0.025	<0.025	<0.025	<0.025	<0.025	<0.025
Zinc	0.49524	0.278	0.194	0.101	0.066	<0.011	<0.011	<0.011	<0.011

Notes: g/L – grams per liter J - Estimated concentration
mg/L – milligrams per liter < - less than

Hazardous Material Determination

Tests were conducted to demonstrate that heavy metals adsorbed onto and incorporated into AAT matrix would not leach out to levels above acceptable limits. A sample of AAT, loaded with heavy metals, was prepared by swirling it in a composite water sample for approximately 48 hours. The mixture was then centrifuged and the AAT solids dried at 60° C for several hours. These metals loaded AAT solid particles were subjected to extraction tests using the CAL-Wet (sodium citrate extractant) procedure and water from the Mine. Water from the Mine was used to determine if the spent AAT would liberate heavy metals if left in contact with Mine water. The results are presented in Table 3 in mg/L. The table also shows the Soluble Threshold Limit Concentration

(STLC) (mg/L) values for comparison. Analysis of the table shows that the metals concentrations were below the STLC values when extracted using the CAL-WET and site-specific untreated Mine water as leaching solutions. The results of these tests demonstrate that the reacted AAT with the sequestered metals removed from the water is a stable, inert, non-hazardous material.

Also, note that the metals loaded AAT continued to remove additional metals from the untreated Mine water after it had been used to remove the metals from the water stream. See Table 3 for the composition of the water that was used to extract the “spent” AAT material. It is a common characteristic of AAT, that over time it removes more metal than expected from normal isotherm tests. Activated aluminum tailings have the ability

in many cases to partially regenerate its surface adsorption capability and thereby continue to adsorb more metals over the long-term. This has favorable implications for the use of AAT in tailings impoundments or for disposal of metals loaded AAT in mine pits. In both cases the reagent will continue to remove additional heavy metals from the water, even after the initial treatment to remove metals is complete.

2008 Bench Tests

The second set of studies for the McLaughlin Mine were bench tests performed on Mine water, and on the same water that was evaporated to 72% of the initial volume. Both solutions were tested to demonstrate the robustness of AAT under differing Total Dissolved Solids (TDS) and sulfate contents. The tests were designed to simulate a natural situation by combining pond sediment and pond water for initial isotherm screening tests and subsequent verification column isotherm tests.

Isotherm screening tests were performed to optimize reagent blend composition and dose rate for use in the column tests.

The 2008 study used GeoBind™ AAT. Various standard proprietary reagent blends were added to portions of the pond water and sediment material, which were combined at the ratio of 1.5 grams sediment to 100 milliliter of pond water. The optimum blend was determined to be delivered at a dose rate of 2 grams GeoBind™ reagent blend per liter. Water samples were collected, filtered and tested for metals. Table 4 shows the analytical results for the untreated initial and evaporated samples for the optimum formulations determined in the screening isotherms.

Table 3. Analytical Results Leaching Tests McLaughlin Mine (2006) Reacted AAT With Metals From Composite Sample

Parameter	Sample/Test Description			
	STLC Value mg/L	AAT Std. Cal-Wet mg/L	Modified Cal-Wet using Mine Water to Extract Loaded AAT mg/L	Untreated Mine Water Used in Modified Cal-Wet mg/L
Silver	5	0.119	<0.022	<0.011
Aluminum		540	<0.055	1.27
Arsenic	5	<0.011	<0.011	0.472
Barium	100	0.13	<0.003	0.018
Beryllium	0.75	0.006	<0.003	<0.003
Calcium		1,952	593	190
Cadmium	1	0.043	<0.003	<0.003
Cobalt	80	1.86	<0.025	0.281
Chromium	5	0.647	<0.025	<0.025
Copper	25	0.150	<0.025	<0.025
Iron		414	15.7	83.2
Potassium		21.9	14.7	18.3
Magnesium		1,426	881	Not Anal.
Manganese		63.4	0.132	4.35
Molybdenum		0.026	<0.025	<0.025
Nickel	350	14.8	0.021	8.67
Phosphorus	20	0.638	0.072	<0.025
Lead	5	0.026	<0.011	<0.011
Sodium		6,708	187	328
Sulfur		541	J 1781	Not Anal.
Vanadium	24	0.194	<0.025	<0.025
Zinc	250	0.509	<0.011	0.076

Notes: Std. - Standard
 < - less than
 mg/L - milligrams per liter
 J - Estimated concentration

Once the optimum dose rate had been established, columns were set up to perform confirmation tests on the pond water at the initial concentration, and on pond water that was reduced to 72% of the initial volume. Seven-foot-tall, 7.5 inch inner diameter (ID) polycarbonate columns were filled with 6 inches of sediment material and 6 feet of pond water for the two different water concentrations. The waters were added gradually, to minimize mixing of the sediment into the water. The columns were allowed to settle for a day to allow continued settling of any sediment which became suspended during the filling process. Initial water samples were collected from ports at 1 foot intervals on each of the columns, filtered and tested for metals. A few samples were also collected for anions (sulfate and chloride).

Based on the isotherm results, a dose rate of 2 g/L was used for these column tests. The total mass of reagents was added to the columns in four equal increments. A quarter of the chosen GeoBind™ reagent blend (0.5 g/L) was mixed with the appropriate pond water to make a 10% slurry. The reagent slurries were mixed for 2 hours and then added to the columns. The reagents were allowed to settle for 18 hours to 3 days before collecting water samples from ports at 1 to 5 feet. Water samples were filtered and analyzed to determine the concentration of selected metals. This process was repeated three more times. Selected samples taken following the final reagent addition were also analyzed for sulfate and chloride.

The column study test results are presented in Tables 5 and 6. Samples were collected from each port of the six ports to determine if there would be a concentration gradient from top to bottom of the water column. All analyte concentrations were constant across all ports. Since the concentrations were constant, average concentrations are presented in the tables. Results are listed for the initial (untreated results) and after each of the 4

reagent aliquot additions. Key results include the following:

- The majority of metals were removed after only 18 hours after the first GeoBind™ addition
- Metals concentrations decreased with additional AAT treatment
- Metals were removed across the complete column and no gradients in concentrations were observed.

Table 4. Analytical Results McLaughlin Mine (2008) Pond Water Metals Fixation Screening Results Selected Formulations^a

Isotherm	Untreated "As Received"	Untreated "Evaporated"
Dose (g/L AAT reagent blend)	0	0
Pond Solution	"As is"	72%.
Pond Water (ml)	--	--
Sediment (g)	--	--
Final pH (s.u.)	6.9	6.9
Aluminum (mg/L)	0.069	<0.056
Arsenic (mg/L)	<0.011	<0.011
Boron (mg/L)	0.309	0.444
Barium (mg/L)	0.023	0.031
Cobalt (mg/L)	0.078	0.104
Copper (mg/L)	<0.026	0.032
Manganese (mg/L)	3.16	4.53
Nickel (mg/L)	0.353	0.501
Zinc (mg/L)	0.168	0.109
Isotherm	Treated "As Received"	Treated "Evaporated"
Dose (g/L AAT reagent blend)	2	2
Pond Solution	"As is"	72%.
Pond Water (ml)	100	100
Sediment (g)	1.5	1.5
Final pH (s.u.)	9.7	9.8
Aluminum (mg/L)	<0.056	<0.056
Arsenic (mg/L)	<0.011	<0.011
Boron (mg/L)	0.053	0.059
Barium (mg/L)	0.020	0.022
Cobalt (mg/L)	<0.026	0.029
Copper (mg/L)	<0.026	<0.026
Manganese (mg/L)	<0.016	<0.016
Nickel (mg/L)	0.024	0.032
Zinc (mg/L)	<0.011	<0.011

^aAll results filtered through 0.45 micron filter.

Notes: g/L – grams per liter; ml – milliliter; g – gram; mg/L - milligrams per liter; s.u. – standard units

The study results show that AAT is effective at removing metals from water under a range of different conditions. The study also shows that the AAT loaded with the metals that were removed from the water is exposed to the CAL-Wet leaching procedure, it is an inert, non-hazardous material. The study further demonstrated that after the initial treatment to remove metals was complete, the reacted AAT continued to remove metals from solution.

Table 5. Analytical Results McLaughlin Mine (2008) Three Inch Column Test; Evaporated Water 72% with 10% AAT Slurry Addition

Analyte	Average Result		
	Initial	1st Addition	2nd Addition
pH (s.u.)	7.1	9.4	9.9
Aluminum (mg/L)	<0.056	<0.056	<0.056
Arsenic (mg/L)	0.011	<0.011	<0.011
Boron (mg/L)	0.467	0.468	0.360
Barium (mg/L)	0.031	0.027	0.026
Cobalt (mg/L)	0.102	0.032	0.029
Copper (mg/L)	0.027	<0.026	<0.026
Manganese (mg/L)	4.54	0.742	<0.016
Nickel (mg/L)	0.493	0.079	0.037
Zinc (mg/L)	0.140	<0.011	<0.011
Sulfate (mg/L)	6360	--	--

Analyte	Average Result	
	3rd Addition	4th Addition
pH (s.u.)	10.1	10.0
Aluminum (mg/L)	<0.056	<0.055
Arsenic (mg/L)	<0.011	<0.011
Boron (mg/L)	0.385	0.334
Barium (mg/L)	0.026	0.023
Cobalt (mg/L)	0.030	0.028
Copper (mg/L)	<0.026	<0.025
Manganese (mg/L)	<0.016	<0.015
Nickel (mg/L)	0.035	0.035
Zinc (mg/L)	<0.011	<0.011
Sulfate (mg/L)	--	6370

Notes: s.u. – standard units mg/L - milligrams per liter

Table 6. Analytical Results McLaughlin Mine (2008) Eight Inch Column Test Initial Water with 10% AAT Slurry Addition

Analyte	Average Result		
	Initial	1st Addition	2nd Addition
pH (s.u.)	6.9	9.3	9.9
Aluminum (mg/L)	<0.056	<0.056	<0.056
Arsenic (mg/L)	<0.011	<0.011	<0.011
Boron (mg/L)	0.337	0.347	0.276
Barium (mg/L)	0.029	0.025	0.023
Cobalt (mg/L)	0.074	<0.026	<0.026
Copper (mg/L)	0.027	<0.026	<0.026
Manganese (mg/L)	3.22	0.346	<0.016
Nickel (mg/L)	0.355	0.041	0.025
Zinc (mg/L)	0.190	<0.011	<0.011
Sulfate (mg/L)	4810	--	--

Table 6. (continued)

Analyte	Average Result	
	3rd Addition	4th Addition
pH (s.u.)	10.1	10.0
Aluminum (mg/L)	<0.056	<0.055
Arsenic (mg/L)	<0.011	<0.011
Boron (mg/L)	0.303	0.278
Barium (mg/L)	0.022	0.020
Cobalt (mg/L)	<0.026	<0.025
Copper (mg/L)	<0.026	<0.025
Manganese (mg/L)	<0.016	<0.015
Nickel (mg/L)	0.025	0.025
Zinc (mg/L)	<0.011	<0.011
Sulfate (mg/L)	--	4705

Notes: s.u. – standard units
mg/L - milligrams per liter

Jamestown Mine

Bench-scale testing was performed on water from the Harvard Pit at the Jamestown Mine in 2007. The Jamestown Mine is a closed gold mine located in the Mother Lode District of the Western Sierra Foot Hills in California. Groundwater and water in the Harvard Pit is

impacted by TDS, sulfate, arsenic, chloride, sodium and other ions emanating from the tailing management facility and the rock storage area. There are multiple potential remedial alternative in which where AAT usage may be considered. One of these is either the spray addition of AAT slurries over the pit or passing the water through an AAT bed to remove heavy metals from the water. The resulting water, which has the heavy metals removed, would be either taken to dryness or significant reduction in total volume by use of an enhanced evaporation process.

Screening level batch tests were performed on using AAT and proprietary AAT blends to determine the formulations to remove metals, in particular arsenic. Two dose rates (1 and 2 g/L) were investigated. The concentrations of arsenic in the Harvard Pit have been measured to be as high a 1.6 mg/L. The results in Table 7 show that AAT treatment was effective at removing the arsenic and other selected metals to below the detection limit.

**Table 7. Analytical Results
Jamestown Mine Harvard Pit Water
AAT Powder Batch Test**

Analyte	Untreated	After Treatment with AAT
	mg/L	mg/L
Arsenic	0.444	<0.014
Nickel	0.036	<0.011
Zinc	0.023	<0.011

Notes: mg/L - milligrams per liter

Chemical Manufacturing Facility

The chemical facility had groundwater with arsenic concentrations in the mg/L range. Laboratory tests and Radius-of-Influence (ROI) pilot-scale test were performed for this site with AAT products. The ROI and subsequent application will be the subject of another paper. This test work is for subsurface in-situ mixing of AAT to form permeable reactive barriers (PRB) or reactive

zones to sequester arsenic and other material of concern to eliminate future arsenic migration.

The laboratory tests consisted of an initial set of isotherms to determine effective formulations and dose rates. These isotherms were followed by column tests which used arsenic containing site groundwater and soil. TCLP and multiple Synthetic Precipitation Leaching Procedure (multiple-SPLP) tests were performed to demonstrate that heavy metals adsorbed onto and incorporated into AAT matrix would not leach out to levels above acceptable limits. The multiple-SPLP consists of nine sequential extractions and simulates leaching by acid rains or mildly acid media for a period of 1000 to 10,000 years. The USEPA East of the Mississippi River SPLP extraction fluid was used since it is more aggressive than the West of the Mississippi River SPLP extraction fluid.

Initial Batch Tests

The initial batch screening tests (isotherms) were performed on 50/50 mixtures of soil and groundwater to determine the effective formulations and dose rates to meet specified target concentrations of 10 to 50 ppb arsenic in the time allotted for the tests. The isotherm leach tests results showed that a dose rate of 1X or 2X g AAT blend per liter soil/groundwater mixtures were necessary to immobilize arsenic at various locations on the site. "1X" is the base dose rate and "2X" is twice that amount in g AAT blend/L media. Column tests were designed in the next phase based on these isotherm results.

Column Studies

The column studies were designed to simulate PRB's, based on the previous isotherm tests and the dose rates of 1X and 2X grams of AAT blends per liter of site soil were investigated. The test objectives were to evaluate whether PRB's would lower arsenic concentrations to below 50 µg/L and

how long the PRBs would last. In order to evaluate these objectives, various lengths of PRB's using a constant groundwater flow rate were used.

One of the primary conclusions of the column study was that the groundwater contained one or more reactive substances that reacted with the AAT surface to lower its long-term capacity and reactivity for arsenic removal. Analysis of the test results indicated that in order to maintain AAT activity, the treatment system would need to be changed to lower the impacts of the competing substance and/or the composition of the AAT blend would be modified to minimize the impact of the competing substance. Based on this analysis, a successful revised column study was designed and is described below

Revised Column Study

The objective of the revised study was to evaluate if soil treated with AAT could maintain its arsenic removal reactivity for 90 days. The column test would evaluate the impacts of modifying the AAT blend formulation to maintain reactivity, while at the same time lowering the competing substance content in the groundwater. Maintaining reactivity for this study meant that the effluent arsenic concentration would not radically increase in a short time period and that the effluent concentration would not exceed 50 µg/L, and preferably be less 10 µg/L, for a minimum of 90 days.

The column design fed the groundwater in an upward flow pattern through two inch diameter by twelve inches long column of soil. The groundwater flow rate was approximately 1.5 feet per day which is the nominal flow rate for most the facility. The design matrix included a control column, arsenic containing site soil without addition of AAT, and treatment columns with 2X or 3X dose rates and two AAT blend compositions.

The column test results show that the 3X g per liter dose rate using an enhanced AAT blend provided the best results. Many metal concentrations were below the detection limit for the duration of the "3X" test. The 3X enhanced AAT treatment blend in Column B1 maintained all metals, including arsenic, concentrations below the MCL. The results show that arsenic concentrations were maintained below the detection limit of 10 µg/L for greater than 90 days. For comparison, the effluent arsenic concentration from the control column was 0.533 mg/L after about one pore volume flowing through the column. The "2X" column effluent arsenic concentration increased to 20 from 10 µg/L (ppb) after about 80 days on line. The effluent concentration did not increase over the remainder of the test. The more conservative "3X" dose rate using the enhanced AAT blend was selected for pilot-studies since it showed no arsenic increase for greater than 90 days.

TCLP and SPLP Leach Tests

Leaching tests using the TCLP and multiple-SPLP were performed to measure the leaching potential of arsenic and other elements from soil treated with the AAT blends. Two different AAT treated soils were used for this investigation. These soils were loaded with arsenic by running PRB tests until the effluent concentrations were essentially the same as the influent arsenic concentration. As such these soils were loaded with high levels of both the competing substance and arsenic.

The TCLP test used buffered acetic acid solution at pH 4.98 as the primary extraction fluid this study. The leaching results are shown in Table 8. The results were below the State risk-based criteria.

**Table 8. Analytical Results
Chemical Manufacturing Facility;
TCLP and SPLP Tests**

Treated Soil Location	Extraction Procedure	Arsenic Leachate Concentration mg/L
Source Area	SPLP	<0.011
Down Gradient	SPLP	<0.011
Source Area	TCLP	<0.010
Down Gradient	TCLP	0.04

Notes: mg/L – milligrams per liter

The multiple-SPLP procedure is used to simulate the chemical durability of a material that is long-term exposure to acid rain. For this project, the procedure used a pH of 5 nitric and sulfuric acid leaching solution. It generally accepted that the multiple-SPLP results show the stability of the treated product for the next 1,000 to 10,000 years. The results are shown in Table 9. All arsenic concentrations were below the detection limit.

**Table 9. Analytical Results
Chemical
Manufacturing Facility Sequential
Extraction Procedure; SPLP Tests**

Extraction Number	pH (s.u.)	Arsenic Leachate Concentration mg/L
1	5.11	<0.011
2	5.98	<0.011
3	5.93	<0.011
4	6.52	<0.011
5	6.72	<0.011
6	6.48	<0.011
7	6.85	<0.011
8	7.02	<0.011
9	6.92	<0.011

CONCLUSIONS

Activated aluminum tailings is a product derived from red mud created when extracting aluminum from bauxite ore. It is an emerging technology that is effective in removing heavy metals, soluble cyanide, as well as iron, aluminum, manganese and silicate from water. This paper describes testing to simulate spray addition of AAT over a water body or flowing contaminated water through a bed filled with AAT to remove metals of concern. The paper also describes testing for in-situ mixing of AAT in with soil to sequester metals and limit or stop migration of metals in the groundwater. Tests were conducted on waters from the McLaughlin Mine and Jamestown Mine sites and a confidential chemical manufacturing facility.

This report shows that AAT is effective at removing heavy metals from impacted groundwater and sequestering them. The AAT treatments were successful at removing metals when AAT slurries were added to the top of water column and allowed to settle and when AAT was mixed into soil to sequester metals of concern. Leaching tests using the CAL-WET, TCLP and multiple-SPLP demonstrate that AAT loaded with metals of concern are stable. In addition, the multiple-SPLP results show that metals loaded AAT successfully retain constituents of concern over the long term. It is recommended that AAT and AAT reagent blends be tested at the bench-scale before proceeding to the field to optimize the formulation, manner of application and costs.

REFERENCES

Genc-Fuhrman, Tjell, McConchie, 2004a, *Adsorption of Arsenic from Water Using Activated Neutralized Red Mud*, Environ. Sci. Technol. 2004, 38, 2428-2434.

Genc-Fuhrman, Tjell, McConchie, 2004b, Arsenic removal from drinking water using activated red mud, *Malaysian Journal of Science* (23): 219-228 (2004).

Genc-Fuhrman, Bregnhøj, McConchie, 2005, *Arsenate removal from water using sand-red mud columns*, *Water Research* 39 (2005) 2944–2954.

McConchie, Clark, Davies-McConchie, Fergusson, 2002, *The Use of AAT Technology to Treat Acid Rock Drainage*, *Mining Environmental Management*, July, 2002.

WETLANDS TREATMENT OF MINE DRAINAGE AT ANTAMINA MINE, PERU

H. Plewes

Klohn Crippen Berger Ltd., Vancouver, British Columbia, Canada

C. Strachotta

Klohn Crippen Berger Ltd., Brisbane, Queensland, Australia

Margaret McBrien

Louis Berger Group, Inc., New Jersey, USA

Laura Rey

Compañía Minera Antamina S.A., Lima, Peru

ABSTRACT: A new water treatment facility was constructed in 2005/2006 to manage drainage from the expanding Tucush Valley waste rock dump at Antamina Cu-Zn-Mo mine, located in the rugged high Andes in Peru, 4,200 m above sea level. The treatment system comprised a combination of sediment ponds, serpentine channels and wetlands. The wetlands cover 6 ha and are designed to treat up to 115 L/s for removal of nitrates, ammonia and metals.

The project is the highest operating wetland in the world and provides an important precedent for water treatment at other operating and abandoned high altitude mines, particularly in the Andes. Monitoring to date indicates the wetland is functioning as designed with effective removal of zinc, molybdenum and ammonia. Further monitoring is required to confirm effective treatment of other target parameters. However, all water parameter concentrations measured at the treatment system discharge point are compliant with established water quality requirements.

INTRODUCTION

The Compañía Minera Antamina S.A. (CMA) copper-zinc-molybdenum mine is located in the Central Andes of Peru, 4,200 m above sea level, 280 km northeast of Lima (Figure 1). Ore is excavated from an open pit and processed to produce a metal concentrate that is piped to the Peruvian coast for shipping overseas. Waste rock generated by the mine is deposited into a number of dumps, including one located in the neighbouring Tucush Valley. The Tucush Valley forms part of the

Ayash River catchment, which is used for drinking water and irrigation by downstream communities.

Prior to installation of the wetland, the water treatment system for the Tucush Valley employed by CMA was a series of sediment control ponds. As this system was to be displaced by the expanding Tucush Valley Waste Dump, a new water treatment facility was required. In addition to the treatment of runoff and discharge from the Waste Dump,

CMA required the facility to accommodate the treatment of tailings seepage water. Design of the water treatment facility aimed to satisfy water quality discharge criteria sent by the Peruvian Ministry of Mines; World Bank Guidelines; and, site specific ecotoxicology assessments, and in doing so protect the receiving environment and downstream domestic and irrigation supply. Table 1 lists the key compliance criteria for water quality in Ayash River downstream of the treatment system.

Table 1. Ayash River Catchment water quality criteria (selected parameters)

Parameter	Guideline concentration	Source
Total Suspended Solids	50 mg/L	MEM ¹
Dissolved Copper	0.025 mg/L	Site ecotoxicology study
Dissolved Molybdenum	0.2 mg/L	MEM ²
Dissolved Zinc	0.215 mg/L	Site ecotoxicology study
Ammonia	10 mg/L	Site ecotoxicology study /US EPA
Nitrate	10 mg/L	Site ecotoxicology study / World Bank

¹ Ministerio de Energía y Minas del Perú (1996)

² Ministerio de Energía y Minas del Perú (2007)

Working with CMA, Klohn Crippen Berger Limited (KCBL) and the Louis Berger Group (LBG) prepared a feasibility study outlining possible alternatives for the project site located downstream from the planned limit of the Tucush Valley Waste Dump. An innovative treatment system was recommended that comprised a combination of sediment ponds, serpentine channel and wetland. This multi-faceted option presented the best solution to fulfill CMA's water discharge objectives while providing a low-

maintenance, cost-effective, aesthetic facility, with maximum flexibility to meet uncertainties in future loading conditions.

Once detailed design plans and specifications were completed, KCBL supervised the integration of local labour and international technical expertise to construct the project within the US \$2 million budget. The completed system is now the highest elevation treatment wetland in operation in the world.

BACKGROUND

Wetland Water Treatment Principles

Wetland treatment of mine drainage is conducted at mining projects across the world. Treatment is undertaken on discharge waters with low pH, high pH, and high concentrations of dissolved metals and nitrogen-species. As a passive treatment system, wetland treatment of mine water has been identified as technically effective, low cost and relatively easy to maintain following establishment, where local conditions provide for their long-term sustainability.

Specific to the treatment requirements in the Tucush Valley, the types of wetlands used for mine drainage treatment can be categorized as aerobic and anaerobic. Generally, aerobic wetlands are used for the treatment of net-alkaline waters through the use of a shallow water column and reed beds. Anaerobic wetlands are used for the treatment of net-acid, metal-bearing waters through the use of a shallow water column with an organic sediment substrate.

During the wetland conceptualisation at Antamina, CMA requested that the wetland should be designed primarily for the removal of ammonia and nitrate from the Tucush

Valley discharge, with secondary capabilities of the removal of zinc and molybdenum. As a result, both aerobic and anaerobic wetland components were incorporated into the Tucush Valley treatment system design. The aerobic wetlands were designed to remove ammonia through plant uptake and nitrification (bacterial oxidation of ammonia). The nitrification process resulted in the generation of nitrate, which is also required to be removed from the discharge water. Nitrate concentrations are also present in the Tucush Valley Waste Dump discharge. Denitrification, the process of removing nitrate from the system, is undertaken by denitrifying bacteria active on the surface of organic anaerobic sediments. In addition to denitrification, anaerobic sediments host sulphate reducing bacteria capable of precipitating sulphide minerals which accumulate in the substrate. As a result, metal concentrations (zinc and molybdenum) in the Tucush Valley discharge may be removed.

Site Setting and Wetlands Design

The gravity-flow driven wetlands system shown in Figure 2 was selected to reduce operating costs at the high-altitude, remote site and to achieve a sustainable long-term, low-maintenance solution. Pre-sedimentation of solids is achieved in an upstream sediment pond supplemented by a serpentine channel formed by rock-filled gabion baskets. The sediment pond and serpentine channel also attenuate flow surges into the downstream wetlands section and enable the wetlands to adjust to variation in runoff water quality and quantity. This was an important consideration to allow for the expected increase in metal loadings during the wet season and to accommodate expansion of the waste dump over time. An upgrade to the existing flood control bypass canal for a 100-year flood was also undertaken to mitigate rainfall runoff

from the adjacent valley slopes into the treatment system.

The wetland component of the treatment system encompasses 6 ha and is designed to treat up to 115 L/s. The wetland cell layout and dimensions were designed to minimise impact on the narrow valley by reducing the amount of excavation required. The upstream section of the wetland incorporates a large sacrificial cell to capture sediments during extreme events and distribute flows to the mid-section of the wetland. The wetland mid-section comprises two parallel shallow cell circuits (0.40 m depth) with a gentle slope (0.5 %-1 % bottom slope) and are linked by cascading spillways. A 15 cm topsoil layer along the mid-section base is used to promote ammonia and nitrate removal. The lower wetland section consist of deeper and flatter cells (0.75 m depth; <0.5% slope) with 15 cm of organic matter and vegetation over the topsoil over the growth medium. The purpose of the lower wetland section is to keep sediments anaerobic, promoting sulphate reduction and aid in the removal of molybdenum and zinc. Construction of the treatment system was undertaken in 2005 during the dry season (Figure 3). Facility commissioning occurred in 2006.

Selection and sourcing of local vegetation was critical for project success and focused on two species; *Scirpus californicus* and *Juncus arcticus*; both of which are adaptable to the local environment and variable hydrological conditions due to the abundance in nearby lake shores. Advantages of using these species include the provision of substrate for microbial attachment; filtration and adsorption enhancement of wastewater constituents; the ability to transfer oxygen to the water column and/or soils to provide the appropriate aerobic environment; and, the capabilities to uptake nutrients and metals.

Wetland vegetation was collected from nearby Lake Pajoscocha. A meticulous procedure and limited timeframe for the transplanting of the vegetation was employed to ensure vegetation establishment and to encourage future seed propagation. Approximately 10,500 plants were transplanted and evenly distributed across the 6 ha wetland area. Generally 60,000 plants would be required to cover an area of 6 ha, however, a phased approach was adopted for the establishment of vegetation in the wetlands to minimize impact on the source lake ecosystem.

This approach comprised seed collection from the established wetland vegetation, germination and transplanting into the treatment wetland. It is anticipated that 3 to 5 years will be required for the wetland to establish from the transplanting phases to mature vegetation.

Provisions were made to allow additional water to be passed through the treatment system to assist wetland vegetation establishment particularly during the dry season. This includes the haulage vehicle maintenance area discharge water, which continues to be transferred today.

SAMPLING PROGRAM

Water quality monitoring is conducted on a weekly basis from monitoring points located across the Tucush Valley. For the assessment of treatment efficiency, the two key monitoring sites are located at the treatment system entry from the Upper Tucush Valley including waste dump discharge (CO45B) and from the haulage vehicle maintenance area (CO43). Discharge of the system is measured at CO39. These sites are shown in Figure 2.

Additional monitoring points located downstream of the treatment system, prior to the confluence of the Tucush Valley and the Ayash River, have been established by CMA to assess water quality from the total Tucush Valley catchment prior to discharge into the Ayash River. Communities along the Ayash River, downstream of the confluence with the Tucush Valley, are dependent upon the Ayash River for non-potable domestic use. Therefore, discharge water quality concentrations from the Tucush Valley are required to be compliant with established water quality criteria (Table 1).

RESULTS

Example monitoring records of the treatment system intakes (CO45B, CO43) and outlet (CO39) for flow, TSS, dissolved zinc and molybdenum, and ammonia, are presented graphically in Figures 4 to 8.

The results indicate that the majority key parameters concentrations are compliant with established water quality criteria in Table 1. Table 2 provides summary parameter comparisons between the treatment system intake and outlet. The effectiveness of the treatment system is confirmed with reductions in parameter concentrations from the system intake to outlet. Additionally, the wetland component of the treatment system is still currently being established; therefore, further reductions in discharge concentrations may occur once the wetland is established and operating at capacity.

Recent data for nitrate in the first 3 months of 2009 does show exceedances for nitrate. These concentrations are associated primarily with monitoring location CO45B, indicating a nitrate source from the Tucush Valley Dump. Early results show that the current treatment system has limited capability to reduce nitrate

concentrations below the guideline criteria, even though a reduction in concentration has been observed. Due to the preliminary nature of the treatment system, the capability of the treatment system to effectively reduce nitrate concentrations is not yet fully understood.

Table 2. Estimated parameter loading reduction – based on average loading rates.

Parameter	Inlet average loading (kg/day)	Outlet average loading (kg/day)	% Reduction
Dissolved Zinc	0.27	0.13	51%
Dissolved Molybdenum	0.23	0.08	65%
Ammonia	1.95	0.80	59%
Nitrate	185	161	13%

CONCLUSIONS

A water treatment system was required by CMA to treat discharge water from the expanding Tucush Valley Waste Dump at the high altitude Antamina Mine. The primary objective of the water treatment system was to treat nitrogen-based parameters (ammonia and nitrate), followed by the treatment of low concentrations of zinc and molybdenum.

Monitoring records indicate the wetland is effectively reducing the current Tucush Valley Waste Dump discharge parameter concentrations. Concentrations of ammonia, nitrate, zinc and molybdenum are being removed from the water column to degrees ranging from 13% to 65%. Considering the preliminary nature of the treatment system, there is potential for further parameter concentration reduction once the wetland has fully established.

The effective operation of this treatment system implies that wetland treatment of waste dump discharge can be undertaken at

high altitude projects. However, the application of this treatment technique is governed by the specifics of the project site, including geochemical characteristics and long-term discharge concentrations. These project components, along with the achievable treatment goals, should be understood prior to committing to this treatment mechanism. Generally this is undertaken via a scoping study, conceptualization and feasibility study process.

ACKNOWLEDGEMENTS

The authors of this paper would like to thank Compañía Minera Antamina for allowing the use of site data in the development of this paper submission.

REFERENCES

- Ministerio de Energía y Minas del Perú. (2007) Guía para la evaluación de impactos en la calidad de las aguas superficiales por actividades minero metalúrgicas, Republica del Perú – Ministerio de Energía y Minas, 4p.
- Ministerio de Energía y Minas del Perú. (1996) Aprueba los niveles máximos permisibles para efluentes líquidos para las actividades minero-metalúrgicas – Resolución Ministerial No 011-96-EM/VMM, Republica del Perú – Ministerio de Energía y Minas, 5p.
- World Bank. (1995) World Bank Environment, Health and Safety Guidelines; Mining and Milling – Open Pit, World Bank, 1p.

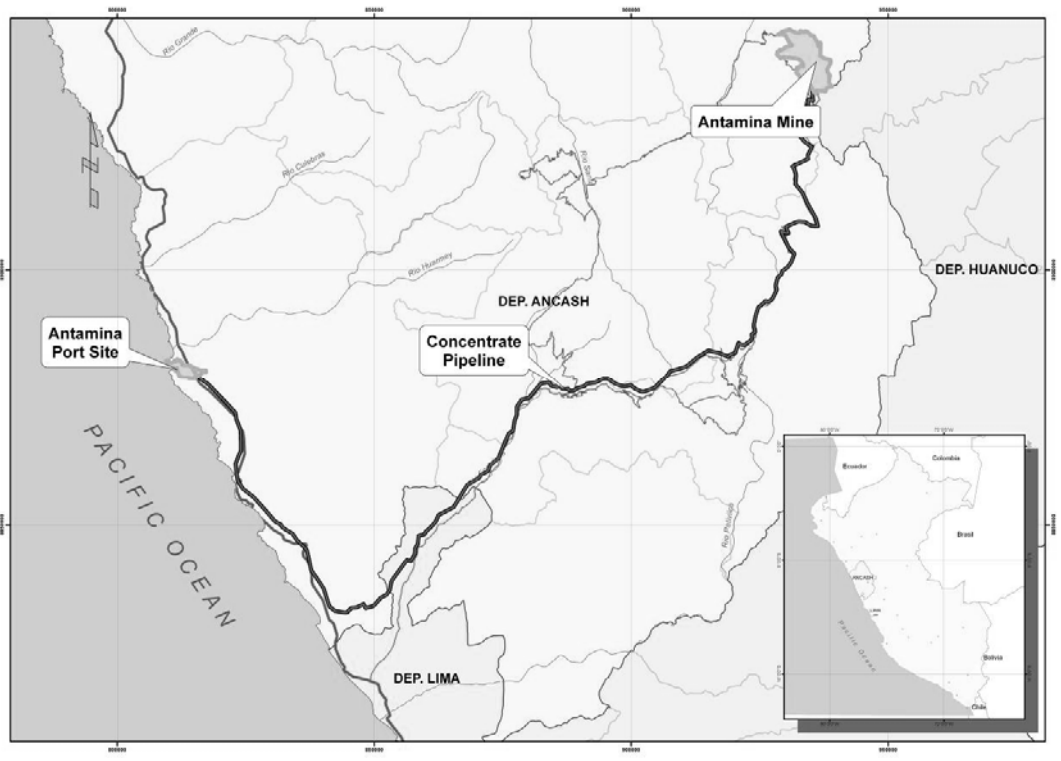


Figure 1. Regional project location map.

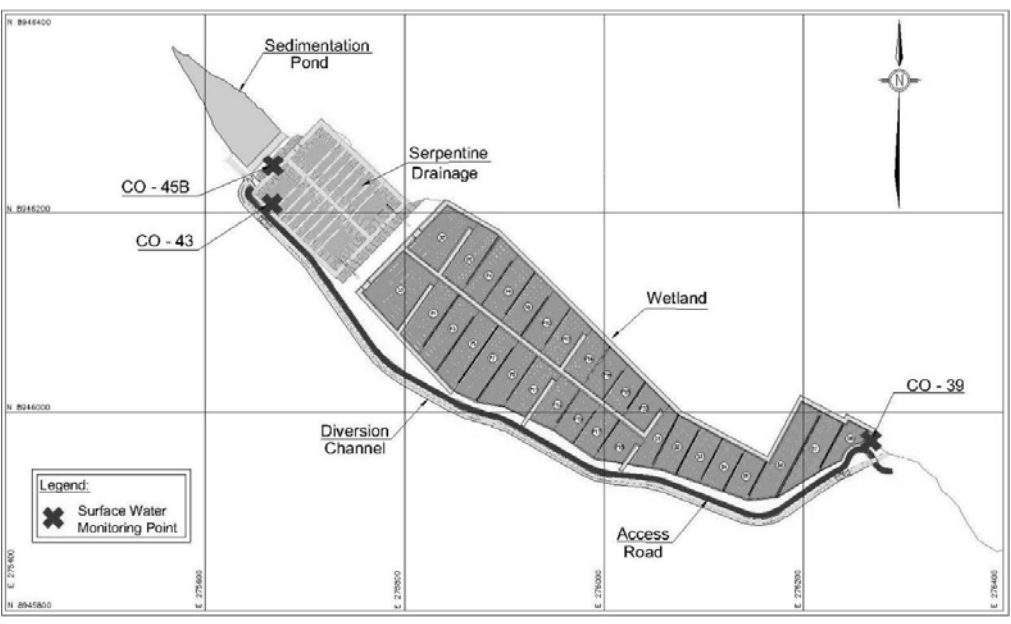


Figure 2. Detail of components of the Tucush Valley water treatment system.



Figure 3. Tucush Valley water treatment system during construction.

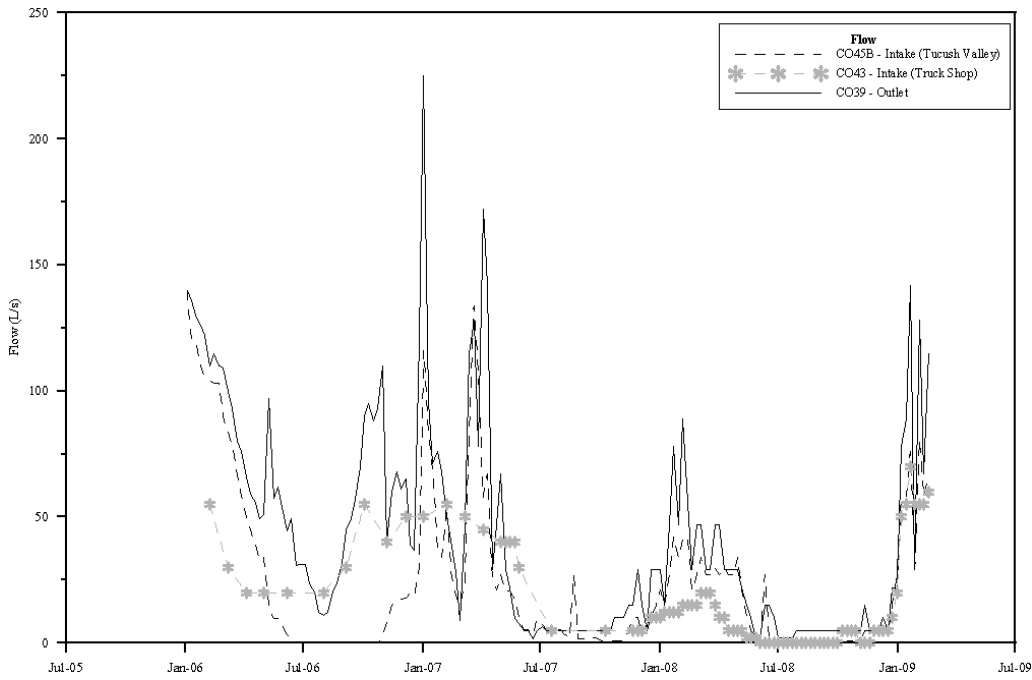


Figure 4. Water treatment system intake and outlet flow measurements (L/s).

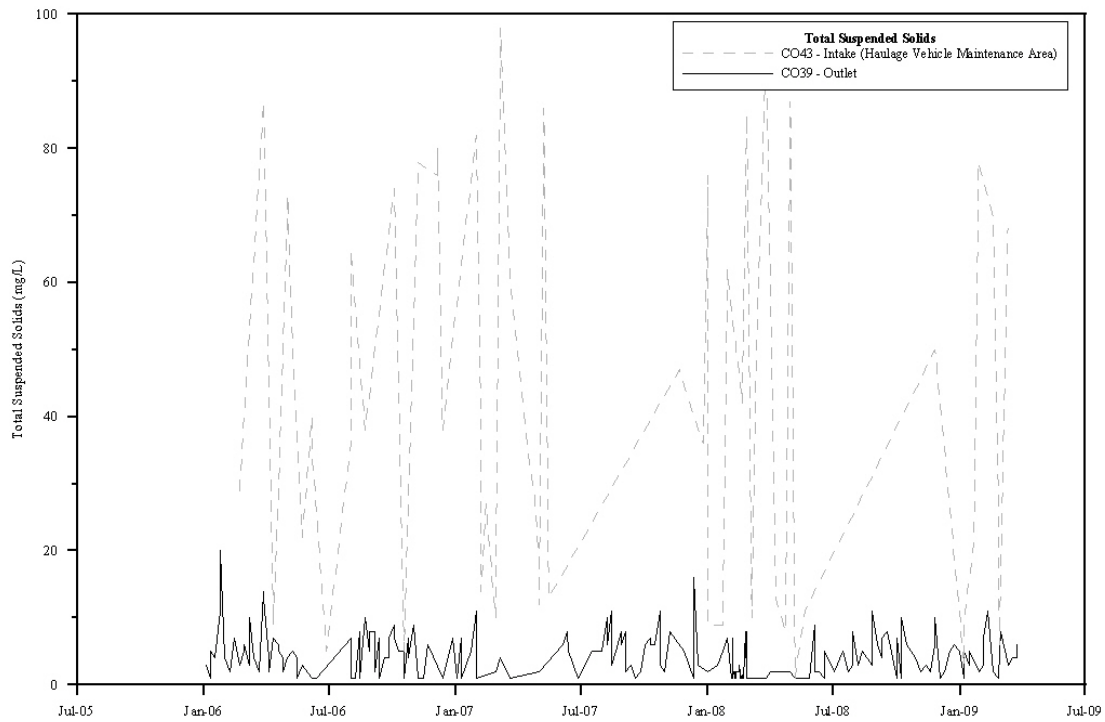


Figure 5. Water treatment system CO43 and CO39 concentration comparison – TSS.

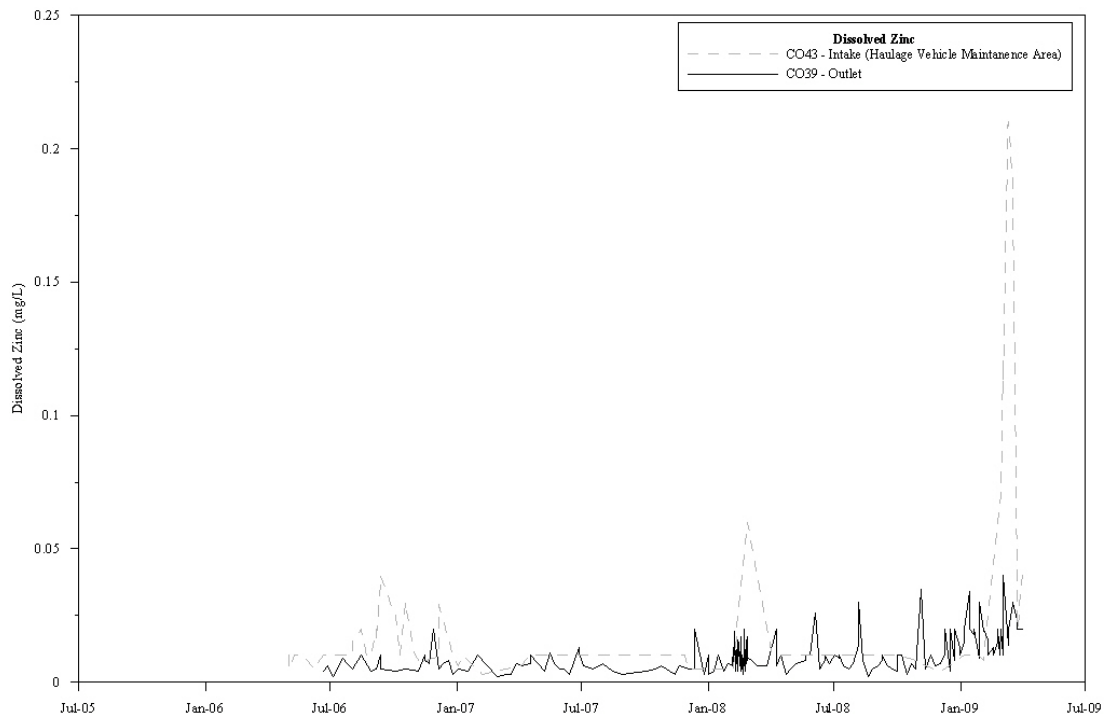


Figure 6. Water treatment system CO43 and CO39 concentration comparison – Zn.

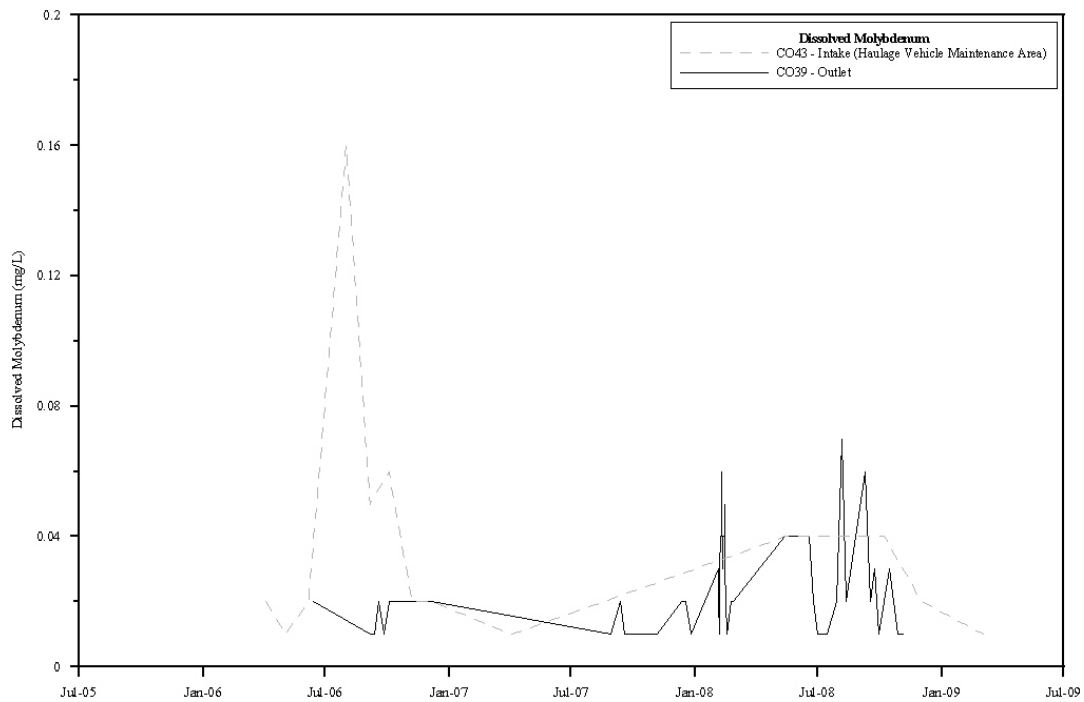


Figure 7. Water treatment system CO43 and CO39 concentration comparison – Mo.

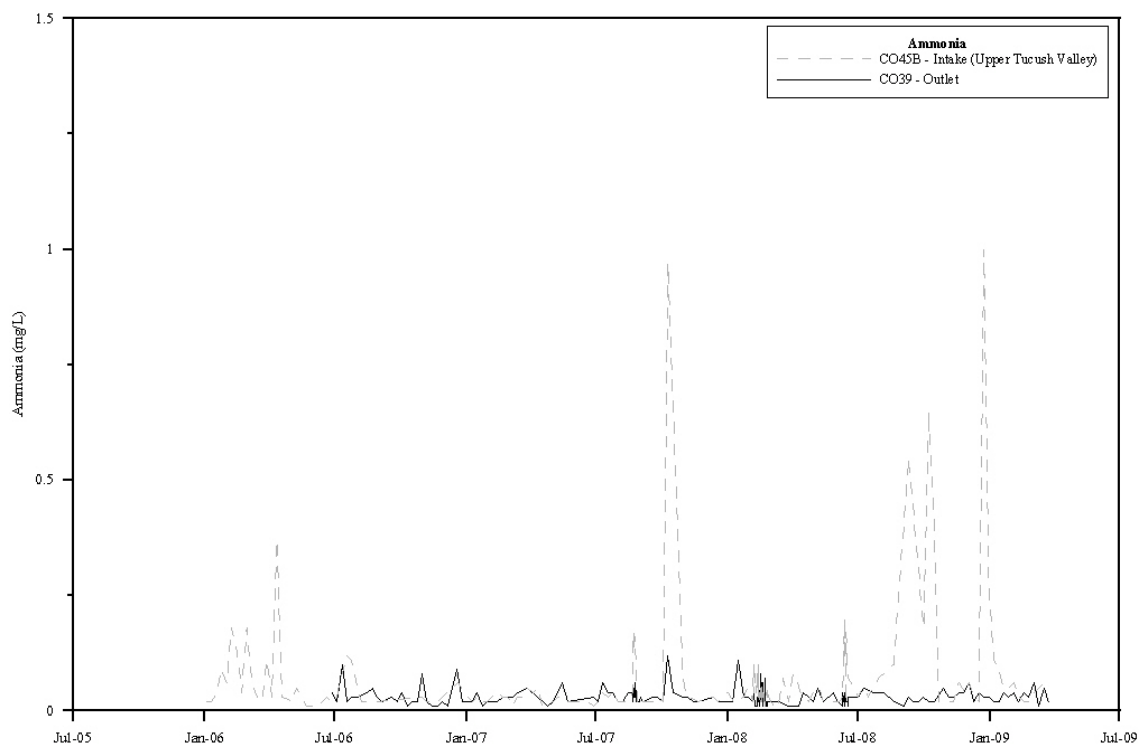


Figure 8. Water treatment system CO45B and CO39 concentration comparison – Ammonia.

LABORATORY THROUGH FULL-SCALE STUDIES ON THE REMOVAL OF NICKEL BY ZERO-VALENT IRON

Thomas Wildeman and Alvaro Pinto

Colorado School of Mines, Golden, CO

Luiz L. Fregadolli

Votorantim Metais, Sao Paulo, SP, Brasil

ABSTRACT: The MSF nickel mine near Fortaleza de Minas in Minas Gerais, Brazil has drainage of mining influenced water from the toe of the waste rock pile. The flow ranges from 20 to 100 L/min; the pH is between 5 and 7; and Ni and Mn concentrations range from 5 and 1 mg/L during the dry season to 20 and 10 mg/L in the wet season. Sulfate concentration in the water averages 1100 mg/L. The environmental limits at the outfall established by the State of Minas Gerais are: Ni, 0.025 mg/L; Mn, 0.10 mg/L; and sulfate, 250 mg/L. Laboratory studies using zero valent iron (ZVI) found that the rate of nickel removal was first order with respect to the concentration of nickel and was rapid enough that larger scale studies would be effective. In addition, spectroscopic evidence showed that nickel removal was not by adsorption but rather Ni is substituted for some of the Fe(II) in the magnetite that is formed from ZVI corrosion.

Based upon the successful laboratory studies, bench-, pilot-, and then small full-scale zero-valent iron (ZVI) treatment systems were constructed and operated to determine the ability of such a system to remove nickel and manganese. Unlike most permeable reaction barriers, these ZVI systems were above ground. The pilot system surface was 3 by 4.5 meters and it was 1.2 meter deep. The drain pipes in the bottom were covered with 10 cm of clean sand. Then 6 alternate 15 cm layers of ZVI and sand were added for the active bed. Over the top of the reactor, 12 L/min of water flowed for one year. During this time, Ni concentrations averaged 18.6 mg/L in the influent and 0.11 mg/L in the effluent; Mn concentrations averaged 6.3 mg/L in the influent and 1.7 mg/L in the effluent. Next, a full-scale system containing 14 m³ of ZVI in a bed 1 m deep was constructed. In this case the complete bed was ZVI. Although Ni and Mn removal averaged 95 % and 80 % respectively, because nothing was added to the system to consume oxygen before the water entered the ZVI, the system cemented and became impermeable after 9 months. Currently, a full-scale system using a mix of ZVI and organic materials is operating with better success.

INTRODUCTION

Nickel is a transition metal that commonly appears in mining influenced waters (MIW).

The term MIW is important when considering the aqueous chemistry of nickel because its hydroxide and carbonate precipitates are soluble enough that even in water at a pH of 7

that is net alkaline, there can be enough nickel in solution that the aquatic toxicity limit of 0.20 mg/L for water with hardness 100 mg CaCO₃ /L can be easily exceeded (Stumm and Morgan, 1996; USEPA, 2004). In addition, nickel sulfide is reasonably soluble and unless conditions are excellent, removal within a sulfate reducing bioreactor (SRBR) is problematic (Stumm and Morgan, 1996; Pinto et al., 2009). This question of nickel removal is precisely the issue at the Mineracao Serra de Fortaleza (MSF) Nickel Mine near Fortaleza de Minas, Minas Gerais State, Brazil. Although there are no acid rock drainage problems at MSF, the aquatic limits for surface waters leaving the site have been set at 0.10 mg/L for Mn and 0.025 mg/L for Ni. As can be seen from the parameters presented in Table 1, the water from the waste rock pile is net alkaline however, the average concentration of nickel ranges from 5 mg/L in the dry season to 16 mg/L in the wet season. Removal of nickel through SRBRs has proved vexing and so it was decided to explore other methods of removal including the use of zero valent iron (ZVI).

The study took two simultaneous paths; laboratory studies on the mechanism of removal were conducted at the Colorado School of Mines (CSM) (Pinto, 2004; Pinto, et al., 2009). Included in the laboratory studies were kinetic experiments to determine the speed of the reaction and what possible constituents control that speed. Also, equilibrium removal experiments as a function of pH were performed to determine whether nickel was being adsorbed or included in the structure of the corrosion products.

Finally, the solids formed during the removal studies were examined by x-ray diffraction analysis, scanning electron microscopy, and Mossbauer spectroscopy to determine whether the phases that were formed contained nickel as a structural entity.

Table 1. Typical chemical characteristics of important mine waters at the MSF mine site

Season Parameter	Waste rock		Lake Surface	
	Dry mg/L	Wet mg/L	Dry mg/L	Wet mg/L
pH*	6.6	6.4	8.26	7.5
Alkalinity*	59	41	130	64
Al	0.020	0.03	0.061	<0.025
Cu	0.006	0.29	0.007	<0.003
Fe	<0.002	0.02	0.11	0.01
Mn	0.17	4.5	0.018	0.009
Ni	5.15	16.5	0.052	0.16
Zn	0.040	0.22	0.005	0.003
Sulfate	751	1588	536	474

The conclusions of the laboratory study were that nickel is removed, apparently by inclusion into a magnetite phase that is a corrosion product. Because removal is by a phase formation, the nickel is not easily released if conditions change. From the kinetic studies, the nickel removal rate showed a first order dependence on the amount of ZVI, and the half time for removal of nickel by ZVI ranged between 35 to 74 hours and this half time should be reduced significantly because the volume ratio of water to ZVI in the field is approximately one, whereas the ratio in the laboratory ranged from 100 to 1000.

The field studies included the construction and operation of bench, pilot and full-scale treatment systems at MSF Nickel. Bench-scale experiments were started in 2001 and lasted into 2002. The pilot-scale project was begun in November of 2002 and lasted for one year. The full-scale project was begun in late 2004 and is still continuing. One important feature of all of the field studies is that they were conducted using surface water and so the treatment systems were ground level reactors where the ZVI could be exposed to the atmosphere. Until this study,

ZVI was almost exclusively used for permeable reaction barriers that were installed below the ground to treat contaminated ground water (Gillham and O'Hannesin, 1994, O'Hannesin and Gillham, 1998). The remainder of this paper is written in a case study fashion. It summarizes the important features and findings (including the failures) of the field studies, and will proceed from the bench, to the pilot, and then to the full-scale projects.

BENCH-SCALE STUDIES

The bench-scale reactors consisted of 10 L of material in 20 L buckets; cell 1 was 50% ZVI by volume and 50% cow manure; cell 2 was 100% ZVI. The ZVI consisted of metal turnings from local machine shops. Water from the toe of the waste rock pile (Table 1) was used. The systems were run for 50 weeks but were sampled intermittently as shown in Figures 1 and 2. The metal analyses were performed by atomic absorption spectrophotometry (AA) at the MSF laboratory. Table 2 gives the average concentrations over the 50 week period, and Figures 1 and 2 show the concentrations in the influent and effluents over the 50 week period.

Nickel and manganese are being removed by both reactors, and the cell with manure is doing better at nickel removal. Investigation of Figure 2 shows that removal of manganese is not as good and both cells remove manganese by approximately the same amount. Investigation of Figures 1 and 2

shows that nickel is immediately and completely removed, whereas manganese removal does not occur immediately. Over the operation period, the pH of the effluents was raised slightly to a value of 7.5 and then at the end, the pH raised to 8. At pH values between 7.5 and 8, the solubility of MnCO_3 (rhodochrosite) is such that the manganese concentration is below 0.10 mg/L (Venot, et al., 2008). So manganese removal could either be by the formation of MnCO_3 or by adsorption onto ZVI corrosion products.

Comparison of sulfate concentrations of the feed and the two effluents shows that bacterial sulfate reduction is occurring in the cell with manure, whereas it is not occurring in the cell with 100% ZVI. The cell with manure also has better removal of nickel. Apparently, precipitation of metal sulfides is aiding the removal of nickel. The environmental limits at the MSF outfall established by the State of Minas Gerais are: Ni, 0.025 mg/L; and Mn, 0.10 mg/L. Neither cell configuration removes manganese to the environmental limits. Examination of Figure 1 reveals that the manure/ ZVI cell removes nickel to below the environmental limits over 50% of the time, whereas the 100% ZVI cell removes nickel to below the environmental limit of 0.025 mg/L less than 50% of the time. Another bench-scale reactor that contained a mix of materials to promote sulfate reduction but contained no ZVI also removed nickel to below the environmental limits less than 50% of the time. The bench-scale studies showed that the best removal system is a sulfate-reducing reactor with an addition of ZVI.

Table 2. Average removal results for the bench-scale reactors.

		Cell 1 50% ZVI / 50% Cow Manure	Cell 2 100 % ZVI
Parameter	Influent	Effluent	Effluent
pH	7.32	7.76	7.87
Total Ni	8.30	0.04	0.42
Total Mn	2.71	0.44	0.71
Sulfate	1332	1195	1292

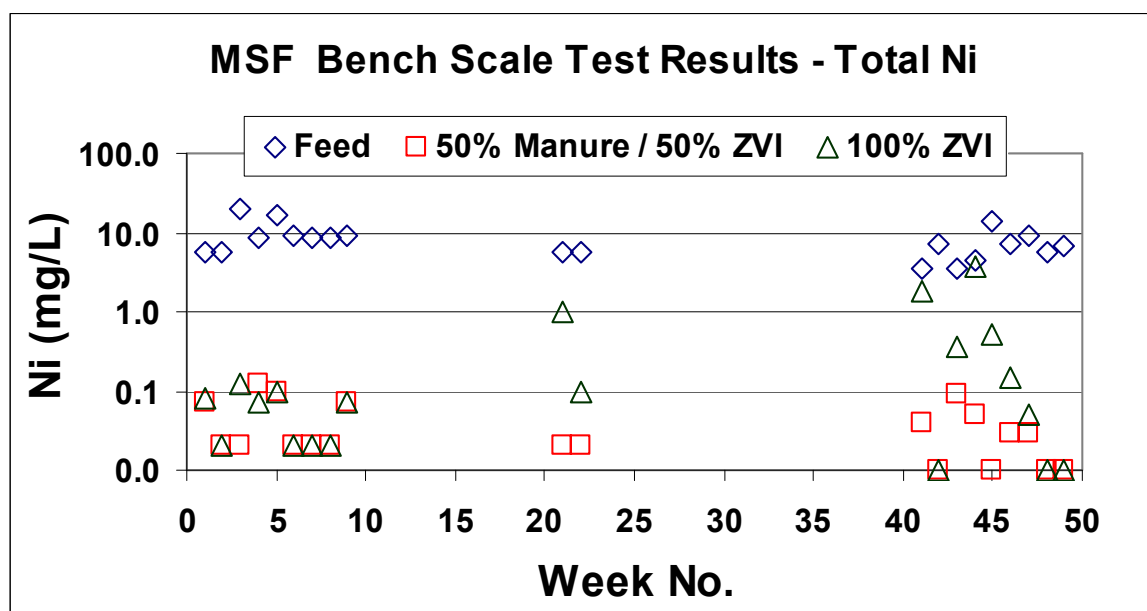


Figure 1. Nickel removal in the bench-scale ZVI reactors.

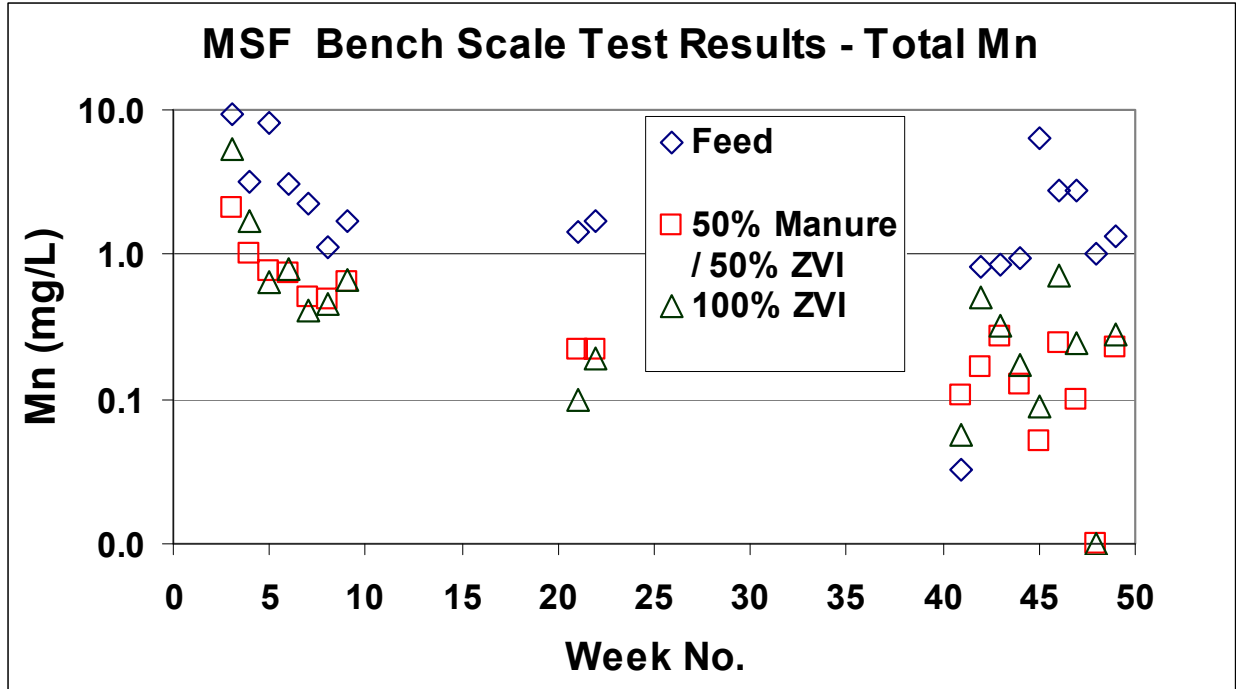


Figure 2. Manganese (Mn) removal in the bench-scale ZVI reactors.



Figure 3. The top of the ZVI pilot cell in the beginning (left) and after 12 months (right).

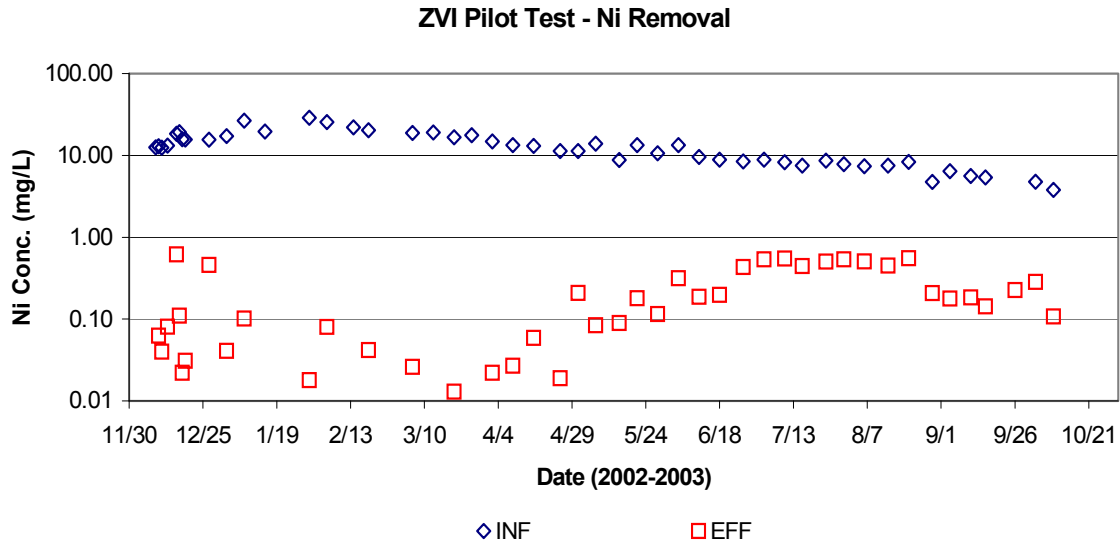


Figure 4. Nickel removal (plotted on a logarithmic scale) in the ZVI pilot cell.

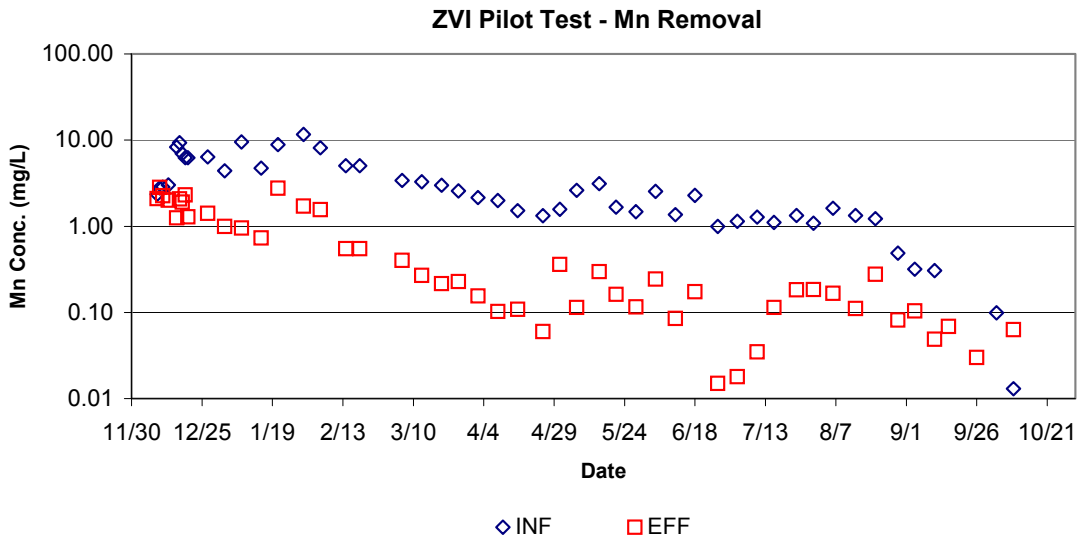


Figure 5. Manganese removal (plotted on a logarithmic scale) in the ZVI pilot cell.

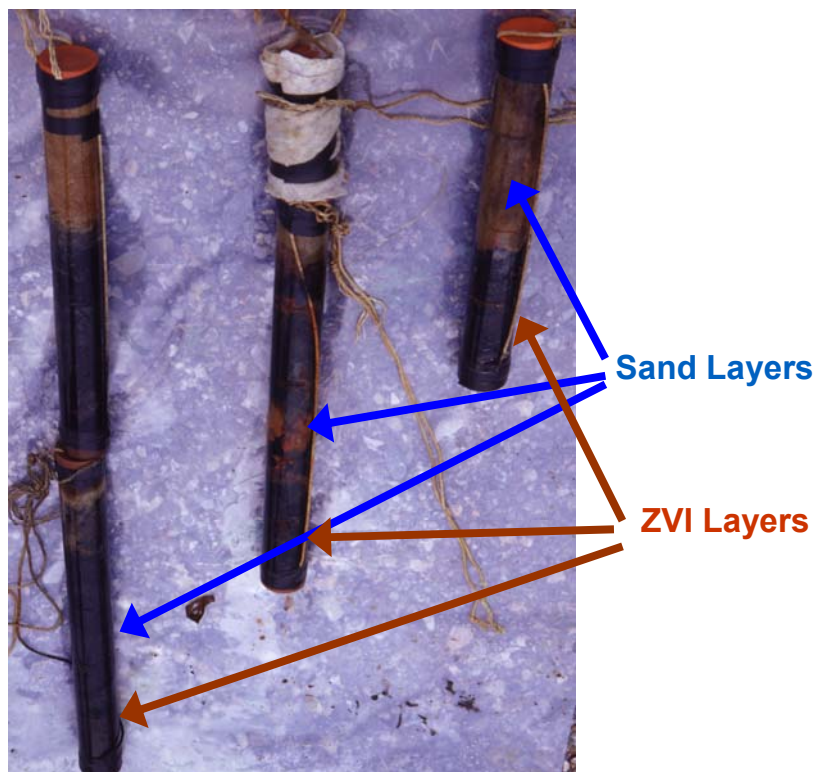


Figure 6. Three separate cores showing reaction products from top to bottom in the pilot ZVI cell taken 6 months into operation.

PILOT-SCALE PROJECTS

The first pilot-scale reactor used to treat the waste rock water (Table 1) contained no ZVI but was a typical sulfate-reducing mixture of wood chips, limestone, alfalfa, and manure. It only removed on average 70% of the nickel, and this was definitely not as good removal as experienced in the bench-scale reactors that contained ZVI. Consequently, it was decided to try a pilot reactor using ZVI, and the decision was made to use a ZVI / sand mix, the sand was used to provide good hydraulic conductivity through the ZVI. The cell was 1.0 m deep and 14 m³ in volume and consisted of alternating horizontal layers of 15 cm of ZVI and 15 cm of sand up to 1.1 m. Again machine shop turnings were used for the ZVI; the flow was set at 12 L per minute. Figure 3 is a picture of the top of the cell at the beginning of operation and after

12 months. Figures 4 and 5 show the removal trends over the 12 months the ZVI cell was operating. As seen in Figure 3, six sampling ports were put in the cell and they contained tubes with the ZVI / sand layers. These were sampled at 6 and 12 months and the solids were sent for a-ray diffraction analysis. Figure 6 is a picture of these cores taken after 6 months.

As in the bench-scale cell, removal of nickel was immediate, and as seen in Figure 4, for the first 5 months, the effluent concentration was below the environmental limit of 0.025 mg/L over 50% of the time. However, in the second six months of operation, removal efficiency dropped. As in the bench-scale reactor, manganese removal was not immediate but after 2 weeks, manganese removal was averaging 90% and was below 0.10 mg/L a number of times. However as

seen in Figure 5, towards the end of operation, removal efficiency decreased. Also, as seen in Figure 3, the level of water in the cell to maintain a flow of 12 L/min is increasing to the point where water is almost overflowing the cell berms. This implies that the permeability of the cell is decreasing.

From measurements taken when the cell was filling, it was determined that at a flow of 12 L/min, it takes 280 min for water to flow through the cell. Using average influent and effluent concentrations of 13.5 and 0.19 mg/L, the concentration has decreased by slightly over 6 half times. This assumes that the first order kinetics observed in the laboratory study applies to this field study (Pinto, et al., 2009). Using the value of six half times, it is estimated that the time to reduce the concentration of nickel by a factor of 2 in the field cell is about 47 minutes.

As seen in Figure 6, examination of the cores taken at 6 and 12 months, shows ferric oxyhydroxides are formed at the top of the cell and at intermediate levels in cell but the bottom of the cell shows that the reaction products are uniformly black. One important feature seen in the cores is that the black precipitate is forming in the sand as well as the ZVI layers. It is clear that ZVI corrosion products can diffuse from the specific site to the general ZVI substrate. This has important implications relative to the reduction of permeability that occurs in a system that has 100% ZVI. The x-ray diffraction analysis of the core material in the sand and the ZVI revealed primarily magnetite (Fe_3O_4), and then wustite (FeO), and hematite (Fe_2O_3), and quartz. Even though permeability and hydraulic conductivity decreased and reaction products have migrated to the sand layers, the material in all layers was not cemented but easily crumbled when handled.

The results of the pilot-scale study show that indeed nickel and manganese can be removed

almost to the environmental limits of 0.025 mg/L for nickel and 0.10 mg/L for manganese. However, the decrease in removal efficiency in the later stages of the study, the loss of hydraulic conductivity, and the obvious migration of corrosion products from the ZVI to the sand layers gave strong signals that long term removal past one year is problematic.

THE FULL-SCALE PROJECTS

The 100% ZVI Cell

In the full-scale system three tanks were built that were capable of containing 169 m³ of substrate at a depth of 1 m. Only one tank was used immediately and that was filled with 100 % ZVI only to a depth of 0.65m. Immediately after filling, the surface of the reactor was black. However, by the next day the surface was covered with $\text{Fe}(\text{OH})_3$. This was a foreboding of future problems. Nevertheless, immediately upon filling the reactor started operating at a flow of 14 m³/hr. By the next day, nickel concentration was reduced from 17 to 0.10 mg/L while Mn concentration changed from 4 to 2 mg/L. For the ten months the system operated, the average values of important parameters are given in Table 3. However, at the end of ten months the ZVI had welded to such an extent that hydraulic conductivity was too low to support a reasonable flow through the system. Again, sampling tubes were put in the reactor so that the state of the ZVI could be assessed. Figure 7 shows the state of the ZVI in the sampling tubes and also a ZVI clod taken from the surface of the reactor. Unlike the cores from the pilot cell, shown in Figure 6, these cores show hematite oxidation all the way to the bottom, indicating significant oxygen concentration in the water all the way down to the bottom of the reactor. The picture of the clod from the surface of the reactor shows every corrosion product

possible from ZVI. The hematite crust is dramatic, and it appears that magnetite or wustite in the center of the clod causes it to weld together. Also, there are patches of green rust in the clod. From the way the ZVI was welding, it would probably be the case that even if the full-scale system was made with layers of ZVI and sand, as in the pilot system, it probably would have lost hydraulic conductivity and failed.

The ZVI / Organic Reactor

The failure of the 100 % reactor led to another attempt to use ZVI for removal. This time, a substrate was mixed that was approximately 40 % by volume ZVI with the remainder being an organic based substrate that would promote sulfate reduction. The hypothesis behind this mixture was that if the ZVI particles in the cell were not touching, then welding would not occur. The organic substrate contained wood chips, sugar cane bagasse, limestone, hay, and manure. Figure 8 shows the reactor being filled and the condition of the top of the substrate after six months of operation. Now the surface is no longer cemented. In 2007, the system was receiving approximately 20 m³ per hour of water and it flowed through a series of two ZVI/organic reactors and then through a limestone filter. Each of the reactors had a

footprint of 8 by 13 meters. Table 4 gives the average concentrations of nickel, iron, manganese, and sulfate from April through December 2007. Figure 9 shows the changes in nickel concentration of the influent water as it leaves each of the three reactors.

Figure 9 shows that, from July through December, the concentration of nickel does indeed fall below the 0.025 mg/L environmental requirement as the water leaves reactors 2 and 3. However, on average, iron and manganese are being released from the ZVI in reactors 1 and 2 and the manganese is not removed in reactor 3. Also, the environmental limit for sulfate is 500 mg/L and although there is some reduction in sulfate concentration, reaching the environmental limit is problematic.

In the lab study of the removal of nickel by ZVI (Pinto, et al., 2009), the mechanism of removal was inclusion of the nickel into the structure of magnetite, which was a product of the iron weathering. However, in the study, the ZVI was not in an organic substrate. In the case of ZVI in an organic substrate, sulfate reduction is the most probable mechanism of removal. In these reactors, there is certainly some FeS that is formed and this may aid in the removal of NiS.

Table 3. Average values of parameters in the influent and effluent of the 100 % ZVI cell for 10 months of operation.

Parameter	Influent	Effluent
pH	7.16	8.40
Average Ni (mg/L)	12.6	1.22
Average Mn (mg/L)	2.99	0.57
Avg. Fe first 2 months (mg/L)	0.33	0.93
Avg. Fe last 8 months (mg/L)	0.076	0.082
Average Sulfate (mg/L)	1530	1482



Figure 7. Pictures of the cores after 10 months in the full-scale ZVI cell and a clod from the surface of the reactor.



Figure 8. The ZVI/organic reactor being filled and the substrate just below the surface after six months of operation.

Table 4. Average concentrations of key constituents in the influent and the three reactors for the period from April through December 2007.

2007 Avg. Concentrations in mg/L				
	Ni	Fe	Mn	SO ₄ ⁼
Influent	6.124	0.13	0.47	1,313
Effluent 1	0.356	4.03	1.01	1,263
Effluent 2	0.258	3.65	0.92	1,268
Effluent 3	0.144	0.10	0.74	1,276

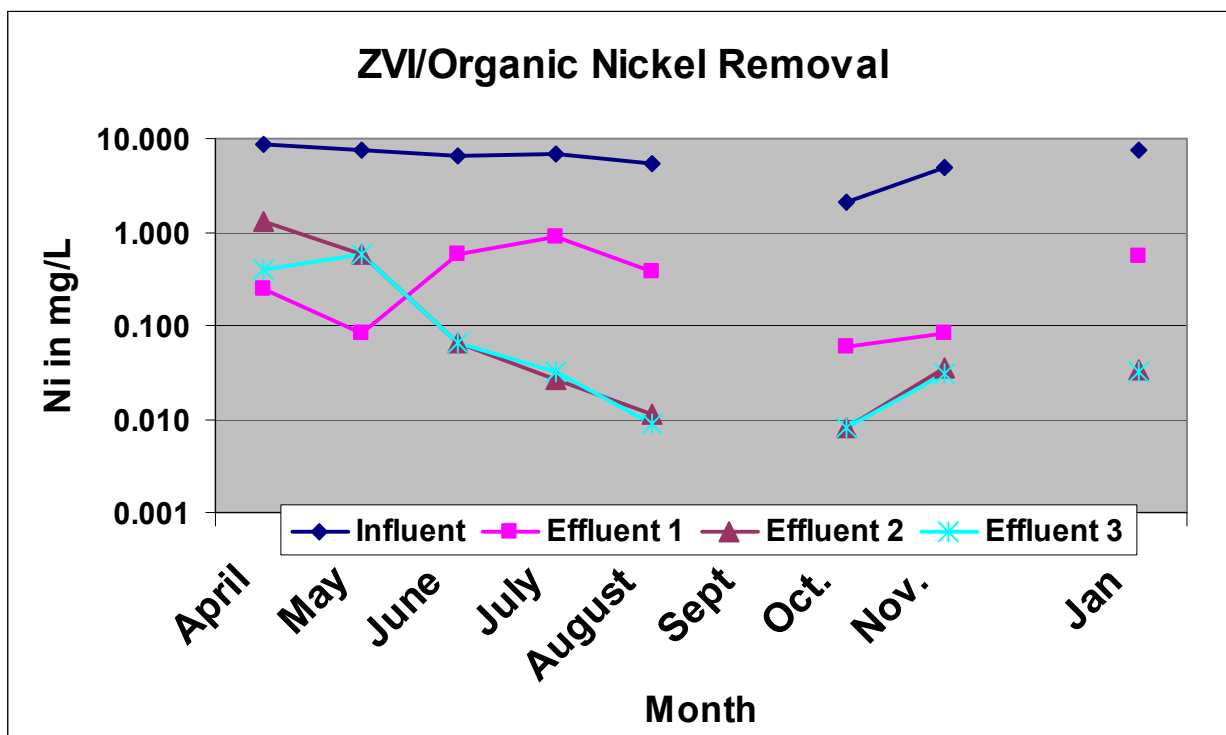


Figure 9. Changes in nickel concentration in the influent and in the effluents of the three reactors.

CONCLUSIONS

This ZVI project is unusual because the iron is in an above ground reactor and is receiving oxygenated water. Consequently, there is an objective of determining whether this type of ZVI reactor would physically work as well as determining whether the nickel and manganese concentrations could be removed

to below the environmental limits of 0.025 and 0.100 mg/L. For the pilot ZVI/sand system, water could flow through the system for 12 months. However, the movement of ZVI weathering products into the sand suggests that this system would eventually clog. For the full-scale system that only contained ZVI, physical failure due to the weathering products welding the ZVI

occurred in less than one year. Using an above ground system of only ZVI is doomed to failure.

Considering removal of nickel, a system of ZVI only can occasionally remove nickel to below the environmental limit of 0.025 mg/L. However, the average nickel concentration from the pilot system was about 0.11 mg/L and from the full-scale system it was 1.22 mg/L. On the other hand, after a three month startup period, the ZVI/organic system was consistently removing nickel to below the 0.025 mg/L environmental limit.

There are two other constituents of concern in MSF mining influenced water, sulfate with an environmental limit of 500 mg/L and manganese with an environmental limit of 0.10 mg/L. For both of these constituents, consistent removal to these limits was not possible. Using ZVI alone, there was some manganese removal and minimal removal of sulfate. For the ZVI/organic system, manganese was added to the water and the removal of sulfate was better, but far from the 500 mg/L target.

The field results suggest that removal by ZVI alone of constituents often found in mining influenced water is physically impossible, if not chemically problematic.

REFERENCES

Blowes, D. W., C.J. Ptacek, and J.L. Jambor. (1997). In-Situ remediation of Cr(VI)-contaminated groundwater using permeable reactive walls: Laboratory Studies. *Environmental Science & Technology*. 31: 3348-3357.

Gillham, R. W., and S. F. O'Hannesin. 1994. "Enhanced degradation of halogenated aliphatics by zero-valent iron." *Ground Water*, Vol. 32, No. 6, pp. 958-967.

O' Hannesin, S. F., and R. W. Gillham, 1998. Long-term performance of an in-situ iron wall for remediation of VOC's. *Ground Water*, Vol. 36, No.1, pp. 164-170.

Pinto, A. P., 2004. Laboratory and field investigation on the removal of nickel by zero-valent iron. PhD. Thesis, Colorado School of Mines, 226 pp.

Pinto, A. P., T. R. Wildeman, and L. Fregadolli, 2009. Laboratory investigations on the removal of nickel by zero-valent iron. *Proceedings of the 8th Int. Conf. on Acid Rock Drainage*, Skeleftea, Sweden, June, 2009.

Stumm, W., and J. J. Morgan. 1996. *Aquatic Chemistry*, 3rd Ed. Wiley-Interscience, New York, New York, 1022 pp.

U.S. EPA (U. S. Environmental Protection Agency). 2004. *National Recommended Water Quality Criteria*. United States Environmental Protection Agency. Office of Water. (4304T) Available at <http://www.epa.gov/waterscience/criteria/wqcriteria.html>.

Venot, C., L. Figueroa, R.A. Brennan, T.R. Wildeman, D. Reisman, and M. Sieczkowski, 2008. Comparing chitin and organic substrates on the National Tunnel waters in Blackhawk, Colorado for manganese removal. *Proceedings, 2008 National Meeting, American Society of Mining Reclamation*, pp.1352-1366.

THE USE OF WASTE ROCK INCLUSIONS IN TAILINGS IMPOUNDMENTS TO IMPROVE GEOTECHNICAL AND ENVIRONMENTAL PERFORMANCE

Michael James

SNC-Lavalin, Montreal, QC, Canada

Michel Aubertin

Ecole Polytechnique, Montreal, QC, Canada

ABSTRACT: This paper describes a tailings and waste rock co-disposal method that consists of placing continuous rows of waste rock within a tailings impoundment prior to each stage of raising to create inclusions. Thin layers of waste rock may also be placed on the bottom and sides of the impoundment prior to tailings deposition. For relatively shallow impoundments, the waste rock inclusions (WRI) may also consist of isolated heaps of waste rock placed before tailings deposition. The use of waste rock inclusions is expected to provide a number of beneficial effects, including: a) accelerated consolidation of the tailings due to the drainage capacity of the waste rock; b) compartmentalization of the tailings to limit the quantity of tailings released in the event of a failure of a dike and to allow for progressive closure; c) containment and submersion of reactive waste rock to limit water flow and oxygen flux; and d) improved seismic performance of the impoundment by reducing excess porewater pressure and deformation of the dike.

A general outline of the WRI method, its advantages and disadvantages compared with the conventional method of raised tailings impoundment construction, as well as some results of a comparative evaluation of the seismic performance of an upstream-raised tailings impoundment with and without waste rock inclusions are presented.

INTRODUCTION

Due to their potential to cause physical and environmental damage, financial loss, and a risk to life in the event of failure, the fact that they do not contribute to profitability, and their long life spans, the design, construction and maintenance of tailings impoundments presents a number of challenges. These challenges include: a) ensuring their stability under static and seismic conditions; b) minimizing the consequences to persons and

property in downstream areas in the event of a failure; and c) reducing the potential for an adverse environmental impact on surrounding areas.

To help reduce these risks, Aubertin et al. (2002a) proposed a tailings and waste rock co-disposal method consisting of placing a thin layer of waste rock on the bottom and sides of a tailings impoundment and then constructing inclusions of waste rock within the impoundment at each stage prior to

tailings deposition. The waste rock inclusion method would accelerate consolidation of the tailings, provide for the disposal of some or all of the waste rock, and result in improved geotechnical behavior of the impoundment.

The purpose of this paper is to further describe the concept of waste rock inclusions (WRI) in tailings impoundments and compare it with conventional tailings impoundment construction methods.

THE CONCEPT

The concept of using waste rock inclusions in tailings impoundments is illustrated on Figure 1, which presents schematics of a tailings impoundment in plan and cross-section. The figure shows a 3-stage, upstream-raised tailings dike and impoundment with four continuous waste rock inclusions, two parallel and two perpendicular to the main dike. Thin layers of waste rock lie on the bottom and sides of the impoundment. The WRI method could also be used with zoned earthfill dikes that are typically used to form impoundments for reactive tailings.

The assumed construction sequence of the conceptual impoundment of Figure 1 is as follows.

1. Construction of the starter dike. For non-reactive materials, this dike can be made from waste rock, with a wide base to provide improved stability.
2. Placement of a thin layer of waste rock on the bottom of the impoundment.
3. Placement of a thin layer of waste rock on the sides of the impoundment and on the upstream slope of the dike.

4. Placement of continuous rows of waste rock along pre-designated routes in the impoundment, up to the level of the current raise.
5. Tailings deposition into the cells created by the waste rock inclusions.
6. Repeat steps 3 through 5 until the impoundment is completed.

For relatively shallow impoundments with only a few stages of tailings deposition, isolated heaps (not shown in Figure 1) can be placed in the impoundment prior to tailings deposition to promote accelerated drainage and consolidation of the tailings (somewhat similarly to sand columns in a clay deposit). The number, configuration, spacing and dimensions of the waste rock inclusions will depend on the quantity of waste rock available relative to the size of the impoundment as well as materials properties, and design and construction considerations.

GENERAL CHARACTERISTICS OF TAILINGS AND WASTE ROCK

The WRI concept was initially proposed for tailings and waste rock from hard rock mining (i.e. from the extraction and processing of base and precious metals), with tailings deposited as a slurry (Aubertin et al. 2002a). The WRI method could also be used for other types of operations (with paste tailings for instance), but this aspect is not addressed here.

The gradation of hard rock tailings tends to vary from colloidal ($< 1 \mu\text{m}$) to sand-sized (0.75 mm to 4.75 mm) with the finer fraction dominating (Bussi re, 2007). These tailings are generally of no to low plasticity based on the Plasticity Index, and are generally classified as silt or sandy silt (ML) by the Unified Soil Classification System.

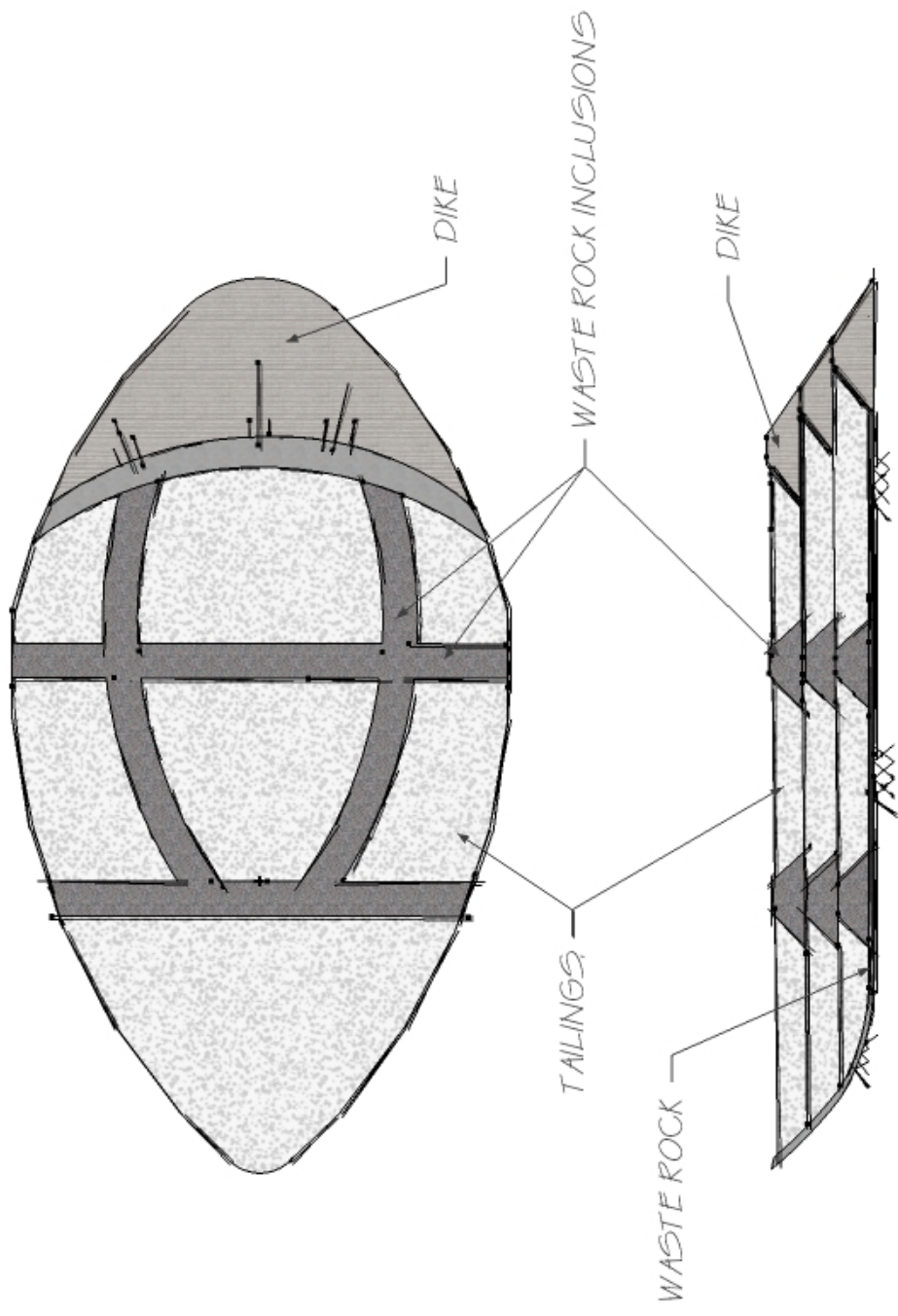


Figure 1. Schematic illustration of a tailings impoundment with waste rock inclusions.

The characteristics of waste rock are determined by the strength (hardness, brittleness) of the rock, by the type and frequencies of discontinuities in the rock mass, and by the excavation method (usually by drilling and blasting). The vast majority of waste rock excavated from hard rock mines consists of silt to boulder sized fragments (Aubertin et al. 2005).

Typical ranges of gradation for tailings and waste rock from hard rock mining are shown on Figure 2. As shown, the particle size distribution of waste rock is typically 3 to 4 orders of magnitude greater than that of tailings. This is reflected in their material properties, including their hydraulic conductivities.

The hydraulic conductivity of tailings generally ranges from 5×10^{-7} to 1×10^{-4} cm/s, with the lower values being associated with the finer fraction of the tailings (slimes) and the higher values with the coarser fraction (sands) (Vick, 1990; Bussi re, 2007). Due to layered deposition as slurry, the hydraulic conductivity of tailings is often much greater horizontally than vertically.

The hydraulic conductivity of waste rock typically varies from 1×10^{-5} to 1×10^{-2} cm/s, depending on the gradation, particularly the fines content (< 0.75 mm) and porosity (Gamache-Rochette, 2004; Martin et al., 2004; Aubertin et al. 2008).

Based on data from various Canadian mines, the ratio of waste rock to tailings produced by dry weight is typically close to 1:8-10 for underground mines, and 2-3:1 for open pit mines (Aubertin et al., 2002b). All or some of the waste rock (and tailings) produced by hard rock mining may be reactive and thus require collection and treatment of the seepage to prevent AMD (acid mine drainage) from affecting the surrounding areas.

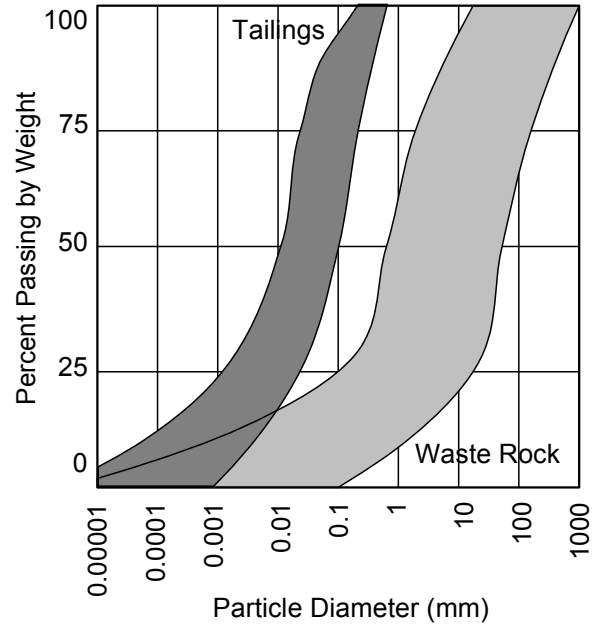


Figure 2. General range of grain size distributions for hard rock mines tailings (Vick, 1990; Bussi re, 2007) and waste rock (Gamache-Rochette, 2004).

Waste rock, even when end-dumped and uncompacted, is strong and incompressible compared to slurry-deposited tailings.

Hydraulically deposited hard rock mines tailings tend to be highly contractive and thus very susceptible to liquefaction under static or seismic loadings (Ishihara et al., 1981; Vick, 1990; Terzaghi et al., 1996).

Figure 3 presents an example of the tip resistance versus depth from cone penetration testing at an active hard rock mine tailings impoundment in the province of Quebec. The variation in the tip resistance is typical of unconsolidated tailings (Stone et al., 1994). The zones of lower tip resistance represent areas of significant underconsolidation that are weak, compressible and highly susceptible to liquefaction (James, 2009). Also shown on Figure 3 is the estimated tip resistance of the tailings

after consolidation, calculated using the method of Chen & Juang (1996) which relates the effective friction angle of compressible sands to the ratio of the measured tip resistance to the vertical effective stress.

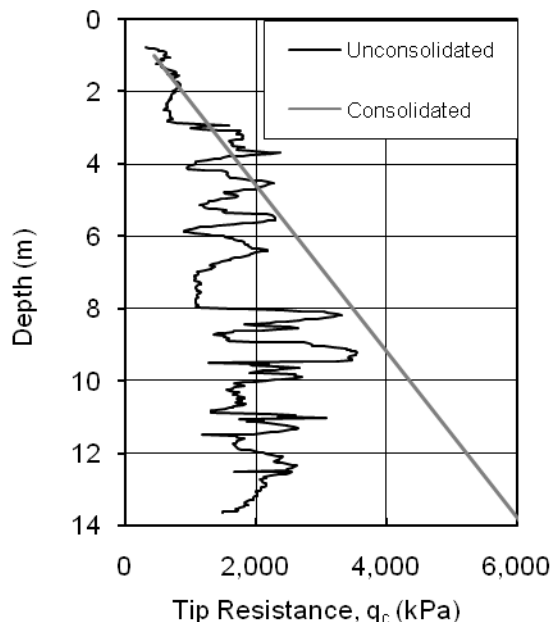


Figure 3. Example of measured tip resistance from cone penetration testing at an active tailings impoundment with estimated tip resistance due to consolidation (from James, 2009).

Consolidation results in increased tip resistance, which is associated with increased strength, stiffness, and liquefaction resistance. This illustrates the potential effects of accelerated consolidation with WRI.

COMPARISON WITH THE CONVENTIONAL METHOD

The use of waste rock inclusions in tailings impoundments can be assessed in a preliminary manner by comparing the

expected response of a tailings impoundment with WRI to that of a conventional tailings impoundment (without WRI). The following sub-sections discuss the behavior of both types of impoundments with respect to specific issues.

Consolidation of the Tailings

The coefficient to consolidation, c_v , for hard rock tailings generally varies between 1×10^{-2} and 1 cm/s^2 (Vick, 1990; Aubertin et al., 1996; Bussière, 2007) and is similar to that of natural soils of similar gradation and plasticity (Holtz & Kovacs, 1981).

The deposition of tailings slurry in conventional impoundments generally results in varying degrees of consolidation within the tailings. Complete consolidation typically takes many years to achieve, depending on the drainage conditions, the rate and sequence of placement, and the thickness of the deposit (Vick, 1990; Stone et al. 1994).

The presence of local or continuous WRI in a tailings impoundment will provide shorter drainage paths for the relief of porewater pressures generated during the placement of successive layers of tailings, resulting in more rapid consolidation relative to that in a conventional impoundment. This is illustrated on Figure 4 where schematic seepage vectors from a conventional raised tailings impoundment and a tailings impoundment with waste rock inclusions are shown. The use of WRI can be very effective in accelerating the dissipation of porewater pressure during and after tailings placement. For instance, recent calculations conducted with an analytical method inspired by Chin's (2004) solution for sand drains, indicates that the rate of consolidation of tailings can be increased by a factor of 5 or more by placing waste rock heaps in a regular pattern in the

impoundment (Aubertin et al., to be published).

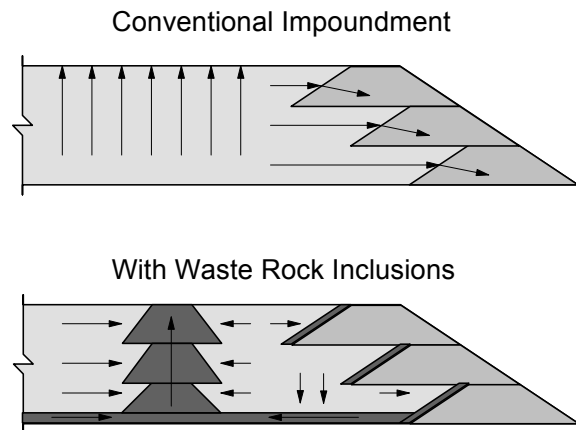


Figure 4. Schematic illustration of the seepage in a conventional impoundment and in an impoundment with waste rock inclusions.

Also, the strength and stiffness of tailings tend to increase with increasing consolidation. Thus, the more rapid consolidation due to the waste rock inclusions could result in some improvement in the stability of the impoundment under static and seismic conditions.

Compartmentalization of the Tailings

Waste rock inclusions can be placed to create partly or fully closed cells within the tailings impoundment (see Figure 1). This compartmentalization would have two main beneficial effects relative to conventional impoundments: 1) the quantity of tailings and water released in the event of a breach of the dike would be limited to that in the cell(s) bordering the breach; and 2) the surface of the impoundment could be progressively reclaimed as cells are filled. In this case, the consolidated tailings would provide a more stable working surface (for cover placement, for instance) than the

under-consolidated tailings of a conventional impoundment.

Improved Static and Seismic Stability

As noted previously, the strength of tailings increases with consolidation (due to porewater dissipation and increased density). When the critical failure surface for static equilibrium passes through the tailings (this is often the case with upstream-raised tailings dikes), the increased consolidation in the impoundment with WRI leads to an increase in the static stability. However, as the consolidation ratio of the tailings in the conventional impoundment approaches that of the impoundment with inclusions, their static stabilities would become equivalent (in the long term).

Another advantage of WRI is that there can also be a reinforcement effect if an inclusion is located within the area encompassed by the failure surface.

James (2009) conducted two-dimensional dynamic numerical analyses of: 1) a tailings impoundment with a rockfill dike; and 2) an impoundment with an upstream-raised tailings dike. Both impoundments were modeled with and without waste rock inclusions.

The dynamic analyses used ground motions that simulated the occurrence of earthquakes with moment magnitudes varying from 6.5 to 7.5 at a distance of 30 km from the dikes. The analyses included simulation of the site response with the development of excess porewater pressures and liquefaction in the retained tailings.

For the impoundment with the rockfill dike, the presence of the inclusions (all located away from the dike) reduced the development of excess porewater pressures

in the tailings adjacent to the inclusions and reduced the deformation of the dike by 30%.

For the impoundment with an upstream-raised dike, the presence of the inclusions (which included an inclusion located very close to the dike) also reduced the development of excess porewater pressures in the tailings adjacent to the inclusions. In this case, the vertical and horizontal deformations of the dike were reduced by an order of magnitude. Without inclusions, significant deformations extended a large distance (over 150 m in some cases) from the dike into the impoundment, indicating the potential for the release of a large portion of the retained tailings in the event of a failure. With the WRI, significant deformations were limited to an area much closer to the dike, pointing to a limited release of tailings in the event of a failure.

It is also worth noting here that the presence of the waste rock inclusions prevented failure of the simulated impoundment for the magnitude 7.5 earthquake.

The failure of a tailings impoundment at the Mochikoshi Gold Mine in Japan in 1978 was attributed to the post-shaking dissipation of excess porewater pressures generated by earthquake loading (Ishihara, 1984). James (2009) also conducted post-shaking analyses of the impoundments with and without inclusions. The results indicated that the WRI led to a more rapid dissipation of the excess porewater pressures generated during shaking. The predominant direction of seepage was to the inclusions rather than though the downstream slope of the dike, which would be a potentially destabilizing occurrence. More details on these analyses are presented in James (2009); additional results will also be published elsewhere.

Containment and Submersion of Reactive Waste Rock

Waste rock used to construct inclusions in a tailings impoundment will be largely encapsulated with saturated tailings and submerged below the phreatic surface as tailings are deposited (if care is taken not to create a water drawdown near the WRI). Such saturated conditions would prevent oxidation, acid production, and metal leaching from sulphidic minerals (such as pyrite and pyrrhotite) in the waste rock. This would be quite advantageous when compared to the unfavorable hydro-geochemical conditions that often prevail in a typical waste rock pile (Martin et al. 2004; Molson et al. 2005; Aubertin et al. 2005, 2008).

Depending on the quantities of tailings and waste rock produced, the reactivity of the waste rock, and the mining sequence, it may be possible to use all of the reactive waste rock to create WRI and thus reduce the need for measures to control AMD at a waste rock pile. Under the most favorable conditions (i.e. a low waste rock to ore ratio, as with some underground mines), it may be possible to completely eliminate the need for a waste rock pile.

Effect on the Consequences of Failure

The stability of tailings impoundments in Canada is generally evaluated based on well established practices such as those defined in the Dam Safety Guidelines of the Canadian Dam Association (CDA, 2007). Using these guidelines, the hydrologic and geotechnical (seismic) loadings, based on recurrence intervals, on an impoundment are determined from the consequences of failure, specifically the risk of loss life, economic loss (to another party), and damage to infrastructure, the environment, or cultural/historic sites.

The area affected by the release of tailings due to an impoundment failure is a function of the quantity of tailings released and the topography of downstream area (Lucia et al., 1981; Jeyapalan et al., 1983).

By compartmentalizing the tailings, the use of waste rock inclusions can limit the quantity of tailings that would be released in the event of a failure and thus the area potentially impacted by the release would be reduced. As a result, the risks would be diminished along with the corresponding consequence category. This could lower the design recurrence interval. Likewise, WRI could also alleviate the need for costly stabilization of dams or renovation of outlet works at closure due to changes in operations, regulations, evaluation criteria, or downstream conditions.

Summary of the Comparisons

Table 2 summarizes the main differences between conventional tailings impoundments and tailings impoundments with waste rock inclusions.

PLANNING, DESIGN AND OPERATIONAL CONSIDERATIONS

There are a number of considerations that should be taken into account in the planning, design and operation of a tailings impoundment with waste rock inclusions. Some major considerations are summarized below. However, each project has its unique characteristics, so this summary is necessarily general.

Planning considerations should begin in the pre-feasibility stage and continue through detailed design. These should include:

- Estimation of the quantity of waste rock and tailings to be produced.

- Evaluation of the reactivity of the waste rock and tailings, and the potential for AMD generation.
- Production schedules for tailings and waste rock.
- Development of mine waste management and closure objectives and criteria (e.g. environmental and geotechnical).
- Development of a preliminary configuration for waste rock inclusions, including the number, size and configuration of the inclusions and whether the inclusions will be continuous or isolated heaps.
- Completion of a trade-off study comparing the use of waste rock inclusions to more conventional alternatives.

As the project proceeds, additional considerations that should be included in the design are:

- Evaluation of the material properties of the tailings and waste rock required for analysis of the impoundment with waste rock inclusions.
- Consolidation analysis; including an estimate of the penetration of the fine tailings into the coarse waste rock of the inclusions.
- Stability analyses using analytical and numerical methods; the latter may be required, particularly for seismic analyses.
- Safety considerations; the width and configuration of the inclusions should be such that the trucks to be

Table 1. Comparison of an impoundment with and without waste rock inclusions.

Issue	Conventional Tailings Impoundment	Tailings Impoundment with WRI
Consolidation of the tailings.	Slow and variable within impoundment.	Relatively rapid and more uniform.
Compartmentalization of the tailings.	None.	Yes.
Stability.	Generally, good static stability and poor seismic stability.	Slight to moderate improvement in static stability (especially with WRI close to dike) and significant improvement in seismic stability.
Containment of reactive waste rock.	None.	Some or all of reactive waste rock contained and submerged. For underground mines, separate waste rock disposal facility may not be required.
Planning and design considerations.	Conventional.	Additional planning required in feasibility and design phases and during operations. Additional waste rock transportation costs can be anticipated.
Closure considerations.	Conventional.	Individual cells created by inclusions allow for progressive closure and reclamation of impoundment; surface of consolidated tailings provides a better working surface.
Consequence of failure.	Failure of impoundment could lead to the release of a significant quantity of tailings and waste water, particularly in the event of liquefaction.	The quantity of tailings and waste water released in the (less likely) event of a failure would be limited by the presence of the WRI.

used to place the waste rock in the impoundment can operate and turn safety.

Operational considerations include:

- Maintaining the correct configuration of the inclusions as the impoundment is raised to prevent drifting of successive stages.
- Monitoring the consolidation of the tailings using piezometers and settlement probes.

RELATED ISSUES

In terms of seismic stability, the use of waste rock inclusions in tailings impoundments is closely related to the use of stone (or gravel) columns in silty or sandy soils to control the effects of seismically-induced liquefaction (Barksdale, 1987; Adalier and Aydingun, 2003; Aydingun and Adalier, 2003). In terms of consolidation, the use of waste rock inclusions in tailings is somewhat similar to the use of wick or sand drains in clayey soils (Hausmann, 1990; Chin, 2004), which serve to promote the dissipation of excess porewater pressures generated by static loading on the clay.

In sandy soils, stone columns prevent the development of high excess porewater pressures by providing for the dissipation of seismically-induced excess porewater pressures as they are generated. This is possible because of the relatively high hydraulic conductivity of the sand and the even higher hydraulic conductivity of the stone columns. However, with respect to tailings and silty soils, the hydraulic conductivities may be too low for general excess porewater pressure dissipation during shaking, even with closely spaced drainage inclusions. Nonetheless, in these types of materials, the stiffness of the inclusions acts

to stiffen the soil mass, resulting in less shear strain during seismic loading, which can result in less excess porewater pressure development.

Also, due to the relative gradations of tailings and waste rock, there would undoubtedly be some penetration of tailings into the waste rock inclusions. The same phenomenon occurs with stone columns in sandy soils. This is dealt with in the analyses by estimating the depth of penetration based on the gradations and reducing the assumed dimensions of the drainage inclusions accordingly. More work is needed on this aspect before general rules can be proposed.

CURRENT AND FUTURE RESEARCH

Research on the use of waste rock inclusions to improve the environmental and geotechnical performance of tailings impoundments is currently being conducted at Ecole Polytechnique, in Montreal, by the Industrial NSERC Polytechnique-UQAT Chair in Environment and Mine Wastes Management.

Research completed to-date includes a numerical study on the use of waste rock inclusions to control the effects of liquefaction in tailings impoundments (James, 2009). As mentioned above, this study indicated that the presence of waste rock inclusions lead to a significant and substantial improvement in the seismic performance of a typical upstream-raised tailings impoundment under a range of earthquake loadings ($M_w=6.5$ to 7.5).

Pepin (2009) presents the results of large-sized shaking table tests that were used to model tailings with rigid and drainage inclusions. These results indicate that the presence or inclusions in tailings retards the development of excess porewater pressures

and liquefaction. Another component of this research addresses the consolidation of tailings with waste rock inclusions. The results of the investigations, and of other related studies, will appear in upcoming publications.

CONCLUSIONS

The use of waste rock inclusions (WRI) represents a valuable option for the design and construction of tailings impoundments, particularly in areas of significant seismicity or when the waste rock is prone to produce a contaminated leachate. In addition to the benefits of improved static stability and seismic performance, the method can provide environmental benefits and reduce the consequences of failure with respect to the safety and security of downstream areas. These aspects are presented and discussed in this paper.

ACKNOWLEDGEMENTS

The authors gratefully acknowledge the financial support of the Industrial NSERC Polytechnique-UQAT Chair in Environment and Mine Wastes Management and of the Mine Reclamation and Geotechnical Services Department of SNC-Lavalin Inc. (<http://www.enviro-geremi.polymtl.ca>)

REFERENCES

Adalier, K. and Aydingun, O. (2003). Numerical Analysis of Seismically Induced Liquefaction in Earth Embankment Foundations – Part I: Benchmark Model. *Canadian Geotechnical Journal*, 40, 753-765.

Aubertin, M., Bussière, B. & Chapuis, R. P. (1996). Hydraulic Conductivity of

Homogenized Tailings from Hard Rock Mines. *Canadian Geotechnical Journal*, 33, 470-482.

Aubertin, M., Bussière, B. & Bernier, L. (2002b). *Environnement et gestion des rejets miniers* [CD-ROM Manual]. Montréal: Presses Internationales Polytechnique.

Aubertin, M. Mbonimpa, M., Jollette, D., Bussière, B., Chapuis, R.P., James, and Riffon, O. (2002a) Stabilité géotechnique des ouvrages de retenue pour les résidus miniers: Problèmes persistants et méthodes de contrôle. *Défis & Perspectives: Symposium 2002 sur l'environnement et les mines*, Rouyn-Noranda, CIM. Proceeding on CD-ROM.

Aubertin, M., Fala, O., Molson, J., Gamache-Rochette, A., Lahmira, B., Martin, V., Lefebvre, R., Bussière, B., Chapuis, R.P., Chouteau, M., Wilson, G.W. (2005) Évaluation du comportement hydrogéologique et géochimique des haldes à stériles. *Symposium Rouyn-Noranda: L'Environnement et les Mines*, CIM, Proc. On CD-ROM.

Aubertin, M., Fala, O., Molson, J., Chouteau, M., Anterrieu, O., Hernandez, M.A., Chapuis, R.P, Bussière, B., Lahmira, B., Lefebvre, R. (2008) Caractérisation du comportement hydrogéologique et géochimique des haldes à stériles. *Symposium 2008 sur l'environnement et les mines*, Rouyn-Noranda, Canada. CIM, Proc. On CD-ROM.

Aydingun, O. & Adalier, K. (2003). Numerical Analysis of Seismically Induced Liquefaction in Earth Embankment Foundations – Part II: Application of Remedial Measures. *Canadian Geotechnical Journal*, 40, 766-779.

- Barksdale, R. D. (1987). *Applications of the State of the Art of Stone Columns – Liquefaction, Local Bearing Failure, and Example Calculations*, Technical Report No. REMR-GT-7, Washington DC: US.
- Bussiere, B. (2007). Hydro-Geotechnical Properties of Hard Rock Tailings from Metal Mines and Emerging Geo-environmental Disposal Approaches. *Canadian Geotechnical Journal*, 44(9), 1019-1052.
- Canadian Dam Association (CDA). (2007). *Dam Safety Guidelines*. Edmonton AB: Canadian Dam Association.
- Chen, J.W. & Juang, C.H. (1996). Determination of Drained Friction Angle of Sands from CPT. *Journal of Geotechnical Engineering*, 122(5), 374-381.
- Chin, J. (2004). Equal strain consolidation by vertical drains, *Journal of geotechnical and geoenvironmental engineering*, ASCE, 130(3): 316-327.
- Gamache-Rochette, A. (2004). Une Etude de caraterisation en laboratoire et sur le terrain des ecoulements de l'eau dans les roches steriles. M.Sc. Thesis (unpublished). Ecole Polytechnique Montreal PQ, Canada.
- Hausmann, M. R., 1990, *Engineering Principles of Ground Modification*. Tonronto ON: McGraw-Hill Publishing Company.
- Holtz, R. D. & Kovacs, W. D. (1981). *An Introduction to Geotechnical Engineering*. Englewood NJ: Prentice-Hall, Inc.
- Ishihara, K., Sodekawa, M. & Tanaka, Y. (1981). Cyclic Strength of Undisturbed Mine Tailings. *Proceedings of the International Conference on Recent Advances in Geotechnical Earthquake Engineering and Soil Dynamics, St-Louis USA*. (pp. 53-58. New York: ASCE.
- Ishihara, K. (1984). Post-Earthquake Failure of a Tailings Dam due to Liquefaction of the Pond Deposit. *Proceedings of the International Conference on Case Histories in Geotechnical Engineering, St-Louis USA*, (pp. 1129-1143). New York: ASCE.
- James, M. (2009). The Use of Waste Rock Inclusions to Control the Effects of Liquefaction in Tailings Impoundments. Ph.D. Thesis (unpublished). Ecole Polytechnique: Montreal QC.
- Jeyapalan, J. K; Duncan, J. M. & Seed, H. B. (1983). Investigation of Flow Failures of Tailings Dams. *Journal of Geotechnical Engineering*, 109(20), 172-189.
- Lucia, P. C., Duncan, J. M. & Seed, H. B. (1981). Summary of Research on Case Histories of Flow Failures of Mine Tailings Impoundments. *U.S. Bureau of Mines Information Circular* (pp. 46-53). Washington DC: U.S. Department of the Interior.
- Martin, V., Aubertin, M., Bussière, B. & Chapuis, R. P. (2004). Evaluation of unsaturated flow in mine waste rock. 57th Canadian Geotechnical Conference and the 5th joint CGS-IAH Conference, 24-27 October 2004, Quebec City, 14-21.
- Molson, J.W., Fala, O., Aubertin, M., Bussière, B. (2005) Numerical simulations of pyrite oxidation and acid mine drainage in unsaturated waste rock piles. *Journal of Contaminant Hydrology* 78(4): 343-371.
- Pepin, N. (2009). Étude du comportement des résidus miniers soumis à un chargement cyclique sur table sismique. Master's Thesis (unpublished). Ecole Polytechnique: Montreal QC.

Stone, K. J. L., Randolph, M. F. & Sales, A. A. (1994). Evaluation of Consolidation Behavior of Mine Tailings. *Journal of Geotechnical Engineering*, 120(30), 473-490.

Terzaghi, K., Peck, R. B., & Mesri, G. (1996). *Soil Mechanics in Engineering Practice* (3rd ed.). Toronto, ON: John Wiley & Sons Inc.

Vick, S. G. (1990). *Planning, Design, and Analysis of Tailings Dams*. Toronto: Bitech Publishers Ltd.

PHASED CLEANUP APPROACH TO ARSENIC CONTAMINATION AT SAGINAW HILL MINING DISTRICT, TUCSON, ARIZONA

Christine Galli LaBerge, P.E.,
Walsh Environmental Scientists and Engineers, LLC;

Richard J. Rudy, P.G.,
Ecology & Environment, Inc.

ABSTRACT: The Saginaw Hill Mining District (Site), located approximately 10 miles southwest of Tucson, Arizona, contains heavily contaminated surface soil, waste rock, and tailings as a result of previous mining and exploration activities. The maximum observed arsenic concentration in surface soil, 47,301 milligrams per kilogram (mg/kg), greatly exceeds the Arizona Department of Environmental Quality soil remediation level for residential exposure of arsenic, which is 10 mg/kg.

The Site is undeveloped; however, it is located within an urbanizing area of Pima County just beyond the Tucson city limits. Prior to closure, the Site was a popular destination for all-terrain vehicle (ATV) riders and hikers. The end goal of the assessment and cleanup efforts is to reopen the Site for recreational use (hiking and ATV).

Funding for cleanup at this Site was limited and a phased approach was necessary that not only presented a reasonable cleanup level for arsenic, but also one that could be constructed in two separate efforts and funded with two different fiscal year budgets. The Dr. John Drexler (University of Colorado-Boulder) *in vitro* method was used to obtain relative bioavailability (RBA) site specific data for arsenic. Based on these results, the risk management criteria for arsenic, adjusted to reflect Site-specific bioaccessibility, resulted in a recreational cleanup criterion of 390 mg/kg.

The on-site repository construction and site stabilization design was completed in two separate bid packages that could be implemented in two separate fiscal years to accommodate funding restrictions. Interim stabilization techniques were used, including soil binders and silt fences to provide remedy protection of completed construction prior to implementation of the second phase. The first phase of the design was constructed in 2007 and the second phase of the design was built successfully approximately 1 year after completion of the first phase.

INTRODUCTION

Site Location and Description

The Saginaw Hill Mining District (Site) is located approximately 10 miles southwest of Tucson, Arizona on Bureau of Land Management (BLM) property, and consists of two areas of contamination: the Saginaw Mine and the Palo Verde Mine (Figure 1). The Saginaw Mine covers approximately 5 acres and contains waste rock, tailings, and smelter slag, while the Palo Verde Mine covers approximately 1 acre and contains primarily waste rock. The Site is located at an elevation of 2,600 feet above mean sea level at the southern end of the Tucson Mountains, and is surrounded by steep hills (Auby 2003). The Saginaw Hill climate and ecology are characteristic of the arid conditions of the area.

The average daily temperatures range from approximately 101 degrees Fahrenheit (°F) in the summer to 39°F in the winter, with daily variations of more than 25°F (Citydata 2005). The average annual precipitation is approximately 12 inches, and the land is covered with Sonoran Desert vegetation.

The Site is undeveloped; however, it is located within an urbanizing area of Pima County just beyond the Tucson city limits. While the Site is now inaccessible to the public (fenced with locked gates), it was historically and recently frequented by all-terrain vehicle (ATV) riders and other recreational users. Additionally, Johnson Primary School is located adjacent to the northeast corner of the Bureau of Land Management (BLM) property boundary.

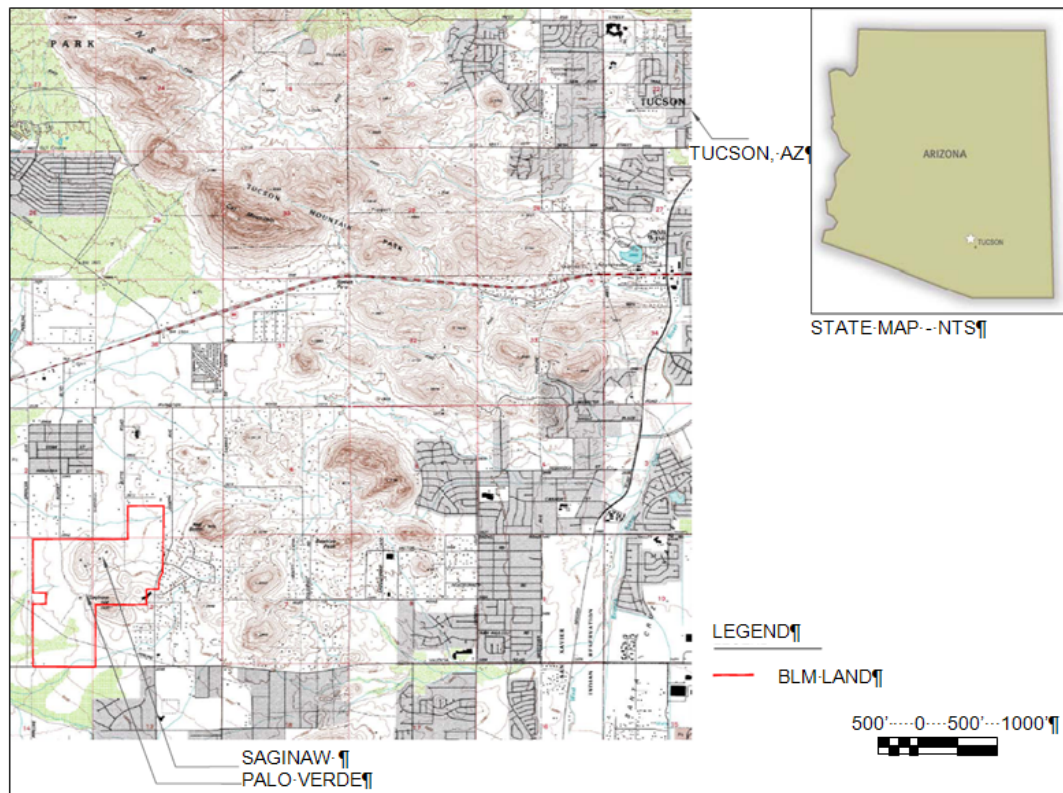


Figure 1. Site Location Map, Saginaw Hill Mining District: Saginaw Mine and Palo Verde Mine

Table 1. Maximum Concentrations Observed for Chemicals of Concern at the Site

Location	Arsenic (mg/kg)	Lead (mg/kg)	Mercury (mg/kg)
Palo Verde Mine	5,348	111,000	1.8
Saginaw Mine	37,400	76,100	15.8
Arroyo between mine sites	2,300	3,700	1,300
Surrounding soils around Palo Verde Mine	1,100	2,400	2,600
Surrounding soils around Saginaw Mine	2,142	15,339	1,300
Auxiliary waste piles southeast of Palo Verde Mine	47,301	25,000	2,300

Note: Results obtained through the use of x-ray fluorescence technology and/or confirmatory laboratory analysis.
mg/kg = milligrams per kilogram

Primary Chemicals of Concern

Primary human health chemicals of concern (COCs) include arsenic, lead, and mercury. Table 1 presents the maximum observed concentrations for these COCs at the Site.

ENGINEERING EVALUATION/COST ANALYSIS (EE/CA)

An Engineering Evaluation / Cost Analysis (EE/CA) was performed at the Site to identify the source, nature, and extent of contamination; evaluate the risk posed by onsite sources of contamination; explore various alternatives; and select the most appropriate removal action alternative for the Site.

Risk Assessment

A human health risk assessment was performed to assess the risk posed by arsenic

to potential receptors. Site-specific risk management criteria (RMCs), based on recreational use, bioaccessibility of arsenic, and Arizona groundwater protection levels, were developed to correspond to a target excess cancer risk level of 1×10^{-5} .

Four composite surface soil samples from the Site were analyzed for bioaccessibility of arsenic. All four samples were collected following the 2000 U.S. Geological Survey methodology published by Kathleen Smith that statistically affirms that a 30-increment composite sample can accurately represent 30 individual grab samples. Dr. John Drexler at the University of Colorado-Boulder has been working cooperatively with EPA Region 8 for a number of years to develop an *in vitro* method that can be used to obtain relative bioavailability (RBA) data for lead, arsenic, and other metals in soils. The Drexler *in vitro* test results indicated a range of bioaccessibility from 3% to 6%. Based on these results, the RMC for arsenic, adjusted to reflect Site-specific bioaccessibility, resulted in a recreational cleanup criterion of 390 mg/kg (LaBerge, et. al. 2008).

Removal Action Objectives

The removal action objectives (RAOs) defined for the Site were as follows:

- Prevent or reduce human exposure (through inhalation, ingestion, and dermal contact) to arsenic, lead, and other metals of concern in material at the Site;
- Prevent or reduce ecological exposure (through inhalation, ingestion, and dermal contact) to arsenic, lead, and other metals of concern in waste material at the Site; and
- Prevent or reduce potential migration of arsenic, lead, and other metals of concern in waste material at the Site via surface runoff, erosion, and wind dispersion.

Alternative Analysis

The following alternatives were considered for the Site. Alternative 1 addresses the entire Site whereas Alternatives 2, 3, and 4 address only surface material and Alternatives 5 and 6 address groundwater.

- Alternative 1: No Action
- Alternative 2: Removal of Contaminated Surface Materials and Consolidation in On-Site Repository
- Alternative 3: Excavation of All Material from Palo Verde Mine, Auxiliary Waste Piles, and Arroyo; Partial Removal of Material at Saginaw Mine; Consolidation in On-Site Repository; and Capping of Remaining Surface Materials
- Alternative 4: Removal of Contaminated Surface Materials to Off-Site Facility (either Hazardous Waste Facility or Commercial Landfill)

- Alternative 5: Groundwater Administrative Action and Long-Term Monitoring
- Alternative 6: Groundwater Treatment through Precipitation and Optional Immobilized Ligand

Selected Alternatives

Alternative 3 was selected to address surface material. The waste rock and tailings from both the Palo Verde Mine and the Saginaw Mine, auxiliary waste piles and arroyo were selected for removal, along with the surrounding soils around Palo Verde. The construction of an engineered repository at the Saginaw Mine near the location of the slag heap was specified and a surrounding cap of crushed rock around soil in the vicinity elevated above risk levels was selected.

The alternative involved five basic actions:

- Removal
- Consolidation
- Capping the Repository
- Capping all excavated portions and the surrounding soil around Saginaw
- Revegetation on Repository Cap

Alternative 3 was selected as it was deemed most protective of human health concerns, would not leave as significant a scar on the land that would require revegetation over a long period of time (crushed rock cap instead of scraping all surface soil), and involved the construction of an on-site repository which proved to be a safe and cost effective way to enclose highly contaminated material.

Alternative 5 was selected to address groundwater considerations at the Site. The alternative called for restrictions on the future use of the Site (administrative action) and long term monitoring of nine on site wells. This alternative was paired with Alternative 3

as decision makers recognized the absence of current human receptors to groundwater and allowed for future modification (such as treatment) if needed.

Benefits of Site Specific Risk Evaluation Results on Implementability and Cost

Background concentrations for arsenic were determined by collecting off-Site unimpacted soils from the surrounding area. The background arsenic concentration was determined to be 30 mg/kg (determined by utilizing the mean plus two standard deviations). If the remedial action cleanup level had been set at the initial value calculated from various risk exposures (23.3 mg/kg), the action level would have potentially been set below background concentrations. If the cleanup level was set to three times the background concentration (as has been done at some BLM abandoned mine sites), the remediation action level would have been four times lower than the value utilized when incorporating bioavailability data.

When utilizing the remediation action level of 390 mg/kg for arsenic, approximately 27,000 cubic yards of material were determined to require some level of remediation. If the bioaccessibility data had not been used and a level of 90 mg/kg was utilized instead (three times the background concentration), cost estimate ranges for the remediation would be expected to increase from approximately \$1.8M-\$2.6M to \$3.8M-\$5.4M (assuming an increase in volume and increase in unit price due to implementability difficulties).

If bioaccessibility data had not been used and remediation costs were increased as shown, these costs may have delayed the start of remediation actions at the Site or, in the extreme case, may have precluded remediation from taking place at all. Risk to

the community was therefore significantly reduced by developing a reasonable and implementable remediation action that was within the funding capabilities of the governmental agency and which protected the public from Site-specific hazards in a responsible manner.

ENGINEERING DESIGN

The following subsections discuss each component of the engineering design.

Auxiliary Piles

The auxiliary waste piles at the site were excavated and transported to the Saginaw mine repository area. Dust control was maintained and the excavated area was stabilized using a temporary soil binder followed by revegetation.

Arroyo

The arroyo was heavily contaminated with sediment exceeding the recreational cleanup criterion established in the site specific risk assessment. The engineering design included excavation of contaminated sediment to the Saginaw mine repository area, maintenance of existing vegetation wherever possible, transplanting Saguaro cacti as needed and constructing an access road along the arroyo for access. In addition, the design called for armoring the arroyo with riprap to prevent erosion and further offsite sediment migration.

Palo Verde Excavation

The engineering design included excavation and transport of waste material at the Palo Verde mine site to the Saginaw mine repository. A crushed rock cap was designed for placement on the excavated area for stabilization.

Saginaw Excavation

The material already located at the Saginaw mine was only excavated if outside of the repository footprint. A crushed rock cap, similar to that specified for Palo Verde, was designed for placement over any excavated area to provide stability.

Repository

The onsite repository was located at the Saginaw mine and included stable slope configurations and a cap design to minimize/eliminate exposure to potential receptors. Run on / run off controls were also designed using diversion channels, and revegetation was specified for the final cap.

Crushed Rock Cap

A crushed rock cap was also designed to be placed on surrounding soils elevated above remediation levels. The decision was made not to excavate this material in order to maintain existing vegetation wherever possible.

Groundwater Monitoring

A groundwater monitoring program was specified and is currently underway.

Figure 2 shows a graphical representation of the auxiliary pile and arroyo sediment consolidation, and Figure 3 presents the design of the repository.

PHASED IMPLEMENTATION

This Site has historically been underfunded and current funding restrictions required that the planned construction be split into two phases to stretch over two governmental funding cycles. The second phase of the construction was completed; however, the

remaining funding proved highly difficult to secure.

Phase I of the engineering design included the following items:

- Consolidate materials from auxiliary waste piles at Saginaw mine repository site
- Excavate contaminated sediments from arroyo and consolidate at Saginaw mine repository site
- Stabilize new material placed at Saginaw mine repository site with soil binder
- Armor arroyo to prevent erosion
- Stabilize excavated areas with soil binder or revegetate

Phase II of the design included the following:

- Excavate waste material from Palo Verde
- Excavate waste material from Saginaw
- Construct Repository
- Place crushed rock cap on excavated areas and surrounding soils
- Construction of run-on / run-off controls around repository and Palo Verde

Figure 4 presents a graphical representation of the activities taking place in each phase.

BENEFITS TO PHASED APPROACH

By phasing the design in two separate and stand alone designs, funding restrictions and budgetary cycles could be accommodated to still implement the selected alternative and meet the needs of the community.

The completion of Phase I resulted in an armored and cleaned arroyo which limited offsite migration of contaminants and a consolidated area of waste material stabilized in place by a temporary spray-on soil binder. The soil binder remained stable throughout the time between completion of Phase I and

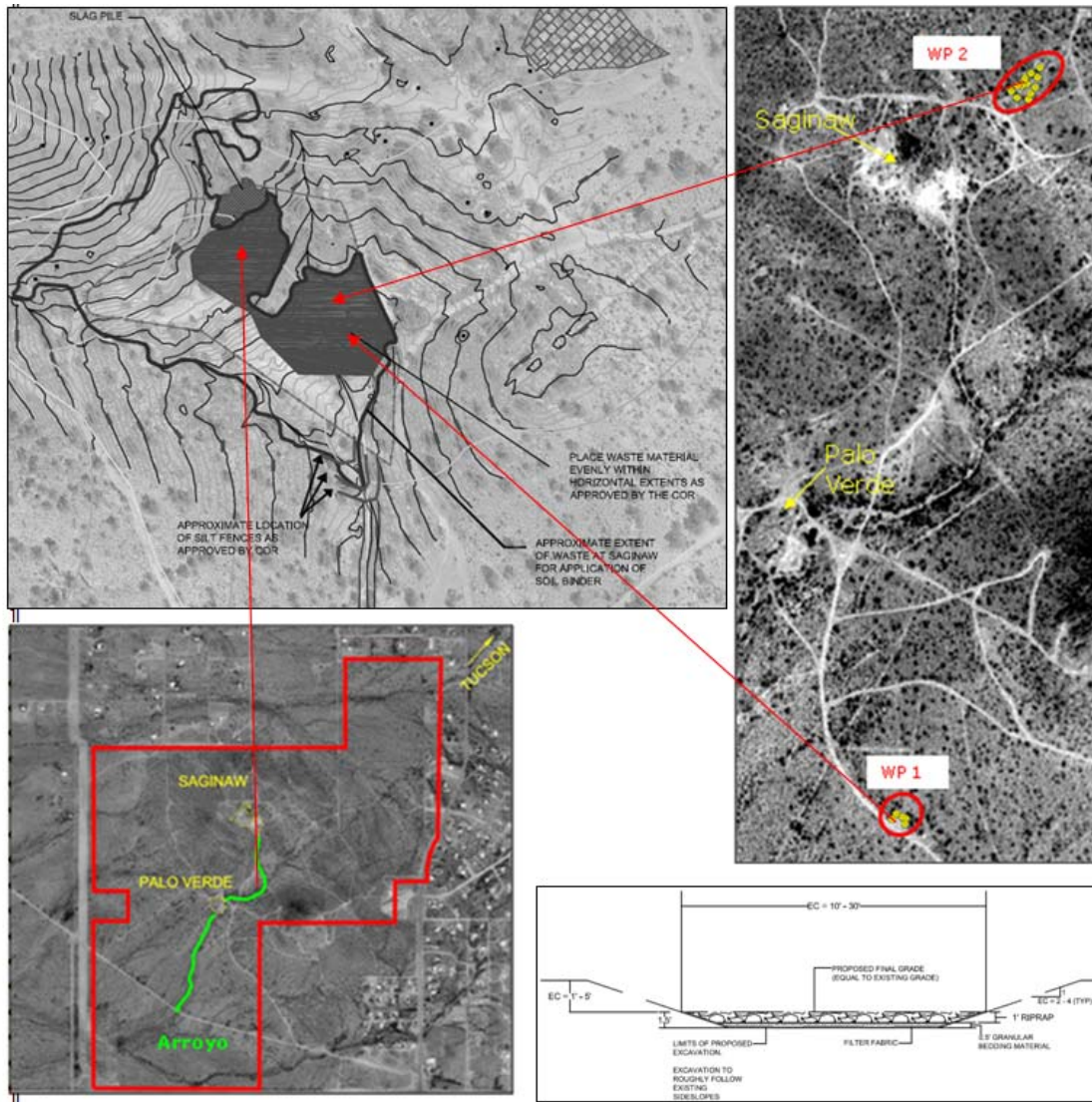
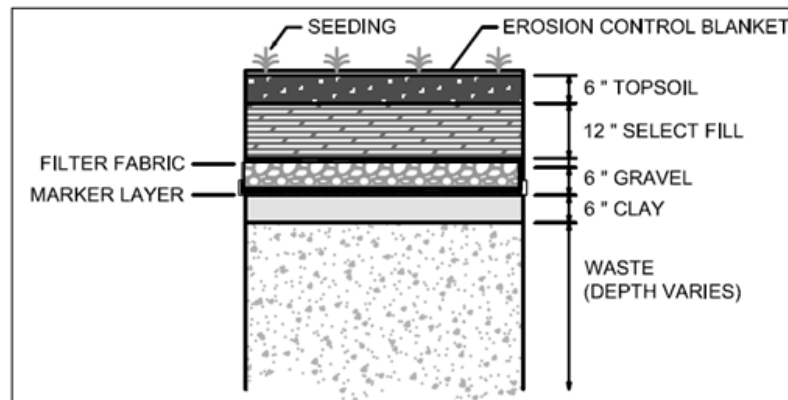
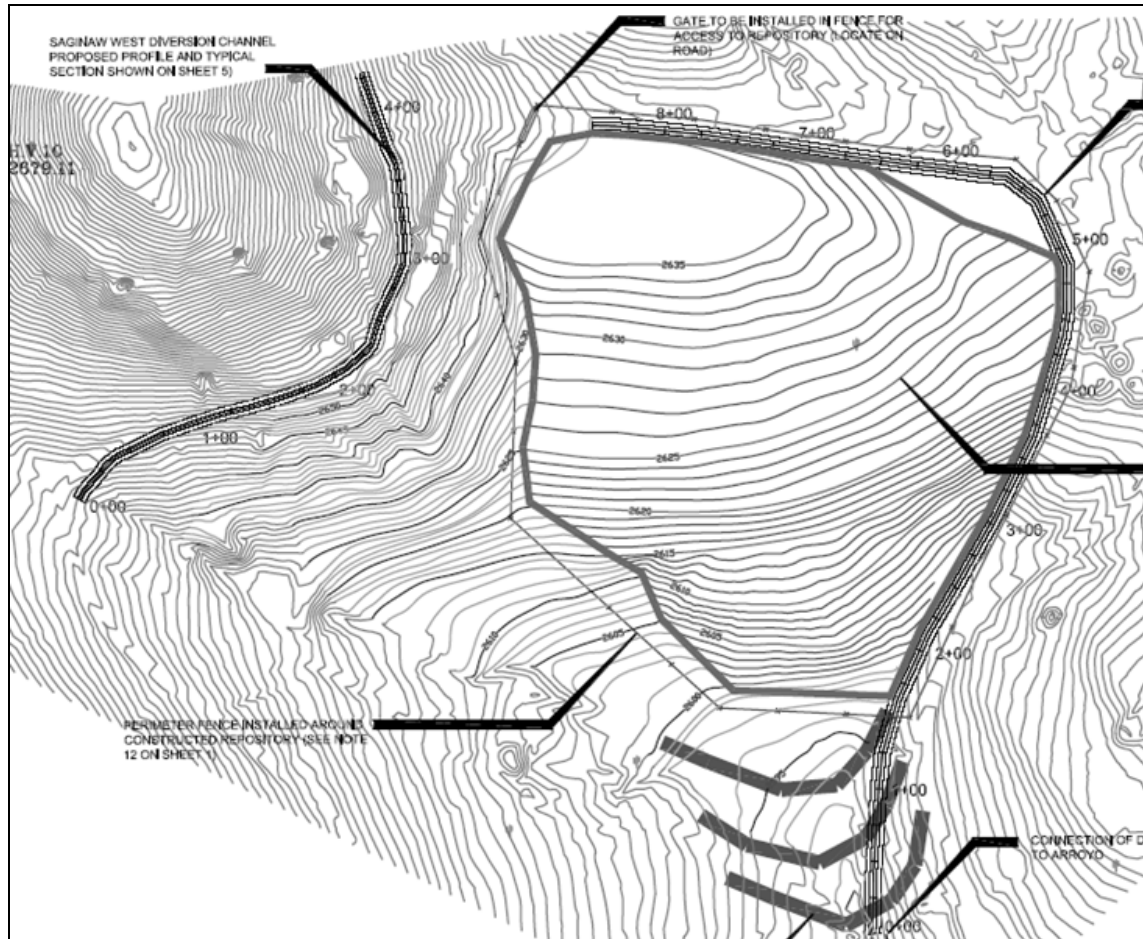


Figure 2: Consolidation of Auxiliary Pile material and Arroyo at the Saginaw mine repository area with Detail of Arroyo Armoring

the commencement of the second phase of construction. No items within the first phase of construction required reconstruction in the second phase, apart from best management practices and storm water controls (i.e. silt fencing) to provide remedy protection for remediated areas down gradient.

The community was significantly involved in the selection of the alternative. By phasing the implementation, community members were able to see progress almost immediately after

the alternative was selected. If the design had not been phased, it is likely that either the alternative selected by the community would not have been implemented due to funding restrictions, or the implementation would have been put off several years to gather sufficient funds. Residents in the area felt that the Bureau of Land Management was taking the Site conditions seriously and appreciated the quick move toward construction.

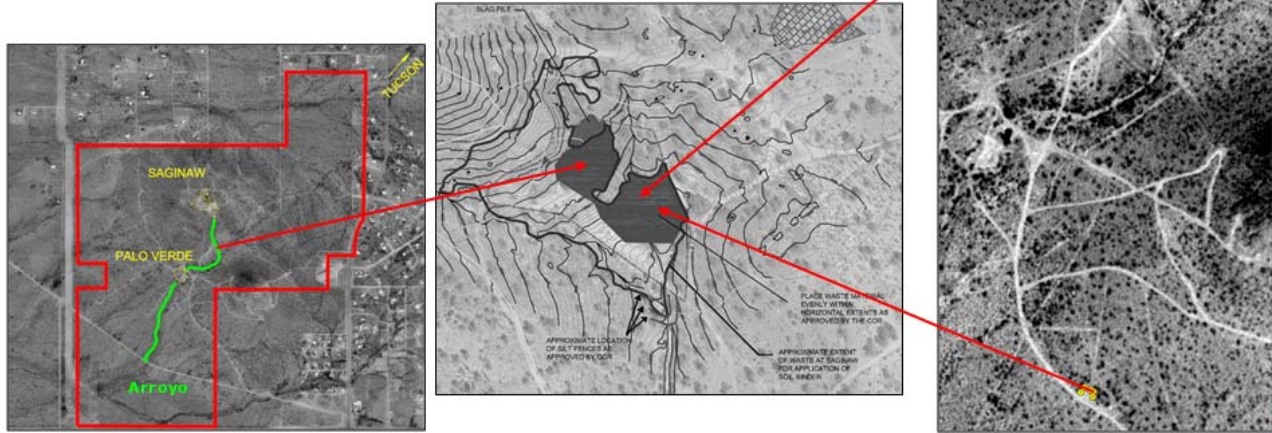


Cap Detail

Figure 3: Repository Design

Phase I

- Consolidate materials from auxiliary waste piles at Saginaw mine repository site
- Excavate contaminated sediments from arroyo and consolidate at Saginaw mine repository site
- Stabilize new material placed at Saginaw mine repository site with soil binder
- Armor arroyo to prevent erosion
- Stabilize excavated areas with soil binder or revegetate



Phase II

- Excavate waste material from Palo Verde
- Excavate waste material from Saginaw
- Construct Repository
- Place crushed rock cap on excavated areas and surrounding soils
- Construction of run-on / run-off controls around repository and Palo Verde

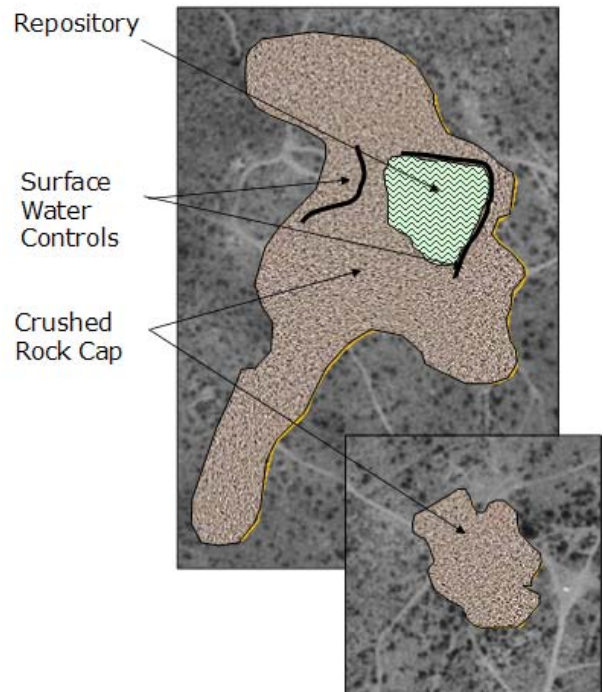


Figure 4: Phased Approach

SUMMARY AND CONCLUSION

The use of bioaccessibility data in the site specific risk assessment allowed for a practical and implementable cleanup level for arsenic of 390 mg/kg. Risk to the community was significantly reduced by developing removal action objectives based on this cleanup level and evaluating alternatives that were effective, implementable, and affordable.

Approximately 27,000 cubic yards of material were determined to require some level of remediation in the selected alternative. This resulted in a cleanup cost estimate of \$1.8M-\$2.6M. Based on government funding restrictions, this budget was not implementable within one funding cycle. Therefore, in order to develop an engineering design that would be protective of the community and achieve the long term objectives at the site, the funding capabilities of the governmental agency had to be accommodated within the design itself.

By establishing a design that could be constructed in two different funding cycles, the Site could be stabilized between implementation phases, the budget could be adjusted to enable funding, and the selected alternative could be implemented without giving up needed protection.

The second phase of construction for Saginaw began less than one year after completion of phase I. The engineering design required no significant modification in either phase of construction and actual costs were within the budgeted range of the design cost estimate.

REFERENCES

- Auby, B., 2003, *Preliminary Assessment of the Saginaw Hill Abandoned Mines*. May 6.
- Citydata, 2005, Website containing population, meteorology, and demographic data for cities and towns. Available at <http://www.city-data.com/city/South-Tucson-Arizona.html>
- EPA (U.S. Environmental Protection Agency), 2002, *Supplemental Guidance for Developing Soil Screening Levels for Superfund Sites*. Solid Waste and Emergency Response. OSWER 9355.4-24.
- EPA (U.S. Environmental Protection Agency), 2004a, *Region 9 Preliminary Remediation Goals, Background Document and PRG Tables*. Available at <http://www.epa.gov/region09/waste/sfund/prg/>
- Ford, K.L., 2004, *Risk Management Criteria for Metals at BLM Mining Sites*, Technical Note 390. BLM/RS/ST-97/0001+1703.
- LaBerge, C.G., Ford, K.L., Freeman, R., Wiman, A. 2008. *Risk Management Criteria Determination Using In Vitro Bioaccessibility Results for Arsenic at Saginaw Hill Mining District, Tucson, Arizona*. EPA National Groundwater Association Conference. Available at: <http://www.ngwa.org/gwol/080183555.aspx>
- Smith, K.S., C.A. Ramsey, and P.L. Hageman, 2000, *Sampling strategy for the rapid screening of mine waste dumps on abandoned mine lands*: Proceedings from the 5th International Conference on Acid Rock Drainage, Society for Mining, Metallurgy, and Exploration, Littleton, CO, p. 1453-1462.

SPATIAL DISTRIBUTION OF SOIL PHYSICAL PROPERTIES IN THE TAILINGS OF SCHNECKENSTEIN (GERMANY)

Taoufik Naamoun and Nejb Kallel

Faculty of Sciences, Sfax, Tunisia

Broder Merkel

TU Bergakademie Freiberg, Germany

ABSTRACT : The present paper resumes data relating to soil properties based on field examinations, on laboratory tests of samples from the uranium tailings of Schneckenstein. The objective of this study was to estimate the infiltration rate of water in uranium residues as well to predict the ability of contaminants to be transported from the survey area. For that purpose four sediment cores were taken at the tailing sites by drilling at four locations to different depths. Two borings were located in each tailing respectively. Samples were collected at 1 m interval. Grain-size-distribution analysis of samples was carried out by sieve and sedimentation method and evaluated using the program WINSIEB. The coefficient of permeability, K_f was obtained by Hazen's formula based on grain size analysis and the triaxial test. The water content, the specific gravity as well as the soil density were determined experimentally, while the total porosity and the degree of saturation were calculated using empirical formula.

In the upper most part of the tailings and the last two samples of the fourth borehole, the soil material consists of a wide range of material ranging from silt to cobbles while in the other part it is made up of only silt and fine sand. In the upper most tailings (cover layers) the coefficient of permeability is approximately 10⁻⁵ m/s and thus considerable permeable. For the tailings material in particular, the coefficient of permeability ranges between 10⁻⁸ and 10⁻⁷ m/s except the two last intervals of the fourth borehole. The dry density is very low and does not exceed 1.8, whereas the grain density exceeds 2.7g/cm³ in almost all analysed materials. The total porosity is very high in almost all tailing parts exceeding 30 %. The heap material is considered as damp, whereas the processed material is mostly moist.

INTRODUCTION

One of the fundamental and most ubiquitous tests undertaken during the analysis of sediments and soils in geological and environmental investigations is that of grain size distribution analysis (Pettijohn et al.

1972; Lewis & McConchie, 1994; Lewis & McConchie, 1994; Nichols, 1999; Morgan & Bull, 2007). The various size ranges and proportions of material identified during grain size distribution analysis encompass materials of sub-micron size through clays, silts, sands and gravels. A variety of different

techniques has been employed during geological analyses to present these distributions (Krumbein, 1934; Folk, 1966).

Additionally, Correlations of hydraulic properties with easily measured physical properties are useful for purposes of site characterization in heterogeneous sites. Also, correlations between various properties of porous media are useful for predicting difficult-to-measure hydraulic properties using properties that are more easily measured. This can provide a practical means for the quantification of the spatial distribution of hydraulic properties (Flint & Selker, 2002).

Moreover, the success of modelling soil flow and transport processes heavily depends on the quality of the model parameters that are used to describe the soil's hydraulic behavior (Ritter et al., 2004). Since the hydraulic conductivity which is symbolically represented as K ; ($K = a(D_{10})^b$ where a and b are empirically derived terms based on the soil type, and D_{10} is the diameter of the 10 percentile grain size of the material) influences runoff, drainage, infiltration, erosion and water quality, accuracy in measuring K is important in monitoring water movement (Perrone & Madramootoo, 1994). Also, its spatial distribution is often required for predictive hydrological models (Vachaud et al., 1988; Braud et al., 1995; Moustafa, 2000).

On the other hand, the hydraulic conductivity and the permeability K_f depend on each other and $K_f = K\mu/\rho g$ (where: K = hydraulic conductivity (cm/sec); ρ = density of water = 0.9982 g/cm³ at 20°C; g = acceleration of gravity = 980 cm/sec²; μ = dynamic viscosity of water = 0.01 g/(cm sec) at 20°C). However, the direct determination of K i.e. K_f requires much effort and is time consuming, because many measurements are

required to represent the intrinsic variation. Thus indirect method, based on other more easily measurable soil properties (such as grain size distribution and using the Hazen approximation), are sometimes preferred (Ahuja et al., 1989).

As water is stored in, and flows through, the interconnected pores of the rock matrix; therefore, porosity is useful for characterizing the hydrologic character of the various soil facies (Flint & Selker, 2002). Thus, the available physical properties, particularly porosity is generally related to porous media hydraulic properties, and can be a useful surrogate for estimation of these properties over a broad range of soil types.

Besides ores from the Schneckenstein area, uranium ores from Zobes, Niederschlema, Oberschlema and the area of Thuringia were treated in the Schneckenstein mill. The 1.96 Mt of residue was stored in two decantation basins adjacent to the site. Thus, the resulting tailings will contain different materials which considered as a potential source of contamination. The focus of this paper is to determine with accuracy the spatial variation of different physical soil properties in uranium residue at the Schneckenstein site, Germany.

SITE DESCRIPTION

The area of investigation is located in the southwest of Saxony, in the Boda valley approximately 3km from the village of Tannenbergstal/county of Vogtland, Germany (Figure1). In the northwest, the Boda valley is surrounded by the Runder Hubel mountain (837m above sea level) and in the southeast by the Kiel mountain (943m a.s.l). The surface of the site is situated at an altitude of 740 to 815m above sea level. It receives an average annual precipitation of 1050mm.

Also, the area of investigation is located on the southwest border of the Eibenstock granite that could be considered as biotite – syenogranite and covered with a weathered surface layer. Southwest of the area follows the contact zone with quartz-schist.



Figure 1: The Area of Investigation, Uranium Tailings, Schneckenstein

MATERIALS AND METHODS

Field Experimental Work

Four sediment cores were taken at the tailing site by drilling to different depths. Two boreholes were located in each tailing (Figure 2). The first and the second boreholes (GWM 1/96; GWM 2/96) terminated at the granite formation in tailing 2 (IAA I). The third boring (RKS 1/96, Tailing 1(IAA II)) was sunk to a depth of about eight meters but the granite formation was not reached due to technical problems. The fourth boring (RKS 2/98, Tailing1) is 12m deep. The cores (diameter 50mm) were cut into slices of 1m length and transported in argon filled plastic cylinders to avoid ambient air contact.

Laboratory Measurements

Grain-size Analysis

The grain size analysis was carried out in the soil mechanics laboratory in the Institute of Geotechnics Based on DIN18 123. The determination of the grain-size-distribution of samples from the tailing sites was carried out by sieve and sedimentation method (wet-sieve analysis before the sedimentation).

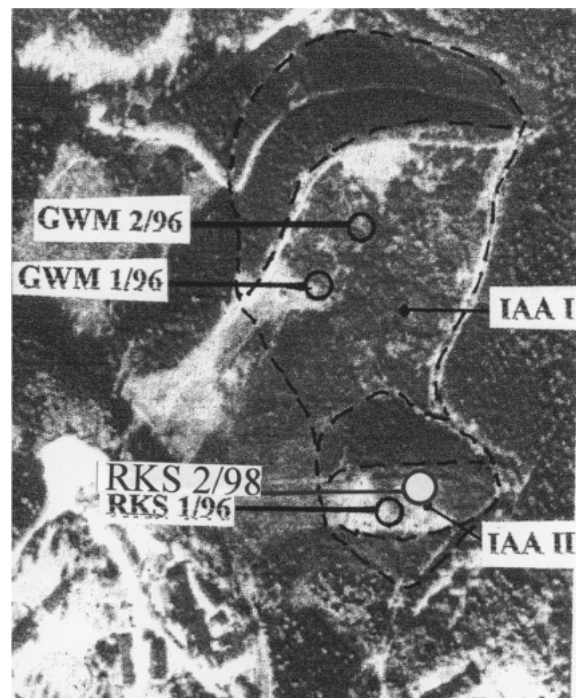


Figure 2: Location of the Borings in the Tailing Sites IAA I and IAA II

The soil materials in the upper layers of the profile from visual observation consist of a mixture medium and coarse grain particles (Figure 3). Therefore it was necessary to use the wet sieve analysis for the part of sample with grain size more than 0,063mm and the hydrometer method (sedimentation) for the part of sample with grain-size less than 0,125mm implementing the methodology described in the paragraph 6.3.2 of the Din 18 123.

For other samples, it was only necessary to involve the hydrometer method because the grain-size of the soil material was less than 0,125mm (Figure 4). The evaluation of the analysis was conducted with the WINSIEB-program.

Coefficient of Permeability

The results of particle-size analysis were used to determine the coefficient of permeability at different depths in the tailing site, thus allowing the prediction of water movement in the soil. The Hazen formula incorporated in the WINSIEB program was applied.

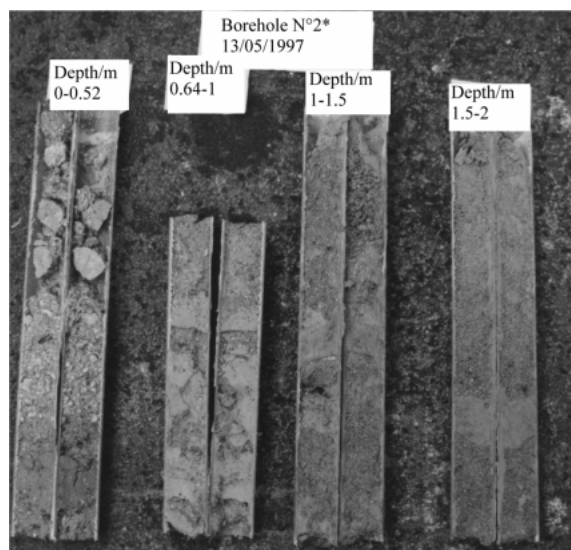


Figure 3: In most tailings the first depth intervals are constituted from heap materials

The coefficient of permeability was also obtained using the triaxial-test carried out according to DIN 18 130 part 1. In this test an undisturbed soil sample about 10cm in length and 46mm in diameter was fitted into a latex hose and placed on a basic-plate of diameter 48mm. The base of the sample was covered with three filter papers of different sizes (1mm, 0,63mm and wide porous filter-paper).

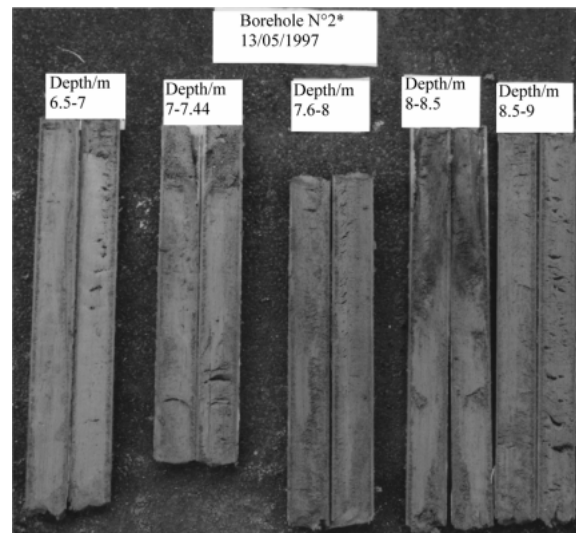


Figure 4: The effect of milling & grinding is clearly demonstrated

Then the sample was then placed on the pedestal. Between the sample-cover and the sample, three filters similar to those mentioned above were also placed as above. By dissolving some Na-fluoride in the water filling the cell, leakage of fluid was well controlled. Finally an inside and outside pressure were applied to the tri-axial-cell. The inside-pressure was calculated using the following formula:

$$P_i = i * L * 0,1 \quad (1)$$

P_i - The inside pressure

i - Hydraulic gradient

L - The length of the sample given in meter

The outside-pressure exceeds the inside pressure by 20 %. The triaxial-test demands a minimum of two weeks for one sample.

The coefficient of permeability (K_f) was calculated according to the following formula:

$$K_f = Q * L / t * F * h \quad (2)$$

Q -flow out water volume

L _ the length of the sample in meters

t _ time interval in seconds
 F _ sample diameter in square meters
 h _ the pressure

Since the coefficient of permeability (K_f) is influenced by the temperature of water, the values determined in the tests were adjusted to a field -temperature of 10°C based on the POISEUILLE formula given as:

$$K_{10} = \alpha * K_T \quad (3)$$

Where:

α - Correction-coefficient.
 K_T - The determined coefficient of permeability corresponding to the test temperature.

The different values of the coefficient of correction (α) for temperature are given in the following table (Table 1):

Table 1: α values at different temperatures

Temperature (T°C)	5	10	15	20	25
α	1,158	1,000	0,874	0,771	0,686

The intermediate values can be linearly calculated.

Water Content Determination

The water content of a soil sample is the amount of water present in a certain quantity of soil in relation to its dry mass:

$$\omega = (M_w / M_s) * 100 \quad (\text{percent})$$

Where:

M_w - mass of water present in the soil mass.

M_s - mass of soil solids.

In order to determine the water-content in the different samples, 10 g of the soil material for the silt or clay material and 200g of sand or gravel, taken at varying depths intervals. The soil material was dried in an oven at a temperature of $105 \pm 5^\circ\text{C}$ to a constant mass for 48 hours. The procedure was repeated several times to determine if a constant mass state has been attained. In order to prevent rewetting by the air moisture, the container with dry the soil was placed in a desiccator as soon as it is cooled. The testing procedure is based on the German Institute for standardisation; DIN 18 121 Part 1.

Specific Gravity

The specific gravity of soil solids ρ_s is defined as the mass of the solid component m_t divided by the volume V_k of the component.

$$\rho_s = m_t / V_k \quad (\text{g/cm}^3)$$

Where: m_t is the mass of dry solids.

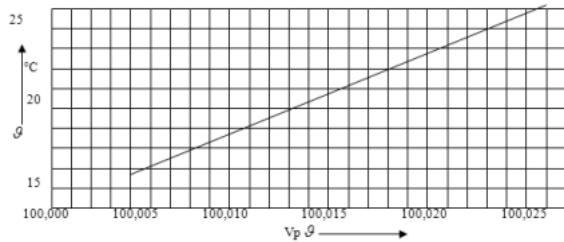
Approximately 20g of pulverised soil sample and dried at a temperature of 105°C was weighed and then filled in a pycnometer. Distilled water was then added until about 2cm above the sample-surface. In order to ventilate the sample, it was heated for about 45 min. The pycnometer was then cooled to room temperature and filled with distilled water up to the brim before it was closed with the plug and weighed. Finally, the temperature of the pycnometer-content θ was recorded.

The V_k was calculated using the formula:

$$V_k = V_p \theta - V_w \theta \quad (\text{cm}^3) \quad (4)$$

Where: $V_p \theta$ is the pycnometer volume at the temperature θ and $V_w \theta$ is the water volume at the temperature θ .

The volume of the pycnometer at the temperature ϑ can be determined using the following temperature-volume-graph:



The volume of water can be calculated using the following formula:

$$V'_w \vartheta = m'_w \vartheta / \rho_w \vartheta = m_2 - (m_p + m_t) / \rho_w \vartheta, (\text{cm}^3) \quad (5)$$

Where: $\rho_w \vartheta$ the density of water at the temperature ϑ can be obtained from the Table 2; (g/cm^3)

$m'_w \vartheta$ the mass of water in the pycnometer at the temperature ϑ ; (g)

m_2 - the mass of the pycnometer filled with the soil material and water; (g)

m_p - the mass the empty pycnometer; (g)

m_t - the mass of the soil material (sample); (g)

Table2: Water density at different temperatures

$\vartheta / ^\circ\text{C}$	$\rho / (\text{g}/\text{cm}^3)$	$\vartheta / ^\circ\text{C}$	$\rho / (\text{g}/\text{cm}^3)$	$\vartheta / ^\circ\text{C}$	$\rho / (\text{g}/\text{cm}^3)$
15,0	0,99913	18,5	0,99853	22,0	0,99780
15,5	0,99905	19,0	0,99843	22,5	0,99768
16,0	0,99897	19,5	0,99833	23,0	0,99757
16,5	0,99888	20,0	0,99823	23,5	0,99745
17,0	0,99880	20,5	0,99813	24,0	0,99732
17,5	0,99871	21,0	0,99802	24,5	0,99720
18,0	0,99862	21,5	0,99791	25,0	0,99707

The procedure described above was accomplished according to the German institute for standardisation; DIN 18 124

Determination of soil density

A cylinder with 50 ml of volume was used to determine the soil density at each depth interval. The cylinder was filled with well pressed soil material and its weight was determined using a balance with an error correction up to 0,1%. Each parameter was determined using the formula below.

The calculation of soil density and related parameters are based on the following mathematical equations:

$$\rho_{\text{wet}} = \text{mass of soil sample } (m_w) / \text{volume of the container } (V_c)$$

If the water content ω of the soil material is well known, the dry unit density of the soil material is:

$$\rho_{\text{dry}} = \rho_{\text{wet}} / 1 + \omega$$

(The water content is determined after the DIN 18 121 part1)

The dry mass is calculated as:

$$m_d = m_w / (1 + \omega) \quad (6)$$

The water volume is calculated as:

$$V_w = (m_w - m_d) / \rho_w \quad (7)$$

The dry volume is calculated as:

$$V_d = m_d / \rho_s \quad (8)$$

(ρ_s is the specific gravity determined after the DIN 18 124)

The pore volume is calculated as:

$$V_p = V_c - V_d \quad (9)$$

The total porosity is calculated as:

$$n = V_p / V_c \quad (10)$$

The saturated porosity is computed as:

$$n_s = V_w / V_c \quad (11)$$

The degree of saturation is calculated as:

$$S_r = V_w / V_p \quad (12)$$

The wet density is determined after the DIN 18 125 Part1.

RESULTS & DISCUSSION

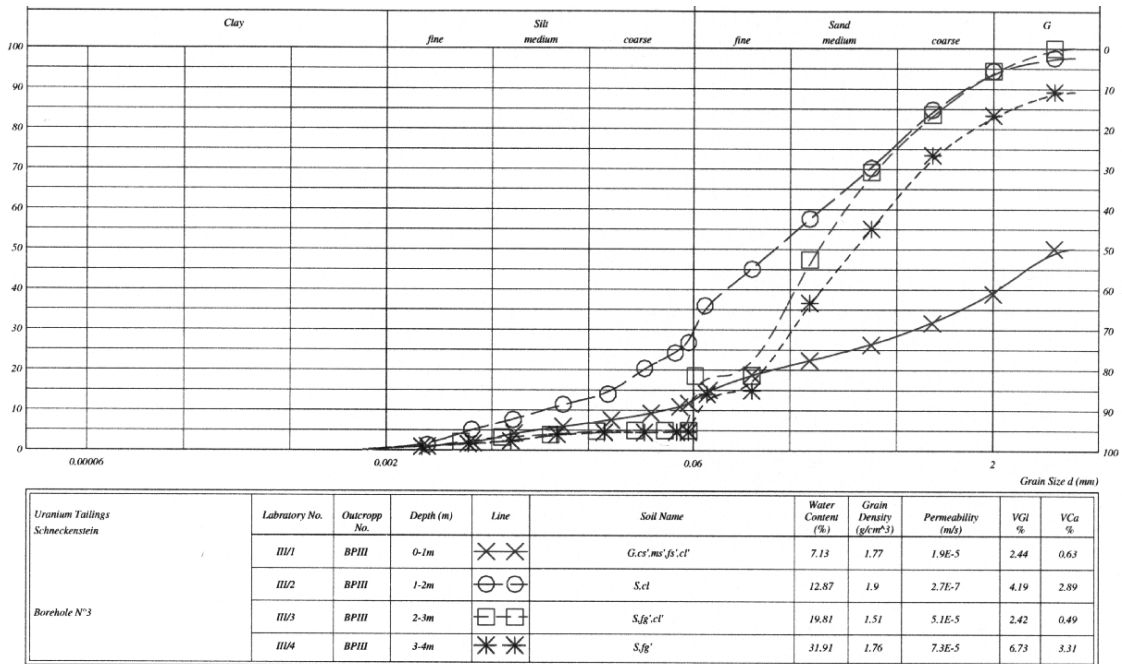


Figure 5: Sieve Analysis (1)

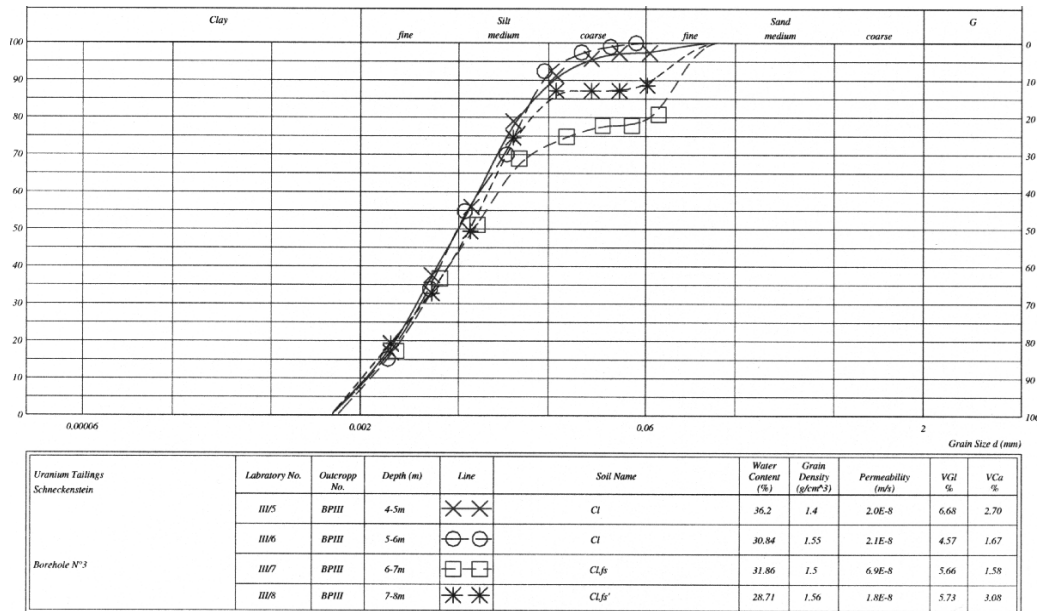


Figure 6: Sieve Analysis (2)

Grain size distribution

On the basis of the coefficient of uniformity defined as d_{60}/d_{10} where d_{60} is size (mm) passing 60 % and d_{10} size (mm) passing 10 %; the soils can be described as well graded/poorly sorted since the values are > 2 especially in the uppermost part of the tailing and the last two samples in borehole N°4. In addition, the values of C_c where $C_c = d_{30}^2/d_{60} \cdot d_{10}$ (Bell, 1992).

Where d_{30} is the size of the grains on the cumulative curve where 30 % of the particles are passing, are generally between 1 and 3. This also places the materials in the well grade class.

Based on the soil classification scheme of Wagner, (1957) and Anon, (1981), the materials of the uppermost part of the tailings and the last two samples from borehole N°4 have a wide range of sizes. This is from silt to cobbles (0.006 and 200mm). In the lower part, the materials are mostly of silt-fine sand (0.006 and 0.2mm), Figure 5 & Figure 6. The uniform grain size in the deeper level may be

due to the uranium leaching process. In this case, it is probably due to alkaline procedure rather than acidic. Alkaline because it requires the crushing of the materials (IAEA, 1993).

The coefficient of Permeability (K_f)

The K_f was computed using the Hazen's relationship. The relationship is in the following form:

$$K_f = C \cdot d_{10}^2, \quad (13) \quad (\text{Kezdi, 1969; Holting, 1996})$$

$$\text{Where } C = 0.7 + 0.03t / 86.4$$

The results show that, high K_f values were recorded in the uppermost tailings with values as high as 10-5 m/s. Thus these materials can be described as moderately permeable (Anon, 1977). However, in the deeper intervals, the K_f values are in the range of $10^{-8} - 10^{-7}$ m/s except in the last two intervals of the fourth borehole. The material is described as slightly permeable Figure 7.

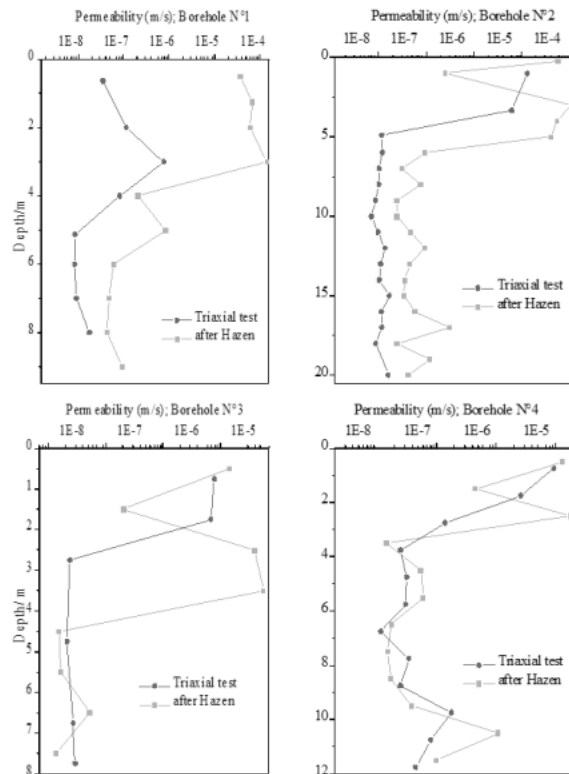


Figure 7: The coefficient of permeability by means of two methods

As shown in Figure 8, the K_f values obtained from the Triaxial test are different compared to those obtained by Hazen formula. The variation is mainly due to the heterogeneity of the tailings material and the different methods used.

The dry density

The dry density is found to be less than 1.8 in all tailings and it is classified as very low after Anon, (1979), (Figure 9).

The grain density

The values of the grain density vary between 2.53 and 2.85 g/cm³ in most of the tailings. According to Bowles, (1992), the high grain density is caused by the presence of high concentrations of minerals containing iron (Figure 9).

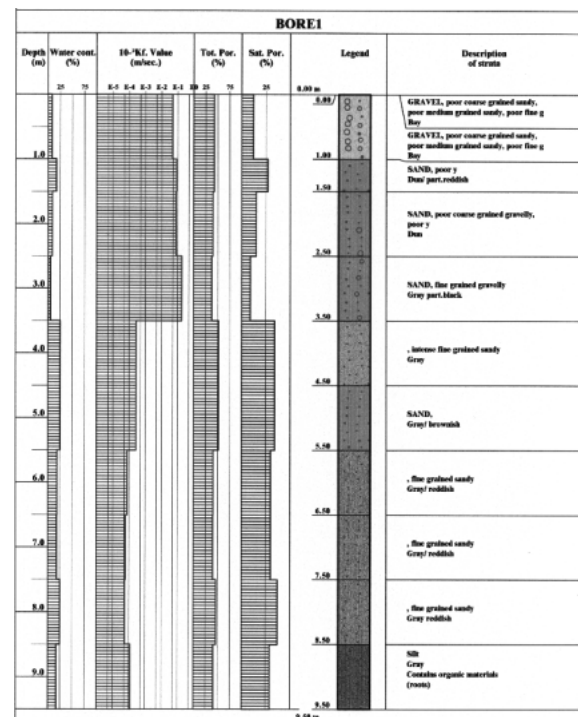


Figure 8: Physical Soil Properties variation with depth (1)

The total porosity

The total porosity is dependent on particle size in boreholes N°3 and N°4 and it increases as the grain size decreases. However, in the other boreholes, the relation is not defined. The values (> 30 %) are considered as very high (Anon, 1979). These values are in good agreement with data from some other locations (Maidment, 1992), (Figure 7).

Degree of saturation (Sr)

The degree of saturation is defined as:
 $S_r (\%) = 100 \cdot e_w / e$; (Terzaghi & Peck, 1967)

Where: e_w the volume occupied by water per unit volume of soil matter and e is the void ratio of the soil.

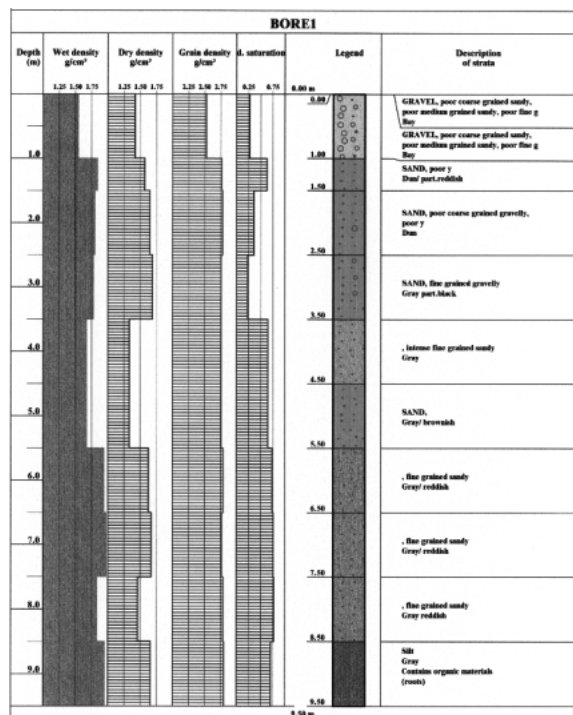


Figure 9 : Physical Soil Properties variation with depth (2)

The values range from 23 to 77 %; 27 to 83 %; 30 to 83 % and from 27 to 74 % with mean values of 57, 64, 58 and 58 % in the first, the second, the third and the fourth boreholes respectively.

In the uppermost part of the tailings and the last two samples from the borehole N°4, the degree of saturation is in the range between 26 and 50 %, this is classified as damp according to Terzaghi & Peck, (1967). In most of the other analysed samples (treated material), the Sr lies between 51-83 %, thus the tailing materials may be described as moist and rarely wet (Terzaghi & Peck, (1967) (Figure 7).

It is noteworthy to point out that the variation of some of the physical soil properties is related to the mineralogical variation in the tailing materials.

CONCLUSION

From the chemical point of view, an increase of the cation exchange capacity of the tailings material is expected since the milling process increase the number of broken bonds around the edges of silica-alumina particles which are considered as a function of grain size; the smaller the particles, the larger the exchange capacity, and the irregularities in the lattice structure (lattice distortions) as well, providing a greater number of unsatisfied valences at surfaces and edges of the soil units (Degens, 1965). Since most of the tailings seem to be stagnant, the probable transport of contaminants is expected to be in relation with the upper parts of the tailings. Besides, the water content is high in most of the tailing sites. Thus an important interaction between the mineral matrix and the pore waters may occur due to the high total porosity and the degree of saturation mainly of the processed materials.

REFERENCES

- AHUJA, L.R. et al., (1989) : Evaluation of spatial distribution of hydraulic conductivity using effective porosity. Soil Sci. 148, 404–411.
- ANON, (1977): The description of rock masses for engineering purposes, working party report, Q.J. Engg Geol., 10, p. 355-88.
- ANON, (1979): Classification of rocks & soils for engineering geological mapping, part I: rock & soil materials, Bull. Inst. As. Engg. Geol., N°19, p. 364-71.
- ANON, (1981): Code of practice on site investigation, BS5930, British standards institution, London.
- BELL, F. G., (1992): Engineering properties of soils and rocks, third edition, Butterworth Heinemann.

- BRAUD, I., et al., (1995) : A stochastic approach to studying the influence of the spatial variability of soil hydraulic properties on surface fluxes. *J. Hydrol.* 165, 283–310.
- BOWLES, J. E., (1992): *Engineering properties of soils & their measurements*, fourth edition McGraw-Hill, Inc.
- DEGENS, E. T., (1965): *Geochemistry of sediments*, A brief survey, Prentice-Hall, Inc.
- FLINT, E.L. & SELKER, J.S., (2002): Use of porosity to estimate hydraulic properties of volcanic tuffs. *Advances in Water Resources* 26 561–571
- FOLK, R.L., (1966): A review of grain-size parameters, *Sedimentology* 6 73–93.
- HÖLTING, B., (1996): *Hydrogeologie – Einführung in die allgemeine und angewandte Hydrogeologie*. 5. Auflage. Enke Verlag Stuttgart, 441 pp.
- IAEA, (1993): Uranium extraction technology, technical reports series N°359: p. 75.
- KEZDI, A., (1969): *Handbuch der Bodenmechanik*, seite 128, VEB Verlag Berlin.
- KRUMBEIN, W.C., (1934): Size frequency distribution of sediments, *Journal of Sedimentary Petrology* 4 65–77.
- LEWIS, D.G. & McCONCHIE, D., (1994): *Practical Sedimentology*, Chapman and Hall.
- LEWIS, D.G. & McCONCHIE, D., (1994): *Analytical Sedimentology*, Chapman and Hal.
- MAIDMENT, D. R., (1992): *Handbook of hydrology*, 6.9, McGraw-Hill, Inc.
- MORGAN, R.M. & BULL. P.A., (2007): The use of grain size distribution analysis of sediments and soils in forensic enquiry. *Science and Justice* 47 125–135
- MOUSTAFA, M.M., (2000). A geostatistical approach to optimize the determination of saturated hydraulic conductivity for large-scale subsurface drainage design in Egypt. *Agric. Water Manage.* 42, 291–312.
- NICHOLS, G., (1999): *Sedimentology and Stratigraphy*, Blackwell Science Ltd., Oxford.
- PERRONE, J. & MADRAMOOTOO, C.A., (1994): Characterizing bulk density and hydraulic conductivity changes in a potato cropped field. *Soil Technology* 7 261-268
- PETTIJOHN, F.J. et al., (1972): *Sand and Sandstone*, Springer-Verlag, Berlin.
- TERZAGHI, K. & PECK, R. B., (1967): *Soil Mechanics in Engineering Practice*, p. 26, Wiley.
- VACHAUD, G. et al., (1998): Stochastic approach of soil water flow through the use of scaling factors: measurement and simulation. *Agric. Water Manage.* 13, 249-261.
- WAGNER, A. A., (1957): The use of the unified soil classification system for the bureau of reclamation, *Proceedings 4th international conference of soil mechanics foundation Engg*, 1, p. 125-34, London.

ENHANCED DEWATERING OF FINE TAILINGS USING ELECTROKINETICS

Andy Fourie

School of Civil & Resource Engineering, University of Western Australia, Perth, Australia

ABSTRACT: There are many initiatives for dealing with soft, fine-grained tailings, including using some form of co-disposal, where coarse and fine tailings are combined before placement into a storage facility. This paper deals with an alternative technique for treating the fine fraction of the tailings to increase the solids content, potentially providing for either in-situ dewatering or as an alternative for deposition of the fine fraction alone. The technique is based on the established concept of electrokinetic dewatering. The novel feature of the work is the use of a conductive polymer as electrodes, which negates the problems of corrosion usually associated with electrokinetic dewatering, where metallic anodes corrode at an extremely rapid rate. The conductive polymer was produced in two forms, namely tubular wells that could be used for in-situ dewatering of deep deposits of fine-grained tailings, and a conductive filter belt for in-plant treatment. Results from both configurations of the polymer electrodes are provided in the paper, and include data for a range of tailings, including mineral sands slimes, smectite-rich diamond tailings and coal tailings. A surprising result was the wide range of tailings for which the technique appears to be viable, with tests on highly saline bauxite residue proving effective. Based on a large number of laboratory benchtop tests, and a limited number of larger field tests, the likely power consumption rates of the polymer electrodes are summarised and compared with data for a conventional clay.

INTRODUCTION

Many tailings disposal facilities contain material that undergoes extremely slow self-weight consolidation. Aside from the dangers posed by such poorly consolidated material (e.g. the potential for flowslides or mudrushes in the event a breach of the impoundment occurs), are problems of rehabilitation of the facility once it is closed. The extremely low undrained shear strength of many such deposits means that earthmoving machinery cannot operate on the surface and thus placement of cover material and establishment of a growing medium is extremely difficult.

In many operations it has been found that it is not adequate to rely on self-weight consolidation to achieve the required degree of dewatering (and thus shear strength gain). As an example, in the phosphate industry in Florida, USA, the tailings have very low solid contents (of the order of 3% to 6% solids) and consolidation to the required solids content of 20 to 25% may take several decades (Shang and Lo, 1997). One solution that has been adopted is the use of prefabricated vertical drains (see Jakubick and Hagen, 2000 and Lersow and Schmidt, 2006). The disadvantage of this approach is that in order to develop significant settlements, a surcharge of imported fill

needs to be placed over the tailings to produce the excess pore pressures that will drive the consolidation process when dissipation of these pore pressures occurs. This process is expensive and time consuming and the imported fill occupies airspace that could otherwise have been used to store additional tailings.

Recourse may be made to a range of other dewatering techniques, including electrokinetic dewatering, as pioneered by Casagrande (1949) for accelerating the consolidation of natural soft clays. Electrokinetic dewatering of fine grained mine wastes has been attempted by Veal et al (2000) amongst others, but with relatively little success. There are no instances of very large-scale implementation of the concept in this type of application. Possible reasons for this were suggested by Shang and Lo (1997) as including high power consumption, indiscriminate use of the technique and improperly designed operating systems. Intrinsic to these difficulties may be a limited understanding of electrokinetics, according to Shang and Lo (1997).

OPTIONS OFFERED BY ELECTROKINETIC DEWATERING

The specific phenomenon of interest in the electrokinetic in-situ dewatering of tailings is that of electroosmosis. Although water molecules possess an overall neutral charge, they are polar. This means that they are attracted to positive particles and ions in solution and orient themselves around the ions. If an electric field is set up within a matrix that is saturated with water (such as in a tailings storage facility) the positive ions tend to move toward the zone of lower potential (the negative electrode for instance). As the ions move, the water molecules surrounding it are dragged with it. Hence in soils, electroosmosis usually involves the flow of pore water to the cathode (negative electrode). In addition to the water molecules surrounding the ion, frictional drag is created by the motion of

the ions, and this helps to transport additional water. (Abiera et al, 1999).

There have been a number of studies evaluating the viability of electrokinetic (EK) dewatering of mine tailings. Details of many of these are given in Fourie et al (2007). Despite the overall effectiveness of the technique in decreasing the water content of the tailings, this usually came at high cost (in terms of energy consumption per unit of tailings dewatered), problems with corrosion of the anodes, and difficulty in collecting and removing water that drained to the cathode.

The recent development of conductive polymers that have been formed into grids and tubes holds the promise of solving the above difficulties. These materials, termed electrokinetic geosynthetics (EKGs) have been tested in a range of laboratory experiments and more recently in some field experiments. A comprehensive background is given by Lamont-Black (2001), with specific field experiments being reported by Jones et al (2008). The EKG used in the experiments described in this paper consists of a mesh made from a metal wire stringer coated in a conductive polymer. When used as a cathode, the tubular electrode is enveloped in a geotextile sleeve such as a nonwoven, heatbonded product. Its great advantage over conventional metallic electrodes used in soil improvement applications is that it overcomes the difficulties of corrosion, sufficient electrical contact and physical removal of water from the system (Lamont-Black, 2001). Properties of the EKG's are given in Table 1.

Table 1. Properties of electrokinetic geosynthetics (EKG) used in laboratory tank tests and field tests.

Property	Test method	Value
Density @ 23° C	ISO R1183	1063 kg/m ³
Tensile strength yield	ISO 527	18 MPa
Tensile strength break	ISO 527	25 MPa
Elongation @ break	ISO 527	160%
Surface resistivity	CABOT-D042	5x10 ² Ω/sq
EKG tube diam.		7cm

LABORATORY TESTING

The majority of the experimental work described in this paper was carried out at laboratory scale, and a range of different issues were investigated, including:

- Whether electrokinetic dewatering was applicable to a range of different tailings materials.
- What the effect of salinity was on the performance of the technology.
- Whether improved performance could be achieved by manipulating the manner in which voltage was applied.
- The effect of electrode orientation.

Electroosmotic (EO) cell tests

Two different sets of laboratory tests were carried out. The initial set of laboratory tests were designed to test the viability of dewatering the tailings electrokinetically and therefore used

conventional metal electrodes. An electroosmotic testing cell based on that described by Hamir et al (2001) was manufactured for this phase of testing. It was made entirely of Perspex and included a pore pressure transducer in the base pedestal and a drainage outlet connected to the top cap. The cell had an internal diameter of 145mm and samples with an initial height of up to 150mm could be tested. The cell was tested at pressures up to 175kPa, although the maximum used in these tests was 30kPa. The electrodes used in these tests were perforated copper discs.

The cathode was always placed at the top of the specimen. A layer of filter paper and a 1.3mm thick non-woven needle-punched polyester disk were sandwiched between the cathode and the loading piston and between the anode and the base pedestal. This was to prevent loss of solid particles through the drainage system. The electrodes were connected to a power supply via coated electric wiring. All measurements of load, displacement, expelled pore water, electrical current drawn and base pore pressure were logged continuously. The pH of samples of expelled pore water was checked periodically.

Tests on various tailings were firstly carried out without the application of an electrical potential across the specimen, i.e. these tests served as control tests (duplicate control tests were carried out in a 150mm diameter Rowe cell and very similar results obtained to those from the electro-osmotic cell).

Tank tests

A simple test was developed to evaluate the viability of EK dewatering of tailings samples. A plastic tub having a capacity of approximately thirty litres was filled with the tailings slurry, electrodes installed into the tailings, the electrodes connected to a

DC power supply, and the power turned on. Most tests used a voltage of 12V (which gave a voltage gradient of about 0.5 V/cm), although some tests used higher voltages (up to 30V) as shown in Table 3. A schematic of the testing arrangement is shown in Figure 1 and a photograph of a test in Figure 2. As soon as the tubular cathode electrode filled with water, the water was extracted and the volume measured. In addition, the mass of the tank was continuously monitored, to provide a measure of the total mass of water lost during the test. This total loss is made up of three components; the recovered water mentioned above, the evaporated water and water lost through electrolysis. In the latter stages of the testing programme, the mass lost through evaporation was minimised by covering the tub with a thin plastic film. In earlier tests, control tests were run in which the rate of evaporation from a tailings-filled tank in the absence of applied voltage was monitored to quantify the evaporation losses, thus providing an indirect measure of the third component, the loss due to electrolysis.

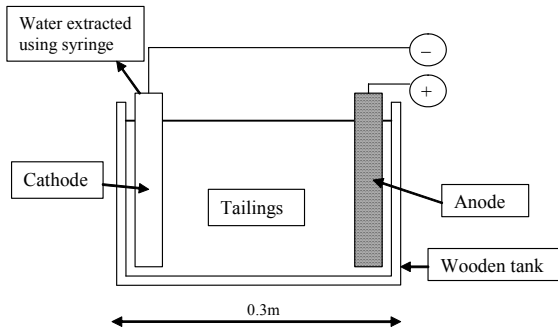


Figure 1. Schematic of laboratory tank test setup.

RESULTS

Effect of voltage on rate of consolidation

The results of tests on mineral sands tailings MS1 using the EO cell are shown in Figure 3.



Figure 2. Photograph of completed test in tank.

The base test was carried out under an imposed vertical stress of 15kPa, with zero applied voltage. Subsequent tests had applied voltages of either 10V or 30V, with the applied vertical stress being either 10kPa or 30kPa.

The test with zero voltage took 50 hours for full consolidation to occur, whereas tests with an applied voltage were significantly quicker. For ease of comparison, the time for 95% consolidation, t_{95} , has been used as an indicator of the effect of applied voltage. These data are summarised in Table 2.

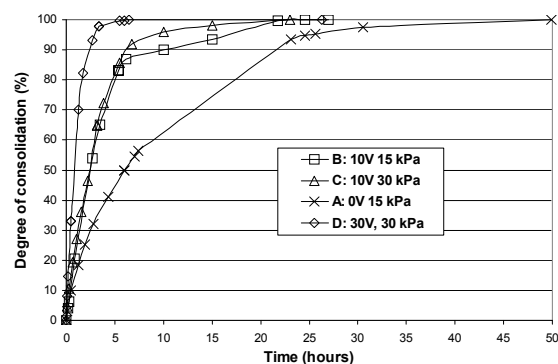


Figure 3. Effect of voltage on consolidation

Table 2. Time to 95% consolidation in EO cell tests on mineral sands tailings MS1.

Test	t_{95} (hours)
A	26
B	17
C	8.5
D	2.5

In all cases, applying a voltage during the consolidation phase resulted in more rapid consolidation. Comparing tests A and B, there is a 35% reduction in time, and between tests C and D a 70% reduction. Clearly the use of electrokinetic dewatering has the potential to dramatically increase consolidation rates of clayey materials. A further advantage is that it is not necessary to apply a surface surcharge (such as a sand fill) to generate consolidation. As shown in the results from the tank tests later in the paper, significant EK consolidation is possible in the absence of any significant vertical stress. Finally, the amount of consolidation is greater in tests where a voltage is applied than in zero volts tests, not just the rate at which consolidation occurs.

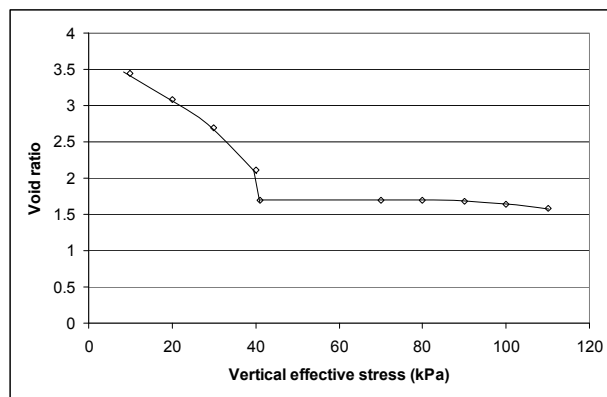


Figure 4. Effect of applying a voltage of 12V (at 40kPa vertical effective stress) on subsequent consolidation behaviour of kaolin.

For example, the result shown in Figure 4 is for an EO test on consolidation, where kaolin was consolidated to a vertical effective stress of

40kPa. Once consolidation was complete, a voltage gradient of 0.5 V/cm was applied, and a further 2mm consolidation occurred, equivalent to 36% increase over the consolidation under the 40kPa load alone. Another interesting observation is that once the voltage was switched off and additional vertical stress applied, there was virtually no further consolidation, as shown by the loading path from 40 to 110kPa in Figure 4. It appears that the application of voltage has provided a significant 'pseudo-preconsolidation' value to the kaolin.

Similar results to those shown in Figure 3 were reported by Fourie et al (2007) for different tailings materials, and it was felt that the results were sufficiently promising to explore the potential application of EKGs for accelerating consolidation of tailings.

Laboratory tank tests

The form of the EKG grids make it virtually impossible to incorporate them in the EO cell. This, together with the fact that we wanted to conduct tests at very low effective stress values, resulted in the use of the simple tank tests for the EKG follow-up study. In these tests, two EKG tubes were pushed into the tailings-filled tub, with one of the electrodes (the cathode) being sheathed with a heat-bonded nonwoven geotextile. Within an hour of installing the EKGs, the required voltage was applied and the tank placed on a scale in the laboratory, to provide a measure of overall mass loss. Soon after the application of voltage, water began to flow into the cathode, irrespective of the type of tailings tested. The cathode was emptied using a syringe as soon as it reached a level near the surface of the tailings in the tank. Measurements included daily current readings, and occasional pH and conductivity readings of the water collected from the cathode.

A typical result from the tank test is shown in Figure 5. The material tested was kaolin clay, which provides a reference result for the mine tailings samples that were tested subsequently. The test was terminated before flow into the cathode ceased completely, in order to provide a turn-around time for tests of about a week. As can be seen, at the time of stopping the test, flow was still occurring, albeit at a decreasing rate. Also shown on this figure is the current drawn by the system. The result is typical of all tests, with an initial spike in current followed by a very rapid decrease until a relatively stable value (in this case 10mA) is reached. The energy consumed during a particular test was calculated by integrating the product of voltage, current and time to produce a unit of kWhour. This was converted to kWhour per dry tonne (kWh/dt) by dividing by the initial dry mass of material in the tank. For the test shown in Figure 5, the value was 2.27 kWh/dt and this result serves as a useful baseline value for discussion of the tailings test results.

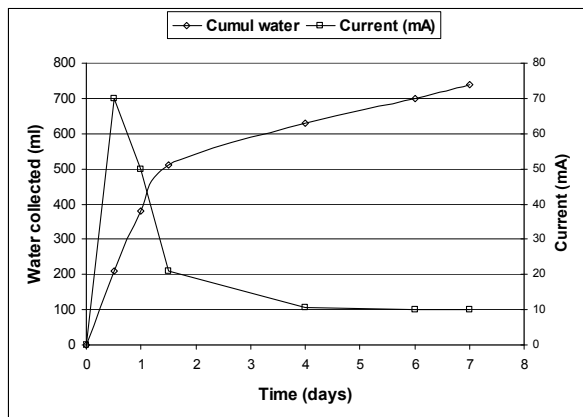


Figure 5. Cumulative water collected and variation of current with time in tank test on kaolin clay.

Effect of salt concentration on dewatering

Before describing results from tests on tailings materials, the change in dewatering effectiveness as a consequence of the salt concentration of the material being tested was evaluated. This was done to compare results with the suggested

limitations of the technology reported in the literature as being equivalent to an electrical conductivity of around 0.5mS/cm (see Casagrande, 1983).

A series of tank tests was carried out in which the molarity of the salt concentration in the water added to kaolin was adjusted by adding swimming pool salt to the mixing water prior to addition to the dry kaolin clay. Molarity values of 0.001, 0.01 and 0.1 were used, in addition to the base test that used tap water only. The resulting conductivity values are given in Table 4. Tests were only run for four days. All tests started at a moisture content of 85% (compared with the liquid limit of 60%), and the average water content measured at the end of four days is also given in Table 4.

Table 4. Molarity of salt solutions and resulting initial conductivity values used in kaolin tank tests, plus the value of final moisture content.

Molarit	Conductivity (mS/cm)	Final moisture content (%)
0	0.2	51
0.001	0.65	56
0.01	1.53	57
0.1	7.6	66

There is clearly a reduction in dewatering rate as the salt concentration of the pore water increases. It would not be meaningful to compare energy consumption rates for these tests, as they all end up at different values of moisture content and thus the amount of water extracted during the four day tests varied. This illustrates that the units used in this paper (kWh/d.t.), although superior to the more commonly used kWh/m³, are still deficient, because they do not indicate the change of moisture content (i.e. the volume of water extracted) during

an experiment. This issue is discussed in more detail later in the paper.

Table 3. Characteristics of tailings tested.

Tailings	Liquid Lin (%)	Plastic Lin (%)	pH	kWh/d.t	Change in wat content (%)	V/cm
Mineral sands (MS1)	66	29	8	1.9	37	0.24
Mineral sands (MS3)	110	34	8.2	3.8	130	0.15
Diamond (D)	76	38	8.5	37.3	47	0.35
Coal (C)	65	24	9.1	9.2	31	0.5
Bauxite (B)	55	27	9.5	11.0	12	0.5
Kaolin (K)	60	28	7.5	2.3	26	0.5

Five different tailings were tested in the laboratory tank and the details of these tests are compared with the results of a test on kaolin in Table 3. Unfortunately the voltage gradient was not the same in all tests. However, the gradients are relatively close and some general observations can be made. Firstly, the use of energy consumption units of kWh/d.t. can be misleading. For example the bauxite tailings only used 2.3 kWh/d.t. compared with 3.8 for the MS3 tailings. However, the comparative decreases in water content were 12% and 130% respectively. Clearly we need to refine this unit of measure to reflect how much water was removed per unit of energy consumed. An alternative measure that is sometimes used, millilitres per milliamp-hour (ml/mA-hr) is better in this regard, but still does not indicate the relative starting and end points of the test. For example, decreasing the water content by 10% for a soil that is already below the liquid limit will be much more difficult than decreasing it by 10% for soil initially above the liquid limit. Perhaps incorporation of the change in liquidity index will ultimately provide a better measure of energy efficiency, but a suitable unit of measure does not currently exist.

One result to stand out in Table 3 is the relatively higher energy consumption rate for

the diamond tailings. All the other material tested had kaolinite as the dominant clay mineral, whereas the diamond tailings were predominantly smectite. As described by Gray and Mitchell (1967), the effect of the clay minerals present in a soil (or tailings) can significantly change the effectiveness of EK dewatering, with a decrease of up to 10-fold between sodium kaolinite and sodium illite at similar values of water content. This result was confirmed by an extensive study reported by Lockhart (1983).

The two mineral sands tailings, which had a high percentage of kaolinite, showed low values of energy consumption for very significant decreases in water content. It is suggested that tailings with a high kaolinite clay content are likely to respond extremely well to EK dewatering. The salinity of the pore water is also a determining factor, but even the bauxite tailings, with a conductivity of 17 mS/cm, responded to EK dewatering, albeit less impressively than some of the other tailings. This points to the technique possibly being attractive for the dewatering of oil sands tailings, where the conductivity is likely to be below 2.5 mS/cm, and which typically has a high percentage of kaolin clay (FTFC, 1995).

Potential application of EKGs for in-situ dewatering of tailings

The large volumes of fine oil sands tailings that are currently stored in impoundments are a major concern for this industry. Although the recently announced directive (ERCB Directive 074) may begin to reduce future volumes, these legacy impoundments require some form of treatment.

Vertical electrodes

The potential of dewatering (and thus stabilising) these impoundments and reducing their volume, using EK dewatering would present some major challenges. Assuming the tailings are responsive to EK dewatering, and the inference from the results presented in the preceding section would seem to indicate it is likely, the logistics of installing EKGs would require careful planning and evaluation. One idea would be to construct a pioneer access causeway onto a section of mature fine tails (MFT), from where crane rigs similar to those used for conventional vertical drain installations could be used. From work carried out by Lockhart and Stickland (1984), amongst others, a suitable arrangement of the EKG electrodes would be a hexagonal array of anodes, centred on a single cathode. The cathode would be sleeved in a geotextile and act as the collector well. Water would have to be collected from the cathodes, to prevent short-circuiting of water back to the anodes.

An outdoor test using a 3m³ tank, filled with MS1 tailings was carried out to trial this concept. The arrangement is shown in Figure 6, and could be expanded to cover any required area simply by adding more arrays. For the installation shown in Figure 6, an electrode spacing of 1m was used. This could be increased to at least 2.5m, although of course a higher voltage would need to be applied to achieve the required voltage gradient. Given the high water content, and thus low undrained

shear strength of the MFT, installation of the tubular EKGs is expected to require relatively little driving effort. A trial field installation could confirm this.

Issues to be addressed with the suggested layout include the need for an adequate DC power supply system, extensive cabling to connect all electrodes, and a system for collecting and removing the drainage water.



Figure 6. View of outdoor experiment after a week of testing, MS1 tailings.

To date there have been no large scale installations of EKG dewatering systems for tailings storage facilities, although over two decades ago Lockhart and Stickland (1984) proved the viability of the technology by dewatering a 5 000 tonne block of coal tailings to a consistency described as 'spadeable', which indicates a significant improvement on the soft slurry that they started with. Why then has the technology not caught on? One issue might be the poor durability of metal electrodes, which were the original material of choice. Rapid corrosion of the anodes was a major problem, with rates as high as 1.1kg/dry tonne reported by Lockhart and Stickland (1984). The advent of EKG electrodes, which are significantly more durable, has alleviated this concern. In addition, the tubular EKGs are able to collect water for subsequent removal, unlike

conventional metal electrodes. Perhaps the biggest impediment to use of the technology is the lack of a demonstration site; everyone wanting to be 'first to be second'. Installation of a full-scale trial EKG dewatering scheme will require a relatively significant commitment, and it is only likely to occur when the potential user is convinced that the likely returns (in terms of water recovery, improved stability and reclamation potential, and reduced volume) are sufficient to warrant the risk of the scheme not working.

Horizontal electrodes

An alternative to the above idea could be the use of sheets of EKG electrodes oriented horizontally. This layout could be used during the tailings deposition phase, whereas the vertical orientation option discussed above is more applicable to situations where an existing impoundment is to be dewatered.

This idea was evaluated by cutting the tubular EKGs lengthwise to form a sheet and placing one of these sheets at the base of the tank described earlier. The tank was filled with tailings, followed by placement of a second EKG sheet on the surface of the tailings. A picture of this arrangement is shown in Figure 7, where the upper sheet was used as the cathode. This meant that EK driven flow was upward and had to overcome gravity-driven hydraulic flow.

This test was found to have a similar energy consumption rate as vertically oriented electrodes tested in the same material, even though water was not removed from the surface as it accumulated during EK dewatering. This gradual build-up of head would have counteracted the EK flow, but did not appear to be significant enough to prevent the electrodes functioning satisfactorily.

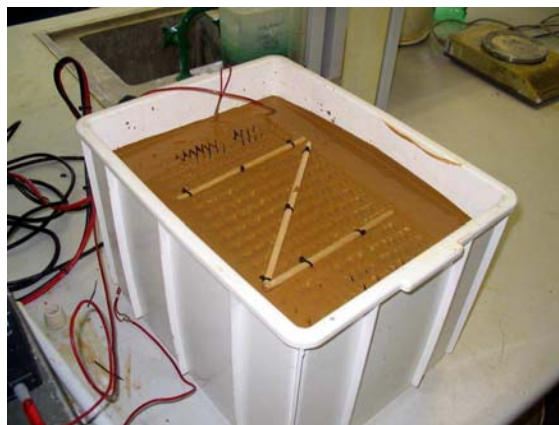


Figure 7. Illustration of layout using horizontal electrodes.

Although only a single test was carried out using horizontally oriented electrodes, the performance of the system was satisfactory and pointed to another possible way of implementing dewatering using EKG electrodes.

Alternative application of EKG technology for dewatering of mine tailings

Most tailings streams undergo a limited amount of thickening in some form of thickening vessel such as a thickening tank. There are some operations, particular examples being coal washeries, where thickening sometimes takes place on a belt filter of some type. This approach is often adopted when the tailings are particularly clayey and settle very slowly under self-weight. Conventional tank-thickening is thus usually unsuccessful. A problem with belt-thickening is clogging of the filter belts and the resulting need to wash the belts regularly, leading to high maintenance and operating costs. In addition, conventional belt filters do not generally achieve very high solids content (low water content) values because their effectiveness is limited by the low hydraulic conductivity of fine tailings.

An EKG belt filter would avoid the problems of clogging and of low hydraulic conductivity because the technique does not rely on conventional pressure-driven flow. In fact, as discussed by Jones et al (2008), the flowrates generated by an electrokinetic system are virtually the same in a bentonite slurry as they are in a fine sand. The phenomenon is not particle size (or void size) dependent. Lamont-Black et al (2006) showed that EKG filter belts could be successfully used to dewater sewage sludge, a material that is notoriously difficult to dewater. Improvements over conventional belt filters were significant, with improvements of the dry solids content from 19% to >30% being achieved. These promising results led to an extended field campaign to evaluate the potential use of EKG belt filters for dewatering mine tailings.

An existing filter belt machine was retro-fitted with a purpose-designed EKG belt. The machine was transported to South Africa, where a diamond tailings similar to the D tailings (see Table 3) studied in this paper, was evaluated. Field trials were run over a period of about nine months, and increasingly impressive results were obtained. As an example, solids contents in excess of 78% were achieved, whereas a similar test using conventional pressure induced flow, without voltage, resulted in a final solids content of 58% after the same residence time. The solids content values were increased to such an extent that the material took on the consistency of soft particle-board after treatment. The resulting tailings could be transported by truck or conveyor to the tailings storage area and, if required, compacted using traditional earth-compacting equipment. The water content corresponding to 78% solids places it close to the optimum water content for maximising density using conventional compaction techniques. This potentially provides a completely new approach to tailings management, obviating the need for large, high-risk tailings storage facilities.

A current limitation of the EKG filter belt machine is the treatment capacity. Typical treatment rates using the small retro-fitted filter belt machine discussed above were about 20 m³/hour. This is orders of magnitude lower than that required to treat typical oilsands tailings volumes. However, there is no reason the filter belt machines could not be scaled up significantly and no reason appropriately sized EKG filters could not be manufactured. Once again, the lack of an existing demonstration site to allay fears about large-scale viability hamper the implementation of the technology in the form described here. An alternative could be to only treat a proportion of the tailings stream using an EKG belt, with the remainder being treated using current techniques. The EKG treated tailings could be used to construct part of the retaining embankments to contain the conventionally treated tailings.

CONCLUDING REMARKS

Strategies for managing tailings have always had to strike a balance between the need to store the material safely while ensuring environmental impact is minimal or zero, but still keep costs down to an absolute minimum. After all, there is usually no money to be made from tailings; they merely represent a necessary evil that must be managed.

The mining industry has been relatively proactive in developing self-regulation procedures for managing tailings storage facilities, with most operations now having Operations Manuals and many site personnel undergoing appropriate training. However, failures and breaches of TSFs continue to occur throughout the world. As public scrutiny of mining operations intensifies in the light of these transgressions, government intervention is likely to occur, as indeed seems to be the case with the recent Tailings Directive in Alberta (ERCB Directive 074). It seems

inevitable that unit costs of tailings management are going to increase with time as a consequence of these developments.

The technology described in this paper, which is based on the principle of electrokinetic dewatering, may provide one of the new technologies for managing problematic fine tailings such as the oilsands fine tailings. It is by no means a developed technology, and there are understandable concerns about its robustness and applicability to the treatment of large volumes of tailings. Nevertheless, in this era of enhanced scrutiny and almost inevitable government intervention, investments in new technologies that address the fundamental problem of managing fine tailings, namely reduction of the volume of water entrained in the tailings, may pay off handsomely in the future.

Five different mine tailings, plus common kaolin clay were tested and the results described in this paper. A striking feature of the data is that it appears to be possible to treat material that is outside the envelope commonly considered appropriate for electrokinetic dewatering processes. Whereas a rule-of-thumb often used in evaluating the likely viability of an EK dewatering scheme indicates an upper limit of electrical conductivity of around 0.5 mS/cm, tailings material having more than twenty times this value (>10 mS/cm) was successfully dewatered. The only limitation appears to be the energy cost that a client may be prepared to bare. Even this factor was found to be of less concern than sometimes believed, with energy consumption rates varying between 1.9 and 37 kWhours per dry tonne. As discussed in the paper, this measure of energy consumption rates can be misleading, because it ignores the effect of the initial and final water content values, but it does provide some measure of comparison.

The particular focus of the EK dewatering described in this paper was the use of new

generation, conductive polymer electrodes (or EKGs), which do not suffer from the problems of corrosion experienced when using metal electrodes. They can be formed into various shapes, and tend to maintain better contact with the material being treated as consolidation occurs. Based on the successful laboratory trials reported in this paper, a range of potential applications for the dewatering of tailings were described. These were in-situ dewatering of existing tailings storage facilities using vertically oriented EKGs, dewatering of tailings during deposition using layers of horizontally oriented EKGs, and in-plant dewatering using EKG filter belts retrofitted to standard filter belt machines.

Although the technology described in this paper shows great promise as a potential means of significantly reducing the water content of stored tailings, it will require an owner or operator being prepared to undertake a large field trial to provide a robust evaluation of the potential offered by EK dewatering. As with most new technologies that offer potentially high rewards, such a field trial does not come without the risk of non-performance, a factor that to date has held back the field testing of this technology.

REFERENCES

- Abiera, H.O., Miura, N., Bergado, D.T. and Nomura, T. 1999. Effects of using electro-conductive PVD in the consolidation of reconstituted Ariake clay. *Geotechnical Engineering Journal*, 30(2), 67-83.
- Bjerrum, L., Mowm, J. and Eide, O. 1967. Application of electro-osmosis to a foundation problem in a Norwegian quick clay. *Geotechnique*, 17, 214-235.
- Casagrande, L. 1949. Electro-osmosis in soils. *Geotechnique*, 1(3), 159-177.

- Casagrande, L. 1983. Stabilisation of soils by means of electro-osmosis. *Journal of the Boston Society of Civil Engineers section, ASCE*, 69(2), 255-302.
- ERCB Directive 074: Tailings Performance Criteria and Requirements for Oil Sands Mining Schemes (February 2009).
- Fourie, A.B., Johns, D.G. and Jones, C.J.F.P. 2007. Dewatering of mine tailings using electrokinetic geosynthetics. *Canadian Geotechnical Journal*, 44, pp 160-172.
- FTFC (Fine Tailings Fundamentals Consortium), Volume 1, Clark Hot Water Extraction Fine Tailings, In: *Advances in Oil Sands Tailings Research*, Alberta Department of Energy, Oil Sands and Research Division, 1995.
- Gray, D.H. and Mitchell, J.K. 1967. Fundamental aspects of electro-osmosis in soils, *Journal of the Soil Mechanics and Foundations Division*, 93(SM6), pp 209-236.
- Hamir, R.B., Jones, C.J.F.P. and Clarke, B.G. 2001. Electrically conductive geosynthetics for consolidation and reinforced soil. *Geotextiles and Geomembranes*, 19(8), 455-482.
- Jakubick, A.T., Hagen M., 2000, "Wismut Experience in Remediation of Uranium Mill Tailings Ponds", in C.K. Rofer and T. Kaasik, Eds., *Turning a Problem into a Resource: Remediation and waste Management at the Sillamae Site, Estonia*, NATO Science Series, 1. Disarmament Technologies – Vol. 28, Kluwer Academic Publishers, Dodrecht/Boston /London, 2000.
- Jones, C.J.F.P., Lamont-Black, J., Glendinning, S., Bergado, D., Eng, T., Fourie, A.B., Liming, H., Pugh, C., Romantshuk, M., Simpanen, S. and Yan-Feng, Z. (2008). Recent research and applications in the use of electrokinetic geosynthetics. Keynote Lecture, EuroGeo4, Proc. 4th European Conference on Geosynthetics, 7-10th September, Edinburgh, UK, pp 1-30.
- Lamont-Black, J. 2001. EKG: the next generation of geosynthetics. *Ground Engineering*, October 2001, 22-23.
- Lamont-Black, J., Huntley, D. T., Glendinning, S. & Jones, C. J. F. P, 2006, Case history: the use of electrokinetic geosynthetics (EKG) in belt press dewatering. 8th International Conference on Geosynthetics, Yokohama.
- Lersow, M. and Schmidt, P. (2006). The Wismut remediation project. Proc 1st International Seminar on Mine Closure, Perth, Australia, September 2006, 181-190.
- Lockhart, N.C. 1983. Electroosmotic dewatering of clays. III. Influence of clay type, exchangeable cations, and electrode materials. *Colloids and Surfaces*, 6: 253-269.
- Lockhart, N.C. and Hart, G.N. 1988. Electroosmotic dewatering of fine suspensions: the efficacy of current interruptions. *Drying Technology*, 6(3), 415-423.
- Lockhart, N.C. and Stickland, R.E. 1984. Dewatering coal washery tailings ponds by electroosmosis. *Powder Technology*, 40, 215-221.
- Mohamedelhassan, E. and Shang, J.Q. 2001. Effects of electrode materials and current intermittence in electro-osmosis. *Ground Improvement*, 5, 3-11.
- Shang, J.Q. and Lo, K.Y. 1997. Electrokinetic dewatering of a phosphate clay. *Journal of Hazardous Materials*, 55, 117-133.
- Veal, C., Johnston, B. and Miller, S. 2000. The electro-osmotic dewatering (EOD) of mine tailings. *Proceedings American Filtration Society Conference*, 2000, 10 pp.

PROJECT CASE STUDY – COMPOSITE SOIL COVER FOR SULPHIDE TAILINGS AT MINE SITE IN NORTHEASTERN ONTARIO, CANADA

Ron Bygness

Industrial Fabrics Association International – Roseville, MN, USA

Bruno Herlin, P.Eng.

Terrafix Geosynthetics Inc. – Toronto, ON, Canada

ABSTRACT: During the Fall of 2006, the Ontario Ministry of Northern Development and Mines tendered a construction project to provide a soil cover over the North Impounded Tailings (NIT) area at the abandoned Kam Kotia Mine site in Northeastern Ontario, Canada. The soil cover would effectively impede the entry of water and oxygen into the high sulphide tailings, substantially reducing acid generation and metal leaching effects from within the tailings. The final design incorporated waste rock, sand, gravel layers, a Geosynthetic Clay Liner (GCL), clay and granular cover soils. During the Fall of 2006 and Winter of 2007, Hazco Environmental & Decommissioning Services implemented the construction of this design. Overall, 800,000 m² of GCL was deployed and covered. Deployment of the GCL was undertaken by Terrafix Environmental Inc. under the supervision of Hazco and Earth Tech Engineering. This paper summarizes the design and construction of this composite soil cover system.

INTRODUCTION

The Kam Kotia Mine in Timmins, Ontario operated intermittently from the 1940s until 1972 producing copper, zinc and gold. Following closure approximately 3 million tonnes of acid-generating sulphide tailings and 500 thousand tonnes of acid-generating waste rock was left on the surface at the site. These waste materials have since evolved to become significant sources of Acid Rock Drainage (ARD) and Metal Leaching (ML), which has had a significant impact on the surrounding environment. The Ontario Ministry of Northern Development and Mines (MNDM) has implemented a multi-staged rehabilitation program at the site to mitigate the ARD-ML

effects of the waste deposits. Several phases have been completed to date. This paper will only look at the composite soil cover system installed during the fall of 2006 and winter of 2007. The MNDM currently collects and treats ARD runoff and seepage and operates a High-Density Sludge (HDS) treatment plant to treat ARD impacted runoff. Wardrop and SENES were retained to design a dry soil cover for the North Impounded Tailings (NIT) in 2004 and 2005. This design was tendered for construction in 2006 and was awarded to Hazco Environmental & Decommissioning Services. The design goal for the project is to provide a “dry” soil cover to minimize the infiltration of water and also limit the ingress of oxygen into the tailings. This construction

design will reduce the quantity, acidity and metal loading of the leachate reporting to the site's drainage collection system to the point where passive treatment technology could be implemented and the HDS plant could be taken out of service.

HISTORY

This abandoned site had approximately 6 million metric tonnes (MT) of unmanaged acid-generating tailings covering more than 500 hectares (1,235 acres). Decades of environmental damage, since closure of the mine in the '70s, were evident as the surrounding soil was burnt orange, the water red, and the area void of vegetation and wildlife. It is considered one of the worst environmental disasters in Ontario history.

The mine was originally developed in the 1940s under the federal government's War Minerals Program. Subsequent to the ending of that program, the mine was operated as a commercial venture intermittently, finally ceasing operations in 1972. Since then, the mining and surface rights to most of the site have reverted to the Crown, leaving the responsibility of rehabilitation in the public realm.

In addition to the physical hazards located on the site, there were about 6 million MT of high-sulfide tailings located within 3 distinct tailings areas, much of which was unimpounded and covered more than 500 hectares.

Acid mine drainage (AMD), and leached heavy metals produced from all 3 of the tailings areas, had a severe impact on nearby land and water. The 3 tailings areas located on the Kam Kotia Mine site are referred to as: (a) the "North Unimpounded Tailings" or "NUT", located in the northeast area of the site; (b) the "North Impounded Tailings" or

"NIT", located in the northwest area of the site; and (c) the "South Unimpounded Tailings" or "SUT", located in the southern area of the site (see Figure 1). For many years, the area to the south of the mine site was known as the "south kill zone." This was an area where virtually all vegetation was destroyed by the site's AMD. In addition, acidic drainage from the SUT area into the Little Kamiskotia River south of the site resulted in severe effects on the biota of that river, with its waters at a pH of 3 or lower. The areas to the north and northeast were similarly affected by contaminated drainage from the NUT area, as was the Kamiskotia River to the north of the mine site.

In response to rising concerns about the effects to the local environment from the contaminated drainage from the site, and the possibility of the contamination of groundwater in the area, MNM contracted a consortium of firms, headed by SENES Consultants Ltd., in 2000. The SENES consortium developed a 5-phase plan to rehabilitate each of the environmental, health, and safety hazards on the site.

Projected rehabilitation costs for the entire site were originally estimated at approximately C\$40M, but that total was also projected to go up to achieve a full cleanup.

MINE OWNERSHIP

Principle exploration: 1926-1928, exploration shaft.

Mining 1943-44: 169,000 MT open pit (mining carried out on behalf of Wartime Metals Corp., a federal government agency).

Mining 1961-1972: 5.84 million MT, mainly underground.

Total production: 6.0 million MT – 1.1% copper, 1.17% zinc, 0.10 oz/tonne silver.

Patented 1932 : Kam Kotia Porcupine Mines Limited (82.5% owned by Hollinger Consolidated Mines Ltd.).

Transferred 1966: Viloamac Mines Ltd./Kam Kotia Ltd.

Transferred 1975: Robison Mines Ltd.

January 1988: land surface rights forfeited to Crown.

March 1998: mining rights forfeited to Crown.

TAILINGS DISPOSTION

1961: 270,000 MT in unconfirmed area north of mill.

1961: 170,000 MT in South Unimpounded Tailings (SUT) area.

1961-67: 2.73 MT deposited in the North Unimpounded Tailings (NUT) area.

1967: Ontario Water Resources Commission (OWRC) required construction of dams to create the North Impounded Tailings (NIT) area.

1967: 1.5 MT deposited in open pit.

1968-1972: 1.4 MT deposited in NIT.

North and east seeps, with a pH of 2-3, drain NUT, east half of NIT and north half of plant site to the Kamiskotia River in the North.

South seep drains SUT, south half of NIT, and plant site to Little Kamiskotia River in the south, which has a pH of 3.5-4.

5-PHASE REMEDIATION PLAN

During fiscal 2000-01, Senes Consulting developed a 5-phase conceptual rehabilitation plan for the Kam Kotia Mine site. Funding for Phases A and B came from the Abandoned Mines Rehabilitation Fund.

Phase A, 2001-02, included construction of a lime addition treatment plant, as well as all of its required infrastructure, and the construction of a new NUT impoundment dam structure, including the stabilization and reinforcement of the existing “north-south” dam. This impounded area was designed to hold all of the remaining unimpounded tailings, which were physically relocated to within the dam area during the subsequent phases of rehabilitation, neutralized with lime, with the impounded area developed as a wetland. Final Cost: C\$10.2M

Phase B, 2002-03, dealt primarily with the relocation of the SUT tailings, estimated at 330,000cu.m., to within the new NUTA impoundment area where they were mixed with lime and neutralized. The completion of this work meant that there would be little new impact to areas south and southwest of the mine site – the areas where there is human habitation.

Upon completion of the work, more than 340,000cu.m. of SUT tailings had been relocated and buffered with EnviroLime. Lime was also spread over the peat/soil surface in the SUT area to buffer residual acidity. Final cost: C\$3.6M.

(A large cost saving was created by using an acid-neutralizing product, EnviroLime, to neutralizing the relocated tailings, instead of the more common hydrated lime. Although a slightly greater amount of the EnviroLime was

required to get the same results as the hydrated lime, the cost for the EnviroLime per unit volume was less than half that of hydrated lime. The EnviroLime was also an easier product to apply to the relocated tailings than hydrated lime, as it can be applied in a dry state and doesn't tend to be as windblown due to its coarser, granular consistency. The constituents of EnviroLime are: CaO 63-75%, MgO 1-8%, SiO₂ 1-2%).

Phase C involves the relocation and buffering of the unimpounded NUT tailings to within the new NUT impounded area. However, due to the large "pond" of acidified, metal-bearing water that collected within the NUT impoundment area, the 611,000cu.m. of the NUT tailings that were relocated during the winter of 2003-04 were stacked around the perimeter of the impoundment area. Approximately 34,000cu.m. of tailings remained to be relocated from the farthest edge of the NUT area and from the various seeps and creeks. Estimated cost: C\$8.2M.

Once the contaminated water project was completed, and the remainder of the NUT area tailings was relocated.

Phase D involved the construction of the wet/moist NUT impoundment area cover. The Phase D work included dealing with the rehabilitation of the north and east seeps and creeks in the northeast area of the site. Estimated cost: C\$3.4M.

Phase E involved the construction of an engineered aggregate "dry" cover over the NIT area, and addressed the physical hazards on the mine site, including the thin crown pillar and the open pit. As Phases C and D could not be completed due to the contaminated NUT pond, the initial 2 layers of the Phase E NIT cover were built during the winter of 2004-05. The remainder of the Phase E work was completed during the winter of 2006-07. Estimated cost: C\$11.4M.

Final construction of a composite cover soil system that includes a Geosynthetic clay liner (GCL) at the former Kam Kotia Mine in Ontario started in November 2006, with an initial deployment of 10,000 sq.m. on day 1 of the project. Over 120,000 sq.m. were deployed by year end in 2006.

Construction resumed in 2007, and when completed in the spring, there was an 800,000 sq.m. soil cover system completed for the Ontario Ministry of Northern Development and Mines at the abandoned mine site southeastern Ontario.

The soil cover is designed to effectively impede the entry of water and oxygen into the high-sulphite tailings, substantially reducing acid generation and metal leaching effects from within the tailings.

DESIGN OF THE COMPOSITE SOIL COVER

Ontario's Ministry of Northern Development and Mines commissioned Wardrop Engineering Inc., and SENES Consultants Ltd. to design a soil cover over the NIT, shown on Figure 1. Earth and rock borrow materials were characterized and preliminary designs were assessed using parameters calculated from standard geotechnical soil testing. Preliminary hydrogeological and geochemical models were run on four design options. The two designs utilizing compacted local clay and geosynthetic clay liners (GCLs) were found to be equivalent in performance and cost. A second round of more detailed laboratory testing was done, including calculating void ratios, freeze-thaw permeability, water retention curves and oxygen diffusion coefficients. After incorporating this data into the analyses, the optimal final design incorporated waste rock, sand, gravel layers, a GCL, clay and granular cover soils.



Figure 1. Aerial view of the abandoned Kam Kotia Mine site prior to implementation of a multi-staged rehabilitation program.

MATERIAL TESTING AND HYDROLOGICAL MODELLING

A comprehensive sampling, geotechnical testing program, and chemical analyses of the waste rock was undertaken to characterize the borrow materials available from the surrounding glaciofluvial (granular) and glaciolacustrine (clay) deposits. In addition to natural aggregate sources, the mine waste rock was also sampled and tested for use in the cover. This material testing and Hydrological Modelling program was conducted under the direction of Mr. Andrew Mitchell, P.Geo., formerly of Wardrop Engineering, and Mr. Jeff Martin, P.Eng., of SENES Consultants Ltd.

Additional detailed testing such as oxygen diffusion, freeze-thaw permeability and moisture retention were conducted under the direction of Dr. Michel Aubertin at Ecole Polytechnique in Montreal, Quebec.

The complete hydrological modelling design and results including the performance of four cover option models was presented at the 58th Canadian Geotechnical Conference in Saskatoon, unfortunately the paper was never

published in the conference proceedings. A request for this paper can be made to the author of this case study paper.

COVER OPTIONS AND FINAL DESIGN

The four cover options which were modelled by Wardrop and SENES are as follows, starting from the tailings surface upward:

- 1: 0.3m rock / 0.25m sand / 0.5m clay / 0.5m sand
- 2: 0.25m rock / 0.3m sand / 1.0m clay / 0.5m sand
- 3: Cover incorporating a geosynthetic clay liner (GCL) with appropriate sand bedding and cover.
- 4: Cover incorporating a synthetic geomembrane (PVC) with appropriate sand bedding and cover.

The final laboratory test program indicated that the silty clay from the site borrow pit was highly frost susceptible and that there could be an increase in the permeability of up to two orders of magnitude with repeated freeze-thaw cycling. This raised concerns for the longevity of a cover designed with clay as the sole water and oxygen barrier. To overcome this propensity of the clay, it was decided that a GCL would be incorporated into the final design. In addition to the GCL, some other final refinements of the design were incorporated to provide a more robust and durable installation. The final cover, for the tailings surface upwards is as follows:

1. A basal layer of crushed mine waste rock of 300mm thickness. This layer formed both an effective capillary break due to its coarse grain size distribution as well as adding structural stability to the design. In addition, using the waste rock in this manner provided an opportunity to deal with this acid-generating waste as part of

another element of the mine site rehabilitation, which precluded needing to cover the waste rock pile in a later phase of work – at additional cost.

2. A layer of granular fill of 300mm thickness. This layer completed the required thickness for an effective capillary break as well as providing a suitable subgrade for synthetic liner installation.
3. A polypropylene coated GCL forms the water and oxygen barrier to effectively isolate the tailings from the ingress of water and air into the tailings mass from above. The polypropylene coated product was selected in the final design since it has an order of magnitude lower hydraulic conductivity than the figures assumed in the modelling, which adds conservatism in the design at little additional cost.
4. A layer of silty clay, 300mm thick is placed directly over the GCL to ensure full hydration throughout the service life of the cover. In addition, the lower permeability of the clay will act as a secondary barrier in addition to the GCL, enhancing the oxygen barrier.
5. A layer of granular soil, 500mm thick isolates the clay and GCL from physical disturbance and also provides a store and release function to mitigate the effects of sustained high precipitation or drought. The thickness of this layer was increased from the preliminary designs to provide greater protection from frost and root penetration. In addition, it provides the required confining stress on the GCL and enhances the durability of the cover.

6. A layer of organic mulch and topsoil, 100mm thick, obtained from the removal of overburden from the clay source will be turned into the upper 50-75mm of the granular layer to provide a growth media for surface vegetation.

The final design incorporated into the cover to provide greater resistance to frost induced disruptions and a layer of the silty clay available locally was incorporated into the sequence to provide continual hydration of the GCL, which is essential to maintaining low gas permeability in the comparatively thin bentonite clay layer afforded by the product.

NEW GEOSYNTHETIC CLAY LINER/ POLYPROPYLENE COATED

A geosynthetic clay liner containing a polypropylene coating was used to provide a unique hydraulic property. This product which has been available since 1999 adopts merging a typical textile coating procedure to that of a needle-punched geosynthetic clay liner. Originating from the textile industry, this process yields a composite clay geosynthetic barrier (GBR-C) / geosynthetic clay liner (GCL) product with unique hydraulic properties and physical performances that make it well suited to many new design approaches. The product includes a polypropylene coating applied to the woven geotextile side of a GCL, providing a low permeability typical for a geomembrane at 5×10^{-13} cm/sec (ASTM E96).

PROPERTIES / TEST METHODS ON POLYPROPYLENE COATED GCL

Testing of the polypropylene coated GCL for this project was done by Sageos/CTT Group (Canada) under the supervision of Earth Tech Engineering (Winnipeg). Hydraulic testing on the coated GCL is a difficult task in the

traditional permeameter due to the lower flow characteristics of this new GCL – attributable to the polymer membrane coating. Whereas, a typical non-coated GCL will yield permeability values on the order of 3×10^{-9} under 35 kPa effective confining stress and 14 kPa head pressure, testing in accordance with the Hydraulic Conductivity Test Method ASTM D5084. Polypropylene coated GCLs have shown to force side wall leakage to occur. Thus making it difficult to measure the performance in the traditional permeameter.

To more accurately determine the true flow through the membrane portion of this type of GCL, a water vapour transmission test was performed. An equivalent hydraulic permeability (k) was calculated using the procedure outlined by Koerner (1997). Via ASTM E96, a value of less than 5×10^{-13} can be expected.

The coating is typically applied to the woven portion of the GCL. This coating has added another dimension to GCLs with an increase in peel values and internal shear values. The fibres which have been needled through the composite are subjected to the coating and as the coating becomes an integral part of the GCL, the fibres are bonded within the coating. Another added benefit of a polypropylene coated GCL is its effectiveness as a root inhibitor (Lucas 2002).

PROJECT OVERVIEW

Construction of the 80 ha composite cover soil system started in early November of 2006 with an initial deployment and completion of

10,000 m² on the first day of the project. Initial plans were to deploy 120,000 m² during the fall prior to closing the project down for the winter. These initial plans were changed and 800,000 m² was deployed from November of 2006 to February of 2007. Deployment rates at times reached over 30,000 m² per day.

Although the rate of deployment of the GCL can reach high deployment rates, this deployment is restricted by the cover soil placement over the GCL. For this project the cover soil used was a silty clay which was available locally at the mine site. Once Hazco's truck fleet was up and running, deployment rates as mentioned reached over 30,000 m² per day (shown in Figure 2).



Figure 2. Hazco's truck fleet carrying the clay from a nearby clay source available on site being transported as a cover soil over the geosynthetic clay liner.

The GCL was deployed over a stable subgrade of granular fill as mentioned previously in Section 2.2. A 0.3m overlap was done, recorded, and supervised by Earth Tech Engineering (shown in Figure 3).



Figure 3. Deployment of the GCL. One foot overlap being done. Polypropylene side of the GCL facing down.

Following the deployment of the GCL, loose bentonite was placed between panel edges. Loose granular bentonite should be placed between the panels at a rate of 2 kg per lineal metre of seam if the GCL is the primary hydraulic seal. The addition of bentonite to the seam is optional when the GCL will be acting as leak isolator for an overlying membrane. Spreading of the loose bentonite is shown in Figure 4.



Figure 4. Spreading of the loose bentonite between GCL sheets.

Following the deployment of the GCL, a 0.3m thick silty clay layer was placed directly over the GCL as shown in Figure 5.



Figure 5. Clay being applied over the GCL.

SUMMARY

One can obtain many types of GCLs: stitched, glued, needle-punched, different bentonite content, different geotextile weight, scrim reinforced, and enhanced polymer etc. This list is long. Over the years and through increased use, this area of geosynthetics engineering seems to see ever-cheaper GCLs being requested for particular projects. This may mean thinner textiles and/or less bentonite, almost to the point of becoming less a GCL than a double-layered textile. What is the lowest mass per unit area of bentonite that a GCL can have and still achieve, for example, the quoted manufacturer's hydraulic conductivity? It's getting to the point where 12 kg/m² seems acceptable from the standard 18 kg/m². The design community originally used 24 kg/m². There has to be a limit, but only specific project engineers will ask for those limits.

Engineers when asking for a geosynthetic clay liner must request for an accurate breakdown of the GCL instead of simply asking for a GCL. The recommended list of data when requesting for a GCL is as follows:

- Top geotextile shall be X g/m² nonwoven.

- Bottom geotextile shall be $X \text{ g/m}^2$ woven or $X \text{ g/m}^2$ scrim-reinforced nonwoven.
- Swell index of the bentonite.
- Fluid loss of the bentonite.
- Bentonite mass per unit area at X moisture content.
- Grab strength of the GCL.
- Peel strength of the GCL.
- Permeability of the GCL.
- Index flux of the GCL.
- Internal shear strength of the GCL.

Scrim = woven.

Scrim-reinforced nonwoven = woven + nonwoven.

Scrim-reinforcement = needle-punching of a woven and nonwoven geotextile together.



Figure 6. Needle-punching board.

All GCLs have a nonwoven top geotextile for needle-punching purposes.

The bottom geotextile is either a required woven on its own or a scrim nonwoven geotextile if required for rough soil conditions or steep slope applications.

The Geosynthetic Research Institute recommends that the bottom geotextile of a GCL must contain a scrim-reinforced

nonwoven geotextile. Possible failures which may occur by not using a scrim-reinforced bottom geotextile are internal erosion of the bentonite through the geotextile in hydraulic head conditions (Rowe and Orsini 2002), and possible shrinkage of the GCL itself in the composite lining system (GRI White Paper – 2005).

As per the Geosynthetic Research Institute's White Paper of April 2005: *Do not use GCLs with needle-punched nonwoven geotextiles on both sides unless one of the geotextiles is scrim-reinforced. There are numerous possibilities in this regard, but all should have a woven component embedded within, or bonded to, the nonwoven component.*

The project described herein contained a bottom woven geotextile. As mentioned, a polypropylene coating is applied to the GCL used in this case study paper to decrease the permeability of the product (GCL) to the range of a geomembrane.

One should never use trade names when requesting an item for a specific project. One should always list the testing values required from a specific product, i.e. ASTM testing values. Products and their names change over time hence the requirement to avoid using trade names. Another factor is to avoid having the purchasing agent and/or general contractor make a decision during the tender process.

Remember, you get what you pay for in life. Want cheap? Expect it, but don't expect quality and performance from it. Someone will sell it to you. Will they provide you with a warning? It's to be hoped that they will provide you with the limitations of the product. Want something reliable? Every company can offer reliability at a reasonable price. Want the "crème de la crème" with all the built-in safeguards and back-up systems? Every manufacturer would love to sell its premium brand, but expect to pay a premium

for that. In our world, however, the cheapest price often prevails. A manufacturer's premium brands probably represent only 10% of their overall sales – if that.

The geosynthetics arena is no different. The variety of available geosynthetic products is great that clients seek advice from a particular distributor, supplier and/or manufacturer. But are clients provided with all of the information? Suppliers would love to provide their particular premium brands, of course; but at the end of the day, the cheapest price frequently prevails. Buyers beware.

Products are never equal when using trade names. Products are equal when values are provided and hence can be compared. Ask for them in your tender request.

ACKNOWLEDGEMENTS

The writer would like to acknowledge the contribution of a number of people and contributors to the paper.

Mr. Andrew Mitchell, Mr. Jeff Martin, and Mr. Christopher Hamblin of the Ministry of Northern Development and Mines for supplying the original design paper for this project, which as mentioned, was never published during the 58th Canadian Geotechnical Conference.

Mr. Patrick Jolicoeur and Mr. Phil Springs of Hazco Environmental & Decommissioning Services, General Contractor of this composite soil cover deployment.

Mr. Troy Shaw, Mr. Blu Alexander, and especially Mr. Leroy Osmond of Terrafix Environmental Inc. for being the GCL installer during -40C to -50C constant weather during the winter.

REFERENCES

ASTM D5084. *Standard Test Methods for Measurements of Hydraulic Conductivity of Saturated Porous Materials using a Flexible Wall Permeameter.*

ASTM E96. *Water Vapour Transmission.*

Bentofix Technologies Inc., "Fix – 412 Features of a Scrim-Reinforced GCL & Manufacturing Process", Barrie, Ontario, Canada, 1992, (*unpublished*).

GRI – Geosynthetic Research Institute – Philadelphia, PA, USA. GRI-GCL3. Standard Specification for Test Methods, Required Properties, and Testing Frequencies of Geosynthetic Clay Liners (GCLs), Geosynthetic Research Institute, 2005.

Koerner, K.R. and Koerner, R.M., 2005. GRI White Paper #5 on In-Situ Separation of GCL Panels Beneath Exposed Geomembranes. Geosynthetic Research Institute.

Lucas, S.N., 2002. Manufacturing of and the performance of an integrally-formed, polypropylene geosynthetic clay barrier, International Symposium on Clay Geosynthetic Barriers, Nuremburg, Germany, 2002, pp. 227-232.

Maubeuge, K.P. von, 2002. Investigation of bentonite requirements for geosynthetic clay barriers. International Symposium on Clay Geosynthetic Barriers, Nuremburg, Germany, 2002, pp. 155-163.

Mitchell, A., Martin, J. and Hamblin, C., 2005. Design of a Composite Soil Cover for Sulphide Tailings at the Kam Kotia Mine Site, Northern Ontario, Canada. 58th Canadian Geotechnical Conference. (*presented but not published*).

Rowe, R.K. and Orsini, C., 2002. Internal erosion of GCLs placed directly over fine gravel. International Symposium on Clay Geosynthetic Barriers, Nuremburg, Germany, 2002, pp. 199-207.

SENES Consultants Ltd., Lakefield Research Limited, ESG International, Denison Environmental Services, "Final Report Kam Kotia Mine Property Rehabilitation Study – Phase 1".

OXIC AND ANOXIC TAILINGS SLURRY AGING STUDIES AT THE HOPE BAY PROJECT, NUNAVUT

Kelly Murphey and Charles Bucknam

Newmont Mining Corporation, Englewood, CO, USA

Thomas Wildeman

Colorado School of Mines, Golden, CO, USA

Kelly Sexsmith and Lisa Barazzuol

SRK Consulting, Vancouver, B.C., Canada

John Chapman

SRK Consulting, Brisbane, Queensland, Australia

ABSTRACT: The Hope Bay Project will strive to meet high standards for environmental compliance, before, during and after mining. Treatment of the excess water may need to be included in the design of the hydrometallurgical circuit. The fate and transport of every contaminant will need to be carefully assessed in order to support environmental assessment, to obtain permits to mine and process the ore, and to meet Newmont's environmental requirements. The geochemical characterization program of the metallurgical products for this project includes extensive static testing, mineralogical analyses and humidity cell tests. Experience has shown that there can be substantial changes in process water quality as the tailings solids equilibrate with porewater and supernatant during storage, and, as residual cyanide and its products degrade. Aging tests on tailings slurry from the hydrometallurgical tests are being conducted to simulate these processes. The tests include oxic (or atmospheric) and anoxic equilibration tests of two and eight month duration respectively. Oxic tests are open to the ambient laboratory atmosphere and are exposed to sunshine to provide temperature fluctuations. Anoxic tests require a very rigorous protocol. Immediately after splitting, samples are purged with nitrogen and placed in glove bags in a nitrogen purged refrigerator until ready for testing. Then, samples are prepared in nitrogen purged glove bags with no head space in the bottles, and placed in anoxic bags equipped with oxygen absorbers. Aging takes place within the anoxic environment in a nitrogen purged refrigerator to simulate cold weather conditions. Preliminary results from the current oxic and anoxic aging tests are presented.

INTRODUCTION

Newmont Mining Corporation is evaluating the Hope Bay project located in Nunavut

Territory about 160 km southwest of Cambridge Bay. The Hope Bay deposits are located in an Archean greenstone gold belt that is up to 20 km wide and that extends

over a roughly 80 km strike length. Three areas with gold mineralization have been identified on the belt thus far: Doris (including the Doris North, Connector and Central deposits), Madrid (including the Suluk, Naartok East, Naartok West and Rand deposits), and Boston. Gold mineralization in the Doris deposits is associated with steeply dipping quartz veins, surrounded by a narrow envelope of intense dolomite-sericite altered rocks and then a sequence of highly folded and metamorphosed pillow basalts. Gold mineralization in the Madrid deposits occurs within zones of multi-phased brecciation, quartz stockwork, and silicification within a broader sericite-albite-dolomite alteration halo where predominantly volcanic rocks have been preferentially altered and sulfidized. Gold mineralization in the Boston deposits occurs within a large iron-rich carbonate altered shear system and is associated with sulfide mineralization within quartz veins and as a halo in the wall rock around the veins.

Both solution and solid products arising from mining and processing must be documented and characterized. Metallurgical testing has generated three separate tailings products for characterization: flotation tailings, detoxified cyanidation residues, and combined tailings that represent a mixture of the flotation tailings and cyanidation residues.

Preliminary static testing indicates that there are abundant amounts of neutralization potential (NP) in the form of carbonate minerals in ore and all three types of metallurgical residues from all three deposits. The laboratory and pilot plant flotation tailings being tested contain relatively little sulfide and are clearly non-acid generating.

To simulate the geochemical evolution of tailings with time, aging tests are often completed using simple “bucket” tests, in which slurries are stored in 20 liter pails and then periodically sampled to establish trends over time. In recent years, some improvements have been made to this type of aging test, particularly for characterization programs in the uranium mining industry. Notably, anoxic tests have been introduced to simulate processes occurring in flooded tailings or in the saturated portion of a tailings facility. There have been improvements in the consistency of the storage conditions, and the slurry is split into separate sample aliquots to minimize disturbance of the remaining tailings samples and to ensure consistent water to rock ratios throughout the test.

For the Hope Bay project, Newmont Metallurgical Services (NMS) in collaboration with Colorado School of Mines, and SRK Consulting have made further improvements to the aging test procedure. So that comparisons can be made, the aging tests will eventually be completed on bulk flotation tailings (BFT), cyanidation detoxified tailings, and the combined tailings. Because the actual storage conditions are uncertain, both oxic and anoxic conditions are simulated. The purpose of this paper is to describe how these studies are being conducted and present preliminary results.

METHODS

Sample Preparation

To date, pilot scale metallurgical tests have been initiated for five ore samples, including Boston (B), Doris Central (DC), Naartok East (NE), Naartok West (NW), and Suluk (S). The pilot plant flotation tailings samples were available from Naartok East

and West and Suluk for sampling, while the bulk concentrates are in storage until further steps in the metallurgical testing program are undertaken to study solution detoxification options. Initial work on the Doris Central and Boston detoxified cyanidation samples were on-going at Lakefield Research when the aging testing program at Newmont Metallurgical Services was initiated on the flotation tailings from previous testing on these deposits.

Using a slurry splitter, the 20 L slurry suspension was split into on 5 L and 12, 1.25 L aliquots at Newmont Metallurgical Services for the following purposes: 5 L for tailings characterization, 5 L (4 splits) for the oxic aging test, 5 L (4 splits) for the anoxic aging test, and the remainder reserved for a possible column study. Figure 1 shows the operation of the rotary slurry splitter, which is an essential piece of equipment for an activity such as this aging study.



Figure 1. Using the slurry splitter to prepare the aging aliquots.

Immediately following sample preparation, a solution sample was taken from the characterization splits for analysis of the parameters shown in Table 1. This sample represents “time zero” for both the oxic and anoxic tests. Once testing of the Naartok East, West, and Suluk cyanide detoxified residues and combined tailings is initiated, the samples will also be subjected to the analyses shown in Table 2. .

Description of the Oxic Aging Test

Immediately after splitting, the four, clear, polycarbonate-2.5 L aliquot bottles were rolled for 15 minutes and then placed on a south facing window sill with caps propped open with a drinking straws so that there was continuous exposure to the atmosphere. Figure 2 shows the samples on the window sill shortly after being split and rolled. No attempt was made to control the temperature, which was recorded, and the temperatures on the sill went through a daily cycle of between 20 and 35°C. Through this variation in temperature, the air above the settled slurry was allowed to equilibrate with the atmosphere. In the respect that these temperatures are higher than the conditions that will actually be encountered on site, these can be considered accelerated aging conditions. At no time during the aging were the sample bottles shaken to re-suspend the tailings solids.

At intervals of 1, 2, 4 and 8 weeks (Table 3), one of the sample aliquots was removed and prepared for analyses.

Table 1. Analytes for Oxic and Anoxic Aging Test – Flotation Tailings

Test	Requested Max DL ¹	Units	Preservative and Volume of Sample needed
pH (unfiltered)	0.5	pH Units	Unpreserved 250-mL
Eh (unfiltered)	50	mV	
pH (filtered)	0.5	pH Units	
EC	0.5	µS/cm	
Total alkalinity	0.5	mg CaCO ₃ /L	
Bicarbonate	0.5	mg CaCO ₃ /L	
Carbonate	0.5	mg CaCO ₃ /L	
Hydroxide	0.5	mg CaCO ₃ /L	
Chloride	0.2	mg/L	
Acidity	0.5	mg CaCO ₃ /L	
TDS	30	mg/L	
Dissolved Phosphorous	0.005	mg P/L	
Sulfate	1	mg/L	
Total organic carbon	1	mg/L	
Total inorganic carbon	1	mg/L	Unpreserved 50-mL
ICP-AES	0.05	mg/L	HNO ₃ , 100-mL
ICP-MS	trace level	µg/mL	
Hg by CVAF	0.02	µg/L	BrCl, 50-mL

¹As requested by SRK

Table 2. Analytes for Oxic and Anoxic Aging Test – Cyanide Detoxified and Combined Tailings

Test	Requested Max DL ¹	Units	Preservative and Volume of Sample needed
All parameters in Table 2			NaOH, 50-mL
Total CN	0.01/0.002	mg/L	
WAD-CN	0.01/0.002	mg/L	
Aquatic Free-CN	0.01/0.002	mg/L	Unpreserved 250-mL
Nitrate (NO ₃ -N)	0.02	mg/L	
Nitrite (NO ₂ -N)	0.002	mg/L	
Ammonia (NH ₃ -N)	0.01	mg N/L	
SCN (Thiocyanate)	0.02	mg/L	
OCN (Cyanate)	1	mg/L	
S204 and S406	1	mg/L	

¹As requested by SRK

Table 3. Sampling times for the oxic and anoxic aging studies. Finished aliquots means all aliquots have been taken through that time point at the time of publication.

Sample Aliquot	Oxic Study time step	Finished Aliquots ¹	Anoxic Study time step	Finished Aliquots ¹
1	1 week		1 month	S
2	2 weeks		2 months	NE, NW
3	4 weeks	S	4 months	DC, B
4	8 weeks	DC, B, NE, NW	8 months	

¹As of June 30, 2009



Figure 2. Oxic aging samples shortly after being split and rolled.

Description of the Anoxic Study

The term anoxic is used here to imply that the atmosphere is devoid of oxygen as much as possible. No attempt is being made to actively generate reducing conditions. Nevertheless, to ensure the maintenance of continuous anoxic conditions, the procedures

used in this study are more involved than those for the oxic aging test.

Prior to splitting the slurry, two glove bags were set up and purged with nitrogen for 15 minutes. To verify that the purge was successful, an oxygen meter that utilizes a solid state probe was used to continuously monitor the oxygen level in the glove bag. Purging was considered complete when the oxygen meter read below 1% of normal atmospheric oxygen.

Immediately after slurry splitting, two of the 2.0 L amber glass bottles which received the 1.25 L slurry splits for anoxic aging, were placed in each of the two glove bags. Then each bottle was nitrogen purged twice for 30 minutes. The purpose of this step was to remove all oxygen from the slurry as well as to ensure a nitrogen atmosphere above the slurry. Figure 3 shows an aliquot being purged to the point where the meter does not detect oxygen in the slurry sample or the glove bag. Once the purging was complete, the bottles were tightly sealed and then transferred to a refrigerator that had been set-up with glove bags where anoxic conditions were maintained by a constant flow of nitrogen through the glove bags. The splitting of the slurry and the purging of the four aliquots to anoxic conditions took about 6 hours, and so the aliquots were left in the refrigerator at least over night.



Figure 3. The glove bag and the oxygen meter showing that the slurry bottle was purged to anoxic conditions.

Within a week of purging the samples, the aliquots were prepared for the anoxic aging test in a glove bag that had been purged with nitrogen so that oxygen was below 1% of normal atmospheric conditions. The suspended slurry was transferred into nitrogen-purged 1.25 L amber glass bottles such that the headspace was eliminated. While in still in the glove bag, each tightly sealed bottle was then transferred into an impermeable anaerobic bag, which also contained an oxygen absorber bag and oxygen indicator pellet to ensure an anoxic atmosphere was maintained. Each of the four anaerobic bags was then tightly sealed and returned to the refrigerator into a glove bag through which nitrogen continuously flowed. The refrigerator temperature was maintained at below 4°C. As with the oxic tests, the sample bottles were never shaken to re-suspend the tailings solids.

The Doris Central BFT slurry was the first sample to be subjected to this protocol and some of the sample bottles froze and broke in the anaerobic bags. After this problem was corrected and the method refined, the oxygen indicator pellets showed that indeed anoxic conditions were maintained throughout the time interval.

At intervals of 1, 2, 4 and 8 months (Table 3), one of the sample aliquots was removed and filtered within a nitrogen purged glove bag so that the anoxic integrity was maintained until aliquots were preserved for specific analyses (Table 1). After filtering, Eh measurements were taken inside the purged glove bag.

PRELIMINARY RESULTS

As of June 30, 2009 none of the anoxic aging studies have been completed (Table 3). For the oxic studies, all tests except Suluk have been finished. Thus, the characterization highlights presented below should be considered preliminary. Because that is the case, only indicative parameters such as pH and major constituents in the solutions will be discussed.

For all tests, whether oxic or anoxic, and all aliquots, pH levels were approximately 8 and alkalinity values were above 100 mg CaCO₃/L. The pH values for the Doris Central and Boston oxic aging studies appear to have increased with aging. Figures 4 and 5 show the trends in the values of the pH and alkalinity over the course of the oxic aging study for the four deposits that have been completed. Clearly over the eight weeks of oxic aging there is no tendency in the four BFT slurries to turn acidic.

In both the oxic and anoxic tests, Eh readings were between 300 and 500 mV, which is in the range where iron would be

present predominantly as ferric hydroxides $\text{Fe}(\text{OH})_3$ (Langmuir, 1997). None of the aliquots had an aroma of hydrogen sulfide or of reduced organic compounds that would be indicative of reducing conditions. In the anoxic tests, the preliminary results indicate that reducing conditions have not developed, and suggest that these samples either do not contain any strong reductants that would impose an appreciable change in conditions, or that they contain some oxide phases that help to stabilize the redox conditions.

With respect to the major cations in the solutions, on an equivalent per liter basis (molarity times ionic charge), magnesium and calcium concentrations are higher than the sodium and potassium concentrations. For anions, the dominant anions on an equivalent per liter basis are sulfate, bicarbonate, and chloride. Figure 6 shows how these major constituents change over

time in the oxic aging test for the Boston BFT solutions. The bicarbonate concentration was calculated assuming that all of the alkalinity is due to that anion (Langmuir, 1997). Using these seven ions, the cation/anion balance is better than 2.5 % in the five water samples (Langmuir, 1997). Figure 7 shows the change in major constituents for the Naartok West oxic aging solutions. In this case, the cation/anion balance is 10 % or better for all five samples.

In Figures 6 and 7, the increases in magnesium and sulfate, particularly in the Boston solutions, are clear. The solutions in the Doris Central and Naartok East oxic aging studies have also shown increases in magnesium and sulfate. Geochemical modeling, trends in the aging test, and results of the mineralogical characterization currently in progress on these samples will be used to determine the likely mineralogical controls on porewater chemistry.

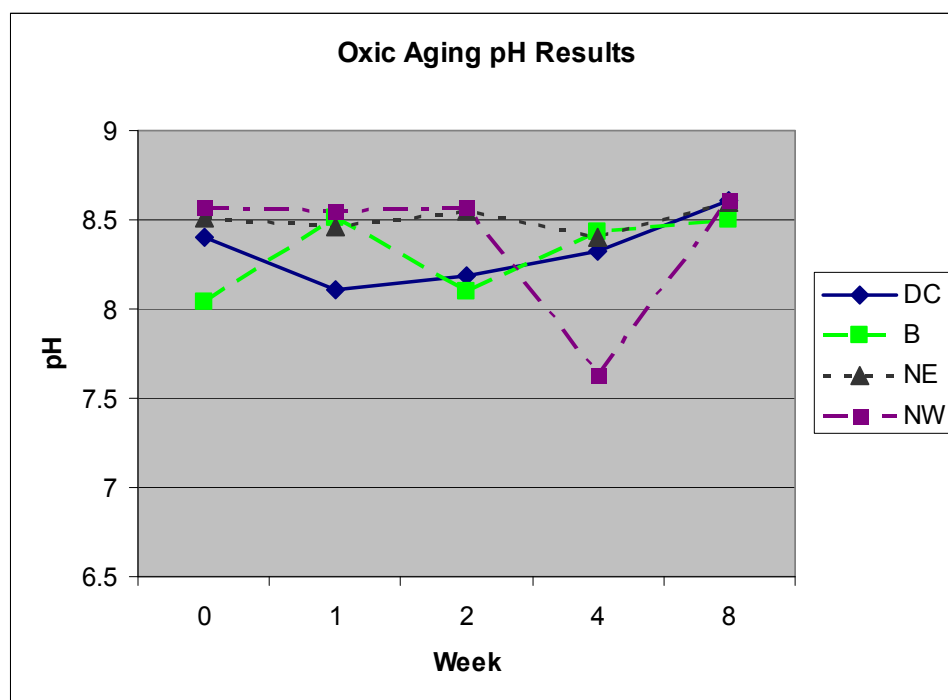


Figure 4. Trends in pH over time for the four oxic aging tests that have been completed.

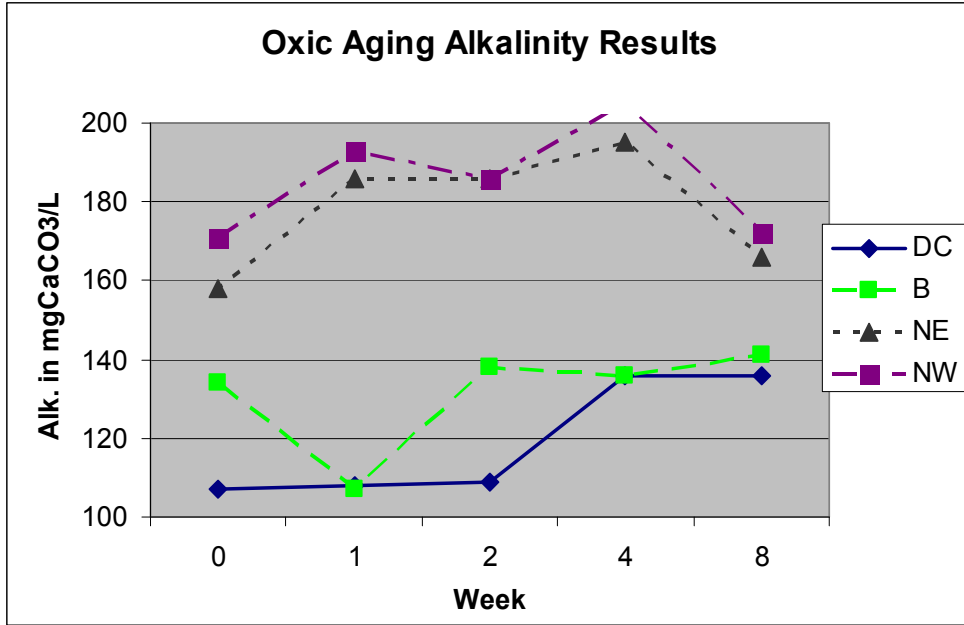


Figure 5. Trends in alkalinity (mg CaCO₃/L) over time for the four oxic aging tests that have been completed.

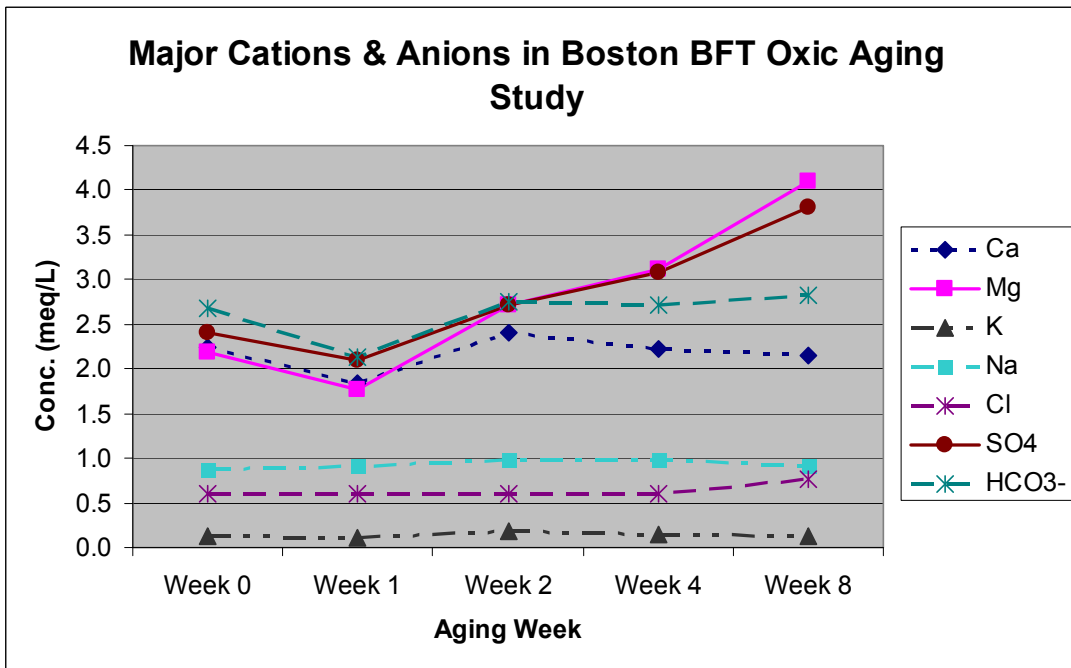


Figure 6. Trends over time in the major constituents in solution during the Boston oxic aging study.

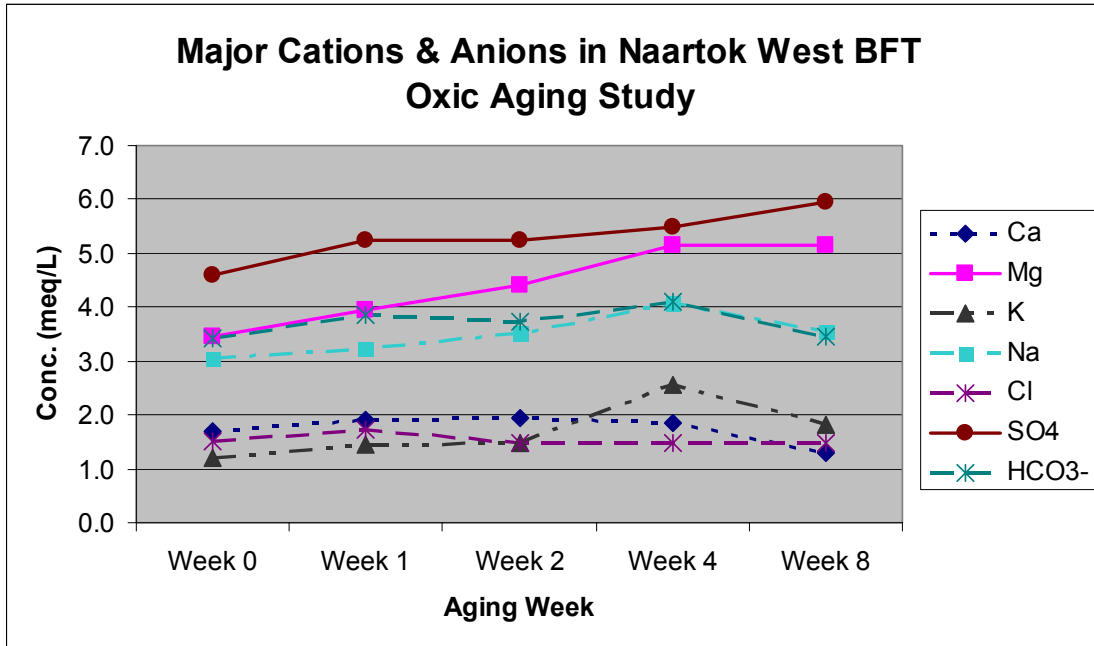


Figure 7. Trends over time in the major constituents in solution during the Boston oxidic aging study.

This increase of magnesium in the oxidic aging solutions is beneficial because it raises the hardness of the water. Several of the cations have aquatic toxicity levels that depend on hardness (CCME, 2007). Both calcium and magnesium compete with other cations for the gill sites that are the receptors for ingestion of cations into the aquatic organism (Di Toro et al., 2001). Thus, when hardness in the water increases, tolerance to metals increases. For all four BFT slurries, the increase in magnesium in solution raises the hardness level to above 180 mg CaCO₃/L, which is very hard water, the highest category.

CONCLUSIONS

Methods for simulating aging of tailings slurries have been developed. Of particular importance, is the development of a robust method for the anoxic aging of tailings slurries. The method takes advantage of the use of glove bags through which nitrogen continuously flows. Because the glove bags

can be placed in a refrigerator, anoxic aging under the conditions that would be encountered in the Nunavut Territory can be simulated.

At this time, preliminary results from the oxidic portion of the aging study show that pHs of the bulk flotation tailings slurries remain at around 8, and alkalinities remain at 100 mg CaCO₃/L. During the course of oxidic aging, the magnesium concentrations in the slurry solutions increase. This increase raises the hardness of the solutions to very hard, the highest category. This increase in hardness helps aquatic organisms better tolerate any metal contaminants that may be in the BFT solutions.

REFERENCES

CCME, 2007. Canadian Water Quality Guidelines for the Protection of Aquatic Life, Update 7.1, December 2007. In: Canadian environmental quality guidelines, 1999,

Canadian Council of Ministers of the Environment, Winnipeg.

Di Toro, D.M., H.E. Allen, H.L. Bergman, P.R. Paquin, and R.C. Santore, 2001. Biotic ligand model of the acute toxicity of metals 1. Technical Basis. *Env. Toxicology and Chemistry*, v. 20, pp. 2386-2396.

Langmuir, 1997. *Aqueous Environmental Chemistry*. Prentice Hall, New Jersey, 600 pp.

U.S. EPA, 2003. USEPA National Primary Drinking Water Standards, USEPA Document 816-F-03-06, June 2003.

ELECTROKINETIC DEWATERING OF GYPSUM CONTAINING TAILINGS

Julie Q. Shang

Dept. of Civil and Environmental Engineering, The University of Western Ontario, London, ON

Angelo R. Fernando and Edmond K. Lam

Innovation & Technology Development - Research Centre, Cameco Corporation, Port Hope, ON

ABSTRACT: Mine tailings are discharged as slurry of low solid contents as the end product of mining and mineral processing. Chemical flocculants, such as polymers and inorganic salts, are often used to assist tailings dewatering for subsequent disposal. However, in cases that tailings contain significant fraction of fine solids (in the micro meter range) and clay minerals, the dewatering process becomes increasingly difficult and time consuming. In this study, the water flow generated by electrokinetics on mine tailings from a mine site in Saskatchewan, Canada is investigated. The tailings contain mainly gypsum, quartz and clay minerals. The tailings are characterized for the geotechnical, physical, chemical and mineralogical properties first, and then electrokinetic cell tests are carried out to measure the coefficient of electroosmotic permeability, a key parameter on the response of tailings to electrokinetic dewatering. Two conductive materials are used as electrodes in the study, i.e., a stainless steel SS316 mesh, which is a high-grade corrosion resistant material; and an electrical vertical drain using a conductive polymer as the conductor. The results of the study show that the electrokinetic dewatering would be very effective on the tailings using SS316 mesh electrodes, indicated by the magnitude of the coefficient of electroosmotic permeability, quantity of water transported through the tailings specimen, duration of water flow, effective current density and applied voltage gradient. The stainless steel 316 mesh electrodes performed well over a period of 800 hours under an applied voltage gradient of 55 V/m and current density of 5 to 8 A/m². The corrosion rate of SS316 mesh anode was measured as 0.2 g/A-hour in this study. On the other hand, the electrical vertical drains performed satisfactorily in the first 100 hours then completely lost conductance. It is also found that the tailings pore water pH is crucial in maintaining the water flow induced by electrokinetics.

INTRODUCTION

Mine tailings are the end product of mining and mineral processing after the mineral has been extracted. The extraction process often involves crushing and grinding, leaching, and separation. The final steps are thickening and subsequent dewatering of tailings before

discharge to the tailings management facility (Figure 1). It is desirable that the tailings have a higher solid content for water conservation and reuse, whereas they can still be pumped through pipe lines for discharge. Chemical flocculants, such as polymers and inorganic salts, are used to assist tailings thickening and dewatering. However, in

cases those tailings contain fine solids (in the micron-meter range) and significant fraction of clay minerals, the thickening and dewatering processes become increasingly difficult and time consuming.

Electrokinetic dewatering of mine tailings has been studied since 1960s. Applications included dewatering of coal and sand washeries and tailings from mineral recovery (Lockhart 1986). The treatments were implemented in tailings disposal ponds, and underground mines (Kelsh and Sprute 1976, 1981). The response of tailings to the electrokinetic treatment depends on the properties of the tailings, which vary in a broad range. Therefore, material characterization is always the first step in a feasibility study for developing an electrokinetic dewatering application. A major challenge in the engineering applications of electrokinetics is anode corrosion due to electrochemical reactions. Relatively inexpensive anode materials, such as steel, copper, aluminum, etc., deteriorate rapidly, leading to the lost of conductance and release of harmful metals to the environment. Stainless steel and silicon cast iron have much lower corrosion rate and can be considered in applications. Conductive polymers such as electrokinetic geosynthetics (EKG) (Fourie et al. 2007) and electrical vertical drains (EVD) (Chew et al. 2004, Rittirong et al. 2008) have been used as electrodes. However, the performance of these products remains to be evaluated, especially over longer terms and under higher electrical current. Another notable anode material is coated titanium, which is virtually corrosion free. However, the issues such as the cost, ability to handle polarity reversal (serving as the anode and cathode alternatively) and durability of coating need to be addressed for large-scale geotechnical applications.

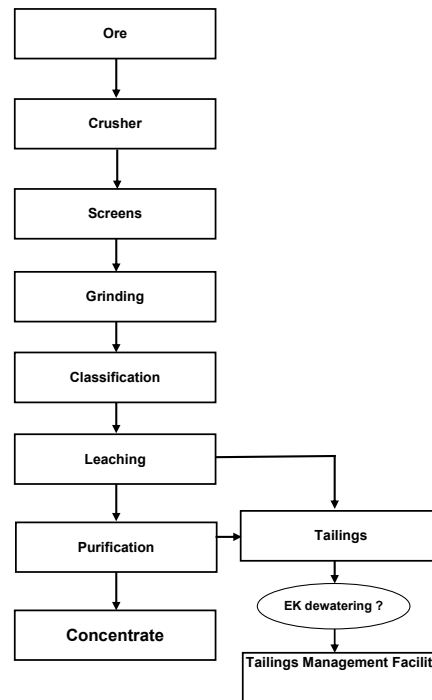


Figure 1. Flow chart of mineral processing

In this study, the effects of electrokinetics on tailings from a mine site in Saskatchewan, Canada, are investigated. The tailings contain mainly gypsum, quartz and clay minerals. At first the tailings are characterized in terms of geotechnical, physical, chemical and mineralogical properties. Electrokinetic cell tests are carried out to measure the coefficient of electroosmotic permeability, a key parameter on the response of the tailings to electrokinetic dewatering. The other factors, such as the voltage loss at the electrode-tailings interface, electrode corrosion, duration and rate of water flow, polarity reversal, and water chemistry, are also studied.

BACKGROUND

Electrokinetics is the general term for the response of fine solids suspended in water when a direct current (dc) is applied, which includes three dominant effects, i.e.,

electrophoresis, electroosmosis and electrochemical reactions. Electrophoresis generates the movement of tailings solids suspended in water, which is predominant in dilute suspensions such as tailings slurry before thickening. Electroosmosis generates water flow in tailings aggregates, which is representative of underflow from a thickener. Electrochemical reactions generate oxygen and hydrogen gases, pH changes at electrodes and reduction-oxidation of electrodes and tailings solids.

For thickened tailings, the coefficient of electroosmotic permeability relates the velocity of the water flow and applied electrical field intensity, also known as the voltage gradient;

$$q_{eo} = k_e E \quad (1)$$

where q_{eo} (m/s) is the flow velocity by electroosmosis, k_e (m²/sV) is the coefficient of electroosmotic permeability, and E is the voltage gradient. k_e represents the water flow velocity induced by a unit voltage gradient (1 V/m). The values of k_e have been reported in the ranges from 1.5×10^{-9} m²/sV for clayey silt to 1.2×10^{-8} m²/sV for Na-Bentonite slurry (Mitchell 1993). Because mine tailings are highly variable in mineralogy, particle size and water chemistry, the coefficient of electroosmotic permeability of tailings must be measured and assessed in the feasibility study of electrokinetic dewatering.

In addition to the electroosmotic permeability, the feasibility of electrokinetic dewatering also depends on the hydraulic conductivity of tailings. It has been reported electroosmosis is effective when the hydraulic conductivity of soil is in the range of 10^{-10} to 10^{-8} m/s (Mitchell 1993, Rittirong and Shang 2005).

The water flow generated by electroosmosis is directly related to the zeta potential of solids. When in contact with water, almost all fine solids carry electric charges on their surfaces, which attract dissolved ions of opposite sign and form an electrical double layer. The response of tailings to an applied dc current depends on the magnitude and polarity of the surface charge on the solids, which can be estimated in terms of the zeta potential, ζ , defined as the electrical potential at the boundary between the absorbed ions on the solid surfaces and mobile ions in water. Theoretically the velocity of water flow induced by electroosmosis is proportional to the zeta potential of solids (Helmholtz 1879). Therefore, the measurement of zeta potential provides an indication of both the direction and magnitude of water flow induced by electroosmosis. The zeta potential of tailings solids is a function of water pH and can be measured through pH adjustment using an acid or base.

Electrochemical reactions associated with the application of a direct current in tailings are complex, including electrolysis of water (generation of oxygen and hydrogen gases), reduction at the cathode and oxidation at the anode. As a result, the pore water pH of tailings decreases at the anode and increases at the cathode; the anode corrodes and/or deteriorates quickly if it is made of a consumable material. The impact of the electrochemical reactions to electrokinetic dewatering of tailings must be considered in the design and implementation.

CHARACTERIZATION

The tailings used in the electrokinetic tests were recovered from a tailings management facility in Northern Saskatchewan, Canada. The tailings and original supernatant were

sent to the laboratory in sealed plastic containers and used in all tests.

The geotechnical, elemental, mineralogical and physical-chemical properties of the tailings are summarized in Table 1.

Table 1. Summary of tailings properties

<i>Geotechnical</i>		<i>Mineralogical</i>	
Specific Gravity	2.62	Quartz	
Liquid limit %	32.5	Gypsum	
Plastic limit %	25.9	Muscovite	
<i>Elemental, %</i>		Clinocllore (chlorite)	
O	52.7	<i>pH</i>	7.3
Mg	2.8	<i>zeta</i>	-14.2
Al	7.7		
Si	19.7		
S	6		
K	4		
Ca	4.5		
Ti	0.2		
Fe	2.7		

The grain size distribution is shown in Figure 2. The tailings have approximately 58% solids finer than 100 μm and 10% finer than 2 μm , indicating that the tailings solids consist of mostly fines. The tailings have low plasticity with a plasticity index of 6.6. Quartz and two clay minerals are identified (muscovite and chlorite) in the tailings, whereas gypsum is the other constituent. The original supernatant of the tailings has pH 7.3. The zeta potential of the tailings solids was measured using Zeta Plus (Brookhaven Instruments Corporation). The measurement was carried out on a tailings suspension, which was prepared by mixing 20 mg wet tailings solids with 100 ml original supernatant. As shown in Table 1, the tailings possess a stable negative zeta potential of -14.2 mV.

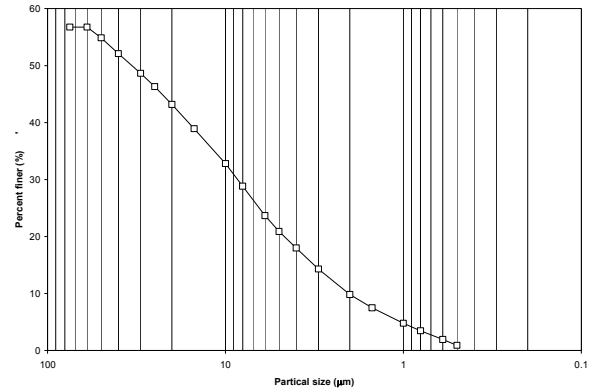


Figure 2. Particle size distribution of tailings for particles finer than 75 μm (passing #200 sieve)

The zeta potential of tailings solids as a function of water pH was measured by titration using 0.1 M NaOH and 0.1 M HNO₃ solutions. The results are presented in Figure 3, which shows that the zeta potentials of the tailings are stable in the range of -12 mV to -14 mV between pH 3 and pH 9. The point of zero charge (pzc) is located at pHo = 10.3. The zeta potential becomes unstable at pH > 9 and turns positive at pH > 10.3.

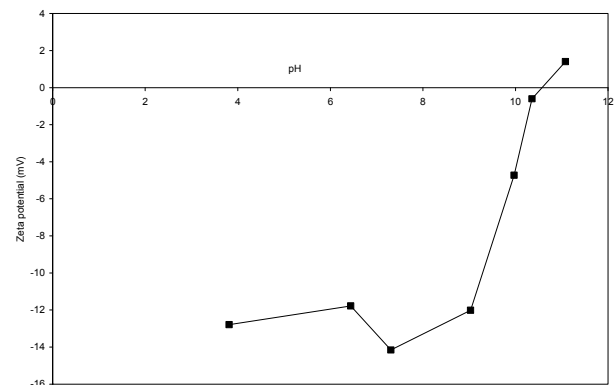


Figure 3. Zeta potential of tailings solids vs. water pH

EXPERIMENT

EK-cell

The Electrokinetic cell (EK-cell hereafter) shown in Figure 4 has been developed to measure the electroosmotic permeability in porous geo-materials under well-controlled boundary conditions (Mohamedelhassan and Shang 2002).

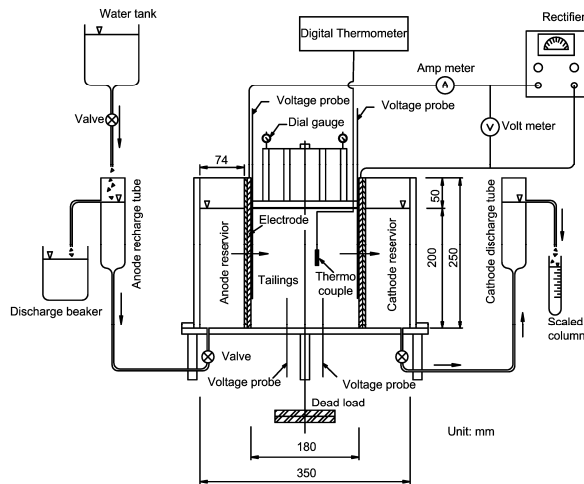


Figure 4. EK-cell

The EK-cell consists of an anode reservoir, a specimen compartment, and a cathode reservoir. The cell is made of 10-mm thick Plexiglas with the inside dimensions of $35 \times 10 \times 25$ cm (Length \times Width \times Height). The tailings are placed in the specimen compartment and a rubber sheet is placed on top of the tailings specimen so that the top and bottom of the EK-cell are impervious boundaries and the water flow through the tailings sample in the cell is one-dimensional (horizontal). The electrodes with the same width and height as the EK-cell (10 cm \times 35 cm) are placed at both ends of the specimen compartment, which are wrapped with a geo-textile for filtering and drainage. A dead load of 15 kg is applied via a loading plate (13.6 cm long \times 10 cm wide \times 2 cm thick) on the top of the specimen compartment, generating a surcharge pressure

of 11 kPa. The purpose of applying the surcharge pressure is to obtain a specific density for the tailings specimen and to ensure full saturation. All EK-cell tests are carried out after the consolidation settlement of the tailings sample has virtually completed under the surcharge pressure of 11 kPa. The water in both reservoirs on the EK-cell is controlled at the same level via recharge and discharge tubes to ensure the hydraulic gradient across the tailings specimen is zero. Therefore, any water flow (discharge) measured during an EK-cell test is solely attributed to the applied dc current. The electrodes are connected to a dc power supply (B&K Precision 1671A 0-30V, 0-5 A) and the dc current and voltage are measured using a high precision multi-meter.

It should be noted that the main objective of an EK-cell test is to measure the electroosmotic permeability defined in Eq. (1). In this case, the tailings specimen in the EK-cell can be modeled as a rigid porous plug with minimum deformation (settlement). The EK-cell tests provide information on the electroosmotic permeability as a function of tailings density (porosity), applied dc current (current density), voltage (voltage gradient), time and water chemistry. In addition, the EK-cell tests provide information on voltage losses at interfaces of electrodes and tailings.

In this study, two types of electrodes were used in the EK-cell tests, i.e., the Electrical Vertical Drain (EVD) and stainless steel 316 mesh (SS316). The EVD, as shown in Figure 5, was originally developed for soil improvement applications. The conductive core of the EVD is made of a copper foil encapsulated in conductive polymer, 6 mm thick and 95 mm wide, which is wrapped with a textile filter. SS316 is the highest grade of corrosion-resistant stainless steel commercially available. The mesh used in the tests has a thickness of 0.7 mm, nominal opening 0.7 mm, and specific opening area

29.2 %. In the EK-cell test, the SS316 mesh is wrapped with the same textile filter as used in the EVD for filtration and drainage.

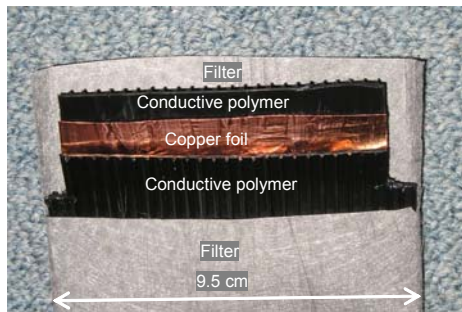


Figure 5. Electrical Vertical Drain (EVD)

Polarity Reversal

Polarity reversal has been applied in applications of electroosmosis in soil improvement applications, mainly to reverse differential settlements (Gray and Somogyi 1977). It is also recognized that polarity reversal may serve an important role in controlling the pore water pH at the anode to prolong the water flow. For the tailings tested, since the zeta potential remains stable and negative in the pH range of 3 to 9, as shown in Figure 3, it is desirable to sustain the pH of tailings pore water in this range. One way of achieving this goal is polarity reversal, i.e. to reverse the anode and cathode periodically. The schematic of polarity reversal is illustrated in Figure 6. Under the normal polarity (NP) mode, the left electrode of the EK-cell is the anode and right electrode is the cathode. Under the reversed polarity (RP) mode, the applied dc voltage is reversed, i.e., the left electrode is the cathode and the right electrode the anode, whereas all other conditions remain the same. The water flow in the tailings reverses direction after the polarity reversal. The quantity of water discharge is measured at either right or left side of the EK-cell, depending on whether the EK-cell is under NP or RP mode.

Experiments and Results

Three EK-cell tests were carried out on the tailings, as shown in Table 2, i.e., EK-EVD, EK-SS316, and Control. The tests were set up in three identical EK-cells and carried out simultaneously. The hydraulic conductivity of the tailings was estimated in the Control cell by seepage under a constant hydraulic gradient, i.e., maintaining a constant total head difference (20 cm) between the left and right reservoirs. It was found that the hydraulic conductivity of the untreated tailings reduced approximately one order of magnitude over a period of 350 hours, Table 2.

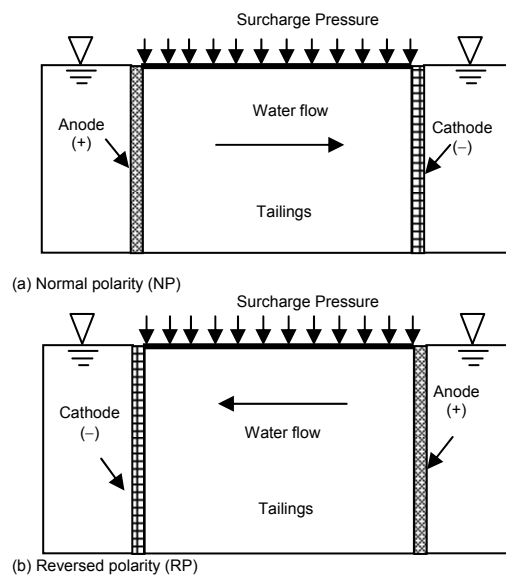


Figure 6. Polarity reversal during EK-cell test

In both EK-cell tests, a constant dc voltage of 10 V was applied across the electrodes, generating constant electric field intensity (voltage gradient) of 55 V/m (with an electrode spacing of 18 cm). The corresponding dc current across the sectional area of tailings specimen (10 cm x 20 cm) was monitored and presented as the current density versus time, as shown in Figure 7, showing the range of current density in the tests was between 5 to 8 A/m², with

exceptions on the EK-EVD test, which will be explained later.

Table 2. Summary of testing conditions

Surcharge pressure, kPa	11
Drainage path	Left and right reservoirs (2-way)
Tailings sample size, cm x cm x cm (height x length x width)	20 x 18 x 10
Applied voltage, V	10
Applied voltage gradient, V/m	55
Hydraulic gradient	0

Properties of Tailings Specimens (Average of three tailings specimens)

Dry density (g/cm ³)	Water content (%)	Degree of saturation (%)	Void ratio	Hydraulic conductivity* (m/s)	
				Before EK-cell test	After EK-cell test
0.95	66.9	99	1.8	1.3×10^{-6}	2.2×10^{-7}

* Estimated by seepage test in the Control test
 Test EK-EVD – EVD electrodes
 Test EK-SS316 – SS316 mesh electrodes
 Test Control – no voltage application

Figure 8 shows the accumulated water flow induced by the dc current. Both EK tests started with the normal polarity (NP) (the left and right electrodes served as the anode and cathode, respectively, see Figure 6). The water flow was triggered immediately towards the cathode, collected at the right side of the cell) and measured in real time by a graduated cylinder. The dc current passing through the tailing specimens in both EK-cells increased with time at first, reached a peak after about 100 hours, and then leveled off (see Figure 7). The water flow stopped in both cells after about 100 hours, as shown in Figure 8. In an attempt to re-activate the water flow, the reversed polarity (RP) mode was applied at hour-191 with the same applied voltage of 10V in both cells.

In Test EK-SS316 using stainless steel electrodes, the water flow resumed immediately (see Figure 8) towards the left side of the cell (cathode) and continued until hour-700 before it stopped again. At this time the electrode polarity was switched back

to NP mode for another 100 hours but it did not trigger further flow. The test was then terminated at hour-800. The total water discharge in Test EK-SS316 was 900 ml, or about 25% of the volume of the tailings specimen, and 40% of the tailings pore volume. In other words, 40% of water filled in the pore space of tailings has been replaced by the water driven into the tailings specimen by the dc current.

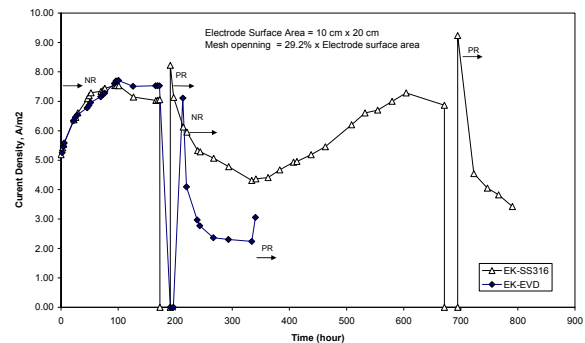


Figure 7. Electrical current density in EK-cell tests, applied voltage = 10 V, voltage gradient = 55 V/m.

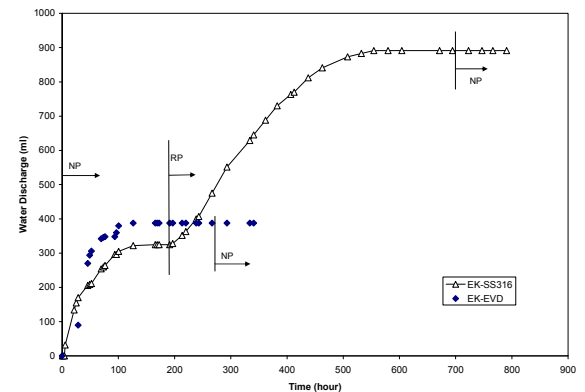


Figure 8. Electroosmotic induced water discharge, NP = normal polarity, RP = reversed polarity (refer to Figure 6)

In Test EK-EVD the current density drastically reduced to 2 A/m² after the polarity reversal, and no further water flow was registered. It is quite obvious that the EVD electrodes have lost the capacity to conduct current. Two more polarity reversals were made at hour-191 and hour-269 without inducing any water flow. Therefore Test EK-

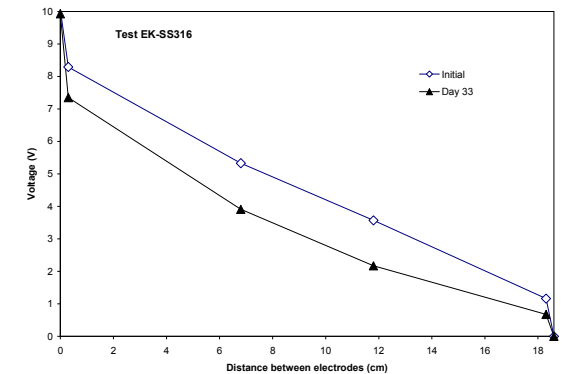
EVD was terminated at hour-340. The total water discharge was 388 ml in Test EK-EVD, which was approximately 10% of the volume of the tailings specimen.

The voltage profiles across the two EK-cells were monitored by voltage probes and are shown in Figure 9. The total voltage loss at the anode and cathode during the normal polarity mode were about 2 V in Test EK-SS316 and 4 V in Test EK-EVD, respectively. The total voltage loss at the SS316 electrodes and tailings interface was about 35% of the applied voltage, which is consistent with previous studies using steel electrodes (Casagrande 1983). The noticeable increase in the voltage loss at the anode (from 2.8 V to 3.8 V) is attributed mainly to the increase in tailings electrical resistivity at the vicinity of the anode. On the other hand, the EVD on the right-hand-side of the EK-cell has lost its capacity of conducting current, as indicated by the sharp voltage drop evident at the tailings electrode interface after 15 days, Figure 9 (b).

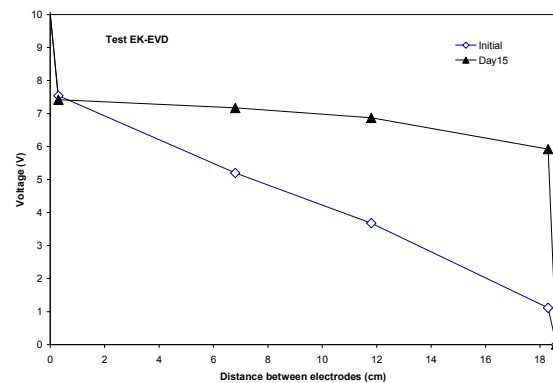
The settlement of the tailings specimens during the EK-cell tests is shown in Figure 10. In all three tests, the settlements of the tailings specimens were measured by two dial gauges mounted on the top of the loading plate, 3 cm from the left and right electrodes, respectively.

Tests EK-EVD and EK-SS316 electrodes showed similar patterns of settlement, i.e., nearly negligible settlement at the right-side of the specimen and about 1.7 ~ 1.8 % at the left side of the specimen. The settlement registered from the Control test during the same testing period was negligible. The higher settlement at the left side of the specimen was obviously induced by the negative pore pressure at the anode due to electro-osmosis. It is of interest to note that in Test EK-SS316, the settlement on the left side of the specimen reached a limit after

150 hours and was not affected by polarity reversal. This indicates that the tailings specimen behaved as a rigid (to some extent, cemented) porous plug for water transport, which may be attributed to cementation generated by electrokinetics (Mohamedelhassan et al. 2005).



a)

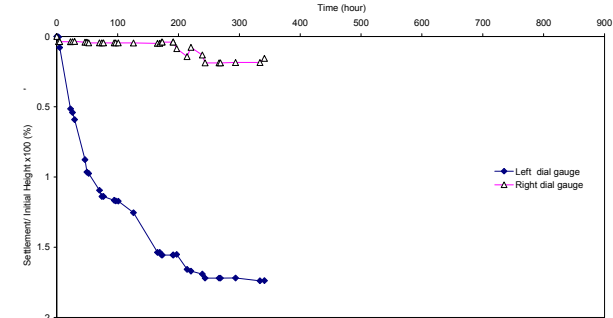


b)

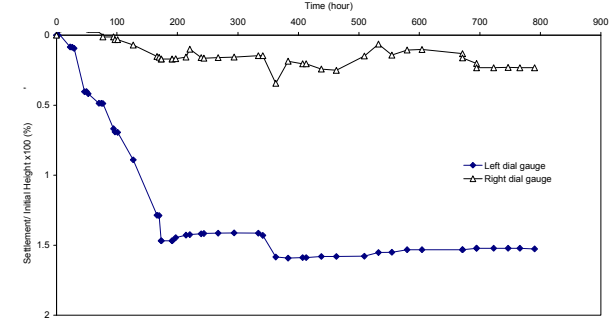
Figure 9. Voltage losses at electrodes-tailings interface and voltage distributions in the tailings specimens: (a) Test EK-SS316; (b) Test EK-EVD

The coefficients of electro-osmotic permeability of two tailings specimens are calculated from Eq. (1) and presented in Figure 11. The initial k_e values measured from tests EK-EVD and EK-SS316 are $6 \times 10^{-9} \text{ m}^2/\text{Vs}$ and $4 \times 10^{-9} \text{ m}^2/\text{Vs}$, respectively, which quickly decreased with time and approaches zero after 113 hours of voltage application. The polarity reversal resulted in further flow in Test EK-SS316, and the k_e values sustained

in the magnitude between 10^{-10} and 10^{-9} m²/Vs over 300 hours, then it gradually decreased to zero. These results show that k_e is highly dependent of time.



(a) Test EK-EVD



(b) Test EK-SS316

Figure 10. Settlement of tailings specimens during EK-cell tests

The hydraulic conductivity of Test EK-SS316, as estimated by the seepage test on the tailings specimen after the test, was 5×10^{-8} m/s, compared to 2.2×10^{-7} m/s on the Control specimen. Again, this maybe attributed to cementation and blockage of pores in the tailings associated with electrokinetics.

The temperature of tailings specimens were monitored during the EK-cell tests and the results showed that under the applied voltage gradient (55 V/m), there was no significant heating effects and the temperature of tailings samples was consistent with the room temperature.

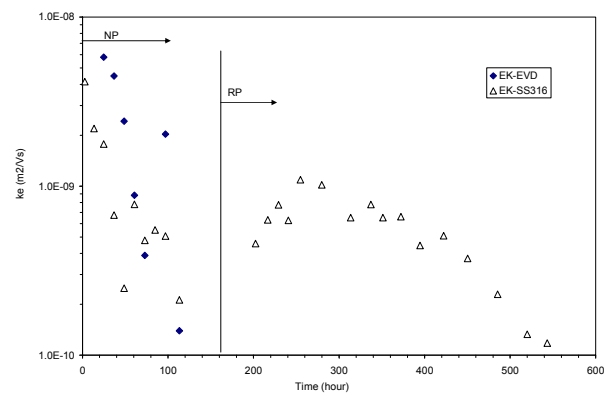


Figure 11. Coefficient of electroosmosis, k_e , versus testing time

The tailings were removed from the EK-cell after test EK-SS316 to measure the tailings pore water pH near the left and right sides of the cell. The tailing pore water pH is 11.5 on the left side and 5.5 on the right side of the tailings specimen, compared to the original water pH 7.3. The changes in the tailings pore water pH provide insight to the stop of water flow during the EK test. As shown in Figure 8, the water flow was from the left side to the right side of the EK-cell under the NP mode; and from the right side to the left side of the EK-cell under the RP mode. The tailings pore water pH increases at the cathode and decreases at the anode. Based on the results of zeta potential measurement shown in Figure 3, the surface charge of tailings solids approaches zero at pH = 10.3 and becomes positive with further increase in the water pH. Therefore it is inferred that the stop of water flow in both EK-cell tests after about 100 hours was caused by the increases in tailings pore water pH at the cathode. The resume of water flow in test EK-SS316 after the polarity reversal is attributed to the decrease in the tailings pore water pH at the right side electrode, which served as the anode under the RP mode. Finally, the water flow stopped again in test EK-SS316 when the tailing pore water pH increases to 11.5 (above pH = 10.3) at the cathode (left side

electrode). The results demonstrate the importance of pore water pH control in the EK dewatering applications. To maintain dewatering effects, the tailings pore water pH must be controlled such that the zeta potential of tailings solids remains negative. This can be achieved by polarity reversal, as shown in this study, as well as other means such as pH adjustment by chemicals (Mohamedelhassan and Shang 2003) and agitating tailings during the dewatering process (Kelsh and Sprute 1975).

The tailings water content after Test EK-SS316 is 55% to 60% throughout the tailings specimen, decreased from the original 67% (Table 2). The decrease in the tailings water content was primarily attributed to settlement during the EK-cell tests (Figure 10). Note this is not representative of EK dewatering effect because the EK-cell is configured to measure k_e , which serves mainly as a porous plug with open drainage at both anode and cathode.

The mass loss of SS316 mesh electrodes were measured after test EK-SS316 and the corrosion rate was calculated, as shown in Table 3. The results show that for the tailings tested the corrosion rate of the SS316 mesh is 0.19 to 0.21 g/A-hour, compared to the corrosion rate of 0.7 ~ 1.04 g/A-hour of mild steel as reported in the literature (Lockhart 1986). In dewatering applications, the electrode material should be selected based on factors such as duration of treatment, cost, environmental considerations, etc.

CONCLUSIONS

A dc current delivered by stainless steel 316 electrodes generated significant water flow in gypsum containing tailings originated from a mine site in Northern Saskatchewan. The water flow across the tailings specimen sustained for more than 400 hours under an

applied voltage gradient of 55 V/m. The corresponding dc current density was in the range of 6 to 8 A/m². The total volume of water discharged by the dc current was equivalent to about 40% of the tailings pore volume. The coefficient of electro-osmotic permeability (k_e) of the tailings was measured in the order of 10^{-10} to 10^{-9} m²/Vs. Combined with the low hydraulic conductivity of the tailings ($\sim 10^{-8}$ m/s), the results indicate the tailings responds favorably to electrokinetic dewatering. The selection of electrode material is crucial in an EK dewatering application. The electrical vertical drain electrodes made of conductive polymer failed to sustain water flow under a voltage gradient of 55 V/m. On the other hand, SS316 mesh electrodes performed reasonably well for 800 hours under the applied voltage and current in the EK test. The corresponding corrosion rate of the SS316 mesh has been established as 0.2 g/A-hour, which was about one order of magnitude lower than mild steel. The pH control for tailings pore water is required to sustain water flow under a dc current. Polarity reversal has proven to be an effective measure to balance tailings pore water pH during EK treatment.

ACKNOWLEDGEMENT

The research is funded by Cameco Corporation and Natural Science and Engineering Research Council of Canada. The contribution of Dr. Amnart Rittirong, Dr. Yanqing (Bruce) Xu, Dr. Patrick Landine and Ms. Anooradha Nursimulu to the research is greatly appreciated.

Table 3. Mass loss of SS316 electrodes and corrosion rate

Mass of Electrode				Operation Time as Anode		Ave current*	Corrosion rate			
Original		After EK test		Loss		h	mA	g/A-hr		
g	g	g	g	g	g			Left	Right	
Left	Right	Left	Right	Left	Right	Left	Right	Left	Right	
101.7	104.4	77.6	64.1	24.1	40.3	273	509	420	0.21	0.19

* Normalized against mesh opening area 29.2 %

REFERENCES

Casagrande, L. (1983). Stabilization of Soils by Means of Electro osmosis - State of the Art. *Journal of Boston Society of Civil Engineers, ASCE* 69(2), 255-302.

Chew, S.H., Karunaratne, G.P., Kuma, V.M., Lim, L.H., Toh, M.L. and Hee A.M. (2004). A Field Trial for Soft Clay Consolidation Using Electrical Vertical Drains. *Geotextiles and Geomembranes*, 22, 17-5.

Mohamedelhassan E, Shang J. Q, Ismail M.A. and Randolph M.F. (2005). Electrochemical Cementation of Calcareous Sand for Offshore Foundations. *International Journal of Offshore and Polar Engineering (IJOPE)*. Vol.15, No.1, 71-79.

Fourie, A. B., Johns, D. G. and Jones, C. J. F. P. (2007) Dewatering of Mine Tailings Using Electrokinetic Geosynthetics. *Canadian Geotechnical Journal*, 44(2), 160-172.

Gray, D. H. and Somogyi, E. (1977). Electroosmotic Dewatering with Polarity Reversals. *J. Geotech. Eng. Div. ASCE* 103 (GTI) 51-54.

Helmholtz, H.L.F. (1879). Studies of Electric Boundary Layers. *Wied. Ann.*,

Vol. 7, pp. 337-382. In Abramson, H.A., Moyer, L.S. and Gorin, M.H. (1942). *Electrophoresis of Proteins*, Reinhold Publishing Corporation.

Kelsh, D.I. and Sprute, R. H. (1975). Limited Field Tests in Electrokinetic Densification of Mill Tailings. U.S. Bureau of Mines RI 8034.

Kelsh, D.I. and Sprute, R.H. (1976). Electrokinetic Consolidation of Slimes in an Underground Mine. U.S. Bureau of Mines RI 8190.

Kelsh, D. I. and Sprute, R.H. (1981). Dewatering Fine Particle Suspensions with Direct Current - Field Applications" 2nd World Congress Chem. Eng. 4, 142-145.

Lockhart, N.C. (1986). Electro-dewatering of Fine Suspensions. *Advances in Solid-Liquid Separation*. 241-274.

Mitchell, J.K. (1993). *Fundamentals of Soil Behavior*. 2nd Ed., John Wiley & Sons, New York.

Mohamedelhassan, E. and Shang, J.Q. (2002). Feasibility Assessment of Electroosmotic Consolidation of Marine Sediment. *Ground Improvement*. Vol. 5, No.2, 1-8.

Mohamedelhassan, E. and Shang, J.Q. (2003) Electrokinetics Generated Pore Fluid and Ionic Transport in an Offshore Calcareous Soil". *Canadian Geotechnical Journal*, Vol.40, 1185-1199.

Rittirong, A. and Shang, J.Q. (2005). Ground Improvement – Case Histories, Edited by B. Indraratna and J. Chu, Chapter 34 (Theme 5), pp. 1127-1162, Elsevier Publishers.

NORTH ZPL DAM – CASE HISTORY OF A FOUNDATION FAILURE AND SUBSEQUENT REMEDIATION AND FOUNDATION STRENGTHENING OF AN EMBANKMENT CONSTRUCTED ON SOFT LACUSTRINE CLAYS

Brad Russell, Iain Bruce and Stephen West

BGC Engineering Inc., Vancouver, British Columbia, Canada

Riley Little

Hudson Bay Mining & Smelting Co Ltd, Flin Flon, Manitoba, Canada

ABSTRACT: A slump of the downstream slope of a reinforcing berm at the Zinc Pressure Leach tailings containment facility in Flin Flon, Manitoba occurred as result of loading the soft lacustrine clay foundation too rapidly. The berm was being built to allow continued raising of a tailings dam that was transitioning from upstream to downstream type of construction. Although the existing dam stability was not compromised, any further dam raising was deemed to require stabilization at the toe. Following the initial movement, a rock fill of mine waste was placed at the toe to stabilize the entire slope. Instruments were installed to monitor the work, the subsequent deformations and pore pressure responses. Annual drilling has occurred since the failure and the results document the strengthening of the clay with time. This allows comparison of calculated strengthening rates from laboratory tests with actual strengthening rates. Additionally, a correlation has been drawn between deformation monitoring and changes in the calculated factor of safety over time. This paper explains the soils stratigraphy, summarizes the failure causes and provides a summary of the remedial works and their effects over time. Actual test and field data are presented that will assist with future designs on similar soils and in similar environments.

INTRODUCTION

The North ZPL Dam is an active structure that contains residue from the Zinc Pressure Leach (ZPL) process. The dam is being raised annually, at a rate of approximately 1 metre per year. The original N ZPL Dam was built using slag end-dumped through water to create a starter embankment that was

then made impervious by placement of an upstream face of clay, also placed through water. The dam has been raised over time with slag, clay, compacted tailings fill and waste rock as described in more detail in Section 2. The general arrangement of the structure is shown in Drawing 01.

In December 2005, during placement of a downstream slag berm along the N ZPL

Dam, a failure, involving the lower downstream shell of the dam, occurred in the soft lacustrine clay foundation beneath the berm. The slip developed over an area approximately 100m wide by 25m long and 18m deep as a result of rapid loading.

While the dam composition is basically uniform throughout its length, the foundation conditions vary with rock foundations on each abutment and various depths of clay along the length of the dam. Section NZPL 1+42 intersects the dam nearly at the center of the slag berm failure and represents the area with the thickest clay foundation. As-built dam cross sections had originally been created from anecdotal information and construction photographs.

The failure initiated a field program in early 2006 to investigate the subsurface conditions, install instrumentation, assess the stability of the structure and establish a plan to stabilise the dam. The information collected and analyses conducted resulted in the construction of a downstream stabilisation toe berm comprised of waste rock in early 2007. The toe berm served to stabilise the dam and allow continued operation.

During the toe stabilisation berm construction in 2007, an additional field and laboratory testing program was undertaken to gather additional information regarding the foundation soil stratigraphy and strength characteristics of the foundation soils. In addition, further instrumentation was installed to monitor the behaviour of these foundation soils. The foundation soil strength parameters have been refined as a result of the additional field and lab testing. Monitoring of instrumentation, including piezometers, slope inclinometers and settlement pins, have provided soil response data and provided insight regarding the time-

dependant behaviour of the soft foundation soils when subjected to load.

The information collected during the two field programs has been correlated with construction history records and has provided sufficient data to allow reassessment of the as-built cross sections and the material properties of the soils in the dam and foundations. This, along with the subsequent instrumentation monitoring has allowed a more detailed stability analysis, which included estimated excess pore water pressure responses, to be conducted.

HISTORY OF N ZPL DAM CONSTRUCTION

The N ZPL Dam was initially constructed as a slag causeway built across the southern portion of the Clarification Pond by connecting between a natural bedrock high on the east with a narrow point of natural ground that protruded into the pond on the west. It was initially constructed by end-dumping slag into the pond, promoting displacement of the natural lake bottom sediments until stability of the embankment was achieved. Very little site specific soil data was gathered for the foundation conditions over which the causeway was being constructed in advance of the construction.

The construction history has been compiled based on various reports and documents submitted by both HBMS and BGC in the past. The dimensions and elevations of features have been provided by various historic survey data and construction notes and compared with the results of borehole investigations. Consolidation and settlement has been considered in assessing variances between the historic values.

The complete history of the N ZPL Dam construction is presented below along with notable features and observations through each sequence. Elevations have previously been reported in mine grid co-ordinates but for the purpose of consistency, the historic values have been converted to UTM NAD83 datum and are reported herein as such.

1992: Slag was end-dumped into the Clarification Pond to create the initial causeway. The structure was built to approximate elevation 317.7m with a crest width between 10 to 12m. The sideslopes have been estimated at 1H:1V.

Clay fill was placed along the upstream face of the slag causeway. Material was mainly placed by end dumping through water and was uncompacted. The upstream slope was estimated at 4H:1V and the width at the crest was approximately 4m.

Clay fill was placed over the crest to raise the structure to approximately elevation 319.1m.

ZPL tailings were initially deposited into the ZPL facility in 1992. Deposition has continued since this time. The material is low plastic and consists of silt sized particles, being deposited at low density.

1996: In winter, clay fill was placed over the entire crest to raise the structure to 320.4m.

Downstream widening of the structure was completed with waste rock. The waste rock was constructed to elevation 318.5m. Cracking and slumping was observed in the fill but these were repaired. The cracking

was attributed to settlement of soft clay foundations under the dam shell.

Longitudinal cracks were observed along the dam crest.

1997: Additional waste rock was placed along the downstream side of the dam to repair deformations and act as a stabilising berm. The resulting waste rock was between 10 to 15m in width. The downstream slope was between 1H to 1.5H:1V above water but due to slumping and lake bottom displacements, the slope likely was flatter below water.

In November and December, clay fill was placed over the entire crest, raising the crest to elevation 321.5m. Slag and sand were placed as a road surfacing.

1999: Compacted tailings fill, obtained from FFTIS borrow pits, was placed over the ZPL tailings beach on the upstream side of the clay fill. The widening was approximately 10 to 12m wide and constructed to elevation 321.9m. Minor settlement was noted following placement.

The clay core was raised to elevation 322.7m with the crest at a width of approximately 10m.

Additional tailings fill was placed over the beach along the upstream side of the dam to the same elevation as the clay crest, 322.7m.

2000: Surveys indicate that the central portion of the dam settled as much as 0.156m between October 1999 and July 2000.

Tailings fill was placed over the upstream portion of the dam, resulting in a 10m wide crest at elevation 323.4m.

2002: Stability analyses undertaken based on information available at the time suggested that the design factor of safety was decreasing as the dam height was raised. A stabilisation berm of slag was placed along the downstream slope of the dam. The slag was end-dumped into the Clarification Pond to encourage the displacement of soft lake bottom sediments and clay. The placement started from the east side and progressed westerly with a width of approximately 60m and being maintained approximately at elevation 319.5m. Waste rock, at times boulder-sized, was included in the fill at various times. As the leading edge of fill approached Section 0+93, large displacements were noted and the fill underwent excessive deformation and settlement. The placement of fill was halted at this location.

2003: Tailings fill was placed over the entire dam crest to raise the dam to elevation 325.0.

2004: In March, placement of slag was reinitiated along the downstream side of the dam and the berm was completed to the natural ground point on the west abutment. Larger deformations were noted in the vicinity of Section 0+93 to 1+42.

As the dam continued to rise and water regularly became trapped against the upstream dam face, piping of the tails and the loose upstream clay face of the dam was recognized

as an increasingly likely failure mode. Filter sand was placed approximately between the contact of the downstream toe of the dam and the downstream slag stabilisation berm. An excavator opened a trench as deep as possible and filter sand was placed within the trench at a width of approximately 1 to 1.5m and a depth of approximately 3m.

Tailings fill was placed over the crest of the dam and in the upstream direction. The crest was widened by approximately 8m upstream over the ZPL tailings beach.

2005: Early in the construction season (likely June or July), one lift of slag was placed over the downstream slag stabilisation berm. The thickness of this lift was likely approximately 1.5m bringing the berm elevation to approximately 320.5m.

In November and December, additional slag was placed on the downstream slag stabilisation berm. The first lift of approximately 1.5m thickness brought the berm to elevation 322.0m over the full width. The downstream slope was approximately 1.4H:1V. Following the completion of this lift, a second lift of approximately 1.0 to 1.5m thickness was placed over the full extent of the berm. Within 24 hrs of the completion of this lift, a failure of the downstream slope occurred. The center of this failure was located at approximately Section 1+42 and extended approximately 50m each side of this.

2006: Large longitudinal cracks were observed along the crest of the dam,

similar in nature to previous cracks observed annually.

To maintain freeboard through the winter, compacted tailings fill was placed over the dam crest and in an upstream direction, raising the crest to elevation 327.4m. Prior to fill placement, stability analyses were undertaken to assess the impacts of the raise. The calculated factor of safety did not decrease and the dam raise was not deemed to be detrimental. Instrumentation was monitored throughout fill placement.

Although placement of the fill did not decrease the factor of safety, analyses suggested that the overall factor of safety of the dam was still low, so construction of an additional downstream toe berm was recommended. In November and December, the construction of a downstream waste rock stabilisation berm was initiated. Waste rock was end-dumped into the Clarification Pond with the intent of displacing the full depth of soft lake bottom sediments and clays. The berm started from chainage 0+44 and progressed in a westerly and northerly direction to displace soft material away from the downstream slope of the dam.

2007: From January through March, waste rock was placed into the downstream stabilisation berm. The berm was completed from approximately chainage 0+44 to the west abutment of natural ground, to a width of 90m and to an approximate elevation of 319.5m. While the intent of the berm was to displace the full thickness of the soft clay deposit, drilling

confirmed that full displacement was not achieved. The soft clay layer was thicker than anticipated and it was found that in-place waste rock varied in thickness between 11 and 13m.

In September, compacted tailings fill was placed on the crest of the dam to maintain freeboard. The crest was raised to elevation 328.8m with a width of 7m and a 3H:1V downstream slope.

2008: A number of raise configurations were considered to ensure the active structure could maintain freeboard. An upstream raise onto the ZPL tailings beach using compacted tailings fill and geo-grid was recommended.

AS-BUILT SECTION UPDATE

As noted previously, the as-built cross sections had originally been compiled from anecdotal information and various construction photographs. While the sections had been generally accurate in regards to composition and materials, details of dimensions and thicknesses were only approximated. The characteristics of the materials placed under water were also estimated, but with even less certainty.

The drilling and interpretation of boreholes that occurred as a result of the latest instability provided more definitive quantitative data for the location and dimension of various materials. The results of the boreholes were correlated with the construction history documents and photographs to reassess the composition and geometry of the dam at the various sections along the North ZPL Dam. As a result, a number of modifications to the dam cross

sections were made. The most notable allowed for increased widths and thicknesses of the slag and waste rock that had been placed between 1992 and 1997. Also of particular importance was the definition of the clay layer and bedrock surface profile beneath the structure. The bedrock was found to be at greater depth than previously assumed and the clay layer thicker on the downstream side of the dam. Beneath the crest, consolidation of the clay has reduced the overall thickness over time. The revised as built section is shown in Drawing 02.

SOIL PROPERTIES

Compacted Tailings Fill and Tailings Slimes

The compacted tailings fill has been assigned a friction angle of 35 degrees based on previous experience with this and similar materials. While laboratory testing has not been conducted on the compacted tailings fill specifically, which is mainly comprised of sand obtained from borrow pits in the FFTIS, direct shear testing has been conducted on the finer-grained tailings slimes. The friction angle of this material has been found to be as high as 35 degrees. A conservative value of 30 degrees was selected for tailings slimes in the analysis. The compacted tailings fill would be placed at a higher density than the hydraulically deposited tailings slimes and therefore bulk unit weights of 20 kN/m³ and 17 kN/m³ were applied respectively.

Slag, Waste Rock and Sand

Unit weights and friction angles for slag, waste rock and sand, including filter sand and sandy till, were selected based on experience with these and similar materials. Unit weights of 22 kN/m³, 20 kN/m³ and 17 kN/m³ were applied, along with friction

angles of 38 degrees, 38 degrees and 35 degrees, respectively.

ZPL Tailings

The drained parameters of ZPL tailings have been determined by a series of direct shear tests. The material exhibited an internal friction angle of approximately 42 degrees with 5 kPa cohesion. The bulk unit weight has been calculated by in-situ density tests and found to be approximately 15 kN/m³.

Lacustrine Clay

The overall dam stability is governed by the soft lacustrine clay foundation soil. The strength and deformation properties of the lacustrine clay foundation have been defined using accumulated data from various field investigations and lab testing conducted over a number of years. The relevant strength and deformation properties are discussed below.

Atterberg Limits

The lacustrine clay has been sampled from a number of locations around the FFTIS and ZPL facilities. Results from various areas have been compiled and data with similar Atterberg limit indices have been combined. The lacustrine clay present in the foundation of the N ZPL Dam is clay with high plasticity that is similar in nature to that encountered in a portion of the South Weir Dam foundation. The plasticity index (I_p) of this clay ranges from 26 to 45.

Drained Parameters

The drained parameters of the lacustrine clay were determined by Triaxial CIU test on samples obtained by Shelby tube. The angle of friction has been determined to be approximately 28 degrees with the material exhibiting 5 kPa of cohesion. The lacustrine

clay foundation has been analysed using only undrained parameters, however the drained properties have been applied to the silty clay material used as dam fill.

Coefficient of Consolidation (c_v)

During loading of a fine grained soil, such as clay, the vertical stress is initially carried as excess pore water pressure in the soil. With time, the excess pore pressure is able to drain out of the soil and the material undergoes a volume change, defined as consolidation.

The rate at which excess pore water pressures dissipate can be represented by the coefficient of consolidation (c_v). This value has been estimated using a number of various methods. Hughes Engineering used Cone Penetration Testing (CPT) in 1999 to obtain an average value of $9 \times 10^{-4} \text{ cm}^2/\text{s}$ for the lacustrine clay. A Shelby tube sample obtained from BGC07-BH26 on the N ZPL Dam was tested in a Triaxial CIU apparatus and exhibited an estimated value of $5.5 \times 10^{-4} \text{ cm}^2/\text{s}$.

Actual piezometric levels in the foundations have been measured at the N ZPL Dam and South Weir Dam during and following periods of construction. The clay at these locations have been subjected to a known load and by analysing the increase in pressure caused by loading along with the subsequent decrease in pore water pressure levels as consolidation occurred, the degree of consolidation and coefficient of consolidation can be estimated. At the N ZPL Dam, an estimated value of $2.5 \times 10^{-4} \text{ cm}^2/\text{s}$ has been calculated.

The consolidation rate obtained using actual piezometric levels best represents the actual field characteristics of pore water pressure dissipation within the lacustrine clay at the N ZPL Dam and therefore, the value of

$2.5 \times 10^{-4} \text{ cm}^2/\text{s}$ has been used to assess pore pressure responses at this location.

Undrained Shear Strength (s_u)

Direct Measurement By Downhole Vane Test

The undrained shear strength (s_u) of lacustrine clay under the N ZPL Dam had not been measured directly prior to 2007 when it was measured in-place using a downhole vane during the 2007 stability investigations. The shear strength was generally found to vary from a high value beneath the dam crest and decreased with distance downstream of the dam centreline. The increase in strength is attributed to additional consolidation under the oldest and highest portion of the dam. The degree of consolidation and hence strength, decreases with distance downstream. Beneath the dam crest where the clay has undergone consolidation since initial dam construction in 1992, the shear strength ranged between 40 to 42 kPa. Below the slag berm that has been in place since 2002 and 2004, the shear strength ranged between 30 to 46 kPa. Beneath the waste rock toe stabilisation berm that had just been placed, the shear strength was low, in the range of 3 to 9 kPa.

The direct measurements of undrained shear strength provide actual strengths of the foundation soil at a particular time. This is useful in assessing the stability because the undrained shear strength is the principal resistance in the clay foundation and directly governs the overall stability of the structure. However, the instantaneous shear strength obtained by downhole vane tests are not inherent soil properties that can be applied to the clay for all instances in time. Due to changes in pore pressure and the degree of consolidation as discussed above, the undrained shear strength of clay varies with time and location.

These instantaneous measurements can assist in the estimation of undrained shear strengths at other instances in time. There exists a relationship between the undrained shear strength and effective stress, which is a function of excess pore pressure. This relationship is discussed below. The actual measurements can provide confirmation of estimates because they serve as a known value at a particular time under a known set of conditions.

Total and Effective Stress Relationship (s_u/σ_v' Ratio)

The relationship between undrained shear strength and the degree of consolidation can be represented using a total stress approach proposed by Ladd (1991). In this approach, the undrained shear strength of the soft clay on which fill is being placed is normalised with respect to the in-situ vertical effective stress (σ_v') or effective overburden stress. The ratio is defined as s_u/σ_v' .

During construction, when fill is placed on to the clay foundations, the initial shear resistance is generated by the undrained strength of the normally consolidated clay. The applied vertical stress is initially carried completely as excess pore water pressure in the soils. With time, as the pore pressures dissipate and the soil consolidates, the shear strength is increased commensurate with the increased effective stresses applied to the soil foundations. By estimating or measuring the s_u/σ_v' ratio beneath the dam, the stability of the dam can be calculated and refined.

Estimation by Skempton's Ratio

The s_u/σ_v' ratio can be estimated using correlations to plasticity index (I_p) as proposed by Skempton (Craig, 1999) and noted below:

$$s_u/\sigma_v' = 0.11 + 0.0037 * I_p$$

Following this correlation and the results of recently obtained Atterberg limits tests, the s_u/σ_v' ratio is estimated to range from 0.21 to 0.28, with an average value of 0.24.

Estimation by Actual Undrained Shear Strengths and Pore Pressures

The ratio can also be attained by comparing actual undrained shear strengths as measured by vane tests in the field with the estimated vertical effective stress at the location and time of the test.

The vertical effective stress was estimated based on the types of material encountered within the borehole and applying applicable unit weights, along with an estimate of the excess pore pressure present at the location of the vane test. In some cases, the estimation of excess pore pressures was assisted by data later obtained from pneumatic piezometers installed within the particular borehole. These values had to be adjusted slightly to account for dissipation between the times of vane testing and pore pressure measurement. In other cases, piezometers were not installed within the borehole and the pore pressure estimation relied upon a review of construction sequence and expected pore pressure dissipations.

Based on nine undrained shear strength measurements at the N ZPL Dam, an average s_u/σ_v' ratio of 0.18 was obtained.

Estimation by Back-Analysis of Slope Stability

The s_u/σ_v' ratio was also calculated using a back-analysis of slopes leading up to and subsequent to the failure at the North ZPL Dam in December 2005.

Back-analyses have been performed using the commercially available computer modelling program Slope/W. This operation again relied upon a review of the construction history to provide an estimation of excess pore water pressures generated within the foundation soil at each instance in time examined.

The factor of safety of the dam had been estimated based on behaviour. As the downstream slag berm was stable after the placement of the first lift of slag in November 2005, the factor of safety at this time was greater than 1.0. However, as failure occurred following placement of the second lift, the factor of safety was slightly less than 1.0. The slope then regained a stable configuration post-failure and at this point, the factor of safety was once again greater than 1.0.

The s_u/σ_v' ratio was adjusted for each of these scenarios to obtain factors of safety that best matched the conditions observed in the field. To maintain stability through the first lift and only achieve failure following the second lift, the s_u/σ_v' ratio had to be equal to approximately 0.22. This ratio also maintained stability of the post-failure configuration. Considering re-moulding of clay could have occurred during the failure, the ratio was reduced in clay that was likely to have undergone shearing. A value of 0.17 was used within the clay downstream of the failed portion of the slag berm. With this reduced value applied to the downstream portion, the post-failure configuration maintained a factor of safety greater than 1.0.

Confirmation of Process

The s_u/σ_v' approach discussed above was confirmed by analysing the slip surface data provided by Slope/W. The program uses a method of slices to determine the driving and

resisting forces generated within the critical failure block. A number of properties are provided but of specific interest is the undrained shear strength present along the base of each slice.

An analysis was conducted for the field conditions in April 2007, the time of the downhole vane shear strength testing. The shear strength along the base of each slice was compared to the actual shear strength values measured in the field at that time. The shear strengths in the analysis were found to be less than the actual measurements. Beneath the slag bench, where vane measurements indicated minimum shear strengths of 30 kPa, the analysis reported a shear strength of 22 kPa. Below the waste rock stabilisation toe berm, where vane measurements indicated shear strengths as low as 3 kPa, the analysis reported shear strengths of only 1 kPa near the contact between the waste rock and the clay. The lower values reported by the analysis indicate that the approach is valid and even slightly conservative.

Design Values

The methods noted above indicate general agreement of the s_u/σ_v' ratio. For the purpose of design, two values will be used to characterise the lacustrine clay foundation. Upstream of the failed portion, where re-moulding has not occurred, a ratio of 0.22 has been applied. Within and downstream of the failed portion, where re-moulding has possibly occurred, a ratio of 0.17 has been applied. Although re-moulding would not have occurred over the full depth of the clay layer, the exact location of the slip surface and re-moulding is not known with certainty and it is considered conservative to apply the reduced value across the full depth of the layer.

The soil properties used for design are summarised in Table 1 below.

INSTRUMENTATION AND MONITORING

The installation and monitoring of instrumentation within the N ZPL Dam has provided invaluable data to aid the assessment of stability of the structure.

A number of piezometers have been installed at the N ZPL Dam at various times. Pneumatic piezometers installed within the soft clay foundation have provided reliable measurements of excess pore pressure and the associated rate of dissipation from past construction activities. This has enabled an accurate estimation of past pore water pressure levels and an assessment of previous stability conditions. The pore water pressure readings have also enabled an estimation of strength gain with time for the soft foundation soil which in turn allowed modelling of future configurations.

Table 1. Soil Parameters Used for Analysis

Material	Unit Weight (kN/m ³)	Drained Shear Strength		Undrained Shear Strength
		c' (kPa)	φ' (°)	s _u /σ _v '
Compacted Tailings	20	0	35	-
Tailings Slimes	17	0	30	-
Slag	20	0	38	-
Waste Rock	22	0	38	-
Sand	17	0	35	-
ZPL Tailings	15	5	42	-
Silt/Clay Fill	17	5	28	-
Lacustrine Clay	17	-	-	0.17 - 0.22
Water	9.8	-	-	-

Two slope inclinometers were installed on the N ZPL Dam in April 2006. These were installed directly along chainage 1+42 with BGC06-BH6 located along the upstream side of the slag berm and BGC06-BH7 located on the downstream side of the dam crest. A third SI was installed at BGC07-BH29 in March 2007 within the waste rock stabilisation toe berm.

Settlement pins have been in place on the surface of the N ZPL Dam since September 2006. There were 16 pins originally installed in the vicinity of the slumped area. This included pins on the dam crest, on the top of the slag berm and near the bottom of the slag berm downstream slope.

Slope inclinometers (SI's) and settlement pins have provided quantitative data to assess movements within and on the surface of the structure. While the instruments have shown movement and deformation, they have provided evidence of a reduced rate of movement to support the concept of strength gain within the foundation and improved stability over time as discussed below.

The slope inclinometer and settlement pin movements can also be used to assess the calculated factors of safety. It is commonly accepted that a relationship exists between deformations and the factor of safety of a structure. As a general rule of thumb, a structure is in distress and likely showing visual deformations if the factor of safety is less than 1.2. Between 1.2 and 1.3, the structure may continue to exhibit deformations but they are likely not visible, surface features. The deformations would likely only be observed by instrumentation monitoring. Over and above 1.3, any deformations would be at a slow rate and would be attributed mainly to ongoing consolidation if placed over a soft foundation such as the N ZPL Dam. Observations

regarding this relationship are discussed in the following section.

The instruments at the N ZPL Dam continue to indicate movement and continue to provide useful data regarding the consolidation characteristics of the underlying soils.

DAM STABILITY OVER TIME

General Assessment

The stability of chainage 1+42, the critical section with the thickest layer of foundation clay, has been assessed at various instances through the past 3 years. The assessment considers both the stability of the downstream slag berm as well as the dam crest itself. Figure 1 illustrates the changes in stability with time and with respect to various construction activities and estimated excess pore water pressures in the dam foundation.

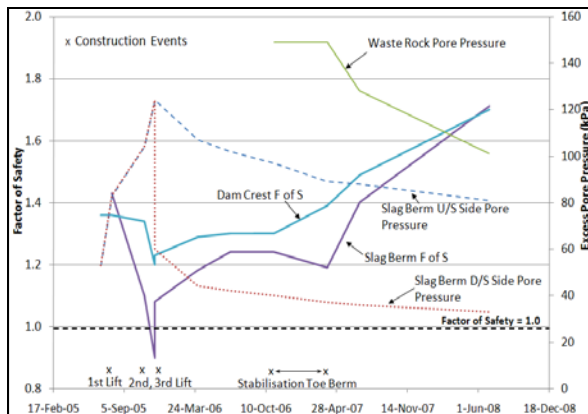


Figure 1: N ZPL Dam 1+42 - Factor of Safety and Excess Pore Pressure versus Time.

The placement of fill on the slag berm in 2005 resulted in the generation of large excess pore water pressures in the clay foundation beneath the berm. As the loading was placed in a relatively short period of time, the dissipation of pore pressures was not possible. This sharp increase in excess

pore pressure corresponds with a steady reduction in the factor of safety, particularly of the slag berm itself.

As can be seen, December 2005 marks a drop in factor of safety of the slag berm below 1.0, coincident with the failure of the slope. Following failure, the slope flattened and naturally regained a stable configuration. The foundation pore water pressure beneath the failed portion decreased as a result of the reduced overlying fill. The calculated factor of safety of the slag berm increased to approximately 1.1 at this instant.

Due to the low factor of safety, the slag berm was maintained in this configuration with no additional loading placed. The excess pore pressures were allowed to dissipate, and this resulted in a gradual increase in calculated factor of safety, with the slag berm reaching slightly greater than 1.2.

A slight drop in the factor of safety of the slag berm was calculated for November 2006 during construction of the waste rock stabilisation toe berm. The clay downstream of the slag berm underwent re-moulding during this period and was subjected to large excess pore pressures. As noted previously, shear strengths were measured as low as 3 kPa within this zone.

The stabilisation toe berm effectively increased the length of any potential slip surfaces. The waste rock itself has a high friction angle and will prevent a slip surface from passing through the berm. Therefore, potential slip surfaces are forced through the underlying clay and only reach surface downstream of the waste rock. While the construction of the berm generated large excess pore pressures and low shear strengths in the clay foundation, the cumulative effect of the increased shear length resulted in an increased factor of safety of the slag berm

and the dam crest. Deformations and rates of movement decreased following the completion of the berm.

Since the completion of the stabilisation toe berm, the shear strength of the foundation clay has slowly increased as the excess pore pressures dissipates. While it is estimated that the excess pore pressure beneath the stabilisation toe berm is only 30% dissipated, the increased shear strength across this full width has resulted in a steady increase in the calculated factor of safety. Based on current estimates of pore water pressures and shear strength gain, the current factor of safety at chainage 1+42 is now calculated to be in excess of 1.5.

Relationship with Deformation Monitoring

As discussed above, a general relationship exists between the factor of safety of a structure and the observed deformations and movements it exhibits. Figure 2 provides a comparison of dam stability and the observed rate of movement at the slope inclinometers over time. Figure 3 illustrates the direct relationship between calculated factor of safety versus rate of movement at the SI's. A vertical error bar illustrates the range of calculated factors of safety for a specific rate of movement on the SI at BGC06-BH7.

Figure 4 and Figure 5 provide similar comparisons, relating the dam stability to the observed rate of movement of settlement pins in the vicinity of chainage 1+42. The rates of movement in Figure 5 have been generalised to account for fluctuations in the data. The ranges in rates of movement for each calculated factor of safety are illustrated by the horizontal error bars.

Slope Inclinometers

At the time of installation of the initial two SI's, the calculated factor of safety of the

dam was approximately 1.2 on the slag berm and approaching 1.3 on the dam crest. The rate of movement within the SI's was observed to be at the maximum observed levels, between 8 to 9 mm/month. Since that time, both instruments have exhibited continuously reducing rates of movement.

The calculated factor of safety of the slag berm showed a temporary drop below 1.2 during the construction of the waste rock stabilisation toe berm and it may be expected that the SI at

BGC06-BH6 on the slag berm may exhibit a corresponding increased rate of movement. This SI however is located toward the upstream side of the berm, and through the original dam, and is likely to exhibit responses that correspond more closely with the dam crest itself, similar to the SI at BGC06-BH7.

The dam crest has shown a general trend of increasing factor of safety since the installation of these two SI's. This increase corresponds to the steady decrease in the rate of movement observed within the two SI's. The direct relationship between calculated factor of safety and rate of movement is shown in Figure 3.

The third SI, at BGC07-BH29, is monitoring movements within and beneath the toe berm. This zone has undergone and continues to exhibit significant deformation as a result of consolidation and settlement of the underlying clay. These deformations to the waste rock above the clay are largely attributed to differential settlements of the clay over an undulating bedrock profile. The rates of these movements are not directly related to the calculated factors of safety of the dam crest or the slag berm.

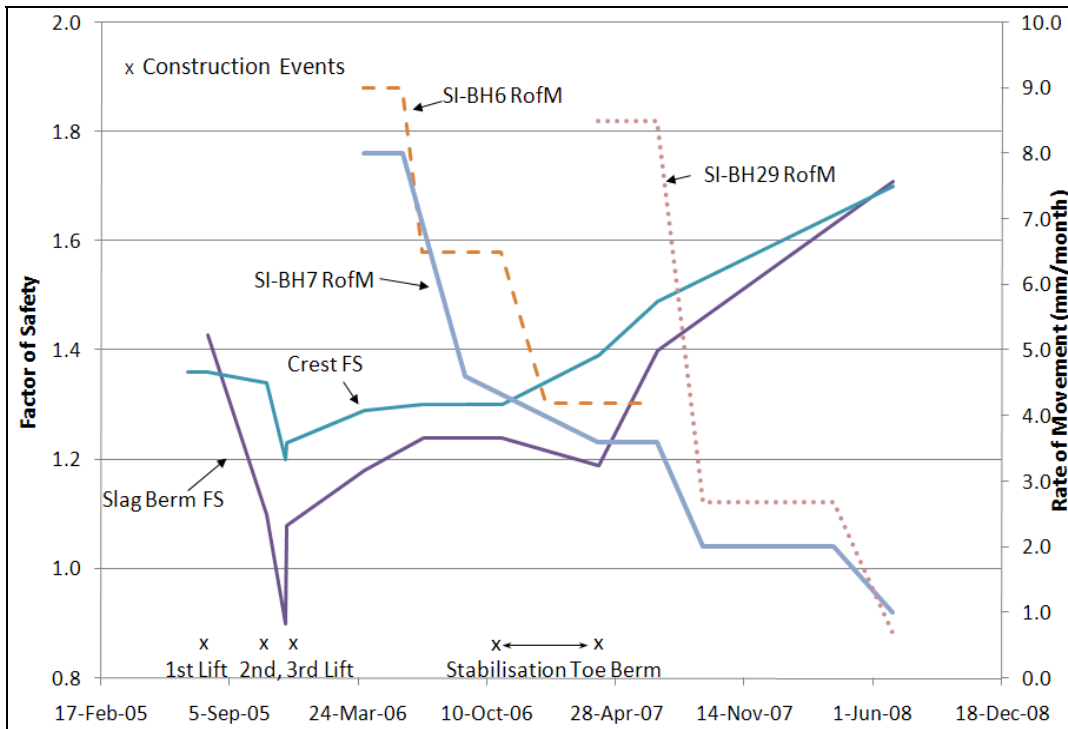


Figure 2 N ZPL Dam 1+42 - Factor of Safety and SI Movement versus Time.

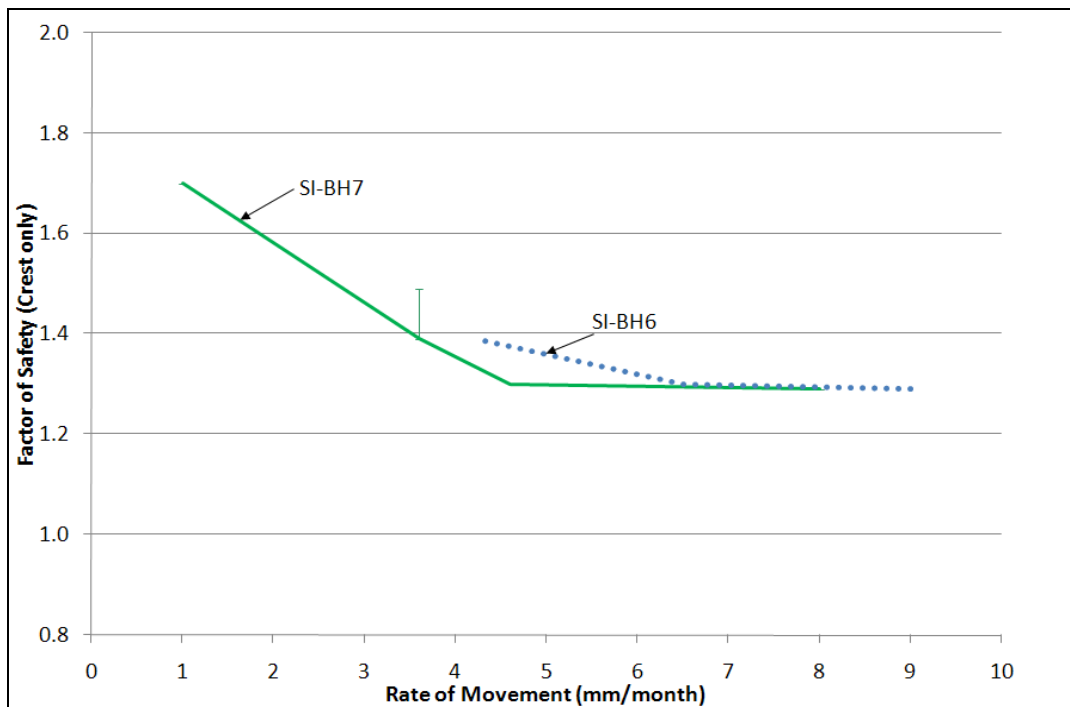


Figure 3: N ZPL Dam 1+42 - Factor of Safety versus SI Rate of Movement.

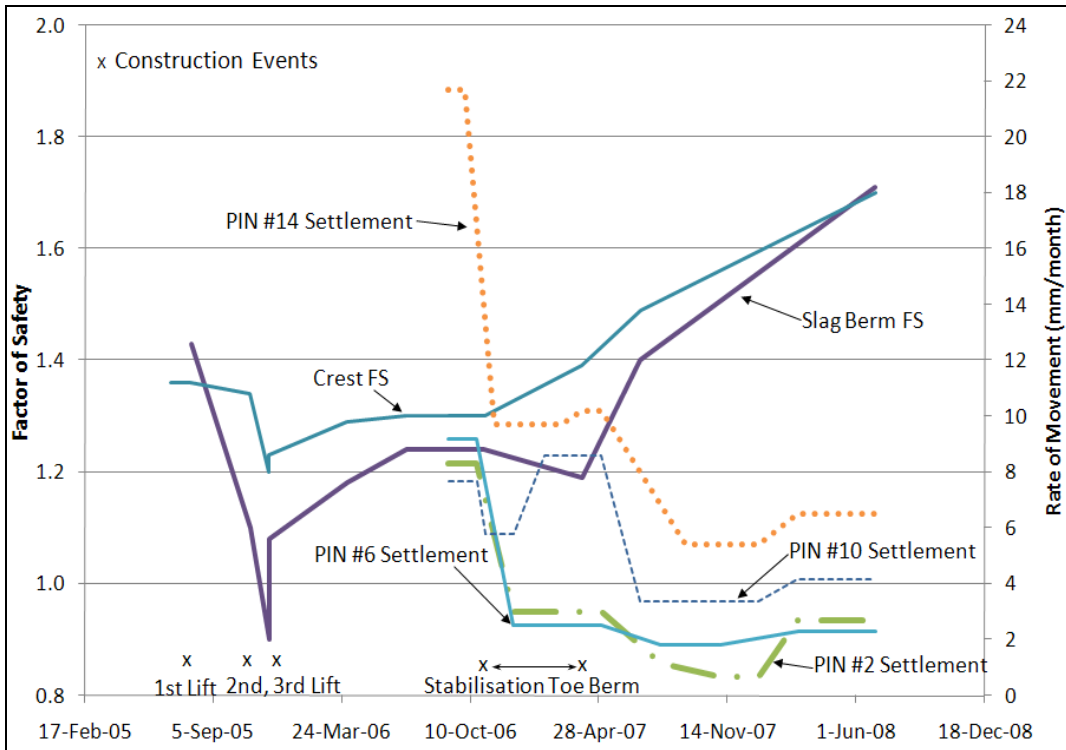


Figure 4: N ZPL Dam 1+42 - Factor of Safety versus Settlement Pin Movement versus time.

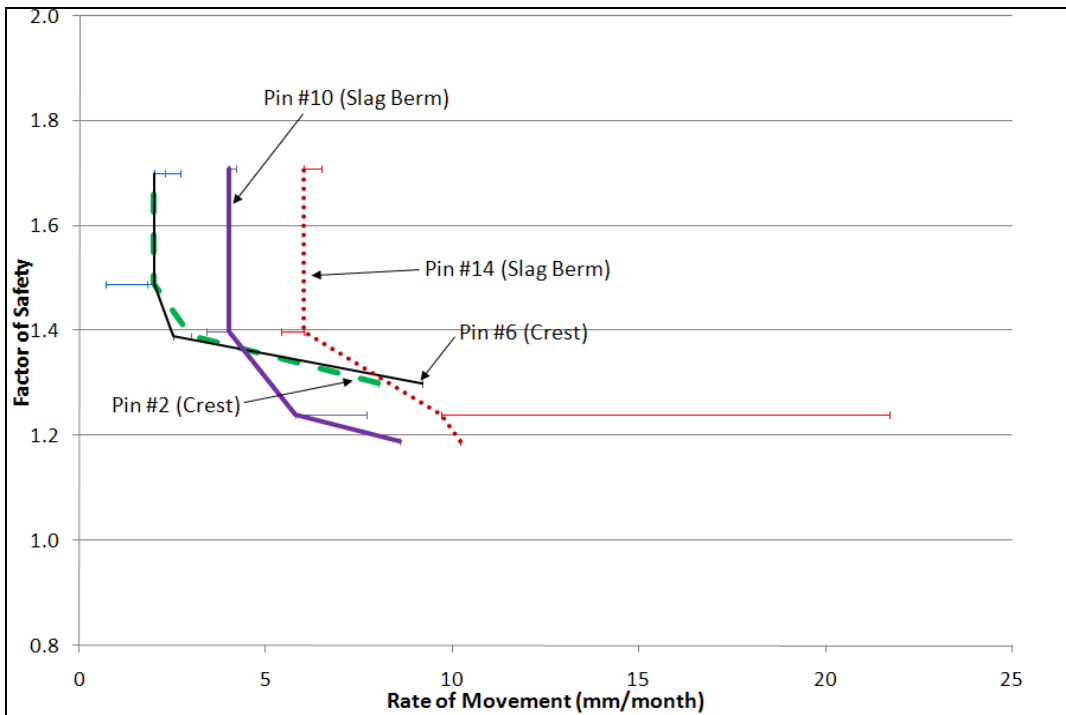


Figure 5: N ZPL Dam 1+42 - Factor of Safety versus Settlement Pins Rate of Movement.

Settlement Pins

Pins #2, #6, #10 and #14 are located directly on chainage 1+42 and as a result, these four pins can be closely related to the calculated factor of safety of the critical section. At the time of installation, the calculated factor of safety was approximately 1.2 on the slag berm and approximately 1.3 on the dam crest. The rate of movement of these pins were at or near their maximum rates, ranging from 8 to 9 mm/month for Pins #2, #6 and #10, to 22 mm/month for Pin #14, located on the lower level of the slag berm within the failed portion.

Pins #2 and #6, located on the dam crest and on the upstream side of the slag berm, respectively, have shown an overall decrease in the rate of movement since their installation, with a current rate of movement fluctuating between 1 to 3 mm/month. This corresponds to the general trend of increasing factor of safety of the dam crest. Pin #6, although installed on the upstream side of the slag berm, is located over the original dam crest and therefore behaves in line with the current dam crest as opposed to the slag berm.

Pins #10 and #14, on the upper and lower sides of the failed slope, respectively, displayed a reduced rate of movement

following their installation but then exhibited an increased rate during the waste rock stabilisation toe berm construction. This time period also corresponds to a drop in factor of safety of the slag berm below 1.2. Since that time, the rate of movement of these pins has generally decreased, as the factor of safety of the slag berm has increased. Currently, the rate of movement for Pins #10 and #14 fluctuate around 4 mm/month and 6 mm/month, respectively.

Figure 5 displays the direct relationship between the calculated factor of safety and the rate of settlement at the settlement pins. This relationship generally indicates that the rate of movement reached a near constant rate when the calculated factor of safety reached approximately 1.4. The subsequent rate is attributed to the ongoing consolidation of the foundation soil.

REFERENCES

- Craig, R. F. 1997. Soil Mechanics. 6th Edition.
- Ladd, C. C. 1991. Stability Evaluation During Staged Construction. Journal of Geotechnical Engineering. Vol. 117, No. 4. April 1991

ENVIRONMENTAL DESULPHURIZATION AND GEOCHEMICAL BEHAVIOUR OF HEMO-ILMENITE MINE PRODUCTS

Virginie Derycke, Mostafa Benzaazoua and Bruno Bussière

Université du Québec en Abitibi-Témiscamingue, Québec, Canada

Mukendi Kongolo

CNRS, INPL-ENSG, Laboratoire Environnement et Minéralurgie, France

Raphaël Mermillod-Blondin

Université du Québec en Abitibi-Témiscamingue, Québec, Canada

Agnico-Eagle Mines Ltd, Technical Services Division, Québec, Canada

Patrice Nadeau

Rio Tinto Fer et Titane, Sorel-Tracy, Québec, Canada

ABSTRACT: Rio Tinto Fer et Titane (RTFT) is a Quebec based society, recognized as a world leader in the production of titanium dioxide feed stock. Hemo-ilmenite ore is extracted from the Tio open-pit mine and transformed in Sorel-Tracy plant. During ore preparation, the hemo-ilmenite ore is first roasted in rotary kilns to ensure its magnetization and desulphurization; this process produces SO₂ emissions. Decreasing those SO₂ emissions is an important environmental objective for RTFT. Desulphurization by flotation is an interesting alternative to achieve Rio Tinto's goal in terms of reduction of SO₂ emissions. The process would consist in reducing the sulphur grade by using flotation of the rotary kiln feed. Desulphurization of hard rock mine tailings has been proven to be an efficient approach to reduce acid mine drainage from several mining wastes. The coarse nature of the rotary kiln feed is one of the major challenges related to the desulphurization process by flotation. Coarse particle flotation is a well known challenge in the ore processing industry and Rio Tinto's sulphide content has a wide particle size range, from 75 µm to 1200 µm. Flotation tests were done using different xanthate type collectors. Results from flotation tests using a Denver conventional cell showed a reduction of sulphur content from 0.74 to 0.14 % corresponding to approximately 80% recovery. Results from kinetic tests showed that the sulphide concentrate has to be managed as a metal-leaching and acid-generating material.

INTRODUCTION

Rio Tinto Fer et Titane extracts and transforms the hemo-ilmenite ore from the Tio mine since 1950. The Tio mine, located

43 km north of Havre St-Pierre (Quebec) is a massive lens-like deposit of intrusive hemo-ilmenite in an anorthosite rock. The ore is crushed at the Tio mine site and sent to the

metallurgical complex of Sorel-Tracy near Montréal.

In the ore preparation plant, the hemo-ilmenite ore is magnetized and roasted in rotary kilns. This process produces large amounts of SO₂ emissions. Decreasing SO₂ emissions during the roasting process is an important objective in the ongoing Rio Tinto's environmental program. Reducing sulphur grade of rotary kiln feed is therefore a very interesting way to decrease SO₂ emissions. Desulphurization of the hemo-ilmenite concentrate by mean of flotation is an alternative to achieve Rio Tinto's goal in reducing SO₂ emissions. Indeed, ore desulphurization using flotation has already been successfully tested on several mining wastes to reduce acid mine drainage (Benzaazoua et al., 2008; Benzaazoua et al., 2000). There is extensive literature on non selective sulphide recovery by flotation for environmental purposes (Benzaazoua et al., 2004; Benzaazoua et al., 2008; Benzaazoua et al., 2000; Benzaazoua and Kongolo, 2003; McLaughlin and Stuparyk, 1994; Yalcin et al., 2004). Moreover, flotation is often used as a process to concentrate sulphide minerals that contain economic values (Blazy and Jdid, 2001; Crozier, 1991).

The work described in this paper is related to the use of froth flotation on a hemo-ilmenite product to produce a low sulphur fraction (non SO₂ generating during roasting) and a sulphide concentrate fraction. The main obstacle to the flotation of Tio ore is its wide particle size range (from 75µm to 1200µm). Coarse particle flotation is a well known challenge that has been thoroughly reviewed in the literature (Gomez, 2000; Jameson, 2005; Tao, 2004).

The main objective of this study consists in evaluating the feasibility of hemo-ilmenite desulphurization using a conventional Denver

lab cell and different xanthates as collecting reagents. It also aims at evaluating the environmental behavior of the desulphurization products with static and kinetic tests.

METHODS AND MATERIALS

Samples

The hemo-ilmenite material was sampled at the ore preparation plant.

Figure 1 represents the simplified existing flow-sheet of the Sorel-Tracy process and shows the position of the sampling point (SP).

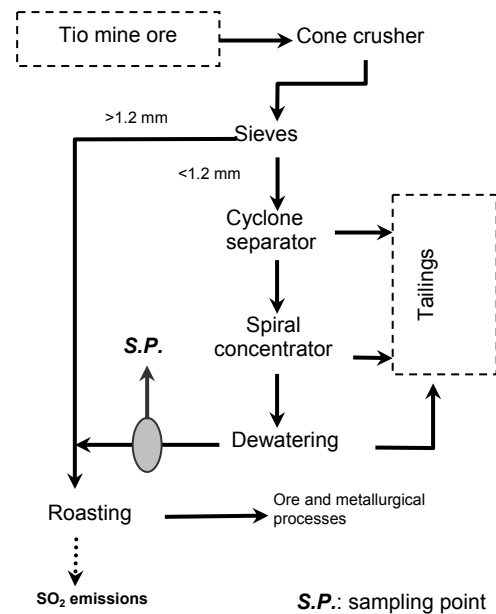


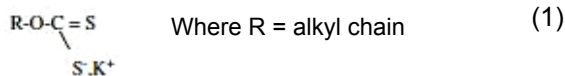
Figure 1: Schematic diagram of the ore preparation plant showing the sampling point.

Before transportation to the laboratory, the sampled hemo-ilmenite ore was stored under process water, in order to preserve the initial physico-chemical pulp characteristics (pH, Eh, etc.) by minimizing air contact. At the laboratory, the process water was drained out and the material was split into one kilogram

equal parts and stored into a freezer to prevent sulphide oxidation. Impact of material aging on desulphurization results was carried out through 5 flotation tests varying from 75 minutes to 49 days from sampling time.

Reagents

Flotation requires different type of reagents to produce the proper surface tension for mineral separation. The choice of collectors was based on preliminary tests conducted by Rio Tinto Technology Department (Dumais, 2000; Sutherland, 1999) and on a literature review. The frother used was MIBC (methyl isobutyl carbinol) from Prospec chemicals Inc. Different collectors were tested, belonging to the xanthate collector family. Their formula is:



Potassium ethylxanthate: KEX-20 with 88% purity; molecular weight 160.0 g/mol; from Prospec chemicals Inc. Its alkyl chain formula is R= CH₂-CH₃.

Potassium amylxanthate: KAX-51 with 62% purity; molecular weight 202.4 g/mol; from Prospec chemicals Inc. Its alkyl chain formula is R= (CH₂)₂-CH-(CH₃)₂.

Potassium tridecylxanthate : with 73% purity; molecular weight 314.0 g/mol; synthesized from tridecanol and carbon disulfide (Rao, 1971) and then purified (Kongolo, 1991). Its alkyl chain formula is R= C₁₃H₂₇

The pH regulator reagent was a 10 vol.% solution of H₂SO₄.

Physical, chemical and mineralogical characterization methods

The chemical composition of the ore was evaluated through a complete digestion in HNO₃/Br₂/HF/HCl; the solution was then analysed using an Inductively Coupled Plasma and Atomic Emission Spectroscopy (ICP-AES, Perkin Elmer). This technique was also used for liquid samples. Mineralogy of the solids was determined using both X-Ray diffraction (Bruker D8 Advance), followed by a quantification based on the Rietveld method (using TOPAS software) (Rietveld, 1993), and with small-scale optical microscopy examinations of the solid samples using a metallographic microscope (Nikon Optiphot2-Pol). Specific gravity (Sg) was determined with a helium pycnometer (Micromeritics, Accupyc 1330). Particle size distribution was determined with standard ASTM sieves (8 sieves between 150µm and 1800µm) as well as by using a Malvern Mastersizer laser particle size analyser for the fraction below 150µm. Xanthate purity was determined using the method proposed by Kongolo (1991) based on ultraviolet spectroscopy measurements (Ultraspec 2100 pro).

Slurry conditioning and flotation procedures

Desulphurization tests were performed both at the URSTM-UQAT laboratory using material sent by Rio Tinto and at the ore processing plant at Sorel-Tracy using fresh material. All flotation tests were done using the same laboratory Denver D-12 cell to avoid any bias related to different wears of the impeller-stator system (Harris and Khandrika, 1985). Experimental procedure is described in

Figure 2. The target in terms of pulp density was 30% solid. Conditioning time was set to 11 minutes for pH regulation followed by collector addition (different type of collector at various concentrations) and frother addition (MIBC at 50 g/t). Speed of the rotor-stator was set at 1900 rpm in order to keep the

maximum of particles in suspension. Even with the high energy employed, coarse particles tend to settle in the corner of the flotation cell. During flotation tests, a manual agitation using a spatula was added to the original mechanical agitation to counteract coarse particle settling in corners. Airflow was fixed at 2.5 L/min. The froth was manually skimmed with a spatula by the same operator, for all flotation tests. pH was measured and adjusted at a value of 6 by addition of a diluted H_2SO_4 solution.

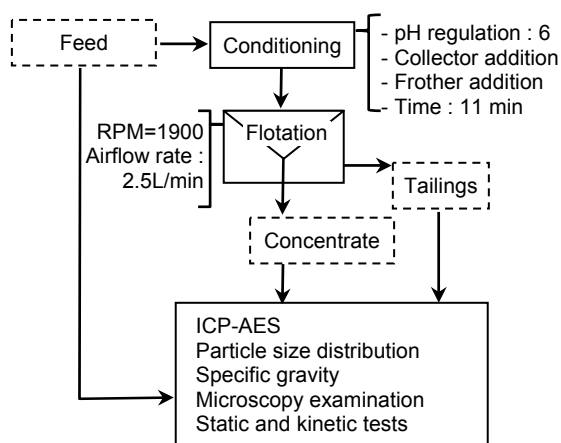


Figure 2: Schematic description of the experimental flotation procedure and subsequent analyses.

Environmental characterization methods

Acid-base accounting (or static) tests were performed using the Sobek method modified by Lawrence and Scheske (Lawrence and Scheske, 1997) to evaluate the acid-generating potential (AGP). The acidity potential (AP) is calculated from the sulphur (under the sulphide form) percentage in the sample, and neutralization potential (NP) is obtained using acid-base titration. The net neutralization potential (NNP) is the balance between NP and AP. A classification criterion commonly used for AGP evaluation (Aubertin et al., 2002; SRK, 1989) was used for this study. It stipulates that if the material's NNP is higher than 20 kg $CaCO_3/t$,

it is classified as non acid generating; and if the material's NNP is lower than -20 kg $CaCO_3/t$, it is classified as acid generating. If the material's NNP is between -20 and +20 kg $CaCO_3/t$, the material is classified as uncertain in terms of AGP. The ratio NP/AP is another classification criterion used for AGP. In this case, the material is classified as non acid-generating if NP/AP is above 2; acid generating if NP/AP is lower than 1; and in the uncertain zone if the ratio is between 1 and 2 (Adams et al., 1997).

When results from static tests are in the uncertainty zone or when a better understanding of the geochemical behaviour of a given mine wastes is needed, kinetic tests can be used to further investigate the environmental behaviour. In this study, weathering cells (Cruz et al., 2001; Villeneuve, 2004) were used on both the hemo-ilmenite material and on the desulphurized final products (flotation concentrate and tailings). Those kinetic tests consist of leaching a thin layer of solid (about 67 g) placed on a filter paper placed in a Buchner funnel. Cyclic leaching was performed with 50 mL deionized water twice a week, on days 3 and 7, and flushing solutions were left in contact with the solid for 3 hours before being extracted by vacuum suction. The solid sample is exposed to ambient air throughout the test period. 24 cycles were performed in this study. More information on weathering cells can also be found in Villeneuve (Villeneuve, 2004).

RESULTS

Characteristics of the hemo-ilmenite ore

The hemo-ilmenite ore has a wide particle size distribution, ranging from 75 μm to 1200 μm . This size distribution is the greatest challenge for the flotation process. Particle size analyses of the hemo-ilmenite ore are

listed in Table 1 and Figure 3. Particle size distribution below 150 μm is shown in Figure 4.

Table 1: Main results of particle size analysis.

	Feed
D10 (μm)	110
D50 (μm)	480
D90 (μm)	1180
Specific gravity, Sg	4.5

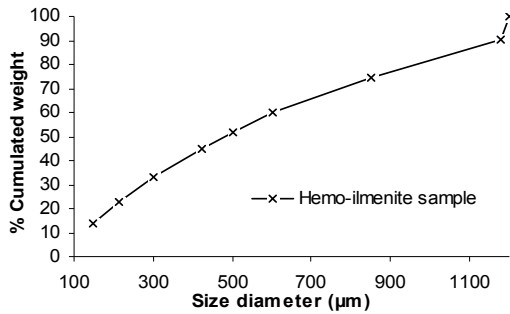


Figure 3 Cumulative size diameter distribution of hemo-ilmenite sample (sieving method).

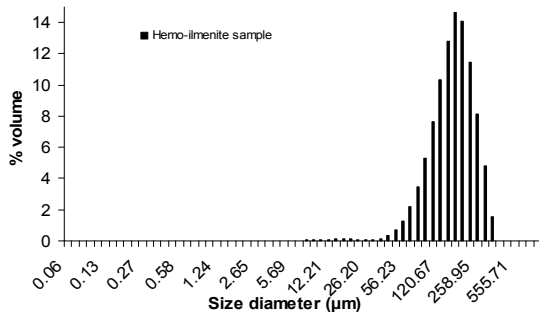


Figure 4 Size diameter distribution for size fraction below 150 μm (Laser based method).

The hemo-ilmenite ore was divided into three particle size fractions for chemical and mineralogical analyses. Main results are listed in Table 2. Sulphate fraction of the total sulphur percentage was not analysed in this study since previous work carried on the hemo-ilmenite ore showed that the sulphur is

essentially contained in sulphide minerals (Bussi re et al., 2005).

Table 2: Main chemical and mineralogical properties of three different size fractions of the hemo-ilmenite sample.

Hemo-ilmenite size fractions			
Parameter	< 150 μm	150-300 μm	> 300 μm
Fraction wt. %	12.6	18.7	68.7
S (wt. %)	1.23	1.06	0.68
Ti (wt. %)	19.1	17.6	20
Fe (wt. %)	34.1	30.5	34.4
Al (wt. %)	1.19	2.49	1.19
Ca (wt. %)	0.55	1.05	0.461
Mg (wt. %)	1.54	1.65	1.58
Mn (wt. %)	0.09	0.08	0.09
Ni (ppm)	520	500	440
Cu (ppm)	360	200	110
Co (ppm)	560	490	480
Cr (ppm)	800	990	1080

Hemo-ilmenite size fractions			
Mineral	< 150 μm	150-300 μm	> 300 μm
Pyrite (%)	4.3	2.9	2.9
Ilm�nite (%)	65.5	56.0	70.0
H�matite (%)	22.6	18.5	21.7
Labradorite (%)	6.4	20.6	5.0
Biotite (%)	1.2	2.0	0.4

Bulk sulphur analysis in the hemo-ilmenite ore is approximately 0.8 wt.%. The fraction above 300 μm seems to contain less sulphur compared to the other fractions analysed, but as it represents the major part of the sample (68.7 wt%), sulphur content of the fraction above 300 μm represents 57 wt.% of the overall sulphur content.

The hemo-ilmenite ore is mainly constituted of hematite and ilmenite. Major gangue minerals are plagioclase (labradorite). Biotite is present in lesser quantity. Metallic sulphides are also present with pyrite being the most abundant. Microscopic examination showed traces of other sulphides like chalcopyrite (CuFeS_2), siegenite ($(\text{Ni},\text{Co})_3\text{S}_4$) and millerite (NiS). It also allowed observation of the specific texture of the hemo-ilmenite ore, which consists of exsolution intergrowths of hematite and ilmenite, as already described in a previous study (Bussi re et al., 2005; Pepin, 2009).

Collector optimization

The effect of hemo-ilmenite ore aging in conditions that prevent sulphide oxidation was evaluated through flotation tests using Kax-51 at 100 g/t concentration. Results are presented in Figure 5.

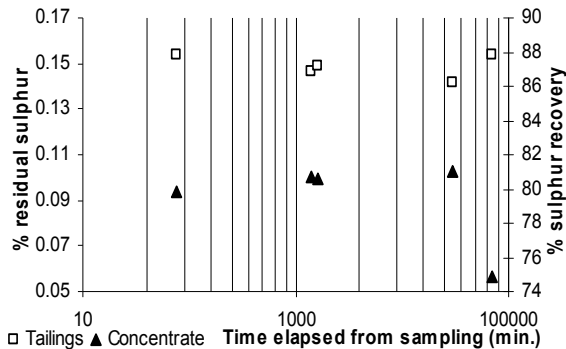


Figure 5: Desulphurization results (% residual sulphur and % sulphur recovery) for a 100 g/t dosage of kax-51 as a function of time elapsed from sampling.

Except for the last test where sulphur recovery was 75 percent, the time elapsed between material sampling and flotation did not seem to have a significant impact on desulphurization results (with a residual sulphur percentage between 0.14 and 0.15 and a sulphur recovery between 80 and 81 percent). Thus, storing the hemo-ilmenite ore in a freezer in the laboratory and under water during transportation was considered a satisfying solution for the preservation of material's physico-chemical properties.

One of the objectives of the flotation tests was to evaluate the effect of the collector's alkyl chain length, and the effect of collector dosage on desulphurization results. Three collectors belonging to the xanthate family were tested. Their alkyl chains had various lengths: 2, 5, and 13 carbons. Three collector dosages (50-100-150 g/t) were tested with

Kax-51 (the reagent that gave the best sulphur recoveries during preliminary testing). Kex-20 and tridecylxanthate were tested at 100 g/t, for comparison with Kax-51 at 100 g/t. It should be mentioned that the tridecylxanthate was difficult to dissolve in water unless heated, due to its high molecular weight. Results in terms of sulphur recovery and residual sulphur content are presented in Figure 6 and Figure 7.

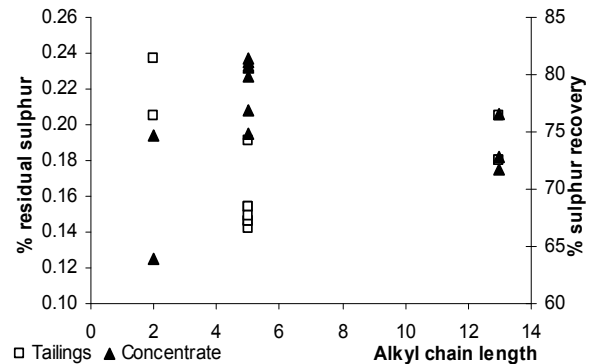


Figure 6: Desulphurization results (% residual sulphur and % sulphur recovery) as a function of alkyl chain length of the collector at 100 g/t concentration.

Desulphurization results seem to be greatly affected by the alkyl chain length of the collector. The best results were obtained with the Kax-51 (alkyl chain of five carbons) and produced desulphurized tailings containing less than 0.15% of residual sulphur in most tests and a corresponding sulphur recovery of approximately 80%. The optimal dosage of Kax-51 was 50 g/t which produced desulphurized tailings containing 0.08% of residual sulphur (88% of sulphur recovery).

Flotation tests using Kax-51 at concentration of 100 or 150 g/t were probably overdosed since they led to lower performances.

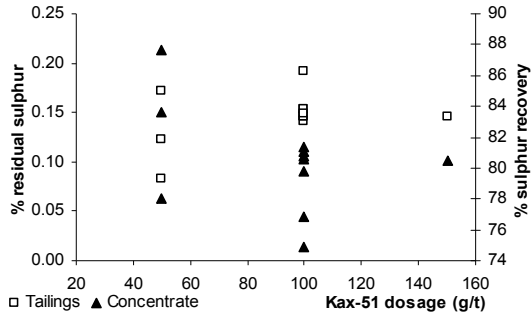


Figure 7: Desulphurization results (% residual sulphur and % sulphur recovery) as a function of Kax-51 concentration.

Particle size effect

Sulphur recovery

Recovery of sulphur as a function of particle size was determined for the three studied fractions (< 150 μm ; 150-300 μm ; > 300 μm). The objective of these tests was to evaluate the effect of particle size on desulphurization performance. Results in terms of sulphur recovery and residual sulphur content are presented in Figure 8 and Figure 9.

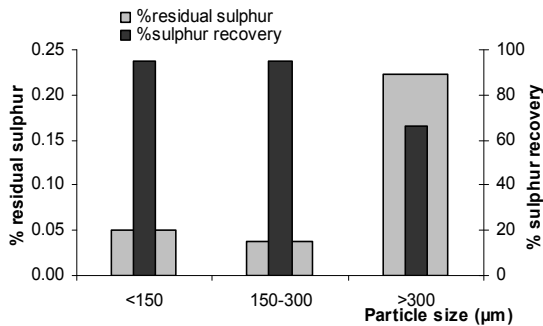


Figure 8: Desulphurization results (% residual sulphur and % sulphur recovery) for a 100 g/t dosage of Kax-51 as a function of particle size.

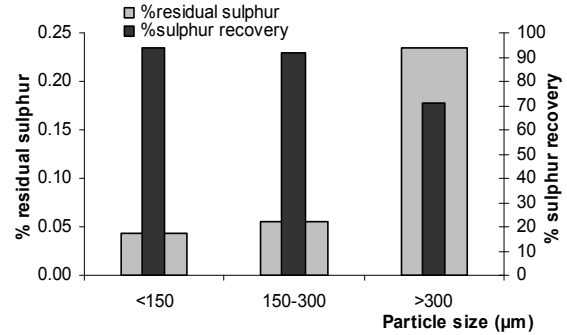


Figure 9: Desulphurization results (% residual sulphur and % sulphur recovery) for a 150 g/t dosage of Kax-51 as a function of particle size.

The sulphur recovery reached 90 - 95 % for fractions below 300 μm . However for the fraction above 300 μm , the sulphur recovery did not exceed 70%. These tests outline the well known limit of coarse particle flotation. Bulk sulphide recovery was 81% for tests with Kax-51 for both dosages (100 and 150 g/t). For the fraction above 300 μm , the flotation test at 150 g/t reached higher sulphur recovery than the one at 100 g/t. However, sulphur recoveries of other fractions were slightly lower at 150 g/t.

Hemo-ilmenite entrainment

Entrainment of hemo-ilmenite in the concentrate should be avoided during the desulphurization process since it leads to a loss in the Rio Tinto's ore recovery. Entrainment of hemo-ilmenite was low in all flotation tests conducted in this study (whatever the collector type or the dosage used). The average value was 0.1%. Entrainment of hemo-ilmenite was also quantified for the three selected fractions. Results in terms of hemo-ilmenite recovery in

concentrate (i.e.: hemo-ilmenite entrainment in concentrate) are presented in Table 3.

Table 3: Desulphurization results (% of hemo-ilmenite recovery in concentrate) with dosage of 100 and 150 g/t of Kax-51 as a function of particle size.

% hemo-ilmenite entrainment in concentrate		
Fraction (µm)	Kax-51; dosage of 100g/t	Kax-51; dosage of 150g/t
<150	0.3	0.2
150-300	0.06	0.09
>300	0.01	0.04

The entrainment of hemo-ilmenite in the concentrate was very low in the upper fraction but increased with decreasing particle size, which is in accordance with literature findings (Zheng et al., 2006).

Mineral liberation

Polished sections of Hemo-ilmenite ore for each selected fraction (< 150 µm; 150-300 µm; > 300 µm) were studied using small-scale optical microscopy to evaluate sulphide liberation. Grains containing sulphides were manually counted, measured, and their sulphide liberation level was estimated. 429 sulphide grains were reported within the three polished-sections studied. Around 90% of those sulphide grains were fully liberated. Results of the sulphide size distribution in terms of grains percentage are presented in Figure 10.

Most sulphide grains had diameters below 300 µm. However, observation of more sulphide grains (> 1000 grains) may allow a more accurate sulphide liberation determination.

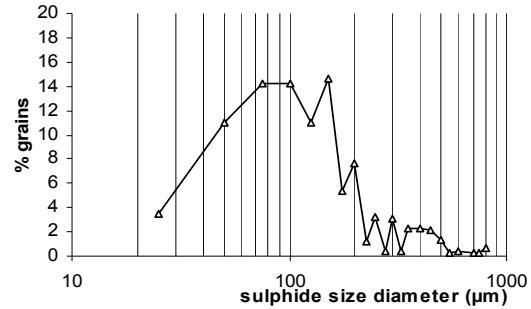


Figure 10: Sulphides size diameter distribution of the hemo-ilmenite ore estimated by optical microscopy examination (grain counting).

Characteristic of the flotation products

Characterization of flotation products (concentrate and tailings) was conducted in the same manner as for the hemo-ilmenite ore. The main results in terms of particle size analyses of the concentrate and the desulphurized tailings are listed in Table 4. The concentrate was finer than the tailings as illustrated in Figure 11. Grain size frequency curve of the tailings was very similar to the one of hemo-ilmenite ore.

Table 4: Main result of particle size analysis.

	Concentrate	Tailings
D10 (µm)	80	110
D50 (µm)	230	450
D90 (µm)	550	1180
Specific gravity, Sg	4.2	4.5

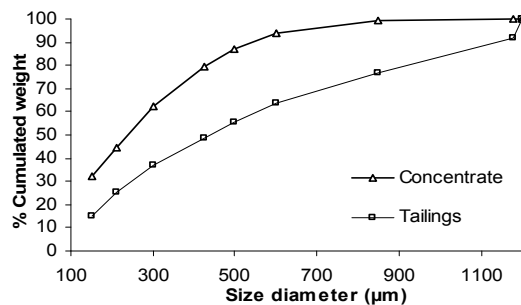


Figure 11: Cumulative size diameter distribution of hemo-ilmenite concentrate and tailings.

The particle size distributions of the concentrate and tailings fractions below 150 μm are presented in Figure 12. Within this fraction, the size frequency curve of the concentrate shows three size populations with respective modes at 0.31 μm (1.0%), 22.5 μm (2.5%), and 190.7 μm (7.2%). Tailings particle size distribution is quite similar to the one of hemo-ilmenite ore in the fraction lower than 150 μm .

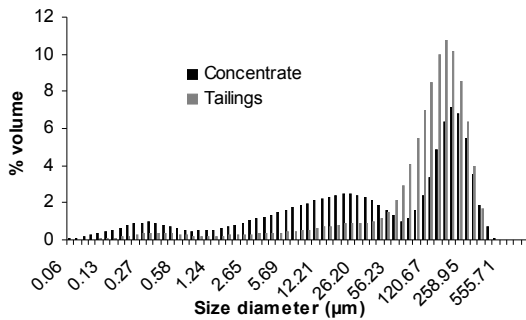


Figure 12: Size diameter distribution for size fraction below 150 μm .

Both tailings and concentrate were analysed by ICP-AES to evaluate the sulphur recovery. The average value of elements, reported in Table 5, was calculated from chemical analysis of concentrates and tailings produced by the flotation tests with best performances (9 tests). Mineralogical content of concentrate and tailings were back calculated from chemical data and minerals stoichiometry.

Table 5 shows the good selectivity during the desulphurization process allowing concentration of sulphur as well as other valuable metals like Cu, Co, Ni, and Cr, and entrainment of hemo-ilmenite was negligible.

Three polished-sections of desulphurized tailings were prepared corresponding to the three fractions chosen (< 150 μm ; 150-300 μm ; > 300 μm) for small-scale optical microscopy, where the residual sulphide occurrences were investigated. 27 grains containing sulphides were reported and approximately 40% of them were larger

than 300 μm . This result may be underestimated due to the small amount of residual sulphide particles found in those cross sections.

Table 5: Chemical and mineralogical properties of the concentrate and the tailings from the 9 top tests. Mineralogical content are calculated from ICP-AES analyses and minerals stoichiometry data.

Parameter	Concentrate	Tailings
Fraction wt. %	1.28	98.72
S (wt. %)	47.38	0.14
Ti (wt. %)	1.24	19.14
Fe (wt. %)	38.64	33.61
Al (wt. %)	0.71	1.84
Ca (wt. %)	0.43	0.70
Mg (wt. %)	0.60	1.59
Mn (wt. %)	0.02	0.09
Ni (wt. %)	1.38	0.03
Cu (wt. %)	1.17	/
Co (wt. %)	0.72	0.04
Cr (wt. %)	0.15	0.10
Mineral	Concentrate	Tailings
Pyrite (%)	86.3	0.3
Hemo-ilmenite (%)	3.9	75.5
Chalcopyrite (%)	3.4	Traces
Labradorite (%)	4.9	7.9
Biotite (%)	Traces	9.4

Acid generation potential

The environmental behaviour of the concentrate was evaluated using static and kinetic tests. The hemo-ilmenite ore and the desulphurized tailings were also studied for comparison although they are not mine wastes. Results of the static tests are presented in Table 6. The concentrate is classified as highly acid generating by both NNP and NP/AP criteria. According to the NP/AP ratio, the hemo-ilmenite ore (i.e. feed) and the desulphurized tailings are acid-generating. However, according to the NNP criterion, which is more realistic for low sulphide tailings (Plante, 2004), they are both in the uncertainty zone.

Table 6: Static test results of hemo-ilmenite (Feed), concentrate and desulphurized tailings.

	Feed	Conc.	Tailings
S (wt.%)	0.73	46.7	0.14
AP (kg CaCO ₃ /t)	22.75	1460.9	4.3
NP (kg CaCO ₃ /t)	3.4	6.5	4
NNP (kg CaCO ₃ /t)	-19.35	-1454.4	-0.3
NP/AP	0.14	0.006	0.92

The analyses of water flushed during the kinetic tests are presented in Figure 13. The leachate pH of the solutions for the hemo-ilmenite ore (i.e. feed) and the tailings tests remained higher than 7 with a low conductivity (lower than 100 $\mu\text{S}/\text{cm}$). Those two materials did not show important mineral dissolution as attested by the water chemistry. Kinetic test on the concentrate confirms its high acid generation potential. Indeed, the leaching pH of the flushed waters quickly dropped down to 4 at the end of the test and conductivity measures decreased with time but remained higher than 200 $\mu\text{S}/\text{cm}$.

Concentrations of two elements of interest in this study (Fe and Ni) are corrected to take into account the recovered volume and are normalized to one kilogram of solid material. Cumulative concentrations of dissolved nickel and iron are presented in Figure 13. The concentrate's kinetic results show that silica, sulphur, nickel and calcium are the main elements that dissolve during testing, with a final cumulative concentration of 1397 mg/kg for silica, 2898 mg/kg for sulphur (essentially as sulphate), 1070 mg/kg for nickel, and 1687 mg/kg for calcium. Release of these elements in leaching solutions slightly decreased after the 100th day and iron started to be detected in flushed waters at the same time, as shown in Figure 13. This observation may attest of a change in mineral dissolution after the 100th day in the concentrate, or of precipitation of iron before the 100th day. Geochemical modelling performed with VMintec attested that iron

species like ferrihydrite or goethite have saturation indices that suggest oversaturation.

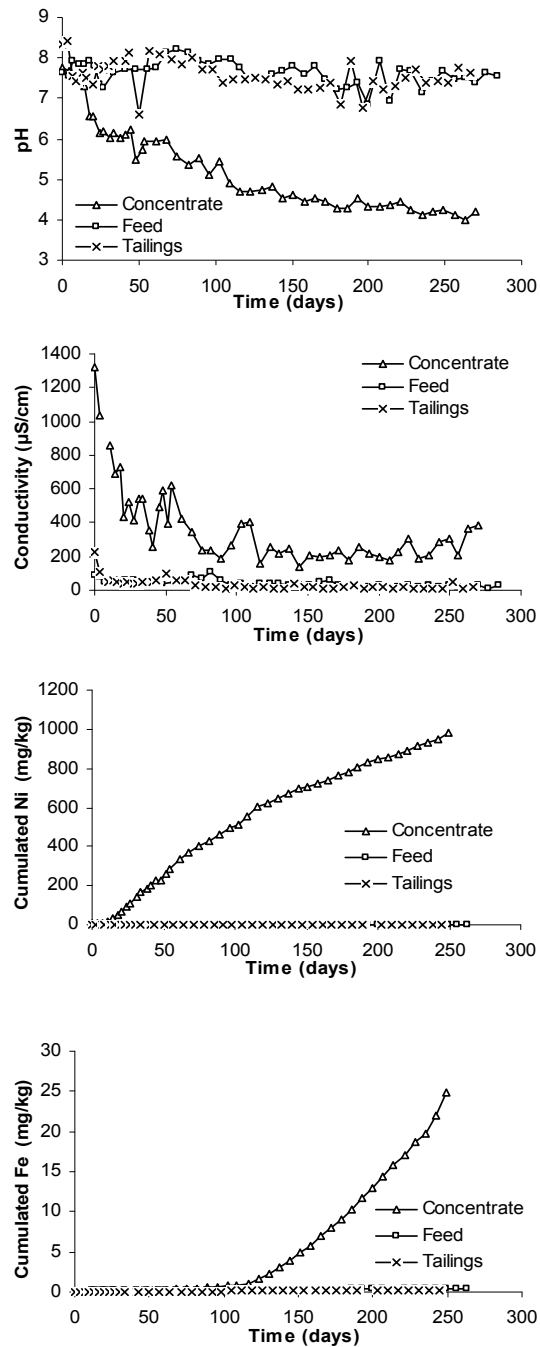


Figure 13: Water quality evolution (pH; conductivity, cumulated Ni and Fe) from the weathering cell tests versus time for Hemo-ilmenite ore (Feed), concentrate and desulphurized tailings.

Kinetic results for the tailings and hemo-ilmenite ore (i.e. feed) showed only weak element dissolution; silica and calcium being the main elements dissolved (between 150 and 170 mg/kg as final cumulative concentration).

Post-testing solid analyses were performed after the end of kinetic tests. The main results are presented in Table 7. NP of hemo-ilmenite ore and desulphurized tailings after post dismantling were 20% to 40% of their initial values. Final NP of the sulphide concentrate was zero. Element depletions were calculated from the chemical analysis of final products and represent the remaining proportion of elements in the final product. Main elements which are depleted in the final product are Ca, Mg, Mn, and Ni for the concentrate. For the hemo-ilmenite ore and the desulphurized tailings, Ca and Mg are the only elements dissolved.

Table 7: Static test results of hemo-ilmenite (Feed), concentrate and desulphurized tailings and % depletion of main elements after dismantling of weathering cells (in curves values correspond to initial value).

	Feed	Conc.	Tailings
S (wt.%)	0.79	47.1	0.20
AP (kg CaCO ₃ /t)	24.72	1472.5	6.5
	(22.75)	(1461)	(4.3)
NP (kg CaCO ₃ /t)	0.8	0	1.7
	(3.4)	(6.5)	(4.0)
NNP (kg CaCO ₃ /t)	-23.97	-1452.9	-4.8
	(-19.35)	(-1454)	(-0.3)
NP/AP	0.03	0	0.26
	(0.15)	(0.0044)	(0.92)
% Depletion	Feed	Conc.	Tailings
Ca	90.0	67.6	88.1
Mg	94.6	74.0	96.4
Mn	/	80.8	/
Ni	/	89.6	/

DISCUSSION

The evaluation of the desulphurization process applied to hemo-ilmenite was the main objective of this preliminary work. The

process was tested using a conventional mechanical flotation cell despite the presence of coarse particles. Elimination of coarse particles by grinding is neither economically nor technically feasible for Rio Tinto, as generating fine particles of hemo-ilmenite represent a loss of ore for Rio Tinto. This study investigated the effect of different collectors at different dosages on sulphide concentration, including a size distribution analysis. The best concentrate produced contains few entrained hemo-ilmenite particles (average value around 0.1 wt.%). So far, Kax-51 was the collector that gave the best sulphur recovery, and Kax-51 dosage below 100 g/t (at pH 6) provided good results in terms of sulphur removal from the hemo-ilmenite ore. Pulp pH was quite difficult to set since it was buffered at pHs between 8 and 9 whatever the volume of acid added. This difficulty can explain the different results between tests having the same parameters (Figure 5, Figure 6, and Figure 7) since it is well known that pyrite flotation has very poor performances in the pH range of 8-9 (Cases et al., 1990; Jiang et al., 1998; Mermillod-Blondin, 2005). It should also be mentioned that the comparison between collector having different alkyl chain length at a dosage of 100g/t was biased by the use of the grams of collector per tons of ore (g/t) unit (as illustrated in Table 8). Tridecylxanthate was added in lesser quantity than the Kax-51 because of its higher molecular weight.

Table 8: Comparison of collector's concentration with the grams of collector per ton of ore and the mole of collector per litre of pulp unities.

Collector	g/t	mol/L
Kax-20	100	2.81*10⁻³
Kax-51	100	2.22*10⁻³
tridecylxanthate	100	1.43*10⁻³
Ore density=4.5; solid percentage=30%		

The environmental study of the hemo-ilmenite ore and of the desulphurization products showed that the concentrate is highly acid generating. The desulphurized tailings and hemo-ilmenite ore can be classified in the uncertainty zone. Oxidation neutralization curves are used for the interpretation of the acid generation potential (Benzaazoua et al., 2004; Demers et al., 2008). Sulphates represent the main oxidation product while the sum

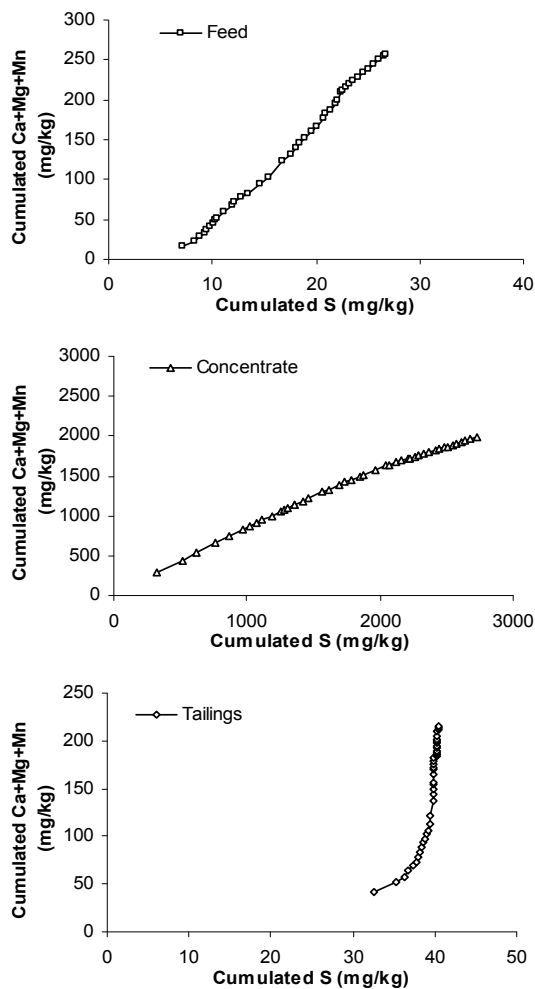


Figure 14: Oxidation-neutralization curves of the hemo-ilmenite ore (i.e: feed), the concentrate and the desulphurized tailings.

of Ca+Mg+Mn represents the main dissolution products. The cumulative mass of sulphur (i.e: sulphate amount) analysed in the

leaching solutions is plotted against the cumulative amount of calcium, magnesium, and manganese. The oxidation-neutralization curves corresponding to the hemo-ilmenite ore and the concentrate have a linear shape showing dissolution of neutralizing elements in response to the acidity produced. On the other hand, the oxidation-neutralization curve of desulphurized tailings shows a passivation shape. There is dissolution of neutralizing elements with little or no acid generation as illustrated in Figure 14.

Thorough interpretation of the geochemical behaviour would need further investigation by geochemical modelisation with programs like Vmintec or Jchess.

CONCLUSION & PERSPECTIVES

This study produces promising results showing the potential of adding a desulphurization process to decrease SO₂ emission in rotary kilns. Flotation produced a sulphide concentrate with a 80 wt.% average sulphide recovery and little entrainment of hemo-ilmenite (approximately 0.1 wt.%). Since it is considered an acid generating mine waste, the sulphide concentrate storage should be managed to prevent acid mine drainage once stored at the site surface. The size by size analysis (< 150 µm; 150-300 µm; > 300 µm), coupled with micro-scale analyses and chemical analyses, attested that sulphide recovery in fractions higher than 300 µm was poor (below 70%). Further work is necessary to optimize the desulphurization of the hemo-ilmenite ore. Further flotation test will be conducted at alkaline pH ranges (Mermillod-Blondin, 2005) to test flotation performances under more stable pH conditions. Flotation tests will include the testing of collectors with carbon chains larger than 5 carbons (Kax-51) that would be more powerful than Kax-51. Those collectors must have alkyl chains

shorter than 13 carbons (tridecylxanthate) for easier dissolution in water.

ACKNOWLEDGEMENTS

The authors would like to thank the NSERC Polytechnique-UQAT Chair in environment and mine wastes management for financial support, and are grateful to Rio Tinto Fer et Titane. for making this research possible. The URSTM personnel must also be acknowledged for their technical support.

REFERENCES

Adams, K., Kourtis, A., Gazea, B. and Kontopoulos, A., 1997. Evaluation of static tests used to predict the potential for acid drainage generation at sulfide mine sites. *Trans. Inst. Min. Metall., Sect A: Min Industry* 106, January-April (A1-A8).

Aubertin, M. et al., 2002. The management of mining discharges in a context of sustainable development and environmental protection, *La gestion des rejets miniers dans un contexte de développement durable et de protection de l'environnement*, pp. 317-326.

Benzaazoua, M., Bussiere, B., Dagenais, A.M. and Archambault, M., 2004. Kinetic tests comparison and interpretation for prediction of the Joutel tailings acid generation potential. *Environmental Geology*, 46(8 SPEC.ISS.): 1086-1101.

Benzaazoua, M. et al., 2008. Integrated mine tailings management by combining environmental desulphurization and cemented paste backfill: Application to mine Doyon, Quebec, Canada. *Minerals Engineering*, 21(4): 330-340.

Benzaazoua, M., Bussière, B., Kongolo, M., McLaughlin, J. and Marion, P., 2000.

Environmental desulphurization of four Canadian mine tailings using froth flotation. *International Journal of Mineral Processing*, 60(1): 57-74.

Benzaazoua, M. and Kongolo, M., 2003. Physico-chemical properties of tailing slurries during environmental desulphurization by froth flotation. *International Journal of Mineral Processing*, 69(1-4): 221-234.

Blazy, P. and Jdid, E.A., 2001. Flottation : Aspects pratiques, *Techniques de l'Ingénieur, Génie des procédés*, pp. J 3360, 25p.

Bussière, B., Dagenais, A.-M., Villeneuve, M. and Plante, B., 2005. Rapport final : Caractérisation environnementale d'un échantillon de stériles du Lac Tio. Présenté à Mme Dominique Beaudry, Conseillère principale – Environnement, QIT-Fer et Titane inc.

Cases, J.M., Kongolo, M., de Donato, P., Michot, L. and Erre, R., 1990. Interaction between finely ground galena and pyrite with potassium amylxanthate in relation to flotation, 2. Influence of grinding media at natural pH, *International Journal of Mineral Processing*, pp. 35-67.

Crozier, R.D., 1991. Sulphide collector mineral bonding and the mechanism of flotation. *Minerals Engineering*, 4(7-11): 839-858.

Cruz, R., Mèndez, B.A., Monroy, M. and Gonzales, I., 2001. Cyclic voltametry applied to evaluate reactivity in sulfide mining residues. *Applied Geochemistry*, 16: 1631-1640.

Demers, I., Bussière, B., Benzaazoua, M., Mbonimpa, M. and Blier, A., 2008. Column test investigation on the performance of monolayer covers made of desulphurized

- tailings to prevent acid mine drainage. *Minerals Engineering*, 21(4): 317-329.
- Dumais, A., 2000. Water-assisted flotation of coarse pyrite using a flotation column. Phase I. Feasibility tests, COG Technologies Inc.
- Gomez, C.O., 2000. Water-assisted flotation of coarse pyrite using a flotation column. McGill University, Montréal.
- Harris, C.C. and Khandrika, S.M., 1985. Flotation machine design: important hydrodynamic effects; slight geometrical causes. *Powder Technology*, 43(3): 243-248.
- Jameson, G.J., 2005. Flotation of coarse and ultra-fine particules, Centre for Multiphase Processes, University of Newcastle, Australia.
- Jiang, C.L., Wang, X.H., Parekh, B.K. and Leonard, J.W., 1998. The surface and solution chemistry of pyrite flotation with xanthate in the presence of iron ions. *Colloids and Surfaces A: Physicochemical and Engineering Aspects*, 136(1-2): 51-62.
- Kongolo, M., 1991. Interactions de l'amyloxanthate de potassium avec la galène et la pyrite finement broyées: conséquences sur la flottation, l'Institut National Polytechnique de Lorraine.
- Lawrence, R.W. and Scheske, M., 1997. A method to calculate the neutralization potential of mining wastes. *Environmental Geology*, 32(2): 100-106.
- McLaughlin, J. and Stuparyk, R., 1994. Evaluation of low sulphur rock tailings production at Inco's Clarabelle Mill, *Innovation in Mineral Processing*, pp. 129-146.
- Mermillod-Blondin, R., 2005. Influence des propriétés superficielles de la pyrite sur la rétention de molécule de type xanthate : application à la désulfuration des résidus miniers. Université de Montréal Thesis.
- Pepin, G., 2009. Évaluation du comportement géochimique de stériles potentiellement générateurs de drainage neutre contaminé à l'aide de cellules expérimentales in situ École polytechnique de Montréal. Montréal, Canada.
- Plante, B., 2004. Comparaison des essais statiques et évaluation de l'effet de l'altération pour des rejets de concentrateur à faible potentiel de génération d'acide, École polytechnique de Montréal. Montréal, Canada.
- Rao, S.R., 1971. Xanthates and related compounds.
- Rietveld, H.M., 1993. *The Rietveld Method*. Oxford University Press.
- SRK, 1989. Draft acid Rock technical Guide. In: R. SRK (Steffen, Kirsten) (Editor), AMD Task Force, Vancouver, Canada.
- Sutherland, A.C., 1999. Flotation of Sulphide Minerals From OPP Spiral Feed and Concentrate Rio Tinto & Titanium Inc. Technology Department
- Tao, D., 2004. Role of Bubble Size in Flotation of Coarse and Fine Particles - A Review. *Separation Science and Technology*, 39(4): 741-760.
- Villeneuve, M., 2004. Évaluation du comportement géochimique à long terme de rejets miniers à faible potentiel de génération d'acide à l'aide d'essais cinétiques. , École polytechnique de Montréal. Montréal, Canada.

Yalcin, T., Papadakis, M., Hmidi, N. and Hilscher, B., 2004. Desulphurization of Placer Dome's Musselwhite Mine gold cyanidation tailings. CIM Bulletin, Online Edition, Vol. 97(No. 1084): November/December, 7 p.

Zheng, X., Johnson, N.W. and Franzidis, J.P., 2006. Modelling of entrainment in industrial flotation cells: Water recovery and degree of entrainment. Minerals Engineering, 19(11): 1191-1203.

CHEMICAL COMPOUND FORMS AND RELEASE OF LEAD IN URANIUM TAILINGS OF SCHNECKENSTEIN (GERMANY)

Taoufik Naamoun and Nejb Kallel

Faculty of Sciences, Sfax, Tunisia

Broder Merkel,

TU Bergakademie Freiberg, Germany

ABSTRACT : The participation of any hazardous heavy metal in the water cycle requires an understanding of the ways of its binding or of its specific chemical forms in the material of investigation. The scope of the present study is to evaluate the release and mobility of lead from uranium residues. For that purpose, a seven steps sequential chemical extraction was the tool to define its different compound forms in the processed sediments. Also, a hydrochemical investigation was carried out. The distribution of lead species and saturation indices were calculated by means of the software PHREEQC. According to the collected data, between 81 and 100% of the non residual fraction is in association with the nodular hydrogenous fraction. Ranging between ~ 1 and 14% is associated with the sulphide-organic phase. From ~ 0 to 14% is associated to the carbonate phase. Whereas, only a trace amount of the non residual Pb is easily released to pores and less than 1% is found to be exchangeable. According to the chemical investigation the lead content ranges from 0.01 ppb and 2.8 ppb in superficial water samples. Also it varies between 0.6 ppb and 1.5 ppb in groundwater. At drainage water, it lies between 0.3 ppb and 12 ppb. Moreover, the recorded lead content in the extracted porewater samples from the processed material is relatively high. It ranges from ~ 0.5 to 85 ppb. According to PHREEQC model, most of the soluble Pb tends to precipitate with carbonate. Also a considerable share from the total aqueous lead is expected to be in its ionic compound form $Pb(CO_3)_2^{2-}$. Also, the co-precipitated $PbCO_3$ complex is its other main form. Therefore, this tendency may limit the contamination risk of the pore water by Pb to the half.

INTRODUCTION

Regretfully, in most of historical cases (and some modern cases too), the exploitation of ore deposits has been accompanied for a negative impact to the environment (mainly to surface and groundwater), (Guogh, 1993; Gray et al. 1994; King, 1995; Carrillo-Chavez et al. 2003). However, during the last two decades,

real problems of high concentration of heavy metals in groundwater around mining areas have been recognized. Since the second half of the 1980s and during all the 1990s the environmental research on the impact of mining activities has increased considerably (Carrillo-Chavez et al. 2003).

In the nineties, after the German reunification, an extensive research program was undertaken to improve the understanding of the geochemical evolution of uranium tailings and to develop more effective predictive and remedial techniques for the environmental problems associated with uranium tailings (Hurst & Glaser, 1998).

The Schneckenstein mill, in the southwest of Saxony in eastern Germany, processed approximately 1.2 Mt of uranium ore between opening in 1947 and final closure in 1957. The mill produced 660 tons of uranium at a capacity of 150.000 tons of ore per year. The resultant 1.96 Mt of tailings are contained in an elevated 108-ha two tailings dam adjacent to the site. These tailings may act as a storage pool for heavy metals including lead, which get into the surrounding rivers by drainage and to the groundwater by infiltration. Effective management and remediation of mine drainage is possible only if the processes that influence metal release and transportation are fully understood.

The Schneckenstein site was selected for this research because these tailings were extensively studied within the frame of a technical cooperation between the chair of hydrogeology of the TU Bergakademie Freiberg and the department of ecology and environmental protection of the TU Dresden (Germany) and because a variety of hydrological conditions are present at this site, and in the vicinity of laboratory facilities. This research program included investigation of the hydrology, hydrogeology, mineralogy and geochemistry of the tailings impoundment.

Lead is one of the most dangerous inorganic contaminants owing to its high toxicity to living organisms (Kelly, 1999; Krieger et al., 1999; Callender, 2005). It is therefore of particular concern with respect to potential chronic risks to human health (Davies et al., 1990; SEGH, 1993; Wixson & Davies, 1994;

Mielke et al., 1997; Mielke & Reagan, 1998). Since mining activity represents an important source of lead to the environment. Hence, the present study was designed to establish baseline levels of lead in ground and superficial waters of the Schneckenstein area. The purpose of this paper is to elucidate the behaviour of lead in the uranium residue and to determine its distribution patterns.

SITE DESCRIPTION AND HYDROLOGICAL SETTING



Figure 1: The Area of Investigation, Uranium Tailings, Schneckenstein

The Schneckenstein tailings are located ~ 3km from the village of Tannenbergsthal county of Vogtland, in the Boda valley, in the southwest of Saxony, Germany (Figure 1). The Boda valley is bordered by the Runder Hubel (837 m a.s.l) and the Kiel (943 m a.s.l) to the Northwest and Southeast respectively. The site of investigation lies in the area of the watershed between the Zwickauer basin and the Eger. It receives an average annual precipitation of 1050 mm. The Boda Bach is considered as the most important Receiving River and all other streams flow into it and subsequently into the 'Pyra' river in the Tannenbergsthal area (Figure 2). The bedrock is the Eibenstock granite covered with a

weathered surface layer. Southwest of the site follows the contact zone with quartz-schist.

The Schneckenstein mill processed ores from different ore bodies; Schneckenstein and Zobes (Vogtland), Oberschlema, Niederschlema (region of schlema) as well as Culmitzsch and Schmirchau (Thuringia).

The major Steps in the milling process were radiometric sorting, gravity separation, grinding and chemical leaching.

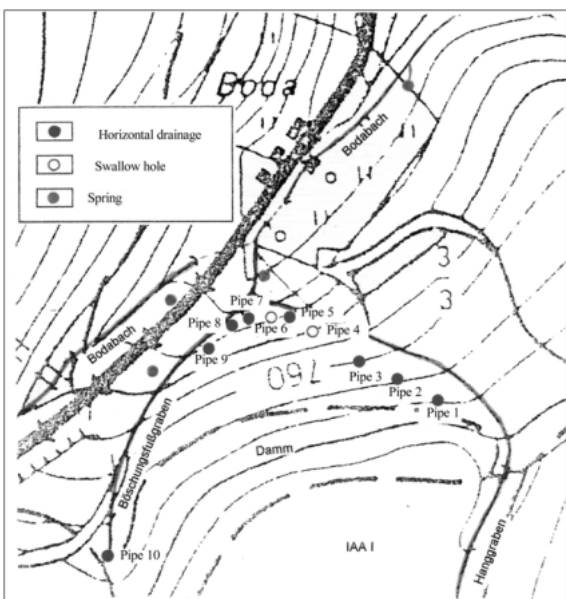


Figure 2: Map of Water Outlets and Springs in the Downwash of the IAA (after Gottschalk, 1997)

EXPERIMENTAL

Field Activity and Sampling

The research was focused on four sediment cores. These cores were taken at the tailings by drilling four boreholes to different depths. Two borings were dug in each tailing (Figure 3). The first and the second borings (GWM 1/96 and GWM 2/96) were drilled down to the granite foundation in Tailing 2 (IAA I). The third borehole (RKS 1/96, Tailing 1(IAA II))

was sunk to a depth of about eight meters. The granite formation was not reached due to technical limitations. 12m deep of the first tailing was sunk for the fourth borehole (RKS 2/98, Tailing 1). The cores (diameter 50mm) were cut into 1m long slices and transported in argon filled plastic cylinders to prevent ambient air contact.

Also water samples were taken at several sampling points as indicated in the Figure 2. E_h and pH were measured in the field with a pH/ E_h -meter (WTW® pH 323) in a closed flow-cell. The pH-meter was calibrated with Merck buffer solutions (CertiPUR, pH 7.00 and 10.00). The E_h -meter controlled against a redox buffer solution (Mettler Toledo, Eh 439, accepted tolerance 5%) and corrected for temperature and to the standard hydrogen electrode. Total alkalinity was determined by titration (Hach® titrator). All samples were filtered (0.2 μ m; regenerated cellulose), anion sample aliquots were stored at +4°C in darkness prior to analysis. For cation analyses, sample aliquots were acidified to pH<2 with HNO₃ (Suprapure®) and stored frozen.

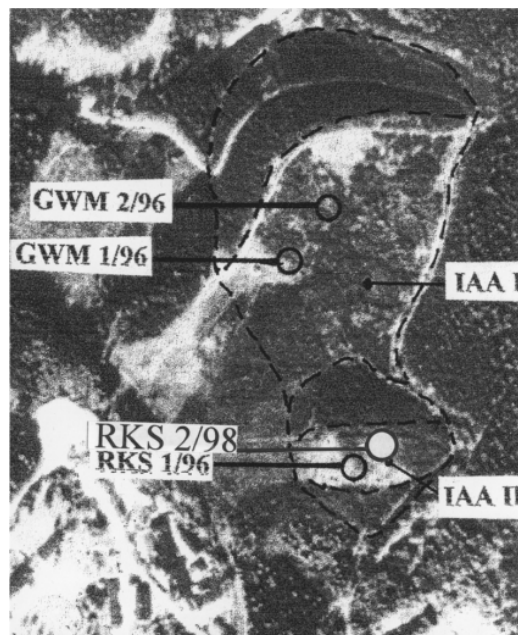


Figure 3: Location of the Borings in the Tailing Sites IAA I and IAA II

Activities in Laboratories and Analytical Methods

Mobility Testing

Basing on the contrast of their mineral contents and metal concentrations, nine samples were selected. A polyethylene spoon was used to avoid any contamination. They were freeze dried. Subsequently, they were ground in agate mortar till a fine size of $\leq 63 \mu\text{m}$ and homogenised. A seven steps extraction procedure was used according to Salomon & Forstner, (1984). The leaching schema and reagents are shown in figure 4.

Pore Water Analysis

Pore water extraction was conducted by means of two different procedures:

- Pore water extraction by means of a high pressure device:

Since most of the processed material has a low permeability, only three samples were analysed. Then the electrical conductivity, the redox potential and the pH values were measured. Also the samples were filtered by a $0.2\mu\text{m}$ membrane filter as well stabilised by diluted nitric acid (1 ml acid/100 ml water) until a $\text{pH} \sim 2$ and finally filled in polyethylene bottles then stored in a refrigerator. The lead content was determined by means of ICP-MS equipment. The detection limit for lead was $1\mu\text{g/l}$.

- Mixed pore water extraction:

The water was extracted from the sediment without any crushing following the first step of the Salomon & Forstner extraction schema illustrated in Salomon & Forstner, (1984).

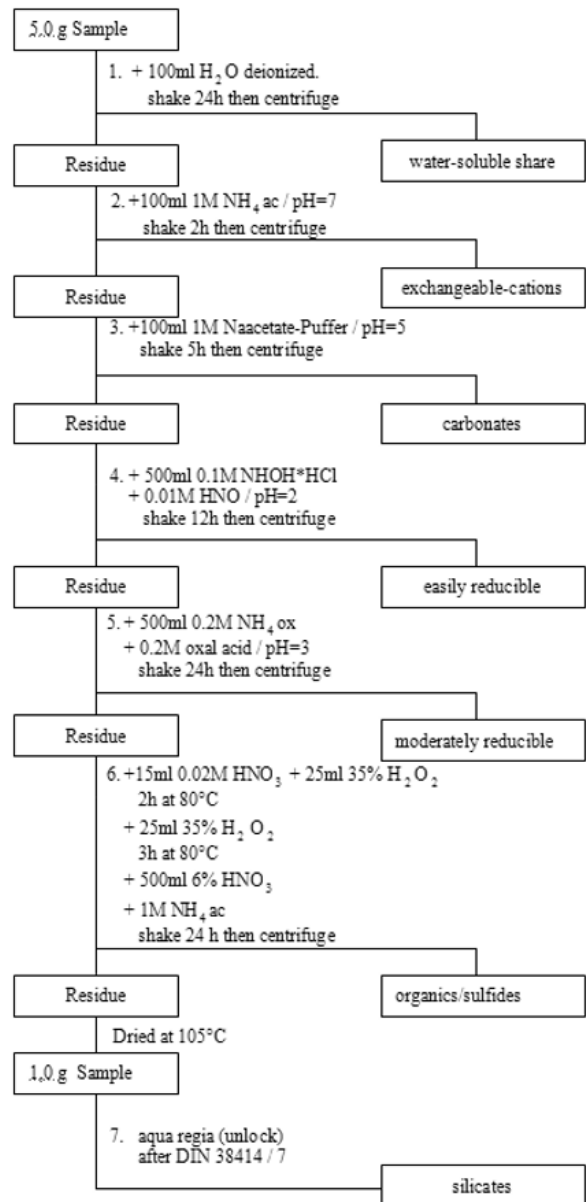


Figure 4: Sequential Extraction - Scheme

Hydrochemical Model

The computer program PHREEQC (Parkhurst, 1995) windows version was used. The software is designated for the simulation of a wide range of geochemical reactions including mixing of water, dissolving and precipitating phases to achieve equilibrium with the aqueous phase and effects of changing temperature. Also, it indicates mineral species and provides estimates of element

concentrations which had not been determined analytically as well as of molalities and activities of aqueous species, pH, pe and saturation indices.

RESULTS & DISCUSSION

Mobility Testing

The Pb content in the tailings material varies between 40 and 190 ppm. Because of the similarity in ionic radius of Pb^{2+} and K^+ a large amount of Pb is incorporated in silicates such as potash feldspars and micas. Thus 33 to 84% of the bulk content is in association with the lithogenous fraction with the dominance of the non clay components.

Although the high affinity of organic substances essentially humic substances to complexation with Pb (Krauskopf, 1956; Goldberg, 1960; Stevenson, 1977; Nriagu & Coker, 1980; McBride, 1994) as well as its extreme tendency to form very insoluble sulfide compounds under reducing conditions due to its chalcophilic property (Lu & Chen, 1977; McBride, 1994; Song & Müller, 1999), no bound Pb to the sulphide-organic phase was recorded in four samples. However, only a certain amount of the non residual Pb is associated with the mentioned phase ranging between ~ 1 and 14%. This may be due to the low humus content in the tailings material and also to the alkalinity of the medium that favour the detachment of Pb-organic complexes (McBride, 1994). Also low content may be due to the dissolution of most Pb -sulfide minerals during the mineral processing accompanied by a high loss of sulphur as observed in its low content in the bulk of analysed sediments.

Further, because of the high affinity of Fe (Kinniburgh & al., 1976; Pickering, 1979; McKenzie, 1980; Laxen, 1983) and Mn (Pickering, 1979; McKenzie, 1980; Cronan,

1976) oxides and hydroxides for Pb mostly at high pHs as well as of the alkalinity of the medium, between 81 and 100% of the non residual fraction is found in association with the nodular hydrogenous fraction.

Furthermore, as the high pH favour the precipitation of Pb with carbonates (McBride, 1994; Salomons & Förstner, 1984), an appreciable amount of the non residual Pb ranging from ~ 0 to 14% is in association with the carbonate phase and these findings are in agreement with those of Salomons & Förstner, (1980) confirming the association of a considerable amount of Pb with carbonates.

Besides, due to the difficult of displacing Pb in exchangeable form clays (Mitchell, 1964), only very little amounts of the non residual Pb is in association with the exchangeable phase which does not exceed 1% in all the samples. Secondly, since lead is the least mobile heavy metal in soils, especially under reducing conditions (McBride, 1994), only a trace amount of the non residual Pb is found in association with the pore water phase.

Lead in Superficial Waters

Under the pH- E_h conditions of the area Pb tends to combine with sulphate or carbonate ions to form PbSO_4 (anglesite) or PbCO_3 (cerussite). In superficial water, it varies between 0.01 $\mu\text{g/l}$ at PNP13 and 2.8 $\mu\text{g/l}$ at PNP17. In groundwater, it ranges from 0.6 $\mu\text{g/l}$ (GWM3) to 1.5 $\mu\text{g/l}$ (GWM1), whereas at drainage water, it varies from 0.3 $\mu\text{g/l}$ at PNP11 to 12 $\mu\text{g/l}$ at PNP7.

Lead in Pore Waters

The lead content is slightly high. It increases with depth. It ranges from 6 to 21 $\mu\text{g/l}$ with a mean value of 11 $\mu\text{g/l}$ and a standard deviation of 8 $\mu\text{g/l}$.

Lead in the Extracted Pore Waters

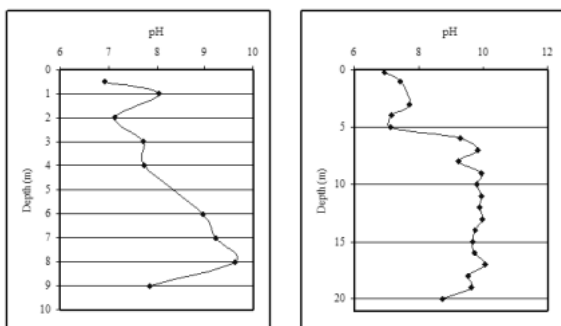


Figure 5: pH Variation with Depth, Core 1 and Core 2 Respectively

Under most probable E_h conditions and at the recorded pH values (Figure 5), most of Pb is expected to be in its crystalline form $PbCO_3$ (Wagman et al., 1982). The lead content is relatively high in most analysed samples mainly from those in the lower tailings. On the other hand, Pb is well known for its high affinity to complexation with organic ligands as well as by its high tendency to form very insoluble sulphide compounds under reducing conditions. Therefore, the current low amount of lead bound to sulphide and organic phase as already emphasised by the selective extraction procedure, on the one hand, and its current high soluble content, on the other hand, may be used as a finger print of the oxidation of Pb bearing minerals during the mineral processing and consequently its mobilisation on its $PbOH^+$ ionic form (Wagman et al., 1982). Thus, almost all the non residual Pb is exposed to mobilisation with time.

In the first and second cores, the extracts ranges from ~ 0.5 to $85 \mu\text{g/l}$ and from ~ 0.5 to $85 \mu\text{g/l}$ with mean values of about 30 and $34 \mu\text{g/l}$ and standard deviations of about 31 and $23 \mu\text{g/l}$ respectively. In the third and fourth cores, it varies from 1 to $16 \mu\text{g/l}$ and from 0.4 to $31.5 \mu\text{g/l}$ with mean values of 5 and $4 \mu\text{g/l}$ respectively. Their standard deviations are close 5 and $9 \mu\text{g/l}$ respectively.

Hydrochemical Model

According to PHREEQC model, with depth, the tailings sediments become under post aerobic or reducing conditions (Figure 6). Since large amounts of Pb are bound to nodules, the anoxic conditions of the treated material favour the dissociation of such compounds i.e. the supplying of the pore water by such hazardous contaminant. Moreover, as the pH of the studied environment is in the alkaline sector, most of the soluble Pb tends to precipitate with carbonates. Thus a considerable share from its total aqueous amount is in its ionic compound form $Pb(CO_3)_2^{2-}$. The co-precipitated $PbCO_3$ complex is its other main form. This tendency may limit the contamination risk of the pore water by Pb to the half.

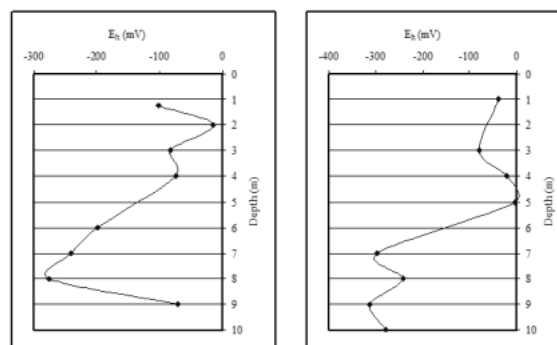


Figure 6: The Calculated E_h Variation with Depth, Core 1 and Core 2 Respectively

CONCLUSION

The Pb contents in pore waters are less important since the solubility of Pb is very low under all weathering conditions. In addition, most of the non residual Pb is an association with nodules. Thus in spite of the dissolution of the compounds under anaerobic conditions which increase its solubility and the presence of sulphur tend to reduce its contents in water. This is because Pb tends easily to form PbS complex irrespective of the pH values.

REFERENCES

- CALLENDER, E., (2005): Heavy Metals In The Environment - Historical Trends. In: Lollar, B.S. (Ed.), Environmental Geochemistry, Vol. 9 Treatise On Geochemistry (Holland, H.D., Turekian, K.K., Eds.), Elsevier-Pergamon, Oxford, Pp. 67-105.
- CARRILLO-CHAVEZ et al., (2003): Environmental Geochemistry Of The Guanajuato Mining District, Mexico. *Ore Geology Reviews* 23 (2003) 277-297
- CRONAN, D. S., (1976): Manganese Nodules And Other Ferromanganese Oxide Deposits. In : RILEY, J. P. & CHESTER, R. (Eds.). *Chemical Oceanography*. Academic, London. New York, 5, 217-263.
- DAVIES, D.J.A. et al., (1990): Lead Intake And Blood Lead In Twoyear- Old U.K. Urban Children. *The Science Of The Total Environment* 90, 13- 29.
- GOLDBERG, E. D., (1961): Chemistry In The Oceans. In: SEARS, M. & WASHINGTON, D. C. (Ed.): *Oceanography*. Amer. Assoc. *Advanc. Sci.*, 67, 583-597.
- GRAY, J.E. et al., (1994): Environmental Geology Of The Summitville Mine, Colorado. *Econ. Geol.* 89, 2006- 2014.
- GUOGH, L.P., (1993): Understanding Our Fragile Environment. Lessons From Geochemical Studies. USGS Circ., 1105.
- HURST, S. & GLESER, K., (1998): Uranbergbausanierung-Eine Herausforderung An Die Fachgremien, Uranium Mining And Hydrogeology II, Proc. Of The Intern. Conference And Workshop, Freiberg, Germany, Verlag Sven Von Loga, Kln.
- KELLY, M.G., (1999): Effects Of Heavy Metals On The Aquatic Biota. In: Plumlee, G.S., Logsdon, M.J. (Eds.), *The Environmental Geochemistry Of Mineral Deposits. Part A: Processes, Techniques, And Health Issues*. . *Reviews In Economic Geology*, Vol. 6A. Society Of Economic Geologists, Inc., Pp. 363-371. Chap. 18.
- KING, T.V., (1995): Environmental Considerations Of Active And Abandoned Mine Lands: Lessons From Summitville, Colorado. USGS Bull., 2220.
- KINNIBURGH, D. G. et al., (1976): Adsorption Of Alkaline Earth, Transition, And Heavy Metal Cations By Hydrous Oxide Gels Of Iron And Aluminium. *Soil Sci. Soc. Am. J.*, 40, 796-799.
- KRAUSKOPF, K. B., (1956): Factors Controlling The Concentration Of Thirteen Rare Metals In Seawater. *Geochim. Cosmochim. Acta.*9, 1-32.
- KRIEGER, G.R. et al., (1999): Bioavailability Of Metals In The Environment: Implications For Health Risk Assessment. In: Plumlee, G.S., Logsdon, M.J. (Eds.), *The Environmental Geochemistry Of Mineral Deposits. Part A: Processes, Techniques, And Health Issues*. . *Reviews In Economic Geology*, Vol. 6A. Society Of Economic Geologists, Inc., Pp. 357-361. Chap. 17.
- LAXEN, D.P.H., (1982): Adsorption Of Pb, Cd, Cu And Ni Onto Hydrous Iron Oxides Under Realistic Conditions. *Proc Intern. Conf. Heavy Metals In The Environment*, CEP-Consultants, Edingburgh, Sept. 6-9, 1082-1085.
- LU, C. S. J. & CHEN, K. Y., (1977): Migration Of Trace Metals In Interfaces Of Seawater And Polluted Surficial Sediments. *Environ. Sci. Technol.*, 11, 174-182.

- McBRIDE, M. B., (1994): Environmental Chemistry Of Soils. Oxford University Press, New York, USA, 406 Pp.
- McKENZIE, R: M., (1980): The Adsorption Of Lead And Other Heavy Metals On Oxides Of Manganese And Iron. *Aust. J. Soil Res.* 18, 61-73.
- MIELKE, H.W. et al., (1997): Associations Between Soil Lead And Childhood Blood Lead In Urban New Orleans And Rural Lafourche Parishes Of Louisiana USA. *Environmental Health Perspectives* 105, 950-954.
- MIELKE, H.W. & REAGAN, P.L., (1998): Soil Is An Important Pathway Of Human Lead Exposure. *Environmental Health Perspectives* 106, 217-229.
- MITCHELL, R. L., (1964): Trace Elements In Soils. In: BEAR, F. E. (Ed.). *Chemistry Of The Soil*. Reinhold, New York, 320-368.
- NRIAGU, J. O. & COKER, R. D., (1980): Trace Metals In Humic And Fulvic Acids From Lake Ontario Sediments. *Enviro. Sci. Technol.*, 14, 443-446.
- PARKHURST, D. L., (1995): PHREEQC, A Computer Program For Speciation, Reaction-Path, Advective-Transport, And Inverse Geochemical Calculations. *Water-Resources Investigations Report 95-4227*. Lakewood, Colorado.
- PICKERING, W. F., (1979): Copper Retention By Soil/Sediment Components. In.: *Nriagu JO (Ed) Copper In The Environment. Part I. Ecological Cycling*. John Wiley, New York, 217-253.
- SALOMONS, W. & FERSTNER, U., (1980): Trace Metal Analysis On Polluted Sediments. II Evaluation Of Environmental Impact. *Environ. Technol. Lett.*, 1, 506-517.
- SALOMONS, W. & FERSTNER, U., (1984): *Metals In The Hydrocycle*, Springer Verlag, Berlin-Heidelberg, 349 Pp.
- SEGH [Society For Environmental Geochemistry And Health], (1993): In: WIXSON, B.G., & DAVIES, B.E. (Eds.), *Lead In Soil: Recommended Guidelines*. Science Reviews, Northwood, ISBN: 0-905927-39-7.
- SONG, Y. & MÜLLER, G., (1999): Sediment -Water Interactions In Anoxic Freshwater Sediments. Springer- Verlag. 111 Pp.
- STEVENSON, F. J., (1977): Nature Of Divalent Transition Metal Complexes Of Humic Acids As Revealed By A Modified Potentiometric Titration Method. *Soil Sci.* 123, 10-17.
- WAGMAN, D. D. et al., (1982): The NBS Tables Of Chemical Thermodynamic Properties. Selected Values For Inorganic And C1 And C2 Organic Substances In SI Units. *J. Phys. Chem.*, 11 (2), 392.
- WIXSON, B.G. & DAVIES, B.E., (1994): Guidelines For Lead In Soil. *Environmental Science And Technology* 28 (1), 26A- 31A.

THIOSALT IN MINING WASTE: REACTION KINETICS MODELLING

Jorge Miranda-Trevino, Kelly Hawboldt, Christina Bottaro and Faisal Khan
Memorial University of Newfoundland, St John's, NL, Canada.

ABSTRACT: The presence of thiosalts in mining wastewaters is an environmental issue due to the resulting pH depression as these species degrade with time. Despite research in the area, reaction kinetics of thiosalt species under different pH and temperature conditions is not fully understood, especially in conditions common in receiving ponds. As a result, it is difficult to design ponds or develop treatment technologies to treat these compounds. Several studies have dealt with the reaction kinetics of major thiosalt species (thiosulphate, trithionate, tetrathionate) under various pH and temperature conditions. However, further research is required to better understand the fundamental behaviours of thiosalt species and identify probable reaction paths in the presence of natural catalysts such as microbes and metals. The overall objectives of our work are to determine the behaviour of thiosalts in mining wastewaters, develop possible treatment technologies, and assess the risk of these species, treated and untreated, in the larger watershed. The work presented here represents the first stages of the study. An extensive review is presented on available reaction kinetics and reaction path data of three major species of thiosalts (thiosulphate, trithionate and tetrathionate) under the conditions of the receiving pond. The impact of natural catalysts and their influence in the reaction of thiosalts is also discussed. Thus far we have studied the individual behaviour of the thiosalts experimentally. This experimental data is presented with a general model development strategy. Finally, preliminary results from kinetics studies on three thiosalts without the presence of catalyst in different conditions are presented. An analysis of the error and uncertainty associated with the capillary electrophoresis (CE) method used to measure the thiosulphate, trithionate and tetrathionate is also presented.

INTRODUCTION

Thiosalts are sulphur compounds generated in mining and metal processing operations (Dinardo and Salley, 1998) or naturally in the presence of Fe^{III} (Kuyucak et al, 2001). These species, also known as polythionates, are intermediates in the oxidation of sulphide (S_2^{2-}) to sulphate (SO_4^{2-}). Based on their stability, the most important species are: thiosulphate ($\text{S}_2\text{O}_3^{2-}$), trithionate

($\text{S}_3\text{O}_6^{2-}$) tetrathionate ($\text{S}_4\text{O}_4^{2-}$) and pentathionate ($\text{S}_5\text{O}_6^{2-}$) (Brimblecome, 2005, Dinardo and Sally, 1998; Kuyucak et al, 2001; Vongporm, 2008). Although these compounds are not considered toxic, their presence in the environment can accelerate environmental problems such as acidification of water bodies and promotion of metal migration from soil and sediment (Kuyucak et al, 2001).

In recent years, thiosulphate has been studied as a substitute for cyanide in the recovery of silver and gold (Ahern et al, 2006; Senanayake, 2007; Zhao et al, 1999). Thiosalts in the mining/metal processing effluents are as a result of oxidation processes associated with the unit operations (Chanda and Rempel, 1987; Kuyucak et al, 2001). Factors that affect the production of thiosalts in such processes are ore characteristics (such as amount and species of sulphur), process pH and temperature, residence time, pulp density, and chemicals used in the process, among others (Kuyucak et al, 2001; Dinardo and Sally, 1998). Although the amount of thiosalts produced will vary according to the process, the concentration in the effluent could be as high as 1200 ppm (Dinardo and Sally, 1998; Kuyucak et al, 2001; Rolia and Tan, 1985).

Once the thiosalts are produced, they usually pass through the different water treatment processes without any significant oxidation. However, once in the receiving pond, several factors promote the oxidation of thiosalts to sulphate such as the presence of *Thiobacillus* bacteria in natural environments, seasonal pH shifts that occur in the ponds (Dinardo and Sally, 1998), and presence of chemical catalysts (Druschel et al, 2003b).

Schwartz et al. (2006) evaluated the toxicity of thiosalts to different fish species. In the study, it shows that the toxicity of thiosalts is low compared to the metal mining effluent regulation (MMER) species, with thiosulphate being the most toxic compound. However, it does identify the decrement in pH as one cause for fatality of *Daphnia Magna* (Figure 1).

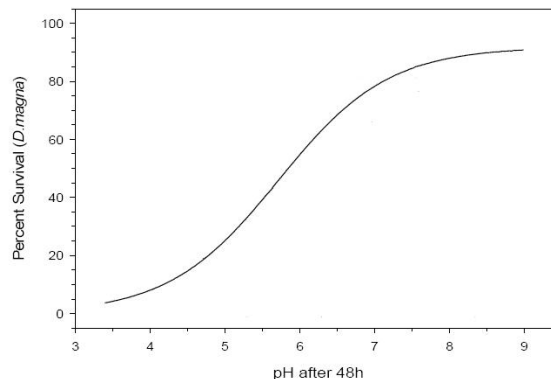


Figure 1. Trend for *Daphnia Magna* survival as result of pH change (modified from Schwartz et al 2006)

The lack of appropriate treatment technique and the pH depression caused by the oxidation of the thiosalts have made them subject to extensive studies to identify their origin in the mining process (Kuyucak et al, 2001; Rolia and Tan, 1985) and their kinetic behaviour under different conditions (Ahern, 2006; Meyer and Ospina, 1982; Mizoguchi et al, 1976; Rolia and Chakrabarti, 1982; Suzuki, 1999; Xu and Schoonen 1995).

The current study is divided in three main areas:

1. Gathering of kinetic information for thiosulphate, trithionate and tetrathionate under different pH and temperature conditions and in the presence of natural catalysts such as *Thiobacillus* bacteria and pyrite.
2. Identification of thiosalt treatment technologies to reduce their discharge to watersheds.
3. Human health and environmental risk assessment for both treated and untreated cases in large watersheds.

This paper outlines work done for the first stage of the research where the global reaction kinetics is proposed for thiosalt oxidation as a function of pH and temperature.

Thiosalts Kinetics Studies

Chemical kinetics can be divided in three areas (Connors, 1990; Steinfeld et al 1999):

- Chemical structure or reaction dynamics, which explains how the atoms and molecules are interacting.
- Thermodynamics, which explains the behaviour of the system or molecules at equilibrium.
- Kinetics, which explain the changes of the molecules considering time as a variable.

The study and determination of reaction mechanisms are based on the understanding of these three areas. The reaction mechanism is the knowledge of the sequence of reactions at the molecular level that take place to transform the reactants into products (Mortimer and Taylor, 2002). The objective of the study is to determine a global reaction rate expression rather than step-by-step reaction mechanism. Nonetheless, it is important to review the information available in the three areas in order to identify the most relevant reactions during the oxidation of thiosalts.

Temperature and pH conditions are important in the studies of thiosalts kinetics. Vongporm (2008) studied the reactivity of thiosalts in temperatures between 4 and 30°C and in pH between 2 to 9 identifying the conditions in which thiosulphate, trithionate and tetrathionate are reactive. Table 1 show the areas where each species is reactive.

Chemical Structures of Thiosalts

The chemical structures for thiosulphate, trithionate and tetrathionate are presented in Figure 1. One of the main characteristic of the chemical structure of thiosalts is the

bounding of sulphur atoms with various oxidation states (Meyer and Ospina, 1982). The atoms of sulphur and oxygen are available for reactions as both are exposed to attacks from other compounds. This information will be important to propose the global mechanism for each thiosalt and the reactions paths for their oxidation.

Table 1 Areas where thiosalts are reactive.

	Temp= 4°C.	Temp= 15°C.	Temp= 30°C.
pH-2	• Thiosulphate	• Thiosulphate	• Thiosulphate • Trithionate
pH-4		• Trithionate	• Trithionate
pH-7		• Trithionate	• Trithionate
pH 9	• Tetrathionate	• Tetrathionate	• Thiosulphate • Trithionate • Tetrathionate

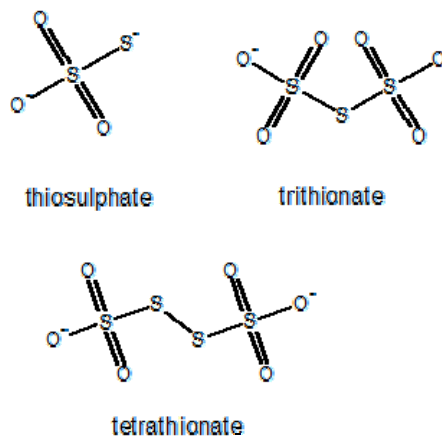


Figure 2. Thiosulphate, trithionate and tetrathionate Structures

Thermodynamic Information

Any given system will be at equilibrium when a minimum energy level is reached. This means that those reactions with lower free energy will be favoured. There is limited thermodynamic information for thiosalts, however Thauer et al. (1977)

reported standard free Gibbs energy for selected reactions. This information can be used to estimate the change in free Gibbs energy of the reaction and propose the equilibrium of the system.

Table 2 and 3 show a summary for free Gibbs energy for different reactions involving thiosalts and other related sulphur compounds.

Kinetic Studies

There have been several studies related to reaction kinetics involving polythionates. However, most of these were carried out under different conditions that make direct comparison challenging. Nevertheless, the studies provide a background for the development of the kinetic model at the receiving pond conditions. The next section gives a brief summary of the pertinent studies grouped on the basis of type of thiosalt and pH range, i.e. acidic or basic.

Table 2. Thermodynamic information related to thiosalts (Modified from Thauer et al 1977).

Reaction	ΔG° (kJ/mol)
$S_4O_6^{2-} + [H_2] \rightarrow 2S_2O_3^{2-} + 2H^+$	-20.2
$SO_4^{2-} + H_2 \rightarrow SO_3^{2-} + H_2O$	+ 5.0
$SO_3^{2-} + 2H^+ + 3H_2 \rightarrow H_2S + 3H_2O$	-172.8
$S_2O_3^{2-} + 4H_2 \rightarrow 2HS^- + 3H_2O$	-174.1
$S_2O_3^{2-} + 2H^+ + 2H_2 \rightarrow 2S + 3H_2O$	-118.4
$3SO_3^{2-} + 4H^+ + H_2 \rightarrow S_3O_6^{2-} + 3H_2O$	-50.2
$S_3O_6^{2-} + H_2 \rightarrow S_2O_3^{2-} + SO_3^{2-} + 2H^+$	-121.8
$S_2O_3^{2-} + H_2 \rightarrow HS^- + SO_3^{2-} + 2H^+$	-1.1
$S_4O_6^{2-} + H_2 \rightarrow S_2O_3^{2-} + 2H^+$	-84.5

Thiosulphate

Thiosulphate is usually stable in neutral and alkaline environments, however, under high temperature conditions (i.e. above 70°C), thiosulphate decomposes to sulphate (SO_4^-) in alkaline media. On the other hand, it is

highly reactive in acid media where it decomposes to tetrathionate ($S_4O_6^{2-}$) in the presence of oxidants such as oxygen (Xu and Schoonen, 1995).

Table 3. Free Gibbs energy of formation (modified from Thauer et al 1977)

Substance	State	ΔG_f° (kJ/mol)
SO_3^-	Aqueous	27.87
SO_4^{2-}	Aqueous	177.97
$S_2O_3^{2-}$	Aqueous	122.7
$S_3O_6^{2-}$	Aqueous	229
$S_4O_6^{2-}$	Aqueous	244.3

Acidic Media

Mizoguchi et al (1976) proposed the following pathway for the degradation of thiosulphate in acid media.

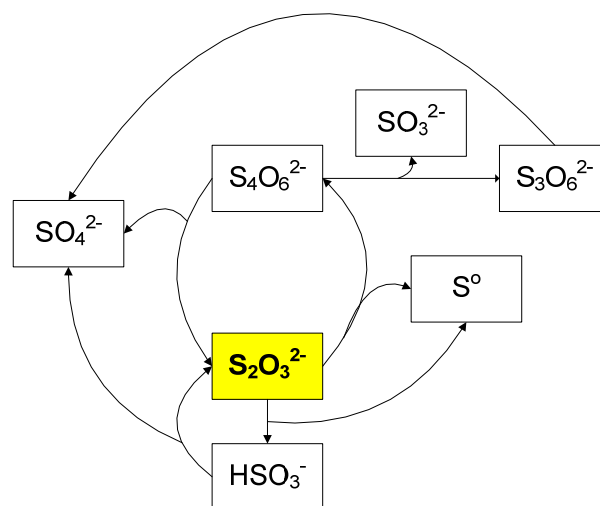
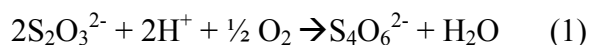


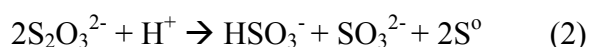
Figure 3. Thiosulphate degradation pathways (modified from Mizoguchi et al, 1976).

Wasserlauf and Dutrizac (1982) reported the degradation of thiosulphate to tetrathionate, as shown in reaction 1, under neutral to mildly acidic conditions.

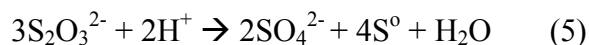
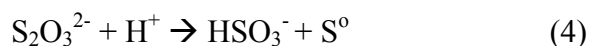
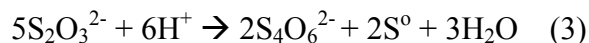


In this case, the protons act to catalyze the reaction. Suzuki (1999) also identified tetrathionate as the main product of thiosulphate dissociation in acid media.

Unlike, the studies mentioned above, Xu and Schoonen (1995) proposed decomposition of thiosulphate at 25°C and pH=2.9 as shown in reaction 2. In this study, the authors identified that tetrathionate could react with O₂ yielding different products than reaction 1.



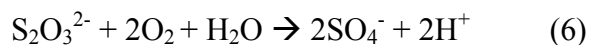
Finally, Mizoguchi et al (1976) studied the reaction at pHs below 2.3 and high temperatures between 70 and 150 °C. The reactions proposed are as follows:



Regarding kinetic information, Xu and Schoonen (1995) proposed a reaction order of 2 for reaction two and a reaction rate constant of $0.66 \pm 0.009 \text{ M}^{-2}\text{s}^{-1}$. The initial rate method was used to obtain the reaction order and constant. Further discussion on this approach is presented in the Data Analysis section.

Basic Media

The oxidation of thiosulphate in alkaline media under atmospheric conditions is usually a slow process which requires a strong oxidant. At 125°C under saturated oxygen conditions, thiosulphate follows is a first order decomposition reaction with a reaction rate constant of $1.48 \times 10^{-3} \text{ s}^{-1}$ as proposed by Rolia and Chakrabarti (1982) in reaction 6:

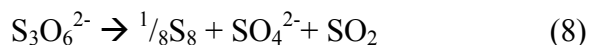
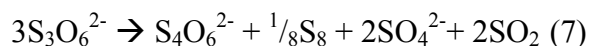


Trithionate

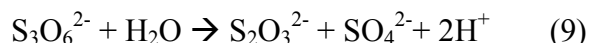
Trithionate is stable at neutral conditions and low pH and its reactivity increases with pH. The products of trithionate oxidation are thiosulphate and sulphate but depending of the conditions of the solutions, thiosulphate could be subject to additional degradation (Meyer and Ospina, 1982; Mizoguchi et al, 1976).

Acid Media

Meyer and Ospina (1982) followed the degradation of trithionate at pH between 3.5 and 4. They reported an initial degradation mainly to tetrathionate and sulphate (reaction 7) and equilibrium to sulphate, sulphur dioxide and sulphur (reaction 8).



For high temperatures, between 70 and 150°C, Mizoguchi et al (1976) proposed the degradation of trithionate to thiosulphate and sulphate according to reaction 9.



This same reaction is proposed by Suzuki (1999) and Wasserlauf and Dutrizac (1982) for the oxidation of trithionate at pH below 7 and by Varga and Horvath (2007) in alkaline solutions. As a result of the acidic conditions, thiosulphate produced in reaction 11 should undergo further oxidation to tetrathionate and sulphite (Mizoguchi, 1976).

Kinetic information available for trithionate in acidic shows that the reaction order is 1 with various reaction rate constant reported

such as $1.2 \times 10^{-2} \text{ h}^{-1}$ (Ahern, 2006), $2.6 \times 10^{-3} \text{ h}^{-1}$ (Vongporm, 2008) and $3.2 \times 10^{-3} \text{ h}^{-1}$ (Meyer and Ospina, 1982).

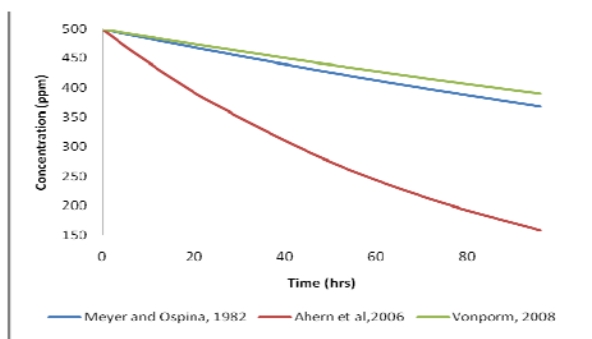


Figure 4. Rate comparisons for trithionate acid media.

Basic Media

Trithionate is more reactive in alkaline conditions. The proposed products of trithionate oxidation in basic solutions are the same as proposed for acid solutions in reaction 11 (Ahern et al, 2006; Rolia and Chakrabarti, 1982; Wasserlauf and Dutrizac, 1982). However, Rolia and Chakrabarti (1982) noted that the reaction did not reach equilibrium during long runs as the thiosulphate generated continue to react to form sulphate.

The reaction order for trithionate in basic environment is reported to be one by Rolia and Chakrabarti (1982) with a reaction rate constant of $4.06 \times 10^{-3} \text{ h}^{-1}$ in experiments at 80°C . Also Vongporm (2008) reported the same reaction rate but with a constant of $1.90 \times 10^{-3} \text{ h}^{-1}$ in experiments at 30°C .

Figure 5 shows a graphic comparison of the kinetic data for trithionate.

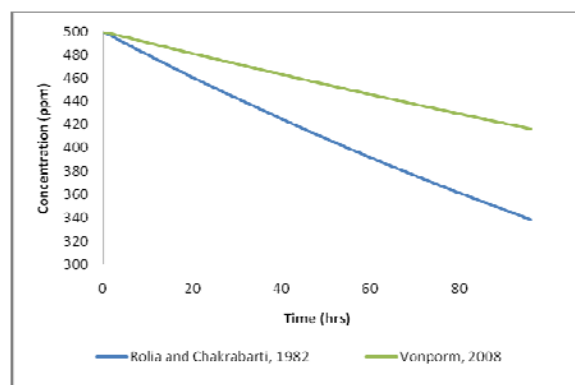


Figure 5. Rate comparison for trithionate basic media.

A proposed pathway for trithionate degradation based on the information available is shown as follows:

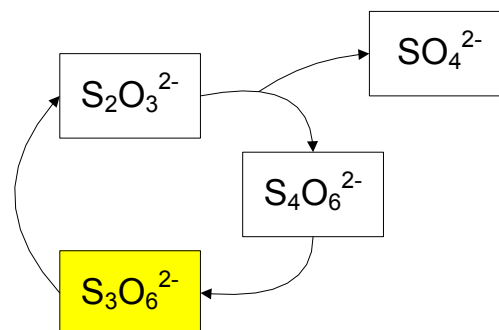


Figure 6. Trithionate degradation pathways

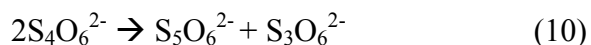
Tetrathionate

Tetrathionate is highly stable in acid conditions. However, it degrades to thiosulphate and sulphate at pH near to neutral (Wasserlauf and Dutrizac, 1982). In the case of alkaline environment, common products of tetrathionate oxidation are thiosulphate and sulphite.

Acidic Media

There is limited information regarding the behaviour of tetrathionate in acid

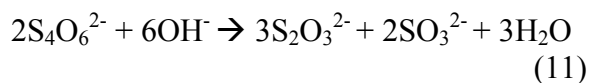
environments. Meyer and Ospina (1982) studied the reaction at pH 3.5 to 4 and temperature of 20 and 70°C proposing trithionate and pentathionate as the products of the reaction:



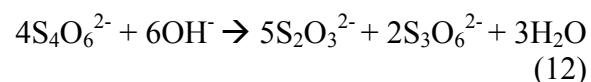
Their kinetic analysis gives that tetrathionate oxidation is a second order reaction with a reaction constant at 20°C of $4.1 \text{ M}^{-1}\text{hrs}^{-1}$.

Basic Media

In the presence of a strong alkaline media, tetrathionate oxidation will yield thiosulphate and sulphite according to reaction 11 (Varga and Horvath, 2007; Zhang and Dreisinger, 2002):



Both authors reported trithionate as a probable intermediate in the reaction similar to the reaction proposed by Rolia and Chakrabarti (1982):



Since thiosulphate is considered a catalyst of tetrathionate oxidation, the equilibrium and the final products will strongly depend on the composition of the solution (Varga and Horvath, 2007).

Various authors agree that the reaction order of tetrathionate in basic media is one (Rolia and Chakrabarti, 1982; Vongporm, 2008; Varga and Horvath, 2007; Zhang and Dreisinger, 2002). However, the reaction rate constant reported varies significant among these authors. The highest constant is reported by Zhang and Dreisinger (2002) at $0.38 \text{ M}^{-1}\text{s}^{-1}$, followed by Varga and Horvath

(2002) with $4.4 \times 10^{-2} \text{ M}^{-1}\text{s}^{-1}$ and finally Rolia and Chakrabarti (1982) with $5.1 \times 10^{-3} \text{ M}^{-1}\text{s}^{-1}$ and Vongporm (2008) with $6.1 \times 10^{-3} \text{ M}^{-1}\text{s}^{-1}$.

Figure 7 shows the comparison of kinetic information for tetrathionate in basic media.

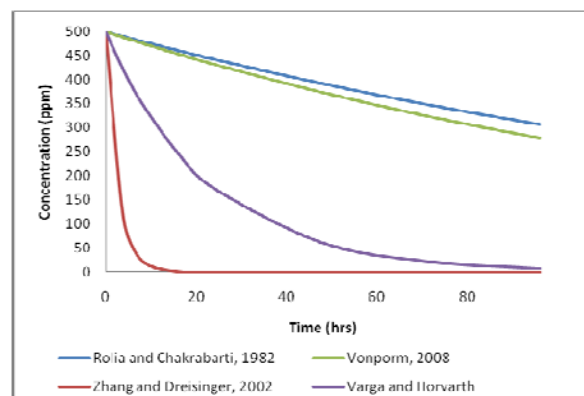


Figure 7. Rate comparison for tetrathionate basic media.

The strong dependency of the reaction on pH could be a partial explanation for the difference in the constants reported among different authors.

A proposed pathway for tetrathionate degradation based on reaction 11 and 12 is shown as follows:

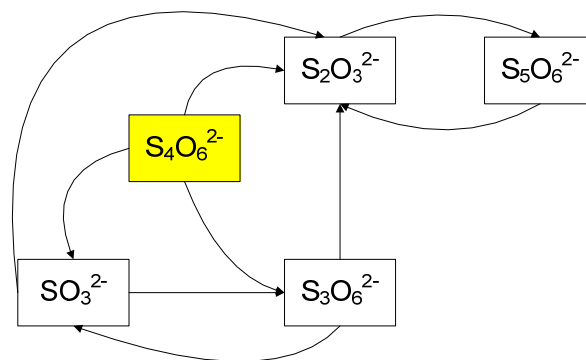


Figure 8. Tetrathionate degradation pathways

Effect of Oxydant and Catalysts

Oxygen

The degradation of thiosalts is an oxidation process, hence, it is expected that the concentration of oxygen available should play an important role in the reaction. Although Zhang and Dreisinger (2002) suggested that the dissolved oxygen in the solution could inhibit the degradation of tetrathionate and trithionate in alkaline media, other studies (Chanda and Rempel, 1987; Druschel et al, 2003; Xu and Schoonen, 1995) identify the role of oxygen in the degradation of tetrathionate in acid environments.

Nevertheless, since the conditions of the tailing ponds are variable in terms of available oxygen, the role of this compound in the degradation of thiosalts should be studied further.

Fe^{3+}

Pyrite and Fe^{3+} -rich environments enhance the degradation of polythionates and in the case of trithionate and tetrathionate, the reaction constant can be orders of magnitude higher (Druschel et al., 2003a; Xu and Schoonen, 1995). The main role of pyrite is to participate in the oxidation of the thiosalts, but it can also generate those compounds (Bribblecombe, 2005), therefore it is important to understand the role of pyrite not only in acid environments but also in neutral and basic conditions.

Hydrogen Peroxide

Druschel et al (2003b) identified hydrogen peroxide as an oxidant for trithionate and tetrathionate oxidation at low pH through the formation of an intermediate compound identified as $\text{S}_3\text{O}_4^{n-}$. Since this approach is

becoming a popular option in the thiosalt treatment, will be important to understand the reaction pathway and possible products of the interactions.

Experimental Procedure

Thiosalts samples will be measured by capillary electrophoresis technique using a modified method of Pobozy et al. (2002). This technique determines the concentration of the salts by an indirect spectrophotometric method, which means that the UV signal will be absorbed most strongly by the background electrolyte, whereas the thiosalts absorb weakly or not at all, thus, by difference we could determine the concentration of the thiosalt.

General set up of the equipment is as follows:

- Capillary Electrophoresis: Agilent 1602 electrophoresis equipped with an onboard UV-visible diode-array detector
- Capillary: bare fused silica, 75 μm inner diameter, 48.5 cm total length and 40 cm effective length (length to the detector).
- Background electrolyte (BGE): Pyromelic acid (benzenetetracarboxylic acid)
- CE conditioning (new capillary):
 - NaOH [1 M] for 60 minutes
 - Ultrapure water for 60 minutes
 - BGE for 60 minutes
- CE conditioning (everyday set up before start working in the equipment):
 - NaOH [0.1 M] for 15 minutes
 - Water for 10 minutes
 - BGE for 10 minutes
- CE settings prior to injection:
 - NaOH [0.1 M] for 1 minutes
 - BGE for 2 minutes
 - Sample Running time for 7 minutes
- The expected migration time for thiosalt peaks:
 - Tetrathionate – 4 minutes

- Thiosulphate – 3 minutes
- Trithionate – 3.5 minutes
- Pentathionate – 5 minutes
- Capillary temperature: 25°C
- Detection wavelengths:
 - 191.2 nm
 - 214.10 nm
 - 254.20 nm
 - 200.20 nm
 -

For the kinetic studies, a sample of 100 mL of each thiosalt solution was placed in 200 mL beakers. Thiosalts concentrations will be varied from 250 ppm to 1000 ppm. The concentrations of thiosalts were followed over time using CE. At specific intervals 3 mL of each solution was sampled and then filtered with a 0.2 μm nylon syringe filter into three different CE vials then treated for storage or submitted for analysis. For storage, the CE vials were frozen in liquid nitrogen, trying to avoid fully submerging the cap was under the liquid; frozen samples were stored in an ultra low temperature freezer. Special attention was taken to avoid keeping the samples at room temperature for more than 5 minutes.

For the CE analysis, the samples were taken out of the freezer and thawed with water at 20°C for 5 minutes, three vials at a time.

For the kinetic studies, the pH conditions used were 2, 4, 7 and 9 and the temperatures 4, 15 and 30°C.

Data Analysis

The data collection and analysis in reaction kinetic studies represent a challenge as every case is unique according to the species, concentrations and conditions that are under study. In a general overview, the approach to determine the kinetics information is presented of Figure 9:

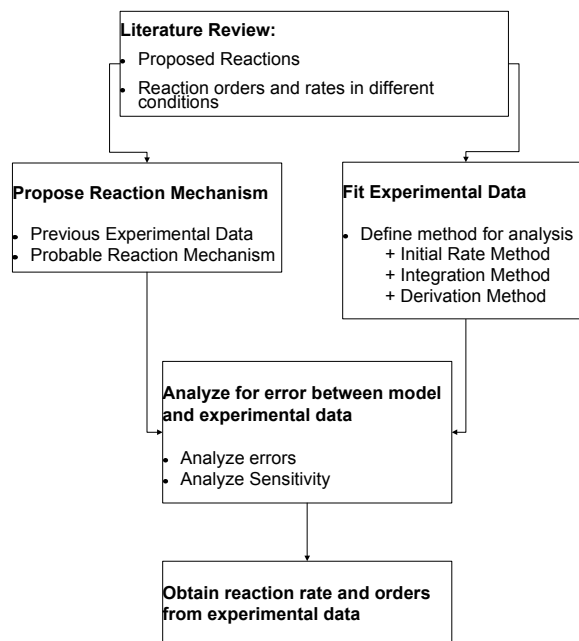


Figure 9. Flowchart for Kinetic Data Analysis.

Thiosalts are known to catalyze their own degradation reactions (Wasserlauf and Dutrizac, 1982), adding complexity to the kinetic study. In order to simplify the global reaction mechanisms, the information regarding the reaction constants and orders will be done by de-coupling the reactions. In other words, each thiosalt will be isolated in different conditions in order to obtain the kinetic information and use this information in the global reaction mechanisms. For example, based on the literature review, thiosulphate in acid conditions will oxidize to tetrathionate and sulphur, however, this reaction is reversible. By de-coupling, the reaction, the rate can be obtained by analyzing the thiosulphate to tetrathionate reaction and then the tetrathionate to thiosulphate reaction. The combination should yield a global reaction rate for thiosulphate. However, following the same reaction path, tetrathionate can degrade to pentathionate and trithionate which undergo further oxidation (see Thiosalt Kinetic Studies).

Hence, a proposed global reaction mechanism should include information about all the thiosalts involved or that are considered to play an important role in the oxidation.

The proposed reaction rates are presented for the thiosalts in acid conditions based on reactions 3, 9, 10 and 12:

$$\frac{d[S_2O_3^{2-}]}{dt} = -k_1[S_2O_3^{2-}]^{\alpha} + k_2[S_4O_6^{2-}]^{\beta}[SO_4^{2-}]^{\epsilon}$$

$$\frac{d[S_3O_6^{2-}]}{dt} = k_3[S_4O_6^{2-}]^{\gamma} - k_4[S_3O_6^{2-}]^{\delta}$$

$$\frac{d[S_4O_6^{2-}]}{dt} = -k_2[S_4O_6^{2-}]^{\beta}[SO_4^{2-}]^{\epsilon} + k_1[S_2O_3^{2-}]^{\alpha} + k_4[S_3O_6^{2-}]^{\delta} - k_3[S_4O_6^{2-}]^{\gamma}$$

Similar to basic conditions, the proposed reaction rates are:

$$\frac{d[S_3O_6^{2-}]}{dt} = k_6[S_4O_6^{2-}]^{\theta} - k_7[S_3O_6^{2-}]^{\eta}$$

$$\frac{d[S_4O_6^{2-}]}{dt} = -k_8[S_4O_6^{2-}]^{\theta}$$

The kinetic information will be obtain using the initial rate method which is based on the principle that the kinetic information gathered in the initial stages of the reaction should apply until equilibrium is reached (Mortimer and Taylor, 2002)

Results

The initial rate method will help to obtain the reaction order and constant of thiosalts oxidation and hence, model the degradation of the compound into the form of:

$$[A] = [A_0]e^{-kt} \quad (a)$$

$$\frac{1}{[A]} = kt + \frac{1}{[A_0]} \quad (b)$$

These equations are valid if the chemical reactions follow a first order (equation a) or second order (equation b) kinetic. However, it is expected that these individual equations

will fail to fully model the thiosalt degradation as secondary reactions are present in the oxidation mechanism.

Figures 10 to 12 show the trend of trithionate and tetrathionate degradation at different concentrations and temperatures, where the straight line is the simulation for each different concentration. The acid condition points are the average values obtained in the studies at pH of 2 and 4 while the basic conditions are the average values obtained at pH 7 and 9.

The Rate expressions for trithionate in acid media (equation c), basic media (equation d) and tetrathionate in basic media (equation e) are presented next:

$$[S_3O_6^{2-}] = [S_3O_6^{2-}]_0 e^{-0.0026t} \quad (c)$$

$$[S_3O_6^{2-}] = [S_3O_6^{2-}]_0 e^{-0.0017t} \quad (d)$$

$$[S_4O_6^{2-}] = [S_4O_6^{2-}]_0 e^{-0.00061t} \quad (e)$$

The simulation using the data obtained for trithionate and tetrathionate with the initial rate method show a good fit during the first 24 hours of the reaction (Figure 10, 11 and 12). Nevertheless, the trend of the original values deviates from the simulation with time, especially for concentrations of 500 and 1000 ppm.

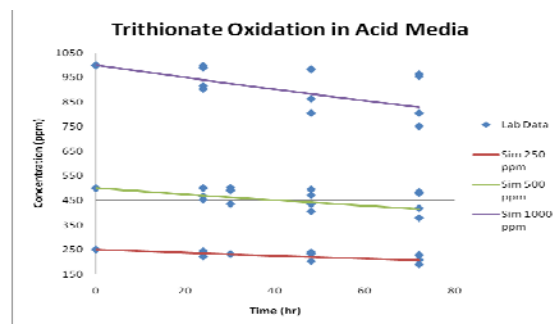


Figure 10. Trithionate Oxidation in Acid Media

The trend of the simulation curves show that the temperature plays an important role in the oxidation of thiosalts suggesting that the

reactions are enhanced by the increase in the temperature above 15°C in the case of trithionate and tetrathionate.

In Figure 10, the difference between the experimental results and the model increases with concentration. In the case of trithionate in acid media, the deviation after the early stages of the reaction is expected as the oxidation of trithionate involves the generation of thiosulphate which can degrade to tetrathionate which can then contribute to the generation of more trithionate.

In Figure 11, trithionate degradation in basic media, the deviation from the simulation is even more obvious at high concentrations and high temperatures, probably because tetrathionate is more reactive in basic media and the secondary reactions affect the behavior of trithionate in the solution.

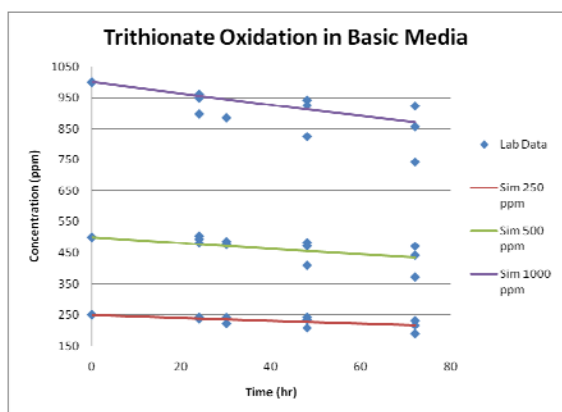


Figure 11. Trithionate Oxidation in Basic Media

Tetrathionate behaviour in basic media shows a significant deviation from the simulation at low temperatures, probably because the secondary reactions that drive the degradation of the thiosalt requires a temperature of 30°C or higher to overcome the activation energy.

Although in the case of tetrathionate, the reaction rate proposed is one of the simple

one, additional runs will have to be done before obtained a good understanding of the mechanisms that it's undergoing during the oxidation as it is clear in Figure 12 that the behaviour in the first stages of the reaction does not hold after 24 hours.

The results presented here are only a preliminary approach for the overall study that aims to identify, from a global perspective, the most important reactions that take place during the oxidation of thiosalts, which could lead to an accurate model of behaviour in tailing ponds.

CONCLUSIONS

Thiosalts kinetics modeling is complex as result of the different interactions between the species according to conditions and composition of the solution. Decoupling of the reactions can be an approach that could lead to insight regarding the global reaction mechanisms of these compounds.

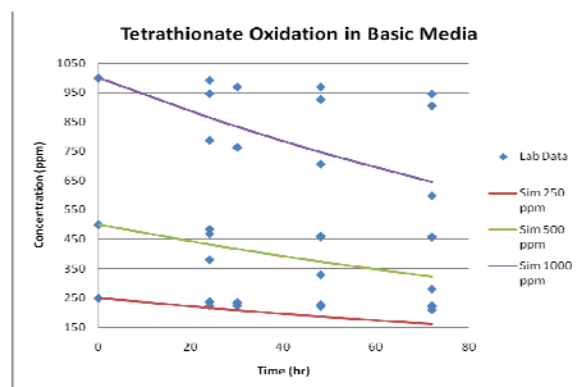


Figure 12 Tetrathionate Oxidation in Basic Media

Preliminary results show that through the initial rate method we can obtain valuable kinetic information for the oxidation of the pure species. Once that information is obtained, the proposed reaction rate can be established and hence, a reaction mechanism proposed and verified.

The deviations from the simulation for trithionate and tetrathionate indicate the presence of secondary reactions that have to be included in the kinetic model. Secondary reactions might involve the generation of species that go on to further participate in reactions with the original thiosalt, e.g., as a catalyst for the original reaction or to further react to regenerate the original thiosalt or to generate other products, depending on the conditions.

The trends of the secondary reactions are expected to be revealed by the de-coupling of the reactions. This means that the study will focus on the gathering of information of pure species in specific conditions and later substitute the kinetic information in the reaction rate proposed. The first approach is presented in the data analysis section, but those equations can be refined with the development of the research and the inclusion of different catalysts.

Thiosulphate should play an important role in the reaction mechanisms for thiosalt degradation as it is present in the degradation reaction pathways of trithionate and tetrathionate. The next step of the research will focus on the determination of the kinetic information of thiosulphate under different conditions. Exploratory studies have indicated a reaction order of two, but further studies are needed to confirm this result.

A global mechanism for thiosalts oxidation could lead to a better understanding of the main reactions taking place and species present in the tailing ponds during specific conditions or over time. This information could be used in the mining process to reduce the generation of thiosalts, in the treatment process to set up conditions that will drive

equilibrium into the more stable species and finally in ponds to establish a more accurate environmental risk assessment and treatment strategy.

ACKNOWLEDGEMENTS

The authors would like to recognize the financial support of the Natural Sciences and Engineering Research Council of Canada and the support provided by Michael Pappoe in the Chemistry Department of Memorial University.

REFERENCES

- Ahern, N., Dreisinger, D., Van Weert, G. (2006). Kinetics of trithionate degradation. *Canadian Metallurgical Quarterly*, 45, 2, 135 – 144.
- Brimblecome, P. (2005). The Global Sulfur Cycle. In: Shlesinger W.H. ed *Biogeochemistry*. London, Elsevier, 645-682.
- Chanda, M., Rempel, G.L. (1987). Catalyzed air oxidation of thiosalts, *Canadian Metallurgical Quarterly*, 26, 3, 227 – 237.
- Connors, K.A. (1990). *Chemical Kinetics*. New York, VCH Publishers.
- Dinardo, O., Sally, J. (1998). Treatment of thiosalts in milling effluent: A review of treatment process. *Mining and Mineral Sciences Laboratories Report*. Thiosalts Consortium-Phase II. CANMET-MMSL
- Druschel, G.K., Hamers, R.J., Banfield, J.F. (2003a). Kinetics and mechanism of polythionate oxidation to sulfate at low pH by O₂ and Fe³⁺. *Geochimica et Cosmochimica Acta*, 67, 23, 4457-4469.

- Druschel, G.K., Hamers, R.J., Luther, G.W., Banfield, J.F. (2003b). Kinetics and mechanism of trithionate and tetrathionate oxidation at low pH by hydroxyl radicals. *Aquatic Geochemistry*, 9, 145-164.
- Kuyucak, N., Antonio Serrano, J.R., Hultqvist, J., Eriksson, N. (2001). Removal of Thiosalts from Mill Effluents. *Waste Processing and Recycling IV*, 481 – 495
- Meyer, B., Ospina, M. (1982). Raman spectrometric study of the thermal decomposition of aqueous tri- and tetrathionate. *Phosphorus and Sulfur*, 14, 23-36.
- Mizoguchi, T., Takei, Y., & Okabe, T. (1976). The chemical behavior of low valence sulfur compounds. X. Disproportionation of thiosulfate, trithionate, tetrathionate and sulfite under acidic conditions. *Bulletin of the chemical society of Japan*, 49(1), 70-75.
- Mortimer, M., Taylor, P. (2002). *Chemical kinetics and Mechanisms*, Cambridge, The Open University.
- Pobozy, E., Jarczynska, M., Trojanowicz, M. (2002). Speciation of sulphur-containing anions by use of capillary electrophoresis. *Chromatographia*, 56, 11/12, 723-728.
- Rolia, E., Chakrabarti, C.L. (1982). Kinetics of decomposition of tetrathionate, trithionate, and thiosulfate in alkaline media. *Environmental Science & Technology*, 16, 852-857.
- Rolia, E., Tan, K.G. (1985). Generation of Thiosalts in mills processings complex sulphide ores. *Canadian Metallurgical Quarterly*, 24, 4, 293 – 302.
- Schwartz, M., Vigneault, B., McGeer, J. (2006). Evaluating the potential for thiosalts to contribute to toxicity in mine effluents. Mining and *Minerals Science Laboratories Report*. Thiosalts consortium. CANMET-MMSL
- Senanayake, G. (2007). Review of rate constants for thiosulphate leaching of gold from ores, concentrates and flat surfaces: Effect of host minerals and pH. *Minerals Engineering*, 20, 1 -15. Steinfeld, J.I., Francisco, J.S., Hase, W.L.(1999). *Chemical Kinetics and Dynamics*. New Jersey, Prentice Hall.
- Suzuki, I. (1999). Oxidation of inorganic sulfur compounds: Chemical and enzymatic reactions. *Canadian Journal of Microbiology*, 45, 2, 97-105.
- Thauer, R.K., Jungermann, K., Decker, K. (1977). Energy Conservation in Chemotrophic Anaerobic Bacteria. *Bacteriological Reviews*, March, 100 – 180.
- Varga, D., Horvath, A.K. (2007). Kinetics and mechanism of tetrathionate ion in alkaline medium. *Inorganic Chemistry*, 46, 7654 – 7661.
- Vongporm, Y. (2008). *Thiosalt behaviour in aqueous media*. Master in Engineering Thesis. Memorial University of Newfoundland.
- Wasserlauf, M., Durizac, J.E. (1982). The chemistry, generation and treatment of thiosalts in milling effluents: A non-critical summary of CANMET investigations 1976-1982. *CANMET Report*. CANMET-MMSL
- Xu, Y., Schoonen, M.A.A. (1995). The stability of thiosulfate in the presence of pyrite in low-temperature aqueous solutions. *Geochimica et Cosmochimica Acta*, 59, 22, 4605-4622.

Zhang, H., Dreisinger, D.B. (2002). The kinetics for the decomposition of tetrathionate in alkaline solutions. *Hydrometallurgy*, 66, 59 – 65.

Zhao, J., Zhichun, W., Chen, J.(1999). Separation of gold from other metals in thiosulphate solution by solvent extraction. *Separation Science and Technology*, 34, 10, 2061 – 2068.

LESSONS LEARNED FROM 30 YEARS OF MINED LAND RECLAMATION

H. T. Williams, MA, CPESC

Walsh Environmental Scientists & Engineers LLC, Boulder, Colorado USA

ABSTRACT: This paper presents ten critical reclamation lessons learned from the authors 30 years of conducting greenhouse trials, field trials, and implementing reclamation plans at mine sites around the world. Each lesson is briefly documented, discussed and its applicability to the reclamation of other projects explored. The projects range from desert to rainforest ecosystems and from sea level to over 12,000 ft above sea level. Some of the lessons were learned on tailings facilities, but all were learned on mine waste facilities and all are applicable to current mining operations. The paper is of value to anyone conducting reclamation and/or revegetation on mining projects.

INTRODUCTION

I have had the opportunity in the last few years to re-visit some of the projects I have designed and built over my career. Although most were completed in the last 15 years, some of these projects go back as far as almost 32 years. The information gained from visiting sites like these is invaluable and most often not documented beyond reports to private companies. A reclamation strategy or plan may seem to work well for three or four years, or may even work well for five or 10 years, but after 15, 20 or more years some interesting things occur. For one, inorganic fertilizers that were applied at construction will be gone. In addition, the original organic amendments as well as any organic erosion and sediment control materials, will be gone. Even organic matter additions from large

particle size materials such as twigs and branches, will be gone after 10 to 15 years in the soil. At this time, when those things we use to kick-start a new community or ecosystem are gone and no longer provide their original functions of stabilizing the soil, a project does one of two things; it either flourishes because those things are no longer needed, or it crashes because those temporary means are gone and their intended replacements or alternative means have not done the job. No amount of short-term testing can provide you with this information and it is not readily available in the literature. The only way to get this information is to go out and observe what has happened on projects where reclamation has occurred over varying lengths of time in the past. This type of training should be a part of every restoration ecologists' acumen.

The following paper provides 10 very important lessons learned from observing reclamation projects from as far back as 30 years. The majority of these lessons will be ones you have learned as well. In fact, I would be happy if this paper only adds one new lesson to the average ecologists' knowledge base, and would be even happier if I were to learn at least one new lesson from its readers. As you read through these lessons, please be inspired to think of your own lessons, share them, and feel free to contact me with them.

LESSON ONE: SMALL SCALE TEST PLOTS DON'T WORK

This lesson didn't take me 30 years to learn. In fact, I learned this lesson the very first time I took 1-square meter test plot data from plots installed at the California Gulch Superfund site near Leadville, Colorado and tried to use it to reclaim a large scale mining project. It made good sense at the time, the statistics clearly showed that plot A was far superior to Plot B. What it didn't tell me was that the edge effects from Plot C had overshadowed both A and B, and that protection afforded by the hill and trees north of the plots were an intervening variable on all of the plots. Shortly afterward, I remember flying over the Midwest and seeing distinctly greener vegetation along fence rows, irrigation ditches streams, hedgerows, and wind shelter fencing and plantings. I realized I was observing an edge effect on farmer's fields that must have been hundreds of feet wide to be visible from 30,000 ft. This practical example has been useful in all of my later test plot designs.

In addition to edge effect, actual reclamation seldom can be done using the exact methods that were used to construct small scale test plots. This may not always be an issue, but

many times it is. On the White Pine Tailings Reclamation Project in the Upper Peninsula region of Michigan, where 6,500 acres of copper tailings too soft to access by typical farm equipment, it was a major issue (Schultz-Stoker, Williams and Duvall, 2001). Test plot research had been conducted on these copper tailings for over 20 years by local universities. A procedure of adding organic matter had been suggested and was later proved out by further testing. However, spreading 100 tons of organic matter over an acre is not as easy as it is to spread over a 1-square meter test plot. Many trials and errors were required to identify equipment that could negotiate the tailings without getting stuck and requiring an even larger piece of equipment to extract. Eventually a mixture of wood chips and paper mill sludge was selected, and methods using special low ground pressure equipment were developed and the site was reclaimed.

Lesson learned: Use test plots of a large enough size to eliminate edge effect and other intervening variables and use the plots to test the same equipment that will be used for the actual reclamation.

LESSON TWO: DIRECT REVEGETATION WORKS

Many existing, historic, abandoned and currently active mining projects were designed and initiated prior to regulations requiring the removal, storage and re-use of topsoil. For these projects, the idea of establishing self-sustaining vegetation, as is currently required for most all mining projects, is daunting. This task is further complicated if the tailings, waste rock or heap leach pad material to be reclaimed is phytotoxic in any way.

The Alta Lakes abandoned mined land project is a primary example (Bellitto and Williams, 1998). This project consisted of over 60 acres of gold mine tailings and waste rock that, in the late 1800s, had been simply released downhill from the mill and had collected in the valley bottoms below. No topsoil had been salvaged or was available for reclamation. The standard methods of revegetating these types of mine wastes was to either excavate and haul out the mine waste, or haul in topsoil and bury the mine waste sufficiently deep to allow plant growth to occur. Either method required hauling topsoil, as the former approach would leave a barren subsoil or bedrock incapable of sustaining plant life. The California Gulch Superfund and White Pine Mine projects, discussed above, were similar in that phytotoxic mine wastes needed to be reclaimed and the standard, permitted method was to bury them with topsoil. In the case of the White Pine Mine tailings, this meant bringing in enough topsoil to cover 6,500 acres of tailings three feet deep, at a cost, even at the conservative assumption of \$3.00 a yard to load, haul and place, of almost 100 million dollars!

Obviously, the realization of these impossibly high reclamation costs has brought about a great deal of research into "Direct Revegetation." Direct revegetation is the modification of mining wastes to allow establishment of vegetation directly into the material rather than into a replaced topsoil. Through projects like the California Gulch Superfund site, the Alta Lakes project and the White Pine Mine, methods are now well developed and proven to do this. Presently, on many mine sites, a practical and cost efficiency limit becomes apparent when attempting to directly revegetate mine wastes with a pH much below 4.5. In these cases, it is often less expensive to remove or bury the

waste than to ameliorate the soil with additives.

In some cases the regulatory process is still catching up, but these and many other precedents are now available. For the White Pine Mine, following greenhouse studies, large scale field trials and initial implementation, the state allowed direct revegetation of the tailings saving the mining company almost 100 million dollars.

Lesson learned: Direct revegetation works and can save millions of dollars.

SPECIES TOLERANCE TESTING WORKS

The California Gulch Superfund Project provided an exceptional opportunity to evaluate species for their tolerance to low pH and high metal levels in the soil. This project, which is located at over 10,000 ft above mean sea level (amsl) has a very short growing season on the order of 45 days. Testing species tolerance in outdoor test plots would have taken years and in greenhouses would have taken many months. In order to quickly move the project forward, and not waste valuable winter time, a quicker method of testing plant species tolerance to difficult conditions was needed. Fortunately, a method exists where agar, as used in microbiological laboratories, is adjusted to varying pH and metals levels simulating what is to be expected in the field. This agar is placed in test tubes and surface sterilized seeds are placed on the surface of the agar. With the tubes placed in a dark, cool place, germination of the seeds takes place in less than a week. From the germination rates and early root growth, comparative information can be obtained on many species', and varieties of species', tolerance to the media. With this method, literally thousands of seeds

can be tested in a few months in a space no larger than a coat closet.

Although there may be many other methods now available, utilizing this In-Vitro Tolerance Testing method, I have identified several species previously undocumented to tolerate low pH and high metals concentrations (Bellitto and Williams, 1998). These species have been useful on many subsequent direct revegetation projects.

Lesson learned: Species tolerance testing works and can identify unanticipated and/or unidentified tolerant plants.

LESSON FOUR: CONCURRENT RECLAMATION IS A MUST

Almost all current mining regulations require concurrent reclamation wherever possible. And for good reason; over the years salvaged and stockpiled topsoil has not shown as good of results as a growth medium as was first thought or anticipated. Salvaged topsoil quickly loses much of its microbiological component as soon as it is disturbed and losses more over time if it is stockpiled too deeply. The value of soil microorganisms is well documented, and in fact, it is now known that there are typically just as many soil microorganism species as surface species. In terms of a soils viability and ability to sustain vegetation, these species may be more important than the larger surface species.

Generally speaking Clayey texture topsoils can't be stockpiled much more than three feet deep without affecting oxygenation and losing microbiological activity. Coarser textures can be stored somewhat deeper, but hardly ever over eight feet deep. However, one rarely sees topsoil stockpiles on a mine site less than 10 feet deep. I first encountered

this issue on the White River Oil Shale Project near Vernal, Utah. Topsoil had been stored on this site at up to 20 feet deep for approximately 10 to 15 years. When the contractor dug into it he found soil no different than surrounding native subsoils at a depth of four or more feet. Of course the chemical makeup was altered from having been leached at the surface for a number of years, but the biological component was completely gone and the soil was essentially devoid of beneficial fungi, bacteria and actinomycetes.

The lesson learned from this experience was to plan for concurrent reclamation and move as much topsoil as possible directly into an area to be immediately reclaimed. Any remaining topsoil, should be stockpiled in very low, spread out stockpiles, and immediately seeded with a cover crop that won't compete with the native species included in the soil seedbank. This stockpiled topsoil may lose some of its viability, but over the years, I have found it loses much less than if stockpiled deeper.

At the Hayden Hill Gold Mining Project in northern California, a reclamation plan was developed which included concurrent reclamation of pit benches as the mine progressed downward (White and Williams, 1993). It became immediately apparent that accessing the pit benches after the pit had progressed down to the next bench was either impossible or extremely dangerous because the benches could and were collapsing. The mine's reclamation manager found that he could immediately spread topsoil from a new area of excavation from the pit wall out onto the pit floor about 15 feet wide and the required 12 inches in depth. Then as the next bench was cut, the equipment operators could see when dark topsoil started to cave off from the bench now above them. This not only

solved the problem of bench access, but helped speed up pit excavation.

Lesson learned: Concurrent reclamation must happen and live handling topsoil is far better than stockpiling it. Although not necessarily standard operating procedure, developing the methods to do this often leads to more efficient and cost savings ways of accomplishing other goals.

LESSON FIVE: GREEN HOUSE AND FIELD TRIALS CAN PAY FOR THEMSELVES

During the green house trials for the White Pine Mine Direct Revegetation project, a boron deficiency was identified in the tailings following the addition of organic matter (OM). It was later determined that the tailings had a sufficient quantity of this micronutrient for normal plant growth prior to the addition of organic matter. However, after OM was added at quantities capable of binding copper adequately to eliminate its phytotoxicity, the deficiency showed up. Apparently, the OM was also binding boron, and binding it sufficiently to cause deficiency symptoms in the plants. The final revegetation specifications for the project included an addition of boron.

The White Pine Mine Tailings Revegetation Project included 500 acres of tailings surface to be reclaimed each year until the entire 6,500 acres were completed. If even the initial reclamation of the first 500 acres had failed, due to not knowing about the boron deficiency, the money spent for this effort would have been wasted. A conservative estimate of \$1,000 per acre for this cost totals \$500,000. Obviously, the second time the area was prepared and seeded would require less effort, but even at half of this effort, a minimum of \$250,000 would be necessary.

The greenhouse trials which identified the boron deficiency were completed at a cost of approximately \$50,000. In this instance, the greenhouse studies saved the client around \$200,000. Obviously, not every green house or field trial produces results so easily related to direct savings. However, in every green house and field trial I have conducted, something was discovered which saved money, time, or effort in the final product. One such study pointed out the need to place mycorrhizal fungi inoculants in a concentrated layer so that the roots of seedlings would have to grow through it, rather than just randomly come into contact with a more disseminated incorporation of the material through the entire six inch depth of the prepared seedbed (Schultz-Stoker, Williams and Duvall, 2001). Numerous other such studies have identified species tolerant of the site conditions and have surely saved the cost of planting seeds which would never grow or thrive. With the minimal cost of greenhouse or field trials, and the potential for large savings, these studies should be a part of every reclamation project.

Obviously, to be worth their costs, preliminary studies must be well thought out and executed. Many such studies just repeat previously conducted studies, or test what is already known, and do not add to the pool of site specific information necessary to complete the project. Prime examples of this are the numerous field studies that test inorganic fertilizer additions; plots with fertilizer, or higher amounts of fertilizer, are obviously going to grow better, at least until the fertilizer runs out. Similarly, species or seed mix tests in green houses rarely simulate the actual climatic conditions a plant will encounter in the field and plants that thrived in the greenhouse do not always do well once planted in the actual soils on the actual site. Better, is to use a few select indicator species

to test soil ameliorant levels in the greenhouse, and then test species and seed mixes in field trials. A very good starting point, to ensure that one is not “re-inventing the wheel,” is to interview local farmers, ranchers and agricultural agents in the area, before designing trials of any sort. This information, combined with a literature search that covers your geographical area and/or specific soil and climatic conditions, will help eliminate duplications of efforts that aren’t really necessary. Trials just for the sake of trials adds nothing to the pool of knowledge and besides wasting time and money, gives the industry an image of being un-organized and disconnected.

Lesson learned: Greenhouse and field trials can pay for themselves and even save hundreds of thousands of dollars over their costs if well thought out and executed.

LESSON SIX: DON’T TRUST SURFACE VEGETATION

About 18 years ago I visited the Lelydorp III Bauxite Mine site in the rainforests of Suriname. My mission at the time was to develop a reclamation plan for the proposed new tailings ponds and related disturbances for the mine. When we arrived, our mine guide took us for an orientation of the site. At one point he stopped at an over look and pointed out the excellent revegetation that they had achieved on a waste rock dump. I had to admit, it looked lush and well covered. And, to learn something from this experience, I asked if I could walk down the slope and see just what had actually grown. I started walking down the slope, carefully watching for the many snakes and plate sized spiders common to the Amazonian rainforests of South America. After about 50 yards of walking down the stable slope, I took a step and suddenly felt like I was walking on a

trampoline. Just as the realization struck that I was no longer walking on soil and should be stepping backward, fast, the vegetation gave way and I fell straight down about eight feet, into a totally grown over erosion gully. Luckily, soft soil, and a lot of dead plant material, bugs and spiders broke my fall. I looked up and saw the hole in the vegetation and root mass quickly closing overhead, and the normal darkness returning to the gully. A few, very, very long minutes later my companions, who had seen me suddenly drop out of site, helped extract me, calm and with great poise I’m sure, from the gully. It was many days later when I stopped having the feeling that “things” were still crawling over me.

There is nothing quite like the thought of deadly snakes, and big spiders to drive home the point that dense vegetation can cover a world of problems below. Vegetation, especially vines and large leafed species, and erosion control netting and thick hydromulches for that matter, can cover up the ground surface but may not be stabilizing the soil sufficiently to control erosion. Or, in the case of the Lelydorp III Mine, vines may be growing from great distances away and covering areas with plant material that are far from the place where the plant is rooted, leaving the majority of the soil unprotected by root mass. It is very important to balance seed mixtures, and be sure that root mass will be sufficient in all areas to hold the soil in place. Of course as natural succession takes place, grass species and small forbs will be displaced by shrubs and eventually trees, but initially a thorough covering of good erosion protection species, such as sod forming grasses, clump grasses and small forbs are necessary.

Lesson learned: Look beyond the surface vegetation and be sure the soil is stabilized...and watch where you step.

LESSON SEVEN: MOST ORGANIC AND SYNTHETIC EROSION CONTROL PRODUCTS WON'T LAST MORE THAN SEVEN YEARS

The general concept behind most erosion control and revegetation products is that if you can stabilize the soils just long enough for vegetation to become established, the vegetation will take over and they will no longer be needed. Given this premise, most products do not persist very long. However, in arid and semi arid areas, and in steep or difficult soil areas even in more humid areas, vegetation may require many years to become established, or may not ever be established sufficient to control erosion. In these areas, other means besides vegetation are necessary to control erosion.

During my master's thesis work in 1978 I installed test plots on haul road cut banks, waste rock piles and simulated pit benches at Homestake Mining Company's Pitch Uranium Project in the central Colorado Rocky Mountains (Williams, 1982). I have visited these test plots over the almost 32 years they have been in place many times, including 2008, and have never failed to learn something more each time.

The plots have provided a very good opportunity to observe the materials we used for mulch and erosion control, as well as species persistence, over a long period of time. On all steep slope plots, we used straw mulch held in place by conwedtm netting. On less steep plots, such as pit benches, we used wood chips as a surface mulch. For erosion control on steep slopes we used a variety of techniques based on available materials on-site. These consisted of wood chips incorporated into the top four inches of soil, logs and rock placed across the slopes to act as slope length breaks, 4- to 6-inch rock

placed on the surface and rock incorporated into the top four inches of soil.

What became very obvious was that the straw and wood materials completely decomposed and stopped providing any protection after less than seven years, but the rock is still present and still providing erosion control 31 years and 10 months after installation. Many of these plots were either very steep (angle of repose or just slightly less), south facing, or both. Natural slopes such as these in the region are typically tallus with no more than 20 percent vegetative cover. Erosion control on undisturbed slopes is provided by rock. Our hopes were that if we could stabilize a surface soil on these steep slopes long enough for vegetation to become established that it would control erosion permanently. This did not prove to be the case when we used wood chips or logs. In those plots, vegetation was established after the first three to four years, but then as the wood chips and logs decomposed, the protection was lost and the slopes unraveled and became too unstable to continue to support the vegetation. From about four to 20 years after planting they declined in vegetation and now, after over 30 years, the soil has eroded away and they are simply tallus slopes of rock with almost no vegetation present.

These plots have taught me to consider erosion protection in reclamation from two viewpoints: what is required to sufficiently stabilize the soil for the period of time necessary to get vegetation established; and, what is required to permanently stabilize the soils for the long-term. On such projects as heap leach pad caps and emergency spillways, permanent or at least very long-term stabilization, is a must. In most cases this has resulted in the addition of more benches or retaining walls, or the addition of rock to increase the coarse fraction of the

soil, then I would have included had I not had the results of these long-term test plots. However, I have not had the failures that I saw in these plots since incorporating these learned lessons.

Lesson learned: In many cases you need long-term erosion control and most erosion control methods and products last less than seven years. Permanent methods and materials are available and should be used where necessary.

LESSON EIGHT: YOU MUST KICK-START THE SOIL SYSTEM WITH A VARIETY OF ORGANIC MATTER FORMS AND SIZES TO GET TO SELF SUSTAINABILITY

In a natural, undisturbed, soil system there are a variety of organic materials in various stages of decomposition, from newly fallen leaves and last years' grass blades to fallen branches and even complete fallen trees. As you progress downward through the soil profile, these various organic materials become less and less recognizable as what they originated from. Numerous microorganisms, and larger organisms such as worms, snails, moles, ground squirrels and others, are assisting in the process of reducing these materials to a point where they can hold water and nutrients in a form available to plants. A soil in balance is one that has a steady supply of new organic materials replenishing those that are lost through decomposition such that a stable organic matter percentage is maintained in the soil. Though a "good" soil maintains between about 2 to 5 percent organic matter, this rate can be above or below this number and still be considered stable and in balance for the area it is in.

Given that a natural soil system has this variety of organic material inputs, how is it that we typically assume we can get a self-sustaining soil, sufficient to produce a self-sustaining vegetative community, by just replacing the A soil horizon, adding a little fertilizer and mulch, and planting with a grass mix? Without the added "coarse fraction" of the O soil horizon, the brush layer, and the yearly leaf fall from a mature vegetation stand, how do we expect to maintain a steady level of organic matter in the soil? In truth, we do not. In the test plots installed at the Pitch Project the organic amendments we used, cow manure and wood chips, were gone within a few short years, with no continued input from vegetation. In contrast, the test plots we installed at the White Pine mine included a variety of organic materials, in varying sizes and shapes, and have become self-sustaining over at least 10 years so far.

The reality is that if you want to establish a truly self-sustaining vegetative community, you must provide a variety of organic materials in varying sizes and shapes sufficient to last until you have adequate vegetation production to provide continued inputs to the system. This concept is a work in progress, and provides support to salvaging every organic material source from a site, not just the topsoil but the O horizon, the brush, trees, downed trees, etc., so that they can be used in the reclamation process later. And it is an indication of why concurrent reclamation works better, as these resources tend to disappear for a variety of reasons if not used immediately.

Of course, doing reclamation in the manner described above costs a little more and so may not be practical in every instance. However, in almost every instance, if you include the cost of failure, and re-doing the work, possibly several times if you never do

it right, the cost may be much less if you do it right the first time.

Lesson learned: If you don't kick-start the soil system with a variety of organic matter forms and sizes emulating nature, you will never get to self sustainability.

LESSON NINE: WASTE PRODUCTS MAKE EXCELLENT AMENDMENTS

Finding a source of organic materials for reclamation is often one of the most difficult parts of the effort. However, if a waste product can be found, the cost can be reduced considerably. Many produced products have waste streams which can be useful in reclamation. For the White Pine Mine tailings revegetation work, we identified paper mill sludge and wood chips as some of the most readily available components in that area. Paper mill sludge is similar in appearance and nature to hydromulch, but is far less clean and consistent, which is actually better for reclamation purposes. Wood chips were also a by-product of the paper industry. After harvesting, trees are run through a debarking machine which produces a product of about 50 percent bark and 50 percent wood chips from just under the bark. The pieces are from about one to six inches in length and vary greatly in width as well. The wood chips were typically being stockpiled or hauled to a landfill. The stockpiles were a fire hazard and could spontaneously ignite when dug into. Therefore, the producers were glad to allow us to take them, free of charge, at our cost to load and haul.

The Paper mill sludge was being hauled to landfills. Our concept was that these trucks could easily be diverted to the tailings site, saving the paper mill the landfill tipping fee. However, the value of the sludge mysteriously escalated when the paper mill

learned of its beneficial use. Negotiations resulted in the mine getting the material for free with a 50 percent sharing of the haul costs. A lesson learned here was that you never want to acknowledge the value of someone else's trash.

Obviously, many areas where reclamation needs to occur are far from paper mills and forests. Although finding suitable materials often takes work, we have never failed to find some material suitable for our needs. It is also important to consider that in areas where there isn't much waste organic matter, such as deserts, you need less organic matter to establish the native vegetation. Other waste organic matter sources we have found and used include biosolids from waste water treatment plants, used hops and grains from the beer brewing industry, saw dust and waste from sawmills, slash from the timber industry, compost (or almost composted) material from landfills, land clearing waste from agricultural properties, wasted hay from cattle and horse operations (watch out for weed seeds), and yard waste from residential areas. Each of these materials has pluses and minuses, but often can form a part of a reclamation projects' needs at a low cost.

In most cases the loading and trucking of the material are the highest cost components. Therefore, finding material at its source, so that you can intercept it after it is loaded on trucks, and diverting it to your site, may be the most cost effective approach. If it had been headed towards a landfill, saving the tipping fees may be sufficient payment for the material. However, it is very important to have a value of the material in mind before you start any negotiations or "tip your hand" to the owner of the material. After evaluating the value of the material, it may become clear that paying more than you anticipated is still a good deal, but you don't want to end up where we did, having a provider ask an

outrageous price for something he was paying to get rid of.

Lesson learned: Waste products make excellent amendments but be careful who you tell this to.

LESSON TEN: PLANT SALVAGE AND ON-SITE PROPAGATION REALLY DO WORK

On almost every reclamation project I have ever done, a lesson learned was that we could have done better had we used site adapted plant materials. We always specify and use seeds and plant materials that are identified as adapted to the site's conditions, but we seldom use seeds collected right from the area or shrubs and trees transplanted from nearby. And, we always look back and think how much better our survival rates may have been if we had used plant materials adapted to our exact soil conditions, our exact climate, and perhaps most importantly, adapted to the specific mycorrhizal fungi strains in our area. There is much research indicating that all of the soil microorganisms, not just the fungi, are site adapted and specific to the plant species, if not the varieties, on a specific site.

On the Alta Lakes Project, we used seedlings procured from an in-state nursery and transplanted trees from the surrounding forest. The survival rate of the seedlings was less than 50 percent, while the survival of the transplanted trees was over 90 percent. Although it could be expected that seedlings would have a lower survival rate than transplanted trees of two feet tall or more, this variance was more than we had expected. No study has been done to determine the exact cause for the survival rate difference. However, I strongly suspect that site specific adaptation to all of the environmental factors,

including the soil microbiology, was a large part of it.

At the Kori Kollo Mine in Bolivia, a program has been in effect for many years to collect native shrubs and succulents for reclamation purposes. At this site, which averages between only three and six inches of precipitation per year, plants are directly transplanted from the surrounding desert onto waste rock dump slopes and other reclamation areas. Seeds are also collected and an on-site nursery is used to propagate additional plant materials for the mine. This project has had very good success, primarily with *Atriplex* species, and is a very good source of information for on-site plant propagation in arid areas.

Lesson learned: Plant salvage and on-site propagation really do work.

CONCLUSION

Reclamationists and restoration ecologists often work in isolation for private companies conducting research and producing reclamation plans that are used for permitting but are not documented in published papers or readily publicly available or catalogued in any academic sense. Because of this, there is a wealth of information out there to be learned from and shared that is not. With this paper I share the lessons I have learned and encourage other practitioners to share their collective experiences. By sharing our learned knowledge, we all benefit by being able to provide a more comprehensive, reproducible and consistent end product. The first stone is cast!

REFERENCES

Bellitto, Michael, and Williams, H. Thomas, 1998, *Reclamation at the Alta Lakes Project*, paper presented at the Land Reclamation 98 Conference in Nottingham, England, September. 1998.

Schultz-Stoker, Jill, Williams, H. Tom, and Elizabeth A. Duvall, 2001, *Erosion and Sediment Control at the White Pine Mine*. Paper presented at the Meeting Challenges: Successful Practices In Fugitive Dust Management conference. Chicago, Illinois. April 2001.

White, Jeffrey S. and Williams, H. Thomas, 1993, *Reclamation at the Hayden Hill Project in Northern California*, SME Mining Environmental Handbook, Littleton, Colorado. 1993.

Williams, H. Thomas, 1982, *High Altitude Soils Biological Response to Enhancement*, paper presented to the Western State College Reclamation Group. 1982.

AUTHORS BIOGRAPHY:

Mr. Williams has over 30 years' experience in conducting baseline studies, analyzing environmental impacts and preparing reclamation plans for large scale development projects such as mine sites, power plants, pipelines and transmission lines. Mr. Williams is a restoration ecologist with specific expertise in the reclamation and revegetation of disturbed land, wetlands remediation, statistical analysis of vegetation, and erosion and sediment control. Mr.

Williams has prepared over 55 reclamation plans for major mining projects. He has prepared reclamation plans in a number of US states, and Ireland, Russia, Turkey, Brazil, Chili, Bolivia, Suriname, Madagascar, Zambia, and Indonesia, internationally. A significant number of these plans were prepared under the US National Environmental Policy Act (NEPA) process and included addressing all of the major components and areas of the project, including wetlands/riparian areas, aquatic systems, power lines, pipelines and access roads, regardless of the main project type. In 1992 he managed the EIS and prepared the reclamation plan for a major gold mining project, which won the California Mining Association's Award for Excellence and contributed to the client's receipt of the prestigious Dupont/Conoco Award for Environmental Leadership. In 1997 he prepared a reclamation plan to restore an abandoned mine property into exclusive mountain property. This project won an Excellence in Reclamation award from the Colorado Department of Mining and Geology. Mr. Williams was the Project Manager for the preparation of the reclamation plan for the Crown Jewel Project in Washington, which has been termed by the involved agencies "the most comprehensive reclamation plan for a gold mine ever developed." In addition, he has managed the revision of reclamation projects, and visualized and developed innovative reclamation concepts, which have saved the owners millions of dollars over the previous designs.

Mr. Williams continues to practice restoration ecology from Walsh's Lakewood office in Colorado, USA.

Oil Sands Tailings I

REDUCTION OF OIL SANDS FINE TAILINGS

B. Ozum

Apex Engineering Inc., Edmonton, Alberta Canada

J.D. Scott

Dept. of Civil & Environmental Engineering, University of Alberta, Edmonton, Alberta, Canada

ABSTRACT: Existing disposal practices of oil sands mining companies over the past five decades resulted in the accumulation of approximately 750 million cubic meters of mature fine tailings (MFT). The Energy Resources Conservation Board of Alberta now requires that oil sands mining companies will reduce production of fluid fine tailings by 50% by 2013. Two procedures for doing this are by changing the bitumen extraction process to produce less fine material and by depositing much of the fines produced into semi-solid nonsegregating sand deposits. For this purpose it is proposed to use CaO (lime) and O_3 (ozone) or CaO and biodiesel (BD) as extraction process aids coupled with nonsegregating tailings (NST) production using CaO or CaO and CO_2 . These processes simultaneously improve the chemistry of recycled release water and geotechnical properties of oil sands tailings without harming bitumen extraction efficiency and bitumen fuel quality.

Use of CaO at about 60 to 150 mg/kg-ore dosages plays the role of caustic $NaOH$ of the Clark Hot Water Extraction (CHWE) process; it increases the pH of the ore-water slurry and promotes the solubility of asphaltic acids present in bitumen which act as surfactants reducing the surface and interfacial tensions. Advantages of CaO over $NaOH$ are that Ca^{2+} introduced by CaO causes clay flocculation, which produces tailings with reduced clay dispersion and eliminates Na^+ accumulation in the recycled release water. Use of O_3 at 50 to 100 mg/kg-ore or BD under 200 mg/kg-ore dosages, supplementary to CaO additive, improves bitumen extraction efficiency especially for low grade-high fines ores. O_3 performs as a super oxidant in the presence of $Ca(OH)_2$ and produces surfactant species from bitumen asphaltenes and BD performs as a surfactant used from an external source.

Also, production of NST is proposed by using CaO or CaO and CO_2 , which improves the recycled release water chemistry and the geotechnical properties of NST. Based on the laboratory scale studies it is speculated that environmental impacts of the existing bitumen extraction and tailings disposal process practices would be reduced or eliminated by the proposed extraction and NST production processes. Pilot scale testing of the proposed processes is needed for the commercial implementation of these processes.

INTRODUCTION

Bitumen Extraction and CHWE Process

Surface minable oil sands are utilized by ore-water slurry based extraction processes which involve three basic phenomena: (i) liberation of bitumen in the oil sands structure; (ii) mobilization of bitumen; and (iii) aeration of bitumen. Experience gained over the decades in bitumen extraction has indicated that reduction of surface and interfacial tensions in oil sands ore-water slurry systems improves bitumen liberation, reduces the attachment of clay particles to bitumen droplets and promotes the attachment of air bubbles to bitumen droplets; which all promotes the bitumen extraction efficiency (Baptista and Bowman, 1969; Bowman, 1967; Leja and Bowman, 1968; Kasperski, 2001; Masliyah et al., 2004). Bitumen mobility increases with reduced bitumen viscosity; it has been experimentally demonstrated that sufficient bitumen mobility is achieved when the temperature is maintained above 35°C.

Dr. K.A. Clark and his co-workers at the Alberta Research Council succeeded in the extraction of bitumen from oil sands ore-water slurry systems with caustic $NaOH$ addition; which eventually resulted in the development of the Clark Hot Water Extraction (CHWE) process (Clark, 1939; Clark and Pasternack, 1932). Some versions of the CHWE processes are being commercially used at all oil sands extraction plants in northern Alberta, Canada.

The mechanism of the CHWE process is also based on the above discussed principles; basically on the liberation, mobilization and aeration of bitumen. Addition of $NaOH$ as an extraction process aid maintains the pH of the ore-water slurry at about 9.0. Elevation in the pH of the slurry increases the solubility of asphaltic acids present in bitumen (partly aromatic, containing oxygen functional groups

such as phenolic, carboxylic and sulphonic types) which perform as surfactant reducing the surface and interfacial tensions; which promotes swelling and dispersion of clay and liberates bitumen trapped in the ore matrix (Speight and Moschopedis, 1977).

Problems Associated with the CHWE Process

Commercial experience gained over four decades demonstrated that the CHWE process provide high extraction efficiency; however, issues associated with the CHWE processes are raising concerns about: (i) increase and eventually accumulation of Na^+ ions in the recycled release water which could affect the bitumen extraction process and the Composite Tailings (CT) process used for tailings disposal; (ii) produces tailings with poor geotechnical properties which causes formation of MFT; and, (iii) possesses low thermal efficiency. To overcome problems associated with the CHWE process; non-additive, low temperature extraction (LTE) processes were developed (Burns et al, 1998). LTE processes were used at Syncrude Canada Ltd.'s Aurora Mine and Albian Sands Energy Ltd.'s Muskeg River Mine plants; however, modifications were made to boost the extraction efficiency. At both plants temperature and pH of the extraction process were increased; therefore, both plants are operating with basically some version of the CHWE process.

Increase in the MFT inventory over the years motivated the oil sands industry to develop the Composite or Consolidated Tailings (CT) process which was implemented in the 1990s (Caughill et al, 1993; Liu et al, 1994). In this practice the tailings is modified into a nonsegregating product by which the fines and the sands settle together in a nonsegregating manner. Production of CT requires maintaining the tailings compositions above critical solids contents, which could be

achieved by passing the whole tailings through cyclones and blending the Cyclone Underflow with MFT with the addition of $CaSO_4$ (gypsum) at about 800 to 1,300 g/m^3 -CT dosages to prevent segregation as depicted in Figure 1.

Production of CT has many short fallings; it produces additional MFT from the Cyclone Overflow tailings, increases Ca^{2+} and Mg^{2+} concentrations in the recycled release water and potentially causes H_2S emission by anaerobic reduction of SO_4^{2-} with the residual bitumen in the tailings.

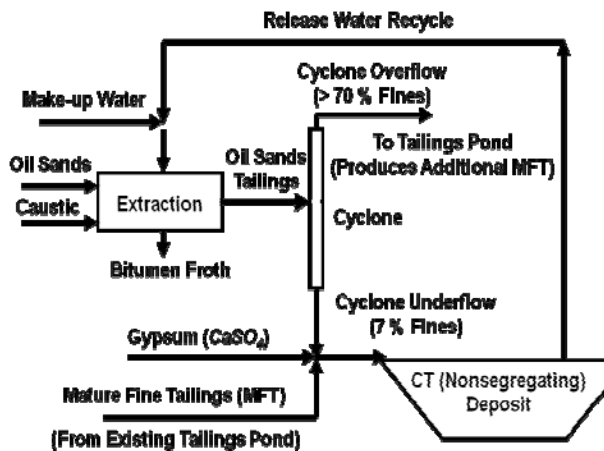


Figure 1. CT production process

In existing practice the use of caustic $NaOH$ or sodium salts of weak acids in extraction processes and $CaSO_4$ in the CT production process continuously increase the salinity of the release water (McKinnon, 2004; Allen, 2008a; 2008b). The ratio of monovalent (mainly Na^+) to divalent (Ca^{2+} and Mg^{2+}) cations and bicarbonate ($CaHCO_3$) concentrations plays important roles both in extraction and CT production processes (Hall and Tollefson, 1982; Jeeravipoolvarn et al, 2008). The bicarbonate ions associated with Ca^{2+} cause clay surfaces to be dominated by Na^+ cations. Also, when the monovalent to divalent cation concentrations ratio is large, then the clay surfaces are dominated by Na^+

and clays become dispersed as in the bitumen extraction process when $NaOH$ is added. When the monovalent to divalent cation concentrations ratio is low the clay surfaces would have an abundance of exchangeable Ca^{2+} cations and clay particles aggregate and flocculate; which is the reason that $CaSO_4$ is used for CT production.

Exchangeable Sodium Ratio (ESR) as expressed in Equation 1 is used to identify possible clay structure status in salt impacted soils (Harron et al, 1983):

$$ESR = \frac{0.015[Na^+]}{\sqrt{\frac{[Ca^{2+}] + [Mg^{2+}]}{2}}} \quad (1)$$

This relation provides a prediction of adsorbed phases based on the concentration of ions in solution; for ESR values greater than 0.1 Na^+ ions occupy adsorption sites on the clay resulting in swelling of the clay with water and clay dispersion (Dawson et al, 1999). The steady increase in ESR of the release water indicates that existing oil sands plants will produce more MFT and reduction of MFT inventory will require higher dosages of $CaSO_4$ addition for the CT production. This trend could be reversed by modification of bitumen extraction and CT production processes.

NOVEL PROCESSES

Solutions for Existing Water Chemistry and MFT Production Problems:

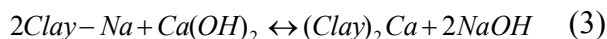
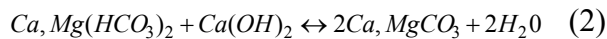
Existing water chemistry and MFT production problems of the oil sands plants evolve from the CHWE process which uses $NaOH$ or sodium salts of weak acids such as sodium citrate as extraction process aid. These additives provide high bitumen extraction efficiency; however they cause dispersion of

the clay booklets which results in the production of tailings with poor geotechnical properties. These problems could be solved by altering the oil sands extraction process, i.e. using different additives to promote bitumen extraction efficiency with limited clay dispersion. Regardless of the additives used in the extraction process, the tailings have to be disposed as nonsegregating tailings (NST).

A *CaO* based bitumen extraction process is being investigated as an alternative to the CHWE process which uses *NaOH* as an additive. A NST production process using *CaO* is also being investigated as an alternative to the present CT process which uses *CaSO₄* as an additive.

Novel Bitumen Extraction Processes by Using *CaO*, *CaO* and Ozone or *CaO* and Surfactants

The bitumen extraction research is focused on the use of *CaO* (lime), which becomes *Ca(OH)₂* in an aqueous environment, as an alternative to *NaOH* for the conditioning of ore-water slurry. When *Ca(OH)₂* is used as an extraction process aid it increases the *pH* of the ore-water slurry, similar to the *NaOH* additive, increases the solubility of asphaltic acids which acts as a surfactant reducing the bitumen-water interfacial tension promoting bitumen extraction efficiency. The advantages of using *Ca(OH)₂* are that it reduces *Ca²⁺* and *Mg²⁺* concentrations which detrimentally effect bitumen extraction efficiency and flocculates the clay particles by the following reactions:



The optimal dosage of *CaO* addition would be in the range of 50 to 200 mg/kg-ore which depends on the fines (fraction of solids with

<45 µm size) content of the ore. For normal grade ores which are about 12% bitumen and <10% fines contents the use of *Ca(OH)₂* alone as process additive provides sufficiently high bitumen extraction efficiency. For low grade ores, however; bitumen extraction efficiency could be boosted by producing additional surfactants by oxidizing bitumen asphaltenes with *O₃* (ozone) or the addition of surfactants such as biodiesel (BD), i.e., fatty acids methyl esters.

The performance of *CaO* on bitumen extraction was tested using a low grade oil sands ore and a typical process water slurry system. Composition (all by mass) of the ore was of 7.7% bitumen, 82.4% solids and 9.7% water as measured by Dean-Stark extraction, 27.7% of the solids were fines (<45 µm). Extraction tests were performed digesting the 300 g ore in 360 g of water slurry in a Denver D-12 Flotation cell for 5 minutes by setting the rotor speed at 800 rpm. Extraction test results and water chemistry data are presented in Table 1 and Table 2. Process water used in these tests is of high alkalinity and high *pH*, which is similar to the process water used in CHWE process.

The data presented in Table 1 and Table 2 show that the use of *CaO* as an extraction process additive at 150 mg/kg-ore dosage works as good as the process water used in the CHWE process when the extraction temperature is 40 °C or higher. About half of the *CaO* is consumed for bicarbonate to carbonate conversion (Equation 2) and a significant portion of the other half is consumed by the ion exchange reaction with clay (Equation 3), improving the geotechnical properties of the tailings. Therefore, the use of *CaO* as an extraction process additive simultaneously improves bitumen extraction efficiency, release water chemistry and the geotechnical characteristics of the tailings.

Table 1. Bitumen extraction with *CaO* additive.

Temperature °C	CaO (mg/kg-Ore)	Froth Yield (g)	Bitumen Recovery (%)
30	0	107.51	53.8
30	0	107.50	55.8
30	150	95.98	50.9
30	150	96.30	47.4
35	0	112.11	56.9
35	0	115.93	58.3
35	150	111.52	58.7
35	150	115.20	59.1
40	0	116.91	60.5
40	0	113.93	61.4
40	150	111.18	62.9
40	150	115.65	62.2
45	0	116.15	60.2
45	0	122.01	61.8
45	150	122.39	65.3
45	150	127.47	67.8
50	0	116.88	62.4
50	0	117.95	63.7
50	150	119.33	67.5
50	150	121.13	67.7
55	0	118.20	69.2
55	0	122.76	67.9
55	150	122.13	69.1
55	150	123.56	70.6

The long term effect of the use of *CaO* as an extraction process additive was also evaluated by recycling the release water five times. In these tests a normal grade ore was used composition (all by mass) of 9.8% bitumen, 85.1% solids and 3.4% water as measured by Dean-Stark extraction. About 14.2% of the solids were fines (<45 µm). In these tests the ore-water slurry composition was kept constant at a water to ore mass ratio of 1.2.

The experimental results presented in Table 3 and Table 4 show that the use of *CaO* at 150 mg/kg-ore dosage in each extraction cycle has no harmful effect on bitumen extraction efficiency and release water chemistry. Geotechnical properties of the tailings produced in these tests haven't been studied; however, it was visually observed that tailings obtained by using *CaO* as the extraction process aid settles faster and decant water contains much less clay size particles. These data indicate that use of *CaO* as an extraction process aid is a viable alternative to the CHWE process which uses *NaOH* for the same purpose. The use of *CaO* as the extraction process additive may require longer retention time for ore conditioning, probably at a cooler temperature.

Table 2. Release water chemistry for extraction tests with *CaO* additive.

Temper. °C	CaO (mg/kg-Ore)	Alkalinity (mg CaCO ₃ /L)			Cations (mg/L)				Anions (mg/L)		
		pH	Total	CO ₃	HCO ₃	Na	K	Mg	Ca	Cl	SO _x
Process Water											
30	0	8.4	412	12	400	361	18	8	7	168	88
30	0	8.4	332	6	326	364	23	13	16	166	159
30	0	8.3	333	2	331	368	23	13	16	167	161
30	150	8.5	313	10	303	361	22	11	14	168	161
30	150	8.5	310	8	302	354	22	11	14	168	161
35	0	8.4	322	4	318	354	23	13	16	169	165
35	0	8.4	322	6	316	367	23	13	15	168	162
35	150	8.5	304	8	296	360	22	10	12	171	164
35	150	8.5	300	8	292	353	22	11	13	169	168
40	0	8.4	308	4	304	272	21	12	13	161	160
40	0	8.4	314	4	310	355	23	12	15	169	166
40	150	8.4	299	8	291	348	22	11	14	170	164
40	150	8.4	296	6	290	350	22	11	13	170	165
45	0	8.4	300	6	294	349	21	11	14	163	159
45	0	8.4	306	4	302	372	21	11	12	167	164
45	150	8.5	283	8	275	359	21	9	11	168	159
45	150	8.5	287	8	279	357	22	9	12	168	161
50	0	8.5	297	8	289	367	21	9	11	170	161
50	0	8.5	300	6	294	355	21	9	10	171	161
50	150	8.5	286	10	276	348	20	10	10	161	166
50	150	8.5	290	10	280	369	20	10	12	165	164
55	0	8.5	287	8	279	358	21	10	12	169	170
55	0	8.5	290	8	282	360	20	9	10	170	169
55	150	8.5	280	10	270	371	20	9	10	167	171
55	150	8.5	272	8	264	363	20	9	11	171	170

The slurry temperature was kept constant at 50°C and *CaO* was used at 150 mg/kg-ore dosage in each cycle. About 1.2 L of release water was taken from each large scale tests; 300 mL was used for release water chemistry analysis, 300 mL was used for one blank (without any additive) extraction and 600 mL was used for two extraction tests, also at 50°C temperature and using *CaO* at a 60 mg/kg-ore dosage. Extraction tests and water chemistry data are presented in Table 3 and 4.

The research also focused on the production of surfactant species to promote bitumen extraction efficiency by in-situ oxidation, sulfonation and sulfoxidation of bitumen asphaltenes by treating the ore-water slurry with *O₃* (ozone) and *SO₂* (sulfur dioxide). Bitumen extraction tests were also performed by conditioning the ore-water slurry before treating the slurry with *O₃*.

Table 3. Effect of release water recycling on bitumen extraction with *CaO* additive.

CaO (mg/kg-ore)	Froth Yield (g)	Bitumen Recovery (%)
First Cycle		
0	126.42	92.3
60	128.71	94.8
60	131.47	96.4
Second Cycle-I		
0	128.58	94.6
60	138.64	95.7
60	136.47	96.2
Second Cycle-II		
0	142.77	92.7
60	138.51	96.7
60	149.65	95.2
Third Cycle		
0	138.96	96.5
60	142.99	93.1
60	151.1	99.7
Forth Cycle		
0	143.21	92.9
60	135.05	96.2
60	128.11	93.3
Fifth Cycle		
0	138.21	94.8
60	143.07	95.9
60	144.32	95.0

Bitumen extraction using O_3 as an extraction process aid was performed mostly on low grade ore, properties of which are presented in Table 5. Bitumen extraction tests were performed at 40 and 50°C. The bitumen extraction tests results and corresponding release water chemistry data are presented in Tables 6, 7, 8 and 9.

Data presented in Tables 6 to 9 show that for low grades ores with high fines contents the combined use of *CaO* and O_3 could improve bitumen extraction efficiency without harming the release water chemistry.

It is known that O_3 performs as an oxidant more effectively at high *pH*, i.e., in the presence of $Ca(OH)_2$ (Hoigne, 1988). Experience has indicated that oil sands ore-water slurry conditioning with both *CaO* and O_3 works better when the slurry is at a low temperature, i.e. at about 5 to 10°C.

Table 4. Effect of *CaO* on recycled release water chemistry.

CaO mg/kg Ore	<i>pH</i>	Alkalinity (mg CaCO ₃ /L)			Cations (mg/L)			Anions (mg/L)	
		Total	CO ₃ ⁼	HCO ₃ ⁻	Na+	Mg ²⁺	Ca ²⁺	Cl ⁻	SO ₄ ⁼
First Cycle									
0.00	8.2	307	0	307	441	8	8	171	158
60.00	8.3	230	0	230	340	9	8	165	174
60.00	8.5	233	6	227	338	10	10	174	184
60.00	8.5	247	6	241	338	10	10	176	185
Second Cycle-I									
0.00	8.1	225	0	225	373	9	10	177	220
60.00	7.7	156	0	156	308	10	9	164	218
60.00	7.8	169	0	169	322	12	13	174	231
60.00	7.9	170	0	170	326	12	13	172	229
Second Cycle-II									
0.00	7.9	230	0	230	401	9	10	174	213
60.00	7.8	152	0	152	300	12	11	175	243
60.00	7.9	171	0	171	335	13	13	176	250
60.00	7.9	171	0	171	312	13	13	181	252
Third Cycle									
0.00	7.7	176	0	176	354	9	12	180	254
60.00	7.8	115	0	115	297	13	12	176	275
60.00	8.1	133	0	133	310	14	15	184	290
60.00	8.0	136	0	136	314	14	15	184	289
Forth Cycle									
0.00	7.4	155	0	155	352	12	15	187	277
60.00	7.9	103	0	103	313	16	15	192	321
60.00	8.1	118	0	118	334	16	14	184	311
60.00	8.1	119	0	119	309	17	17	191	320
Fifth Cycle									
0.00	7.5	137	0	137	358	13	15	187	293
60.00	7.8	93	0	93	316	18	15	196	343
60.00	7.8	109	0	109	303	19	18	195	339
60.00	7.8	111	0	111	330	18	18	187	324

The effect of the use of O_3 as an extraction process aid on the total acid number (TAN, mg KOH/g bitumen) of bitumen was also tested. TAN for different bitumen samples and corresponding release water chemistry are presented in Tables 10 and 11. These data suggest that O_3 as an extraction process additive has no harmful effects on bitumen or on release water. Low TAN numbers are attributed to neutralization of the oxidation products, probably asphaltic acids, with $Ca(OH)_2$, which could be another advantages for the use of *CaO* for ore conditioning.

Table 5. Oil sands properties for extraction tests with CaO and O₃.

	Bitumen	Moisture	Solids	Fines in Solids
Ore ID	(%)	(%)	(%)	(%)
XXL0107	8.1	6.6	84.8	17.3
ATL0407	7.7	9.7	82.4	27.7

Table 6. Bitumen extraction with CaO and O₃.

Test ID	Temperature	CaO	O ₃	Froth Yield	Bitumen Recovery
	oC	(mg/kg ore)	(mg/kg ore)	(g)	(%)
ATL0407-1	40	-	-	116.9	60.5
ATL0407-2	40	-	-	113.9	61.4
ATL0407-33	40	150	-	102.6	53.6
ATL0407-34	40	150	-	107.6	56.7
ATL0407-35	40	150	38	109.2	63.5
ATL0407-36	40	150	38	111.4	61.9
XXL0107-87	40	150	41	125.6	55.3
XXL0107-88	40	150	42	123.8	56.4
XXL0107-89	40	150	-	120.7	53.1
XXL0107-90	40	150	-	122.2	54.3
XXL0107-91	40	-	-	117.8	52.2
XXL0107-92	40	-	-	123.3	51.5

Table 7. Release water chemistry, bitumen extraction with CaO and O₃.

Test ID	pH	Alkalinity (mg CaCO ₃ /L)		Cations (mg/L)					Anions (mg/L)	
		Total	HCO ₃	Na	K	Mg	Ca	Cl	SO ₄	
RW Oct 31-06 (*)	8.5	412	400	361	18	8	7	168	88	
ATL407-1	8.4	308	304	353	21	12	13	161	160	
ATL407-2	8.4	314	310	355	23	12	15	169	166	
ATL407-33	8.5	297	287	356	21	12	13	165	173	
ATL407-34	8.6	301	291	353	22	12	14	170	176	
ATL407-35	8.5	266	260	361	21	11	13	168	186	
ATL407-36	8.5	274	268	361	22	11	13	168	176	
XXL0107-87	8.1	218	218	354	27	22	26	170	335	
XXL0107-88	8.1	226	226	355	27	21	25	173	324	
XXL0107-89	7.7	262	262	359	27	21	25	173	304	
XXL0107-90	8.1	257	257	362	27	22	26	174	317	
XXL0107-91	8.0	250	250	362	27	21	24	174	313	
XXL0107-92	8.0	250	250	354	27	20	23	172	299	

(*) Recycle Water

Table 8. Bitumen extraction with CaO and O₃.

Test ID	Temperature	CaO	O ₃	Froth Yield	Bitumen Recovery
	°C	(mg/kg ore)	(mg/kg ore)	(g)	(%)
XX0107-93	50	-	-	155.1	80.8
XX0107-94	50	-	-	153.2	85.9
XX0107-95	50	150	-	141.3	85.7
XX0107-96	50	150	-	158.6	92.5
XX0107-97	40	-	-	162.6	87.3
XX0107-98	40	-	-	154.2	81.9
XX0107-99	40	150	-	136.6	74.1
XX0107-100	40	150	-	150.3	81.2
XX0107-101	40	150	38	151.2	85.8
XX0107-102	40	150	42	152.1	87.3
XX0107-103	40	-	35	144.7	73.8
XX0107-104	40	-	38	148.1	81.3
XX0107-105	50	150	41	148.0	88.4
XX0107-106	50	150	42	139.5	81.2
XX0107-107	50	-	41	140.9	82.9
XX0107-108	50	-	42	150.0	85.6

Table 9. Release water chemistry, bitumen extraction with CaO and O₃.

Test ID	pH	Alkalinity (mg CaCO ₃ /L)		Cations (mg/L)					Anions (mg/L)	
		Total	HCO ₃	Na	K	Mg	Ca	Cl	SO ₄	
RW (*)	8.7	424	402	348	22	7	10	180	95	
XX0107-93	8.4	300	294	333	24	11	13	171	193	
XX0107-94	8.6	310	296	365	23	10	12	174	181	
XX0107-95	8.6	302	288	371	23	8	9	176	181	
XX0107-96	8.7	304	284	374	22	8	9	176	177	
XX0107-97	8.5	334	326	379	23	11	13	174	175	
XX0107-98	8.5	331	323	371	23	11	13	175	178	
XX0107-99	8.6	317	303	379	22	10	13	163	172	
XX0107-100	8.6	320	304	371	23	10	13	173	174	
XX0107-101	8.5	307	295	366	23	11	16	191	176	
XX0107-102	8.5	302	290	384	23	9	10	172	170	
XX0107-103	8.3	301	301	354	22	11	14	162	169	
XX0107-104	8.4	306	298	361	23	10	13	171	177	
XX0107-105	8.5	280	268	363	22	8	9	175	178	
XX0107-106	8.5	271	259	370	22	8	9	173	180	
XX0107-107	8.5	287	279	330	24	10	12	180	183	
XX0107-108	8.5	297	289	368	23	9	10	173	171	

(*) Recycle Water

As another alternative to improve the bitumen extraction efficiency the use of surfactants from external sources as extraction process aids was also investigated. For this purpose the performance of biodiesel (BD) such as fatty acid methyl esters (FAME) and fatty acid monoglycerides (FAMG) with chemical formulas of $C_nH_m-COO-CH_3$; $m < 2n+1$ and $C_nH_m-COO-CH_2-CHOH-CH_2OH$; $m < 2n+1$ as extraction process additives were evaluated. BD has hydrophilic and hydrophobic functional groups which make BD attractive to process water (PW) more than bitumen, also attractive to bitumen more than PW. Photographs of BD and PW drops on bitumen coated glass plates are depicted in Figure 2. Similarly, photographs of BD and bitumen on PW are depicted in Figure 3. The shapes of BD and PW on bitumen and BD and bitumen on PW indicate that bitumen-BD interfacial tension is much lower than bitumen-PW interfacial tension and BD-PW interfacial tension is much lower than bitumen-PW interfacial tension. These properties make BD as surfactant reducing the interfacial tension between bitumen and PW provided that BD is sufficiently dispersed in PW.

Table 10. TAN of different bitumen samples.

Sample ID	Sample Treatment	Average TAN (mg KOH/g Bitumen)
ARC1107-Ore-2	Bitumen from Ore	3.52
ARC1107-25	80 ppm CaO+O ₃	3.03
ARC1107-27	80 ppm CaO	3.15
ARC1107-29	O ₃	2.96
ARC1107-31	Blank (No Additive)	3.13

ppm: mg additive/kg ore

Table 11. Release water for TAN of different bitumen samples.

Sample ID	pH	Alkalinity (mg CaCO ₃ /L)			Cations (mg/L)				Anions (mg/L)	
		Total	CO ₃	HCO ₃	Na	K	Mg	Ca	Cl	SO ₄
APW-Augy-08	8.5	370	8	362	243	20	9	13	185	6
ARC1107-25	8.5	224	4	220	232	18	8	18	189	121
ARC1107-27	8.6	238	8	230	233	18	8	17	191	117
ARC1107-29	8.5	231	8	223	225	18	8	19	179	116
ARC1107-31	8.6	244	8	236	226	19	9	18	184	111

APW: Artificial Proces

The bitumen extraction test results and release water chemistry data for the use of BD as a surfactant additive are presented in Table 12 and 13. The oil sands ore used for these tests was composed of 8.1% bitumen, 5.1% water, 86.5% solids (19.2% of which are fines), which is classified as high fines ore. All extraction tests were performed at 40°C temperature. Since BD is also a fuel which presumably recovered with bitumen, the bitumen recovery efficiency is corrected excluding the BD added into the ore-water slurry.

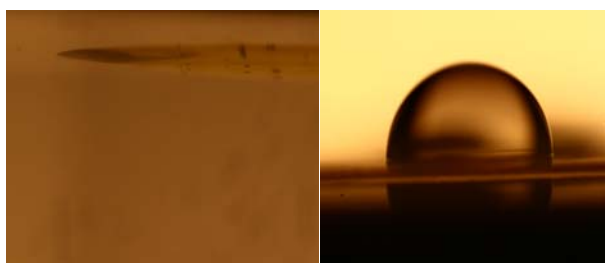
Further tests were performed by dispersing the BD in process water using a high shear mixer. Extraction tests performed by effectively dispersing the BD in process water showed that BD as low as 200 mg/kg-ore dosages performs as an effective surfactant additive without harming release water chemistry or fuel quality of bitumen. We are speculated that the BD addition could be reduced to under 100 mg/kg-ore dosages if BD is properly dispersed in process water.



BD on bitumen

PW on bitumen

Figure 2. Photographs of BD and PW drops on bitumen.



BD on PW

bitumen on PW

Figure 3. Photographs of BD and bitumen drops on PW.

Table 12. Performance of BD as surfactant additive for bitumen extraction.

Test ID	BD (mg/kg-ore)	Froth (g)	Bitumen Recovery (%)	Corrected Recovery (%)
ARC1107-3 Blank	-	87.2	72.5	72.5
ARC1107-4 Blank	-	91.6	74.6	74.6
ARC1107-7 BD	433	96.1	81.7	81.2
ARC1107-8 BD	433	100.8	81.9	81.4
ARC1107-5 BD	867	91.9	83.6	82.5
ARC1107-6 BD	867	94.0	81.8	80.8
ARC1107-1 BD	1667	95.8	80.7	78.7
ARC1107-2 BD	1667	98.6	84.3	82.3
ARC1107-9 BD	3333	89.7	84.4	80.3
ARC1107-10 BD	3333	94.3	83.1	79.0

In summary, the above presented research findings offer to the oil sands industry novel bitumen extraction processes using CaO , CaO and O_3 or CaO and BD as alternative to conventional CHWE process. Implementation of these findings could be the cost effective solutions for the oil sand tailings disposal and water chemistry problems. Performance of these novel process concepts have to be tested using a bench scale extraction plant. Ore conditioning with CaO would deserve more detailed study because of the complexity

involved with the conditioning of oil sands ore-water slurries (Friesen et al, 2004).

Table 13. Release water chemistry, bitumen extraction with BD.

Test ID	pH	Alkalinity (mg $CaCO_3/L$)			Cations (mg/L)				Anions (mg/L)	
		Total	CO_3	HCO_3	Na	K	Mg	Ca	Cl	SO_x
PW (*)	8.6	392	16	376	269	23	11	12	187	24
ARC1107-3 Blank	8.6	278	10	268	369	22	11	17	170	120
ARC1107-4 Blank	8.6	283	10	273	356	23	11	17	180	125
ARC1107-7 BD	8.5	295	8	298	363	24	11	19	182	123
ARC1107-8 BD	8.6	290	8	282	336	26	11	20	189	128
ARC1107-5 BD	8.5	291	8	283	353	23	11	19	176	123
ARC1107-6 BD	8.5	298	8	290	367	25	12	17	183	126
ARC1107-1 BD	8.6	270	10	260	353	22	11	17	171	132
ARC1107-2 BD	8.6	277	10	267	335	24	11	16	185	132
ARC1107-9 BD	8.5	291	8	283	338	22	12	20	174	121
ARC1107-10 BD	8.5	298	8	290	354	23	11	18	183	126

(*) Process Water

Nonsegregating Tailings Production using CaO or CaO and CO_2

Oil sands plants using ore-water slurry based extraction processes produce a tailings effluent in the form of a slurry, which is hydraulically transported and deposited in the tailings ponds. This slurry is a mixture of sand particles, dispersed fines, water and residual bitumen, which is composed of about 55% solids, of which 82% sand, 17% fines (<45 μm or 325 mesh) and 1 w % is residual bitumen. When the tailings is discharged, the coarse sand particles segregate quickly and form a beach, the remaining fine tails of 6 to 10 w % solids accumulate in the tailing ponds. Fine tails settle quickly to 20 w % solids content (99% of which is fines) and over a few years to 30% solids (86 % by volume water) with a stable slurry structure which is called mature fine tails (MFT). This MFT will remain in a fluid state for decades because of its very slow consolidation rate (Kasperski, 1992; McKinnon, 1989).

Material balance on oil sands plants shows that the total tailings produced is 30 to 40% greater than the volume of mined oil sands

which makes the production of MFT unavoidable if the fines and sand are not settling together. It is predicted that if the existing tailings management practice is continued, the accumulated volume of MFT would increase to over one billion cubic meters by the year 2010. Accumulation of large volumes of MFT causes environmental concerns and long-term liability.

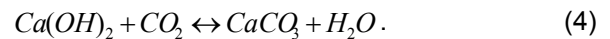
Elimination of the MFT production and eventually reduction of the MFT inventory could happen by: (i) discharging the oil sands tailings as nonsegregating tailings (NST); and (ii) consuming the existing MFT in the NST production. Production of the CT as depicted in Figure 1 could not eliminate the MFT inventory since additional MFT would be produced from the Cyclone Overflow tailings.

Segregation boundaries of oil sands tailings are presented in Figure 4, which shows that production of NST could be possible by: (i) increasing the solids content; (ii) increasing the fines content; and (iii) using additives preventing segregation. The purpose of the use of cyclones in the CT process was to produce tailings with sufficiently high solids contents preventing segregation.

Elimination of the MFT production would be possible by producing the NST as depicted in Figure 5, which involves thickening the Cyclone Overflow using suitable thickeners, blending the Thickener Underflow with Cyclone Underflow into a NST mix and treating this mix with *CaO* (lime) or *CaO* and *CO₂*. Existing MFT could also be added to the NST mix provided that the final product would have sufficient permeability for the recovery of the release water. Use of thickeners for the thickening of Cyclone Overflow tailings saves thermal energy by recycling the release water as warm as

possible. This is an advantage if the excess thermal energy is not available around the extraction site.

Production of NST depends on the properties of the tailings which are controlled by the additives used in the extraction process. Regardless of the type of extraction process, chemical additives are used to shift the segregation boundary line of the tailings towards lesser solids contents, as depicted in Figure 4, by formation of the yield stress in fines-water matrix. The additive used to prevent segregation, like the additive used in extraction process, should not have harmful effect on the release water chemistry. The research findings suggest that *CaO*, or *CaO* and *CO₂* prevents segregation and improves water chemistry by chemical reactions expressed by Equations 2 and 3. The excess *CaO* used in NST production cause the precipitation of *CaCO₃* by the following reaction (Chalaturnyk et al, 2002):



Performance of *CaO* as an additive for the NST production has been tested on Albion Sands' Muskeg Rive Mine and Syncrude Canada Ltd.'s Aurora Mine tailings (Scott et al, 2007; Donahue et al, 2008). Segregation data for the tailings with 59% solids contents of different sand to fines ratios (SFR) without and with *CaO* additives at different dosages are presented in Figures 6 and 7. As seen from these figures, addition of *CaO* as low as 0.6 g/L NST dosage prevents segregation.

The release water recovered from the NST produced by using *CaO* is presented in Table 14.

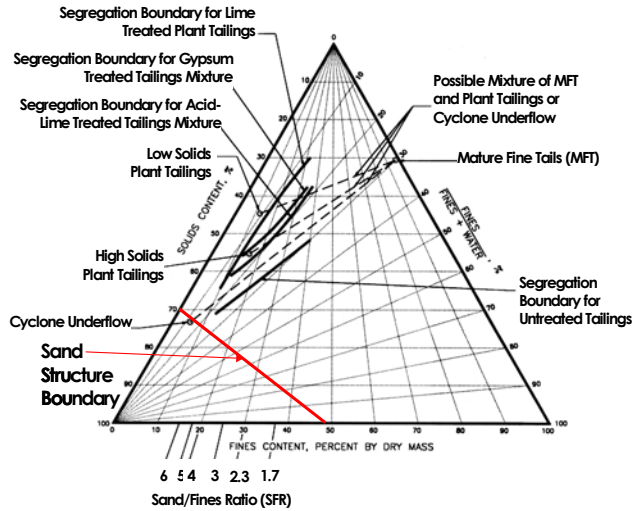


Figure 4. Segregation boundaries for the oil sand tailings.

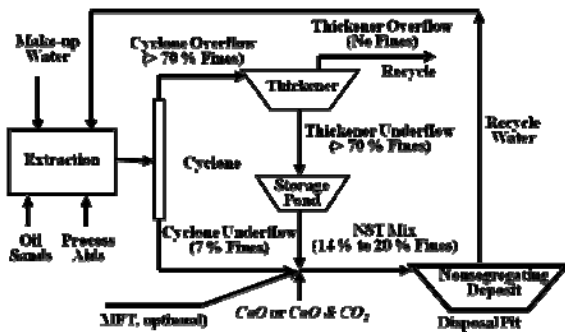


Figure 5. NST production process.

The release water produced by the addition of CaO for the production of NST contained lesser Ca^{2+} and Mg^{2+} ions due to the chemical reactions expressed in Equations 2 and 3. Excess amounts of $Ca(OH)_2$ in the release water, i.e. when CaO dosages were greater than 0.6 g/L NST, would react with the atmospheric CO_2 by the reaction expressed in Equation 4. Excess amounts of CaO in the release water could also be used to reduce the bicarbonate hardness of the make-up water with the chemical reaction expressed in Equation 2. These are the advantages of using CaO as an additive to produce NST.

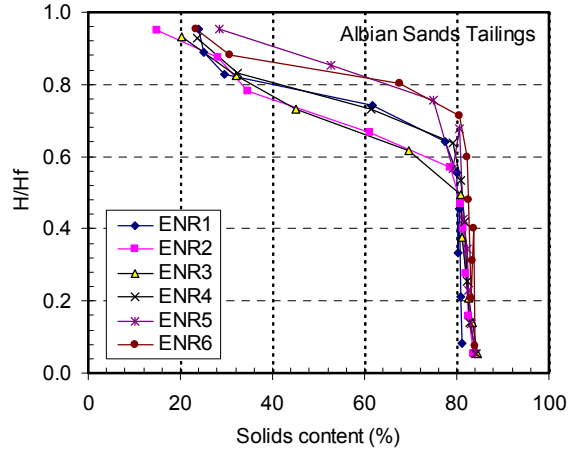


Figure 6. Segregation data without additives.

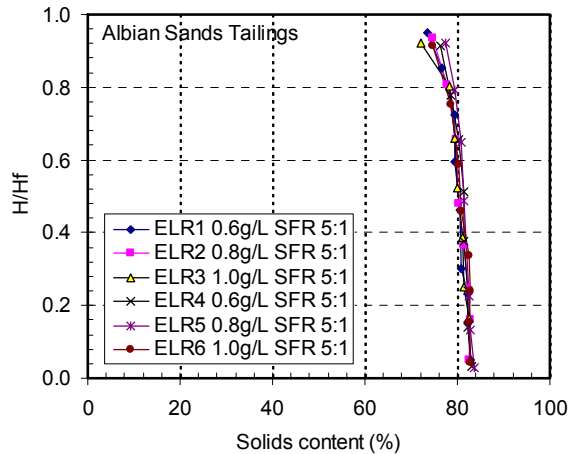


Figure 7. Segregation data with CaO additive.

Table 14. Release water chemistry, NST production using CaO .

CaO (g/m^3)	CO_2	Conduc. (mS)	pH	Ca^{2+} (mg/L)	Mg^{2+} (mg/L)	Na^+ (mg/L)	Fines Capture (%)
0	No	0.999	7.8	44	24	131	82
200	No	0.733	8.8	20	6	115	75
400	No	0.727	9.5	24	1.8	114	87
600	No	0.917	10.9	40	0.2	118	97
800	No	1.449	11.4	80	0.1	126	97
800	Yes	0.777	10.4	30	0.3	116	93

CONCLUSIONS

The existing MFT and water chemistry problems of ore-water slurry based extraction plants could be solved by using CaO and O_3 or CaO and BD as additives in bitumen extract and using CaO or CaO and CO_2 as additives to produce NST for the disposal of tailings. Pilot scale tests are needed further evaluation of the performance of these additives.

ACKNOWLEDGMENTS

Apex Engineering Inc. acknowledges the funding provided by the IRAP-NRC and the AERI. Discussions, suggestions and collaborations by Mr. B. Komishke, Dr. D. Wallace and Mr. R.K.O. Birkholz of Calgary Research Centre-Shell Canada Ltd. and T.M. Dereniwski and T.G. Paradis of the Canadian Natural Resources Ltd. are appreciated. Collaborations with the Department of Civil & Environmental Engineering, University of Alberta and the Alberta Research Council are acknowledged.

REFERENCES

- Allen, E.W. 2008a. "Process water treatment in Canada's oil sands industry: I. Target pollutants and treatment objectives", *J. Environ. Eng. Sci.* 7: 123-138.
- Allen, E.W. 2008b. "Process water treatment in Canada's oil sands industry: II. A review of emerging technologies", *J. Environ. Eng. Sci.* 7: 499-524.
- Baptista, M.V. and C.W. Bowman, 1969. "The Flotation Mechanism of Solids from the Athabasca Oil Sands", 19th Can. Chem. Eng. Conf. Edmonton, Alberta, Canada.
- Bowman, C.W. 1967. "Molecular and Interfacial Properties of Athabasca Tar Sands", *Proceedings of the Seventh World Petroleum Congress, Mexico City, Vol. 3:* 583-604.
- Burns, R., R. Tipman, K. Firmin, R.J. Mikula, V.A. Munoz, K.L. Kasperski and O.E. Omotoso, 1998. "Bitumen Release Mechanisms and New Process Development", *Seventh UNITAR International Conference on Heavy Crude and Tar Sands, Paper No. 1998.226, October 27-30, 1998, Beijing, China.*
- Caughill, D.L., N.R. Morgenstern and J.D. Scott. 1993. *Can. Geotechnical Journal*, Vol. 30(5): 801-811.
- Chalaturnyk, R.J., J.D. Scott and B. Ozum, 2002. "Management of Oil Sands Tailings", *Petroleum Science and Technology*, 20(9&10), 1025-1046.
- Clark, K.A., 1939. "The Hot Water Method for Recovering Bitumen from Bituminous Sand", *Report on Sullivan Concentrator, Alberta Research Council, Alberta Canada.*
- Clark, K.A. and D.S. Pasternack, 1932. "Hot Water Separation of Bituminous Sand", *Ind. Eng. Chem.* 24, 1410.
- Dawson, R. F., D.C. Seago and G.W. Pollock, 1997. "Freeze Thaw Dewatering of Oil Sands Fine Tails", *Canadian Geotechnical Journal*, 36: 587-598.
- Donahue, R., S. Jeeravipoolvarn, J. D. Scott and B. Ozum. 2008. "Properties of Nonsegregating Tailings Produced from the Aurora Oil Sands Mine Tailings", *International Oil Sands Tailings Conference, December 7-10, Edmonton, Alberta, Canada.*

- Friesen, W.I., T. Dobras and T. Kwong, 2004. "A Bench-Scale Study of Conditioning Behaviour in Oil Sands Slurries", *Can. J. Chem. Eng.*, 82, 743-751.
- Hall, E.S. and E.L. Tollefson, 1982. "Stabilization and Destabilization of Mineral Fines-Bitumen-Water Dispersions in Tailings from Oil Sands Extraction Plants that use Hot Water Process", *Can. J. Chem. Eng.*, 60, 812.
- Harron, W.R.A., G.R. Webster and R.R. Cairns, 1983. "Relationship Between Exchangeable Sodium and Sodium Adsorption Ratio in a Solonchic Soil Association", *Can. J. Soil Sci.*, 63; 461-467.
- Hoigne, J. 1988. "The Chemistry of Ozone in Water", pp. 121-143, *Process Technologies for Water Treatment*, Edited by Samuel Stucki, Plenum Publishing Corporation.
- Jeeravipoolvarn, S., J. D. Scott, R. Donahue and B. Ozum. 2008. "Characterization of Oil Sands Thickened Tailings", *International Oil Sands Tailings Conference*, December 7-10, Edmonton, Alberta Canada.
- Kasperski, K.L., 2001. "Review of Research on Aqueous Extraction of Bitumen from Mined Oil Sands", *Natural Resources Canada, Western Research Centre, Division Report May 2001, CWRC 01-17*.
- Leja, J. and C.W. Bowman, 1968. "Application of Thermodynamics to the Athabasca Tar Sands", *Can. J. Chem. Eng.*, 46; 479-481.
- Liu, Y.B., D. Caughill, J.D. Scott and R. Burns. 1994. Paper Presented at 47th Canadian Geotechnical Conference, September 21-23, Halifax, Nova Scotia.
- MacKinnon, M.D. 2004. "Oil sands water quality issues: properties, and discharge options", *CONRAD Water Usage Workshop*, February 24-25, 2004.
- Masliyah, J., Z. Zhou, Z. Xu, J. Czarnecki and H. Hamza, 2004. "Understanding Water-Based Bitumen Extraction from Athabasca Oil Sands", *Can. J. Chem. Eng.*, 82, 628-654.
- Scott, J.D., R. Donahue, J.G. Blum, T. G. Paradis, B. Komishke and B. Ozum, 2007. "Production of Nonsegregating Tailings with CaO or CaO and CO₂ for Improved Recycle Water Quality", *CONRAD Water Usage Workshop*, November 21 & 22, Calgary, Alberta, Canada.
- Speight, J. G. and S.E. Moschopedis, 1977/78. "Factors Affecting Bitumen Recovery by the Hot Water Process", *Fuel Technology*, 1: 261-268.

THE DEVELOPMENT OF CENTRIFUGAL SEPARATION TECHNOLOGY FOR TAILINGS TREATMENT

Peter Mundy

Alfa Laval Inc., Calgary, Canada

Bent Madsen

Alfa Laval AB, Soborg, Denmark

ABSTRACT: The recent Energy Resources Conservation Board (ERCB) directive states new industry-wide criteria for managing oil sands tailings and specific enforcement actions if tailings performance targets are not met. The directive applies to all existing and future oil sands operators. The consequence of this is that environmental demands balanced with production growth and efficiency are more critical to project viability than ever before.

Either as an independent solution or in combination with more traditional techniques, such as Consolidated Tailings (CT), Decanter Centrifuges for the accelerated dewatering of fine tailings is seen by many as a leading solution to this issue. Decanter centrifuges have been used in oil sands treatment for over 30 years, but the application of this technology to tailings treatment has needed certain developments to accommodate the requirements of this new duty.

This presentation describes the decanter centrifuge basic principles and combines the experiences gained from comparable duties to form a new generation of centrifuge. With reference to full scale test-work carried out in 2008, the presentation will review a working solution and describe the changes necessary to meet the recent market demand.

CENTRIFUGE TECHNOLOGY

Centrifuges have developed from 10s of liters per hour at 100s of rpm in the late 19th century to what we have today. 300 m³/h at up to 8000 rpm and numerous applications including the separation of cream from milk, purifying beer and wine, cell separation in the biotech industry and the purification of bitumen in oil sand.

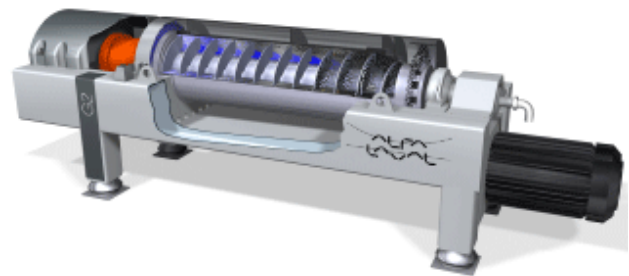


Figure 1. Decanter centrifuge

For separation applications with comparatively high solids loading the decanter centrifuge is the most suitable. Decanter centrifuges were originally developed for industrial applications in the late 1940s. Its design is based on a horizontally driven bowl to induce

accelerated sedimentation. This combined with a conveyor, running with a speed differential to the bowl, transports separated solids up a conical beach and discharges solids in the form of a dry cake. The clarified liquid phase is discharged at the opposite end of the centrifuge over weir plates.

BASIC PRINCIPLES

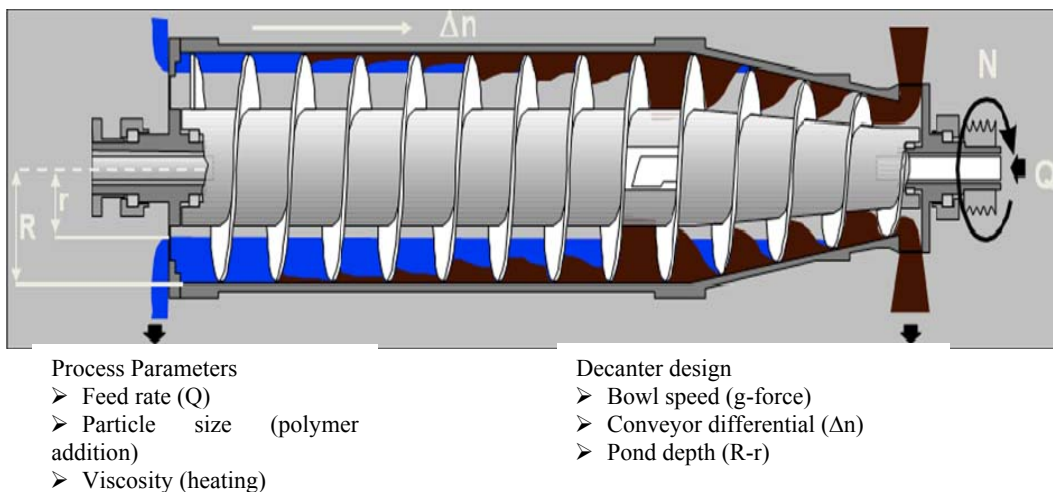


Figure 2. Decanter cross-section

Process parameters such as feed rate, particle size and viscosity, together centrifuge configuration, for example bowl speed, conveyor to bowl differential speed, liquid pond depth and cone beach angle will directly affect separation performance and solids removal.

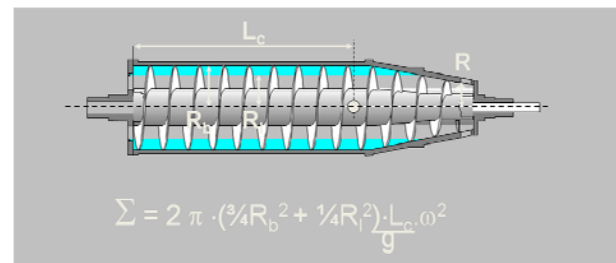


Figure 3. Sigma factor & centrifuge performance

TECHNOLOGY DEVELOPMENT

Sigma factor (developed in 1948). Used in the very early days of decanter development, where sedimentation was the only factor been considered and any practical information from various applications was very limited.

Despite limitations of this formula it has still been used for a large number of old designs. Some of these decanter centrifuges have been upgraded, but they still have a very large radius to the liquid surface. As it is noted, the formula states that this should give a high capacity. In reality, a larger radius to the liquid surface will reduce the capacity of a decanter! In the late 1980s a

number of studies revealed the limitations of the Sigma factor and in general it was realized that the solids handling capacity was the real limiting factor for most decanter applications. Since then the main focus for decanter development has been to improve solids handling capacity. In this context, solids handling capacity means two things: the capability to achieve high cake dryness and to discharge large volumes of cake at the same time. For example Alfa Laval, a leading supplier of decanter centrifuges, switched focus to solids handling ability as a general guide to equipment design. The result was a clear increase in solids handling ability in a variety of processes, from drilling mud treatment to fish and meat dewatering.

Again, using the Alfa Laval products as an example, a couple of important designs demonstrate the development since then. The LYNX 40 decanter normally runs on drilling mud where the main goal is to discharge as much solids as possible and dryness is less important. The solids in drilling mud are relatively large and dense, so residence time is not so critical and it is therefore run with a high differential speed. The shallow cone angle of 6 degrees allows the solids to travel up the beach more easily for high solids removal. General belief would suggest designing such a decanter with a large radius to the solids discharge ports, but instead the LYNX 40 has the same radius to the solids discharge ports as a deep pond decanter and the deeper pond is used to increase the scrolling capacity of this unit. All internal solids passages are designed for high solids handling capacity and the small solids discharge radius has not limited the capacity.

In mature fine tailings, MFT the demand is to achieve a dry cake and still operate at a high solids load (tonne/h). In order to

capture the fine particles in MFT we need to add polymer. This will give solids with a cake like behavior and this will not readily allow liquid to drain off. In order to get a dry cake it will be necessary to operate with a deep layer of solids and with low differential speed. This way of operating a decanter is very similar to the way decanters for dewatering of municipal sludge is operated. Sludge dewatering also involves flocculated suspensions and here Alfa Laval introduced a new design in 2003 under the name "G2", generation 2. The scrolling efficiency of the G2 range is so high that most decanters of this type are designed with a 20 degree cone angle without any negative effect on solids handling capacity.

To design a suitable machine for MFT involves a lot of detailed knowledge about cone angles, flight pitch variation and inclination, pond depth, G-level and differential speed coupled with the conveyability of the solids as a function of dryness. The optimized decanter design is based on experience gained in testing the LYNX 40 on MFT in 2008.

Controlled levels of shear are needed for effective distribution of the polymer in the feed to the decanter. Low shear in the decanter gives the driest cake and highest quality centrate. High cake discharge radius result in a limited possibility for deeper pond depths and separation performance. A large liquid surface radius will automatically introduce a high shear in the decanter feed zone and the lower pond depth will limit the solids handling capability, particularly with flocculated solids. Incidentally, the larger discharge radii on both solids and centrate discharge areas will also cause high shear and hence high wear in those areas. It is therefore predictable that discharging both solids and liquids at smaller radii will reduce

discharge velocities, limit wear in those areas and reduce power draw as a result.

HANDLING WEAR EFFECTIVELY

The nature of a separation process with high solids loading and centrifugation will promote the possibility of increased wear. In the design of the decanter there is a trade-off between component life and the use of higher cost, wear resistant materials to limit wear. The choice of materials must meet acceptable component life and cost of ownership for the centrifuge. Using material

inserts in the known wear locations help to meet market expectation. An example of this is the use of tungsten carbide wear liners in the decanter feed zone. The benefits of this are to limit material change only to the affected area and to keep the time necessary for repair to a minimum.

Wear due to the differential speed between the decanter conveyor and bowl can be effectively handled with the simple inclusion of ribs, welded to the bowl of the decanter centrifuge.

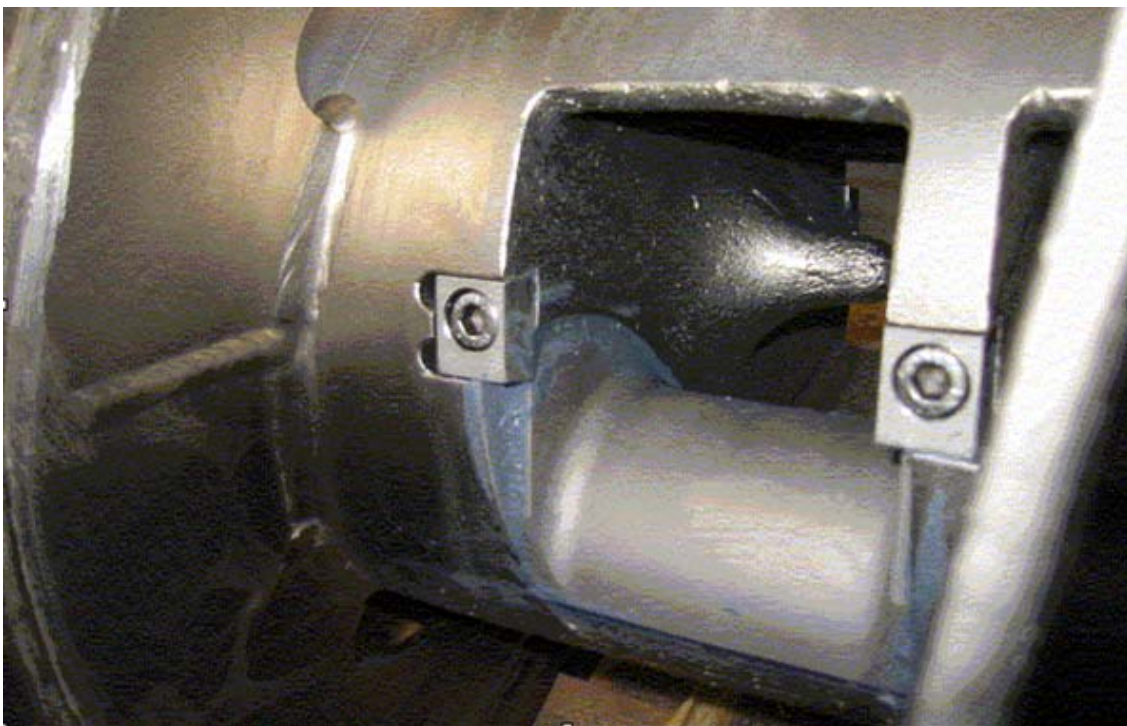


Figure 4. Erosion protection with inserts in the decanter feed zone

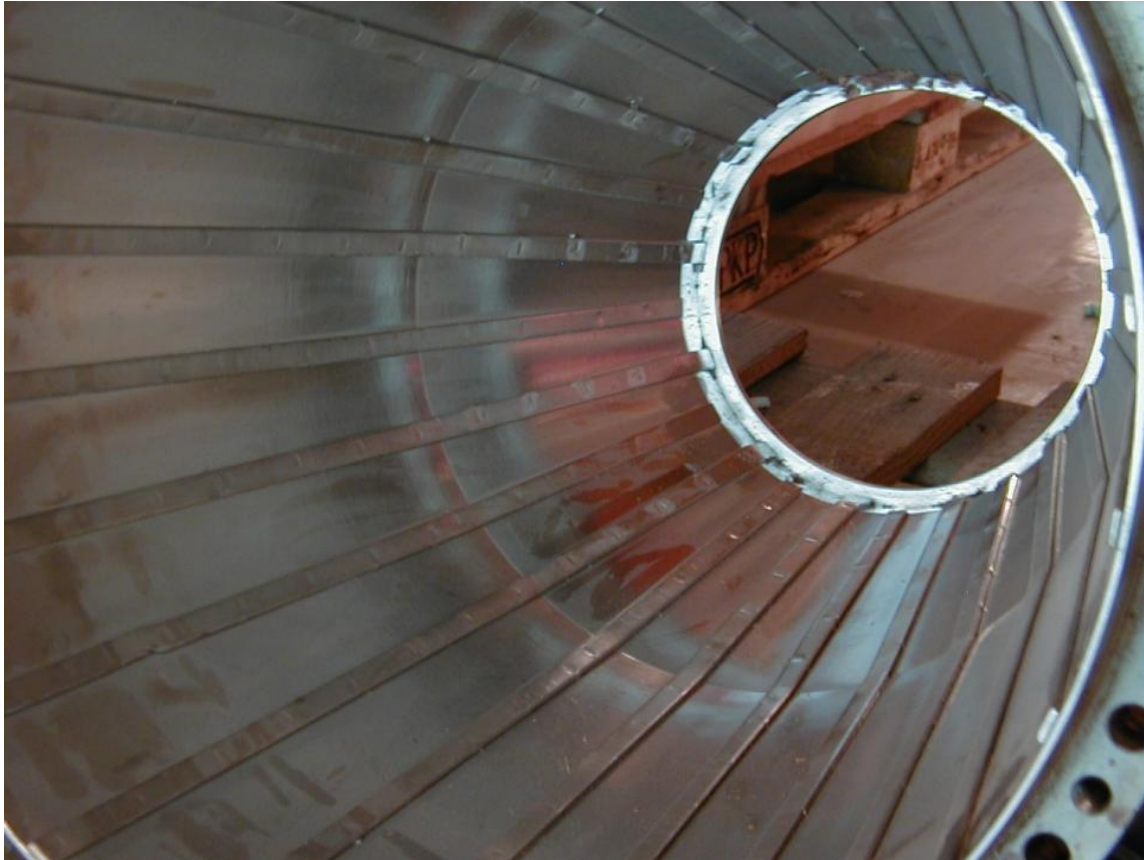


Figure 5. Ribs in the centrifuge bowl

Solids naturally collect between the ribs providing a layer of protection. The positive effects of this design are increased wear protection of the bowl and conveyor, and improved solids transportation.

For added protection of the conveyor, tungsten carbide tiles are attached to the conveyor flights.

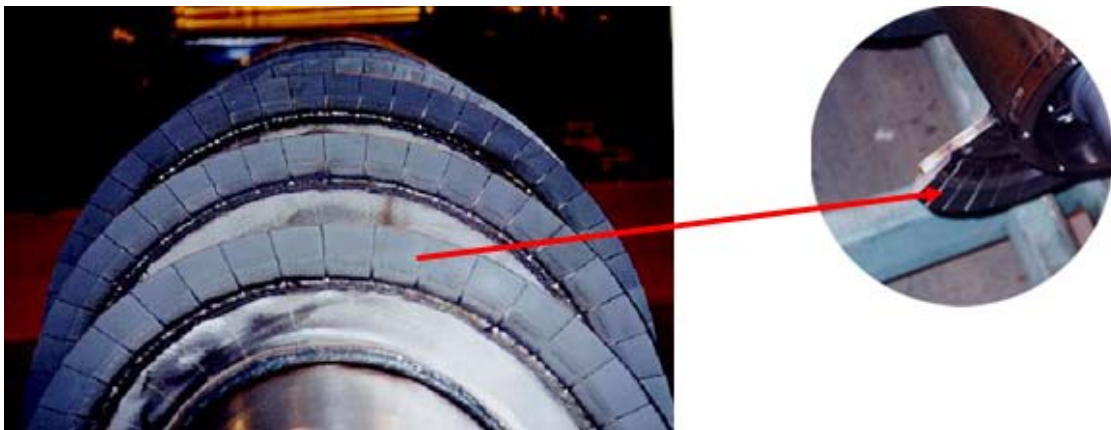


Figure 6. Tiles protect the conveyor flights

CENTRIFUGE CONTROL

With a fixed differential speed decanter a reduction in the solids loading in the feed to the centrifuge will cause a reduction in cake dryness. With tailings treatment the centrifuge will typically be solids limited, so an increase in solids loading in the feed to the centrifuge will increase the risk of over-torque on the unit.

Monitoring the torque between the bowl and conveyor and automatically varying their differential speed make it possible to maintain the optimal performance of the

centrifuge and consistent cake dryness. Variable differential speed control will also protect the centrifuge against the possibility of over-torque.

PROCESS VISION

Step 1 in the process is for MFT dewatering using flocculent addition and centrifugal separation to form two streams. The ultimate aim is for the centrate to be recycled as process water and help reduce the need for fresh water.

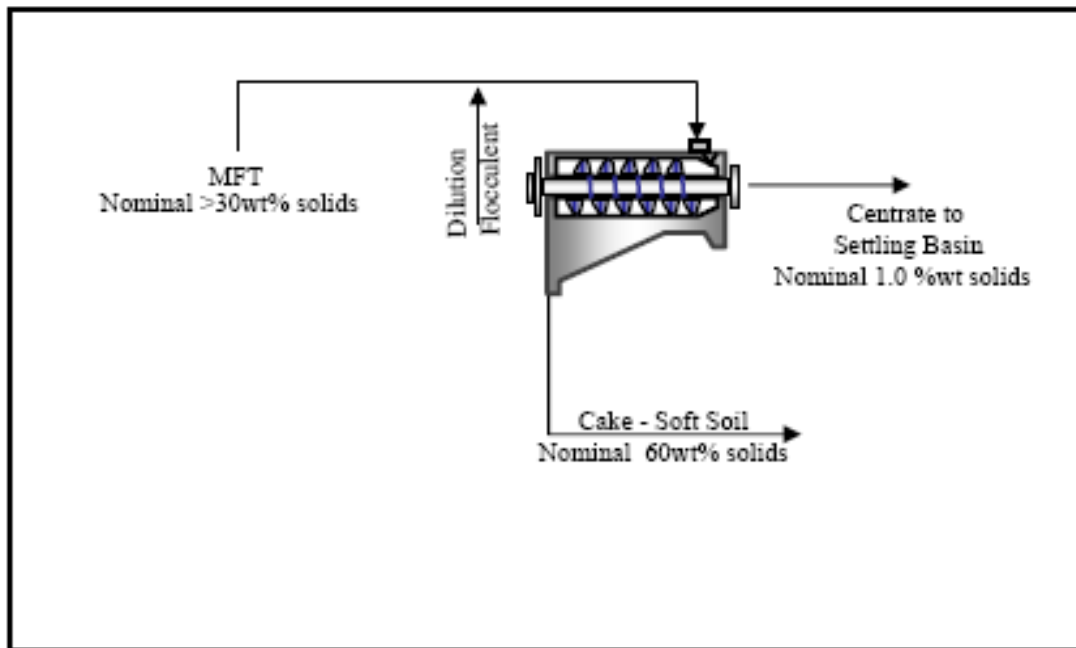


Figure 7. The decanter in the process

Step 2 is the subsequent dewatering of the cake by natural processes, with the final goal

of land reclamation.

ACHIEVABLE PERFORMANCE

Decanter centrate quality <0.5% wt solids
Produced decanter cake with 60% wt solids dryness

Polymer dosage 600 g/dry tonne achievable
Scaling from the test indicate that 54 dry tonnes/hour, 270 m³/h wet feed can be treated by a single centrifuge. For the scale of intended projects multiple centrifuges will be needed.

CONCLUSIONS

Decanter centrifuges are a well established, heavy duty technology and initial tests have achieved positive results showing that this technology can contribute to the viable dewatering of MFT. There is however no 'silver bullet'. The treatment of MFT will require a major investment for both initial accelerated dewatering and distribution of produced dry cake for final drying and land reclamation.

TAILINGS RESEARCH AT SHELL'S MUSKEG RIVER MINE TAILINGS TESTING FACILITY

J. Matthews

Shell Canada Energy, Calgary, Alberta, Canada

S. Masala

Klohn Crippen Berger, Calgary, Alberta, Canada

ABSTRACT: The Tailings Testing Facility (TTF) was constructed at the Shell Albian Sands (SAS) Muskeg River Mine (MRM) site to support evaluation and development of innovative tailings technologies. Since 2007 various field programs have been advanced at the TTF, including field-testing of paste thickening and non-segregating tailings (NST) processes. Paste thickening produces a high density, high fines content non-segregating thickener underflow product and the NST process mixes the thickener underflow product with aggressively dewatered coarse tailings to produce non-segregating mix with a higher sand content. Paste tailings thickening and the NST process are being developed to support the objective of reduced fluid fine tailings inventory accumulation and more rapid reclamation of mined areas to terrestrial land uses. The paper presents depositional and geotechnical insights gained from NST and paste thickener underflow deposition trials. Technical insights discussed include: deposit performance monitoring during filling and consolidation, field characterization, and investigation of shear strength.

INTRODUCTION

The Athabasca Oil Sands Project (AOSP) is owned by Shell Canada Energy (60%), Chevron Canada Limited (20%), and Marathon Oil Sands L.P (20%). Shell Canada Energy acts as the AOSP project manager on behalf of the owners. Assets of the AOSP include the Muskeg River Mine (MRM) and the Scotford Upgrader with a production capacity of 155k bpd of bitumen. The AOSP Expansion, currently under construction, will add an additional 100k bpd bitumen recovery and upgrading capacity. The Muskeg River

Mine (MRM) is an open-pit mining operation that recovers bitumen. The oil sand ore is comprised of bitumen, water, and mineral solids (primarily sand and clay minerals). The ore is mined, mixed with warm water and fed to process vessels where the bitumen is separated from the water and mineral solids before transport to Scotford for upgrading.

As part of Shell's commitment to sustainability and continuous improvement, Shell Canada commissioned the Tailings Testing Facility (TTF) at the MRM site in June 2007. The TTF is used to demonstrate

the viability of various novel oil sands tailings treatment options at pilot scale. Shell's focus at the TTF has been on continued development of tailings thickening, and non-segregating tailings (NST) processes. These processes are being developed with the aim of reducing the rate of fluid fine tailings (FFT) inventory accumulation, improving water recovery from tailings, and providing suitable substrates to support long-term terrestrial reclamation objectives.

TTF operations in 2008 were successful in providing proof-of-concept for the NST process. Proof-of-concept was based on success of pipeline transport and placement of unconventionally high-density slurry to produce a homogenous deposit with very high fines capture and rapid consolidation characteristics. The NST development program has moved into a demonstration of the fully integrated NST flow sheet in 2009 to better evaluate overall system reliability and operability. Each of these technologies are showing promise to support fluid fine tailings inventory reduction and progressive reclamation objectives.

PRE-PILOT RESEARCH

Since 2005 Shell has been actively engaged in evaluation of novel tailings technology development opportunities at the laboratory and field pilot scale. These development efforts covered three scales of testing: laboratory, intermediate scale, and field pilot work.

Laboratory experimentation was the key to develop improved understanding of oil sands tailings behaviour with special focus on the segregation mechanisms in dynamic shear environments and assessment of rheological characteristics of tailings slurries.

Intermediate scale testing was used to further develop technology components at larger time and length scales. The research effort culminated in a 2006 decision to construct a pilot rated for 20 tonnes-per-hour dry solids capacity paste thickening and 100 tonnes-per-hour dry solids capacity NST production rates.

TTF TESTING

TTF Plant

The TTF layout is presented as a simplified block flow diagram in Figure 1.

Plant on-line monitoring

The TTF plant was instrumented to facilitate on-line monitoring of the characteristics of the tailings slurries produced. In addition to on-line monitoring, representative samples were collected and analyzed to determine slurry composition and to assess rheological properties. Data collected for geotechnical purposes included:

- Tailings slurry density and volumetric flow rates of product deliver to deposition sites; and,
- Index and soil classification test data obtained on samples taken from the TT and NST lines, including: composition (oil-water-solids), slurry density (solids content), particle size distribution, and methylene blue index as an indicator of mineral solids surface activity.

Cell layout and instrumentation

Deposition cells were excavated in in-situ overburden and oil sands to a depth of 5 m depth. Each deposition cell had a rectangular base measuring 20 m x 50 m, and with sloping sides H:V = 1:1.7. A 1 m high

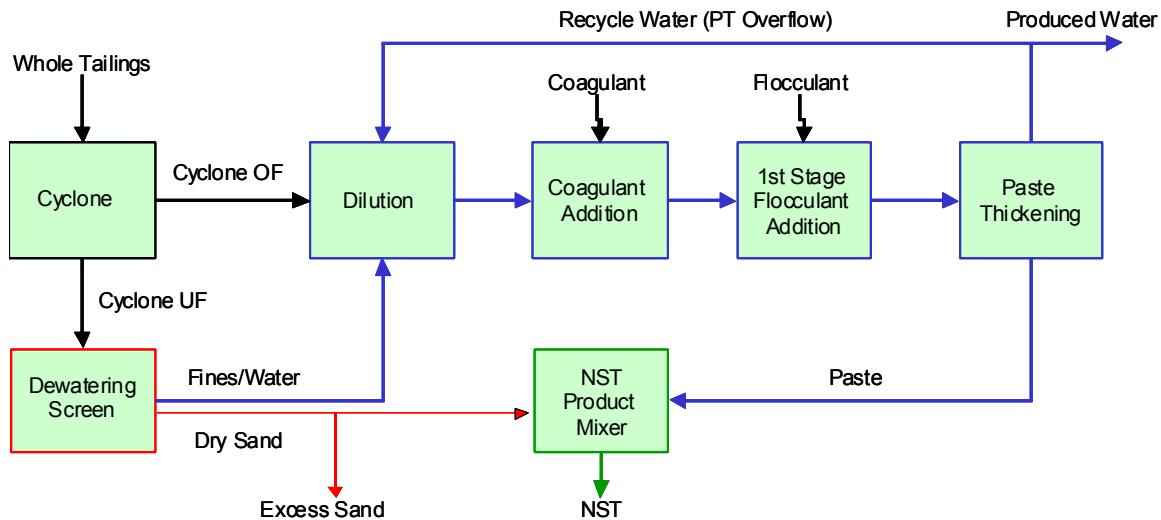


Figure 1. MRM TTF Process Block Flow: NST Production Mod

perimeter dyke was constructed around each cell.

Each cell was instrumented with:

- Two graduated posts for visual monitoring of deposit surface elevation. These were located at 1/3 and 2/3 of the cell length, labelled A and B. Post A was located closest to the tailings discharge point;
- Five stadia along the cell sides for supplementary tailings height measurements, one at each cell end and three evenly spaced along the cell length;
- One vibrating wire (VW) total pressure cell near Post A at the pond bottom;
- Six VW piezometers at 1 m vertical spacing from the base of the cell on Post A; and,
- Three VW piezometers on Post B, at heights of 1.4, 2.5 and 3.5 m from the bottom.

The instrumentation was connected to a data acquisition system for automatic data collection and storage. A typical instrumented cell is shown in Figure 2.

DEPOSITION AND MONITORING

Deposition

Three cells were filled with tailings material during testing programs in 2007 and 2008.

Cell 1 was filled with paste thickener underflow in 20 discrete deposition episodes from September to December 2007. This material is referred to as treated thickened tailings (TTT). The thickening process used gypsum and anionic flocculant to affect rapid settling and high overflow clarity in the paste thickener operation. A radial diffuser was used to reduce the slurry discharge velocity and limit the amount of shear during slurry placement. The thickener feed had variable sand-to-fines ratio (SFR), and variability in the particle size distribution of the thickener feed is reflected in the thickener underflow deposit.

The average composition and particle size distribution (PSD) data for Cell 1 TTT are presented in Table 1. In this paper, fines are defined as particles finer than 0.044 mm, in-line with industry convention.



Figure 2. Typical TTF cell instrumentation

Cell 6 was filled with high density NST slurry in 12 discrete deposition episodes over a span of 8 days in November 2007. The Cell 6 NST product data are shown in Table 1.

Table 1. In-line properties of deposited tailings

Cell	Tailings type	Bitumen content	Solids content	SFR ₄₄ =f ₄₄ /(f ₄₄ +w)	C _{f44}
		%	%		%
1	TTT	1.62	58	0.68	0.45
5	NST	1.85	77	4.73	0.37
6	NST	1.85	77	4.06	0.40

NST slurry with a higher SFR was deposited in Cell 5 in 19 discrete deposition episodes in May and June 2008. The Cell 5 tailings data are shown in Table 1. Figure 3 illustrates the use of tailings diffuser for placement of all NST and TTT material deposited in the test cells.

Monitoring

Monitoring data for the first 260 days after the start of deposition in Cell 6 are presented in Figure 4. The sub-aerially exposed surface slope measured during deposition in Cell 6 varied within 1% - 2%.

The data suggests correlation between deposit thicknesses on rate of excess pore pressure dissipation; for a deposit thickness less than two metres, excess pore pressures dissipated in a matter of two to three days whereas the rate of excess pore pressure dissipation decreased exponentially with increasing deposit thickness (see excess pore-pressure decay post-deposition). This demonstrates the highly non-linear relationship between rate of pore-pressure dissipation and average drainage path length. This effect becomes particularly significant when extrapolating pilot scale consolidation behaviour to commercial scale deposits with thicknesses of up to a hundred metres.

The monitoring results were initially back-analyzed using compressibility and hydraulic conductivity values as were derived from large-strain consolidometer testing of NST samples of similar composition and PSD. The time for excess pore-pressures to dissipate was found to be faster in the field testing program than was predicted using the laboratory derived compressibility and hydraulic conductivity values. In order to emulate the field performance it was necessary to increase the hydraulic conductivity values by an order of magnitude to get a close fit with field-scale performance.

Examination of the differences in surface settlement and excess pore pressure dissipation (Figure 4) demonstrates that, although surface settlement rates may decay to imperceptible rates, excess pore pressures will persist in the deposit and the full dissipation of excess pore-pressures lags obvious changes in surface elevation change. This strongly suggests that surface settlements should not be used to assess the extent of deposit consolidation and that the measurement of excess pore-pressure is a more reliable means of monitoring the extent of deposit consolidation.



Figure 3. Start of NST deposition in Cell 5

Effective stress is calculated by subtracting the excess pore-pressure in a soil element from the total stress applied to that soil element. Thus, when excess pore-pressures are high, effective stresses are low and when excess pore-pressures are fully dissipated then effective stresses are increased. This is very important since the strength of soils (i.e. resistance to deformation when subjected to stresses) is proportional to the effective stress in the soil element. Figure 4 illustrates the development of effective vertical stress at the bottom of the NST deposit in Cell 6, where the total pressure cell was installed.

DEPOSIT CHARACTERIZATION

Geotechnical characterization of the TTF deposits was performed in September and October 2008. This represents nine months since the end of deposition for the TT in Cell 1 and six months since the end of deposition for the NST in Cell 5.

The goals of characterization were the following:

- Assess the homogeneity of the deposits with respect to deposit density and particle size distribution;
- Assess the shear strength of the deposits as a function of density.

Deposit testing was done in three locations on the deposit:

- Site A (upstream of Post A);
- Site B (middle of the cell); and
- Site C (downstream of Post B).

Ponded water was present at the toe of each deposit – close to test location C – resulting in the softest ground conditions at this site for all deposits. This area was always damp and was periodically inundated by ponded water. The upper 0.3 – 0.4 m of the NST deposit surface was unsaturated at locations A and B, and the NST deposits were readily foot trafficable where the unsaturated crust was noted. This foot trafficability was adequate to access to these deposits with lightweight, manually operated testing equipment without any special load bearing mats or rafts. There was no unsaturated zone noted at the deposit surface at location C in the NST deposits; the decreased bearing capacity manifested itself as deeper indentations in the surface due to foot traffic.

The TTT deposit could only be accessed by foot traffic in some areas and even then with soft underfoot conditions. Most of the surface of the TTT deposit was desiccated with fissures extending to a 10-15 cm depth in all areas except the downstream ponded water area. Piezometers indicated that pore-pressure dissipation was not complete and the deposit was fully saturated to within 5 to 10 centimetres of the surface. Given that the surface was very soft, even for foot traffic, a floating platform was used to access and sample this deposit.

The characterization for each of the three deposits included the following field and laboratory testing methods.

Density profiling

Density profiling was performed by continuous sampling using the Cyre soft soil sampler. The core was extruded and cut at specified lengths for immediate weight measurement; the material was then used for moisture content testing. The core determined density was controlled by a more accurate push-in cylinder measurement at the surface. The cylinder densities differed less than 2% from the core densities at the same depths.

Sampling for laboratory testing

Collection of material for laboratory testing was done using the Cyre soft soil sampler, by repeated manual pushing adjacent to the locations where density profiling was performed.

Laboratory analyses

Laboratory analyses of core sub-samples included:

- Dean-Stark analysis for oil- water- solids percentages;
- Particle size distribution by sieve-hydrometer;
- Methylene blue adsorption; and
- Atterberg limits (for TTT only, as NST was found to be non-plastic).

These properties for NST in Cell 6 are shown in Figure 5. It can be seen that NST densifies from an initial 77% solids at discharge to about 84% solids in a consolidated state. These values are for fully saturated solid conditions and the mass of bitumen is

included as mineral solids mass after oven drying; therefore the densities are marginally higher than would be reported for bitumen-free samples.

A measure of fines storage efficiency (FSE), expressed in kilograms of fines per m^3 of stored tailings, can be calculated for each tailings deposit type. The FSE for TTT in Cell 1 is about 700 kg/m^3 , while the FSE values for NST in Cells 5 and 6 are about 300 and 350 kg/m^3 , respectively. Therefore, TTT can store about two times more fines than NST.

Cone penetration

Cone penetration testing (CPT) was performed to assess deposit stratification and provide continuous profiling of soil mechanical and hydraulic properties. The testing was conducted with pore pressure, natural (passive) gamma and seismic longitudinal and shear wave measurements (SCPTu). Pore pressure dissipation tests were conducted at selected depths. The SCPTu results for NST in Cell 6 are shown in Figure 6, with all 3 tests sites shown on each plot.

Important characteristics of CPT results in NST materials are high generated extra pore pressures and unusually low longitudinal wave velocities. The former is explained by a high percentage of fines in the pores of the coarse fraction in NST. The latter may be the result of air entrained in tailings in the NST mixing plant and during pumping.

Shear strength estimate from SCPTu data for Cell 6 is shown in Figure 7 and discussed in section 5.9. The strength values are calculated using a constant strength parameter value $N_k = 15$ for all cells. The N_k is usually varied between 10 and 20.

Continuous Surface Wave System (CSWS)

The CSWS testing uses surface Rayleigh waves to determine shear wave velocities at various depths. The use of computer-controlled vibration source and multiple receivers makes it more accurate and repeatable than the conventional SASW testing.

The setup consisted of six geophones spaced one metre apart, with the vibrator 2 m away from the geophone string. The wave frequency was varied from 7 Hz to 150 Hz. The depth of penetration was 5 m, to the bottom of the cell. Tests were performed on areas that had and had not been disturbed by foot traffic. Slight differences in the velocities measured were evident in the upper 30-40 cm of the deposits. The CSWS velocities in NST in Cell 6 are shown in Figure 6, together with the seismic CPT data.

Ball penetration

Ball penetration is a novel testing technique for continuous shear strength profiling of soils. It does not require the correction for overburden pressure and the results are more sensitive due to a large probe area. Ball penetrometer testing has the potential to provide more accurate undrained shear strength estimates in soft sediments than CPT. It also allows determination of residual (fully remoulded) strength by cyclic push-pull action, which is not possible with CPT.

Ball penetration testing was done to assess sensitivity and accuracy of shear strength determination relative to CPT. Residual strength tests were conducted at two depths in each hole by repeated push-pull action over a stroke of 0.5 m. The strength values for the ball penetration were calculated using the constant strength parameter value $N_{ball} = 10.5$. The N_{ball} value usually varies within the

range of 9 to 13. Ball penetration shear strengths are shown in Figure 7 and discussed in section 5.9.

Vane shear testing

Vane shear is a traditional undrained shear strength measurement technique. Vane shear testing was conducted for comparison with shear strengths obtained by the CPT and ball penetrometers. The rotation speed was initially about 0.5-1.0°/s until peak strength, and then the rate was increased to about 3°/s for residual values. Measured strengths were not normalized to a unique rotation rate. Vane shear strengths are shown in Figure 7.

Marchetti dilatometer (DMT)

Marchetti dilatometer was used to determine tailings compressibility and strength parameters including constrained modulus; undrained strength or friction angle (depending on the type of deformation assumed – undrained or drained); and overconsolidation ratio (OCR). Dilatometer reading were recorded every 25 cm until the bottom of the cell. The DMT shear strength data in Cell 6 are shown in Figure 7.

Shear strength method comparison

Comparison of all shear testing methods in Figure 7 allows for several interesting observations.

Continuous peak strength curves of CPT and ball penetration methods show linear increases with depth, a distinctive feature of normally consolidated (NC) soils. There is a 30-40 cm thick surface crust, created by drying and freezing, with increased shear strengths on all 3 testing locations.

Peak shear strengths from ball penetration are consistently highest in magnitude for the

same depths on all 3 testing locations A, B and C. Vane peak strengths are in overall good agreement with the ball peak data, while CPT strengths are consistently lower than both ball and vane peak strengths. The CPT strengths were calculated using a constant value of the strength factor N_k and that this parameter can be adjusted to better fit CPT strengths to other data.

The ball and vane methods predict similar residual strengths, with minor differences at location C, where the ball data are slightly higher. It can be seen in Figure 7 that the DMT method produces residual shear strength data. The DMT measured strengths are similar in magnitude to residual strengths determined from the other three applied testing methods.

The data suggests slightly reduced shear strengths for deposit material at the toe of the deposit relative to material in the higher and drier positions, where a 30-40 cm thick surficial unsaturated crust was noted at testing locations A and B.

Minimum peak strengths in Cell 6 are recorded by the CPT method just below the surface crust, and they are all above the 5 kPa threshold. The residual strength varies linearly from about 1-2 kPa near surface to about 5 kPa at 5 m depth. The sensitivity (ratio of peak to residual strength) of Cell 6 NST varies in the range 4-5.

FIELD LOAD TESTS

As a next step in the bearing capacity testing of the TTF tailings deposits, surface load tests were performed in Cell 6 using concrete blocks laid on the tailings surface (as a simple static loading assessment) and, in Cell 5, using the plate load test equipment.

A large concrete block was used to provide a contact load of 35 kPa directly to the surface of the consolidated NST deposit surface in Cell 6. The block was supported by a stiff desiccated surface crust, and negligible settlement was observed after load application. Another test with using the same block in a different orientation exerted contact pressure of about 17 kPa to freshly uncovered NST deposit at a depth of 30 cm below the deposit surface. Several centimetres of 'creep' settlement were observed in this test over a year after load application. These two tests roughly bounded the range of static bearing capacity for the surface loading problem of a two-layer NST deposit.

Four plate load tests (PLT) were performed in Cell 5, with a rigid 30 cm diameter plate. The testing procedure with settlement stabilization at each load increment was favouring drained deformational behaviour. Two tests were performed at tailings surface, two on fresh, soft tailings about 30 cm below it. The bearing capacities varied roughly between 20 kPa at depth to 50 kPa at the surface. The lower end PLT bearing capacities match the minimum peak shear strength values obtained in penetration values.

At the ends of two tests, a series of loading-unloading cycles was performed, with maximum stress less than the bearing capacity. Incremental settlements in the cycles were not decreasing in magnitude, which indicated potential for accumulation of pore pressures under dynamic loading.

TRAFFICABILITY

Two trafficability tests were performed with heavy mine dozers on NST in Cell 6 in the summer conditions, with a desiccated surface crust, and in winter conditions, with a frozen

ground layer at the surface. The testing consisted of two steps, the first with static, the second with dynamic, cyclic loading of tailings surface. Pore pressure build-up was measured under the trucks of test dozers; piezometers were located in soft tailings under the harder surface crust. It was found that cyclic loading causes accumulation of pore pressures up to a complete liquefaction. Therefore, trafficability is related solely to the properties of stiff surface crust, and further testing will be directed toward investigation of relevant climatic factors governing the behaviour of tailings surface layer.

CONCLUSIONS

The following conclusions were made based on the field observations to date:

- The TTT and NST produced at the TTF had very high fine capture efficiency and were deemed to be non-segregating. Geotechnical index testing showed overall spatial homogeneity of the TTT and NST deposits.
- Fines capture was 300 to 350 kg of fines per cubic metre of NST deposit and approximately 700 kg of fines per cubic metre of TTT deposit.
- Consolidation of the NST deposits occurred more rapidly than predicted based on finite strain model predictions that were based on compressibility and

hydraulic conductivity data derived from large strain consolidation testing.

- The TTT and NST deposits demonstrated typical normally consolidated soil behaviour; after dissipation of excess pore pressures, resistance to shear was negligible near the surface and linearly increasing with depth except where the near surface deposit showed overconsolidation characteristics due to drying, desiccation, and freeze-thaw effects.
- Load-deformation response to surface loads and during trafficability testing of NST tailings is of the undrained type, as a result of slow dissipation of excess pore pressures due to large amount of fines in the sand pore space. Cyclic loading has tendency to accumulate generated excess pore pressures up to a complete liquefaction.

ACKNOWLEDGEMENTS

The authors wish to thank Shell Canada Energy for permission to publish the information contained in this paper. Thanks also to Hatch, Klohn-Crippen Berger Ltd., Golder Associates, Geoforte, David Taplin Consultants, Barr Engineering, and ConeTec for providing essential engineering and technical support to the project. Special thanks are extended to Shell's entire TTF team and the Shell Albian Sands operations and management team for their continued support.

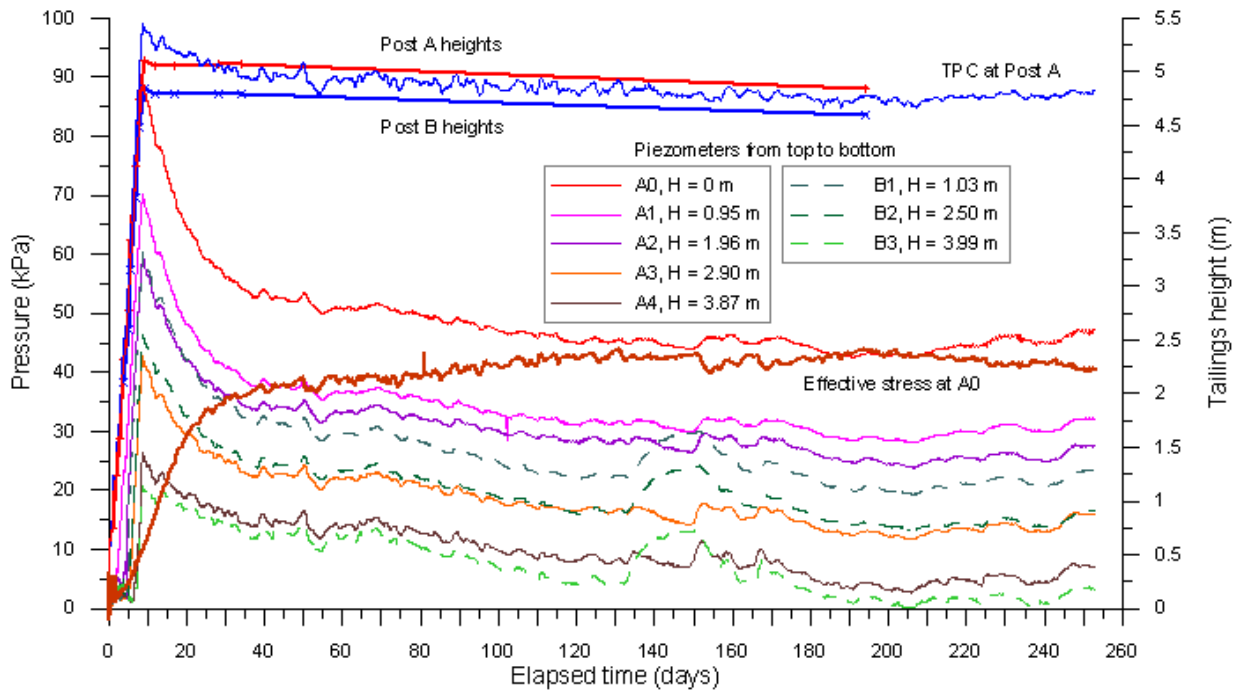


Figure 4. Cell 6 monitoring data: tailings heights, pore pressures and total pressure at cell bottom

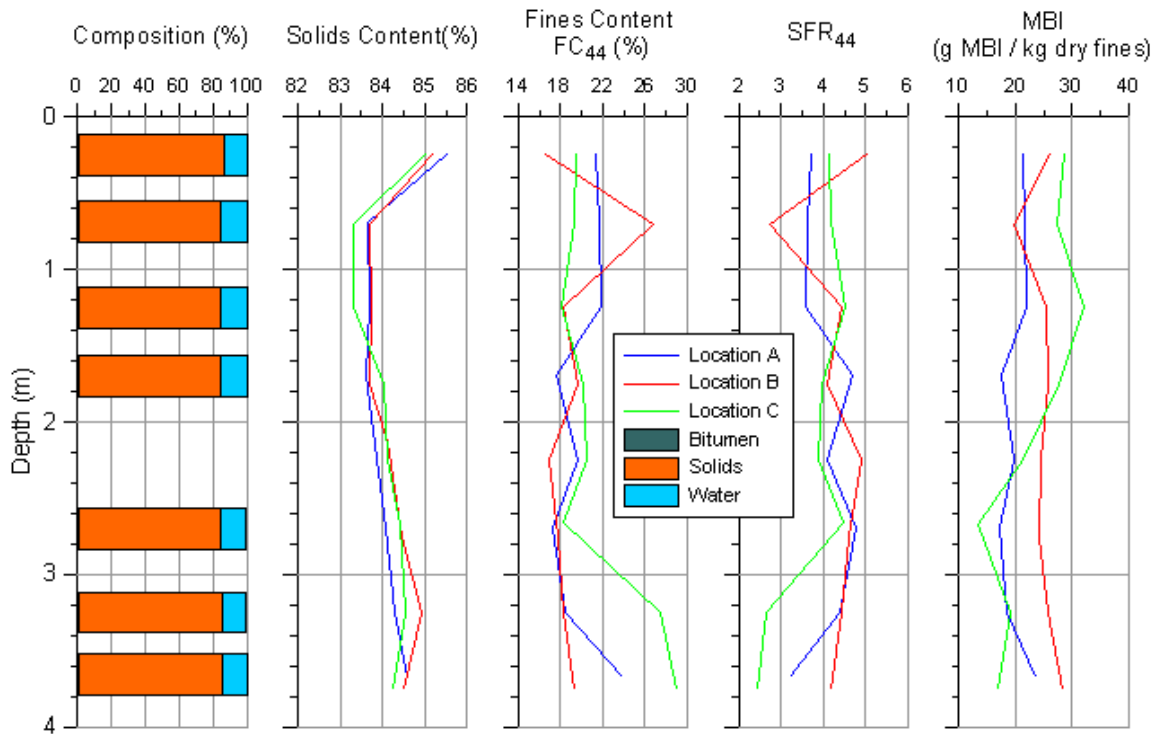


Figure 5. Cell 6 laboratory testing: composition and geotechnical index properties

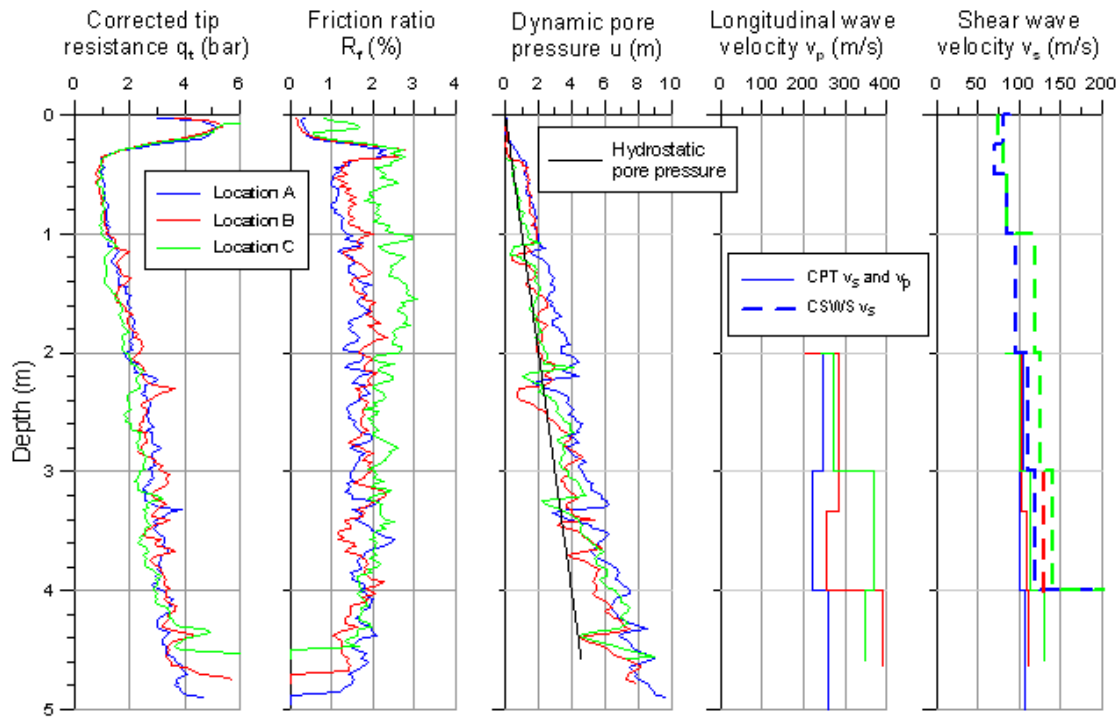


Figure 6. Cell 6 CPT and CSWS testing

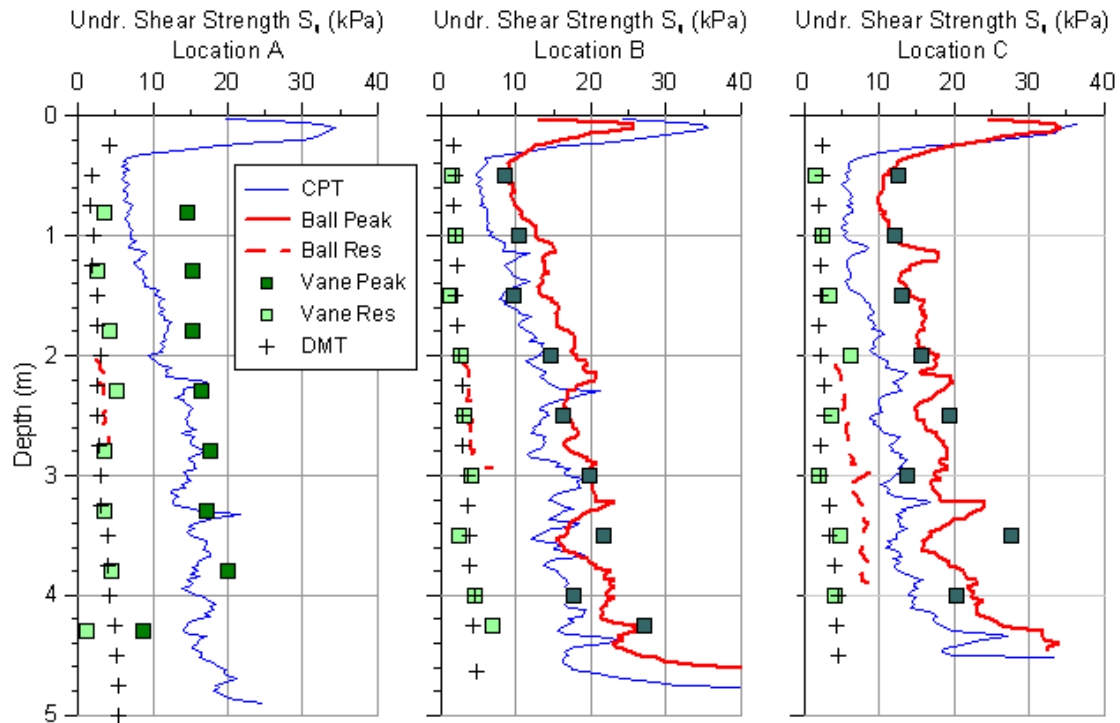


Figure 7. Shear strength investigation in Cell 6: CPT, ball, vane and DMT data

PASTE PUMPING AND DEPOSITION FIELD TRIALS AND CONCEPTS ON SYNCRUDE'S DEWATERED MFT (CENTRIFUGE CAKE)

I. Ahmed, M. Labelle & R. Brown

Golder Paste Technology Ltd., Sudbury Ontario, Canada

R. Lahaie

Syncrude Canada Ltd., Fort McMurray, AB, Canada

ABSTRACT: Syncrude Canada Ltd. (Syncrude) continues to investigate alternative tailings management technologies, in search for a commercially viable method of dewatering mature fine tailings (MFT) at their Mildred Lake facility. Syncrude developed a novel approach, processing MFT with a centrifuge pilot plant that resulted in cake consistencies of 55 wt% solids and a centrate of less than 0.5 wt% solids. The centrifuge cake, once produced must be transported, deposited and ultimately placed for reclamation. Golder Paste Technology Ltd.'s (Golder PasteTec) role was to assess the pumpability of the centrifuge cake. This was accomplished in two stages, first by conducting on-site bench scale rheological tests to characterize the centrifuge cake. Yield stress and slump values for sheared and unsheared centrifuge cake samples, produced under different conditions, were obtained. The results lead to the understanding that centrifuge cake behaved similar to paste, following a Bingham plastic model and when sheared, the material can be pumped. PasteTec then designed and implemented an on-line mobile flow loop system to verify the material's pumpability. Using a positive displacement pump, centrifuge cake was transported through a nominal 100 mm diameter pipeline (about 50 m long) to evaluate the friction losses under various operating conditions. The tests illustrate that an estimated 10 and 5 kPa/m friction factor can be expected for a 200 mm (at 1.4 m/s) and 350 mm (at 1 m/s) diameter pipe, respectively. These values are scaled up from the field data and based on a centrifuge cake of 54.5 wt% solids. Syncrude and Golder PasteTec have demonstrated that dewatered MFT of paste consistency can be transferred using positive displacement pumps. The challenge that remains is in engineering the means to place the considerable volume of paste generated.

INTRODUCTION

The oil sands of northern Alberta, are mined and processed for the production of bitumen. Oil sands exist as a mixture of mineral material (sand, silt and clay), bitumen and

water. Resulting from the bitumen extraction process are tailings that mainly consist of sand, silt, clay and water with minor amounts of bitumen. The coarser sand is used to form dykes and beaches, whereas the fine clays and other solids, form Mature Fine Tailings or

MFT (Liu et al, 2006). MFT does not readily densify in the pond environment. Even after 10 years or more of placement, MFT only settles to about 30 to 35 wt% solids. Currently, about 600 million m³ of MFT exists within the tailings ponds of northern Alberta's oil sand producers (Houlihan et al, 2008). This poses the following issues:

- MFT will indefinitely occupy a large area of the mine site with the need for continued containment;
- At times the tailing pond's footprint sterilises oil sand reserves;
- Potentially available recycle water for the extraction process is tied up in the MFT;
- MFT does not accommodate traditional approaches to closure using cover material because of its high water content and low bearing capacity; and
- Mitigative efforts are required to ward off waterfowl and shorebirds from MFT ponds.

Syncrude's existing approach is to dredge some of the MFT from the disposal pond (after 3 or more years of settling) and blend these with new tailings and a chemical agent to produce Consolidated Tailings (CT). The CT forms a non-segregating mixture which may be reclaimed to a solid deposit. However, with this method, residual fine tailings that are still produced, require further treatment or placement. As well, only a portion of the MFT is used in the CT process. Different technologies for MFT treatment remain very necessary.

There has been a great deal of research in terms of methods of processing MFT and, in recent years, much focus has been placed on the use of thickening/filtration techniques with flocculant addition (Yuan and Shaw, 2006; Wang et al, 2008; Li et al, 2008).

Others have studied more fundamental parameters in an attempt to understand the mechanisms that affect solids settlement (Omotoso et al, 2002; Liu et al, 2006; Uhlik et al, 2008). Syncrude continues to investigate alternative technologies for a commercially viable method of treating MFT. At their Mildred Lake facility in Fort McMurray, Syncrude commissioned a centrifuge pilot plant to study the dewatering of dredged MFT from their pond. Golder Paste Technology Ltd.'s (Golder PasteTec) role was to assist Syncrude in examining the pumpability of the resulting centrifuge cake. As this was the first attempt at pumping MFT at such a dewatered level, a two step approach was undertaken. First, evaluate the centrifuge cake's rheological behaviour, to assess the potential to pump as well as to examine the centrifuge pilot plant layout for subsequent flow loop set up. Second determine the centrifuge cake's transportation characteristics via actual flow loop testing, using a positive displacement pump.

The initial testing focused on examining the centrifuge cake's yield stress under a variety of conditions (solids content, flocculant dosage). Yield stress is a measurable parameter that indicates the effort required to pump a certain fluid or in this case paste. Once yield stresses were obtained, it became apparent that if the centrifuge cake was to be pumped, then it should be sheared first, since the sheared values were significantly lower; i.e., shearing the centrifuge cake to produce a more flowable paste. As a result of understanding the centrifuge cake's rheological behaviour, a flow loop was designed to verify pumpability. It was confirmed that the centrifuge cake can be successfully pumped with positive displacement pumps. The centrifuge cake's rheological characteristics were determined, following a Bingham plastic model, exhibiting similar behaviour to paste. This allowed for the calculation and estimation of friction factors for larger diameter pipes.

BACKGROUND

The development of paste technology began 30 years ago with the objective of processing mill tailings from metal mines into a cemented mixture for engineered backfill applications. Ground support for the underground operations can be provided by the paste backfill. In the last 10 years the use of paste technology has become more wide spread and the preferred backfill method of mines world wide. In the early 1970's dewatering metal mine tailings to a paste consistency for surface disposal was also being considered and it was first used in a mill located in northern Ontario (Robinsky, 1999). However, it was not until 2000, with the success of Bulyanhulu in Tanzania that paste concepts for surface disposal gained increasing acceptance in the metal mining industry (Landriault, 2006). As Bulyanhulu became the first operation to incorporate both surface and underground paste disposal methods for the complete treatment of mill tailings (Landriault et al, 2001).

Paste is defined as a densified uniform material of such mineralogical and size makeup, that it will bleed only minor quantities of water when at rest, experience minimum segregation and can be moved in a pipeline at line velocities well below that of critical velocities for similar sized materials at lower pulp densities. A true paste, without cement, can remain sitting in a pipeline for extended periods of time.

The paste's slump is normally measured with an ASTM 30.5 mm (12 inch) slump cone, a standard tool used in the concrete industry; values in the range of 6 to 10 inches are typical. Paste can generally be produced from materials with a wide range of size distributions; however, pastes usually contain a minimum of 15% by weight of minus 635 mesh (20 μm) material. Mineralogical makeup is sometimes important, as not all materials within the outlined size distribution make a paste. With Syncrude's MFT, testing conducted under a different program

indicated that 66% by weight of the material passes 20 μm .

MFT CENTRIFUGE CAKE BENCH SCALE RHEOLOGY – PHASE 1

The objective of this phase of the study was to assess the rheological characteristics of the resulting centrifuge cake from the MFT centrifuge pilot plant. Also, to evaluate whether the cake could be transported via positive displacement pumps.

Material and Procedure

Bench scale rheological characterisation of the centrifuge cake was performed on sheared and unsheared grab samples and the static yield stresses (or simply termed yield stress in this paper) obtained from Syncrude's pilot plant. Along with the yield stress, the initial slump of the centrifuge cake was also measured. These slump tests were performed with a concrete industry standard, ASTM 30.5 mm slump cone. With smaller sample sizes, a mini cone was used to assess the slump and correlate back to the actual slump value.

Yield stress was determined by the yield vane technique using a Brookfield viscometer (DVII). This method uses a sensitive rheometer to slowly turn a vane (spindles V71, V72 and V73) immersed in the material, while constantly monitoring the torque on the spindle. Once the maximum torque is registered, the peak or 'yield' stress is calculated. This method was carried out on several samples produced under different centrifuge operating conditions, balancing flocculant dosage with centrate quality. Each individual sample was split into 5 to 6 beakers. Here, a calculated amount of water is carefully blended into the sample for dilution purposes, creating successively lower solid contents. A relationship between yield stress and solid content was then developed. Each sample was then sheared and retested,

thus constructing a new curve indicative of the material's sheared yield stress values. Slump tests were performed with a concrete industry standard, ASTM 30.5 mm slump cone for each initial grab sample. Due to the small quantity of the diluted samples, a mini cone was used to assess the "mini slump" and the value was correlated back to an approximate actual slump value. Solids content for each sample was tested using a Mettler Toledo HR 83 Halogen Moisture Analyser.

Results and Discussion

Yield stress is defined as the minimum force required to initiate flow. It is also indicative of material consistency once the relationship is established. The yield stress curves illustrated in Figure 1 were obtained from centrifuge cake samples produced from different operating conditions. The relationship between solids content and yield stress is usually exponential for stable mineral pastes.

The results of these tests indicate that unsheared samples exhibit unusually high yield stresses at a given solids content compared to typical metal mine pastes. This is due to a combination of fine particle size, clay mineralogy, pore water chemistry, flocculant dosage and solids content. In comparison, sheared tests had a significant reduction in yield stress, especially under higher and tested flocculant dosages of 1360 g/tonne (samples a and b). Other sheared tests (samples c and d) resulted in yield stresses of less than 600 Pa, at solids content of less than 55%.

These results were evaluated against Golder PasteTec's database of tailings samples tested and the analysis led to the understanding that it would be possible to use positive displacement pumps to transport centrifuge cake under sheared (i.e. paste) conditions. Therefore, a plan was developed to conduct flow loop testing on site, to ultimately gather

data for pump and pipeline scale up and design.

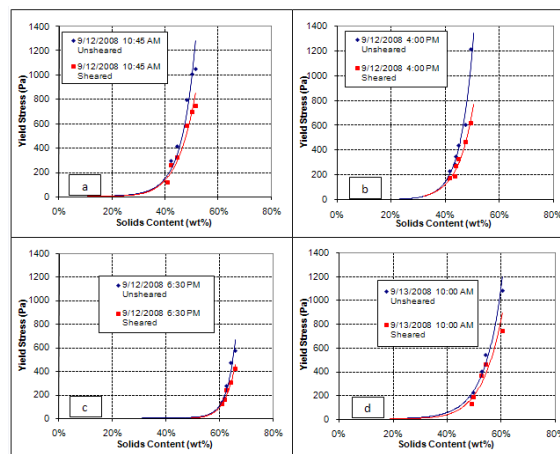


Figure 1. a) Initial solids 51.4%, flocculant dosage 1360 g/tonne; b) Initial solids 49.3 wt%, flocculant dosage 1360 g/tonne; c) Initial solids 65.73 wt%, flocculant dosage of 400 to 770 g/tonne; d) Initial solids 60.6 wt%, flocculant dosage 780 g/tonne.

ON SITE FLOW LOOP TESTING WITH CENTRIFUGED MFT – PHASE 2

A flow loop was designed such that live feed could be received from the centrifuge pilot plant. Pressure loss and volumetric flow rate data can be captured in real time through the flow loop. Tests were conducted under various conditions.

The pumped centrifuge cake was then deposited within a contained area for further geotechnical testing by Syncrude.

Rheology

Rheology is defined as the science concerning flow and deformation of matter. Many rheological models have been investigated to better understand the flow properties of paste or thickened tailings. Attempts to theoretically treat thickened tailings and paste

using slurry rheology models have not yet been greatly successful.

Many parameters contribute to the measured friction losses, including particle size distribution, particle angularity, solids density and the general nature of the suspension. Stable mineral pastes are usually considered to be non-Newtonian fluids as they possess a yield stress, and their flow properties change at different shear rates.

PasteTec's test program is designed to gather a fundamental understanding of the centrifuge cake's rheological behaviour under specific pilot plant operating conditions. In this case, it was determined that the Bingham plastic model suitably characterised the fluid/paste. This is because the paste possessed a defined shear stress, also known as yield stress, (when shear rate = 0) and exhibited a linear shear rate to shear stress relationship.

FLOW LOOP SETUP AND TESTING PROCEDURE

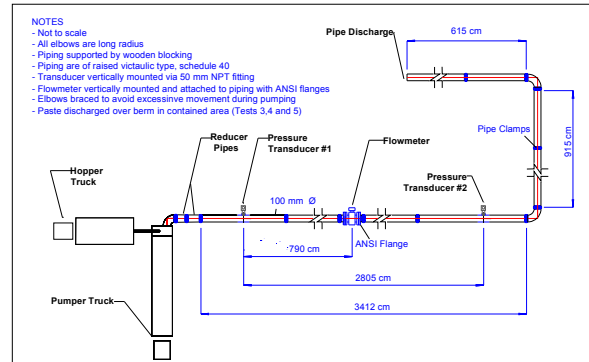
Piping Layout

The flow loop was conducted on relatively flat ground on the eastern side of the MFT centrifuge pilot plant. The loop was surveyed by Syncrude. The elevation difference between the two transducers was 14 mm and thus the pressure differential due to static head contribution is negligible.

Five individual test runs were completed and the piping layout is illustrated in Figure 2. The pump discharge is 150 mm in diameter. It is immediately connected to a 150 mm diameter elbow. From the elbow, two reducers, one from 150 mm to 125 mm (length of 70 cm) and another from 125 mm to 100 mm (length of 100 cm) were used to bring the line diameter down to 100 mm. The pipes (3.048 m each length) themselves were of the Schedule 40 raised Victaulic type. These were secured with gaskets and clamps.

Couplings were fabricated to join the raised Victaulic pipe to the ANSI flanged flowmeter.

Figure 2. Flow loop set up for tests 3, 4 and 5. Note that for tests 1 and 2, the 615 cm discharge pipe and the preceding 90°



elbow were not installed.

Hopper and Pump Trucks

The centrifuge cake was deposited into a hopper truck first and then discharged into the pumper truck. The hopper truck was a modified volumetric concrete mixer. It provided suitable surge capacity and a high rate shearing auger to handle the centrifuge cake.

The pipe was connected to a trailer mounted Concord CML 120 positive displacement pump (situated on the pumper truck) that was in good operating condition. A new cutting ring and wear plates were installed prior to testing to ensure a tight seal and to allow the pump to perform efficiently.

Data Logging Equipment

The data logging equipment consisted of a DAQCard data logger inserted into one of the PCMCIA slots of a laptop computer running Virtual Bench Logger software. The pressure transducers were installed in the pipeline and connected to the data logger. Two transducers were used in total with the 100 mm diameter pipe. The transducers have a range of 0-600 psi (4136.85 kPa) and are

safety rated to double this pressure to reduce the risk of damage to the diaphragms from pressure spikes during pumping. The Endress and Hauser transducers are self-calibrating and have proven to be reliable in the field.

A typical set of pressure transducer and flow velocity output measurements is presented on Figure 3. Data from the two transducers and flowmeter were gathered at 0.05 s intervals. The strokes made by the positive displacement pump are clearly evident as abrupt reductions in pressure. The “flat” pressures between the strokes are indicative of the paste being pumped at a constant rate. The pressure losses were calculated by first, averaging the “flat” sections of the chart for each of the transducers and then subtracting the differences between the two. The pressure differentials are then divided by the distance between the transducers to provide a pressure loss per length.

Material

Up to approximately 12 m³ of material was provided by Syncrude for each test. The centrifuge cake was deposited in a pit for Tests 1 and 2. Subsequently (Tests 3, 4 and 5), the spent material was deposited into a contained area where further geotechnical testing can later be performed by Syncrude.

Procedure

Centrifuge cake was conveyed via a short 60 foot (18.3 m) transfer conveyor onto a 180 foot (54.9 m) telescopic stacker. Discharge from the telescopic stacker was received in the flow loop system by a 7 m³, mobile hopper. From here the centrifuge cake was transported via a screw conveyor to a mixing auger located on the concrete pumper truck. The pump’s output velocity was varied while a consistent material feed was charged to the flow loop.

For the duration of each test, the conditions at the pilot plant were closely monitored to

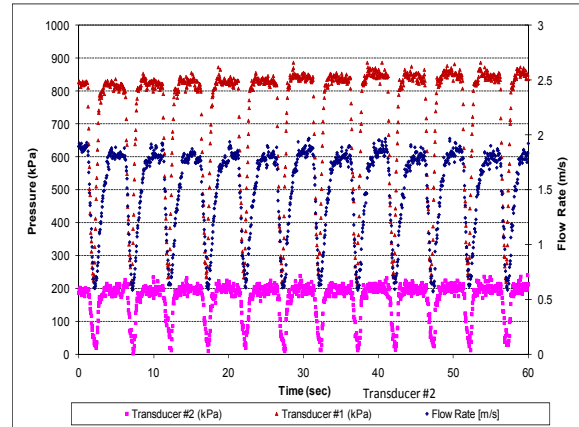


Figure 3. Typical data set for a flow loop run at constant pumping rate

maintain operating conditions that were as constant as possible, such that material entering the flow loop system was consistent. The mobile hopper acted as surge storage for the centrifuge cake. It took roughly 1.5 hours to fill the hopper, when flocculant was applied and over 2 hours without flocculant. Each flow loop run required 2 full hoppers of material. As the flow loop testing program progressed, grab samples from the screw conveyor discharge were taken and analysed for solids content (using a Mettler Toledo HR 83 Halogen Moisture Analyser). In doing so, the feed material was confirmed to be consistent for the duration of the test. Because the centrifuge cake was transported via a screw auger to the concrete pumper’s mixer, shearing was introduced to the material prior to pumping. The shearing rate was held constant for all tests.

Each data set during testing is comprised of one minute of data for each flow rate for a particular centrifuge cake production run. Once a data set was completed, the flow rate was adjusted and another data set was taken. Over 10 data sets per test were recorded. In order to assess flow properties shear stress and nominal wall shear rate, a ramp up, then ramp down of flow rates were carried out. Slump tests before and after pumping were also taken to assess qualitatively the material’s transportation characteristics.

At the end of testing each day, the pipes were flushed to remove any material in the lines.

FLOW LOOP RESULTS

Data Analysis – Flow Velocity versus Pressure Loss

The raw data obtained directly during testing was analyzed statistically to remove pressure fluctuations and pump spikes. The remaining data was averaged to generate one data point for pressure loss and flow velocity. Plotting out all data points obtained during testing for a particular centrifuge plant operating condition provides an assessment of the

materials shear properties over time. Table 1 describes the different centrifuge cakes tested. The legends referred to in the following figures correspond to references made in Table 1. An additional test was attempted, where half (approximately 650 g/tonne) of the flocculant dosage was used. The resulting centrifuge cake was watery and would not have been contained in the hopper truck as the material would have leaked out of the flashing underneath. The consistency of the material would have been suitable for pumping.

Figure 4 illustrates the pressure loss data obtained at different flow velocities (Tests 3, 4 and 5)

Table 1. Centrifuge cake material characteristics for each test

Run	Slump (mm)	Solids Weight %	Flocculant Dosage (g/tonne solids)
Test 1	100	54.3	1300
Test 2	100	54.6	1300
Test 3	100	54.5	1300
Test 4	113	52.1	1300
Test 5	175	68.9	0

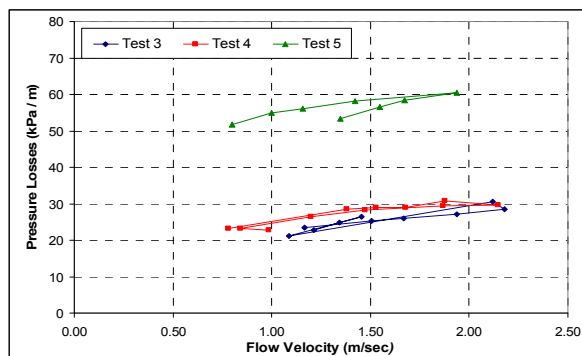


Figure 4. Pressure loss vs. flow velocity for a 100 mm diameter schedule 40 pipe

Wall Shear Stress versus Nominal Wall Shear Rate

The centrifuge cake followed the Bingham Plastic flow model closely, and exhibited very little shear thinning. The flow curve data fit the applied linear trendline with a

reasonable R^2 value, indicating minimal variance of the data points from the applied regression.

In order to scale up data from smaller diameter pipelines, the fluid must be characterized according to its flow properties, which can be determined by analyzing shear stress versus shear rate data. If there is a linear relationship between shear stress versus shear rate data, and the y-intercept is not equal to zero, the material is classified as a Bingham fluid. Once the fluid is characterized, the correction for shear rate can be calculated. The typical method for determining shear rate is simply the $8V/D$ relationship, which is $8 \times \text{flow velocity} / \text{inner diameter of pipeline}$. This equation works well for fluids exhibiting Newtonian behaviour in the laminar flow regime. To account for non-Newtonian behaviour of the

paste, a correction must be applied to the $8V/D$ shear rate. The equation to calculate the wall shear rate for non-Newtonian Bingham fluids is;

$$\dot{\gamma}_w = ((1+3\dot{\eta})/4 \dot{\eta}) \times (8V/D) \text{ Equation 1}$$

where;

$$\dot{\gamma}_w = \text{Nominal Wall Shear Rate}$$

$$\dot{\eta} = \ln(T_w) / \ln(8V/D) \text{ Equation 2}$$

$$T_w = D(dP)/4L \text{ Equation 3}$$

D = Inner Diameter of Pipeline

L = Length of Pipe

Once the raw data from the flow loop is reduced to pressure losses, and the flow velocities are converted to shear rates the flow curve graphs can be generated. From these graphs, the trendline equation is used for the scale up model. The actual data used from the trendline equation typically does not involve the extrapolation of the results since the shear rate in larger diameter pipelines is less than smaller diameter pipelines. A sweep of flow rates is assessed to make available experimental data for low shear rate conditions. Figure 5 shows the nominal wall shear rate versus shear stress results for Tests 3, 4 and 5.

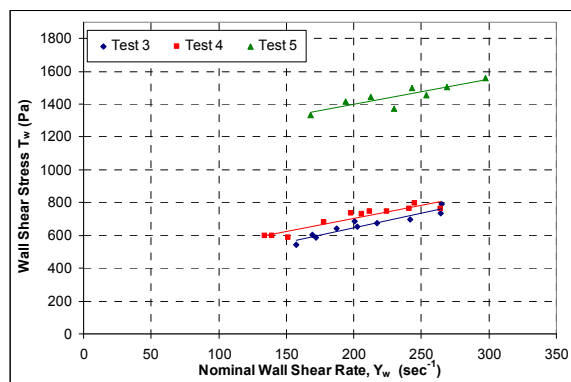


Figure 5. Wall shear stress vs. nominal wall shear rate for a 100 mm diameter sched 40 pipe

Pipe Pressure Loss Scale Up Calculations

Once the operating conditions are established, the corrected shear rate can be calculated using the above equations, and the corresponding shear stress (T_w) can be selected off the flow curve graphs. By substituting T_w , D and L into Equation 3, dP can be solved for and the scaled up pressure losses obtained. For these calculations, it is assumed that incompressible plug flow conditions exist in the pipeline.

OBSERVATION AND DISCUSSION ON FLOW LOOP

Material Transportation Behaviour

The centrifuge cake was easily cleaned out each night by pumping water through the lines along with some soap. The pipes were inspected at the end of each day as well as individually at the end of the flow loop testing program and were found to be clean and free of material build up.

Slump testing was performed prior to pumping, as the material entered the pump truck's hopper and at the end of the pipe discharge. A small change in slump was observed. For example in Test 1 the measured slumps before and after pumping were 100 mm and 113 mm, respectively. This suggests that the material exhibited only slight shearing or shear thinning while being transported in the pipe. Further, upon leaving the sample for extended periods of time (approximately 24 hours), there was no observable water bleeding or segregation of material within the centrifuge cake structure.

Scaling Up Pipe Pressure Loss

This section details the pipe pressure loss analysis that is scaled up from the actual 100 mm diameter, schedule 40 pipe flow loop

tests performed on site. This is based primarily on the centrifuge cake or paste being produced at a hypothetical 1.8×10^6 tonne/year or 268 tonne/h solids at a target flow velocity of 1 m/s. Trials 1, 2 and 3 correspond to the operating conditions for the centrifuge plant that yielded high solids content in the centrifuge cake and an acceptable amount of solids in the centrate. Scaled up pipe pressure loss values for the various tested conditions are presented for comparison (Table 2).

Figure 6 illustrates the pressure loss variations with flowrate for Tests 3, 4 and 5 scaled up to a 350 mm diameter schedule

40 pipe. Normally, flow loop testing using the actual pipe size is necessary prior to installation.

It is also evident that pressure losses are greatest when flocculant is not used in the centrifuge process (Test 5). It represents more than twice the unit friction loss compared to targeted plant operating conditions (Tests 1, 2 and 3). Should a positive displacement pump system be used for transporting centrifuge cake, it would be important to note that failure of the flocculant delivery system means that the pipeline could plug, therefore the plant should be shut down and pipes flushed out.

Table 2. Predicted pipe pressure losses for 200 mm and 350 mm diameter schedule 40 pipe, based on 100 mm diameter schedule 40 pipe data

Parameter	Test 3		Test 4		Test 5	
Weight % Solids	54.5		52.1		68.9	
Calculated Solids Flow rate [tonne/h]	268		268		268	
Paste (solid and liquid) Volumetric Flow rate [m ³ /h]	329		352		226	
Pipe Diameter for Schedule 40 Pipe	2 pipes x 200 mm	350 mm	2 pipes x 200 mm	350 mm	2 pipes x 200 mm	350 mm
Paste (solid and liquid) Flow Velocity [m/s]	1.4	1.0	1.5	1.1	1.4	1.0
Pressure Loss [kPa/m]	10	5	12	6	26	15

Overall, the centrifuge cake's transportation characteristics are similar to that of other metal mine pastes. When compared to these other pastes, in general, the centrifuge cake has a lower solids content with a lower

slump. The quantity of flocculant used in this pilot plant testing, greatly impacts the rheological behaviour of the material and therefore the pressure loss profile of the resulting centrifuge cake.

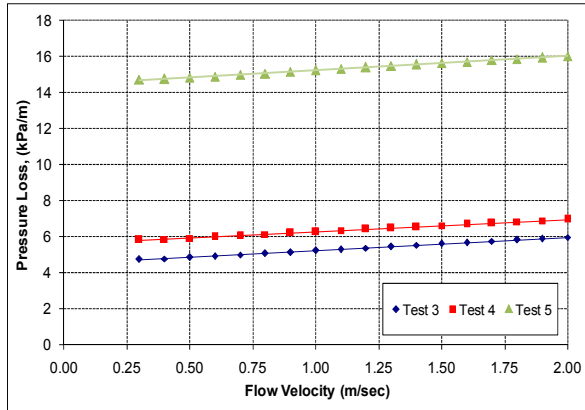


Figure 6. Scaled up pressure loss vs. velocity for a 350 mm diameter sched 40 pipe

Material Deposition

The centrifuge cake was deposited into a bermed surrounding (Figure 7). The material formed an intermediary cone. This cone took shape and collapsed periodically but resulted in a flowing paste pile, creating a sloped deposition. The paste appeared to expand as it was discharged from the pipe. Near the toe of the paste pile, cracks were formed on the surface. This feature is particularly interesting as the paste is then exposed to the air with a greater surface area and the potential for natural desiccation.

CONCLUSION

Through field pumping trials, it was confirmed that MFT centrifuge cake can be pumped with a positive displacement pump, provided the cake was first sheared in a mixer.

The rheological characteristic of the centrifuge cake, similar to paste, follows a Bingham Plastic model. With this understanding, it was possible to model and predict the friction loss values for study purposes from field data to pipes of larger diameters. For example, with 54.5 wt% solids in the centrifuge cake an estimated 10 kPa/m can be expected for a 200 mm

diameter pipe at a flow velocity of 1.4 m/s. Similarly, a 5 kPa/m friction factor can be expected for a 350 mm diameter pipe at a flow velocity of 1.0 m/s



Figure 7. Paste discharge and illustration of deposition angle. Note surface cracking of deposited paste

When deposited, it was apparent that the paste formed a sloped surface with minimal water bleed. Surface cracking of the deposited paste was also visible as the deposition front advanced.

REFERENCES

R.Houlihan, H.Mian, and the ERCB Tailings Team, “Past, Present, Future Tailings Regulatory Perspective” in “First International Oil Sands Tailings Conference”, Edmonton, Alberta, Canada, Dec 7-10, Oil Sands Tailings Research Facility Canadian Oil Sands Network for Research and Development, addendum.

D.Landriault, D.Welch and J.Frostiak, "Bulyanhulu Mine: Blended Paste Backfill and Surface Paste Deposition / The State of the Art in Paste Technology" in "Minefill 2001: Proceedings of the 7th International Symposium on Mining with Backfill", Seattle, Washington, USA, Sept 17-19,

Society for Mining, Metallurgy and Exploration (SME), Littleton, Colorado (USA), pp 403-416.

D.Landriault, “They Said It Will Never Work – 25 Years of Paste Backfill 1981-2006” in “9th International Seminar on Paste and Thickened Tailings”, Limerick, Republic of Ireland, April 3-7, Australian Centre for Geomechanics, pp 277-292.

H.Li, J.Zhou and R.Chow, “Comparison of Polymer Applications to Treatment of Oil Sands Fine Tailings” in “First International Oil Sands Tailings Conference”, Edmonton, Alberta, Canada, Dec 7-10, Oil Sands Tailings Research Facility Canadian Oil Sands Network for Research and Development, pp 77-84.

Q.Liu, Z.Cui and X.S.Yuan, “Electrokinetic and Settling Behaviors of Aurora Oil Sands Tailings” in “Met Soc: Interfacial Phenomena in Fine Particle Technology, The Sixth UBC-McGill-UA International Symposium, 45th Annual Conference of Metallurgists of CIM”, Montreal, Quebec, Canada 2006, pp 179-195.

O.Omotoso, R.J. Mikula and P.Stephens (2002), “Surface Area of Interstratified Phyllosilicates in Athabasca Oil Sands from Synchrotron XRD” JCPDS – International Centre for Diffraction Data, Advances in X-Ray Analysis (45), pp 391-396.

E.I. Robinsky (1999), “Tailings Dam Failures need not be Disasters – The Thickened Tailings Disposal (TTD) System”. CIM Bulletin volume 92 (1028), pp 140-142.

P.Uhlik, H.Hooshiar, H.A.W. Kaminsky, T.H. Etsell, D.G. Ivey and Q.Liu, “Cation Exchange Capacity and Total Surface Area of Clay Fractions from Oil Sands Process Streams” in “First International Oil Sands Tailings Conference”, Edmonton, Alberta, Canada, Dec 7-10, Oil Sands Tailings Research Facility Canadian Oil Sands Network for Research and Development, pp 64-72.

X.Wang, Z.Xu and J.Masliyah, “Polymer Aids for Settling and Filtration of Oil Sands Tailings” in “First International Oil Sands Tailings Conference”, Edmonton, Alberta, Canada, Dec 7-10, Oil Sands Tailings Research Facility Canadian Oil Sands Network for Research and Development, pp 73-76.

X.S.Yuan and W.Shaw, “Novel Process for Treatment of Syncrude Fine Transition and Marine Ore Tailings” in “Met Soc: Interfacial Phenomena in Fine Particle Technology, The Sixth UBC-McGill-UA International Symposium, 45th Annual Conference of Metallurgists of CIM”, Montreal, Quebec, Canada 2006, pp 477-489.

VERTICAL “WICK” DRAINS AND ACCELERATED DEWATERING OF FINE TAILINGS IN OIL SANDS

Patrick Sean Wells

Suncor Energy Inc., Fort McMurray, AB

Jack Caldwell

Robertson GeoConsultants, Vancouver, BC

ABSTRACT : Suncor Energy Inc. is committed to a programme of accelerated research and field trials of tailings technologies with a focus on the closure and final reclamation of soft tailings areas. The work described in this paper was undertaken specifically with regard to Ponds 5 and 6, located in Suncor’s Lease 86/17 area to the north of Fort McMurray, AB, Canada. The tailings in these ponds are soft materials that are the product of commercial development of tailings treatment technologies, ongoing since 1995.

One line of research evaluated the potential for the use of petroleum coke (a by-product of upgrading operations) to build a trafficable cap on the soft tailings. A second line of research evaluated the use of enhanced soft tailings dewatering systems (vertical “wick” drains) in the capped, soft materials. Together these technical approaches may decrease the consolidation time of the soft tailings within these ponds, allowing for an accelerated placement of a final reclamation cover.

This paper discusses 2009 field trials of vertical “wick” drains installed in very high fines, low density tailings in Pond 5. A description of the trial operations is provided, along with preliminary data and conclusions. Findings so far indicate that vertical drains can be an important component in the dewatering of soft fine tailings in oil sands deposits.

BACKGROUND

Closure and reclamation of oil sands tailings areas has been a focus of industry and academic research efforts for over thirty years. One of the key areas of interest is the dewatering of low density, high fines materials which are the result of oil sands ore

processing. Such materials are currently contained within tailings storage facilities, and may benefit from some measure of dewatering through enhanced methods such as vertical (or “wick”) drains, capping and long-term storage such as end-of-mine lake capping, or long-term consolidation monitoring and surface water removal.

DISCUSSION

Material Description

The primary component of interest in oil sands soft tailings is Mature Fine Tailings or MFT. This material is described in several publications, including a number through the Fine Tailings Fundamentals Consortium, and is not detailed here. Large volumes of this material remain within tailings storage facilities and hence the development of methods to deal with either the initial formation or the eventual dewatering of this material is important to the industry.

Consolidated Tailings (CT) has been the principal technology in the industry to process MFT into a trafficable deposit. In this process, MFT is combined with coarse sand (at a known Sand-to-Fines Ratio defined by the 44 micron size split (SFR_{44})) and with a gypsum slurry to form a non-segregating material that releases water and consolidates relatively quickly under well-controlled conditions. In practice, however, large scale CT deposition typically result in the generation of volumes of low SFR_{44} and segregating CT, in addition to deposits within the target SFR_{44} range. Perimeter placement of higher SFR_{44} CT results in areas of soft, non-trafficable surfaces. Methods of remediation are important as the time required to produce a solid, reclaimable deposit can be longer than current regulatory requirements envisage.

Suncor's Pond 5 is located north of Fort McMurray, Alberta, Canada and is the first production-scale CT pond in the oil sands industry. Twelve years of process and depositional system development have resulted in a variety of deposit types within the pond area, with approximately 40% of the pond surface area exposing low-strength, high-fines tailings.

Dewatering trials starting in mid-2009 were conducted on the soft materials at the south-west corner of the pond. The materials are characterised by the following:

- Sand-to-Fines Ratios (SFR_{44} defined at 44 micron particle size) between 0.4 and 3:1
- Percent solids by weight: 34 to 70%
- Void ratios ranging from 0.65 to greater than 5.5
- In-situ shear strengths from 0.1 to 2 kPa

SFR_{44} , % solids, and in-situ shear strengths tend to increase with depth below the pond surface. Table 1 lists the basic in-situ material properties with depth in the test area. The behaviour of these materials ranges from that of a fluid to a semi-fluid state. In terms of standard stress behaviours, these properties result in the following:

- Piezometric readings are equivalent to total stress at depth and are a function of the material densities and depths of the overlying fluid. This is what would be expected for a fluid as compared to a solid where grain-to-grain contact occurs.
- Field measurements consistently indicate zero effective stress for all material below a critical void ratio of approximately 0.65; thus implying an absence of grain-to-grain contact.

Because the tailings are essentially a fluid, the driving force providing the pressure differential which promotes water flow from the tailings into the vertical drain is equal to the total head (hydraulic potential) within the tailings column, minus the total head within the individual drains. Note that because of the fluid nature of the tailings, when the wick drains are installed, for tailings with density (ρ_t), the expected fluid pressure hence

potential (P) at a depth (h_t) in the tailings is equal to the density of the tailings times the depth ($P = \rho_t * h_t$). Within the drain the potential is $P = \rho_w * h_w$. In that the density of water is less than the density of the tailings, there is a net pressure differential between the outside and the inside of the wick drain and hence flow of tailings water from the tailings into the wick drain.

In theory, this process continues until the soft tailings approach their liquid limits and begin to generate effective stresses, acting as a soil as opposed to a slurry. Once the fluid-like tailings begin to experience grain-to-grain contact the hydraulic conductivity of the soil-like tailings begins to exert an influence on the flow of tailings water into the wick drain. This is the phenomenon referred to as “cake formation.”

This concept is shown in Figure 1. The result is pressure/potential differentials that increase with depth and density of the semi-fluid tailings. For the trial site, Figure 2 shows the differentials. These conditions are applicable as long as there is no grain-to-grain contact between the soil particles, which occurs near void ratios of 0.65 in these low SFR44 tailings. This void ratio corresponds to the point where effective stresses can be generated in this type of material, and beyond which standard soil mechanics principles apply.

LABORATORY TESTING

Laboratory testing was undertaken at the University of British Columbia by R.J. Fannin, Professor of Civil Engineering, and Atitep Srikongsri. The tests were designed to evaluate the potential for Suncor’s soft tailings to clog the geotextiles commonly used in wick drains. The tests also provided an opportunity to measure the consolidation and hydraulic conductivity

properties of the reconstituted tailings samples. This work was done using a UBC designed and constructed permeameter¹.

Tailings samples obtained from the test site area were collected using two different methods. The first sample, AR7, was obtained using a back-hoe from the soft tailings surface just off the dyke. The second sample, DTA, was obtained from directly below the coke cap surface area, 450ft from the dyke, between a depth of 10 and 15ft.

A known volume of each sample was placed in the permeameter between geotextiles of differing apparent opening sizes. The sample was then placed under a controlled load producing a stress of 10kPa. The total volumes of released water, settlement, and pressure with depth were measured as a function of time. A summary of the material properties is provided in

Table 2. Permeability (k) and Coefficient of Consolidation (C_v) values resulting from analysis of these data fall into expected ranges for this type of low SFR₄₄ material.

In summary the laboratory testing provided the following general conclusions:

- There was no evidence of clogging of nonwoven geotextiles with Apparent Opening Sizes (AOS) of 90 and 210 micron
- There was some evidence of very minor piping of woven geotextile, with AOS = 300 micron
- Tailings exhibit a very low hydraulic conductivity, which appears to control the dewatering phenomenon

Figure 3 shows the calculated changes in the permeability of the AR7 sample during the test procedure.

VERTICAL DRAIN FIELD TESTS

Figure 4 &

Figure 5 show a plan view of the field test site as well as a centreline cross section under the floating coke cap on which the test was conducted. Material properties were determined through a combination of shallow surface sampling, CPT profiling, vane shear testing, and piezometer monitoring.

The vertical drain trial programme consisted of two installations. The first installation, Individual Drain Area (IDA), is designed to determine tailings dewatering rates as a function of depth. The second installation, Vertical Drain Field (VDF), is designed to investigate dewatering and consolidation effects on soft tails using full profile, close-spaced vertical drains.

At this point there has been insufficient time to fully establish and quantify the performance of the VDF. Significant outflow was observe from the wick drain on initial installation and there is some evidence of overall settlement of the area which may be an indicator of dewatering-induced volume change and consolidation.

Within the IDA, monitoring instruments have been installed. including nested piezometers, Horizontal Settlement Pipes (HSP), and CPT probing. Piezometers are used to monitor changes in total stress in the fluid tailings as well as pore water pressure dissipation if and when the drains dewater the soft material to the point that they behave as a soil. The HSP units are flexible plastic pipes installed at the base of the coke; by passing a probe through the pipe it is possible to determine the elevation of the pipe and hence to quantify the settlement of the coke into the soft tailings. The CPT probing was used to determine the strength, density, and general stratigraphy of the tailings column.

The IDA units consist of a 5-ft long strip of the vertical drain installed at specific depths with “duck bill” attachments that provide for expulsion and capture of over-pressured release water at the surface of the coke cap. This installation is shown in Figure 6 and Figure 7. The pressure within the tailings column is determined from piezometric measurements obtained during the CPT testing. The water column pressure is based on the calculated hydrostatic head measured from the top of the discharge pipe on the coke cap. The pressure/potential differences between the two are shown in Figure 2.

The coke cap is water-saturated to within 10 to 20 cm of the top surface, and shows hydrostatic conditions. The positions for each test profile (C01 & C02) are shown in Figure 4.

Shortly after installation of the individual vertical drains, water flow was observed and measured from most of the discharge tubes. Select flow rates vs. time are shown in Figure 8. Drain titles consist of the installation depth below the assumed bottom of the coke cap in feet, with each of three drains at the depth differentiated by the letter A, B, or C. Rates appear to be a function of depth, with the shallower (10 to 15 ft) drains producing minimal flow that increases with depth. The deepest drains, however, did not producing any flow.

It is possible that the shallow drains (<15ft below the coke cap) either daylight into the lower hydrostatic conditions within the coke cap layer, thus discharging into the coke rather than the collection buckets, or do not have sufficient pressure differences to sustain long-term flow. This could be resolved through additional loading of the coke cap to increase the pressure differential sufficiently to promote flow. The deeper drains below 40 ft have been installed into sandy materials

which are under hydrostatic pore water pressure conditions. These areas are unlikely to have sufficient pressures to drive fluids to the coke cap surface. Drainage may, however, be occurring downward into the underlying sands.

Using radial well equations and measured flow rates and pressure differentials, the apparent permeability of the tailings was estimated. While this method is approximate and based on an assumption of radial flow through a porous medium to a well, it nevertheless provides an interesting set of results (Table 3) that are comparable to results obtained from the UBC laboratory testing and from more rigorous analyses using the computer code FLAC as described below.

LONG-TERM EFFECTIVENESS

Given a soft tailings deposit with an average density of 50% solids by weight, a target density of 70%, an SFR₄₄ of 0.5:1, a depth of 10 m, and a single 10 m vertical drain installed for every 4 m² surface area, the total amount of water that needs to be removed by a single drain is 16,540 litres. At a nominal drainage rate of 1 L / day / 5 ft length of installed vertical drain, this gives a total drainage time of 504 days. It is, however, unreasonable to assume a continuous flow rate over any reasonable period of time given the decreasing permeability of the surrounding tailings as the density increases with dewatering. In order to account for this more properly, alternate detailed analysis is required.

Modelling of the conditions using Fast Lagrangian Analysis of Continua (FLAC) in the 10m column shown in Figure 1 looked at the time required to dewater soft tailings both with and without vertical drains, with a number of drain spacing conducted. Material

property parameters used in the model were taken from the results of the UBC lab tests, and the preliminary dewatering rates measured in the first 30 days in the field appear to match predictions made by the model. The placement of vertical drains is predicted to decrease the dewatering time from more than 100 years with no installed vertical drains, to nine years at a 2-m drain spacing, and to less than a year at 0.6 m (2-ft) spacing. Predicted flow rates and total time for consolidation are shown in Figure 9 and Figure 10. While the predicted flows for the 6 m spacing installations appears high, it is unlikely the longer flow path would result in flows this high. Further analysis will refine these predictions.

CONCLUSION

Vertical drains are proving to be capable of dewatering very soft, fluid tailings within oil sands CT ponds. The mechanism under which this dewatering occurs may be described through the pressure differentials which initially results from the difference in fluid potential of the tailings outside the wick drain and the hydraulic potential within the drain. As the water is drained from the tailings, solid-like tailings begin to form around the wick drain and hence the hydraulic conductivity of these materials begins to impact flow rates into the wick drains. These factors may be modeled via calculations based on simple field measurements, laboratory tests, and computer modelling. Although the work done to date is preliminary with longer measurement of wick drain flow rates and more detailed analyses required, it is reasonable to conclude that vertical drains can be an important component in the dewatering of soft fine tailings in oil sands deposits.

Table 1 - In-Situ Test Site Material Properties

Sample No-Depth (m)	Water (wt %)	Solids (wt %)	SFR (44)
450-0.5	64.26	33.69	1.94
450-3.0	63.12	34.07	0.72
450-4.0	48.74	46.65	0.82
450-8.0	41.51	54.77	0.89

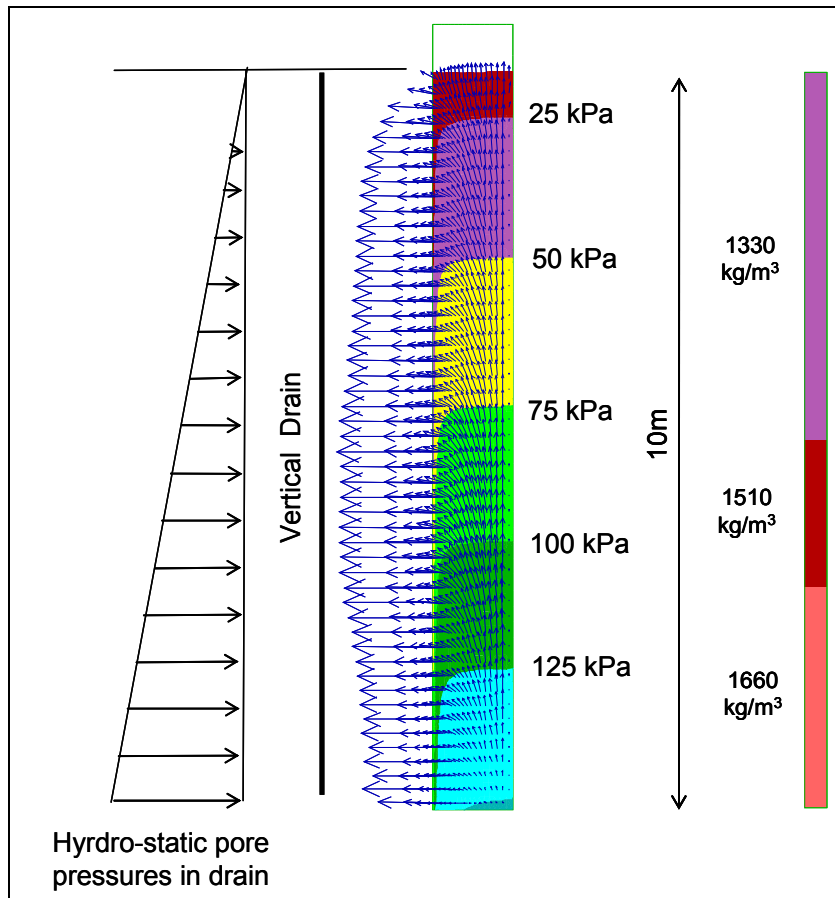


Figure 1. Vertical Drain Pressure & Flow Vectors

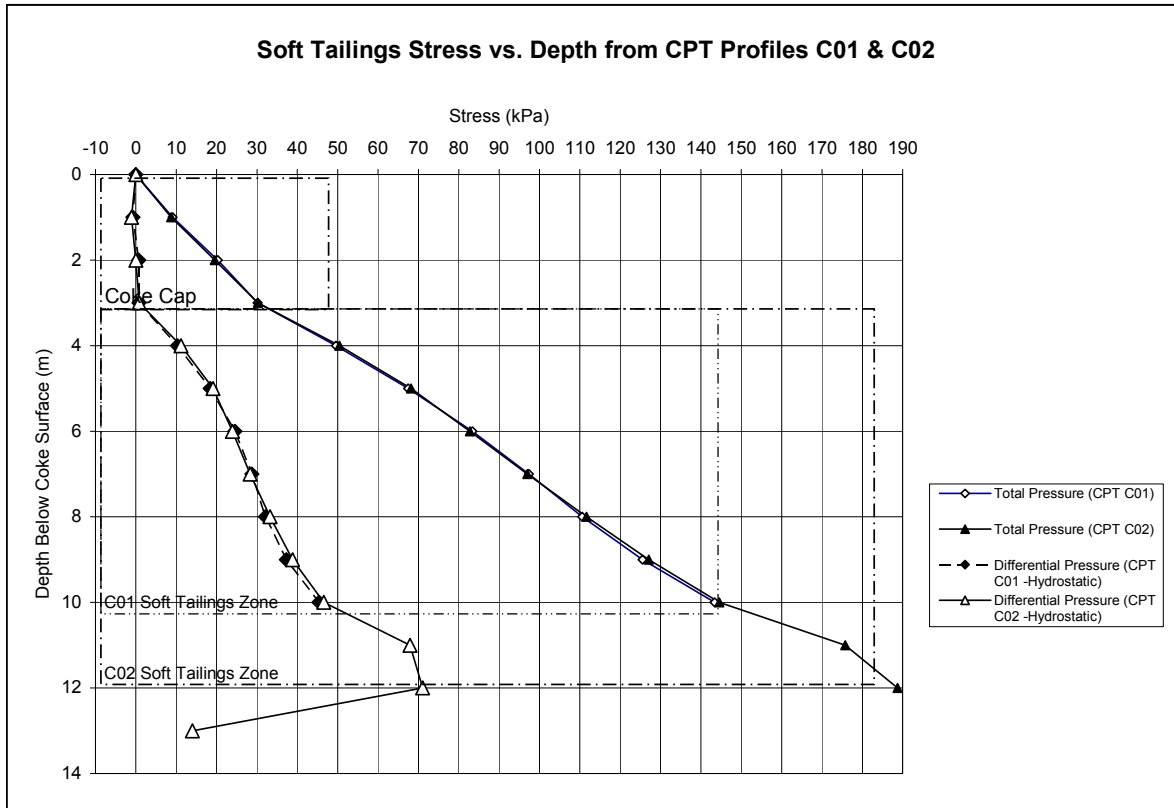


Figure 2. Total Stress and Vertical Drain Stress Differentials

Table 2- Laboratory Sample Properties from UBC Testing

Sample	Initial solids by weight (%)	Final solids by weight (%)	Sand-to-Fines Ratio (SFR(44))	Bitumen content (wt %)	Clay Content (wt %)	Cv (m ² /yr)	k (m/s)
AR7 (SGS-SA3)	62%	76%	1.0	6%	10%	0.11	7E-10
DTA (MDH-A1786 450-3.0)	34%	65%	0.7	7%	15%	1.63	1E-08

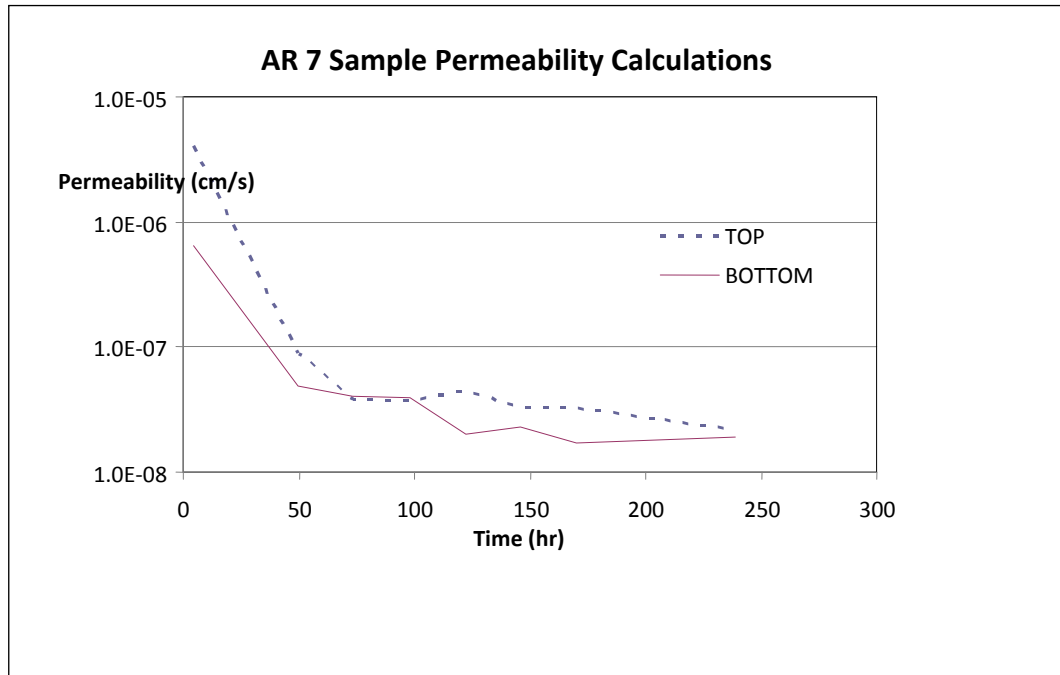


Figure 3. AR7 Sample Permeability

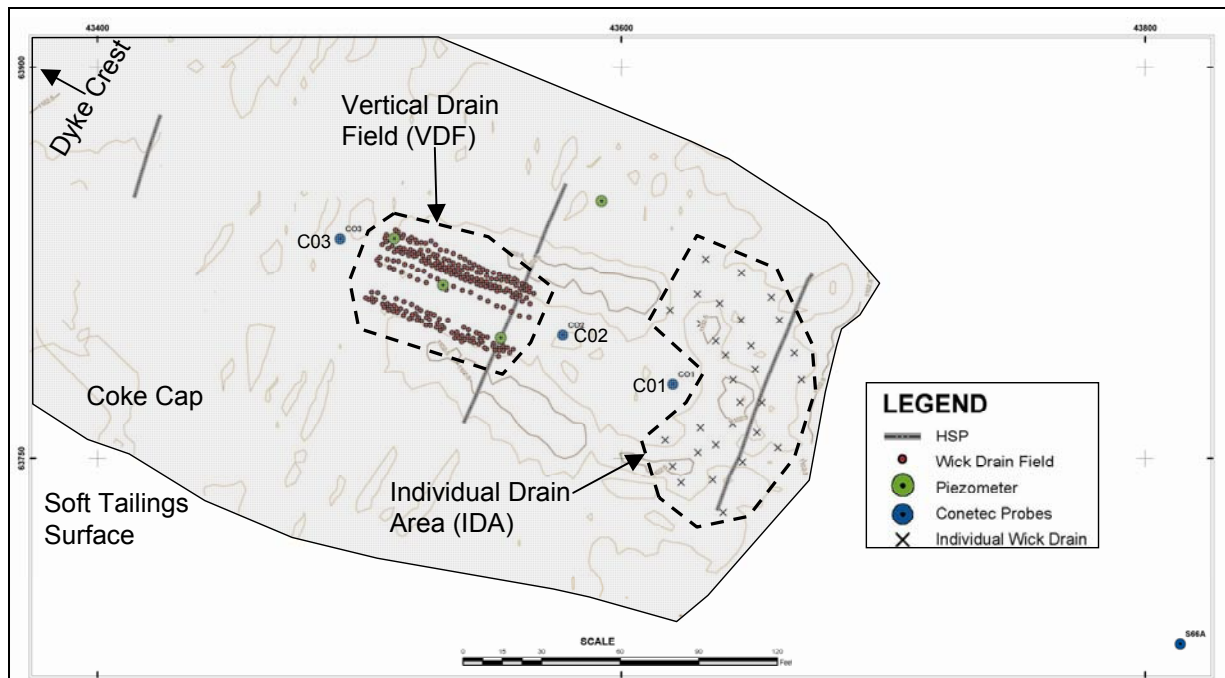


Figure 4. Plan View of Test Site, Pond 5

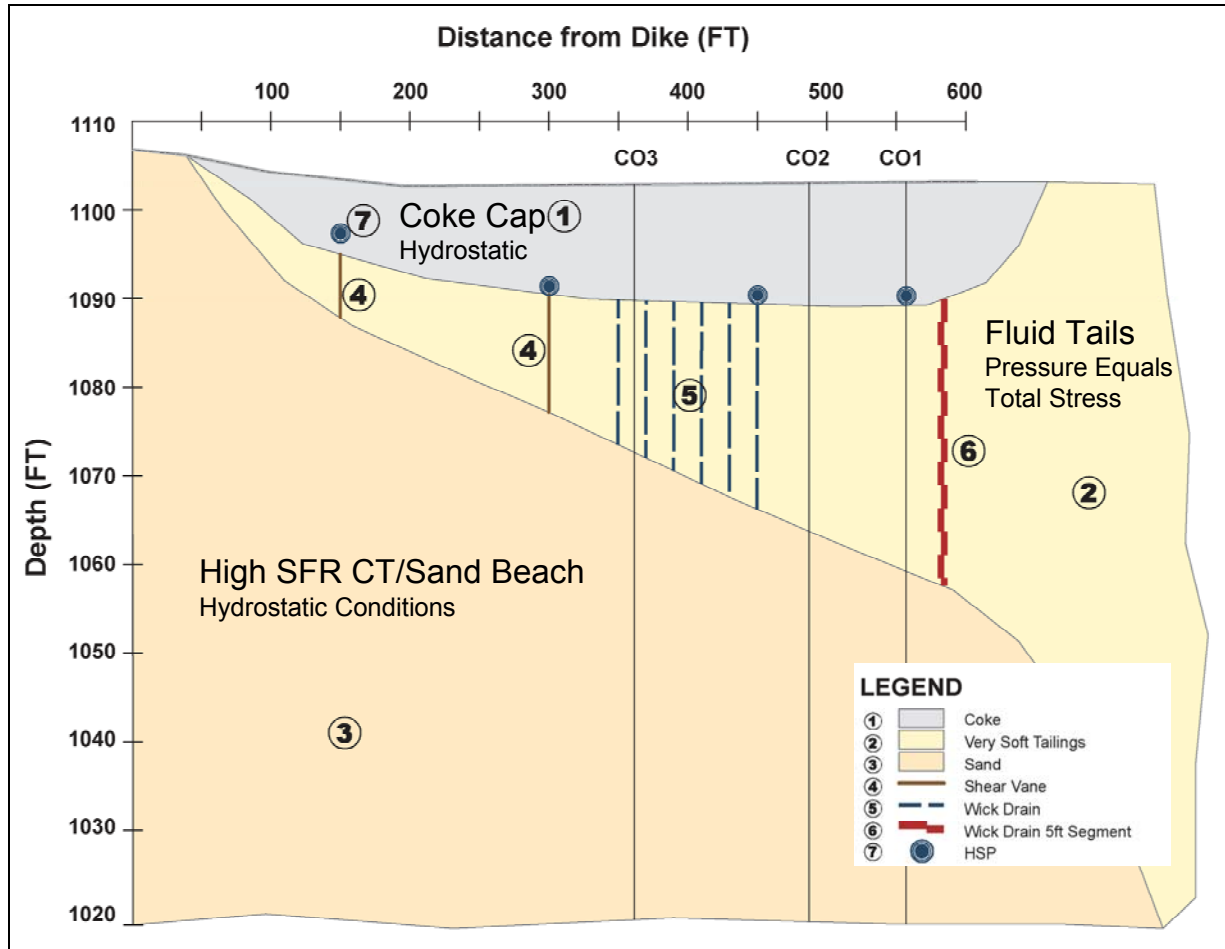


Figure 5. Centreline Test Site X-Section

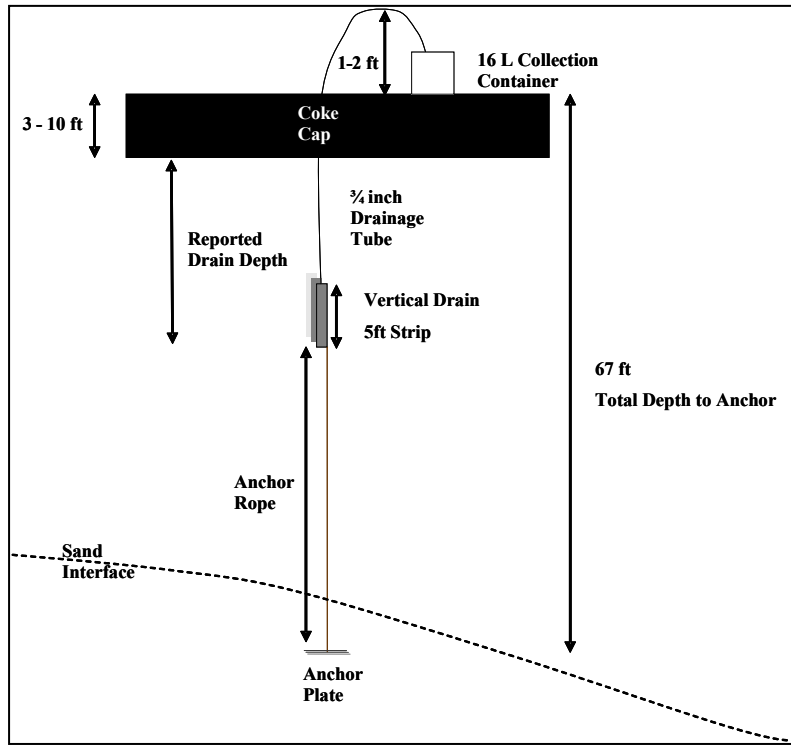


Figure 6. Individual Drain Test Installation

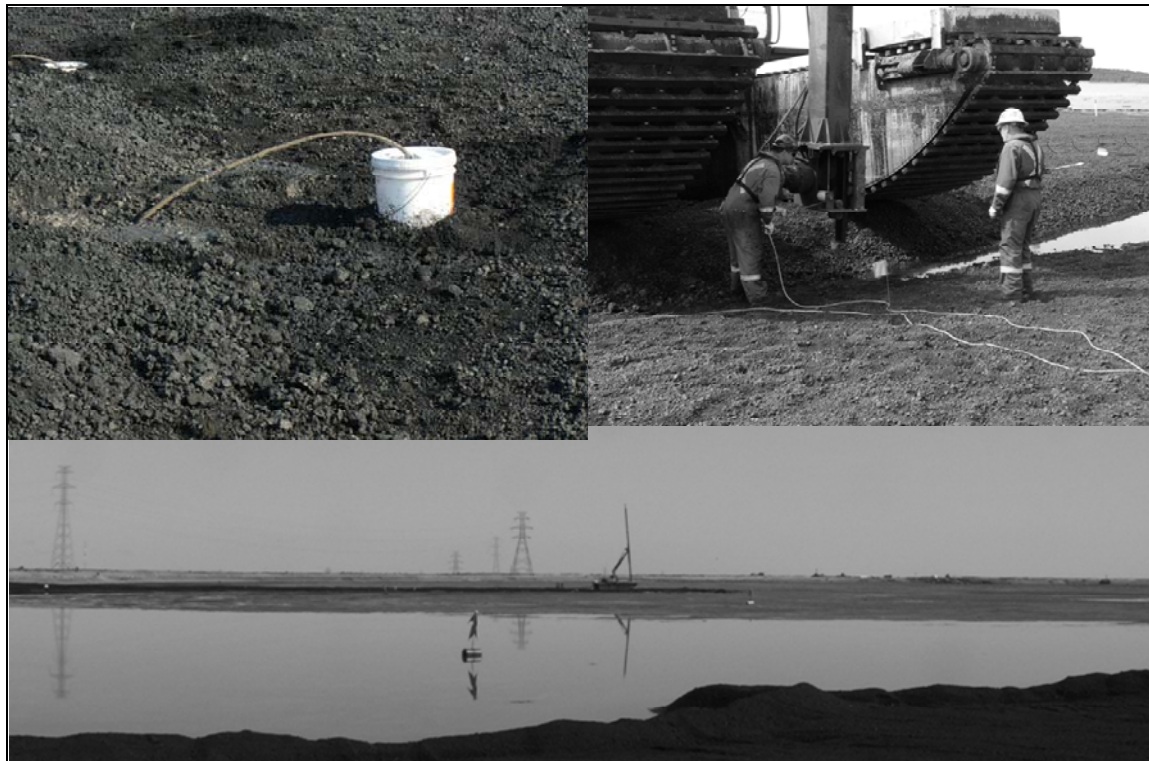


Figure 7. Installation Photos

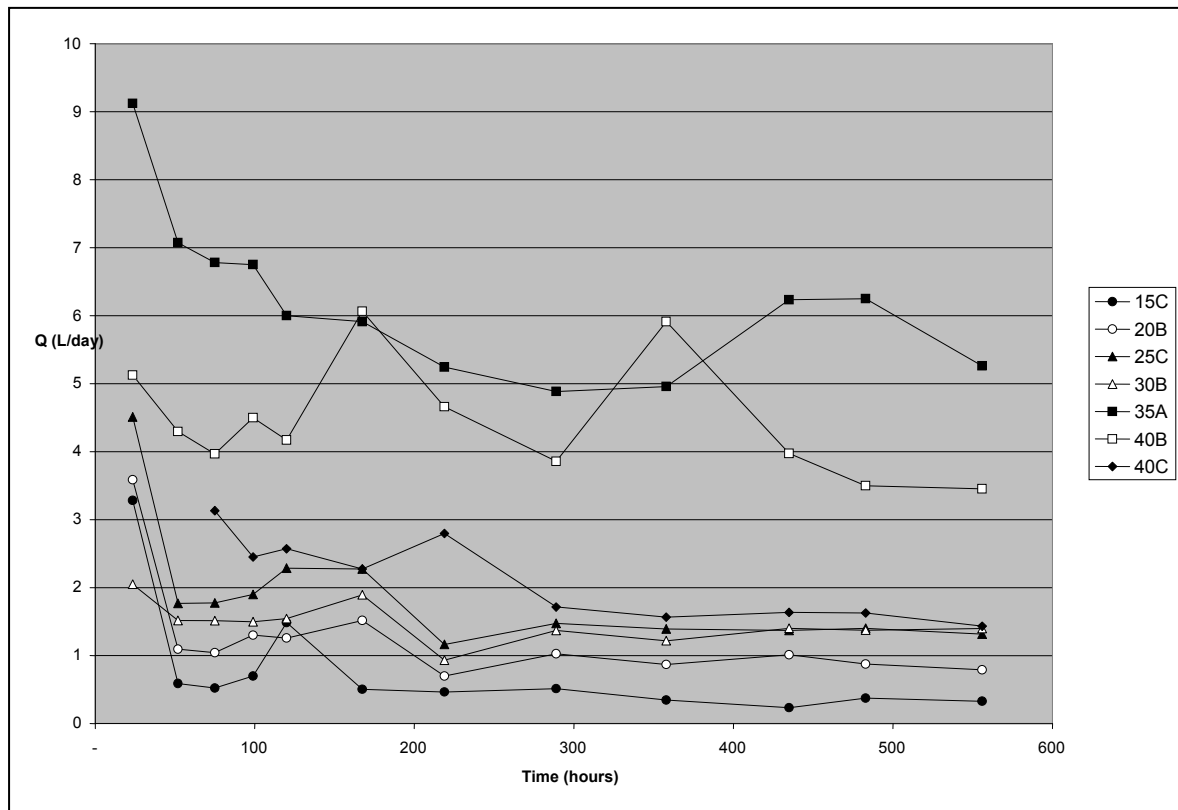


Figure 8. Flow from IDA Test Drains vs. Time

Table 3 - In-Situ Permeability Estimates from Radial Flow Calcs

Drain Depth (ft below coke btm)	Radial K (m/s)
15	6.1E-10
20	1.2E-09
25	1.1E-09
30	7.6E-10

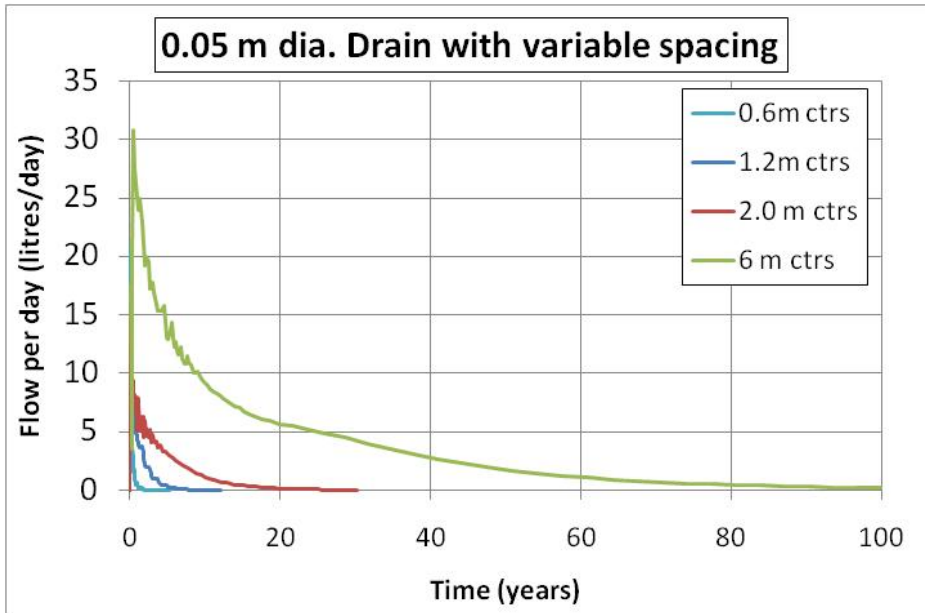


Figure 9. Modelled Drain Flow Rates vs. Time

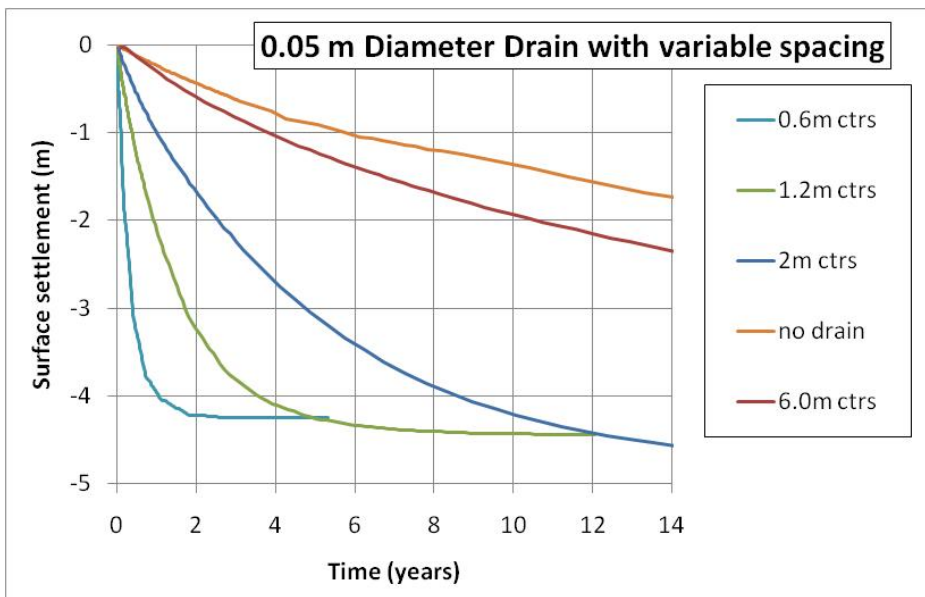


Figure 10. Modelled 10 m Column Surface Settlement

REFERENCES

ⁱ A study on the behaviour of soil-geotextile systems in filtration tests, E.M. Palmeira, R.J. Fannin, and Y.P. Vaid, Canadian Geotechnical Journal 33, (1996)

DYNAMIC SIMULATION OF TAILINGS MANAGEMENT OPTIONS

Nicholas Beier, David Segó & Norbert Morgenstern

University of Alberta, Edmonton, Alberta, Canada

ABSTRACT: Mining and mineral processing ultimately lead to the production of waste by-products including waste rock and a finer grained slurry called “tailings”. These tailings are managed through the implementation of a tailings management system (TMS), consisting of tailings treatment/dewatering at the mill, thickening, transport to and construction of storage impoundments, natural dewatering within the impoundments, water recovery and recycle, effluent treatment, and restoration of the site.

Evaluating all the options available to develop a reliable management system or understanding the implications of modifications to an existing TMS can be time consuming and expensive. A sound, well designed TMS will help fulfill the mining industry’s commitments to sustainability and to apply the best available technologies. A dynamic systems modeling approach was used to develop a model/tool capable of guiding the tailings planner/regulator through the process of tailings management to attain the most practical and environmentally sound solution. A prototype model of a simple metal mine TMS, comprising a suite of sub-models representing the various components outlined above has been developed. The paper will present the prototype dynamic simulation model development. The model will allow the tailings planner to simulate the tailings system over time, demonstrate various outcomes by alternating management practices, and conduct sensitivity analyses to determine which options have the largest impacts on the system.

INTRODUCTION

Mining and mineral processing ultimately lead to the production of waste by-products including waste rock and a finer grained slurry called “tailings”. Management of the tailings and waste rock currently results in environmental challenges and financial burdens for operators. Environmental pressure has increased as of late to reduce the storage of fluid tailings ultimately

minimizing risk from releases and leading to the timely reclamation of these deposits.

In a recent technical publication, the Australian Government, (2007) defined tailings management as “managing tailings over their life cycle, including their production, transport, placement, storage, and the closure and rehabilitation of the tailings storage facility.” The selection of a particular tailings treatment train and management method will depend upon the objectives of

the operator/regulator or applicable regulations for the mine site. Typically, operators look for efficient and cost effective systems that provide sufficient protection of the environment and satisfy regulations. The tailings management system (TMS) must also be dynamic to cope with a tailings facility whose geometry and operational considerations change over the life of the mine (decades). Facilities should be constructed and operated in an orderly fashion to ensure the main objectives of the TMS are achieved. These objectives may include the following (Houlihan and Mian, 2008; McKenna, 2008; Scott and Lo, 1992; Vick, 1983):

- Energy efficiency: processes and transportation (pumping of tailings, water and sand slurry);
- Cost effectiveness: minimize disruption to mine operations, ensure adequate storage is available for tailings and overburden materials, minimize disposal active area, reduce/eliminate long term containment of fine tailings; process flexibility and robustness;
- Safety and integrity of impoundment: maximize integrity and stability of the tailings impoundment to ensure no release of tailings;
- Environmental protection: minimize seepage, total disturbed area and detrimental effects to local species and habitats; and
- Reclamation: tailings surface suitable to sustain reclamation activities; create a trafficable landscape at the earliest opportunity to facilitate progressive reclamation

In Alberta's Oil Sands industry, current tailings management practices resulting in continual accumulation of fine tailings has prompted the Energy Resource Conservation

Board (ERCB) to regulate fluid fine tailings through performance criterion. In February 2009, the ERCB issued Directive 074: Tailings Performance Criteria and Requirements for Oil Sands Mining Schemes. The aim of the directive is to reduce fluid tailings accumulation and create trafficable surfaces for progressive reclamation (Houlihan and Mian, 2008). To meet the new Directive 074, operators are looking to alternative tailings management options and technologies to reduce their inventory of fluid fine tailings and expedite the reclamation process.

This research aims to assist in the assessment of tailings management options through the development of a dynamic simulation model. The model will simulate the tailings system behaviour and complex relationships from production to the onset of reclamation. The initial stage of model development (focus of the current paper) will investigate a simple metal mine tailings management scenario. The complexity and scale of the proposed tailings management plan is suitable for the development and calibration stages of the simulation model structure and components. Once the model has been proven robust for the simple scenario, an oil sands mine will be simulated. Fine tuning of the model will be required to reflect the management scheme and material flows at oil sands operations.

OBJECTIVE

Evaluating all the options available to develop a sound management system or understanding the implications of modifications or upsets to an existing TMS can be time consuming and expensive. A sound, well thought out TMS will help fulfill the mining industry's commitments to achieve sustainability and to apply the best available technologies to minimize the risk of failures. There currently is no single

simulation model available to assist the planner or regulator in evaluating the management options quickly and efficiently.

The objective of the proposed research is to develop a dynamic simulation model (tool) that will guide the tailings planner/operator/regulator through the process of tailings management to attain a practical, economical, and environmentally sound solution. The model will allow the tailings planner to simulate the tailings system over time, demonstrate various outcomes by alternating management practices, and conduct sensitivity analyses. Essentially, the simulation model is a what-if tool to experiment with various operating strategies or design alternatives to support technology assessment, scenario-analysis, fore-sighting and mine planning (Scaffo-Migliaro, 2007; Halog and Chan, 2008). Sensitivity/uncertainty analyses could also be used to strategically guide further research and resource expenditure.

TAILINGS MANAGEMENT ANALYSIS

The intent of the TMS modeling is not to mimic or predict the exact behaviour but rather to identify the properties and processes (i.e. consolidation, solids content, treatment options) that are most significant. These significant processes would have the greatest impact on the overall success of the tailings management system and would be the target of further research, or more detailed design. Performance measures have been defined to assess the management strategies in the simulation model (Table 1). For example:

- What is the required impoundment storage volume (for both solids and water)?
- How much material is required to construct impoundments?
- What is the available storage volume?

- How much material is available for construction of impoundments?
- What is the available recycle water volume and quality?
- What is the seepage rate to the environment and its quality?
- Time frame to produce a stable tailings deposit?
- Sensitivity/flexibility of disposal option?

Table 1. Simulation Model Performance Measures

Variable (function of time)	Symbol
Available storage volume/height	$Q_{available}$
Required storage volume/height	$Q_{required}$
Recycle volume available	$Q_{recycle\ avail}$
Recycle quality	$C_{recycle,i}$
Seepage rate	$Q_{seepage}$
Seepage quality	$C_{seepage,i}$
Deposit Strength	$Su(t,z)$

SYSTEMS MODELING

Tailings management systems are typically multifaceted, interrelated and complex. Additionally, mining operations are constantly evolving with time due to inherent changes within ore bodies and subsequently extraction processes as well as economic conditions. Dynamic system analysis and modeling or dynamic simulation modeling (DSM) is therefore appropriate to capture and represent the complex, evolving system through time.

The proposed research will use the object orientated, systems dynamic modeling software called GOLDSIM as the “simulation engine” (Figure 1). Goldsim is a highly graphical, object orientated simulation platform used for dynamic systems modeling. It allows flexible inputs, outputs, time stepping, and coupling of processes

(Wickham et al. 2004). The Goldsim platform is like a “visual spreadsheet”. The user can visually and explicitly create and manipulate data, equations and relationships (Kossik and Miller, 2004). The simulation model can be constructed from process-based, empirical or even qualitative formulations based on a tentative relationship between two parameters. Probability can even be incorporated within the model to represent uncertainty in processes, parameters and events. Goldsim also has the ability to dynamically link with external programs such as excel to enhance the simulation capability (Kossik and Miller, 2004).

A spreadsheet will be used as the data entry/interface for all model inputs such as site properties, tailings properties, mining and extraction rates, environmental data and pertinent management decision variables (i.e. constraints on the system). The user will have the option to utilize built in functions and sub-models or implement their own models. Implementation of user specific models/data would be completed either in the data input spreadsheet or the Goldsim model directly. Model output will be displayed in a spreadsheet and can be visualized via GIS where needed (i.e. deposition modeling).

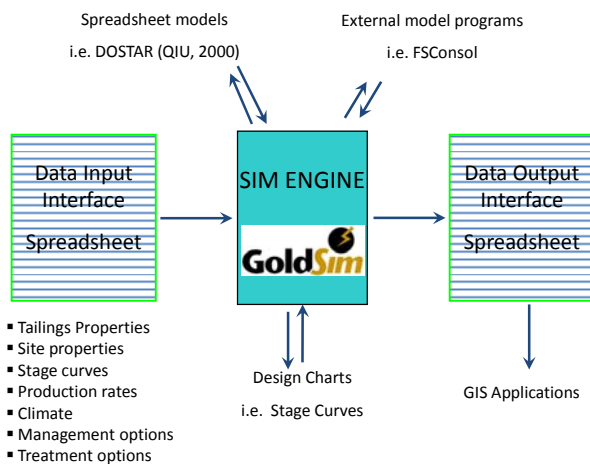


Figure 1. Model structure (Beier et al. 2008)

TAILINGS MANAGEMENT SIMULATOR

Conceptual Model

A dynamic systems model was developed for the simulation and evaluation of tailings management systems. The systems model will track the stocks and flows of mass (solids [mineral including both fine and coarse], water, and chemicals) throughout the TMS. A simplified conceptual model of a typical TMS is depicted in Figure 2 and will represent the highest level of the TMS simulation model. The TMS model will be composed of a suite of sub-models representing individual components such as the extraction plant, tailings treatment, impoundment and the environment. Critical processes (such as consolidation, evaporation or seepage) within each component will dictate mass transfer between components.



Figure 2. Conceptual Simulation model.

Mine/Extraction Sub Model

The sub-model components representing the mine pit and extraction plant will essentially drive the model. Time trajectories for the relevant material flows will be specified by

the user in the data input spreadsheet and transferred to the GOLDSIM model via the Mine/extraction sub model (Table 2).

Table 2. Required Time Trajectories

Variable (function of time)	Symbol
Tailings	Q_{Tails}
Pulp Density	ρ_{Tails}
Particle size distribution equation*	PSD
Chemical Species in tail pore fluid	C_i
Overburden (OB) Mass	Q_{OB}
OB Water Content	W_{OB}
OB Bulk factor	B_{OB}
Fresh water make-up	Q_{Fresh}
Recycle water	$Q_{Recycle}$
Miscellaneous water (i.e. pit dewatering, runoff into pit, etc.)	Q_{Misc}

*Specified as an equation based on Fredlund et al. (2000).

Other material specific properties required for volume calculations include specific gravity (Gs) of tailings solids and overburden materials.

Impoundment Sub Model

The impoundment component consists of several interrelated sub-models and will distribute mass of water and solids within the system through time, taking into account the inflows and outflows (Figure 3). The available storage will be influenced by tailings deposition and impoundment construction methods (represented by stage curves), and the various inflows and outflows from the impoundment.

Stage Curves

At this phase in the model development, the stage curves will be uncoupled from the simulation model.

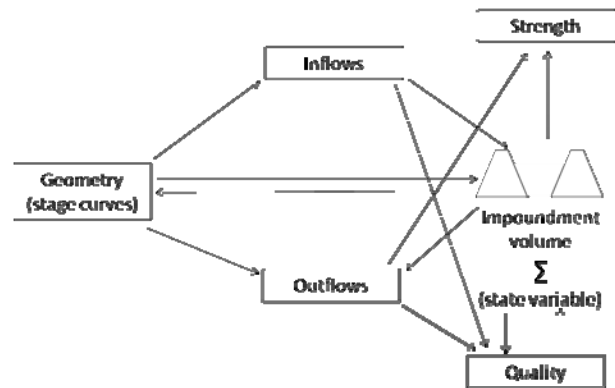


Figure 3. Impoundment Model

Using the relevant tailings production data, proposed impoundment design, and estimated tailings beach slopes, stage curves representing area/volume relationships will be developed to represent the impoundment structure. Based on the available overburden or tailings material available for construction, the stage curves will represent the performance measures $Q_{available}$ or $H_{available}$.

Estimates of the tailings deposit slope may be based on operational experience or calculated based on an acceptable method. Some examples of methods to determine deposit slopes and profiles can be found in Fitton (2007). A simple empirical model developed by Fitton (2007) using solids content (S% by weight) and flow rate will be used for the initial phase of simulation modeling (equation 1).

$$l = \frac{26.6S^2}{\sqrt{Q_{Tails}}} \quad (1)$$

Inflows/Outflows

To determine the storage volume within the impoundment, the model must track the volume of material (water and solids) stored through time, including inflows and outflows (Table 3). The tailings discharge and miscellaneous inflows as well as recycle outflow are specified in the mine/extraction sub-model.

Table 3. Inflows/Outflows

Variable (function of time)	Symbol	Flow
Tailings	Q_{Tails}	In
Precipitation (rain/snow)	$Q_{precipitation}$	In
Miscellaneous water (i.e. pit dewatering, pit runoff, etc.)	Q_{Misc}	In
Recycle water	$Q_{Recycle}$	Out
Pond Evaporation	$Q_{pondevap}$	Out
Tails Evaporation	$Q_{Tailsevap}$	Out
Seepage	$Q_{seepage}$	Out

Applicable climatic data will be specified by the user in the input spreadsheet and will include precipitation ($Q_{precipitation}$) and evaporation parameters (for modified Penman equation).

Pond evaporation ($Q_{pondevap}$) will be calculated (equation 2) based on the potential evaporation (PE) as determined by the modified Penman method (Rykaart, 2002) with A_{pond} as determined from the stage curves.

$$Q_{pondevap} = PE * A_{pond} \quad (2)$$

Evaporation from the tailings beach surfaces ($Q_{Tailsevap}$) will be less than from free pond surfaces. The actual evaporation (AE) and subsequently $Q_{Tailsevap}$ can be calculated using PE and the following equations (Qiu and Segó, 2007):

$$AE = PE * \left(Ar \left[\frac{1}{1 + (\alpha T)^p} \right]^q + Br \right) \quad (3)$$

$$Q_{Tailsevap} = AE * (A_{total} - A_{pond}) \quad (4)$$

The parameters for AE (Ar and Br related to residual evaporation rate, α related to air-entry value, and p and q related to material properties) can be determined by regression methods from curves of evaporation rate

versus drying time (T) as described in Qiu and Segó (2007). The area of the exposed tailings beach can be determined from the stage curves.

Seepage losses ($Q_{seepage}$) from the impoundment will include both basal seepage ($Q_{seepageBase}$) and seepage through the dike ($Q_{seepageDike}$). Basal seepage can be estimated as follows (Wels and Robertson, 2003):

$$Q_{seepageBase} = k_{tails} * i * A_{base} \quad (5)$$

Where k_{tails} is the hydraulic conductivity of the tailings and “ i ” is the vertical hydraulic gradient within the pond.

Dike seepage can be estimated using the method described by Chapuis and Aubertin (2001) and Rykaart (2002). For each dike cross section (Figure 4) and given hydraulic conductivity of the dike (k_{dike}) a simple expression for $Q_{seepagedike}$ may be determined in the form of equation 6:

$$\frac{Q_{seepagedike}}{k_{dike}} = \alpha 1 + \frac{\alpha 2 \Delta h^2}{L} + \alpha 3 \left(\frac{\Delta h^2}{L} \right)^2 \quad (6)$$

Where Δh and L are geometric parameters that can be determined from the stage curves. A series of seepage calculations are completed for different geometries characteristic of the dike evolution. The data is plotted as $\frac{Q_{seepagedike}}{k_{dike}}$ vs. $\frac{\Delta h^2}{L}$ and $\alpha 1$, $\alpha 2$, and $\alpha 3$ are curve fitting parameters. Therefore for any given dike configuration and pond elevation an estimate of seepage may be determined.

Impoundment Volume

Reservoir elements, unique to GOLDSIM, will be utilized within the impoundment sub-model to sum the inflows and outflows from the impoundment.

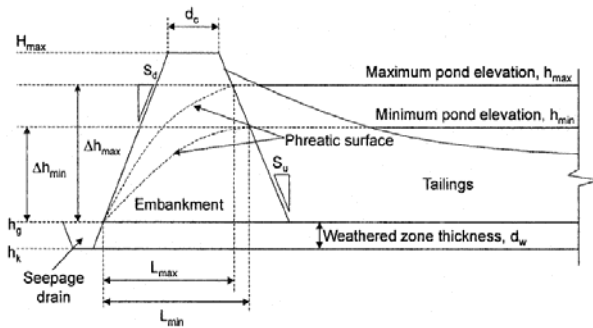


Figure 4. Simplified cross section of dike used for seepage determination (modified from Rykaart, 2002).

Essentially, the storage volume required (both solids and liquids) at any given time can be calculated from:

$$Q_{required} = Q_{inflows} - Q_{outflows} \quad (7)$$

To determine the amount of free recycle water available ($Q_{recycle_avail}$) one must now differentiate between the volume of material in the tailings deposit and the free water pond. The volume occupied by the tailings deposit ($Vol_{deposit}$) at any given time can be determined with conventional large strain consolidation software such as DOSTAR (Qiu and Sego, 2007) or FSConsol (GWP Software, 1999). The volume of the pond or available recycle volume can be calculated by:

$$\frac{Vol_{recycle_avail}}{(Vol_{pond})} = Q_{required} * T - Vol_{deposit,T} \quad (8)$$

Water Quality

The chemical composition of the fluid streams in a TMS can have a profound effect on extraction efficiency and tailings behaviour such as the settling characteristics and suspension rheology (Mikula and Omotos, 2006). There are four main chemical mechanisms that may govern the distribution of ions between the water phase

and solid phase (exchangeable surfaces or mineral precipitates) (Wallace et al., 2004):

- Mixing.
- Ion Exchange.
- Precipitation.
- Dissolution or degassing of CO₂

Integration of all these geochemical processes can be quite complex and data intensive (equilibrium constants and kinetic rates for each process and chemical species). Therefore, the initial scope of TMS model will only look at mixing of ions which is assumed to occur instantaneously. During extraction, mixing will occur between the water phase in the ore, process water and any additives. Mixing may also occur during tailings treatment and within the impoundment. Ions initially distributed separately in each stream, mix rapidly and completely to achieve a new chemical equilibrium. Essentially, mixing of the fluid streams will lead to dilution of mass in various components of the TMS. The kinetics of mixing are assumed to be much greater than the other three processes. Exchange processes only occur on surfaces with active exchange sites (clays), therefore it is likely not significant for hardrock mining operations.

Simulating mixing should be sufficient to understand the major trends of chemical mass transfer between the many components of the TMS. Future research could fine tune the water chemistry system modeling to include more complicated reactions such as surface exchange with clays and eventually solubility/precipitation reactions.

Array functions in GOLDSIM can be used to track the chemical species of each stream within the simulation model. The arrays can be manipulated by the following mixing function to calculate the chemical

concentrations in the pond/recycle water with time:

$$C_{i_{pond}}(t + \Delta t) = \frac{C_{i_{pond}}(t)Vol_{pond}(t) + \sum_{j=1}^n c_{ij}q_j\Delta t}{Vol_{pond}(t) + \sum_{j=1}^n q_j\Delta t} \quad (9)$$

Where c_{ij} is the chemical species “i” in stream “j” and q_j the volumetric flow rate of stream “j”.

Steady state flux (J_x) of chemical species from the tailings pond into the environment may be estimated from a simple 1-dimensional flux calculation.

$$C_{seepage} = \left(k \frac{\Delta h}{\Delta L} C_i + \tau n D_o \frac{\Delta C}{\Delta L} \right) * A \quad (10)$$

Where k is the hydraulic conductivity of the tailings or dike, $\Delta h/\Delta L$ is the hydraulic gradient in the direction of flow, $\tau n D_o$ is the effective diffusion coefficient and $\Delta C/\Delta L$ is the concentration gradient. The seepage chemistry calculations are simple and therefore useful for comparison purposes only. Detailed contaminant transport modeling may be completed separately by using the stage curves, dike configurations and pond concentrations to more accurately assess the seepage quality.

Strength

For typical cohesive tailings deposits normally consolidated conditions will apply. Therefore, an estimate of the undrained shear strength (S_u) may be estimated by the ratio S_u/σ' . Therefore changes in the deposit strength with time can be tracked by evaluating the consolidation of the deposit. The ratio can be correlated with plasticity index (PI) as in the following equation (Shiffman et al., 1988):

$$S_u/\sigma' = 0.11 + 0.0037PI \quad (11)$$

For cohesionless, hard rock tailings, effective stress parameters cohesion, c' , and friction angle, ϕ' , are used to evaluate the shear strength. Therefore changes in cohesionless, tailings deposit strength with time can also be tracked by evaluating the consolidation (gain in effective stress) of the deposit and loading conditions (Bussiere, 2007).

LIMITATIONS AND FUTURE WORK

The initial TMS model will be developed using publically available data representing a simple metal mine. Inherently, there will be limitations to the capabilities of this model. To the best of the researcher’s knowledge, this is the first attempt at developing a high level model for simulation of tailings management systems using public data sources. As such, there will be some degree of simplifications and assumptions required in absence of available data. Additionally, due to the numerous systems and networks involved in the simulation model, the level of detail in the model may be somewhat limited for ease of use. This simulation model will be the first stage in the development of a robust TMS simulation model.

The next stage of the simulation model development will be to add a treatment sub-model (Figure 5). It will be used to represent dewatering and strength enhancement of the tailings stream prior to deposition.

Essentially the user will have to specify a relationship between the feed tailings properties and the underflow/overflow properties (Figure 6).



Figure 5. Conceptual Simulation model with treatment component.

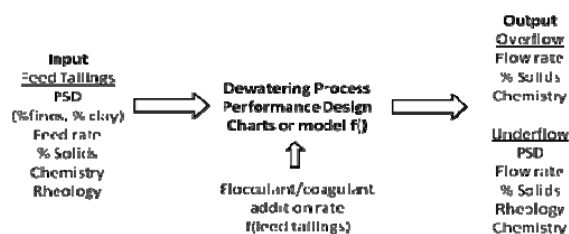


Figure 6. Treatment sub-model components.

Once the model has been proven robust for the simple scenarios, an oil sands mine will be simulated. Fine tuning of the model will be required to reflect the management scheme and material flows at oil sands operations.

CONCLUSION

Tailings management is a complex issue, especially for large operations such as the oil sands. The proposed dynamic simulation-modeling approach will assist TMS decision makers (designers/operators/regulators) to determine the relative influence of various parameters and processes on the tailings system behaviour. It will also allow the user to forecast and compare outcomes by alternating management practices and

investigating the impact of novel and innovative technologies.

ACKNOWLEDGEMENTS

The authors are thankful for the financial assistance from National Sciences and Engineering Research Council of Canada and the Oil Sands Tailings Research Facility. Thanks also to Alberta Research Council and Prairie Mines and Royalty Ltd. for the financial support of Mr. Beier.

REFERENCES

- Beier, N., Segó, D. and Morgenstern, N. (2008). Developing a Dynamic Simulation Model for Tailings Management and Planning. 1st International Oil Sands Tailings Conference, Edmonton, Alberta, December 7-10, 2008. 192-199.
- Bussiere, B. 2007. Colloquium 2004: Hydrogeotechnical properties of hard rock tailings from metal mines and emerging geoenvironmental disposal approaches, Canadian Geotechnical Journal, **44**:9 1019-1052.
- Chapuis, R. and Aubertin, M. 2001. A simplified method to estimate saturated and unsaturated seepage through dikes under steady-state conditions. Canadian Geotechnical Journal, **38**: 1321-1328.
- Fitton, T. 2007. Tailings Beach Slope Prediction. PhD thesis, School of Civil, Environmental and Chemical Engineering, RMIT University, Melbourne, Australia.
- Fredlund, M.D., Fredlund, D.G. and Wilson, G.W. 2000. An equation to represent grain-size distribution. Canadian Geotechnical Journal, **37**: 817-827.

GWP Software (1999). "FSConsol User's Manual", GWP Software Inc.

Halog, A. and Chan, A. 2008. Developing a dynamic systems model for the sustainable development of the Canadian oil sands industry. *International Journal of Environmental Technology and Management*, **8**(1): 3-22.

Houlihan, R. and Mian, H. 2008. Past, Present, Future Tailings – Regulatory Perspectives. First International Oil Sands Tailings Conference, Edmonton, Alberta, December 7-10, 2008. 8 pp.

Kossik, R and Miller, I. 2004. A probabilistic total system approach to the simulation of complex environmental systems. Proceedings of the 2004 Winter Simulation Conference.

McKenna, G. 2008. Landscape design for oil sands tailings. First International Oil Sands Tailings Conference, December 7-10, 2008, Edmonton, AB, Canada, pp. 51.

Mikula, R. and Omotoso, O. 2006. Role of clays in controlling tailings behaviour in oil sands processing. *Clay Science*, **12**(2): 177-182.

Rykaart, E.M., 2002. A methodology to describe spatial surface flux boundary conditions for solving tailings impoundment closure water balance problems. PhD thesis, Department of Civil and Environmental Engineering, University of Saskatchewan, Saskatoon, Canada.

Qiu, Y. and Segó, D.C., 2007. Optimum Deposition for Sub-Aerial Tailings Disposal:

Concepts and theories. *International Journal of Mining, Reclamation and Environment*, **20**(4): 272-285.

Scaffo-Migliaro, A. 2007. Modeling and simulation of an at-face slurry process for oil sands. MSc thesis, Department of Mechanical Engineering, University of Alberta, Edmonton, Alberta.

Scott, M.D. and Lo, R.C. 1992. Optimal tailings management at highland valley copper, *CIM Bulletin*, **85**: 85-88.

Shiffman, R.L., Vick, S.G., and Gibson, R. 1988. Behaviour and properties of hydraulic fills. Hydraulic fill structures. Geotechnical Special Publication no. 21, ASCE. Colorado State University, Fort Collins, Colorado, August 15-18, 1988, pp. 166-202.

Vick, S.G. 1983. Planning, design, and analysis of tailings dams. Wiley, New York.

Wallace, D., Tipman, R., Komishke, B., Wallwork, V., and Perkins, E. 2004. Fines/water interactions and consequences of the presence of degraded illite on oil sands extractability. *The Canadian Journal of Chemical Engineering*, **82**: 667-677.

Wels, C. and Robertson, M. 2003. Conceptual model for estimating water recovery in tailings impoundments. *Tailings and Mine Waste '03*. Pp. 87-94.

Wickham, M., Johnson, B., and Johnson, D. 2004. Dynamic systems-modeling approach to evaluating hydrologic implications of backfill designs. *Mining Engineering*, **56**:1 52-56.

ZONED STRENGTH MODEL FOR OILSANDS UPSTREAM TAILINGS BEACHES

Scott Martens and Tyler Lappin

Klohn Crippen Berger Ltd., Calgary, Alberta, Canada

Tim Eaton

Shell Canada Energy, Calgary, Alberta, Canada

ABSTRACT: Tailings dam design in the oilsands industry frequently uses upstream constructed dykes to contain ponds of fine tailings and water. These upstream dykes comprise compacted outer shells and un-compacted beaches of coarse tailings sand. The beach densities vary, and in some cases the beaches are sufficiently loose so as to be vulnerable to flow liquefaction. The design standard is generally to assess the dyke stability using post-liquefaction strengths for all potentially liquefiable materials. In these cases, the loose beaches may limit the ultimate height of the containment dykes. Shell Canada Energy and Klohn Crippen Berger Ltd. (KCBL) have conducted several detailed investigations of the properties of the beach sands at the Muskeg River Mine. Initial data indicated that much of the upstream beaches were potentially liquefiable, and post-liquefaction strengths were therefore used for the beaches in the dyke designs. More recent investigations indicated that densification of the beach sands was gradually occurring due to the gravity imposed shear stresses within the beaches, and that some layers within the beach sands were not vulnerable to flow liquefaction. KCBL developed a zoned beach tailings strength model to account for the effects of the loose and dense sand layers on the dyke stability, based on extensive cone penetration testing in the beach sands. This innovative model maintains an appropriate level of safety against potential instability related to beach liquefaction, while accounting for the strength available in the denser sand layers. The beach properties and the tailings strength model used for the dyke design are described in this paper.

INTRODUCTION

Site Description

The Shell Canada Energy (SCE) Muskeg River Mine (MRM) is an oilsands mine 60 km north of Ft. McMurray, Alberta. Tailings from the bitumen extraction process are currently stored in the External Tailings Facility (ETF), a tailings impoundment contained by a ring dyke with a perimeter

length of approximately 12 km. For the majority of that distance, containment is provided by an upstream construction tailings dyke. Construction of the ETF is complete to the design elevation, with a maximum height of 52 m. Future expansion is planned to higher dyke elevations in order to increase the storage capacity of the ETF.

Upstream tailings dams in the oilsands mining industry rely on a compacted shell of

coarse tailings sand and beaches of non-liquefiable sand to contain the pond and internal loose beach deposits. A typical section illustrating the materials in an upstream construction oilsand tailings dyke is shown on Figure 1. Energy to densify the sand in the shell is provided by dozers which compact the sand through the vibration of trafficking repeatedly across the sand surface, together with the downward drainage of construction water through the sand.

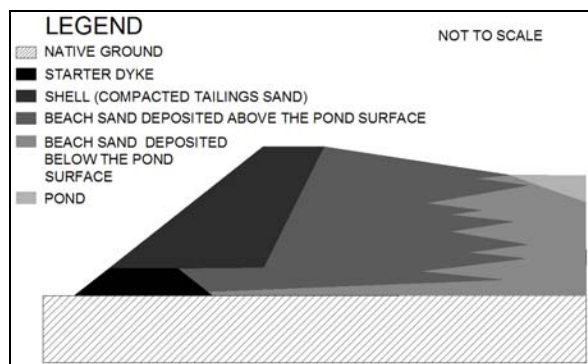


Figure 1. Upstream construction oilsand tailings dyke – typical section.

Design Basis

Large tailings dams must be safe from instability for all foreseeable combinations of loading conditions and resistances (material strengths) within the dyke and foundation.

The design basis typically used for upstream constructed tailings dykes in the Alberta oilsands industry is to use post-liquefaction strengths for all materials that are vulnerable to liquefaction. Potential liquefaction triggers include rapid shell or beach construction, foundation straining, and seismic ground motions. Seismicity studies in the area (KCBL, 2006) have indicated that the seismic ground motions for the return periods considered for tailings dam designs are low. Seismic triggering is considered very unlikely for most oilsands tailings dams. However, due to the very high consequences of a flow slide, if liquefaction triggering from other

(static) sources cannot be ruled out, post-liquefaction strengths are used for potentially liquefiable materials.

The initial design of the ETF considered that the beach sand deposited above the pond water elevation, denoted the beach-above-water (BAW) zone, would be sufficiently dense to not be vulnerable to static liquefaction. The deposition mode of the tailings (above water versus below water) has been understood to substantially affect the density of the deposited tailings in other oilsands mines, with BAW being sufficiently dense to resist static liquefaction, and beach-below-water (BBW) being loose and vulnerable to static liquefaction. However, in the case of the MRM tailings beaches, Cone Penetration Test (CPT) and Standard Penetration Test (SPT) data indicate that there is no clear distinction between the density of the BAW and BBW, with many instances of loose BAW, and occasional instances of dense BBW.

CPT and SPT testing after the first several years of operation and construction indicated that in most cases, the tailings beach sand beyond a 20 m distance from the upstream crest of the compacted shell did not meet the target density to be considered safe from static liquefaction. As a result, post-liquefaction strengths were used for the beach sands beyond this 20 m limit for planning further raises of the dykes.

Tailings Properties

The primary method used at the ETF to assess the tailings sand density and liquefaction susceptibility was the CPT.

Annual CPT programs starting in 2003 have been conducted at the MRM ETF to assess the state of the newly deposited beaches, and any changes in state of the older beach deposits.

Recent CPT results indicated increases in the density of the tailings beaches, when comparing the results of the annual test programs at the same locations. This improvement is believed to be a result of the increasing shear stresses under the slope of the tailings dyke gradually causing shearing and densification of the beach sand as the dyke is raised.

In general, the beach density decreases with increasing distance upstream from the compacted shell, with the density of the beaches nearest the compacted shell generally exceeding the criterion used to assess if the sand is vulnerable to flow liquefaction. However, the most recent CPT data suggests that some loose layers do still exist at all distances from the upstream edge of the compacted shell. The presence of liquefiable and non-liquefiable layers are addressed in the model described in this paper.

Throughout the paper the term “non-liquefiable” is used. In the context of this paper, this denotes sand that is dense of the contractant-dilatant boundary and not vulnerable to flow liquefaction. Such a material could, however, undergo cyclic liquefaction or cyclic mobility under dynamic loading of sufficient amplitude and duration.

ASSESSMENT METHODOLOGY

Post-Liquefaction Strength

The post-liquefaction strength of the liquefiable beach sand was characterized with an undrained shear strength dependent on overburden pressure, and a liquefied shear strength ratio $s_u/\sigma'_{v0} = 0.1$, based on the CPT data, and correlations by Olson and Stark (2002). A typical CPT plot is shown on Figure 2, together with the calculated post-liquefaction strength using the method of Olson and Stark (2002).

Flow Liquefaction Susceptibility

Several criteria were used to assess the vulnerability to flow liquefaction. Primary emphasis was placed on the Fear and Robertson (1995) contractant-dilatant boundary, which is based on a combination of theoretical understanding and case history data, and agrees reasonably with the results by other researchers. This criterion is recommended for use in practice by Olson and Stark (2003).

The equation of the flow liquefaction boundary used (contractant-dilatant boundary), based on Fear and Robertson (1995) and as stated by Olson and Stark (2003), inverted to show $(N_1)_{60}$ as a function of vertical effective stress was:

$$(N_1)_{60} = \left(\frac{\sigma'_v}{9.58 \times 10^{-4}} \right)^{\frac{1}{4.79}} \quad [1]$$

where:

σ'_v is in kPa

This boundary line was originally expressed in terms of SPT $(N_1)_{60}$. Olson and Stark (2003) have translated this criterion into terms of CPT q_{c1} using a fixed ratio of $q_c/N_{60}=0.6$. KCBL have found that the conversion between CPT and SPT recommended by Lunne et al. (1997) and also by Wride et al. (2000) is a better fit for the MRM tailings sand. Because the Lunne et al. (1997) correlation incorporates several parameters from the CPT data, it cannot practically be used to convert the liquefaction criteria from SPT to CPT terms. Therefore, we converted the CPT data to equivalent SPT $(N_1)_{60}$ to check against the boundary line, rather than converting the boundary line from SPT terms to CPT.

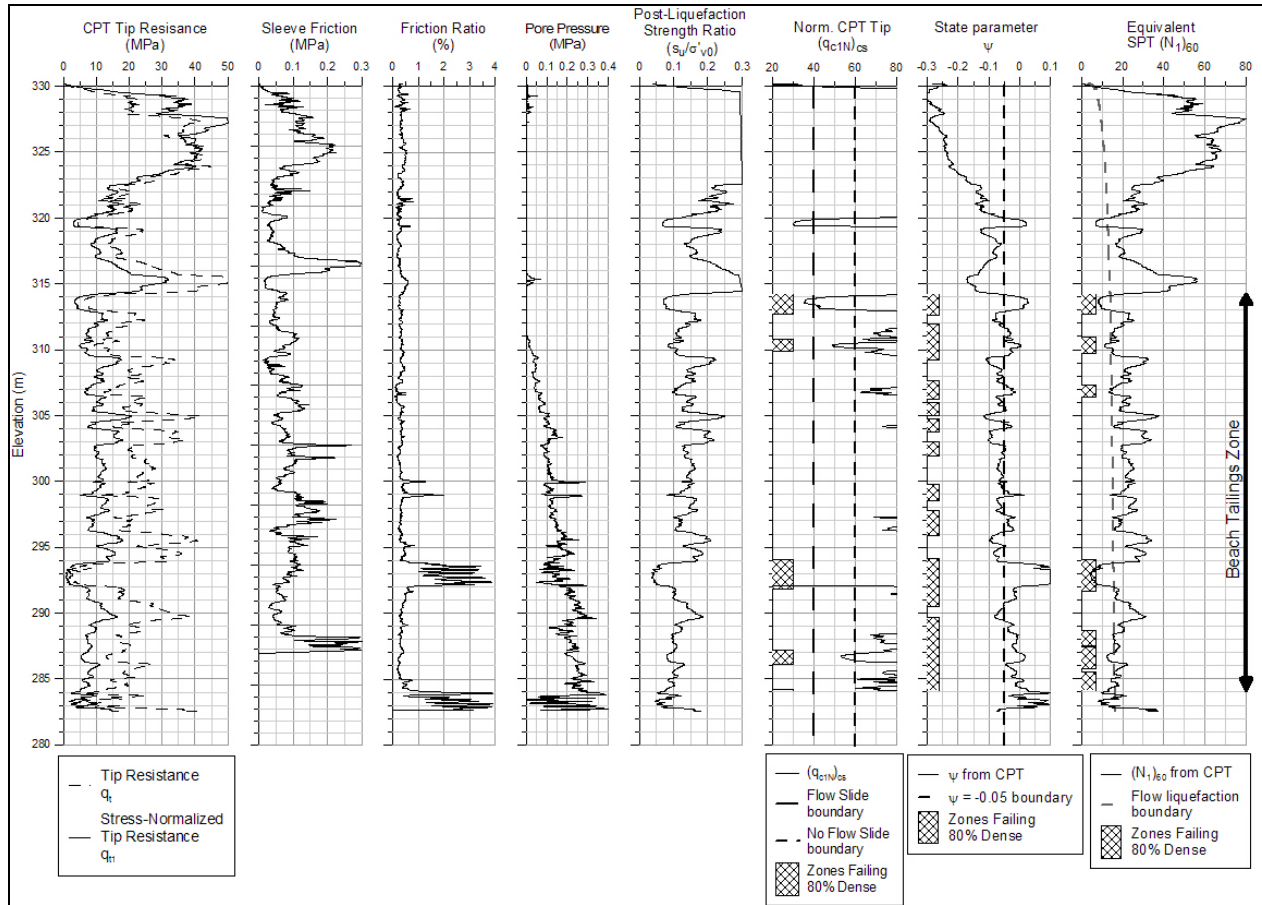


Figure 2. Typical CPT data from upstream oilsands tailings beach

The equation used to calculate the equivalent SPT $(N_1)_{60}$ was

$$(N_1)_{60} = \frac{\frac{q_{t1}}{P_a}}{8.5 \times \left(1 - \frac{I_c}{4.6}\right)} \quad [2]$$

where:

q_{t1} = stress normalized CPT tip resistance

P_a = atmospheric pressure, in units consistent with q_{t1}

I_c = CPT soil behaviour type index

The CPT data converted to equivalent SPT $(N_1)_{60}$ are plotted on Figure 2, together with

the Fear and Robertson (1995) liquefaction flow failure criteria.

To verify the suitability of the equivalent $(N_1)_{60}$ as calculated from the CPT, SPT boreholes were drilled adjacent to 18 CPT holes. The SPT holes were drilled using a mud-rotary drill, 98 mm diameter borehole, an upward discharge drill bit, AW rods, an automatic trip hammer and a standard sampler without a sample retainer in the shoe or liners. Energy measurements were taken on all of the SPT tests for two boreholes in the comparison program, and an average energy ratio of 85% was calculated for the automatic trip hammer used in the tests. A sample of the SPT and equivalent $(N_1)_{60}$ results are plotted on Figure 3. As seen from this figure, the equivalent $(N_1)_{60}$ values calculated from the CPT are generally a good

match to the measured SPT $(N_1)_{60}$ values. It isn't clear if the differences result from the correlation between the test types, lateral variability within the tailings sand over the distance (typically less than 3 m) between the CPT and SPT boreholes, or from variability within the SPT itself. Jefferies and Davies

(1993) have claimed that the inherent variability within the SPT is so great that the equivalent $(N_1)_{60}$ values calculated from the CPT are at least as reliable as the values directly obtained from the SPT.

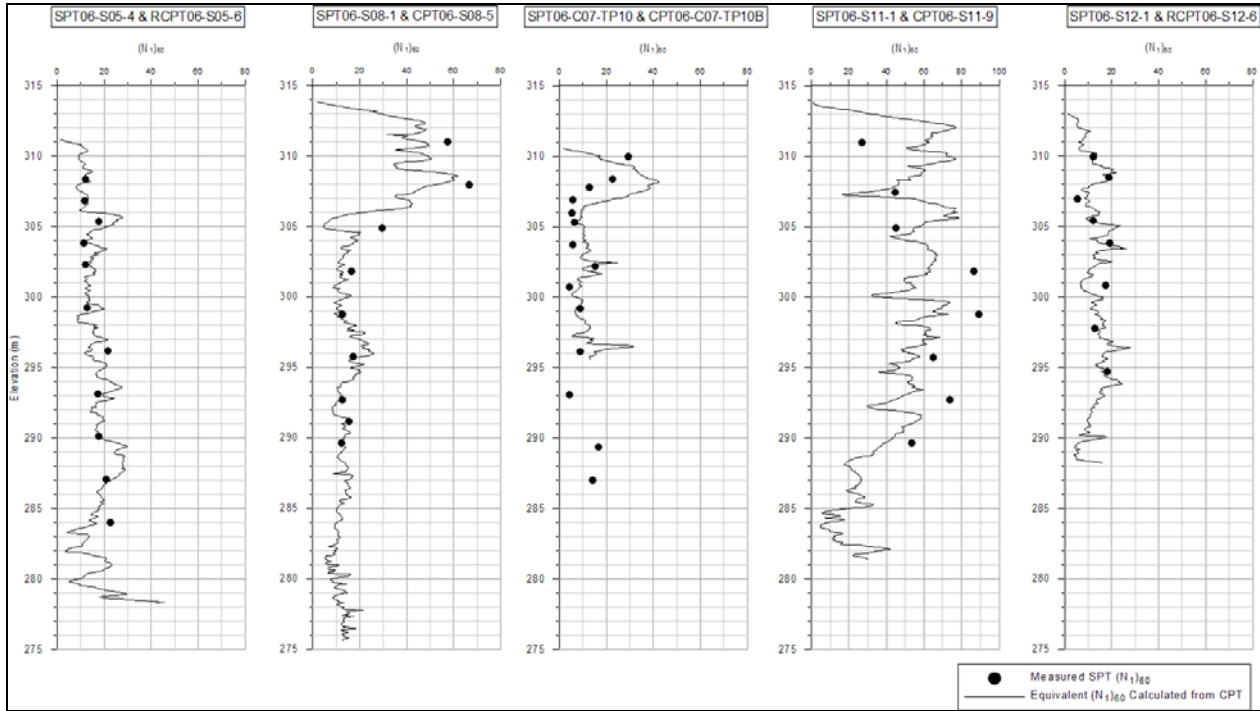


Figure 3. Comparison between SPT $(N_1)_{60}$ and equivalent $(N_1)_{60}$ calculated from CPT

A second criterion, by Yoshimine et al. (1999), expressed in terms of normalized CPT tip resistance $(q_{c1N})_{cs}$ was used as a check of the susceptibility to flow liquefaction. Yoshimine et al. (1999) indicated that sands with $(q_{c1N})_{cs} > 60$ were generally not vulnerable to flow liquefaction. This criterion is based on liquefaction case histories and not theoretical considerations. This criterion is not stress-dependent (although the CPT tip resistance is stress-normalized) and likely results in a conservative estimate of liquefaction susceptibility for shallow sands, and an unconservative estimate for deep sands. The Yoshimine et al. (1999) liquefaction

susceptibility criterion generally indicates a much lower percentage of liquefiable material than the other criteria. The CPT data are plotted against the Yoshimine et al. (1999) flow liquefaction criteria on Figure 2.

A third method to assess the susceptibility of the tailings sand to flow liquefaction was based on the state parameter, which was calculated directly from the CPT using the method of Plewes et al. (1992), modified to use the slope of the critical state line (λ_{10}) from triaxial testing on Albion tailings sand performed by KCBL. The calculated state parameter for much of the recent CPT data in Albion tailings sand beaches is in the range of

$\psi = -0.1$ to $\psi = 0$, but rarely exceeds $\psi = 0$. This would indicate that the tailings sand is dilative. However, Jefferies and Been (2006) recommend that sand should have a state parameter $\psi < -0.5$ to $\psi < -0.08$ to be confident that flow failure would not occur. This is sufficiently dense such that shear dilation dominates volumetric compression, and prevents generation of positive pore pressures during shear. If a criterion of $\psi < -0.05$ is used, most of the tailings beaches would be considered liquefiable. If the criterion was taken as $\psi < -0$, as per Fear and Robertson (1995), however, a much lower percentage of liquefiable material would be calculated. The calculated state parameter is plotted on Figure 2.

This assessment of the tailings beach liquefaction susceptibility was based primarily on the Fear and Robertson (1995) criterion, with the CPT data expressed as equivalent SPT $(N_1)_{60}$. The other criteria were used as a check of these results and to form an appreciation of the range of uncertainty in the assessment, but were not used to quantify the proportion of the beach that is vulnerable to a flow slide.

Zoned Tailings Model

An examination of the CPT data indicated that within the upstream tailings beaches, layers of sand were present that were both loose and dense of the flow liquefaction state boundary. The proportion of loose sand typically increased with distance upstream along the beach.

In order to characterize the extent of loose sand at each CPT location, the state of the beach tailings in each CPT hole was examined over a running 1 m average window with depth, where the sand at a given depth was assessed as liquefiable unless 80%

of the data points within the 1 m window were dense of the Fear and Robertson (1995) boundary line. Work by Jefferies and Been (2005) and Popescu et al. (1997) support the use of an 80% criteria for liquefaction susceptibility assessment. A 1 m averaging window was considered to be most appropriate based on the data set.

The effect of using a running 1 m window was to broaden the zones of materials considered to be liquefiable, compared to only counting the data points that failed to meet the criterion. This was considered reasonable to account for the potential for pore fluid migration following liquefaction of a loose layer, which could in turn result in loosening and loss of strength of an overlying, denser layer.

The CPT data were recorded at 1 cm depth intervals, and so each 1 cm depth was assigned a liquefiable or non-liquefiable status based on this criterion. The percentage of liquefiable sand was then summarized for each CPT hole. An average post-liquefaction strength was assigned to the beach sand at the location of the CPT, weighted by the proportions of liquefiable and non-liquefiable sand.

The details of the windowing scheme are shown on Figure 4, and an example of the method application is shown on Figure 5. The CPT data at this example borehole location indicated that approximately 70% of the vertical distance in the beach zone was non-liquefiable.

The results of characterizing the sand as being vulnerable or not vulnerable to flow liquefaction using this method are shown on Figures 2 and 5, where the depths that are highlighted have failed the criteria and are considered vulnerable to flow liquefaction.

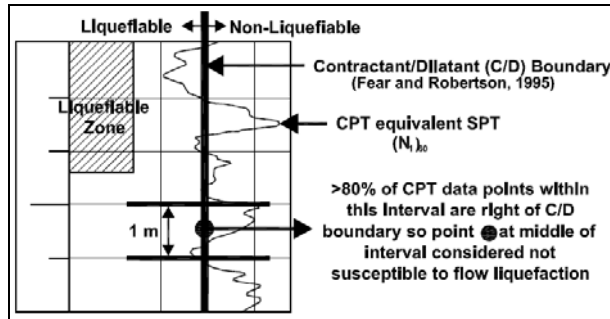


Figure 4. Liquefaction susceptibility assessment method.

Following this assessment, the beach was then divided into zones based on the percentage of liquefiable sand at each CPT location. Increments of 20% were used, and the percentage of non-liquefiable beach at each CPT location was rounded down to the nearest even 20%. For example, a CPT hole that indicated 36% non-liquefiable sand would be grouped into the 20% non-liquefiable zone. This rounding procedure was set to introduce conservatism into the assessment and account for uncertainty in the actual tailings behaviour.

A plot of the CPT data along a section, showing the characterization of the tailings into liquefaction susceptibility zones is shown on Figure 6.

An example plan of a dyke beach area showing the locations of the CPT holes and the interpreted plan extents of the various liquefaction zones is shown on Figure 7.

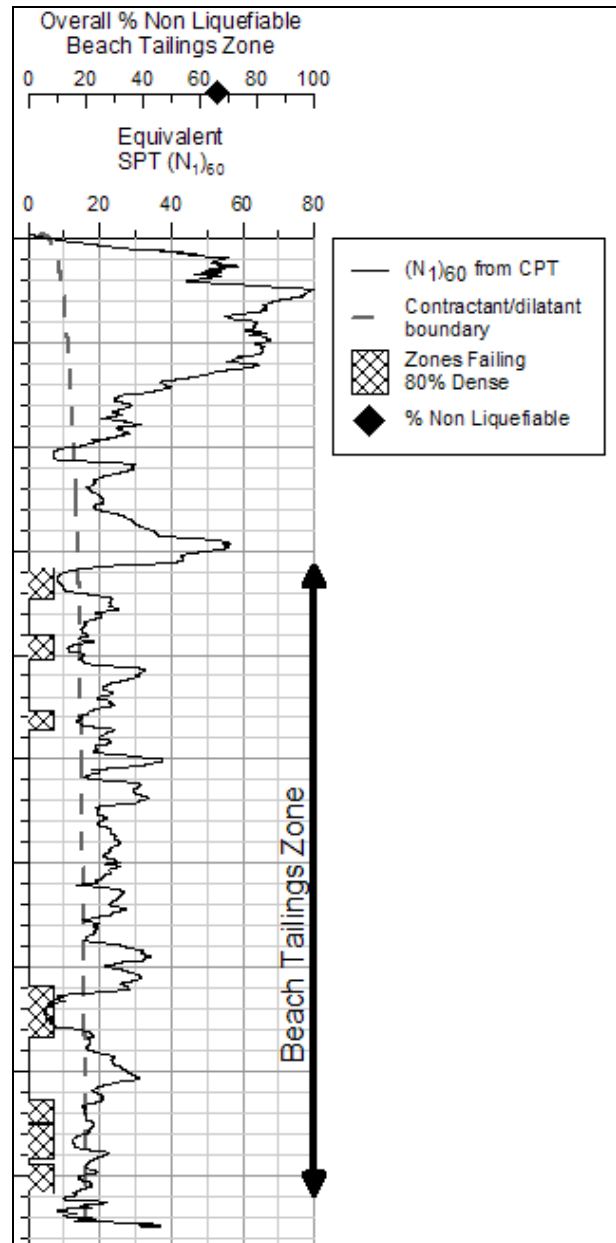


Figure 5. Liquefaction susceptibility characterization

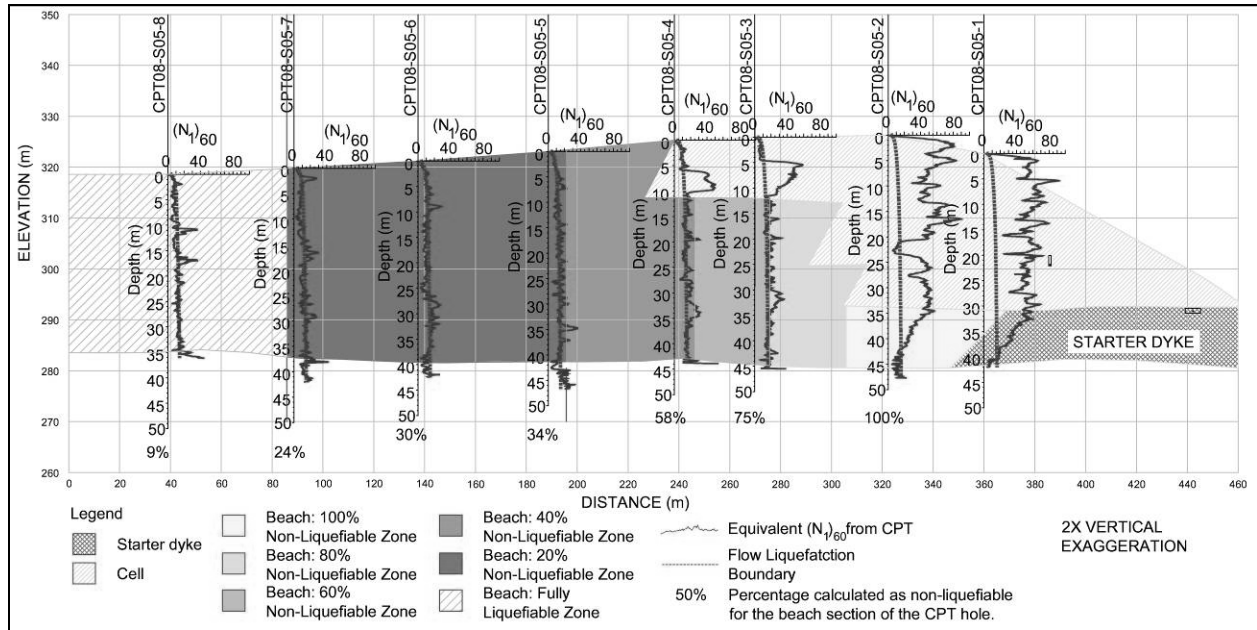


Figure 6. Cross section with CPT data and applied tailings zonation model

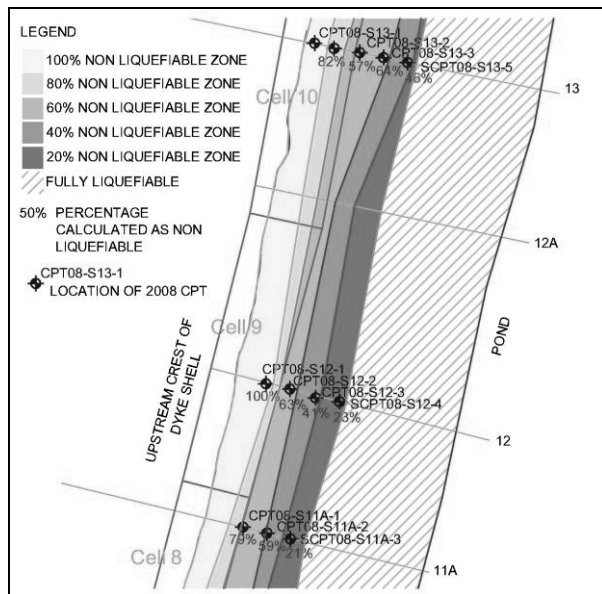


Figure 7. Typical extents of sand zonation along dyke beach

Strength Assignment for Zoned Tailings

The proportion of sand vulnerable to flow liquefaction was assigned a post-liquefaction

undrained strength ratio $s_u/\sigma'_{v0} = 0.1$, while the proportion of sand not considered vulnerable to flow liquefaction was assigned an effective stress, constant volume friction angle of $\phi' = 30^\circ$. A vertical section through the beach sand was assigned a weighted average friction angle based on the proportions of these materials, using the following expression:

$$\sigma'_{avg} = \arctan \left[\frac{LP * 0.1 + (100 - LP) * \tan(30^\circ)}{100} \right] \quad [3]$$

where:

LP = percentage of liquefiable sand in a vertical section

The strengths assigned to each tailings zone, based on the above formula, are summarized in Table 1.

Table 1 Summary of equivalent strength parameters

Beach Tailings Strength Zone (% Non-liquefiable along a Vertical Section)	Strength Parameter
100 (Completely non-liquefiable)	$\phi' = 30^\circ$
80	$\phi' = 26^\circ$
60	$\phi' = 21^\circ$
40	$\phi' = 16^\circ$
20	$\phi' = 11^\circ$
0 (Completely liquefiable)	$s_u/\sigma'_{v0} = 0.1$

Validation of Conceptual Model

The validity of the conceptual zoned tailings model was examined with numerical analyses using the FLAC version 6.0 finite difference software. The purpose of the numerical modelling was to check for a kinematically feasible failure mechanism that may occur if continuous layers of liquefiable tailings sand are present, that would be missed if the strengths of the liquefiable and non-liquefiable zones were blended according to Equation 3. Two models were compared to assess the validity of the weighted average strength concept for the tailings sand: one model with continuous horizontal weak

layers through the tailings beach, with the proportional of liquefiable and non-liquefiable layers grouped into zones of even 20% increments, and a second model with blended strengths for each zone. The factor of safety for each model was computed using the shear strength reduction technique in FLAC. This method for computing the factor of safety requires no prior assumptions on the geometry of the failure surface, and allows the minimum kinematically feasible failure surface to be found. Highly complex but realistic failure surfaces may be found that would not be identified using traditional limit equilibrium methods.

The two models used in FLAC are shown on Figures 8 and 9.

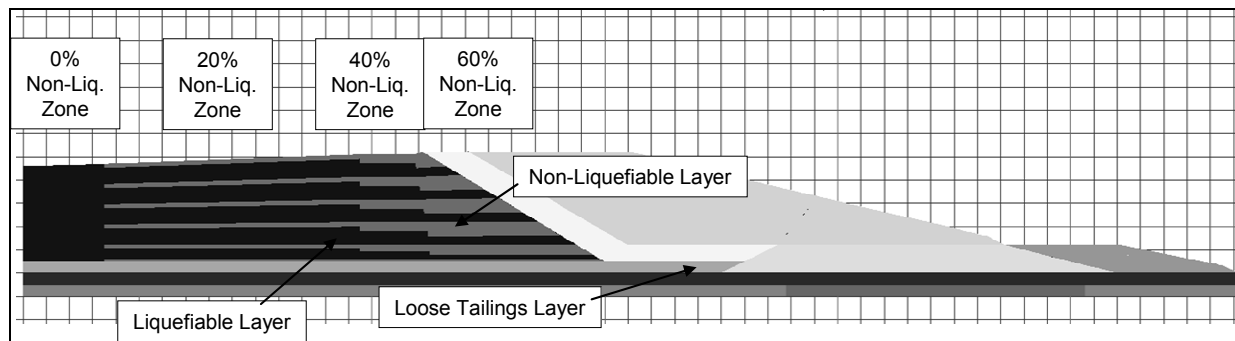


Figure 8. FLAC discrete layer model

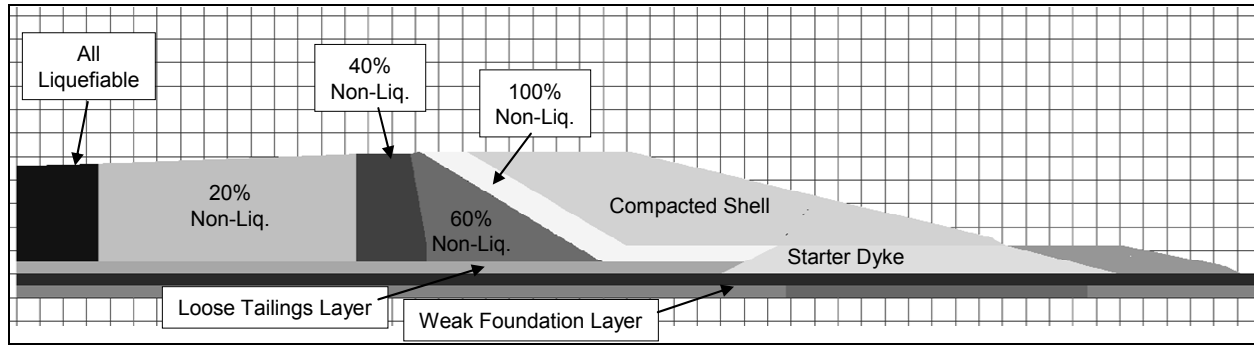


Figure 9. FLAC blended strength model.

Several trial analyses were performed using different patterns of liquefiable and non-liquefiable sand layers in the beach, while matching the overall proportions of these materials with the blended strength model. The factors of safety computed using the two methods differed in the range of 2% to 3%, with the model using the discrete zones in each case having a slightly lower factor of safety. A closeup plot showing shear strain rate contours of an incipient failure state for the case of the discrete material layers are shown on Figure 10. It is evident from Figure 10 that the failure surface cuts across the liquefiable and non-liquefiable layers in the beach, and then follows the weakest layer along the base of the sliding mass, which includes both a loose layer at the base of the tailings, and weak clay shales

in the foundation. The FLAC model shows the development of two shear zones through the tailings; one in the 40% non-liquefiable zone, and a second in the 80% non-liquefiable zone. These multiple shear zones are not predicted using the limit equilibrium model, and the FLAC results provide a better understanding of the potential mechanisms of failure even though the calculated factors of safety are similar.

We conclude from these analyses that the blended strength model reasonably approximates the more complex real system, with the difference in factor of safety well within the range of uncertainty in other input parameters.

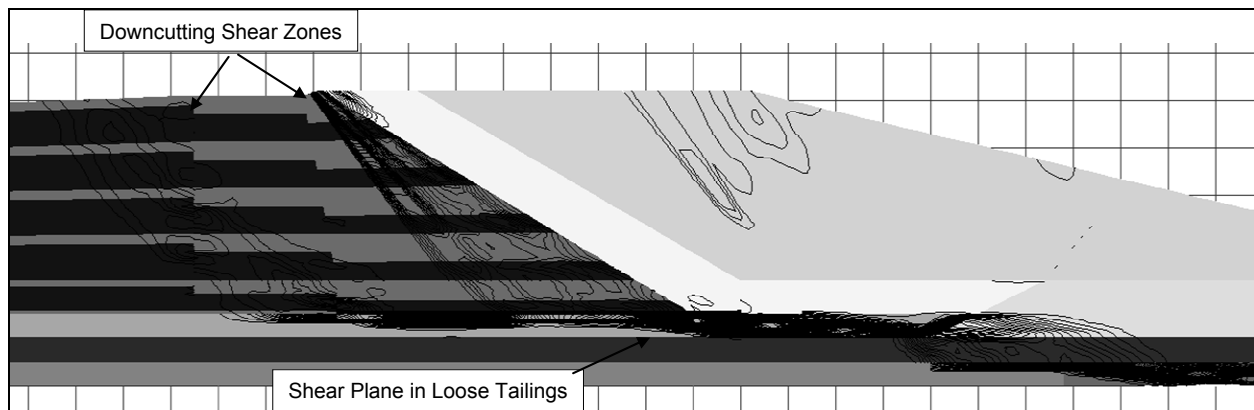


Figure 10. Shear strain rate contours showing shear surface development for discrete layer model

LIMITATIONS ON MODEL APPLICABILITY

The tailings beach sands comprise a stacked sequence of near-horizontal layers of varying density. The weighted average scheme discussed above is reasonable to characterize the tailings strength for the portion of the failure envelope where the slip surface downcuts across the various dense and loose layers of the tailings sand, since the mobilized strength will incorporate the strength of both the dense and loose layers. This weighted average strength, however, would not be appropriate for any portion of the slip surface that runs horizontally, where the slip surface would run along the weakest available layer.

The proposed tailings zonation strengths were incorporated in the ETF design analyses only where the slip surface downcuts across the tailings beach layers. A loose layer of tailings sand is present at the base of the ETF. As a potential shear surface could run along this loose layer, it was modeled using a post-liquefaction strength.

CONCLUSIONS

Incorporation of the zoned tailings strength model has allowed successful construction of the ETF to the design elevation, with a maximum height of 52 m, while reducing the size of toe berms that would otherwise be required had all of the tailings sand containing loose zones been treated as liquefiable.

ACKNOWLEDGEMENTS

The authors acknowledge and appreciate the permission of Shell Canada Energy to publish the information contained in this paper.

REFERENCES

- Fear, C., and Robertson, P., 1995. "Estimating the Undrained Strength of Sand a Theoretical Framework." *Canadian Geotechnical Journal*, 32: 859-870.
- Jefferies, M., and Been, K. 2006. *Soil Liquefaction: A Critical State View*. Routledge, Taylor and Francis Group, Oxford, UK.
- Jefferies, M., and Davies, M. 1993. Use of CPTu to Estimate Equivalent SPT N_{60} . *ASTM Geotechnical Testing Journal*, 16(4): 458-468.
- Klohn Crippen Berger Ltd. 2006. Ft. McMurray Region Seismic Hazard Study. Report submitted to the Ft. McMurray Seismic Hazard Working Group, October.
- Lunne T, Robertson, P. and Powell J. 1997. *Cone Penetration Testing in Geotechnical Practice*. Blackie Academic & Professional (Chapman & Hall), Glasgow, UK.
- Olson, S., and Stark, T. 2002. Liquefied strength ratio from liquefaction flow failure case histories. *Canadian Geotechnical Journal*, 39: 629-647.
- Olson, S., and Stark, T. 2003. Yield Strength Ratio and Liquefaction Analysis of Slopes and Embankments. *ASEC Journal of Geotechnical and Geoenvironmental Engineering*. 129(8): 727-737.
- Plewes, H., Davies, M., and Jefferies, M. 1992. CPT based screening procedure for evaluating liquefaction susceptibility. In *Proceedings of the 45th Canadian Geotechnical Conference*, Toronto, Ont., 26-28 October 1992. Canadian Geotechnical Society, Alliston, Ont. Vol. 4, 1-9.

Popescu, R., Prevost, J. H. and Deodatis, G. 1997. Effects of spatial variability on soil liquefaction: some design recommendations. *Geotechnique* 47, No. 5, 1019-1036.

Wride (Fear), C., Robertson, P., Biggar, K., Campanella, R., Hofmann, B., Hughes, J., Küpper, A., and Woeller, D. 2000. Interpretation of in situ test results from the CANLEX tests. *Canadian Geotechnical Journal*, 37: 505-529.

Yoshimine, M., Robertson, P. and Wride (Fear), C. 1999. Undrained shear strength of clean sands to trigger flow liquefaction. *Canadian Geotechnical Journal*, 36: 891-906.

IN PIT DYKE CONSTRUCTION PLANNING

Duane Treacy and Laura Bowie

Shell Canada Energy, Fort McMurray, Alberta, Canada

Tim Eaton and Robin Fauquier

Shell Canada Energy, Calgary, Alberta, Canada

Jay Horton

Norwest Corporation, Vancouver, British Columbia, Canada

ABSTRACT: Shell Canada Energy operates the Muskeg River Mine located 70 km north of Fort McMurray, Alberta. Mining and extraction have a production capacity of 155,000 bpd of bitumen from oilsand. Production started in early 2003 and mineral tailings produced from separating bitumen and mineral solids are stored in the External Tailings Facility (ETF). The majority of mineral tailings production will be stored in-pit by the end of 2010 for the life of mine.

The tailings storage plan requires in-pit dykes to be designed, constructed and operated on a continual basis throughout the life of mine. Six in-pit dykes will be constructed and operational between 2007 and 2013. Dyke construction fills come from mine wastes removed to expose oilsand that are sent for processing. Dyke construction fills and their properties are forecast using a geology model. Since 2005 a full time planner has been dedicated to preparing short-term dyke construction plans and material placement schedules.

Mining, extraction, tailings production and dyke construction occur on a continuous basis 24 hours per day 365 days a year. Materials have to be placed in dykes during the extreme cold of winter, spring thaw and in the wet summer months. Mine wastes that are not suitable for placement in the dykes go to mine waste storage dumps.

This paper describes the experience gained to date from applying the geology model, design premises, planning process; and from construction using mine waste. Proposed improvements will be described.

INTRODUCTION

Tailings sand and mine waste are used as dyke construction materials. Tailings sand has large advantages over mine waste in that it is:

- Readily available in large quantities,
- Has consistent properties and behaviour, and
- Has placement methods that are well suited to dyke construction.

The purpose of the paper is to describe the use of mine waste materials in dyke construction. Mine waste can be highly variable because its genesis is the result of deposition in varying aqueous conditions. These depositional environments are in themselves complex and not described in detail here.

Site Description

The Shell Canada Energy (SCE) Muskeg River Mine (MRM) is located 70 km north of Fort McMurray, Alberta. Oilsand is mined by truck and shovel operation. Since operations started in 2003 mineral tailings from the bitumen extraction process have been stored in an out of pit tailings impoundment with a perimeter ring dyke length of approximately 12 km. Construction and filling of the ETF is complete to the approved design elevation, with a maximum height of 52 m. Except for the ETF starter dykes constructed using mine waste, the perimeter dyke was constructed with tailings sand.

Starting in 2010 the majority of tailings produced will be stored in pit until the end of mining in about 30 years time.

Once tailings storage operations move in pit highly integrated planning of material movement is required to ensure:

- Supply of consistent bitumen feed to the extraction plant,
- Excavation and clean up of dyke footprints,
- Supply of construction fills to dykes,
- Scheduling of non-suitable mine wastes to disposal locations,
- Scheduling dyke construction to meet tailings filling schedules,
- Placement of dyke construction fills according to geotechnical specifications

and geotechnical performance constraints, and

- Scheduling the above activities in a northern climate with temperatures ranging from minus 35°C to plus 35°C.

The integrated planning process at MRM began in 2006; about three years before in pit tailings were scheduled for the first in pit storage cell, Cell 1. Typically in pit walls and dykes up to 80 m high, as shown in Figure 1 form tailings storage cells.

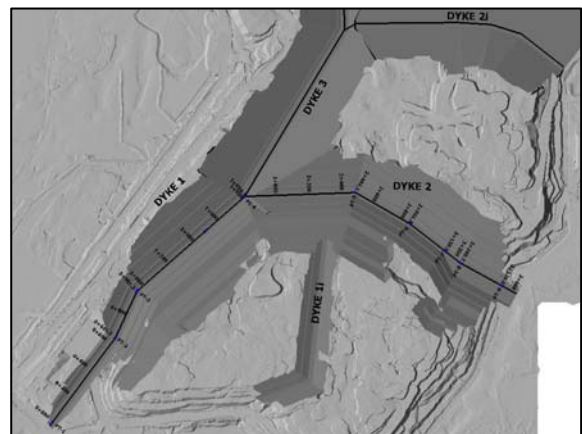


Figure 1. In pit tailings storage cells formed by dykes and pit walls.

Oilsand Tailings Storage Requirements

Oilsand mines operate for many years and move large quantities of material every day. MRM moves 150 Mt annually and neighboring operations move up to 400 Mt annually. This requires large fleets of excavators, trucks, dozers and support equipment. The mine must have enough space to allow the mining fleet to operate safely and efficiently. The mine must maintain an inventory of:

- Bitumen feeds for blending,
- Construction materials for dyke zones and seasonal constraints; and
- Also be large enough to allow access to dyke footprints for construction, and

- Provide the tailings space required by the integrated plan.

Regulatory Requirements

The Energy Resources Conservation Board (ERCB) regulates the energy industry in Alberta with a mandate to maximize recovery of the resource. In some instances the ERCB has to consider sterilization of bitumen in order to allow oilsand mining to proceed due to the geometry of the bitumen resource and the lack of sufficient barren ground for locating site facilities within a given mining lease.

The ERCB coordinates oilsand project reviews for regulatory agencies and public stakeholders. Approvals issued by the ERCB will contain conditions from other agencies and public input, in addition to conditions for energy recovery efficiency. Environmental conditions will support objectives of sustainability, protecting air, water, habitat and wildlife, reducing industry use of water from the Athabasca River, minimizing surface disturbance and progressive reclamation to landforms (with equivalent capability to that which existed prior to mining).

Tailings Properties

Mineral tailings from bitumen extraction are pumped to storage areas in slurries that may contain up to 60 percent solids by weight. The MRM life of mine bitumen feed has a fines content range of 13 percent to 14 percent (non-diluted, less than 44 microns by laser diffraction). The coarser sand fraction settles quickly near the discharge point and is often used for construction of containment dykes, as it is readily available in large quantities right at the construction dyke site. The finer fraction takes longer to settle and a significant component will remain in fluid suspension for many years

based on historical performance at older oilsand operations. The MRM ETF fluid tailings that remain in suspension are dominated by the clay fraction less than 2 microns.

The net effect of bitumen mining and extraction on overall waste volumes of material mined is a swelling of material volumes by up to 120 percent; depending on the geology. The swelled volume must remain stored on site and reclaimed, and is dominated by the fluid tailings component (largest swell factor and most difficult to manage and reclaim).

PLANNING

MRM in pit dyke construction planning currently involves a team of people working on a common goal of building the dykes on time, within budget and within the design specifications. The planning team (mining, dyke construction and tailings) works closely with mine operations supervision, field engineering, geotechnical engineering, the design consultant and construction monitors. The dyke can only be built with suitable materials available from the mine as the shovels expose ore inventory and remove waste.

Short Range Planning

Before the dyke can be built three-dimensional solids are constructed with Vulcan (Figure 1), an AutoCAD based proprietary drafting program. The weekly dyke planner requires a centerline, stations and typical cross sections from the designer. From this information the solids are created. Then survey lines and corresponding control points are used to survey stake lines in the field.

The weekly dyke plan and the longer 90-day dyke plan are created based on tonnage projected by the shovel planner from the geological block model for weekly and 90 day intervals. The short-term dyke plans have to follow what is happening in the field and the issues that must be dealt with on a daily basis.

Each week the lowest mined pit surface and the in pit dyke surface are as built by survey. This information is incorporated into two separate as builds. These are merged together by the weekly planner using Vulcan. Based on discussions with the departments involved with dyke construction the solids are cut to the as built surface to determine tonnages available for placement. This is an important step because it gives a good idea of progress and where to go visually on the computer and in the field. Any issues during this step are addressed with the stakeholders before the plan can be finalized.

The placement tonnages are tracked in dispatch and in a proprietary program named Powerview. The weekly planner uses a pivot table linked to Powerview that will give tonnages during any time period. The tonnages from Powerview are coded to the dyke placement locations such as downstream, upstream, toe berm (Table 1).

The weekly in pit dyke planning meeting is on a Thursday. This is a critical meeting with stakeholders for communicating and implementing the plan and resolving short-term issues. It is important that stakeholders agree the plan is achievable.

The survey for the dyke is on a Monday. The Pivot table is used to subtract the material tonnage placed between the Monday and the Thursday meeting to ensure the tonnages presented are accurate. When the pivot table is used the coding for the last week is checked to ensure accurate coding.

The planner creates source construction material solids using Vulcan and the geological block model to provide projected tonnage available from the pit where waste shovels are working. Information is also used from the field tours, knowledge of the pit and familiarity with the geology in the mine.

When tailings sand is used for dyke construction the short range mine waste construction planner relies on the short term tailings planner to address details related to tailings sand placement.

Table 1. In pit dyke placement tonnages extracted from Powerview.

DUMP_LOCATION_CD	MATERIAL_DESC	PROD_TONNES
DY_INPIT D2 US		382
	Type4	382
DY_INPIT D2 TOEBERM		107,113
	Dump Waste	352
	Type1	18,628
	Type4	88,133
DY_INPIT D2 DS		238,397
	Dump Waste	363
	Type4	238,034
GRAND TOTAL		345,892

The weekly plan can be created from information gathered with the In Pit Dyke Team, the placement tonnage and the construction source material tonnage. The weekly Mud Map (Figure 2), is a plan view of the cleanup requirements, placement areas, placement elevation targets, special instructions, priorities and projects involved. In the final plan proper wording is crucial. All communication references the Mud Map and must be followed through in the field every shift seven days a week.

Extraction plant requirements, ore properties (bitumen grade and particle size distribution),

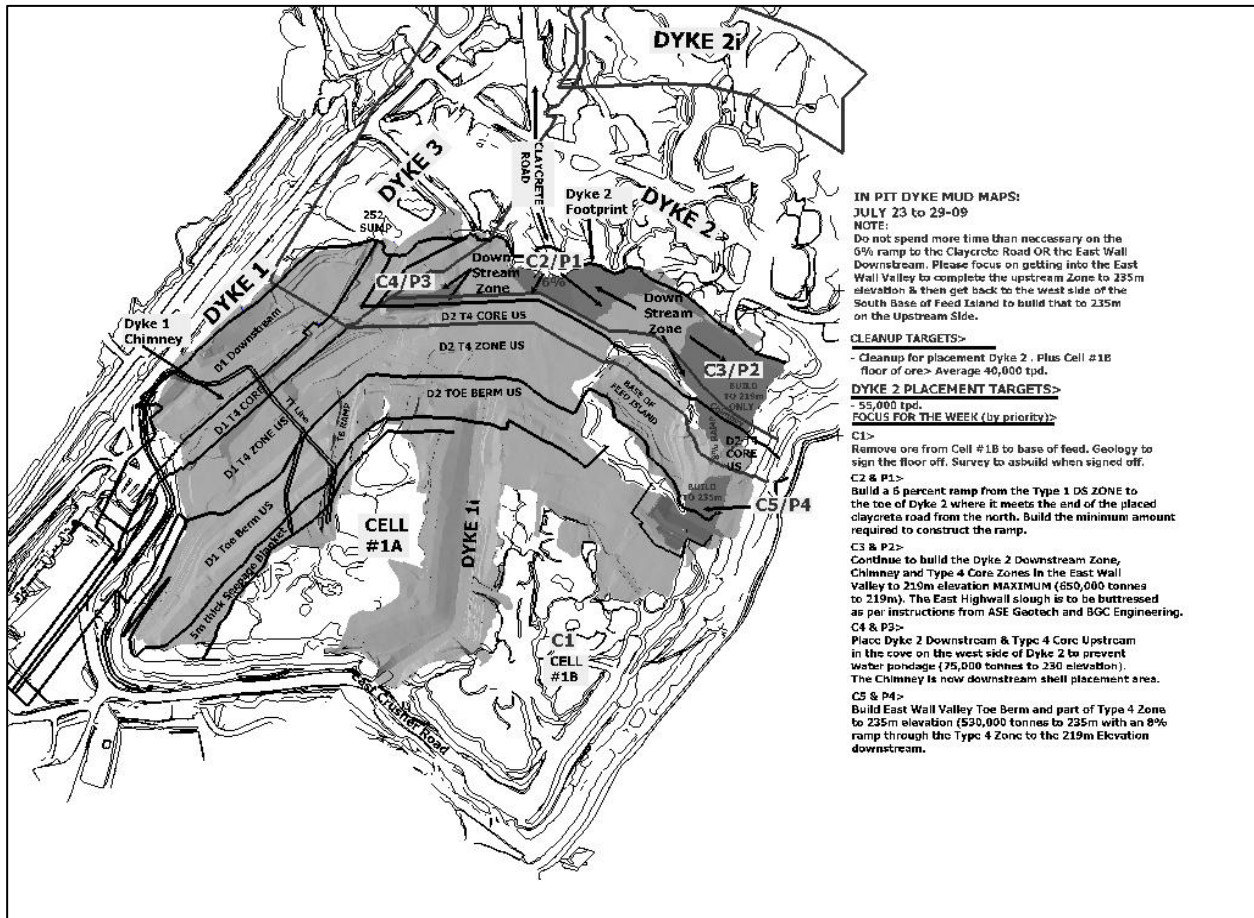


Figure 2. Weekly Mud Map.

available construction material types, equipment availability, weather, footprint availability and cleanup before material placement govern dyke placement progress. The construction quality control and quality assurance monitors are responsible to record all downtime on the dyke. The type of downtime is recorded in the construction monitoring reports. The information is linked to a waterfall chart that shows total available placement hours, delay time and net monthly placement hours (Figure 3). All short-term issues must be addressed with available resources. New trends are fed up to mid range planning. Note that ‘Truckers break’ in the figure reflects all shift changes and coffee breaks during the month and affects all mining and construction activity.

Mid Range Planning

At MRM the mid range tailings and in pit dyke planning is based on the mine plan for the same period of time. The mid range plan may extend out five years with detailed mining, filling and construction schedules. The outputs of ore tonnage to the crushers and the waste tonnage dug to access the ore are the main two inputs needed. The ore tonnage is used to determine the amount of tailings to be generated and therefore the storage capacity required to hold the tailings. The waste tonnage is divided into materials suitable for dyke construction and material to waste dumps. The dykes are then built in order to maintain storage capacity that meets or exceeds the expected tailings volumes. Dyke construction schedules strive to provide

6 months of tailings storage contingency. The mine plan also determines the footprint

available for dyke construction.

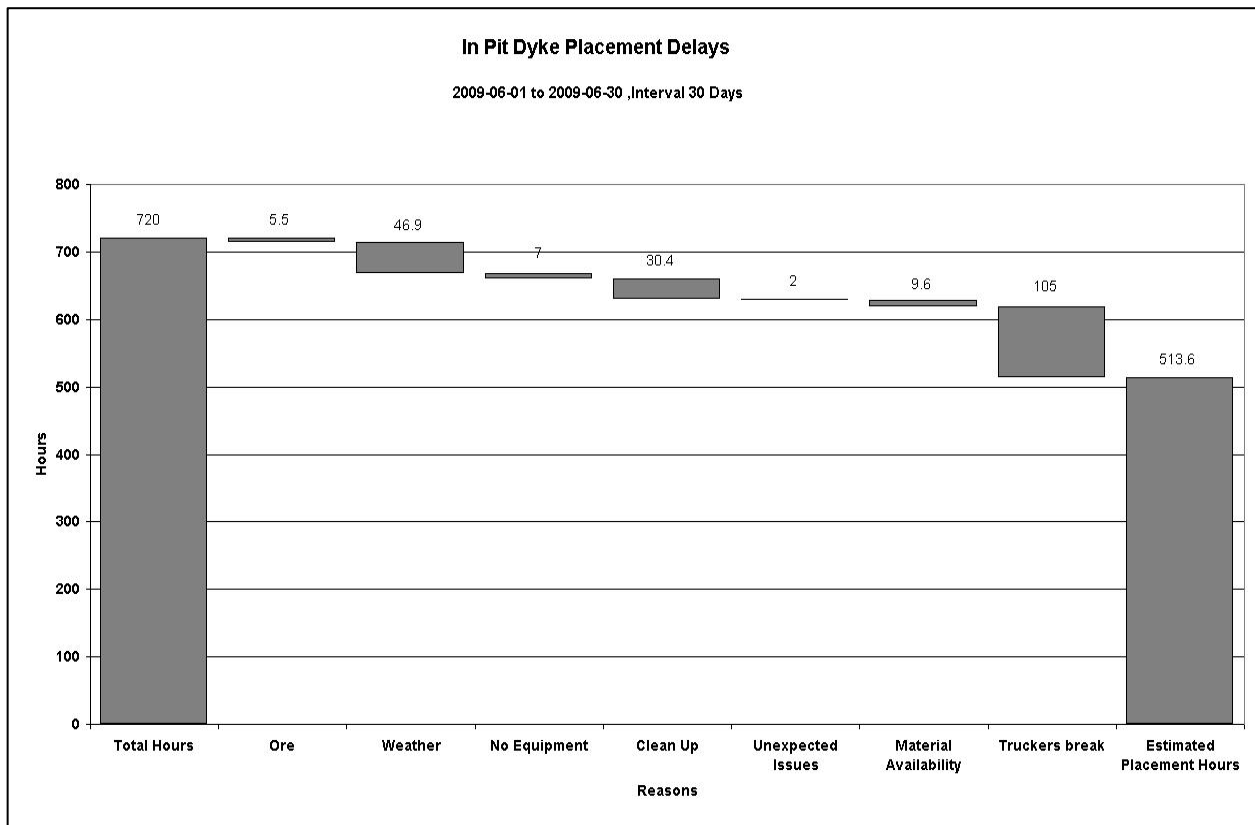


Figure 3. Waterfall chart of dyke placement delays.

If a mine plan shows footprint is not available soon enough the resulting outcome likely create potential for a tailings storage pinch point, congested placement areas or unacceptable build rates. The dyke planner must work with the mine planner to open up dyke footprints as soon as possible. The dykes are then planned based on the design cross sections. In pit dykes generally have an upstream and downstream zone, a core zone, internal drainage-seepage control elements and geotechnical specifications for each zone. The zones of the dyke need to be planned in a sequence that can be achieved in the field, for example the sand chimney is not planned to rise faster than the upstream side that it leans against. Certain drainage elements, abutment

clean up and fill placement must be scheduled in non-winter

Iterative Process

The resulting plan may work the first time but this is not usually the case. Often the in pit dyke planner finds problems with not having dyke footprint available when needed or not enough construction material to maintain capacity required for tailings. When this discrepancy happens, the planner must then coordinate efforts with the mine planner to allow for more footprint or waste tonnages. The resolution process takes time because the mine plan needs to meet targets related to ore feed. The number of iterations varies as

fixing one problem can reveal issues not considered in previous passes.

This iterative process takes place with the geotechnical side as well. The footprints being mined out are based on dykes being built at a certain slope. The slope is based on a number of factors, one being the in-situ material for the foundation. Although geotechnical investigations are performed to support the design the expected foundation material is not always present. Less favourable foundation conditions can result in additional foundation excavation and preparation or changes to the slope of the dyke (increased fill volume). Positive changes can result as well when weak foundation clays are not as extensive as identified by the borings. The geotechnical team monitors dyke foundation and fill performance. When performance is less favourable than anticipated additional construction fills may be required to buttress slopes and stabilize foundations. These changes always require further iterations of the plan.

The planning is completed using the Chronos component of Vulcan software. Chronos is Excel based and allows the planner to control inputs and what outputs are generated for reporting.

Constraints

There are considerations for dyke construction depending on the season. The main factors are placement of fills against pit walls and placement of drainage elements. Both of these areas of the dyke are only planned between April/May to October/November. When these areas are not built to plan potential for placements constraints in winter occur. Seasonal utilization factors are applied to account for frozen material that must be wasted in the winter and wet material that must be wasted

to due rain in the summer. (Rain softens haul roads lowering truck productivity. That results in more trucks assigned to the bitumen haul to keep the plant operating at full capacity.) Long periods of adverse winter or summer weather will impact longer term planning as it slows construction progress. Equipment productivity is addressed by using historical factors.

When equipment availability and utilization for dyke construction become serious and a threat to tailings containment the planning team resolves the issue with mine maintenance and mine operations. Maintenance schedules may have to be changed and mining priority may have to shift from ore feed to construction fills. Additional equipment purchases above those planned for may be required.

In pit infrastructure such as haul roads, tailings and water reclaim pipelines; booster pump stations, drainage controls and power lines are other constraints for how the dykes will be built. Roads and pipelines will cross active construction areas of dykes and eventually need to be relocated in order to keep the dyke construction ahead of the tailings filling schedule. Often there are multiple processes/activities occurring in the same location. Extra coordination and care is necessary to ensure interaction between heavy equipment routes, pipeline operation and maintenance activities have properly considered access, safety and efficient operation.

Material Descriptions

The materials used in dyke construction at MRM are derived from overburden and interburden seams that are mainly composed of the Lower Cretaceous McMurray Formation (Km) with a small proportion made up of surficial (Quaternary) materials. At MRM, the Km has been informally

divided into three members. These informal members are Lower (LM), Middle (MM) and Upper McMurray (UM) and exhibit an overall transgressive and deepening succession of depositional environments, the lower most of which eroded into Devonian strata. For planning purposes, the informal members are further subdivided into upper and lower units (i.e. MM1 and MM2). These three McMurray members reflect environments of sediment deposition that grade from continental-fluvial (Lower), through middle to outer estuary (Middle), and into a marine sequence (Upper).

Figures 4, 5 and 6 provide a representation of the laboratory data by member and facies at MRM. The grey bars represent the 10 percent to 90 percent range of data for each facies type within a geological member. A horizontal line indicates the average data content. The values at the top of the bars represent the percentage of the total core length of the member made up of that facies group. Minor facies in each group are not included hence the total for each group does not equal 100 percent.

Figure 4 shows a wide range of fines contents are present with averages ranging from 30 percent to 50 percent fines for various channel facies and 70 percent to 90 percent fines in the quiescent facies. Fines are measured by laser diffraction (LD). The intent here is to show the geotechnical fines limit of 74 micron whereas geology, mine and tailings planning use a 44 micron limit.

Water content range is quite consistent throughout the McMurray deposit. Figure 5 provides the geotechnical water content (weight of water over weight of solids) by member and facies. The data shows that the water content in most of the MM1, MM2, and LM2 facies average near 12 percent to 13 percent except the Estuarine Channel facies which averages near 14 percent. The

UM tends to be wetter with water contents in the 14 percent range.

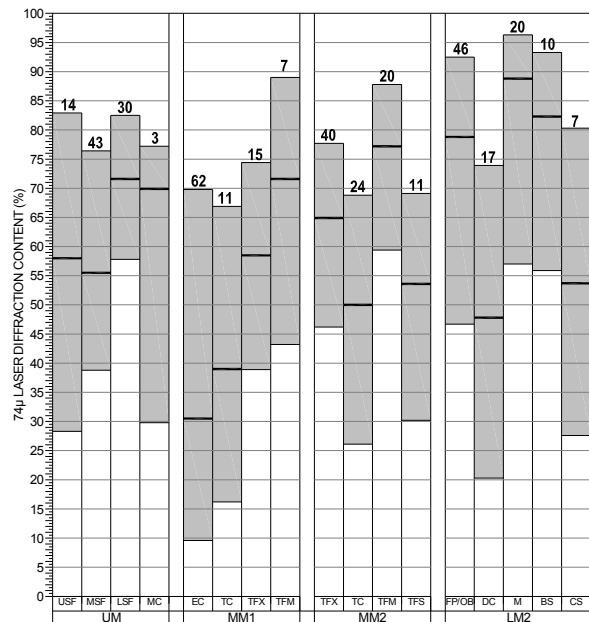


Figure 4. 74µ laser diffraction content of McMurray Formation waste materials.

Facies consisting of porous, clean sands typically have the highest bitumen content (weight of bitumen over total weight) whereas less porous, fine-grained sands and silts have lower bitumen content. Argillaceous minerals are generally barren. Figure 6 provides the total bitumen content of the waste material by member and facies. Most of the waste facies in the MM1, MM2 and UM members are between 3 percent to 5 percent bitumen content on average with the exception of TFM which has about 1 percent. The fine-grained facies of the LM2 are, on average, less than 1 percent bitumen content.

Material Classifications

Dyke construction material planning is carried out using a block model containing geological information where each block is assigned a waste type corresponding to a design material type. In modelling to date it had been decided that it was reasonable to

assign particle size and fluid properties in the geology block model based on facies descriptions and not on direct measurement of particle size distributions and fluid contents at regular sampling intervals.

The basis for the properties was the geology logs which have been acquired over a decade by dozens of different core hole loggers. All of the descriptions are subjective and were not corrected with actual lab data. This practice has been corrected and replaced with actual properties obtained from laboratory testing. At present, potential construction materials are classified into six main categories:

- Type 1 – Good quality sandy fill
- Type 2 – Good quality clayey fill
- Type 4 – Moderate quality sandy fill
- Type 4w – Oxidized ore
- Type 5 – Moderate quality clayey fill
- Type G – General fill

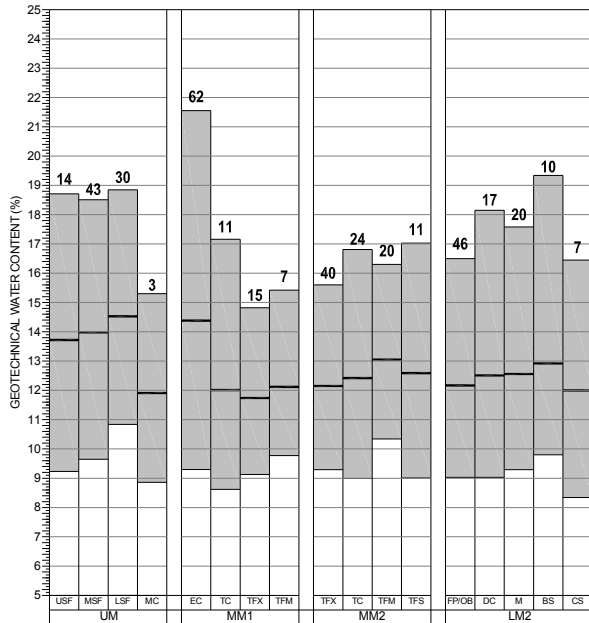


Figure 5. Geotechnical water content of McMurray Formation waste materials.

The construction specifications currently in use are based on the dyke design zonation requirements and are based mainly on clay and or sand content, bitumen and water content. The waste typing process, used for dyke construction planning will become more reliable in the near future when modelling scripts are converted to rely on actual hard data and not subjective facies descriptions.

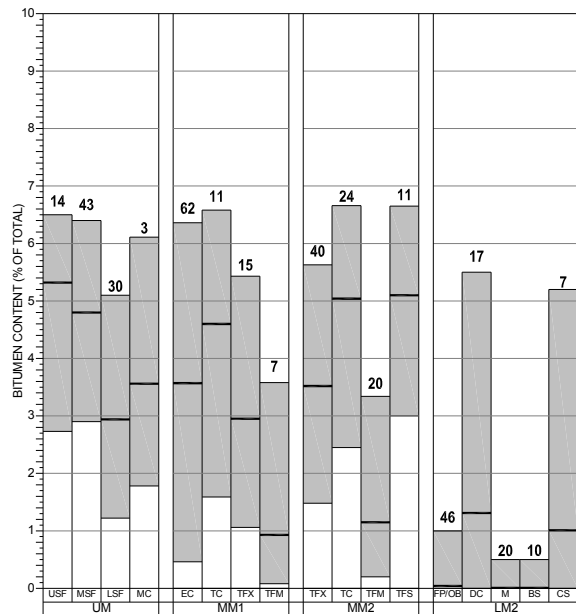


Figure 6. Bitumen content of McMurray Formation waste materials.

The construction monitors to account for the conditions as seen in the field use modified specifications. Construction monitors are not allowed to closely inspect or sample from the shovel faces for safety reasons. Therefore initial field calls must be made from a distance and a monitor must develop a keen eye after significant experience is obtained. Only after mine waste is placed as a construction fill can monitors make detailed assessment, sample and test. The fill types are differentiated by general material descriptions, bitumen content, moisture content, total fluid content, loaded haul truck (Cat 797) rut and roll, and compaction characteristics.

Shovels mine the waste materials from the various geological horizons in bench faces that range from 10 m to 20 m high. Significant material blending occurs during excavation and placement producing much more homogeneous material properties than the individual facies. Shear strengths and pore pressure response will exhibit a range depending blended particle size distribution, moisture and bitumen contents, and the level of compaction energy delivered to the fill.

Geology Model Refinements

Historically oilsand operators did not collect a lot of data on mine waste from geology exploration programs because of cost and the priority was to prove reserves. This was also the case at MRM prior to start up in 2003 and the early years of operation. For the last three years mine waste sampling and laboratory testing guidelines have been followed for the geology exploration programs at MRM and SCE's new Jackpine Mine (2010 planned start up). The real data set on mine wastes has increased significantly and will allow modelling of construction materials with greater precision and confidence.

Work is currently underway to refine these material types to better make use of the typical materials present in the mining area. These new material types are expected to move away from a typing method reliant on facies determination toward an approach defined by the material geotechnical characteristics such as grain size, water and bitumen contents. It is also expected that construction modelling will factor the mixing of materials in the shovel face to permit the use of lower quality materials when they are present in reasonable proportions in blended materials.

Field Trials

Field trials are in progress to optimize material placement specifications and visual calls by construction monitors. Monitors have been provided with additional resources to test and calibrate visual judgement of the material types, compaction effort and haul truck rut and roll performance with the geotechnical design specifications. Ability to place suitable construction materials may be limited by trafficability of the fills by loaded Cat 797's.

CONCLUSIONS

The integrated dyke planning process is described for the Muskeg River Mine operated by Shell Canada Energy. The process is complex with many internal participants and stakeholders that must work as a team to achieve success and meet common goals. Tailings sand is a practical dyke construction material. Demand to use mine waste in dyke construction has increased. Currently established practice now requires all geology exploration programs to acquire geotechnical data from mine waste zones. The mine waste data is used to support dyke construction material modeling and planning. Recent internal studies and field trials, in progress and ongoing, are providing insights how the data will allow better material characterization and utilization in dyke construction. This paper has not attempted to explain the details of dyke construction with tailings sand or the use of tailings sand to comply with new regulations.

ACKNOWLEDGEMENTS

The authors acknowledge and appreciate the permission of Shell Canada Energy to publish the information contained in this paper. Particular thanks are extended to the teams in Mine Technical Services and Mine Operations at Muskeg River Mine who work closely to make this process a success.

REFERENCES

2006-2009. Internal discussions, dyke construction studies and planning data, Muskeg River Mine. Shell Canada Energy Limited.

FLUORESCENCE CHARACTERIZATION OF OIL SANDS NAPHTHENIC ACIDS

A.M. Ewanchuk, M. Alostaz, A. C. Ulrich & D. C. Segó

University of Alberta, Edmonton, Alberta, Canada

ABSTRACT: The process affected (PA) water from oil sands production plants is known to contain naphthenic acids (NAs) that are produced during the extraction process. Presence of NAs is an environmental concern as they are corrosive to the refinery unit and are toxic to various organisms in the tailings pond. Oil sands NAs contain functional groups that when exposed to ultraviolet wavelengths between 260-350nm emit unique fluorescence signals that can be presented as fluorescence excitation-emission matrices (EEMs). The fluorescence signal produced is a distinctive characteristic of the electron structure for that particular NA. The uniqueness of the fluorescence signal produced allows for using them as fingerprints or signatures to characterize NAs in PA waters, track changes that occur to NAs from the bitumen to the storage in tailings ponds and identify changing concentrations, speciation, the source or refining process, degradation and aging processes of the NAs in PA water.

INTRODUCTION

Naphthenic Acids in the Oil Sands

The oil sands deposits in northern Alberta, Canada, represent one of the largest oil deposits in the world with reserves of 173 billion barrels proven to be recoverable (Alberta Government 2009). The Athabasca oil sands contain large amounts of naphthenic acids from the biodegradation of a mature petroleum deposit (Clemente & Fedorak 2005). Bitumen extraction is currently done via modified versions of Clark Hot Water Extraction method (Allen 2008). The raw ore is digested with warm water (50-80°C) and NaOH that acts as a conditioning agent (Yen et al. 2004; Holowenko et al. 2002). During the extraction process the naphthenic acids are released and carried throughout the

extraction plant into the process water (Janfada et al. 2006).

Up to 85% of the water used in the extraction process is recycled water (Allen 2008). The water not recycled that contains sands and clays, is referred to as the tailings, and is then hydraulically transported to a tailings pond; impoundments where the particles within the slurry are allowed to settle (Headley & McMartin 2004). The naphthenic acids are then concentrated and contained within the impoundments. A zero discharge policy has been implemented for the water used in the mining industry to minimize impact to the surrounding environment; however at the end of the mine lifespan there is a requirement to remediate and return the land back to its original state, with the intent to facilitate a sustainable ecosystems (Allen 2008). Naphthenic acids have been shown to be toxic

to various organisms and cause corrosion issues within the refinery units in the extraction process (Allen 2008; Clemente & Fedorak 2005; Headley & McMartin 2004; Slavcheva 1999; Babaian-Kibala 1994).

Concentrations of naphthenic acids within the tailings ponds have been found in the range of 40-120 mg/L, while nearby groundwater concentrations are typically lower in the range of 0.4-51 mg/L (Holowenko et al. 2001; Clemente & Fedorak 2005). In the surrounding area surficial waters contain natural occurring naphthenic acids due to contact with the oil sand ore body in the range of 0.1 to 0.9 mg/L (Clemente & Fedorak 2005).

Current methods of identifying and characterizing naphthenic acids are complex, time consuming and do not have the ability to isolate individual species. Due to the inherent properties of the naphthenic acids there is a demand for a more rapid and accessible analytical technique in order to adequately characterize the presence of these compounds. Recently fluorescence technology has been shown to generate unique signatures that can be used to identify individual naphthenic acid compounds. This paper summarizes some of the fundamental research on the characterization of naphthenic acids, and describes the ability of fluorescence spectrometry as an alternative for quantitative analysis of naphthenic acids.

NAPHTHENIC ACIDS

Characteristics of Naphthenic Acids

Naphthenic acids are monobasic carboxylic acids and are composed primarily of alkyl-substituted cycloaliphatic carboxylic acids (Brient et al. 1995). Naphthenic acids are considered to be of the form $C_nH_{2n+Z}O_2$,

where n is the number of carbons and Z is a zero or negative, even integer that specifies the homologous series (Clemente & Fedorak 2004). The Z value ranges from 0 to -12 and indicates the hydrogen deficiency resulting from the ring formation. Ring structures typically contain five or six carbons with each multiple of -2 signifying another ring (Brient et al. 1995). Figure 1 shows some typical structures of naphthenic acids, with R representing the alkyl functional group.

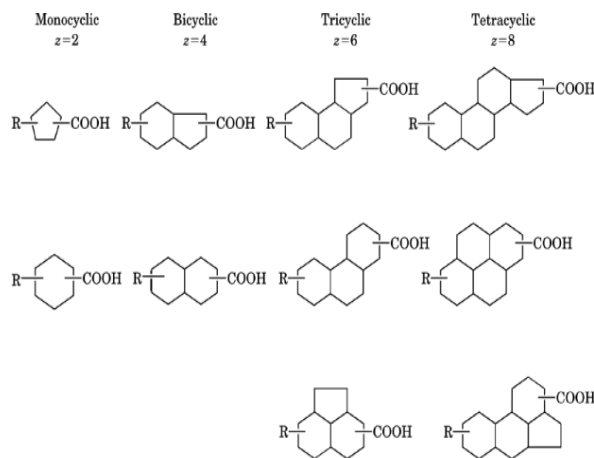


Figure 1: Naphthenic Acid Structures (adapted from Brient et al. 1995)

However, the naphthenic acids derived from petroleum products have been shown to contain various levels of impurities, and do not fall within the general formula $C_nH_{2n+Z}O_2$. Using thin layer chromatography the presence of phenol, nitrogen and sulphur were found within the naphthenic acid fraction of a Californian crude oil (Seifert & Teether 1969). Similarly UV and IR analysis on a Californian crude oil found the presence of pyrroles, thiophenes, and phenols in the naphthenic acid portion (Seifert et al. 1969). More recently mass spectrometry methods were able to determine compositions containing oxygen, ozone, tetraoxygen (O_4), O_2S , O_3S and O_4S within a South American heavy crude (Headley et al. 2009).

ISSUES WITH NAPHTHENIC ACIDS

Toxicity

Naphthenic acids have been found to be the source of toxicity within the tailings pond water using the Environmental Protection Agency Toxicity Identification and Evaluation protocol (Allen 2008). The toxicity is generally associated with surfactant properties associated with naphthenic acids (Headley & McMartin 2004). Many organisms will experience toxic effects from exposure to the acids. Concentrations in the range of 2.5-5 mg/L have been found to be acutely toxic to fish (Clemente & Fedorak 2005). Other organisms that experience toxic effects include plants, plankton, rats and some bacteria (Allen 2008; Clemente & Fedorak 2005). The naphthenic acid compounds have been shown to induce acute toxicity effects to aquatic animals, and pose a risk to terrestrial animals (Janfada et al. 2006). Acute poisoning in mammals was found to be unlikely even under worst case scenarios (Headley & McMartin 2004). Rats were found to have detrimental effects which manifested in the liver when exposed to the naphthenic acids through oral consumption of dissolved species (Clemente & Fedorak, 2005). The toxic dosage is found to be 3.0 to 5.2 milligrams per litre for rats, which correlates to about 11 grams per kilogram for humans (Janfada et al. 2006). This leads to the belief that though acute poisoning may not be a risk for mammals, the repeated exposure will have adverse health effects (Allen 2008; Headley & McMartin 2004). Though acute and long term effects have been associated with the toxicity of naphthenic acids, other toxicity tests have ruled out mutagenic and carcinogenic toxicity (Headley & McMartin 2004). Some research has also indicated that there may be some evidence of

endocrine disruption characteristics (Hao et al. 2005).

Several works have established that the lower molecular weight naphthenic acid molecules were the culprits of its toxicity (Janfada et al. 2006; Headley & McMartin 2004; Holowenko et al. 2002). The naphthenic acids found in freshly deposited tailing waters were dominated with lower molecular weight and lower carbons, and contained the highest levels of toxicity (Allen 2008). As the naphthenic acids were degraded, compounds with high numbers of carbon were found and the toxicity decreased (Allen 2008). Therefore toxicity is not solely related to naphthenic acid concentration, but to the complexity and content of the naphthenic acids (Headley & McMartin 2004). Research completed by Allen (2008) determined that there was still a significant acute toxic effect at low concentrations, depending on the receptor. However there is also significant amount of evidence that shows as the naphthenic acid content decreases, so does the level of toxicity (Headley & McMartin 2004). This leads to further complications in analysis of the environmental risks naphthenic acids pose.

Corrosion

A second issue with naphthenic acids in the oil sands industry is corrosion within the refinery units. Corrosion due to naphthenic acids was first apparent in the early 1920s (Slavcheva 1999). The corrosive reactions involve the chelation of the metal ions present within the refinery units, such as iron, by the carboxylic functional group (Clemente & Fedorak 2005). Other work suggests that the naphthenic acids react with iron surfaces of the piping in the refinery, and form iron naphthenate salts (Babaian-Kibala 1994). The high solubility of these compounds then allows them to detach from the piping

surface, and subsequently expose the surface for more corrosion attack (Babaian-Kibala 1994).

The elevated temperatures that are found in the extraction process can favour the corrosion reaction, however at temperatures above 400°C naphthenic acids are susceptible to decay and can actually form a film surrounding the alloy that can protect it (Clemente & Fedorak 2005). This residue is thought to be the composition of iron naphthenates (that originally caused the corrosion) precipitating from solution (Babaian-Kibala 1994). This cycle is due in part to the recycling of process water within the system. The concentration of the naphthenic acids in the corrosion cycle will increase and the cycle will keep repeating itself, which can lead to large amounts of metal loss within the pipes. Other factors contributing to corrosion by naphthenic acids are 1) The total acid number 2) The velocity and turbulence within the system 3) The physical state of the crude oil (vapour or liquid) and 4) The type of piping materials within the refinery (Slavcheva 1999).

The high boiling point of the naphthenic acids lead them to maintain presence in the hotter parts of the refinery system (Babaian-Kibala 1994). Since the naphthenic acids are able to withstand the high temperatures, the extent of the corrosion is widespread. Areas affected by naphthenic acid corrosion include atmospheric and vacuum furnace and tower bottoms, pumps, valves, fittings and transfer lines (Slavcheva 1999; Babaian-Kibala 1994). In addition there can be localized corrosion attack on any area that is exposed to high velocities (Slavcheva 1999).

Studies to date have not found a correlation between the concentration of the naphthenic acids and the amount of corrosion experienced, but is instead related to the composition of the naphthenic acids present

(Babaian-Kibala 1994). Improved characterization of naphthenic acids could perhaps give better insight as to the mechanisms behind the corrosion process, and help mitigate the problem.

METHODS OF CHARACTERIZATION

Fourier Transform Infrared Spectroscopy

One possible method used to characterize naphthenic acids in the industry is through the use of Fourier transform infrared (FTIR) spectroscopy. This involves the acidification of an aqueous sample, which is then exposed to dichloromethane which quantitatively extracts the naphthenic acids (Yen et al. 2004). The dichloromethane with the extracted naphthenic acids is then analyzed using the FTIR equipment, which measures the absorbance of the monomeric and dimeric forms of the carbonyl groups at their respective wavelengths of 1743 and 1706 cm^{-1} (Clemente & Fedorak 2005). The results are then quantified by calibration curves derived from commercially available naphthenic acids. This method is unable to give insight into individual naphthenic acids and resolve carbon numbers and Z families (Holowenko et al. 2002).

Mass Spectrometry

Other methods used to characterize naphthenic acids have been based on mass spectrometry. Mass spectrometry separates the sample into charged particles which can then be analyzed and sorted according to mass. A method of detection is then used to determine the quantity of the mass present in the sample. Mass spectrometry methods such as gas chromatography (Holowenko et al. 2002), high performance liquid chromatography (HPLC) (Bataneh et al. 2006), electrospray ionization (Martin et al.

2008; Clemente and Fedorak 2005), fast atom bombardment (Fan 1991), and chemical ionization (Zhenbo et al. 2005) have been used.

In gas chromatography an inert gas is passed through an inert column, where naphthenic acids are separated at various retention times. As the number of carbons and rings in the structure are increased, their retention time in the chromatography column is increased (Hao et al. 2005). The analysis gives a nominal mass that could then be used to predict the carbon number and subsequent empirical formula for the naphthenic acids. One of the issues noted with this method is the massive amount of ions that are measured in the sample. The ions measured are then used to determine the compounds present in the sample. The complexity of the naphthenic acids can make this a tedious process, of which data can be misleading (Clemente & Fedorak 2004). Another issue with the test was found to be column bleed, as the samples were exposed to prolonged retention times the presence of higher carbon numbered naphthenic acids were found to increase. Another limitation of this method is the misinterpretation of the data. Due to unpredicted changes in the sample there maybe cleavage of the heavier weighted isotopes which would appear as a low end molecular mass and thus the individual concentrations of the naphthenic acid compounds would be shifted (Clemente and Fedorak 2004). In work completed by Hao et al. (2005) it was shown that part of the issue with gas chromatography was the fact that the column would become overloaded with elevated levels of injection volume.

High performance liquid chromatography (HPLC) can also be used to characterize naphthenic acids. NAs are separated according to carbon number, degree of cyclization, and the degree of alkyl branching

(Bataineh et al. 2006). The retention times of the NAs are dependent on the number of carbons, n , and the degree of cyclization, Z . This method requires a large amount of sample preparation. HPLC can be used in conjunction with mass spectrometry methods, such as high resolution mass spectrometry (HRMS) (Martin et al. 2008).

Electrospray ionization is a method used for determining concentrations of aqueous samples, through solid phase extraction using a sorbent (Clemente and Fedorak 2005). The samples are eluted from the sorbent and subsequently analyzed by the electrospray ionization-mass spectrometry unit, a method that is very similar to gas spectrometry. Electrospray ionization has been coupled with HPLC, in order to increase the sensitivity of NA detection (Martin et al. 2008). Fast atom bombardment uses an inert gas and separates the compounds into protonated and deprotonated molecules. In the case of naphthenic acids, an abundance of deprotonated molecules are formed, from which the molecular weight and subsequent molecular structure can be found (Fan 1991). Fan (1991) found that gas chromatography was not suitable for compounds that were of low molecular weight or volatile, and that naphthenic acids fell into neither of these categories. Fast atom bombardment had been shown to successfully categorize carboxylic acids in previous work when Fan (1991) decided to apply the concepts to naphthenic acids.

Chemical ionization mass spectrometry has shown some use in characterization of naphthenic acids when modified. The general chemical ionization method was found to not be suited to naphthenic acids as the fragmented ions in the method make determination of molecular weights and identification difficult (Zhenbo et al. 2005). They found that modifying the naphthenic

acids to their ester form and using isobutane as a reagent improved the general chemical ionization method. The issue with this method is the amount of sample preparation that is required in order to analyze the naphthenic acids. As with other mass spectrometry methods only the relative distribution of the naphthenic acids can be determined, not individual species (Zhenbo et al. 2005).

Mass spectrometry methods have been applied to the study of naphthenic acids as it allows the quantification of all the isotopes present, however, as previously mentioned this only allows for the categorization of the naphthenic acids according to carbon number and homologous series. The individual naphthenic acids and their isotopes cannot be determined individually.

The determination of the total naphthenic concentration in a sample does not adequately explain the toxic or the corrosive effects, and gives very little detail into the makeup of the sample (Clemente & Fedorak 2005). The use of mass spectrometry can give some insight as to whether or not the sample is made up of heavy molecular weight compounds, or light molecular weight compounds. One of the main issues with this method is the high number of extraction and purification steps that are necessary in order to separate the hydrocarbons from the naphthenic acids (Clemente & Fedorak 2005). The lengthy testing process is an issue in the oil sands industry, and would prove to be an issue in the case of urgent measurements. This facilitates the need for a fast and reliable method for characterizing NAs. Recently fluorescence technology has been applied to naphthenic acids and unique signals have been generated.

FLUORESCENCE

Principles

Compounds will exhibit a fluorescing nature due to their electron structure and chemical bonds within aromatic components (Alostaz et al. 2008a). When exposed to an energy source, such as UV light, electrons can be excited to a higher energy level. Electrons will return to their original ground state through various radiative and non-radiative mechanisms, which include fluorescence (Díaz-García & Badía-Líaño 2005). Aromatic components contain both single and double bonds. The single bonds contain a shared electron pair, which forms a σ bond containing low energy levels. In a double bond the first shared electron pair forms a σ bond and the second electron pair forms a π bond (Alostaz et al. 2008a). The π bond exhibits weak binding forces that when subjected to UV light allow electrons to absorb the energy and are subsequently promoted to a higher energy level.

The fluorescence signals obtained are unique to each particular compound, and thus can be used in identification for analytical purposes (Lackowitz 2006). The fluorescence spectra can be obtained from two different scanning techniques, emission and excitation fluorescence spectra. In the emission spectrum the excitation wavelength is held constant and the emission fluorescence radiation is measured. Conversely in the excitation spectrum the observation wavelength is held constant and intensity is measured as a function of excitation wavelength (Alostaz et al. 2008b). Combining the information obtained from the two spectra enables the construction of a three dimensional plot known as an excitation-emission matrix (EEM) (Rho & Stewart 1978). An example of a typical

3-dimensional (3D) EEM is shown in Figure 2.

In cases where multiple components are present the fluorescence signals obtained can overlap and be difficult to resolve. Alternative methods such as synchronous fluorescence spectrometry (SFS) and time resolved fluorescence spectrometry are used. In SFS both the excitation and emission wavelengths are scanned simultaneously while keeping a constant wavelength interval between them (Vo-Dinh 1978). Time resolved fluorescence spectrometry utilizes the varying fluorescent times of each of the multiple components. The intensity contributions of each compound can then be resolved by time or frequency (Alostaz 2008).

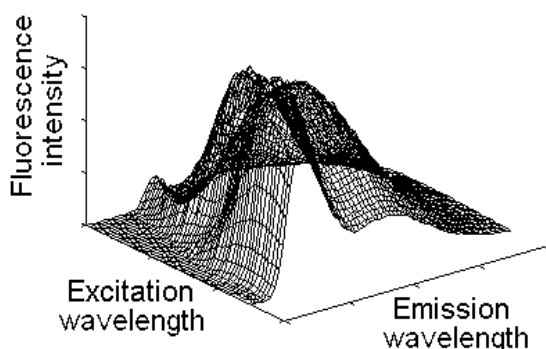


Figure 2: Typical 3D Excitation-Emission Matrix (adapted from Alostaz 2008)

Fluorescence spectrometry has been used as an analytical technique in several different areas of application. Fields of application have included biochemistry, medicine and molecular biology to determine biomolecules, metal ions and organic compounds (Díaz-García & Badía-Líaño 2005). Fluorescence has been used to determine trace levels of species in clinical, biological and environmental samples. Petroleum products such as gasoline, diesel, and heavy crude oil that contain polycyclic aromatic

hydrocarbons (PAHs) have been shown to produce unique EEMs that can be used to track and determine contamination (Alostaz et al. 2008a). Synchronous fluorescence spectrometry has been used for detecting natural organic matter, as well as PAHs and petroleum contaminants (Kavanagh et al. 2009).

Benefits

Fluorescence spectrometry as an analytical technique has many benefits. The methods are highly sensitive and can be used to identify trace components in small sample sizes (Díaz-García & Badía-Líaño 2005). Samples do not require preparation and are not affected or destroyed during measurement, nor are hazardous by-products generated (Alostaz et al. 2008). In addition fluorescence methods are readily reproducible, simple and are cost effective (Brown et al. 2009). The signatures generated are unique and offer the ability to identify individual compounds, making fluorescence techniques a powerful characterization tool.

Applications to Naphthenic Acids

Recently fluorescence technology has been applied to naphthenic acid measurements in oil sands process affected waters. The general formula used to describe traditional naphthenic acids, $C_nH_{2n+Z}O_2$, does not indicate that fluorescence will occur. However, as previously stated, the naphthenic acids extracted from oil sands are known to contain impurities that exhibit fluorescence due to various levels of unsaturation and aromaticity (Headley et al. 2009). Mohammed et al. (2008) demonstrated this ability and determined a linear response in UV light absorbed and naphthenic acid concentrations from 1-100 mg/L.

Brown et al. (2009) used fluorescence EEM for process affected water samples from different oil sand companies and groundwater samples in the Athabaskan area. The EEMs obtained demonstrated that fluorescent signatures differed between each of the companies sampled and exhibited less intensity in the groundwater samples. The difference between the process affected water samples was attributed to the differing refining methods that are used by each company, and the age and storage of the samples (Brown et al. 2009). It is suggested that lower molecular weight naphthenic acids will fluoresce at shorter emission wavelengths than the higher molecular weight. Previous characterization methods have confirmed that the naphthenic acid concentrations in the ground water are lower than those found in the process affected water. In order to confirm that the intensity observed in the EEMs was correlated to concentration, Brown et al. (2009) performed a series of dilutions. The resulting emission spectrum showed that as the sample was diluted to lower concentrations, the observed intensity was also lowered.

Similar excitation peaks were observed at approximately 290nm for process affected water in both studies performed by Brown et al. (2009) and Mohammed et al. (2008). The excitation peak for groundwater samples was found to be lower at an excitation wavelength of approximately 260nm (Brown et al. 2009). Emission peaks were observed at 305nm and 340nm for fresh process affected water samples in the study completed by Brown et al. (2009) and a similar peak was observed at 346nm in the study completed by Mohammed et al. (2008). In an aged sample the first observed peak was observed at a lower emission wavelength of 290nm, and the second peak was again observed at 340nm though not as prominent (Brown et al. 2009). Similar results have been determined using

synchronous fluorescence spectrometry by Kavanagh et al. (2009). Samples were scanned at an offset wavelength interval of 18nm and fluorescence peaks were established at wavelengths of 282.5nm and a broad peak in the range of 320 to 340nm (Kavanagh et al. 2009).

Future

Further research into the fluorescing nature of naphthenic acids is required. Due to the complex nature of the naphthenic acid mixture the signals produced are overlapping and complex. In the case of overlapping signals a decomposition method can be used, such as parallel factor analysis (PARAFAC). PARAFAC is a multivariable statistical procedure that can be used to decompose EEM data and differentiate the components of the mixture (Alostaz et al. 2008b). The method uses an alternating least squares approach and offers the advantage of providing a unique solution (Bro 1997). The use of PARAFAC in fluorescence analysis has been demonstrated in fluorescence signals obtained from the characterization of petroleum products and crude oil where overlapping signals have been obtained (Alostaz et al. 2008a,b). In samples that do not fluoresce sufficiently for detection or contain other substances that interfere with fluorescence, success has been demonstrated using fluorescence tagging. Samples can be modified with various reagents that increase the sensitivity and selectivity of detection (Toyo'oka 2002). These reagents can be tailored to suit the detection and selectivity needs of the mixture to enhance the recognition and quantification of the molecules (Díaz-García & Badía-Líaño 2005). Toyo'oka (2002) demonstrated the value of fluorescence tagging with various types of carboxylic acids, under which naphthenic acids fall.

CONCLUSION

Due to the inherent toxic and corrosive properties of naphthenic acids there is a need for a quick, reliable and cost effective characterization technique. Current methods of characterization are time consuming and do not have the ability to separate individual naphthenic acid components. Fluorescence spectrometry methods have been demonstrated to be successful in analyzing environmental samples, and more recently has been applied to naphthenic acids. Fluorescence offers many benefits over the current analytical methods and would provide benefit to the characterization of naphthenic acids in oil sands process affected waters and surrounding surface and ground waters.

REFERENCES

- Alberta Government. 2009. Alberta's Oil Sands. [online] Available from <http://www.oilsands.alberta.ca/> [accessed August 27, 2009]
- Allen, E.W. 2008. Water treatment in Canada's oil sands industry I: Target pollutants and treatment objectives. *Journal of Environmental Engineering and Science*, 7: 123-128.
- Alostaz, M. 2008. Improved ultraviolet induced fluorescence (UVIF)-standard cone penetration testing (CPT) system to detect petroleum hydrocarbon contaminants. PhD thesis, University of Alberta.
- Alostaz, M., Biggar, K., Donahue, R., and Hall, G. 2008a. Petroleum contamination characterization and quantification using fluorescence emission excitation matrices (EEMs) and parallel factor analysis (PARAFAC). *Journal of Environmental Engineering and Science*. 7: 183–197.
- Alostaz, M., Biggar, K., Donahue, R., and Hall, G. 2008b. Soil type effects on petroleum contamination characterization using ultraviolet induced fluorescence excitation-emission matrices (EEMs) and parallel factor analysis (PARAFAC). *Journal of Environmental Engineering and Science* 7: 661–675.
- Babaian-Kibala, E. 1994. Phosphate ester inhibitors solve naphthenic acid corrosion problems. *Oil and Gas Journal*, 92: 31-35.
- Bataineh, M., Scott, A.C., Fedorak, P.M., and Martin, J.W. 2006. Capillary HPLC/QTOF-MS for Characterizing Complex Naphthenic Acid Mixtures and Their Microbial Transformation. *Analytical Chemistry*, 78: 8354-8361.
- Brient, J.A.; Wessner, P.J.; Doyler, M.N. Naphthenic acids. In *Kirk-Othmer Encyclopedia of Chemical Technology*, 4th ed.; Kroschwitz, J.I., Ed.; John Wiley and Sons: New York, 1995; 1017–1029.
- Bro, R. 1997. PARAFAC Tutorials and Applications. *Chemometrics and Intelligent Laboratory Systems*. 38(2):149-171.
- Brown, L.D., Alostaz, M., and Ulrich, A.C. 2009. Characterization of Oil Sands Naphthenic Acids in Oil Sands Process-Affected Waters Using Fluorescence Technology. In *Proceedings, 62nd Canadian Geotechnical Conference*, Halifax, Nova Scotia, September 20-24, 2009.
- Clemente, J.S. and Fedorak, P.M. 2004. Evaluation of the analyses of tert-butyl dimethylsilyl derivatives of naphthenic acids by gas chromatography – electron impact mass spectrometry. *Journal of Chromatography*, 1047(2004): 117-128.

- Clemente, J.S. and Fedorak, P.M. 2005. A review of the occurrence, analyses, toxicity, and biodegradation of naphthenic acids. *Chemosphere*, 60(2005): 585-600.
- Díaz-García, M.E., and Badía-Líaño, R. 2005. Fluorescence: Overview. 97-106.
- Fan, T.P. 1991. Characterization of naphthenic acids in petroleum by fast atom bombardment mass spectrometry. *Energy Fuels*, 5 (3): 371-375.
- Hao, C., Headley J.V., Peru, K.M., Frank, R., Yang, P., and Soloman, K.R. 2005. Characterization and pattern recognition of oil sand naphthenic acids using comprehensive two dimensional gas chromatography/time of flight mass spectrometry. *Journal of Chromatography*, 1067: 277-284.
- Headley, J.V. and McMartin, D.W. 2004. A Review of the Occurrence and Fate of Naphthenic Acids in Aquatic Environments. *Journal of Environmental Science and Health*, A39(8): 1989-2010.
- Headley, J.V., Peru, K.M., and Barrow, M.P. 2009. Mass Spectrometric Characterization of Naphthenic Acids in Environmental Samples: A Review. *Mass Spectrometry Reviews*, 2009, 28, 121– 134.
- Holowenko F, MacKinnon M and Fedorak P. 2001 Naphthenic acids and surrogate naphthenic acids in methanogenic microcosms. *Water Resources*, 35:2596–606.
- Holowenko, F., MacKinnon, M. and Fedorak, P. 2002. Characterization of naphthenic acids in oil sands wastewaters by gas chromatography-mass spectrometry. *Water Research*, 36, 2843–2855.
- Janfada, A. et al. 2006. A Laboratory Evaluation of the Sorption of Oil Sands Naphthenic Acids on Organic Rich Soils. *Journal of Environmental Science and Health*, A41: 985-997.
- Kavanagh, R.J., Burnison, B.K., Frank, R.A., Soloman, K.R., Van der Kraak, G. 2009. Detecting oil sands process-affected waters in the Alberta oil sands region using synchronous fluorescence spectroscopy. *Chemosphere* 76: 120–126.
- Lakowicz, J.R. 2006. Principles of Fluorescence Spectroscopy, 3rd Ed. Springer Science+Business Media, LLC, New York, NY.
- Martin, J.W., Han, X., Peru, K.M., and Headley, J.V. 2008. Comparison of high- and low-resolution electrospray ionization mass spectrometry for the analysis of naphthenic acid mixtures in oil sands process water. *Rapid Communications in Mass Spectrometry*, 22: 1919–1924.
- Mohammed, M.H., Wilson, L.D., Headley, J.V., and Peru, K.M. 2008. Screening of oil sands naphthenic acids by UV-Vis absorption and fluorescence emission spectrophotometry. *Journal of Environmental Science and Health Part A* 43: 1700–1705.
- Rho, J.H., and Stewart, J.L. 1978. Automated Three-Dimensional Plotter for Fluorescence Measurements. *Analytical Chemistry*, 50(4), 620-625.
- Slavcheva, E., Shone, R., Turnbull, A., 1999. Review of naphthenic acid corrosion in oil refining. *British Corrosion Journal* 34, 125-131.

Seifert, W., and Teeter, R. 1969. Preparative Thin-Layer Chromatography and High Resolution Mass Spectrometry of Crude Oil Carboxylic Acids. *Analytical Chemistry*, 41(6), 786-795.

Seifert, W., Teeter, R., Howells, W.G., and Cantow, M. 1969. Analysis of Crude Oil Carboxylic Acids after Conversion to Their Corresponding Hydrocarbons. *Analytical Chemistry*, 41(12), 1639-1647.

Toyo'oka, T. 2002. Fluorescent tagging of physiologically important carboxylic acids, including fatty acids, for their detection in liquid chromatography. *Analytica Chimica Acta*, 465: 111-130.

Vo-Dinh, T. 1978. Multicomponent Analysis by Synchronous Luminescence Spectrometry. *Analytical Chemistry*, 50(3) :396-401.

Yen, T.W., Marsh, W.P., MacKinnon, M.D., and Fedorak, P.M. 2004. Measuring naphthenic acids concentrations in aqueous environmental samples by liquid chromatography. *Journal of Chromatography A*, 1033 (2004) 83-90.

Zhenbo, L. Et al. 2005. Determination of naphthenic acids in crude oil by chemical ionization mass spectrometry. *Chinese Journal of Geochemistry*, 24(1): 67-72.

CAPACITY FOR SORPTION OF NAPHTHENIC ACIDS FROM OIL SANDS PROCESS-AFFECTED WATER TO SOILS FROM ATHABASCA OIL SANDS REGION

Lisa D. Brown, M. Alostaz and A. Ulrich

Department of Civil and Environmental Engineering, University of Alberta, Edmonton, Canada

ABSTRACT: Tailings impoundments present a significant challenge in the mining industry worldwide, not only with regard to waste management, but also safety and environmental protection. Naphthenic acids, the polar organic carboxylic acids that are present in crude oil deposits, are the primary source of acute toxicity in oil sands process-affected water. The high concentrations of naphthenic acids found in oil sands tailings ponds, averaging 110 mg/L, pose great risk for impacting surface and groundwater. Sorption of naphthenic acids represents a potential subsurficial attenuating mechanism. Preliminary batch sorption tests using native soils from the Athabasca oil sands region, including organic rich soil (muskeg), clays, and sands, were conducted to determine the capacity for uptake of oil sands naphthenic acids from process water collected from an oil sands company property lease. Fluorescence spectrophotometry was utilized as a screening tool for detecting changes in process-affected water fluorescence signals due to sorption. The muskeg exhibited the greatest capacity for sorption of naphthenic acids, as indicated by 80% reduction in fluorescence signal. Clay also appeared to adsorb naphthenic acids, exhibiting 40% reduction in signal, while the sand possessed little capacity for sorption, as shown by only 10% reduction in signal. Organics detectable by fluorescence were released from the soils during the batch sorption testing. Research is required to further delineate the interactions of the organics in the oil sands process-affected water and the complex soil systems.

INTRODUCTION

The Athabasca oil sands deposit represents a portion of one of the largest global reserves, with over 1.7 trillion barrels of proven recoverable oil available (Alberta Government 2008). To protect surface waters in the region, oil sands operations cannot discharge process-affected water to the surrounding environment (Allen 2008). The Clark Hot Water Process utilized for bitumen extraction generates approximately 1.25 m³

of tailings for every barrel of oil produced (Alberta Chamber of Resources 2004). The extraction process enhances the release of naphthenic acids in oil sands process-affected water, which is stored in tailings impoundments that occupy over 70 km² of land (Allen 2008).

The term “naphthenic acids” is used to collectively describe the polar organic carboxylic acids that are present in crude oil (Brient et al. 1995). Naphthenic acids are a

complex mixture of alkyl-substituted acyclic and cycloaliphatic carboxylic acids with the general chemical formula $C_nH_{2n+z}O_2$, where n indicates the carbon number and Z specifies a homologous series, or the degree of cyclization (Brient et al. 1995). The Z variable is an even negative integer between 0 and -12, which indicates the loss of covalently bonded hydrogen due to the presence of ring structures (Marsh 2006). The saturated ring structures predominantly contain five or six carbon atoms, and each multiple of -2 indicates the presence of another ring.

MacKinnon and Boerger (1986) identified naphthenic acids as the primary source of acute toxicity when aquatic life is exposed to oil sands process-affected water. Studies have also shown that toxicity is greatly attributed to naphthenic acids with less than 22 carbon atoms (Holowenko et al. 2002, Lo et al. 2006, Frank et al. 2008). Although naphthenic acids are found in many crude oil deposits (Tissot and Welte 1984), development in the Athabasca oil sands presents unique challenges due to the concentration of naphthenic acids in large wastewater storage ponds where the potential for significant impacts on the surrounding environment is immense. Reported naphthenic acid concentrations in tailings ponds have averaged 110 mg/L (Headley and McMartin 2004).

Building an understanding of the behavior of naphthenic acids in the subsurface is necessary to develop a successful risk management approach to managing seepage from oil sands tailings ponds. In the subsurface, sorption of contamination to soils is a significant potential attenuating mechanism. To date, batch sorption experiments have been conducted on commercially available clays and organic-rich overburden, clean aquifer material, and soil cores from the oil sands region.

However, very few studies have been completed on the sorption of naphthenic acids to the variety of soils encountered in the Fort McMurray region, and results from previous studies have not yet been proven reproducible.

Both Peng et al. (2002) and Janfada et al. (2006) utilized organic soils, also referred to as muskeg, in adsorption batch tests. Muskeg is typically the top layer of overburden covering the Athabasca oil sands deposit and is recovered during soil salvage operations for use in reclamation on oil sands leases. Peng et al. (2002) found that the adsorption of single-ring model naphthenic acids was best described by a linear isotherm, although measured adsorption coefficients were low, in the range of 0.2 mL/g. Concentrations of surrogates ranged from 10 to 100 mg/L, and other manipulated variables included temperature (4 and 23°C), pH (2.9, 6.8, 10), fraction of organic carbon in soil (0.016, 0.027), and ionic strength (0, 10, 30 mM $CaCl_2$). Molecular structure, whereby both cis- and trans-isomers were tested, and temperature had little effect on adsorption, indicating that weak physical adsorption is the likely mechanism. Ionic strength and pH of the solution had a statistically significant impact on adsorption due to the change in naphthenic acid solubility. The strongest sorption occurred at low pH and high ionic strength.

In contrast, Janfada et al. (2006) observed considerable sorption of naphthenic acids extracted from oil sands process affected water to the two same soils utilized by Peng et al. (2002), obtaining values of K_d between 1.3 and 17.8 mL/g from a linear isotherm. Concentrations of naphthenic acids ranged from 80 to 200 mg/L, as determined by negative ion electrospray ionization-mass spectrometry, and batch sorption tests were conducted at a temperature of 4°C, pH of 8, and with both deionized water and synthetic

groundwater. The K_d values increased by an order of magnitude when the synthetic groundwater was used instead of deionized water. Janfada et al. (2006) hypothesized that this dramatic increase in sorption could have been the result of naphthenic acids “salting out” with the increased ionic strength.

Gervais (2004) conducted batch sorption experiments on material sourced from an active sand pit on Syncrude’s property, with both stock naphthenic acids extracted from process-affected water and surrogates in a synthetic, high ionic strength groundwater. Tested concentrations of stock naphthenic acids ranged from 10 to 100 mg/L while the mixture of surrogate naphthenic acids included individual concentrations that ranged from 1.5 to 10 mg/L. Because the pH of the batch reactors was between 7 and 8, it can be safely assumed that the ionized form of the naphthenic acids was prevalent. The Freundlich isotherm, with $n > 1$, provided the best fit to the adsorption data from the stock naphthenic acid mix and indicated that sorption increases with increasing sorbate concentration.

Gervais (2004) analyzed fluid from the stock naphthenic acid using gas chromatography-mass spectrometry to determine if a change in “signature” could be observed following exposure to the aquifer material, which would indicate the preferential sorption of a particular range of naphthenic acid isomers. Gervais (2004) concluded upon visual examination of the three dimensional plots generated that sorption does not result in signature change in the naphthenic acid mixture.

Gervais (2004) and Oiffer (2006) collected data in field studies in hopes of observing evidence of attenuation of naphthenic acids. Of the three cases examined by Gervais (2004), attenuation of naphthenic acids was detected at only one site and this was

attributed to aerobic biodegradation. At this location, a plume of groundwater from the McMurray Basal Aquifer was monitored, and naphthenic acid concentrations decreased with distance while sodium and chloride did not. Also, a relative decrease of lower molecular weight naphthenic acids was observed, providing evidence of biodegradation occurring. In the other two scenarios, tailings fluid was seeping to surficial aquifers; groundwater monitoring showed no indication of attenuation of naphthenic acids in the subsurface. Meanwhile, Oiffer (2006) observed minimal sorption of naphthenic acids in a sandy aquifer, but did note a reduction in acute toxicity of groundwater samples, which was credited to a decrease in naphthenic acid concentration via weak sorption and dispersive dilution, and not biodegradation.

Typically, soils with low permeability, high organic content, and/or charge are more likely to sorb organic compounds (Dubus et al. 2001). Marsh (2006) tested both pure clay minerals and soils, consisting predominantly of sand (greater than 95%), from oil sands operations. Naphthenic acids concentrations were determined using high pressure liquid chromatography and ranged from 10 to 200 mg/L. Batch sorption tests performed with clay minerals (sodium- and calcium-saturated kaolinite, illite, and montmorillonite) and commercial naphthenic acids resulted in K_d values ranging from 18 to 57 mL/g at pH of 6, versus 0 to 10 mL/g at pH of 8. When batch sorption tests were conducted with oil sands process affected water-sourced naphthenic acids, only at a pH of 8, sorption was only observed with calcium saturated montmorillonite. No sorption was observed with soil cores from the oil sands region. It must be noted that Marsh (2006) only indicated if a linear sorption isotherm could be observed and reported only significant changes in naphthenic acid concentrations.

It is not surprising that Gervais (2004) observed minimal sorption of naphthenic acids to a clean aquifer sand as sand does not have properties that would indicate sorption capacity. High sorption to muskeg, as observed by Janfada et al. (2006), is expected due to the organic content. Marsh (2006) did not show any conclusive results as some sorption to clay minerals did occur and little sorption occurred with the soil cores, but these soils were predominantly sands and so major conclusions regarding sorption potential of oil sands process-affected water naphthenic acids could not be reached. Batch sorption tests need to be conducted with those soils likely to interact with oil sands process-affected water in order to gain a sufficient understanding of sorption potential in the subsurface.

The main objective of this research is to determine the sorption capacity of soils collected in the Athabasca oil sands region for oil sands acids, including naphthenic acids, found in process-affected water.

METHOD

Sources and preparation of samples

For this study, process-affected water was collected directly from an oil sands company tailings pond in the winter of 2009, refrigerated at 4°C and stored in the dark in glass bottles at the Applied Environmental Geochemistry Research Facility at the University of Alberta. The naphthenic acid concentration in the oil sands process-affected water was on the order of 10 mg/L, as measured by a commercial laboratory using Fourier transform infrared spectroscopy.

Soil cores were collected from the same oil sands company that supplied process affected water. Drilling occurred in the summer of

2006 and cores were stored in lexan liners and frozen until required. Three soil samples were utilized for this study: a sand, a clay, and an organic rich soil (muskeg). The sand was collected from a depth of approximately 22.5 m below ground surface and is fine to medium grain with trace silts. The clay was collected from a depth of about 10.5 m below ground surface and is grey, low plasticity with trace sand and rocks. The muskeg was collected from the surface of an undisturbed area of the oil sands company lease. A coal-based granular activated carbon (GAC), AquaSorb 1500, was purchased from Jacobi Carbons (Varvsholmen, Sweden).

Unless stated otherwise, all supplies were obtained from Fisher-Scientific (Edmonton, AB). All laboratory glassware was rinsed with methanol and air-dried prior to use.

Batch sorption testing

The batch test method was utilized for this study to determine the sorption capacity of native soils from the Athabasca oil sands region. ASTM methods D4646 and E1195 were referenced in developing methodology for batch sorption testing.

Prior to batch testing, six inch long soil cores were thawed at 4°C. Each soil sample was homogenized and stored in amber glass bottles at 4°C.

The batch tests were conducted in 44 mL clear glass EPA vials fitted with Teflon coated septas. The soil to water ratio was fixed at 1:5 for the clay, sand, and GAC samples and 1:10 for the muskeg, on a dry mass basis. Soils were used at native moisture content conditions. Tests were completed in triplicate. Soil, then water, was added to a vial, which was then placed on a wrist-action shaker for 24 hours at 20°C. pH measurement was taken both before and after agitation. Sodium azide was added to each

vial at a concentration of approximately 500 mg/L as a microbial inhibitor.

GAC was used as a positive control to determine if the experimental method facilitated favourable conditions for sorption to occur. Negative controls consisted of process-affected water with no soil and deionized water with each of the soils.

All samples were filtered using vacuum filtration to 0.45 μm . Both the filtrate and the soil were retained for analysis.

Fluorescence and absorbance measurements

Mohamed et al. (2008), Kavanagh et al. (2009), and Brown et al. (2009) demonstrated the use of fluorescence technology for naphthenic acid detection and measurement. Fluorescence is thus utilized in this study as a screening tool.

A Varian Cary Eclipse fluorescence spectrophotometer was used with right angle detection for sample analysis. A collection of emission scans from 250 to 600 nm with 1 nm increments were obtained at excitation wavelengths ranging from 260 to 450 nm with 10 nm increments. The bandwidth (slit width) was 10 nm for excitation and 5 nm for all samples. The scan rate was 600 nm/min, allowing for a scan time of approximately 20 minutes per sample. Both excitation and emission filters were set to automatic and the PMT voltage was 600 V for all scans.

Absorbance measurements were conducted using a Shimadzu UV2401-PC UV-VIS Recording Spectrophotometer, coupled with Shimadzu UVProbe software. Absorbance readings were obtained for wavelengths from 250 to 600 nm with 1 nm increments.

Samples were processed in clear quartz 1.24x1.24x4.5 cm cuvettes supplied by Varian.

Data preparation

Absorbance measurements were obtained to correct for both primary and secondary inner filtering effects, using the method described by Tucker et al. (1992). The corrected intensity values were then used to develop Excitation-Emission Matrices and emission spectra. Excitation-Emission Matrices were generated using the Scan function of the Varian Cary Eclipse software and emission spectra.

Light scatter, an artifact of fluorescence spectroscopy due to reflection of excitation light by impurities in the analyzed samples, was not removed from the data, but is seen as a 45° line across the Excitation-Emission Matrix and is also observed in the emission spectra.

RESULTS AND DISCUSSION

Fluorescence spectrophotometry was used as a screening tool to determine if soils collected from an oil sands operator's facility have the capacity to adsorb naphthenic acids from oil sands process-affected water. Fluorescence was utilized as a quick, non-destructive analytical technique for screening the samples from this preliminary batch sorption test. Excitation-Emission Matrices and emission spectra at different excitation wavelengths were prepared for the three soil-process water batch tests, as well as the positive and negative controls. All matrices are shown with the same contour intervals to facilitate comparison between samples.

The results indicate that fluorescence is an effective screening tool to indicate sorption of oil sands naphthenic acids to soils, which

may be employed prior to using more expensive, time consuming, and consumptive analytical techniques for naphthenic acid measurement.

Moisture and organic matter content of the soil samples were analyzed using facilities available in the Department of Civil and Environmental Engineering, University of Alberta. The moisture contents of the clay, sand and muskeg were 19.6%, 16.3% and 50.5%, respectively, on a dry basis. Organic matter was 3.5%, 0.73%, and 84.9% for the clay, sand, and muskeg.

The test condition with oil sands process-affected water and no soil, shown in Figure 1, served as both a benchmark from which to compare the soil test conditions and a negative control to detect interferences due to experimental methodology.

Figure 1A shows that the peak intensity of the process water signal occurs around excitation wavelength 280 nm and emission wavelength 350 nm. The intensity of the signal is greater than 1000, as seen in Figure 1B. The fluorescence signal is characteristic of this process-affected water sample and is assumed to be indicative of the oil sands naphthenic acids concentration. If sorption of oil sands naphthenic acids to the soil occurred, it is expected that the intensity of the fluorescence signal peak, seen clearly on the emission spectra, would decrease and that the shape of the Excitation-Emission Matrix may also change.

In addition, deionized water mixed with each of the soils was analyzed to determine if naturally occurring organic compounds would desorb from the soils during the batch sorption tests that would be detected by fluorescence. These samples are shown in Figures 3, 5, and 7.

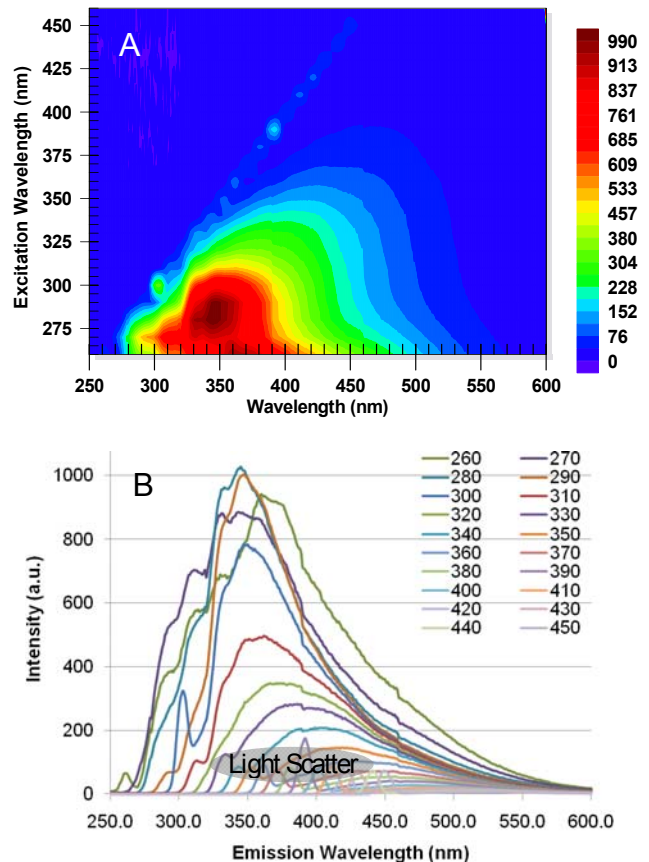


Figure 1. A. Excitation-Emission Matrix. B. Emission spectra at different excitation wavelengths in nm for process-affected water after 24 hour batch sorption testing with no soil

The clay soil sample appears to have the capacity to sorb naphthenic acids. The intensity of the process water signal peak, seen in Figure 2A, has reduced from about 1000 to less than 700 and this is attributed to the retention of naphthenic acids by the clay. Thus, the concentration of oil sands naphthenic acids was reduced by almost 40% in the process-affected water due to interaction with the clay soil sample. When comparing Figure 2A with Figure 1A, the signals appear to be similar, but Figure 2A spreads further into the higher excitation and emission wavelengths. Figure 3 shows that the clay soil released organic compounds,

detectable by fluorescence, to the deionized water, and it is assumed that these organics

organic material was released from the sand to the deionized water.

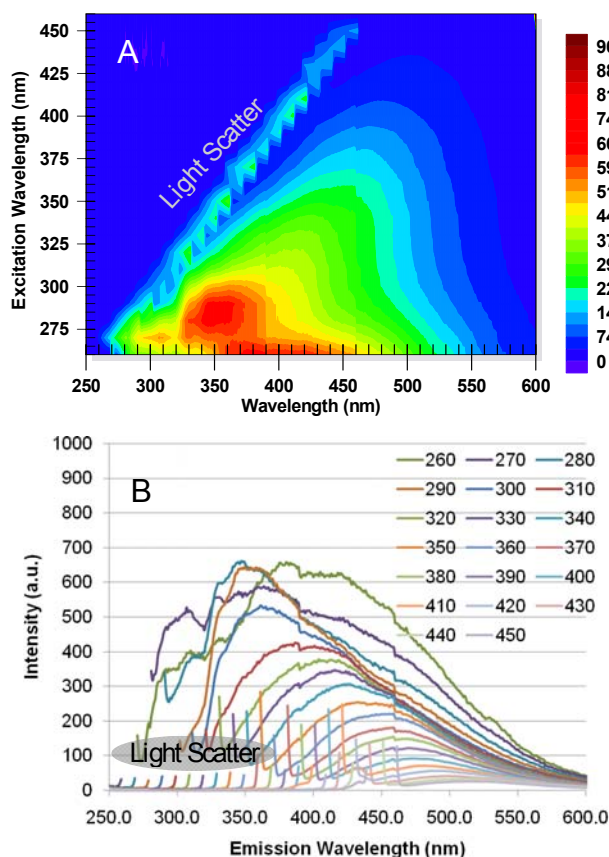


Figure 2. A. Excitation-Emission Matrix. B. Emission spectra at different excitation wavelengths in nm for process-affected water after 24 hour batch sorption testing with clay

increased the intensity of the signal at the greater wavelengths in Figure 2.

The process-affected water peak intensity is reduced to only 900 from greater than 1000 after interaction with the sand soil sample, as shown in Figure 4B, indicating approximately a 10% reduction in oil sands naphthenic acid concentration in the process-affected water following sorption with sand. Very little difference can be seen between Figures 1 and 4, indicating that the sand has little sorption capacity. Figure 5 show that very little

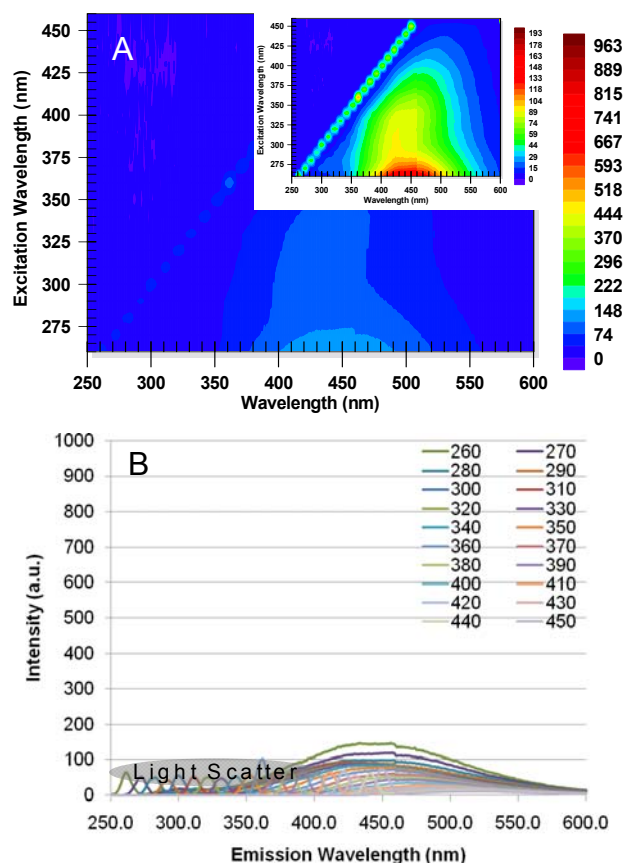


Figure 3. A. Excitation-Emission Matrix. B. Emission spectra at different excitation wavelengths in nm for deionized water after 24 hour batch sorption testing with clay

Of the three native soils tested, the batch test condition with muskeg appears to have shifted the fluorescence signal of the process-affected water most significantly. The peak seen in Figure 6B does not resemble that seen in Figure 1B, indicating that sorption of naphthenic acids by the muskeg was considerable. Figure 7 shows that a significant amount of organics was released by the muskeg to the deionized water, which is expected as muskeg is an organic rich soil type.

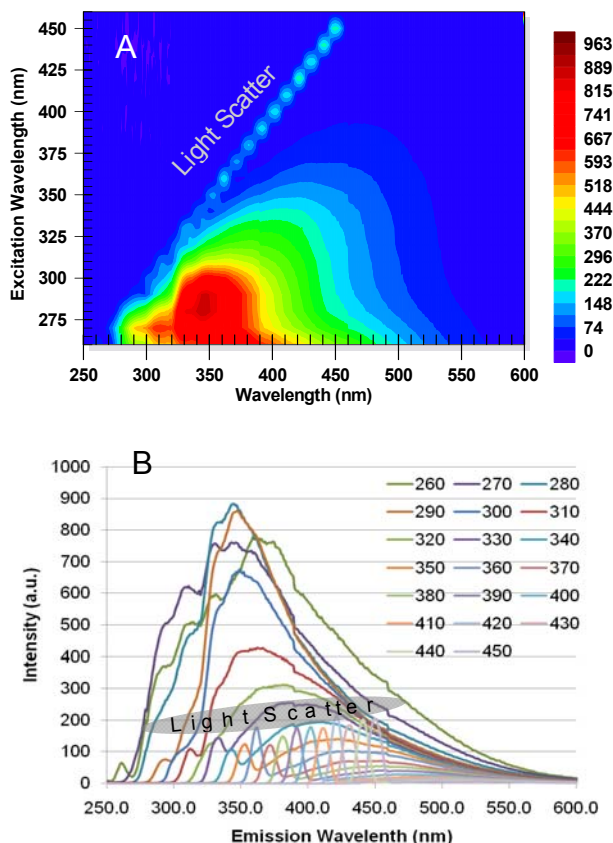


Figure 4. *A.* Excitation-Emission Matrix. *B.* Emission spectra at different excitation wavelengths in nm for process-affected water after 24 hour batch sorption testing with sand

The intensity of the fluorescence signal of the process-affected water at excitation wavelength 280 nm and emission wavelength 350 nm reduced by approximately 80% following sorption with muskeg. The assumption that the increased signal intensity at the greater excitation and emission wavelengths is caused by naturally occurring organic compounds releasing from the muskeg soil sample will need to be verified analytically.

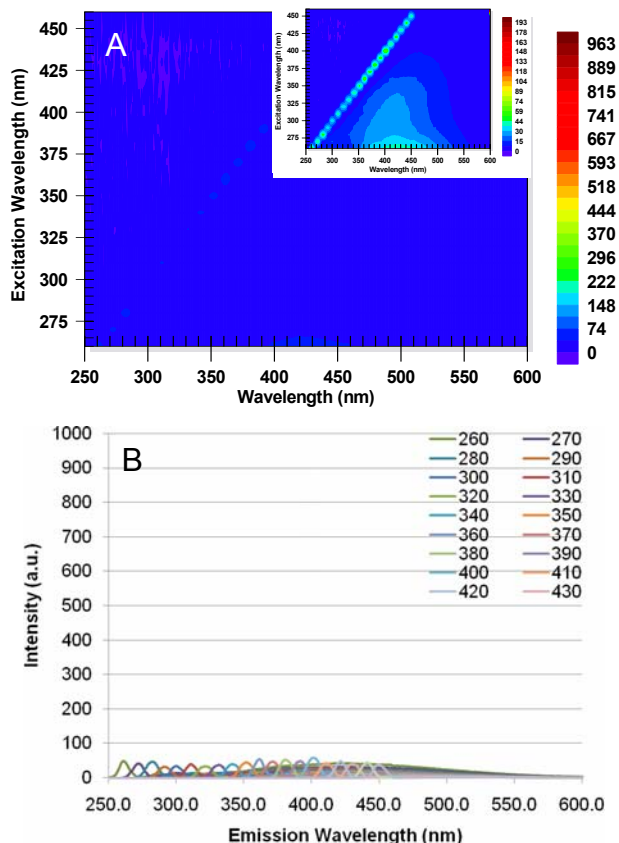


Figure 5. *A.* Excitation-Emission Matrix. *B.* Emission spectra at different excitation wavelengths in nm for deionized water after 24 hour batch sorption testing with sand

The positive control condition consisting of oil sands process-affected water and granular activated carbon demonstrated that the methodology facilitated complete sorption, as shown by the absence of a fluorescence signal in Figure 8.

The results from the preliminary batch sorption tests are consistent with general assumptions regarding sorption capacity of clays, sands, organic-rich soils, and GAC.

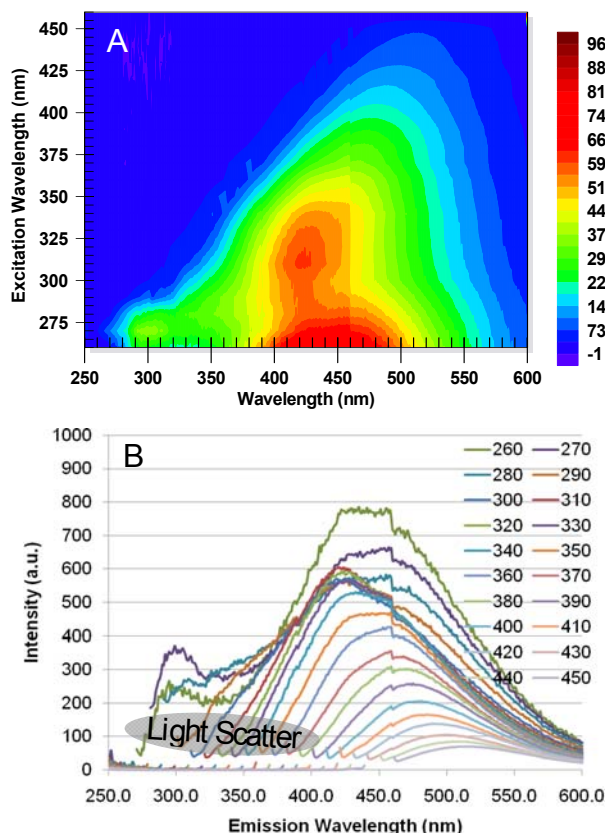


Figure 6. *A.* Excitation-Emission Matrix. *B.* Emission spectra at different excitation wavelengths in nm for process-affected water after 24 hour batch sorption testing with muskeg

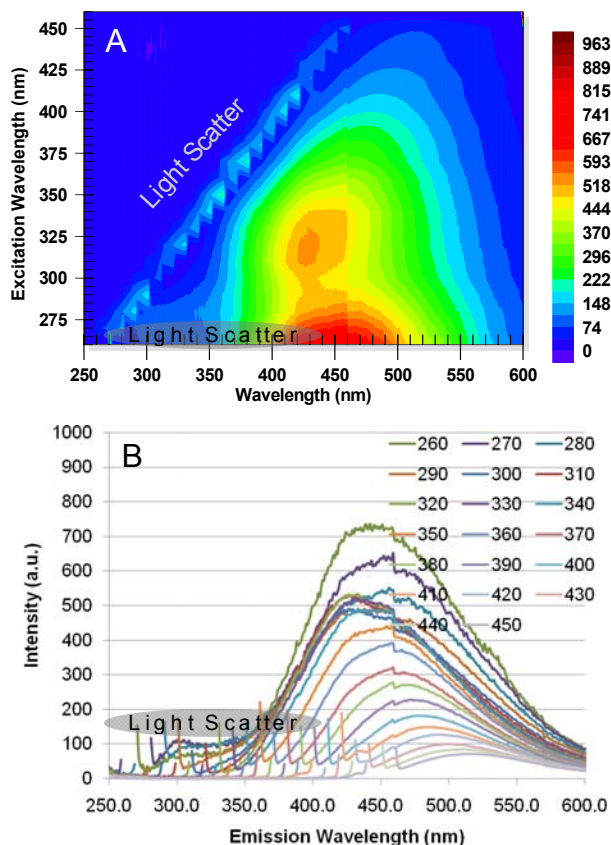


Figure 7. *A.* Excitation-Emission Matrix. *B.* Emission spectra at different excitation wavelengths in nm for deionized water after 24 hour batch sorption testing with muskeg

The release of organics from the soils during the batch testing is also consistent with the measurements of organic matter content.

Table 1 summarized the percent reduction of the peak intensity of the fluorescence signal of process-affected water following batch sorption testing with the three native Athabasca oil sands region soils and GAC. This reduction in the fluorescence signal is credited to the removal of oil sands naphthenic acids from process-affected water due to soil sorption.

Table 1. Percent reduction of peak intensity of process-affected water fluorescence signal following batch sorption testing

Soil	% Reduction
Clay	40
Sand	10
Muskeg	80
GAC	100

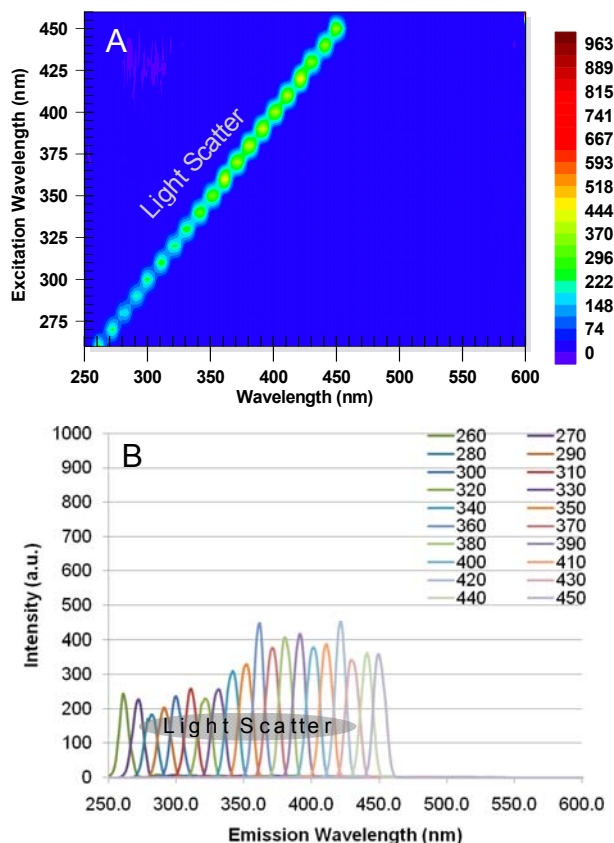


Figure 8. *A.* Excitation-Emission Matrix. *B.* Emission spectra at different excitation wavelengths in nm for process-affected water after 24 hour batch sorption testing with GAC

CONCLUSIONS

Preliminary batch sorption tests were conducted with clay, sand and muskeg soil samples native to the Athabasca oil sands region and oil sands process-affected water to assess soil sorption capacity for naphthenic acids. The muskeg exhibited the greatest sorption capacity, followed by the clay and then the sand, as expected based on soil properties. Fluorescence spectrophotometry was an effective screening tool for detecting sorption of naphthenic acids following batch sorption testing. Continued research will further delineate the interactions of the organic compounds present in both the oil

sands process-affected water and the native soils. Naphthenic acid analysis will be completed to determine sorption coefficients and changes in toxicity and other properties, due to sorption.

ACKNOWLEDGEMENTS

The writers would like to acknowledge the contributions of S. Holden, J. Burkus and M. Demeter, of the University of Alberta, Charity Zayonc and Mike Bowron of Suncor Energy Inc., and the Oil Sands Tailings Research Facility.

Special acknowledgement is given to the University of Alberta WISEST program, and Nicole Baker and Kathyln Moores for their enthusiasm and hard work on this research.

Funding for this project has been provided by Suncor Energy Inc. L. Brown would also like to thank Alberta Ingenuity for funding support.

REFERENCES

- Alberta Chamber of Resources. 2004. Oil sands technology roadmap: unlocking the potential. Edmonton, AB.
- Alberta Government. 2008. Alberta oil sands: resourceful. responsible. Edmonton, AB.
- Allen, E.W. 2008. Process water treatment in Canada's oil sands industry: I. Target pollutants and treatment objectives. *Journal of Environmental Engineering and Science* 7: 123-138.
- Brient, J.A., Wessner, P.J., and Doyle, M.N. 1995. Naphthenic acids. *In* Encyclopedia of Chemical Technology, 4th Ed. Edited by J. I. Kroschwitz, John Wiley & Sons, Inc., New York, pp 1017-1029.

- Brown, L.D., Alostaz, M., and Ulrich, A. C. 2009. Characterization of oil sands naphthenic acids in oil sands process-affected waters using fluorescence technology. Proceedings of the 62nd Canadian Geotechnical Conference & 10th Joint CGS/IAH-CNC Groundwater Conference, Halifax, NS, in press.
- Clemente, J.S. and Fedorak, P.M. 2005. A review of the occurrence, analyses, toxicity, and biodegradation of naphthenic acids. *Chemosphere* **60**: 585-600.
- Dubus, I.G., Burriuso, E. and Calvet, R. 2001. Sorption of weak organic acids in soils: clofencet, 2,4-D and salicylic acid. *Chemosphere* **45**: 767-774.
- Frank, R.A., Kavanagh, R., Burnison, B.K., Arsenault, G., Headley, J.V., Peru, K.M., Van Der Kraak, G., and Solomon, K.R. 2008. Toxicity assessment of collected fractions from an extracted naphthenic acid mixture. *Chemosphere* **72**: 1309-1314.
- Headley, J.V. and McMartin, D.W. 2004. A Review of the Occurrence and Fate of Napthenic Acids in Aquatic Environments. *Journal of Environmental Science and Health Part A* **39**(8): 1989-2010.
- Kavanagh, R.J., Burnison, B.K., Frank, R.A., Solomon, K.R., and Van Der Kraak, G. 2009. Detecting oil sands process-affected waters in the Alberta oil sands region using synchronous fluorescence spectroscopy. *Chemosphere* **76**: 120-126.
- Lo, C.C., Brownlee, B.G., and Brunce, N.J. 2006. Mass spectrometric and toxicological assays of Athabasca oil sands naphthenic acids. *Water Research* **40**: 655-664.
- MacKinnon, MD, and Boerger, H. 1986. Description of two treatment methods for detoxifying oil sands tailings pond water. *Water quality research journal of Canada* **21**(4): 496-512.
- Marsh, W.P. 2006. Sorption of naphthenic acids to soil minerals. M.Sc. Thesis, Department of Civil and Environmental Engineering, the University of Alberta, Edmonton, AB.
- Mohamed, M.H., Wilson, L.D., Headley, J.V., and Peru, K.M. 2008. Screening of oil sands naphthenic acids by UV-Vis absorption and fluorescence emission spectrophotometry. *Journal of Environmental Science and Health Part A* **43**(14): 1700-1705.
- Tissot, B.P. and Welte, D.H. 1984. *Petroleum formation and occurrence*, 2nd Ed. Springer-Verlag, Berlin, Germany.

POTENTIAL USE OF CARBONACEOUS MATERIALS FOR THE TREATMENT OF PROCESS-AFFECTED WATER

Christina C. Small, Zaher Hashisho and Ania C. Ulrich

University of Alberta, Department of Civil and Environmental Engineering, Edmonton, Alberta, Canada

ABSTRACT: Naphthenic acids found in process-affected mine tailings water are known to be highly toxic organic by-products; promoting corrosion in oil production and refining. The use of adsorption onto activated carbonaceous media has been successful in removing the naphthenic acids from the waste water. Using oil sands coke (a waste product of the bitumen extraction process) to treat the process-affected water is presented in this paper as a potential technique for naphthenic acids removal. Batch tests were completed using 500 mL of process-affected water and 5-30% of material by weight of either non-activated delayed coke or granular activated carbon (GAC). GAC removed 90-100% of dissolved organic carbon from process-affected water. Though non-activated, the delayed coke removed 13-30% of dissolved organic carbon from process-affected water. Such analyses provide a preliminary knowledge base for understanding the adsorptive behaviour of petroleum coke.

INTRODUCTION

The Canadian oil sands located in Fort McMurray, Alberta, generates over 1 million barrels of oil per day; requiring large volumes of water, and producing substantial quantities of waste (Allen, 2008a). Due to the zero discharge policy adapted in the area, the water utilized in the oil sands operations is recycled. The wet waste fraction is stored in large tailings ponds. Over $4 \times 10^8 \text{ m}^3$ of tailings is currently stored in the Athabasca region, wherein roughly $0.1\text{--}0.2 \text{ m}^3$ of tailings is generated per tonne of processed oil sands (Headley et al, 2009).

The wet tailings waste itself contains a sizable amount of coarse and fine sediments (sands and clays), water, dissolved inorganic

and organic by-products, as well as fractions of non-recoverable bitumen. The fine sediment fraction precludes the efficient settling of the material, and the dissolved organic fraction is known to contain toxic components. The accumulation of waste over time corresponds to various environmental implications, representing a large challenge for the oil sands industry.

After the bitumen extraction, upgrading produces considerable amounts of coke through either delayed or fluid coking processes. Due to the minimal understanding and current use of this material, the majority of the coke is stored on-site. Consequently, the oil sands coke represents another waste by-product generated by the industry.

The literature suggests that petroleum coke (like granular activated carbon) may be used as an adsorbent due to its chemical composition and arrangement of molecules (Barczak et al, 2005). Granular activated carbon is a common material known for its adsorptive capabilities. Depending on the properties of the raw carbon used, GAC has the potential to adsorb organic material (whether in vapour or liquid form). The large surface area (due to its micro-porous structure) and range of functional groups on the carbonaceous material permit attraction, leading to the direct removal of organics from the surrounding fluid (Karanfil and Kilduff, 1999). Due to its high carbon content of about 80-85% by weight (Furimsky, 1998), the oil sands petroleum coke may be an effective alternative for adsorption of toxic components from the waste.

This paper summarizes some of the fundamental research on the primary components of the oil sands waste, and describes the use of oil sands coke and GAC for the adsorption of select pollutants from process-affected water.

PROCESS AFFECTED WATER

During oil processing, fresh and recycled water are used to separate the bitumen from the sand and clay fractions, typically through flotation during hot water extraction (Allen, 2008a). The final composition of the process affected (PA) water differs across the Athabasca region depending on the unique geology of the mining area; however, the overall trend is the creation of saline water that is high in inorganic compounds and organic acids (Beier et al, 2007). More specifically, a cubic meter of oil sands mined within the Athabasca region will require approximately 3 m³ of water (whether fresh or recycled) for the extraction of bitumen,

resulting in almost 4 m³ of unusable slurry waste (Headley et al, 2005). This slurry waste is stored on site in constructed tailings ponds. Dewatering of the tailings ponds through densification procedures allows for the partial settling of sediments and the release of water-allowing for the recycling and continued use of water throughout the operations (Headley et al, 2005).

As the water becomes contaminated with by-products of the extraction procedures, additional clean water is required; increasing the demand for imported fresh water. Since not all of the water used in operations can be recycled, three barrels of river water per barrel of water are imported from nearby resources (Allen, 2008a). Within the Athabasca region, the main water sources come from the Athabasca River, groundwater, run-off, and connate water. Whether the water withdrawal can support the industries within the area in the future is questionable (Allen, 2008a).

Certain constituents within the PA water contribute to corrosion within the oil production and refining stages of the operations; the same components have also been found to increase the toxicity of the water (Allen, 2008a). This presents both industrial and environmental concerns for the oil sands companies. As the PA water is recycled, it becomes more concentrated with waste by-products, decreasing the volume of reusable resources. Conversely, the PA water toxicity poses a health risk to the environment and will require remediation (mainly at mine closure). In order to prevent the possibility of corrosion within the facilities, it becomes more practical for companies to import more fresh water than risk harm to the operations.

The removal of toxic components from the PA water would primarily result in more

efficient water recycling, and a decrease in the imported supply. With appropriate treatment, various industrial and agricultural applications may also utilize the water as well (Butler et al, 2006). Lastly, the effective treatment and reduction of PA water toxicity may lead to the allowable release of water to the environment.

Given that the recycled PA water is not typically treated before use in extraction, appropriate treatment strategies may be applied at this stage to minimize any concerns of scaling, corrosion, fouling, and to improve bitumen recovery (Allen, 2008a). This would increase the volume of recycled water, reducing the water import costs. Therefore, a good understanding of the toxic and corrosive components within the PA water is needed for the optimal development of treatment technologies.

ORGANICS

The organic material within the tailings ponds PA water includes the following compounds: organic acids, aromatic compounds, and bitumen; where the dissolved organic matter content ranges from 50-100 mg/L (Allen, 2008a). These components are waste by-products from the oil extraction processes, and contribute to the poor water quality of the tailings ponds. Of the organic acids, 80% consists of naphthenic acids which contribute to the major source of toxicity within the tailings ponds (Allen, 2008a). It is the naphthenic acids that also contribute to the corrosion in oil processing and refining.

NAPHTHENIC ACIDS (NAs)

NAs are naturally occurring compounds within the oil sands bitumen (Barbour et al,

2006), and are released during the oil sands extraction processes due to the aqueous digestion methods used within the industry (Clemente et al, 2003). Depending on the geology of the area in which the ores are mined, different concentrations and compositions of NAs can be expected.

NAs represent a class of alkyl-substituted acyclic and cycloaliphatic carboxylic acids; where, the structure varies depending on the number of hydrogen atoms lost, as linear hydrocarbon chains are gained (Barbour et al, 2006). Consequently, there is a variety of NAs, and depending on the functional groups; some are more toxic than others. It has been determined that the aging of tailings water as well as microbial activity can reduce the toxicity of NAs; however, it is still not possible to establish which compounds are responsible for the toxicity itself (Clemente et al, 2003). This presents an issue for designing treatment technologies, as it is not known whether the toxic NAs are being completely removed from the tailings water. It has been established that NAs are typically dominated by carbon numbers 13-16; increasing time and degradation will produce carbon numbers of C₂₂₊, where decreased toxicity has been observed (Allen, 2008a). This may have an important implication in monitoring and classifying NAs for the industry. Until the NAs can be uniquely characterized, techniques which aim to sufficiently remove all of the NAs in process-affected water may reduce any environmental or industrial concerns.

Though the NAs are naturally occurring, their concentrations in tailings pond waters have been found to range from 40 to 120 mg/L (Barbour et al, 2006). As the oil sands industry expands within the Athabasca region and more water is recycled, it can be assumed that these concentrations will increase with time as well. In contrast, the natural concentrations found within the Athabasca

river (travelling through the oil sands deposits) was determined to range from 0.1 to 0.9 mg/L (Clemente and Fedorak, 2005). If the high concentrations of NAs within the tailings ponds become mobile, this potential leaching may result in a large environmental impact.

The literature indicates that the solubility of NAs in water is affected by pH, and is greatest above neutral conditions. Depending on the functional groups present on the NAs, preferential sorption is likely to occur within the environment (Barbour et al, 2006). These characteristics favour the mobility of NAs in surface waters contaminated with petroleum (Clemente and Fedorak, 2005). As a result, the NAs are available for transport and uptake by plants and animals. However, the NAs have been confirmed to be toxic to a variety of aquatic organisms, especially at concentrations exceeding 2.5 to 5 mg/L (Clemente and Fedorak, 2005). If the NAs are not removed from the tailings ponds, this toxicity will have to be considered during mine closure and reclamation. Though NAs have been demonstrated to biodegrade with time (Allen, 2008a), it is not certain how long it may take for the toxic compounds to degrade.

The corrosion of infrastructure by the presence of NAs presents a large concern to the oil sands industry. This occurs through the formation of hydrogen gas at operating temperatures favouring corrosion (220-400°C), causing the chelation of metal ions due to the presence of carboxylic acid groups (Clemente and Fedorak, 2005). This process is highly dependent upon the types of NAs that are in the PA water during processing as well as their unique molecular composition. Temperature also plays an important role in determining whether the NAs will affect the equipment and machinery. Due to the lack of control on the

types of NAs within the PA water and the temperatures necessary for extraction and processing, it becomes more important for treatment technologies to be incorporated into oil extraction and refining.

PETROLEUM COKE

Petroleum coke is a by-product of the upgrading of bitumen to synthetic crude oil. Syncrude and Suncor Energy are cumulatively producing over 5 million tonnes of coke per year through either delayed or fluid coking processes (Coy and Fedorak, 2006). However, the cokes produced by these companies differ in composition due to the coking processes used during the bitumen upgrading process. Overall, the processes are dependent upon the thermal treatment; delayed coking generally occurs at a temperature range of 415-450°C, whereas fluid coking uses temperatures between 480-565°C (Coy and Fedorak, 2006). This heating affects the separation of the oil from the waste fractions as well as the degree of volatilization. Consequently, the volatile fractions measured in delayed and fluid cokes are 7-13% and 4-6% respectively; at the same time, the heating also generates varying ash contents (Coy and Fedorak, 2006).

The use of the petroleum coke differs between companies as well, where the majority of the coke is considered a waste product due to minimal use. Syncrude stockpiles the bulk of their coke on site (exceeding over 30 million tonnes); whereas a large amount of Suncor coke is burnt in boilers in order to raise steam and electricity (Furimsky, 1998). Research shows that the coke has a calorific value equal to that of medium grade coal of approximately, 29.5 MJ/kg (Coy and Fedorak, 2006). Until this becomes an economically viable option

for the industry, alternative uses of the petroleum coke have been investigated.

An alternative application of the coke has included the use of petroleum coke for adsorption purposes. This may be a viable option due to the high carbon content within the material. With activation, the coke has been shown to develop large surface area and porosity, where the adsorption capacities are 10 times that of raw coke (Sego et al, 2001). The use of this property within the Athabasca region is of interest to the oil sands industry to improve water quality within the tailings ponds.

ADSORPTION

Adsorption occurs due to the attraction forces existing between the adsorbent's surface functional groups and the adsorbate molecules. These interactions generally result from weak chemical bonds (Yang, 2003), allowing for the future desorption of the sorbed material.

The effectiveness of adsorption is based on the following factors: the nature of the adsorbent; the nature of the adsorbate; and, the conditions of the solution in which both reside (Barczak et al, 2005). If the appropriate functional groups exist to permit attraction and sufficient sites for the adsorbate to inhabit exist, adsorption will occur. However, the pH and ions within the solution will affect the availability and number of sites; and ultimately, the adsorption potential. More specifically, a decrease in pH will lead to the increase in hydrogen atoms within the solution, resulting in the alternative adsorption of protons (Barczak et al, 2005). As a result, higher pH solutions may be necessary for effective adsorption.

The pore size distribution and surface area of the adsorbent can affect the adsorption capacity, as more adsorption is likely to occur on a solid with a larger surface area. Pores that are spherical in shape also allow for a greater interaction with the adsorbate (the material adsorbed); allowing for a higher rate of adsorption (Yang, 2003).

Adsorption has been regarded as one of the more efficient technologies for organic contaminants removal from water due to the following: low impact on the environment; minimal production of associated wastes; and, their capacity for full or partial removal of organics (Allen, 2008b). As a result, this technique may be one of the more economical options for PA water treatment. It is also possible for this method to be teamed up with another remediation technique, for optimal organic and pollutant removal. However, finding an economically feasible adsorbent with the appropriate characteristics of high adsorption capacity for organics within the PA water is of interest to the oil sands industry.

Activated carbon has been classically used to adsorb organic contaminants (Stavropoulos and Zabaniotou, 2009). Activation (whether physical or chemical) produces a material that contains a greater number of pores of varying shapes and sizes through the degradation of non-carbon impurities. The range of pores existing within the micropore to macropore range, all depend on the raw parent material, the reaction conditions, and the temperature at the time of activation (Barczak et al, 2005).

Studies have shown that activated carbon has the ability to remove naphthenic acids from PA waters (Allen, 2008b). Therefore, adsorption as a treatment technology should be considered for the remediation of PA water. Other experiments using UV-Vis

absorbance and fluorescence spectrophotometry indicated that GAC is effective in adsorbing naphthenic acids at pH =9 (Headley et al, 2008). However, it is not known whether naphthenic acids removed were of the toxic form. Nevertheless, these results provide the appropriate stepping stones for developing a treatment technology suitable for the oil sands industry. Though GAC has been seen as an effective adsorbent in the literature, the commercially available product can become expensive for large scale projects. It will be more beneficial to find a more economically viable option for large reclamation projects.

APPLICATION TO PETROLEUM COKE

Petroleum coke is a common organic by-product used for the production of activated carbon throughout the literature. When activated, petroleum coke has a higher activation yield and surface area than most raw materials (Stavropoulos and Zabaniotou, 2009). Therefore, coke has the potential to be a viable alternative to GAC. The costs to generate this material through either physical or chemical activation tend to be the highest; however, the greater yield provides a lower overall total investment cost (Stavropoulos and Zabaniotou, 2009). Lower overall costs may be associated with a smaller production of activated petroleum coke required for usage; with respect to other common raw materials. There is also a lower cost in obtaining the coke raw material, as it is an abundant waste material and typically cheap (Stavropoulos and Zabaniotou, 2009). Since oil sands companies produce this waste material daily; there is no direct cost in obtaining the petroleum coke. These low costs (if at all) in obtaining the material may allow companies to invest the higher costs associated with activation. As a result, the

material may represent the most economically viable source to industries on a longer term scale.

Activated coke is commonly used to treat organic contaminants within industrial wastewaters, as the product is high in organic carbon and low in inorganic components (Barczak et al, 2005). The process of activation leads to the formation of an assortment of pores. As a result, it has been observed to adsorb both low and high molecular weight compounds, depending on the preparation and creation of the material. The composition and structure of the coke highly depends on the technology utilized for bitumen upgrading. Accordingly, the adsorptive behaviour of the coke is expected to differ as well. For example, delayed coking, utilized by Suncor Energy produces a coke with a higher H/C ratio than coke produced through fluid coking utilised by Syncrude Canada (Furimsky, 1998). When produced, delayed coke can be found in lump form; whereas, fluid coke is a very fine powder. As a result, the delayed coke would need to undergo sufficient grinding to achieve an initial surface area comparable to fluid coke.

The mode of activation may also control the development of pores within the petroleum coke; and ultimately, its adsorption capacity. Studies have shown that activation of delayed coke with steam at 850°C for 4 hours produces an activated coke with a maximum adsorption capacity for methylene blue of 100.5 mg/g (Sego et al, 2001).

Activated petroleum coke has been used to remove chlorinated organic compounds from waste water in the pulp mills industry, and the success of the activation led to the removal of >90% (Sego et al, 2001). Thus, petroleum coke is an excellent candidate for organic acid removal from tailings pond PA

water. Since the coke has a considerable surface area when activated, it may be appropriate to observe the natural adsorptive characteristics of the petroleum coke before activation. Non-activated fluid coke added at 15- 30% by weight to PA water was reported to reduce the organic carbon content by 70 to 90% (Chung et al, 2009). It is of interest to the oil sands industry to observe whether non-activated delayed coke has the same adsorptive behaviour as non-activated fluid coke.

This paper will examine the ability of GAC and non-activated delayed coke to remove dissolved organic carbon from oil sands process-affected water.

LABORATORY EXPERIMENT

Materials And Methods

Delayed petroleum coke and oil sands PA water were obtained from Suncor Energy. Before testing, the coke was ground to pass sieve mesh # 40 (aperture 425 μm) with a mortar and pestle. Grinding the coke to a fine powder allows for the optimal comparison to the fluid coke understood to have an efficient adsorptive capacity.

The PA water was initially centrifuged and filtered through 0.45 μm filters in order to remove the fine clay particles. This technique was completed to prevent the naphthenic acids from adsorbing to the clays, giving a false representation of the coke adsorption potential. Decreasing the clay/ coke competition also established a baseline for the coke adsorption.

Initial testing of the PA water was completed at room temperature and consisted of the following measurements and analyses: pH; electrical conductivity (EC); alkalinity; dissolved organic carbon (DOC); ion

chromatography (for major cations and anions); and, inductively coupled plasma mass spectrometry analysis (for trace metals). More specifically, alkalinity values were determined through the use of potentiometric titrations with 0.02N H_2SO_4 . Method HACH- DR/2400 for mid-range organic carbon (15-150 mg/L carbon) was used to obtain the DOC values. The method assumed that the filtration of the samples through 0.45 μm filters allowed for the direct translation of DOC readings, typically obtained as total organic carbon readings. Before treatment, the PA water was stored at approximately 4 °C.

Batch tests were completed by mixing the delayed coke with the PA water (500 mL) in 5, 10, 20, 30 weight % intervals. Procedures for the batch testing were obtained from ASTM D 4646 (ASTM, 2008). Samples were left to agitate for 24 hours, as it was proposed to be the efficient time necessary to reach equilibrium (ASTM, 2008). The agitation speed was altered to 160 rpm, in order to efficiently mix the petroleum coke with the water; ensuring contact with every surface. Afterwards, the samples were filtered through 0.45 μm filters to remove the coke, and the water was re-analyzed for the same initial parameters. The same experiment was completed with a coal-based GAC, as the research showed that GAC has a high adsorptive capacity. As a result, the GAC represents a positive control within the experiment. Both the GAC and coke were also mixed with ultra-pure (DI) water to obtain a negative control with respect to species in the PA water.

Results And Discussion

Table 1 shows the outcome of coke and GAC when mixed with ultra-pure (DI) water. In comparison to the blank DI water sample, coke and GAC were observed to alter the pH,

alkalinity, and EC. With the addition of coke, the pH dropped from an initial value of 8.3 to new values ranging from 7.2-7.6. Alternatively, the addition of GAC resulted in an increase in pH where values ranged from approximately 9.7-10.4. The results of the EC testing showed that coke and GAC both added salts to solution after the completion of the batch tests. The quantity of salts in solution tended to increase with increasing additions of coke and GAC. Overall, the GAC showed higher EC values than the coke, where the numbers are orders of magnitude higher than that of the original DI water samples. The DOC values for both the coke and GAC mixed with DI water were all under-range, indicating the expected absence of organic compounds.

Table 1. The analysis of ultra-pure (DI) water mixed with the addition of coke and granular activated carbon. Values include the mean of two replicates ± one standard deviation.

Sample	pH	EC (µS)	Alkalinity (mg CaCO ₃ /L)	DOC (mg/L)
DI Water Only	8.3 ± 0.6	1.9 ± 0	3.50 ± 0.7	0 ± 0
5% Coke	7.2 ± 0.03	41.1 ± 3.3	20.25 ± 0.4	1 ± 1.4
10% Coke	7.3 ± 0.03	55.9 ± 6.4	18.00 ± 3.5	0.5 ± 0.7
20% Coke	7.3 ± 0.02	96.5 ± 11.0	17.75 ± 3.9	6.5 ± 3.5
30% Coke	7.6 ± 0.02	155.1 ± 4.2	35.38 ± 0.2	1 ± 1.4
5% GAC ^a	10.0 ± 0.04	83.1 ± 4.6	47.25 ± 2.5	1.5 ± 0.7
10% GAC ^a	10.3 ± 0.03	140.1 ± 0.5	69.50 ± 0.7	2.5 ± 0.7
20% GAC ^a	9.7 ± 0.07	152.8 ± 1.2	72.75 ± 1.8	4 ± 4.2
30% GAC ^a	10.4 ± 0.08	170.3 ± 6.0	74.00 ± 4.9	1 ± 1.4

^a GAC = granular activated carbon.

The results of the IC and ICPMS analyses of DI water mixed with coke and GAC showed trends in major ion concentrations within the solutions (Figure 1). Increases in Ca, SO₄, and Na are associated with the salts measured through the EC analysis. The GAC was observed to add higher amounts of Ca than the coke. However, the coke added

significantly higher amounts of SO₄ and Na with increasing weight percentages. The trace metals observed as dominating throughout the coke solutions were Mn and Sr (88) with average concentrations of 3.8 µg/L and 4.1 µg/L, respectively. In contrast, Mn was not observed within the GAC solutions; however, the average concentration for Sr (88) was 66.7 µg/L. These results provide a control for the basis of the experiment with PA water.

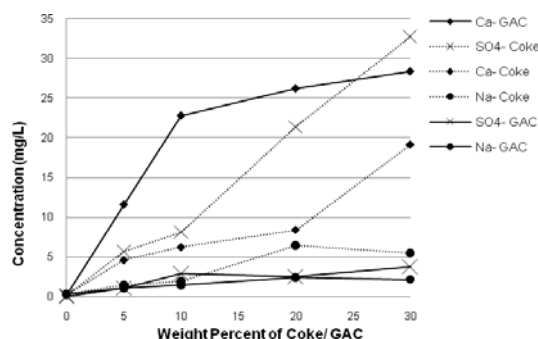


Figure 1: Major increasing trends in the ultra-pure water chemistry once mixed with granular activated carbon and coke. Values contain the mean of two replicates.

Table 2 shows that the pH of the PA water when mixed with coke remains relatively constant throughout the different treatments; with the exception of the 20% by weight coke addition. Here, the pH is higher than that of the initial PA water, and is associated with increasing ion concentrations (as seen in Figure 2). In contrast, the pH of the PA water mixed with GAC was observed to increase with increasing weight additions. The pH of the GAC is approximately within the same range as that measured with the DI water.

The alkalinity was seen to increase with increases in the amount of GAC added to the PA water (Table 2). These values were higher by an order of magnitude than those measured from the DI water samples.

When added to the PA water, the GAC has consistently higher EC values than the coke samples. This results in a higher quantity of salts within the final water solutions. Overall, these values are greater than those measured with DI water and may be associated with the ions existing in the PA water.

Overall, the DOC values decreased with the addition of coke and GAC to PA water (Table 2). DOC is the fraction of the total organic carbon found in aqueous form. It is assumed that the dissolved fraction participates in adsorption, and is the portion of organic carbon that includes the naphthenic acids. For the GAC samples, all measured values were under-range with use of the HACH method, showing adsorption of 90 to 100% of dissolved organic carbon (including naphthenic acids). This indicates that GAC is an effective adsorbent. The coke samples, though non-activated, depicted a 13 to 30% decrease in DOC. Since naphthenic acids are a percentage of the measured DOC, the adsorption of naphthenic acids is less than the measured range.

Table 2: The analysis of process affected (PA) water mixed with the addition of both coke and granular activated carbon; based on percent weight. Values include the mean of two replicates ± one standard deviation.

Sample	pH	EC (mS)	Alkalinity (mg CaCO ₃ /L)	DOC (mg/L)
PA ^c Water Only	8.46 ± 0.06	3.11 ± 0.01	565 ± 0	53 ± 0
5% Coke	9.06 ± 0.07	3.12 ± 0.01	571.3 ± 12.4	45 ^a
10% Coke	9.09 ± 0.04	3.14 ± 0.01	547.5 ± 17.7	46 ^a
20% Coke	8.74 ± 0.01	3.12 ± 0.01	572.5 ± 14.1	42 ^a
30% Coke	9.07 ± 0.03	3.13 ± 0.01	520.5 ± 13.4	37 ^a
5% GAC ^b	9.80 ± 0.01	3.23 ± 0.07	700.0 ± 0	5.5 ± 7.7
10% GAC ^b	10.12 ± 0	3.24 ± 0.04	735.0 ± 42.4	0 ± 0
20% GAC ^b	10.39 ± 0.08	3.22 ± 0.01	818.8 ± 5.3	1 ± 0.7
30% GAC ^b	10.52 ± 0.03	3.25 ± 0.03	892 ± 4.2	4.5 ± 1.4

^a One value obtained from the testing.

^b GAC = granular activated carbon.

^c PA = process affected

The following cation concentrations were obtained through IC and ICPMS testing, and were found to be relatively constant throughout the varying coke treatments when mixed with PA water: Mg (5.8 ± 0.4 mg/L); K (9.9 ± 0.9 mg/L); Ca (5.5 ± 1.3 mg/L); Na (652.8 ± 4.9 mg/L); Rb⁸⁷ (0.09 ± 0.01 mg/L); As (0.08 ± 0.01 mg/L); and, V (0.2 ± 0.05 mg/L). The major associated anions observed as consistent throughout the different trials were as follows: Cl (561.2 ± 2.8 mg/L); F (1.99 ± 0.05 mg/L); SO₄ (261.8 ± 18.9 mg/L); and, Mo (3.2 ± 0.7 mg/L). Altogether, these values were comparable to those obtained from the blank PA water samples. As a result, the previous cation and anion concentrations can be said to have mainly originated from the PA water.

In contrast to the coke samples mixed with DI water, the addition of coke to PA water did not result in increasing trends in Na, Ca, and SO₄ concentrations. The higher ionic strength of the PA water may have prevented the additional release of these ions. Consequently, the ions do not add to the salt content in the PA water. The Sr (88) concentrations were observed to be consistent throughout the weight % additions with an average concentration of 25.9 µg/L. This is significantly higher than the values measured from the coke and DI water samples; however, the observed concentration is comparable to that of the blank PA water (20.0 µg/L).

Major trends observed in the water chemistry analysis of PA water showed an overall increase in B and a decrease in NH₄ and Mn with increasing added weights of coke (Figure 2). At a 20% weight addition of coke, B showed an abrupt increase in concentration, while the pH decreased; this anomaly has yet to be confirmed as a true observation or experimental artefact.

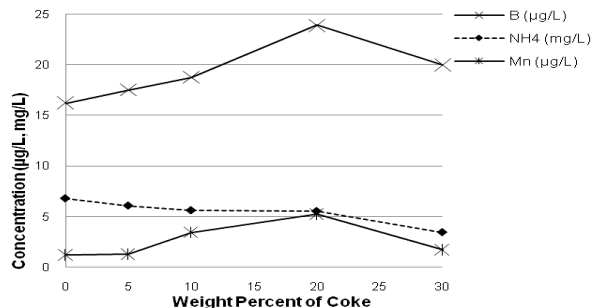


Figure 2: Major trends in the process affected water once mixed with coke. Values include the mean of two replicates.

The steady decrease in ammonium (NH_4) with the addition of coke indicates that it may have adsorbed to the coke; reducing the overall concentrations in solution. Within the coke and DI water solutions, the NH_4 concentrations were lower and consistent in value throughout the weight % additions, with an average concentration of 0.15 ± 0.01 mg/L. A 56% reduction of NH_4 was observed for the 30 weight percent coke and PA water treatment. The trace metal, manganese (Mn) was observed within the PA water samples, which was also measured within the DI water samples. Unlike the invariable concentrations observed in the analyses of DI water samples, the concentrations for the PA water treatments ranged from 1.3 to 5 $\mu\text{g/L}$. This trend is also considered to be an anomaly, where the average concentration is similar to that of the DI water samples.

The following cation concentrations measured were recurrent throughout the varying GAC treatments (based on percent weight additions) when mixed with PA water: K (8.9 ± 1.2 mg/L); and Na (686.2 ± 7.3 mg/L). The major associated anions concentrations also observed to be consistent throughout the tests were as follows: F (1.9 ± 0.05 mg/L); and SO_4 (220.4 ± 10.6 mg/L).

In contrast to the GAC samples mixed with DI water, the Ca concentrations decreased

and the Na and SO_4 concentrations were unvarying over the weight percent additions to solution. However, the Na and SO_4 concentrations are an order of magnitude higher than those measured in the DI water samples. As a result, there are more salt-forming ions in the PA water solutions before the addition of the delayed coke. The trends for the Na and SO_4 concentrations are comparable to the coke samples mixed with PA water. This explains the higher EC values within the PA water samples than the DI water samples.

The non-detectable Mn concentrations measured when GAC was mixed with PA water were similar to that of the GAC samples mixed with DI water. In contrast, the average Sr (88) concentrations had a 50% reduction in comparison to the DI water samples, where values decreased from 66.7 $\mu\text{g/L}$ to 33.7 $\mu\text{g/L}$.

Ions of interest showing increasing trends (Figure 3) not seen in the blank PA water include arsenic, vanadium, and phosphate ions. These additions to the final solutions were not observed within the DI water samples. Since the concentrations of these ions were low within the blank PA water, the higher concentrations measured throughout the weight additions may have been contributed from the GAC itself. With the greater use of GAC, the concentrations of arsenic and vanadium may require an alternative remediation technique due to their association with animal and plant toxicity. The iron had an overall increasing trend where the concentration was observed to peak around the 10% weight addition of GAC. Though iron appears to be added to solutions in the presence of GAC, the range of concentrations observed is not significant.

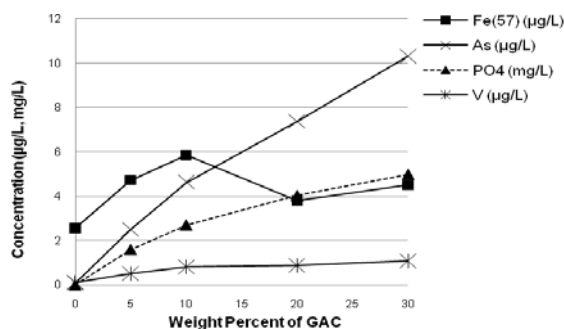


Figure 3: Major increasing trends in the process affected water chemistry once mixed with granular activated carbon. Values contain the mean of two replicates. Ion values correspond to an increase in pH (9.8-10.52).

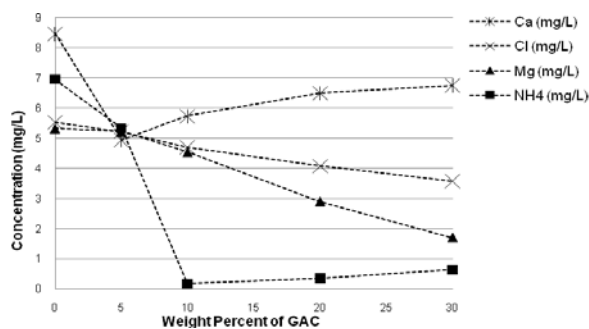


Figure 4: Major decreasing trends in the process affected water chemistry once mixed with granular activated carbon. Values contain the mean of two replicates. Ion values correspond to an increase in pH (9.8-10.52).

The concentrations of Cl (0.22 mg/L), Mg (1.1 mg/L), and NH₄ (0.09 mg/L) were persistent across the different weight additions when the GAC was mixed with DI water. Since all of the initial concentration values of these ions were higher in the blank PA water (Figure 4), the GAC significantly affected their presence in solution. Decreasing trends observed when GAC is mixed with PA water are more abundant than that of the coke samples. The reductions may likely be attributed to the direct adsorption onto the GAC itself. However, if the ions are available in excess within the solution, the saturation may favour the formation of

precipitates. These precipitates would have been removed with filtration after the completion of the batch test; explaining the decreasing trends. The reduction in these salt-forming ions is significant as well as desirable for the oil sands industry.

CONCLUSIONS

The preliminary batch experiments showed that the addition of non-activated delayed coke to process affected water at 15 to 30% by weight reduced the dissolved organic compounds (and associated naphthenic acids) by 13 to 20%. This is encouraging seeing that the as-produced coke, a widely available waste by-product of bitumen upgrading, have the ability to remove organic contaminants from bitumen extraction. While granular activated carbon depicted higher adsorption capacity for dissolved organic compounds, it is more expensive than non-activated coke.

Unlike the DI water, when carbonaceous media is added to PA water, the higher ionic strength was observed to prevent the additional release of major salt-forming ions. Due to the concentration of dissolved ions within the PA water, the EC values are much higher than the DI water mixed solely with GAC or coke. With increasing carbon weight additions one can expect higher associated pH and alkalinity values, where trace metals may become a concern when higher amounts of coke or GAC are added to the PA water.

FUTURE WORK

Activation of the delayed coke is needed to increase its porosity and surface area and enhance its adsorption capacity and removal efficiency. Future experiments should also examine whether changes in pH alter the coke adsorption as this may increase the removal efficiency of organic contaminants.

ACKNOWLEDGEMENTS

The authors would like to acknowledge the University of Alberta; funding from NSERC; and the coke samples, process affected water, and funding provided by Suncor Energy.

REFERENCES

Allen, E.W. 2008a. Process Water Treatment in Canada's Oil Sands Industry: I. Target Pollutants and Treatment Objectives. *Journal of Environmental Engineering and Science*; 7: 123- 138.

Allen, E.W. 2008b. Process Water Treatment in Canada's Oil Sands industry: II. A Review of Emerging Technologies. *Journal of Environmental Engineering and Science*: 7: 499-524.

ASTM. 2008. Standard Test Method for 24-h Batch-Type Measurement of Contaminated Sorption by Soils and Sediments. ASTM International. PA, USA; D 4646-03.

Barbour, S.L., Headley, J.V., Janfada, A., and Peru, K.M. 2006. A Laboratory Evaluation of Sorption of Oil Sands Naphthenic Acids on Organic Rich Soils. *Journal of Environmental Science and Health Part A*; 41: 985-997.

Barczak, M., Dąbrowski, A., Hubicki, Z., and Podkościelny, P. 2005. Adsorption of Phenolic compounds by Activated Carbon- A Critical Review. *Chemosphere*; 58:1049-1070.

Beier, N., Biggar, K., Donahue, R., and Segó, D. 2007. Trickle-Freeze Separation of contaminants from Saline Waste Water. *International Journal of Mining, Reclamation and Environment*; 21(2): 144-155.

Butler, D., Memon, F.A., Murphy, R., and Vlasopoulos, N. 2006. Life Cycle Assessment of Wastewater Treatment Technologies Treating Petroleum Process Waters. *Science of the Total Environment*; 367: 58- 70.

Chung, K., Mackinnon, M., and Zubot, W. 2009. Method of Treating Water Using Petroleum Coke. Canada. Patent No. 20090101574; 04-23-2009.

Clemente, J.S., Fedorak, P.M., MacKinnon, M.D., and Prasad, N.G.N. 2003. A Statistical Comparison of Naphthenic Acids Characterized by Gas Chromatography- Mass Spectrometry. *Chemosphere*; 50: 1265- 1274.

Clemente, J.S., and Fedorak, P.M. 2005. A Review of the Occurrence, Analyses, Toxicity, and Biodegradation of Naphthenic Acids. *Chemosphere*; 60: 585-600.

Coy, D.L., and Fedorak, P.M. 2006. Oil Sands Cokes Affect Microbial Activities. *Fuel*; 85: 1642-1651.

Fedorak, P.M., and Scott, A.C. 2004. Petroleum Coking: A Review of Coking Processes and the Characteristics, Stability, and Environmental Aspects of Coke Produced by the Oil Sands Companies. Report Submitted to Suncor Energy Inc., Syncrude Canada Ltd, and Canadian Natural Resources Ltd; 66p.

Furimsky, E. 1998. Gasification of Oil Sand Coke: Review. *Fuel Processing Technology*; 56: 263-290.

Headley, J.V., Hill, G.A., Nemati, M., and Paslawski, J.C. 2009. Biodegradation Kinetics of Trans-4-methyl-1-cyclohexane Carboxylic Acid. *Biodegradation*; 20: 125-133.

Headley, J.V., Peterson, H.G., and Quagraine, E.K. 2005. In Situ Bioremediation of Naphthenic Acids Contaminated Tailing Pond Waters in the Athabasca Oil Sands Region- Demonstrated Field Studies and Plausible Options: A Review. *Journal of Environmental Science and Health Part A*; 40: 685-722.

Karanfil, T., and Kilduff, J.E. 1999. Role of Granular Activated Carbon Surface Chemistry on the Adsorption of Organic Compounds. 1. Priority Pollutants. *Environmental Science and Technology*; 33(18): 3217-3224.

Sego, D.C., Shawwa, A.R., and Smith, D.W. 2001. Color and Chlorinated Organics Removal from Pulp Mills Wastewater Using Activated Petroleum coke. *Water Resources*; 35(3):745- 749.

Stavropoulos, G.G., and Zabaniotou, A.A. 2009. Minimizing Activated Carbons Production Cost. *Fuel Processing Technology*; doi: 10.1016/j.fuproc.2009.04.002.

Yang, R. T. 2003. Adsorbents: Fundamentals and Applications. John Wiley and Sons, New Jersey; 410 pp.

GEOCHEMICAL INTERACTIONS BETWEEN PROCESS-AFFECTED WATER AND NATIVE SOILS IN FORT MCMURRAY

Holden, A.A. and Ulrich, A.C.

Dept. Of Civil & Environmental Engineering, University of Alberta, Edmonton, Canada

Donahue, R.B.

Professional Engineer, Edmonton, Alberta, Canada

ABSTRACT: Exchangeable Cation, Cation Exchange Capacity and Batch Sorption experiments were conducted to assess the potential environmental impact of process-affected (PA) water seepage into the subsurface from an oil sands tailings pond in Fort McMurray, Alberta. Studies focussed on the geochemical interactions in the surficial glacial till and underlying sand channel. Due to the abundance of carbonate and sulphate salts present in the soil, the Ammonium Acetate method was found to be unsuitable for exchangeable cation analysis. Cation exchange capacity was approximately 10meq/100g in the till and 5meq/100g in the sands. Batch studies predict that the influx of PA seepage will induce the dissolution of sulphate salts. Sodium present in the PA water will exchange with pre-bound calcium and magnesium, with the divalent ions subsequently precipitating – likely as a carbonate mineral phase solid solution.

INTRODUCTION:

Every cubic metre of synthetic crude oil produced, generates 1.5 cubic meters of mature fine tailings (tailings = sand, fines and water mixture) [1]. These tailings must be stored in large settling ponds rather than be released, as oil sands tailings operations presently operate under a policy of zero water discharge to the environment [2]. There are a number of locations on oil sands leases in northern Alberta where existing or proposed tailings ponds will be sited atop buried sand channels, relicts from previous glacial rivers. Preliminary hydrogeologic modeling suggests that seepage from these ponds will infiltrate through the overlying glacial till and into the sand channels; however, the development and

extent of this impact is not known [3]. The Suncor Energy Inc. South Tailings Pond (STP), the first such facility to be studied from its inception, offers the opportunity to increase understanding for what is to become an industry-wide issue.

The research described herein seeks to clarify the geochemical response of the native soil-pore water system to the ingress of process-affected seepage water from a tailings pond in Fort McMurray, AB, so that future remediative strategies can be designed accordingly. This will be addressed through a series of sub-objectives, namely:

1. To assess the capacity of in-situ soils in binding potential contaminants

- (cation exchange capacity experiments);
2. To characterize cations, initially bound to the soil, that may be displaced and released through interaction with incoming PA water (exchangeable cation experiments); and
 3. To establish a preliminary understanding of the adsorptive strength and ion exchange reactions within local soils when exposed to PA water (batch sorption experiments) .b. To additionally investigate 3. using a novel modification of batch sorption experiments featuring less disturbed soil samples.

Cation exchange capacity in clays is dependent upon clay mineralogy and to varying extent pH. At pH 7, approximate values of CEC range from 3 to 15 meq/100g for Kaolinite, 10 to 40 meq/100g for Illite and Chlorite, and 80-150 for Smectite-Montmorillonite [4]. Across Alberta, including in the vicinity of the STP, surficial geology includes glacial till deposits which are derived from, and therefore reflective of, the underlying bedrock material – in this case the Clearwater Formation. [5,6]. To the best of our knowledge, no studies have examined the local clay mineralogy of the Pleistocene till; however, the most surficial stratum of the Cretaceous Clearwater Formation was found to have a composition of 13/13/38/38 at the Suncor SE Waste Dump and 20/15/50/15 at the Syncrude site (Montmorillonite/Chorite/Illite/Kaolinite) [5]. The predominantly Illite, Kaolinite composition predicts the CEC of glacial tills in Fort McMurray will be between 3 and 40meq/100g.

Ion sorption affinity is governed by 1) ion charge and valence; 2) ion size – particularly the hydrated radius; 3) properties of the solid exchanger; 4) the quantity and ratios of the

various solutes; and 5) the total solution concentration [7]. Being a predominantly electrostatic process, at equal concentrations, ions with a greater charge will be preferentially adsorbed for example, in the order of: $\text{Al}^{3+} > \text{Ca}^{2+} > \text{Mg}^{2+} > \text{K}^+ > \text{Na}^+$. Furthermore, species with smaller effective ion size are able to come nearer to the exchanger surface and hence will be preferentially absorbed, thus for monovalent cations at equal concentrations: $\text{Cs}^+ > \text{Rb}^+ > \text{K}^+ > \text{Na}^+ > \text{Li}^+$ [8]. The groundwater concentrations at the time that soil samples were collected suggest that in decreasing order of abundance, the dominant cations are: $\text{Na}^+ > \text{Ca}^{2+}$ (although sometimes $\text{Ca}^{2+} > \text{Na}^+$) $> \text{Mg}^{2+} > \text{K}^+ > \text{NH}_4^+ > \text{Li}^+$. Together this suggests that exchangeable cations will primarily consist of calcium, magnesium and sodium. Bound calcium is expected to exceed bound magnesium; however, the relative abundance of sodium is unclear.

PA water includes high concentrations of sodium, chloride, sulphate and alkaline species. It is therefore expected that the interaction of PA water with the native soil/pore water will result in the sorption of sodium and subsequent displacement of pre-bound cations such as calcium and magnesium. Depending on the saturation indices of the mineral phases with the resultant solution, this could lead to precipitation of chloridic, sulphidic or carbonate salts.

METHODS

Laboratory experiments utilized soil at its native moisture content in order to avoid dissolution complications with sparingly soluble salts, such as gypsum, thought possibly present, based upon previously conducted saturated paste extraction experiments [9] (data not shown). Initially dissolved within the pore fluid, such salts

may not re-dissolve sufficiently quickly or to their initial extent, if the soil is first dried and then re-hydrated. To investigate the soil response across the vertical extent of the till, samples were selected from the upper, middle and lower glacial till (3.4 - 4.6, 6.1 – 6.4, and 8.2 – 9.1 meters below ground surface (mbgs)), and for additional interest, from the lower portion of the clay till-Wood Creek Sand Channel transition zone (12.2 - 13.7 mbgs) and deep in the Wood Creek Sand Channel (37.7 and 38.7 mbgs). A brief description of the soils is presented in Table 1. South Tailings Pond site details, including geology and soil core sampling information are described in a companion paper (Holden et al., this conference).

Exchangeable Cations:

Exchangeable cations were characterized based upon the methods of Sheldrick [10] and EPA 9081 [11]. A slurry was formed by mixing 2.5g of undried soil with 25g of 1N ammonium acetate, adjusted to pH 7.0. The mixture was shaken for 30 minutes (Burrell Wrist-Action® Laboratory Shaker, Model BB, at 10° amplitude, 400±20 Osc/Min) and subsequently centrifuged at 4150 rpm for 10 minutes (Heraeus Multifuge® 3 L-R). The resultant extract was filtered (0.2µm), diluted by 10 times using de-ionized water (18.2MΩ cm 0.7µS/cm Barnstead), and analyzed by Ion Chromatography at the University of Alberta Applied Environmental Geochemistry Research Facility. Experiments were conducted at room temperature (20.0°C). Tests were conducted in triplicate.

Lithium, sodium, ammonium, potassium, magnesium and calcium concentrations were analyzed using a Dionex ICS-2000 Ion Chromatography System and Chromeleon Client v6.50 software. Fluoride, chloride, nitrite, bromide, nitrate, phosphate and sulphate concentrations were analyzed using

a Dionex 2500 Ion Chromatography system (Dionex GP50 Gradient Pump, Dionex CD25 Conductivity Detector) and Chromeleon Client v6.50 software. Quality control included a check standard and blank after every 10-15 samples, and 5 calibration standards.

Cation Exchange Capacity:

EPA method 9081 was used to estimate the cation exchange capacity [11]. Briefly, 4-6g of undried soil was mixed four times with 1.0N sodium acetate (pH 8.2) to replace the pre-existing, bound cations with sodium ions. Next, the soil was rinsed three times with 2-propanol Optima (Fisher Scientific) to remove remaining free-phase ions. Lastly, the soil was mixed three times with 1N ammonium acetate (pH 7.0), with the washings retained. The concentration of displaced sodium in the combined 3 washings (diluted by 10 times) was quantified by Ion Chromatography and used to estimate the cation exchange capacity of the soil. Experiments were conducted at room temperature (20.0°C). Tests were conducted in triplicate.

Batch Sorption Experiments:

A total of four different treatments were applied using a combination of the standard batch sorption method or a new soil cube sorption method and simulated process-affected water or PA water collected on-site.

Process-affected water was collected from a discharge line feeding directly into the South Tailings Pond. In-house analytical speciation of this water was used to guide the creation of a simplified, inorganic, simulated process-affected water, whose principle constituents were sodium, bicarbonate, chloride and sulphate (Table 2).

Standard Batch Sorption Experiment:

Sorption and ion exchange behaviour were investigated as a function of process-affected water concentration. Six different simulated PA solutions were used: deionized water to a conservatively- selected maximum of 1.2 times the highest concentration of Suncor PA water observed to date (0, 20, 40, 60, 80, 100% by volume). Similarly, hereafter denoted “real” PA water stock solutions were prepared to 0, 20, 40, 60, 80 and 100% by volume (no dilution) of the water collected on site.

Batch samples were prepared in 50mL plastic centrifuge vials¹, by mixing 15g of undried soil with 30g of solution (1:2 soil:solution ratio). Preliminary experimentation found that a) ionic potential, an important determinant of geochemical behaviour, was dictated by the PA water and not by the soil; therefore, a representative model of the in-situ response to incoming PA water was not critically dependent upon the relative soil content; and b) final solution concentrations were more perceptible, particularly for less abundant ions, at higher solids content. Vials were agitated at room temperature (20.0°C) for 24 hours [12] using a wrist-action shaker. Subsequently, samples were centrifuged at 4150rpm for 15min. Any changes to the physical characteristics of either the soil or solution such as color, opacity, etc. were noted. A portion of the resultant supernatant was analyzed for pH and alkalinity, while the remainder was filtered (0.2µm) and major ion and trace metal speciation ascertained by Ion Chromatography and Inductively Coupled Plasma Mass Spectrometry², respectively. Two fluid-only blanks were prepared at each concentration – one before batch vials were

created, one after – to measure non-adsorptive losses in the system. Mass measurements were taken throughout the experiment to further record any such losses. Tests were conducted in triplicate.

Following the conclusion of the sorption experiment, desorption experiments were conducted on the remaining soil. The desorption method was simply an extension of the latter portion of the CEC experiment; in short, three rinses with 2-propanol followed by three rinses with 1N ammonium acetate solution (pH 7.0).

Cube Batch Sorption Experiment:

A new method is proposed to investigate sorption and ion exchange behaviour as a function of process-affected water concentration - by diffusive equilibrium with an intact soil section. The applied solutions are the same as above.

A 15g cube of undried soil (approximately 2x2x2cm) was carefully cut from the soil core section using a stainless steel palette knife, placed within a 4oz. glass jar³ and topped with 30g of solution. A preliminary simulation of 1-dimensional diffusive transport using PHREEQC [13] predicted that equilibration would be achieved in 5 days for a cube of these dimensions. The jar was then sealed and left in the dark, at 20.0°C, for 5 days. After this period, any changes to the physical characteristics of either the soil or solution were noted. The equilibrated solution was decanted and analyzed for pH, alkalinity, major ions by Ion Chromatography and trace metals by Inductively Coupled Plasma Mass Spectrometry analyses. A fluid-only control was prepared at each concentration. Mass measurements were conducted throughout the

¹ Plastic containers were deemed suitable given our focus on inorganics and the short-term 24h duration

² Samples were preserved in 1% nitric acid, and analyzed via PerkinElmer SCIEX ELAN 9000 – results not shown.

³ Given the greater duration of this experiment, glass jars were used to minimize the sorption of organics onto container walls, which could have altered the inorganic system response.

experiment to record evaporative losses to the system. Tests were conducted in triplicate.

Soil samples were retained during each of the exchangeable cation, CEC and batch experiments, and dried at 100°C for 24 hours for gravimetric water content analysis (Table 1). These values were later used to correct for the presence of pore water in the undried soil samples.

Two commonly used models in batch sorption experiments are the linear and Langmuirian sorption models. The linear sorption model is specified as

$$K_d = C_s / C_w$$

with K_d representing the non-equilibrium 24 hour distribution coefficient [12], C_s the solute mass sorbed per unit mass of dry soil (mg/kg) and C_w , the solute concentration remaining in solution (mg/L).

The Langmuirian model in turn, is given by $C_s = (bN_{\max}C_w) / (1+bC_w)$

where b is a constant, and N_{\max} the maximum possible sorption by the solid [4].

RESULTS

CEC / Exchangeable Cations

Cation exchange capacity values ranged from approximately 10 meq/100g in clay samples, to about 5 meq/100g in sand samples. The sum of exchangeable cations exceeded the cation exchange capacity for each soil region tested. Resulting calcium concentrations were the largest, near 15-20 meq/100g, while potassium and sodium were the smallest at approximately 0.05 to 0.3 meq/100g (Table 3).

Batch Sorption Experiments

Across cube and standard batch experiments, the difference between initial stock solution and final fluid control sample concentrations was less than 10% for all major cations except for calcium, suggesting that linear partitioning coefficients calculated for calcium may be unreliable [12].

Batch Sorption – Deionized Case

Batch sorption samples created using deionized water are conceptually similar to saturated paste extractions outlined by Janzen [9], and serve to identify the distribution of chemical species available to interact with incoming PA seepage. Each of the soils tested showed that interaction with deionized water led to the dissolution of calcium and magnesium sulphate and carbonate salts. The concentration of released ions was greatest in the sand channel (most abundantly Ca^{2+} 9.09 meq/kg_{dry soil}, SO_4^{2-} 10.15 meq/kg_{dry soil}), and weakest in the lower clay till and adjacent till/sand interface region (for the latter, most abundantly Ca^{2+} 2.12 meq/kg_{dry soil}, alkalinity 2.71 meq/kg_{dry soil}).

Cube batch samples tended to show an identical response to the standard (ground) batch samples, although to a lesser extent (approximately 70% of the magnitude of the ground samples' response), likely reflecting that the sample stirring and shaking inherent to the ground experiment procedure exposes a greater soil surface area and may also introduce particle grinding and milling effects, etc. causing an increased amount of dissolution to occur.

Batch Sorption – Zero to Full Strength PA Cases

Cation sorption was best represented by a

linear isotherm only for sodium (Table 4), and selectively for ammonium and lithium. The sodium response was linear from 0 to full strength (100%) PA water, with possible evidence of beginning to approach a Langmuirian plateau by full strength. Lithium was well characterized by simple linear desorption for all solution strengths, although only for simulated PA experiments. Samples mixed with real PA water, which includes aqueous lithium, displayed more complicated sorption behaviour than samples mixed with lithium-devoid, simulated PA water. The ammonium response was variable, but showed evidence of linear desorption from 0-100% for simulated PA samples and occasionally also for real PA, standard batch samples.

For the majority of cation species, including calcium, magnesium and potassium, neither the linear nor Langmuirian models suitably captured the system behaviour. Figure 1 illustrates an example dataset showing cations both well and poorly characterized by the linear sorption model.

The experimentally-determined, final, equilibrium solutions were modeled using PHREEQC [13], to ascertain their degree of saturation with respect to carbonate and sulphate mineral phases. Results consistently found equilibrium solutions to be oversaturated with respect to calcite and dolomite, at all PA strengths except, usually, the deionized case. Solutions from all PA strengths tended to be very near the saturation point of magnesite, typically crossing into oversaturation at higher PA strengths. All solutions were well undersaturated with respect to gypsum. These results generally suggest that regardless of PA strength, in reaching the equilibrium state, carbonate salts would be precipitated out of solution, while sulphate salts, if present, would dissolve, being released into solution.

The trends of equilibrium solution ion concentrations with increasing PA strength were examined for each batch sample created. Mass balance calculations permitted a comparison of a predicted final concentration, based upon non-adsorptive losses, initial pore fluid and added PA solution chemistries, with the observed final equilibrium concentrations. A positive value for the difference between the predicted and observed values is indicative of uptake of that ion while a negative value represents release (e.g. by dissolution, desorption, etc).

Consistent findings were observed in the ion trends - across soil treatment (cube vs. ground), PA solution (real vs. simulated) and soil type (clay vs. sand) tested (Figure 2). Chloride was minimally present in all samples, with a constant, near zero response across PA strengths. Sulphate showed evidence of a constant to slightly increasing extent of release with PA strength. The amount of sulphate released was much greater than the chloride response, but smaller than the calcium or magnesium release, except in the Sand Channel. Magnesium typically showed a constant release across all PA strengths. Calcium behaviour was similar, with a constant to slightly increasing extent of release with PA strength, although at approximately twice the magnitude of magnesium. By contrast, sodium showed evidence of increasingly large uptake with PA strength, occasionally beginning with a near-zero or very slight release in the Deionized case. The alkalinity response tended to begin with release at low PA strengths, quickly switching into often large uptake by high PA strengths. Here, again the Sand Channel response was slightly different, showing a more significant release of alkalinity-based species with PA strength.

DISCUSSION

Cation Exchange Capacity

Cation exchange capacity varied from approximately 10meq/100g in the till, to 5meq/100g in sand samples, with initial indications suggesting a close association between sample-specific variability and the physical characterization of each soil. Grain size analysis from each of the core sections tested, is currently ongoing and will be used shortly to further examine the CEC data. Qualitatively, while creating samples, those from the lower till were noticeably more clayey, while those from the middle till samples were much grittier by comparison; the higher suggested sand content would explain the relatively lower CEC in that region (4.02 vs. 15.50meq/100g). Likewise, transition zone samples consisted of very sandy soil, and correspondingly had the lowest observed CEC (3.51meq/100g).

The geology of the Wood Creek Sand Channel follows a general progression with depth from silty sands, to clean sands, to coarser grained sands and gravels [5]. Similarly, lithology of the sampled cores notes that M2-38 originated from a section of very silty, fine-grained sand with some fine gravel and occasional clay lenses (CEC 6.50meq/100g), while that of M2-39 was not silty, and coarser, with fine-medium grained sand and medium to coarse gravel – reflected, as expected, by a relatively smaller CEC of 5.59meq/100g.

To the best of our knowledge, very few studies have investigated the CEC of Pleistocene soils near Fort McMurray. Peng et al. [14] reported values of 16.2 to 19.4meq/100g for peat-augmented reclamation/salvage soils at the Syncrude site, which is comparable to the value of 11.32meq/100g observed in the upper till. In Northwestern Alberta, in the Peace Lowland

ecoregion, Cathcart et al. [6] reported a mean CEC of 29.5meq/100g in the B Horizon (15-30cm below surface). Similar to the present site, high clay content in those soils is attributed to tills derived from Cretaceous marine shale. Whalen et al. [15] analyzed surficial (0-15cm) soils from Fort Vermillion and Beaverlodge in the Peace River region of Alberta, reporting CEC's of 59.0 and 38.2meq/100g respectively. The observed values therefore appear plausible in the context of these findings.

Exchangeable Cations

The results suggest that Ammonium Acetate extractions are unsuitable for analyzing exchangeable cation behaviour on South Tailings Pond soils. Since soil cores were collected as baseline samples prior to interaction with PA water, this finding should not be specific to the STP, and would be expected to extend to surrounding areas in the oil sands region. (The Ammonium Acetate method had been selected in the present study because it is one of the most commonly used methods [16, 17] and because mineralogical analysis of the soils on-site had not yet commenced, identifying the presence of any potential confounding mineral phases). In the present study, the value of exchangeable calcium alone exceeded the CEC for each soil sample tested. Similarly, exchangeable magnesium values may be elevated, often accounting for one quarter to one third of the CEC. These findings suggest dissolution of a mineral phase(s) occurred in conjunction with exchange reactions.

Several possibilities for correcting the data were explored, though none were found to be successful. For example, exchangeable cation samples were analyzed for anion content by Ion Chromatography as a means of identifying a divalent cation salt source. Only sulphate was detected however, although by nature of the eluent used, our IC system

cannot measure carbonate species, while other anions, such as chloride, if present, were indistinguishable from the overwhelming acetate peak. The sulphate concentrations observed represented only a small fraction of those recorded for calcium (about 2% in a mmol/L comparison) – discounting the dissolution of sulphate salts as the primary source of excess calcium or magnesium ions.

To examine the validity of a CEC or exchangeable cation method, Dohrmann [17] proposed the Carbonate and Sulphate Field (CSF) Model – predicated upon the principle that CEC or exchangeable cation values should remain approximately the same despite variations in soil to solution ratios. On the other hand, a method is unsuitable, if, for soils containing partially soluble mineral phases (carbonates and sulphates in particular), a greater relative amount of solution imparts a higher degree of solubilization. To test the applicability of the current method with STP soils, the Ammonium Acetate exchangeable cation extraction [10,11] was repeated at a second soil to solution ratio (5g undried soil per 25g solution) and the results combined with the initial dataset and analyzed using the CSF model. Results found that, of the three major cations detected, exchangeable sodium and magnesium values were marginally susceptible to the variation in soil:solution ratio; however, the derived values are likely a suitable approximation of the true exchangeable concentrations. However, the CSF model revealed that this method is not suitable for analyzing exchangeable calcium, believed due to the presence of partially soluble calcium mineral phase in STP surficial soils.

In this context, the present findings are supported by several authors. Sheldrick [10] and Carter [16] note that the Ammonium Acetate method is unsuitable for

exchangeable calcium and magnesium quantification in calcareous clays. Similarly, Dohrmann cautions against the application of either the Ammonium Acetate or Barium Chloride methods to calcareous clays, because of the tendency for the exchanging solution to partially dissolve the minerals contained therein [17]. As a solution, Dohrmann [18] proposes pre-saturating the exchange solution with the confounding mineral of interest, e.g. calcite, to minimize unwanted dissolution of that salt. However, this technique can compensate for only a single mineral phase, whereas Fort McMurray soils are believed to include calcite, gypsum and magnesium salts.

Lithium Chloride extractions may offer a suitable alternative for characterizing exchangeable cations within STP soils. Lithium Chloride offers the advantage, over extracting agents like ammonium acetate, of preserving the initial soil pH and its findings have been found to correlate well with both Calcium Chloride and Barium Chloride methods [19]. However, the likelihood that this high strength ionic solution too will dissolve the calcium and magnesium salts is unclear. In addition, the method characterizes only exchangeable cations and not CEC. Initial experiments have been conducted using this alternate extraction agent with STP soils and early results appear promising (Table 5): notably, the sum of exchangeable cations does not exceed the overall cation exchange capacity, and using the CSF model [17], similar, though not identical concentrations of exchangeable cations were achieved at different soil to solution ratios. (Limited sulphate salt dissolution did occur, but did not significantly impact the results).

A simple PHREEQC [13] simulation was run to check whether or not the LiCl experimental results were plausible. The simulation equilibrated groundwater chemistry with the number of exchange sites predicted by CEC

experiments, in order to characterize the assemblage of bound cations. For comparison, LiCl experimental data were expressed in terms of equivalent fractions,

$$\beta_I = \text{meq}_{I-X_i} / \text{sum}(\text{meq}_{I-X_i})$$

with I as the exchangeable cations possessing charges i [20]. The results of the comparison are quite similar (Table 6), both granting credibility to this experimental method, and suggesting that it is not largely influenced by salt dissolution.

Batch Sorption

In descending geological order, the linear sorption partitioning coefficients for sodium range from about 0.45 in the till, to 0.15 in the interface region and 0.19 deep in the Wood Creek Sand Channel. This suggests that significant sodium attenuation may be possible in the till. However, if, as suspected, the Wood Creek Sand Channel acts as a preferential pathway for seepage from the STP, most incoming ions in full strength process-water seepage, where sodium concentrations near 600mg/L, will remain in solution, and unchecked, may represent a threat for release into neighbouring aquatic environments.

Linear sorption does not explain the behaviour of most ions in the soil-water systems; however, important clues to their behaviour can be inferred from simple plots of the equilibrium solution response versus input PA strength (Figure 2). Plots across all batch samples revealed strikingly similar behaviour between the trends of sulphate, the more abundant calcium, and also to a lesser extent, magnesium. Plots further show that all 3 species are released and that their concentrations remain relatively constant despite the interaction with increasingly concentrated PA water. Together, these behaviours suggest the dissolution of pre-

existing salts within the soil: calcium, and to a lesser extent, magnesium sulphates. Saturation indices of equilibrium solutions support this interpretation as gypsum was undersaturated at all PA strengths. Finally, the minor increases in the amount of calcium and sulphate released with PA strength that were observed could reflect a greater extent of salt dissolution at higher ionic strength.

The plotted alkalinity trends, corroborated by the saturation indices of calcite in the equilibrated solutions, suggest that except at low PA strengths, alkalinity is lost from the system – believed to be by the precipitation of carbonates. (At low strengths, for example in the Deionized case, both the plots and the saturation indices instead suggest alkalinity release – likely the dissolution of pre-existing carbonate salts).

A proper understanding of the divalent cations' behaviour is not immediately obvious from the graphs. Comparing ion trends with increasing PA strength, calcium behaviour, mild release, is opposite to the strong sorption of sodium, and the amount of calcium and magnesium released is greater than can be attributed to sulphate salts alone – both, as ion exchange would require. Confusion arises though, as the trends suggest calcium release, while saturation indices instead propose calcite precipitation. However, if the divalent ions' responses are combined, subtracting out the quantity believed released by sulphate salt dissolution, and using precipitated carbonate (alkalinity) to estimate additional calcium and magnesium that may have been exchanged, then precipitated, the resultant curve (Ca+Mg-SO₄+Alk) is almost identical to the sodium response. Therefore, it is hypothesized that calcium and magnesium are released into solution both by dissolution of pre-existing sulphate salts and by sodium-induced desorption, followed by limited precipitation as a carbonate mineral phase.

Overall, the results of the newly proposed cube batch sorption experiments were very similar to those of the traditional set-up featuring highly disturbed ground soil samples. The magnitude of ion concentrations in the equilibrium solutions was noticeably smaller for cube samples; however, this did not impact the analysis in any apparent manner. For example, the calculated sodium partitioning coefficients, the shape and magnitude of ammonium, sodium and lithium linear isotherms, and the shape and magnitude of batch sorption ion trends versus PA strength were all essentially the same across both methods. Thus the new method may offer a viable alternative to standard batch experiments and a conceptual improvement in simulating sorption behaviour within unperturbed geologic settings.

CONCLUSION

It is hypothesized that with the arrival of incoming PA water, sulphate concentrations will increase due to salt dissolution, while soluble sodium will exchange with bound calcium and magnesium, with the released divalent cations subsequently co-precipitating as a solid solution carbonate mineral phase.

ACKNOWLEDGEMENTS

We wish to thank Suncor Energy Inc. for permission to publish this work.

REFERENCES

Alberta Chamber of Resources. (2004). *Oil sands technology roadmap: unlocking the potential*. p.3. Retrieved August 4, 2009, from http://www.acr-alberta.com/Portals/0/projects/OSTR_report.pdf

Extraction Technical Projects Group, *Understanding process water - workshop*, CONRAD Connections.

Hall, T., Mugo, R., Digel, M., Gibson, C., Gulley, J.R. (2004). *Water quality modelling report for the Suncor south tailings pond project*. Golder Associates Ltd.: Calgary. p.23-24.

Langmuir, D. (1997). Adsorption-Desorption Reactions. In R. McConnin (Ed.), *Aqueous Environmental Geochemistry*, (pp.343-402). New Jersey: Prentice-Hall, Inc.

Klohn Crippen Consultants Ltd (2004). *Millennium mine, design of the South Tailings Pond*. prepared for Suncor Energy Inc.

Cathcart, J., Cannon, K., Heinz, J. (2008). Selection and establishment of Alberta agricultural soil quality benchmark sites. *Can. J. Soil Sci.*, 88, 399-408.

Fonstad, T.A. (2004). *Transport and fate of nitrogen from earthen manure storage effluent seepage*, in *Department of Civil and Geological Engineering*. (Doctoral dissertation, University of Saskatchewan, 2004) p. 271.

Deutsch, W.J. (1997). *Groundwater Geochemistry: Fundamentals and Applications to Contamination*, (p50). CRC Press LLC, Boca Raton, FL.

Janzen, H.H. (1993). Soluble Salts. In M.R. Carter (ed), *Soil Sampling and Methods of Analysis*, (pp161-166). Can. Soc. Soil Sci., Lewis Publ., Ann Arbor, MI.

Sheldrick, B.H. (ed). (1984). Method 84-005 - 1N Ammonium Acetate Extractable Ca, Mg and K. *Analytical Methods Manual 1984*. Retrieved from <http://sis2.agr.gc.ca/cansis/publications/manuals/analytical.html>

United States Environmental Protection Agency (USEPA) (1986). Method 9081 Cation-Exchange Capacity of Soils (Sodium Acetate). Retrieved from <http://www.epa.gov/solidwaste/hazard/testmethods/sw846/pdfs/9081.pdf>

ASTM Standard D4646, 2003. Standard Test Method for 24-h Batch-Type Measurement of Contaminant Sorption by Soils and Sediments, ASTM International, West Conshohocken, PA.

Parkhurst, D.L., Appelo, C.A.J. (1999). User's guide to PHREEQC (version 2)--A computer program for speciation, batch-reaction, one-dimensional transport, and inverse geochemical calculations: U.S. Geological Survey Water-Resources Investigations Report 99-4259, p312.

Peng, J., Headley, J.V., Barbour, S.L. (2002). Adsorption of single-ring model naphthenic acids on soils. *Can. Geotech. J.*, 39, 1419-1426.

Whalen, J.K., Chang, C., Clayton, G.W., Carefoot, J.P. (2000). Cattle Manure

Amendments Can Increase the pH of Acid Soils. *Soil Sci. Soc. Am. J.*, 64, 962-966.

Simard R.R. (1993). Ammonium Acetate-Extractable Elements, In M.R. Carter (ed), *Soil Sampling and Methods of Analysis*, (pp39-42). Can. Soc. Soil Sci., Lewis Publ., Ann Arbor, MI.

Dohrmann, R. (2006). Cation exchange capacity methodology I: An efficient model for the detection of incorrect cation exchange capacity and exchangeable cation results. *Appl. Clay Sci.*, 34, 31-37.

Dohrmann, R. (2006). Cation exchange capacity methodology III: Correct exchangeable calcium determination of calcareous clays using a new silver-thiourea method. *Appl. Clay Sci.*, 34, 47-57.

19. Husz, G. (2001). Lithium chloride solution as an extraction agent for soils. *J. Plant Nutr. Soil Sci.*, 164, 71-75.

Appelo, C.A.J., Postma, D. (2005). Ion Exchange. *Geochemistry, groundwater and pollution, 2nd Edition* (pp.241-309). The Netherlands:A.A. Balkema Publishers.

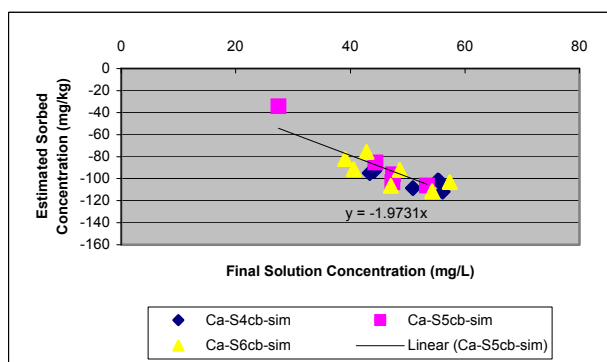
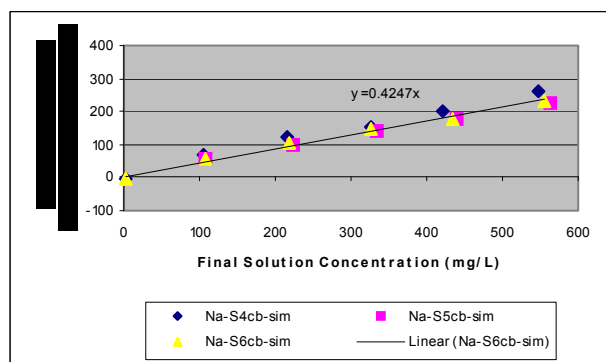


Figure 1. Applying linear sorption isotherms to experimental data for MW3-4 (upper clay till) batch cube samples (15g undried soil mixed with 30g simulated PA water) (sodium – left, calcium - right).

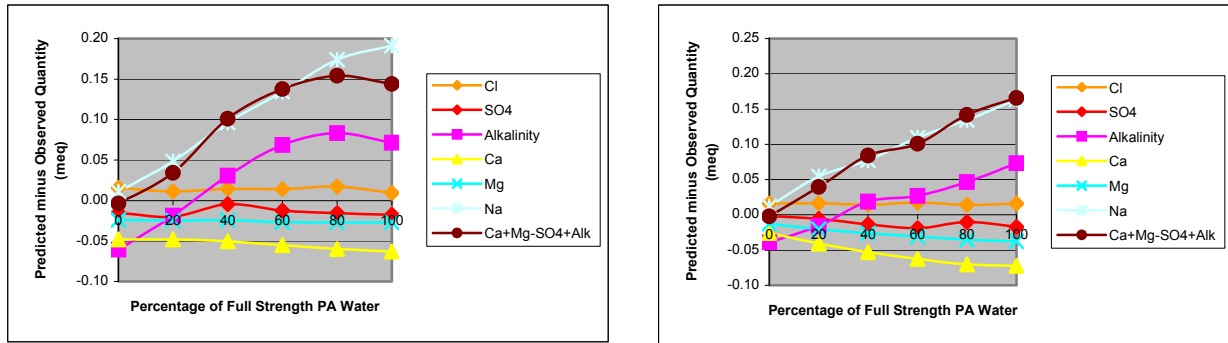


Figure 2. Example trends of equilibrium ion concentrations with PA strength (MW3-9 (lower clay till) soils: 30g of simulated PA water mixed with 15g of undried, ground soil, sample #1 in triplicate series (left); 30g of real PA water mixed with 15g undried soil cube, sample #1 in triplicate series (right)).

Table 1. Physical Properties of the Tested Soils

Experiment Assigned ID	Soil Core Sampling Location	Gravimetric Water Content	% FOC by weight	Description from Borehole Logs
MW3-4	Monitoring well 3B, 3.4 to 4.6 mbgs	0.142	1.530+0.057	Clay (till), silty, sandy, low-medium plastic, brown, moist
MW3-6	Monitoring well 3B, 6.1 to 6.4 mbgs	0.121	3.690+0.028	See above
MW3-9	Monitoring well 3B, 8.2 to 9.1 mbgs	0.124	0.986+0.018 ^A	See above
M4-13	Monitoring well 4B, 12.2 to 13.7 mbgs	0.056	0.978+0.028 ^B	Transition zone, clay till to sand (silty)
M2-38	Monitoring well 2A, 37.7 mbgs	0.169	not tested	Sand, dark grey, fine-grained, very silty, wet, some fine gravel, trace coarse gravel, occasional pebble sub-angular, occasional CL clay lens 4-6" thick with high amount of gravel (till-like)
M2-39	Monitoring well 2A, 38.7 mbgs	0.103	not tested	Sand/gravel, dark grey, fine to medium-grained, clean, gravel medium to coarse-grained, occasional small cobble

^A Tested sample came from a marginally lower elevation of 9.1 to 9.8mbgs

^B Tested sample came from a marginally higher elevation of 11.0 to 12.2mbgs

Table 2. Average Chemical Composition of Full Strength Process-Affected Waters used in Batch Sorption Experiments

Cation Species	Simulated PA water (mg/L)	Real PA water (mg/L)	Anion Species	Simulated PA water (mg/L)	Real PA water (mg/L)
Calcium	16.07	7.62	Chloride	398.00	374.51
Magnesium	12.14	4.17	Fluoride	0.01	2.21
Potassium	12.59	10.05	Bromide	none	0.93
Sodium	720.62	591.35	Nitrite	none	nd
Ammonium	0.47	2.02	Nitrate	none	4.65
Lithium	none	0.16	Phosphate	none	nd
pH	8.3	8.6	Sulphate	228.03	150.39
			Alkalinity (as CaCO ₃)	709	491

nd = not detected

Table 3. Results from the CEC and Exchangeable Cation Experiments

Sample ID	Region	CEC (meq/100g)	Exchangeable Cations (meq/100g)			
			K	Ca	Mg	Na
MW3-4	upper till	11.32	0.04	19.48	1.48	0.06
MW3-6	middle till	4.02	nd	17.07	1.09	0.14
MW3-9	lower till	15.50	nd	22.24	3.51	0.20
MW4-13	till/sand transition zone	3.51	nd	16.48	1.17	0.07
MW2-38	deep sand channel	6.50	nd	13.68	1.37	0.32
MW2-39	deep sand channel	5.59	0.07	16.82	1.97	0.32

nd = not detected

Table 4. Linear Sorption Model Partitioning Coefficients (Kd) for Sodium (units: mg/kg / mg/L)

Sample ID	Geology	Solution = Real PA Batch Experiment Type = Ground	Solution = Simulated PA Batch Experiment Type = Ground	Solution = Real PA Batch Experiment Type = Cube	Solution = Simulated PA Batch Experiment Type = Cube
MW3-4	upper clay till	0.51±0.01	0.57±0.08	0.46±0.03	0.44±0.04
MW3-6	mid clay till	0.26±0.06	0.15±0.04	0.25±0.03	(a)
MW3-9	lower clay till	0.58±0.07	0.60±0.03	0.63±0.01	0.73±0.01
MW4-13	clay/sand interface	0.12±0.01	0.17±0.07	0.16 (b)	0.17±0.15
MW2-38	deep sand channel	0.22±0.01(d)	0.27±0.02 (d)	(c)	(c)
MW2-39	deep sand channel	not measured	0.14±0.04 (d)	(c)	(c)

(a) data was non-linear (b) only one sample so no standard deviation possible (c) soil too cohesionless for cube batch tests (d) isotherm possesses non-zero intercepts

Table 5. Results from Preliminary Extractions using Lithium Chloride

Sample ID	Method Used	CEC (meq/100g)	Exchangeable Cations (meq/100g)			
			K	Ca	Mg	Na
MW3-4	NH ₄ OAc	11.32	0.04	19.48	1.48	0.06
	LiCl		0.12	5.81	1.14	nd
MW3-6	NH ₄ OAc	4.02	nd	17.07	1.09	0.14
	LiCl		0.08	2.32	0.62	0.001

nd = not detected

Table 6. PHREEQC-Modeled [13] and LiCl Experimental Exchange Fractions for MW3-6 Soil

Bound Species	PHREEQC-predicted Exchange Fraction	LiCl-predicted Exchange Fraction
CaX ₂	0.745	0.788
MgX ₂	0.238	0.211
NaX	0.12	0.0003

FATE AND TRANSPORT OF PROCESS-AFFECTED WATER IN OUT-OF-PIT TAILINGS PONDS IN THE OIL SANDS INDUSTRY IN CANADA

Holden, A.A., Perez, L., Martin, J.W., Mendoza, C., Segó, D.C. & Ulrich, A.C.
University of Alberta, Edmonton, AB, Canada

Tompkins, T. & Barker, J.F.
University of Waterloo, Waterloo, ON, Canada

Haque, S. & Mayer, K.U.
University of British Columbia, Vancouver, BC, Canada

Sutherland, H. & Bowron, M.,
Suncor Oil Sands, Fort McMurray, AB, Canada

Biggar, K.W.,
BGC Engineering, Edmonton, AB, Canada

Donahue, R.B.,
Applied Geochemical Engineering Solutions Inc., Edmonton, AB, Canada

ABSTRACT: In Northern Alberta, an increasing trend will be the placement of out-of-pit tailings ponds atop natural buried sand channels, relicts from previous glacial rivers. The sand channels, if unchecked, have the capacity to act as potential flow paths for process-affected (PA) water, facilitating discharge into the environment. Preliminary flow and transport modeling of such a site suggests that PA seepage will occur into the underlying sand channel, but the development and extent of this impact is not known. Suncor Energy Inc.'s South Tailings Pond (STP), with approximately 8km of its dyke atop the Wood Creek Sand Channel, represents the first such facility, and offers the opportunity to develop better understanding and management techniques for what is to shortly become an industry-wide challenge. In 2006, a 5 year research initiative began between the Universities of Alberta, Waterloo, and British Columbia and Suncor Energy Inc., with the principle objectives being 1) to understand the fate and transport of PA water through native sediments; and 2) to explore different remediation strategies for groundwater, ranging from monitored natural attenuation to in situ chemical oxidation. This paper describes the design and construction of key field research facilities supporting the research initiatives of this project.

INTRODUCTION

Due to operational necessities in the oil sands industry, out-of-pit tailings ponds are constructed to store tailings and PA water before their ultimate placement within the excavated open-mine pits. Containment within these impoundments, and the protection of the surrounding sediments, surface water and groundwater are critical design issues, with current legislation requiring that oil sands tailings operations operate under a policy of zero water discharge to the environment [1].

In Northern Alberta, the South Tailings Pond is the first of several [2], to be placed atop buried glaciofluvial outwash channels. These channels, if unchecked, have the capacity to act as potential flow paths for PA water, facilitating the release of tailings pond seepage into adjacent surface or ground waters. Preliminary flow and transport modeling of these sites suggests that PA seepage will infiltrate into the underlying sand channel [3]. However, the development and extent of this impact is not known and is complicated by many factors including local geology, dyke construction, pond fluids and filling history [4].

Suncor Energy Inc.'s (Fort McMurray, AB) STP, with approximately 8km of its dyke situated atop the Wood Creek Sand Channel, offers the first opportunity to study such a facility from its inception and thereby provides a unique research and knowledge transfer opportunity for the entire Athabasca oil sands industry.

In 2006, a 5 year research initiative was established between the Universities of Alberta, Waterloo, and British Columbia and Suncor Energy Inc., with the principle objectives being 1) to understand the fate and transport of PA water through native sediments (including hydrogeologic

behaviour and biologically and geochemically-mediated transformations); and 2) to explore different remediation strategies for groundwater, ranging from monitored natural attenuation to in situ chemical oxidation.

This paper introduces the key field instrumentation supporting this project, namely, a groundwater monitoring network to track the progress and evolution of PA water in the subsurface, an Infiltration Pond to permit study of infiltration rates and geochemical and biological reactions induced by PA seepage beneath a small-scale constructed impoundment, and the In Situ Aquifer Test Facility, enabling first a field evaluation, using controlled input of PA water, of natural attenuation in the sand channel aquifer, and later, an evaluation of the viability of in situ chemical oxidation to destroy toxic organic compounds contained in the PA water once they have migrated into the sand channel.

SOUTH TAILINGS POND SITE DETAILS [4,5]

The STP (Figure 1) covers an area of approximately 2300 ha with an approved, current tailings holding capacity of 230Mm³, but with application under review to increase the dyke elevation to allow for an ultimate tailings holding capacity of 350Mm³. The STP is to be used for storage of water and fine tailings, and initial deposition began June 29, 2006. The footprint of the STP is irregularly-shaped and runs approximately 5 km East to West and 4km North to South. The height of the overburden starter dyke was approximately 14m, and the maximum tailings dyke height will be approximately 42m. Three continuous retaining dykes make up the North, West and South portions of the STP. Containment to the East is provided by naturally elevated ground. Approximately

8 km of the South and West Dyke walls, and 50% of the STP footprint, overlies the Wood Creek Sand Channel, a buried, permeable, glaciofluvial channel.

GEOLOGY/HYDROGEOLOGY [4,5]

Hydrogeological conditions have been characterized through a combination of field mapping, air photo interpretation, drilling logs and surface geophysics [4].

In descending order, the geology at the STP consists of Holocene organic soil, Pleistocene glacial till, Pleistocene glacial outwash channels (in some areas only), and the Cretaceous Clearwater, Cretaceous McMurray, and Devonian Waterways bedrock formations. The Holocene organic soils are typically 1-2m deep, and are muskeg-based, featuring silts, peat, organic soil with roots and wood pieces, and trace clays.

The Pleistocene glacial till is approximately 8-15m deep (when atop the Wood Creek Sand Channel), and may include each of clayey tills, sandy tills, silty tills, and Clearwater rafted, ice-thrusted or derived tills. Deposition is generally uniform, although thin (<5m) or altogether absent coverage has been observed at several locations across the site [4]. Upper regions can be sandy with a progressively higher clay fraction found with depth.

Discontinuous lenses, approximately 2 m deep, of Pleistocene glaciolacustrine soils (silts, clays, fine sands) are occasionally present atop the glacial till layer.

The Wood Creek Sand Channel is a Pleistocene glaciofluvial feature that is approximately 20-30m deep and consists of dense sands and gravels. In the area of the STP, the Wood Creek Sand Channel is

broadly oriented from SE to NW, although it is joined near the middle of the West Dyke by a secondary branch aligned SW to NE (Figure 1). These branches are approximately 1000m wide. A third segment of the Channel underlies the body of the STP; however, initial data suggests it is not a major flow channel and was perhaps an overbank or flood feature [4]. Further characterization of the Wood Creek Sand Channel morphology and orientation towards the SE is ongoing [5]. With depth, the Channel stratigraphy typically changes from silty sand to clean sand to coarse sands and gravels. The Wood Creek Sand Channel principally rests atop the Clearwater clay shales although in some areas it rests directly atop the McMurray Formation.

The remaining formations include the Clearwater Formation, of marine origin, which is principally composed of clay shales and thin, carbonate-cemented siltstone beds. The McMurray Formation includes oil sands, water sands and clays and exists between 32m and 98m at depth below ground surface. The Devonian Waterways Formation consists of calcareous rocks. Approximately 300m thick, it begins between 82m and 175m at depth below ground surface.

The eastern/southeastern edge of the STP is bounded by a deposit initially classified as a kame during surficial mapping, that topographically rises towards the East. More recent investigations reveal the unit to be a fluvial feature that is fine-grained along the exterior and coarse-grained at its centre [5]. Although the SE portion of the WCSC may be in hydraulic contact with the edge and base of this feature, the “kame” is extensively layered, with bulk permeability similar to that of glacial till, limiting vertical recharge into the Wood Creek Sand Channel and the unit’s involvement in local and regional groundwater flows [4].

The principle flow feature in the vicinity of the STP is the SE to NW branch of the Wood Creek Sand Channel. This channel also maintains groundwater conditions in the connecting Wood Creek Sand Channel offshoots. Groundwater flow in the main channel is from SE to NW, at an estimated rate of between 6L/s to 60L/s. Conversely, in the SW branch of the Wood Creek Sand Channel, which is narrower and less permeable, groundwater flows towards the southwest at an estimated rate of 1L/s to 10L/s [4]. Groundwater flow in the same is from East to West [5]. Slug tests have reported a median hydraulic conductivity of 0.021m/d in the glacial till, 2.0m/d in the same and 56m/d (or 36m/d by pumping tests) in the Wood Creek Sand Channel [5]. A “spill-point” of the Wood Creek Sand Channel into the McLean Creek, a tributary to the Athabasca river, exists beyond the NW corner of the STP dyke. Prior to dyke construction, the Wood Creek Sand Channel was predominantly confined, except for the NW (where it encounters the McLean Creek) and SE sections of the main channel [4].

ENVIRONMENTAL CONTROLS

A key design criterion identified by Suncor in the establishment of the STP has been to ensure the protection of the nearby McLean Creek and the surrounding, off-lease groundwater resources against contamination by PA seepage. Suncor has identified three potential locations for seepage discharge into the environment – from the NW branch of the Wood Creek Sand Channel into the McLean Creek, or along either SW or SE extensions of the Wood Creek Sand Channel and thereafter entering the regional groundwater system. Discharge along these potential exits is mitigated by the following controls: an interception pumping well field to the NW (groundwater is pumped into the STP), a cutoff wall to the SW, where hydraulic

gradients are minimal, and once required, a proposed pumping well system to the SE (under investigation) (Figure 1) [5]. This closed-loop containment of contaminated waters on-site, permits aquifer injection experiments critical to this research project.

INSTRUMENTATION

There are three principle instrumented field research facilities at the STP site: a groundwater monitoring network, a field-scale infiltration pond, and a system of injection/sampling wells in the Wood Creek Sand Channel – the In Situ Aquifer Test Facility.

GROUNDWATER MONITORING NETWORK

In the Spring of 2006, critical groundwater monitoring infrastructure was installed to permit tracking of the migration and evolution of PA seepage over time. This research transect was established in the northwestern portion of the STP dyke (Figure 1), downstream of the STP according to local and regional groundwater flow patterns. Here, the sand channel underlies the dyke, thus permitting early detection of PA release in the geology of interest. Furthermore, its boundaries had been precisely defined by previous electrical resistivity tomography mapping [6].

The groundwater monitoring transect consists of 4 nests of multilevel groundwater monitoring points that span the width of the sand channel, underlying the West wall of the STP dyke. Nests are instrumented at a series of elevations, vertically spanning the top of the glacial till through to the base of the underlying Wood Creek Sand Channel (Figure 2). Nests 1 and 2 were installed west of, and in the middle of the starter dyke

respectively while Nests 3 and 4 are positioned east of the starter dyke, within the STP itself.

Monitoring Well Installation Details

Nests 1 and 2 were instrumented with seven monitoring wells each, to permit the quarterly collection, and geochemical analysis¹, of groundwater samples from several elevations across the subsurface. Boreholes were drilled using a 0.11m casing on a 1503 Nodwell SONIC Drill Rig. Each monitoring well was constructed from 50mm nominal I.D. Schedule 80 PVC solid pipe, with a 1.5 m well screen consisting of 0.5mm slotted well casing (except for the deepest sand channel wells, 1A and 2A, which had 3m well screens). Sand (10/20 Frac) was used as a filter pack, extending beyond the well screen by at least 0.3m in either direction. Bentonite chips were used to grout the remaining void space up to ground surface.

After construction, monitoring wells were developed using a Well Wizard compressed air development pump in order to flush out suspended soil in the well and filter pack, introduced during drilling operations. This ensures a properly graded filter pack that adequately filters out subsequent suspended solids and retains its hydraulic conductivity to allow for inflow and high quality water samples.

Monitoring wells (MWs) were installed from the base (MW 1A, 2A) through to the top of the saturated portion of the Wood Creek Sand Channel (MW 1E, 2E), in the lower clay till (MW 1F, 2F), and in the upper clay till (1G, 2G) (Figure 2).

¹ All water samples are analyzed for pH, Electrical Conductivity, temperature, alkalinity, iron and sulfide content, BTEX and F1 hydrocarbons, Dissolved Oxygen, major cations and anions and trace metals

Monitoring well 1C was damaged during construction (punctured and filled with bentonite) and unsuccessfully replaced by well 1H. Wells 1D and 1E were incorrectly installed at the same elevation. Monitoring wells 1C and 1D were ultimately replaced as wells 1J, 1I in April 2007. With the onset of the pumping by well fields in the northwest to contain potentially impacted waters on-site, the water table was drawn down, desaturating the upper layer of the Wood Creek Sand Channel and hence wells 1E and 2E. Monitoring wells 1C, 1D, 1E and 2E were therefore filled with argon gas and capped on June 2006, to prevent exposure of anaerobic regions to oxygen and unwanted geochemical reactions that could impact the ongoing research program.

Level Logger Installation Details

Nests 3 and 4, located within the STP, were each instrumented with four grouted LTC (level, temperature, conductivity) data loggers (Solinst 3001), in Spring 2006, to permit real-time monitoring of contaminant migration. Monitoring wells were not initially constructed here, given the likelihood of their being damaged during dyke construction. Once dyke construction in the vicinity is complete, a series of monitoring wells, similar to those present in Nests 1 and 2, will be installed on the ultimate downstream face of the dyke, at Nests 3 and 4 (Fall 2009) (Figure 2).

LTC data loggers were installed in the upper and lower regions of both the clay till, and the saturated portion of the Wood Creek Sand Channel. Two boreholes were drilled in Nest 3 from April 11 to 12, 2006 and two in Nest 4 from May 2 to 3, 2006, using a 0.11m casing on a 1503 Nodwell SONIC Drill Rig. Two level loggers were then installed within each borehole. Sand (1.2m, Frac 10/20) was deposited around each logger to act as a filter pack/well screen and bentonite chips were

used to fill void spaces both between paired logger installations and up to the ground surface. Loggers were field-calibrated and programmed for hourly measurements.

Installation difficulties ultimately necessitated an alternate LTC data logger implementation. Coaxial cable from the loggers consistently became tangled during installation, leading field staff to inappropriately attempt to splice the cables. Unsuccessful splicing resulted in malfunctions and data gaps for several units, until all were deemed non-operational by 2008. In order to recapture the ability to monitor groundwater conditions in real-time, 4 replacement LTC loggers (Schlumberger Water Services CTD-Diver) were installed within monitoring wells 1B, 2A, 2B, 2G (Nests 3 and 4 were inaccessible because of dyke construction). Probes were situated at the approximate centre of wellscreens. Probes are connected to the surface using Diver Data Cables so that they may be read or programmed without being retrieved. A barometric data logger (Schlumberger Water Services Baro Mini-Diver) was installed in well 1B so that air pressure conditions may be compensated for within the LTC logger-recorded groundwater measurements [7].

Soil Samples

Soil samples were collected during the drilling of boreholes in Nests 1 to 4, in preparation for a laboratory program to study the geochemical and biological interactions of PA water with the clay and sand soils beneath the tailings pond. Jarred soil samples were collected from boreholes 1A, 2A, 3A and 4A at approximately 1m depth intervals. Soil core samples were collected from boreholes 1B and 2B in 1.5m (5 foot) lengths at the same depth interval as the monitoring wells screens for all monitoring wells, and also from 3B and 4B in 1.5m (5 foot) lengths at the same depth interval as the initially installed LTC loggers. Soil cores were

collected using drilling rig-mounted Lexan liners and capped at the surface to maintain the redox conditions, then shipped to the University of Alberta Cold Regions Geoenvironmental Research Facility for storage at -20°C.

INFILTRATION POND

A second key component of the field research infrastructure is a field-scale analogue of the STP - the Infiltration Pond. Excavation began late March 2008 with final pond filling completed by late August 2008. (Double ring infiltrometer experiments were conducted on the exposed floor between initial excavation and pond filling). The pond was sited just outside the SE portion of the STP dyke, adjacent to another research facility, the In Situ Aquifer Test Facility (Figure 1). This location was selected for a) its proximity to nearby roadways and hence ease of access for construction machinery and vehicles, b) possessing a known deposit of competent clay till of sufficient depth for completion of the pond, and c) its proximity to the In Situ Aquifer Test Facility (<50m) - to act as a potential source of injectable water for that facility. The Infiltration Pond permits field-scale examination of the rate of infiltration of PA water into the clay till, the biochemical and geochemical evolution of infiltrating PA water over time and depth, and also provides a source of authentic PA water for the Wood Creek Sand Channel aquifer tests.

Construction Details

The Infiltration Pond is 10m x 10m at its base, and was excavated approximately 1.3 m deep into competent clay till. Sidewalls rise at a slope of 1:1, and crest with a berm approximately one third of a meter above the original grade (Figure 3). In descending order, the site-specific shallow geology

consists of surficial roots and vegetation, 0.5m of muskeg, 0.5m of dirty sand, and approximately 12m of silty clay (CL classification) before the Wood Creek Sand Channel is encountered. During excavation, the surficial vegetation, muskeg and sand layers were stripped and removed and the pond floor excised to a depth of 1.3m into the clay till, or a total of 2.3m below ground surface. The 1.3m deep pond was placed below the base of the lowest surficial sand layer, in order to prevent lateral leakage of PA water through a highly conductive stratum into the surroundings. Excavated clayey material was deposited around the perimeter of the excavation and compacted with the backhoe to a) replace the removed organic and sand layers (restoring the initial ground level) b) line the sidewalls with a low permeable material to contain pond contents and c) establish a berm 0.2-0.3m above initial grade.

Thirty 10cm (4-inch) diameter, 1.8m (6 foot), slotted casing pipes were evenly placed across the base of the pond to facilitate collection of future soil cores for lab analysis. The PVC casings (Rice Engineering) were arranged in a 6 by 5 grid pattern. Pipes were recessed only deep enough to fix the screens in place to a maximum of 0.15 m depth, then covered with geotextile filter socks (Nilex Nonwoven 4545). Tailings sand was deposited about the pipes and compacted to set the casings in place. A water truck was later used to flood the site with the PA water so that approximately 0.2 m of free-standing water lay atop the saturated sand. In the summer of 2009, an LTC data logger (CTD-Diver) was placed within a perimeter casing to monitor changes in pond elevation and chemistry. Casings were not capped to exclude rain, snow, or evaporation effects, in order to keep conditions as similar to the real STP as possible.

The selected design allows casings to fill with pond water, while preventing the influx of tailings sand. This simplifies the collection of water samples from the pond floor, from just above the point of infiltration and also facilitates subsequent core sampling by preventing tailings sand sloughing during drilling.

Soil Samples

Initial samples for characterizing background soil conditions were collected by continuous sampling of the clay till to a depth of 12 m below ground surface, at 4 separate locations (each corner of the pond). To preserve the subsurface redox conditions, moisture content and undisturbed state of the soil, samples were retrieved via direct push drilling with acrylic liners, which were promptly capped, taped and labelled before being placed in an ice-filled cooler. Samples were temporarily stored in on-site freezers then transferred to the University of Alberta for storage at -20°C in the Cold Regions Geoenvironmental Research Facility.

Boreholes were grouted using a weak cement grout in preference of other, more traditional materials. Bentonite was discounted since it would present an active geochemical surface that would confound studies investigating the geochemical behavior beneath the pond floor. Sand was similarly discounted, since it could potentially create a preferential flow conduit through the clay till both nullifying experiments examining infiltration rates in the clay till and potentially introducing PA water unnecessarily into the Wood Creek Sand Channel. Although cement, as an alkali material, will induce local pH changes or possibly pH “halos” this was nonetheless deemed the best alternative. At the surface, boreholes were covered with a few centimeters of clay till material.

Future samples to quantify both the progress of infiltration by isotope tracking and the microbially-mediated and geochemical impact of PA water ingress upon the clay till are planned for collection as follows – 9 per year, during 2009, 2010 and 2011. These cores, 5.1cm (2-inch) diameter and 0.6 m (2-feet) long, will be collected by direct-push methods using a gasoline-powered vibrating hammer (Pionjar Model 120 Hand held gas powered drill, modified with specially machined drive heads).

IN SITU AQUIFER TEST FACILITY

Construction Details

The In Situ Aquifer Test Facility was created as a predictive field-scale model for characterizing the interaction of PA water with a sandy aquifer in the Athabasca oil sands region. The In Situ Aquifer Test Facility is situated near the SE portion of the STP dyke, where the Wood Creek Sand Channel aquifer is unconfined and has a flow rate of ~5-10cm/d. The facility is comprised of a system of injection and monitoring wells, positioned within the Wood Creek Sand Channel. Two injection/monitoring wells were constructed in March-April 2007: one screened at 15.5-17.0 mbgs within yellowish-red sand (STP-07-158-SS), the other deeper within grey sand at 27.5-29.0 mbgs (STP-07-159-SS). This zonation, which may reflect differences in redox conditions, provides a means of monitoring the interaction of PA-injectate within two chemically distinct layers of the aquifer. Falling head permeameter results (not included) and observations made while logging lithology suggest that here the Wood Creek Sand Channel is a relatively homogeneous feature comprised of fine to medium sand with trace to little silt, interrupted by silt/clay seams and with an

increased occurrence of coarse sand and gravel with depth.

A nest of multilevel monitoring points was constructed in the estimated down-gradient direction from each injection well, in June 2008. These wells improve the researchers' ability to identify local groundwater flow direction and velocity and permit study of injectate-aquifer interactions over greater residence times. Nest STP-08-158A was installed 3.7m from STP-07-158-SS and STP-08-159A was positioned 8.6 m from STP-07-159-SS, at an approximate bearing of 200 degrees S/SW from the injection wells (Figure 4). Difficulty in precisely characterizing local groundwater patterns owing to a) negligible hydraulic gradients b) a limited number of nearby monitoring points and c) conflicting observations at a local versus regional scale, precluded more distal placement of these nests. Boreholes were drilled using a roto sonic rig, fitted with a 10cm (4-inch) O.D. bore barrel. The barrel was trailed by a 14cm (5.5-inch) casing; inserted to prevent borehole collapse during core barrel withdrawal.

Each nest was instrumented with three, 2.5cm (1-inch) diameter, Schedule 40 PVC wells. Wellscreens are 1.5m long and were hand-slotted using a hacksaw as prefabricated components were not available. Wellscreens were wrapped with filter fabric to prevent influx of sand. Wellscreens in each nest were separated by a vertical distance of 0.5m. To facilitate installation of each screen at the target depth, a section of 2.5cm (1-inch) Schedule 40 PVC riser was subtended to the wellscreen. A PVC cap was mounted between the base of the wellscreen and the riser top, to prevent the accumulation of water in this section beneath the screen. Because the risers correctly elevated each wellscreen relative to one another, all of the multilevel wells could be installed concurrently, atop the floor of the borehole. Sandpack was placed about the

screens in the shallow nest and the formation allowed to collapse to backfill the annular space during retrieval of the drilling rods. The top 1.25 m was backfilled with hydrated granular bentonite to seal the borehole. Nest STP08-159A was similarly installed, with a filterpack comprised of Target® filter sand placed from the base of the borehole to 1.25 m above the uppermost wellscreen (24.5 mbgs), and topped with hydrated bentonite pellets to 19.8 mbgs. The formation was allowed to collapse into the annular space near to the ground surface, with residual space also capped with hydrated bentonite pellets.

Additional multilevel monitoring may be installed at greater distances (and travel times) from the injection wells in the future – permitting injectate interactions with greater volumes of aquifer material and for prolonged residence times.

Injection Assembly

Aquifer injections are accomplished using a 1,041 litre (275 gallon) polyethylene tank tied into the injection wells via 5.1cm (2-inch) PVC piping, a flow valve and a garden hose (Figure 5). A platform was constructed to raise the base of the tank above the ground surface, ensuring complete drainage from the system into the well during injection. An earthen mound was formed using a bulldozer, and later leveled by hand (~0.75 m(tall) x 3 m x 3 m). A platform made of 4x4 lumber was seated atop the mound, so that when included with the tank's pre-existing base support, the piping exiting the tank is approximately 1.2 m above the ground surface.

Each injection well is instrumented with an inflatable packer, pump and data logger to aid in the aquifer injection experiments. The data logger (Schlumberger Water Services CTD-Diver) provides a means of continuously recording pre- and post-injectate

groundwater temperature, pH and electrical conductivity. The RST Instruments N-Packer is used to seal the wellscreen from the overlying stagnant water in the well, following an injection. A Grundfos Redi-flo 2 submersible pump is used to sample water during injection experiments. [Aquifer injections, on the other hand, are driven by the approximately 15 m difference in hydraulic head between the discharging tank and the water table]. The components were assembled in-house such that tubing and wiring pass through the packer (positioned just above the wellscreen) to the probe and pump (aligned within the wellscreen), thereby allowing for samples and measurements to be taken with the packer inflated and in place.

Similarly, each down-gradient multilevel well is equipped with a CTD-Diver to monitor water levels, temperature and conductivity.

All injected process water is recovered by pre-existing, down-gradient pumping well fields and discharged into the STP as part of Suncor's strategy to ensure no adverse, off-lease, environmental impact. [5]

Soil Samples

Continuous core samples were collected within the Wood Creek Sand Channel for subsequent laboratory testing, including grain size, hydraulic conductivity (falling head permeameter), fraction of organic content, calcite and dolomite content, ion exchangeable metals, trace element concentrations associated with five operationally defined fractions within the sediment (easily exchangeable, poorly crystalline iron oxides, well crystallized iron oxides, organic matter and sulfides, and residual primary minerals) [8,9], major cations, amorphous oxyhydroxides and microbial activity. Core sections were recovered in 0.76 m (2.5 foot) lengths, and following retrieval, immediately encased

within split PVC tubes. Tubes were capped and taped across their entire length to minimize exposure to the atmosphere. Samples were then frozen and transported to the University of Alberta for storage at -20°C.

OTHER AVAILABLE SUNCOR FACILITIES

Geotechnical engineering controls on the STP dyke, and facilities associated with environmental compliance or remaining from preliminary site surveys offer additional sources of information. Between August and November 2008 Suncor installed a system of pressure relief wells around the perimeter of the STP, as a geotechnical measure to reduce pore pressures in the Wood Creek Sand Channel at the toe of the dyke. Internal drains installed within the dyke itself, discharge water into a perimeter drainage ditch. Suncor has an extensive network of monitoring wells across the site, set both into the Wood Creek Sand Channel and the glacial till, which are regularly sampled over the course of the year. Samples are also collected regularly, and by request, directly from discharge lines feeding into the STP or under more equilibrated conditions – skimmed from the surface of the STP. Suncor has made both the use of these installations and their historical sampling records available to this project, offering researchers the means to further corroborate and extrapolate findings beyond the localized boundaries of the groundwater transect, Infiltration Pond and In Situ Aquifer Test Facility.

CONCLUSION

This research initiative will further understanding of the fate and transport of chemicals of concern through clay till and sand aquifers in the Athabasca oil sands region, promoting sound groundwater

management and remediation in the oil sands mining industry.

ACKNOWLEDGEMENTS

We wish to thank Suncor Energy Inc. for permission to publish this work and Klohn Crippen Consultants Ltd. for their advice and technical assistance.

REFERENCES

Extraction Technical Projects Group, *Understanding process water - workshop*, CONRAD Connections.

Morgenstern, (2005), Personal communication between Dr. N.R. Morgenstern and Drs. K.W. Biggar and C. Mendoza.

Hall, T. Mugo, R., Digel, M., Gibson, C., Gulley, J.R. (2004) *Water quality modelling report for the Suncor south tailings pond project*. Golder Associates Ltd.: Calgary. p. 23-24.

Klohn Crippen Consultants Ltd, (2004), *Millennium mine, design of the South Tailings Pond*, prepared for Suncor Energy Inc.

Stephens B., Langton C., Bowron, M. (2006), *Design of Tailings Dams on Large Pleistocene Channel Deposits A Case Study – Suncor’s South Tailings Pond*,

http://www.klohn.com/news/technicalpapers/%5CCDA_2006-Paper_No.074.pdf

Komex International Ltd., (2003), Communication to Mike Bowron, Suncor, Re: Millennium Mine Tailings Dyke Geophysical Investigation E00080801

Schlumberger Water Services
<http://www.swstechnology.com/pdfs/brochures/Diver-Series-Brochure-English.pdf>

Tessier, A., P.G.C. Campbell, and M. Bisson (1979), Sequential extraction procedure for the speciation of particular trace metals. *Anal. Chem.* 51: 844–851.

Herbert JR, R.B. (1997), Partitioning of heavy metals in podzol soils contaminated by mine drainage waters, Dalarna, Sweden. *Water Air Poll.* 96: 39-59.

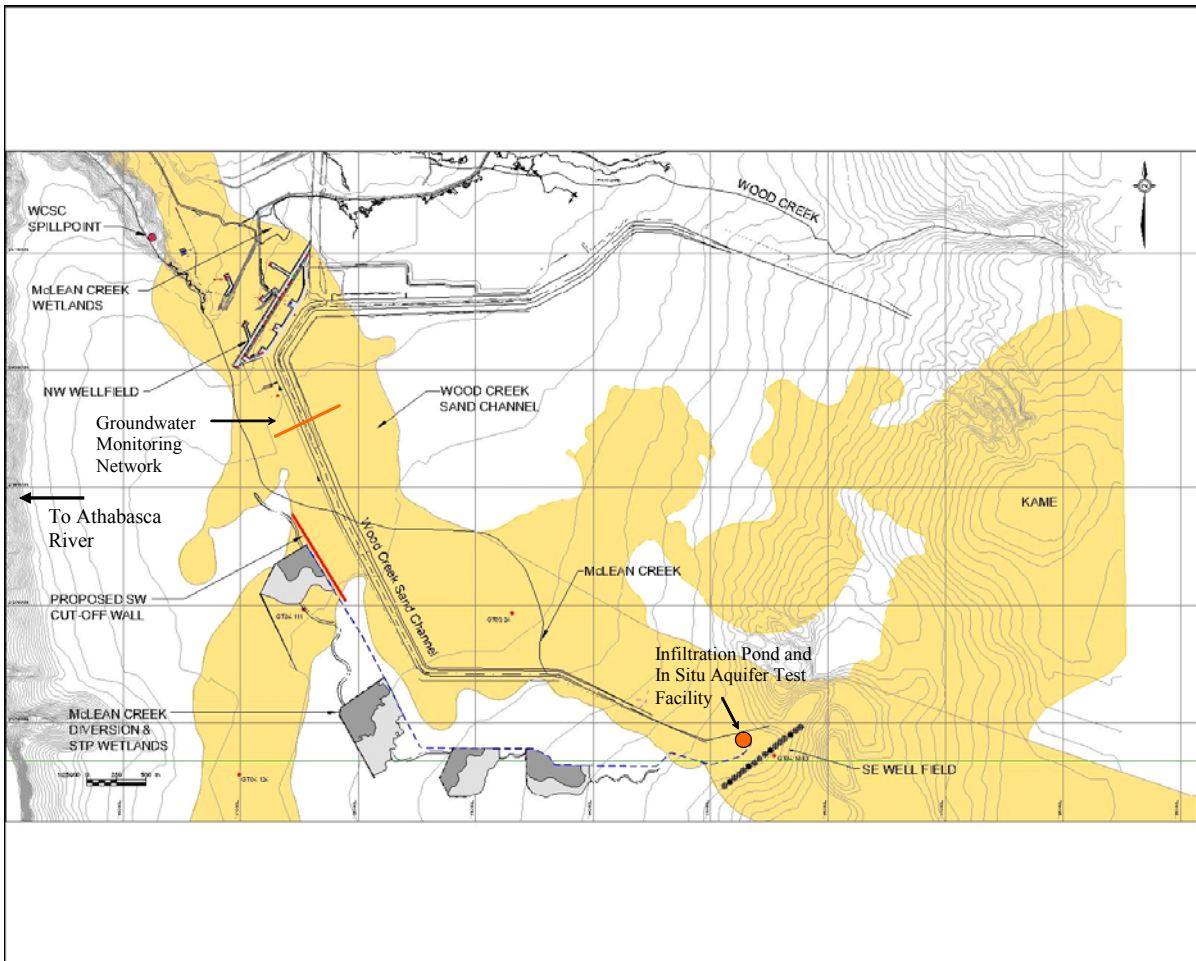


Figure 1. Schematic of the South Tailings Pond, showing the underlying Wood Creek Sand Channel (WCSC) and the approximate locations of the Infiltration Pond, Groundwater Monitoring Transect and In Situ Aquifer Test Facility. (Reprinted and modified from [5])

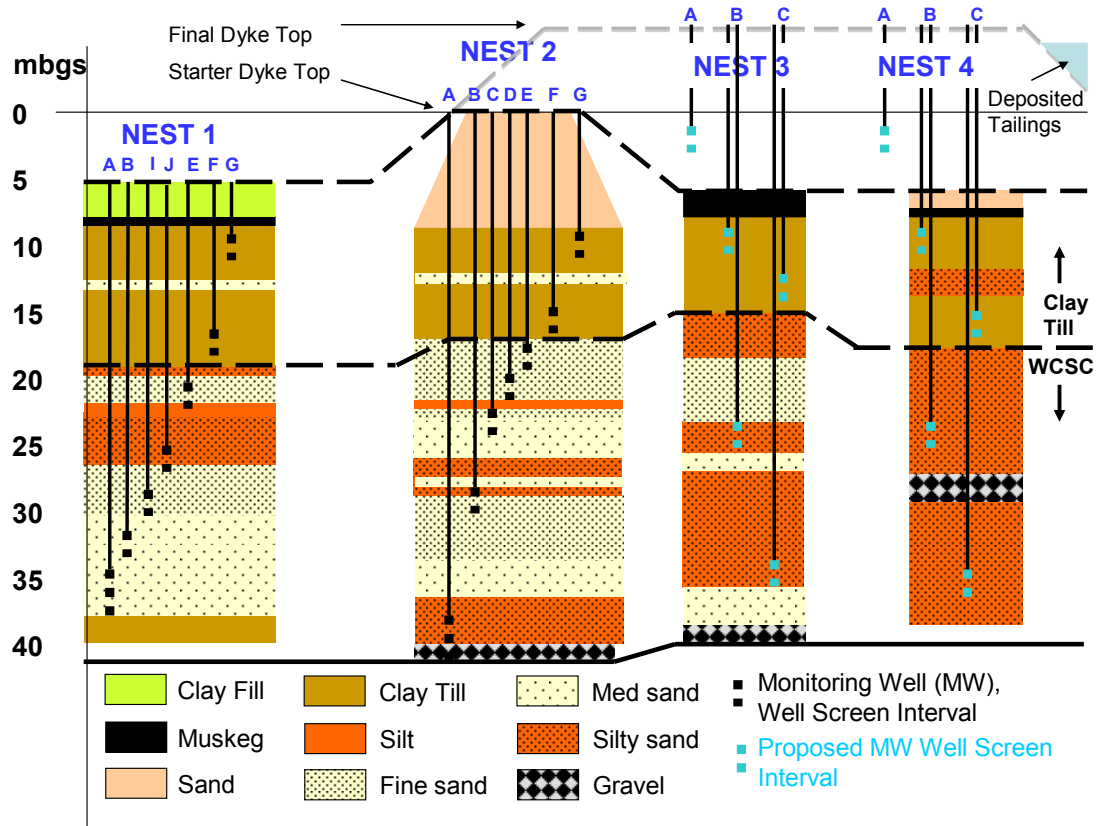


Figure 2. Schematic of the vertical delineation of the surficial geology by monitoring wells at the groundwater monitoring research transect.

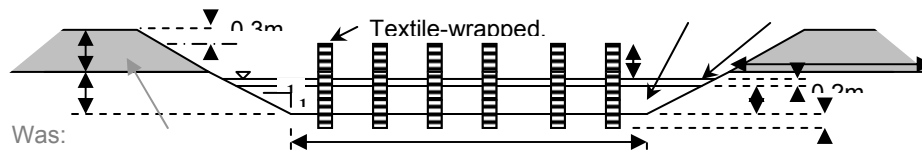


Figure 3. Cross-section schematic of the Infiltration Pond.

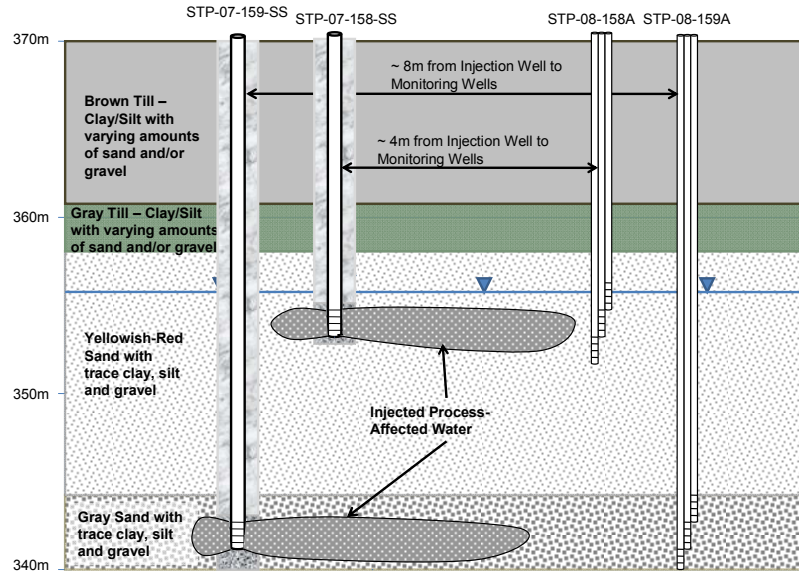


Figure 4. Cross-section schematic of the aquifer injection wells and associated multilevel monitoring wells at the In Situ Aquifer Test Facility. (Elevation as meters above sea level). Borehole and well diameters not to scale.

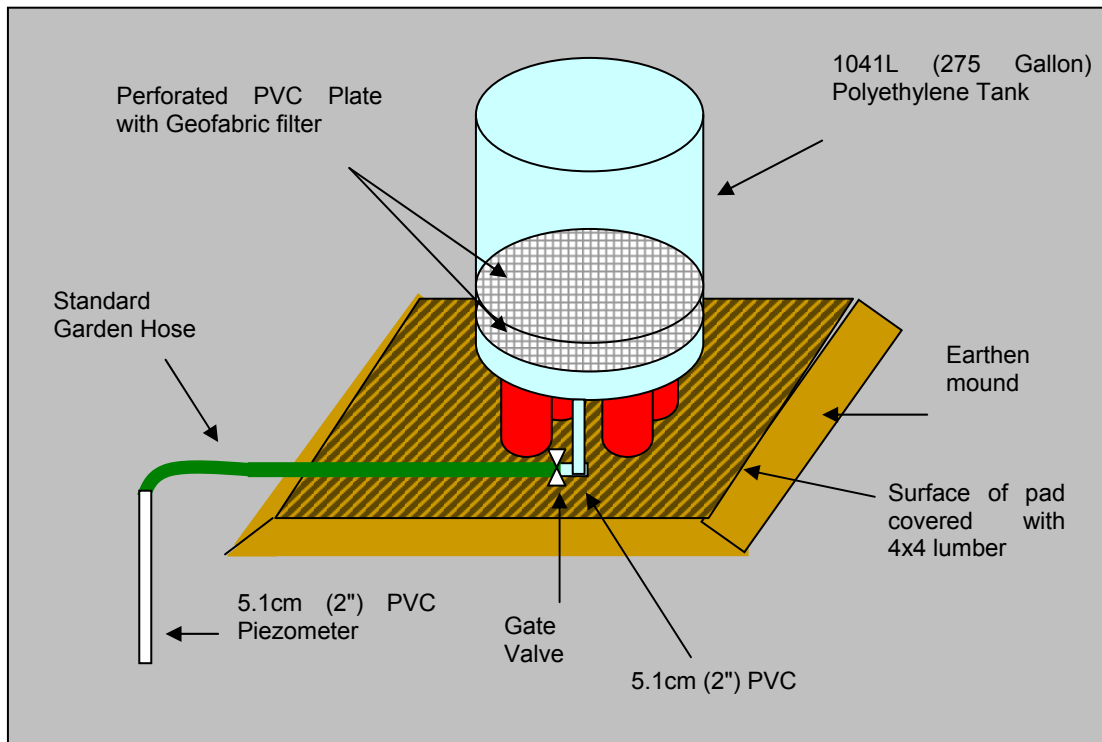


Figure 5. Initial concept schematics for the injection assembly at the In Situ Aquifer Test Facility

HEIGHTENED OIL SANDS EXTRACTION BY PRESSURE CYCLES

P.K. Andrew Hong, Zhixiong Cha

Department of Civil & Environmental Engineering, University of Utah, Salt Lake City, USA

ABSTRACT: Hot water extraction of bitumen from oil sands has been commercially applied for decades. The extraction process is greatly aided by the addition of caustics and other reagents, which can adversely impact handling and disposal at process end. Recent attention has been on increasing process efficiency by reducing temperature, which might lead to longer conditioning time and additional chemical additives that require further treatment downstream. Utah oil sands with high bitumen viscosity are expected to require more intensive agitation and caustic wetting agent such as with sodium hydroxide. We have invented a new heightened oil sands extraction (HOSE) process that greatly accelerates release and collection of bitumen from oil sands, while requiring no intensive agitation, caustics, or other chemical additives that aggravate hydrocarbon contamination of process water and subsequent treatment and disposal needs. The technique involves compression and decompression cycles, delivering gas and oversaturating it in the sands/water mixture during compression; this creates expanding microbubbles during decompression that helps dislodge bitumen from the sands. The new process results in high yields without requiring chemical additives that are prone to creating problematic end products, thus it has potential in reducing environmental impacts from oil sands operation.

INTRODUCTION

Oil sands (tar sands or bituminous sands) are a combination of clay, sand, water, and bitumen. The bitumen extracted from oil sands has chemical structures similar to conventional crude oil, but has greater density (a lower API gravity) and viscosity [Schramm et al. 2002; Wikipedia on tar sands]. On average bitumen

contains 83.2% carbon, 10.4% hydrogen, 0.94% oxygen, 0.36% nitrogen, and 4.8% sulfur [Wikipedia on tar sands]. Oil sands are found in over 70 countries throughout the world and represent 66% of the world's total reserves of oil, but about 75% of the world's reserves are in Venezuela (1.8 trillion barrels) and Canada (1.7 trillion barrels) [Wikipedia on tar sands]. In the US, tar sands (oil sands)

resources are primarily concentrated in Eastern Utah, where the in-place tar sands oil resources are estimated at 12 to 20 billion barrels. The United States has little experience with producing oil from tar sands [Veil and Puder, 2006].

The selection of recovery and treatment processes for different oil sands deposits are influenced by the properties and composition of the oil sands and bitumen. Canadian Alberta oil sands are “wet sands” because the sand grains are surrounded by a layer of water and bitumen that partially fills the voids between the wet grains. Most oil sands in US are “oil-wet sands” because the bitumen is directly in contact with sand grains without an intervening water layer. As a result, extraction methods for US oil sands could be different from those of Alberta [Veil and Puder, 2006; Daniels et al., 1981; Bukka et al., 1992].

Hot water extraction has been used commercially to recover bitumen from surface mined oil sands ore by exploiting the differences in their surface properties [Schramm et al., 2002; Spaeks et al., 2003; Nibogie et al., 2006]. The separation of bitumen from Utah oil sands requires more intensive shearing force and caustic wetting agent such as sodium hydroxide [Sepúlveda, 1977]. Another issue with current hot water process is the high pH water that can emulsify hydrocarbons in the aqueous phase, especially when the oil sands contain a high concentration of fines. We have developed a new, heightened oil sands extraction (HOSE) process for extraction of bitumen from oil sands. This process applies alternate compression and decompression cycles to the mixture of hot water and oil sands. It combines separation and

floatation in one step without chemical additives.

EXPERIMENTAL

The operation of heightened oil sands extraction (HOSE) is performed at elevated pressure. In a 150-mL, low-pressure vessel with a mechanical stirrer (175 psi grade reactor), one volume of water (20-40% of vessel capacity) is added into the reactor. After the water is heated to over 90°C by injecting steam into the aqueous phase or via heating element, 0.1 – 1.5 volume oil sands are added into the vessel. The vessel is then closed and pressurized to a designated pressure of 50 – 150 psi. The temperature of the water/sands mixture is controlled between 50°C – 105°C. Elevated pressure in the vessel, 50 – 150 psi, can prevent boiling at or over 100°C. After the water temperature reaches the designate temperature, the headspace pressure of the vessel is quickly released by venting. Thus, oversaturated dissolved gas in the aqueous phase generates microbubbles during decompression (pressure release). The rate of pressure release is controlled by opening of a valve to prevent bitumen from being expelled especially when the temperature is over the boiling point.

The bitumen content of oil sands from Asphalt Ridge, Utah is measured by Soxhlet extraction method. The oil sands are subsequently extracted with hexane and toluene for 48 hours (2 times 24 h). Mass balance calculation shows that Asphalt Ridge oil sands contain 12±1.7% bitumen. Utah oil sands contain [Sepúlveda, 1977] less fines (7-8% by weight) than Canadian oil sands (> 15% by weight). The

recovered bitumen has ultra high viscosity. The remaining hydrocarbon content in the oil sands following HOSE is measured by Soxhelt extraction to calculate the recovery efficiency.

RESULTS AND DISCUSSION

Figure 1 shows the oil sands before (Fig. 1A) and bitumen after the HOSE process; with the collected bitumen (Fig. 1B, right) and process water and settled sands (Fig. 1B left) as shown. Extraction was performed with 20 compression and decompression cycles with air up to 100 psi and completed within 10 min. No chemical additives were used. A separate experiment without pressure cycles conducted with the same sample with strong stirring at 95°C showed 95% bitumen recovery from the sands after 3 h; extraction with pressure cycles achieved similar recovery in a much shorter time (10 min) at slightly lower temperatures (85°C).

Figure 2 shows the extraction of bitumen at different numbers of pressure cycles at compression pressures of 100 and 150 psi, respectively. As shown, both the pressure and the number of pressure cycles exerted an effect on the degree of extraction. Higher extraction was achieved with increasing number of pressure cycles, and similar extraction could be achieved in fewer pressure cycles when a higher compression pressure (150 psi) was used.

Figure 3 shows the effects of a different compressing gas, i.e., CO₂, on extraction according to varied temperature and pressure. Again, higher extraction was observed with increasing pressure cycles, as well as with

increasing extraction temperature and pressure. In comparison to air, CO₂ effected similar extraction amounts at milder conditions, i.e., reduced temperature and pressure.

The relationship between solid loading and extraction efficiency was examined, as the required number of pressure cycles could be affected by solid loading. Results showed that when the volume ratio of water to oil sands was > 2, enough liquid volume in the mixture was allowed for the generation of bitumen froth. To increase process and energy efficiency, high oil sands loadings were attempted. In reduced water volume, additional hot water was added as necessary after bitumen separation to ensure separation of the bitumen froth layer from the solids. Figure 4 shows bitumen extraction with different solid/water ratios after different pressure cycles. The results suggested faster separation of bitumen was achieved when more water was used (T ~ 100°C); however, this difference disappeared when 5 or more cycles were used when near complete extraction occurred.

The applications of pressure cycles in enhanced extraction of contaminants from soil as well as in enhanced treatment of contaminants have been demonstrated [Hong et al., 2009; Hong et al., 2008a; Hong et al., 2008b]. We attribute the enhanced extraction of bitumen from oil sands for these reasons:

- 1) Water carrying dissolved gas during pressurization enters into small pore spaces of the oil sand particles and their aggregates; subsequent expansion of gas bubbles during depressurization breaks up aggregates of oil sands, increasing the exposure of bitumen within oil sands.

- 2) Water carrying dissolved gas penetrates during pressurization into small spaces between the bitumen and the sand particles; subsequent gas expansion acts to pry open the spaces, resulting in separation of bitumen from the sand surface.
- 3) Elevated water temperature decreases the viscosity of the bitumen, changing it into a viscous liquid that allows penetration and dissolution of CO₂ into the bitumen; subsequent gas expansion from within the bitumen pry the bitumen from the sand particles and lift the bitumen globs into the water column and to the water surface via flotation.

HOSE is a new water-based technology for extraction of bitumen from oil sands. The unique contact technique appears to provide these advantages:

- 1) High product yield – 95% of bitumen extraction from oil sands.
- 2) Reduced heating energy – Extraction temperature as low as 65 °C when CO₂ is used.
- 3) Rapid process speed – Bitumen release and recovery in a single step; total contact time for bitumen release and recovery < 20 min.
- 4) No caustics or other chemical additives are necessary, resulting in less problematic end products



Figure 1A. Raw oil sand samples (12 % bitumen by wt.) of Asphalt Ridge, Utah (left) and collected bitumen (right).

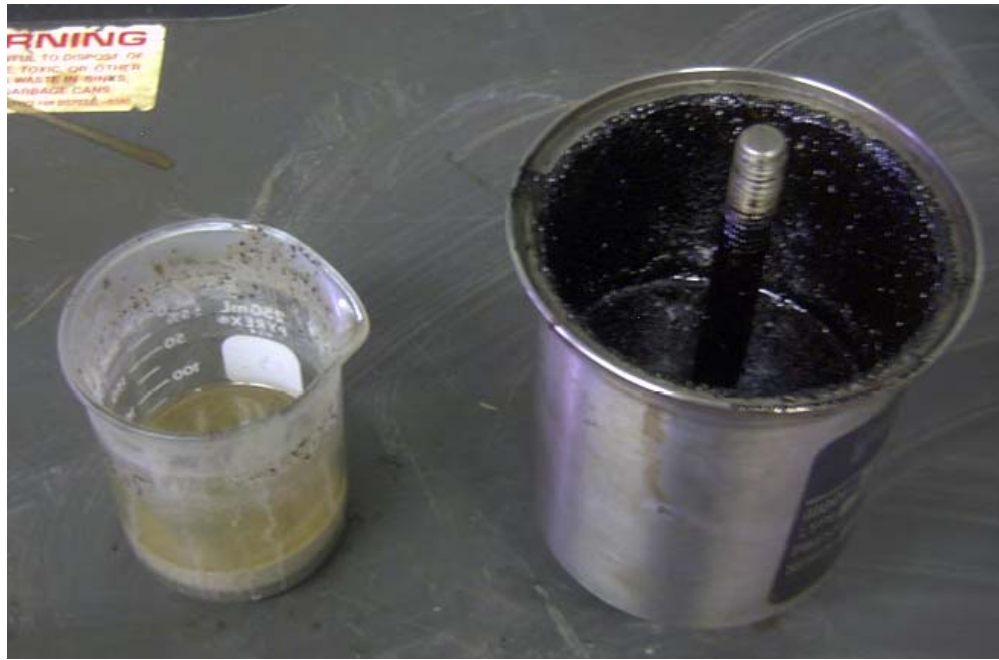


Figure 1B. Depleted, settled oil sands (left) and collected bitumen via pressure cycles (right).
 Extraction conditions: T = 85 °C; P = 100 psi; 20 cycles; total extraction time: 10 min.

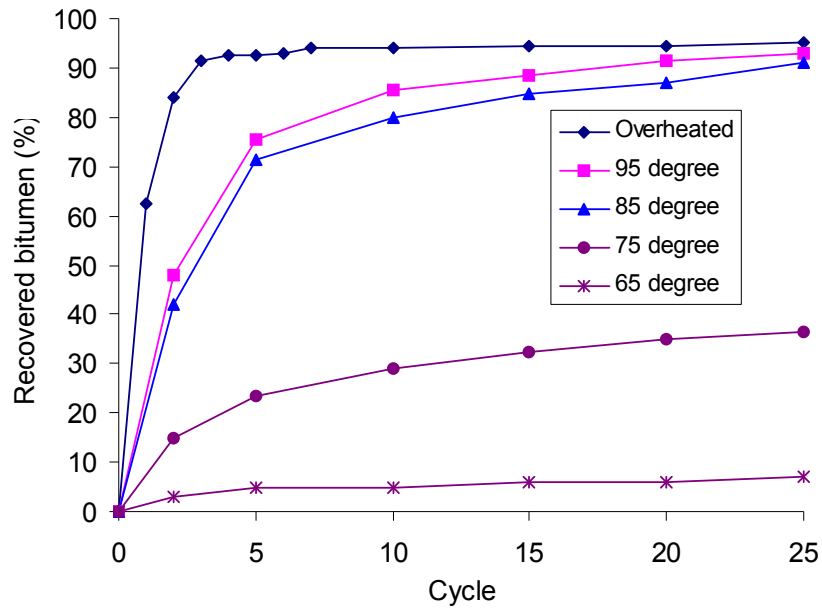


Figure 2A. Bitumen recovery according to the number of pressure cycles with air (150 psi). (Solid-to-water volume ratio at 0.5:1.)

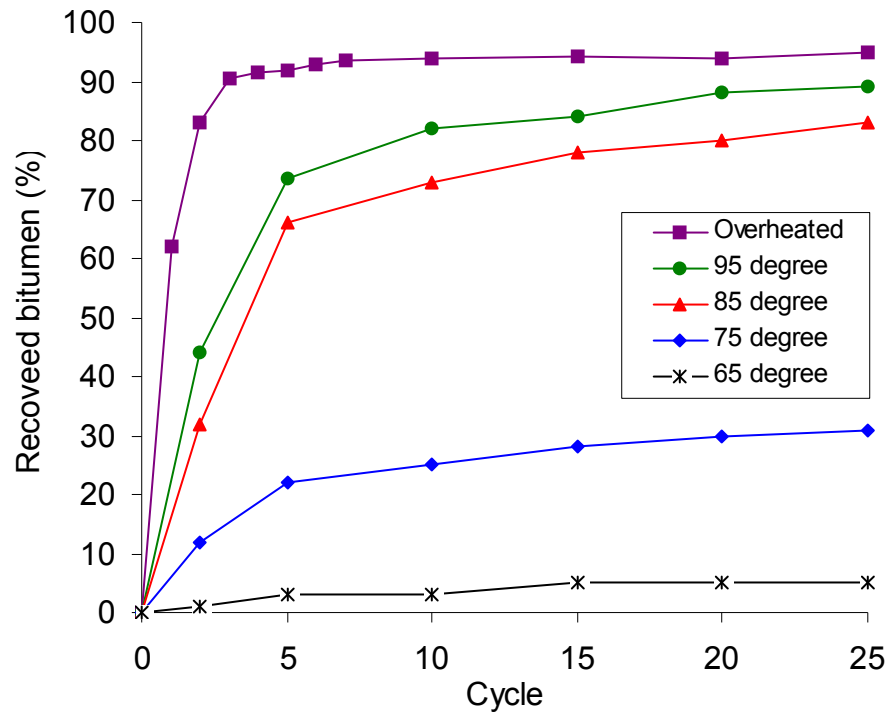
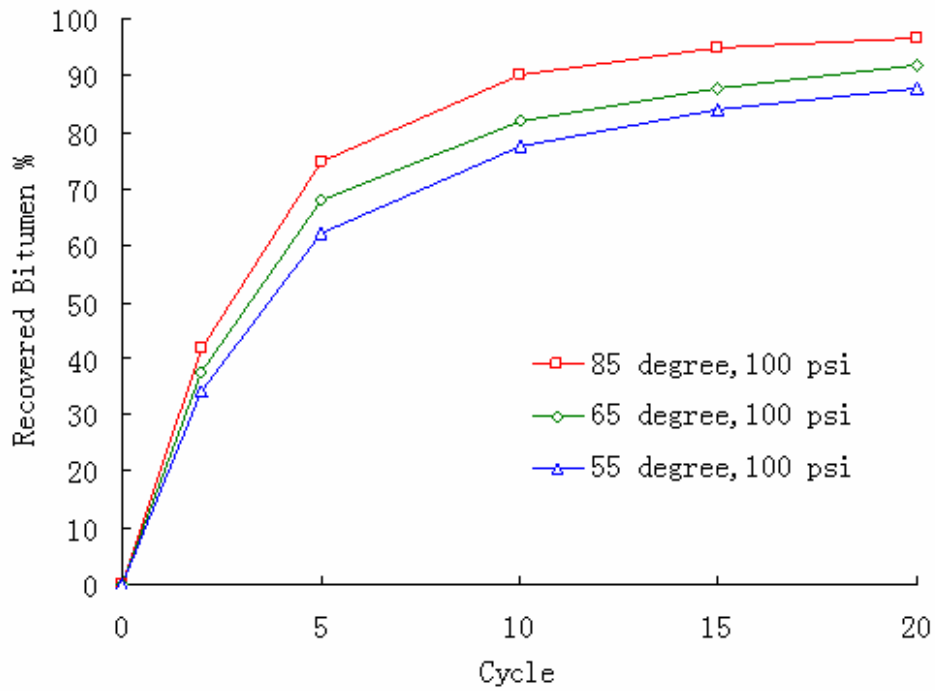
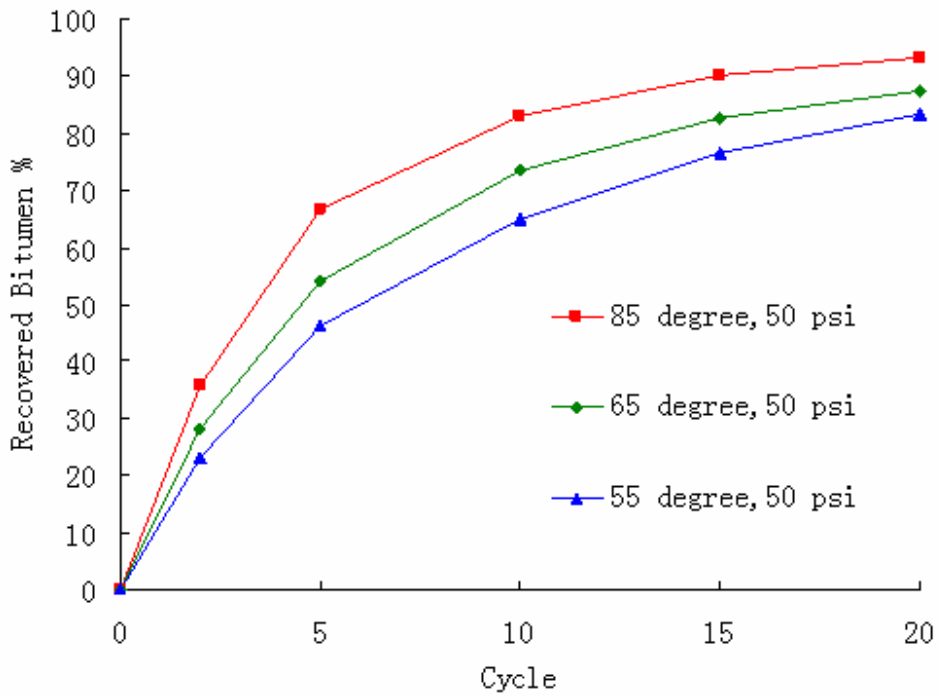


Figure 2B. Bitumen recovery according to the number of pressure cycles with air (100 psi). (Solid-to-water volume ratio at 0.5:1)



(A)



(B)

Figure 3A (top) and 3B (bottom). Bitumen recovery in hot water with pressure cycles of CO₂ at different temperature, pressure, and number of pressure cycles.

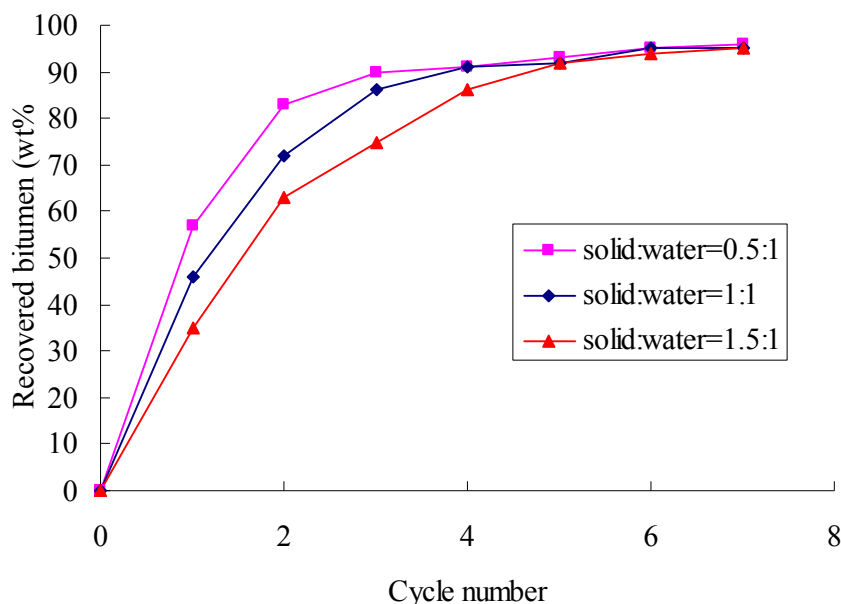


Figure 4. Bitumen recovery efficiency (wt%) vs. cycle number. The solid water ratios are volume ratios.

REFERENCES

- Hong, S. Nakra, J. Kao, D. Hayes. (2008a) Pressure-Assisted Ozonation of PCB and PAH Contaminated Sediments, *Chemosphere* 72 (2008) 1757–1764.
- A.. Hong, S. Nakra (2009) Rapid extraction of sediment contaminants by pressure cycles, *Chemosphere* 74 (2009) 1360–1366.
- A. Hong, X. Cai, Z. Cha (2008b) Pressure-assisted chelation extraction of lead from contaminated soil, *Environmental Pollution* 153 (2008) 14-21.
- B. D. Spaeks, L. S.Kotlyar, J. B. O'Carroll, K. H. Chung. Athabasca Oil Sands: Effect of Organic Coated Solids on Bitumen Recovery and Quality. *Journal of Petroleum Science & Engineering*, 2003, 39, 417-430.
- J. A. Veil, M.G. Puder. Argonne National Lab report: Potential Ground Water and Surface Water Impacts from Oil Shale and Tar Sands Energy-Production Operations. Available at http://www.ead.anl.gov/pub/doc/ANL-EVS-R06-9_oil_shale_report.pdf, 2006
- J. E. Sepúlveda. Hot-Water Separation of Bitumen from Tah Tar Sands. Thesis, University of Utah, 1977.
- J. I. Daniels, L. R. Anspaugh, Y. E. Ricker. Technology Assessment: Environmental, Health, and Safety Impacts Associated with Oil Recovery from U. S. Tar-Sand Deposits, October 13, 1981.

<http://www.osti.gov/energycitations/servlets/purl/6093147-w3acwe/6093147.PDF>

K. Bukka, F. V. Hanson, J. D. Miller, and A. G. Obladi. Fractionation and Characterization of Whiterocks Tar Sands Bitumen. *Energy & Fuels* 1992, 6, 160-165.

L. L. Schramm, E. N. Stasiuk, H. Yarranton, B. B. Maini. Temperature Effects in the Conditioning and Flotation of Bitumen from Oil Sands in Terms of Oil Recovery and Physical Properties. Canadian International Petroleum Conference, Paper 2002-074.

United States Patent 4532024. Process for Recovery of Solvent from Tar Sand Bitumen.

R. Nibogie, R. Buske, J. Overstreet, J. Dick, Hughes Christensen. New Technology Improves Economics in Canada's Extensive Alberta Oil Sands Region. 2006 SPE Annual Technical Conference and Exhibition held in San Antonio, Texas, U.S.A., September 24–27, 2006.

Tar sands, From Wikipedia, the free encyclopedia, Available at http://en.wikipedia.org/wiki/Tar_sands.

ANVIL POINTS OIL SHALE TAILINGS MANAGEMENT RIFLE, COLORADO

Richard Rudy PG,
Ecology and Environment, Inc.;

Christine LaBerge PE
Walsh Environmental Scientists and Engineers, LLC

Jon McClurg,
Walsh Environmental Scientists and Engineers, LLC

ABSTRACT

Early experimental attempts to recover petroleum hydrocarbons from oil shale led to current environmental issues that have had to be addressed by the U.S. Department of Interior, Bureau of Land Management (BLM). The Defense Authorization Act of 1998 transferred administrative jurisdiction of Naval Oil Shale Reserves 1&3 (NOSR) from the U. S. Department of Energy, to the BLM. NOSR 1&3 are adjacent oil shale reserves located within the rugged highland country of western Colorado. The Anvil Points Facility is located within the boundary of NOSR # 3, and was constructed to pioneer oil shale mining, processing and environmental research and development by government and private industry. Between 1947 and 1982 the Anvil Points Facility mined and processed approximately 400,000 cubic yards of oil shale. However by 1983 private sector interest in oil shale research waned and the facility was placed in standby mode. Although the decommissioning of Anvil Points Facility addressed certain environmental concerns and physical hazards, the Site had environmental concerns, particularly those associated with the waste shale pile left from the experimental processing of oil shale. These include: inorganic contaminants, waste shale pile stability, potential contamination of the “relic and waste disposal ponds” and erosion of waste shale pile materials into West Sharrard Creek (a tributary of the Colorado River).

To address these potential environmental issues associated with the shale pile, BLM conducted an investigation and preliminary engineering design. The results of a streamlined risk assessment concluded that arsenic concentrations in the waste shale tailings significantly exceed risk based guidelines. Furthermore, this analysis showed that the shale tailings were unstable and could result in catastrophic failure and collapse thereby creating a potential for migration into West Sharrard Creek. Thus the removal action addressed by the preliminary engineering design focused on elimination of potential arsenic exposure and elimination of the collapse threat.

An extensive engineering evaluation was performed of potential shale tailings remedies with the final decision for the pile to be relocated to an on site repository. Given this was a planned major federal action an analysis of the selected alternative also had to also undergo a Demonstration of NEPA Adequacy to be consistent with BLM's existing Resource Management Plan for this management unit. Recently the construction of the repository and retort tailings relocation has been completed.

INTRODUCTION

Background

The Anvil Points Facility (APF) is located within the boundary of the past U.S. Naval Oil Shale Reserve (NOSR) Number 3, approximately 7 miles west of Rifle, Colorado (Figure 1). The APF occupies approximately 365 acres within the NOSR Number 3, which has a total area of 20,171 acres.



Figure 1. Location of the Anvil Points Facility

The site is located within the rugged highland country of western Colorado and is comprised of semi-arid land in the southeast Piceance Creek basin. Elevations range from 5,500 feet near the Colorado River to 9,000 feet above sea level at the top of the Roan Cliffs. The APF was constructed to pioneer oil shale mining, processing and development by government and private industry. Development of the site was

initiated in the spring of 1945 by the U.S. Bureau of Mines. Construction of the first retorts and the installation of the crushing and screening equipment were completed by the spring of 1947. Operations using a number of different oil shale processing techniques were conducted at the site between 1947, when the first batch of oil shale was retorted, to July 1955, when the APF was shut down due to the expiration of the Synthetic Fuels Act. Between 1956 and 1964, the APF was inactive with only minimal workers on site to maintain the facility. Experimental oil shale production operations were restarted by the Colorado School of Mines Research Foundation, which leased the APF between 1964 and 1968, when operations ceased again. In 1972, Development Engineering, Inc., a subsidiary of Paraho Corporation, leased the APF and operated the facility intermittently between 1973 and 1982, when their lease expired. Between 1947 and 1982, approximately 400,000 cubic yards of oil shale were mined and processed at the APF. By 1983, private sector interest in oil shale research waned and the facility was placed in standby mode. In 1984, the Department of Energy (DOE) had assumed responsibility of the facility from the Navy and decided. In 1997, Congress transferred administrative jurisdiction of NOSR 3 from the DOE to the Department of Interior, BLM.

Shale Pile

Spent (retorted) shale and raw shale fines (excluded from the retorting process) were disposed of from the Plant Site at the top of the bench west of West Sharrard Gulch onto

the steep slope descending to the gulch (Figure 2). The waste shale pile extends for approximately 900 feet along the terrace bench above the gulch, and is 150 feet high at its highest point. The surface of the shale pile has a slope of about 1.4:1, and contains several areas of material sloughing. The course of West Sharrard Creek was altered to make additional space for the spent shale pile and for construction of several spent shale process lagoons. During plant operations, retort wastewater was disposed on the shale pile (NEESA 1985). Water and wastewater flowing through the shale pile have probably leached soluble salts and organic compounds, which may have entered ground water or seeped into West Sharrard Gulch.

The raw shale fines and spent shale piles eventually merged. A fire (in-situ combustion) was observed in the pile of raw shale fines in 1978, later attributed to residual heat from the retort process. The raw shale fines and spent shale piles eventually merged. A fire (in-situ combustion) was observed in the pile of raw shale fines in 1978, later attributed to residual heat from the retorted shale (Lavery 1985). High temperatures (approaching 500°C), and cracking and venting of hot gases were observed for several years. The waste shale pile reportedly burned until it was extinguished in the late 1980s or early 1990s.

Local surface geology is composed of early Tertiary sedimentary formations (deposited 65-38 million years ago) and Quaternary formations (deposited less than 3 million years ago). The Eocene Uinta Formation forms the top of the plateau above the APF and contains sandstones and siltstones.



Figure 2. View of the Shale Pile in 2003, looking to the south.

Underlying the Uinta are the Parachute Creek and Anvil Points members of the Eocene Green River Formation. These units form the Roan Cliffs and contain oil shale, marlstone, siltstone, sandstone, and limestone. Underlying the Green River Formation is the Paleocene-Eocene Wasatch Formation. It forms the lower portion of the Roan Cliffs and is exposed on the ridges and mesas southward to the Colorado River. The Wasatch is composed of interbedded clays, mudstones, sandstones, and conglomerates. The sandstones are predominantly channel deposits and are laterally discontinuous. Quaternary alluvium flanks the Colorado River. The strata at the APF generally dip slightly to the west (NEESA 1985). The oil shale mined and processed at the APF is from the Mahogany Ledge Unit of the Parachute Creek Member of the Green River Formation. The Mahogany Ledge Unit in this area is approximately 70 feet thick.

The location of the shale pile in West Sharrard Gulch is an area composed mainly of unconsolidated colluvial and alluvial deposits that tend to interbed and form gradual contact zones with one another. The alluvium varies in thickness from the upper to lower reaches of the gulch, with a maximum thickness of about 40 feet below the APF. The alluvium is a poorly sorted mix of clay,

silt, sand, cobbles, and boulders with minor inclusions of well-sorted lenses of sand and sandy gravel.

Hydrogeology

Ground water is found within the alluvium of West Sharrard Creek and in the Green River Formation up gradient of the APF. Based on data from an existing ground water monitoring network, ground water flow in the alluvium is irregular in the vicinity of West Sharrard Creek and is poorly suited as a potable water source because of the poor water quality and limited storage.

Several aquifers exist in the Uinta Formation and upper member of the Green River Formation within the area delimited by the Roan Plateau. Several springs and seeps were noted by NEESA (1985), but “the water does not readily infiltrate into the less permeable rock formations below.” NEESA noted that ground water movement in these formations follows local stratigraphic dip, which is to the northwest (i.e., away from the APF).

At the APF, shallow ground water tends to remain perched in the alluvium above the less permeable silty sandstone and shale layers of the Wasatch Formation. Due to the steep topographic gradient, seepage velocities are high. The off-site migration time was estimated to be days, at least to the point where ground water and surface water reaches the Sharrard Park alluvial fan (ORNL 1991). Ground water at the site varies from 14 feet below ground level (bgl) just east of the shale pile to 30 feet bgl at a location about 250 feet south of the shale pile.

There are no municipal ground water wells nearby; communities with water supply wells downgradient are at least several miles away. The wells are completed in shallow alluvium,

and are considered drawing from “ground water under the influence of surface water”.

There are five permitted domestic water wells within 3 miles of the APF Plant Site. These wells are adjacent to or within 0.3 miles of the Colorado River and are completed at depths ranging from 48 to 270 feet. Those nearest the Colorado River are presumably drawing from alluvium; those higher up on the valley floor may be drawing from bedrock.

Vegetation Resources

The immediate vicinity of the shale pile was historically vegetated with pinyon-juniper woodlands interspersed with slopes of mountain sagebrush shrub lands and occasional shale outcrops barrens. However, vegetation throughout the entire APF area has been seriously impacted through a number of human actions, including those associated with APF operations, as well as roads and well pads developed more recently for natural gas extraction. The results of these activities are large areas that have been cleared of woody vegetation and are now dominated by weeds and planted reclamation species.

The shale pile is bounded to the west and north by roads and cleared areas dominated by bare soil or patches of the noxious weed, cheatgrass (*Anisantha tectorum*), non-native reclamation grasses such as crested wheatgrass (*Agropyron cristatum*) and western wheatgrass (*Pascopyrum smithii*), and scattered native saltbush shrubs (*Atriplex* spp.). The bench terrace between the shale pile and the West Sharrard Creek gulch also supports these weedy and reclamation species with scattered Utah juniper (*Sabina osteosperma*) and pinyon pines (*Pinus edulis*) near the south end. The shale pile itself supports very little vegetation. The adjacent slopes are dominated by cheatgrass, with numerous shrubs, including saltbush,

greasewood (*Sarcobatus vermiculatus*), rabbitbrush (*Chrysothamnus viscidiflorus*) and scattered Utah juniper. Areas of riparian wetlands occur along the three creeks that flow through the APF. West Sharrard Creek traverses the eastern portion of the site. An additional 1,700 acres of riparian wetlands occur along the 15-mile long segment of the Colorado River downstream of the confluence with West Sharrard Creek; these could be impacted should the shale pile release contaminants to the Colorado River via West Sharrard Creek. These areas provide important habitat for a number of bird species. The in-stream portions of this corridor provide crucial habitat for various fish species, including a number of sensitive species listed below, as well a number of waterfowl, wading birds, and shorebirds, some of which are also considered sensitive.

In the vicinity of the shale pile, the West Sharrard Creek floodplain was altered in the past when the creek bed was moved to make additional space for the spent shale pile and process lagoons. The creek is usually dry, carrying water only in response to precipitation events, snow melt, and occasional interception of ground water. The stretch of West Sharrard Creek in the vicinity of the shale pile is deeply down cut, with steep banks that support sparse upland vegetation. Little vegetation occurs within the gulch, along the flow channel. No wetlands, nor riparian areas, exist in this reach of the creek.

Wildlife Resources

Much of the APF site, including the area of the shale pile, lies within lands mapped by the Colorado Division of Wildlife (CDOW) as big-game winter range for mule deer and American elk. Some timing limitations for protection of big-game resources are applied to the area by BLM. Large carnivores that occasionally move through the APF study

area include black bears and mountain lions. Other predators in the APF vicinity include the bobcat, coyote, red fox, American badger, long-tailed weasel, short-tailed weasel, and mink. Raccoons, ringtails, striped skunks, and western spotted skunks probably also occur.

White-tailed jackrabbits and desert cottontails occur in the area. Rodents occurring on site include porcupine and several members of the squirrel family.

A variety of mouse species are likely to be present. Non-rodent ground-dwelling small mammals documented or expected include Preble's shrew and the masked shrew, montane shrew, dwarf shrew, and water shrew. Several bat species also occur or would be expected. These include five BLM sensitive species. Raptor species hunt and nest within the APF study area.

Reptiles known or likely to occur within the APF study area include a number of lizards and snakes, including two snake species listed as sensitive.

Given the physical and ecological conditions in the vicinity of the shale pile, it is unlikely that this area supports nesting or feeding habitat for any wildlife, with the exception of an occasional rodent or reptile.

Sensitive Species and Environments

Sensitive species had to be addressed by any remedial action at the shale pile. BLM is directed to ensure that no action that requires federal approval should contribute to the need to list a species as threatened or endangered under the Endangered Species Act (ESA). This protection also applies to species that are proposed or candidates for listing and to species designated by each state director as sensitive.

A list of potential sensitive species for the APF study area was compiled from these studies. Species considered for inclusion in this assessment are known to occur within the APF study area.

Sensitive Environments

Sensitive environments within the APF include 1,700 acres of critical habitat for various fish and bird species (ORNL 1994). However, none of this habitat occurs within the immediate vicinity of the shale pile. A number of sensitive or endangered bird species and bats are present that could potentially be impacted by contaminated surface water (derived from leaching from the shale pile) through ingestion of water or the aquatic food chain. Seasonal streams can be an important source of water for livestock as well as wildlife, including mule deer, and may be used for breeding by amphibians. Additionally, riparian vegetation may uptake contaminants from the shallow ground water associated with the stream, and any contaminants transported into some of the streams may be transported to the Colorado River or nearby Fravert Reservoir. These latter two habitats support game fishes, nesting by a variety of water birds, and other terrestrial and aquatic wildlife.

The APF also includes habitat for several sensitive plants species, including the federally listed DeBeque Milkvetch. Due to the inhospitable soil condition of the shale pile and impoundments, it is unlikely that any of the sensitive plants occur on these contaminated materials. Field observations made during May 2004 observed no sensitive plant species on the waste shale pile, impoundments, or plant area.

Sensitive wildlife habitats within the larger APF area include critical mule deer winter range, riparian corridors along ephemeral drainages, the Colorado River riparian

corridor, the Colorado River aquatic habitat, Fravert Reservoir, and any seasonal pools used for breeding by amphibians or as wildlife/livestock watering holes. Mule deer winter range includes most of the habitat types within and near the site. Riparian habitats along ephemeral drainages and the Colorado River receive disproportionate wildlife use throughout the year. Numerous species, including migratory birds present in the area only seasonally, concentrate in the relatively lush and structurally complex riparian habitat that is downstream from the shale pile.

Previous Removal Actions

Previous removal actions at the shale pile and impoundments have been generally limited in scope and were performed when the APF was operational or during demolition of the Plant Site. No information is available about the amount of time or money spent on these previous removal actions, and no removal actions on the shale pile or impoundments were performed under CERCLA authority by the Bureau of Mines, Department of Energy, or BLM.

In response to releases of oil from the *in-situ* retorting that was occurring within the shale pile in 1979, a channel was constructed at the base of the shale pile to divert oily runoff to a Process Pond. During decommissioning and demolition of the APF (1984-1986), approximately 700 barrels of oil were skimmed from the Process Pond and transferred to tanks. All impoundments were also filled in with native soil between the mid-1970s and 1986. The course of West Sharrard Creek was altered to make room for the shale pile during operations, and work was also performed to prevent the shale pile from reaching the creek during plant operations.

In addition, current estimates of the volume of the shale pile are significantly less than what would be expected from approximately 400,000 cubic yards of raw shale which was processed at the APF (E&E 2004). Current estimates of the amount of material within the shale pile range between 70,000 and 130,000 cubic yards. Although no written documentation was available on this subject, it is believed that significant quantities of shale fines were used as road material within the APF.

Location of Contaminated Materials

Waste shale, composed of spent (retorted) shale and raw shale fines (excluded from the retorting process) were disposed from the Plant Site at the top of the bench west of West Sharrard Gulch onto the steep slope descending to the gulch. The waste shale pile extends for approximately 900 feet along the floor of the gulch and reaches 150 feet in height at its highest point. The surface of the shale pile has a slope of about 1.4:1 and contains several areas where sloughing has occurred. Industrial waste treatment ponds were formerly located at the base of the waste shale pile and to the south of the pile.

Volume of Contaminated Materials

Calculations of spent shale resulting from disposal of 425,000 tons of raw shale (NEESA 1985) yield a volume of spent shale of about 393,500 cubic yards assuming a specific gravity of 1.08 tons per cubic yard. However, all recent estimates of the volume of spent shale remaining at the APF have been substantially lower, ranging from 60,694 to 178,000 cubic yards.

Due to uncertainty about irregularities in the natural hillside where the waste oil shale was deposited, 130,000 cubic yards of waste shale were used for cost estimating purposes.

STREAMLINED RISK EVALUATION

Oil shale mining activities from the APF have probably influenced the surrounding environment since the creation of NOSR #1 in 1916. Processed shale generated from mining activities has contributed inorganic elements into the waste shale pile and impoundments; and inorganic and organic (attributed to *in-situ* combustion within the waste shale pile) elements into the ground water and the surface water through leaching of waste materials. The area is used year-round for oil and gas exploration and production. Hunting and cattle grazing also occur on the property.

Risk Assessment Results

While several metals of concern were found to be present at concentrations exceeding three times background in soil, three metals exceeded established soil screening levels. Arsenic concentrations in waste shale and native material beneath the waste shale significantly exceeded the Colorado soil clean-up guidelines for residential or unrestricted land-use, and the EPA risk-based concentrations for both industrial and residential sites. Beryllium concentrations in waste shale and native material beneath the waste shale exceeded the EPA risk-based concentration for residential sites, but not the risk-based concentration for industrial sites. Based on the results of a 2000 CDPHE study, iron concentrations in waste shale exceeded the EPA risk-based concentrations for residential sites. However, iron concentrations were found to be less than the risk-based criterion (RBC).

Aluminum, arsenic, boron, cadmium, chromium, iron, lead, manganese, nickel, and vanadium exceeded one or more risk based ground water guidelines for human health, agricultural use, or tap water (CDPHE 2000). No metals of concern exceeded established

Colorado surface water risk based guidelines; however, potassium and sodium were found at concentrations three times background.

REMOVAL ACTION CRITERIA

While several metals of concern were present at the site, arsenic concentrations in waste shale and native material beneath the waste shale significantly exceeded risk-based guidelines. Furthermore, it was shown that the waste shale pile was unstable and could result in catastrophic failure and collapse creating the potential for migration of contaminants into West Sharrard Creek. Arsenic concentrations in the waste shale therefore posed a potential threat to human health and the environment.

The proposed removal action criterion was the reduction or elimination of the threat to human health and the environment posed by ingestion, inhalation, and dermal contact with arsenic in the waste shale as well as elimination of the potential for collapse of the pile into West Sharrard Creek.

Comparative Analysis of Removal Action Alternatives

A comparative analysis of the Removal Action Alternatives with respect to the effectiveness, implementability, and cost criteria is described below. All of the removal action alternatives were expected to be technically implementable. They all involved proven technologies, and equipment and services were expected to be available.

Alternative 1 — Stabilization and Closure in Place

The Stabilization and Closure in Place alternative will be effective in stabilizing the pile to prevent potential collapse and migration of sediments into West Sharrard Gulch. Furthermore, the cap will reduce

exposure of contaminants via air pathways and ingestion and serve as a barrier between the waste shale and potential receptors. However, since the pile will remain in place, the potential for migration of contaminants into ground water is not completely mitigated. In addition, the possibility of erosion due to the steep slope of the regraded area also poses a risk for potential migration of sediments into surface water. Finally, this alternative would require extensive long-term monitoring to adequately monitor the effectiveness of the alternative and to comply with Colorado Solid Waste regulations.

Alternative 2 — Placement in an On-Site Repository

The excavation and placement of the waste shale into an on-site repository carries many of the same benefits as those presented in Alternative 3. As the pile would actually be excavated to another site, the risk of collapse of the pile into West Sharrard Creek is no longer applicable. Furthermore, the placement of the material into a location removed from the West Sharrard Gulch would lessen the risk of possible erosion and sediment transport into surface water; as well as reduce the potential for leaching of metals-contamination into ground water. A principal critical issue in implementing this alternative is locating a suitable site. The site should be accessible, be uncontaminated from previous APF operations, and have sufficient area to accommodate the waste shale materials. The constructed on-site repository will have to comply with Colorado Solid Waste regulations including long-term post-closure monitoring.

Alternative 3 — Placement in an Off-Site Commercial Landfill Facility

The excavation and placement of the waste shale materials in an off-site commercial landfill facility is an effective and

implementable removal action. The principal difference between this alternative and Alternatives 2 and 3 is cost. Landfill and/or hauling fees are significantly higher than stabilizing in place or building an on-site repository for the waste shale. Furthermore, the long-term liability of placing the material in a commercial facility remains to be determined.

REMOVAL ACTION

Based on the evaluation criteria, the recommended removal action was the placement of the waste shale materials in an on-site repository. This alternative represented a high level of overall protectiveness of human health and the environment and achievement of the remedial action objectives. It was technically and administratively feasible and was potentially the lowest cost alternative considered. The off-site commercial landfill alternative would be as protective of human health and the environment; was technically and administratively feasible; and would eliminate the need for BLM to design, construct, and maintain a landfill at the Anvil Points property. However, the difference in cost was significant, with the principal cost elements being landfill and transportation fees. However, if landfill fees at the nearby West Garfield Landfill could have been negotiated to a price acceptable to the BLM (this was not achieved), this alternative would have been more desirable in the long term.

NEPA ADEQUACY ANALYSIS

The APF project followed the Council of Environmental Quality (CEQ) guidance on potential impacts to the human environment. An Environmental Assessment (EA) level analysis was conducted that assessed the potential impacts of the removal action alternatives within the larger context of the

BLM's Roan Plateau Resource Management Plan, which prescribes how the BLM will manage the various resources present in the area that includes NOSRs 1 and 3. All critical elements addressed by NEPA were addressed in this analysis, A Finding of No Significant Impacts was reached by this NEPA adequacy analysis.

CONCLUSIONS

In spite of previous closure activities, the spent shale pile left from experimental extraction of hydrocarbons from oil shale at the Anvil Points Facility still presented threats to human and ecological receptors if left in place in West Sharrard Creek. A variety of remedial alternatives were investigated, including placement in a commercial landfill, creation of an on-site repository, stabilization and closure in place. It would have been preferable to remove the shale material to a nearby commercial landfill to minimize long-term maintenance costs, but the quantity of material made this cost-prohibitive. The selected remedial action incorporates the safety of placement in an engineered repository on-site, and results in removal of all shale material from potential sloughing and leaching into West Sharrard Creek and the nearby Colorado River.

REFERENCES

Lavery. 1985. Determination of Particle Deterioration and Collapse Susceptibility of Retorted Oil Shale Piles Caused by Potential Internal Combustion, Prepared by U.S. Army Corps of Engineers Waterways Experiment Station for U.S. DOE Laramie Project Office, December, 1985. McCarthy 1986. Synfuels Engineering and Development, Letter dated September 24, 1986 (reference from CDPHE 2000).

Naval Energy and Environmental Support Activity (NEESA). 1985. *Site Characterization of the Anvil Points Facility, Rifle, Colorado.*

Oak Ridge National Laboratory (ORNL). 1991. *Geology and Hydrology of the Shallow Alluvial Aquifer, West Sharrard Gulch,*

Colorado. Prepared by David R. Smuin, Oak Ridge National Laboratory, ORNL/TM-11467, March, 1991. Prepared for the U.S. Department of Energy.

ORNL. 1994. *Preliminary Assessment Spent Shale and Drum Area West Sharrard Gulch Anvil Points Facility.*

TREATMENT OF PRODUCED WATER BY PRESSURE-ASSISTED OZONATION AND SAND FILTRATION

P.K. Andy Hong, Zhixiong Cha and Chia-Jung Cheng

Department of Civil and Environmental Engineering, University of Utah, USA

Cheng-Fang Lin

Graduate Institute of Environmental Engineering, National Taiwan University, Taiwan

ABSTRACT: Ever increasing energy demand worldwide necessitates energy production from heavy petroleum sources such as oil sands and oil shale. Extraction of bitumen from oil sands and in situ extraction of kerogen from oil shale result in large quantities of water containing hydrocarbon contaminants. The contents of dispersed and dissolved oils and other organic contaminants present problems for subsequent water uses and disposal. When discharged near shoreline, produced water with even trace oil results in sheen formation at the water surface.

This research employs a new ozonation technique to treat water to remove oil and prevent oil sheen. Unlike ordinary ozonation practice, the new technique incorporates rapid, successive cycles of compression and decompression during ozonation. Nano/micro bubbles are created that provide reactive zones at the gas-liquid interface, resulting in heightened chemical conversions—most notably the conversion of hydrophobic hydrocarbon molecules into hydrophilic organic acids. This study examined the reduction of dissolved and dispersed hydrocarbons as well as prevention of oil sheen according to treatment extent and varied treatment parameters. Experimental results from a 2-stage treatment system suggest effective oil reduction and oil sheen prevention. Specifically, when a synthetic produced water containing 120 ppm of crude oil (100 ppm of dispersed and 20 ppm of soluble oil at a total COD of 320 mg/L) was subjected to 10 pressure cycles (reaching 100 psi; 20 s each) of ozonation and sand filtration at 6 cm/min as the first stage and then repeated by 20 cycles of ozonation and sand filtration, it resulted in removal of oil to 20 ppm as water-soluble organic acids, decrease of turbidity from 200 NTU to 2 NTU, and complete sequestration of surface sheen. Treatment results and removal mechanisms are discussed. The new technique has potential for treating produced and tailings waters, allowing safe discharge to the environment as well as making high-value reuses of the water possible.

INTRODUCTION

Produced water containing hydrocarbons is produced concomitantly when oil or gas is produced (Veil et al. 2004), reaching 3 billion

tons annually in the U.S. alone (Veil et al. 2004; Sullivan et al. 2004). It is increasingly produced as an oil well approaches its end. Development of unconventional sources such as extraction of bitumen from oil sands and

in situ extraction of kerogen from oil shale result in large quantities of water with hydrocarbons. Dispersed and dissolved oils in these waters pose treatment and disposal challenges, often preventing beneficial uses (Veil et al. 2004; Yang and Nel 2004; ERIN Consulting Ltd. and OCL Services Ltd. 2004). In many regions, sustainable energy supply and new development will critically depend on availability and sound management of water.

When discharged near shoreline, produced water with trace oil results in oil sheen at the water surface, which is a concern due to its potential impact on plankton and birds in addition to aesthetics (ERIN Consulting Ltd. and OCL Services Ltd. 2004). Hydrocarbon concentrations at 20 to 40 ppm or even lower have been found to cause oil sheen, while at times higher hydrocarbon concentrations (> 50 ppm) do not result in surface sheen (McCay 2002). Removal of dispersed and dissolved hydrocarbons from water is challenging. Produced water treatment technologies were recently reviewed (Hayes and Arthur 2004). While API separator, hydrocyclone, flotation, filtration, and membrane processes had been shown to remove constituent oil with various degrees of success, none were without drawbacks such as the ability to handle soluble or high oil contents or susceptibility to fouling (ERIN Consulting Ltd. and OCL Services Ltd. 2003; Tibbetts et al. 1992; Simms et al. 1992; Reed and Johnsen 1996). While ozonation had been well established for treatment of chemical wastes, only a few studies were reported for produced water (Klasson et al. 2002; Corrêa et al. 2009; Walker et al. 2001). In no cases were successful removals of free and soluble oils by ozonation reported.

Neither conventional ozonation nor sand filtration alone had been shown to treat

produced water effectively. We demonstrate, however, a new ozonation technique coupled with sand filtration for removal of oil and prevention of oil sheen. This study examines the removal of dispersed and dissolved hydrocarbons with a focus on sheen prevention according to treatment extents and varied treatment parameters. An important goal is to promote safe discharge and reuse potential of process waters.

EXPERIMENTAL

Synthetic produced water (SPW) – Preparation and characteristics

The test synthetic produced water (SPW) was prepared by mechanically stirring 1.5 mL of Rangely crude oil (CO, USA) with 2000 mL of DI water at room temperature at 500 rpm for 30 min. Vacuum filtration (ASTM D1888) of oil samples through a 0.45- μ m glass filter paper was used to distinguish the dispersed oil from the dissolved. Dispersed oil was estimated by the total suspended solids (TSS), i.e., the retained “solids” on the filter. The total and dissolved hydrocarbon concentrations were calculated from COD measurements before and after vacuum filtration. In this study, iridescent oil sheen was observed for COD between 50 ± 10 to 100 ± 10 mg L⁻¹ (i.e., hydrocarbon concentration of 20 – 40 mg L⁻¹), and brown oil sheen was observed for COD > 120 ± 15 mg L⁻¹.

Following treatment, suspended solids were found on the water surface and were collected and included in mass balance calculation. The ratio of COD to the total hydrocarbon concentration was determined by mass balance calculation to be 2.8 (i.e., COD/total hydrocarbon concentration = (COD before filtration – COD after filtration)* liquid volume/ weight of solids

retained on the filter paper). Dispersed and dissolved hydrocarbons in SPW were delineated by filtration. The filtrate was extracted by hexane (200 mL of filtrate by 50 mL of hexane twice). The hexane extract was concentrated to 1 mL by a gentle nitrogen stream and analyzed by GC/MS. Hydrophilic compounds in the treated sample were extracted by SPE method. For samples with low COD, the samples after filtration were adjusted to pH > 12 and concentrated 10 times by boiling before passing the concentrate through the SPE column (IST ISOLUTE C18 (EC)). The SPE column was eluted with 20 – 30 mL of methanol, and this solution was reduced to 0.5 mL by a nitrogen stream before GC/MS analysis.

Analyses were by a GC/MS system with a GC 6890N (Agilent Technologies) installed with a capillary column (HP-5ms, non-polar column, 30 m x 0.25 mm x 0.25 μ m, Agilent Technologies) coupled with a MSD 5973 (Agilent Technologies) and controlled by the MSD Productivity ChemStation software (Agilent Technologies). One μ L of sample was injected into a splitless inlet at 250°C. The sample was carried by helium gas at 35 cm/s and the mass range from 50 to 550 m/z was scanned. The oven temperature was programmed from 50°C (initially held for 1 min) to 100°C at 25°C min⁻¹, followed by 100°C to 350°C at 5°C min⁻¹ and at the end the temperature was maintained for 5 minutes. The NIST Mass Spectral Library – G1033 was used for species identification.

Two-stage treatment by ozonation in pressure cycles and sand filtration

The SPW was treated by a new ozonation technique involving pressure cycles as well as by conventional bubbling ozonation for comparison. Ozone was generated by an ozone generator (Model T-816, Polymetric Corp.) from dry, filtered air at 100 V.

Different ozone flowrates at 5, 10, and 20 L min⁻¹ were used, corresponding to gas phase ozone concentrations of 0.52%, 0.29%, and 0.16% (v/v), respectively, as determined by Indigo colorimetric method (Hoigné and Bader 1982). Bubbling ozonation was carried out in a 2-L beaker containing 1.8 L of water. Solution pH at 11 was maintained by manually adding 4-M NaOH solution. Pressure-assisted ozonation (i.e., ozonation in pressure cycles) was performed at room temperature of 23±2 °C in a closed reactor of stainless steel as previously described (Hong et al. 2008). The pressure reactor featured a gas vent, a pressure gauge, and a magnetically coupled stirrer at the top and an inlet and an outlet at the bottom (Figure 1). To start, the reactor was loaded with SPW to be treated; a pressure cycle began with the compression stage when the inlet valve was opened to allow entrance of an O₃/air mixture driven by a compressor (GAST) at the desired flowrate. The gas passed through a diffuser plate at the reactor bottom and through the liquid to pressurize the closed headspace to reach a designated pressure (e.g., 690 kPa or 100 psi); once the designated pressure was reached, the pressure was released via rapid venting by opening the outlet solenoid valve at the reactor top. The time for compression to reach designated pressure depended on the headspace volume and gas flowrate (e.g., reaching 150 psi in 28, 15, and 7 s at 5, 10, and 20 L/min, respectively); the time for decompression varied with gas venting rate but typically in 2 – 3 s. The pressure cycles could be repeated as many times as prescribed. During ozonation, the magnetic stir operated at about 60 rpm. At the conclusion of pressure cycles, the water was allowed to sit for 3 min following pressure release. Additionally, a 2-stage treatment for SPW was tested that consisted of a first stage involving ozonation in pressure cycles followed by sand filtration and a second stage repeating the tandem

processes once. The sands were of 0.25 – 0.42 mm. The circular sand filter was of 10 cm in depth and 9 cm in diameter operated at 6 cm/min via vacuum.

RESULTS AND DISCUSSION

Physicochemical Treatment of Synthetic produced Water – Ozonation and Sand Filtration

Table 1 shows the SPW before and after various treatments. Before treatment, SPW was highly turbid (200 NTU) with total and dissolved CODs at 320 and 48 mg/L, respectively, and sheen appearance was obvious at the water surface. Both soluble COD (i.e., COD of filtrate through 0.45 μm filter) and total COD were measured; while soluble COD was mostly indicative of dissolved oil, the total COD represents both dispersed and dissolved oils. Subjecting the SPW to pressure cycles with O_3 at different numbers of pressure cycles and flowrates (effecting different compression times to reach 100 psi) resulted in varied degrees of changes in pH, turbidity, CODs, and presence or absence of sheen. As shown, desirable outcomes would occur when sufficient compression time and pressure cycles were used, eliminating sheen appearance at 1 h and 1 d following treatment. As BOD_5 could provide an indication of biodegradability, it was measured following treatment and compared to total COD; higher BOD_5/COD ratios were achieved under favorable treatment conditions.

Effluent quality improved when ozonation in pressure cycles was followed by sand filtration (SF) (bed depth of 10 cm, diameter of 9 cm, and filtration rate of 6 cm min^{-1}). For example, results of No. 14 with SF showed improvements over those of No. 5 without SF in terms of turbidity (21 vs. 100

NTU), total COD (73 vs. 150 mg/L), BOD_5/COD (0.58 vs. 0.48), and sheen formation (negative vs. positive after 1 h). The effectiveness of oil removal was further examined by a 2-stage ozonation-sand filtration process in which the treatment of ozonation by pressure cycles and sand filtration was repeated once more. The 2-stage ozonation-filtration process showed significant improvements in turbidity, total COD, BOD_5/COD , and sheen formation (e.g., No. 18 demonstrated turbidity of 2.1 NTU, total COD & sol. COD of 59 & 55, respectively, BOD_5/COD of 0.58, and absence of sheen after 24 h). Figure 2 shows pictures of SPW before and after the 2-stage treatment process. It should be noted that ozonation treatment increased soluble COD, which indicated increased dissolved hydrocarbons that were likely organic acid products from ozonation of dissolved oil. The changes in total and soluble CODs showed a change in water compositions, i.e., a decrease in dispersed oil and increases in water-soluble organic acids. Apparently, these organic acid products placed lesser strain on the biodegradability of the treated SPW, as indicated by a higher BOD_5/COD ratio of 0.58.

Chemical Conversion by Ozonation in Pressure Cycles

Figure 3 shows chromatograms of major species in the SPW before and after different treatments. These species were extracted by non-polar solvent hexane and tentatively identified by GCMS as long-chain aliphatic compounds with C-C double bonds, but were not authenticated. After 10 min of bubbling ozonation at ambient pressure, there were little changes or slight decreases in the SPW's contents. After 50 min of like treatment, significant conversions of the aliphatic compounds to aldehydes as oxidation products while the bulk of

hydrocarbons and their long chains remained. However, when the SPW was ozonated in 30 pressure cycles completed within 20 min, all of the long-chain hydrocarbons disappeared, suggesting that the non-polar crude oil compounds might have been degraded or converted into polar hydrocarbon products that were not extractable by hexane. Thus, the treated SPW was further extracted by SPE method and analyzed. Figure 4 shows chromatograms of compounds as extracted by SPE before and after ozonation in pressure cycles. Before ozonation, relatively small amounts of hydrocarbons were collected by SPE (lowest line), and increasing hydrocarbons were collected with 20 and 40 cycles of ozonation (middle and upper lines, respectively). These products were hydrophilic compounds that were absent in the hexane extract but collected by SPE. Among the compounds tentatively identified by GCMS were compounds with keto, hydroxyl, and carboxylic groups.

Mechanism of Heightened Removal

Ozonation in pressure cycles appears to be more effective than conventional bubbling ozonation in converting non-polar hydrocarbons to hydrophilic compounds that are more amenable to removal by sand filtration. We attribute the heightened interaction of ozone with hydrocarbons to the appearance of expanding microbubbles during pressure cycles:

1. “Sweeping” of contaminants: During compression the bulk of ozonation gas dissolves into water, saturating it under pressure (e.g., 7 atm); during decompression the now oversaturated gas exits the liquid phase by formation and growth of microbubbles throughout. The expanding gas-liquid interface of microbubbles acts to “sweep” the water

body thoroughly and accumulate contaminants at the interface.

2. Confluence of contaminants and O₃ at the interface: To fill the expanding gas volume of microbubbles during decompression, O₃ molecules are drawn across the interface where hydrophobic and amphiphilic contaminants (i.e., dispersed and dissolved hydrocarbons) are accumulated. This results in heightened contact and reaction of O₃ with contaminants that otherwise exist at diffuse state throughout, thus leading to heightened ozonation treatment.
3. Non-polar droplets of suspended oil are converted at the surface into organic acid groups (e.g., carboxylic groups that can interact with one another via hydrogen bonding) that cause the small droplets to agglomerate and more readily retained by rapid sand filtration, thus providing rapid removal without prolonged ozonation treatment necessary for degradation.

Results of this work show that ozonation in pressure cycles when coupled with sand filtration provides an alternate technique for rapid removal of oil from process waters and prevention of oil sheen after discharge. Oil removal is primarily via chemical conversion that alters interfacial properties of the oil droplets, rendering them abatable by conventional sand filtration. A 2-stage system appears most effective in which the first stage with fewer ozonation cycles can target removal of the bulk of dispersed oil and the second stage with more ozonation cycles in converting the remaining dispersed and dissolved hydrocarbons to organic acids, thus lowering residual oil and eliminating sheen. It is anticipated that accumulated oil in the sand bed can be thermally regenerated (e.g., 550°C) and be available for redeployment.

REFERENCES

- Corrêa, A.X.R., E.N. Riepo, C.A. Somensi, R.M. Sperb, and C.M. Radetski. Use of Ozone-Photocatalytic Oxidation ($O_3/UV/TiO_2$) and biological remediation for treatment of produced water from petroleum refineries. *Journal of Environmental Engineering*. (In Press) doi:10.1061/(ASCE)EE.1943-7870.0000111
- ERIN Consulting Ltd. and OCL Services Ltd. Sheens Associated with Produced Water Effluents – Review of Causes and Mitigation Options. Environmental Studies Research Funds Report No. 142. Calgary. (2003) pp. 46.
- Hayes, T. and D. Arthur. 2004 Overview of emerging produced water treatment technologies. The 11th Annual International Petroleum Environmental Conference, Albuquerque, New Mexico, U.S.A., October 12-15, 2004
- Hoigné, J. and H. Bader. Colorimetric method for the measurement of aqueous ozone based on the decolorization of indigo derivatives. In: *Ozonization Manual for Water and Wastewater Treatment*, W.J. Masschelein (ed.). John Wiley & Sons. Inc., New York (1982).
- Hong, A., X. Cai, and Z. Cha. Pressure-assisted chelation extraction of lead from contaminated soil. *Environmental Pollution* 153 (2008), pp. 14-21.
- Klasson, K.T., C. Tsouris, S.A. Jones, M.D. Dinsmore, D.W. DePaoli, A.B. Walker, S. Yiaccoumi, V. Vithayaveroj, R.M. Counce, and S.M. Robinson. Ozone treatment of soluble organics in produced water. Petroleum Environmental Research Forum Project 98-04. ORNL/TM-2002/5 OAK RIDGE NATIONAL LABORATORY, U.S. Department of energy contract DE-AC05-00OR22725. (2002).
- McCay, F. Development and application of an oil toxicity and exposure model. *OilToxEx. Environmental Toxicology and Chemistry*. 21 (2002), pp. 2080-2094.
- Reed, M. and S. Johnsen (Eds). Technology for Mitigation. In: *Produced Water 2: Environmental Issues and Mitigation Technologies*. Plenum Press, New York, 1996, 413-532.
- Simms, K., A. Zaidi, and O. Bhargava. Method Development and New Technology. In: *Produced Water: Technical/Environmental Issues and Solutions*, J.P. Ray and F.R. Engelhardt (Eds). Plenum Press, New York, 1992, 455-604.
- Sullivan, E. J., R. S. Bowman, L. Katz, and K. Kinney. Water treatment technology for oil and gas Produced water. Identifying Technologies to Improve Regional Water Stewardship: North-Middle Rio Grande Corridor, Albuquerque, New Mexico, U.S.A., April 21-22, 2004.
- Tibbetts, P.J.C, I.T. Buchanan, L.J. Gawel, and R. Large. Chemical Characterization. In: *Produced Water: Technical/Environmental Issues and Solutions*, J.P. Ray and F.R. Engelhardt (Eds). Plenum Press, New York, 1992, 97-174.
- Veil, J.A., M.G. Puder, D. Elcock, and R.J. Redweik, Jr. A White Paper Describing Produced Water from Production of Crude Oil, Natural Gas, and Coal Bed Methane. National Energy Technology Laboratory, U.S. Department of Energy contract W-31-109-Eng-38. (2004).

Walker, A.B., C. Tsouris, D.W. DePaoli, and K.T. Klasson. 2001. Ozonation of soluble organics in aqueous solutions using microbubbles. *Ozone: Science & Engineering*, 23 (1) (2001) pp. 77 – 87.

Yang, M and T. Nel. Oil in produced water analysis and monitoring in the North Sea. SPE Annual Technical Conference and Exhibition, San Antonio, Texas, U.S.A., September 24–27, 2006.

Table 1. SPW characteristics after sand filtration (SF) following pressure-assisted (PA) ozonation under different conditions (triplicate or quadruplicate results with std. dev. shown)

No. & Treatment	Flowrate (L/min)	Comp. Time (s)	Characteristics after PA treatment						
			pH	Turbidity (NTU)	Tot. COD (mg/L)	Sol. COD (mg/L)	BOD ₅ /COD Ratio	Sheen at 1 h	1 d
1 No treatment	-	-	6.9± 0.1	196± 13	325± 34	48±4	0.45	Y	Y
2 PA/air/10 cy	10	15	6.9±0.1	98± 11	142±23	42±7	0.45	Y	Y
5 PA/O ₃ /10 cy	10	15	6.2±0.2	101±10	152±17	50±7	0.48	Y	Y
8 PA/O ₃ /10 cy	5	28	5.8±0.2	55±8	120±9	52±4	0.48	Y	Y
11 PA/O ₃ /10 cy	20	6	6.4±0.1	124± 10	179±15	46±6	0.50	Y	Y
14 PA/ O ₃ /10 cy/SF	10	15	7.6± 0.2	21±4	73±14	48±3	0.58	N	Y (50%)
16 PA/ O ₃ /10 cy/SF & PA/O ₃ /10 cy/SF	10	15	7.6± 0.2	3.8±1.1	58±11	51±7	0.55	N	Y (25%)
18 PA/O ₃ /10 cy/SF & PA/O ₃ /20 cy/SF	10	15	7.5	2.1±0.3	59±8	55±6	0.58	N	N
20 PA/air/10 cy/SF & PA/air/20 cy/SF	10	15	7.6	79±8	112±11	38±5	0.51	Y (50%)	Y

Note: The notation of “PA/ O₃/10 cy/SF & PA/O₃/20 cy/SF” indicates pressure-assisted ozonation with 10 pressure cycles and then sand filtration, which is immediately followed by a 2nd stage ozonation with 20 pressure cycles and then sand filtration.



Figure 1. The feature of pressure reactor. There is a gas vent and a pressure gauge at the top, inlet and outlet at the bottom, and a magnetically coupled stirrer.



Figure 2. SPW before (left) and after treatment (right) by PA/O₃/10 cy/SF and PA/O₃/20 cy/SF (flowrate = 5 L/min).

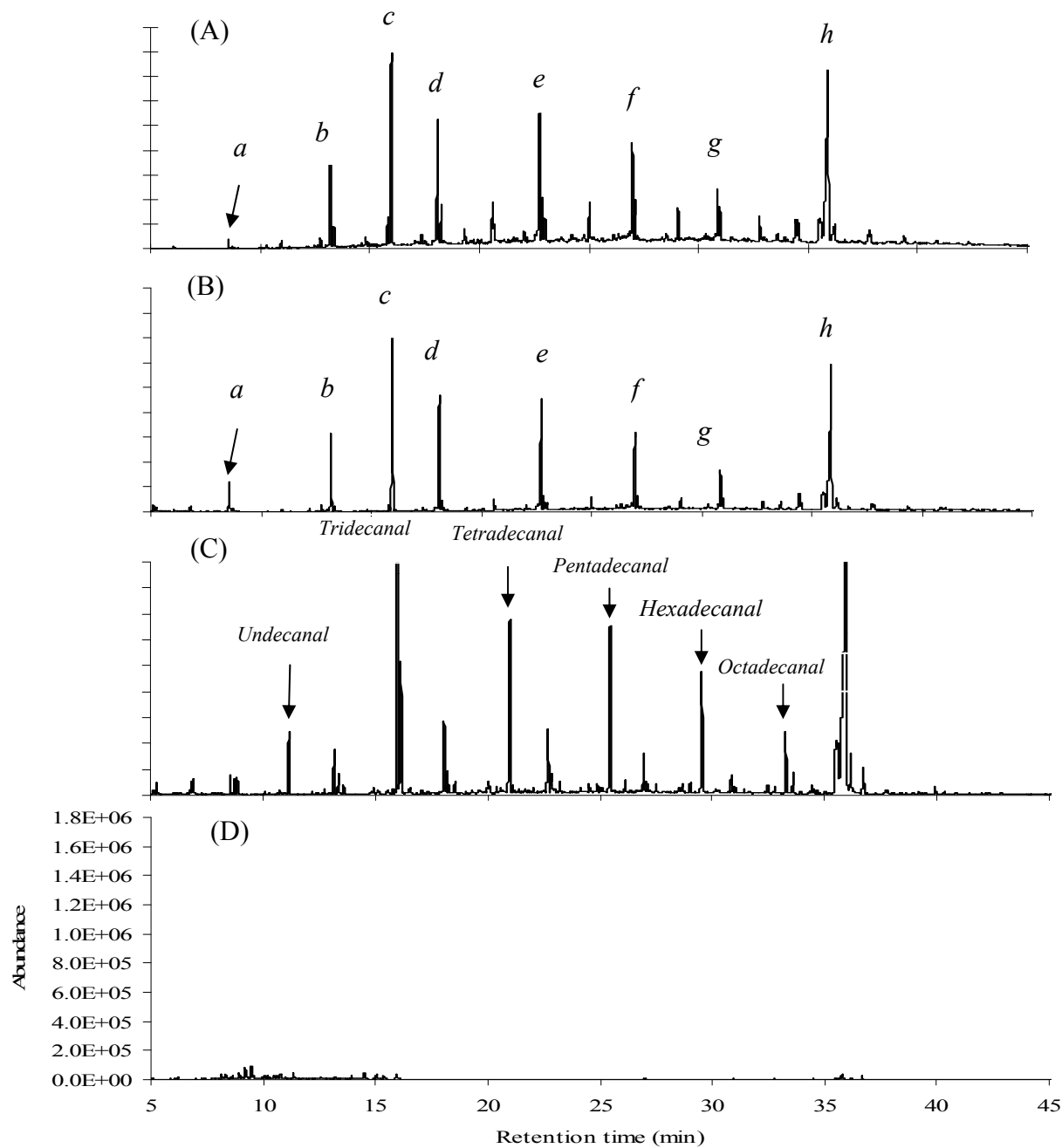


Figure 3. GC/MS chromatograms of hexane extractable organics in filtered SPW samples after various ozonation at 5 L min^{-1} flow rate: (A) No treatment, (B) bubbling ozonation (10 min), (C) bubbling ozonation (50 min), and (D) PC ozonation (30 cycles, ~19 min). Identified compounds: *a*, 1-dodecene; *b*, 1-tetradecene; *c*, 2,4-bis[1,1-dimethylethyl]phenol; *d*, 1-hexadecene; *e*, 1-octaadecene; *f*, 1-nonadecene; *g*, 1-decosene; *h*, diethylene glycol dibenzoate.

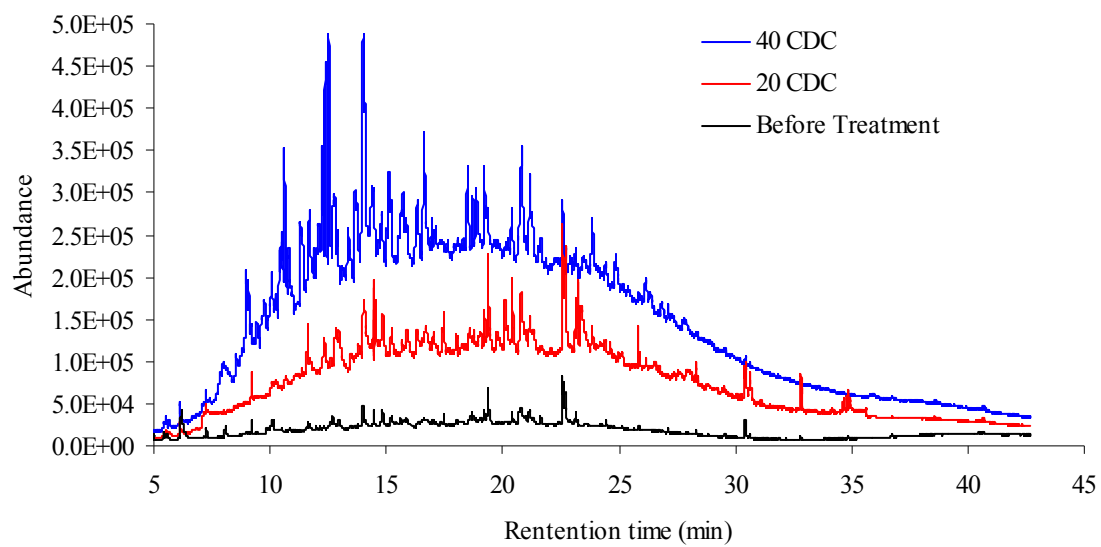


Figure 4. GC/MS chromatograms showing increasing abundance of hydrophilic organics as extracted by SPE method in SPW before treatment (lowest chromatogram), after PA/O₃/20 cy (middle), and PA/O₃/40 cy (upmost).

DETERMINATION OF PARTICLE SIZE DISTRIBUTION OF OIL SAND SOLIDS USING LASER DIFFRACTION METHOD

Robert Mahood, Jessica Norgaard and Tim Eaton

Shell Canada Energy.

Bill Liu and Mark Nixon

Golder Associates Ltd.

ABSTRACT: Sieve and hydrometer test method has been used to determine particle size distributions (PSD) of soil samples for over 70 years. It follows standardized sample preparation and testing procedures, which are rigorous but time consuming.

The oil sands industry has been exploring alternative testing methods in determining particle size distributions for the past two decades because of the large numbers of samples that must be processed for ore characterization. Laser diffraction method has been used as the main tool for particle size determination by some Oil Sand Operators as this method requires significantly shorter turn-around time compared to the sieve and hydrometer method. Particle size distributions from the laser diffraction method are converted to equivalents of the sieve/hydrometer method using correlations developed in a comparative study. Observations and anecdotal evidence during the early stage of the laser diffraction application seemed to suggest higher variations of the test results. A detailed study program was recently conducted to compare particle size distributions between the laser diffraction and sieve/hydrometer methods.

The results of the comparative study program are presented in this paper, together with discussions on the background of both the testing methods and the uncertainties associated with each method.

INTRODUCTION

In the field of geotechnical engineering, particle size distributions of soil samples have traditionally been determined using the sieve/hydrometer method. The oil sands industry has been exploring alternative methods of particle size analyses due to the large number of the samples that need to be tested for ore characterization and mine

planning (Cowles 2000) and to a lesser extent for geotechnical engineering requirements. Laser diffraction method is one of the alternatives that have been used to analyze particle size distributions in preference over sieve/hydrometer due to shorter turn-around time. However, it is recognized that this method is less commonly accepted by the geotechnical community. To assess the suitability of laser diffraction as a method for

particle size analyses, the method was compared against the more conventional and standard sieve/hydrometer methodology through a comprehensive testing program in which 290 samples were analyzed using both methods.

SAMPLE PREPARATION

Prior to sizing analysis, an oil sand sample is sampled to an approximately 100g-sample size. The sample undergoes a dean stark extraction (hot toluene extraction), to remove the water and bitumen from the solids. The hot extraction tends to leave the solids quite compacted and with a minor organic coating on the solids (making it difficult to disperse the extracted solids). Determination of particle size distribution in oil sand samples is challenging due to the need to remove the bitumen prior to particle size distribution analysis. Several methods can accomplish this, including Dean Stark, Soxhlet, "cold-wash" and "skimming the bitumen". Each of these methods may introduce errors into the respective method due to the possibility of fine matter being removed with the bitumen. This is an entirely separate issue and not discussed further in this paper.

The solid sample is disaggregated using a rubber pestle and mortar to break apart the aggregates, but preserve the original particle sizes as much as possible. At this stage it is common for many samples to be mixed together and then sub sampled further. Sub sampling of the oil sand solids is typically done using a Jones riffle splitter until the desired sample size is achieved. Samples will require further disaggregation once dispersed in the water and dispersant materials required for each sizing method.

SIEVE/HYDROMETER TEST METHOD (ASTM D 422-63)

The sieve/hydrometer test involves mixing a small amount of soil (30g to 50g) into suspension and measuring how it settles with time. The sample is disaggregated by mortar/pestle and soaked in concentrated aqueous dispersant. The slurry sample is processed in a mixer for further disaggregation. It is then placed in the sedimentation cylinder with additional water added to form a one-liter thin slurry. The sample is shaken and inverted for one minute; readings using the hydrometer are taken at set intervals for 24 hours. The sample is washed through a No. 200 sieve that retains sand particles greater than 75 microns. The particles are sieved through a sieve stack thus providing the percent passing of the coarse fraction and completing the full particle size distribution.

The hydrometer method is a weight based test where heavier (large) particles settle faster than lighter (small) particles, following Stokes Law. A hydrometer is lowered into the soil-water slurry and the buoyancy force of the slurry balances the weight and suspends the hydrometer. The amount of the hydrometer projecting above the suspending fluid is a function of the density of the slurry. As the soil particles fall the density of the slurry decreases, and as a result the hydrometer is suspended lower in the slurry.

The diameter of the particle at a certain time is calculated based on the viscosity of the slurry, the depth below the surface, the unit weight of the water and the specific gravity of the soil particles. There are several factors that can affect the overall particle size distribution of the oil sand solids using the sieve/hydrometer methods including:

- The ASTM procedure is intended for soil samples. The hot toluene extracted, disaggregated solids have different characteristics than undisturbed soil samples. These characteristics will apply to both a sample tested by the sieve/hydrometer method or the laser diffraction method when directly comparing testing techniques.
- Hydrometer readings require adjustments for the following:
 - The temperature of the slurry
 - The viscosity of the slurry
 - The location of hydrometer reading; hydrometers are calibrated to be read at the bottom of the meniscus, since that is not possible, readings are made at the top, the impact of this on the final result may be small.

There are two assumptions in the calculation of the hydrometer test using Stoke's law:

- 1) Particles are free falling spheres
- 2) The particles do not collide during the test

These assumptions could arguably cause the hydrometer test to overestimate clay sized particles (less than 2 microns) as clay particles may have large aspect ratios and would behave more like plates rather than spheres.

It is apparent that the results of the sieve/hydrometer test can be affected by sample preparation, variations of samples (soil vs. oil sand solids), room conditions and clay properties. These have been quantified as part of this study.

The sieve/hydrometer is a weight-based test that follows the Stoke's law, which assumes that the particles falling within the viscous

fluid are spherical and do not interfere with one another. The sieve component of the test does allow for possible overestimating of the smaller particle sizes as the sieve allows particles with high aspect ratios to pass through. A sieve/hydrometer test uses 30g to 50g, which allows for less chance of misrepresentation of any one-particle size than laser diffraction, as discussed below.

LASER DIFFRACTION TEST METHOD (ISO 13320-1)

The laser diffraction method works on the basis of a single particle of a sample passing through a fixed window of a laser while suspended in a liquid. When the particle passes by the laser, the light is diffracted around the particle. The size of the particle will dictate the diffraction pattern of the light. As such, this is a volume based test that is independent of the density of the particle. The laser diffraction apparatus does not measure the particle size directly; it measures the scattered light patterns and converts that pattern to particle size.

There are two algorithms that are currently used to convert the diffracted light patterns to particles size distributions; Fraunhofer theory and Mie theory (Wen et al. 2002). Conversion from light scattering data to particle size distribution assumes that particles are perfect spheres. Both methods stem from an analytical solution of Maxwell's equations for the scattering of electromagnetic radiation.

When particles pass through the window of laser for a set amount of time, the intensity of a certain sized light pattern dictate how many times that particle size has been measured by the laser diffraction apparatus. The number of readings taken by the laser diffraction apparatus adds a statistical element to the laser diffraction test.

Samples are prepared for laser diffraction testing (5g to 8g vials) using a similar procedure as sieve/hydrometer tests. A sub sample of the solids (half to one gram) is added to a small beaker with a surfactant to assist in water wetting the solids and a dispersant to ensure the solids are not re-agglomerating in the aqueous solution. The wet solids are gently mixed for further disaggregation and then added to a reservoir of water. The slurry is pumped through the laser diffraction machine, passing through the laser light window. The standard operating procedures (SOP) used by the technician dictate the pump rate, the amount of sonication and the duration of the test. The operating procedures also include the solid absorption (estimated or experimentally obtained) and refractive index properties that can affect the results of the laser diffraction test. Each of these parameters and operating procedures can vary within laboratories if guidelines for testing are not explicitly provided.

It is known that the results of the laser diffraction tests can be affected by variables including test apparatus (different pumps, attachments, models and brands), sample preparation, operating procedures and data analyses (algorithms and assumptions). It is known from historic laser diffraction testing in poorly controlled situations that these numerous variables can impact the repeatability and reliability of the test as a viable particle sizing technique.

Laser diffraction requires samples to be prepared with adequate care and diligence such that half to one gram of soil is representative of a larger sample. The relatively small sample size does not allow for inaccurate sampling (i.e. too many sand grains being scooped out of the vial). To overcome the small sample size, routine duplicate runs are required to ensure that sub sampling technique is repeatable.

Laser diffraction is a relatively recent method of measuring particle size distributions, compared to sieve/hydrometer that has a longer history of application (since the first ASTM publication in 1935). Laser diffraction is a statistical based test that is established upon the physics of light and the results are independent of the specific gravity of the particles being tested. The particles are assumed to be spheres in order to solve the analytical equations that convert scattered light patterns into particle sizes (Campbell 2003). The laser diffraction test averages the particle size based on spherical volume as any particle passes through the laser enough times that each face of the particle will be measured. The laser diffraction test is supported by an International Standards Organization (ISO) document, ISO 13320-1, which was first published in 1999. ASTM has supported the light scattering method for metal powders since 1992 (ASTM B822) where it states that “although each type of testing equipment uses the same basic principles for light scattering as a function of particle size, different assumptions pertinent to application of the theory, and different models for converting light measurements to particle size, may lead to different results for each instrument. Therefore, the use of this test method cannot guarantee directly comparable results from different types of instruments.” This statement regarding the use of light scattering methods for metals would appear to also apply to the use on soil solids.

DIRECT COMPARATIVE STUDIES

A testing program was conducted to directly compare the sieve/hydrometer and laser diffraction test methods using 290 disaggregated core samples. Each of the samples was sampled (using a Jones riffle splitter) to generate two sub samples of equal characteristics, one for laser diffraction and

one for sieve/hydrometer. The laser diffraction testing of the 290 samples was completed using a single laser diffraction machine and operating procedures; the sieve/hydrometer test was completed at one laboratory using the ASTM procedures.

The results of the laser diffraction and sieve/hydrometer testing are compared at discrete points along the particle size distribution curve. The percent passing for the two testing methods are plotted against each other at 150, 80, 44, 22, 10, 5, and 2 microns (see Figures 1 – 7). Each of the scatter plots of laser diffraction percent passing versus that of the sieve/hydrometer test includes a 1:1 line which helps to identify whether a trend is noticeable at a given particle size.

There is a close correlation, near one to one, between the two testing methods for each of the particle sizes compared. There is a trend of laser diffraction reporting slightly higher percent passing at 80, 44, 22, 10 and 5 microns than sieve/hydrometer. At 150 and 2 microns the trend is of laser diffraction reporting slightly lower percent passing than sieve/hydrometer.

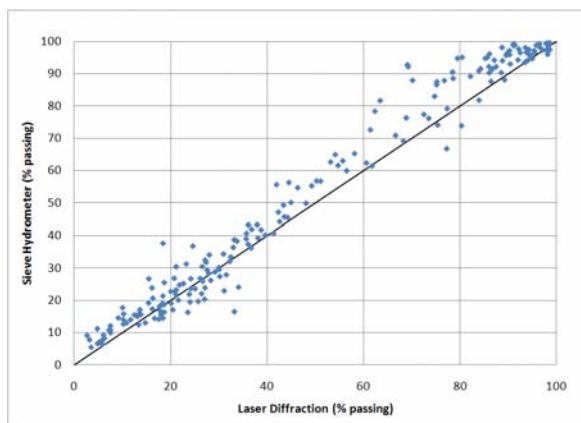


Figure 1. Sieve Hydrometer versus Laser Diffraction for 290 samples at 150 microns.

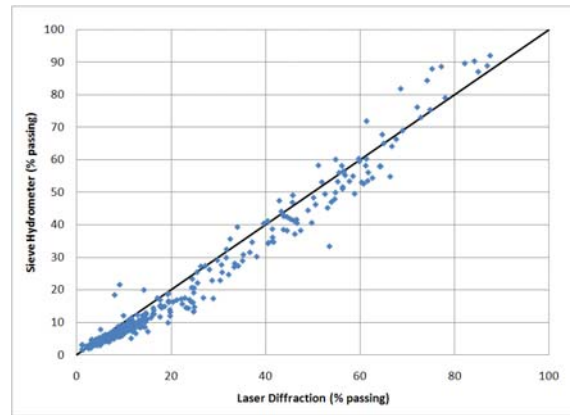


Figure 2. Sieve Hydrometer versus Laser Diffraction for 290 samples at 80 microns

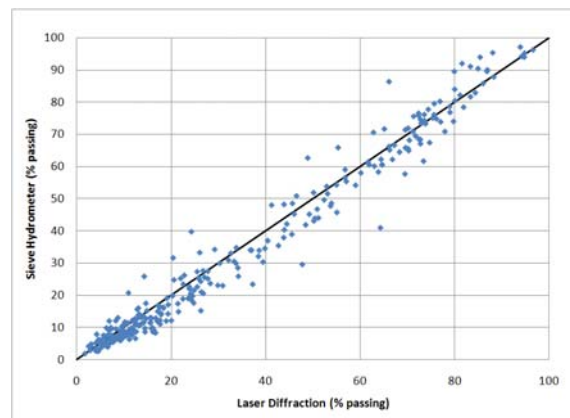


Figure 3. Sieve Hydrometer versus Laser Diffraction for 290 samples at 44 microns

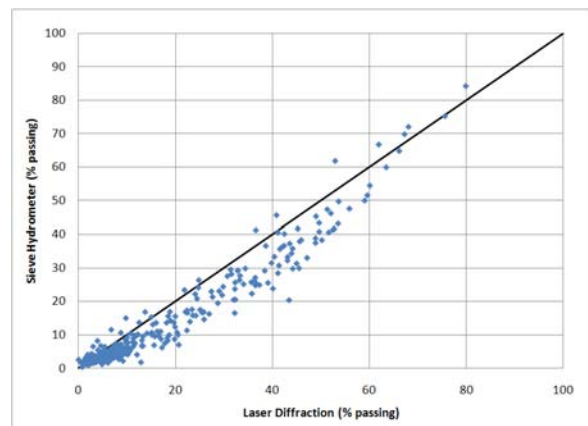


Figure 4. Sieve Hydrometer versus Laser Diffraction for 290 samples at 22 microns.

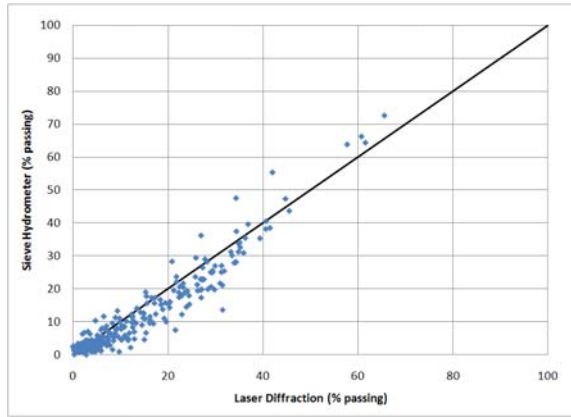


Figure 5. Sieve Hydrometer versus Laser Diffraction for 290 samples at 10 microns.

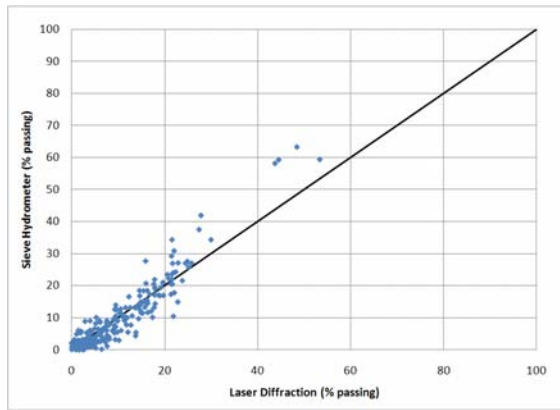


Figure 6. Sieve Hydrometer versus Laser Diffraction for 290 samples at 5 microns.

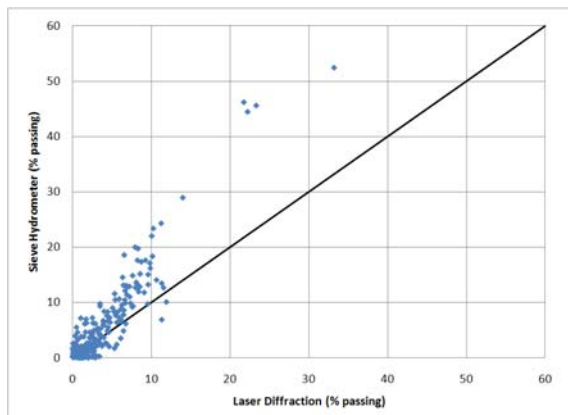


Figure 7. Sieve Hydrometer versus Laser Diffraction for 290 samples at 2 microns.

Frequency plots of the difference in percent passing of sieve/hydrometer minus laser diffraction are shown on Figure 8 - 10. The differences are broken into 2 percent passing intervals.

The frequency plots of the difference between sieve/hydrometer and laser diffraction illustrate a normally distributed curve, centred near zero displaying a good correlation between the two test methods. The trend of sieve/hydrometer returning higher percent passing can be seen at 2 microns, with the median of the dataset being positive. At 80 and 44 microns the bell curve appears to be centred on the negative side of zero indicating that at these discrete particle sizes the laser diffraction returns a larger percent passing than the sieve/hydrometer.

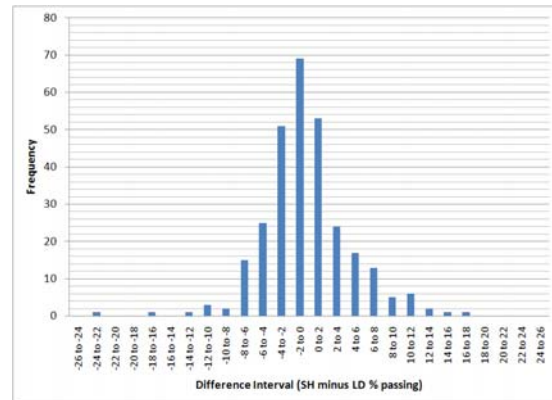


Figure 8 Frequency distribution of difference of percent passing sieve/hydrometer minus laser diffraction at 80 microns

SUMMARY

Due to the large number of samples that need to be analysed for particle size distributions in oil sands development, it is often preferred to use an alternate method to the traditional sieve/hydrometer method that can complete particle size analyses quickly, efficiently and accurately. A direct comparison of sieve/hydrometer and laser diffraction on 290 samples suggests that the two methods

can generate comparable results. Under controlled conditions, the laser diffraction method can return similar results to sieve/hydrometer at particle sizes greater than 2 microns, suggesting that laser diffraction can be a suitable alternative for particle size analyses of solid oil sands samples.

the laser diffraction test method needs to be effectively managed through implementation of consistent sample preparation and testing procedures, training of operating personnel, enforcement of QA/QC procedures, and on-going comparison between different laboratories and testing methods.

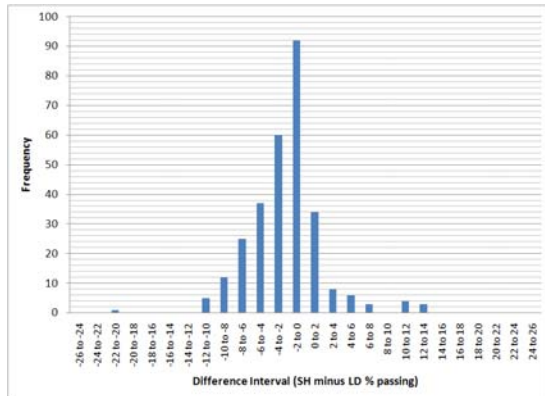


Figure 9. Frequency distribution of difference of percent passing sieve/hydrometer minus laser diffraction at 44 microns

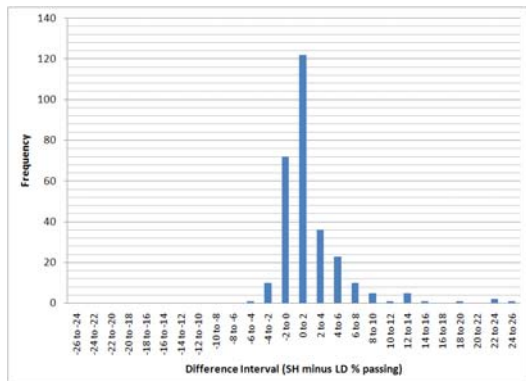


Figure 10. Frequency distribution of difference of percent passing sieve/hydrometer minus laser diffraction at 2 microns

Variations in testing procedures, equipment type/model and settings, sample preparation, and small sample sizes are some of the factors that impact the accuracy and consistency of the laser diffraction results. The variability of

REFERENCES

ASTM Standard D422-63, “Standard Test Method for Particle-Size Analysis of Soils,” ASTM International, West Conshohocken, PA, United States.

ASTM Standard B822 – 02, “Standard Test Method for Particle Size Distribution of Metal Powders and Related Compounds by Light Scattering,” ASTM International, West Conshohocken, PA, United States.

Campbell, J., 2003, “Limitation in the laser particle sizing of soils,” *Advances in Regolith, Cooperative Research Centre Landscapes Environments and Mineral Exploration*, Canberra Australia.

Cowles, R., 2000, “Particle characterization for oil sand processing, particle size measurement by laser diffraction,” *Petroleum Science and Technology*, Vol. 18, 203-220.

ISO International Standard 13320-1, 1999, “Particle size analysis – laser diffraction methods,” ISO, Geneva, Switzerland.

Wen, B., Aydin, A., and Duzgoren-Aydin, N., 2002, “A comparative study of particle size analyses by sieve-hydrometer and laser diffraction methods,” *Geotechnical Testing Journal*, 2002, Vol. 25, No. 4.

ACKNOWLEDGEMENTS

We would like to acknowledge the following people whose valuable assistance was instrumental to this study. Mohamad Audel with Shell Albian Sands provided the samples from the Muskeg River Mine. John Innis with Shell Mine Development selected the

remaining samples. Nancy Renaux with Shell Global Solutions Analytical Chemistry was a key team member as Nancy was the key interface with Golder to provide samples as well as the data that was compiled in a transparent manner that expedited the study. All of the staff at the Golder soils laboratory.

BREAKTHROUGH RESULTS IN OILSANDS PROJECTS

A. Siddiqi

Bantrel, Calgary, Alberta, Canada

ABSTRACT: Recently, major projects have been running into serious difficulties. Projects are running over budget, behind schedule, and fail to meet stakeholder expectations. Tailings projects have the additional demands of complying with regulations with tight deadlines. This additional demand puts enormous pressure on project execution timelines, which inevitably results in cost escalation, if not properly managed.

Therefore, to properly manage project execution and achieve **Breakthrough** results in the process the following project aspects should be considered:

- Thorough front end planning (EPC execution strategies)
- Getting the initial estimate right (Balancing Board demands for ROI with execution realities)
- Project Manager/ Director leadership style (Right decisions at the right time) and the decision making process
- Empowered Project Execution Team

Some of the benefits associated with implementing the above factors are:

- Reduced costs,
- Improved schedule performance,
- Improved quality, and
- Yes, delivering “**Breakthrough**” results

INTRODUCTION

Market research indicates that approximately 79% of major Oil Sands projects (projects with a total cost of \$500 million or more) miss at least one of their key targets, either they are:

- Not on time,
- Not on budget, or
- Not delivering what they’ve set out to do

Upon project completion it is quite evident which project requirements were met, and which were not. In the case of failed projects aspirations to save costs, meet or beat the schedule, deliver excellent quality and a safe optimum producing plant are confronted with the stark reality of cost overruns, being behind schedule, delivering poor quality, an unsafe site, an unfriendly operating facility and less than expected production. And it doesn’t take long for these failures to hit the rumour mill, with the media benefiting at everybody else’s expense. Unfortunately, the

result is that senior management loses credibility in the eyes of analysts and shareholders, and worst of all the morale of team members goes down the tubes.

The primary challenge, then, for project management is to achieve all of the project goals and objectives while managing the preconceived project constraints.

The key is to realize that project management is an “ART” as well as a “SCIENCE”. While 79 % projects have missed the mark, 21 % have not. In my project management experience, which includes executing billion dollar projects in the oil sands, it feels good to stand before you, knowing that my team and I have consistently managed project constraints. Every time it happened we called it a **Breakthrough**. This paper will explore the **Breakthrough** Execution Model and the key factors, which lead to success in project execution. The focus of this paper is to deal with the “ART” side of Project Management; I look forward to sharing the “SCIENCE” side of the equation with you in the future.

Project management is the discipline of planning, organizing, and managing resources to bring about the successful completion of specific project goals and objectives. A project is a temporary endeavor, having a defined beginning and end, usually constrained by date, undertaken to meet particular goals and objectives, usually to bring about beneficial change or added value.

In 1950, the modern Project Management era began. Project management was finally, formally recognized as a distinct discipline in the management arena. Prior to the 1950s, projects were managed on an ad hoc basis.

With the rapid growth of the Oil Sands in Alberta and the need to execute major projects, Project management expertise was in high demand, as it was recognized that for multi-billion dollar projects to be successful right project management was the key. However, the question arises, is there a right template or business model to achieve success? The answer is **yes, there is..**

BREAKTHROUGH MODEL

Let’s consider the example of Jane an expert pianist. She was not always an expert. The first thing Jane did was learn the basics. Second, she practiced playing piano for a long time. Playing Piano made Jane a master in understanding the potential for each key and each stroke. With a strong mindset, Jane succeeded in creating beautiful music and breakthrough tunes. To create a new tune you require a mind set of “going beyond.”

Keeping this analogy in mind, I have tried to capture the key strokes of Project management and developed the following **Breakthrough** visual.

What is a **Breakthrough**? A **Breakthrough** is an extraordinary accomplishment, which despite being viewed as unrealistic or unlikely by stakeholders at the time, goes beyond stakeholder expectations.

We need to do it different to achieve different results. The discussion which follows provides a brief description of each element of the **Breakthrough** model.

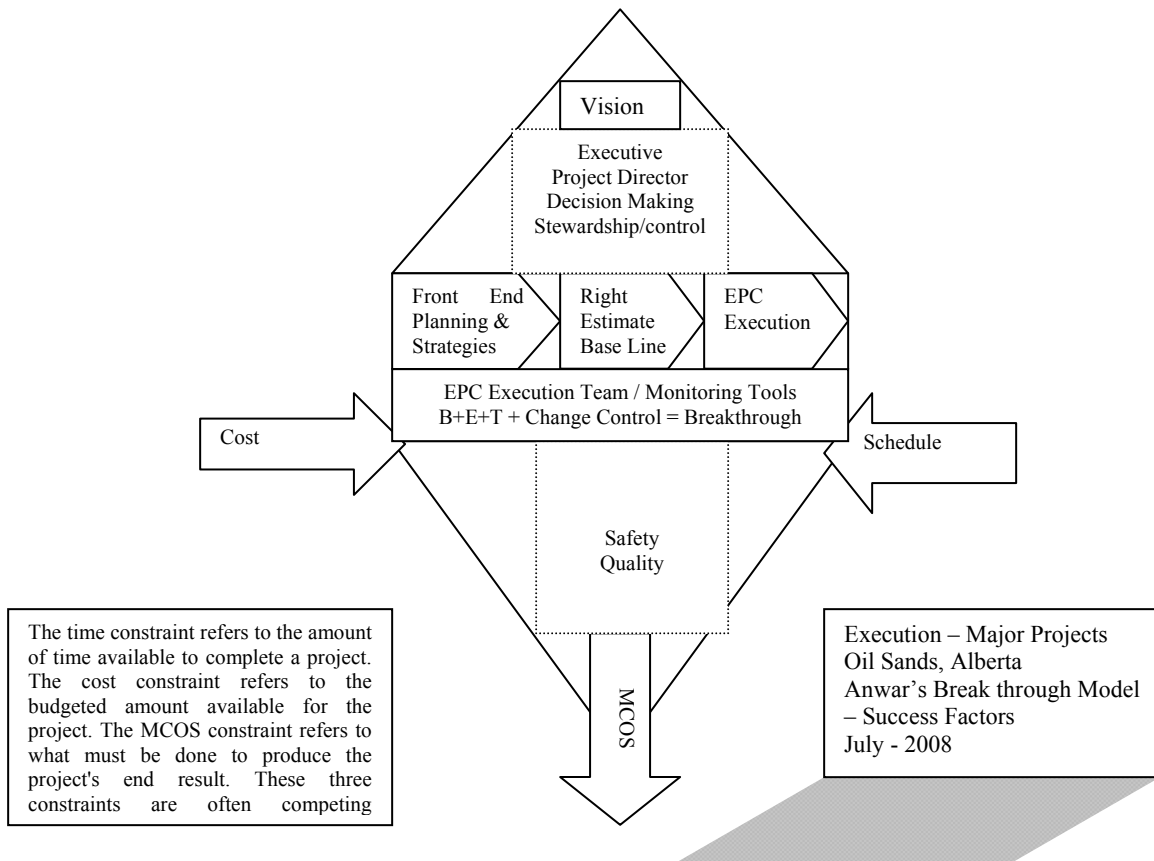


Figure 1. Model-Break Through in Major Projects Execution

“The definition of insanity is doing the same thing over and over again, and expecting a different result “
Rita Mae Brown

VISION

Executive

The Executive’s role is to provide a broad vision and strategic direction, rather than setting specific management initiatives. The Executive identifies the parameters of the sand box, and leaves the invention of sand box games to the Project Director and his team.

The seed for success or failure is sown at the Executive level. The Executive sets everyone for success through the following key factors: vision statement, decision making process, delegating authority to the appropriate levels of management, endorsing front end planning/strategies, and appointing a competent project director along with key team members. During project execution, it is imperative that any strategic changes in these key factors are communicated to and approved by the Executive.

Project Director

The Project Director is accountable for executing the Executive's vision and accomplishing the stated project objectives.

The Executive must exercise due care and diligence in choosing a competent Project Director. A great Project Director must be knowledgeable, reputable, and a good decision maker who delivers results through his team. In other words, the Project Director must know how to skilfully play the piano (you know what I mean...).

The Project Director is so critical to the success of the project that often the project takes on the same personality as the Project Director.

“Looking like a winner “Regardless of how you feel inside, always try to look like a winner. Even if you are behind, a sustained look of control and confidence can give you a mental edge that results in victory “ Arthur Ashe

Pick battles enough to matter, small enough to win Jonathan Kozol

FRONT END PLANNING & EXECUTION STRATEGIES

Proper front end planning (“FEP”) enhances project execution in all-subsequent phases of a project. Experience confirms that the time spent in FEP is time well spent. Almost always cost overruns and schedule delays have their roots in inadequate FEP. Proper FEP is one of the best investments to guarantee successful project completion.

Further, proper FEP defines:

- Project drivers/objectives,

- Project MCOS (Minimum Conditions of Satisfaction), and
- EPC strategies (Engineering , Procurement , Construction including Contracting)

These FEP/EPC strategies need to be well thought out, along with naming the project organization, and developing roles and responsibilities.

The Project Director, collaborating with the project team, should initiate the EPC execution plans in a timely manner.

The EPC execution plan must align with the project objectives, and is a:

- Tool for strategic planning;
- Means to get all the parties involved, working as a team;
- Living document;
- Communication tool for internal and external stakeholders;
- Guidepost for state-of-the art project management execution; and
- Baseline against which changes are measured.

Proper FEP ensures consistency in execution, coordination, project control, and communication.

“Nothing is really hard if you divide it into small jobs” Henry Ford

RIGHT ESTIMATE

It cannot be overemphasized how important it is to get the estimate right, on which appropriations are made. It sows the seed for success and failure. All too often, for whatever reason, the Executive expect estimates to be low. Perhaps this need is driven by stakeholder desire to achieve high ROI, or the need to get a speedy approval.

This mind set is unintentionally communicated to the team resulting in lower estimates than what reality demands.

A low cost estimate combined with constant changes in scope, fluctuating commodity prices, changes in execution strategies and schedule delays (including winter impacts in Northern Alberta) result in increased execution costs. That's why it's so important to get the initial estimate right. Unneeded focus on justifying cost increases debilitates and demoralizes an already overextended project team.

Thus, it is of utmost important to get the Initial Estimate (that is both the base line cost estimate and schedule) right (neither too high nor too low). Additionally, a high level of analysis should be undertaken to ensure that the estimate is reasonable; and a management reserve should also be allotted to take into account potential uncontrolled changes. These amounts should be included in ROI calculations and should be considered when making investment/cap-ex decisions.

EPC EXECUTION & S-T-R-E-T-C-H TARGETS

EPC Execution is the process of implementing activities as per the FEP and baseline estimate, in accordance with budget and schedule objectives. A stretch target is the process whereby one develops the mindset to surpass these objectives and thereby increases the probability of achieving the same.

People don't like to set goals because they don't like to fail. But we get through by setting goals. Go to push the envelope to find out how far you can go.

The key is to set stretch targets, and to work diligently each and every day to achieve them.

EPC EXECUTION TEAM (Breakthrough)

The challenge here is how we get eagles to fly in-sync. It is the Project Leader's responsibility to prepare, train and enroll the team into **Breakthrough** execution. Once the EPC team is enrolled and committed, a different behavior pattern emerges and the winning starts.

"There is a difference between interest and commitment. When you are interested in doing something you do it only when it is convenient. When you are committed to do something you accept no excuses, only results" **Kenneth Blanchard**

"Start by doing what is necessary, then what is possible and suddenly you are doing what is impossible" **St. Francis of Assisi**

Breakthrough = Behavior (B) + Experience (E) + Technology (T) + Change Control (CC). In other words, **Breakthroughs** = B+E+T + CC

Here are the basic steps:

1. Enroll - the team in the vision, strategies and plan. Thereby, setting the tone for a **Breakthrough** mindset.
2. Stick your neck out – publicly declare and commit to the results you will deliver
3. Lead by example- Inventories can be managed. People are led by example
4. Look for possibilities
5. Take actions – place yourself in the future and think back to the present.
6. Remove barriers

7. Live in the gap, scared
8. Recognize the breakdowns
9. Make decisions - be a leader.
10. Make it happen
11. Celebrate, and
12. Record lessons learned for the next job / team

Keep completion in mind, as it drives different behaviors. It is important to get complete even with failure.

When you have confidence, you're fearless. Confidence is contagious and the result is magnificent team accomplishment. Confidence also adds to your credibility. So, approach your project with greater confidence than you've ever had before. Work more easily under pressure. Make faster and better decisions. Get greater commitment from your entire staff. And do far more to achieve your project goals within the frame work of your organization's overall objective and EPC Execution plan.

Monitoring Tools

Monitoring and controlling consists of those processes performed to observe project execution so that potential deviations from their plan can be identified in a timely manner and corrective action can be taken. The key benefit is that project performance is observed and measured regularly to identify variances from the project execution plan.

Utilizing the best tools for EPC execution, cost control and schedule control will allow us to timely identify deviations or departures from the baseline.

Change Control

Change is a normal and expected part of the EPC execution process. Over the course of EPC execution, the work scope, time frame

requirements and key personnel change very often. Changes can be the result of necessary design modifications, differing site conditions, material availability, contractor-requested changes, value engineering and impacts from third parties, to name a few. The change needs to be documented and approved as per project approval matrices. The impact to cost, schedule, scope and quality must be evaluated and communicated in project reports, on a monthly or quarterly basis, depending on the nature and magnitude of the change. During the process of Change Control, it is important not to lose sight of the initial project parameters and targets set in FEP.

Training / Communication

Projects that succeed regardless of changing conditions are the ones that provide their people with the right training and development opportunities to match the challenge of any given project condition.

A successful manager communicates clearly and effectively; works well within a team; and is comfortable with leadership, the planning process and the terms and execution of Projects. Goals that are not written down are just wishes. We need to get out of our comfort zone, set goals, set stretch targets, stick our neck out, make public declarations, make promises, commitments and deliver.

MEETING MCOS (Minimum Conditions of Satisfaction)

Delivering MCOS with respect to plant production targets, along with meeting safety, cost, schedule and quality will be the best gift for everybody involved in the project. It does not only give self satisfaction at all levels but makes the company, community and oil sands industry better.

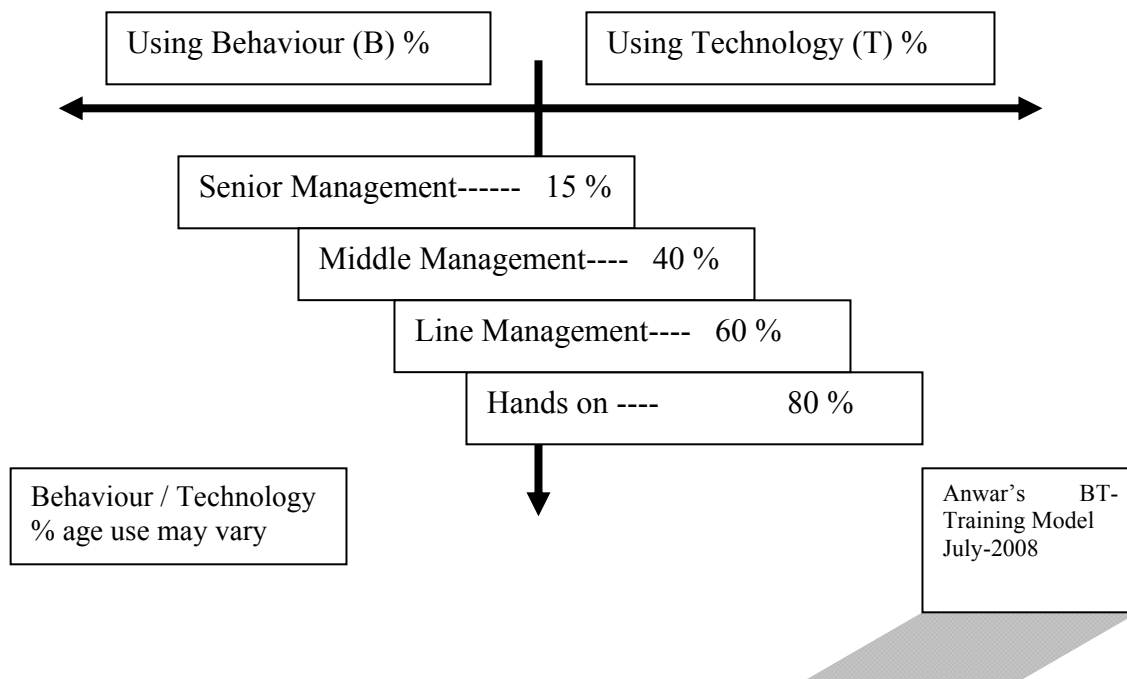


Figure 2. Behaviour/Technology Training Model

CONCLUSION

These are the lessons I have learned during the past few decades in executing major projects in the Oil Sands. My experiences have convinced me that ownership pays and credibility works.

Although many projects have been managed well, *“The most exciting breakthroughs of the 21st century will occur not because of technology, but because of an expanding concept of what it means to be human.”*

To summarize, if we need to narrow down the scope of this paper to the 4 most significant insights, they would be:

1. Ensuring that the Right Estimate is developed;
2. Selecting the right Project Director for the job;
3. Fostering a Breakthrough Mindset for execution; and

4. Realizing of what it takes to appropriately train different levels of management.

To attain success the project team should develop a unique culture that fosters communication, job ownership and trust amongst team members. Following the model of behaviour % and technology %, appropriate trainings programs will need to be organized for Executives, senior management and project team members so that they can effectively and predictably deliver on project requirements (i.e., safety, schedule, cost, quality, smooth start-up, commissioning, MCOS) and of course deliver **Breakthrough** results.

A new tune will be created and a mind set will be there for “going beyond”.

SAFELY DELIVERING QUALITY WITHIN COST & SCHEDULE CONSTRAINTS

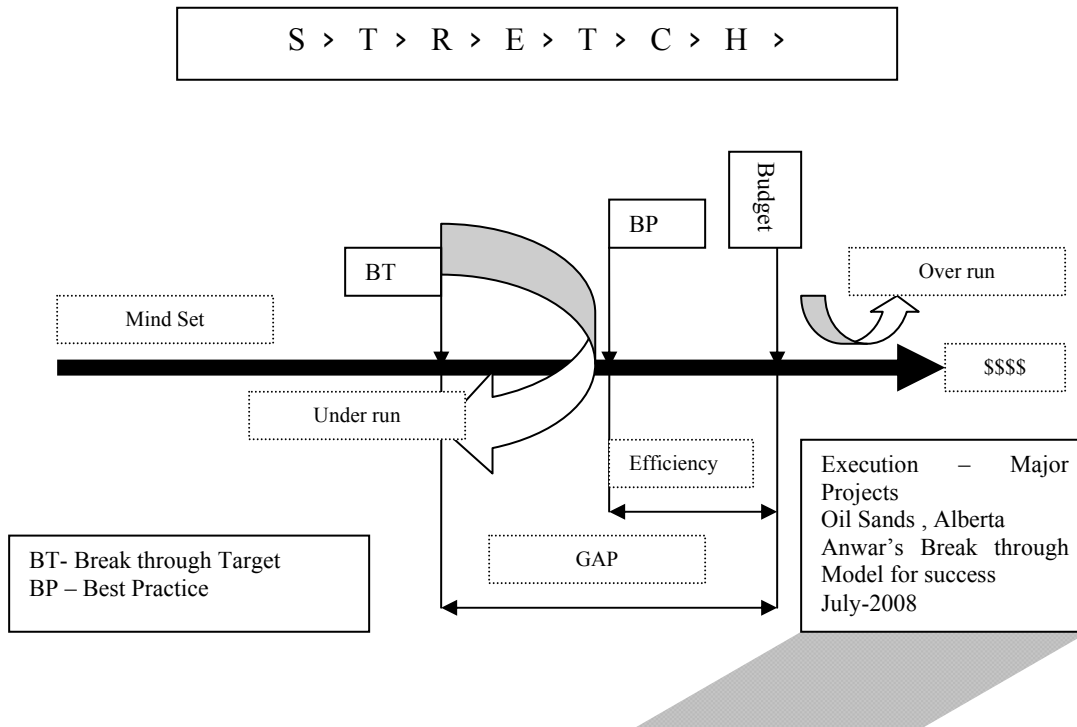


Figure 3. Setting Stretch Targets, Break Through Performance

“You can let it happen, make it happen or wonder what happened” Tommy Lasorda

Envision it, Lead it, drive it, deliver it – Make it happen

FUTURE WORK

1. Today we explored the fundamental “Art” of Project Management. Although there is also a “SCIENCE” to Project Management, in order to do justice to this topic I will continue to work on detailed approaches

ACKNOWLEDGEMENTS

1. Faraz Siddiqi , Contracts Manager – North American
2. Faisal Siddiqi , Projects Control Lead – Worley Parsons @ Shell job
3. Sumair Siddiqi, Mgr. Projects Control - Aecon
4. Murray Smart , senior vice president Retd. – Syncrude Canada Ltd.
5. John McVey , senior vice president – Bantrel Canada

Tailings and Mine Waste Management II

A NEW, DYNAMIC, INTERNET- BASED MINE SITE WATER AND SOLUTE MANAGEMENT TOOL

James R. Kunkel and Victor Lishnevsky
Knight Piésold and Co., Denver, Colorado, USA

ABSTRACT: Water and solute management at a mine site are critical components for environmental permitting, mine facility design and operation, and mine facility closure. A new, dynamic, Internet-hosted model uses site specific daily and monthly climatological data, site-specific operational conditions, such as loading plans, filling curves, leaching curves, upset solute concentrations, financial targets, reclamation needs, and other mine site properties. The model provides the ability to enter actual operational and climatological data, automatically verifies input data, and provides interactive process schematics that allow the user to easily identify pipelines, ponds, plants, heaps, waste-rock piles, tailings storage facilities, open pits and other mine facilities. Model results are provided in three formats: color-coded summary tables, graphical outputs, and spreadsheet formats. The model can be run for both short-term (60 days of operation) and long-term (many years of operation) and can be operated with a user-designated design storm event and a probabilistic analysis to estimate water volumes and solute mass and concentrations from various mine facilities.

This Internet-hosted model has been applied to several complex mine projects throughout the world. Our contribution to modeling of mine facilities predicts water volumes and solute concentrations in a deterministic and probabilistic format. The advantages of having the model hosted on the Internet are that (1) access can be from any computer connected to the Internet, (2) the model only requires an Internet browser to run, and (3) technical people in different locations can simultaneously run the model and view output. The model can be set up to run automatically and email results to users in order to provide early warning of possible system upsets or uncontrolled releases. The Internet code is efficient (programmed in ASP), gives simulation results in seconds, and multiple scenarios can be quickly modeled. Operational decisions based on actual values or probabilities can be made in real time.

INTRODUCTION

A dynamic water and solute management tool (Knight Piésold Minder™) is one which accounts for the water and solute components of a mining process in a stepwise fashion on a reasonably small time step, utilizing site-

specific climatological and operational information. Many water balances have been prepared using spreadsheet applications, which have many limitations. Depending on the complexity of the system and the life of mine, it is not unusual to exceed the number of fields and records supported by a single

spreadsheet and the formula length supported by a single cell. Some analysts try to utilize Monte Carlo stand-alone models to add sophistication to the water balance and to overcome the limitations of spreadsheet models. However, these models are often cumbersome, run slowly, and cannot manage the large amounts of water and solute information typically used in a dynamic model. Stand-alone models often require more troubleshooting and more on-site support.

The Internet-hosted model proposed herein accounts for water and solutes primarily in an operational mode, but also can be used for initial sizing and design of the process components. Trautwein (2009) suggests that water and solute balance tools must have the following nine features: (1) a process schematic; (2) complexity; (3) climatological and process information; (4) functionality; (5) performance; (6) output; (7) maintenance; (8) value; and (9) extensibility. The Internet-hosted model Knight Piésold Minder™ provides these features in an easy-to-use, fast running package.

Rather than try to assign cumulative probability or probability density functions to *a priori* to the climatological and process variables, the Internet-hosted model performs many equally likely runs resulting in many equally likely outcomes, which are then analyzed in a *posterior* fashion using probability theory to provide the potential operational risk to the operator or owner.

The purposes of an operational water and solute management tool include: (1) to establish optimal and cost-effective pond storage and water treatment or make up (where applicable); (2) to identify flows to and from the heap/tailing facility allowing for appropriate sizing of process circuit pipelines; (3) to identify solute concentrations at various locations within the process circuit; (4) to

identify potential fluctuations in the process circuit over time to aid forecast planning; (5) to quantify potential flow and volume of treated and make up water in order to calculate associated costs; and (6) continuing permit compliance. Each of the nine features of the Internet-hosted water and solute management tool listed above are explained by an example problem.

PROCESS SCHEMATIC AND COMPLEXITY

For purposes of this paper, the example for the water and solute balance model will be a heap leach operation with an open pit mine, and SX-EW metal recovery. The basis of the operational and solute management model is shown on a complex schematic as Figure 1. Not all schematics must be complex.

Figure 2 shows a much more simplified process schematic which may be sufficient for operational water and solute management, especially during pre-feasibility.

If the water and solute management model appears to be too complex, most people agree that it is never utilized in the operation of the process. The beauty of an Internet-hosted model is that it offers a simple user interface which requires minimal input information (the complex “stuff” is already programmed in) which is easily changed or updated as operating data become available.

THE WATER AND SOLUTE MANAGEMENT MODEL

The water and solute management model is a computer program which is set up on the Internet. Precipitation runoff, plant site water, the heap leach pad and ponds, outside source makeup water, pit dewatering, water supply requirements will all be components in the

site-wide model. Knight Piésold's philosophy of design, operation and closure of water and solute management modeling is that (1) all possible climatological and operational scenarios should be considered; (2) operational considerations will govern the "best" design for our clients; and (3) client interaction is important to understanding the "best" design or operation.

The traditional water balance model often seeks to find a "critical period" of wet or dry climatological sequences which result in a "maximum" pond storage volume or a "minimum or maximum" water demand using a systematic climatological record and identifying the critical periods by assuming that the historical record will repeat itself. Hydrologists often use synthetically generated time series of climatological data to extend the historical record and use these synthetic sequences to identify a critical period, a maximum or a minimum pond size, or other operational variable such as makeup water volume. The problem with this approach is that the designer usually does not know when the project will come on line in relation to the historical record. To avoid this pitfall, Knight Piésold uses a more robust approach.

The basic assumption of letting the historical climatological record repeat itself over the life of the project is still used. However, the water and solute management calculations begin in each year of the historic climatological record. This method results in the same number of water and solute computational runs (or cases) as the number of years of climatological record. The data for the years prior to the start date will be transposed to the end of the cycle so all analyses will be for the full period of record. In this way, sequences of wet and dry years which occurred historically are still preserved; however, the initial project start date could be in any year.

Results of this type of analyses guarantee that the critical period (maximum or minimum) will be found, if one assumes that the historical climatological record repeats itself, or if a synthetic time series is used. We then estimate the *posterior* probability of a specific operationally-caused event (such as a given makeup water demand) occurring once or more during the project's life. This probability includes the operational and climatological components of the process water balance rather than an *a priori* probability climatological input.

Because the Internet-hosted computer program calculates the flow rate or volume and solute concentrations for all of the facilities of interest, outputs by facility or process (such as makeup water, solute concentration, or total discharge water) are available. Because each of these outputs is associated with an identically distributed random realization, the probability of the flows, concentrations, or volumes for each can be estimated. This will allow the operator/owner to make informed decisions related to the risk at a given facility. Some typical processes which are often of use to owners/operators are: pond sizes (volume in m^3), metal concentrations (g/L), and quantity of makeup or return water (m^3/hr).

Figures 3 through 5 show the computational process schematically for a 33-year period of monthly climatological data and a 6-year mine life.

CLIMATOLOGICAL AND PROCESS INFORMATION

Climatological Inputs

The climatological inputs include not only the daily or monthly precipitation, evapotranspiration, air temperature, and other data, but also runoff curfew numbers, heap

loading sequences, leaching curves, and upset limits for pond storage, solute concentrations and other data that will serve as “alarms” during the simulations. Based on experience with many similar heap leach projects, we have found several areas that require additional analysis such as the effects of increasing precipitation with elevation, runoff factors, and storm event precipitation values.

More specifically for example, the daily 24-hr precipitation data will be used to establish storm events for various return periods. Since the 24-hour precipitation can fluctuate significantly from month to month, storm events were also calculated on a monthly basis. This is more appropriate for the project than applying annual data because annual data tend to be overly conservative in some months and because the specific operational conditions change on a monthly basis (e.g., where loading and leaching are occurring, solution flow rates, pond fluctuations, etc.). An example of the variation in 24-hr precipitation by month is shown on Table 1.

Regression analyses are typically developed using the site and nearby site precipitation records to established long term, monthly design precipitation record for the site. Potential evaporation, evaporation from leached and unleached areas of the heap leach pad, and evaporation losses due to the method of application will be established based on theoretical equations which use the site precipitation and temperature data. Surface runoff and base flow from offsite and onsite areas are determined using the U.S. Natural Resources Conservation Service (NRCS) methodology.

Process Information

The operational and process parameters input in the water and solute balance model are very important for analyzing the process and predicting water requirements and solute

concentrations. These input parameters include physical characteristics of the heap ore (bulk density, porosity, hydraulic conductivity, gradation and other characteristics), loading rates, leach rates and recovery curves, solution application rates, ore moisture contents before, during and after leach, operational restrictions such as maximum flow rates, and the closure concepts. Additional data such as pit dewatering and water supply requirements are also be input into the model. If some data do not yet exist, these operational parameters are included in the water and solute management model as estimates which are changed as more data become available. How the model handles heap loading curves is shown on Figure 6; and how the model utilizes typical leach recovery curves are shown on Figure 7.

FUNCTIONALITY AND PERFORMANCE

Functionality

The Internet-hosted water and solute program can be utilized for both design and operation. For design the program is typically run on a monthly time step, but may be run on a daily time step as needed. The fully dynamic solute concentrations for metals recovery may require a daily time step to observe changes in recover. The advantage of the model is that many years of data may be run quickly and the probabilities calculated for given design variable to assess which variables are the most sensitive and where money should be spent in additional data collection such as metallurgy or mine planning for better loading plans, or evaporation data.

During operation, the model is typically run on a daily time step to predict over the next 60 days or so what the outputs will be. This provides the opportunity to run many “what if?” scenarios like “What if there is a 10 year

storm event next week?” or “What if my leaching curves change?” or “What if there is a one-month drought and makeup water is limited?”

During operation, data are typically collected on the process variables. The Internet-hosted model can provide easy updating of climatological and process data; especially leaching curves based on heap leaching history. The probabilities of consequences, as shown on Figure 8 for pond volumes with draindown over the mine life, given selected process or climatological data changes can be easily calculated. This will allow managers to make informed business decisions with minimal effort and training. Additionally, the Internet hosted model can be accessed anywhere one can log on to the Internet. Multiple users can be running the model at the same time.

Performance

The speed of the Internet-hosted model results in most analyses being completed in seconds even for long climatological records and complex process flow sheets. This makes a practical model for use in daily forecasting and futurecasting in the time frame of years, even using daily data.

OUTPUT

Outputs can include summary tables and graphs as shown on Figures 9 and 10 with color coding to indicate near overtopping of a pond, for example. Remote notification of exceedances via e-mail or alarm also can be part of the output.

Newer solutions provide a summarized “dashboard” with the ability to access more detailed output on demand. Spreadsheet-compatible exportable tables are available for

each process component (see for example, Figure 11.)

MAINTENANCE, VALUE, AND EXTENSIBILITY

Maintenance

Updating climatological data and changes in process logic are easily done via re-programming if needed. Stand-alone and Internet-hosted models offer similar results; however, stand-alone models often require more troubleshooting on individual work stations and more on-site support.

Value

The value of the Internet-hosted model is in its ability to avert failures such as pond overflows or lack of carry-over water in storage.

Extensibility

An Internet-hosted water and solute management model doesn’t end with avoidance of environmental and safety hazards. The proposed Knight Piésold Minder™ model allows the operator to quickly, accurately, and remotely (if necessary) forecast potential environmental and safety consequences.

CONCLUSIONS

The Internet-hosted dynamic water and solute management model is (1) powerful; (2) easy to use; (3) easy to deploy at a given site; and (4) cost effective compared to stand-alone models. In summary the model has the following features:

- Web-based application,

- Clients can avoid going back to consultant to make operational changes,
- Information can be shared online,
- Fast computations,
- Supports visualization,
- Easy to customize the system once the process logic has been developed,
- Programming language is not as limited as spreadsheet and other commercial solutions,
- Simple user interface,
- Export input data to make changes quickly in familiar spreadsheet applications,
- All code and data stored in single location,

- System accessible through web browser,
- Many users can use the system simultaneously,
- Same consulting effort as other solutions, and
- No annual software licensing fees.

REFERENCES

Trautwein, A., 2009, "Using water balance tools for site design, operation and expansion management," In: Tailings and Mine Waste '08, London: Taylor and Francis Group, ISBN 978-0-415-48634-7, pp. 265-268.

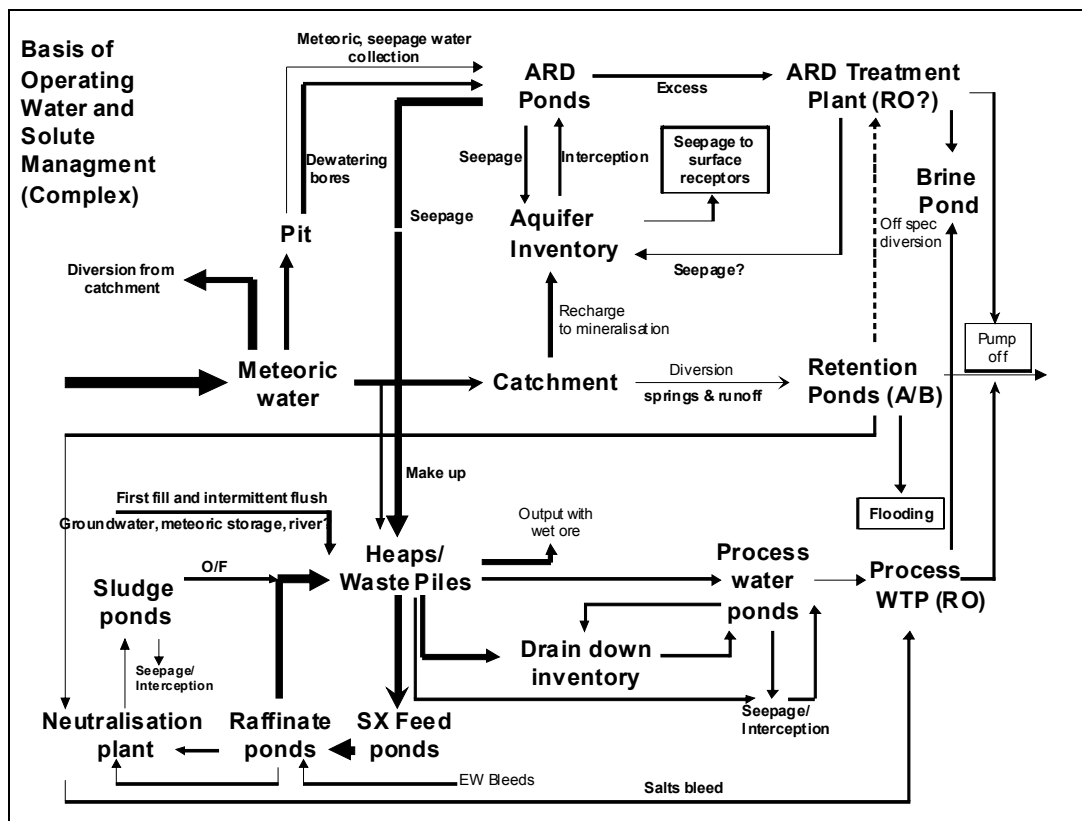


Figure 1. Complex Operational Water and Solute Management Schematic

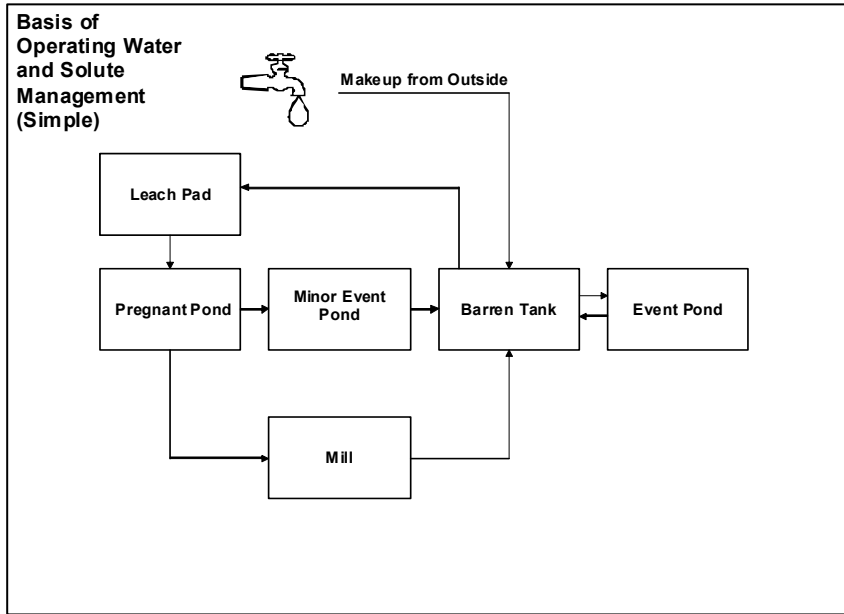


Figure 2. Simplified Operational Water and Solute Management Schematic

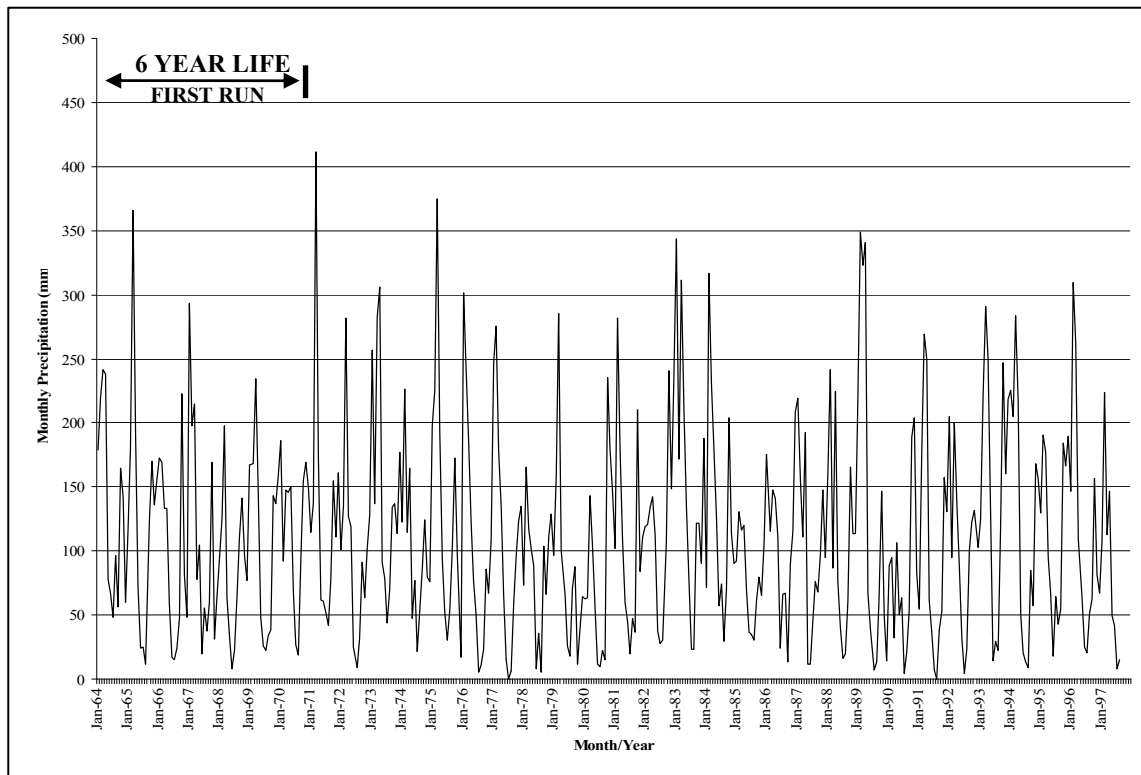


Figure 3. Computational Schematic for First 6-year Simulation

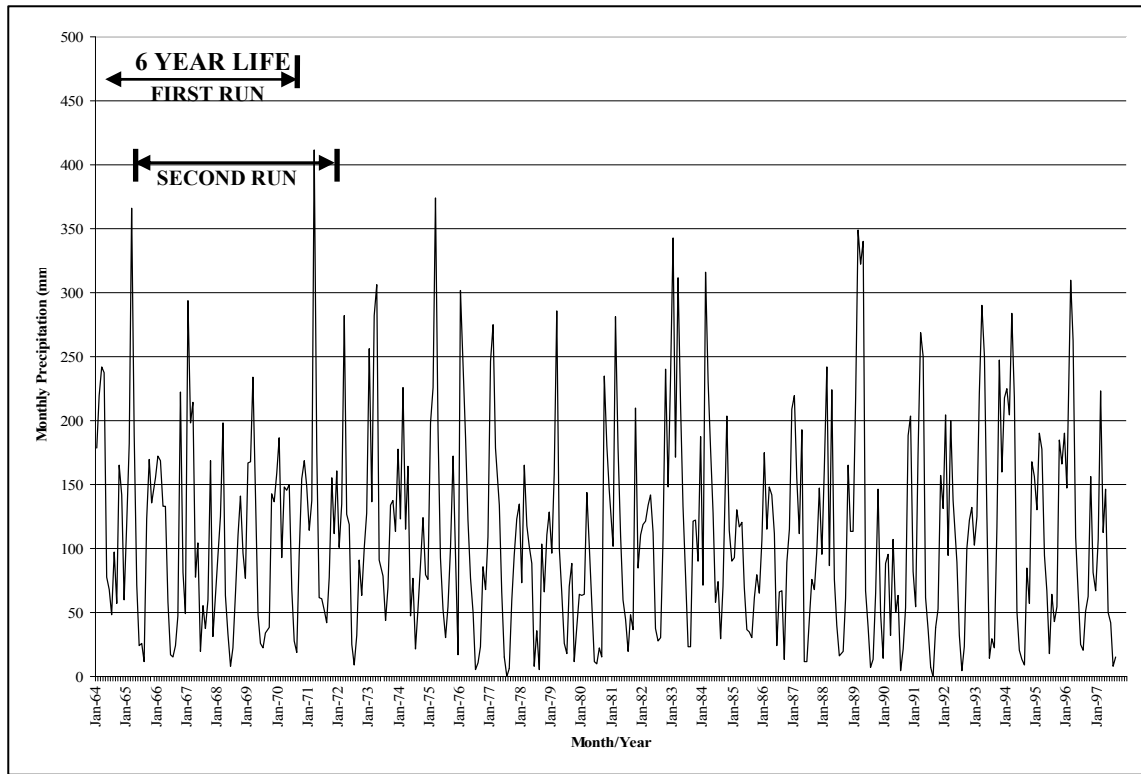


Figure 4. Computational Schematic for Second 6-year Simulation

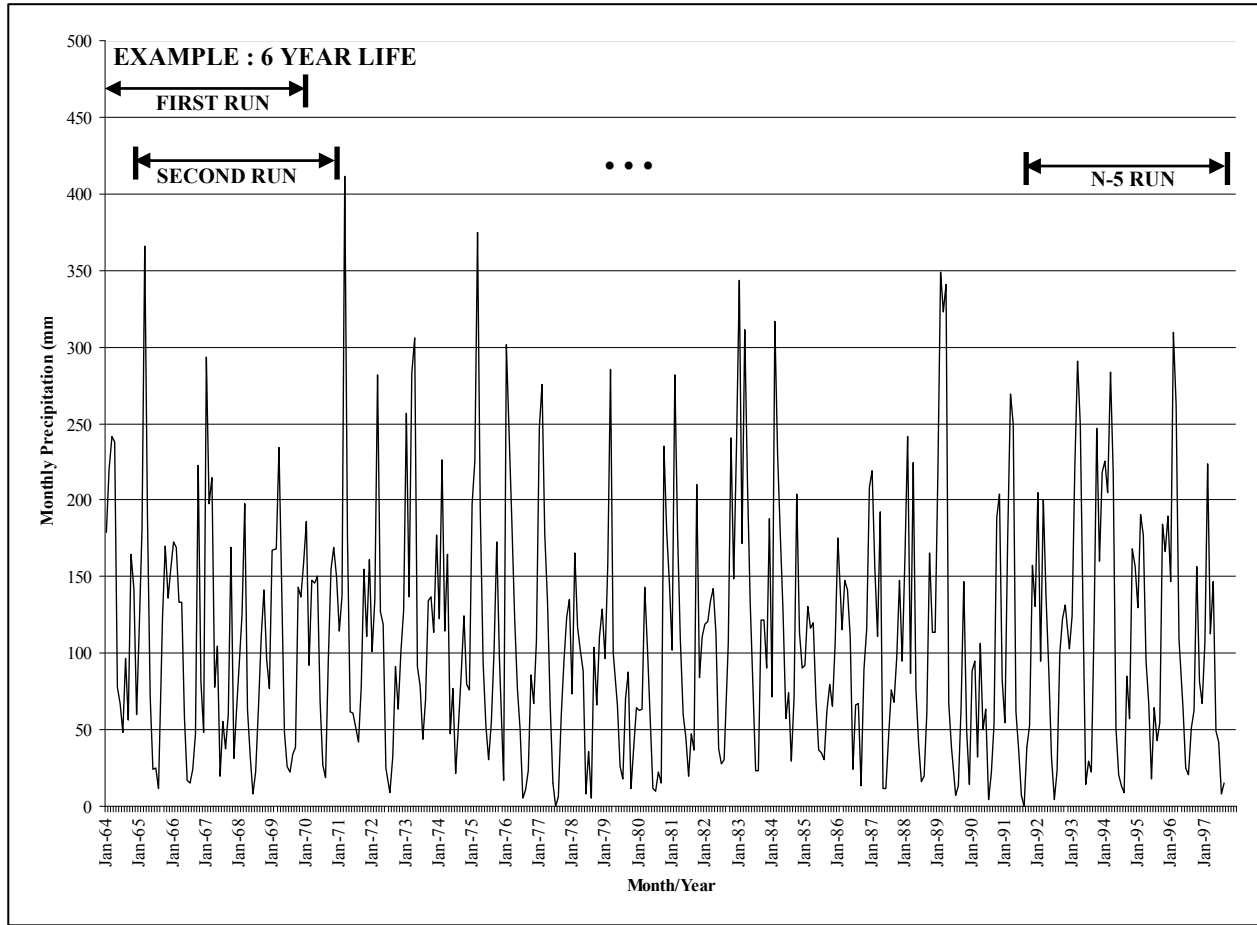


Figure 5. Computational Schematic for Nth 6-year Simulation

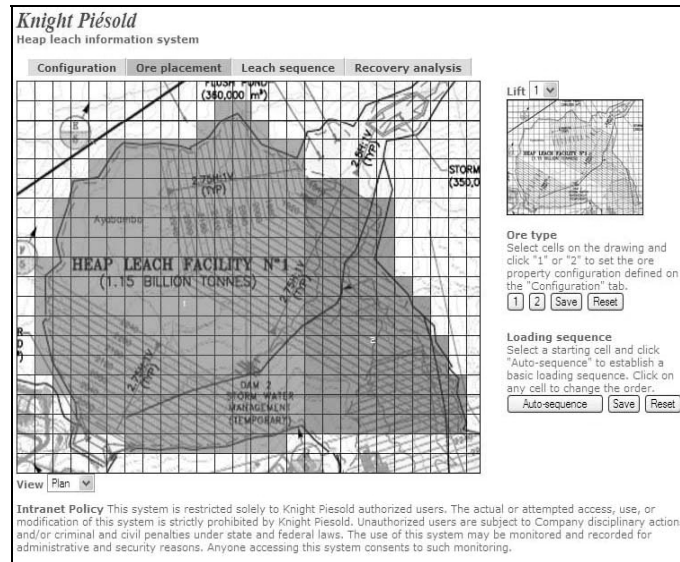
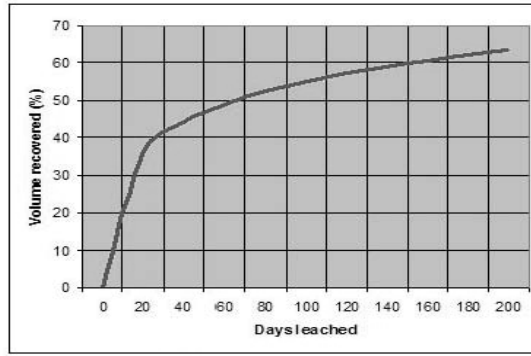
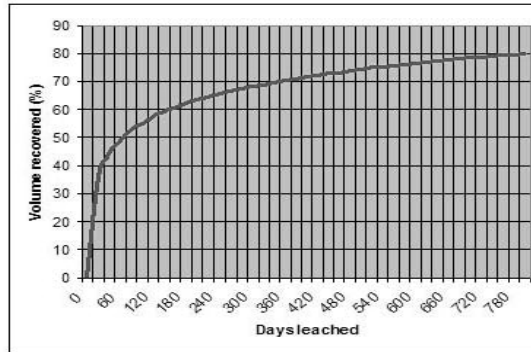


Figure 6. Typical Heap Loading Sequence



Recovery chart for Lift 1, Cell 3



Recovery chart for Lift 1-4, Cell 3

Figure 7. Typical Leaching Curves

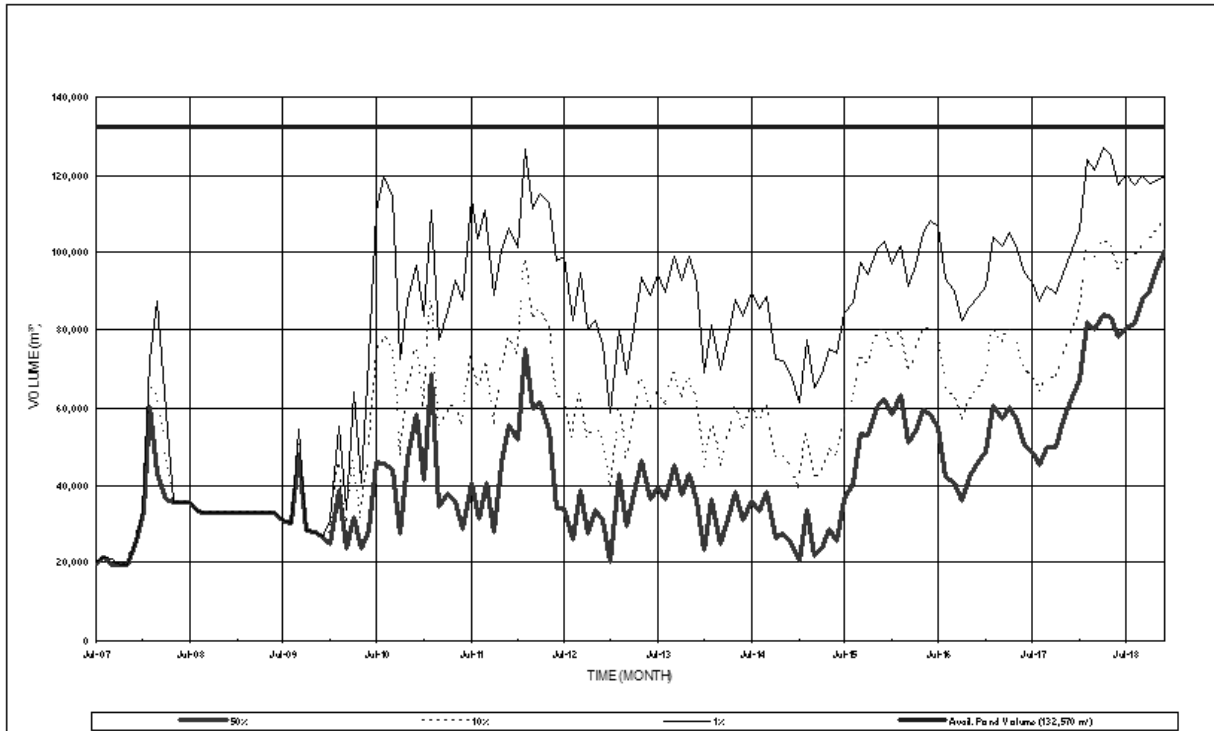


Figure 8. Probabilities of Pond Volumes with Draindown

Output	Minimum	Maximum
Sol From Barren Tank To Leach Pad (gpm)	0	1,000
Sol From Pregnant Pond To Mill (gpm)	0	1,000
Sol From Pregnant Pond To Minor Event Pond (gpm)	0	1,168
Sol From Minor Event Pond To Barren Tank (gpm)	0	1,171
Sol From Mill To Barren Tank (gpm)	0	990
Sol From Event Pond To Barren Tank (gpm)	0	813
Makeup From Outside (gpm)	0	806
Sol From Barren Tank To Event Pond (gpm)	0	1,177
Pregnant Pond Depth (ft)	1	2
Minor Event Pond Depth (ft)	2	2
Barren Tank Depth (ft)	1	2
Event Pond Depth (ft)	2	21

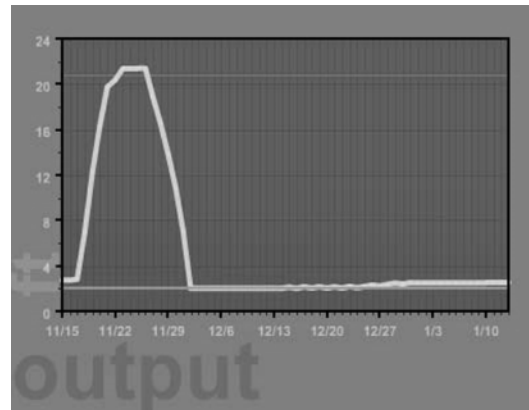


Figure 9. Example of Color-Coded Output

Figure 10. Example of Graphical Output

Water Balance Forecasting Tool		knight piésold minder™						
Demonstration Project								
Input		Short Term	Long Term	Gold Recovery	Manage	Help	Logout	
Gold		Solution	Export					
Date	Total solution flow (m ³ /hr)	Tonnes	Grade (g/tonne)	Contained gold (g)	Pregnant solution grade (mg/l)	Monthly gold recovery (g)	Total gold recovery (g)	Retained gold in solution (g)
08/09	377	10,986,914	1.50	21,650,720	0.3023	96,882	13,805,936	1,380,644
09/09	445	11,014,130	1.50	21,692,910	0.6115	200,637	13,840,523	767,591
10/09	451	11,042,253	1.50	21,733,733	0.6261	209,715	13,868,580	636,664
11/09	449	11,070,375	1.50	21,775,917	0.6451	211,932	13,895,152	576,425

Figure 11. Spreadsheet Compatible Exportable Table

Table 1. Monthly 24 Hour Precipitation Storm Event for Various Return Periods

Return Period	Jan	Feb	Mar	Apr	May	Jun	Jul	Aug	Sep	Oct	Nov	Dec	Annual
2-year	0.76	0.62	0.71	0.68	0.93	0.82	0.36	0.37	0.55	0.67	0.73	0.79	0.93
5-year	1.13	0.94	0.92	0.94	1.25	1.16	0.77	0.69	0.89	1.07	1.00	1.16	1.25
10-year	1.37	1.15	1.07	1.12	1.47	1.40	1.04	0.90	1.11	1.34	1.18	1.41	1.47
25-year	1.70	1.43	1.27	1.35	1.77	1.71	1.38	1.18	1.41	1.69	1.43	1.74	1.77
50 yr	1.94	1.63	1.42	1.53	1.99	1.94	1.63	1.37	1.63	1.95	1.61	1.98	1.99
100-year	2.18	1.84	1.58	1.71	2.22	2.18	1.89	1.58	1.85	2.21	1.80	2.23	2.23

USE OF THE HYDROGEOSPHERE CODE TO SIMULATE WATER FLOW AND CONTAMINANTS TRANSPORT THROUGH MINING WASTES DISPOSED IN A SYMMETRIC OPEN PIT WITHIN FRACTURED ROCK

Farouk Ben Abdelghani, Richard Simon and Michel Aubertin

École Polytechnique Dept of Civil, Geological and Mining engineering, Québec, Canada .

John Molson and René Therrien

Université Laval, Département de Géologie et Génie Géologique, Québec, Canada.

ABSTRACT: Mining wastes are usually disposed into open pits or underground excavations. The adjacent rock mass is often fractured with single fractures or fracture network. These discontinuities control flow of water and transport of contaminants from mining wastes. Numerical simulations have been carried out to assess the influence of joints on underground flow in and around symmetric mine openings. The influence of hydraulic regional gradient is also analyzed. Contaminant transport and unsaturated flow modelling was performed using HydroGeosphere, a 3D numerical flow and transport model (Therrien and al., 2005). A parametric analysis was conducted by simulating various 2D cases using experimentally obtained material properties and controlled boundary conditions. The effects of material hydraulic properties (i.e. the water retention curve and hydraulic conductivity function), fracture network characteristics, variable recharge rates and saturated hydraulic conductivity of the joints are investigated. The parametric analysis illustrates how water and contaminants may migrate around waste disposal areas created in fractured rock at mine sites.

INTRODUCTION

The mining industry contributes significantly to the economy of many countries throughout the world. Mining operations also generate significant volumes of wastes that must be managed properly to limit their environmental impact. Over the last few years, the mining industry and various governmental and research organisations have expended

significant effort to develop tools and geo-environmental methods to help improve solid and liquid waste management at mine sites, and to develop more effective rehabilitation strategies.

Quantitative studies of groundwater flow and solute transport in fractured media are now commonly conducted. These studies have been motivated by a variety of practical issues

including locating and evaluating water supplies and geothermal and petroleum energy resources. In addition, the search for safe storage of hazardous wastes, where the primary concern is the release of contaminants to the ecosphere through interconnected conductive discontinuities, has led to studies of low-permeability rock formations (e.g. Xu and Hu, 2005). Mining wastes are potential sources of contaminants that are sometimes disposed of in fractured rock masses. If the fracture network is sufficiently interconnected, water flow and contaminant transport can be significant. Describing the movement of solutes or chemicals in such domains is a major challenge.

In this paper, numerical simulations are presented using the 3D code HydroGeosphere (Therrien et al., 2005) for water flow and contaminant transport through mining wastes disposed of in symmetric open pits created in fractured rock masses. Results for two cases with different types of waste material are presented and discussed. The effect of a hydraulic regional gradient is investigated. The influence of an orthogonal fracture network is also presented and discussed. Finally, a scenario with a variable surface recharge is presented.

WATER FLOW AND CONTAMINANT TRANSPORT IN FRACTURED ROCK

Water Flow In A Single Fracture

Water flow in fractures is described by the ‘‘cubic law’’ which is an analytical solution of the Navier-Stokes equation for laminar and steady state water flow. It can be written as (Witherspoon and al., 1981; Tsang, 1984):

$$Q_f = V_f A_{sec} = -[\rho_w g b^3 w \Delta h / 12\mu_w L] \quad (1)$$

$$\text{where } A_{sec} = b w \quad (2)$$

- Q_f : fracture discharge (m³/s).
- V_f : mean water flow velocity in fracture (m/s).
- A_{sec} : area of fracture perpendicular to water flow (m²).
- b : fracture opening (m).
- w : fracture width perpendicular to water flow (m).
- L : fracture length parallel to water flow (m).
- Δh : hydraulic head difference along the flow direction (m).
- ρ_w : water density (kg/m³).
- g : gravity acceleration (m²/s).
- μ_w : water dynamic viscosity (kg/m/s).

Equation (1) was validated for laminar flow in microfractures composed of planar surfaces. This equation can be modified with additional parameters to take into account influence factors such as surface rugosity, tortuosity, and the Reynolds number (e.g. Gale, 1990; Indraratna and Ranjith, 2001).

For transient and partially saturated water flow conditions, eq.1 can be used to determine the continuity equation of flow discharge and the equation of partially saturated water flow in fractures (Wang et Narasimhan, 1993). Under these conditions, it is very important to correctly define the unsaturated hydraulic functions of the fracture and all materials used in the selected code.

Contaminant Transport

Contaminant transport in fractured rock is an important but difficult aspect to take into consideration due to the complexity of fracture networks and the role of fractures affecting contaminant migration.

For reactive and non-reactive contaminants the principal modes of transport are advection and mechanical dispersion. Advection is the contaminant migration by water flow in

response to a hydraulic gradient. Mechanical dispersion is the process of contaminant migration due to a concentration gradient and water tortuosity.

The general advection-diffusion equation for contaminant transport in fractures can be written as (Freeze and Cherry, 1979):

$$dC/dt = D_e(d^2C/dx^2) - q/n(dC/dx) \quad (3)$$

where C is the concentration, t is the time, q is the specific discharge (constant), D_e is the effective diffusion coefficient and n is the porosity. Typical values for D_e under saturated conditions in soils range between 1×10^{-9} and 2×10^{-9} m^2/s (Sharma and Reddy, 2004). The value of D_e takes into account the effect of tortuosity and can be related to the free solute diffusion coefficient D_0 by:

$$D_e = \zeta D_0 \quad (4)$$

where ζ is the tortuosity coefficient ($\zeta < 1$) and usually varies between 0.01 and 0.5 (Freeze and Cherry, 1979).

The Hydrogeosphere Code

The numerical model HydroGeosphere (Therrien et al., 2005) is used for simulations presented here. It is a three-dimensional control-volume finite element model that simulates variably-saturated subsurface flow and advective-dispersive mass transport in discretely-fractured or non fractured porous media. The model simulates flow and transport in three dimensions in the porous medium and in two dimensions in fractures. Variably-saturated flow is described by a modified form of Richards' equation, where the storage term is expanded to consider water and soil compressibility (Therrien and Sudicky, 1996). Fractures are idealized as two-dimensional parallel plates, implying uniform total head and concentration across the fracture width,

and flow velocities are determined by the cubic law (Witherspoon et al., 1980). Retention and relative permeability curves for both the fractures and the matrix are given either by van Genuchten's (1980) functions or they are specified in a tabular form, but hysteresis is not considered. In the model, the porous medium is discretized with 3D finite elements and fractures are discretized with 2D finite elements. The nodes forming the 2D fracture elements are common with nodes forming the 3D porous medium. It is assumed that there is continuity of hydraulic head and concentration in the fracture and matrix at these common nodes, which corresponds to instantaneous fluid and solute exchange between the domains. For solute transport, the effective diffusion coefficient for solutes in the matrix is given by the product of the free water diffusion coefficient and the tortuosity. Mechanical dispersion in the fractures and the matrix is described by longitudinal and transverse dispersivities. For transverse dispersivity in the 3D porous medium, HydroGeoSphere accounts for a horizontal and a vertical component.

SIMULATION OF A CONCEPTUAL OPEN PIT MODEL

Figure 1 presents the conceptual 2D model of an open pit simulated with the HydroGeosphere code. The open pit is symmetric about the axis at $x = 0$ m. It has a depth of 150 m and the wall slope is 68 degrees. The lower limit of the model is 200 m below the pit base. The left and right limits of the model are located respectively at -400 m and $+400$ m from the origin. Two types of mine wastes are considered: waste rock resulting from mining operation and tailings from the milling process.

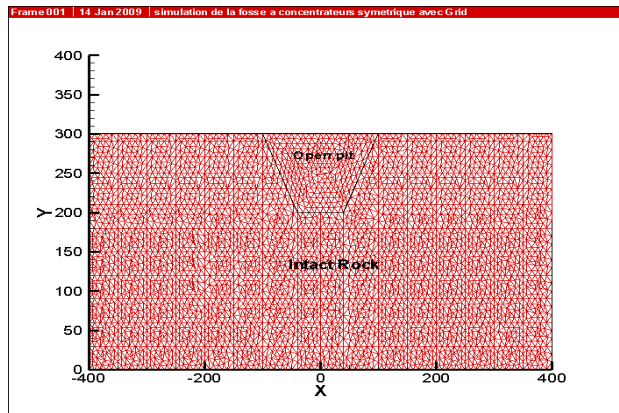


Figure 1. Open pit conceptual model.

Material hydraulic characteristics

The water retention curves representing the variation of the degree of saturation versus suction for the mill tailings, waste rock, and intact rock are shown in Figure 2 (semi-log graph).

Table 1 lists the different hydraulic parameters of these materials. These functions are defined by using experimental data from Aubertin et al. (2005) for mine waste rock, from Cifuentes (2005) for tailings and from Wang and Narasimhan (1985) for the rock matrix.

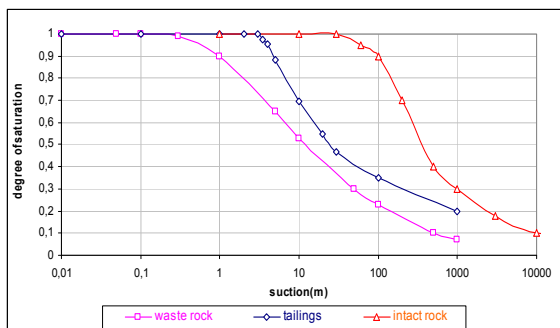


Figure 2. Material water retention curves.

Table 1 Material hydraulic parameters

Parameters	Waste rock	Mill tailings	Intact Rock
Porosity	0.34	0.43	0.02
Air entry value (m)	0.3	3.5	35
Ksat(m/s)	1×10^{-5}	1×10^{-8}	3.2×10^{-8}
Residual volumetric water content	0.03	0.1	0.0015

Figure 5 shows that as suction increases, the rock mass remains at a higher degree of saturation than the tailings and waste rock, due to its low porosity and higher AEV.

RESULTS AND DISCUSSION

Open Pit Filled With Waste Rock

For all simulations, the initial water table is fixed at an elevation of 220 m. To generate a regional gradient, a decreasing hydraulic head between 220 m and 210 m is imposed at the base of the model for x between -400 m and $+400$ m (which gives a regional gradient of 0.0125). The left and right boundaries are pervious with fixed hydraulic heads of 220 m and 210 m respectively. The base of the model is assumed impervious. A constant recharge rate of 1.5 mm/d is fixed at the surface for 10 days followed by a period of 10 days without rain in alternation for a period of 20 years. To simulate contaminant migration, a constant unit concentration is fixed within the open pit, and is initially set to zero within the surrounding host rock. The contaminant is assumed inorganic and non reactive with a free diffusion coefficient of 2×10^{-9} m²/s. All transport model parameters are summarized in Table 2. Two cases are presented here: a homogeneous rock mass, and a rock mass with

an orthogonal fracture network. All simulations are made under unsaturated and transient flow conditions. The Gridbuilder V.5.6 code (McLaren, 2005) is used to generate mesh network and the Tecplot code (Amtec, Inc.) is used for data extraction and visualization. This simulation has generated 8128 nodes and 7906 elements.

Table 2 Model parameters used in transport simulation

Parameter	Value
Tortuosity	0.1
Matrix longitudinal dispersivity(m)	0.1 m
Matrix transverse dispersivity	0.01 m
Fracture longitudinal dispersivity	0.5 m
fracture transverse dispersivity	0.05 m

Case 1: Homogeneous rock

Figures 3 and 4 show simulated profiles of suction and degree of saturation as a function of time and distance within a horizontal section at $y = 280\text{m}$. Figure 3 shows that the initial suction variation is linear and varies between -60 m and -70 m for x varying between -400 m and $+400\text{ m}$. With time and due to precipitation, the suction decreases greatly and especially within the rock mass. The variation of suction remains linear in the open pit. Due to the regional gradient, values are more important at the left side of the model than its right side.

As shown in Figure 4, the low porosity rock mass remains at a high degree of saturation with values between 90 and 100 %, whereas, wastes remain at a lower degree of saturation near their residual value. We can also notice an increasing of degree of saturation in the waste with time with values varying from 28%

to 38%. This is due to a progressive filling of the open pit.

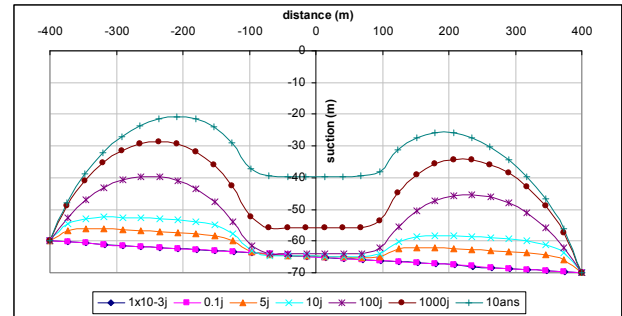


Figure 3. Simulated water suction profiles at $y = 280\text{m}$, open pit filled with waste rock, homogeneous rock mass.

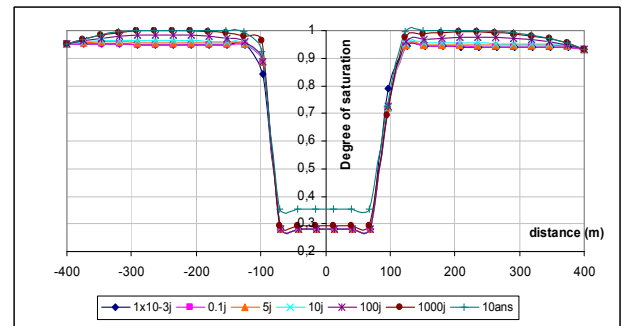


Figure 4. Simulated degree of saturation profiles at $y = 280\text{m}$, open pit filled with waste rock, homogeneous rock mass.

Figure 5 shows results of contaminant concentration evolution with time. This figure shows that concentration remains constant and equals unity inside open pit (which is the initial condition). Contaminant migration is slowest at early simulation times. As time increases and due to precipitations effect, migration becomes more significant especially with depth.

Due to the low value of the regional gradient, the contaminant outlet is quite symmetric.

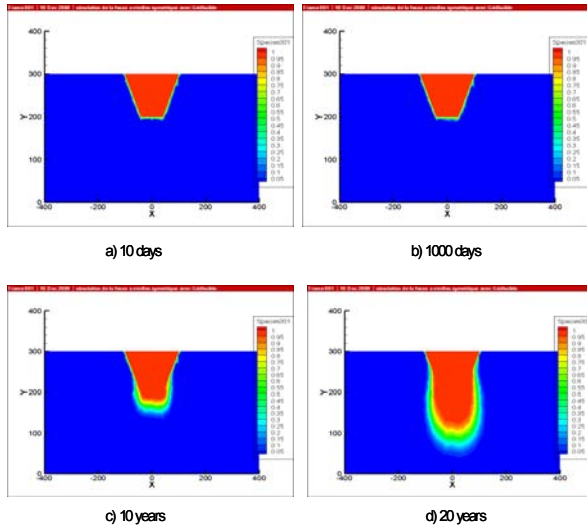


Figure 5. Simulated contaminant concentrations, open pit filled with waste rock, homogeneous rock mass.

Case 2: effect of vertical fractures

Here, vertical fractures are introduced into the rock mass. All fractures have an aperture of 0.3 mm and they are located at $x = 350$ m, 300 m, 250 m, 200 m, 150 m, 100 m, 40 m, -350 m, -300 m, -250 m, -200 m, -150 m, -100 m, -40 m and 0 m (Figure 6).

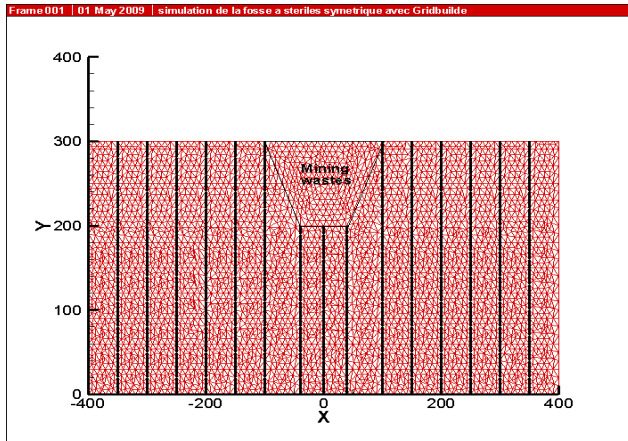


Figure 6. Open pit with vertical fractures (not to scale).

Figures 7 and 8 show simulated profiles of suction and degree of saturation as a function of time and distance.

Figure 7 shows clearly the effect of vertical fractures on suction profiles. Initially, suction variation is linear, but with time this variation becomes sinusoidally due to fractures. We can notice the variations of suction are less important here in comparison with the homogenous rock mass. Also, as shown by Figure 8, the variation of degree of saturation is very low and is constant with time.

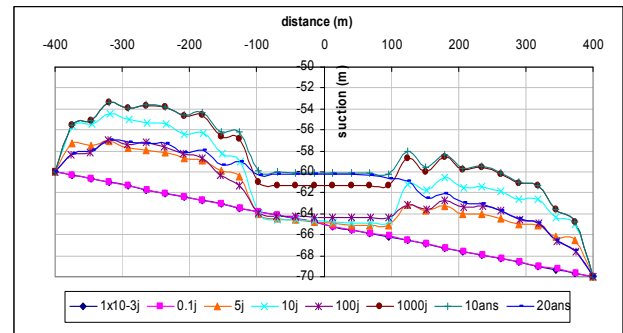


Figure 7 Simulated water suction profiles at $y = 280$ m, open pit filled with waste rock, rock mass with vertical fractures.

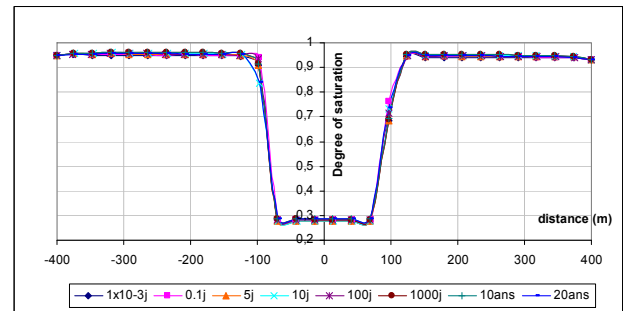


Figure 8. Simulated degree of saturation profiles at $y = 280$ m, open pit filled with waste rock, rock mass with vertical fractures.

For contaminant migration, the resulting concentration evolution with time is shown in Figure 9. This figure shows a preferential contaminant migration through vertical fractures. Indeed, contaminants use fractures to migrate rapidly and reach a great depth. We can assume that contaminants migrate more by advection process due to the great fracture hydraulic conductivity,

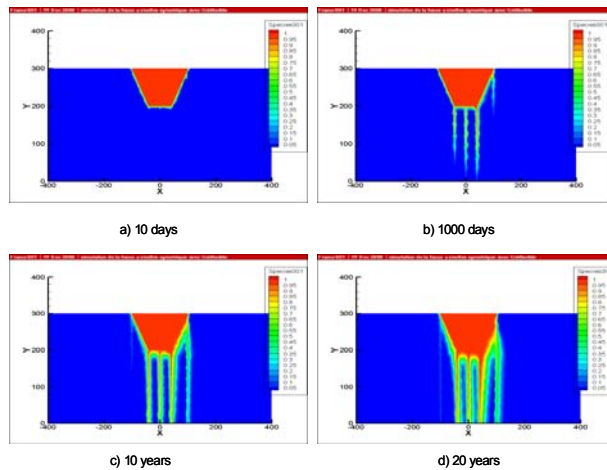


Figure 9. Simulated contaminant concentrations, open pit filled with waste rock, rock mass with vertical fractures.

Case 3: Effect of orthogonal fractures

Here, an orthogonal fracture network is introduced into the rock mass. All fractures have an aperture of 0.3 mm. The horizontal fractures are located at $y = 30$ m, 60 m, 90 m, 120 m, 150 m, 180 m, 210 m, 230 m, 250 m, 270 m and 290 m (Figure 10).

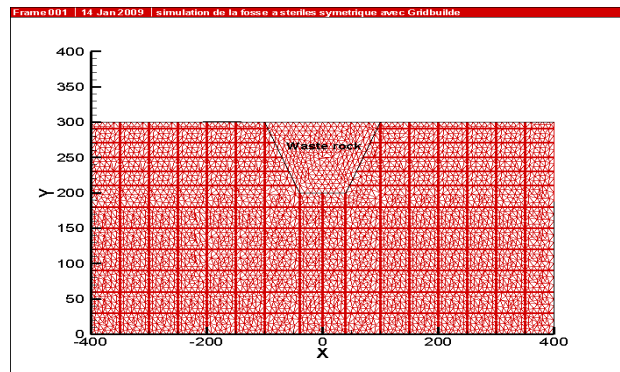


Figure 10. Open pit with orthogonal fracture network (not to scale).

Figures 11 and 12 show simulated profiles of suction and degree of saturation as a function of time and distance.

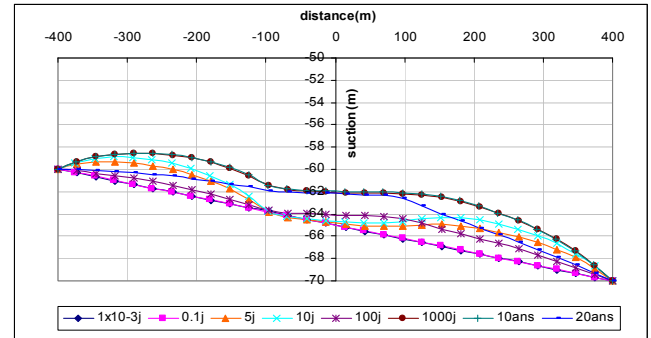


Figure 11. Simulated water suction profiles at $y = 280$ m, open pit filled with waste rock, rock mass with orthogonal fracture network.

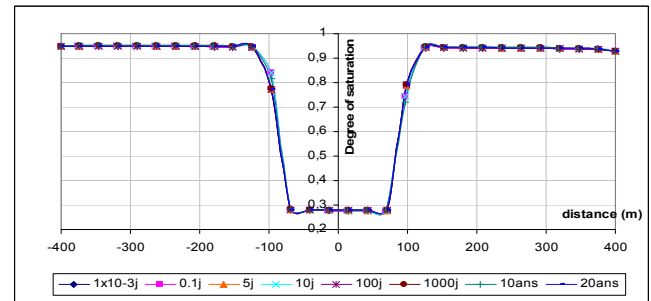


Figure 12. Simulated degree of saturation profiles at $y = 280$ m, open pit filled with waste rock, rock mass with orthogonal fracture network.

It can be seen from Figures 11 and 12 that orthogonal fractures amplify vertical fracture effect on water flow network. Figure 11 shows that variations of suction are less important here in comparison with the homogenous rock mass and case with vertical fractures only. Also, as shown by Figure 12, the variation of degree of saturation is very low and is constant with time. We can therefore say that introducing orthogonal fracture network causes a desaturation effect. This is due to significant water flow through the fracture network and water hasn't enough time to accumulate.

For contaminant migration, the resulting concentration evolution with time is shown in Figure 13. This figure shows a significant

difference in contaminant migration share in comparison with Case 1 (homogeneous rock mass). Indeed, migration is more important here and contaminant transport occurs primarily through fracture network. In contrast to Case 1 (no fractures), contaminants migrate more rapidly along the regional gradient direction. So, if we assume the existence of a surface water plane near the open pit, the risk of contamination at this plane will increase by the existence of fractures in the rock mass.

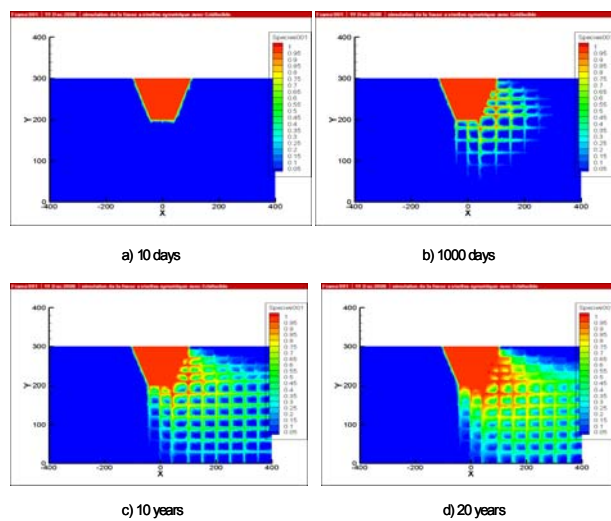


Figure 13. Simulated contaminant concentrations, open pit filled with waste rock, homogeneous rock mass.

Case 4 Effect of variable surface recharge rate

In this case, the recharge rate imposed on the surface varies with time. Data from the Latulipe meteorological station located in northern Quebec was used to establish the recharge rate, as shown in Figure 14 (Cifuentes, 2005). As can be seen in Figure 14, the first period of precipitation starts at day 120, a maximum is reached at day 273 and the last period of precipitation is at day 303. For our simulations, we consider a repetitive cyclic period of 1 day of precipitation followed by

2 days without precipitation for each month of the year for a period of 2 years.

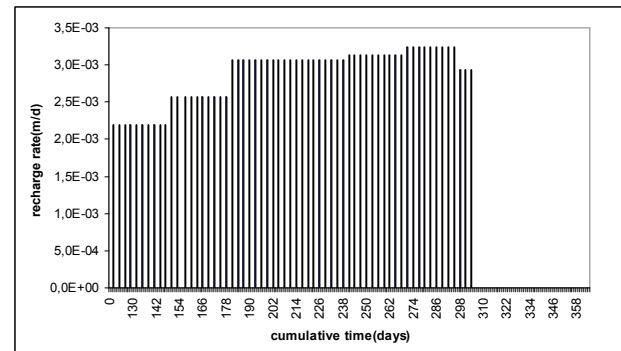


Figure 14. Precipitation distribution, Latulipe station, variable recharge case.

For this simulation, the initial water table is deeper being located at an elevation of 50 m. Hydraulic heads of 50 m and 40 m are imposed respectively at the left and right boundaries. The hydraulic regional gradient is therefore identical to that in cases 1 and 2. Also, the rock mass is homogeneous and no fractures are present.

Figures 15 and 16 show the simulated profiles of suction and degree of saturation as a function of time and distance.

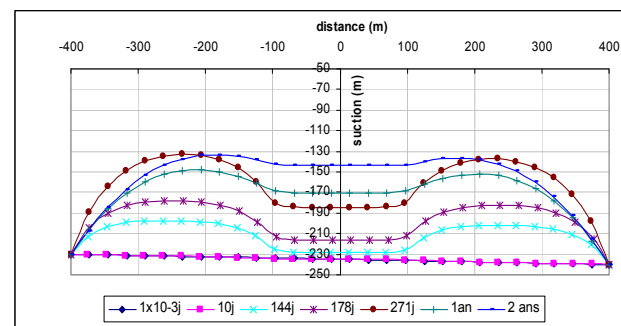


Figure 15. Simulated water suction profiles at $y = 280\text{m}$, open pit filled with waste rock, variable recharge case.

Figure 15 shows that the suction variation is more important here with the variable recharge

rate, especially within the open pit in comparison with case 1 (Figure 3). This is due to the short period without rain relative to the raining period. As shown by the results of Figure 16, the variation of the degree of saturation is more pronounced especially in the rock mass.

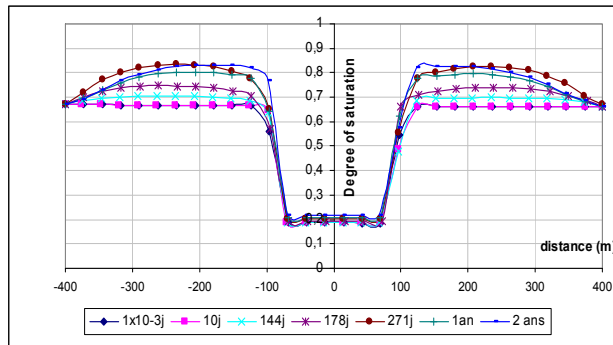


Figure 16. Simulated profiles of the degree of saturation profiles at $y = 280\text{m}$, open pit filled with waste rock, variable recharge case.

Open Pit Filled With Tailings

In this case, the open pit is filled with mill tailings which have a saturated hydraulic conductivity of the same order of magnitude as the intact rock matrix but lower than the waste rock. The same initial and boundary conditions used in Case 1 of the open pit filled with waste rock are used here. The rock mass is homogeneous and no fractures are present here. The simulated results of suction and degree of saturation as a function of time and distance along a horizontal section at $y = 280\text{m}$ are shown in Figures 17 and 18.

From Figures 17 and 18, we can notice that fluctuations are more important here than for case 1 with the open pit filled with waste rock. Figure 17 shows a significant decrease in suction within the open pit and rock mass. In contrast to case 1, the suction decrease is more significant in the tailings relative to the rock mass.

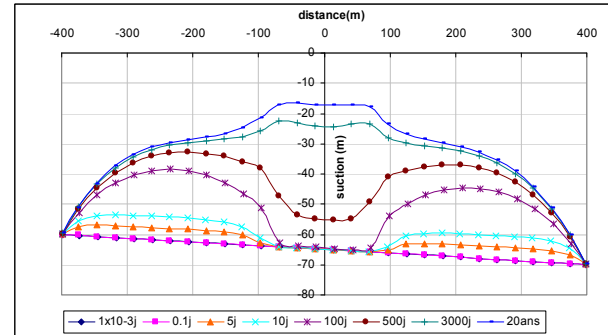


Figure 17. Simulated water suction profiles at $y = 280\text{m}$, open pit filled with tailings.

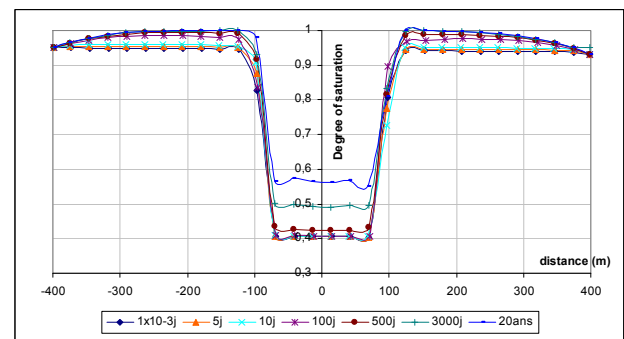


Figure 18. Simulated profiles of the degree of saturation profiles at $y = 280\text{m}$, open pit filled with tailings.

Figure 18 shows a significant increase in degree of saturation in tailings with time, with saturations near 58% after 20 years. This value is greater than for the case with waste rock. The degree of saturation in the rock mass fluctuates between 93% and 100%.

Contaminant concentration evolution with time is shown in Figure 19. With time, contaminant migration becomes more important and contaminant migrates from open pit to rock mass. In comparison with waste rock, lateral migration is more important here. The contaminant shape is quite oriented in the direction of regional gradient.

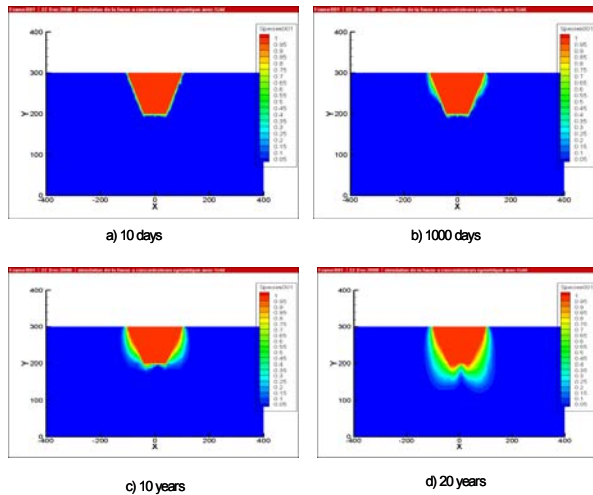


Figure 19. Simulated contaminant concentrations, open pit filled with tailings, homogeneous rock mass.

Introducing an orthogonal fracture network with 0.3 mm aperture (see Figure 10 for fracture network), we obtain concentration results as shown by Figure 20.

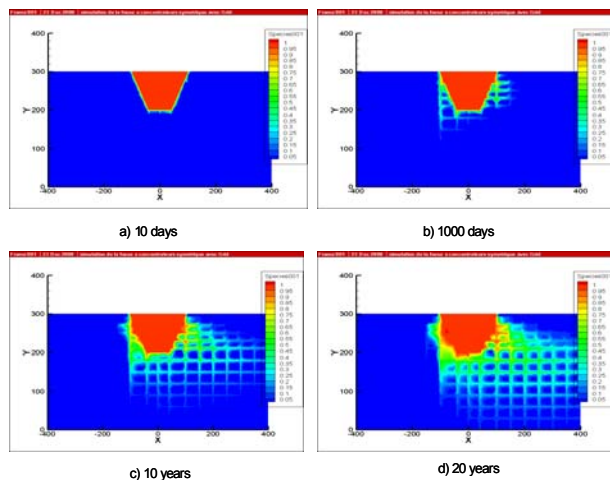


Figure 20. Simulated contaminant concentrations, open pit filled with tailings, fractured rock mass.

As was the case for the open pit with waste rock, fractures have a great influence on contaminant transport. In fact, we can see from Figure 20 that the contaminant migrates rapidly through the fracture network thus reaching greater distances than when the rock mass is homogenous.

CONCLUSIONS

This study highlights that many factors affect water flow and contaminant transport from mine wastes stored in open pits in fractured rock. Simulations with the 3D HydroGeosphere code show that:

- Water flow and contaminant transport are largely affected by the type of open pit filling material, the type and nature of initial and boundary conditions and the nature of the rock mass (homogeneous or fractured). For a homogeneous rock mass, water accumulates in the open pit due to water infiltration. This induces a suction decrease over time and an increasing degree of saturation within the open pit and rock mass.
- When a fracture network is added to the rock mass, water will flow preferentially through the fractures and will not have enough time to accumulate. This leads to a certain desaturation of the system and especially in the rock mass. Variations in the suction and degree of saturation over time become less important.
- Fractures also have a great effect on contaminant transport. Contaminants will migrate through the fracture network and can reach greater distances. The contaminant plume is more affected by the regional gradient when fractures are present. Thus, the degree of fracturing is an important aspect to consider in any evaluation of contaminant transport in fractured rock mass.
- A regional gradient can have a great effect on the water flow network and on contaminant transport. Contaminant concentrations are greater in the direction of the regional gradient. This difference in concentrations becomes more importance with time.

- Imposing a variable rate of precipitation at the surface will introduce a variation in the suction and degree of saturation.

REFERENCES

Amtec Engineering Inc. 2003. Tecplot Version 10. États-Unis Amtec Engineering Inc. Fichier informatique sur CD-ROM.

Aubertin, M., Fala, O., Molson, J., Rochette, A.G., Lahmira, B., Martin, V., Lefebvre, R., Bussière, B., Chapuis, R.P., Chouteau, M. and Wilson, W.G. 2005. Évaluation du comportement hydrogéologique et géochimique des haldes à stériles. Symposium en Environnement et Mines.

Aubertin, M., Bussière, B., Aachib, M., Chapuis, R.P. 1996. Une modélisation numérique des écoulements non saturés dans des couvertures multicouches en sols. *Hydrogéologie*, 1, p. 3-13.

Ben Abdelghani, F. 2008. Simulation numérique des écoulements et du transport de contaminants dans les rejets miniers entreposés dans les massifs rocheux fracturés. Thèse de doctorat (in preparation), École Polytechnique de Montréal.

Ben Abdelghani, F., Simon, R., Aubertin, M., Molson, J. 2007. Analyse numérique des écoulements et du transport de contaminants autour des rejets miniers entreposés dans les massifs rocheux fracturés. GéoOttawa conférence. Ottawa, Canada.

Cifuentes, E. 2005. Modélisation numérique des écoulements non saturés dans les couvertures à effets de barrière capillaire inclinées. M. Ing Génie Minéral, École Polytechnique de Montréal.

Chapuis, R.P., Chenaf, D., Bussière, B., Aubertin, M., Crespo, R. 2001. A User's Approach to Assess Numerical Codes for Saturated and Unsaturated Seepage Conditions. *Canadian Geotechnical Journal*, 38(5), p. 1113-1126.

Freeze, R.A and Cherry, J.A. 1979. *Groundwater*. Prentice Hall, Upper Saddle River, N.J. 604p.

Gale, J. 1990. Hydraulic behaviour of rock joints. *Proceedings of the International Symposium on Rock Joints*. Balkema, Rotterdam. Barton and Stephansson Eds. p. 351-362.

Indraratna, B. and Ranjith, P. 2001. Hydromechanical aspects and unsaturated flow in jointed rock. Lisse. A.A. Balkema. 286p.

Priest, D.S. 1993. *Discontinuity Analysis for Rock Engineering*. London. Chapman and Hall. 473p.

Rosenbom, E. A., Therrien, R., Refsgaard, C.J., Jensen, H.K., Ernstsen, V., Klint, S.E.K. 2009. Numerical analysis of water and solute transport in variably saturated fractured clayey till. *Journal of Contaminant Hydrology*. 104. 137-152.

Sharma, D.H. and Reddy, R.K. 2004. *Geoenvironmental engineering, site remediation, waste containment, and emerging waste management technologies*. Contaminant Transport and Fate, chapter 8. John Wiley and Sons Eds, Hoboken, New Jersey. p. 167- 211.

Therrien, R., Sudicky, E.A., 1996. Three dimensional analysis of variably saturated flow and solute transport in discretely fractured porous media. *Journal of Contaminant Hydrology* 23, 1-44.

- Therrien, R., McLaren, R.G. and Sudicky, E.A. 2005. HydroGeosphere, A three-dimensional numerical model describing fully-integrated subsurface and surface flow and solute transport. Draft eds. 252p.
- Tsang, W.Y. 1984. The effect of tortuosity on fluid flow through a single fracture. *Water Resources Research*. 20: 9. 1209-1215.
- Van Genuchten, M.Th., 1980. A closed-form equation for predicting the hydraulic conductivity of unsaturated soils. *Soil Science Society of America Journal* 44, 892–898
- Wang, J.S.Y. and Narasimhan, T.N. 1993. *Unsaturated flow in fractured porous media. Flow and Contaminant Transport in fractured rock.* (Bear, J, Tsang C. F. and Marsily, G. Eds) San Diego. Academic Press, Inc. p.169-236.
- Witherspoon, A.P., Tsang, W.Y., Long, S.C.J. and Noorishad, J. 1981. New approaches to problems of fluid flow in fractured rock masses. *Proceedings of the 22nd US Symposium on Rock Mechanics. Rock Mechanics from research to application.* Massachusetts. Institute of Technology. June 28-July 2. p. 3-22.
- Witherspoon, P.A. 1986. Flow of groundwater in fractured rocks. *Bulletin of the International Association of Engineering Geology*. No 34, Paris, France. 103-115.
- Witherspoon, P.A., Wang, J.S.Y., Iwai, K., Gale, J.E., 1980. Validity of cubic law for fluid flow in a deformable rock fracture. *Water Resources Research* 16 (6), 1016–1024.152
- A.E. Rosenbom et al./*Journal of Contaminant Hydrology* 104 (2009) 137–152
- Wang, J.S.Y. and Narasimhan, T.N. (1985). Hydrologic mechanisms governing fluid flow in a partially saturated, fractured, porous medium. *Water Resources Research*. 21-12. p. 1861–1874.
- Xu, J. and Hu, B.X. 2005. Stochastic analysis of contaminant transport through non stationary fractured porous media: a dual-permeability approach. *Water Resources Research*. 41-5.

WATER BALANCE MANAGEMENT APPROACH TO MINE CLOSURE AT THE ROYAL MOUNTAIN KING MINE, COPPEROPOLIS, CA

Adam Whitman

Meridian Beartrack Company, Reno NV

Ian Hutchison, Jim Juliani and Sarah Bortz

Strategic Engineering and Science Inc., Irvine CA

ABSTRACT: This case history outlines a water balance management approach to closure of the Royal Mountain King Gold Mine near Copperopolis, California.

The Royal Mountain King Mine operated from 1988 through 1994. It includes three open pits, a 150-acre flotation tailings reservoir, 250 acres of over burden disposal systems, a leached concentrate residue facility, and a process water pond.

As a result of the mine's location in the mineralized Hodson fault zone, the groundwater and low flow conditions in the local creeks are impacted by elevated levels of total dissolved solids, chloride, sulfate, and traces of arsenic and selenium. During mining, water quality conditions at the Site improved due to the fact that the pits acted as large extraction sumps for groundwater and reduced poor quality spring flows to the creeks. The pits filled after mine closure, forming lakes. Water quality has worsened, both because the extraction sumps are no longer present and because of the effects of the various mine waste management units.

The waste management units have been closed either in accordance with regulatory prescriptive closure standards or engineered alternatives to these standards. In recognition of the naturally occurring poor quality water at the Site, consideration is being given to re-classifying the designated beneficial uses of groundwater. This will facilitate regulatory approval of closure of those waste management units which were temporarily closed using engineered alternatives to the regulatory prescriptive standards.

The major focus of closure is on site-wide water management. This involves collecting seepage from the toes of the overburden disposal systems, in addition to collecting the water in the flotation tailings reservoir and transferring it to one of the pits for seasonal storage. A discharge permit has been obtained allowing pit water to be released to the local creek during infrequent high flow rainstorm conditions. An automated computer controlled discharge system has been installed.

This case history is an example of achieving a moderate life cycle cost solution by satisfying regulatory agency concerns and thereby avoiding the high costs of the fully prescriptive regulatory closure requirements.

INTRODUCTION

In the summer of 2008, the authors toured the Royal Mountain King Mine (RMKM) site with the staff of the Regional Water Quality Control Board (RWQCB). As a result of a change in regulatory staff, there was a new motivation to finalize the mine closure after almost 13 years of closure and reclamation construction. In what turned out to be a breakthrough, the regulator purveyed the Site (Figure 1) and finally concurred that; “this mine closure is an exercise in water balance management, not in containment of mine waste under the prescriptive requirements of the California regulations.” As a result, the approaches of the mining company and the regulators were aligned and a plan for mine closure was agreed upon.

The RMKM, operated by Meridian Beartrack Company (MBC) between 1988 and 1994, is located in the foothills of the Sierra Nevada near Copperopolis, California, in Calaveras County. MBC has been performing management, reclamation, and closure construction of the Site from the onset of mining to the present.

The RMKM Site includes the following areas:

- Three engineered waste management units (WMUs): a six million, 150-acre flotation tailings reservoir (FTR), a six-acre process water pond (PWP), and a 0.4 million ton, 18- acre leached concentrate residue facility (LCRF). In accordance with California Title 27 prescriptive requirements, the LCRF and PWP have been closed with geomembrane and soil caps. The FTR was graded for drainage,

and covered with topsoil and vegetated. During the final years of mining tailings deposition was managed to maximize surface slope toward the drainage outlet.

- The FTR is a clay lined valley fill impoundment and both groundwater and rainfall infiltration accumulate in the stored tailings. The water contained in the tailings was initially discharged from the FTR Leachate Collection and Recovery System (LCRS) to Skyrocket Pit Lake. However in an effort to reduce the amount of poor quality water accumulating at the Site, the LCRS was closed in 2002 and hydraulic pressure was allowed to build up in the FTR. At best this experiment was anticipated to reduce groundwater inflow and increase evapotranspiration sufficiently to avoid having to remove water from the FTR. At worst, it is expected to reduce the amount of water that has to be removed. A small surface seep appeared near the edge of the FTR in 2008 indicating that at least some water will need to be transferred out of the FTR.
- Three overburden disposal sites (ODSs) covering approximately 250 acres and containing 54 million tons of waste rock: FTR ODS, West ODS, and Gold Knoll ODS. The ODSs have been reclaimed by grading, placement of topsoil cover and vegetated. The RWQCB also considers their closure as an engineered alternative to the Title 27 requirements.
- Two former pits filled with water: Skyrocket (55 acres) and North Pit (23 acres) Lakes.
- One backfilled pit: Gold Knoll.

The Skyrocket and North Pits have filled with groundwater and runoff from adjacent areas. Water levels in both pit lakes have reached equilibrium, with levels fluctuating seasonally from year to year, depending on the amount of rainfall. A 35-foot high earthen dam (Skyrocket Dam) has been constructed across the low point of the Skyrocket Pit Lake rim to contain the stored water without spillage (Figure 2). The dam is a jurisdictional structure, and is operated and maintained under a permit from the California Division of Safety of Dams.

Three seeps emanate from locations at the toes of the Gold Knoll and West ODSs (Figure 3). Water from these seeps is managed by collection and storage in Skyrocket Pit Lake. Water removed from the FTR is also placed in Skyrocket Pit Lake. This dewatering reduces the potential for seeps occurring along the sides of the FTR.

SITE CONDITIONS

Climate

The Site has a Mediterranean climate with warm, dry summers, and cool, wet winters. The average winter temperature is about 43 degrees Fahrenheit (°F) and the average summer temperature is about 71°F. Mean monthly extremes vary from 33°F to approximately 92°F. The mean annual precipitation is 25 inches, approximately 80% of which occurs in the winter months of November through March. The mean annual gross pan (Type A) evaporation at the Site is 68 inches.

Geology

The mine is in the western portion of the foothills metamorphic belt in Western Calaveras County. Gold mineralization occurs locally along a northwest-trending,

east-dipping thrust fault zone, dominated by the Hodson and Littlejohns Faults (Figure 4). These structures juxtapose Upper Jurassic carbonaceous phyllite (shale and slate) against the greenstone (altered mafic metavolcanic units) of similar age.

There is extensive alteration, with the occurrence of quartz, pyrite, sericite, mariposite, serpentinite and ankerite, within the fault zone. This alteration resulted in the deposition of gold, both as free gold and within pyrite and arsenopyrite. The three pits are located within this fault zone.

The regional strike and structural grain of the major rock units in the Hodson district are northwest. Well-developed foliation dips 50 to 80 degrees to the northeast.

Groundwater

Groundwater occurs in bedrock fracture systems and migration generally follows the surface topography from the northeast to the southwest. There are three general groundwater zones defined by the geologic conditions: the phyllite, the fault zone, and the greenstone.

The phyllite has the lowest rate of movement due to limited fracture systems and the relatively plastic nature of this rock. The hydraulic conductivity ranges from 2×10^{-7} to 5×10^{-4} cm/sec.

The fault zone and greenstone have more extensive fracture systems and therefore experience higher groundwater migration rates. The hydraulic conductivity of these zones ranges from 5×10^{-5} to 5×10^{-3} cm/sec.

Because the least transmissive rock is located along the downgradient boundary of the RMKM, the phyllite acts as a barrier to westward groundwater flow. Groundwater backs up within the fault zone and

greenstone, resulting in a relatively flat gradient in the Skyrocket Pit Lake area. The depth to groundwater becomes very shallow, and surface springs occur at low points such as the bed of Littlejohns Creek, which flows through the Site. From 1994 through the early 2000s, during and after mining while the pit lakes filled, groundwater at the Site migrated into the deep dewatered mine pits where the water was collected and used for mining purposes. As a result, these surface springs largely dried up during the mine's operating life and for a period thereafter.

Groundwater quality at the Site depends upon the chemical composition of the host geologic formations, the extent to which the groundwater migration pattern has been modified by the WMUs and the pits and to some extent by seepage from the WMUs.

The greenstone formation that underlies the eastern portion of the Site contains groundwater of relatively good quality with lower total dissolved solids (TDS) concentrations and few detections of metals. The fault zone that traverses the western and central portion of the RMKM contains significant natural mineralization, which results in poor quality groundwater containing elevated TDS and sulfate concentrations and a greater frequency of detection of arsenic, iron, manganese, nickel, and selenium. The phyllite formation along the western portion of the Site has the highest TDS concentrations and detections of chloride and sulfate and metals such as iron and manganese. (See Table 1)

There have been changes in groundwater quality, particularly in areas around former mine facilities. These changes generally consist of increases in TDS, sulfate, and in some cases nitrate concentrations.

Littlejohns Creek flows across the Site and into Flowers Reservoir just downstream.

Numerous ephemeral drainages around the Site flow into Littlejohns Creek. Significant flows in these tributary drainages occur for periods during and after significant rainfall. During the summer months spring flows occur in the creek bottoms and at the ODS-2, ODS-5 and Gold Knoll.

There is extensive anecdotal and quantitative information that indicates that the Site had a year-round presence of poor quality surface water well before mining occurred. Historically, poor quality seeps and springs were observed in the area where the current pit lakes are located. The results of archeological investigations in the area of Skyrocket Lake indicate that the area was continuously occupied by pre-historic Native Americans due to the year-round availability of water from local springs and the value of salt that was abundant in the area. Pre-project water quality data indicates baseline surface water quality at and around RMKM was poor and did not meet all the applicable water quality goals for potential beneficial uses that are currently designated in the relevant Basin Plan, a document that describes the beneficial water uses in the area and applicable water quality goals and standards. The principal constituents that are typically elevated include TDS, mineral constituents, i.e., sulfate, chloride, sodium, calcium, and magnesium, as well as manganese and iron. Traces of arsenic were also detected.

The quality of the RMKM surface water flows is influenced by the groundwater quality. During low flow periods in the spring, summer and fall, water in the creeks is predominantly spring flow, and the quality is similar to that of groundwater in the fault zone and phyllite. During the high flow season, particularly in the winter months, the effect of spring flows on creek water quality is diluted by the better quality surface runoff entering the creeks.

Figure 4A presents a chart of TDS concentration over time for Littlejohns Creek at monitoring locations at the downstream boundary of the RMKM. It clearly illustrates how surface water quality was improved during mining with the dewatering of the pits.

The results of salt load evaluations indicate that if the ODS spring flows are discharged, the salt loading will be of the same order of magnitude as the pre-mine salt loadings. This is not surprising, as the salt load is determined by the amount of rainfall infiltration and poor quality groundwater that emerges as springs. Mining has not significantly changed the quality or amount of this spring flow.

Pit Lakes

The long-term average rate of groundwater migration into the pit is a function of how much lower the level in the pit lake is, relative to the surrounding groundwater levels. Where pit lake levels and the surrounding groundwater levels are higher than the creek bottoms, there is potential for groundwater to migrate to and discharge into creeks. Lowering the pit lake level can therefore reduce or eliminate discharge of groundwater into Littlejohns Creek during the dry season.

Skyrocket Pit Lake water quality (Table 1) is determined by the quality of the groundwater, since this is the primary source of constituents in the pit lake. The water quality is stable. In addition, water quality depth profile data collected for Skyrocket Pit Lake indicates that there is stratification, with a shallow seasonal thermocline (typically within the top 25 feet) and a deep pycnocline at approximately 150 feet. Below the pycnocline, conditions are anoxic and sulfate reduction appears to be taking place. In addition, TDS and arsenic concentrations are

higher below the pycnocline than at the surface of the pit lake.

North Pit Lake reached equilibrium levels relatively rapidly, and the water level typically varies seasonally. Both TDS and arsenic concentrations are lower in North Pit than those in the Skyrocket Pit. The pit water quality appears to be stable and there is no stratification.

MINE CLOSURE

Development of Closure Concepts

Initially the regulatory agency, the RWQCB, reviewed the mine closure as a need to require compliance with the prescriptive closure requirements outlined in Title 27. These requirements included impermeable clay/soil or geomembrane/soil covers of the 400 acres of the ODSs and the FTR at a net present value (NPV) cost of approximately \$80 million. MBC would also be required to maintain the FTR and ODSs in a drained state, with treatment and discharge of any groundwater that migrated into these WMUs and out through the drains or to the seepage collection areas, resulting in a cost of another \$50 million NPV.

This initial viewpoint was held because of the following:

- During mining poor quality spring flow into Littlejohns Creek was minimized. After cessation of mining, as the pits filled and the seeps re-appeared, and much of the apparent worsening water quality was incorrectly attributed to leakage from the WMUs.
- Pre-mining background data was collected during a dry period when there was less of an impact to surface water from poor quality groundwater seeps.

Less poor quality groundwater was available to flow into Littlejohns Creek as springs. As the pits filled and the seeps re-appeared, average water quality conditions were worse than even during the pre-mining period, again this worsening was incorrectly attributed to leakage from the WMUs.

- The RWQCB felt uncomfortable in allowing engineered alternatives to the prescriptive standard necessary to approve the closure that had been completed, particularly in light of seemingly worsening water quality that occurred in the late 1990's and early 2000's (Figure 4A).
- Under the circumstances, it was difficult for MBC to commit to the significant cost of the comprehensive field investigations and study programs that would have been needed to demonstrate that pre-mining conditions were poor and closure allowing for some sort of residual impact was the only feasible approach. As a result, the closure plan development was piece-mealed and several closure plans, RWQCB's orders, and in one instance an appeal to the overseeing State Water Resources Control Board were needed before the current closure plan approach was developed and accepted by the RWQCB.
- The late appearance of the seep from the FTR in 2008, even though it was stated that drain closure was to be a test, continues to introduce uncertainties into how effective the final closure plan will be.

MBC has demonstrated to the RWQCB that because of the way the WMUs were constructed, the prescriptive approach would be infeasible. Furthermore, because water quality can be managed to improve conditions it is not necessary to achieve complete containment of all the surface

wastes, making a water management approach to closure the only feasible solution. Also, contingency plans can be established to deal with any uncertainties associated with the water management approach.

Water Management Closure Approach

The water management closure approach essentially formalizes the interim closure construction and operations that MBC had already installed. The elements include: (Figures 3 and 4).

- Ongoing collection of seepage flows from three locations at the toes of the ODSs and the storage if these flows in Skyrocket Pit Lake.
- Transferring sufficient water from the FTR LCRS to maintain water levels within the FTR below an elevation where surface seeps can occur. This water is also stored in the Skyrocket Pit Lake.
- Periodically discharging water from Skyrocket Pit Lake during high flow conditions under a National Pollution Discharge Elimination System permit.
- Maintaining the existing WMU covers and the surface water diversion facilities.

While closure procedures are simple, long-term closure feasibility had to be demonstrated. For this purpose, extensive field data on seepage volumes and natural flows in the creeks were collected and used in conjunction with a series of computer models to demonstrate the plan's feasibility. These computer models were also useful in demonstrating that whether or not the prescriptive covers were installed, a water management system would still have to be put in place. Models were developed for the ODSs, the two pit lakes, and Littlejohns Creek. These simulated monthly water mass balances, as well as TDS and arsenic concentrations. During the closure period,

the ODS seepage flows were applied to the surface of the ODSs with some of this water re-infiltrating and being recycled as continually increasing seepage flows. The ODS models were useful in removing this recycling effect from the measured data and in predicting future realistic seepage rates.

Some of the more innovative closure features that were provided include the following:

- During the closure period 12 acres of available lined surface was used to evaporate the initial 90 acre-feet of very poor quality process water without having to resort to costly physical/chemical treatment. Spray systems were installed in the lined surface of the LCRF, sprinkler systems were used to wet the sides of the PWP and a turbo-mister was used in the North Pit Lake. This was coupled with removal of accumulated salts and the cleaning of the PWP liners so that winter rainfall could be discharged. A covered water storage system was constructed in the PWP through the placement of tailings to hold the water and the construction of a temporary cover over the top of the tailings.
- Construction of a 35-foot high fill dam across the lower end of the Skyrocket Pit Lake, to provide for poor quality water storage during the closure period.
- Installation of a fully automated discharge system that allows up to 30,000 gpm to be discharged to Littlejohns Creek during short storm periods when flood flows occur and receiving water quality standards can be achieved.

It is intended that in time, the above approach will also improve the existing surface water quality. It is also intended that the Skyrocket Pit Lake level will be lowered to a level at

which the seepage of groundwater to Littlejohns Creek is minimized.

Resolving the groundwater quality issues has been another topic of discussion. The Basin Plan for the area is general and it considers groundwater to be suitable for municipal and agricultural supply without recognizing that naturally occurring poor quality water exists. MBC has been able to demonstrate to the RWQCB that there is no need, nor is it feasible, to attempt to restore the poor quality groundwater zone to what it was before mining. Furthermore, to address the Basin Plan issue, MBC is proposing to apply for an amendment to the plan that incorporates recognition of the existing poor quality groundwater in the area.

Contingency plans have been established to cope with unforeseen issues should they arise; these include:

- Construction of an evaporation pond system on the surface of the FTR should too much water accumulate in Skyrocket Pit Lake, resulting in the need for transfers from the FTR to be curtailed.
- Land-application and evaporation as methods to reduce water inventory on a sporadic basis.

CONCLUSIONS

A reasonably cost-effective approach to mine closure has been achieved and while long-term active care has not been eliminated, it has been minimized. The need for active water treatment and costly covers has been avoided. Certain closure activities, including finalization of the closure of the PWP and the long-term operational procedures, and obtaining Basin Plan Amendment, are still ongoing.

While this closure approach is generally consistent with what was envisaged at the time the mine was planned in the early 1980's, the significant effort required in conducting the necessary studies and in obtaining the regulatory approvals was not anticipated. In hindsight, the following activities that would have allowed closure to occur more rapidly and possibly at a lower cost could have been completed earlier:

- During the permitting process, more extensive background water quality data could have been obtained through more frequent monitoring of quality and flow. A site and surface water conceptual model could have been prepared. This model would have highlighted the impact of groundwater on surface water quality and the fact that the data collected represented unusually good water quality because of the initially dry conditions followed by the dewatering of the pits, and that after mining water quality would again worsen. Having this information up-front would have made it significantly easier to obtain approvals for the current closure plan.

- A closure preliminary design could have been produced. This would have required consideration of how surface and subsurface drainage was to be managed and might have resulted in the ODS and FTR footprints and designs being modified, and would certainly have resulted in more realistic closure costs being determined.
- More comprehensive waste characterization testing would have indicated that the ODS leachate would pose a threat to water quality even though it does not have a net acid potential. This would have facilitated a better design for the waste location and the infiltration and drainage controls.

ACKNOWLEDGEMENTS

The approval of Meridian Beartrack Company to publish this paper is gratefully acknowledged.

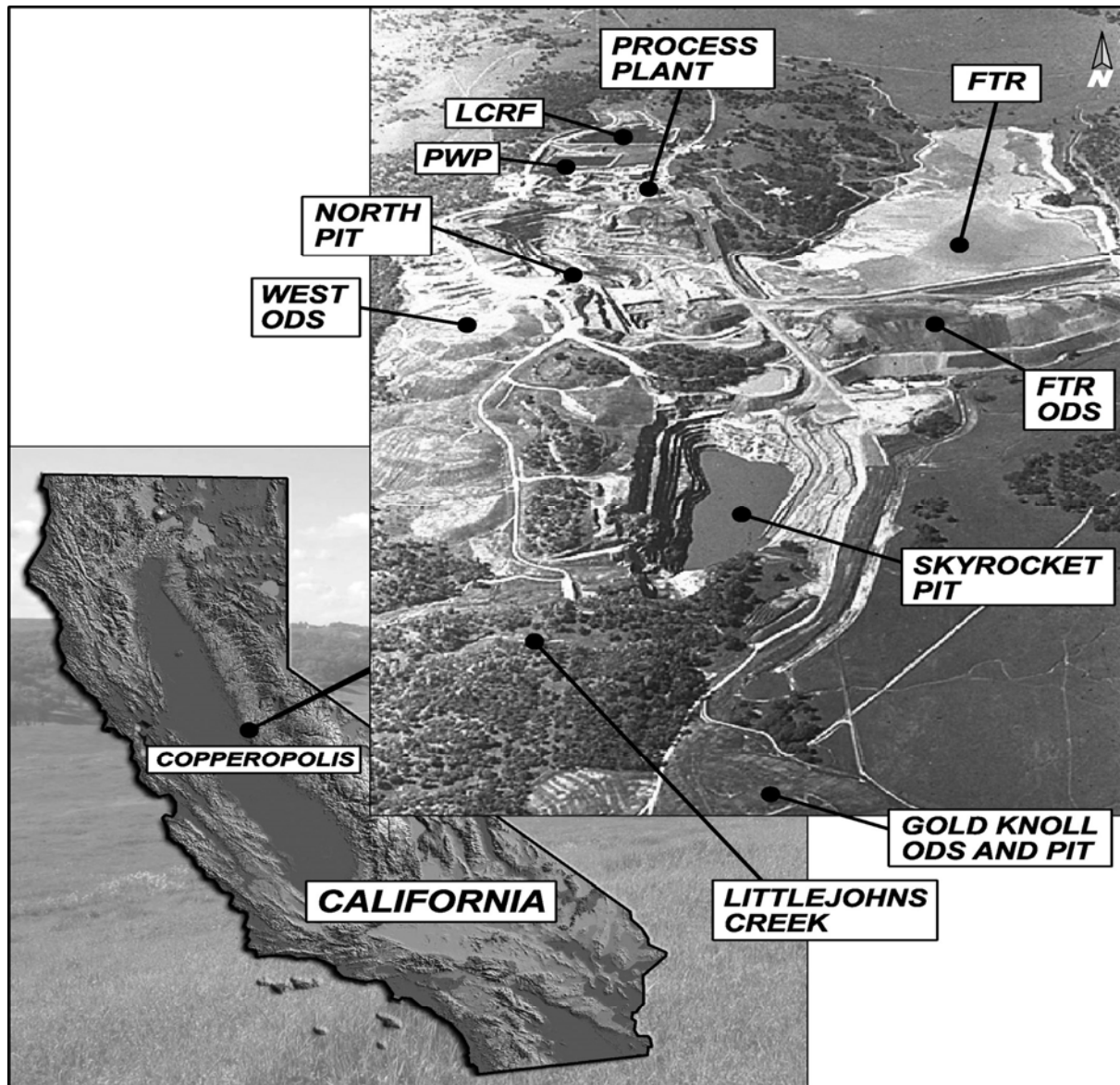
TABLE 1: TYPICAL WATER QUALITY (mg/L)

Medium		TDS	Sulfate	Chloride	Arsenic	Selenium	Nitrate
Pre-project Groundwater ⁽¹⁾	-Greenstone	153	10	8	<0.01	<.005	2.0
	-Fault Zone	1,036	155	231	0.033	<.005	1.2
	-Phyllite	8,909	2,773	2,810	<0.01	<.005	<1.0
Pre-project Surface Water ⁽²⁾	-Upgradient	50 - 490	6 - 131	<2 - 213	<0.01	<.005	<0.1 - 0.42
	-Downgradient	265 - 15,150	44 - 3,400	54 - 5,629	<0.01 - 0.03	<.005	<0.1 - 1.1
FTR Water ⁽³⁾		4,350	2,294	300	0.016	N/A	0.10
ODS	-West ODS-2	3,280	1,960	108	0.002	0.012	24.7
	-West ODS-5	3,920	2,580	134	0.007	0.022	9.5
	-Gold Knoll	8,110	4,995	272	0.026	0.070	32.1
Skyrocket Pit Lake		2,460	1,125	326	0.103	0.007	4.36
North Pit Lake		1,650	930	128	0.007	0.002	0.17

⁽¹⁾ Average for three representative wells.

⁽²⁾ Ranges for several upgradient and downgradient sampling stations.

⁽³⁾ Average since beginning of 2004.



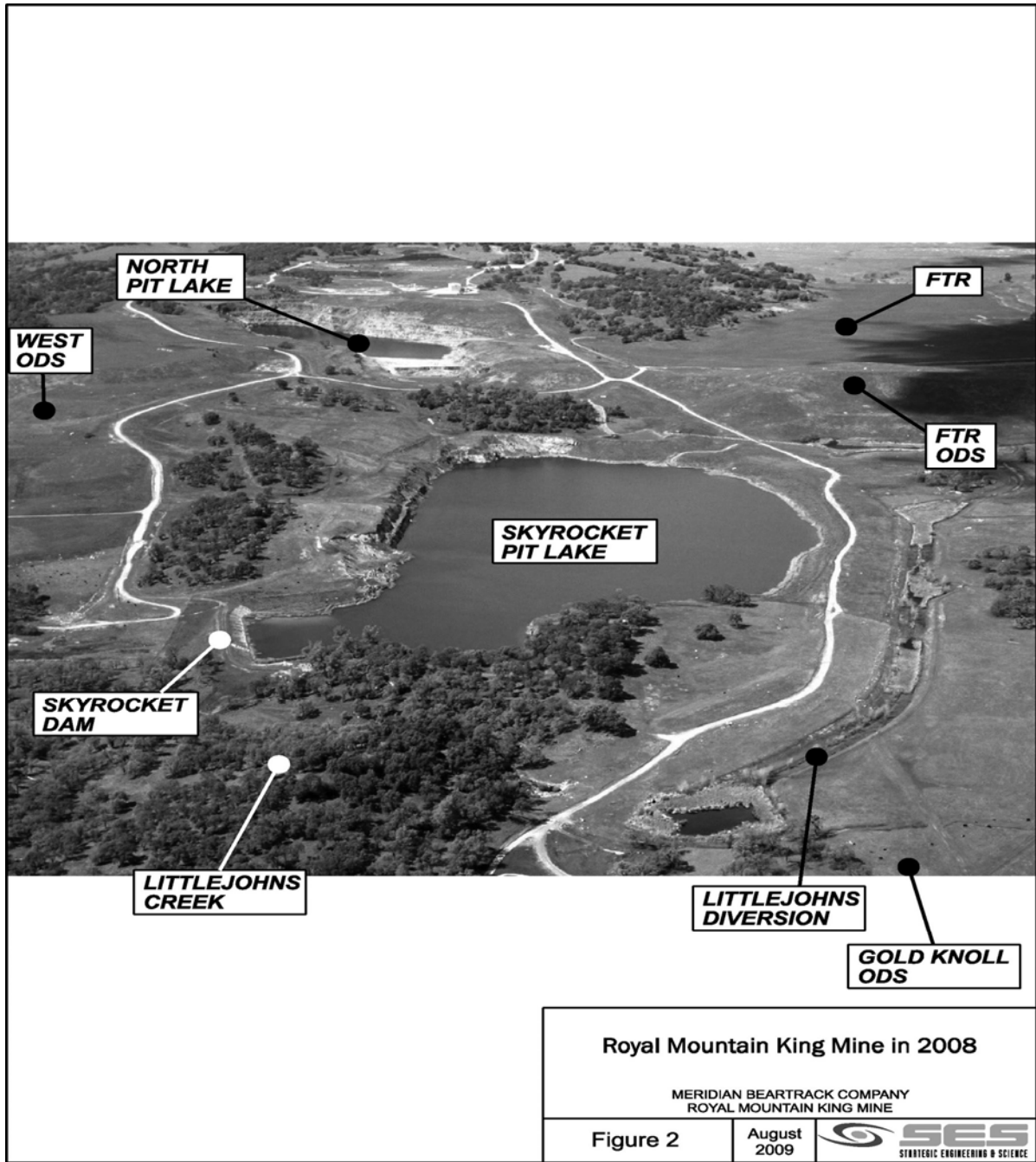
Royal Mountain King Mine in 1994

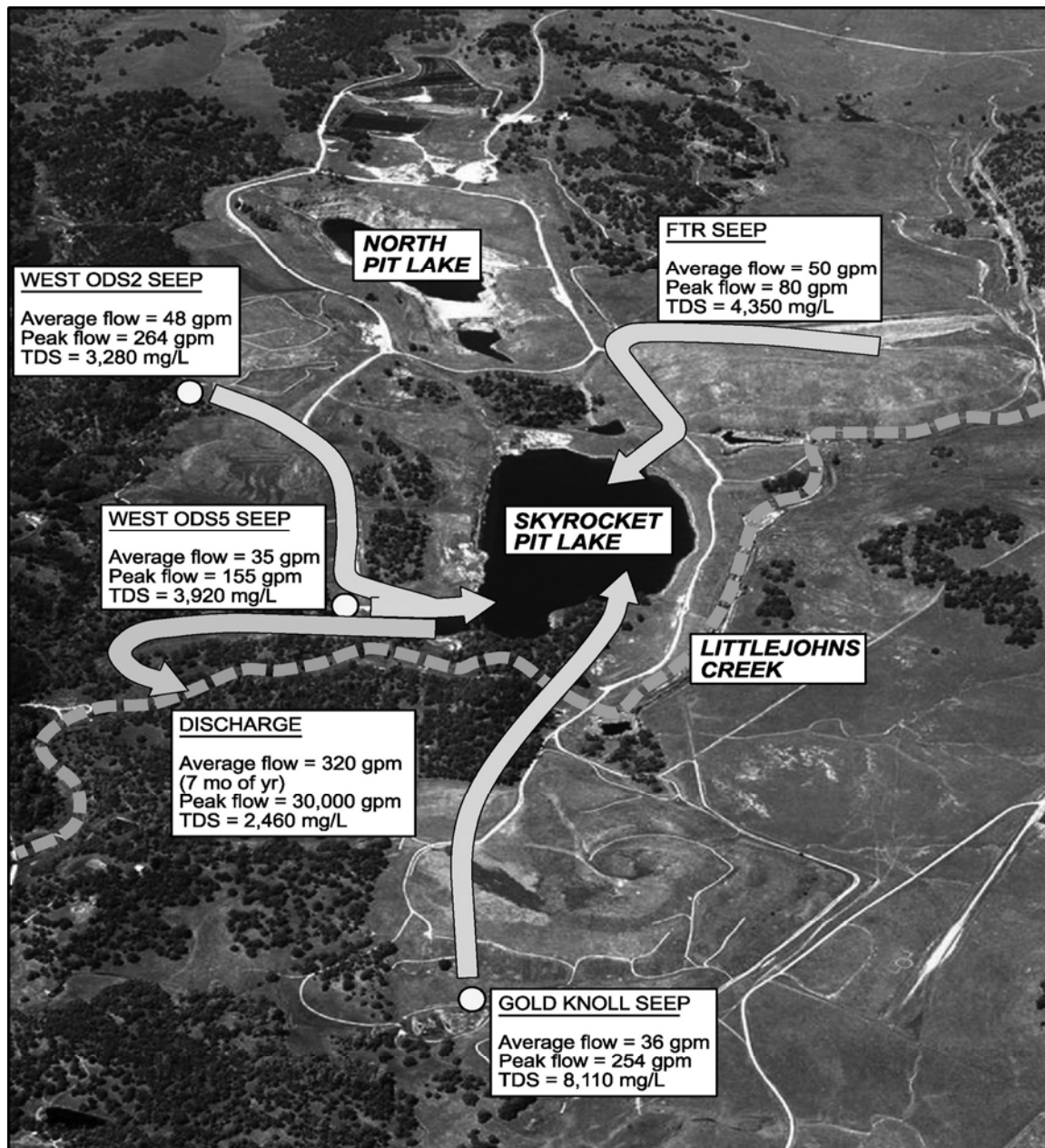
MERIDIAN BEARTRACK COMPANY
ROYAL MOUNTAIN KING MINE

Figure 1

August
2009







Water Transfers

MERIDIAN BEARTRACK COMPANY
 ROYAL MOUNTAIN KING MINE

Figure 3

August
 2009



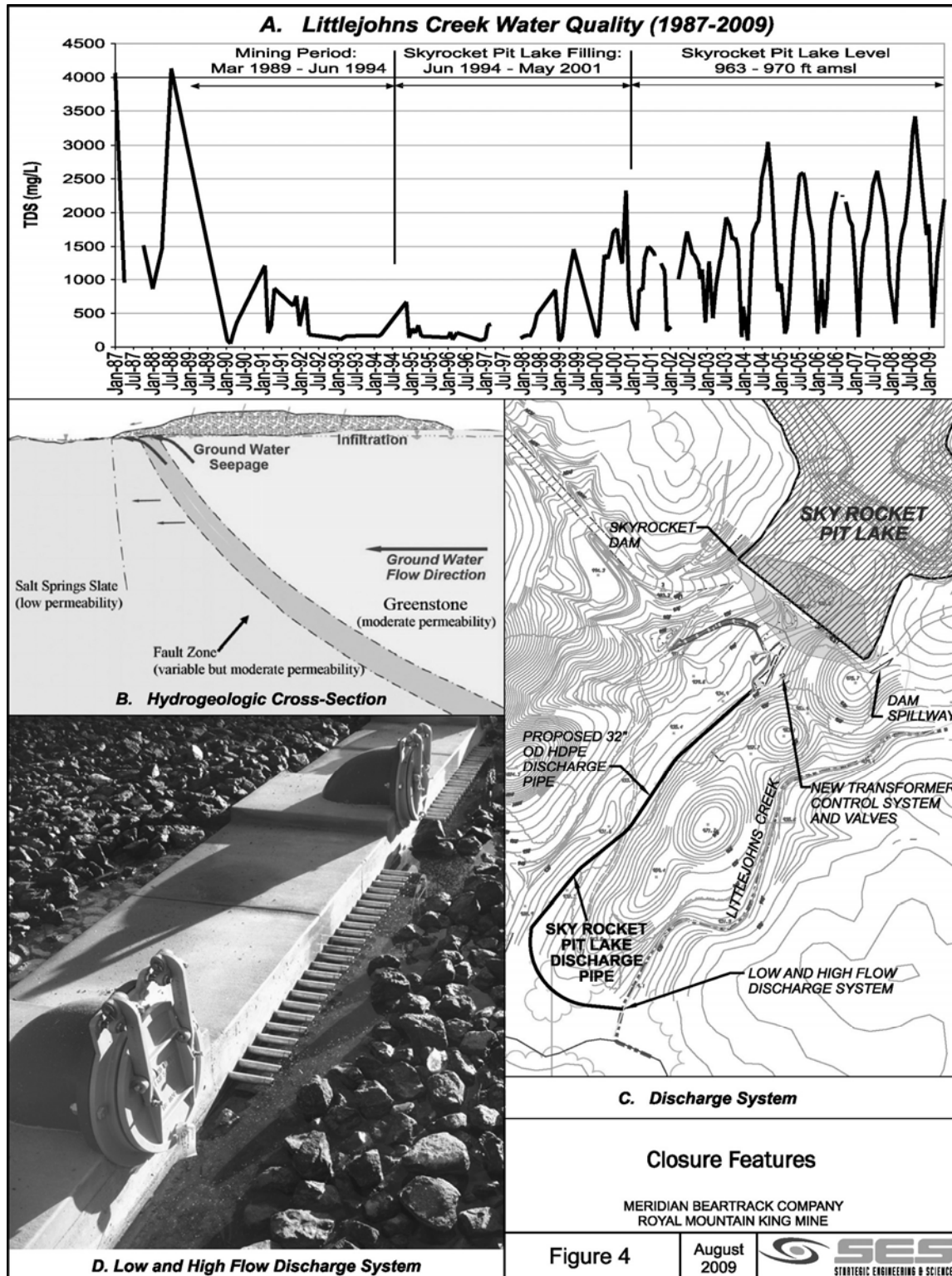


Figure 4

August 2009



SUBAQUEOUS DISPOSAL OF SULPHIDE TAILINGS – RECLAMATION OF THE SHERRIDON ORPHAN MINE SITE, MANITOBA, CANADA

Doug Ramsey

Wardrop Engineering Incorporated, a Tetra Tech Company, Winnipeg, Manitoba, Canada;

Jeff Martin

SENES Consultants Limited, Toronto, Ontario, Canada

ABSTRACT: The Sherridon Orphan Mine Site is a large abandoned Cu-Zn mine site in northwestern Manitoba, Canada. The site is the responsibility of the Province of Manitoba and has been identified as a priority for the remediation of environmental and human health and safety risks associated with the acid generating tailings and waste rock on the site. The reclamation concept, which provides a walk-away solution, involves placement of the ARD materials under a water cover. This presentation will present the detailed design and review the progress of implementation.

INTRODUCTION

The Sherridon Orphan Mine site, located in northwestern Manitoba, Canada (Figure 1) has been identified as one of five high-risk orphaned or abandoned mines sites in Manitoba. The site is the responsibility of the Province of Manitoba and has been identified as a priority for the remediation of environmental and human health and safety risks. This paper provides an overview of the studies completed to develop a remedial design for the site and details the final design and predictions of the environmental improvements expected to result from the project. Construction of the project began in October 2008 and will continue through to October 2012. This project was commissioned by the Mines Branch of the Manitoba Department of Science, Technology, Energy, and Mines. The remediation plan has been developed by Wardrop Engineering, Inc., as the prime contractor with technical assistance from SENES Consultants Limited.

SITE HISTORY

The Sherridon VMS copper-zinc deposit was discovered at Cold Lake (55°08'22"N 101°06'25"W), approximately 65 km northeast of Flin Flon, in 1922. Sherritt Gordon started mining the deposit in 1928. Mining was suspended in 1932, re-started in 1937, and ceased in 1951 when the ore deposit was depleted. The Sherridon Mine initially recovered copper and minor amounts of silver and gold. Zinc recovery was added in 1942. The adjacent communities of Sherridon and Cold Lake developed to support the mine operation and the communities remain to the present. Overall, 7.7 million tonnes of pyretic ore were mined, and 7.4 million tonnes of tailings generated. Tailings disposal was primarily subaerial, with the tailings pile covering approximately 47 ha adjacent to Camp Lake (Figure 2). Tailings are 60 % sulphides mainly consisting of pyrite and pyrrhotite.

Exposure of the sulphides in the tailings to oxidizing conditions has resulted in the production of acidic drainage which has leached heavy metals from the tailings and has acidified Camp Lake. The current pH of Camp Lake is approximately 3.2, with total zinc concentrations in the range of 0.5 to 1.0 mg/L and total copper concentrations in the range of 0.1 to 0.2 mg/L. The lake no longer supports a fish community. Camp Lake discharges to the Cold Lake arm of Kississing Lake (Figure 2), a large lake in

the Churchill River watershed with important sport, commercial sport, commercial and domestic fisheries. Water and sediment contamination and altered benthic invertebrate and fish communities have been documented throughout the Cold Lake arm of Kississing Lake (Wardrop 2009) and approximately 9.5 km² of lake sediment have elevated concentrations of metals attributable to the Camp Lake discharge (UMA/SENEC 2004).

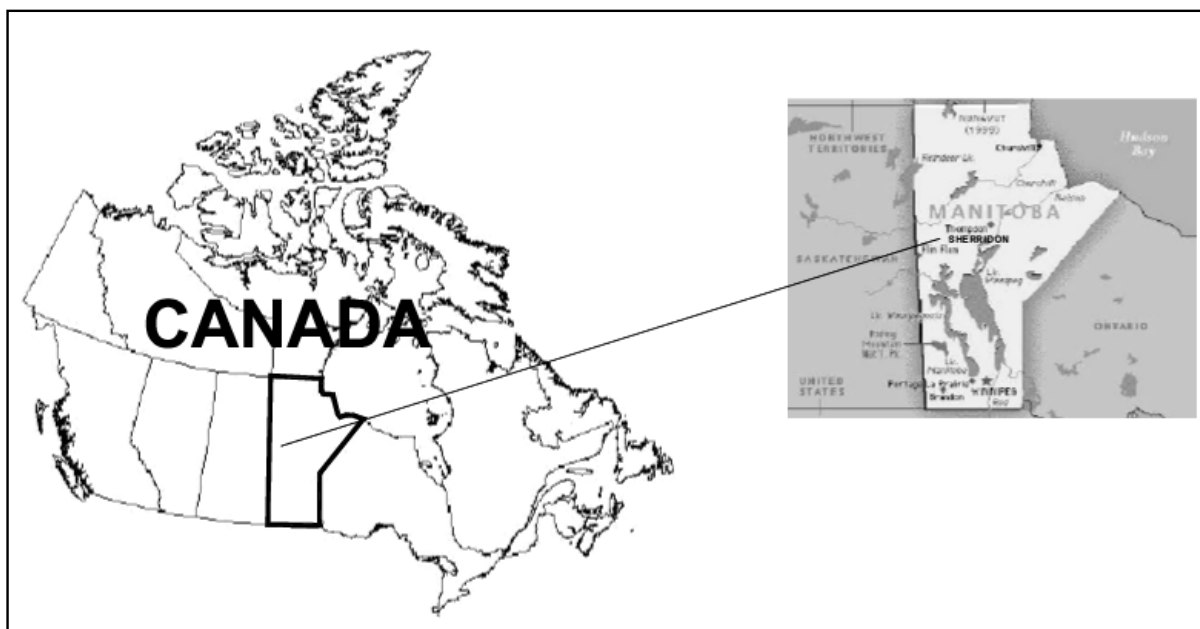


Figure 1: General site location of the Sherridon Orphan Mine site, Manitoba, Canada.

The tailings also are subject to wind suspension, creating dust clouds over the tailings pile during wind events and resulting in localized contamination of the terrestrial environment up to 500 m from the tailings pile (UMA/SENEC 2004).

A human health and ecological risk assessment (UMA/SENEC 2004) determined that the tailings dusting was not a significant risk to human health or the natural environment. The discharge of acid and metal contaminated water to Kississing Lake was identified as a significant ecological risk.

REMEDATION OBJECTIVES

The Manitoba Mines Branch applies a risk-based management approach to the orphan mine sites for which they are responsible. Remediation is therefore considered effective if all significant risks to human health, safety, and the natural environment associated with the site are controlled. Remediation or “clean-up” for purely aesthetic considerations is not an objective of the orphan mine site management program.

Based on the human health and environmental risk assessment completed

for the site (UMA/SENES 2004), the primary risk to be managed is acid and metal loading to Kississing Lake via the Camp Lake discharge. Tailings dusting is a quality of life issue of concern for the local residents but was not found to be a risk to human health, either directly in the dust or indirectly via the consumption of local plants or wildlife. Similarly, adjacent terrestrial contamination resulting from tailings dusting was not found to be a significant risk to the natural environment. Consequently, control of acid and metal

loading to Kississing Lake and elimination of tailings dusting were selected as the primary remediation objectives for the site. These objectives were to be achieved at the lowest possible cost, based on a net present value determination, and preferably would minimize or eliminate any requirement for continuing active treatment. Finally, Manitoba requested that the remedial works be completed by 2012 in accordance with a directive of the provincial auditor.

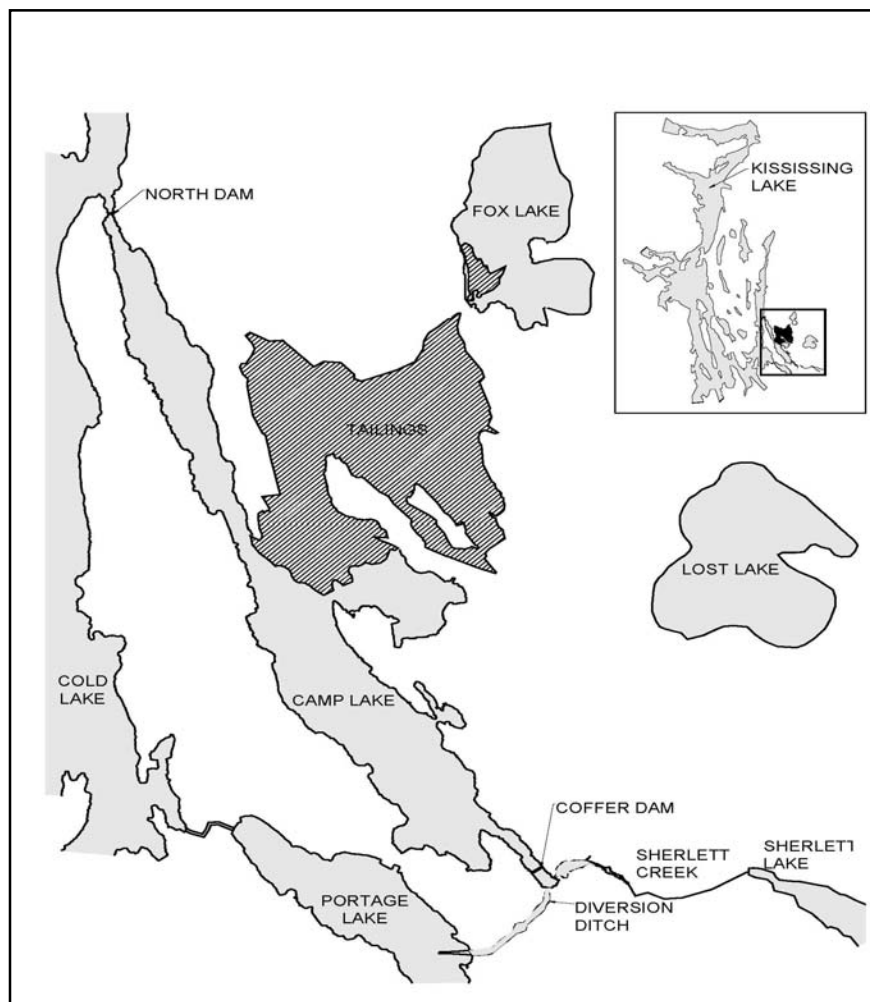


Figure 2: Location of Sherridon tailings in relation to Camp Lake, Manitoba, Canada.

REMEDATION DESIGN PROCESS

The remediation project was designed using a multi-step process. The first step involved the identification of potential remedial approaches and a screening-level analysis to identify fatal flaws and general applicability to the remedial objectives. The remedial options considered in the screening analysis were reduced to a short-list of three options, all of which had the potential to meet the primary remedial objectives, for which preliminary cost estimates were developed, leading to the recommendation of a preferred remedial option (Wardrop 2007).

The preferred option and the process followed in reaching that recommendation were reviewed by a Technical Advisory Committee (TAC) comprised of representatives of all provincial and federal departments and agencies with a potential interest in the project. Based on this TAC review, Manitoba approved the development of the detailed project design for the preferred remedial option. The detailed design process began with consultation with the adjacent communities of Sherridon and Cold Lake to explain the process, describe the preferred remedial option, and solicit questions or concerns. The community consultation and information sessions have since been held at approximately six month intervals, initially to provide reports on design progress and forthcoming construction plans and this information/consultation schedule will be maintained throughout the construction phase of the project.

REMEDIAL CONCEPTS SCREENING

The remediation design study initially identified and screened six remedial concepts for their suitability on the basis of

the site remediation requirements and effective application elsewhere. The options considered at the screening level are summarized in Table 1.

Based on the screening comparison, three options (the base case, engineered cover, and subaqueous disposal in Camp Lake) were identified for further detailed evaluation. The terraced flooding option was eliminated on the basis of high permeability of tailings and expected difficulty in maintaining water cover. Disposal in the underground workings was eliminated on the basis of inadequate capacity, foreclosure of future mining options, and complexity and cost of a multiple remedial approach concept. Raising the Camp Lake water level to flood tailings was eliminated on the basis of the extensive dam development required, the related long term dam safety concerns, potential difficulty in maintaining water cover during drought conditions, and increased advective flux of contaminants at the elevated water level.

DETAILED OPTION EVALUATION

A description of the short-listed closure options and their expected environmental performance is provided below, followed by a cost comparison, and an evaluation of the options. Quantities and unit costs employed in the analysis are detailed in Wardrop 2007.

Vegetated Cover and Treatment of Camp Lake

This is the “base case” option, considered to represent the minimum level of remediation necessary to achieve the reclamation objectives.

Table 1: Screening level comparison of remediation options.

REMEDATION OPTIONS	CONCEPT	DETAILS	ADVANTAGES	DISADVANTAGES	COMMENTS
1 Base Case – Re-vegetate Tailings Pile and Treat Camp Lake Outflow on a Seasonal Basis	<ul style="list-style-type: none"> - minimum cover to enable re-vegetation - treat and discharge excess water from Camp Lake on a seasonal basis 	<ul style="list-style-type: none"> - grade tailings for drainage, place capillary break, soil cover, vegetation - divert Sherlett Creek flow around Camp Lake - construct perimeter dams as needed to direct runoff and control run-on - construct treatment plant to treat discharge on a seasonal basis - construct polishing pond and sludge storage 	<ul style="list-style-type: none"> - relatively low capital cost - decreases contaminant flux to Kississing Lake - prevents dusting - improves aesthetics of tailings basin - southern portion of Camp Lake could be reclaimed 	<ul style="list-style-type: none"> - active treatment required in perpetuity, operating cost offsetting lower capital cost - sludge management required - tailings pore water quality remains poor - Camp Lake remains in a substantially degraded state serving primarily as a treatment pond 	<ul style="list-style-type: none"> - essentially "manages" the tailings problem but does little to actually remediate the area - requires care and maintenance in perpetuity
2 Raise Water Level in Camp Lake to Flood Tailings	<ul style="list-style-type: none"> - construct perimeter dams around Camp Lake and tailings pile - raise water level of Camp Lake to flood the tailings in perpetuity - batch treat initial pulse of contaminants 	<ul style="list-style-type: none"> - dams required to bridge all topographic lows, including a dam across the south basin of Camp Lake - divert Sherlett Creek flow around Camp Lake - require seepage cutoff (e.g., grout curtain) to control advective flux from the basin - minimal relocation of existing subaerial tailings beaches - temporary batch treatment plant at outlet - may require alkalinity barrier cover on tailings 	<ul style="list-style-type: none"> - minimize future tailings oxidation - minimal requirement for relocation of existing tailings - oxidized tailings would act as a diffusion barrier in the long-term - short-term post-flooding treatment of discharge - may be able to reclaim the southern portion of Camp Lake 	<ul style="list-style-type: none"> - increased water level will increase the advective flux of contaminants from the tailings pile - relatively large dams required - increased risk associated with dam failure - tailings pore water remains highly contaminated in the long-term 	<ul style="list-style-type: none"> - small catchment area for Camp Lake may be problematic for maintaining water cover, requiring provision of supplementary water from Kississing Lake during periods of extended drought - high tailings permeability may be problematic at Sherridon
3 Terraced Tailings with Seepage Control to Encourage Full Saturation	<ul style="list-style-type: none"> - re-contour tailings surface to create multiple flooded terraces (similar to the Quirke Tailings Basin in Elliot Lake) 	<ul style="list-style-type: none"> - re-contour tailings into multiple terraces - construct low dams and cut-off trenches to ensure complete saturation of the tailings - could incorporate oxygen diffusion cover to minimize requirement for water cover - divert Sherlett Creek flow around Camp Lake - construct water control structure at north end of Camp Lake - construct treatment plant to treat Camp Lake outflow for uncertain period 	<ul style="list-style-type: none"> - maintains tailings saturation and inhibits oxidation - prevents dusting and erosion of the tailings surface - shallow berms and cut-off trenches are relatively easy to construct - may be able to reclaim the southern portion of Camp Lake 	<ul style="list-style-type: none"> - increased flushing of tailings pore water into Camp Lake - susceptible to drought conditions - effectiveness of a cut-off trench within the tailings is uncertain - active treatment required for long period of time 	<ul style="list-style-type: none"> - would continuously flush the highly concentrated tailings pore water (high treatment demand) - long term stability of structures built in tailings uncertain - water quality in Camp Lake would take a long time to improve - small catchment area for Camp Lake may be problematic for maintaining water cover, requiring provision of supplementary water from Kississing Lake during periods of extended drought
4 Subaqueous Disposal in Camp Lake	<ul style="list-style-type: none"> - excavate all tailings below elevation 314.5 m ASL and relocate to Camp Lake - neutralize tailings during relocation - establish 1.5 m water cover over the tailings, maintained by the Sherlett Creek watershed 	<ul style="list-style-type: none"> - temporary diversion of Sherlett Creek around Camp Lake - relocate all tailings above 314.5 m ASL - add excess neutralizing potential during relocation to precipitate soluble metals - temporary treatment plant to treat Camp Lake water before and during tailings relocation - may require alkalinity barrier cover over tailings - reclaim and re-vegetate exposed areas 	<ul style="list-style-type: none"> - water quality of Camp Lake would be expected to improve, potentially to the degree that fish habitat may re-establish in lake and lake may be suitable for some recreational uses - tailings dusting eliminated - as close to a "walk away" solution as can be reasonably achieved - most likely to eliminate requirement for continuing water treatment 	<ul style="list-style-type: none"> - Camp Lake becomes a uniformly shallow lake 	<ul style="list-style-type: none"> - technically superior provided sufficient subaqueous storage capacity available
5 Tailings Relocation to the Underground Workings	<ul style="list-style-type: none"> - excavate and relocate tailings to the underground mine workings 	<ul style="list-style-type: none"> - divert Sherlett Creek around Camp Lake – uncertain duration - relocate all tailings above 314.5 m ASL to underground - engineer controls to minimize contaminant migration - reclaim and re-vegetate exposed areas - construct treatment plant and treat Camp Lake until water quality stabilizes 	<ul style="list-style-type: none"> - improved water quality in Camp Lake - remove significant load of contaminants to Lake Kississing - may be able to reclaim the southern half of Camp Lake 	<ul style="list-style-type: none"> - inadequate underground capacity to accommodate all tailings - prevents any further mining of the deposit - balance of tailings would require reclamation using one of the other approaches 	<ul style="list-style-type: none"> - involves the complexity of multiple reclamation approaches
6 Engineered Cover	<ul style="list-style-type: none"> - cover the entire tailings pile with an impervious cover to minimize infiltration 	<ul style="list-style-type: none"> - re-contour tailings surface and cover with a high quality liner - permanent diversion of Sherlett Creek to isolate Camp Lake and install controlled discharge to the north - construct treatment plant and treat water from Camp Lake 	<ul style="list-style-type: none"> - may be possible to reclaim the southern portion of Camp Lake - improved water quality in Camp Lake 	<ul style="list-style-type: none"> - active treatment required for long term - sludge management required - tailings pore water quality remains poor - Camp Lake remains in a substantially degraded state serving primarily as a treatment pond 	<ul style="list-style-type: none"> - tailings porewater remains long term source of contamination (albeit much lower advective flux) - essentially "manages" the tailings problem but does little to actually remediate the area - requires care and maintenance in perpetuity

Acid rock drainage release rates in the Sherridon tailings are anticipated to continue to rise as neutralisation potential in the tailings is depleted and the higher strength cores of the existing acidic contaminant plumes within the tailings reach adjacent surface water bodies. Under this option, Sherlett Creek flows would be isolated from Camp Lake because the creek represents approximately 95% of the hydraulic load to Camp Lake and it is more efficient to treat as small a volume of water as practical. The existing tailings and waste rock surface would be regraded where required to establish a vegetative cover. A cover would be required to minimize windblown tailings and to improve the aesthetics of the site.

Establishment of a vegetation cover would require the placement of a phreatic break to control the upward movement of contaminants. The break would consist of 30 cm of coarse material (gravel and possibly some of the existing waste rock), covered with 30 cm of a finer material such as till. The cover would be seeded and maintained as necessary until the vegetation becomes self sustaining.

A high-density sludge (HDS) lime treatment plant would be constructed adjacent to Camp Lake to treat accumulated precipitation and local watershed runoff before discharge of the treated water to Kississing Lake. A sludge disposal facility would be needed for long term management of the produced metal hydroxide sludge.

The treatment plant would be required to remain in operation for centuries. As noted in Moncur (2004) without “an effective remedial program, sulphide oxidation in the vadose zone will continue to release acid, elevated concentrations of metals and sulphate to the tailings pore water for many decades to centuries. Once in the tailings pore water, the metals will be transported to surface waters for even longer”. In the

Camp Tailings, the highest concentrations of metals and sulphates occur in the tailings farthest inland from Camp Lake (Moncur 2004).

Over time it is expected that groundwater quality will deteriorate along the flow paths within the tailings, such that pore water quality discharging to Camp Lake will worsen over time. Consequently, loadings to Camp Lake will increase in the future under this long-term treatment scenario, resulting in increasing lime costs and rates of sludge production over time. For the purpose of the cost comparison, it was assumed that loadings from the tailings area double over the next 100 years and that operation of the treatment plant would be required for at least 100 years – a conservative estimate in consideration of the above. A detailed study would be required to improve on this prediction.

Implementation of this option would have a dramatic effect on water quality in Kississing Lake, as the treated water discharged for the HDS plant would be of good quality. Water quality would continue to be poor in Camp Lake and in ponds adjacent to the tailings pile. The simple cover over the tailings areas and mine/mill area would control tailings dusting improve the aesthetics of the site.

Engineered Cover

A variety of engineered covers could be applied to the tailings, each with different infiltration rates and oxygen barrier properties. For the Sherridon tailings, the performance of the cover as a barrier to infiltration is considered to be more important than its performance as an oxygen barrier. This is due to the large existing inventory of sulphide oxidation products in the porewater and, to a lesser extent, in the hardpan. Discharge of the existing inventory will only be decreased by reducing infiltration. A reasonably good engineered cover could reduce infiltration

by 80% over current levels. For the Sherridon tailings, the current infiltration is estimated at 108 mm/year, or a discharge of 50,760 m³/year for the entire area. A reduction by 80% would result in infiltration of 22 mm/year, or a discharge of 10,150 m³/year.

For the purposes of this comparison, a conceptual cover design has been employed that consists of the following layers, from top to bottom:

- 0.5 m layer of vegetated, un-compacted granular material;
- 1.0 m layer of compacted low permeability clay till; and,
- 0.5 m capillary break layer consisting of coarse gravel and/or processed waste rock.

Alternatively, a cover could be constructed containing a synthetic barrier layer such as high density polyethylene (HDPE) or a geosynthetic clay liner (GCL). The final cover design would be determined through a detailed study, which would consider performance, cost, and the availability of construction materials such as granular and low permeability clay tills. Covers that are good barriers to infiltration typically are also good oxygen barriers, so improvements in one area usually result in improvements in another area. With the engineered cover in place, there could still be some ongoing sulphide oxidation however it will likely be reduced significantly. Even with no ongoing sulphide oxidation, the current porewater inventory will result in long-term loadings.

After installation of the cover, the discharge of contaminated porewater from the tailings pile would continue at pre-cover levels for some time. Discharge would then gradually decline, as the hydraulic gradient and the stored porewater in the tailings (above the level of Camp Lake) both decrease in response to the cover. This process would take years to

decades. Once discharge volumes stabilise at a lower level, loadings would increase in a similar fashion as described above for the base case, due to the migration of the core of the contaminant plume toward Camp Lake.

The environmental benefit of an engineered cover mainly depends on how effective the cover is in reducing infiltration. As discussed above, a reduction of infiltration by 80% would be reasonable to expect. However, the expected future degradation of porewater would partially negate any improvement (reduction) in loading due to reduced infiltration. If the contaminant concentrations in the porewater discharging to the water bodies eventually double, then the reduction in loading would only be 60% of current levels. If left untreated, this level of loading would result in continued degradation of Camp Lake and Kississing Lake. The engineered cover would effectively eliminate dusting and deal with visual impairment. For the engineered cover to provide environmental benefits comparable to the base case, above, a treatment system would be required over the long-term. Sherlett Creek also would be permanently diverted as described for the base case.

Consequently, both the capital and operating costs of this option would be relatively high as both a cover and some form of continuing treatment would be necessary.

Subaqueous Disposal in Camp Lake

Subaqueous disposal in Camp Lake has been considered in a manner that does not require raising the lake level above 316 m ASL, the nominal natural lake level, on completion of the tailings relocation into the lake basin. This requires the excavation of all tailings to elevation 314.5 m ASL in order to ensure at least 1.5 m of water cover over the relocated tailings.

The benefits of relocation and flooding of the tailings include:

- minimize or eliminate the hydraulic gradient that is currently driving the discharge of contaminated porewater from the tailings;
- minimize further oxidation of the tailings;
- eliminate the need for long-term treatment; and,
- stabilise the tailings surface from wind and water erosion.

The hydraulic gradient in the flooded tailings is expected to be flat, therefore eliminating gradient-driven porewater discharge to Camp Lake. Groundwater mounding in the surrounding bedrock ridges is unlikely to provide a significant head to drive ongoing groundwater discharge, as the bedrock is for the most part a relatively impermeable gneiss and the watershed area is small. Instead, it is expected that precipitation in the bedrock ridges would tend to flow mainly as surface runoff to Camp Lake.

In preparation for tailings relocation, Camp Lake would need to be isolated from Sherlett Creek flows by a dyke and diversion channel to route flows around the south end of the lake and reduce the hydraulic load, both to facilitate treatment and level management for tailings placement. Once this structure is in place, Camp Lake and other acidic water bodies in the watershed would be batch-treated with lime to reduce existing acidity and precipitate metals. When water quality becomes acceptable for discharge to Kississing Lake, the level of Camp Lake can be managed as needed by pumping out the treated water. Potential pumping requirements range from moving the water displaced by tailings to pumping the basin empty to allow tailings placement in the dry. Requirements for the addition of neutralization potential to relocated tailings vary with the tailings properties and the

method of placement. Similarly, some tailings benefit from the placement of an alkalinity barrier over the tailings.

Cost Evaluation

Comparative costs of three approaches were developed on the basis of physical and chemical characteristic of the tailings and on typical unit costs for materials and earth moving. These are detailed in Wardrop (2007). For purposes of cost comparison among dissimilar approaches, the long term operating costs were estimated for a period of 100 years using a 3% discount rate. Although the long term operating costs of the continuing treatment options would likely extend for longer than 100 years, costs beyond that horizon do not materially affect such a cost comparison. On this basis, the estimated net present value costs (in millions of 2007 CAD) for the three options are:

- Minimal Cover and Long-term Treatment of Camp Lake \$35.4
- Engineered Cover with Long-Term Treatment of Camp Lake \$35.1
- Subaqueous Disposal in Camp Lake \$34.4

All three options carry effectively the same net present cost, although subaqueous disposal brings additional advantages including no requirement for a long term presence on the site and reclamation of Camp Lake, in addition to providing protection for Kississing Lake and controlling tailings dusting, which all three options address. On this basis, and considering that long-term treatment would likely be for much longer than 100 years, subaqueous disposal was recommended as the remedial approach for the site.

DETAILED DESIGN

The overall objective of the remedial design process is to achieve water quality

in Camp Lake that is in compliance with the Manitoba Water Quality Standards Objectives and Guidelines (MWQSOG; Williamson 2002) for the protection of aquatic life and to do so with a minimum of post-relocation water treatment, all at the lowest possible cost. The base case for the remedial design included:

- Diversion of Sherlett Creek around Camp Lake for period of remedial works
- Neutralization of Camp Lake to pH 9 prior to the initiation of tailings relocation
- Maintenance of neutralized lake water through the period of tailings relocation.
- Relocation of all tailings above elevation 314.5 m ASL to the Camp Lake basin; and,
- Cover all the tailings with a 1.5 m deep water cover on completion of relocation to bring the Camp Lake level to elevation 316.0 m ASL, which is within the historic natural range of lake levels.

The neutralization specification for Camp Lake of pH 9 was determined from a PHREEQC simulation run on Camp Lake water at one unit pH increments between pH 7 and pH 10 and indicated that concentrations of both copper and zinc dropped significantly between pH 8 and 9 (Table 2).

Beyond the base case, the following four specific design variations were evaluated:

- Tailings relocated without neutralization, no barrier cover;
- Tailings relocated without neutralization, covered with an alkalinity barrier;

- Tailings relocated with neutralization, no barrier cover; and,
- Tailings relocated with neutralization, covered with an alkalinity barrier.

The expected effects of each design variant on water quality in the post-remediation Camp Lake were evaluated using the Reactive Tailings Program for Base Metal Tailings (RATAP.BMT) (MEND/NRCan 1990). Model input included tailings dimensions (size, depth, depth to water table), tailings particle size distribution, gaseous transport characteristics (diffusion coefficient, gas filled porosity), precipitation (hydraulic flows), mineralogy (bulk density, reactive sulphide minerals, other primary minerals, secondary minerals, buffering minerals), water quality (background water quality, porewater quality), pond option (pond size, depth, pond water quality, inflow water quality), and dry cover option (number of cover layers, cover diffusivity, cover thickness). Input data are subjected to statistical analysis to identify outliers and significant data clusters. All water quality data were checked for ion balance and solid/solution equilibrium by employing US Geological Survey's PHREEQC water quality program. The model was run at a one month time step for a period of 600 months (50 years) following completion of the remedial works. Specific model inputs are detailed in Table 3.

The key water quality parameters for assessment of the effectiveness of the design variations were identified as pH, sulphate, total zinc, and total copper. The RATAP-estimated post-remediation water quality indicates that both neutralization of the tailings is adequate to achieve all the remediation objectives but that the additional placement of an alkalinity barrier improves performance with respect to zinc and sulphate (Figures 3, 4, 5,

and 6). The applicable chronic exposure MWQSOG for total zinc is 129 µg/L at a total hardness of 108 mg/L and the objective for total copper is 9.9 µg/L. In comparison, the estimated total Zn concentration in Camp Lake the first year following completion of tailings relocation is 70 µg/L. The estimated total Cu

concentration in Camp Lake the first year after tailings relocation is 6.2 µg/L. Both neutralization and an alkalinity barrier reduce sulphate release over neutralization alone during the first approximately 150 months after tailings relocation (Figure 4), indicating sulphide reduction may also be better controlled as well.

Table 2: Camp Lake Neutralization – PHREEQC simulation of parameter concentration response to pH adjustment (SENES 2008).

pH		3.2	7	8	9	10
Temp	°C	4	4	4	4	4
Ca	mg/L	13.7	81.5	92.1	96.4	110.7
Mg	mg/L	7.4	7.4	7.4	7.4	7.4
Na	mg/L	2.6	2.6	2.6	2.6	2.6
K	mg/L	1.8	1.8	1.8	1.8	1.8
Al	mg/L	1.9	0.06	0.5	1.4	1.9
Ba	mg/L	0.01	0.01	0.01	0.01	0.01
B	mg/L	0.01	0.01	0.01	0.01	0.01
Cd	mg/L	0.002	0.002	0.0006	0.0005	0.0005
Cu	mg/L	0.14	0.14	0.018	0.001	< 0.001
Fe	mg/L	34	0.03	0.01	0.001	0.001
Pb	mg/L	0.0005	0.0005	0.0005	0.0005	0.0005
Mn	mg/L	0.3	0.3	0.1	0.07	0.001
U	mg/L	0.0003	0.0003	0.0003	0.0003	0.0003
Zn	mg/L	0.77	0.77	0.77	0.27	0.18
Cl	mg/L	6	6	6	6	6
Si	mg/L	1.2	1.2	0.8	0.5	0.1
SO ₄	mg/L	165	165	165	165	165
NO ₃	mg/L	2.2	2.2	2.2	2.2	2.2
NH ₃	mg/L	0.3	0.3	0.3	0.3	0.3

Table 3: RATAP model input data – surface and tailings porewater quality, Camp Lake hydrology and morphometry, tailings solids mineralogy (SENES 2008).

		Tailings Porewater	Camp Lake	Surface Water	Ground Water	Woods Lake	Neutralized Tailings Porewater
pH		3.24	3.2	7.6	8.2	2.4	6.12
Temp	°C	4	4	4	4	4	4
Ca	mg/L	170	13.7	9.8	49.3	320	575
Mg	mg/L	7.4	7.4	3.1	20.3	290	17.6
Na	mg/L	2.6	2.6	2.1	41.3	40	5
K	mg/L	1.8	1.8	1.5	11.7	5	10.3
Al	mg/L	1,000	1.9	0.193	0.007	140	0.62
Ba	mg/L	0.01	0.01	0.01	0.05	0.2	0.03
B	mg/L	0.01	0.01	0.03	0.04	0.3	0.06
Cd	mg/L	0.002	0.002	0.0001	0.0002	0.027	0.004
Cu	mg/L	0.35	0.14	0.006	0.001	1.1	0.004
Fe	mg/L	31,000	34	2.45	0.2	2,430	0.5
Pb	mg/L	0.0005	0.0005	0.0001	0.0001	0.01	0.00004
Mn	mg/L	36	0.3	0.014	0.37	19	0.17
U	mg/L	0.0003	0.0003	0.0001	0.0001	0.017	0.0003
Zn	mg/L	754	0.77	0.076	0.007	38	0.05
Cl	mg/L	6	6	2.3	6	6	6
Si	mg/L	1.2	1.2	1.2	7.4	38	0.3
C(4)	as						
C	mg/L	8	8	8	60	8	8
SO ₄	mg/L	60,000	165	12	56.1	7,520	1,445
NO ₃	mg/L	0.5	0.5	0.05	0.15	0.15	0.01
NH ₃	mg/L	0.25	0.25	0.03	0.8	1.97	0.01
Ion	Balance						
(%)		0.88	0.42	0.5	-0.09	-0.07	0.06

Camp Lake Post Relocation		Lake	
Total Outflow :	17,490,000 m ³ /yr	area :	1,300,000 m ²

Tailings Solids Mineralogy(mol/m³)					
Pyrite	Pyrrhotite	Chalcopyrite	Sphalerite	Arsenopyrite	Pentlandite
2,610	4,860	51	441	1.5	0.6
Calcite	Dolomite	Siderite	Gypsum	Al(OH)₃	Fe(OH)₃
3.2	2.5	0	975	0	412
Mica	Pyroxine	Quartz	Ymg	YK	YNa
679	939	4,050	2	1	0.5

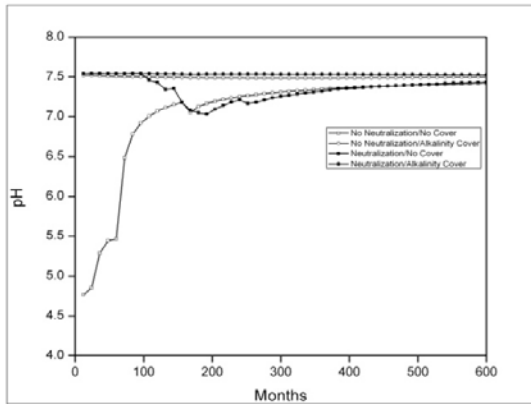


Figure 3: RATAP model results - pH

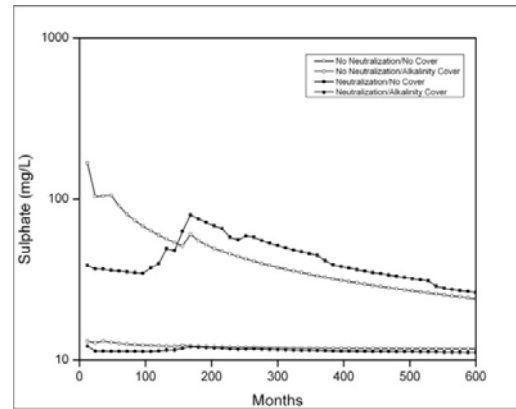


Figure 4: RATAP model results – Sulphate

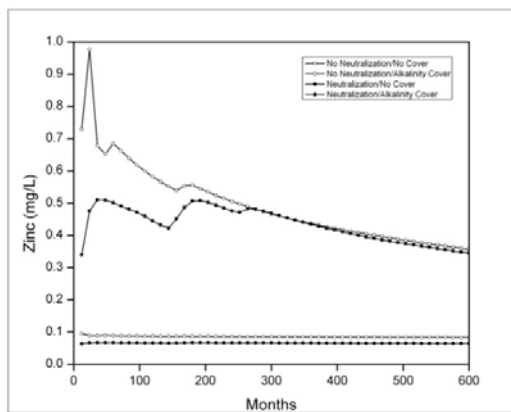


Figure 5: RATAP model results – Zinc

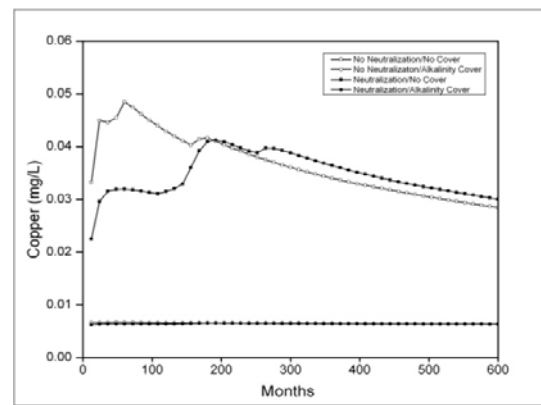


Figure 6: RATAP model results – Copper

Figure 4: RATAP model results – Sulphate

REFERENCES

MEND and Natural Resources Canada (NRCan). 1990. Critical review of the reactive tailings assessment program (RATAP.BMT2).

Moncur, M.C. 2004. Release transport, and attenuation of metals from an old tailings impoundment, Sherridon, Manitoba. M.Sc. Thesis. Department of Earth Science, University of Waterloo, Waterloo, ON.

SENES Consultants Limited. 2008. Geochemical and hydrogeological assessment in support of Sherridon rehabilitation. Prepared for Wardrop Engineering. 34 pp.

UMA Engineering Inc. and SENES Consultants Limited. 2004. Site-specific

assessment of human health and ecological risks from the abandoned mine site, Sherridon/Cold Lake, Manitoba. Report prepared for Manitoba Conservation.

Wardrop Engineering Inc. 2007. Sherridon Orphan Mine site reclamation plan. Report prepared for Manitoba Science, Technology and Mines.

Wardrop Engineering Inc. 2009. Aquatic resources baseline study. Report prepared for Manitoba Science, Technology and Mines.

Williamson, D. 2002. Manitoba Surface Water Quality Standards, Objectives, and Guidelines, Final Draft. Manitoba Conservation Report 2002-11.

MODELLING TECHNIQUES FOR EVALUATING NET PERCOLATION THROUGH SOIL COVERS FOR SOLID AND HAZARDOUS WASTE – A COMPARATIVE CASE STUDY

B.S. Dobchuk, M.A. O’Kane, & R.E. Shurniak
O’Kane Consultants Inc., Saskatoon, Saskatchewan

G.P. Newman
Newmans Geotechnique Inc., Saskatoon, Saskatchewan

S.L. Barbour
University of Saskatchewan, Saskatoon, Saskatchewan

ABSTRACT: Design methodology for soil covers for mine waste has evolved to the point that the use of numerical simulations to evaluate performance is common place. There are a number of numerical models capable of simulating moisture dynamics in surficial soils in response to climate and vegetation. These numerical models are used to study the mechanisms controlling soil cover water balances, and to estimate cover saturation levels and net percolation rates into underlying mine waste. This study evaluated two of these numerical modelling programs: HYDRUS-1D and VADOSE/W. Two verification examples are given for the two models followed by a case study, which compares the predicted model results to measured data for a site in an arid climate in the tropical Southern Hemisphere. Detailed in situ soil moisture measurements and site meteorological data were measured over a number of years. Field-response simulations using both models were compared to measured suction and volumetric field data at depth, to total volume of water in the cover, and to measured net percolation. Both models reasonably predicted the field responses and, for the same input parameters, predicted virtually identical field responses. A variation of the calibrated models using higher intensity rainfall events produced improved matches to the field-response data.

INTRODUCTION

Mine waste cover systems typically represent the single largest component of a mine closure plan, not only with respect to environmental impact and cost but also public and regulatory scrutiny. The climate and

vegetation conditions at each mine site are different and consequently the cover system must satisfy site specific design objectives.

A typical design methodology for a cover system starts with a conceptual design based on existing site data and a limited program of

material characterization. The numerical modelling is used to compare various cover design alternatives to determine the basic cover design. One or more of these alternatives are then constructed and instrumented as field-trials. These trials are used to ensure that the processes relied upon in the design are operative at the field scale. The measured field responses are used to develop a calibrated field response model, which can then be used to evaluate long-term performance of the proposed cover system design.

The development and calibration of a field response model is a complex and vital component of the cover system design process. Figure 1 provides the general steps used to calibrate a field response model.

There are a number of commercially available codes for predicting the water balance of vegetated covers in the vadose zone that are applicable for a field response model calibration. Few studies have been conducted comparing different numerical modelling results with detailed field measurements. The models UNSAT-H, VADOSE/W, HYDRUS, and LEACHM were compared to field data in a study by Bohnhoff et al. (2009).

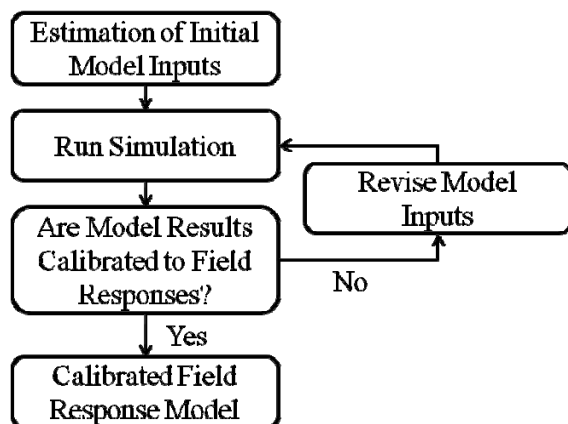


Figure 1. Flow chart of field response model calibration steps

The objective of this study was to compare two numerical models, VADOSE/W and HYDRUS. Theoretical and experimental examples are used to verify elements of model performance followed by a comparison of the calibration of the models to detailed field measurements.

MODEL VERIFICATION

The terms verification and calibration are sometimes used interchangeably in reference to numerical modelling techniques. However, there is a fundamental difference between model calibration and model verification. Model verification is testing a model by having it solve problems with known inputs and solutions to ensure that the model is programmed correctly (i.e. includes the correct (stated) set of mathematical formulations, implements algorithms properly and does not contain errors, bugs and oversights). In contrast, model calibration is the incremental adjustment of model inputs (generally material properties) until the model is able to simulate a set of observational data.

To verify VADOSE/W and HYDRUS, two simple models with known solutions were evaluated. The first model was the Kisch (1959) solution for steady-state infiltration through a clay liner into an underlying layer of unsaturated sand. The second model was based on Wilson et al. (1994) laboratory evaporation measurements.

Kisch Solution

The Kisch solution is a good verification test for a model because the entire solution is in unsaturated soil and it is numerically challenging to obtain a converged solution. The model consists of 0.5 m of clay with 2.0 m of underlying sand, representing a

situation in which there is a clay liner over a sand drainage layer. The moisture retention curves (MRCs) and hydraulic conductivity functions (k-functions) are shown in Figure 2. The van Genuchten (1980) estimation equation was used in both VADOSE/W and HYDRUS to approximate the Kisch (1959) hydraulic properties.

While Kisch is a steady-state solution, it can be solved as the final solution for an extended transient simulation. This is the only option provided for in the HYDRUS model, so transient simulations were completed using both models. The boundary conditions were pressure equal zero at both the top and base of the model. The initial conditions were a hydrostatic pressure profile in the sand above the lower pressure equal zero boundary and then linearly decreasing from -2 m at the base of the clay to zero pressure at the top of the clay.

Actual Evaporation Solution

The second verification test was based on the results of a laboratory evaporation study published by Wilson et al. (1994). An initially-saturated column of sand (Beaver Creek sand) and a water-filled pan were placed in an environmentally-controlled chamber. Both the sand column and the evaporation pan were placed on scales. The chamber was maintained at 38°C and approximately 15% relative humidity. Over a period of 40 days, the evaporation rate from both the column and the water-filled pan were measured based on the change in mass of the column and pan. The MRC and k-function of the sand are presented in Figure 4.

As shown in Figure 4a, the sand has a steep MRC. This gives the sand a distinct drying

front that develops soon after evaporation begins.

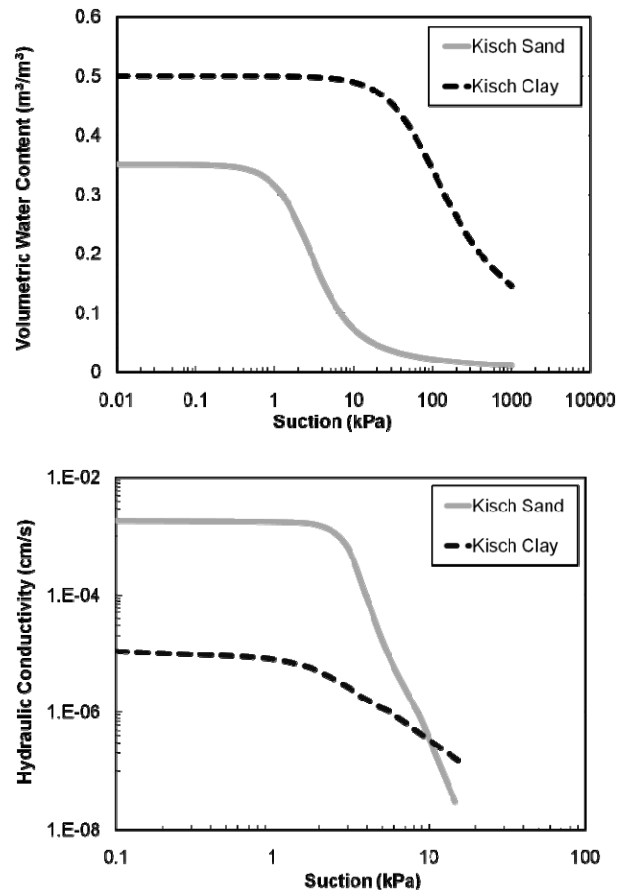


Figure 2. Moisture retention curves (a) and hydraulic conductivity functions (b) for sand and clay in Kisch (1959) solution.

This model is more complicated than the Kisch model in that the boundary condition applied to the surface of the model is a loss of water (i.e. evaporation). The model must solve for the appropriate rate of evaporation to apply to the surface. As the soil suction increases at the surface, the model must decrease the actual evaporation rate calculated.

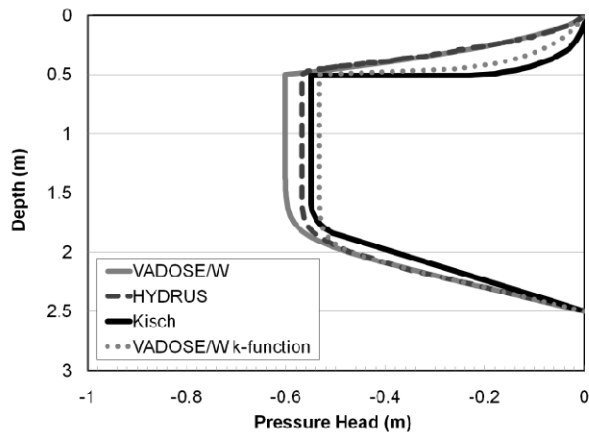


Figure 3. Solution for steady-state infiltration through a clay liner from Kisch (1959) compared to solutions from VADOSE/W and HYDRUS. The VADOSE/W k-function pressure profile used a spline-fit k-function to better predict the pressure profile.

There is a difference in the methodology that VADOSE/W and HYDRUS use to calculate actual evaporation. VADOSE/W uses the Penman-Wilson (Wilson et al. 1994) formulation where actual evaporation (AE) is calculated as a function of soil vapour pressure, suction, and temperature. HYDRUS uses a semi-empirical approach that requires the user to input a maximum allowable suction value for the soil. HYDRUS allows evaporation to occur at the potential rate (calculated using the Penman-Montieth equation) until the user-specified suction is reached. Once this suction is reached, the potential evaporation boundary condition is replaced with a fixed suction boundary condition at the user-specified value. The actual evaporation is then assumed to be equal to the water removed by this pressure boundary condition.

To simulate this experiment, a 0.3 m one-dimensional model geometry was used. The initial condition was a free-drained condition

with a zero flux lower boundary condition and a climate boundary as the surface boundary condition. The climate condition had constant surface temperature of 38°C, daily relative humidity of 10%, and no wind. Daily potential evaporation was the quantity as measured by the pan in the laboratory experiment (Wilson et al. 1994).

The results of the VADOSE/W simulation are presented in Figure 5. The small variation in the measured AE at the start of the experiment can be attributed to variation in the chamber relative humidity as discussed by Wilson et al. (1994). The VADOSE/W model predicts actual evaporation well with a slight under-prediction during days 6-8. Total evaporation over the 40 days was 82.5 mm for the column measured AE and 85.6 mm for the VADOSE/W predicted AE.

Convergence could not be attained using the HYDRUS model for the evaporation experiment due to the steep moisture retention curve of the sand. To evaluate the ability of the model to predict actual evaporation, a similar model was set-up with less extreme hydraulic functions. However, measured laboratory data was not available for this material type. Given the match between the Wilson experiment and the VADOSE/W model, it was concluded that the VADOSE/W model could be used to verify the results of the HYDRUS simulation in this case.

The same geometry and initial and boundary conditions were used for the second evaporation model but the material used was clay-till with the same moisture retention and hydraulic conductivity functions shown in Figure 2 for the Kisch clay.

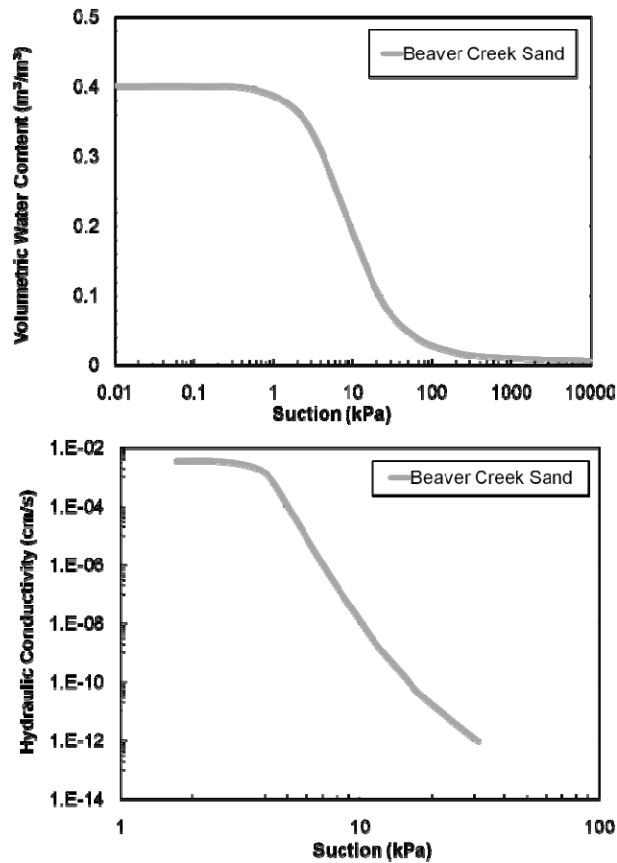


Figure 4. Moisture retention curve (a) and hydraulic conductivity function (b) for Beaver Creek sand from Wilson et al. (1994) column evaporation study.

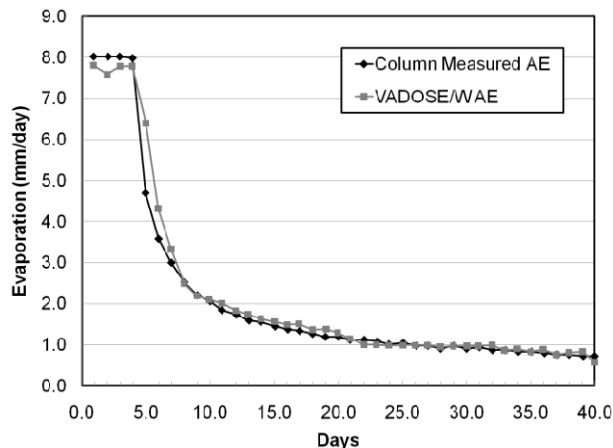


Figure 5. VADOSE/W solution for actual evaporation from a sand column compared to measured data from Wilson et al. (1994).

The evaporation results from both models are shown in Figure 6. Both models predict similar initial evaporation rates (potential rate) ranging between 7.5 and 8 mm/day. By day 9, VADOSE/W starts to predict a drop in evaporation rate due to surface drying but HYDRUS maintains the potential rate through day 11. A large difference in evaporation rate is shown between the two models between days 12 and 16, with differences of 2-3 mm/day. The two models converge to the same evaporation rate by day 28. Total evaporation rate calculated over the 40 days was 98.4 mm for HYDRUS and 104.0 mm for VADOSE/W.

To illustrate the differences in how the two models calculate actual evaporation, the suction at the surface node for both models is presented in Figure 7. On day 11, the surface materials in HYDRUS could no longer supply water at the potential rate. The model computes a rapid increase in the suction to the user-specified maximum suction value and then proceeds through the remaining timesteps with a fixed pressure head surface boundary condition. For this reason, evaporation in HYDRUS does not decline as gradually as VADOSE/W and therefore evaporation is under-predicted for a time period during initial drying.

MODEL CALIBRATION

Calibration of a field response model is a valuable tool for predicting long-term performance of a cover. Calibration of a field-response model requires detailed climate data, material properties, layer thicknesses, vegetation parameters, upper and lower boundary conditions, and initial conditions. A detailed instrumented field cover trial provides observational data against which the developed field-response model can be compared.

Calibrated field-response models from the same field site were developed in both VADOSE/W and HYDRUS to evaluate the similarities and differences between the models.

Site Description

The field site is situated at a mine site in a semi-arid tropical climate in Western Australia with a mean annual rainfall of approximately 320 mm. There are two distinct seasons, a hot, wet summer (December to April), followed by more temperate and drier conditions for the remainder of the year. It is common for rainfall to occur over short periods and with high intensity. Annual potential evaporation typically exceeds 3000 mm.

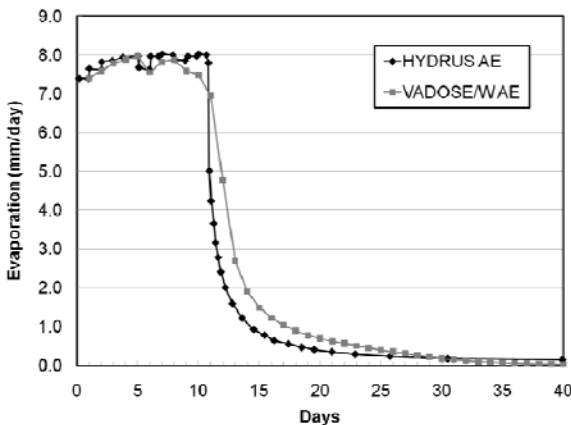


Figure 6. VADOSE/W and HYDRUS solutions for actual evaporation from a clay-till column.

The cover design at the field site consists of a 2.0 m thick monolithic layer of a coarse oxidized run-of-mine material overlaying potentially acid generating waste rock. Field test plots (1 ha in size) were constructed in 1997 on a relatively horizontal surface. The test plots were constructed with common operational considerations. An undulating surface created by ‘paddock’ dumping was used to ensure short surface run-off paths during the life of the test plots.

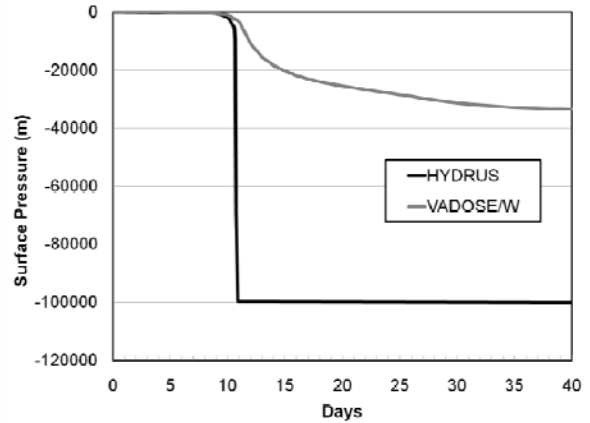


Figure 7. VADOSE/W and HYDRUS solutions for actual evaporation from a clay-till column.

A field performance monitoring system was installed to measure actual evaporation, potential evaporation, rainfall, net percolation (using large-scale lysimeters), and in situ temperature and moisture (suction and volumetric water content) conditions. The in situ monitoring profiles included sensors installed into the overlying cover material as well as into the underlying reactive waste rock.

Model Inputs

The following sections discuss each of the various model inputs for the case study field-response model.

Climate

Water balance models require daily inputs of precipitation amount and duration, maximum and minimum temperature, maximum and minimum relative humidity, average wind speed, and net radiation. All of these parameters are measured at the monitored field trial. This is extremely advantageous as it removes most of the uncertainty in these inputs

Material Properties

Each material layer defined in the field response model requires a unique set of

material properties. The material properties required to characterize moisture movement are the moisture retention curve (MRC) and the hydraulic conductivity function (k-function).

Field measurements of volumetric water content and pore-water pressure measured at similar depths within the field trial can be plotted together to provide an estimate of a portion of the MRC used to define each monitored depth. The porosity of a monitored location can be estimated based on field density measurements or laboratory testing. The parts of the MRC not defined by field data (such as above 1,000 kPa and below 10 kPa) should be systematically adjusted during the calibration process to determine their influence on the simulated field responses.

The k-function is difficult to measure. As a result, prediction methods are frequently used to estimate the shape of the k-function from the more easily measured moisture retention data. Hence, initial estimates of k-functions for field response models are usually estimated using measurements of field saturated hydraulic conductivity (k_{sat}) and a prediction method such as van Genuchten (1980) or Fredlund et al. (1994).

The instantaneous profile method (Eching et al., 1994) is recommended to estimate a range of unsaturated hydraulic conductivity values for a given material layer. The instantaneous profile method uses the measured changes in water content and suction to calculate the hydraulic conductivity. The data points provide an envelope of observational responses within which the estimated k-function should ideally remain.

The MRCs and k- functions used for the calibrated field-response modelling in both VADOSE/W and HYDRUS are presented in Figure 8. Both the cover and waste materials

had similar geotechnical characteristics and thus were simulated with the same hydraulic functions.

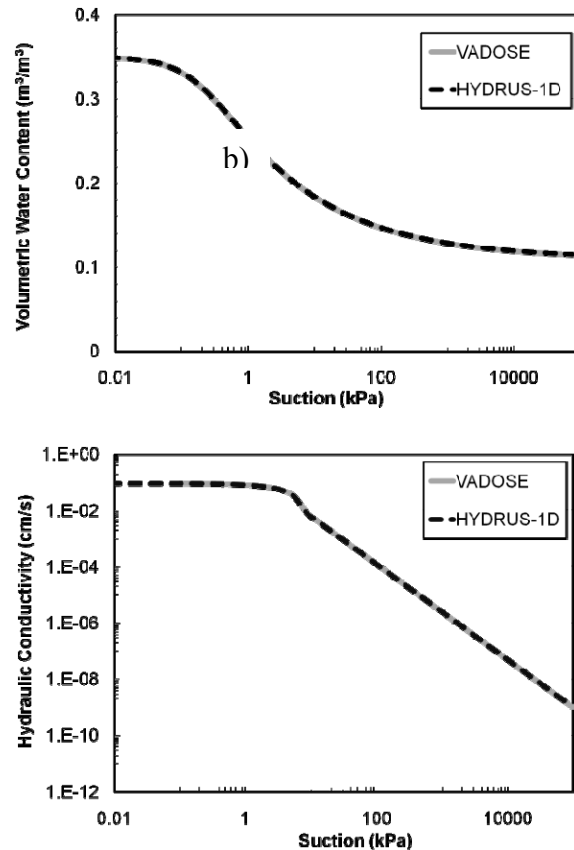


Figure 8. Moisture retention curve (a) and hydraulic conductivity function (b) for cover and waste materials from a semi-arid site in Western Australia.

Vegetation and Runoff

Vegetation is one of the most difficult variables to define in a field response model and also limits the certainty with which material inputs can be defined. During the field response modelling calibration process it can be difficult to define whether or not the observed field responses are due to vegetation or material properties. Hence, the field site chosen for this calibration case study had minimal vegetation, which simplified the calibration process.

Runoff can also be difficult to predict, and as shown by Bohnhoff et al. (2009), is an important variable in developing a successful calibrated field-response model. Given the hummocky terrain and the coarse cover material, little runoff occurs at the case study field site. However, field observations have shown that during high intensity storm events, some runoff occurs throughout the year.

Initial and Boundary Conditions

Initial conditions are defined by the field measurements on the first day of the simulation period. However, it is the authors' experience that the model needs to run for a long enough period of time so that initial conditions are not influencing model predictions. If the model is calibrated and the initial conditions reasonably defined, this period will show the model and field results converging.

The field site was on a relatively horizontal surface, so a one-dimensional simulation was considered adequate. A lower unit gradient boundary condition was specified in both models at a sufficient depth as to not influence the model predictions. A unit gradient boundary condition assumes that at the lower boundary the soil suction (and, as a result, water content and hydraulic conductivity) are constant with depth although they are allowed to change with time in response to changes in net percolation.

Calibration Procedure

As shown in Figure 1, an iterative process is used to develop a calibrated field-response model. Initial estimations of the material characteristics and vegetation parameters are input into the model and the resulting predicted suction and water content results are compared to those measured in the field. Depending on the match of the simulated response to the measured data, the input

functions are refined until a reasonable match is made.

As discussed in Shurniak & O'Kane (2009), no field response model can be calibrated to perfectly predict all field responses. Nuances of the soil-plant-atmosphere flow regime cannot be (and likely will not ever be) accounted for and different models may lead to equally acceptable representations of field responses; a condition referred to as equifinality (Beven, 2006). At some point during the calibration process, no additional changes will enhance the model predictions. At this point the model can be considered reasonably calibrated and its inputs can be used as a basis for evaluating long-term mine waste cover system performance.

The iterative calibration process for this study was first completed with VADOSE/W. Once the authors were satisfied with the calibrated model, the functions used in the VADOSE/W model were input into HYDRUS. However, HYDRUS is only able to incorporate estimation equations such as the van Genuchten (1980) MRC and k-function relationships. This differs from VADOSE/W where both the MRC and k-function can be entered as a series of data points and fitted with a spline function, or estimated using an estimation equation.

The hydraulic property equations used in both models as presented in this paper were based on the input requirements of HYDRUS. These were developed based on the closest match to the equations developed from the initial VADOSE/W calibration and are the functions presented in Figure 8.

RESULTS AND DISCUSSION

Field-response simulations with both the HYDRUS and VADOSE/W models were run for a 250-day period between December 10,

1999 and August 16, 2000. Identical material properties, boundary conditions, and initial conditions were used in both models. Output results were generated for all depths corresponding to field sensor locations; however, only a selection of the output is presented in this paper. The predicted volumetric water content at a depth of 0.6 m in the cover compared to the measured volumetric water content at the same depth is shown in Figure 9.

Both models predict similar water content profiles with time. A slight variation between the initial measured and predicted water contents is due to the estimated initial water content profile used in the models. Neither model captures the range of variation that is measured in the field but the response and timing of the events are well predicted. The field data shows slightly greater drying occurring during long dry spells, such as those occurring in February and during the dry season beginning in May.

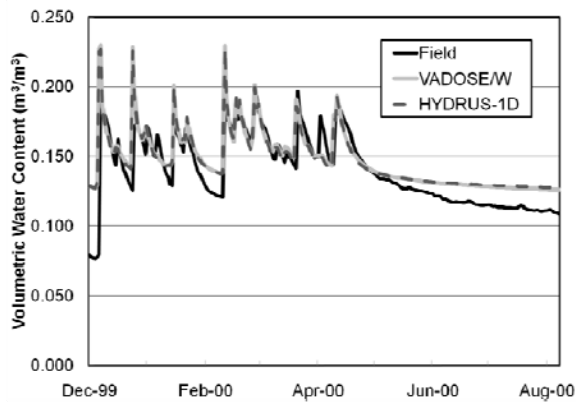


Figure 9. Field-response modelling results comparing simulated to measured volumetric water content at a depth of 0.6 m in the cover.

The predicted matric suction at a depth of 0.6 m in the cover compared to the measured matric suction at the same depth is presented in Figure 10. As with the volumetric water content, the two models predict similar suction profiles with only slight variations at

the beginning of the simulation and a slight divergence occurring at the end of the simulation.

Both models slightly over-predict the magnitude changes in the suction with time, compared to the measured results. However, it is important to note that the matric suction sensors (Campbell Scientific CS-229) have reduced accuracy at suctions less than 10 kPa, so the models may be capturing variations in suction that the field sensors do not.

The predicted suction response is also slightly ahead of that measured in the field. This may also be partially due to the CS-229 sensors, which require a ceramic cylinder to come into equilibrium with the surrounding soil. This would introduce a slight delay in the field sensor response.

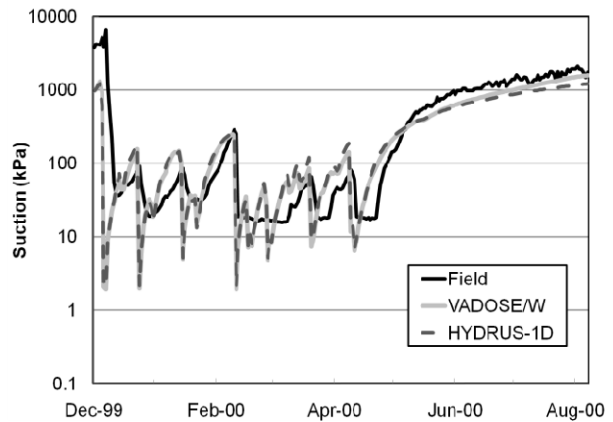


Figure 10. Field-response modelling results comparing simulated to measured matric suction at a depth of 0.6 m in the cover.

A common predictor of cover performance is the quantity of stored water in the cover that is available for vegetation. The total water in the cover is estimated using the volumetric water content. Each sensor (or nodal measurement) is assumed to represent an “element” of the cover material and the total

water in each “element” is calculated and summed to develop a value representing total water in the cover (mm). The total water calculated from the field volumetric water content sensor measurements is compared to that calculated based on the model predicted volumetric water contents in Figure 11.

Again, both VADOSE/W and HYDRUS produce similar predicted response to each other. Both models tend to over-predict the storage during wetting events, but during the more critical drying events, the magnitude is reasonably predicted. The change in storage over the entire simulation is well quantified (VADOSE/W $R^2 = 0.65$; HYDRUS $R^2 = 0.66$). The observed change in storage over the 250-day period was an increase by 39 mm. VADOSE/W and HYDRUS showed little to no increase over this period.

Net percolation was measured at the field site using two large-scale field lysimeters. The total net percolation measured by the lysimeters over the 250-day period was 138 mm (12% of rainfall). The predicted net percolation from the models over the simulation was 232 mm (20% of rainfall) in VADOSE/W and 190 mm (17% of rainfall) in HYDRUS.

Calibration Modifications

To further improve the calibration, some model modifications were made and simulated. It was observed that neither VADOSE/W nor HYDRUS were predicting runoff during the simulations. Field observations have shown that some runoff occurs during high intensity rainfall events. VADOSE/W allows the user to input the duration of storm events and input the shape of the intensity versus time function (a sinusoidal, step, or slope function). HYDRUS allows the user to input hourly rainfall

amounts versus daily amounts to tweak the intensity.

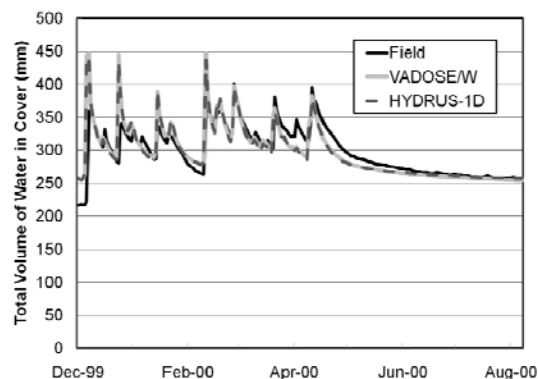


Figure 11. Field-response modelling results comparing simulated to measured total volume of water in the cover (mm) (VADOSE/W $R^2 = 0.65$; HYDRUS $R^2 = 0.66$).

By increasing the intensity of the storm events, the VADOSE/W simulation predicted runoff (238 mm = 21% of rainfall). The field-response also improved ($R^2 = 0.75$), as shown in Figure 12 for total water in the cover compared to the field data. The predicted net percolation was also reduced to 139 mm (12% of rainfall), which is an improved match to the measured value of 138 mm.

By changing the rainfall from daily to hourly, the HYDRUS simulation also predicted runoff (218 mm = 19% of rainfall). The field-response improved ($R^2 = 0.71$) as shown in Figure 12. The predicted net percolation was also reduced to 113 mm (10% of rainfall), which is an improved match to the measured value of 138 mm.

Based on the response of both VADOSE/W and HYDRUS, rainfall storm intensity is a critical parameter for developing a well-calibrated field-response model. This is in agreement with the findings of Bohnhoff et al. (2009), who determined that accurate representation of runoff is a critical parameter

in developing a calibrated field-response model.

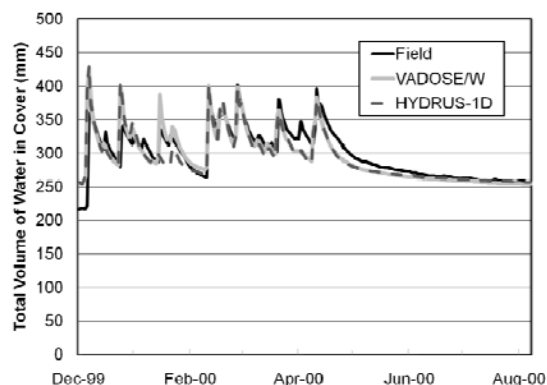


Figure 12. Field-response modelling results comparing simulated to measured total volume of water in the cover (mm) for higher intensity rainfall events (VADOSE/W $R^2 = 0.75$; HYDRUS $R^2 = 0.71$).

Model Comparison

VADOSE/W and HYDRUS differ in a number of ways. Calculation of actual evaporation is treated differently in the two models. VADOSE/W directly calculates the actual evaporation using the Penman-Wilson (Wilson et al. 1994) formulation as a function of soil vapour pressure, suction, and temperature. HYDRUS uses a semi-empirical method where evaporation occurs at a potential rate (Penman-Montieth) until the suction at the surface drops to a user-specified value. The suction is then maintained at this value and actual evaporation is a function of the hydraulic conductivity at this suction value. By having the user specify this value, the user is required to have a good understanding of the evaporation rate that should occur. This is also an additional variable that adds complexity to a calibration process.

Another difference between the models is the way in which the hydraulic functions (moisture retention curve and hydraulic conductivity function) can be entered.

VADOSE/W allows both functions to be entered independently as data points (fit with a spline curve) or using a number of estimation equations. HYDRUS requires the user to input the moisture retention curve using an estimation equation. The hydraulic conductivity is calculated directly from the moisture retention curve with few adjustment parameters. This limits the user's ability to tweak these functions during a model calibration or input field- or laboratory-measured functions. The 2D/3D version of HYDRUS allows the user to enter the functions as data points in a look-up table.

For the climate and material properties of the field site presented in this study, intensity of rainfall events was a critical parameter in calibration of the field-response model. VADOSE/W allows the user to specify the duration and the shape of the intensity function over the event. HYDRUS allows the user to specify hourly precipitation versus daily, which gives the user some control over intensity. By increasing the intensity of rainfall events, the calibration of both models was improved.

General observations of the models were that VADOSE/W has a more powerful interface for entering and modifying soil hydraulic functions and for controlling the rainfall intensity. VADOSE/W calculates actual evaporation with a more rigorous method, which is a critical parameter for predicting cover system performance. HYDRUS, however, has a faster solver than VADOSE/W. HYDRUS also has a number of alternative options (such as hysteresis and dual-porosity models) that were not utilized in this study.

SUMMARY

The prediction of long-term cover performance is an important criterion in cover design for mine waste. VADOSE/W and HYDRUS are two models capable of simulating moisture dynamics in surficial soils in response to climate and vegetation. Both models were used to develop a calibrated field-response model for a monolithic cover system in a semi-arid Australian climate.

Field-response simulations using both models were compared to measured suction and volumetric field data at depth, to total volume of water in the cover, and to measured net percolation. Both models reasonably predicted the field responses and, for the same input parameters, predicted virtually identical field responses. A variation of the calibrated VADOSE/W and HYDRUS models using higher intensity rainfall events produced an improved match to the field-response data. Increasing the intensity of the rainfall resulted in some runoff occurring, which correlated to field observations.

Further comparison of these models is required to better understand their abilities and limitations so that recommendations can be made on ways in which water balance models may be improved.

REFERENCES

Beven, K.J. 2006. A manifesto for the equifinality thesis. *Journal of Hydrology*. 320: 18–36.

Bohnoff, G.L., Ogorzalek, A.S., Benson, C.H., Shackelford, C.D., and

Apiwantragoon, P. 2009. Field data and water-balance predictions for a monolithic cover in a semiarid climate. *Journal of Geotechnical and Geoenvironmental Engineering*. 135(3): 333-348.

Eching, S.O., Hopmans, J.W., & Wendroth, O., 1994. Unsaturated hydraulic conductivity from transient multistep outflow and soil water pressure data. *Soil Science Society of America Journal*. 58: 687-695.

Fredlund, D.G., Xing, A. & Huang, S. 1994. Predicting the permeability function for unsaturated soils using the soil-water characteristic curve. *Canadian Geotechnical Journal*. 31: 533–546.

Kisch, M. 1959. The theory of seepage from clay-blanketed reservoirs. *Geotechnique*. 9: 9–21.

Shurniak, R.E. & O’Kane, M.A. 2009. Methods for simulating measured field responses for long-term performance of mine waste cover systems. *Proc. Fourth International Conference on Mine Closure*, Perth, Australia, 9-11 September 2009.

van Genuchten, M.T. 1980. A closed-form equation for predicting the hydraulic conductivity of unsaturated soils, *Soil Science Society of America Journal*. 44(5): 892–898.

Wilson, G.W., Fredlund, D.G., & Barbour, S.L. 1994. Coupled soil-atmosphere modelling for soil evaporation. *Canadian Geotechnical Journal*. 31: 151-161.

TECHNIQUES FOR CREATING MINING LANDFORMS WITH NATURAL APPEARANCE

Gord McKenna

BGC Engineering, Vancouver, British Columbia, Canada

ABSTRACT: Building on the successes of mine reclamation, some mining companies, regulatory agencies, and stakeholders are starting to require that reclaimed mining landscapes and mining landforms have a more natural appearance. At present, there is little guidance on meeting this new requirement. While most stakeholders aren't clear just what they want, they are often vocal in expressing what they don't want – monuments to mining such as terraced pyramid-like waste rock dumps, long linear drainage ditches, peneplain plateaus, trees planted in straight lines (“plants on parade”), rectangular ponds, and flume-like wetlands. Fortunately several strategies and tools are available to designers and operators to create reclaimed landscapes that better meet society's expectations for natural appearance.

One such approach, landform design, offers a more holistic approach to design of mining landscapes that incorporates a variety of specialists including geotechnical, surface water, groundwater, soils, vegetation, and wildlife. The landform design toolkit includes tools like landform grading, use of natural analogs, terrain analysis for anthropogenic landscapes and new surface water design and construction techniques that result in more sustainable landscapes that more closely resemble natural ones – ideally where form follows function.

One tool is a cafeteria-style list of elements that can be incorporated into reclamation designs. Many of these elements are simple and cost-effective to incorporate into designs and help to provide greater landscape diversity and variety and contribute to breaking up some of the linear and planar patterns inherent in mining activities. Architectural rendering techniques are being applied in the design stages to get stakeholder buy in and to better answer the question up front, “Will the reclaimed landscape be natural-looking?” Designers and operators need to remain vigilant that the proposed changes to designs and construction techniques do not adversely affect environmental performance (and in particular, geotechnical stability) for the sake of aesthetics. Methods, tools, and examples of successful projects are included in this paper.

INTRODUCTION

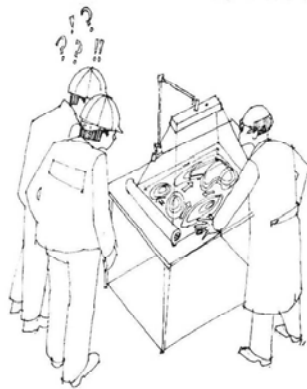
The notion of designing mining landscapes to be aesthetically pleasing is somewhat troubling to many miners. Perhaps it is because mine design involves constraints and

trade-offs and is ultimately a compromise of performance and economics – some may feel that including aesthetics means compromising on performance or cost or perhaps that it goes against the effective spartan business demeanor of many miners.

Talking about industrial design, Gelernter (1997) notes that “to pay money for elegant technology is to seem unserious, self-indulgent, and arguably incompetent.”

Perhaps concern about agreeing to create natural-looking landscapes relates to a lack of direction and experience. And while beauty is in the eye of the beholder, there is a general trend for regulators and stakeholders to ask (or require) mines to produce reclaimed landscapes that are more natural-looking – to reduce the use of straight lines and planar slopes, to use native species for revegetation with trees and shrubs planted in less regular patterns and in patches of size and shape that mimic the surrounding terrain.

Discussion of natural appearance is often framed in terms of visual aesthetics. Related experiences, such as auditory or olfactory aesthetics may also be important or implied. This paper minces the terms natural appearance and aesthetics, and thus overlooks the fact that an elegant concrete arch dam can have high visual appeal, very strong aesthetic appeal, but rather unnatural appearance. Rolston (1998) and especially Cronon (1995) provide good philosophical discussions of our historic and modern meaning of the words “nature” and “natural” and explore the implications for policy and decision making that are important to understanding such topics as environmental protection, mine reclamation, and have bearing on the present topic.



This paper provides some background to the issue, discusses the need for a more holistic and multidisciplinary approach to landform

design, and more practically provides a cafeteria-style list of landform design elements that can be employed to make mining landforms have a more natural appearance. Most of these elements are also useful in creating habitat and diversity in the landscape – embodying the idea of “form follows function” from architecture and industrial design.

Learnings that went into this paper are largely based on hands-on experience at two large oil sands mines in northern Alberta (Syncrude Canada and Suncor Energy), and reclamation tours at about 100 mines in North America, Australia, and Europe. The author has been influenced by numerous colleagues, notably Horst Schor of HJ Schor Consulting, Les Sawatsky of Golder Associates, Marie Keys of Syncrude Canada, Andy Robertson of Robertson Geoconsultants, and Professors Dave Seg0 and Nordie Morgenstern of the University of Alberta. Artwork in this paper is provided by provided by Derrill Shuttleworth of Studio Two in Edmonton.

STATE OF PRACTICE

Most mining landforms (dumps, dykes, tailings ponds, channels, open pits) are designed for geotechnical stability and efficiency of construction (McKenna, 2002). They usually consist of rectangular shapes, evenly-spaced benches (terraces) with linear crests and toes, with angle-of-repose slopes between them, and constant elevation crests (peneplains). Reclamation involves regrading the intermediate slopes between the berms to constant planar slopes (say 2H:1V or 4H:1V), smoothing out any irregularities, covering with constant thicknesses of soil, and planting vegetation at constant densities (stems per hectare), often in long rows. Surface water drainage features, where employed, are usually retrofit during reclamation or

afterwards, and consist of long, linear, trapezoidal channels, often of constant grade, often lined with uniform riprap.

However, most mines have at least one location that breaks these rules. For example, a roughened and sculpted dump slope, rockpiles placed haphazardly on the landscape to provide rodent habitat, a wetland with a shallow irregular shoreline, a grove of shade trees, or a meander in a watercourse. Usually individuals (artisans) are responsible and take pride for these special areas. These areas are often featured in a mine’s promotional materials. A few mines have adopted natural appearance criteria in the design of all new landforms. See Table 1 for examples of each.

Why natural appearance?

There are several reasons for trying to create mining landforms that have natural appearance:

- to meet promises made to stakeholders
- to meet regulatory requirements
- for public relations value
- to create diversity in the landscape which in turn promotes resiliency – a useful element of landscape performance (Holling, 1973)
- to follow a mantra of “form follows function” – a landscape that is design to exhibit similar landscape performance (function) as the natural environment ought to look natural too (form).

The idea that “form follows function” was coined by Sullivan (1896) while reflecting on the design of high-rise office buildings. Sullivan explains, *“It is the pervading law of all things organic and inorganic, of all things physical and metaphysical, of all things human and all things superhuman, of all true manifestations of the head, of the heart, of the soul, that the life is recognizable in its*

expression, that form ever follows function.” Slightly more down to earth, Gelernter (1997) states, *“a useful object has a natural form which when it is in complete harmony with its function is perceived as having a special ‘rightness’ or ‘fit’ that borders on art ... its shape seems less designed than at long last discovered.”*

Table 1. Selected examples

Location	Examples of elements employed
*Anaheim residential, CA	Landform grading
Falconbridge, ON	Preservation of historic areas
Faro, YT	Roughening
Highland Valley Copper, BC	Roughening, meandering creeks
Island Copper, BC	Sculptured shorelines, snags
*Line Creek Coal, BC	Dump roughing, sculpted coal waste piles
*MiBrag Coal, Germany	Sculpted shorelines for pit lakes
Millennium Chemicals, W. Aust.	Slash spread on reclaimed areas
Molycorp, NM	Angle of repose planting
*Premier Coal, W. Aus.	Sculpted beaches, natural revegetation planting
*Price Coal, UT	Slope roughening, diagonal swales
SF Phosphate, UT	Slash
*Suncor, AB	Landform grading, ridge mounds, irregularly shaped wetlands, native vegetation
*Syncrude, AB	Landform grading, roughening, ridge mounds, rockpiles, native vegetation
*TransAlta Highvale, AB	Landform grading, irregular ridgelines, tailored planting
* indicates sites where most new landforms are designed to have natural appearance.	

And why not?

There are cases where designers may chose to build landforms that don’t have natural appearances:

- Non-natural land uses. While many mine landscapes are reclaimed back to natural

areas for wildlife habitat or forestry, some are reclaimed to gardens, industrial areas, or held for later re-mining. In these cases, natural appearance may be undesirable.

- Preservation of historic resources. Miners are often proud of the pits and dumps they have constructed, and value their anthropogenic nature above “hiding” them with regrading and vegetation. Similarly, “ruins” of mining buildings are often preserved as historic facility as a reminder of a previous age.
- Ease of monitoring dams. In some cases, planar slopes with linear crests, with slopes simply grassed are easier to monitor than sculpted landforms with diverse swales and large trees. Similarly, flat benches provide access to read and re-drill geotechnical instruments.
- Avoiding geotechnical instability. There may be instances where slopes that are marginally stable could be affected by changes in slope geometry – any changes for the purposes of natural stability must honour the need for geotechnical (and erosional) stability. Often natural appearance and stability will go hand in hand, if done well.
- Hardrock pit walls. Most benched pitwalls are generally considered too expensive to reclaim and remain as unusual scenery.

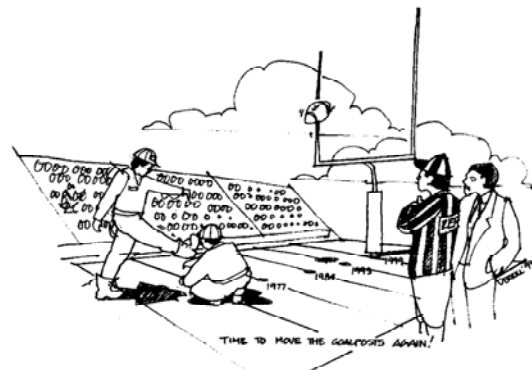


Pitwalls are generally left unreclaimed

Other objections include: too expensive (not usually the case), that beauty lies in the eye of the beholder (yes, but there is often general agreement on whether a particular design is acceptable), efforts would be unmeasurable (yes, though there have been attempts, doesn't show once trees have grown (often largely true, but can be considered in design), and people like the “mining” look (as some miners do), and that one will never be able to fool everyone (but this is not usually the intent).

Trends

Some regulatory agencies are mandating activities to “improve” aesthetics. This is accomplished by requiring mines to present closure plans showing what final reclamation will look like, and then requiring public approval for the plans. If the proposal does not meet the approval of stakeholders, the mine must adjust the plan. This is one mechanism to address the subjectiveness of aesthetics. Typically it is found that building for natural appearance has the same cost as traditional reclamation, can be done with medium to large equipment, and is usually simpler than traditional reclamation. Results are always appealing to stakeholders and regulators, staff and management. The trend is for more and more sites to desire or require design and construction for a more natural appearance and the need to defend traditional approaches in some situations.



Time to move the goalposts again!

ASSESSING NATURAL APPEARANCE

There have been numerous attempts to score natural appearance systematically and quantitatively. The literature offers guidance for those interested. Among the more famous, Leopold (1969a,b) developed a system for rating natural appearance of river valleys using 46 factors in three broad categories (physical factors, biologic and water quality factors, and human use and interest factors) and rated these factors on a scale of 1 to 5. See also Carlson (1977), Litton et al., (1974) and Wilson-Hodges (1978) for other systems.

Quantifying visual appearances has been examined for other industries. For example, highway engineering, transmission lines, quarries, barriers and walls, and cell phone towers. While much of the effort is directed towards halting proposed projects or litigation with respect to real estate values being degraded, the literature offers advice on public perceptions and provides landform designers with useful design information. Much of the most useful information for miners is available in methods and tools of mitigating visual impacts of logging (e.g. British Columbia Ministry of Forests, 1995).

Items that score highly in some of these schemes include:

- Open vistas
- High, steep terrain
- Colourful terrain
- Open water and rivers, especially clear water
- Exposed bedrock, riverbanks
- Rapids, falls
- Rare or scarce scenery
- Historic features

It is perhaps ironic that unreclaimed mining landforms and landscape will often score quite high in quantitative visual appeal systems, especially when they offer scarce

historic scenery in otherwise natural areas. In contrast, a mining landscape that is reclaimed to have a natural appearance will often be indistinguishable from natural landscapes to the casual observer, particularly in forested regions.

Because most people know what they don't want, and aesthetics is highly personal and cultural, the author has found it more useful to take a qualitative approach – using visual aids to communicate what the landscape will look like when reclaimed and seek input from stakeholders and regulators. Accepting input, and making changes, usually leads to acceptance of plans, with a new onus on the miners to deliver what is promised. Such a system forms the basis for approval of municipal developments – architectural renderings of the proposed designs are presented, modified, and if approved, the owner is responsible to live up to the presentation. Renderings are often done in watercolours, or three-dimensional models, or more recently computer-generated artwork. The mining industry uses all of these approaches, but inconsistently.

DESIGN AND CONSTRUCTION APPROACHES

There are several approaches to creating landscapes with natural appearances.

Artisan approach

At most mines, there are one or more individuals (often biologists, reclamation specialists, or heavy equipment operators) that create areas in the reclaimed landscape that are natural-looking and have high aesthetic appeal for most visitors and staff. Examples are provided in Table 1. These examples tend to be one-off approaches to a few areas of the mine site. Many are done “under the radar.” Some win awards. These

approaches can be effective, sometimes costly, but are difficult to apply at the landscape level (in other words, across the whole minesite).

Landform design

If we argue that to achieve a natural appearance that involves aspects of geotechnical, surface water, groundwater, soils, vegetation and wildlife, a multidisciplinary approach is needed.



The multidisciplinary landform design team

Landform design (McKenna, 2002) is one such approach to the design and construction of mining landscapes. Beyond the specialists listed above, it also involves mine planners and operations people and other specialists. The focus is on setting clear, simple and achievable landscape performance goals, then involving designers, planners, managers, and operators to build landscapes that can be reasonably expected to meet these goals. This paper argues that one of the goals that deserves to be considered is natural appearance.

Landform design draws heavily on practical mine reclamation experience, but also brings to bear such disciplines as geomorphology, soil science, wildlife science. The use of natural analogs (Keys et al., 1995) is an important design tool – the idea is to design

mine plateaus, slopes, and streams to mimic natural features in the region, arguing that the natural features are products of the local materials, climate, and processes over thousands of years.

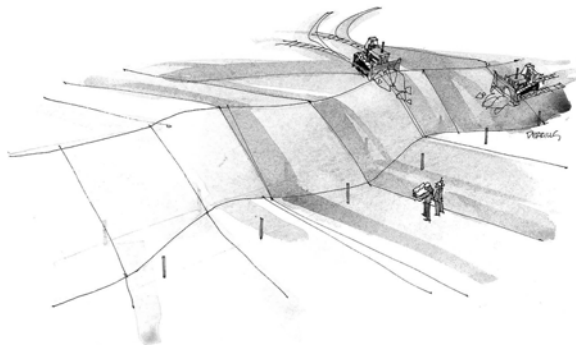
This formal approach to the design of landforms and landscapes offers transparent and integrated efforts, drawing on the weight of the engineering design approach and the knowledge and creativity of a wide variety of specialists.

In many cases, the integration of surface water drainage into the design of dumps and dykes and their associated plateaus, along with the use of revegetation species found in the local environment and planted logically (moisture-loving plants in the swales, plants that tolerate drier conditions on the ridges) following ecosite patterns similar to the natural environment, will produce largely natural-looking landscapes as an output of the design (rather than an explicit input).

Landform grading

Landform grading was invented by Horst Schor a generation ago and is applied to various large residential and mining projects (Schor and Gray, 1995; Schor and Gray, 2007). Landform grading attempts to mimic stable natural hillslopes and involves shaping slopes to have natural geomorphic patterns (swales and ridges) that fit with the local geography and climate, supported by vegetation compatible with slope hydrogeology. Landform grading has been extended in the oil sands region to also include dump plateaus and tailings beaches, shaping these otherwise nearly flat and planar features to having nested watersheds and drainage patterns to support the local land uses, vegetation, surficial hydrology and groundwater hydrology.

Landform grading is one of the major tools employed by landform design teams. Experience has shown landform grading to be practical and indistinguishable in cost from conventional grading. It results in mining landforms that have natural appearance and landscape performance that is similar to the natural surrounding environment.



Landform grading includes sculpting slopes into microwatersheds using swales and ridges.

Landform grading applied to civil project often required very tight survey control and extensive monitoring and sign-off. In a mining environment, there is more flexibility; much of the finer features (swales, ridges, planting schemes, etc) can be (and should be) field fit by a qualified field supervisor and conscientious operators. While the field construction costs are typically no higher with landform grading, the level of engineering design can be about double that of conventional design, but still a tiny fraction of the project cost.

DESIGN ELEMENTS

Table 2 provides design elements that can be used as a cafeteria-style list for the design of landforms with natural appearance. Some typical dimensions are provided. All elements need design (either in the office or the field) by qualified individuals and signoff that regulations will be met, geotechnical stability is assured, and that the elements will work

well together to provide the promised landscape performance.

Table 2. List of landform design elements for natural appearance

Item	Example
1. Meandering creek	<ul style="list-style-type: none"> Irregular 100-300 m wavelength, Minimum amplitude = 1 to 2 creek widths
2. Connect swales with natural watercourses	<ul style="list-style-type: none"> Drain swales into adjacent watercourses. Carry vegetation patterns from natural gullies up onto the dyke or dump slopes.
3. Coversoil and revegetate bare areas, creeks	<ul style="list-style-type: none"> Opportunity for aggressive reclamation of exposed areas near roads and creek slopes – allow early reclamation and general greening up of area.
4. Watershed berm at crest	<ul style="list-style-type: none"> Push up dump material and round the downstream crest as final design feature. Horizontal wavelength 200 to 400 m, zigzag 0 to 20 m, vertical height 2 to 4 m, 2.5 to 4H:1V sideslopes with 3 to 5 m crest width Australians call these “bunds.” They can be built by using large mining trucks and later shaping the resulting line of spoil piles.
5. Irregular ridge mounds	<ul style="list-style-type: none"> To add diversity to skyline profile, add irregularly shaped mounds at the downstream crest Mounds can be 3 to 5 m high, 3H:1V sideslopes or flatter, 20-30m wide, 30-80m long (2000 to 10,000 m³ each) Consider planting schemes to enhance appearance. Mound heights should be designed to be 5-15% of the landform height to break up sightlines. Mounds can be placed near the crest – acting like false storefronts in a Western town.
6. Reslope benches	<ul style="list-style-type: none"> When finished with benches, reslope by regrading substrate or adding additional reclamation material. Make sure that access to place reclamation material is left.
7. Wetlands at	<ul style="list-style-type: none"> Enlarge toe ditch (toe creeks!)

Item	Example
toes	<ul style="list-style-type: none"> to create shallow wetland, 2 m deeper than toe ditch invert (where ditch invert is shallow) • Consider 10-20 m wide, 30 to 60 m long (1000-5000 m³) • Use irregular shoreline, very shallow slopes, create mounds with spoil
8. Tailored planting	<ul style="list-style-type: none"> • Follow ecosite planting schemes – tailor the planting to fit conditions • Consider planting swaths of trees for visual patterns on slopes • Use this scheme to mimic natural vegetation patterns elsewhere
9. Swales on slopes	<ul style="list-style-type: none"> • Construct swales and ridges of slopes to carry runoff safely to the toes of dumps. Use diagonal, elbow, and curvilinear shapes. Hydrologic design required above threshold watershed areas and slope gradients.
10. Reclaim erosional fans and gullies in place	<ul style="list-style-type: none"> • Once gullies are stabilized, instead of ‘erasing’ them, simply repair them in place • Allows increased diversity, reduced cost • Need to remove the ‘cause’ of the gully prior to fixup in most cases
11. Irregular shoreline	<ul style="list-style-type: none"> • Irregular shoreline should be integrated with construction for lakes, wetlands, marshes, and fens.
12. Littoral zone	<ul style="list-style-type: none"> • Build large littoral zones (typically less than 2m deep) into design of lakes
13. Add additional fill at toe	<ul style="list-style-type: none"> • Adding fill at toe to break up straight lines and add topographic diversity may be desired • Similar effect achieved by reclaiming erosion fans in place • Expensive if not a short haul / short overhaul
14. Mounds on plateaus, benches, slopes	<ul style="list-style-type: none"> • Small mounds on berms and slopes for topographic diversity • Can be pushed up or placed or cut/fill from other projects • Typically 10-30 m diameter, 3-5 m high (300-4000 m³)

Item	Example
	<ul style="list-style-type: none"> • Field fit where practical.
15. Brushpiles / snags	<ul style="list-style-type: none"> • Temporary habitat improvements can be made by having small brush piles for small animals or standing snags for raptors
16. Rockpiles	<ul style="list-style-type: none"> • Build rock piles from siltstone for animal habitat • 6 to 15 m diameter, 2 to 4 m high
17. LFH placement	<ul style="list-style-type: none"> • Place forest floor salvage in islands to promote early biodiversity • Slash (coarse woody debris) also enhances diversity and habitat.
18. Microtopography	<ul style="list-style-type: none"> • Roughen slope to create microtopography to enhance soil moisture and diversity
19. Coversoil diversity	<ul style="list-style-type: none"> • Use different prescriptions in different areas to enhance diversity
20. Access controls	<ul style="list-style-type: none"> • Establish a plan for long-term access to area • Provide good access, but restrict number of roads and type • Use aesthetic design principles from trail guides to guide designs.
21. Viewing platforms / photo locations	<ul style="list-style-type: none"> • Install viewing platforms for tours and future recreational opportunities.



Landform grading of a mine dump

FINAL COMMENTS

Creating natural-looking mining landforms and mining landscapes is a creative challenge. Successful reclamation of these landscapes will involve a multidisciplinary team using a variety of design tools and analyses. The results are rewarding personally, for the team, the mining company, and society. Formal design processes are needed for many elements to avoid triggering unintended consequences and for managing costs. Ideally form will follow function, and the landscapes will be both more visually appealing and exhibit better landscape performance.

REFERENCES

- British Columbia Ministry of Forests, 1995. Visual impact assessment guidebook, British Columbia Ministry of Forests, Victoria, BC.
- Carlson, A.A., 1977. On the possibility of quantifying scenic beauty. *Landscape Planning*, 4: 131-172.
- Cronon, W. (Editor), 1995. *Uncommon ground: toward reinventing nature*. W.W. Norton & Co., New York, 561p.
- Gelernter, D.H., 1997. *Machine beauty: elegance and the heart of technology*. MasterMinds. Basic Books, New York, 166p.
- Holling, C.S., 1973. Resilience and stability of ecological systems. *Annual Review of Ecology and Systematics*, 4: 1-23.
- Keys, M.J., McKenna, G., Sawatsky, L. and Van Meer, T., 1995. Natural analogs for sustainable reclamation landscape design at Syncrude. In: COGEMA Resources Inc (Editor), *Environmental Management for Mining*, Saskatoon.
- Leopold, L.B., 1969a. Landscape esthetics: how to quantify the scenics of a river valley. *Natural History*(October): 36-45.
- Leopold, L.B., 1969b. Quantitative comparison of some aesthetic factors among rivers, U. S. Geological Survey, Reston, VA, United States.
- Litton, R.B., Tetlow, R.J., Sorensen, J. and Beatty, R.A., 1974. Water and landscape: an aesthetic overview of the role of water in the landscape. Water Information Center, 314p.
- Rolston, H., 1998. Technology versus nature: what is natural? *Journal of the University of Aberdeen Centre for Philosophy Technology and Society*, 2(2).
- Schor, H.J. and Gray, D.H., 1995. Landform grading and slope evolution. *Journal of Geotechnical Engineering*, 121(10): 729-734.
- Schor, H.J. and Gray, D.H., 2007. *Landforming: an environmental approach to hillside development, mine reclamation and watershed restoration*. John Wiley & Sons, Hoboken, NJ. 354p.
- Sullivan, L.H., 1896. The Tall Office Building Artistically Considered, *Lippincott's Magazine*.
- Wilson-Hodges, C., 1978. The measurement of landscape aesthetics. Working paper - Institute for Environmental Studies, University of Toronto ; no. 2. University of Toronto, Institute of Environmental Studies, Toronto, 52p

COMMUNITY PERCEPTIONS AND CONSULTATION FOR TAILINGS DISPOSAL FACILITIES IN THE DEVELOPING WORLD

Mark Thorpe and Rammy Oboro-O'fferie

Golden Star Resources, Denver

ABSTRACT: The disposal of tailings, especially tailings from a process using cyanide, is controversial in developed countries. However, there are specific challenges for mining operations in developing countries that are often associated with lower standards of education and understanding, especially in the remote and impoverished areas where mines are often developed. There is a general lack of knowledge about modern mining and even more suspicion about tailings disposal facilities.

In such areas, operations need to focus efforts on understanding the concerns and perceptions of their stakeholder communities, so enabling them to incorporate addressing these concerns into the development and operation of the tailings disposal facilities. This starts with the community consultation and environmental permitting and continues through the construction, operation, and the eventual closure of the tailings disposal facility.

The initial community consultation for environmental permitting often focuses on jobs, the development of infrastructure and training and other benefits to local communities. However, little is included on the operation of the mine, processing plant and tailings disposal facility. This is a particular concern where open pit mines are being developed in areas that are new to mining or do not traditionally have large tailings disposal facilities. An operation needs ongoing community support; therefore, the company must provide information to educate at least the community leaders on the development of the entire operation, including the controversial areas of land-take and the disposal of the tailings.

More specifically, the perception of tailings that uses cyanide in the processing plant in the developing world is often one of fear and mistrust. However, by implementing an education program, which may include visits to operating facilities in other parts of the country, a project proponent can provide information on which community leaders can then form opinions. Key among this approach is to provide time for the community leaders to interact with experienced people without the intervention of the project proponent.

Our work in Ghana provides an insight into community perceptions on tailings. Even operating in an area where mining has been ongoing for over 100 year, the majority of the community do

not have a good understanding of tailings disposal. The community feels that the company should provide more information so that community members can understand the risks and take the necessary precautions to minimize any adverse effects.

Our ongoing community consultation has been enhanced to include an educational component on our operations. This improved understanding resulting in a request from local leaders that the company establishes a committee that includes community members that would have input to the management of the tailings disposal facility. This is currently being reviewed by senior management to determine the best way to establish a community consultation / input process for the tailings disposal facilities. The key to the ongoing success of our operations is the continued consultation, coupled with the understanding that our consultation must continue through the life of mine and to closure and post-closure.

INTRODUCTION

Tailings disposal facilities are controversial both in the developing and developed world. In the developed world, there are normally appropriate channels by which concerned stakeholders are able to voice their concerns and a multitude of communications methods is available. However, in the developing world, communications can be challenging thus, either Companies are unable to define appropriate communication channels to reach out to people, or for lack of education and / or inability to write, the people are often unable to articulate concerns to government for redress.

When entering into developing nations, especially in areas where mining is a new form of economic development, project proponents often overlook the very local concerns of stakeholder communities and focus on regulatory and feasibility study requirements. Often, a consultation component is part of the permitting process. However, this may be controlled by the regulatory authorities and require written submissions from concerned stakeholders.

This paper examines the operation and management of Golden Star's two tailings disposal facilities in Ghana, West Africa and

provides an insight into perceptions on tailings disposal facilities in an area with a history of mining. We then take our lessons and provide some guidance that can be used to broaden the understanding of both companies and stakeholder communities in the operation and management of tailings disposal facilities.

GOLDEN STAR RESOURCES

Golden Star Resources Limited (GSR) is a Canadian, federally-incorporated, international gold mining and exploration company producing gold in Ghana.

Through a 90% owned subsidiary, Golden Star (Bogoso/Prestea) Limited, GSR owns and operates the Bogoso / Prestea gold mining and processing operations near the town of Bogoso using bio-oxidation technology to treat refractory sulphide ore and a carbon-in-leach processing facility to treat oxide ores as they are available. Bogoso/Prestea produced and sold 170,499 ounces of gold in 2008.

Through another 90% owned subsidiary, Golden Star (Wassa) Limited (Wassa), GSR owns and operates the Wassa open-pit gold mine and carbon-in-leach processing plant,

located approximately 35 km east of the Bogoso/Prestea operation. Wassa produced and sold 125,427 ounces of gold in 2008. Wassa also owns 90% of the Hwini-Butre and Benso concessions (the “HBB properties”) in southwest Ghana. The Benso mine began shipping ore to Wassa late in 2008, and the Hwini-Butre mine began shipping ore to Wassa in April 2009. The Hwini-Butre and Benso concessions are located approximately 80 km and 50 km, respectively, by road south of Wassa.

GOLDEN STAR TAILINGS DISPOSAL FACILITIES

Both the Bogoso/Prestea and Wassa operations produce tailings that are placed in the engineered tailings disposal facilities. The GSR operations work closely with the tailings engineering consultant and the Ghana Environmental Protection Agency (EPA), and independent reviews are carried out quarterly to ensure the safety of the facilities.

The following sections provide a description of the respective tailings disposal facilities.

Bogoso/Prestea

The tailings produced by Bogoso/Prestea are of two distinct types: flotation tailings and CIL tailings. Processing the sulphide ores requires a flotation circuit to produce a concentrate that is then fed into the BIOX[®] circuit. In the BIOX[®], the sulphide is oxidized at about pH 1.5 by bacteria before the product is washed and neutralized and forwarded to the CIL circuit for leaching.

The two processes result in two different tailings: about 8,000 tonnes per day of flotation tailings and about 700 tonnes per day of CIL cyanide tailings. The tailings are directed to two different areas of the tailings

disposal facility so that water can be recycled to the BIOX[®] circuit without affecting the bacteria.

The tailings disposal facility consists of four areas: TSF I, cell 1, which is inactive and is currently being decommissioned; TSF II cell 1/2 for CIL tailings; TSF II cell 2A for CIL tailings and TSF II cell for flotation tailings. The total area is about 380 ha with 60 ha in active rehabilitation (

Figure 1).



Figure 1. Tailings disposal facility at Bogoso

Deposition of the tailings is sub-aerial via a large main line with spigots to distribute the tailings to form beaches). By rotating the spigotting areas around the facility, the beaches are allowed to dry and consolidate. Water is collected in the supernatant pond and, is returned from the flotation cell to the processing plant for re-use.

Wassa

Tailings at the Wassa CIL processing plant at generated at about 7,000 tonnes per day and are pumped as a slurry to the tailings disposal facility behind the processing plant. The same deposition technique as the Bogoso facility is used at Wassa where spigots deposit the tailings on beaches and



Figure 2. Bogoso/Prestea Tailings Disposal Facility showing spigots and beach

the supernatant is collected in a pond and then pumped back to the processing plant for re-use. The Wassa tailings disposal facility covers 116 ha and it is expected to last the remainder of the mine life. The beaches on the Wassa facility are extensive and provide excellent consolidation even during the rainy season.



Figure 3. Deposition of tailings at the Wassa tailings disposal facility

ECOLOGY AND LAND USE

The Golden Star operations are in, in the wet, semi-equatorial climatic zone of the Western Region of Ghana that is characterized by an annual double maxima

rainfall pattern occurring in the months of April to July and from September to November. Approximately 60% of the total rainfall occurs during the first rainy season.

GSRs operations are in the Moist Evergreen vegetation zone of Ghana. The structure of vegetation is varied; generally, the vegetation is a mosaic of intensively cultivated farmlands, fallows, and secondary forest moist evergreen forests. Major recognizable vegetation cover types are: Moist Evergreen Forest with a discontinuous upper canopy; some of the trees reaching up to 40 m in height; Forb Re-growth - an early stage of ecological succession following soon after abandonment of farming; Thickets, mostly vegetation reaching up to 4m in height with abundant climbers and young trees, which shade out and kill the light-demanding herbaceous species; and secondary forests, low, broken canopy forest that reaches 10 to 15 m in height, with dense climber tangles in the undergrowth.

The land use patterns in the western region of Ghana form a mosaic of subsistence farmland, abandoned farmland (fallow land recovering), cash tree crops, extensive plantations and forest reserves (both working and preserved). As such, most mining development is in areas that has been affected by farming or is currently being farmed. Concurrent with the areas of farmland are small hamlets or villages where the local farmers live.

The land use immediately around our tailings disposal facilities is primarily farmland along with one of the Golden Star oil palm plantations. The farmland is a mix of cash and food crops and other areas that are fallow. The general pattern of agriculture around the tailings disposal facilities is to farm until the soil is depleted and then move the cropping area to a newly cleared patch of

secondary vegetation. Cash crops in the Bogoso and Wassa areas are mostly oil palm and cocoa, respectively.

Where land is required for operation, the consent of the landowner and/or the farmer is sought; the farm is then surveyed and a negotiated (crop & land) rate is used to compensate the farmer for both loss of crops and deprivation of use of land (which includes the long-term productivity of the crop). In general, farmers want to receive the compensation payments as there is plenty of other land to farm and they receive a windfall cash settlement. We have even had the local MP intervene against a program where we proposed providing land, start up costs and a development fee for affected farmers.

STAKEHOLDER COMMUNITIES

Our stakeholder communities vary greatly from isolated farms to towns of up to 20,000 people. The larger towns are associated with longer-term development. For example, the towns of Bogoso and Prestea developed following mining development in the 1920s and 1890s, respectively. These towns continue to benefit from mining in the area and are where many of our employees live.

In general, the usual community services are present, if somewhat poor, including schools, health clinics and a small hospital, shops, electricity and water services, and a market. The general infrastructure and roads are in poor condition but the people in the larger communities are familiar with mining and many derive their living from mining either directly through employment or indirectly as support services to our operations. Additionally, we sponsor, through our Golden Star Development Foundation, the construction of infrastructure and support other community

areas, such as providing scholarships for upper year schoolchildren and post-secondary students.

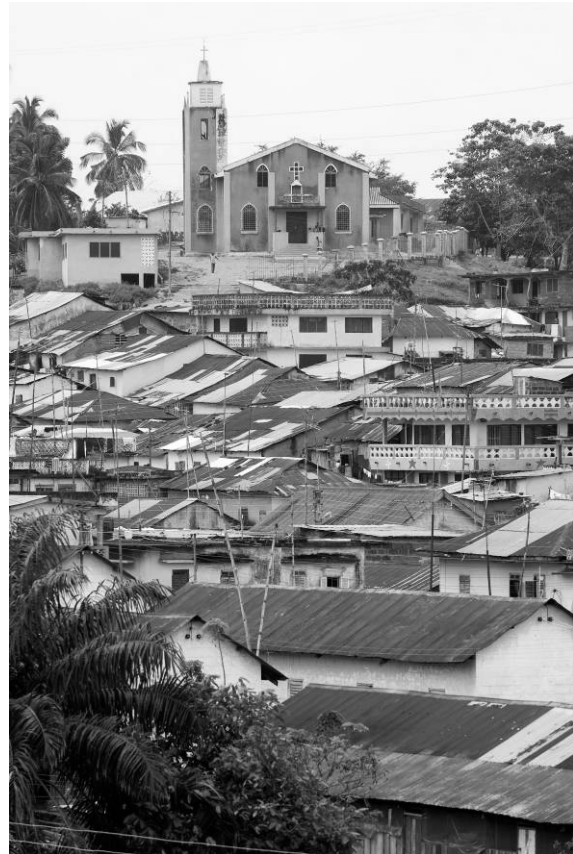


Figure 4. A section of the Prestea town

Although the majority of people live in the larger centres, many people still rely on farming as a source of subsistence food and in some cases income. The location of our operations means that we abut farmland and there are several small farming communities within a kilometre of our operations. These communities are characterized by limited infrastructure development, poor water and sanitation, limited access to schooling and usually no electricity.

Education levels in the communities vary greatly due to access to schools and the demands of farm life that tends to keep older

children working on the farm and not completing their education.

This work addresses the broader community perceptions about tailings disposal facilities. However, the location of our specific operations means that we have the potential to affect a very limited number of communities directly (within 500 m of an operating facility).

For the Bogoso operation, the Anikoko community is within 0.3 km of the tailings disposal facility. This community is a loose association of farmers consisting of about 200 people in 13 compounds.

At Wassa, the Togbekrom community is located in a valley to the north of the tailings disposal facility. Although they are not affected by the facility, there is a certain degree of concern about its operation. Poorer community conditions and the inability to communicate concerns in English exacerbate these concerns.

FIELD WORK AND DATA COLLECTION

Golden Star has been operating in the Bogoso/Prestea area since 1999 and in the Wassa area since 2004. During this time, work has been carried out in many communities for the reasons including the following: community consultation, community outreach and development, investigate complaints, environmental permitting, project development, and community resettlement.

During many of these interactions, community members have expressed opinions or concerns about the tailings disposal facilities operated by Golden Star. These were documented and included in reports presented to management and the

regulatory authorities if the investigation was related to an environmental or other permit.

More specifically, community leaders were invited to discuss the tailings disposal facility in an informal setting where they had the opportunity to exchange opinions in a safe environment. These discussions afforded GSR opportunity to understand in detail community concerns over the tailings management. This information will then be used to develop the outreach education programs to address these concerns by providing the key information.

COMMUNITY PERCEPTIONS

There is considerable variation in the understanding associated with the tailings disposal facility. In general, a better understanding of the facilities are found in the more educated population and in areas that are traditionally mining areas. In general, community members understood that the tailings disposal facility received the wastes from the processing plants at both Wassa and Bogoso. However, beyond that preliminary understanding, there was a contrast in perceptions between the Bogoso / Prestea and Wassa areas. At Bogoso / Prestea, there was a generally good understanding of the facility and its management. Mining has been a part of life in that area for many years, although for the original operations (early 1900s) the discharge of tailings was not controlled but went into valleys and then into the local rivers.

However, at the Wassa mine where the first tailings disposal facility was commissioned by GSR in 2004, there was a lack of understanding about tailings operations and the management of the facility.

There is also a difference in the level of knowledge based on socioeconomic and

cultural status. The Chiefs are generally better informed than their subjects are. This is probably because the Chiefs interact more frequently with our operations and are included in the Community Mine Consultative Committees (CMCC) where informal conversations present questioning opportunities allowing a better overall understand of the mining operations including the tailings disposal facilities.

The informal meeting with the 17 Bogoso opinion leaders from 8 local communities provided additional insight into the understanding of the tailings disposal facilities.

Only 40% of the participants felt that they had adequate knowledge about the tailings disposal facility and that the knowledge was gained from a variety of informal sources as well as from the company during



Figure 5. Community Mine Consultative Committee meeting at Wassa

the community education work carried out in 2004 following a spill. During the conversation, it was clear that there was a similar split in the understanding about the facility with 40% being able to describe the operations associated with the facility.

It was generally felt increased knowledge about the tailings disposal facility would help community members avoid the dangers associated with the facility and that community forums organized by Golden Star would best facilitate this knowledge transfer.

There were disease concerns associated with the facility as it was thought to cause TB, stomach problems and skin rashes as well as reduce the quality and quantity of crops on adjacent lands.

The discussions about the tailings disposal facility finished with a suggestions from the community that a committee, comprising of the communities and the company, should come together to see how the tailings should be managed to reduce its effect on the surrounding communities.

In summary, local community perceptions about the tailings disposal facilities are as follows:

- Adversely affect farm yields
- Cause skin reactions to people working on adjacent farms
- Supernatant water is highly poisonous
- Cause respiratory diseases including tuberculosis
- Cannot be rehabilitated to a proper final land use
- Dams are unsafe and will collapse

In spite of their concerns associated with the tailings disposal facilities, farmers continue to plant crops as close as possible to the facility with a view to receiving compensation should there be need to use adjacent areas of land. In concert with this concern, we established a demonstration farm adjacent to the tailings disposal facility to provide evidence that the tailings disposal facility would not affect the surrounding farmland.

As there is general access to the tailings disposal facilities (they are not fenced), community members use the roads and embankments as transportation corridors from their farms to other areas (e.g. local market). The embankment roads are generally well maintained and travel on them is easier than on the footpaths that wind through the adjacent areas.

COMMUNITY CONSULTATION

In Ghana, there is a requirement for community consultation as part of the environmental permitting process. However, the Environmental (EPA) Agency has the responsibility to organize the consultation. There is also no requirement for ongoing community consultation.

At each of our operations, we established CMCCs. The areas around the Bogoso/Prestea and Wassa operations are broadly divided along traditional lines – the CMCCs pertain to a traditional area (known as a stool) – so that there is general cohesion amongst the participants in each CMCC. It is advisable to understand any fundamental differences within your stakeholder communities before establishing committees that include more than one community. In Ghana, we found that there are considerable differences and rivalries between traditional areas, especially when competing for limited resources, which in this case is funding from the Golden Star Development Foundation for community programs.

The CMCCs now act as the fundamental conduit for information flow to and from our operations. Meetings are held regularly (at least quarterly) and topic of discussion include community development programs, mine development activities, infrastructure funding, community concerns and, to a limited extent, stakeholder complaints. We

established a complaints and grievances mechanism at each operation to ensure a timely response to stakeholder complaints.

During the past few years, Bogoso/Prestea stopped development in the Prestea area while working in other areas, while continuing exploration to define additional resources. During that time, the CMCC was disbanded and was not reconstituted until there was a need for permitting. However, the local community was not receptive to a resumption of mining having been ignored for about 2 years. Consequently, a lot of work was required to re-establish cordial relations with the community and to move the permitting process forward. As in most cases, the limited costs in time and money associated with maintaining the CMCC would now be considered worth the investment due to the current project delays.

During the expansion of the Bogoso tailings disposal facility, the small community of Anikoko was identified but was not affected by the facility albeit they were relatively close (0.3 km) to the flotation tailings impoundment embankments. There were some initial complaints about the facility, which were addressed through mitigative measures including the provision of potable water in an area where stream water was the original water source.

However, the Anikoko community felt left out of the process and started a complaints campaign to the EPA. Rather than meet with the community and determine the way forward, Bogoso / Prestea elected to follow the legal path and complete a socioeconomic impact assessment and was then required by the EPA to complete a resettlement action plan, which was then to be implemented. The resettlement of the Anikoko community is currently ongoing.

A preferable alternative to the resettlement of the community away from their farmlands would have been to work with the community to understand their wants and then to develop a mutually beneficial package to address, as far as possible, the community aspirations. This would have reduced the amount of time and money devoted to the community and would have provided a more sustainable future for the Anikoko community.

Following a review of the community concerns associated with the tailings disposal committees, we are now establishing a program to improve the overall understanding of the mining operations, including tailings disposal.



Figure 6. Typical dwelling within the Anikoko Community

LESSONS LEARNED

In the developing world, companies often underestimate the amount of community education required to bring stakeholders to a level of understanding that allows them to understand and assess the effects of a mine development or changes to an existing operation. For tailings disposal facilities, many stakeholders cannot understand the

concept of a facility to store mud containing with chemicals. Additionally, the lack of understanding makes stakeholders nervous and they may attach an unreasonable level of importance to rumour and other information received for sources beyond operational control.

The poor initial level of understanding means that extra effort is required to provide the adequate information in a tangible format. It is not a case of leaving a copy of the socioeconomic and environmental impact statement at the local library. Many communities are oral in their communication and history as there are a limited number of people who are able to read, let alone understand the highly technical language of most such documents. Therefore, providing this information in a culturally sensitive manner will increase the probability of the success of the project.

In the development or expansion of a facility (tailings or other mining infrastructure), an open, early, and documented approach will generally yield better results for both the proponent and the community. By engaging the community early in the process, a project proponent is able to understand the level of community knowledge about the venture and then take appropriate steps to provide the materials to allow informed community decision making.

For project development, consultation should be early and often and should generally occur before the regulatory authorities require such a process. By documenting the consultation and providing the information to the stakeholder leaders and community, the project proponent raise the level of awareness and ease the permitting process. This concept should be carried through to operations and the consultation continued.

In general, positive actions by reaching out to communities allow companies to understand concerns and then incorporate addressing these concerns in their plans rather than having a development project or operation disrupted.

Although more common in the developed world, operations should consider establishing a community committee to provide local insight into the operation and management of contentious facilities such as their tailings disposal facility.

MINING COMPANY CORPORATE LIFE CYCLE CLOSURE COST (CL3C)

D. van Zyl

University of British Columbia, Vancouver, BC, Canada

ABSTRACT: An important aspect of mine closure cost allocations, as presently applied, is that accounting provisions for future closure costs are included on the balance sheet; however, no cash is set aside to pay for those closure costs when incurred. Therefore, the closure cost of a mine is always carried by the operating income from other mines in a company's portfolio. Discounted cash flow analysis is used for investment decisions however this approach is not helpful in understanding mining company closure liabilities. The "Corporate Life Cycle Closure Cost" (CL3C) is introduced as a concept to account for the closure cash flow liability of a company over the life of its ongoing projects. Sinking fund is presented as an approach to fund closure and post-closure cash flow for companies having one or two mines.

INTRODUCTION

Regulatory agencies, mining companies, and consultants have made significant progress during the last two decades by better understanding the importance of accurately calculating closure costs. New accounting standards introduced in the late 1990's and recent failures of large corporations have elevated the importance of this issue even further. In a recent comprehensive review Parshley, et al (2009) clearly defines and describes three types of closure cost estimates commonly used by the international mining industry:

- Financial assurance cost estimate (FACE) to satisfy regulatory requirements;
- Life of mine (LOM) closure cost estimate; and,

- Asset retirement obligation (ARO) cost estimate for financial reporting requirements.

This paper will focus on the LOM closure cost estimates as these are used by the mine operator and the mining company for planning, budgeting and cost tracking. Typical applications of these are for feasibility studies, due diligence reports, accrual allocation, annual planning and budgeting and cost tracking (Parshley, et al, 2009). The focus of the present paper is not on the details of the cost estimation but on their application in the strategic planning of a company.

A major aspect of LOM closure costing is that it is done on a cash flow basis and the values are then included in the operational cost model. Discounted cash flow (DCF) is used

to obtain the present value (PV) of future costs or the net present value (NPV) for the project. The latter, as well as the internal rate of return (IRR), are two important performance indicators for mining investment decisions. But it is argued below that they are not useful in developing a better understanding of the closure liabilities of a mining company. The concept of a corporate life cycle closure cost (CL3C) is introduced as a simple tool to provide more insight in the closure cost liabilities of mining companies and to support mine development decisions and strategic planning.

CONCEPT

DCF analysis is used in the mining and other industries to evaluate the economic feasibility of projects and to obtain financing for these projects. This is standard practice, extensively used and respected by financial institutions and will continue to be used as such. When two or more projects are potential investment opportunities then DCF analysis is used to obtain the key performance indicators (e.g. NPV, IRR) for this comparison. Corporate decision criteria are then used to make the trade-off decisions.

Closure costs that occur at the end of the mine life, say after 15 years or more of operations, are significantly discounted using DCF and may not contribute much to the overall economics of the project. This is true even if large amounts of cash may be required at the closure stage. The DCF analysis therefore does not provide insights on the impact of different closure costs and their distribution when comparing NPV, IRR or other indicators for multiple projects.

LOM closure cost is regularly updated for all projects in the corporate portfolio. This financial obligation is carried on the financial

statements of the company and provisions are made for this future expenditure. However, the company typically does not develop a sinking fund or other mechanism to provide these cash flows at the end of operations. The closure costs for a specific mine are paid by the company from profits made in their other operations. In short: other mines in the corporate portfolio pay for the closure of a specific mine.

The cash flow needs of a mining company to support multiple ongoing mine closures may be significant and it seems to make sense to also use this future cash flow need as a key performance indicator in long-term planning including project evaluation for investment decisions.

The concept of this paper is that such a cash flow evaluation of closure and post-closure cash flow obligations can be useful input to strategic planning. The term corporate life cycle closure cost (CL3C) is used to describe this evaluation methodology.

IMPLEMENTING CORPORATE LIFE CYCLE CLOSURE COST (CL3C)

The implementation of CL3C is demonstrated through an example. Consider a small to medium sized mining company with 4 mines in various life cycle stages. The company is considering the development of a new mine that will become operational 7 years into the future. Table 1 provides a summary of the mines in the corporate portfolio and includes the new mine under consideration. Year 1 is the present time.

Mine 1 is operating and is expected to do so until the end of year 6 after which it will go into closure. Mine 2 is under development and will start operating in year 4. It will go into closure in year 15. Mine 3 is operating

and will do so until the end of year 8 after which it goes into closure. Mine 4 is operating for another 4 years after which it will close. The new mine, if developed, is expected to go into development in year 3 and start operating in year 7, it will close in year 14.

Table 2 provides estimates of the annual cash flow requirements for mine closure and post-closure for each mine as well as the total cash needs for the whole portfolio. Such costs would be based on the updated LOM closure costs.

Table 1. Corporate Profile of Operating and Proposed Mines

Years	Mines				
	1	2	3	4	5 (new)
1	O	D	O	O	
2	O	D	O	O	
3	O	D	O	O	D
4	O	O	O	O	D
5	O	O	O	C	D
6	O	O	O	C	D
7	C	O	O	C	O
8	C	O	O	C	O
9	C	O	C	C	O
10	C	O	C	PC	O
11	C	O	C	PC	O
12	PC	O	C	PC	O
13	PC	O	C	PC	O
14	PC	O	C	PC	C
15	PC	C	PC	PC	C
16	PC	C	PC	PC	C
17	PC	C	PC	PC	C
18	PC	C	PC	PC	C
19	PC	C	PC	PC	C

D – mine development; O – operations; C – closure; PC – post-closure

The following observations can be made from Tables 1 and 2:

- The total operating life of mines 1, 3 and 4 are not known, similarly the environmental conditions at these mines are not known;
- The cash flow requirements for closure and post-closure costs range from \$1.5M (year 19) to \$60M (year 9) and for three years it exceeds \$30M;
- In year 9, when \$60M is required, only two mines are operating, including the

one under evaluation. Depending on their profitability this extra cash burden may reduce the corporate profit, or may even result in a loss;

- The income contribution from the new mine may be essential for the corporation to generate the required cash flow to cover closure and post-closure costs; and,
- The new mine increases the corporate cash flow needs by about 30 percent when it closes.

Table 2. Closure and Post-Closure Cash Flows (\$M)

Year	Mine					<i>Total Cash Needs</i>
	1	2	3	4	5 (new)	
1	O	D	O	O		
2	O	D	O	O		
3	O	D	O	O	D	
4	O	O	O	O	D	
5	O	O	O	2	D	2
6	O	O	O	4	D	4
7	6	O	O	10	O	16
8	10	O	O	25	O	35
9	15	O	20	25	O	60
10	5	O	20	1	O	26
11	5	O	25	2	O	32
12	2	O	15	2	O	19
13	2	O	10	3	O	15
14	2	6	5	2	5	22
15	2	5	3	1	5	16
16	2	4	2	1	5	14
17		2	1		3	6
18		1			2	3
19		0.5			1	1.5

Next consider the effect of DCF on the closure cost estimates. Using 8 percent interest rate the DCF closure costs in Table 3 are calculated. Year zero for these calculations is the year before operations start, this assumes that all the cash flow needs must be contributed during the operating life of a mine, regardless how long that is. The total operating lives of the mines are listed in Table 3. As expected the DCF costs are much less than the total cash costs. The significance of the discount period is clear when the total and DCF costs for Mine 3 (20 year mine life) are compared. The difference in total and DCF costs will be even larger if the operating life was 25 or 30 years.

It is possible that some companies are already using the CL3C concept in their internal evaluations however such information is not public. It is not known how significant a role this approach is currently playing in making investment decisions. However, it is obvious that it has a number of advantages:

- CL3C evaluations force companies to understand the portfolio wide cash flow requirements for closure and post-closure commitments;
- CL3C can be used as an important indicator when comparing investment strategies on projects, by including an analysis of the closure and post-closure cash flow needs of the new project as it relates the overall closure and post-

closure cash flow obligations of the company can provide valuable input to decision-making;

- CL3C can be used to make decisions about overall investment strategies, e.g. additional mining operations can be acquired and placed in operation to help cover high cash flow needs; and,
- CL3C may also be an important tool to evaluate mergers and acquisitions, e.g. the company portfolio in Tables 1 and 2 is clearly not sufficient to cover the closure costs from operations during years 14 to

19 as there are no operating mines during that period and the total closure cash needs amount to \$62.5M. If this company cannot acquire other operating mines by year 14 then it must have a cash reserve to cover the remaining closure and post-closure costs. Otherwise it may be a better strategy to sell the company at an earlier stage when it still has significant market value.

Table 3 Total and DCF Closure and Post-Closure Costs

Mine	Operating Mine Life (years)	Closure and Post-Closure Costs (\$M)	
		Total	DCF
1	15	51	12.2
2	10	18.5	7.2
3	20	101	17.1
4	12	78	21.7
5	7	21	10

CLOSURE COST STRATEGIES FOR COMPANIES WITH ONE OR TWO MINES

The general model of the mining industry, where income from future mines provide the cash flow for closure and post-closure commitments at the company’s closed mines, is obviously not workable if a company only owns a few mines. It becomes even less applicable if a company owns only one mine.

A sinking fund investment approach can be used to provide the closure and post-closure cash flow obligations of companies. The annual amount of the sinking fund is calculated using:

$$A = F [i / ((1 + i)^n - 1)]$$

Where

- A – uniform amount per period
- F – future value
- i – interest rate
- n – number of periods

Using this expression the annual payments required during the operating stages for the mines in Tables 1, 2 and 3 above are obtained for investment interest rates of 5, 8 and 10 percent, see Table 4. This will accumulate to the total closure and post-closure cash flow needs at the end of the operating life. This is a conservative approach as the total closure and post-closure cash flow is spread out over a number of years following operations and a more sophisticated analysis can be performed to account for that. The annual amounts for

the sinking fund investment are quite low and dependent on the investment interest rate. Because of this uncertainty it may require that the sinking fund investment vary from year-

to-year to make sure that the total amount of cash flow can be covered.

Table 4 Annual sinking fund amounts (\$M) to provide total cash flow costs for closure and post-closure activities

Mine	Interest Rate (%)		
	5	8	10
1	2.36	1.88	1.61
2	0.86	0.68	0.58
3	4.68	3.72	3.18
4	3.61	2.87	2.45
5	0.97	0.77	0.66

Payment to a sinking fund will obviously reduce the company profits and may not make all the shareholders happy, or may make the company less attractive to new investors. However, in some cases this will be the only approach that the company can use to satisfy the closure and post-closure obligations.

There are no regulatory requirements for companies to set up a sinking fund to provide closure and post-closure cash flow, even if the company only owns one or two mines. It can be argued that as long as there is sufficient financial assurance in place that closure can always be done using those funds

if the company defaults. However, this should not be the preferred approach as it may result in inefficiencies and other hidden costs that will have to be carried by society.

CONCLUSIONS

This paper describes the simple concept of corporate life cycle closure cost (CL3C). It consists of a cash flow summary for closure

and post-closure costs for all mines in the portfolio of a company. CL3C can be used as an indicator in the evaluation of new projects as well as for strategic planning such as requirements for the company to make new investments or even consider divesting.

Companies owning only one mine will not be able to fund the closure and post-closure cash flow for that mine from the income of other existing operations. In this case a sinking fund investment can be used during operations to fund the future mine closure and post-closure cash flow needs.

REFERENCES

Parshley, J.V., Bauman, W. & Blaxland, D. 2009. An evolution of the methods for and purposes of mine closure cost estimating. In Andy Fourie and Mark Tibbett (eds.), *Mine Closure 2009; Proc. Fourth International Conference on Mine Closure, Perth, 9-11 September 2009*. Perth: Australian Centre for Geomechanics, pp. 187 – 200.

STRUCTURED GEOMEMBRANE LINERS IN MINING BASE AND CLOSURE SYSTEMS

Clark West

Agri America Inc., Georgetown, SC, USA

ABSTRACT: Structured or embossed HDPE and LLDPE geomembranes have been available to Mine owners and designers for over 10 years and their use in new mines, expansions and final closure designs has been steadily increasing, especially over the past 10 years as owners and designers discover and demand the consistent high quality characteristics of this type of geomembrane due to the unique manufacturing process. This paper will discuss the structured or embossed geomembrane concept and manufacturing process as well as present comparative testing, illustrating the major advantages to the implementation of this type of product in these types of applications. Both technical and economic advantages will be illustrated.

Materials are available for double lined and final cover systems that are revolutionizing the way ponds, pads and final closures are constructed using structured liners. The cost savings are coming in various forms such as material savings, lower installation costs and third party inspection times along with better performance. These new systems will be presented.

INTRODUCTION

In the liner manufacturing industry there are basically two different processes for the manufacture of the textured surface on high density polyethylene (HDPE) and linear low density polyethylene (LLDPE). One is by the blown film method which injects an inert gas, nitrogen, in to the liner at the die under pressure and when it is exposed to normal pressure it will rapidly expand and burst like a bubble creating a texturing on the surface of the sheet. The embossed or structured texturing is created by extruding molten polyethylene between two precisely engineered rollers that have an embossing on one or both of the rollers creating a pattern of spikes on the sheet.

The advantages of the embossed sheet are:

- The core or base thickness of the material is not affected by the process, it is virtually a smooth sheet with spikes. This is seen in the performance of the embossed material as its specifications are closer to a smooth sheet than blown film texturing.
- Consistency between materials is constant because of the simple nature of manufacture.
- Tensile and Strain properties are not affected.
- Completely homogeneous
- Integral textured profile embedded in sheet

- Integral drain profile embedded in sheet

Consistent interface friction
no yes

Disadvantages of blown film

- Non Uniform Surface Asperity Heights, difficult to guarantee friction angle.
- Non Uniform Area Coverage once again difficult to predict interface angles consistently
- Variable Core Thickness an effect of the texturing method
- Reduced Tensile and Strain Properties
- Variable specifications within a Roll and from Roll to Roll

Affect on mechanical properties
yes no

Affect on stress crack potential
yes no

Manufacturing Method

- Horizontal Flat Die Calendar Extrusion
- Precision Machined Profile Rolls
- Consistent Quality Sheet
 - Polymer
 - Thickness
 - Structure
 - Smooth Edge Textured/Structured Sheet
 - Continuous Production QC Testing

STRUCTURED GEOMEMBRANES

Because of the way the material is embossed to form structured liners between two machined rollers it is a simple procedure to remove a single roller or set of rollers to be replaced by roller or rollers with specialized embossing to create liners for a wide variety of applications.

Comparative Properties for Design Consideration

- Blown film co-extruded textured surfaces vs. Micro Spike structured surfaces

Consistent core thickness
no yes

Consistent surface texture
no yes

Consistent asperity height
no yes

- Smooth liner for regular use in leach pads, ponds and tailings dams.
- Microspike textured liner for when a greater interface is needed on lopes etc
- Grip Liner - lower surface spikes for high lower interface but a possible slip plane if needed
- Drain Liner - upper surface studs as a drainage medium to replace nets in double lined situations such as hazardous ponds or leak location systems.
- Super Gripnet - drain studs upper and spike surface lower for high interface lower for steep slopes and a drainage medium for use on landfill or mine closures.
- Micro Drain – upper surface studs lower surface textured for use on top of a fabric or geosynthetic clay with a drainage medium built in.

Transmissivity Cap Profiles

- Transmissivity of the drain stud profile with an overlying non woven heat set geotextile ranges from 1.6E-03 to 3.6E-03 m²/s.
- Laboratory Transmissivity values are dependent on the boundary layer (soil), geotextile, normal loading and gradient

Interface Sheer – Cap Loading

Soil / Grip Liner Surface (degrees)

- Sand 35P
31LD
- Glacial Till 38P
34LD
- Sandy Clay 28P
26LD
- Non Woven GT 31P
26LD
- Course/Fine Sand 51P
44LD

Soil / Drain Liner Surface w/GT

- Sand 30P 30LD

Case History – Gilt Edge Mine – Superfund Site – Ruby Waste Rock Dump Cap

- 80 mil Super Gripnet LLDPE
- 65 Acre Cap System for prevention of ARD
- Valley Fill - 1800 ft long slope with 9 - 25 ft wide benches (40 ft vertical), perimeter ditches, subsurface and surface drainage
- Short Construction Season (high elevation)
- High water flow rate and high interface shear resistance required for geomembrane system

Cover System Layers

- 75 mm (6 in): Topsoil Vegetation Layer
- 1.0 m (36 in): Processed Soil/Rock Layer
- 0.5 m (18 in): Processed Cover Drain Layer

-
- - 335 g/sm (10 oz/sy) NW Heatset Geotextile
 - 2.0 mm (80 mil) LLDPE Structured GM

-
- - 0.3 m (12 in): Processed Base Layer

Interface Characteristics

- Processed Base vs. Bottom Spike Texture
32 deg Peak and 32 deg LD
- Processed Cover Soil vs. Top Drain Structure with Heat Set Geotextile
37 deg Peak and 37 deg LD
 - Water Flow Rate under 550 psf – 2.6 gpm/ft (10 oz/sy NW Heat Set Geotextile)

Structured Geomembranes – Waste Cell Advantages

Bottom Lining System

- Increased Cell Capacity
- Increased Cell Stability
- Reduction in Layers (Integral Drain Layer)

Cell Closure System

- Increased Slope Stability
- Composite (Integral) Drain System
- Ease of Installation on Slope

SUMMARY

- Cost Effective Solution for Slope Stability and Drainage
- Consistent Quality Texture or Structure
- Reduction in CQA costs

CONCLUSION

Structured Flat Die extrusion methods provide a wide variety of materials to give engineers and designers a wider range of materials that can more closely fit the requirements of the project they are designing for creating a greater factor of safety which is a benefit to all.

INNOVATIVE APPROACH TO CLOSURE OF A MIXED WASTES PROCESS WATER POND

Adam Whitman

Meridian Beartrack Company, Reno Nevada

Tarik Hadj-Hamou and Jim Juliani

Strategic Engineering & Science, Inc. Irvine, California

ABSTRACT: This paper describes an alternative approach to final closure of a process water pond (PWP) that was used for hazardous waste water storage during operations of the Royal Mountain King Mine. Upon cessation of mining activities the PWP contained approximately 90 acre feet of hazardous waste water and was therefore considered a waste management unit in accordance with California regulations. Various treatment studies were conducted at the time to dispose of the water but it was finally determined that the most cost effective approach was evaporation. A sprinkler system was installed along the perimeter of the pond and used to atomize the salt-laden water and sprinkle it on the black HDPE lined sloping sides of the pond. To stabilize the remaining concentrated waste water, and as a temporary measure, 39,000 cubic yard (cy) of flotation tailings were placed into the PWP. The flotation tailings were intended to “soak up” the waste water and provide a platform for a temporary geomembrane cover.

The regulatory final closure for the PWP was clean closure which meant removal of the waste water trapped in the tailings, the tailings, the liner system, the leachate collection and recovery system, the subdrain, and all other appurtenances. However, the cost and challenges associated with clean closure lead the authors to propose in-place closure as an engineered alternative final closure to the Regional Water Quality Control Board, the lead regulatory agency. The proposed design consists of encapsulating the waste (water and tailings) by placing a new HDPE geomembrane and a protective soil cover and regrading the berms to restore the area to near the original topography.

INTRODUCTION

Background

The Royal Mountain King Mine (RMK) mine is approximately 5 miles north of the town of Copperopolis in Calaveras County, California. Mining started in May 1988 and continued through April 1994. During the mining period, approximately 56 million tons

of ore and overburden materials were removed from three pits. The overburden material was stockpiled in overburden disposal sites (ODS) while the ore was stockpiled for processing. The ore was processed by crushing, grinding, gravity separation, and flotation. The flotation concentrate (approximately three percent of the ore milled) was further beneficiated by regrinding and leaching with cyanide. The

leached concentrate residue (LCR) was deposited in the Leached Concentrates Residue Facility (LCRF). Water contained in the LCR slurry was drained from the LCRF to the Process Water Pond (PWP) via a decant drain and the leachate collection and recovery system (LCRS) of the LCRF. Upon cessation of mining the three pits, the overburden stockpiles, Flotation Tailings, Reservoir (FTR), the LCRF, and the PWP were classified as Waste Management Units (WMU) and as such needed to be closed in accordance with state and federal regulation. The three pits, overburden stockpiles, LCRF, and FTR were closed whereas the PWP was only temporarily closed by the year 2007. This paper focuses on closure of the PWP.

Configuration

The PWP covers approximately six acres and was permitted to store Group A liquid mining waste. The final design provided for a capacity of 115 acre-feet. The PWP was built by excavating into the native formation on the western edge, northern edge, and portion of the southern edge. An embankment with 2:1 slopes (Horizontal: Vertical) was built along the eastern edge and a portion of the southern edge. Figure 1 shows the PWP in early 2007 prior to final closure construction

The PWP includes a double composite liner system, an LCRS, and an underdrain system. The liner system on the bottom of the PWP consists, from bottom to top, of:

- A 2-ft thick layer of clay;
- A 150-mil geotextile;
- An 80-mil HDPE geomembrane;
- A 150-mil geotextile;
- A 1-ft thick layer of crushed and washed rock;
- A 150 mil geotextile; and
- An 80-mil HDPE geomembrane.

The liner system on the side slopes of the PWP consists, from bottom to top, of:

- A 150-mil geotextile;
- An 80-mil HDPE geomembrane;
- An HDPE drain net; and
- An 80-mil HDPE geomembrane.

A cross-section of the double liner system installed at the PWP is shown on Figure 2. This composite liner system meets the regulatory requirements for Group A mining waste management units.

The LCRS consists of a drainage layer underneath the bottom and side slope of the PWP and a collection system. The drainage layer underneath the bottom of the PWP is the one-foot thick layer of 3/8-inch to 1/2-inch gravel. The drainage layer on the side slope consists of an HDPE drain net. The bottom drainage layer slopes toward a sump equipped with a slotted 6-inch diameter pipe and a riser pipe. The sump is equipped with a submersible pump and is emptied on a regular basis.

The PWP is further underlain by a spine drain system consisting of two diagonal drains across the footprint of the PWP. The drains consist of perforated six-inch diameter pipes encased in gravel filled trenches. The spine drain provides for leak detection monitoring under the pond.

Interim Closure Work

In the summer of 1999, Meridian performed interim closure of the PWP. The purpose of the interim closure was to minimize the amount of water requiring management. The interim closure work included:

- Removal of residual process water from the PWP by vaporization and evaporation;

- Consolidation/stabilization of residual liquids in the PWP by mixing in the residual liquids with approximately 39,000 cubic yards (cy) of flotation tailings;
- Placement of a geomembrane on top of the flotation tailings to allow management of stormwater; and
- Reduction of the embankment on the southeast corner to provide access to the PWP.

Final closure

Final closure and post-closure maintenance of the WMUs at RMK ARE regulated by the Regional Water Quality Control Board (RWQCB), the lead environmental control agency, through Waste Discharge Requirement (WDR) Order. In 2007, when this work was begun, WDR Order No. 5-01-040 issued in 2001 was in effect and closure of the PWP was governed by the following articles:

- **71.** The PWP will be clean closed after the excess water has been removed and the pond is no longer needed to collect and evaporate LCRF/LCRS flows. The liner material, LCRS material and solidified residue will be removed prior to closure and placed in the LCRF.
- **72.** Closure of the PWP requires removal of free liquid and any residual sludge that may be present. During the summer and fall of 1999, the Discharger completed an interim closure of the PWP which consisted of evaporation of wastewater in the PWP to approximately 8 acre-feet, solidification of this remaining brine by placing flotation tailings into the PWP, covering the solidified brine with an impervious liner to prevent contact between rainfall and the underlying materials, construction of a small (1.3

acre) evaporation pond on the lined surface to collect and evaporate the LCRF/LCRS flows.

- **74.** The pond depression area will be graded to establish a natural looking hollow and allowed to fill with runoff and function as a natural seasonal pond. Inflow will occur by a surface drainage swale graded to drain runoff into the pond from the north, and outflow from the hollow will be via the existing open cut rip-rapped spillway which will be maintained.

ALTERNATIVE TO CLOSURE OF PWP

General

Clean closure of PWP as described in the WDRs in the previous section was predicated on the availability of another WMU to dispose of any materials contained in the PWP, including waste, the liner system, and the LCRS. However, the schedule of closure activities led to the closure of all other WMUs prior to closure of the PWP. Reopening a closed WMU to place new waste material could affect the integrity of the cover system and could also adversely affect the surface drainage pattern. Consequently to clean close the PWP would require hauling the solid and liquid wastes as well as the liner, LCRS, and drain materials offsite.

Moving and hauling these materials would pose logistic and environmental challenges not mitigated by the potential benefits of a clean closure. Removal and transport would have first required reducing the in-situ moisture content of the 39,000 cy of flotation tailing material in the PWP classified as silty sand/sandy silt to a value such that the material passes the “paint filter test” or is at moisture holding capacity (the regulatory moisture content allowed for disposal of wet

waste at regulated facilities). Reduction of the moisture content could have been achieved by either pumping the water out of the tailings or mixing in more solids.

Based on available information, the 39,000 cy of flotation tailing were near saturation with volumetric moisture content ranging from 36.5 to 40.5 with an average of 38.5 percent. Assuming that the moisture holding capacity of the tailings is on the order of 8 percent then to reduce the volumetric moisture content of the 39,000 cy of tailings in the PWP from 38.5 to 8 percent approximately 24,000 cy of water would have had to be pumped out or 240,000 cy of similar, but dry, material would have had to be mixed with the 39,000 cy. Dewatering the fine tailings through pumping would have required years whereas the challenges posed by either the approach include:

- Locating 240,000 cy of adequate material;
- Finding an area where the wet materials and dry materials can be mixed;
- Controlling the run-off of the liquid from the mixing area (this liquid is classified as Group A Waste);
- Locating an off-site facility within reasonable distance; and
- Loading and transporting the 279,000 cy (the in-place 39,000 cy plus 240,000 cy) of material safely to an off-site facility.

It was estimated that to haul 279,000 cy (approximately 420,000 tons) of material, the lining system and the LCRS system will require over 19,000 truck trips hauling approximate 22 tons each. The risk for spillage of waste or accidents during these 19,000 trips is not negligible. It was therefore proposed to consider alternatives to the approved clean closure of the PWP by an in-place closure in accordance with the provisions of Title 27. A feasibility study

was conducted to evaluate options to close the PWP. Five alternatives were evaluated:

- Alternative I: Clean closure with off-site disposal of the tailings and the liner system;
- Alternative II: Clean closure with disposal of the tailings and the liner system in the LCRF;
- Alternative III: Clean closure with disposal in a new WMU built on top of the flotation Tailings Reservoir (FTR);
- Alternative IV: In-place closure with dewatering; and
- Alternative V: In-place closure with solidification.

Following the methodology developed in U.S. EPA (1988) the five alternatives for closing the PWP were screened and evaluated. These five alternatives were initially screened and found to meet the short and long-term aspects in terms of effectiveness, implementability, and cost.

Each alternative was analyzed against each of eight major criteria listed in the following. The relative or absolute performance of each alternative was scored against each criterion. Note that all the alternatives selected meet the criteria:

- Overall Protection of Human Health and the Environment;
- Compliance with Applicable or Relevant and Appropriate Requirements (ARARs);
- Long-term Effectiveness and Permanence;
- Reduction of Toxicity, Mobility, and Volume Through Treatment;
- Short-term Effectiveness;
- Implementability;
- Cost; and
- Community Acceptance.

Results of the analysis are summarized in Table 1. Table 2 reports the estimated capital cost to implement each alternative. Space limitation precludes the insertion of the detail analysis of each alternative in terms of the criteria listed previously. The analysis indicates that Alternative IV (in-place closure and dewatering) is the highest scoring alternative. Alternative IV will provide protection of the environment by keeping the waste encapsulated in a cell that meets current Title 27 requirements and which has been documented over the years to function as intended.

Advantages of Alternative IV are:

- No solid waste handling;
- Minimum waste water handling;
- No truck traffic on public roadways;
- No air quality impact; and
- Meets Title 27 requirements as an alternative closure.

A disadvantages associated with Alternative IV is the fact that the WMU remains at RMK. However, this disadvantage is mitigated by the fact that monitoring of the WMU will be on-going as the Post closure Monitoring Plan at RMK will require monitoring of other facilities and the added cost of mentoring the WMU is insignificant when compared to the cost associated with the annual monitoring required at the site for the other WMUs.

Rationale

Consequently, it was proposed to the RWQCB to implement Alternative IV: in-place closure and dewatering to close the PWP. This alternative is acceptable because follows the closure requirements detailed in Title 27 of the California code of Regulations, namely:

- Article 21400(b) allows consideration of options other than clean closure when clean closure is not feasible.
- Article 21400(b) (2) allows RMK to propose, for approval, an alternative to final closure to the RWQCB.
- Article 21400(b) (2) (A) allows to consider closure as a landfill.
- Article 22510(k) allows PWP to be closed in place because the outer liner of the double liner system is clay.
- Article 22510(k) further stipulates that a cover designed per Section 21090(a) shall be constructed.
- Article 21090 provides the design requirements for a landfill cover. Based on the existing liner system, the final cover for PWP will include a geomembrane.

The RWQCB approved the alternative and a detail closure approach and design was developed and implemented.

Approach

Closure of the PWP entailed evaporating the free water that has accumulated on top of the flotation tailings, building the final cover per Title 27 requirements, and dewatering the flotation tailings to bring the in-situ moisture content to regulatory value (i.e. the moisture holding capacity).

The schedule for regulatory final closure was predicated on reducing the water within the flotation tailings to moisture holding capacity

Both free water and the water within the flotation tailings were considered Group A waste through contact, and the optimal method of disposal was evaporation. The free water that accumulated on top of the PWP evaporated during the dry season (April through October). Upon construction of the cover system, the water within the flotation

tailings was pumped out of the tailings and directed towards a newly constructed evaporation pond installed on top of the PWP for evaporation. Dewatering of the flotation tailings will continue until the maximum allowable head of liquid on the liner system will be 30 cm (12 inches) or less as stipulated by the Code of Federal Regulations (CFR), Subpart D, paragraph 258.40(a) (2).

ALTERNATIVE CLOSURE DESIGN

There were three design elements to achieve closure of the PWP:

- Final cover;
- Dewatering system; and
- Evaporation pond.

Final Cover

The PWP was graded to match the surroundings. Following removal of excess water from the tailings, fill was placed in the PWP to provide a subgrade for construction of the final cover. The final grading plan for closure of the PWP provides positive surface water drainage to direct surface water run-off away into existing surface water management system collection and conveyance structures. This final grading plan also mitigates the potential for surface water ponding.

The final cover grading plan for closure of the PWP is presented in Figure 3. The final grading plan conformed to the existing lines and grades of the site, thereby minimizing the amount of earthwork necessary for closure construction and providing an aesthetic final look.

Cover

The final cover for the PWP is the same cover as used for closure of the LCRF and consists of, from bottom to top:

- Fill as needed to reach the elevation of the base grading plan
- Foundation layer at least six inches thick;
- A 60-mil high-density polyethylene (HDPE) geomembrane;
- A geocomposite drainage layer;
- An erosion protection layer at least one foot thick; and
- A vegetative layer at least six inches thick.

The vegetative layer was then hydroseeded with the approved seed mix.

A typical cross-section of the final cover system at the PWP is shown on Figure 4.

Dewatering System

Dewatering sumps and well points were installed in the tailings during construction of the final cover. The well points can be connected to a vacuum system and activated during the dry season. The water pumped out of the tailings placed into the evaporation pond built on top of the PWP. During the rainy season, water is not pumped from the tailings. It is anticipated that two dewatering sumps could be installed. A typical dewatering sump and well point cross section is shown in Figure 5. A boot will be installed around the dewatering sump to connect with the liner and provide a watertight seal. Upon conclusion of dewatering the well points will be removed and the sumps permanently capped.

Evaporation System

The liquid extracted from the PWP is Group A mine waste and consequently needs to be disposed of properly. The optimum approach, and the approach currently used at the RMK mine, is evaporation.

A new lined evaporation pond was built on top of the PWP within the final cover. Thus the evaporation pond benefits from the existing double composite liner system of the PWP. The evaporation pond will be used during the dry season to evaporate the liquid extracted from the tailings in the PWP and the liquid pumped from the LCRS. At the end of the dry season, the residue (i.e., the by-product of evaporation) that may have accumulated in the evaporation pond will be disposed of in accordance with current regulations.

The grading plan and the cover system of the PWP were designed to accommodate injection and/or burial of the residue from the evaporation pond into the PWP.

Placing the new lined evaporation pond above the PWP offers the following advantages:

- The LCRS and spine drain of the PWP are available to collect any leakage;
- The new lined evaporation pond is within the footprint of an existing permitted WMU;
- The residue accumulated in the evaporation pond at the end of the dry season will be disposed of in accordance with current regulations including injection and /or burial into the PWP; and
- Upon completion of dewatering of the tailings, the lined evaporation pond will be cleared and filled with clean soil and incorporated in the grading plan of the final closure of the PWP.

From an operational stand point, monitoring evaporation, controlling the dewatering system, and managing the residue from evaporation, a pond on the order of half an acre is the optimum size. The newly lined evaporation pond is therefore approximately 3 feet deep at the deepest end with a base of 150 ft by 150 ft. Assuming 1 ft of freeboard

and 3H:1V (Horizontal to Vertical), the approximate available storage for evaporation of the pond is approximately 2,700 cy (545,000 gallons).

The pond was built during grading of the final cover of the PWP and was formed by building a 3-ft tall berm. The evaporation pond was lined with a 60-mil HDPE geomembrane. The berms were lined with 60-mil HDPE geomembrane as well. Figure 6 shows a picture of the closed PWP with the evaporation pond.

It is anticipated, that during the dry season (April to October) the net pan evaporation is approximately 44 inches. Assuming an efficiency of 80 percent (pan to lake evaporation), the design evaporation for the dry season is 35 inches $[44 \times 0.8]$. Consequently, a volume of approximately 2,350 cy (475,000 gallons) could be evaporated in one dry season $[35 \text{ in.} \times 0.5 \text{ acre} \approx (35/12) (43560) (0.5) (1/27) = 2,352.8 \text{ cy} \approx 2,350 \text{ cy}]$. Based on the estimated volume of water in the tailings of the PWP and the relatively low draining rate of the tailings, it may take seven to ten years to bring down the level of water in the tailing such that the measured head on the liner is 12 inches or less as indicated on the tentative closure schedule shown in Table 3.

Upon dewatering of the tailings, the perimeter berms will be removed, the geocomposite extended and the soil cover placed over the area of the pond so that all of the PWP will be covered with the components of the final cover described in previously.

CONCLUSION

Working within the framework of the California regulations for closure of WMU, the authors proposed an alternative final closure to the PWP, one of the WMUs at

RMK that was both technically advantageous and economically beneficial. The RWQCB as the lead agency approved the proposed alternative which relied on constructing a regulatory final cover and dewatering the tailings over a seven to ten year period.

REFERENCES

EPA, (1988) “Guidance for Conducting Remedial Investigations and Feasibility Studies under CERCLA,” OSWER Directive No. 9355.3.

Table 1: Ranking Of Alternatives

Description	Grade
Alternative I - Clean Closure - Offsite Disposal	1+
Alternative II - Clean Closure - LCRF Disposal	0
Alternative III- Clean Closure - FTR Disposal	3-
Alternative IV - In Place Closure and Dewatering	6+
Alternative V- In Place Closure and Solidification	3+

Table 2: PWP Closure – Cost Of Alternatives

Description	Cost (million \$)
Alternative I - Clean Closure - Offsite Disposal	15.9
Alternative II - Clean Closure - LCRF Disposal	5.3
Alternative III- Clean Closure - FTR Disposal	6.3
Alternative IV - In Place Closure and Dewatering	1.9
Alternative V- In Place Closure and Solidification	7.4

Table 3 Tentative Schedule for Closure of PWP

Phase	Description	Year
1	<ul style="list-style-type: none"> • removal of free water • filling of PWP up to base grade • placement of geosynthetic components <ul style="list-style-type: none"> ○ 60-mil HDPE over PWP except footprint of evaporation pond ○ 100-mil HDPE over footprint of evaporation pond ○ Geocomposite over PWP except evaporation pond • construction of the evaporation pond • installation of the dewatering system for the tailings • check pumping system • closing the LCRS from the LCRF 	2007
2	<ul style="list-style-type: none"> • dewatering of tailings through pumping and evaporation 	2008 to 2014/2017 ¹
3	<ul style="list-style-type: none"> • closure of the evaporation pond • geocomposite over footprint of evaporation pond • final grading of the cover of the PWP • installation of drainage control, slope protection and erosion control measures on the final cover 	2018 to 2019 ¹
<p>Note</p> <p>1- Actual date will depend upon the rate of dewatering of the tailings</p>		



Figure 1. PWP Prior to Construction (March 2007)

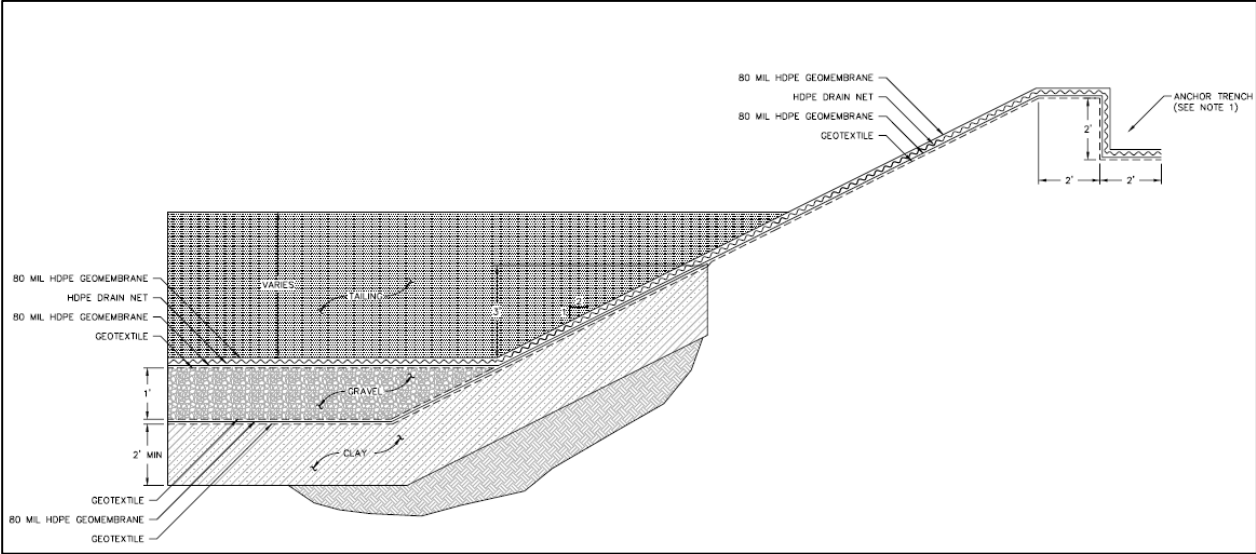


Figure 2. Existing Liner System at PWP

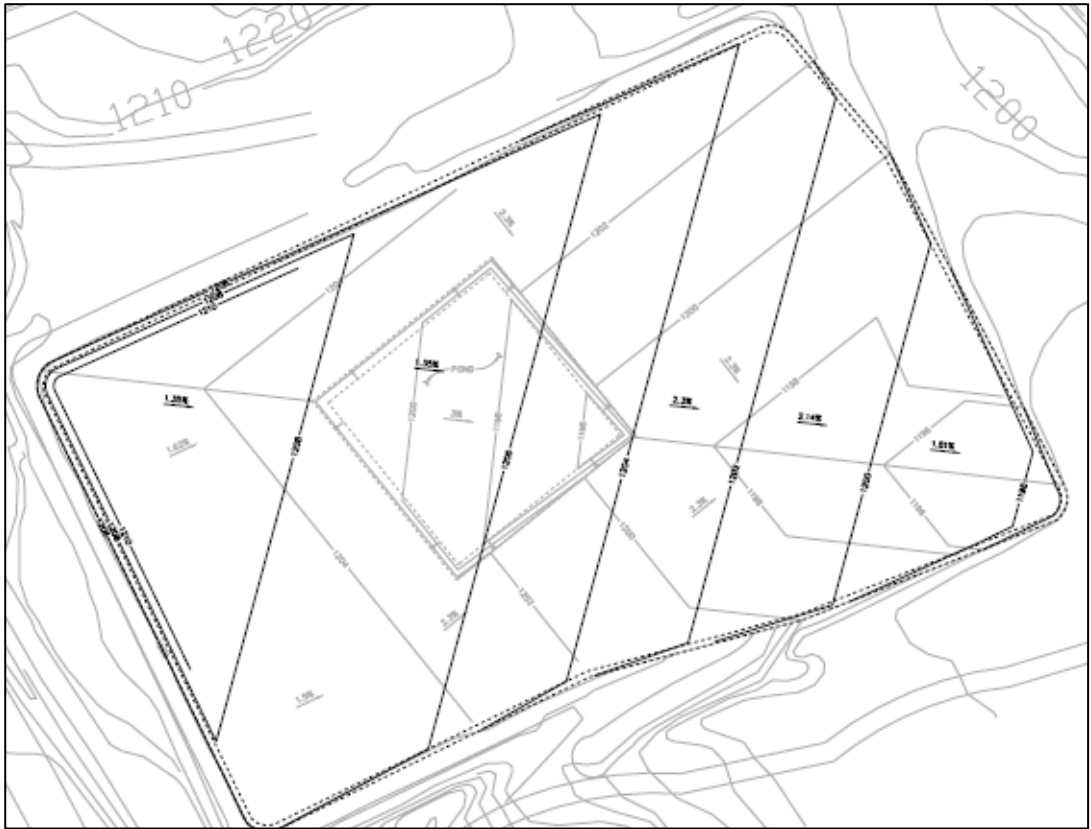


Figure 3. Final Grading Plan

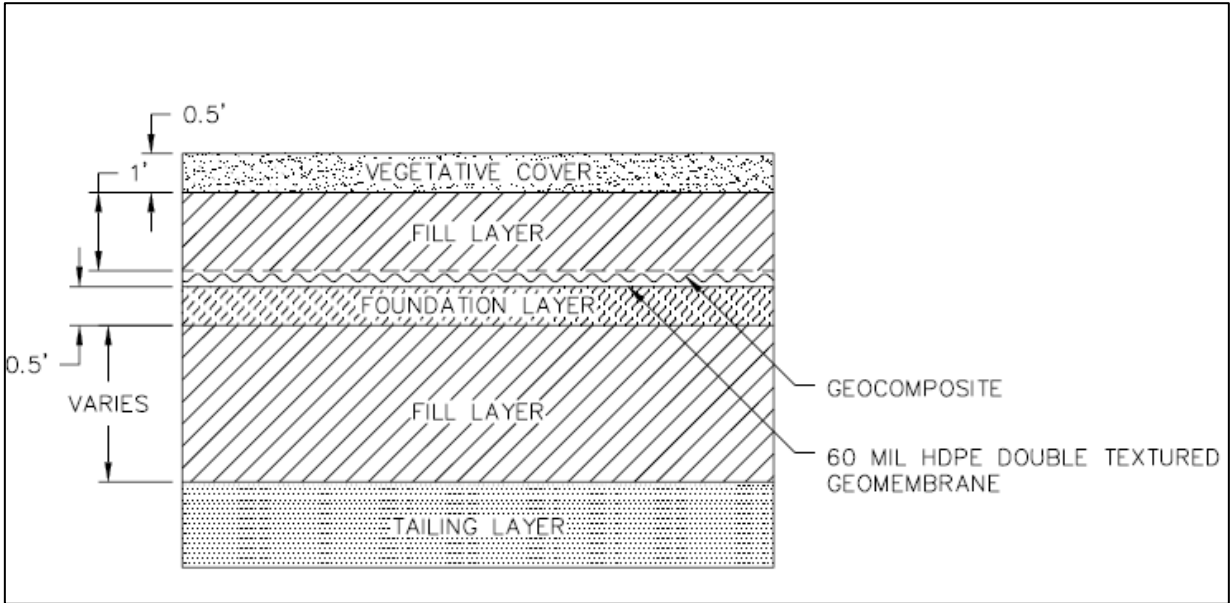


Figure 4: Cross Section of Final Cover

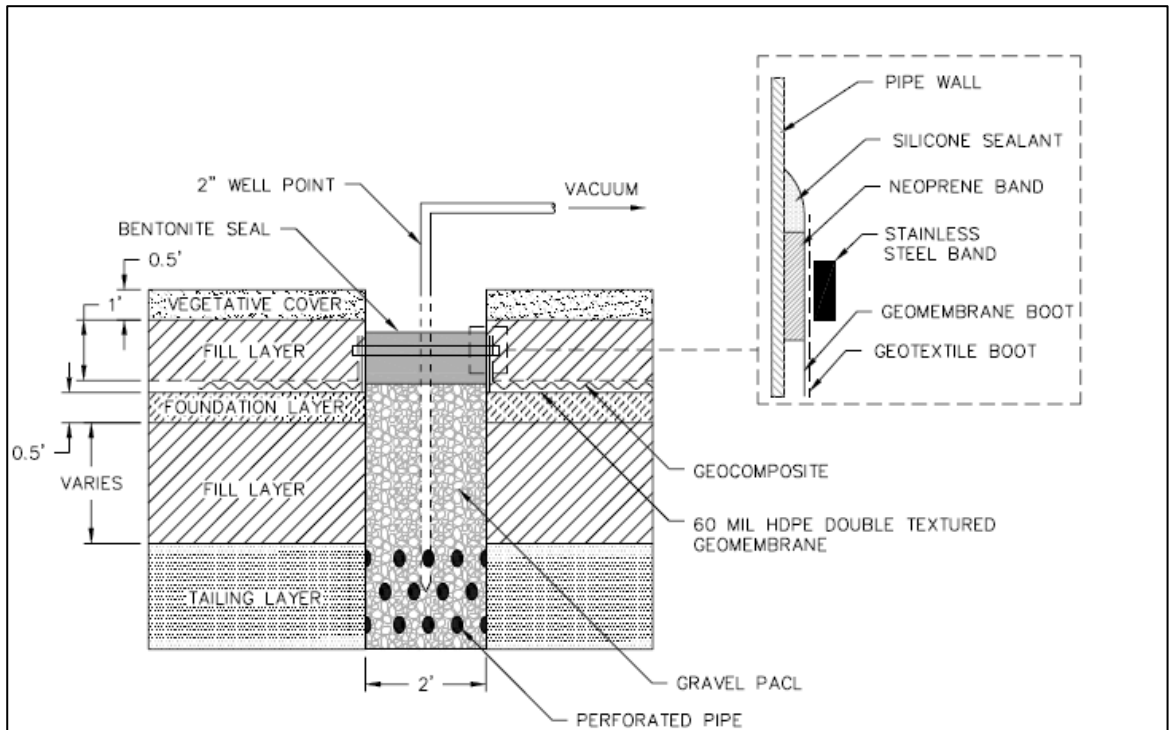


Figure 5. Typical Dewatering Sump



Figure 6. Closed PWP with Evaporation Pond (September 2008)

OPTIMIZATION OF TAILINGS POND DESIGN FOR EFFECTIVE EFFLUENT QUALITY MANAGEMENT

Stephen Daughney, Tom Plikas, Jianping Zhang and Lowy Gunnewiek
Hatch Ltd., Mississauga, Ontario, Canada

Tim Miller, Andr ea Lagac e and David Yaschyshyn
Xstrata Copper Canada - Kidd Metallurgical Site, Timmins, Ontario, Canada

Abstract: Settling ponds represent a relatively low cost and adaptable solution that is commonly applied to mine tailings management. Particular attention must be paid to the design of the pond to ensure that the desired removal of metals and suspended solids are achieved for compliance with effluent water quality regulations. An advanced computational fluid dynamics (CFD) model has been developed to assist in this regard by simulating pond hydraulics and solids settling performance. This tool can be used to assist with pond operation and maintenance planning and to identify pond improvement and optimization projects. The model incorporates the major fluid dynamic processes occurring in the pond: pond hydraulics, flow short-circuiting, particle settling, and sludge re-suspension. Model predictions of total suspended solids (TSS) concentration were compared with data collected from the Kidd Metallurgical Site Tailings Management Area of Xstrata Copper, and found to be within 5% of the measured data. The modeling work has demonstrated that the addition of coagulants to the inflow can significantly reduce the pond outlet TSS concentration during high flow conditions. This information, together with coagulant plant trials, can be used to define a pond management strategy to limit operating costs for chemicals whilst achieving the effluent water quality requirements. The model has also been successfully utilized to assess proposed changes to the pond configuration.

INTRODUCTION

The mining industry must manage and treat wastewater arising from waste rock and tailings impoundments such that environmental discharges meet water quality regulations. Treatment involving lime addition followed by flow through large, shallow settling ponds is frequently applied to limit particulate and metal emissions to the environment. However, lime treatment tends to form a dispersed sludge with finely sized particles (i.e. median particle size

$d_{50} < 10 \mu\text{m}$), so solids removal requires long settling times. The sludge produced is of low density and can easily be re-suspended under critical flow conditions (Mian and Yanful, 2003). Therefore, optimization of pond design and treatment performance is a common goal for many mining facilities in order to minimize impact from TSS carryover on the downstream ecosystem and receiving waters.

The design and operation of settling ponds must consider multiple elements including: pond geometry (i.e. inlet/outlet configuration,

water depth and aspect ratio), properties of solid particles, seasonal influence on flow rate, and environmental factors such as wind and ice cover (Marsalek et al., 2000; Adu-Wusu et al., 2001; Mian and Yanful, 2003). However, quantitative evaluations of the effects of these factors on settling pond performance through a numerical modeling approach are uncommon. Most of the reported studies pertain to lab-scale experimental investigations focused on obtaining empirical equations to predict solids settling and re-suspension behavior in tailings ponds (Mohamed et al., 1996; Mian and Yanful, 2003). While these empirical methods can provide general predictions of pond performance, they are not able to integrate all the key factors in one model. More importantly, these empirical models ignore the complex three-dimensional hydrodynamic characteristics (e.g. short-circuiting and formation of dead zones) that can significantly affect settling efficiency.

These shortcomings can be overcome by the use of computational fluid dynamics (CFD) modeling. CFD is a branch of computational physics that involves the numerical solution of the governing equations that describe the transport of mass, momentum and energy of a fluid. CFD has been applied recently for evaluating municipal wastewater solids settling and river/reservoir hydrodynamics (Lakehal et al., 1999; Kleine and Reddy, 2005). However, the application of CFD to full-scale mine tailings pond design and performance has not been reported.

The primary objective of this study was to characterize tailings pond hydraulics and solids settling using CFD modeling. In particular:

- predict detailed flow patterns throughout the entire pond

- predict the residence time distribution of solids in the pond
- predict the total suspended solids (TSS) concentration at the pond outlet for comparison with established objectives.

The model will help investigate engineered improvements to the pond design and adjustments to operational strategies for the purpose of achieving reductions in the pond outlet TSS concentration.

DESCRIPTION OF STUDY SITE

Kidd Metsite commenced operations in 1966 to process the copper and zinc ore from the nearby Kidd Mine. Operations consist of a concentrator, copper smelter and refinery, as well as zinc, indium, cadmium and sulphuric acid plants. In late 2004, nickel ore from the Montcalm Mine was introduced in a separate milling circuit in the Concentrator. The majority of waste products from metallurgical operations are discharged to the Tailings Management Area (TMA). The TMA covers about 1250 ha, with about 650 ha actively used for tailings disposal. Annual tailings quantities vary, with 2.78 million tonnes disposed in 2008. The tailings are centrally discharged as thickened slurry from spigot points at the apex of a gradually sloped, inverted cone. The spigot points are periodically alternated to evenly distribute the slurry over the cone surface and limit acid generation from the sulphidic waste rock.

Wastewater streams, including acid rock drainage from the tailings cone, process wastewater from the Metsite and runoff from rain and snowmelt events, collect in perimeter ditches to be conveyed to two storage ponds, Pond A and Pond C. Lime is added at the outlet of each pond for pH adjustment and metals precipitation. Ditch 10 is a separate,

unattenuated contributor of process wastewater and runoff, merging with the main flow after the Pond A lime station.

As shown in Figure 1, all lime treated wastewater flows into Pond D, where primary solids settling occurs. Water volumes stored in Ponds A and C are

modulated to respond to precipitation and melt events and regulate the release of water to Pond D. Pond E, downstream of Pond D, is used for final polishing and residual solids removal. The Pond E discharge is adjusted to a pH below 9 by CO₂ injection before flowing into the Porcupine River.

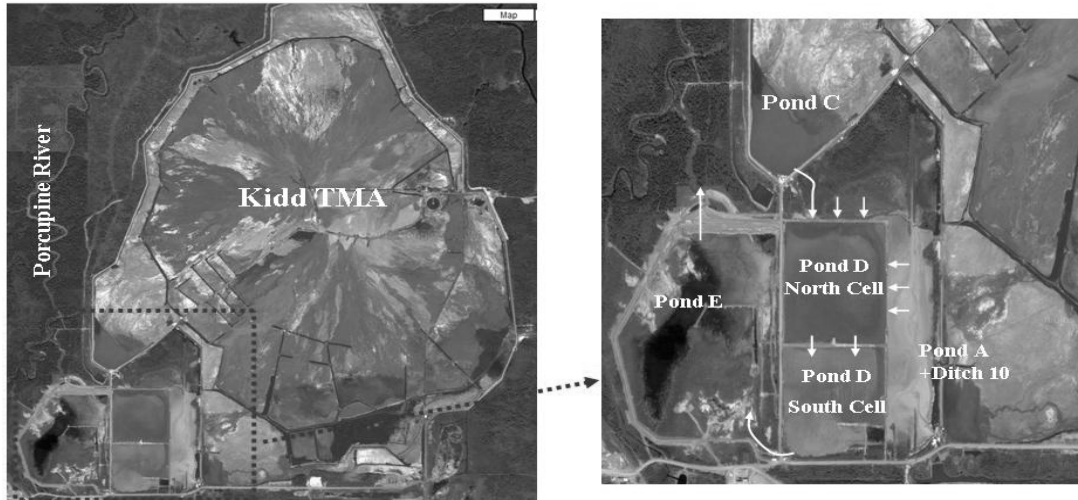


Figure 1 Kidd TMA general layout (left) and TMA pond system (right)

The main role of Pond D is to capture the suspended solids and precipitated metals present in the pond influent. As shown in Figure 1, Pond D is subdivided by the Split Dyke into North and South Cells. The dyke is partially submerged during peak flows. Ponds D measures roughly 500 m in width and 950 m in length.

Operational experience under adverse conditions has revealed higher than desired TSS concentrations at the outlet from Pond D. High solids carryover is most commonly associated with high flows or strong winds. Although the presence of Pond E assures that environmental objectives are satisfied, solids carryover from Pond D in excess of internal control targets is undesirable as this increases the Pond E dredging frequency, with consequent costs and difficulties. Therefore, there is a strong desire to

understand the flow hydraulics and settling performance in Pond D and develop engineering solutions that ensure that Pond D performance goals are achieved for all conditions.

NUMERICAL MODELING APPROACH

A comprehensive CFD model has been developed and implemented in the commercial software package Ansys-Fluent, which is based on the finite volume numerical method as described in Versteeg and Malalasekera (2002). The model incorporates the major fluid dynamic processes occurring in the pond: pond hydraulics, flow short-circuiting, particle settling, and sludge re-suspension.

Modeling of Pond Flow Hydrodynamics

The Reynolds averaged Navier–Stokes equations are solved to determine the flow hydraulics. Turbulence is modeled using the standard k-ε turbulence model of Launder and Spalding (1974).

Modeling of Solids Settling

Suspended solids transport and settling is calculated by solving a convection–diffusion equation as follows:

$$\frac{\partial c}{\partial t} + (u \frac{\partial c}{\partial x} + v \frac{\partial c}{\partial y} + w \frac{\partial c}{\partial z}) + v_s \frac{\partial c}{\partial z} = \frac{\partial}{\partial x_j} (\Gamma \frac{\partial c}{\partial x_j}) \quad (1)$$

where c is the suspended solids concentration in water, u , v and w are water velocities in the x , y and z directions, respectively, v_s is the particle settling velocity that is calculated through application of Stokes Law, and Γ is the diffusion coefficient due to turbulent mixing. In the present study, a steady Pond D feed TSS is assumed. Therefore, the first term in the above convection-diffusion equation can be ignored. The third term can be considered as an extra convection term in the vertical direction, which is caused by the fall velocity of solid particles.

Modeling of Sludge Re-suspension

Sludge re-suspension involves complex physical processes. Zeigler and Lick (1998) and Partheniades (1986) performed experimental studies and suggested the following expression be used to predict the re-suspension rate of cohesive materials, such as fine particles in settling ponds:

$$E = \begin{cases} M \left(\frac{\tau_0 - \tau_c}{\tau_c} \right)^n & \text{if } \tau_0 > \tau_c \\ 0 & \text{if } \tau_0 \leq \tau_c \end{cases} \quad (2)$$

where E is the re-suspension rate ($\text{kg/m}^2 \text{ s}$), τ_0 is the total bed shear stress (N/m^2), τ_c is the critical bed shear stress for re-suspension (N/m^2), and M and n are experimentally determined coefficients.

The above equation indicates that sludge re-suspension only occurs in high velocity areas where the bottom shear stress, τ_0 , exceeds the critical shear stress, τ_c . Re-suspension tests performed by Yanful and Catalan (2002) and Peacey and Yanful (2003) using particles from different tailings ponds with varying particle size distributions, showed that coefficients of $M = 1/6$, $n = 4/3$ and $\tau_c = 0.058 \text{ N/m}^2$ are suitable for estimates of sludge re-suspension in tailings ponds. These values are adopted in this study.

BOUNDARY CONDITIONS

Pond Inflow

Maximum flows to Pond D from Pond A, Pond C and Ditch 10 were calculated based on the 100-year storm event for Timmins using a continuous event hydrology model. A combined Pond D inflow of $620,000 \text{ m}^3/\text{d}$ is anticipated for this circumstance. A reduced flow of $270,000 \text{ m}^3/\text{d}$, representative of the high flows normally encountered in operations during the spring freshet, was selected for model validation purposes. The incoming water was distributed between the 17 culverts on the north dam and low points on the northern and eastern dams, where overtopping occurs during peak flow events, by solving hydraulic equations. This complex distribution for water entering Pond D was programmed into the CFD model using Fluent's User Defined Function (UDF) and applied as a model input at inlet boundaries.

A suspended solids concentration of $1,500 \text{ mg/L}$ was used for the Pond D influent.

This was determined based on historical monitoring data and a correlation developed from testing results in 2007. The selected value represents a conservative, worst-case assumption. The particle size distribution (PSD) for incoming solids was based on Kidd Metsite TMA sludge data contained in a Canadian Mine Environment Neutral Drainage (MEND) report (1997). As shown in Figure 2, the sludge particles ranged in size from 0.5 μm to 25 μm . Five particle sizes (2 μm , 4 μm , 7 μm , 10 μm and 15 μm) were selected for modeling. Each represents the midpoint of a 20% cross-section of the PSD.

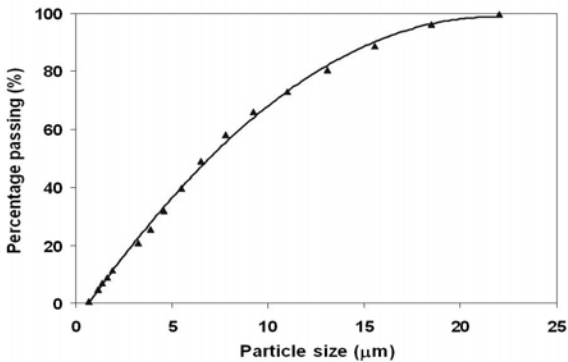


Figure 2: Particle size distribution of Kidd TMA sludge (MEND, 1997)

Water Surface

The pond water surface was modeled as a rigid surface with zero shear and zero diffusive solids flux. Change in pond inventory was not permitted; thus, outflow is equal to inflow. The South Cell water elevation was fixed in all modeling cases at a suitable level to maintain sufficient freeboard below the spillway invert. Water elevation in the North Cell was estimated by solving basic hydraulic equations accounting for inputs such as South Cell water elevation, total flow, Split Dyke elevation profiles and open/closed status of Split Dyke culverts.

Pond Bottom

The pond bottom was defined numerically as a boundary wall. The sludge re-suspension rate was as described by Equation 2 with re-suspended particles adding to the solids concentration at the specific pond location and behaving according to Equation 1. Wind and wave induced sludge re-suspension has not been incorporated in this study. The sludge PSD was adjusted as a function of travel distance from the north dam on the assumption that larger, faster settling particles will be disproportionately deposited closer to the inlet. Pond bathymetry for the CFD model was based on surveys performed prior to dredging campaigns, representing the case with minimum pond residence time. For this work, the North Cell uses the 2007 spring pre-dredge bathymetric data and the 2006 fall survey information is used for the South Cell. The average water depths above the settled sludge layer in the North Cell and South Cell are 0.2 m and 0.5 m, respectively.

RESULTS AND DISCUSSION

Model Validation

Model validation was performed for a combined Pond D inlet flow rate of 270,000 m^3/d . The distribution of flow entering Pond D via the north dam culverts and overtopping on the north and east dams is 2.14 m^3/s , 0.97 m^3/s and 0.02 m^3/s , respectively.

Figure 3 presents the comparison between CFD model predictions and actual measurements for TSS at the Split Dyke location and at the outlet of Pond D. Good agreement was observed between the predicted and measured results. The percentage error between the model and actual

data at the Split Dyke and outlet locations is less than 5%.

Figure 3 also provides an explanation for the seemingly illogical increase in TSS at the pond outlet relative to the intermediate Split Dyke location. The TSS concentration contours show western sections of the Split Dyke where flow overtopping occurs, resulting in a more direct route between the pond inlet and outlet than that which passes through the gap in the Split Dyke. The outcome is a shorter residence time for flow entering Pond D from the western edge of the north dam and, as consequence, higher TSS at the Pond D outlet than at the Split Dyke.

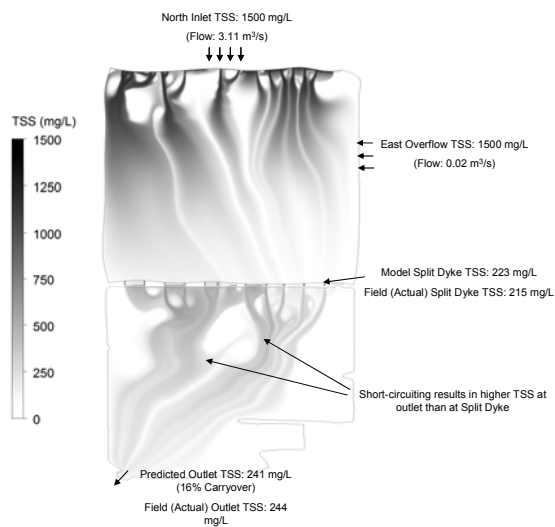


Figure 3: Suspended solids profiles in Pond D at a flow rate of 270,000 m³/d

The results also suggest that the two smallest particle size fractions (2 μm and 4 μm) account for 98.7% of the TSS present at the pond outlet. Particles of greater than 7 microns are effectively deposited in the pond as intended.

Effect of Inlet Flow Rate

After successful validation of the model, several sensitivity simulations were

performed to evaluate the impact of different operating conditions and modifications to the pond design on solids settling performance. An important consideration is the impact of total inlet flow on the outlet TSS concentration, as the inlet flow rate is a variable operating parameter throughout the year. The modeling showed that there is a linear relation between the inlet flow and outlet TSS as given in Figure 4. This performance curve is useful for estimating outlet concentrations based on the particular flow rate through the pond at any given period.

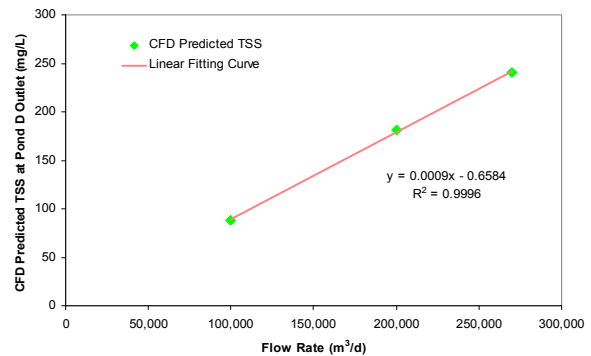


Figure 4: Effect of total inlet flow rate on outlet TSS concentration.

Effects of Coagulation Treatment on Pond Settling Efficiency

The modeling results indicate that small particles (i.e. particle size < 4 μm) in the pond inflow have a dominant influence on the effluent TSS concentration. For better solid/liquid separation, coagulant chemicals can be added to increase particle sizes and thereby improve settling performance.

The effect of coagulant addition on Pond D performance was evaluated for the same flow conditions as imposed in the validation case. The PSD of a coagulated sludge from a similar facility employing lime treatment was used for CFD modeling (MEND, 1997). Figure 5 compares the particle size

distribution of the Kidd TMA sludge with the coagulated sludge.

Figure 6 shows that the TSS concentration in the effluent is lowered to 47 mg/L with the addition of coagulant chemicals, a reduction of 81% compared to the non-coagulated condition as shown in Figure 3. This emphasizes the usefulness of coagulation treatment for high Pond D flow conditions. CFD model output may be coupled with PSD information from bench-scale coagulation trials to define the optimal flow value at which to initiate coagulant use and appropriate coagulant dosage in order to minimize costs for chemicals and Pond E dredging. Such an operational strategy will result in better defined pond management procedures and reduced environmental risk.

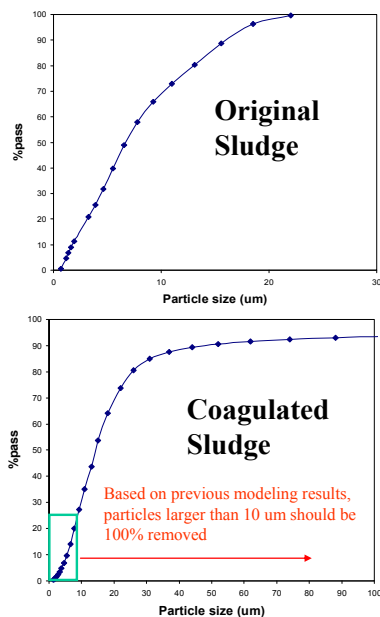


Figure 5. Comparison of particle size distribution between Kidd TMA sludge and coagulated sludge

Effects of Baffles on Pond Hydraulics and Settling Efficiency

Adding baffles to Pond D was considered as

an option to improve pond settling performance. The intent is to channel the flow and reduce flow short-circuiting, thereby increasing pond residence time. Installation of two baffles was proposed in each cell, with the baffles dividing each cell into thirds in the north-south direction and the length of each baffle being equal to half of cell width. The baffles were assumed to be perfect barriers with no potential for overtopping.

In this study, the CFD model was used to predict pond hydraulics and settling efficiency with and without the baffles.

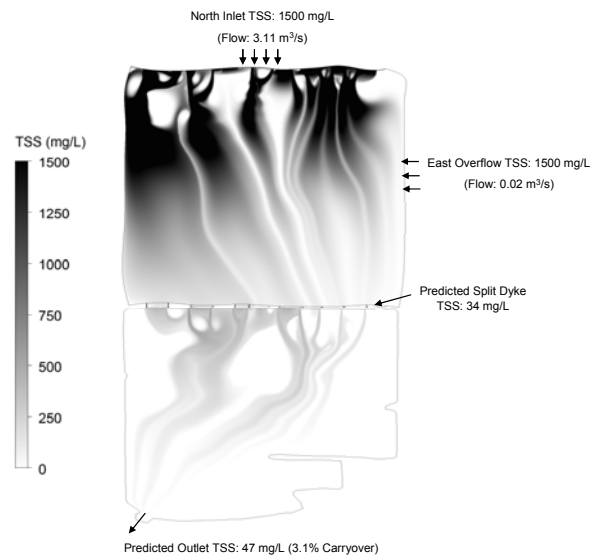


Figure 6. Suspended solids profile with coagulant addition

Simulations were performed at the maximum design flow of 620,000 m³/d. Figure 7 shows the velocity fields for both cases. The results indicate that, contrary to the intent of reducing short-circuiting in the pond, the addition of baffles in the proposed configuration actually compounds the short-circuiting issue. Bigger dead zones are also produced in the pond, particularly on the downstream edges of the baffles, resulting in less effective utilization of the pond volume.

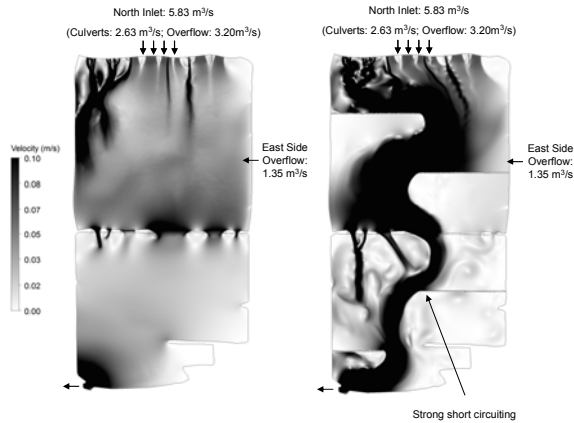


Figure 7. Velocity field comparison for cases without (left) and with baffles (right).

Residence time distributions (RTD) were calculated for tracer particles injected at different locations in the pond. Figure 8 shows a comparison of the RTD between the un-baffled and baffled cases. The tracer released from the north dam moves through the pond much more rapidly when baffles are present resulting in lower residence times. The mean residence time was calculated to be 5.24 hrs with baffles and 7.28 hrs without baffles.

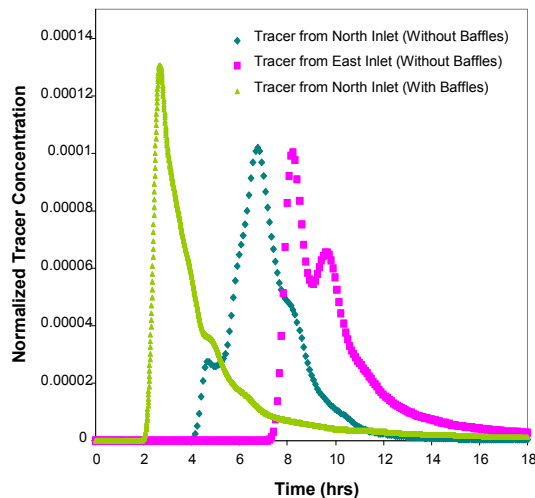


Figure 8. Comparison of residence time distribution (RTD) for the un-baffled and baffled cases.

CONCLUSIONS

A comprehensive three dimensional CFD model has been developed to predict settling pond performance for the treatment of acid rock drainage. A model validation exercise demonstrates good agreement between the predicted and measured outlet TSS concentration data (<5% difference).

The simulation results indicate that adding coagulants can significantly lower the TSS concentration at the pond outlet. CFD output can be used with results from coagulant trials to define a pond management strategy to limit operating costs for chemicals and dredging while minimizing environmental risk. Application of the CFD model to evaluate engineering modifications to the pond has also been demonstrated. This study showed that inappropriate design and placement of baffles has the potential to compound flow short-circuiting issues, resulting in poorer settling performance.

In summary, the model has been demonstrated to be a powerful and flexible tool for predicting pond settling performance. In particular, it can be used for: managing settling pond operation, developing strategies to deal with adverse process and environmental conditions, and providing low cost evaluations of engineered pond improvement options.

ACKNOWLEDGEMENTS

The authors would like to acknowledge the contributions of Mr. Dave Scott at Xstrata Copper Kidd Metallurgical Site for his continuous support to this study. We would also like to express our thanks to Ms. Lori Smith of Xstrata for her assistance with data collection and field measurements, and Mr. Mark Orton of Hatch for his technical

support with pond flow calculations. Finally, we express our gratitude to Xstrata for agreeing to publish the results of this study.

REFERENCES

- Adu-Wusu, C., E.K. Yanful and H. Mian. 2001. Field evidence of resuspension in a mine tailings pond. *Canadian Geotechnical Journal*. 38: 796–808.
- Ansys Fluent 2007. *Fluent 6.3 User's Guide*
- Kleine, D. and B.D. Reddy. 2005. Finite element analysis of flows in secondary settling tanks. *International Journal for Numerical Methods in Engineering*. 64(7): 849 – 876.
- Lakehal, D., P. Krebs, J. Krijgsman and W. Rodi. 1999. Computing Shear Flow and Sludge Blanket In Secondary Clarifiers. *Journal of Hydraulic Engineering*. 125(3): 253-262.
- Launder, B. and D. Spalding. 1974. The numerical computation of turbulent flows. *Computer Methods in Applied Mechanics and Engineering*. 3, 269-289.
- Marsalek, P.M., J. Marsalek, W.E. Watt and B.C. Anderson. 2000. Winter flow dynamics of an on-stream stormwater management pond. *Water Quality Research Journal of Canada*. 35(3):505-523.
- MEND Report. 1997. *Characterization and Stability of Acid Mine Drainage Treatment Sludges*. Mine Environment Neutral Drainage (MEND).
- Mian, M.H. and E.K. Yanful. 2003. Tailings erosion and resuspension in two mine tailings ponds due to wind waves. *Advances in Environmental Research*. 7: 745–767.
- Mohamed, A.M.O., R.N. Yong, F. Caporuscio and R. Li. 1996. Flooding of a mine tailings site: suspension of solids — impact and prevention. *International Journal of Surface Mining, Reclamation and Environment*. 10(3): 117–126.
- Partheniades, E. 1986. A fundamental framework for cohesive sediment dynamics. In *Estuarine cohesive sediment dynamics*. Edited by A.J. Mehta. Springer, Berlin, Germany. pp. 219–250.
- Peacey, V. and E.K. Yanful. 2003. Metal mine tailings and sludge co-deposition in a tailings pond. *Water, Air, and Soil Pollution*. 145: 307–339.
- Versteeg, H.K. and W. Malalasekera. 2002. *An Introduction to Computational Fluid Dynamics: The Finite Volume Method*. Addison-Wesley.
- Yanful, E.K. and L.J.J. Catalan. 2002. Predicted and field measured resuspension of flooded mine tailings. *Journal of Environmental Engineering*. ASCE, 128(4): 341–251.
- Ziegler, C.K. and W. Lick. 1998. The transport of fine-grained sediments in shallow waters. *Journal of Environmental Geology*. 11(1): 123-132.

APPLICATION OF QUANTITATIVE MICRO-MINERALOGY TO TAILINGS AND MINING WASTE

Karin Olson Hoal and Jane G. Stammer

Colorado School of Mines, Golden, Colorado USA,

Kathleen S. Smith and Katherine Walton-Day

U.S. Geological Survey, Denver, Colorado USA,

Carol C. Russell

U.S. Environmental Protection Agency, Denver, Colorado USA

ABSTRACT: The potential of acid and metal release into the environment from mining waste and tailings is a function of the mineralogy, mineral associations, and textural relationships within the rock-waste material. Hence, mineralogical information is vital to interpretation of predictive tests conducted by the mining industry. The quantitative micro-mineralogy technique discussed in this paper is able to rapidly quantify mineralogical information over large sample sets and is being increasingly used by the mining and energy industries. Quantitative micro-mineralogy datasets are now well integrated into geometallurgical applications, but are not yet well integrated into mining geoenvironmental applications. With this technique it is possible to quantify thousands of data points and characterize key mineral attributes such as mineral distribution and composition, elemental composition, mineral assemblages and textural associations, mineral liberation/encasement relationships, and porosity of materials. Some mining geoenvironmental applications are provided in this paper through examples from mine waste, tailings, and soil.

INTRODUCTION

One of the key components in materials characterization for the mining industry is the ability to be able to predict how minerals will break down in the environment on the basis of mineralogical and textural information. Mineralogy and texture currently form the foundation for the geometallurgical characterization of mining and metallurgical materials at many projects; these parameters should also form the basis for evaluating the geochemical information derived during

environmental studies. Current prediction testing using geochemical tests, such as acid-base accounting and the 20-week humidity cell test, bracket potential releases of acid and elements but commonly fail to adequately characterize the relative reactivity of acid-producing and acid-neutralizing minerals. In contrast to geochemical tests, micro-mineralogical methods are capable of quantifying and characterizing parameters such as mineral modal abundances, phase associations, grain-size distribution and texture, and

liberation/encasement characteristics. In cases where mining waste or tailings piles contain sulfide minerals, for example, the degree to which the sulfides are encased in silicate minerals can provide an estimate of the time it would take for the constituent elements to be liberated. Leach tests may not adequately reproduce the natural behavior of minerals under variable conditions such as temperature fluctuations, snowpack, wet/dry cycles, and episodic runoff rates. Incorporating mineralogical information into predictive testing will help meet the goal of predicting the breakdown of sulfide minerals and the release of elements of concern into the environment.

QUANTITATIVE MICRO-MINERALOGY

Scanning electron microscopy (SEM)-based quantitative mineralogy has been in development for over 20 years for the metals mining industry. Its application to environmental materials is relatively new. The method we employ utilizes an SEM platform with backscatter electron (BSE) acquisition and multiple energy dispersive x-ray spectrometer (EDS) detectors for rapid acquisition of backscatter and x-ray data that are coupled with a powerful specialized software package. The x-ray and BSE data are collected at intervals across the sample at a user-defined stepping distance (typically 2 to 30 micrometers). Two systems are currently in use: the QEMSCAN and the MLA, both of which are produced by FEI Company.

The analyses are correlated with a library of mineral definitions that is developed for each project such that each point is mapped as a mineral composition. Proper identification of the mineral phases present in the sample is necessary for accurate quantification. The

product of the analysis is a false-colored image accompanied by quantifiable data sets so that parameters, such as mineralogy, texture, modal abundances, mineral associations, grain size and shape, and alteration products, can be quantified and assessed statistically.

A range of sample types can be analyzed including particles on carbon tape or mounted in 30 mm resin blocks, and solid materials such as thin sections, offcuts, rock chips, or core up to 10×10 cm in size.

CHARACTERIZATION OF ENVIRONMENTAL MATERIALS

Mineral characterization of naturally occurring materials is conducted in many industries, but most commonly in the mining industry where understanding of sulfide mineral behavior is critical for extractive metallurgy and mineral processing. The same data that are gathered by exploration geologists, mine geologists, metallurgists and operating engineers may also apply to the environmental arena (Figure 1).

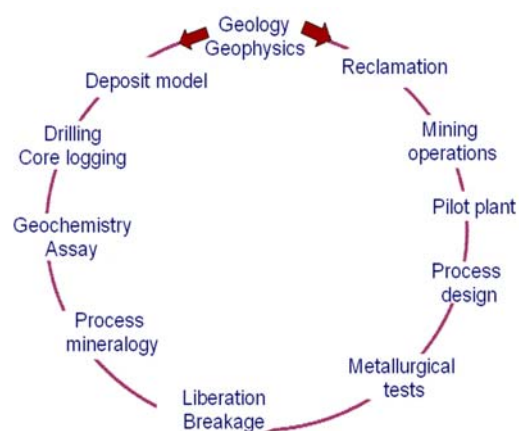


Figure 1. The flow of mineralogical information throughout a project includes reclamation and environmental considerations.

The metallurgical and mineral-processing applications of quantitative micro-mineralogy have been well documented (Gottlieb et al., 2000; Hoal et al., 2009), and the economic benefits of enhanced characterization of materials has been utilized by many companies (e.g., Kendrick et al., 2003).

Environmentally relevant solid materials include waste rock, tailings, spent ore, and the solid products of milling, flotation and mining. These are geological materials that can be described in terms of mineralogy and texture. Thus, similar parameters used for metallurgical and mineral processing also apply to mining waste. These parameters include:

- Mineral and elemental composition
- Elements of concern
- Mineral encasement
- Liberation
- Grain size
- Texture
- Grade
- Sulfide content and distribution
- Carbonate content and distribution

In addition, the relative volumes of material that needs to be characterized increase from metallurgical and mineral-processing products to mine operation and environmental materials. For example, mining waste generated by a copper or gold mine can be 300 times the volume of the valuable material extracted (U.S. Bureau of Mines, 1994).

The role of quantitative micro-mineralogy in allowing companies to both document ore-gangue composition and to predict the potential environmental impact from weathering of minerals provides new opportunities for cost savings and risk reduction. This is true both for increasing the efficiency of operations as well as for posting bonds for cleanup, particularly

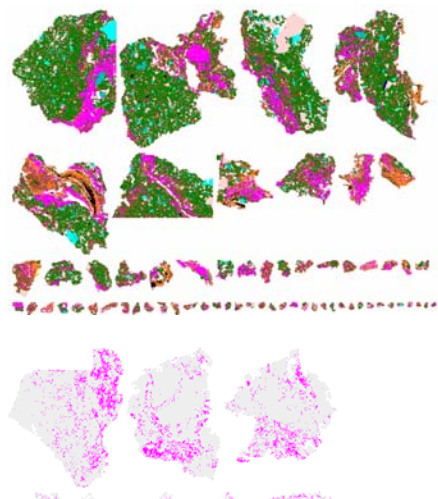
where the worst-case scenario may be assumed in the absence of such documentation. Current characterization of mine-waste material is dominated by established geochemical prediction methods. However, element behavior is controlled by mineralogy and mineral texture. Below we demonstrate how micro-mineralogical information in these materials can be characterized and quantified.

As an example of an environmental application, Figure 2 illustrates soil particles analyzed for a wastewater precipitate project (J. McKinley, CSM PhD, pers. comm.). The upper images show mineral distributions in soil particles that are arranged by size, and the distribution of one phase, Fe-Ca phosphate, which provides additional textural information. The mineral list utilized is also shown.

In the environmental application of quantitative micro-mineralogy, it also is important to understand the origin of the materials studied and their potential relationship to the geologic source materials.

This is necessary in order to correlate host rocks, mining waste, soil erosional products, tailings, and potential downstream dispersal. Figure 3 illustrates a Colorado location in which igneous and metamorphic bedrock samples were taken several kilometers apart.

Soil samples also were taken at some distance from the two localities. It can be seen from the soil samples that they retain the mineralogical characteristics of the bedrock materials, even while the geochemical characteristics of the materials might not be as distinguishing (Botha et al., 2008).



- Illite/Muscovite
- low-S Al-Fe-P-Ca-Mg-Silicate
- Quartz
- high-S Al-Fe-P-Ca-Mg-Silicate
- Plagioclase
- Fe-Ca-Phosphate
- K-Feldspar
- Chlorite
- Ti-Al-S-Silicate
- Biotite
- Fe-sulphide
- Pyroxene
- Amphibole
- Apatite
- Others

Figure 2. Illustration of quantitative micro-mineralogy applied to soil particles from a wastewater precipitate project. The particles are sorted by size and the occurrence of Fe-Ca-phosphate is illustrated, as well as a mineral list (J. McKinley, CSM PhD research, pers. comm.).

TAILINGS AND MINE-WASTE APPLICATION

Figure 4. illustrates tailings material in which the silicate (gangue) minerals are gray-scale in color in order to highlight the distribution of sulfide and sulfate minerals in the material. This image demonstrates the importance of texture in understanding mineral and element behavior. In this case, sulfide and sulfate minerals occur interstitially to silicates and

are not encased, thus indicating their availability to the environment. The lower parts of Figure 4 show mineral associations and grain size and shape of the sulfides in this tailings project. The size and shape of sulfide grains are digitally extracted images of grains from a thin section of the tailings material, preserving in-situ textures. Thus, the textural controls (size, shape, angularity, mineral association) can be quantified as potentially important controls on element release and availability from these tailings materials.

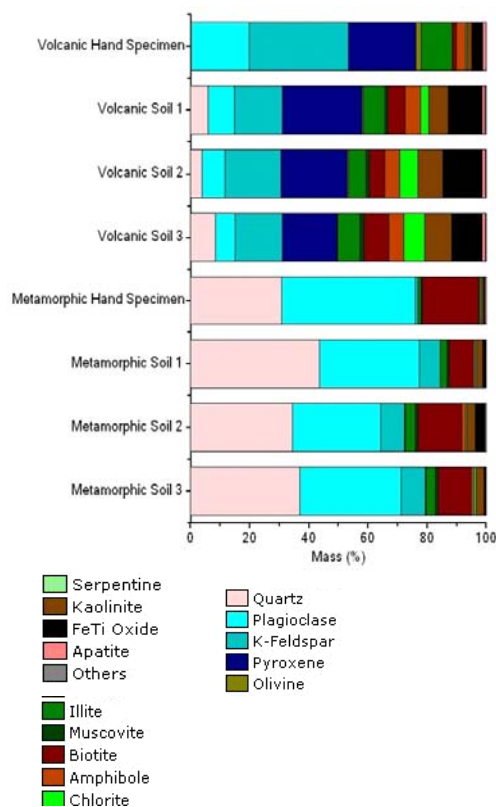


Figure 3. An example of soil samples that retain the mineralogical characteristics of upgradient bedrock materials (Botha et al., 2008).

Figures 5 through 8 illustrate the mineralogy of fluvial tailings material collected downstream of Leadville, Colorado along the Arkansas River (USGS and J. Stammer,

research). This sample was collected from a core taken in the terrace deposits of the river.

In this sample, there is an abundance of Zn in the form of sphalerite (ZnS), Pb in the form of galena (PbS), and As associated with a variety of minerals. Sulfur is strongly associated with iron oxyhydroxides that infill and coat a majority of the grains. Figure 5 shows Pb and As associated with the sulfur-rich iron oxyhydroxide phase. Figure 6 illustrates the adherence of sphalerite and galena to the surface of a potassium feldspar grain. Sphalerite and galena occur both as discrete, liberated particles and as particles adhering to silicate phases. Figure 7 shows sphalerite and goethite adhering to the surface of a biotite grain. The main silicates are quartz, plagioclase, potassium feldspar, biotite, and muscovite. Minor silicate phases include zircon, epidote, hornblende, pyroxene, aluminosilicates, and tourmaline. The major clay component is kaolinite. Accessory phases include gypsum, ilmenite, and pyrite. Figure 8 shows cementation of a variety of grains by the sulfur-rich iron oxyhydroxide phase.

FUTURE CONSIDERATIONS

Incorporating micro-mineralogical information into predictive testing will help meet the goal of predicting the breakdown of sulfide minerals and the release of elements of concern into the environment. Costs can better be anticipated, and uncertainty and potential risks reduced with the inclusion of mineralogical characteristics in predictive testing and in environmental impact assessments at an early stage in project development.

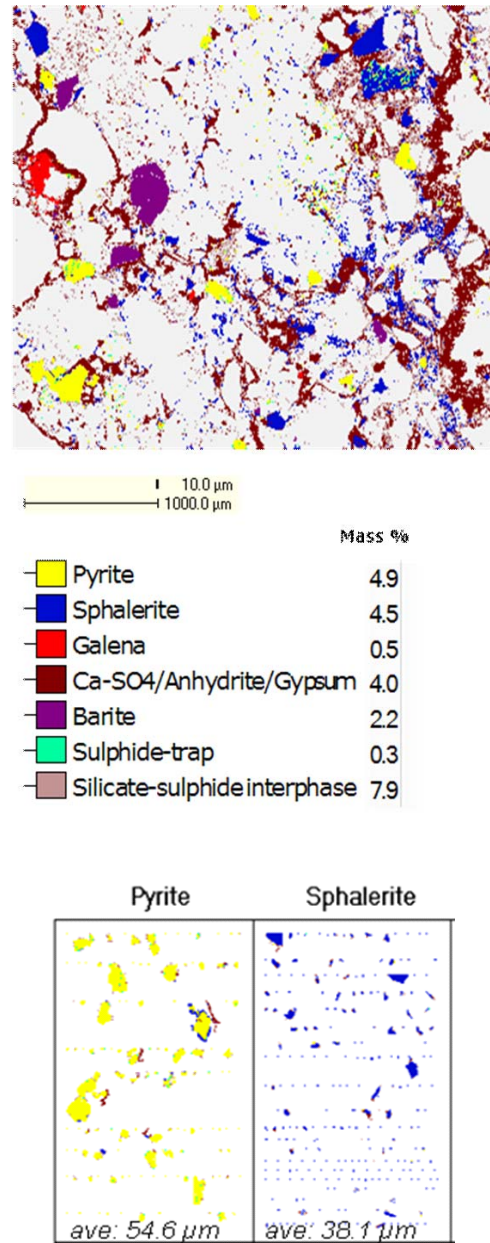


Figure 4. Tailings material showing texture and the interstitial nature of sulfide/sulfate mineral distribution, mineral associations, and size and shape of particles.

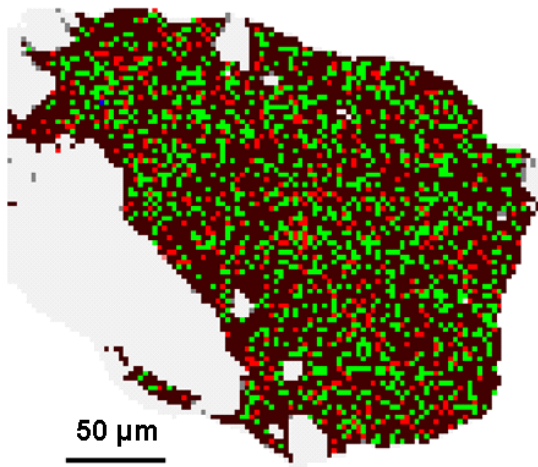


Figure 5. False-color image showing sulfur-rich iron oxyhydroxide (maroon) with associated Pb (green) and As (red).

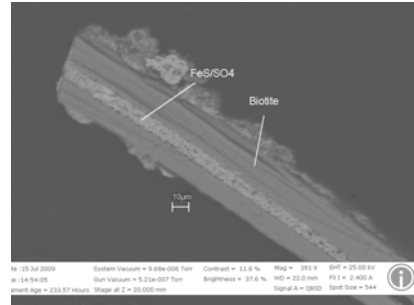


Figure 7. Biotite grain (green) with sulfur-rich iron oxyhydroxide (gray) infilling a cleavage fracture and also surrounding the mica particle. Sphalerite (blue) and goethite (orange) adhere to the biotite surface.

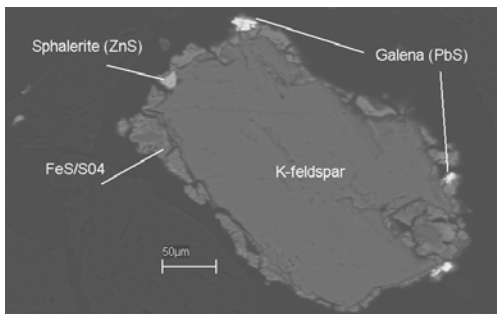


Figure 6. Potassium-feldspar grain (aqua) with sulfur-rich iron oxyhydroxide (gray) surrounding the particle. Galena (red) and sphalerite (blue) adhere to the grain surface.

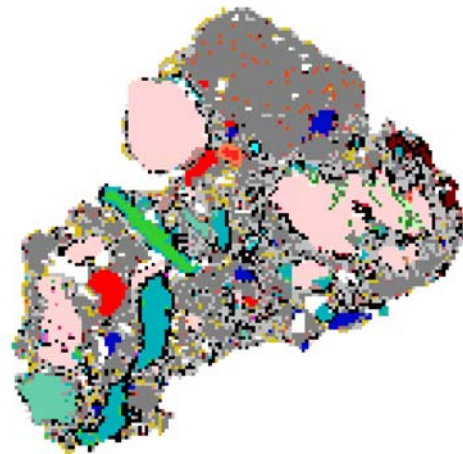


Figure 8. Sulfur-rich iron oxyhydroxide (gray) acting as a cement and surrounding other silicate and metal phases (sphalerite (blue), galena (red), quartz (pink), biotite (green), potassium feldspar (aqua), and plagioclase (light blue)). Black and white areas are voids.

An ongoing goal of the application of quantitative micro-mineralogy to tailings and mine-waste studies is to be able to develop a mineralogical guide to better predict the environmental behavior of in-situ and exposed mining waste. The guide should be developed at the very beginning of a mining project, and be populated with increasing numbers of data and information throughout the project and into closure. Much of the required mineralogy and textural data are already being collected during the early stages of mining for geometallurgical applications. Each part of the mining operation will utilize different aspects of the data for different purposes. Developing a mineralogical guide for prediction of potential environmental concerns will require well-chosen samples that represent the true variability of the environmental materials.

In the future, pressure and constraints from regional economies, financial institutions, and environmental regulations will require better predictions of potential mining environmental effects. As the availability of improved technologies increase, mineralogy should become more important for constructing predictive models, a process which begins with the exploration geologist and is carried through by a chain of specialists who can utilize the mineralogical and textural information throughout development of the mining project. Quantitative micro-mineralogy is a promising environmental assessment tool for mining environmental applications.

ACKNOWLEDGEMENTS

Smith and Walton-Day acknowledge the U.S. Geological Survey Toxic Substances Hydrology Program for funding their portion of this research. The quantitative mineralogical work for this study was

conducted at the Advanced Mineralogy Research Center, Colorado School of Mines.

REFERENCES

Botha, J., Botha, P., Skinner, C., and Hoal, K., 2008, Biological and environmental applications of quantitative mineral analysis, [abst] Automated Mineralogy, MEI, August.

Gottlieb, P., Wilkie, G., Sutherland, D., Ho-Tun, E., Suthers, S., Perer, K., Jenkins, B., Spencer, S., Butcher, A., Rayner, J., 2000. Using quantitative electron microscopy for process mineralogy applications. *Journal of The Minerals, Metals & Materials Society (JOM)* April, p. 24–25.

Hoal, K.O., Stammer, J.G., Appleby, S.K., Botha, J., Ross, J.K., and Botha, P.W., 2009, Research in quantitative mineralogy: Examples from diverse applications, *Mineral Engineering*, Volume 22, Issue 4, p. 402-408.

Kendrick, M., Baum, W., Thompson, P., Wilkie, G., Gottlieb, P., 2003. The use of QemSCAN automated mineral analyzer at the Candelaria concentrator, In: Gomez, C.O., Barahona, C.A., (Eds.), COPPER-2003-COBRE 2003 III-Mineral Processing, Santiago.

U.S. Bureau of Mines, Mineral Commodity Summaries 1994 and Minerals Yearbook, Volume I: Metals and Minerals, 1992.)

FULCRUM: AN INNOVATION IN HYDROLOGIC DATA MANAGEMENT

C.M.S. Butt

Project Scientist, Knight Piésold Ltd., Vancouver, Canada

R. Martel

Environmental Superintendent, Mount Polley Mining Corporation, Canada

ABSTRACT: Numerous data management challenges are confronted when processing, analyzing and interpreting large amounts of data from stream gauging stations within any project site. In an effort to overcome unavoidable constraints imposed by conventional data management and processing techniques, Knight Piésold is developing specialized software specifically designed for undertaking highly repeatable data storage and processing tasks. FULCRUM is a web-based integrative data management system designed to expedite storage, processing and preliminary analysis of hydrometric data. This, in turn, has facilitated much-needed standardization in many aspects of hydrology field data collection and analysis. Many believe that the development of a specialized system such a FULCRUM is prohibitively expensive, would offer no substantial benefits, and potentially jeopardize day-to-day business operations. As a consequence, advances in hydrologic data analyses have been continually constrained by the persistent use of inadequate and inappropriate data management software. FULCRUM is not burdened by these limitations.

INTRODUCTION

Knight Piésold Ltd. (Knight Piésold) is actively involved in many aspects of tailings, waste, and water management for mine development projects around the world. Hydrological data obtained from site specific gauging stations, and associated analysis and interpretation, are often the keystone upon which many of these projects are made viable and subsequently developed. Many important aspects of these projects, such as engineering design of structures, and environmental

assessments and permitting, are directly dependent upon the quantity and accuracy of site specific hydrology data. In fact, water availability is often among the first non-resource related considerations that are given in determining project viability. As importantly, any change in hydrological condition while the mine is in operation is important to document. As such, it is fundamentally important that these data collection activities be undertaken in a logical, systematic, and standardized manner,

and that every effort is made to reduce any cause of error or miscalculation. Left unnoticed or unrestrained, these can jeopardize the success of a project.

As is typical of many organizations around the world, data management in such fields as hydrology is viewed as a necessary burden, is often a significant challenge, is rarely optimized to avoid recurring problems between projects, and surprisingly, is too often viewed with an attitude of indifference. Effective data management is not recognized or acknowledged for the singular importance it has on project success and viability.

This paper will discuss conventional data and file management systems and demonstrate the limitations of such systems in hydrometric data collection and analysis. The discussion will focus on the development of FULCRUM, a specialized web-based data management software solution designed and implemented by Knight Piésold. The FULCRUM system is routinely used Knight Piesold to manage valuable data collected for mining projects and is provided free of charge to clients. A study of the Hazeltine Creek gauging station (operated by Mount Polley Mining Corporation), and the applicability of FULCRUM for undertaking such detailed hydrologic analysis, is provided.

CONVENTIONAL DATA MANAGEMENT

In order to be cognizant of the need for developing and implementing a data management system designed to effectively handle high volumes of data and to control and standardize scientific data collection, a brief discussion of conventional tools is necessary.

Project File Management

Conventional file and data management is often undertaken through the use of network file and folder paths on shared company servers. These are legacy systems that have been implemented over time, and have become the preferred file management systems for many organizations and agencies around the world. Such systems, include Windows Explorer (Explorer) and Microsoft Excel (Excel). These generic systems come at very little, if any, recognized cost to an organization as they are typically already installed for routine file management, reporting and communication. It is an underlying expectation that with minimal training, technical staff can readily use these systems to process and analyze any and all technical data.

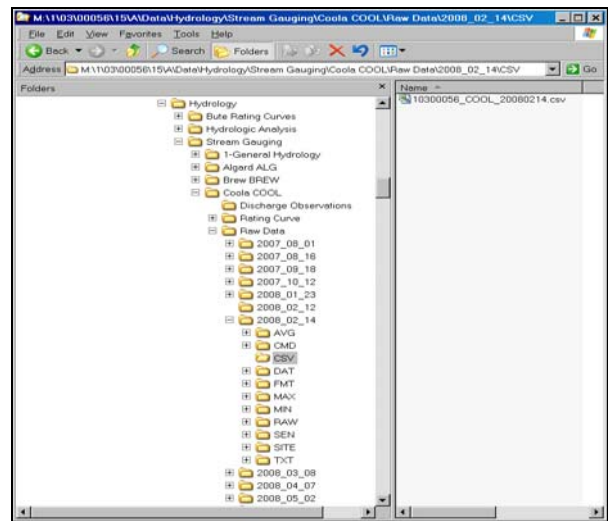


Figure 1. Conventional file and folder structures common to many Projects.

Standard practices in file and folder structuring are often initiated at a functional or project level within these network drives, in order to control the storage and management of collected data, as shown on Figure 1. Like many organizations, Knight Piésold has extensive experience in this methodology, having developed and

maintained numerous project folder structures for routine data collection purposes. It is widely accepted and expected that a certain degree of flexibility in conventional file management structures is fundamental to the successful completion of project data collection.

Calculation Files

As with many data types, hydrometric data often require complex preprocessing in order to calculate and extract vital information to be used for further analyses. Many of these calculations are either highly repetitious or utilize specific formulae readily created and replicated by spreadsheet software such as MS Excel (Excel). As such, Excel has become a standard tool for data management and processing in engineering. Complicated spreadsheets are common in almost all studies, and are conventionally viewed as an ideal data analysis tool as users can write and access the specific formula used to process the raw data and generate the resultant information. The calculation of data within spreadsheets is not viewed as mysterious because every component of the calculation is available for analyses. Reviewers can assess the suitability of specific calculations for a required output and either make corrections or recommend alterations. The use of spreadsheets is thus viewed as a form of transparency, both internally and externally.

In hydrometric studies, complex spreadsheet files are used to calculate discharge, store and correct time-series data, store site visit information, conduct time-series flow calculations, develop rating curves, calculate flow, as well as undertake bench mark and cross-section survey calculations. Due to the volume of data and the amount of processing required, these calculations are rarely able to be managed within a single spreadsheet file and, as such, multiple files, distributed over

multiple folder systems, are typically developed and maintained.

LIMITATIONS IN CONVENTIONAL DATA MANAGEMENT

The conventional techniques for data management and processing described above are cumbersome and frequently result in costly data confusion and a significant lack of quality control. The reason why conventional data management tools are ineffective is due to inherent weaknesses that cannot be avoided without significant programming skill and user-familiarity with the program. As this is

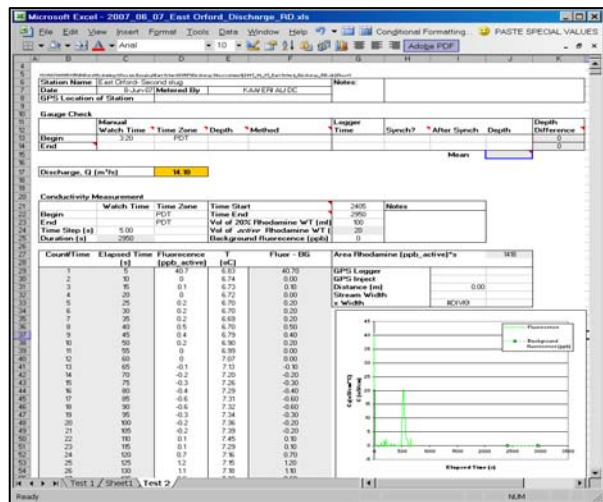


Figure 2. Conventional data processing spreadsheet file, common to many Projects

unlikely in most circumstances, the use and acceptance of the limitations of such data management and processing software is considered a necessary and unavoidable fact of life by many users. In fact, so ingrained is the use of Excel and Explorer in data management that these significant limitations go largely unrecognized as limitations.

File Management

Using conventional file management tools, users can modify and delete files, or even entire folder structures, with minimal tracking and recompense. This can effectively disable a project or seriously compromise aspects of project design. The convoluted and ad-hoc arrangement of data files and folders which develop over time, and which began at Project inception as an idealized structure, make auditing and quality assurance highly impractical. Multiple users, with multiple ways of approaching the same problem, combined with a lack of procedural control, can result in the storage of data in multiple forms. Raw and processed data is frequently replicated without control, and this expends great amounts of time, energy and money. Typical folder and file accessibility is shown on Figure 3.

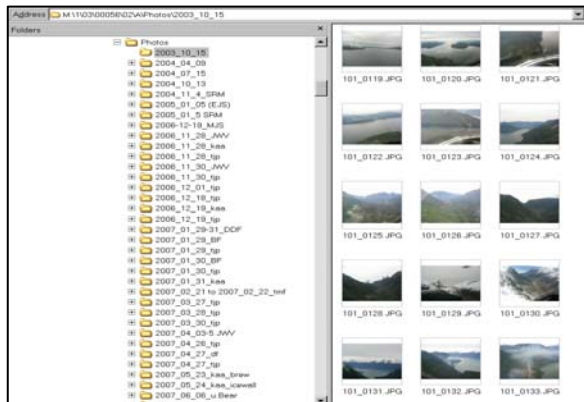


Figure 3. Conventional file management systems.

Calculation files

Excel spreadsheets, inherently prone to alteration and corruption, can have a dramatic impact on resultant calculations. Errors in calculations are not often identified unless the calculated information is grossly erroneous. Vital links to other workbooks can be broken if the linked workbook is renamed, relocated, or altered in some other way. There are very

few ways in which specialists can be expected to review individual calculations to any given detail. As a direct result, reviewers often have little choice but to trust in the integrity and skill of users when undertaking reviews.

Hundreds, and sometimes up to tens of thousands of unstable, unprotected formula are contained within each spreadsheet file. Furthermore, each spreadsheet file is often dedicated solely to the processing of a single aspect of routine data entry (e.g. a single discharge measurement), and this entry may be for an instant in time for one station in a single project. The potentials for errors are exacerbated when processing files are used to calculate data for multiple periods over multiple gauging stations and multiple projects.

The dependency on this antiquated, conventional tool of data management has resulted in users being unable to fully understand and comprehend hydrology data interpretation. The science of hydrology at the primary level of data collection can become stale, and by virtue of the limitation imposed upon itself, obdurate and ill-informed, and in some cases actually regress to a state of ignorance of some of the most basic concepts. Vital information and principles have become lost because high *volume* data collection using conventional tools cannot sustain the requirements and demands of high *quality* data collection.

Put simply, the transparency of Excel is an unjustified assertion based on limited tangible evidence and often made in spite of obvious weaknesses and inadequacies. Dependency upon the use of Excel, in an industry which must base scientific interpretation on standardized, repeatable and controlled scientific data, should be acknowledged and, where possible avoided.

The effect on Project Management

As projects develop, data is gathered at an ever-increasing rate. Datasets quickly become maelstroms of folder systems, files, text documents, photos, field notes and reports. Progressively overwhelmed with an unorganized, non-integrated, non-relational file management system, many project managers can easily recall rapidly losing touch with the status of data collection in their project. As such, they are unable to maintain control of some of the most basic aspects of the project. Similarly, specialists find it increasingly difficult to effectively guide staff in the fulfillment of project and site objectives, and to bring the most out of their data, as they are unable to readily access and interpret the quality of existing work. As a consequence, field personnel undertaking data collection lose control of the purpose and scope of site investigations, and become confused by misinformation and lack of direction and leadership. As such, it becomes increasingly difficult for all parties to maintain control of data collection and interpretation, and consequently, the accuracy in projects may suffer.

INNOVATIVE RESEARCH, AND THE NEED TO STANDARDIZE

When undertaking any aspect of pioneering research, the development and application of standards and guidelines are fundamental in achieving high quality, scientifically valid and repeatable results. The use of conventional file management methodology is not conducive to this development and growth. As projects develop and the need for the employment of innovative techniques is recognized, they are applied without quality control or a structured review and assessment process. Innovation thus becomes a burden to data analysis and review, which often must

occur much later in the process. As such, innovative data collection techniques are never fully analyzed or understood because data management is inefficient and disorderly, and innovation is unable to be successfully carried over into other projects.

Using the current conventional methods, quality control is attempted without controllers recognizing that very little valid quality assurance is undertaken throughout the project data collection life-cycle.

Through the persistent use of conventional file and data management, important and sometimes fundamental aspects of scientific studies such as hydrology, have become misguided and/or lost. Researchers and quality controllers expend a great deal of effort analyzing collected data in order to better understand hydrologic systems, giving little if any thought to the defensibility of the raw data that contributes to their analysis and sometimes basing scientific conclusions on inadequately interpreted data.

When confronted with the rapid accumulation of enormous amounts of hydrometric data, Knight Piésold began to consider non-conventional methods of data storage, processing and analysis. In early 2008, Knight Piésold engineers, scientists and developers met to consider the development of a system that would create a generic, relational database structure applicable to any project, anywhere in the world. This proposed system would not only act as an effective and efficient data storage warehouse, but would be designed to standardize every aspect of hydrometric data collection. This system is known as FULCRUM, a name symbolic of the leveraging advantage provided by this unique and powerful data management and analysis tool.

FULCRUM DATA MANAGEMENT SYSTEM

Hydrology

Knight Piésold currently manages over two hundred (200) gauging stations within FULCRUM, with a virtually limitless capacity for expansion. There are over one thousand nine hundred (1,900) individual discharge measurements stored and calculated in an orderly manner using specialized calculators, nine thousand (9,000) site photographs, one thousand six hundred (1,600) scanned field sheets, and nearly twelve million (12,000,000) data points. This latter is equivalent to over 330 years of continuous data. All hydrometric data, for every Knight Piésold project, is now stored and processed within FULCRUM.

Hydrology data is comprised of both discrete sample and time-series data, as demonstrated on Figure 4. As a result of this, conventional data and file management is unsuitable for detailed hydrological analysis because hydrometric data is not by its very nature composed of unrelated data. Hydrology is the recreation of historical fact through the accurate interpretation of specific time-series and discrete sample data types. These specific data types do not, on their own, provide the basis upon which to recreate this history. Instead, they must be used in conjunction with one another, and only in this way can the data be considered fully defensible. The hydrological history of any project can often be filled with complex and interrelated issues and complications, and all data are required to be collected in a logical, systematic and consistent manner. This Process is made simple through effective data management. Conversely, the process can be impossible if data management is ineffective. Furthermore, analysis and interpretation of hydrometric data is often not a linear process.

It is an iterative process requiring all relevant data to be available. Only when all valid observed and documented data fit the unraveling history can the researcher be fully confident in their analyses. Using conventional methods this can become an onerous, expensive and, at times, a virtually impossible task.



Figure 4. Integration of all data using simple FULCRUM interface

Purpose & Structure

From the commencement of development, the purpose of FULCRUM was to provide a user-friendly interface in which to undertake effective data management using consistent and repeatable forms and controls. Database developers, working in conjunction with Engineers and Scientists, are continually optimizing the system to enhance its functionality and applicability in all aspects of project data management.

The purpose of this project was not to invent a new method of undertaking hydrology studies through developing FULCRUM. Rather, the purpose was to control the science of hydrology in order to ensure that data collection was to an acceptable standard by providing simple and intuitive tools. What has emerged from the implementation of FULCRUM has allowed Knight Piésold to provide a much more robust understanding of

the science of hydrology and of hydrology data. Data analysis is undertaken to a much greater level of detail than was previously possible.

The storage of data in FULCRUM, and the FULCRUM interface, are structured according to the relational manner in which data are collected. This interface is built

around a simple, yet robust, logic and as such FULCRUM integrates previously disparate information (disparate using conventional techniques), and renders the iterative task of data processing faster, more convenient and highly repeatable. Data storage within FULCRUM is, as a result, orderly and clean, as shown on Figure 5.

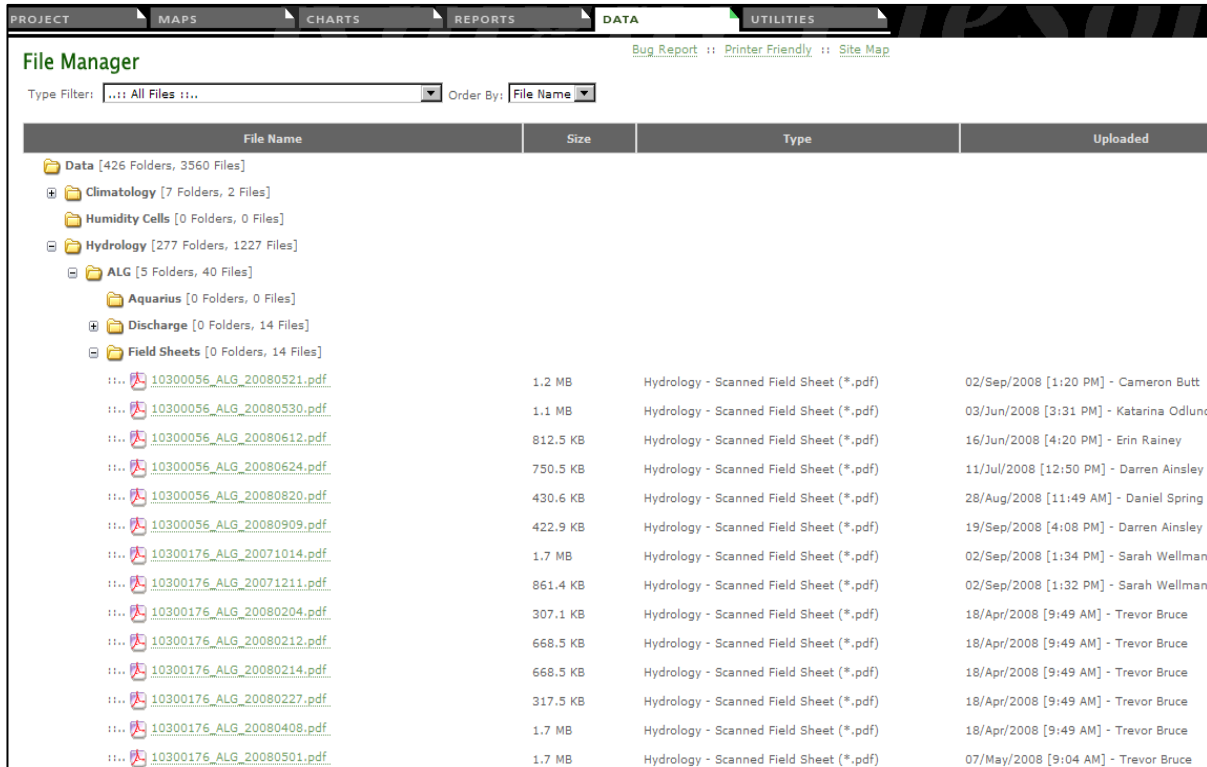


Figure 5. FULCRUM Data storage

FULCRUM and Aquarius

There are numerous hydrometric time-series data software packages available for data analysis and correction which are gradually making a positive impact on the industry. These excellent programs, including Aquarius (Aquatic Infomatics) and Hydstra (Kisters), are very useful for undertaking detailed data analysis. At this stage of development, these programs require that the user has already

undertaken a certain degree of effective data management prior to use. This is not often the case, though, and this is where FULCRUM fulfills a niche role, providing controlled storage and management of all collected data. Through creating seamless integration between FULCRUM and Aquarius, Knight Piésold and Aquatic Infomatics have been able to develop a data management and correction solution package which is unprecedented in its usefulness and

applicability as a complete data management package.

Control & Standardization

Knight Piésold developed clear and concise field operation guidelines which provide very simple data collection protocols. Through these protocols, database auditing tools allow users of FULCRUM to conduct integrity checks on the entire database, in order to provide clients with ongoing quality assurance and quality control. Unlike conventional data management, where alterations and additions to folders are common and file tracking is unable to be effectively maintained, every file within FULCRUM is accounted for as a key component of the integrated data collection program. The purpose of this auditing process is to leave no data unassociated with a station and/or station visit.

Files within FULCRUM cannot be uploaded and left unassociated or unprocessed without being flagged for further investigation by intermediate and/or specialist reviewers. This effectively avoids the undesirable situation of having hundreds or perhaps thousands of files created, modified, stored, copied or deleted within complex folders on a network drive. File allocation is through association of data with site visits, as shown on Figure 6. Simple protocols eliminate subjectivity and the inevitable variability that results from different users attempting to undertake the same task. The ability to quickly comprehend the nature and requirements of data collection allows for sharing of knowledge and experience and has resulted in a greater depth of understanding of hydrological data collection, processing, analysis and interpretation.

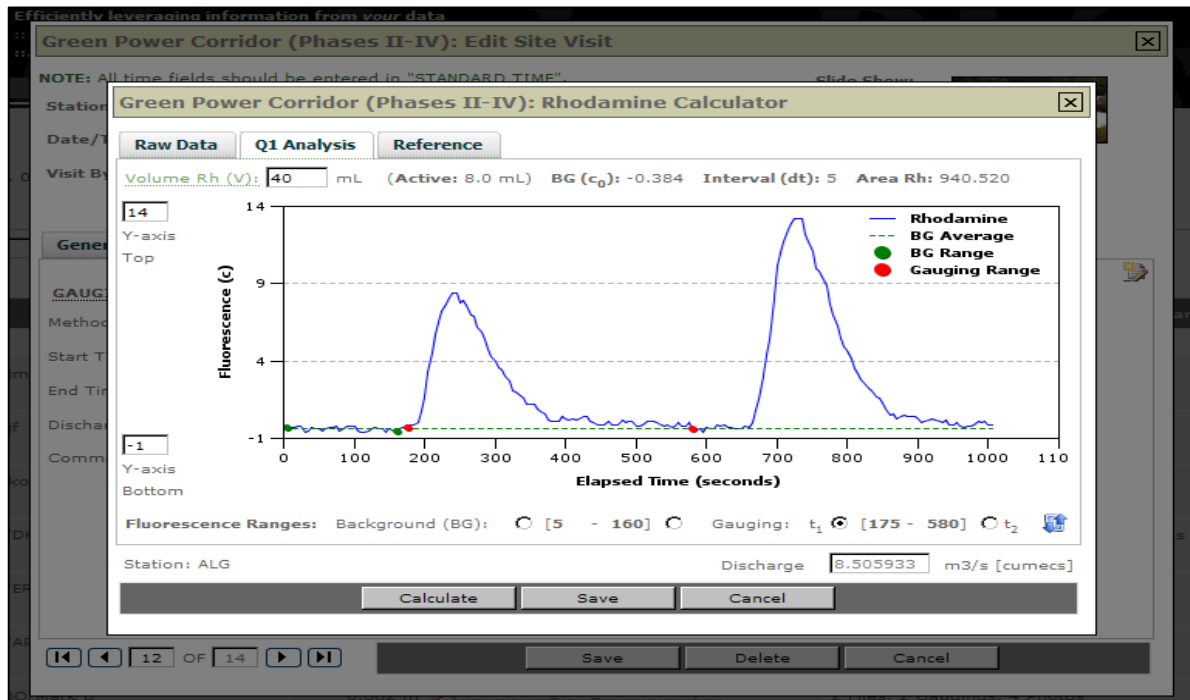


Figure 6. FULCRUM Site Visit master file manager

Repetitious Data Processing

All data collection programs involve a large amount of routine data collection and processing. It is important for any scientific data collection program to contain minimal subjectivity. Hydrometric data should be collected, stored and processed using controls and protocols that are as objective and logical as possible, and disassociate subjectivity from the process. This is a significant impact that FULCRUM has had on the operations of the hydrology group of Knight Piésold. As a result, clear data collection guidelines have been implemented to allow users to apply repeatable data collection logic to all aspects of field operations, creating standards where once standards did not, or were too

constrained to exist. More cumbersome data management tools such as Excel and Explorer are unable to satisfy this important scientific requirement. Through FULCRUM, users are able to better undertake effective field data collection operations because data collection is undertaken in a manner which FULCRUM demands. This control may initially appear constricting to the freedom too often incorrectly associated with hydrometric data collection. However, to be truly scientifically valid and defensible, this freedom, to a greater extent than is often acknowledged, should not exist and is required to yield wherever standardization offers a more robust and defensible methodology.

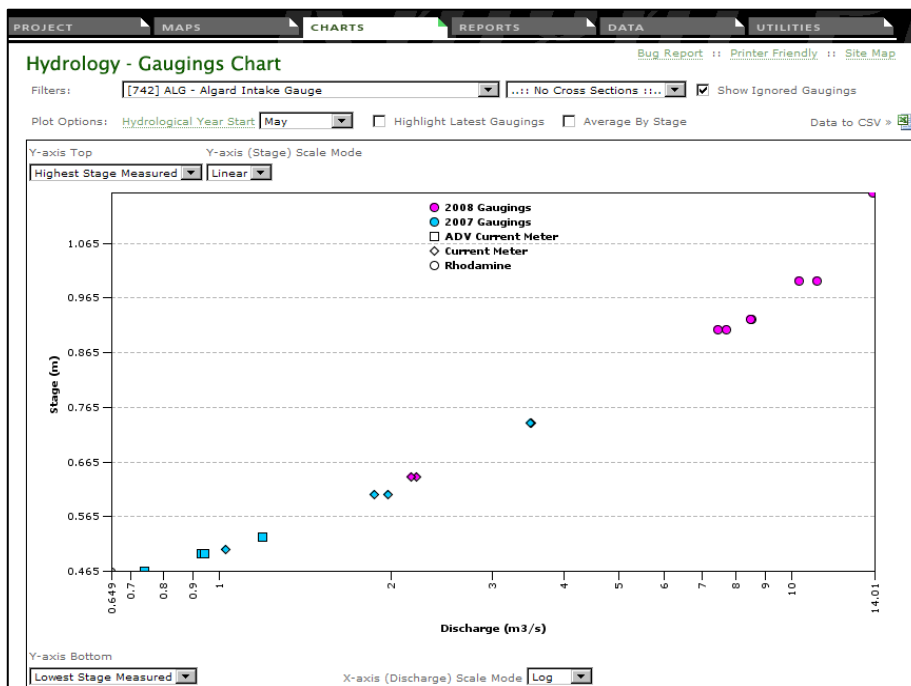


Figure 7. FULCRUM Discharge calculator controls and simplifies repetitive procedures

FULCRUM undertakes repetitive data processing tasks that can be prone to human error, including uploading and importing stage data from field dataloggers, and the calculation of discharge measurements.

Discharge calculation was previously undertaken using cumbersome, low-quality and high-maintenance Excel spreadsheets. Discharge calculators within FULCRUM are consistent, simple, stable, efficient and visually friendly, as shown on Figure 7. The

FULCRUM interface allows for ready access to scanned field sheets and photographs and rapid quality assessments can be made on all data. Users can compare calculated discharge values to all historical measured values at a station, without the tedium and instability associated with transposing fragile data and updating tentative data links spread over multiple spreadsheets.

Efficiency and Effectiveness

A comparative assessment was made of conventional storage and processing methods against the efficiency and accuracy of FULCRUM. FULCRUM consistently

demonstrated a 2500% increase in data processing efficiency over conventional methods, in addition to significant improvements in accuracy, consistency and confidence. The calculation of a rhodamine dye discharge measurement for example, using a conventional Excel file, takes approximately 30 minutes to complete. The FULCRUM Rhodamine Dye discharge calculator takes less than 1 minute to achieve a more accurate result in a quality controlled, repeatable and stable format.

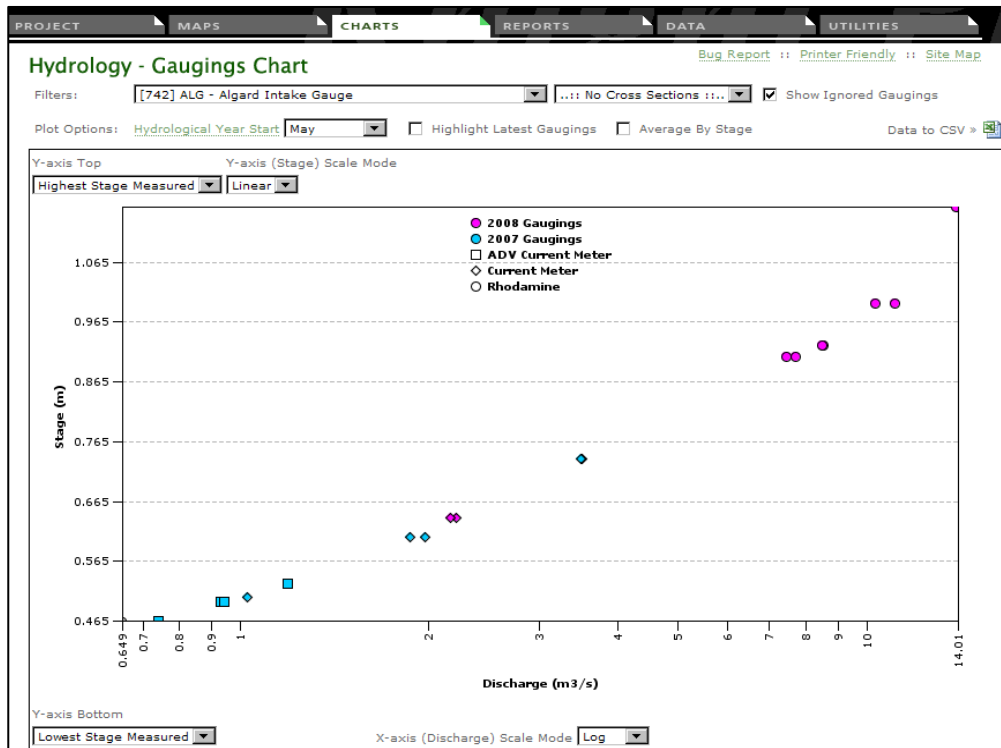


Figure 8. FULCRUM Discharge measurement Chart

The implications of this increased accuracy and efficiency in data collection and processing cannot be underestimated, with the potential for significant time and cost savings for clients, and improvements in the quality of project deliverables. Users found

that understanding the FULCRUM interface was straightforward, with the process streamlined to the bare essentials of the calculation. When challenged, users did not understand the spreadsheet calculations for the equivalent Excel file, and were daunted

by the possibility of having to fully disclose the specific Excel calculations and sequence of calculations which determine discharge. This observation further demonstrates the limitations of Excel in its capacity to provide full transparency.

Quality Assurance and Quality Control

Instrumentation used to collect hydrology data is too often thought of as inherently reliable and stable. In truth, instrumentation is frequently exposed to environments which can result in significant impacts on accuracy and quality. Management of site instrumentation and calibration records is an integral part of the FULCRUM data management system. Using simple instrumentation records, FULCRUM is able to implement controls designed to significantly reduce the opportunity for both human error and errors caused by instrument malfunctions.

Staff Training and Development Plan

Training of staff in correctly and consistently undertaking field data collection and processing can be a daunting and costly task for any organization. This is exacerbated when the protocols of data collection are not properly understood, as is often the case when an organization is dependent on conventional data management tools. As a result training is invariably limited and field staff are often ill-prepared to undertake reliable data collection, having had minimal education in practical hydrological data collection. The implementation of FULCRUM has had a significant impact on the training and education of field staff, allowing senior staff to undertake regular training and assessment, and has further provided project managers and specialists with opportunities to standardize aspects of training and development. This training has

had a resounding influence on the quality of hydrometric data collection, processing, analysis and interpretation.

The future of the FULCRUM Data Management System is multifaceted. Knight Piésold have begun to develop a complete project data management package, applicable to any data-intensive engineering-related industry, which comprises a user-friendly, consistent interface, logical data structure, and standardized data management protocols. Knight Piésold are committed to standardizing data collection programs and to providing ongoing, detailed training programs to both staff and clients. This is viewed as an integral component of maintaining quality management and the provision of superior service. Project data management modules that are planned to be completely contained, managed, shared and processed within FULCRUM include:

- Climatology
- Water Quality
- In Stream Flow Requirements (Fish Habitat Studies)
- Hydrogeology
- Fisheries
- Geochemistry
- Geotechnical Programs
- Embankment Performance Records
- Construction Management
- Air Quality Monitoring
- Green House Gas Assessments
- Document Control and Management
- GIS mapping interfaces

Project Scheduling (for Data Collection Activities).

Web-based GIS functionality, through integration of .NET applications, is allowing FULCRUM to mature into a complete project management package. Complete transparency allows users to access any aspect of a project

to determine the status of data collection. Web-based data management provides complete accessibility and transparency to users, project managers, specialists, interest groups, and clients, anywhere in the world. Data managers and reviewers can coordinate, assess and quality control data collection for any project, wherever they themselves may be. Customizable email notifications can alert users to the addition or alteration of vital information pertaining to any aspect of any project, thus further allowing project managers to become fully cognizant of the state of any project.

CASE STUDY – HAZELTINE CREEK, MOUNT POLLEY MINE

The following is one example of the functionality and usefulness of the FULCRUM system for collected and evaluating hydrology data.



Figure 10. Hazeltine Creek Gauging Station

In the Quesnel region of British Columbia, Mount Polley Mining Corporation (MPMC), 100% owner of the Mount Polley Mine, recently applied for a permit to release treated seepage pond water into Hazeltine Creek, a largely seasonal stream whose primary flows originate from Spring melt runoff from the

surrounding hills, and influenced by the attenuating affects of Polley Lake, situated several kilometers upstream of the gauging station, Hazeltine Creek.

In order to accurately quantify the potential impact of the proposed water release on flora, fauna, and water quality, it was fundamentally important that the surface water hydrology be understood in as much detail and accuracy as possible. These important data would underpin other important data interpretation for this project.

Hazeltine Creek (H7) gauging station was installed by Water Survey of Canada (WSC) in late 1994, and consists of a compound weir constructed of treated pine. A Stevens Chart recorder with a simple float and counterweight system was installed within a galvanized iron stilling well upstream of the hydraulic control, within the gauging pool. The station is shown on Figure 10. This device has been monitoring continual stage for almost fourteen (14) years, with the exception of winter periods, when instrumentation is removed. A one meter staff gauge plate was installed to obtain accurate gauge height readings, and three bench marks were installed and surveyed to this staff gauge. WSC undertook a series of discharge measurements in the initial year of operation (1995) in order to calibrate the theoretically derived rating. This was followed by an extensive period where no discharge measurements were undertaken. Mine personnel assumed that, once established, the curve would apply throughout data collection. Several gaugings were undertaken in 2001, presumably as a result of the identification of leaks that were beginning to form within the weir. Rather than demonstrate a minor deviation from the curve due to these leaks, these gaugings identified a substantial deviation. This deviation was then thought to have been the result of weir settling and/or

the leakage through the base of the weir and/or in the cracks between the lumber (The lumber comprising the weir had, since installation, been progressively deteriorating). In an effort to prevent further leakage, and perhaps even to restore the weir to its original rating, a layer of geotextile fabric was placed over the weir notch. No further gauging work was undertaken to quantify the effect of this geotextile on the rating curve. Field technicians assumed that the rating would have returned to its original state. Additionally, processed stage data demonstrated a prominent downward trend which had caused a reduction in calculated flows. Less flow was being measured each year, in contrast to regional stations, which did not demonstrate this same negative trend. Through the years, the inconsistencies observed stage and calculated discharge data became an increasing concern to MPMC. A series of discharge measurements throughout 2007 and 2008 was undertaken by Knight Piesold and MPMC to validate discharge data from Hazeltine Creek and to identify the cause of this trend.

Conventional methods of data management and processing were employed in an attempt to unravel this complicated problem. This process resulted in generation of over sixty separate excel files dedicated to the calculation of discharge measurements. Numerous additional excel files were generated to handle the processing of the entire stage record, and more still were generated to consolidate discharge and stage data for further analyses and rating development. Due to the significant period of time-series data, and the over two hundred separate site visits to the station, data was not able to be effectively processed. Inadequate data processing power resulted in generation of 14 rating curves, one applicable to each year of operation, as shown on Figure 11.

A more robust data management system was required in order for all data to be used cost-effectively and decisively in this analysis. Following a study using conventional methods, FULCRUM was utilized in coordinating all site visit information into its user-friendly and intuitive interface. Time-series data were imported into data tables and available as a single data string over 200,000 records in length. Easy to use discharge measurement calculators were used to calculate all historical gauging information using a consistent and repeatable format. Previous inconsistencies were revealed and reconciled using this consistent format, and calculation errors, common in the conventional file management methods, were resolved.

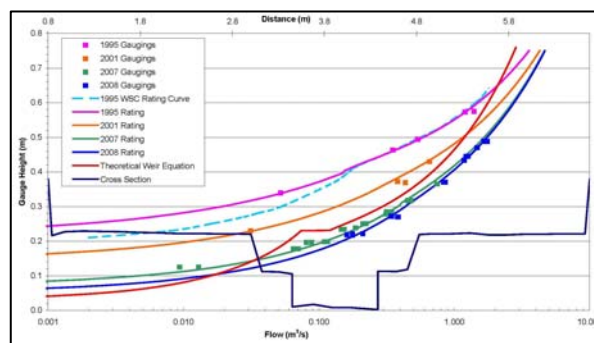


Figure 11. Hazeltine Creek Rating Development using conventional techniques.

In short order, the entire period of record was accurately recreated within FULCRUM. Knight Piesold was able to simultaneously study multiple site visit data, including the original installation data obtained from WSC. These data were directly compared these data collected in 2008. Comparison of the 1994 site installation benchmark survey and the 2008 bench mark inspection survey data, as well as site installation photographs and 2008 photographs, indicated that over twenty (20) centimeters of upward vertical movement in the staff gauge had occurred over the entire period of data collection.

Through FULCRUM, Knight Piesold and MPMC were able to readily determine that erosion and degradation on the weir, though a significant influence itself under idealized conditions, could not account for the significant shift that had occurred. The shift was determined to be the result of the staff gauge (from which all stage data was derived) was gradually being pushed out of the bed, likely as a result of frost heave. Without ongoing maintenance, this displacement had resulted in a substantial alteration in calculated flow values. Close inspection of Figure 12 reveals this vertical displacement.

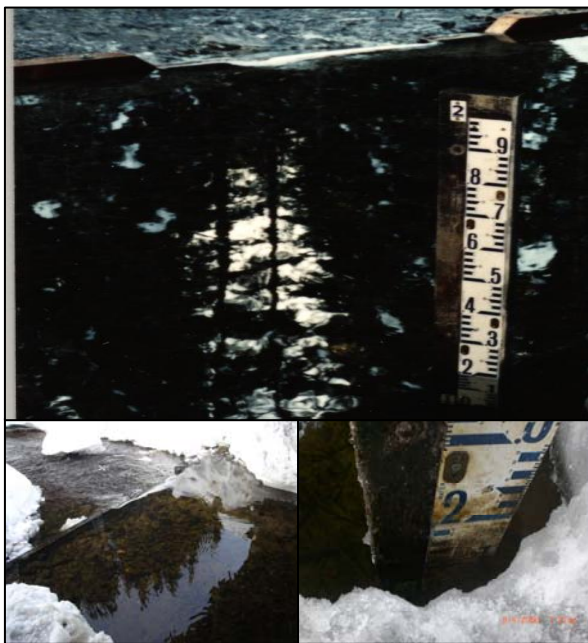


Figure 12. Top: Gauge Height and Control, 1994 (note level of water on weir). Bottom Right: Gauge Height reading in 2008. Bottom Left: Control from same 2008 site visit, 2008 (note level of water on weir)

The result of the study was to retroactively normalize all stage data, in order to produce a single applicable rating curve, as shown on Figure 13. In addition to determining a single rating curve, it was also determined that flow backup of the control was clearly evidenced to occur on an annual basis. More work is

being undertaken to determine the consistency of this backup. Knight Piesold provided MPMC with clear directions on ways of restoring data collection to a high quality standard.

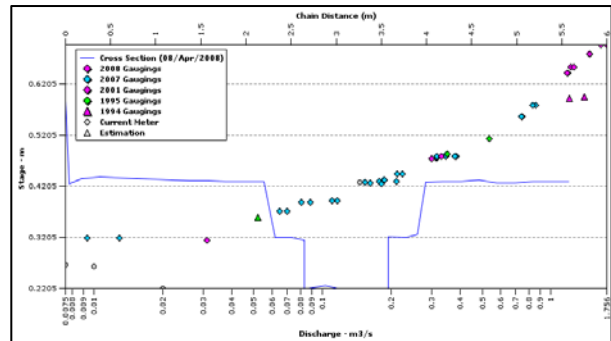


Figure 13. Hazeltine Creek Normalized Rating Curve using FULCRUM

Normalizing the discharge and stage dataset revealed an additional characteristic of the data which had previously been only assumed to occur, primarily due to the low stream gradient and the low point of zero flow of the weir.

During high flows, the stream is subject to substantial backup from downstream influences (likely vegetation). This results in the weir drowning out and causing the rating curve to bend sharply up, as shown on Figure 13. This is contrast to what would be expected from the generalized shape of this weir, where a downward trend would be considered normal. The occurrence of backup is concerning because the causes and veracity of backup is unpredictable from year to year and requires continual maintenance in order to monitor potential shifts.

All of these factors combined to reinforce the importance of reconstructing this weir. Weir reconstruction is an important component of MPMC continuing to collect high quality discharge data. An example of high flows observed during 2008 is given on figure 14.



Figure 14. Backup and drowning of weir during high flows.

FULCRUM has been useful in revealing these and many other subtle idiosyncrasies in these data which have aided in interpretation and defensibility. FULCRUM has provided MPMC and Knight Piesold with an unparalleled level of detail for Hydrometric data analysis for the current water release application.

CONCLUSIONS

It is essential to the success of any project that users are able to rapidly process and quality control collected data. The implementation or adoption of efficient and logical specialized data management systems should be an integral component of hydrometric data collection programs. The limitations and problems that are inherent in conventional data management tools should be acknowledged. The use of conventional software such as Explorer and Excel can result in significant issues of data integrity and confusion.

The development of FULCRUM requires that users examine data in a manner that is innovative and unconventional and completely dissimilar to that of conventional

data management tools. The development or adoption of such systems constitutes a significant alteration in the status-quo of any organization that undertakes data collection activities. Naturally, this presents challenges as major alterations are rarely perceived as productive or even viable, and are often met with resistance. Knight Piesold maintains a strong emphasis on quality systems and management and the development and adoption of such innovations as FULCRUM is a logical extension of this. FULCRUM has been instrumental in allowing Knight Piesold to take control of all hydrometric data associated with numerous projects around the world and as a direct result have developed operating standards where conventional file management and processing systems would not allow. Project managers, engineers, field staff, and clients have all significantly benefitted from the stability, functionality, repeatability and accessibility of FULCRUM. Project managers are more easily and quickly able to assess the status of the collected data, while engineers and specialists can more efficiently review information and direct further analyses. This allows for constructive feedback to be given to field staff, who is then better equipped to more confidently collect and record ongoing data. Clients are able to be given access to all aspects of data collection through robust security privileges, thus enhancing transparency, and enabling these parties to directly see the data that will ultimately determine the viability of their project.

FULCRUM is offered as a free utility that Knight Piesold provides to its clients. It incorporates exceptional GIS functionality and is continually upgraded and optimized to store, process, and present data from multiple disciplines within any given project.

Tailings and Mine Waste Management III

LARGE-STRAIN 1D, 2D, AND 3D CONSOLIDATION MODELING OF MINE TAILINGS

M.D. Fredlund and M. Donaldson

SoilVision Systems Ltd., Saskatoon, SK, Canada

G.G. Gitirana

Praca Universitaria, Goiania, GO, Brazil

ABSTRACT: The management of the consolidation process in mine tailings is central to the long-term behavior of tailings management areas (TMA). The capacity of such TMAs as well as the long-term environmental impacts of such facilities all originate from the consolidation process which will occur over time. The typical slurried deposition of such tailings causes large potential consolidation of the tailings and therefore large-strain theory applies to this problem. The software tools for the application of large-strain theory have been slow in coming given that the mathematical theory was defined in the 60's and 70's. This paper examines the application of a 1D, 2D, and 3D software finite element tool to the solution of large-strain consolidation as applied to TMAs. Expected differences between small-strain and large-strain tools are outlined. Differences between a 1D, 2D, and 3D analysis will be examined and the question "Is a 1D analysis sufficient?" will be answered.

INTRODUCTION

The theory of small-strain consolidation theory was first defined by Terzaghi (1923, 1936) and is recognized to be based on a number of simplifying assumptions. The difficulty of the theory was i) developing methods of solution of the equations (prior to the computer) and ii) applying the theory to real-world problems. The Terzaghi solution assumes no relevant change in permeability as the soil deforms and therefore renders the governing partial differential equation easy to solve.

Early work by the phosphate industry in the 60's and 70's extended the consolidation

formulations to deal with multiple deposition layers and large-strain consolidation. It was generally recognized that the large consolidation deformations when starting with initial void ratios as high as 15 became problematic when working with small-strain formulations. Formulations also allowed for the non-linear behavior of void ratio and therefore permeability which are necessary for the analysis of large-strain problems. A number of researchers in this time period developed 1D large-strain formulations in which the non-linear changes in permeability and void ratio are taken into account (Davis and Raymond, 1965; Schiffman, 1958; and Bardon and Berry, 1965). Additional theoretical formulations where the changes in

self-weight are accounted for may be found in the equations developed by (Mikasa, 1965; Gibson et al, 1967, 1981; and Lee and Sills, 1979).

The difficulty of these early formulations is that many were formulated in terms of void ratio in 1D and therefore not consistent with general stress / deformation formulations.

SoilVision Systems Ltd. has undertaken a research effort in the past few years in order to extend the large-strain formulations to 2D and 3D in a manner consistent with traditional stress-deformation formulations based on stress-states rather than void ratios. The developed formulations are ideal for the prediction of long-term consolidation of mine tailings. Their application to the estimation of long-term tailings behavior through use of a 2D and 3D large-strain consolidation software tool is a relatively new applications field. It is therefore the intent of this paper to i) demonstrate reasonable consistency with existing benchmarks and ii) answer basic questions related to the application of such a tool to tailings management.

BENCHMARKING/VERIFICATION

Benchmarking of software implementing new theory is a crucial yet difficult part of any new software package. Benchmarking is a fundamental part of QAQC which ensures that a computer code can correctly reproduce known solutions to problems generated using both analytical and numerical methods. The theory was added to an internal version of the SVFLUX / SVSOLID coupled software packages as developed in the context of the SVOFFICE 2009 geotechnical software office suite. Each package has been extensively benchmarked in the areas of flow and stress deformation as viewable in their respective verification manuals. Therefore the

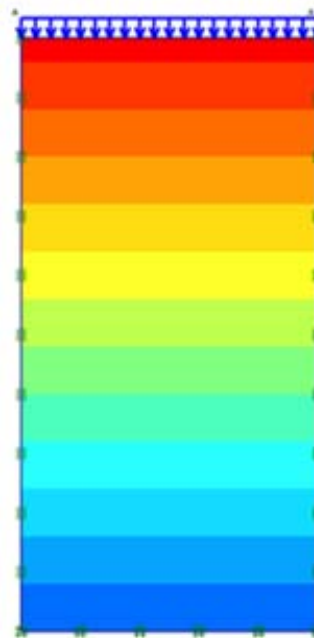
benchmarking effort focused on the new areas of implementation; specifically i) large-strain deformation and coupled consolidation analysis.

A series of benchmarks are presented in the following sections which illustrate benchmarking of the various components of the large-strain consolidation solution. The benchmarks selected consisted of the following:

- i) Large-strain uncoupled theory
- ii) Coupling of small-strain / large-strain equations
- iii) 1D Coupled Large-Strain Benchmark

The solution of the benchmarks form the basis for reasonable confidence that the coupled software is i) performing reasonably and ii) is consistent with previously documented work.

Small-strain/Large-strain Uncoupled



Of foremost and fundamental importance is determining that the uncoupled large-strain theory is being properly solved. Large-strain theory involves the solution of the stress / deformation equations using a lagrangian reference frame.

Figure 1. Example 1D geometry used for Large-strain verification.

This inherently means that the mesh nodal points move with the deformations.

In order to test the correct implementation of large-strain analysis a simple 1m high column model was created in the FLAC software, in a mixed Eulerian-Lagrangian software, and in the SVSOLID software. An example of the 1D column may be seen in. A sufficient load was applied to the column such that large-strain deformations were initiated (> 10%).

After the model was run it was found that a small-strain model produced a deformation = 0.5m. FLAC produced a deformation of 0.4m and the Mixed Eulerian-Lagrangian software produced a deformation of 0.33m. SVSOLID could be set to duplicate any of the small-strain or large-strain solutions simply by adjusting aspects of its formulation. The SVSOLID software matched the answers of the other software packages exactly.

It is also important to note that a small-strain solution to a large-strain model will tend to over-estimate the deformations. This is demonstrated in this example model in which the small-strain model estimates the highest amount of deformations (0.5m).

Coupled Benchmarking – Mandel / Cryer

An important and difficult aspect of a consolidation solution to document is the coupling mechanism. For this part of the software the Mandel-Cryer benchmark was chosen. In this benchmark a sphere with zero pore-water pressure is abruptly loaded. The load is transferred to the pore-water. The areas near the sphere boundary are allowed to drain faster than the regions closer to the center. The consolidation of the outer layers causes shrinkage of a thin cap, which transmits extra loading to the sphere core. As a result, pore-water pressures at the center of the sphere rise during a period of time higher

than the external load. This effect can only be simulated by solving the fully coupled consolidation equations. The effect can graphically be seen in Figure 2.

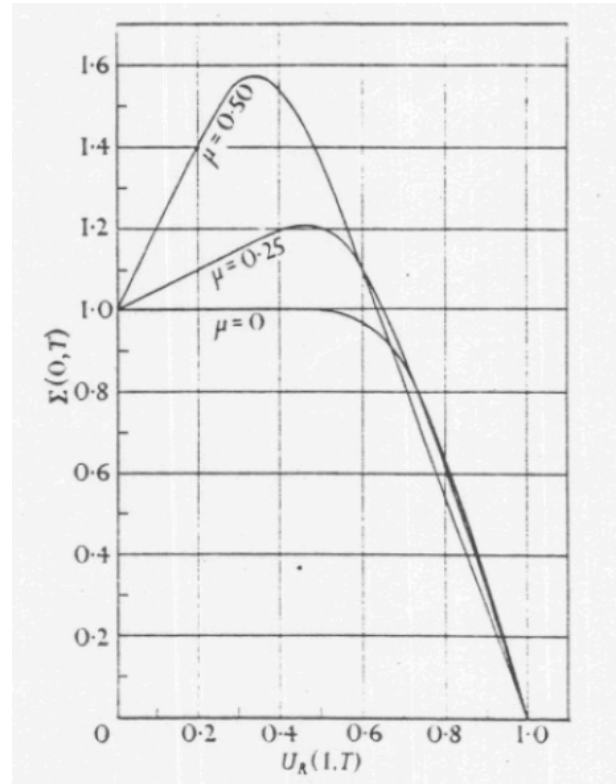


Figure 2. Normalized strain (y-axis) versus normalized time (x-axis) may be seen in Cryer's (1963) Figure 2.

It should also be noted that the amount of rise in pore-water pressures changed based on the Poisson's Ratio used for the analysis.

The coupled SVSOLID / SVFLUX numerical model was able to demonstrate reasonable comparison with the published answers as seen in Figure 3. The answers differ primarily in presentation as a different normalization technique for time was used in Cryer's original paper (a logarithmic technique). Cryer's original paper also does not present loading times where the SVFLUX/SVSOLID results present loading times. Overall the comparison is reasonable and demonstrates

that the coupling in SVSOLID/SVFLUX is implemented properly.

Gibson (1990) review the potential impact that the Mandel-Cryer would have on large-strain formulations with variable permeability. The effect was known to raise pore-water pressures to approximately 60% higher than applied loads in a small-strain problem.

The study by Gibson found that the differential decrease in permeability during consolidation is of dominant importance. Both the magnitude and the rate of dissipation of pore pressure diminish with increasing stress. This is likely due to the throttling effect of a sudden drop in the skeleton permeability close to the drainage surface.

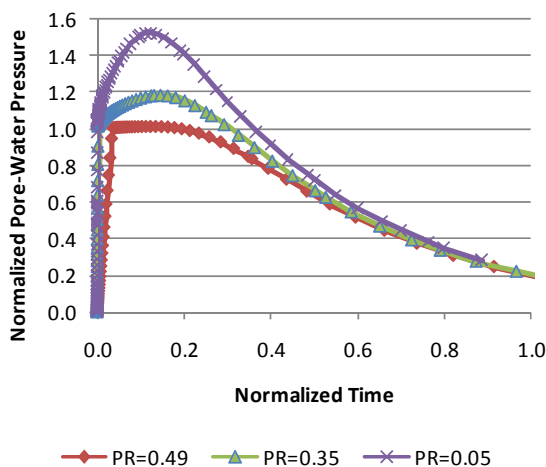


Figure 3. Demonstration of Mendel-Cryer effect with the SVSOLID / SVFLUX software.

1D Coupled Large-Strain Benchmarking

The majority of previous large-strain consolidation formulations developed by Gibson and Schiffman for the phosphates industry took the form of 1D formulations developed in terms of void ratio (rather than stress-state variables). It is therefore important to demonstrate continuity with previous formulations as the current

formulation is developed in terms of stress-state variables.

The “Scenario A” example as presented by Townsend (1990) is utilized for benchmarking purposes. In this example a 1D soil column at an initial void ratio of 14.8 is allowed to consolidate under its own self weight. The bottom boundary is a no-flow boundary and therefore flow of water can only be in the upward direction. The benchmark is extreme from the sense that the material may change from a void ratio of 15.0 to approximately 7.0 with a very small change in stress. The example is therefore highly non-linear and a challenging benchmark to solve. This benchmark was previously solved with a group of 1D academic codes which were largely based on the Gibson (1967) formulation. The geometry of the benchmark is shown in Figure 4.

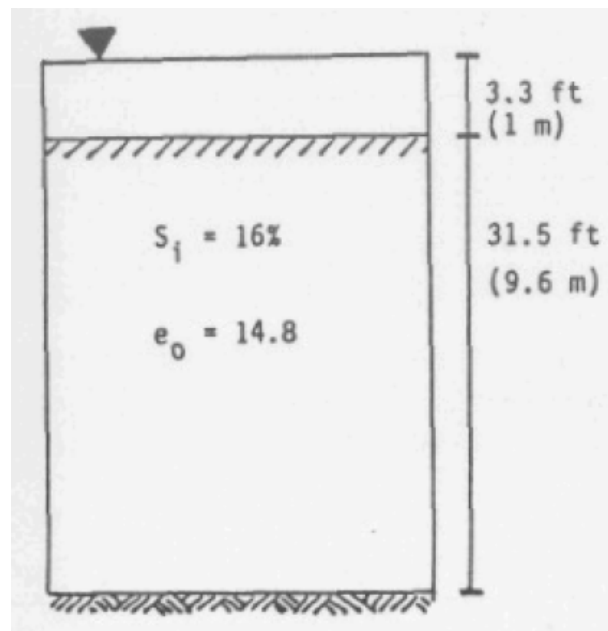


Figure 4. Townsend (1990) Scenario "A" benchmark

The results of the Townsend benchmark were compared to the SVSOLID/SVFLUX software package on three different aspects; i) height of the tailings, ii) pore-water

pressure profile at the end of a 1-year period, and iii) void ratio profile at the end of a 1 year period. The results may be seen in Figure 5, Figure 5 and Figure 7. From these results it can be seen that there is reasonable comparison to existing Gibson-based 1D formulations. Small differences exist but may be attributed to unknowns which are not presented in the Townsend paper such as mesh resolution, time-step size, or the behavior of the upper boundary condition. For example, it is not mentioned in the paper if the upper boundary head deforms down during the consolidation process or is kept constant at its original height. In the SVSOLID / SVFLUX solution it is assumed that the upper head boundary condition is kept constant ov.

WHY 2D AND 3D ANALYSIS?

Typical analysis of tailings areas for some mine sites has involved the use of a 1D large-strain numerical model. Such a model as a series of 1D profiles and the results may or may not be interpolated in some manner.

The primary difficulty with such an analysis is that it misses the fundamental processes of the influence of lateral strains on the solution outcome. It is therefore impossible to represent Mandel-Cryer type of effect using a 1D numerical model.

It is also possible for lateral drainage to occur in many TMAs. Drainage through lateral boundary conditions can only be truly represented in a 2D or 3D numerical model and directly influences the resulting profiles of excess pore-water pressures.

In summary, a 2D or a 3D analysis is warranted for the following reasons:

1. **Lateral flow:** In a 2D or a 3D model it is possible to track lateral flow. This may be of particular importance if the

hydraulic conductivity of deposited layers is different in a lateral direction as opposed to a vertical direction.

2. **Side boundary conditions:** The amount of lateral drainage and its influence on pore-water pressures and void ratios within a TMA can only be determined with a 2D or 3D model. In many large pits the true drainage around the pit is irregular and is best modeled in 3D.
3. **Mandel-Cryer effect:** The Mandel-Cryer effect is only present in a 2D or 3D analysis and can result in a decreased dissipation of pore-water pressures due to the throttling of boundaries where drainage is occurring.
4. **Variable depositions:** Tailings may be deposited in a manner which yields defined zones of coarse, medium, and fine materials. If this is the case then zones can cause areas of differential settlement which are best modeled in 2D and 3D.

In summary a 2D or a 3D analysis is warranted in most situations because of the demonstrated influence of lateral strains. A calibrated 2D or 3D model can provide a significantly greater understanding of the fundamental processes involved over the lifetime of a TMA. Once the fundamental process is determined the ability to run multiple simulations and extend TMA lifetime is present.

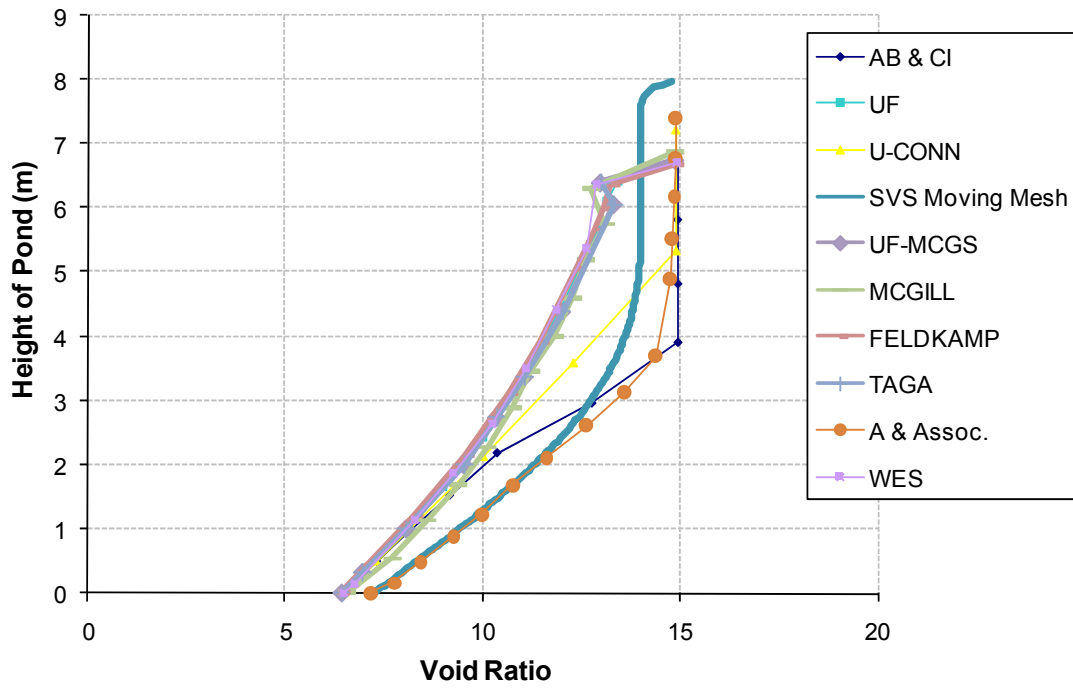


Figure 5. Comparisons to Townsend Scenario A for a void ratio profile after 1 year

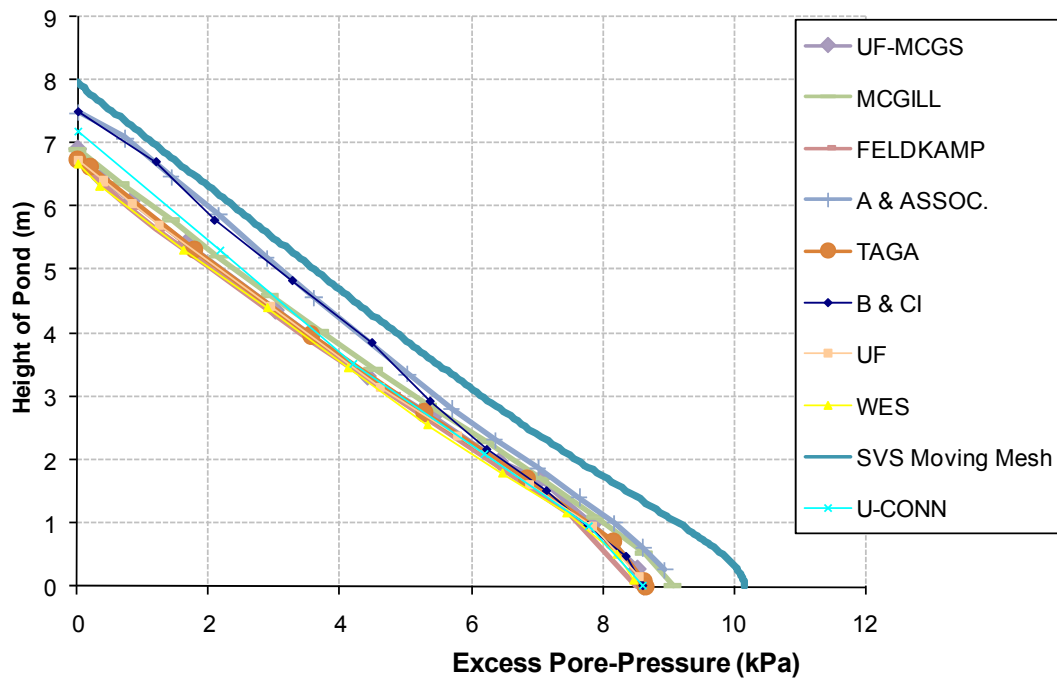


Figure 6. Comparisons to Townsend Scenario A for excess pore-water pressures after 1 year

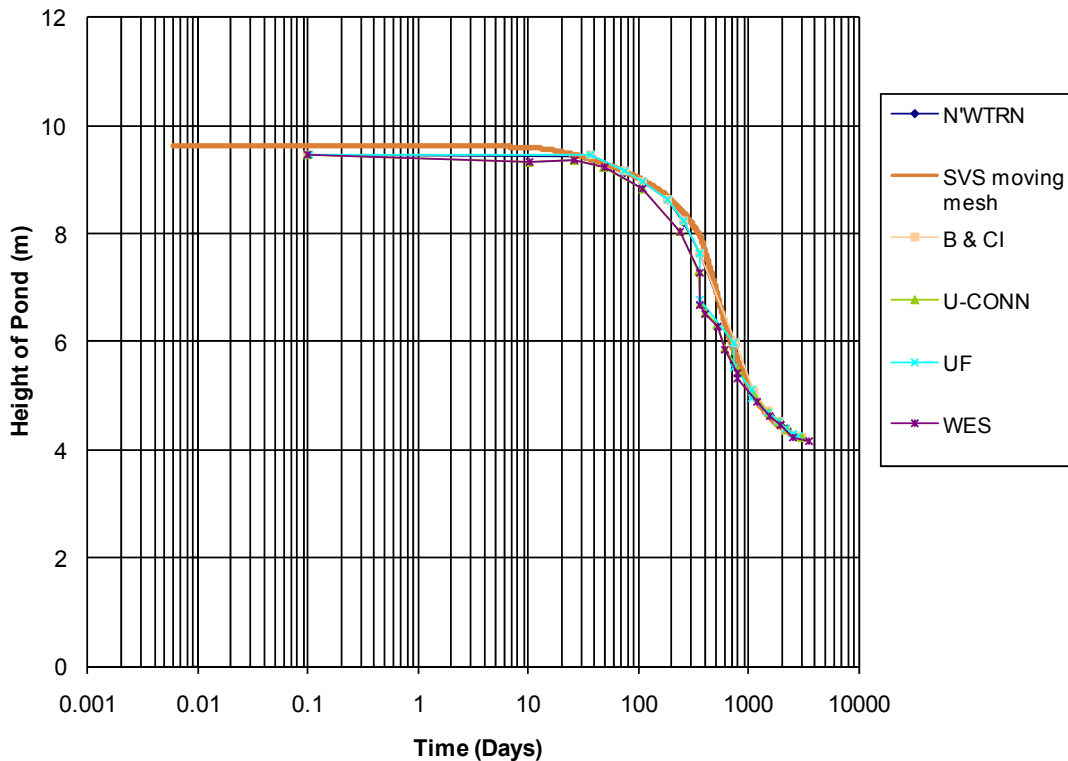


Figure 7. Height of surface of tailings versus time (Townsend, 1990)

LAYERED TAILINGS PIT ANALYSIS

The large-strain consolidation analysis is ideal for the evaluation of tailings when deposited in a pit. Such a storage facility is common for phosphate, copper, and uranium mine tailings. Tailings are typically deposited in a slurried form in somewhat of a continuous fashion. Therefore one of the issues is how to numerically model the continuous deposition of tailings. For the SVFLUX/SVSOLID large-strain implementation the deposition process can be replicated through the use of layers of materials which are phased in over a specific time period. For example, annual layers can be created and then applied to the numerical model at the start of each year. Each layer starts with specified initial properties and is allowed to consolidate due to its own self

weight through the year. Such a phase/layered approach is consistent with previous recommended approaches (Gibson, 1958).

A typical setup of a series of layers is illustrated in. In this particular model each year can be represented by an individual layer of material. The thickness of each layer is determined by the volume of slurried tailings deposited in a particular year. Boundary conditions of this numerical model can be represented by a variety of standard load / fixed / free / head / flow boundary conditions as relevant to the individual flow and stress distribution components of the analysis.

Average material properties were input for the current analysis with void ratio as a function of net normal stress and hydraulic conductivity as a function of void ratio.

The model at various times may be seen in the series of following figures. The flow out of any side of the numerical model can be tracked to determine reasonable discharges to the environment. The upper flow boundary can be represented as a head or flux boundary conditions which could be used to represent tailings deposited subaqueously or exposed to the atmosphere.

Once the model is solved the results can be viewed in terms of total deformations at any time, height of tailings with time, and pore-water pressure and void ratio profiles vs. time and depth

CONCLUSIONS/DISCUSSION

It can be seen from the results of the benchmark models that the new SVSOLID/SVFLUX software can successfully replicate published results for individual large-strain examples as well as fully coupled examples. The code duplicates previous implementations of the 1D large-strain formulation and then extends these same formulations to 2D and 3D.

The use of this formulation is ideal for the estimation of the long-term performance of mine tailings. The use of 1D theory only will compromise the analysis such that pore-water pressures would be under-estimated and tailings consolidation times would be under-estimated. A 2D or 3D analysis will allow inclusion of the Mandel-Cryer effects and allow improved representation of the underlying physical processes. Once the underlying physical processes have been understood the model can aid in improved storage capacity for TMAs.

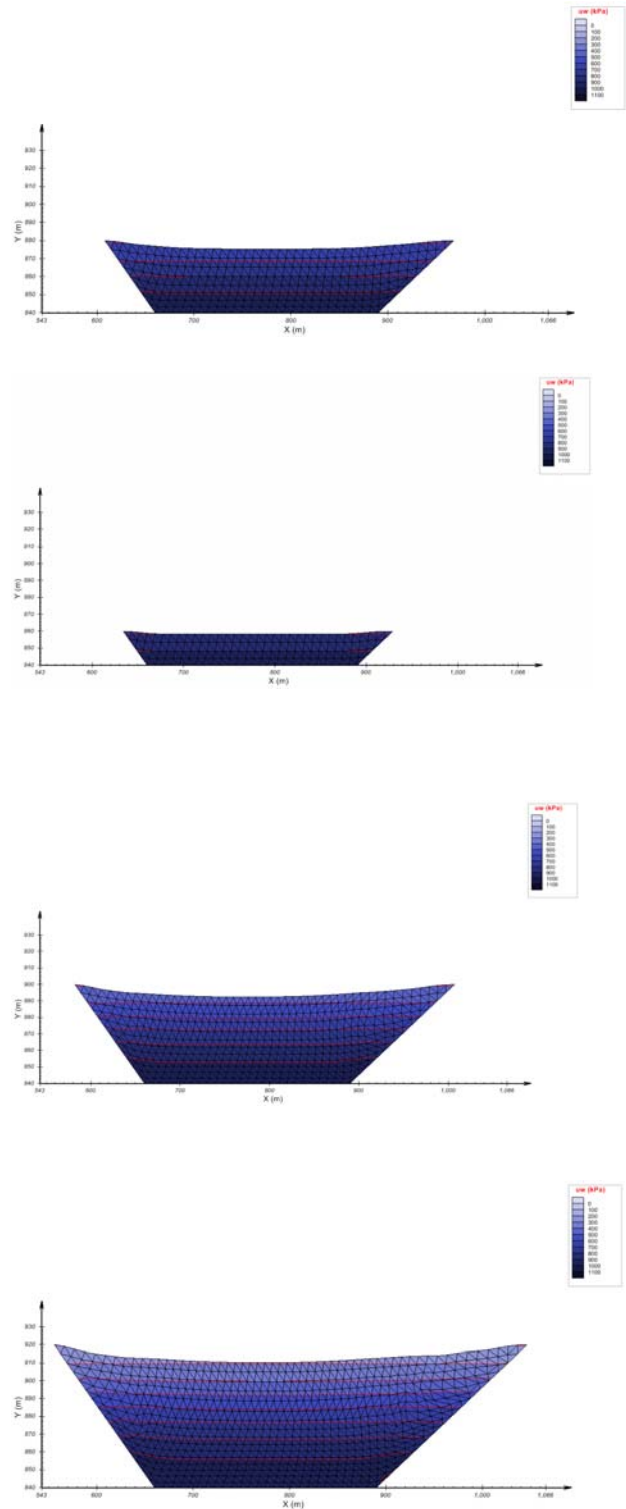


Figure 8. Example analysis of a tailing pit implementing annual layers.

REFERENCES

Barden L. and Berry. P. L. (1965). "Consolidation of normally consolidated clay". Journal of Soil Mechanics and Foundations Division. ASCE, Vol. 95(1p) p. 1-31.

Davis, E. H., and Raymond, G. P. (1965). "A Non-Linear theory of Consolidation", Geotechnique Vol. 15,, pp. 161-173

Lee K. and Sills G. C. (1979). "A Moving Boundary Approach to Large Strain Consolidation". Proc. 3rd International Conference on Numerical Method on Geomechanics pp. 163-173.

Mikasa M. (1 965). "The Consolidation of Soft Clay, A New Consolidation Theory and its Application", Japanese Society of Civil Engineers, pp. 21-26.

Gibson R. E.. England G. L. and Hussey M. J. L., (1967) The Theory of one- Dimensional Consolidation of Saturated Clay. 1 Finite Non-Linear Consolidation of Thin Homogenous Layers". Geotechnique, pp. 261-273

Gibson. R. E.. and Lumb. P.. (1953). "Numerical Solution of Some Problems in the Consolidation of Clay". Proc. I.C.E. Vol. 2, pp. 182-198.

Gibson, R. E., (1958), The Progress Of Consolidation In A Clay Layer Increasing In Thickness With Time, Geotechnique, v8:1

Gibson R. E.. Schiffmann R. L. and Cargill K. W., (1981). "The Theory of One-Dimensional Consolidation of Saturated Clays. II: Finite Non-Linear Consolidation of Thick Homogenous Layers", CanGaedioiatenc hnique J., pp. 280-293.

Schiffman R.,L., 1958. ' Consolidation of soil under time-dependent loading and varying permeability.' Proc. Highw. Res. Wash., 37 : 584-617.

SVFlux Manual, 2009, SoilVision Systems Ltd.

SVSolid Manual, 2009, SoilVision Systems Ltd.

Terzaghi K. (1923). "Die Berechnung der Durchlassig Keisziffer des Tones ans dem Verlauf der Hydrodynamischen Spannungserscheinungen Reproduced in Terzaghi K. (1960), From Theory to Practice in Soil Mechanics", John Wiley & Suns. New York

Terzaghi K. (1943). Theoretical Soil Mechanics", John Wiley & Sons. New York.
Townsend, F.C., McVay, M.C., 1990, SOA: Large Strain Consolidation Predictions, Journal of Geotechnical Engineering, Vol. 116, No. 2, February

INNOVATIVE EXPANSION OF A CENTERLINE CONSTRUCTED TAILINGS STORAGE FACILITY - SETTLEMENT MODELING

Gordan Gjerapic, Kimberly F. Morrison and James M. Johnson

Golder Associates Inc., Lakewood, Colorado USA

Bert Doughty

Thompson Creek Metals Co., Challis, Idaho USA

Dobroslav Znidarcic

University of Colorado at Boulder, Boulder, Colorado, USA

ABSTRACT: The Bruno Creek Tailings Impoundment, located in seismically-active central Idaho, retains settled tailings behind the second tallest centerline-raise cycloned tailings sand dam in the world. The dam is proposed to be raised from its current height of 168 m to nearly 230 m based on projected Life of Mine (LoM) ore reserves. The facility is owned and operated by Thompson Creek Mining Company. An alternatives evaluation indicated the preferred option for expansion of tailings storage capacity is to raise the existing facility using the centerline raise method over most of the dam alignment, but modifying the design to employ a partial realignment of the dam crest at the left abutment. This change will result in a length of the previously centerline-raised dam being constructed over an existing tailings beach. The design also includes steepening of the downstream dam slopes from 3H:1V (horizontal:vertical) to 2.75H:1V, as well as addition of a 12 m (40-foot) raise on the existing rock toe dam. For the portion of the dam alignment to be constructed over the existing tailings beach, a settlement evaluation of tailings was required to obtain more accurate estimates of construction volumes and to predict in-situ levels of saturation and associated material properties for input to seepage and stability analyses.

This paper discusses a closed-form settlement calculation approach that was used to rapidly evaluate embankment settlements for selected embankment and foundation geometries. The discussed methodology was developed specifically to evaluate relatively coarse beach tailings as dam foundation materials under both submerged and unsaturated conditions.

INTRODUCTION

Project Background

The Thompson Creek Mine (TCM) is a molybdenum mine located in Custer County, Idaho. Since 1983, TCM has mined molybdenum ore from an open pit, which is milled into molybdenum concentrates for transportation offsite and subsequent processing.

Mine tailings produced at TCM are stored in the Bruno Creek drainage using a cycloned sand dam and centerline-raise technique (Figure 1). Tailings are piped as a 35 to 40 percent solids by weight slurry from the mill to the tailings impoundment and are either cycloned to separate sands for dam construction (with slimes deposited into the impoundment) or directly deposited into the impoundment (as whole tailings) from perimeter discharge points. Current operations include cyclone construction of the tailings dam for six months each year with a total of approximately 24 percent of the tailings stream consisting of sand for dam construction.



Figure 1. Cycloned sand dam construction.

Operation of the tailings impoundment at Thompson Creek commenced in August 1983. With the exception of temporary

shutdowns in 1991 and from December 1992 to March 1994, the tailings impoundment has been in continuous operation (SRK 1995). At the time of this study, the sand dam was approximately 168 m (550 feet) high and retained approximately 140 million tonnes of tailings, which includes the tailings sand used to construct the dam. However, the facility was designed and permitted to contain up to 180 million tonnes of tailings. This study included development of the Life of Mine (LoM) design and permitting for the facility, which incorporated an additional 90 million tonnes of tailings, bringing the total storage in the facility to approximately 270 million tonnes (300 million tons).

Alternatives Evaluation

An alternatives evaluation was conducted which indicated that the proposed LoM expansion (i.e., approximately 90 million tonnes) could not be stored within the existing Bruno Creek Tailings Impoundment without making modifications to the existing embankment configuration. Otherwise, an alternative storage facility would need to be considered. The selected alternative consisted of realigning the crest of the centerline-raise sand dam at the left abutment (see Figure 2) to contact the ridgeline further upstream, which allows the embankment to be raised without overtopping the ridgeline. This alternative was selected because it allowed for the anticipated tailings through the LoM to be stored in one location, eliminating the need to develop a new tailings impoundment downstream or within another site drainage. Also, past geotechnical, geological, and hydrological studies in the Bruno Creek drainage area were abundant, and could be used to reduce the cost and time associated with new studies.

Proposed Design Concept

The selected concept includes construction of a raise on the existing Bruno Creek Tailings Dam with the crest elevation of approximately 2360 m (7742 ft) above mean sea level.

To limit downstream impacts as well as reduce the volume of sand required for dam construction, a downstream dam slope of 2.75H:1V (horizontal: vertical) was proposed for the structure, as controlled by stability considerations. To further limit downstream impacts, a downstream raise on the existing rock toe dam was proposed.

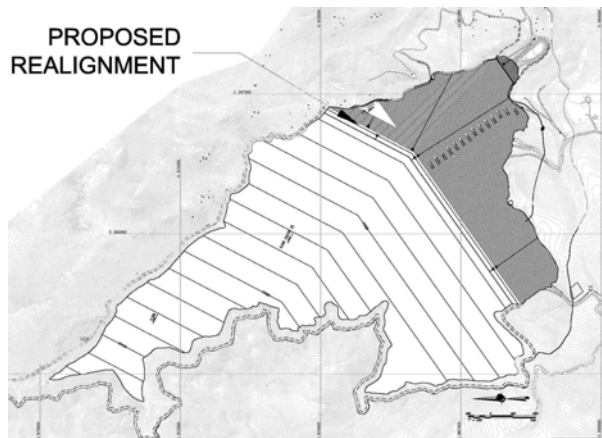


Figure 2. Proposed LoM embankment geometry.

The raise would include realignment of the dam centerline with construction of a starter dike near the left abutment as controlled by topography (i.e., the existing left abutment elevations are too low to accommodate the LoM raise), and continued construction of the existing centerline raise dam along the remainder of the alignment.

FIELD AND LABORATORY TESTING

A geotechnical investigation was conducted to evaluate the subsurface conditions present

within the tailings dam and proposed LoM expansion areas. Specifically, investigations took place along the existing dam centerline and proposed LoM crest realignment, at the left and right abutments, at the dam toe, and within identified construction borrow areas. The investigation program consisted of cone penetration test (CPT) soundings, drillholes, and a series of test pits.

Eight CPT soundings were conducted into the tailings impoundment, including three along the existing dam centerline and five along the proposed crest realignment, each advanced to a depth of 61 m (200 feet) below ground surface unless cone refusal was met prior to reaching the proposed depth. Based upon the pre-tailings impoundment topography, refusal was met in three of the locations as a result of encountering native soils.

Two of the CPT soundings which were advanced along the proposed crest realignment were later paired with conventional drillholes to assist development of site-specific correlations. Within these paired boreholes, geotechnical samples in the form of Shelby tube, modified California barrel sampler, or Standard Penetration Test (SPT) split spoon sampler was performed at 3-meter (10-foot) intervals while drilling.

Pairing of the CPT soundings with boreholes allowed for development of site-specific correlations between SPT blow counts and the CPT data. SPT N_{60} values (i.e., SPT blow counts corrected for energy, only) were calculated from the normalized cone tip resistance and normalized friction ratio based on the methodology proposed by Jefferies and Davies (1993). As their equation was developed based on the results of calibration chamber testing and a limited number of site investigations, it is good standard of practice to place a couple of boreholes and CPTs side by side to verify an acceptable fit to the data collected for the soil deposit being

investigated, or make site-specific modifications.

Tailings samples collected during the field investigation were sent to the laboratory for additional testing, i.e. geotechnical characterization testing (sieve, hydrometer and Atterberg), strength testing (triaxial), and consolidation testing (slurry consolidation, and permeability).

SETTLEMENT MODELING

Selection of Material Parameters

Typically, tailings settlement characteristics differ according to location within the impoundment. Sandier tailings, primarily encountered within and near the dam, are more easily drained (have higher hydraulic conductivities) and will typically compress less when compared to finer grained tailings further away from spigot locations. Finer grained tailings encountered toward the center of the impoundment typically have lower hydraulic conductivities, higher void ratios, and higher moisture contents. These tailings generally experience the greatest consolidation and resulting surface settlements. Although field explorations indicated the presence of alternating layers of slightly finer and coarser tailings, variably both in plan view and depth, no obvious or pervasive delineation boundaries were observed. Accordingly, the tailings material encountered at locations proposed for the LoM embankment raise did not show appreciable variation with respect to the distance from the embankment crest. In particular, tailings materials collected from the drillholes in the tailings dam vicinity (e.g., BH-07-07) and from CPT locations further away from the dam (e.g., BH-07-06) indicate similar compression properties (see Figure 3).

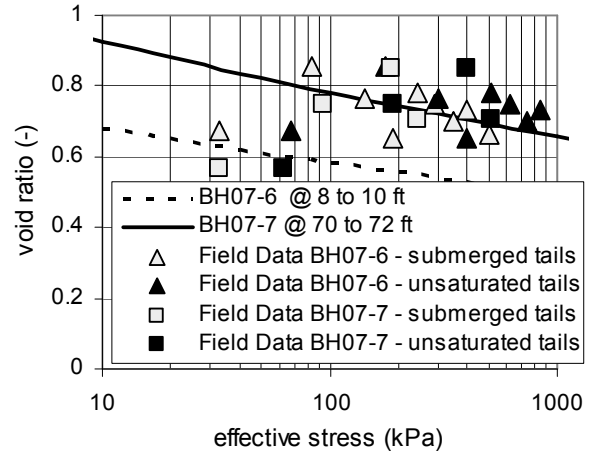


Figure 3. Tailings compressibility results.

Noting that differences in material types for the proposed LoM dam expansion are subtle and are within the expected range considering both horizontal and vertical extents (i.e. similar variations in material properties were observed in the vertical direction within a single borehole and horizontally along the proposed dam centerline), a modeling effort employing several material types was deemed impractical. After a detailed review of the field investigation and laboratory test results, it was concluded that the tailings properties for BH-07-07 sample collected from 21.3 to 21.9 m (70 to 72 feet) provide a good representation of on-site materials (see Figures 3 and 4).

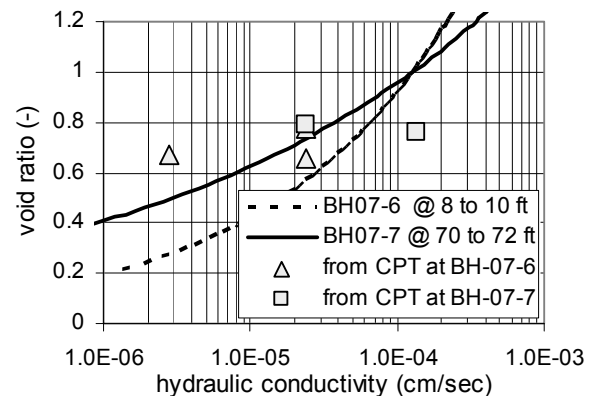


Figure 4. Tailings permeability results.

The compression properties for the representative sample were determined by reconstituting the tailings at slurry consistency and measuring the permeability and void ratio throughout the loading process with the maximum effective stress of 1,400 kPa (see compressibility curves for samples BH-07-6 at 8 to 10 ft and BH-07-7 at 70 to 72 ft on Figure 3). A comparison between laboratory-derived and CPT-interpreted results shown in Figure 3 indicates possible tailings stratification at the surface. For conservatism, somewhat lower compressibility of surface tailings (indicated in Figure 3 for stresses below 80 kPa) were disregarded in settlement analysis.

In Figures 3 and 4, hydraulic conductivity and compressibility relationships for samples BH-07-6 at 8 to 10 ft and BH 07-7 at 70 to 72 ft were expressed as functions of the void ratio based on the measured laboratory data. The adopted void ratio-effective stress ($e-\sigma'$) and permeability-void ratio ($k-e$) relationships (see e.g. Abu-Hejleh and Znidarcic, 1994, 1996) can be written as:

$$e = A(\sigma' + Z)^B \quad (1)$$

and

$$k = Ce^D, \quad (2)$$

where A , B , C , D and Z are material parameters determined from laboratory measurements. Material parameters used for modeling, i.e. parameters for the selected representative sample BH 07-7 @ 70 to 72 ft, are given in Table 1.

Table 1. Material parameters for representative sample (BH 07-7 at 70 to 72 ft).

G_s (-)	A (kPa ^{1/B})	B (-)	Z (kPa)	C (m/yr)	D (-)
2.68	1.103	-0.075	0.506	40.1	5.4

Parameter G_s in Table 1 denotes specific gravity.

Modeling Approach

LoM tailings dam settlements were estimated using a three-part approach:

1. Determine existing tailings height at borings and CPT locations along the crest of the tailings dam and along the estimated crest realignment. The existing tailings height is calculated as a difference between the existing and the pre-mining topography.
2. Determine LoM loading conditions as a difference between the proposed embankment raise and the existing tailings.
3. Determine settlements for the LoM expansion relative to the existing conditions based on geometry from Step 1 and loading conditions from Step 2.

Two extreme groundwater scenarios were considered:

- Case 1 - Phreatic surface coincides with the tailings surface (i.e., saturated/submerged conditions); and
- Case 2 - Phreatic surface coincides with the base of the tailings impoundment (i.e., unsaturated conditions).

When considering field data in Figure 3, the Case 1 scenario was applied to calculate effective stresses using the buoyant/effective unit weight, (calculated as a difference between the wet unit weight, γ_{wet} , and the unit weight of water, γ_w , i.e., implicitly assuming full tailings saturation). The effective stresses for Case 2 scenarios were calculated by assuming that the effective stress gradient is equal to the wet weight ($\gamma = \gamma_{wet}$), i.e. neglecting the influence of capillary pressures.

Densification (settlement) of tailings can be divided into three stages: sedimentation, consolidation, and desiccation. As the tailings are deposited, sedimentation slowly separates the tailings solids from the fluid through gravity, forming a weak solid structure with low strength properties. As new tailings are subsequently placed above the existing tailings, the existing tailings are subjected to the increased overburden pressure, and undergo the consolidation process, a process where pore fluid is expelled from the pore space between tailings particles. Lowering of the water surface above or within the tailings can also induce the consolidation process. Finally, after tailings fluids have been removed from above the solids surface, the tailings solids desiccate as they continue to dewater through evaporation. Desiccation is characterized by an increase in negative pore water pressure (soil suction) and soil tensile stresses, which results in surficial cracking. Based on the results of the LoM geotechnical field investigation and preliminary modeling results (see Figure 5), tailings settlement modeling was conducted assuming instantaneous consolidation and disregarding the effects of desiccation.

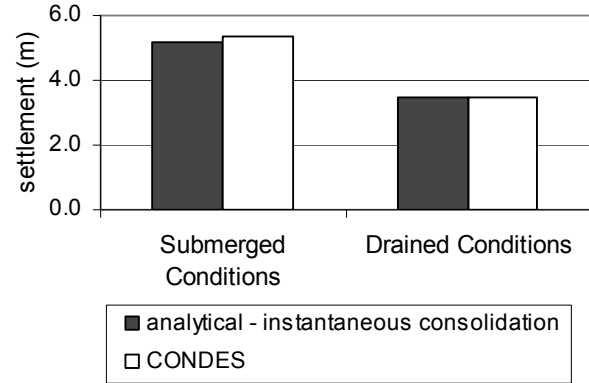


Figure 5. Preliminary modeling results.

Analytical Solutions for Instantaneous Consolidation

Relatively large deformations, typical for tailings materials disposed in a slurry form, can be calculated by using computer programs based on large-strain consolidation theory (Gibson et al., 1967). The governing equations for one-dimensional large-strain consolidation can be written as:

Velocity function:

$$v_u = \frac{K \cdot (G_s - 1)}{1 + e} + \frac{K \cdot (1 + e_o)}{\gamma_w (1 + e)} \frac{d\sigma'}{de} \frac{\partial e}{\partial a} \quad (3)$$

Conservation of mass:

$$\frac{\partial v_u}{\partial a} = \frac{-1}{1 + e_o} \frac{\partial e}{\partial t} \quad (4)$$

where:

- t = time
- a = Lagrangian coordinate
- e_o = void ratio at zero effective stress
- G_s = specific gravity of soil particles
- v_u = velocity function
- γ_s, γ_w = unit weights of soil solids and water, respectively.

To determine final settlements for a given known amount of dry tailings, one can disregard the consolidation process and perform settlement calculations relying solely on the tailings compressibility values. Consequently, such an approach implies instantaneous consolidation (no development of excess pore pressures) and is applicable for relatively fast draining materials and/or for relatively slow deposition rates. Considering the field measurements and the unsaturated conditions of the coarse tailings encountered below the proposed dam realignment, analytical solutions for both submerged and unsaturated tailings were used to calculate settlements.

For the compression properties defined by Equation (1), an analytical solution for the height of submerged tailings at the end of the consolidation process (Case 1 scenario) can be expressed as (see Gjerapic and Znidarcic, 2007):

$$H = H_s + \frac{e(0)[\sigma'(0) + Z] - e(H_s)[\sigma'(H_s) + Z]}{(1 + B)\gamma_w(G_s - 1)} \quad (5)$$

where $e(0)$ and $\sigma'(0)$ denote the void ratio and the effective stress at the base of the soil column, and $e(H_s)$ and $\sigma'(H_s)$ denote the void ratio and the effective stress at the surface, respectively. The total height of solids in the tailings column is denoted by H_s . A general expression for the effective stress at any height within the tailings column can now be determined as a function of the solid height at the same elevation, λ , as:

$$\sigma'(\lambda) = \gamma_w(G_s - 1)(H_s - \lambda) + \sigma'_{top} \quad (6)$$

where:

$$\lambda = a/(1 + e_0), \quad 0 \leq \lambda \leq H_s \quad (7)$$

In Equation (6), σ'_{top} denotes the effective stress at the surface while the void ratios $e(0)$ and $e(H_s)$ are calculated from the corresponding effective stresses based on Equation (1):

$$e(\lambda) = A[\sigma'(\lambda) + Z]^B \quad (8)$$

Similarly, the tailings height for the Case 2 scenario can be expressed as:

$$H = H_s + \frac{e(0)[\sigma'(0) + Z] - e(H_s)[\sigma'(H_s) + Z]}{(1 + B)\gamma_w G_s (1 + w)} \quad (9)$$

where w stands for the gravimetric moisture content and the effective stress is determined as:

$$\sigma'(\lambda) = \gamma_w G_s (1 + w)(H_s - \lambda) + \sigma'_{top} \quad (10)$$

Equations (5) and (9) were used to determine the height of solids for a given height of the tailings column for both groundwater scenarios. Note that equations (5) and (9) can also be used to determine the void ratio profile for the tailings column with constant loading conditions undergoing instantaneous consolidation, a condition necessary for Step 3 of the settlement calculation process.

Verification and Modeling Results

Based on the available field data from the recent geotechnical field exploration and previous reports (Woodward Clyde, 1997), one can determine the range of the expected gravimetric moisture content for both the cycloned sands and the beach tailings materials. Woodward Clyde (1997) data indicate the average dry density of the cycloned sands of about 15 kN/m³ and the average moisture content of approximately 10 percent. Hence, the loading on the existing tailings caused by LoM dam expansion was assumed to equal 16.5 kN/m³

for every meter of fill above the current tailings configuration. Based on the recent geotechnical field exploration, the average gravimetric moisture content of beach tailings is 19.6 percent (maximum of 32.0 percent and minimum of 9.5 percent).

For a given modeling scenario and the material parameters in Table 1, one can now calculate settlements for an arbitrary tailings column within the existing impoundment subjected to a construction load defined by an embankment raise and for a specific set of boundary conditions. To verify applicability of the analytical solutions, settlement results for an existing 160 m high tailings column based on equations (5) and (9) were compared with the results from the computer program *CONDES* (see Yao and Znidarcic, 1997) as shown in Figure 5.

CONDES is a one-dimensional finite difference computer program used to model impoundment filling, consolidation and desiccation utilizing large-strain consolidation theory (Gibson et al., 1967). The program solves a non-linear second order partial differential equation formulated for one-dimensional compression, three-dimensional shrinkage, and propagation of vertical cracks in soft fine-grained soils. It provides the one-dimensional time-dependent solutions of void ratio distribution (solid content distributions), layer thickness, and gives information on propagation and volume of cracks. *CONDES* results in Figure 5 were based on the three-dimensional impoundment filling procedure described in Gjerapic et al. (2008) and the tailings production rate of 11,800 tonnes/day (total tailings production corrected for the amount of cyclone sands used for construction).

Settlements calculated using the large-strain consolidation theory (program *CONDES*) and settlements determined from the analytical solutions indicate close agreement, implying

validity of the applied analytical solutions and confirming negligible effects of excess pore pressure. Consequently, the assumption of instantaneous consolidation is applicable for LoM tailings settlement modeling, for the given tailings parameters, impoundment geometry, boundary conditions and imposed filling rates.

CONCLUSIONS

In specific cases, tailings settlement modeling may be greatly simplified by using presented analytical solutions applicable to both submerged and unsaturated tailings conditions. The presented analytical solutions enable rapid evaluation of tailings settlements for arbitrary impoundment and embankment/loading geometries while rationally accounting for the non-linearity of the tailings compression curve. The presented solutions assume instantaneous consolidation, i.e. are valid only for relatively coarse tailings and/or slow filling rates.

The fact that some tailings exhibit negligible excess pore pressures may be exploited for both the analysis and the design purposes. However, one should keep in mind that the assumption of instantaneous consolidation should be verified against tailings parameters, impoundment geometry, boundary conditions and imposed filling rates. Changes in any of these factors may potentially lead to a scenario where the influence of excess pore pressures on the calculated settlement is significant, thus rendering the assumptions of the presented analytical solutions invalid.

REFERENCES

Abu-Hejleh, A.N. and Znidarcic, D. (1994). "Estimation of the Consolidation Constitutive Relations." *Computer Methods and Advances*

in Geomechanics, Siriwardane & Zaman (eds) Balkema, Rotterdam, pp. 499-504.

Abu-Hejleh, A.N., and Znidarcic, D.Z., and Barnes, B.L. (1996). Consolidation Characteristics of Phosphatic Clays. ASCE Journal of Geotechnical Engineering Vol. 122, No. 4.

Gibson, R.E., England, G. L., and Hussey, M.H.L. (1967). The theory of one-dimensional consolidation of saturated clays, I. finite non-linear consolidation of thin homogeneous layers. Geotechnique, 17(3), 261-273.

Gjerapic, G., Johnson, J., Coffin, J. and Znidarcic, D. (2008) "Determination of Tailings Impoundment Capacity via Finite-Strain Consolidation Models", in GeoCongress 2008: Characterization, Monitoring, and Modeling of GeoSystems (GSP 179) conference proceedings, A. N. Alshawabkeh, Krishna R. Reddy and Milind V. Khire Eds., March 9-12, New Orleans, Louisiana, pp. 798-805.

Gjerapic, G. and Znidarcic, D. (2007) "A Mass-Conservative Numerical Solution for Finite-Strain Consolidation during

Continuous Soil Deposition", Geo-Denver 2007: Computer Applications in Geotechnical Engineering (GSP 157) conference proceedings, Siegel, T.C., Luna, R., Hueckel, T. and Laloui, L., Eds., Denver, Colorado, February 18-21, Geo-Denver 2007 "New Peaks in Geotechnics" CD-ROM.

Jeffries, M.G. and Davies, M.P. (1993). "Use of CPT values to estimate equivalent SPT N_{60} ", ASTM Geotechnical Testing Journal, Vol. 16, No. 4, pp. 458-467.

Steffen Robertson & Kirsten (SRK). (1995). *Embankment Seepage and Stability Issues*. Technical Memorandum from R. Dorey to B. Doughty (TCMC). 13 September 1995.

Woodward Clyde Consultants. (1997). "Final Design Report – Tailings Embankment Toe Drain, Thompson Creek Mine", report No. 24226 prepared for Thompson Creek Mining Company, June.

Yao, D.T.C. and Znidarcic, D.Z. (1997). User's Manual for Computer Program CONDES0. Florida Institute of Phosphate Research (FIPR) Publication No. 04-055-134.

GENERIC PREDICTIONS OF DRYING TIME IN SURFACE DEPOSITED THICKENED TAILINGS IN A “WET” CLIMATE

P. Simms, A. Dunmola and B. Fisseha

Department of Civil and Engineering, Carleton University, Ottawa, Canada

ABSTRACT: Thickening tailings prior to deposition has been implemented at various sites around the world for different kinds of residuals. Evaporation is an important phenomenon in thickened tailings deposits that may strongly influence both the development of shear strength and the quantity of seepage. Recent research has shown that the rate of evaporation can be reasonably predicted using unsaturated flow codes, of the type that are widely available to consultants. This paper reviews this research, highlights some important issues, and discusses some hypothetical modeling for tailings deposition under relative wet regions, such as might be encountered in parts of Canada.

INTRODUCTION

Surface disposal of thickened tailings has been used around the world for many different residuals. “Thickened” denotes that the tailings have been dewatered to the point where the tailings will exhibit a yield strength upon deposition and therefore can form gently supporting stacks, which do not necessarily require containment by dams (Robinsky 1999). This makes thickened tailings deposition an attractive alternative to conventional slurry deposition, due to the significant risk and consequences of dam failure (ICOLD 2001) associated with the latter. Thickened tailings offers other comparative advantages, including ease of closure due to earlier trafficability afforded by the higher density at deposition, and the benefits of recycling the recovered water.

Potential disadvantages include greater exposure to the environment due to lack of water cover, the potential for remobilization of the stack during seismic events (Al-Tarhouni et al. 2009, Li et al 2009), and difficulties in managing deposition geometry (Shuttleworth et al. 2005). The absence of a water cover increases the risk of acid generation in sulphidic tailings (Bryan & Simms 2008), while rain-driven erosion may also be a concern in very humid climates. Directing tailings during deposition to control layer thickness and the overall the geometry of the stack can be difficult due to variability in the rheology the tailings coming out of the pipe, as well as lack of understanding of the overland flow, though this is improving through increased operational experience and research (Shuttlewoth et al 20005, Fitton et al. 2008, Henriquez & Simms 2009).

The technology for dewatering and pumping thickened tailings is now well-established and becoming increasingly cost-effective, as evidenced at the recent international conferences on thickened tailing and associated publications (Jewell & Fourie 2008). However, the behaviour of tailings post-deposition is less understood. Evaporation is a particularly important phenomenon, as it can significantly control the performance of the tailings both in terms of shear strength and the quality and quantity of seepage. This paper briefly illustrates how evaporation may influence deposition planning, and discusses some aspects of the deposition of thickened tailings in relatively humid climates.

BACKGROUND

Conceptual model for tailings evolution post-deposition

Subsequent to deposition, the density of the tailings will decrease by at least three different phenomena: settling, desiccation, and consolidation. Settling can be very significant, even in tailings deposited at already heavily dewatered state. For example, in gold tailings deposited at a gravimetric water content (GWC) of ~40%, the void ratio can decrease from 1.4 to 1.0 over 48 hours due to settling alone (Fisseha 2008). The rate of settling decreases exponentially and can be described as a hindered settling process (Cuthbertson et al. 2008). In arid climates and for relatively dewatered tailings deposited in thin layers, the rate of settling is quickly overtaken by evaporation; however, in humid climates settling may be very important to densification of tailings.

Desiccation is driven by evaporation as well as by seepage into underlying tailings.

Evaporation occurring from tailings is similar to classic evaporation behaviour in soils, and can be distinguished by at least two stages. The first, Stage I, denotes when evaporation occurs at the potential rate, which can be calculated from climatic parameters using the well-known Penman equation or similar expressions. Stage II evaporation occurs when the total suction at the surface reaches a certain value such that the gradient in relative humidity between the soil surface and the overlying atmosphere begins to decrease. Past this point, the rate of evaporation becomes a function of the total suction of the soil surface and decreases below the potential rate (Wilson et al. 1997). The rate of Stage II evaporation depends on a number of factors, including the material properties of the tailings, the relative wetness of the underlying tailings, as well as climate. The various factors affecting evaporation from tailings are visualized in Figure 1. Both Stage II evaporation and seepage can be evaluated using conventional unsaturated flow models, given proper characterization of the tailings. The use, applicability, and limitations of such models are discussed extensively elsewhere (Simms et al. 2007, Fisseha et al. 2009 a & b), one important limitation being the suppression of evaporation by salts for tailings that have a high ionic concentration in their pore-water (Fisseha et al. 2009a, Fujiyasu & Fahey 2000). While unsaturated flow analysis requires some work and care, it is important to establish a necessary maximum layer thickness for a given deposition scheme in a given climate: For too thick of a layer, Stage II evaporation may commence at the surface too early, such that the surface of the tailings will dry out, but the mass of tailings in the layer will remain wet and not develop significant shear strength, therefore limiting the angle of deposition and the overall stability of the stack. We will now attempt to illustrate this problem through generic analyses. We also will show that

evaporation can still contribute significantly to strength gain in deposits in wet climates.

MATERIALS AND METHODS

Materials

For our analyses we use a range of generic tailings parameters. The important properties for unsaturated analysis are the shrinkage curve, the water-retention curve (WRC), and the saturated hydraulic conductivity. The shrinkage curve, WRC, and a typical variation in undrained strength in thickened gold tailings are shown in Figure 2 and 3. The WRC can be fitted by a number of theoretical equations, which use parameters such as the air-entry value (AEV), the slope of the WRC,

and the residual water content. In our generic analysis, we investigate the variation of the WRC in terms the typical range of air-entry values observed in tailings.

A very important point is to distinguish between the two types of WRC – one gives the variation in water content with suction, the other the variation in degree of saturation, S . The latter, in most tailings, must be defined using volume change measured during WRC tests. The true AEV is then taken from the S vs suction curve. There are several different definitions of the AEV, we have chosen the value of suction when $S=0.85$ to be the AEV in this paper. In our analysis, we shift the given WRCs by the AEV, varying the AEV between 50, 100, and 500 kPa. Our WRC is otherwise defined by the Fredlund and Xing

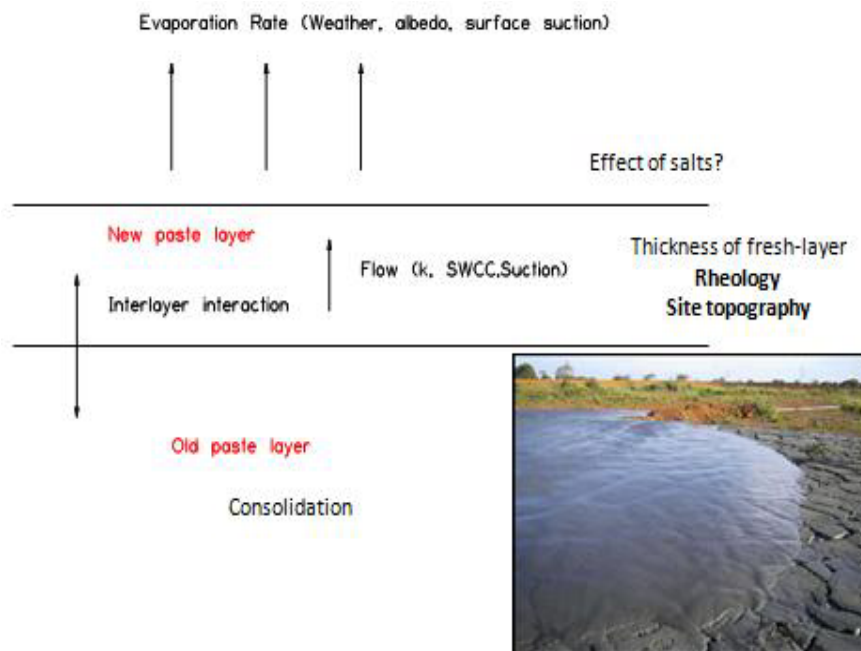


Figure 1. Factors influencing the rate of drying of a freshly deposited layer of thickened tailings (After Simms et al. 2007)

equation (Fredlund & Xing 1994), employing the value of parameters n and m as 2 and 1 respectively. We also vary saturated hydraulic conductivity between 5×10^{-7} m/s and 5×10^{-9} m/s. This range of values encompasses hard

rock tailings as well as CT oil sand tailings (Fisseha 2008, Qui & Segó 2001, Aubertin et al. 1996).

Simulation

We simulate the desiccation of a 0.25 m lift of tailings, deposited at 40% GWC. We ignore settling behaviour and downward seepage. The bottom boundary condition is non-flux and the top boundary condition is the soil-atmosphere coupling that predicts evaporation as a function of suction at the soil surface (Wilson et al. 1997). The potential evaporation is 8 mm/day. We employ the unsaturated flow code SVFlux, which optimizes time stepping and mesh refinement.

We also simulate the desiccation of this same lift for a wet climate: 3 days of initial drying at a potential evaporation rate of 4 mm/day is followed by two days of rain at 20 mm/day, followed by 5 more days of evaporation, also at 4 mm/day. In one simulation,, the WRC is changed after the first drying period, to reflect the permanent volume change that occurs in the tailings following initial drying.

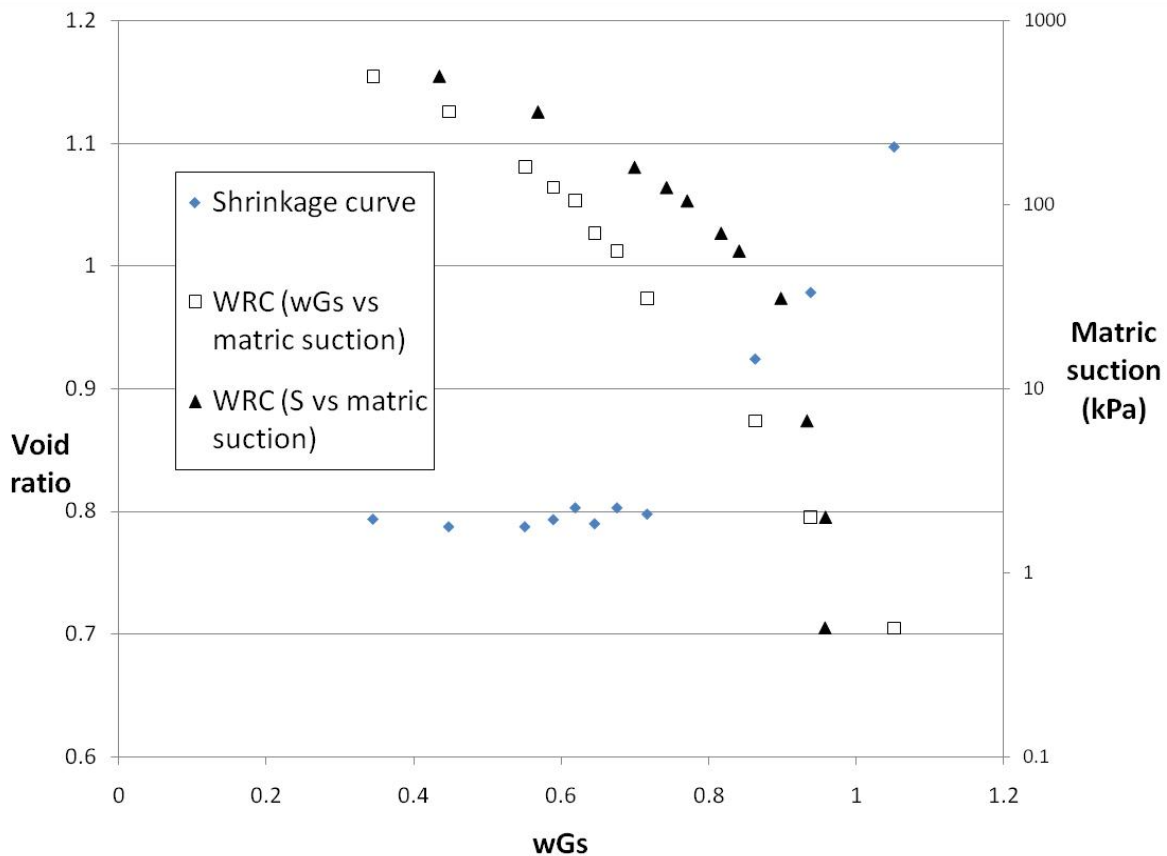


Figure 2. Shrinkage curves and water retention curves of a thickened gold tailings deposited at 40% GWC

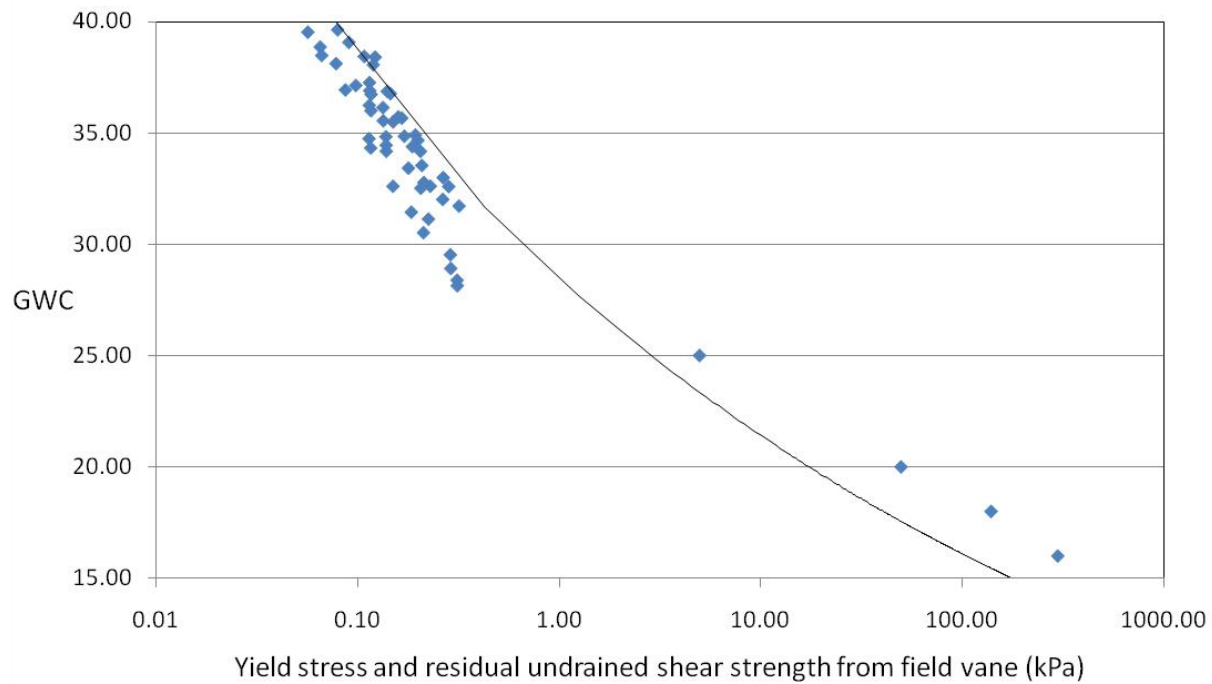


Figure 3. Yield stress and undrained shear strength of a thickened gold tailings

RESULTS

Simulation of deposition with only evaporation

The results are summarized in Figures 4 and 5, which shown the average gravimetric water content over 10 days of drying as a function of the saturated hydraulic conductivity and AEV. It can be seen that hydraulic conductivity is an especially important parameter affecting the drying time - the lower the saturated hydraulic conductivity, the earlier the start of Stage II evaporation, and the longer the time required to dry a layer of tailings to a given water content. Readers may refer to Figure 3 on shear strength to give an idea on the importance of arriving as close as possible to

the shrinkage limit. The relative insensitivity to AEV is heartening in the sense that consultants can rely on databases of WRCs for similar tailings, or use methods to estimate the WRC from grain size (Fredlund et al. 2002, Aubertin et al. 2003) for preliminary analyses of deposition plans. Care should be taken with the value of saturated hydraulic conductivity- the value of this parameter can change significantly with the change in void ratio experienced during drying, so modellers should be sure to use a representative or conservative value.

Simulation of deposition in a wet climate

Though it is often believed that any advantage occurring by evaporation would be minimal in a wet climate (where

precipitation exceeds potential evaporation), three issues should be considered:

1. The tailings will increase in density due to settling, regardless of the climate
2. As tailings have a relatively low hydraulic conductivity, the amount of potential infiltration removed by runoff will be significant (even though most tailings crack during desiccation, these cracks only persist in the surface layer)
3. Volume change hysteresis of the WRC – many tailings that have desiccated to below their shrinkage limit will not subsequently swell back to water contents above the shrinkage

limit. An example of this hysteresis is shown for a gold tailings in Figure 6.

Figure 7 shows the evolution of GWC for the scenario where precipitation is greater than potential evaporation during the deposition period. Despite the overall water balance, the tailings do dry significantly over the simulated deposition period. This is in part due to the simulation of runoff by the model, which occurs when the tailings become resaturated. In the simulation where permanent volume change during drying is taken into account, the amount of runoff is naturally much greater, and the final water content therefore significantly lower.

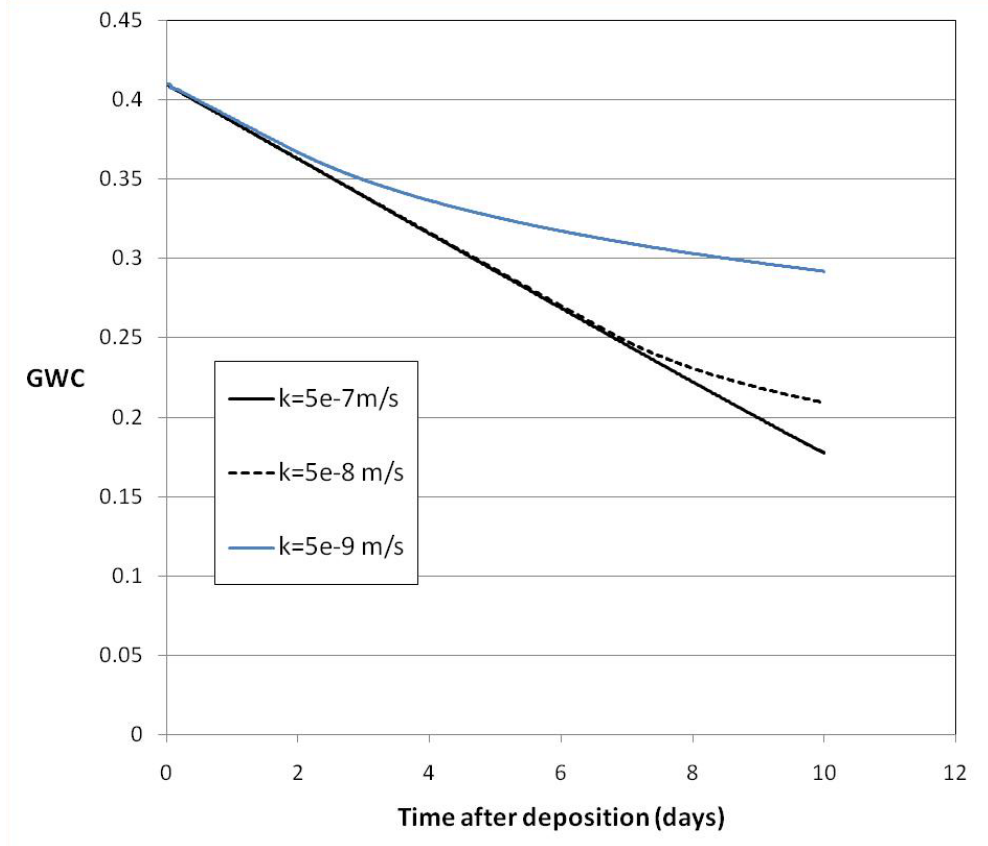


Figure 4. Simulation of drying of 25 cm thick layer with an AEV of 100 kPa, under a potential evaporation of 8 mm/day

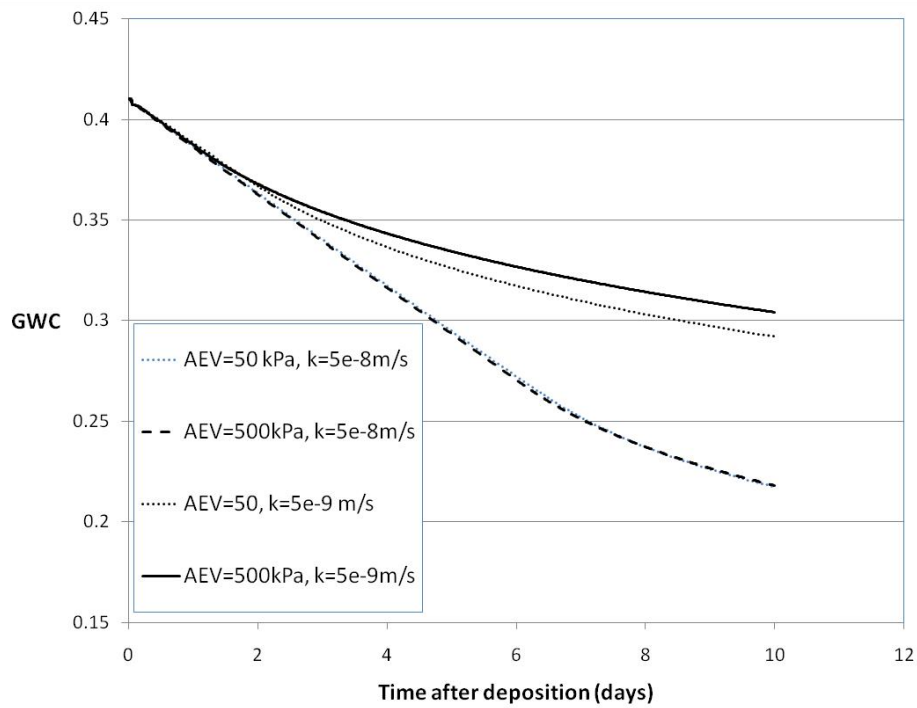


Figure 5. Simulation of drying of 25 cm thick layer, sensitivity to AEV

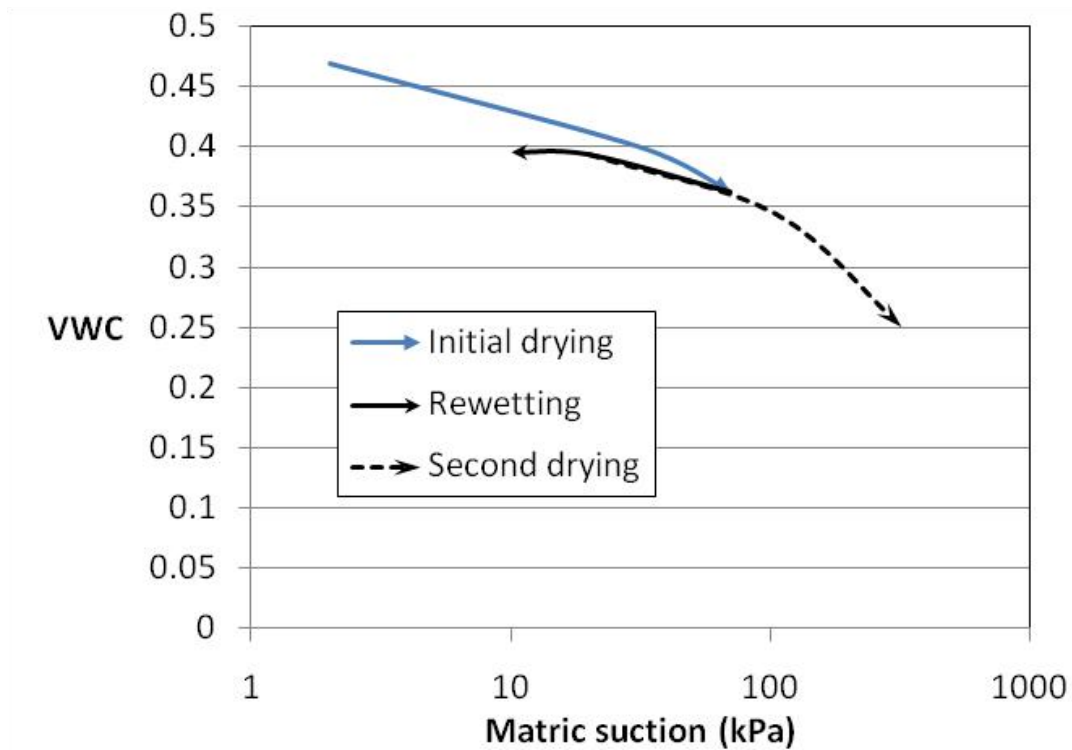


Figure 6. Example of volume change hysteresis in a gold tailings WRC

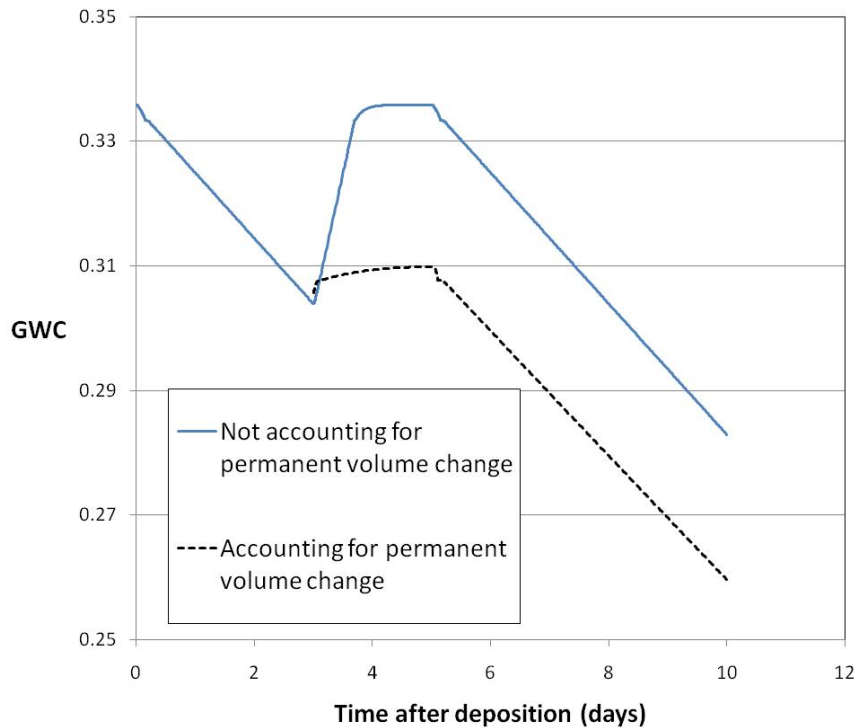


Figure 7. Simulation of 3 days of drying (PE= 4 mm/day), followed by 2 days of rainfall (40 mm over 2 days), and then further drying in a 25 cm thick layer

SUMMARY AND CONCLUSIONS

Predicting the rate of drying using the Penbman equation alone will not suffice to estimate the drying time of a layer of thickened tailings, and some analysis of unsaturated flow in the tailings is required to accurately predict the drying time. The generic analyses undertaken in this paper were very sensitive to the saturated hydraulic conductivity of the tailings, but relatively insensitive to the variation in the AEV between 50 and 500 kPa. Evaporation can still be an important mechanism to maximize strength in a thickened tailings stack, even for wet climates, especially if one considers the influence of settling, runoff, and volume change hysteresis on the post-deposition behaviour.

ACKNOWLEDGEMENTS

Barrick Gold, Golder Associates, and NSERC are gratefully acknowledged for their contribution to this research.

REFERENCES

- Al-Tarhouni, M., Simms, P., & Sivathayalan, S. 2009. Seismic behaviour of thickened gold mine tailings. *Proceedings of the 12th International Seminar on Paste and Thickened Tailings*, Viña del Mar, Chile, April 21st -24th, 2009.
- Aubertin, M., Bussiere, B., & Chapuis, R.P. 1996. Hydraulic conductivity of homogenized tailings from hard rock mines. *Canadian Geotechnical Journal*, 33: 470-482.

- Aubertin, M. Mbonimpa, M., Bussiere, B., & Chapuis, .P. 2003. A model to predict the water-retention curve from basic geotechnical properties. *Canadian Geotechnical Journal*, 41:1104-1122.
- Bryan, R. & Simms, P. 2008. Drying and Oxidation during Surface Disposal of Paste Tailings. *Proceedings of the 23rd International Conference on Solid Waste Technology and Management*, Pittsburgh, Pennsylvania, USA, March 30 - April 2, 2008
- Cuthbertson, A., Dong, P., King, S., & Davies, P. 2008. Hindered settling velocity of cohesive /non-cohesive sediment mixtures. *Coastal Engineering*, 55: 1197-1208
- Fisseha, B., Bryan, R., & Simms, P. 2009a. Evaporation, unsaturated flow, and salt accumulation in multilayer deposits of a gold “paste” tailings. In review, *ASCE Journal of Geotechnical and Geoenvironmental Engineering*.
- Fisseha, B., Bryan, R., & Simms, P. 2009b. Evaporation, unsaturated flow, and oxidation in multilayer deposits of a gold paste tailings. *Proceedings of the 12th International Seminar on Paste and Thickened Tailings*, Viña del Mar, Chile, April 21st -24th, 2009
- Fisseha, B. 2008. Evaporation and unsaturated flow in multilayer deposits of gold paste tailings. Master of Applied Science Thesis, Department of Civil and Environmental Engineering, Carleton University, May 2008.
- Fitton, T.G., Bhattacharya, S.N. & Chryst, A.G.2008. Three-dimensional modeling of tailings beach shape. *Computer-aided Civil and Infrastructure engineering*, 23: 31-44.
- Fredlund, M.D., Wilson, G.W., & Fredlund, D.G. 2002. Use of grain-size distribution for estimation of soil-water characteristic curves. *Canadian Geotechnical Journal*, 39: 1103-1117.
- Fredlund, D.G., & Xing, A.1994. Equations for the soil-water characteristic curve. *Canadian Geotechnical Journal*, 31: 521-532.
- Fujiyasu, Y. & Fahey, M. 2000. Experimental study of evaporation from saline tailings. *ASCE Journal of Geotechnical and Geoenvironmental Engineering*, 126: 18-27.
- Henriquez, J. & Simms, P. 2009. Dynamic imaging and modelling of multilayer deposition of gold paste tailings. *Minerals Engineering*, 22(2): 128-139.
- ICOLD & UNEP. 2001. Bulletin 121: Tailings dams - risk of dangerous occurrences, Lessons learnt from practical experiences. Paris.144
- Jewel, R.J & Fourie, A.B. 2006. *Paste and thickened tailings –A Guide*. Western Australia, Australian Centre for Geomechanics
- Li, A.L, Ritchie, D. & Welch, D. 2009. Stability of large,. Thickened, non-segregated tailings slopes. *Proceedings of the 12th International Seminar on Paste and Thickened Tailings*, Viña del Mar, Chile, April 21st -24th, 2009.

Shuttleworth, J.A., Thomson, B.J., & Wates, J.A. 2005. Surface disposal at Bulyanhulu-practical lessons learned. *6th International Conference on Paste and Thickened tailings*, Santiago, Chile, April 20th-22nd.

Simms P., Grabinsky M.W., & Zhan, G. 2007. Modelling evaporation of paste tailings from the Bulyanhulu mine. *Canadian Geotechnical Journal*, 44: 1417-1432.

Qiu, Y., & Segó, D.C. 2001. Laboratory properties of mine tailings. *Canadian Geotechnical Journal*, 38:183-190.

Robinsky. E.I. 1999. *Thickened tailings disposal in the mining industry*. Robinsky Associates, Toronto, Canada.

Wilson, G.W., Fredlund, D.G., & Barbour, S.L. 1997. The effect of soil suction on evaporative fluxes from soil surfaces. *Canadian Geotechnical Journal*, 34: 145-157.

STORM-WATER MANAGEMENT AT MINE SITES USING SEDIMENTATION PONDS

J.P. Clark

Prince George, British Columbia, Canada.

ABSTRACT: Sedimentation control during mine construction/ operation/closure is attracting increasing regulation over the past decade. The significance of this for mine operators and regulators suggests the need for a guidance document which defines testing required prior to mine construction for activities that could potentially generate sediment and necessitate installation of a sedimentation pond. Designing the appropriate pond size is typically based on a “traditional” approach and methodology which has assumed that the surface area of the pond should be large enough to settle out approximately 10 micron and larger particles for the maximum ten-year, 24-hour rainfall event. This approach is not typically related to the particle size distribution of the soils to be disturbed, nor the soil erosion rates, and therefore cannot predict the (approximate) pond discharge quality. Modification to this “traditional” approach is suggested so that mine operators can predict the optimum surface area of the sedimentation pond, the need to use settling aids, and determine whether the pond discharge will meet local statutory requirements. The appropriate time to perform these predictions and testing is recommended during the environmental assessment phase for new mines. Although this approach is not novel, it will hopefully enable the more blatantly problematic soils to be identified and receive more focus prior to actual construction (e.g. preparations to select and obtain approval for the use of effective and non-toxic flocculants well ahead of the construction taking place, and placing more emphasis on planning erosion control strategies). This approach should yield cost savings for the proponent and ensure a lower risk relative to exceeding discharge and downstream regulatory water quality requirements. The objective is to provide more certainty associated with pond design and performance.

INTRODUCTION

Mining activities during the construction, operational and post mining phases may generate suspended solids in runoff entering receiving waters at soil erosion rates which may increase above “natural” erosion rates significantly in terms of “soil loss”/“sediment yield” quantification using RUSLE (Revised Universal Soil Loss Equation) type methodologies (Goldman, et al, 1986). Application of erosion control strategies may

significantly reduce the sediment load entering adjacent water courses, but typically will not be sufficient to avoid the necessity of installing sedimentation ponds. The mining industry applies significant resources to construct and operate sedimentation ponds and this warrants development of a Best Management Practice (BMP) methodology which strives to yield cost savings for the proponent and ensure a lower risk relative to exceeding both pond discharge quality and downstream water quality requirements. A

cost/efficiency optimization approach is suggested for the application of erosion control techniques and the design and operation of ponds.

BASIS FOR BMP METHODOLOGY

The most important factors which may cause excessive sediment discharges to receiving waters is the presence of abundant unsettleable fine particles in the soils being excavated, or otherwise disturbed, and the soil erosivity characteristics. Whether such soils become problematic with respect to pond discharge quality, regulatory permit compliance and impact on receiving water quality, is generally dependant on:

- (a) The mass loading and concentration of TSS in the influent to the pond, and the portion of this loading which is unsettleable particles, i.e. the eroded soil fraction which is finer than the *critical settling particle size* (Slater et al, 1968).
- (b) The size “split”, or the particle separation size, which the pond is capable of achieving (at various inflow rates) (Clark, 1998 and Howie, 1981).

Hence, the design of a sediment pond should be based on the size distribution of the soils at a specific mine site (and the soil erosivity) in order that the pond discharge quality can be predicted and the design parameters adjusted to meet the discharge and receiving water requirements.

Drawing from past design methodologies, many jurisdictions specify a minimum pond area, or volume e.g. 0.0001 m³/s/1.0 square metre of pond area, which will remove 10 micron and larger particles (Clark, 1998). Some US jurisdictions require pond sizing in terms of pond volume and geographical location (e.g. Maryland, 0.5 inches/acre, or a

pond size of 1,300 yd³/acre drained (Hill EPA, undated), while others may require a specified removal efficiency of the TSS input (e.g. remove 95% of pond input TSS).

CALCULATING POND AREA

Once constructed, the pond area A (m²) is fixed and is the most important pond size design parameter (the function and choice of pond depth is required to create quiescent conditions and store sediment, but does not determine the particle separation size of the pond).

The flow pattern between pond inlet and outlet is influenced by influent geometry, pond shape, wind action, inflow rate, pond depth, outflow geometry, etc. The pond flow pattern should therefore fully utilize the entire pond area, minimizing “dead spots”.

The inflow rate Q (m³/s) determines the “separation” particle size of the pond, since $A = Q/V$ (V cm/s = the settling velocity of the particle with a diameter which is the minimum particle size settled out for a given inflow rate into the pond – calculated using Stoke’s equation, or determined by settling tests on upslope soils, or determined by a particle size analyzer in conjunction with settling tests, etc).

Pond depth and retention time, without the appropriate calculated pond area could result in an “under-designed” pond. Stoke’s settling equation is no longer applicable for a mineral particle finer than the critical settling particle size – i.e. Stoke’s settling equation does not take into account the effects of Brownian motion. It is suggested that the critical settling particle size can be reliably determined by performing settling tests on representative soil samples. In addition, pond discharge quality “failures” may be acceptable occasionally (at pond inflow rates

in excess of the 24-hour, 10-year rainfall event, for example) provided the receiving water objective for TSS concentration is still achieved downstream of the pond discharge. Therefore, calculating pond area is specific to the local regulatory requirements and soil conditions at the mine site.

REGULATORY REQUIREMENTS FOR POND DISCHARGE QUALITY

Expectations for settling pond discharge quality vary based on local regulatory requirements, and are typically linked to a specified rainfall event determined by the regulatory authorities – e.g. the 24-hour, 10-year rainfall event is common. Rationalizing the basis for this “critical rainfall event”, or design pond inflow rate, varies by location, and regulators will hopefully base this requirement on some type of risk analysis - this then forms part of the regulatory definition of BMP. Higher rainfall events would be expected to generate higher TSS in the pond discharge (and naturally in the adjacent water course); whether local regulatory authorities provide relaxed discharge quality at the higher rainfall events will be variable, but if there is a relaxation, then it is suggested the relaxation could logically be linked to achieving the required receiving water quality standards (which are typically higher during higher stream flows, or the so called “turbid flow conditions”). Pre-mining background TSS conditions at various precipitation rates could logically be utilized to contribute to a more “scientific” and site-specific pond design area calculation/requirement by regulators. Mining companies are typically required to meet discharge quality requirements based on one, or sometimes all, of:

(a) BMP, with the BMP being defined by the local regulatory authority; and/or,

- (b) local regulatory requirements (which may not necessarily relate to BMP); and/or
- (c) whatever is necessary to comply with the downstream water quality standards.

As an example, in British Columbia (BC), Canada, requirement (a), relative to non-metal mines, is typically a pond discharge quality requirement of 50 mg/L TSS and is applicable to a pond inflow rate corresponding to, or lower than the 10-year, 24-hour rainfall event; in addition, (a) relative to metal mines and federal requirements (which supersedes the BC requirement), is approximately a 30 mg/L TSS in any discharge from the mining operation (including “runoff”); and (c) is based on BC receiving water quality guidelines. Determination of the applicable peak rainfall event and the return period should logically be based on a correlation of rainfall events and receiving water impacts on a site specific basis; the BC example would be based on so-called “turbid flow conditions” of the water quality guidelines. The following is an example, using BC receiving water quality guidelines (shortened version):

Clear Flow Periods - Induced (downstream of the pond discharge) suspended sediment concentrations should not exceed background levels by more than 25 mg/L during any 24-hour period.

Turbid Flow Periods - Induced suspended sediment concentrations should not exceed background levels by more than 25 mg/L at any time when background levels are between 25 and 250 mg/L. When the background concentration exceeds 250 mg/L, suspended sediment should not be increased by more than 10% of the measured background level.

SOIL PARTICLE SIZE AND POND DISCHARGE TSS

The portion of the particle size distribution of soils that will be eroded, and yield the TSS concentration into the pond, should be defined, since this may have the greatest influence on how the pond will be required to perform. As an approximation assume that the minus 5 mm portion of the soil particle size distribution will be the particle size distribution eroded into the pond, as a conservative approach. Scoping out the mine site soil characteristics will initially serve to define the general approach to designing the pond. This task should be performed diligently, and strive to accurately predict the operational phase of the pond inflow TSS size distributions. This will, for example, avoid installing a flocculant system which in practice turns out to be redundant; or conversely, the predictive testing may incorrectly determine that a flocculant system is not required – this may then lead to a lengthy period of exceeding pond TSS discharge levels, until a flocculant system can be retrofitted. Both these examples imply “unexpected” and additional costs.

As a generalization, and assuming discharge quality requirements similar to (a), (b) and (c) above, the approach to pond design will be linked, in particular, to the amount of (approximately) the % by weight of the minus 10 micron particle size fraction – or more logically, the particle size which is unable to settle in the pond (which, for soil mineral particles of similar density to quartz, may be even finer, e.g. 1 to 5 microns). Focusing on the “10 micron particle size fraction”, I suggest, is also based on economic considerations, since the pond area requirement is proportional to the square of the particle size to be captured in the pond: if BMP selected (say) a 2 micron particle size removal requirement, the pond size would

become 25 times larger in area (compared to being sized for a 10 micron particle removal).

As an example relative to regulatory requirements downstream of a sediment pond discharge:

Clear Flow Periods - The pond discharge (T mg/L TSS) shall not increase the upstream watercourse water quality by more than 25 mg/L TSS (downstream of the pond, where T_{DS} TSS = the downstream TSS at the “compliance point”) when the upstream water quality is ≤ 250 mg/L TSS – i.e.:

$$T \leq T_{DS} + 25(D - 1),$$

where D = the dilution of the pond discharge in the watercourse; this would typically apply for pond inflow rates up to the 10-year, 24-hour rainfall pond inflow rates.

Turbid Flow Periods - The pond discharge (T mg/L TSS) shall not increase the upstream watercourse water quality by more than 10% (downstream of the pond) when the upstream water quality is ≥ 250 mg/L TSS – i.e.:

$$T \leq T_{DS}(D + 10)/11;$$

this would typically apply for pond inflow rates exceeding the 10-year, 24-hour rainfall pond inflow rates.

Note that this approach also lends itself to “locating” the downstream compliance point at (say) a point of compliance significantly further downstream than the pond discharge – for example if there were natural elevated inputs of TSS downstream of the pond, then the compliance point could be downstream of the natural elevated inputs of TSS and downstream of multiple watercourse inputs; or, if the pond is located near the headwaters with low dilution, these equations may be used in the regulatory permit to provide a flexible solution.

For pond inflow rates below the 10-year, 24-hour rainfall pond inflow rate, additional capture of minus 10 micron particles would be achievable, but only for particles above the critical settling particle size. If we assume the critical settling particle size is approximately 2 microns (varying based on particle mineral S.G., shape, etc.), it becomes apparent that even small amounts of fines in the soils becomes problematic in terms of achieving 50 mg/L (and that soil particle size analyses requires analysis down to approximately the two micron particle size, or whatever is the critical settling particle size determined from soils testing and settling tests). For example, if the 10-year, 24-hour rainfall pond inflow rate contained 5000 mg/L TSS, and the soils eroded into the pond contained more than 5% of minus 10 micron particles, the estimated pond discharge would be 250 mg/L, or higher.

PARTICLE SETTLING LIMITATIONS IN THE POND

For discrete particles (i.e. un-agglomerated) in the pond fluid, the critical settling particle size to be aware of for pond design is that particle which is unable to settle based on the “energy” imparted to the particle from the water molecules in the pond, and this “energy” will counteract gravitational settling (this is, of course, the “Brownian Motion” phenomena). Hence the limitation of applying the Stoke’s settling equation to particles smaller than the critical settling particle size.

Other aspects affecting particle settling that we should also consider is the (typical) predominance of elevated particle charge (elevated Zeta potential) as it may affect agglomeration of particles (which, if this occurs, may significantly increase settling rate for particles smaller than the critical settling particle size). Typically, particle Zeta potentials in runoff appear to be elevated –

for example -50 mv for quartz particles at the expected pH range of many runoffs is quite sufficient to prevent agglomeration of fine particles (in particular, the particles smaller than the critical settling particle size). Lower Zeta potentials of approximately -10 mv (or +10 mv) are typical thresholds for allowing agglomeration to take place. This agglomeration is made possible by the universal presence of the van der Waals attractive force. While the van der Waals attractive force acts constantly, the Zeta potential is a function of pH, and the presence of potentially-determining ions in the pond water. Hence the usefulness of knowing the Zeta potential of the particles in the runoff at the pH of the pond, and knowing the zero point of charge of these particles. For example, at about pH = 7.0 for quartz, the typical particle charge is -50 mv, while the charge decreases with lowering pH, reaching approximately zero at pH = 2.0. Thus, quartz particles which are smaller than the critical settling particle size will be observed to agglomerate and settle at about pH = 3.0 (corresponding to a Zeta potential of -10 mv). This example for quartz serves as a useful surrogate for “typical” mineral particles entering the pond; the -10 mv may be assumed, in this context, to be the “critical” Zeta potential allowing the onset of agglomeration to occur. While pH lowering is not typically a viable “settling aid”, potentially determining ions, which may include cationic flocculants, are utilized as a useful settling tool, and it is suggested that when using the positive-negative flocculant combinations, that the Zeta meter may be required to be used on site to minimize the addition of “excess” cationic flocculant as a preventative against toxicity risk developing in the pond discharge.

Other factors affecting particle settling are the particle shape, surface “roughness”, mineral density, etc. These factors all conspire to require the pond area to be larger than if soil

particles were “perfect smooth spheres”. It is worthy to note that highly cohesive soils should be tested in such a way as to “preserve” fine particles in the soil being bound together and possibly remaining “bound” when entering the pond.

WHEN TO USE FLOCCULANTS?

The term “flocculant” is used to cover high molecular weight polymer settling aids (e.g. polyacrylamides) to distinguish them from “coagulants”, inorganic settling aids (e.g. lime, aluminum salts, etc.) and both are distinct from any “natural” agglomeration that may occur in the pond. The application of flocculants (or settling aids in general) to a sedimentation pond inflow is typically a result of the presence of “elevated” minus 10 micron particles in the soils eroded into the pond; less often, flocculants may be applied because the pond area is too small to remove the plus 10 micron particle size fraction – for example, there may not be sufficient space down slope of the land disturbance/runoff to provide a pond of adequate size. Or, the use of flocculants may be intentional to drastically reduce the capital costs of constructing a pond to accommodate the 24-hour, 10-year rainfall runoff event, and this may be particularly valid when the ponds are only required for one or two years, such as for the construction phase.

Flocculant manufacturers can typically assist in selecting the appropriate flocculant(s) efficiently. In addition, it is crucial to select the “correct” flocculant(s) and design and construct the flocculant addition system well ahead of operation of the pond. Flocculant testing on suspensions of “simulated runoff” samples, prepared from collecting representative soil samples and site water (depends whether site water contains any potentially determining ions that could enhance settling) and then preparing

suspensions (of the minus 5 mm size cut is suggested) with a ratio of solids to liquids which is representative of projected TSS concentrations expected to enter the pond. For example, storm events may generate approximately 500 to 5,000 mg/L TSS into ponds (and higher). The ratio (solids:water) may be refined if a RUSLE soil loss calculation can be applied. I suggest not performing settling tests on samples with unrealistically high TSS loading, as this may promote agglomeration, and settling that may not be duplicated at the more realistic storm runoff TSS loadings at the site.

Typically, the particle charge of the runoff particles is assumed to be negative. This is an important factor to be aware of when selecting flocculants. In addition, flocculant-induced toxicity (e.g. for Rainbow Trout, *Oncorhynchus mykiss*) appears to be clearly related to the fish gill being negatively charged (similarly for the predominant particle charge on particles in most receiving waters). Therefore, in order to achieve pond discharges which will pass the 96 Hour LC₅₀ test, we can assume that pond discharges should not contain significant amounts of positively-charged flocculant (and to a lesser extent, should not contain positively charged particles, e.g. due to excess addition of positively charged flocculant, which may then “convert” negatively charged particles in the runoff into particles which have an affinity to adhere to the fish gill and cause mortalities due to “smothering”).

Hence the importance of striving for the selection of flocculants of relatively low toxicity. This is a challenge, both in the searching and testing of flocculants, and then during the operation of a pond. In addition, there is an implied increased cost component when using higher toxicity flocculants, and an increased risk of generating a toxic discharge from the pond.

There is therefore a need to have a methodology/approach to estimate the risks associated with using flocculants at a mine site; establishing the risks associated with using specific flocculants then guides toward the necessary flocculant addition system which will provide an acceptable level of risk which minimizes the likelihood that the pond discharge will fail a 96 Hour LC50 test. Not surprisingly, regulatory authorizations for ponds using flocculants may have the requirement to perform a bioassay within the time frame it takes for the flocculated runoff entering the pond to emerge at the pond discharge.

As an example to determine a “risk assessment” methodology for a specific flocculant application, if the flocculant(s) addition dosage = C_{flocadd} mg/L, and the 96 Hour LC50 concentration of the flocculant(s) = C_{floc} mg/L, then if:

$[C_{\text{flocadd}}] / [C_{\text{floc}}] \geq 1.0$, consider this a high risk.

$[C_{\text{flocadd}}] / [C_{\text{floc}}] \leq 0.05$, consider this a low risk.

Note that the “1.0” is also 1.0 Toxic Units (T.U.), and the “0.05” is 0.05 T.U.

For flocculant proposals in the 1.0 T.U. range of risk, I suggest a more elaborate and sophisticated addition system is pertinent – metering pumps feeding flocculant(s) into the runoff flow, more frequent measurement of runoff flow rate, additional sampling of pond inflow TSS (correlated with on site turbidity measurements), etc. Particle charge measurement as a guide to avoiding the addition of excess cationic flocculant may be necessary when using higher toxicity flocculants. Costs may increase further if the use of higher toxicity flocculants requires a two/three pond system to better control the addition of flocculants(s): for example, a pre-

settlement pond to remove (say) plus 20 micron particles (and to provide a more consistent and less fluctuating flow rate); followed by a second pond where the flocculant(s) are added and rapid settling occurs; a third pond (if required) would be for the purpose of adding additional anionic flocculant to ensure that there is no excess cationic flocculant – a Zeta Meter would be an appropriate instrument to measure that excess flocculant(s) are not added.

Conditioning time is a crucial time aspect of flocculant application; when performing the preliminary settling tests with flocculants, a plot of conditioning time vs. clarification of supernatant is established; occasionally, some flocculants added beyond the optimum dosage may result in progressive worsening of clarity. The conditioning time established for a flocculant (or a flocculant pair – add the cationic followed by the anionic flocculants) must be provided between the runoff entry into the pond and the last flocculant addition location. To satisfy this conditioning time requires a physical flow length which provides the required conditioning time at the highest expected runoff rates. Failure to provide adequate conditioning time may result in added flocculant remaining in the fluid phase and not adsorbed onto the TSS entering the pond. Once the (flocculated) runoff enters the pond, the quiescent conditions do not allow significant “transfer” of flocculant onto the particles, nor does it promote further floc growth. The flocculant remaining in the dissolved state then moves through the pond to the pond discharge and can contribute to toxicity in the pond discharge. In addition, it is imperative that subsequent to the flocculant(s) addition, the runoff is receiving adequate and continuous mixing before entering the pond.

For flocculant addition proposals in the 0.05 T.U. range of risk, I suggest a more basic addition system is pertinent, and the

system may become even simpler and smaller when flocculants in the powder form are used. For flocculants in the 0.05 to 1.0 T.U category, setting the maximum risk potential could utilize the dilution, D, available in the receiving water course: e.g. the T.U. of flocculant added and entering the watercourse ≤ 0.05 as determined by $(T.U.)/(D+1)$. This measure of toxicity should be comparable to the 96 Hour LC10 (on Rainbow Trout) and could be usefully calibrated to *Daphnia magna* bioassays using the “rapid” mine site toxicity measurements (utilizing the induced fluorescent method for *Daphnia*). This method justifies more testing for application to flocculants, although it is successfully utilized for a variety of other toxicants.

“Operational Manuals” are suggested to be in place to guide operators of sediment ponds. While the operation of such ponds not using settling aids is virtually “passive” and requiring minimum attention, once flocculants are required, pond operation during storm events may require a considerable amount of attention. The frequently changing flow rates into the pond, coupled with a variability in the influent TSS (and the variability in the size distribution of the sediment entering the pond) necessitates an appropriate response in terms of the amount of flocculant added. The logistics of the flocculant addition may vary drastically from one site to another, increasing the difficulty of achieving adequate conditioning time. Also, one or both flocculants may be in the powdered form. When flocculants are added together, they need to be mixed together accurately in the correct proportions, based on the initial laboratory testing design. The locations of where the flocculants are added relative to the pond inlet requires careful planning and design. In addition, settling tests may reveal variations in the conditioning time as a function of the TSS concentration (and the variations in the particle size distribution). For example, at the

lower end of TSS concentration in the runoff entering the pond (e.g. 60 mg/L TSS) this lower density of particles may retard the formation of floc-growth rate significantly. Consequently, it is worth the effort to perform sufficient testing prior to pond design to select flocculants which allow a simpler flocculant addition system: lower toxicity flocculants; rapidly acting flocculants; higher molecular weight flocculants which are effective at lower concentrations, etc.

Consideration should also be given to drawing ponds down after the rainfall event in readiness for the next rainfall event to provide “additional” storage capacity. Pond drawdown can be performed as a flow-paced discharge rate coinciding with the requirement to meet downstream discharge quality for TSS. In addition, when the pond is filling up during a rainfall event, discharge from the pond at a lower rate than the storm event inflow rate provides an addition tool to have a lesser impact downstream of the pond.

The flocculant management plan and flocculant selection should focus on minimizing the risk of producing a toxic pond discharge. Some useful tools that provide an onsite measure to guide the flocculant addition/modulation are: a turbidity meter, a Zeta Meter, a rapid settling testing set-up, a mobile particle size analyzer, flow rate measurement of the runoff, flocculant addition metering, etc. On-site rapid TSS determination remains a challenge. Pond operators should receive the appropriate level of training to coincide with the particular type of flocculant addition system selected. A rapid onsite bioassay method may also be an asset when higher-toxicity, higher-risk flocculant systems are used (and calibrating to Rainbow Trout toxicity testing). Turbidity and TSS calibration curves may also be useful.

CONCLUSIONS

It is apparent that there are a number of options available to determine how a proposed sedimentation pond will perform (or to trouble shoot existing pond discharges with elevated TSS) by performing various tests on representative soil samples. Supplementary tools and tests that may gain better control are:

- (a) Perform sufficient testing to predict pond discharge quality, and whether settling aids are necessary (recommend doing this at least 6 months prior to pond construction).
- (b) If settling aids are unavoidable, perform testing to locate low toxicity settling aids.
- (c) Design an operating system which will assist in minimizing the addition dosage of settling aids.
- (d) Measurement of Zeta potential, both for synthetic suspensions using soil samples, and for actual inflows to existing ponds, and at times, for discharges from ponds, particularly when there are discharge toxicity problems occurring.
- (e) Use of a “mobile” particle size analyzer, applied to synthetic sample suspensions from soil samples, and on pond inflows and discharges.
- (f) On-site capability to perform rapid settling tests, to aid in ongoing optimization of flocculant addition (and to ascertain under what runoff conditions the application of flocculants should commence).
- (g) Turbidity measurements of settling test jar supernatant and runoff into the pond, the pond discharge and receiving waters.
- (h) On-site (“rapid”) bioassay capability to detect excess flocculant addition.
- (i) A flocculant addition management plan.
- (j) An erosion control management plan pertinent to the mine site upstream of the pond.
- (k) The pond discharge should pass a 96 Hour LC50 using Rainbow Trout (i.e. 5, or more fish, out of 10 tested should survive 96 hours).
- (l) Establish a Turbidity/TSS correlation.
- (m) Draw the pond water level down after the previous storm event (consistent with not exceeding receiving water quality and ensuring that settled solids in the pond are not being remobilized) to maximize the retention capacity of the pond and minimize the use of flocculants.
- (n) Bioassay frequency requirements should be based on the risk assessment of the actual flocculant(s) (toxicity) being used.
- (o) Flocculants being used which present a low toxicity only require the “basic” type of flocculant addition system, while the use of flocculants which present a high toxicity risk require a more elaborate flocculant addition system.

Figure 1 illustrates suggested testing and calculations which may be useful starting points to gain site specific information of how the soil particles at a mine site will respond in the settling pond, and then assist in the decision for the use of settling aids.

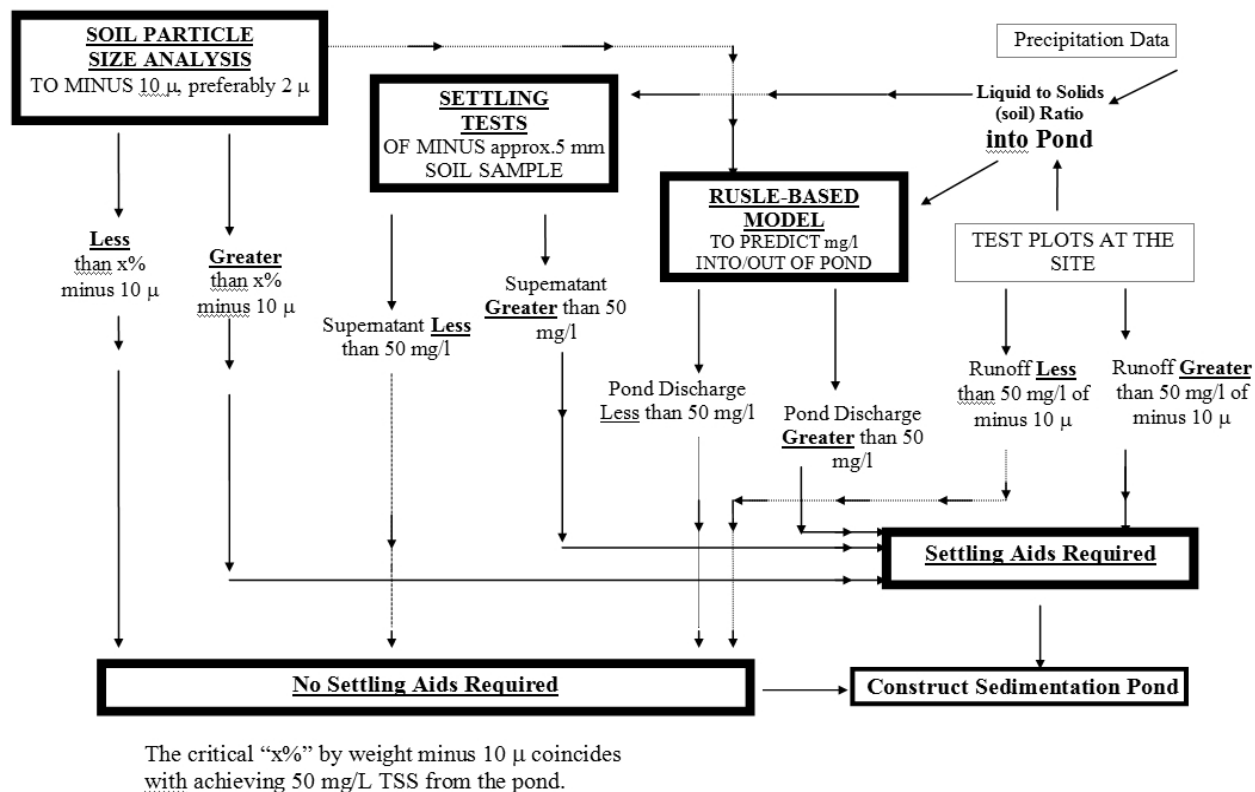


Figure 1. Methodology to determine need for settling aids.

REFERENCES

Alberta Environmental Centre, 1985, Effects on Fish of Effluents and Flocculants from Coal Mine Waste Water.

Allan R.B., and Davidge D.A., April 1985, An Evaluation of the Efficiency and Toxicity of Two Cationic Liquid Flocculants, Environment Canada.

Biesinger K. E. and Stokes G. N., March 1986, effects of Synthetic Polyelectrolytes on Selected Aquatic Organisms, Journal WPCF, Volume 58, Number 3.

Clark J.P., Treatment Of Runoff Containing Suspended Solids Resulting From Mine Construction Activities Using Sedimentation Ponds. Proceedings of the Twenty-Second

Annual British Columbia Mine Reclamation Symposium, September 1998, Penticton.

EPA Technology Transfer Seminar Publication, 1976., Erosion and Sediment Control (a handbook) - Surface Mining in the Eastern US, volumes I and II.

Goldman S.J., Jackson K. and Bursztynsky T.A., 1986, Erosion and Sediment Control Handbook, McGraw-Hill Book Company. Gray D., and Leiser A.T., 1982, Biotechnical Slope Protection and Erosion Control, Van Nostrand Reinhold Company.

Hall W.S. and Mirenda R.J., Acute Toxicity of Wastewater Treatment Polymers to Daphnia Pulex and the Fathead Minnow (Pimephales Promelas) and the Effects of Humic Acid on

Polymer Toxicity, Research Journal WPCF, Volume 63, Number 6, September/October.

Hill R.D., undated, Sediment Ponds - A critical Review, EPA.

Howie, H.J., Draft 4, 1981, Guidelines for the Design and Operation of Settling Ponds Used for Sediment Control in Mining Operations, Ministry of Environment, BC.

Kitchener, J.A., Principles of Action of Polymeric Flocculants, 1972, Br. Polym. J. 1972, 4, 217-229.

Oscanyan P.C., 1975, Design of Sediment Basins for Construction Sites, National Symposium on Urban Development, University of Kentucky, Lexington.

Slater R.W., Clark J.P. and Kitchener J.A. 1968, Chemical Factors in the Flocculation of Mineral Slurries with Polymeric Flocculants, VIII International Mineral Processing Congress, Leningrad.

Spragg L.D., Gehr R. and Hajinicolaou J., Polyelectrolyte Toxicity Tests by Fish Avoidance Studies, Wat. Sc. Tech. Volume 14, pp 1564 - 1567.

Yarsolav S., 1986, A cost-Sensitive Approach to Sediment Pond design, CIM.

Ward A.D., Haan C.T. and Barnfield B.J., 1979, Prediction of Sedimentation Basin Performance, Trans. ASAE.

Wolanski A., 1997, Environmental Considerations of the Use of Synthetic Polymers in the Treatment of Wastewater at Coal Mines in Alberta, Luscar Ltd., Edmonton, Draft.

NANISIVIK MINE TAILINGS DISPOSAL AN EXAMPLE OF A MINING BEST PRACTICE

Jim Cassie

BGC Engineering – Santiago, Chile

Geoff Claypool

BGC Engineering – Calgary, Canada

Bob Carreau

Breakwater Resources – Toronto, Canada

ABSTRACT: The phrase “best practices” simply refers to the best way of doing things. Regarding mining and environmental management, it refers to an on-going and integrated process of sustainable resource extraction from exploration through operations and to closure. The concept of best practices recognizes the requirement for avoidance or minimization of environment impacts, along with other important principles.

Nanisivik Mine was opened in 1976 at the northern end of Baffin Island in Canada’s North, in arguably one of the remotest and harshest environments in the world. With very little high Arctic mining experience, the mine staff and related consultants developed a design for sulphidic tailings that used the natural topography, the accessible construction materials and the cold climate to its maximum advantage. As the operations proceeded, design and construction practices were amended to reflect site experiences and knowledge that was gained. For years, test covers were monitored to collect site specific performance data to assess the proposed closure cover design for the tailings. In 2002, the economic ore reserves were depleted and the mine entered the closure and reclamation phase. As part of this process, the natural process of permafrost aggradation was incorporated into the construction of engineered covers over the sulphidic tailings and waste rock.

Reclamation has been substantively complete since 2007 and results from on-going monitoring indicate that the engineered covers are performing as designed; the deposits are physically stable and no negative environmental impacts have been noted. In the end, it appears that the design, operation and closure of the Nanisivik Mine tailings area constitutes a mining best practice for sulphidic tailings in cold regions. The paper reviews some of the design, operations and closure constraints, issues and performance indicators for the facility, which operated for some 26 years.

INTRODUCTION

Best Practices

Environment Australia (2002) refers to the phrase “best practices” simply as a “best way of doing things”. In relation to environmental management in mining, the following elements are noted:

- An on-going and integrated process of sustainable resource extraction from exploration through operations and to closure.
- Buy-in and commitment from all levels and groups within a mining company.
- The recognition and related avoidance or minimization of environment impacts.

These best practices cross all areas from technical to community relations to staff training and responsibilities. Cassie et. al. (2005) provides another example of mining best practice related to staff training.

Some selected important principles of mining best practices included the following:

- Ecologically sustainable development.
- Use of the Precautionary Principle.
- Use of well informed and trained staff.
- Communication and openness.
- Flexibility and continual improvement.

As such, mining best practices can change through time and vary from locations and specific conditions. As such, best practices might be further defined as simply the best way of doing mining for local conditions and communities. The current paper provides an example of such a mining case history from

Canada’s North and attempts to provide evidence for the noted principles.

Mine History and Closure

Nanisivik Mine was located at the northern end of Baffin Island in the Territory of Nunavut in the Canadian Arctic, as illustrated on Figure 1. The mine site operated between 1976 and 2002 in which time it processed over 17 million tonnes of ore to produce over 150,000 and 2,500,000 tonnes of lead and zinc concentrate, respectively. In addition, approximately 10,000,000 m³ of sulphidic tailings were produced.



Figure 1. Location Map for Nanisivik Mine

Prior to mid-2002, the Nanisivik Mine was scheduled to operate until the depletion of economic ore reserves in 2004 or 2005. However, depressed base-metal prices necessitated a re-evaluation of the mine production plan in mid-2001. This assessment resulted in a reduction of economic ore reserves such that these reserves were depleted in September 2002. Mining operations were permanently ceased at that time.

The Final Closure and Reclamation Plan (FCRP) for the mine was submitted to the

various regulatory bodies in March 2004. Approval of the plan was granted in July 2004 and reclamation activities began in August 2004. Reclamation of the tailings disposal area was undertaken between 2004 and 2006 with substantial completion by 2007. Performance monitoring of the reclamation measures is currently ongoing.

Site Conditions and Constraints

In order to understand the challenges of this site, it is important to note and acknowledge the significant site constraints described briefly below:

Remoteness – The site is located at 73°N latitude and is over 3,000 km north of Ottawa, the capital of Canada. Nanisivik was fortunate to have one of only two deepwater port sites in the Canadian High Arctic, but service is limited to the short open water shipping season. In addition, a gravel airstrip with 737 jet service was located at Nanisivik.

Cold – The mean annual air temperature is approximately -15°C which is extremely cold. Open water season is only 2 to 3 months long.

Dry – The mean annual precipitation equals 280 mm per year while evaporations averaged 200 mm per summer. Hence, the site is very dry.

Permafrost – The site is located on continuous permafrost to a depth of greater than 400 m.

Soils – The cold and the dryness result in very little soil development. As such, the primary construction material was derived from bedrock outcrops which constrained the

possible construction materials for operations and closure.

Tailings – The proposed tailings from this Mississippi Valley Type zinc-lead deposit contained extensive sulphide minerals. In fact, the tailings contained approximately 80% pyrite and had a Neutralization Potential (NP) to Total Acid Potential (TAP) Ratio of only 0.29.

Hence, the mine site staff were faced with undertaking the operations and storage of sulphidic tailings in one of the coldest, remotest and barren locations in the world, before any other such experience existed in the western world.

WTDA DESIGN AND OPERATIONS

The tailings disposal area was centered on West Twin Lake, which is situated approximately 6 km inland from the coast. The West Twin disposal area (WTDA), as it is known, is situated in a topographic low just east of Mt. Fuji, which is the highest landmark in the immediate vicinity, as shown in Figure 2.

West Twin Lake is mirrored by East Twin Lake, where potable water was derived for the mine. In order to prevent possible hydraulic connection between the two lakes, the level of West Twin Lake was kept lower than that of East Twin Lake. Initial environmental survey work in mid-1974 noted no fish population was observed within the Twin Lakes system. In addition, the tailings were potentially acid generating as noted previously. As such, in late 1976, the tailings deposition began in West Twin Lake under the lake level to limit potential oxidation of the tailings.

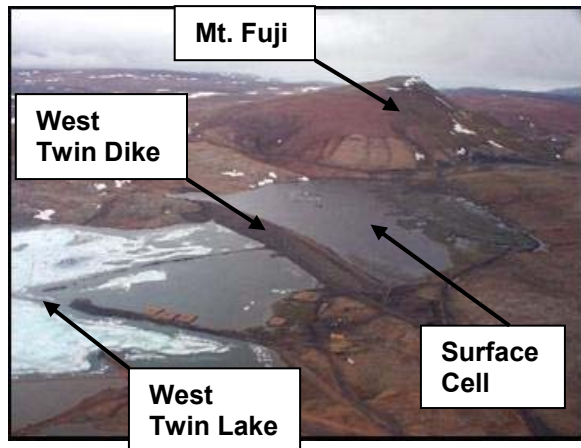


Figure 2. View of WTDA before reclamation (2000)

When the mine initially began, the proposed mine life was 12 years. The original ore reserves were estimated to be 6.5 million tonnes, which was expected to result in the generation of approximately 5 million tonnes of tailings over this initially specified mine life. By mid-1989, 6 million tonnes of tailings had been generated and placed in West Twin Lake and 2.6 million tonnes of proven ore reserves were still remaining. At that point, it became apparent that the tailings volume that would be generated over the eventual life of the mine would exceed the original lake volume and that additional storage capacity would be required for future tailings.

During the placement of tailings within West Twin Lake, two tailings “causeways” developed from the beaching of tailings solids. Terratech (1989) undertook an initial review of potential options for increasing the storage potential of West Twin Lake. Five potential containment dike alternatives were provided; two of which used these existing tailings causeways. Two boreholes were drilled into the tailings causeways in June 1989 and frozen conditions were encountered to a depth of 12 to 13 m.

It was therefore decided to divide West Twin Lake into two sections using a frozen earthen

dike, situated on top of the frozen tailings causeways. The eastern portion of the lake, the Reservoir, would maintain its near-original lake level and include one deep pocket of water for emergency tailings deposition during mid-winter conditions. The western part of the lake, the Surface Cell, would become the main deposition area for the tailings and would rise above the original West Twin Lake level. Initially, it was proposed to place tailings in the lake to a maximum height of 5 to 6 metres (Elevation 376 m) above the original lake level.

The dike was placed along a pre-existing north-south tailings causeway, which prior to being used as the foundation for the dike, extended to within 50 to 75 m of the south shoreline of the lake. Based on subsurface temperature readings within the causeway, the 0°C isotherm was at least 10 m below the original lake level (Terratech 1990). Thus, a frozen foundation for the dike was in place for a majority of its length.

In 1990, the initial lift of the West Twin Dike was constructed, providing additional storage capacity for tailings disposal. The dike was constructed of frozen shale fill and was built in an upstream manner. Each annual lift construction begins on top of beached tailings material deposited in the previous year’s construction and sealing phase. During the late winter, weathered shale rockfill was hauled and dumped, spread with a dozer, moisture conditioned and compacted (with construction traffic) in 30 to 40 cm lift thicknesses to permit freezing of water in the void spaces and nominal compaction to take place. The dike was raised approximately 2 m annually between 1990 and 2000, to an ultimate height of approximately 18 m. Additional details on the specific construction methodology developed by the mine site staff and a related seepage event account is provided in Cassie and LeDrew (2001).

Construction of the West Twin Dike divided West Twin Lake into two cells; the sub-aerial cell (Surface Cell), and the sub-aqueous cell (Reservoir), thereby creating the West Twin Disposal Area (WTDA), as shown on Figure 2.

The presence of the West Twin Dike permitted the sub-aerial deposition of tailings in the Surface Cell. During operations, a water cover of varying thickness was applied to the tailings in the Surface Cell to limit oxygen exchange and to provide dust control. Water was transferred manually from the Surface Cell to the Reservoir using siphons. The Reservoir was further divided with the construction of the Test Cell Dike, which created a Test Cell devoted to studying reclamation cover options. The Reservoir contained mostly subaqueously confined tailings, with a small area of sub-aerially exposed tailings along the base of the West Twin Dike and Test Cell Dike. Water was released seasonally from the Reservoir to the environment, once deemed to be compliant with water quality requirements, through an outlet control structure into Twin Lakes Creek which discharges into the Arctic Ocean approximately 10 km downstream from the WTDA.

WTDA CLOSURE

General

Progressive reclamation planning was undertaken for the mine site throughout the 1990's. Due to their sulphidic nature, the tailings posed potential negative environmental impacts, if not reclaimed appropriately. As such, the following reclamation objectives were developed for the WTDA:

- Isolate the potentially acid generating tailings from the atmosphere to

minimize the risk of acid rock drainage;

- Minimize the risk of physical movement of the tailings to the environment; and,
- Provide a safe and useable surface environment that corresponds to the natural surroundings.

The reclamation objectives were to be achieved by encapsulating the sub-aerial tailings in the Surface Cell and Test Cell in permafrost, thereby using the harsh climatic conditions experienced by the site as a benefit. It was proposed this be done by constructing a permafrost aggradation cover consisting of natural materials and providing adequate surface drainage through the area such that water would not pond on the tailings covers. The sub-aqueous tailings in the Reservoir were to remain under water cover.

Reclamation planning included development and monitoring of a test cover program, development of a final reclamation cover design (including geothermal modelling with climate change considerations), geothermal assessment of the tailings deposit and completion of a site hydrology study for input into the design of various hydraulic structures. The following sections provide details regarding the test cover program and the development of the reclamation plan for the WTDA.

Cover Design

The design process for the reclamation cover for the tailings deposit involved the following:

- Test Cover Construction and Monitoring 1990 – 1997;
- Geothermal Modeling – 2001 and 2002; and

- Development of Final Cover Design – 2003.

A test cover program was initiated in the early 1990's, when it became evident that on-land deposition of tailings would be necessary and that subsequent reclamation of these on-land tailings would eventually be required. As such, a number of test covers were constructed using various designs. The test covers were constructed primarily of granular shale fill derived from locally occurring outcrops and were surfaced with lighter coloured, coarser granular material sourced from local overburden deposits of re-worked glacial materials. The shale fill is comprised primarily of cobble, gravel and sand sized particles. The shale material exhibits low potential acidity and high Neutralization Potential and is considered an acid consuming material (Lorax 1998).

The test covers were then instrumented with geothermal monitoring instruments to assess the geothermal performance of each individual cover design. The test covers were monitored between 1992 and 1997. The annual progression of the active layer thaw in each test cover was monitored using frost gauges and thermocouples. The results were used to determine the sensitivity of active layer thaw penetration to the design variations.

The results of the test cover program indicated that the active layer thaw was confined within the cover materials (a depth of less than 1 m) within three years of cover construction. The ability of the cover to restrict the migration of the thawing front is related to the development of an ice-saturated layer at the base of the cover. For migration of the thawing front to occur into the underlying tailings, the ice-saturated layer at the base of the cover must be melted. Due to the latent heat of fusion effect, a greater amount of energy is required to melt the ice.

The ice-saturation along the base of the cover prevents the underlying tailings from thawing, thus preventing any oxidation of the tailings and any leaching of metals from the tailings.

The results of the test cover program were used to calibrate a geothermal model in order to develop a final cover design that included global warming forecasts. The modeling was intended to provide a final cover design that would maintain the underlying tailings in a perennially frozen state under various global warming scenarios. The climate warming scenarios considered are summarized as follows:

- Mean annual air temperature = -15.1°C
- 1 in 100 year warm year = -13.3°C
- Best estimate warming (2100) = -12.3°C
- High sensitivity warming (2100) = -10.1°C

Based on the geothermal performance of the test covers and the results of geothermal modelling conducted, it was determined that the final design of the reclamation cover for the tailings would be comprised of 0.25 m of armour material (coarse-grained, granular materials) overlying 1.0 m of granular shale fill.

The shale portion of the cover provides the main thermal barrier effect due to its insulating properties. The armour portion of the cover has various purposes. Due to its coarse grain size, it provides erosion protection for the underlying shale materials. In addition, due to its light colour, it provides additional geothermal benefits by reflecting some visible light radiation. Based on the results of the modeling, this proposed cover design provided adequate protection to resist both the estimated 1 in 100 year warm event and the High Sensitivity estimate of global warming over the next 100 years.

Reclamation Construction

The permafrost aggradation covers were constructed at the WTDA in 2004 and 2005. In total approximately 750,000 m³ of granular shale fill and 175,000 m³ of armour material was placed during cover construction. The shale was typically placed in 0.5 m thick lifts and was often applied in stages to allow for dissipation of pore pressures within the underlying tailings. The shale fill was often observed to contain various amounts of entrained ground ice due to the presence of in-situ ground-ice seams encountered within many of the quarries. As such, the armour material was not applied until September 2005 to allow for the melting of any entrained ground ice within the shale fill and application of additional shale fill, where required. This staging would limit deformation of the final graded surface of the cover after placement of the surficial armour material. A photograph of the WTDA following completion of all reclamation measures is provided on Figure 3.

A spillway sized to convey the Probable Maximum Precipitation event (140 mm/24h) was constructed to passively transfer water from the Surface Cell to the Reservoir. The spillway is approximately 550 m in length, 6 m wide at the base and was excavated through a combination of frozen soils and frost affected dolostone bedrock.

PERFORMANCE

Instrumentation

The Surface Cell and Test Cell are instrumented with thermistors, vibrating wire piezometers, frost gauges and ground water

monitoring wells. The instrumentation has two main purposes;

- Assess cover performance by monitoring the depth of the active layer thaw; and
- Monitor the ground temperatures, pore pressures and water quality in the thawed tailings during freezeback.

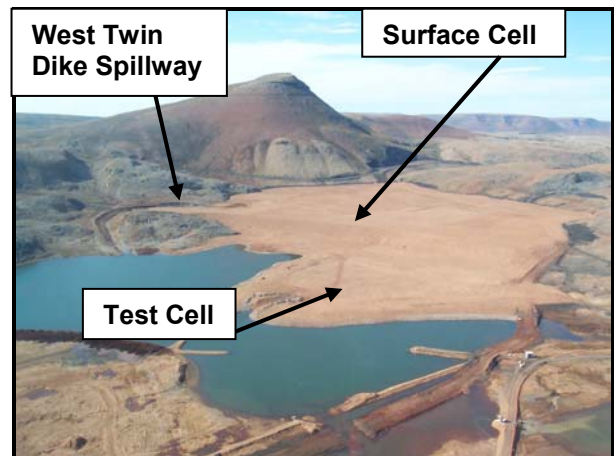


Figure 3. West Twin Disposal Area Post-Reclamation (August 2006).

In addition, the water quality of the run-off from the Surface Cell cover and the water flowing out of the WTDA to the receiving environment is assessed on a bi-weekly basis during open water periods between July and September. The following sections review the monitoring data collected to-date and its significance in assessing the cover performance and the freezeback of the underlying tailings.

Cover Performance

The data collected throughout 2008, the third year since completion of the reclamation covers in 2005, provides an indication of the progression of the active layer thaw throughout the year, as illustrated by the graph provided on Figure 4.

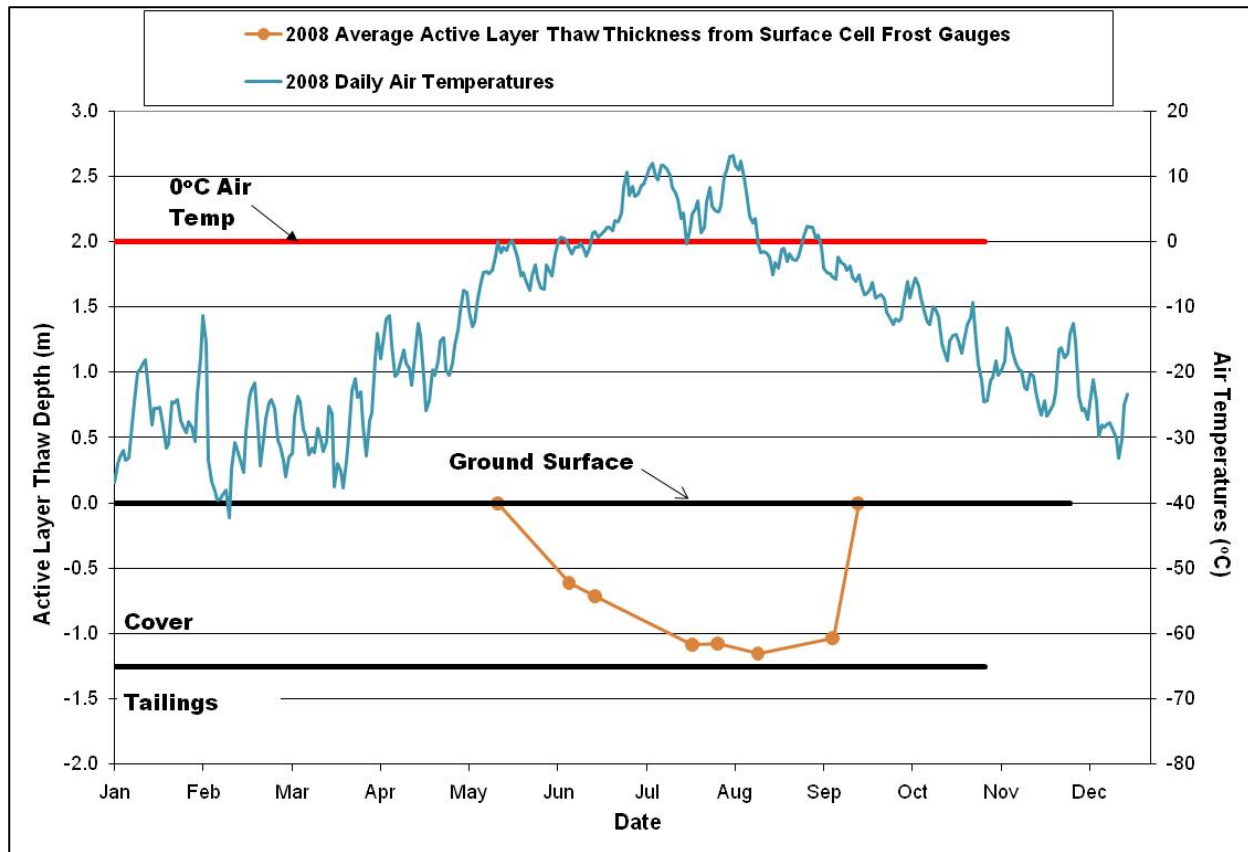


Figure 4. 2008 Geothermal Monitoring Data from Surface Cell Cover

As can be seen, the active layer migration into the cover begins by early May. The thaw depth had reached approximately 1.1 m bgs by early July. The cover had fully frozen back by late September. The results of the geothermal monitoring of the active layer indicate the average maximum thaw depth was approximately 1.15 m, approximately 0.1 m above the base of the cover.

The design provides a contingency in cover thickness to account for extreme warming events and long term global warming effects. However, short term performance following construction was expected to be variable until ice saturation at the base of cover is completed. This is expected to take time due to low amounts of precipitation typically experienced by the site. In addition, the first few years following construction have been abnormally warm, slowing the development

of the ice saturated layer at the base of the cover. Given the warm years following construction, the cover performance is as good, or better, than expected in the short term and is anticipated to get better with time.

Water Quality

During the summer months, samples are collected from the spillway inlet, to monitor the quality of the run-off from the Surface Cell cover, and at the West Twin Outlet Channel where water from the Reservoir flows into Twin Lakes Creek. Water samples are testing for a number of parameters, but of primary interest is the total zinc concentration due to its importance with respect to regulatory discharge criteria. Figure 5 provides the total zinc concentrations observed at the spillway inlet since completion of the Surface Cell cover in 2005.

In 2005 and 2006, the first two years following construction, the total zinc concentration was observed to increase later in the summer, when the active layer thaw was at its deepest amount. In 2007 and 2008, the zinc concentrations were observed to

remain low throughout the year. These results suggest that the improved performance of the cover in confining active layer thaw within the cover materials has had a beneficial effect on the quality of the surface water run-off.

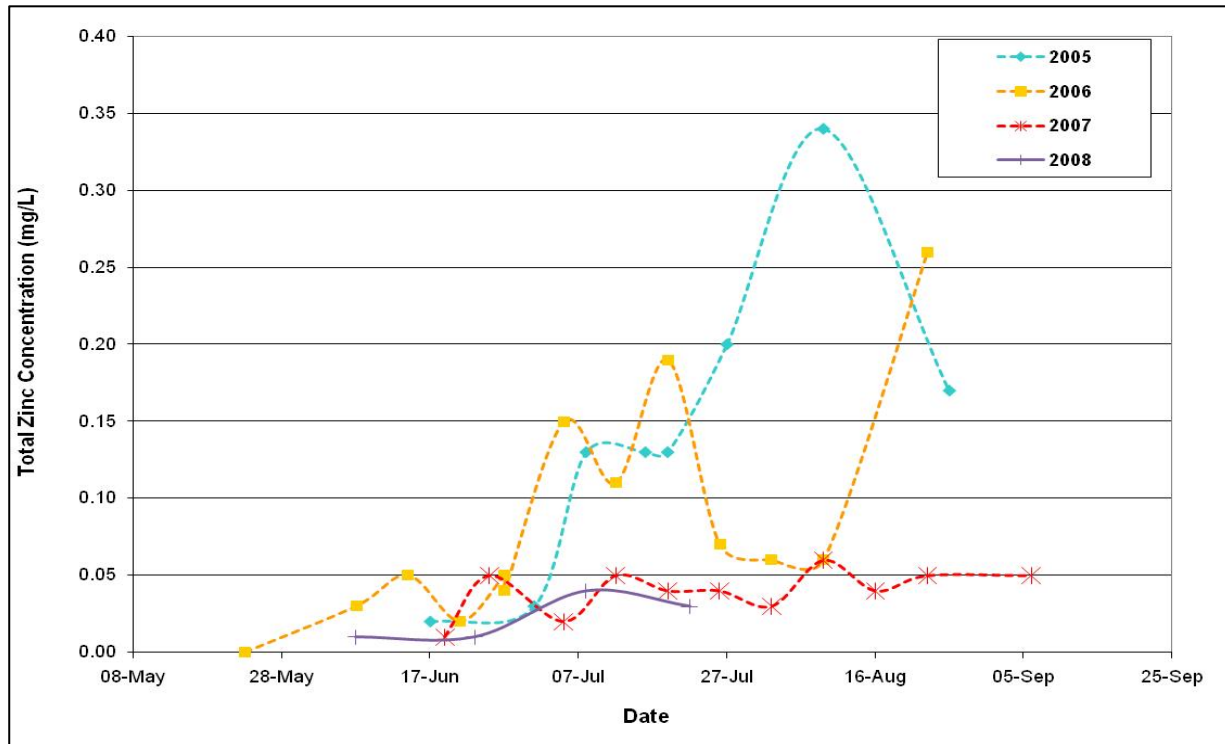


Figure 5 Water Quality Monitoring – Surface Cell Run-off

Figure 6 provides the water quality monitoring data from the West Twin Outlet Channel. As can be seen, the total zinc concentrations have been measured to be within regulatory discharge criteria every year since completion of the cover systems at the WTDA. Some improvement in the water quality has been observed at this location as well, particularly early in the thaw season.

CONCLUSIONS

This paper describes the design approach, test cover program and the reclamation measures

undertaken for a sulphidic tailings area at a remote location within the Canadian Arctic. In terms of best practices, the project took the following steps:

- The mine selected a non-fish bearing lake for the initial subaqueous disposal of sulphidic tailings, surrounded within a basin of permafrost. Subaqueous disposal is still one of the most practical and effective methods of dealing with potentially acid-generating tailings.
- Prior to full lake capacity, the mine staff and their consultants formulated a new approach that accommodated all aspects

and conditions including the frozen tailings causeway, the constrained water

level relative to East Twin Lake and the limited construction materials.

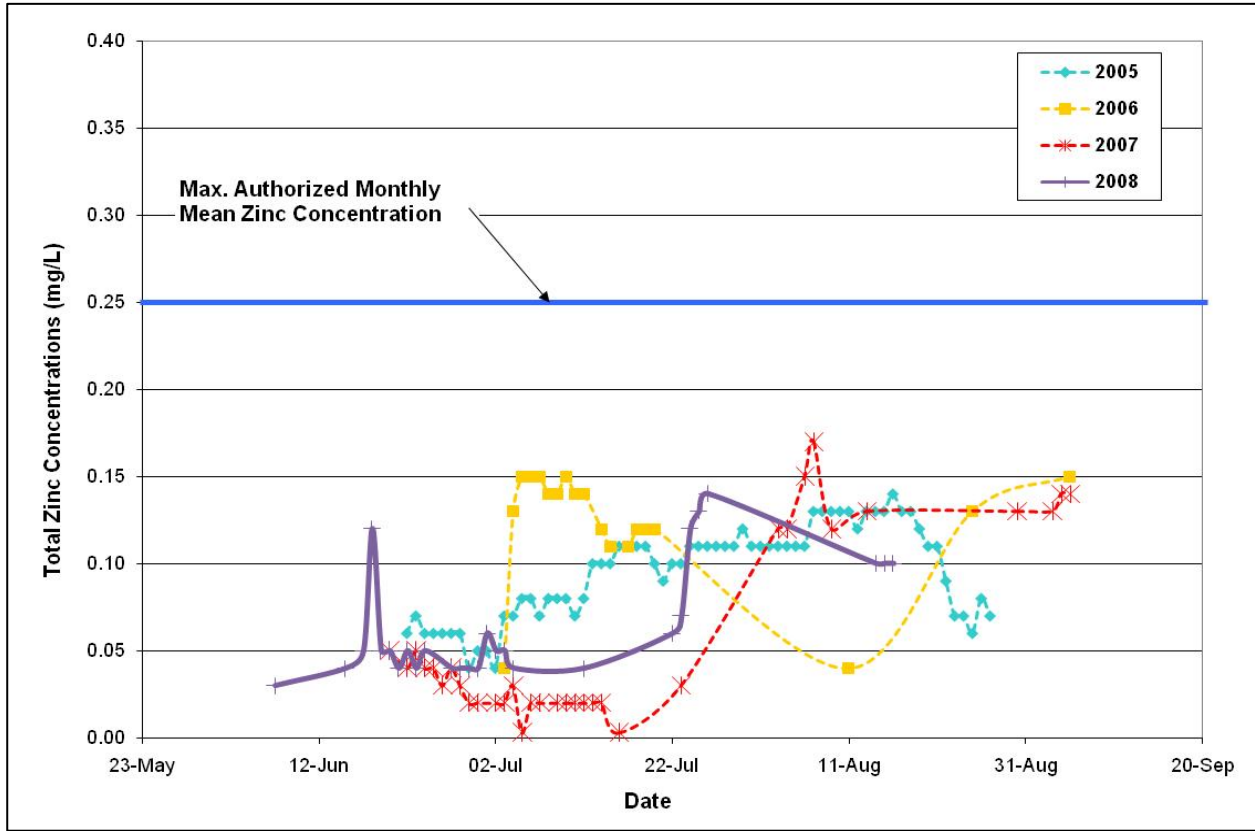


Figure 6. Water Quality Monitoring Results

- The West Twin Dike design and construction respected the use of weathered shale materials constructed within the cold environment. Operations staff determined and laid out a practical construction basis for building this frozen dike during the late winter season. This upstream-constructed frozen dike is unique to the authors' knowledge.
- Test cells with various cover configurations were constructed 12 years before the mine was closed and 7 years of field data was collected to support their proposed cover design.

- Permafrost aggradation covers, designed using local materials and with an allowance for climate change, were used to encapsulate the tailings (and the waste rock as well) in permafrost and thus isolate the sulphidic mine waste from the arctic environment.

The results of performance monitoring undertaken to-date suggest that the covers have been successful in achieving the design objectives by maintaining the tailings in a perennially frozen state. Surface water runoff from the tailings area meets regulatory discharge criteria and continues to improve with time. In the end, the design and closure

met the challenges of the remote and challenging locations and meets the definition for a mining best practice.

ACKNOWLEDGEMENTS

The authors would like to acknowledge Breakwater Resources Ltd. for their permission to publish this paper. BGC would also like to acknowledge the vision of the former mine staff and their consultant Mr. Frank Tordon, P.Eng. in developing and implementing the tailings area design and closure concepts. Further, the recent site staff should be commended for their meticulous efforts in collecting the monitoring data under challenging conditions.

REFERENCES

Cassie, J.W. and LeDrew, K., 2001. Tailings Deposition and Dike Construction at Nanisivik Mine, Nunavut. Presented at the 6th International Symposium of Mining in the Arctic, Nuuk, Greenland, May 28-31, 2001.

Cassie, J.W., Haggard, D. and Sedgwick, D., 2005. Geotechnical Staff Training at Closed Mines – A New Mining Best Practice. Presented at the Northern Latitudes Mining Reclamation Workshop, Dawson City, Yukon, May 24-26, 2005, Paper #3.

Environment Australia, 2002. Best Practice Environmental Management in Mining. Commonwealth of Australia, August 2002.

Lorax Environmental 1999. Acid Generating Potential of Tailings and Shale Cover Materials – Kinetic Testing Final Report. Prepared for Nanisivik Mine, September 1999.

Terratech, 1989. Geotechnical Investigation, Proposed Tailings Containment Scheme, Nanisivik Mine. Report No. 1359-1, submitted to Nanisivik Mines Ltd.

Terratech, 1990. Geotechnical Investigation, Permafrost Aggradation, Nanisivik Mine, NWT. Report No. 1434-1, submitted to Nanisivik Mines Ltd., November 14, 1990.

Oil Sands Tailings II

HIGH PORE PRESSURES WITHIN EMBANKMENT CONSTRUCTED OF LEAN OIL SANDS

J.T.C. Seto and K.W. Biggar

BGC Engineering Inc., Edmonton, Alberta, Canada

G.W. Ferris

BGC Engineering Inc., Calgary, Alberta, Canada

T. Eaton

Shell Canada Ltd., Calgary, Alberta, Canada

ABSTRACT: At the Muskeg River Mine, a series of dykes up to 70 m high are being constructed within the mined-out open pit to store tailings. These dykes are constructed with mine site equipment using earthfill with low-grade bitumen, i.e. lean oil sands. After approximately 20 m of fill was placed, piezometers were installed and high pore pressures were observed at several locations. The pore pressures have been very slow to dissipate. A field and laboratory investigation program was carried out to determine the effect of these pressures on dyke stability. High pore pressures were found to have developed where heavily-compacted fill was placed near its optimum fluid content. Triaxial compression tests showed that the dense fill behaves dilatatively and gains strength with increasing strain. Thus, total stress stability analyses were considered more appropriate than effective stress analyses and undrained strengths of the dyke fills exhibiting high pore pressures were determined.

INTRODUCTION

Shell Albian Sands' Muskeg River Mine, located approximately 8 km northeast of Fort McKay, Alberta, is currently being developed. As part of the mine waste management plan, a series of dykes, designed with an ultimate height of 70 m, are being constructed within the mined-out open pits to store tailings from the extraction process. These dykes are being constructed with mine site equipment and mine waste materials that contain low-grade bitumen (also referred to as "lean oil sands").

After approximately 20 m of fill was placed in Dykes 1 and 2, some piezometers installed within these dykes recorded pore pressures higher than expected in the design. Figure 1 shows the locations of the piezometers, including those exhibiting high pore pressures. Fill placement in these areas was suspended and pore pressures were monitored. After more than a year, the high pore pressures had not dissipated appreciably and there was concern about the implications of these high pore pressures on dyke stability.

A detailed study was carried out to answer the following questions:

- What was causing the high pore pressure?
- How extensive were these high pore pressure areas?
- How should the high pore pressures be considered in current and future dyke design and construction?

What design strengths should be used for these areas with high pore pressure?

The study included a review of construction monitoring data and a field and laboratory investigation program.

BACKGROUND

Dyke Design

The dykes were designed as earthfill embankments with a full-height sand chimney drain, an upstream seepage control blanket, and a downstream sand drain blanket. The design of the dykes evolved over time as the tailings management plan changed, and as experience was gained from construction and performance monitoring (Klohn-Crippen Berger Ltd., 2005; 2008).

The dykes were constructed of waste materials from the mining operation. Dyke design was intended to be sufficiently flexible such that the waste materials could be used as fill as required by the dyke raising schedule. The waste materials include lean oil sand, clayey facies, and mixed facies. These waste streams were split into categories based on the expected geotechnical performance. The embankment is largely constructed of Types 1 and 4 fills. The design values for these fills are listed in Table 1.

Construction History

The dyke fills were intended to satisfy a “rut and roll” criteria to ensure proper compaction of thick fill lifts (up to 1.5 m thickness) using 400 ton haul trucks.

Table 1. Material specifications for Types 1 and 4 Fills.

Fill Type	Description	Friction Angle (°)	Design r_u
Type 1	Good quality sandy fill	33	0.3
Type 4	Moderate quality sandy fill	28	0.5

The pore pressure ratio, r_u , is defined as:

$$r_u = u/\sigma_v \quad (1)$$

where u = pore water pressure and σ_v = overburden pressure.

The maximum rut and roll were specified to be 50 mm and 100 mm for each the Types 1 and 4 fills, respectively. In addition, minimum compacted dry densities of 1700 kg/m³ and 1650 kg/m³ were specified for the Types 1 and 4 fills, respectively.

Construction of Dykes 1 and 2 began in November 2005. During the first construction season, April to July 2006, approximately 20 m thick fill was placed. Nine vibrating wire (VW) piezometers were installed within the fill in July 2006, a number of which indicated piezometric elevations greater than allowed for in the design and showed very little pore pressure dissipation over time, even after several months. Fill placement was temporarily suspended. In March 2007, an additional twelve piezometers were installed within the dyke fill to verify that the measured pore pressures from the previously-installed piezometers were dependable. The results of these installations validated the earlier measurements. In October/November 2007, 7 m of fill was added in the areas around the piezometers where high pore pressures were recorded. Most piezometers experienced an increase in pore pressure but a decrease in pore pressure ratio because the increase in

over-burden pressure. Subsequent load increments (applied only to portions of the

structure) did not further increase the pore pressure ratio.

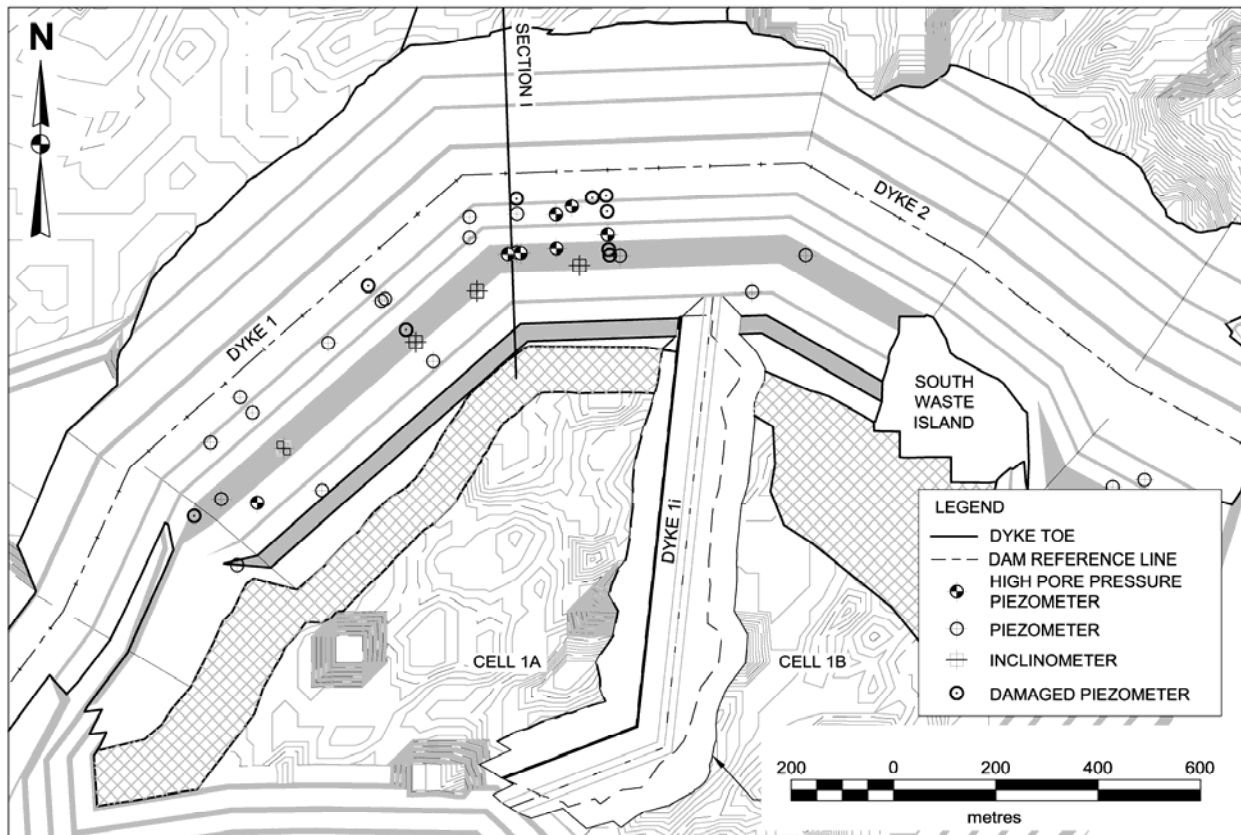


Figure 1. Dyke and instrumentation layout.

Only one of the fifteen piezometer tips installed in Dyke 1 exhibited high pore pressures with slow dissipation. In contrast, Dyke 2 showed more piezometer tips measuring pore pressures exceeding the design pore pressure ratio of 0.5. Figure 2 shows a typical section and the current measured piezometric elevations through the high r_u area of Dyke 1.

Construction Monitoring

Examination of QA/QC monitoring data during construction indicated that the fill materials are uniformly to poorly-graded

Sand and Silt, with trace to some clay. There is little difference in the as-placed particle size distribution between the Types 1 and 4 fills.

Figure 3 shows the Standard Proctor maximum dry density (SPMDD) versus fluid content results for Types 1 and 4 fills. Note that fluid content is de-fined in this paper as the ratio of mass of fluids (bitumen and water) divided by the mass of solids (Lord & Cameron, 1985). Compaction-wise, there is little to discern between the two fill types. The SPMDD varies considerably, with the

majority of tests ranging from 1600 to 1900 kg/m³. On average, the SPMDD appears to correspond to the 6% air voids line.

Figure 4 shows the Troxler field density versus fluid content measurements for Dykes 1 and 2. On average, the fill was compacted to a dry density of 1750 kg/m³ and a fluid content of 13%. Approximately 27% of the Troxler measurements indicated dry densities above 1800 kg/m³ in each dyke. Approximately 53% and 60% of the Troxler measurements indicated dry densities above 1750 kg/m³ in Dykes 1 and 2, respectively. For a given fluid content, Troxler-measured dry densities are lower than the laboratory Standard Proctor maximum dry densities. The “line of optimums” for the dyke fills generally corresponds to the 10% air void line, as shown in Figure 4.

The archived records from Environment Canada’s meteorological station at Fort McMurray Airport were also reviewed to determine if portions of dyke construction occurred during periods of abnormally high rainfall during the construction seasons of 2006 and 2007. Both years were noted to be dry compared to the normal period of 1971-2000.

LITERATURE REVIEW

Lean Oil Sand

Lean oil sand has been widely used by others in the oil sands industry as construction material for engineered structures, including embankments and dykes (e.g. Lord & Cameron, 1985; Cameron et al., 1995a; 1995b, Ashton & Cameron, 1995; and Cameron & Fong, 2001).

Lean oil sand is a four-component system of bitumen, water, gases and solids. Bitumen has a specific gravity of approximately 1.03 (Lord & Cameron, 1985). It also has a higher viscosity than water, and thus is not as mobile a fluid.

Lord & Cameron (1985) found that the geotechnical characteristics of lean oil sand were generalized as follows:

- bitumen content decreases with increasing fines content;
- optimum fluid content and maximum dry density varies with bitumen content and inherent grain size distribution; and
- increased bitumen content reduces the maximum dry density obtainable from a Standard Proctor, reducing it from, on average, 1805 kg/m³ at zero percent bitumen to 1700 kg/m³ at 9% bitumen.

Lord & Cameron also reported that compacted oil sand has very poor trafficability characteristics when the fluid content is wet of optimum. When dry, roll (waving of surface under moving load) was observed with the higher grades of oil sand. Even under proper compaction, the compacted oil sand can become slick when wet and the surface deteriorates rapidly when subjected to vehicular traffic.

Pore Pressure Development During Embankment Construction

When earthfill is compacted in an embankment, the water content is usually controlled to be near Standard Proctor optimum to facilitate compaction. The fill is typically compacted to a relatively high degree of saturation and heavily overconsolidated.

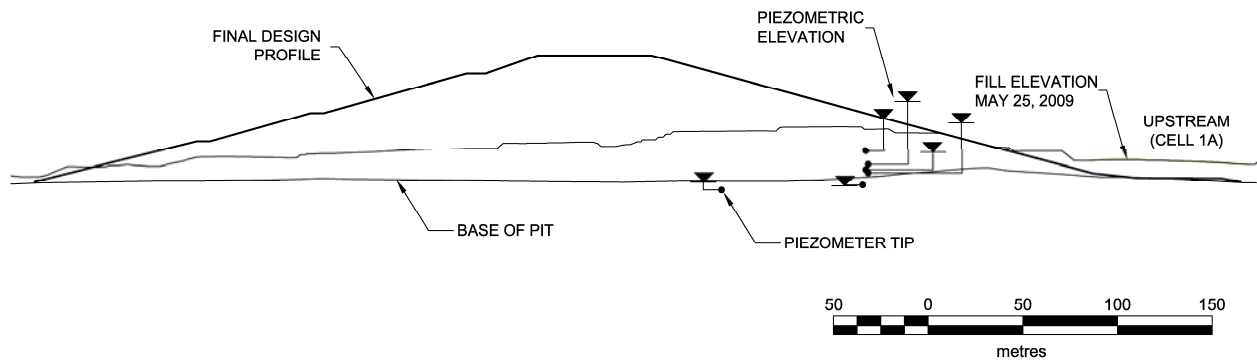


Figure 2. Section 1: dyke cross section showing piezometric levels across high pore pressure zone.

The partially-saturated, compacted soil will initially exhibit negative pore pressures. As additional fill is placed, the load imposed on the earthfill lower in the embankment will produce an increase in pore pressure, resulting eventually in positive pore pressures (Fell et al., 2005).

Pore pressure generation during embankment construction has been widely studied (e.g. Bishop, 1954; Sherard et al., 1963; Li, 1967; Sherman & Clough, 1968; Rivard & Goodwin, 1978; Matheson et al., 1991). It is widely acknowledged that the pore pressure ratio magnitude at the end of construction is affected by: a) placement water content; b) drainage conditions; c) fill height and permeability; d) degree of compaction; and e) rate of construction.

While there has been little published information about the permeability characteristics of compacted lean oil sand, there have been numerous published reports on the effects of compaction effort and degree of saturation on the hydraulic conductivity of glacial tills and compacted clay liners (e.g. Leroueil et al., 2002; Daniel & Benson, 1990). Increasing the compactive energy decreases the hydraulic conductivity of the soil. Furthermore, the hydraulic conductivity of a fine-grained soil can

decrease by several orders of magnitude between a state just dry of the optimum water content to a state just wet of optimum.

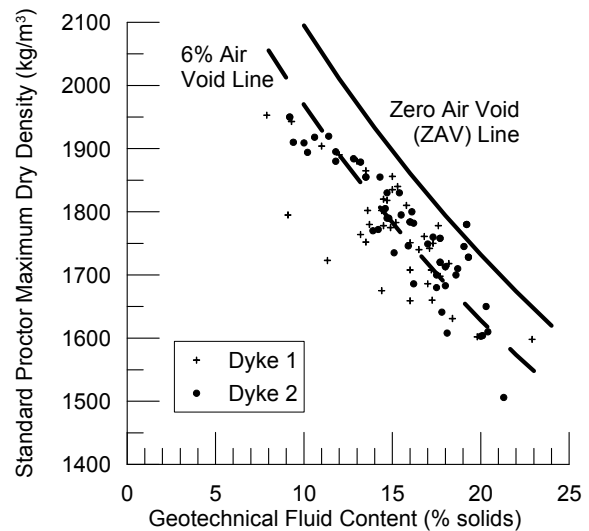


Figure 3. Standard proctor maximum dry densities during dyke construction.

Reported Case Histories

Nipawin Dam, Saskatchewan

Matheson et al. (1991) reported on the performance of two earthfill dams for the Nipawin Hydroelectric project constructed with a non- to low-plastic sand and silt. The embankment was well-instrumented with

piezometers, slope inclinometers, and survey monuments to monitor pore pressures and displacements during and after construction.

During the first two years of construction, 1983 and 1984, the fill was compacted to an average density just below its SPMDD and, on average, 1% dry of optimum. Construction pore pressure ratios were well below design limits (0.4). During the spring of 1985, rainfall was higher than average and during that period, water contents increased to, on average, 0.2% wet of optimum. Measured pore pressures in the embankment fill indicated a relatively steep increase in pore pressure ratio with increasing water content, which was attributed to the rapid rate of construction and the low compressibility of the compacted fill.

The reservoir was impounded to full supply level in the fall of 1985. Deformations were closely monitored and stabilized, as required. Pore pressure measurements from within the embankment fill showed continued slow dissipation of construction pore pressures, with little response to reservoir loading. It was estimated that it would take approximately five years for the construction pore pressures to dissipate.

Medellin Hydro Development, Columbia

Li (1967) reported on the construction and performance of three earth dams for the Medellin Hydro Development. The three dams, located in a humid tropical zone in the Central Andes mountains, ranged in height from 29 m to 50 m, and were constructed with a low-plastic, sandy silt. As the dry season was only 3½ months long, considerable effort was spent to place the fill during the dry season.

A wide range of densities and moisture contents was adopted for compaction control to fit the existing moisture content of the

borrow material and the short construction schedule. Compaction was monitored to ensure that there were no concentrated areas of material with either high or low densities.

High construction pore pressures developed in two of the three earth dams. The two dams exhibiting high pore pressures were planned to be constructed over two dry seasons, but were instead constructed over one dry season.

Stability analyses using effective stress and considering the high measured construction pore pressures indicated that the upstream slopes were unstable and required flattening of the slopes to be stable. Additional analyses were carried out using the total stress or “ $\phi = 0$ ” method. Undrained shear strength parameters were determined from unconsolidated-undrained triaxial compression tests of undisturbed samples taken from critical areas of the fills. The results of the total stress analyses indicated that the slopes were stable. For added stability, toe berms constructed of waste fill were placed at the toes of the dams showing high pore pressures.

Li (1967) attributed the development of high pore pressures to the silty material with high water content during placement coupled with excessive compaction and, to a lesser extent, the rate of construction. The development of high pore pressures was considered unavoidable unless the rate of placement was extremely slow or extensive drainage features were incorporated in the fill.

Highway 63 Berm, Alberta

Syncrude's Highway 63 Berm (Highway Berm) located near Fort McMurray is a 2.5 km long, 62.5 m high dam that retained up to 35 m of differential head of water in a mined out pit and served as a highway and utility corridor to replace the corridor in the

area being mined (Cameron & Fong, 2001). The Highway Berm included a range of fills compacted to various degrees of compaction (Ashton & Cameron, 1995).

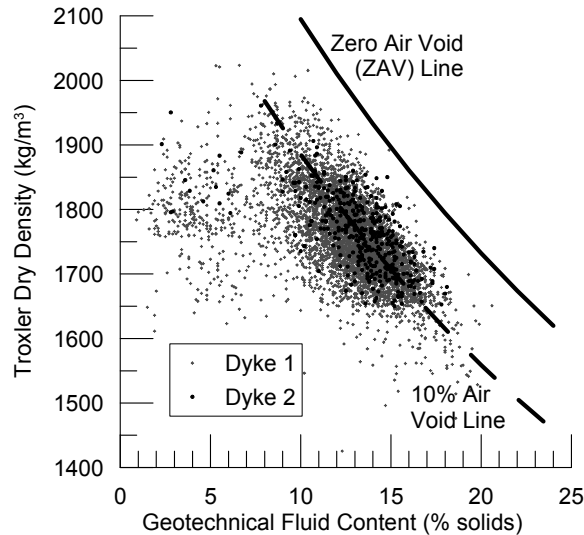


Figure 4. Troxler field dry densities during dyke construction

Pore water pressures within the berm were monitored and the pore pressure ratio was found to be mostly affected by the natural fluid content of the fills and the degree of compaction (Cameron & Fong, 2001). Cameron et al. (1995b) observed that when the fill was densely compacted to 98 percent SPMDD, the pore pressure ratio was largely dependent on the fluid content. Under-compaction was found to reduce the pore pressure ratio and over-compaction was found to increase it.

Up to fifteen out of a total of 53 piezometer tips installed in the Shell fill showed pore pressure ratios above design, with eight of these showing no pore pressure dissipation. The high pore pressure areas were found to be composed mostly of wetter fill and occurred only in local pockets that did not compromise the overall stability of the berm.

Summary of Background Review

The background review indicated that the dykes were constructed of fine sand and silt fill with trace to some clay and approximately 4% bitumen content. The bitumen content influences the compaction characteristics of lean oil sand, and as such, there is a wide spread of obtainable densities that could vary with fluid content. Reported cases where high construction pore pressures developed and were sustained were related to the placement of densely-compacted, uniformly to poorly-graded silty fine sands with high saturation levels. Local climatic records did not indicate unusually high amounts of rainfall during the 2006/2007 construction seasons.

2008 INVESTIGATION PROGRAM

In 2008, a geotechnical investigation program was carried out that comprised the following activities:

- seven coreholes penetrating through the dyke fill and into the foundation,
- downhole geophysical logging within each drilled borehole;
- piezometer installations; and
- cone penetration test (CPT) holes probed adjacent to the drilled boreholes and penetrated to refusal.

The objectives of the field program were to collect samples for specialized geotechnical testing and to characterize the state of the dyke fills. Subsequent to these activities, additional piezometers and slope inclinometers were installed within the dykes for performance monitoring.

The boreholes were located in targeted areas both with and without high pore pressures, based on previous measurements. High pore

pressure ratios ($r_u > 0.5$) were observed in three of the fourteen installed piezometer tips.

Continuous cores were recovered using wireline coring with a mud rotary system. Casing was driven into the top 2 to 3 m of the borehole. Core was typically recovered in 3 m long sections. Field core recovery varied from 0 to 100 percent. Core recovery was generally good (on average, 70%) for the fill materials and better for the bedrock foundation (90% and greater recovery). The fill materials were generally cohesive and the cylindrical shape of the core was mostly retained. Better-quality cores were set aside for specialized geotechnical testing.

Cone penetration tests were carried out using a 25-ton rig. The test holes were probed within 8 m of the drilled borehole. Cone penetration generally met refusal close to the bedrock surface.

Pocket penetrometer tests were carried out on the outer portion of the core at approximately 0.5 m depth intervals. Select core samples that retained a cylindrical shape were trimmed, weighed and the length and diameter measured to calculate core densities. Select samples were tested, including: a) gravimetric moisture content; b) bitumen-mineral-water distribution by the Dean Stark method; c) Atterberg Limits; d) washed sieve and hydrometer; e) flexible-wall permeability; and f) consolidated/unconsolidated undrained triaxial compression tests.

FINDINGS FROM 2008 INVESTIGATION PROGRAM

Fill Characteristics

The dyke fills were observed to be compacted to an average bulk density of approximately 2080 kg/m³ and an average dry density of approximately 1770 kg/m³. This compares to the minimum specified dry density of 1700 kg/m³ and the SPMDD of 1775 kg/m³.

The measured gravimetric water contents (average 13%) and geotechnical fluid contents (average 18.5%) were observed to be greater than those previously reported during construction monitoring of the dykes from the Troxler density measurements.

Permeability testing on five core samples taken from areas where high pore pressures were measured showed hydraulic conductivities ranging from 1 x 10⁻¹⁰ m/s to 3 x 10⁻⁸ m/s. The low values were attributed to a combination of a large percentage of fines, the fine nature of the sand fraction, the presence of bitumen in the voids, and the dense state of compaction.

The CPT data indicated that the dyke fills are dense or very stiff with normalized tip resistance generally exceeding 5 MPa. The cone tip occasionally picked up thin layers of relatively weaker/softer materials, but these were generally less than 0.3 m thick and occurred in local pockets.

Figure 5 shows the dry density-fluid content data for the samples collected during the 2008 investigation, as measured from bulk density and bitumen-mineral-water tests of the cores.

Core densities from samples recovered from the high r_u areas generally plot very close to the Zero Air Void line, and indicate higher densities and saturation levels than samples compacted using Standard Proctor energy (see Figure 3). As described in Section 3.4, silty fine sands that are densely compacted and at high saturation levels are susceptible to developing high construction pore pressures. For this study, dyke fills were considered potentially high r_u if the dry density-fluid content state was such that it plotted on or to the right of the 6% Air Void line for undisturbed core samples or laboratory-compacted specimens

Strength Testing

A series of CU (Consolidated, Undrained) and UU (Unconsolidated, Undrained) triaxial compression tests were carried out on representative core samples to assess the shearing behaviour of high r_u fill across a range of dyke pressures. Tests were carried out for effective confining pressures ranging from 241 to 948 kPa.

Targeted cores were those that were considered dense and wet of optimum, the material that was thought to be exhibiting high r_u in the field. Index tests were conducted after the triaxial compression tests were completed to confirm that the fluid-density state of the samples were indeed susceptible to developing high pore pressures. An additional CU triaxial compression test (CU-6) was carried out on a reconstituted lean oil sand specimen that was compacted wet of optimum and a relatively low dry density, to assess the shearing response of low density, potentially high r_u fill. As shown in Figure 5, five of the six tested specimens plotted above the 6% Air Void line, i.e. are considered potentially high r_u .

A back pressure was applied to all CU samples to saturate. The consolidation characteristics of the test samples varied considerably between samples, owing to differences in particle gradation, initial density, and bitumen content.

All CU tests on the dense intact cores showed a small increase in pore water pressure as the sample was sheared, followed by a sharp decrease and negative induced pore water pressure with increasing strain, i.e., dilative behaviour.

Figure 6 shows a typical test result. All test specimens failed on a distinct shear plane. The CU test on the low-density reconstituted core, test CU-6, also showed a rise and drop in pore water pressure with increasing strain, but the induced pore water pressures remained positive.

Limit equilibrium stability analyses of the dyke slopes based on effective stress and measured r_u 's do not consider this strength gain from the drop in pore water pressure, which can result in conservative de-sign and flat side slopes. Therefore, total stress analyses using undrained shear strengths are considered more appropriate for those sections of the dyke with high pore pressure.

The dilative tendencies of the intact cores and the lack of a clearly-defined peak strength make it difficult to define a failure point in these undrained tri-axial compression tests. In this regard, they likely behave similar to dilative, low-plastic silts.

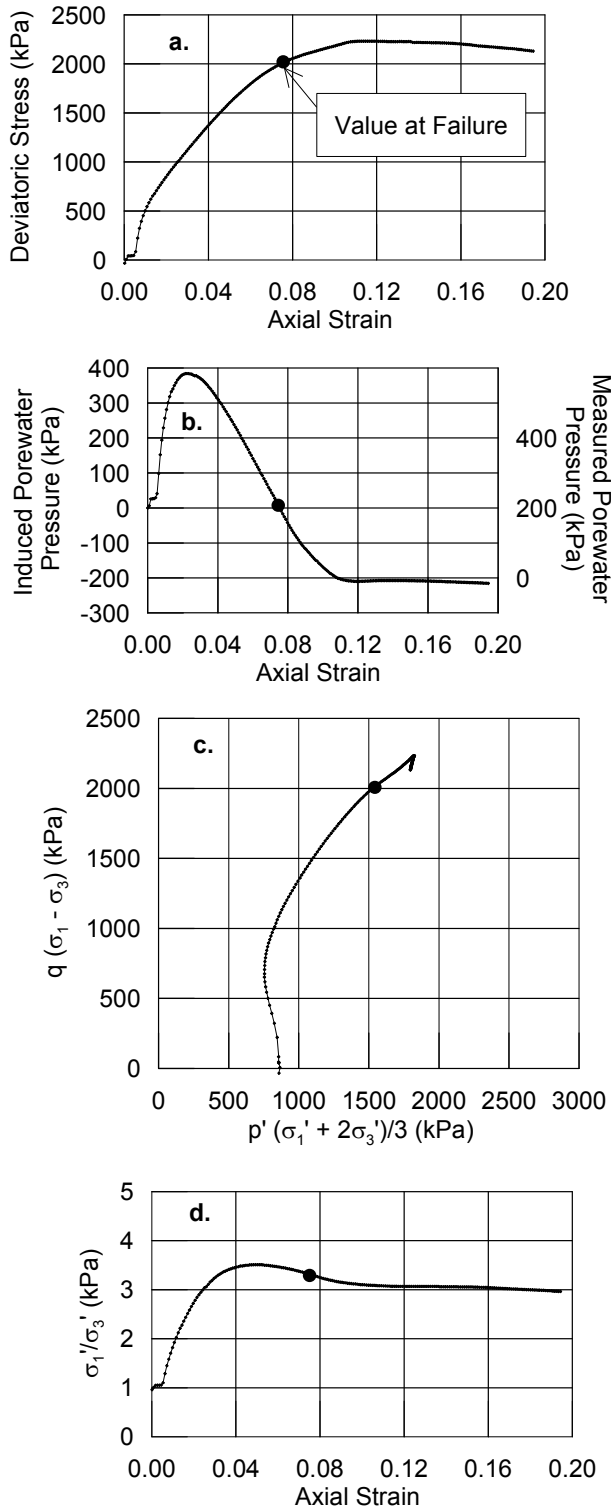


Figure 5. Density-fluid content data from undisturbed cores. Data from vicinity of piezometer tip showing high pore pressures or low permeability also shown.

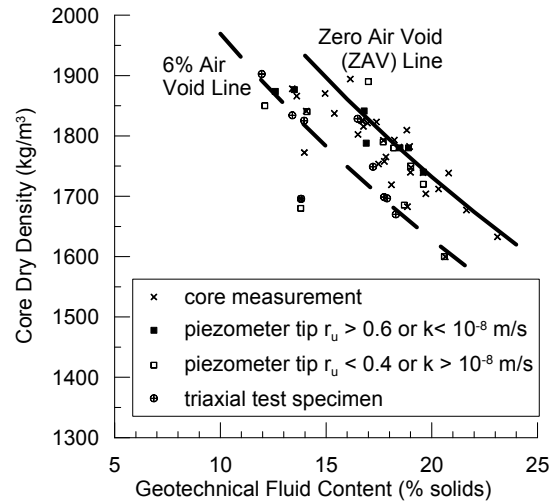


Figure 6. Typical triaxial test results (test CU-3): a) deviatoric stress-strain; b) porewater pressure-strain; c) stress path; d) principal stress ratio-strain. Values at failure ($\Delta u = 0$) also indicated.

Brandon et al. (2006) studied the undrained strengths of low-plastic silts and found that failure defined at the point where the pore pressure during the test de-creases back to the back pressure at the start of the test (i.e., $\Delta u = 0$) allowed unambiguous determination of the point of failure from the test data. The advantage of this criterion is that strength attributable to negative pore pressure is conservatively ignored. Furthermore, in the field, no back pressure is applied to the sample as was done in the laboratory, so the ability of the dyke fills to sustain negative pore pressures in the field is much more limited.

Figure 7 presents the Mohr's circles for the CU tests, based on total stresses determined using the $\Delta u = 0$ failure criterion. The results indicate an undrained strength defined by a friction angle, ϕ_u , of 26° .

Extent of High Pore Pressure Areas

The possible extent of high pore pressure areas was evaluated by examining the field Troxler density test results. As previously described, for a given fluid content, the Troxler-measured field densities are generally lower than the dry density determined from laboratory compaction tests as well as the measured densities of the recovered cores.

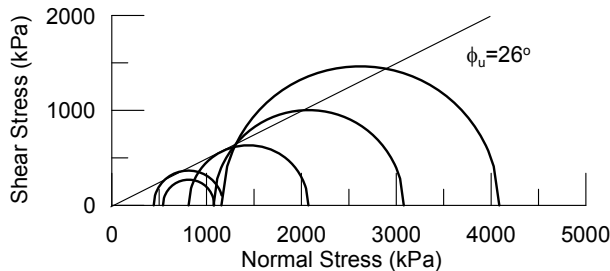


Figure 7. Mohr's circles for CU triaxial tests.

This implies that the dyke fills are denser and more saturated than inferred from the Troxler data. Therefore, the line of optimums represented by the 6% Air Void line for actual cores is considered equivalent to the line represented by the 10% Air Void line from Troxler data.

Each field density measurement recorded during construction was examined relative to the 10% Air Void line. For a measured fluid content from the Troxler, the maximum dry density was calculated assuming 10% air voids and a specific gravity of 2.65. If the Troxler dry density at this fluid content exceeded the dry density of the assumed line of optimums, a flag of "1" was assigned to this data point, representing wet-of-optimum compaction, otherwise a flag of "0" was applied, representing dry-of-optimum compaction. Figure 8 shows this method.

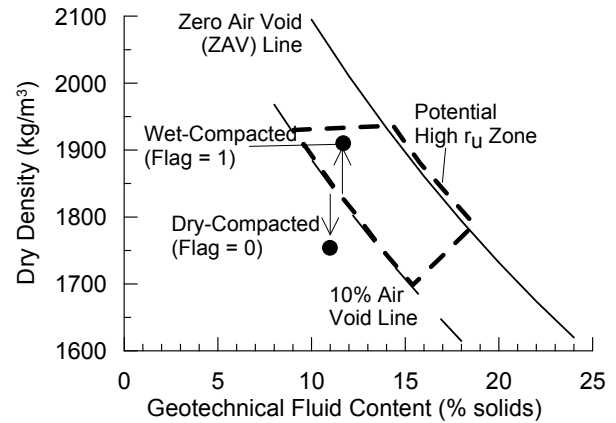


Figure 8. Relative compaction from Troxler density tests.

When this method was applied to the field compaction data and the results plotted spatially according to the locations of the Troxler tests, it was evident that both dry-compacted and wet-compacted fills were placed in both dykes.

Subsequently, the historical placement of wet-compacted/dry-compacted fills was examined. Figure 9 shows the 0/1 flags representing dry-of-optimum compaction and wet-of-optimum compaction, respectively, plotted against time since dyke construction began. Given the high number of data points collected (greater than 5500), no clear trends are apparent. However, after applying a 40-point moving average to the data points (also shown on Figure 9), a clearer trend is observed. The moving average curve is interpreted as follows:

- Where the curve has a low value (e.g. average 0.2 from January through March 2006), this is indicative of a period when the placed fill was largely compacted dry of optimum.
- Where the curve has a high value (e.g., exceeding 0.6 from May through early-June 2006), this is indicative of a period

when the placed fill was largely compacted wet of optimum.

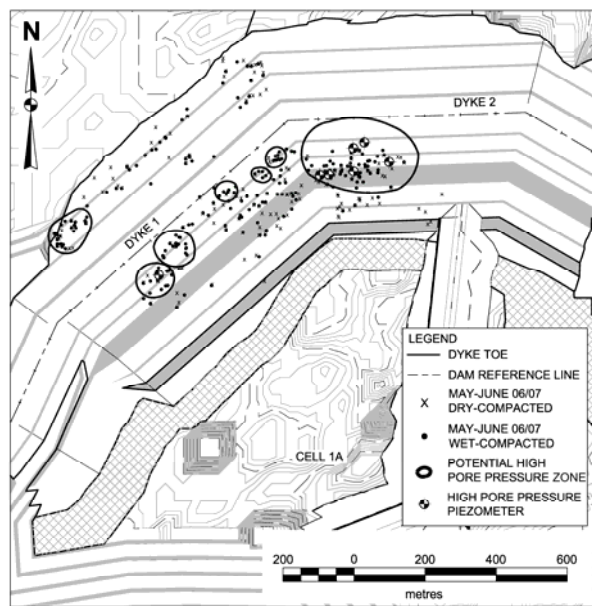


Figure 9. Relative compaction history from Troxler tests.

A threshold value of 0.6 (i.e. at least 60% of the 40 points in the running average were compacted wet-of-optimum) was selected as an indicator of fill being consistently wet-compacted in the rolling average period. As shown in Figure 9, during the periods of May 1 to June 6, 2006, and May 14 to June 8, 2007, a higher proportion than normal of fill was believed to have been compacted wet of optimum. These periods are highlighted in Figure 9. Other periods that showed narrow spikes above the 0.6 threshold have been interpreted as periods where fill placed wet of optimum was more localized.

Figure 10 shows the locations of the field density measurements during these two periods with consistent wet-compaction. The locations of these measurement points coincide very well with the locations where high r_u 's have been recorded. The high density of Troxler data points in these areas suggests that much wet-compacted fill was

placed in a concentrated area during this period. The similar time of year that wet-compaction was observed (May-June 2006 and 2007) suggests that a combination of snowmelt and frost (which may have inhibited drainage) resulted in wetter fill being used for dyke construction than those obtained during other times of the year.

CONCLUSIONS

High pore pressures in the in-pit dykes at the Muskeg River Mine are believed to have developed in areas where thick lifts of fill were rapidly and consistently placed wet of optimum and heavily compacted. Examination of the Troxler density test results from dyke construction indicate that areas with high r_u fill appear to be localized.

Triaxial compression testing indicated that the dense, high r_u fills are dilative. The high pore pressures dissipate with increasing strain, which results in an increase in effective stress. Consequently, limit equilibrium analyses that require input of effective stresses and design r_u 's result in conservative designs because they do not consider the strength gain during shear. Stability analyses using total stress undrained strength parameters for the high r_u fills are considered more appropriate. The undrained shear strength of the dense, high r_u fills was determined from the triaxial test results.

ACKNOWLEDGEMENTS

The authors thank Shell Canada Ltd. for permission to publish this study. Dykes 1 and 2 at Muskeg River Mine were designed by Klohn-Crippen Berger Ltd.

REFERENCES

- Ashton, C. and Cameron, R., 1995. Syncrude's Highway Berm: Part 4 of 5 – Significant construction procedures and quality control data. *Proceedings of the 48th Canadian Geotechnical Conference*. Vancouver: 819-828.
- Bishop, A.W., 1954. The use of pore pressure coefficient in practice. *Geotechnique* 4(4): 148-152.
- Brandon, T.L., Rose, A.T., and Duncan, J.M., 2006. Drained and undrained strength interpretation for low-plasticity silts. *Journal of Geotechnical and Geoenvironmental Engineering* 132(2): 250-257.
- Cameron, R., Ashton, C., Strueby, B., and Fong, V., 1995a. Syncrude's Highway Berm: Part 2 of 5 – Soil parameters (shear strengths and their selection). *Proceedings of the 48th Canadian Geotechnical Conference*. Vancouver: 799-808.
- Cameron, R., Fong, V., Ashton, C., and Strueby, B., 1995b. Syncrude's Highway Berm: Part 3 of 5 – Soil parameters (pore pressure parameters and settlement from inundation). *Proceedings of the 48th Canadian Geotechnical Conference*. Vancouver: 809-818.
- Cameron, R., and Fong, V., 2001. Performance of a quasi-homogeneous earthfill dam retaining 35m of tailings fluid with no filters or clay core: Syncrude's Highway Berm. *Proceedings of the 54th Canadian Geotechnical Conference*. Calgary, 16-19 September 2001: 297-304.
- Daniel, D.E. and Benson, C.H., 1990. Water content – density criteria for compacted soil liners. *Journal of Geotechnical Engineering, ASCE* 116(12): 1811-1830.
- Fell, R., MacGregor, P., Stapledon, D., and Bell, G., 2005. *Geotechnical Engineering of Dams*. London, UK, A.A. Balkema Publishers. 912 p.
- Klohn-Crippen Berger Ltd., 2005. *Muskeg River Mine, In-Pit Dyke 1 Geotechnical Design Report*. Report submitted to SCE Sands Energy Inc., June 14, 2005.
- Klohn-Crippen Berger Ltd., 2008. *Muskeg River Mine, In-Pit Dykes 1 and 2 Design Summary Report Revision 1*. Draft report submitted to SCE Sands Energy Inc., June 2, 2008.
- Leroueil, S., Le Bihan, J.-P., Sebaihi, S., and Alicescu, V., 2002. Hydraulic conductivity of compacted tills from northern Quebec. *Canadian Geotechnical Journal* 39(5): 1039-1049.
- Li, C.Y., 1967. Construction pore pressures in three earth dams. *ASCE Journal of the Soil Mechanics and Foundations Division* 93(SM2): 1-26.
- Lord, E.R.F. and Cameron, R., 1985. Compaction characteristics of Athabasca tar sand. *Proceedings of the 38th Canadian Geotechnical Conference*, Edmonton: 359-368.
- Matheson, D.S., Morgenstern, N.R., Nussbaum, H., 1991. Design, construction and performance of the Nipawin Dams. *Proceedings of the 40th Canadian Geotechnical Conference*, Toronto: 141-170.

Rivard, P.J. and Goodwin, T.E., 1978. Geotechnical characteristics of compacted clays for earth embankments in the Prairie provinces. *Canadian Geotechnical Journal* 15(3): 391-401.

Sherman, W.C. and Clough, G.W., 1968. Embankment pore pressures during construction. *Journal of the Soil Mechanics and Foundations Division* 94 (SM2): 527-553.

Sherard, J.L., Woodward, R.J., Gizienski, S.F. and Clevenger, W.A., 1963. *Earth and Earth-Rock Dams*. New York, John Wiley and Sons.

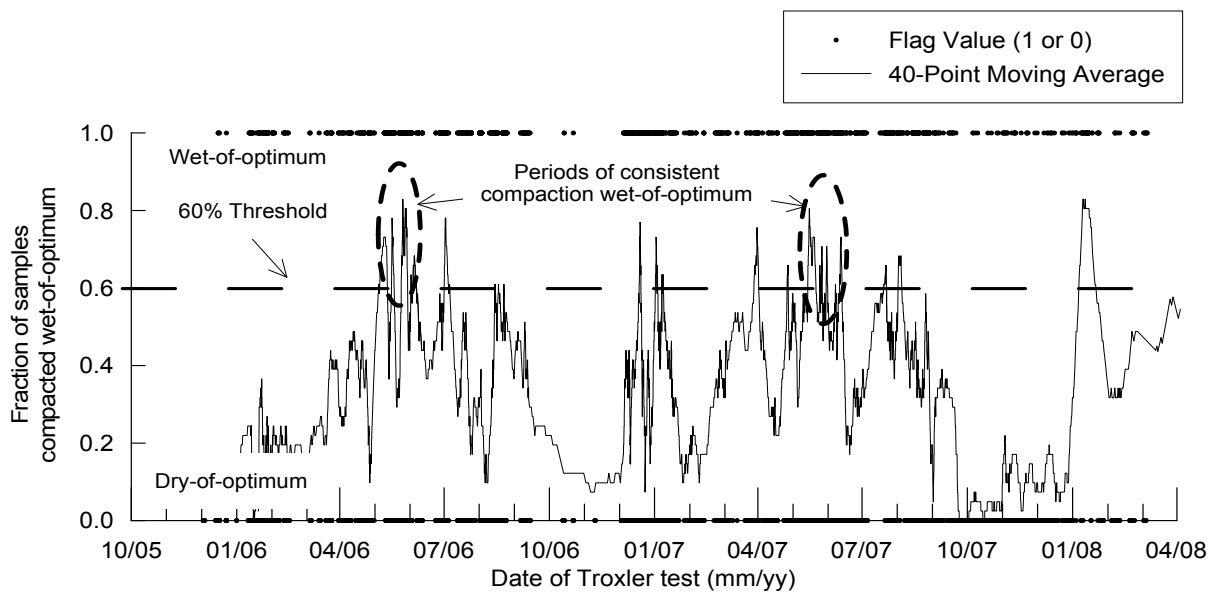


Figure 9. Estimated extent of potential high pore pressure zones.

CROSS FLOW FILTRATION OF OIL SAND TOTAL TAILINGS

C. Zhang, M. Alostaz, N. Beier & D. Segó

University of Alberta, Edmonton, Alberta, Canada

ABSTRACT: Oil sand tailings are disposed in storage ponds with an initial solid content around 55wt%. Due to its characteristics and disposal technique, coarse particles segregate during deposition to form pond beaches, while the finer materials remain suspended in fluid with a solid content around 8wt%. The fines eventually settle and form mature fine tailing (MFT) with 30wt%-35wt% solid content. MFT has poor consolidation characteristics delaying reclamation. Increasing the solid content of oil sands total tailing stream before depositing into tailings pond may be one solution to prevent segregation and thus formation of MFT. Cross flow filtration is a promising technology to achieve this objective. Cross flow filtration tests are presented to illustrate the increase of solids content as well as retention of fines in the total tailings. This paper presents the finding of laboratory scale study that was set up to investigate different factors that could affect the filtrate quality and quantity, such as tailings composition, and filter properties.

INTRODUCTION

Oil sand tailings are deposited as a slurry, which has 55wt% solid content and 17wt% fines content (<44 μ m). The whole oil sand tailings are characterized as heterogeneous or segregating (Sanders et al., 2004). After discharge from the pipeline into the disposal area, coarse particles (sand) settle quickly and form a beach, leaving 6-10wt% fines in the fluid flowing to the pond (Beier and Segó, 2007; Morgenstern and Scott, 1995). After a few years of settling, the remaining fines achieve 30-35wt% solid content with a stable structure, which is called mature fine tailings (MFT). Due to its very slow consolidation rate, MFT needs decades to settle and then will not achieve a trafficable surface (Beier and Segó, 2007; Chalaturnyk et al., 2002).

To describe the segregation issue in tailings management, the ternary diagram illustrated by Azam and Scott (2005) is a useful tool (Figure 1). The area below the segregation boundary represents non-segregating mixture and the combined oil sand tailings are above this boundary. Therefore, either shifting the segregation boundary or increasing the solid content leads to a non-segregating material for deposition.

Consolidated/composite tailings (CT) technology has been implemented by industry to reduce segregation by combining together MFT, gypsum (CaSO_4) and coarse sand (cyclone under flow). Although CT technology provides non-segregating tailings, it still segregates unless carefully deposited. Another concern of CT is the addition of gypsum. Accumulation of Ca^{2+} resulting from gypsum addition in the recycle water may

negatively affect bitumen extraction efficiency (Chalaturnyk et al., 2002).

To avoid adding chemicals and to prevent segregation, increasing total tailings solid content to over 70wt% before deposition is a potential solution. Cross flow filtration is a technology to achieve this dewatering objective and has been demonstrated by Yan et al. (2003) and Beier and Sego (2008).

CROSS FLOW FILTRATION

Working Mechanism

In cross flow filtration, the slurry to be filtered flows parallel to the filtrate membrane. The working mechanism of cross flow filtration is shown in Figure 2. The flow direction in cross flow filtration is perpendicular to the building-up of the filter cake, therefore the shear stress generated by the flow limit the cake thickness and maintains high filtrate flux rate compared to dead-end filtration. Filtrate flux rate ($\text{m}^3/\text{s}\cdot\text{m}^2$) is a measure of how much volume of filtrate liquid flows across a given area of the filtrate membrane during a given time interval. It is calculated as (filtrate flow rate)/(filtrate area).

Oil sand total tailings are classified as a heterogeneous slurry and could be represented by the Saskatchewan Research Council (SRC) Two-Layer model (Beier and Sego, 2008; Sanders et al., 2004). This model considers a fully stratified flow with a high velocity low solid concentration upper layer and a slow moving high solid concentration lower layer, while fines are considered as part of the carried flow (Beier and Sego, 2008). Based on the settling characteristic of oil sand tailings, it is expected that coarse particles within the tailing settle down on the filter pipe membrane at the beginning of cross flow filtration operation. Some fine particles, which are smaller than the filter pipe pores,

drain with filtrate. As operation continues, coarse particles settle and form a stable cake on the filter pipe. The filtration seepage force holds fine particles on the side and top of the filter pipe forming a finer and thinner filter cake (Beier and Sego, 2008).

During the cross flow filtration operation, more and more fine particles are brought to the filter cake because of seepage forces in the filtrate water. These fines increase the filter cake specific resistance and reduce filtrate flux rate. As filtrate flux rate decreases, the filtration seepage force caused by filtration decreases and leads to fewer but finer particles deposited in cake structure, which further decreases the filtrate flux rate. This process continues until the filtrate flux rate decreases to a constant value and cross flow filtration operation attains steady state (Lu et al., 1993, Hwang et al., 2006).

Application of Cross Flow Filtration

The cross flow filtration technology has been used in many fields such as purification or regeneration of process liquids containing fine suspensions (Murkes and Carlsson, 1988; Yan et al., 2003). It is widely used with fine particle slurries and few studies have successfully demonstrated its application to coarse tailings. Yan et al. (2003) applied cross flow filtration to a gold mining waste using a 48mm diameter flexible woven hose. The slurry sample used had a D_{80} of $35\mu\text{m}$ and a solid density of 2730 kg/m^3 . From their lab test, an increase in solid content, from 44wt% to 53wt%, was obtained over a 96m length under 160 kPa transmembrane pressure and 130 L/min feed flow rate.

Beier and Sego (2008) examined the possibility of using cross flow filtration to dewater mine tailings (mixture of sand and kaolinite). Their tailing mixture was similar to the oil sand total tailings (55wt% solid content with 15wt% fines content). They

operated the cross flow filtration experiments using two different filter pipes. One was a polyethylene porous pipe with 40 μ m pore size and the other one was a PVC bottom slotted pipe with 250 μ m wide and 55mm long slots. For both cases, suitable filtrate water quality could be achieved but the bottom slotted pipe required longer to obtain clean filtrate water due to larger pore size. The filtrate flux rate generated from porous pipe was nearly an order of magnitude greater than from slotted pipe in their study. This could be attributed to the larger open surface (porosity) of the porous pipe (34%) compared to the bottom slotted pipe (3%). They operated another cross flow filtration test using porous pipe and high solid content tailing (70wt% with 15wt% fines content). The filtrate water quality was also acceptable and a slightly higher transmembrane pressure was required to produce a similar filtrate flux rate as the test using 55wt% solid content tailing. Based on their experiment results, they concluded that approximately 450m of 55mm diameter porous pipe would be required to dewater the oil sands total tailing stream from 55wt% solid content to 70wt% under 2.26L/s feed flow rate. The performance of cross flow filtration carried out by Beier and Segó (2008) was successful with acceptable filtrate quality and quantity, and indicated that it is a promising method to dewater the actual oil sands total tailings.

PARAMETERS RELATING TO CROSS FLOW FILTRATION

Slurry Velocity

Slurry velocity is a fundamentally important factor in cross flow filtration (Murkes and Carlsson, 1988). Generally, higher velocity generates higher shear rate, which reduces cake thickness and results in higher filtrate flux rate (Yan et al., 2003). Dahlheimer et al. (1970) did experiments using a fibre hose and

kaolin slurry at the concentration of 80 g/L. They concluded that there was a direct correlation between the filtrate flux rate and flow velocity. Yan et al. (2003) demonstrated a linear relationship between slurry velocity (from about 0.7m/s to 2.4m/s) and filtrate flux rate (from about $1.5 \times 10^{-2} \text{L/s} \cdot \text{m}^2$ to $8 \times 10^{-2} \text{L/s} \cdot \text{m}^2$).

Transmembrane Pressure

Transmembrane pressure is an important factor because cross flow filtration is essentially a pressure-driven process (Yan et al., 2003). Transmembrane pressure represents the pressure difference across the membrane from inside to outside of the filter pipe. Higher transmembrane pressure forces more filtrate through the membrane and increase the filtrate flux rate. Higher transmembrane pressure can also compact the cake structure resulting in reduced filtrate flux rate. It was reported by Murkes and Carlsson (1988) that filtrate flux rate will increase with transmembrane pressure up to a maximum, after which the filtrate flux rate may decrease with the rising of transmembrane pressure. However Yan et al. (2003) reported that for large particles (>1 μ m), filtrate flux rate is linearly increased with transmembrane pressure.

Another concern of increasing the transmembrane pressure is the filtrate quality. Beier and Segó (2008) described that although increasing pressure led to higher filtrate flux rate, fines within the filtrate liquid also increased. Therefore the optimal transmembrane pressure should maintain both good filtrate flux rate and filtrate liquid quality.

Slurry Particle Size Distribution

Particle size distribution appears to have a strong relationship with filtrate flux rate. Ripperger and Altmann (2002) described that

for a given slurry the percentage of particles within the 50-500nm size range would determine the steady state filtrate flux rate. This is because particles within this size range have a minimum effective back-transport mechanism, which means if these particles are deposited it is difficult to re-suspend the particles.

Slurry Solid Concentration

Generally, cross flow filtration is relatively insensitive to the slurry solid concentration (Murkes and Carlsson, 1988). Yan et al. (2003) concluded that, high slurry velocity in cross flow filtration produced high shear force, which limits cake thickness and maintains a constant filtrate flux rate in high slurry density.

According to Beier and Segó (2008), tailings with higher solid content required a higher transmembrane pressure to attain similar filtrate flux rate as tailings with lower solid content. They expected as solid content increases along the filter pipe length, an increased transmembrane pressure is needed to maintain constant filtrate flux rate.

Filter Membrane Property

Ripperger and Altmann (2002) outlined that both the filter membrane pore size and porosity are important in cross flow filtration. Membrane pore size should be small enough to ensure that enough particle retention and a clean filtrate are achieved. Although the ultimate filtrate flux rate is controlled by the cake property, more time to form the cake and generate clean filtrate liquid may be required if the pores are large. Higher membrane porosity leads to higher filtrate flux rate even under low pressure. Further requirements are membrane strength, chemical and thermal stability.

Yan et al. (2003) concluded that if the filter pipe radius is not sufficiently large compared to the cake thickness, filtrate flux rate will increase with filter pipe radius even under the same shear rate.

Temperature

Since the flow rate through a filter membrane pore is inversely proportional to the fluid viscosity (Yan et al., 2003), the low viscosity caused by higher operation temperature leads to higher filtrate flux rate (Murkes and Carlsson, 1988). Dahlheimer et al. (1970) reported that, from their observation using fibre hose and kaolin slurry concentration at 20 g/L, the temperature affected the filtrate flux rate significantly, from 0.141 L/s·m² at 20 °C to more than 0.377 L/s·m² at 55 °C.

EXPERIMENTAL PROCEDURE

Materials

The oil sand total tailings used in this study consisted of beach sand, MFT and tap water with 55wt% solid content and 15wt% fines content. The MFT samples were from Albion Sands. The beach sand samples were from Syncrude Canada Ltd. and Suncor Canada Ltd. because beach sand from Albion Sands was not available for this study. The particle size distributions of these materials are shown in Figure 3. The particle size distribution of beach sand was determined using sieve analysis and the particle size distribution of MFT was determined using hydrometer tests (ASTM D422-63).

There were two different experimental tailings used in this study. Tailing 1 was made with Syncrude beach sand, Albion Sands MFT and tap water. Tailing 2 was made with Suncor beach sand, Albion Sands MFT and tap water. The particle size distributions of these two synthetic tailings

are shown in Figure 4. Tailing 2 had a coarser grain size distribution compared to Tailing 1.

Filter Membrane

There were two different filter pipes used in this study. One was a stainless steel porous pipe with nominal 40 μ m pore size and 49% porosity. The other one was a stainless steel slotted pipe with 250 μ m slot width and 13% porosity. The details and photos of these two filter pipes are shown in Table 1 and Figure 5.

Test Setup

Figure 6 shows the sketch of cross flow filtration experiment setup and Figure 7 shows the photo of the experiment setup. The system is a closed circuit pipe loop. Beach sand, MFT and water were mixed in the cone feed tank using a drill mixer. After all materials are fully mixed, the prepared tailing was then delivered into the pipeline and filter pipe using a progressing cavity slurry pump. The dewatered tailing returned back to the feed tank through a soft return tube. There was a trough underneath the dewatering pipe to convey filtrate water to a small pail. Filtrate water was then deposited back into the feed tank to be recycled, or removed depending on test requirements. The pipeline was equipped with a flow meter to measure feed slurry flow rate. Two pressure gauges were used on the ends of the dewatering pipe to measure the transmembrane pressure. A gate valve was placed at the discharge end of the filter pipe to adjust the transmembrane pressure.

Filtrate water samples were collected at 15 to 60 minutes intervals. At each sample interval, filtrate flow rate was measured using a graduate cylinder, and feed flow rate and transmembrane pressure were recorded using the flow meter and pressure gauges.

RESULTS AND DISCUSSIONS

A summary of different test conditions in this study is included in Table 2. Filtrate data (filtrate flux rate) of all cross flow filtration tests are shown in Figure 8. Figure 9 illustrates the filtrate quality data (solid content) of all tests except Test 2.

Effect of Tailing Particle Size Distribution

Tailing 1, made with Syncrude beach sand and Albion MFT, was used in Test 1 and Tailing 2, made with Suncor beach sand and Albion MFT, was used in Test 2. In both tests, stainless steel porous pipe was used and the filtrate water was recycled to maintain feed tailing solid content.

As shown in Figure 8, higher filtrate flux rate was generated in Test 2. It was obvious that coarser tailing composition improved filtrate quantity during these tests.

This was due to the filter cake. At the beginning of cross flow filtration, coarse particles settled on the filter membrane and form a cake. Therefore the coarser the tailing, the coarser and higher permeability within the filter cake. A coarser grained cake allows more filtrate water to flow through under the same transmembrane pressure condition. Therefore a coarser tailing is expected to generate a higher filtrate flux rate.

It was observed that clean filtrate water was produced in Test 2 at the beginning of the cross flow filtration test. This demonstrated that although coarse particles formed a coarse cake, it provides high quality filtrate water.

Effect of Tailing Solid Concentration

Tailing 1 and stainless steel porous pipe were used in both Test 1 and Test 3. The difference between these two tests was that in Test 1 the filtrate water was completely recycled while

in Test 3 the filtrate water was removed at a rate of 4 L/hour.

As shown in Figure 8, the filtrate flux rate data of both tests were similar. It appears that increasing tailing solid content during cross flow filtration operation does not affect the filtrate quantity, and a higher transmembrane pressure and higher slurry velocity may be needed to maintain the filtrate flux rate under high solid content condition (Beier and Segó, 2008; Yan et al., 2003).

As shown in Figure 9, it is obvious that both tests generated high quality filtrate water. Even under high solid contents (>150 minutes in Test 3), the filtrate water quality was good.

Effect of Residual Bitumen

It was observed that a layer of bitumen formed on the top of the cone feed tank during the cross flow filtration test operation. Therefore most of the residual bitumen in the experiment tailing did not enter the cross flow filtration system. Therefore, a cylinder shape tank with a side outlet hole was used instead of the cone tank (Figure 10) for future tests. A paddle mixer was installed in the tank and kept mixing during whole operation to have bitumen flow with tailings.

Tailing 1 and stainless steel porous pipe were used in both Test 1 and Test 4. A cone shape feed tank was used in Test 1 while a cylinder shape tank with paddle mixer was used in Test 4. Filtrate water was recycled during both tests.

As the residual bitumen flowed with the experiment tailing, it was observed that in Test 4 bitumen froth formed on the top of the filter pipe, which could blind this filtrate area during operation and reduce filtrate flux rate. About 30% decrease in filtrate quantity was observed in Figure 8.

The reason for the filtration loss in Test 4 was not only the presence of bitumen, but also the decrease in transmembrane pressure, 109 kPa in Test 1 and 79 kPa in Test 4. Since Test 4 was operated almost one year later than Test 1 and more than 20 cross flow filtration tests had been operated during this time, it is expected that some pores got plugged and could attribute to the reduction in filtrate flux rate. Experiments are underway to investigate how transmembrane pressure affects the filtrate flux rate and compare with existed data to find the effect of residual bitumen on the cross flow filtration performance.

Figure 9 shows that the residual bitumen did not affect the filtrate water solid content. Both tests produced high quality filtrate water within 10 minutes operation time.

Effect of Filter Membrane

Filter membrane property plays a significant role in cross flow filtration. Filter pipe inner diameter is one important factor as it controls the filtrate area (Yan et al, 2003). If the inner diameter does not change, pore size and porosity control the filtrate quality and quantity (Ripperger and Altmann, 2002).

In Test 4 a stainless steel porous pipe was used while a stainless steel slotted pipe was used in Test 5. Tailing 1 and cylinder shape tank with paddle mixer were used in both tests. During both test operations, filtrate water was kept recycling.

A slightly higher filtrate flux rate was produced in Test 5 than in Test 4 even though the porous pipe had a much higher porosity (49%) compared to the slotted pipe (13%). This observation was not consistent with Beier and Segó (2008), who reported higher porosity leading to higher filtrate flux rate.

The reason could be the presence of residual bitumen in tailings and plugged problem in

porous pipe. Because the porous pipe had higher porosity and smaller pores, more filtrate area could be reduced by bitumen compared to slotted pipe. Since more than 20 tests had been operated before Test 4, the porosity of the porous pipe in Test 4 could be lower than the original value. Experiments are underway to confirm this observation.

Clean filtrate water could be obtained in both tests within 10 minutes as shown in Figure 9. The initial filtrate water solid content in Test 5 was higher than in Test 4. The slotted pipe had larger slot size and filter cake required more time to stabilize. Fines were easily pushed out through the filter membrane at the beginning of test until filter cake developed.

CONCLUSIONS AND FUTURE WORK

Several experiments were carried out to assess the effect of filter membrane property, tailing composition, tailing solid content and residual bitumen on the performance of cross flow filtration of oil sands total tailing.

It was found that different tailing particle size distributions formed different cakes and affected cross flow filtration performance. A coarser tailings formed a coarser cake on the bottom of filter pipe and resulted in higher filtrate flux rate with good filtrate water quality.

Increasing tailing solid content did not affect the cross flow filtration performance. According to Beier and Sego (2008), a higher transmembrane pressure may be needed to maintain the filtrate flux rate under high solid content condition.

The presence of bitumen in oil sands total tailing is believed to affect the performance of cross flow filtration. About 30% of filtrate flux rate loss on the cross flow filtration performance was observed and this could be

due to the residual bitumen, decreased transmembrane pressure and pores plugged. The filtrate water solid content was not affected by the residual bitumen in tailings

The membrane affected both the filtrate quantity and quality. Although higher porosity always generated higher filtrate flux rate, the slotted pipe (lower porosity) produced slightly higher filtrate flux rate than the porous pipe with higher porosity. One reason was the residual bitumen in tailings and another reason was the problem with plugging in porous pipe. Both porous pipe and slotted pipe could generate clean filtrate water, but larger pore/slot size required time to form a stable filter cake and to produce clean filtrate water.

Other experiments currently underway are investigating the influence of transmembrane pressure and tailing slurry velocity on the performance of cross flow filtration.

ACKNOWLEDGEMENT

The authors would like to thank Christine Hereygers and Bret Shandro from University of Alberta for technical assistant, and Saidul Alam for providing MFT particle size distribution data.

The financial support from the Oil Sands Tailings Research Facility (OSTRF) is gratefully appreciated.

REFERENCES

Azam, S., Scott, J.D. 2005. Revisiting the ternary diagram for tailings characterization and management. *Geotechnical News*, December 2005: 43-46.

Beier, N., Sego, D. 2007. The oil sands tailings research facility. *Proceedings of the*

60th Canadian geotechnical conference, Ottawa ON.

Beier, N., Segó, D. 2008. Dewatering of oil sands tailings using cross flow filtration. Proceedings of the 61st Canadian geotechnical conference, Edmonton AB.

Chalaturnyk, R.J., Scott, J.D., Özü. B. 2002. Management of oil sands tailings. Petroleum Science and Technology, Vol. 20(9&10): 1025-1046.

Dahlheimer, J.A., Thomas, D.G., Kraus, K.A. 1970. Hyperfiltration. Application of woven fiber hoses to hyperfiltration of salts and crossflow filtration of suspended solids. Industrial & Engineering Chemistry Process Design and Development, vol. 9(4): 566-569

Hwang, K.J., Hsu, Y.L., Tung, K.L. 2006. Effect of particle size on the performance of cross-flow microfiltration. Advanced Powder Technology, vol. 17(2): 189-206.

Lu, Wei-ming., Hwang, Kuo-jen., Ju, Shang-Chung. 1993. Studies on the mechanism of cross-flow filtration. Chemical Engineering Science, Vol. 48(5): 863-872.

Morgenstern, N.R., Scott, J.D. 1995. Geotechnics of fine tailings management. GeoEnvironment 2000, ASCE Specialty Conference, New Orleans, 1663-1683.

Murkes, J., Carlsson, C.G. 1998. Crossflow filtration: theory and practice. New York : John Wiley & Sons Ltd.

Ripperger, S., Altamnn, J. 2002. Crossflow microfiltration – State of the art. Separation and Purification Technology, 26: 19-31.

Sanders, R.S., Schaan, J., Hughes, R., Shook, C. 2004. Performance of sand slurry pipelines in the oil sands industry. The Canadian Journal of Chemical Engineering, 82: 850-857.

Yan, D., Parker, T., Ryan, S. 2003. Dewatering of fine slurries by the Kalgoorlie Filter Pipe. Minerals Engineering, 16: 283-289.

Table 1. Summary of Dewatering Pipes

Pipe Type	Porous	Slotted
Length (m)	3.48	3.49
Pore Size/Slot Width (µm)	40	250
Inner Diameter (mm)	42	52
Porosity	49%	13%
Filtrate Area (m ²)	0.46	0.57

Table 2. Summary of Experimental Conditions

Test	Tailing	Pipe	Velocity (m/s)	Pressure (kpa)	Other Conditions
Test 1	Tailing 1	Porous	0.89	109	
Test 2	Tailing 2	Porous	0.95	115	
Test 3	Tailing 1	Porous	0.92	115	Remove filtrate 4L/hour
Test 4	Tailing 1	Porous	0.92	79	
Test 5	Tailing 1	Slotted	0.84	70	

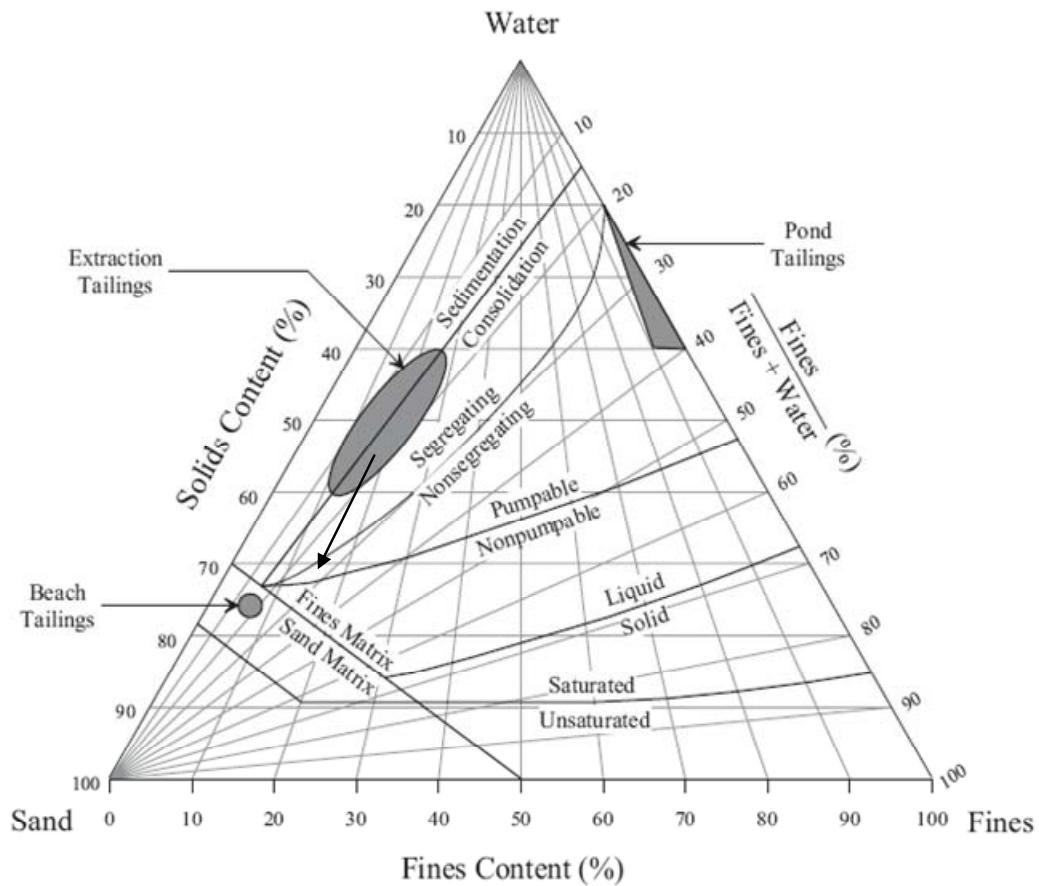


Figure 1. Ternary Diagram of Oil Sands Tailing (modified after Azam and Scott (2005) and Beier and Segó (2008)).

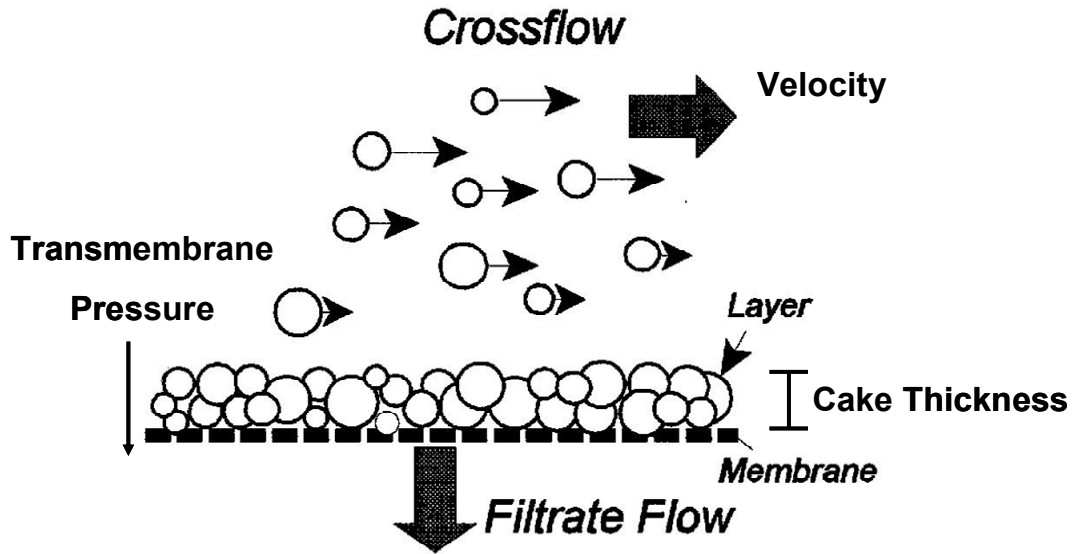


Figure 2. Cross Flow Filtration Working Mechanism (modified after Ripperger and Altmann (2002))

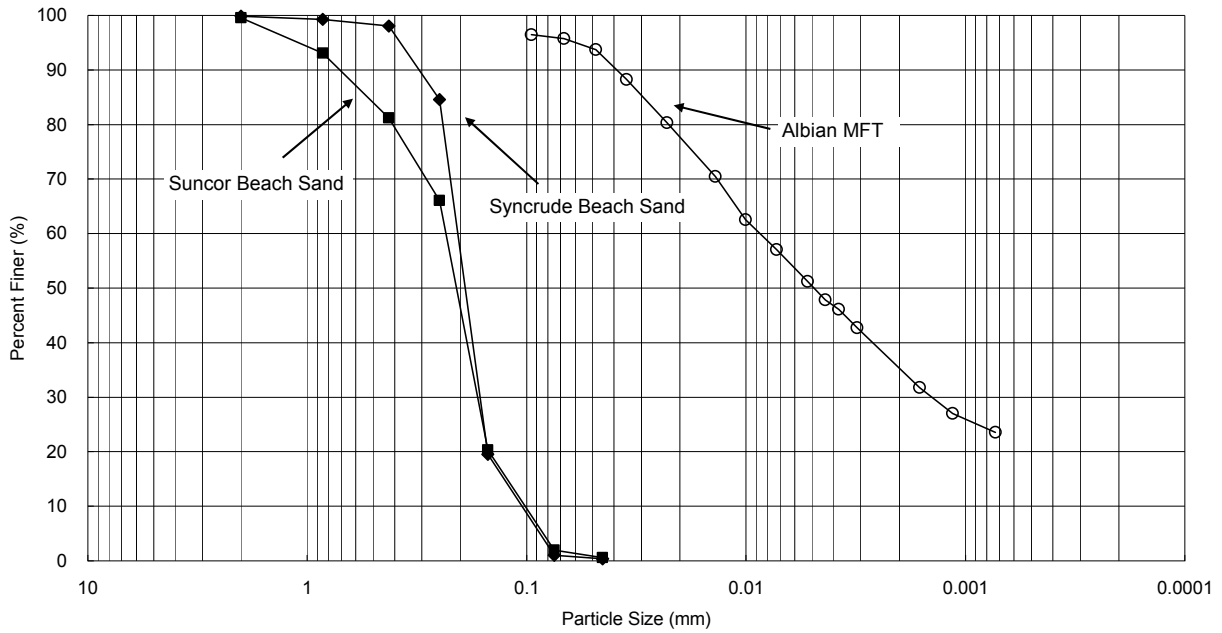


Figure 3. Particle Size Distribution of Beach Sand and MFT

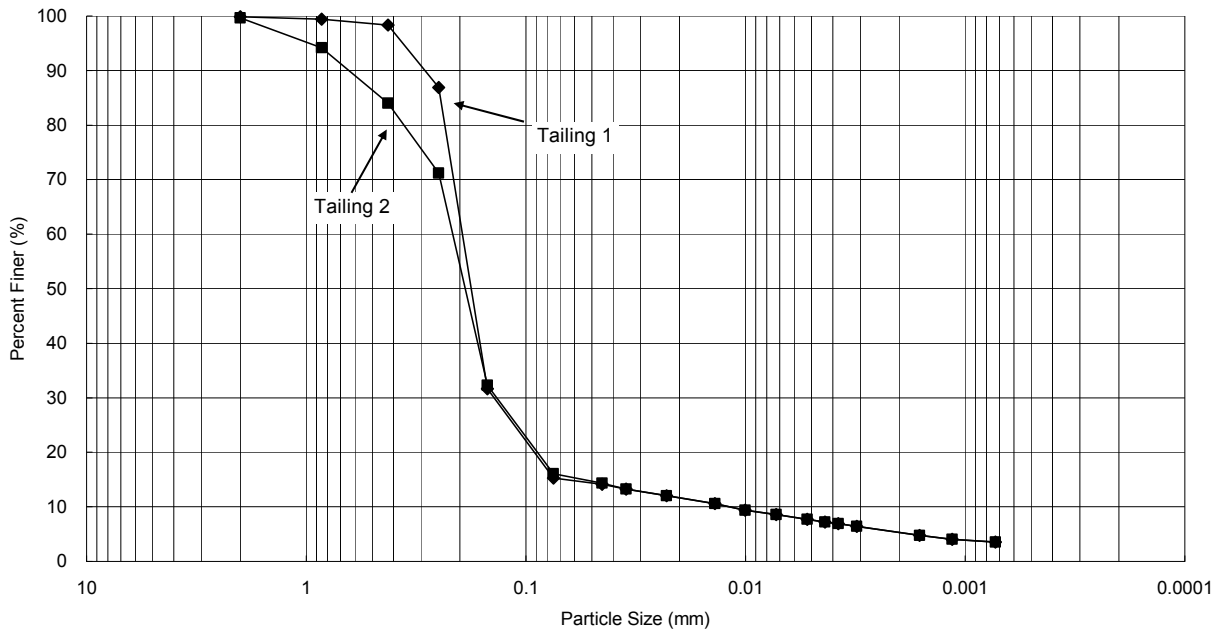
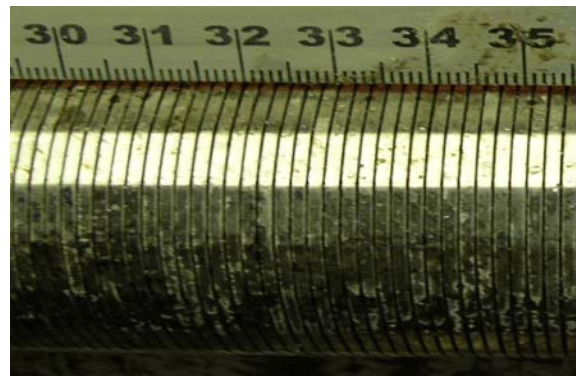


Figure 4. Particle Size Distribution of Experiment Tailings



Stainless Steel Porous Pipe



Stainless Steel Slotted Pipe

Figure 5. Photo of Filter Pipes

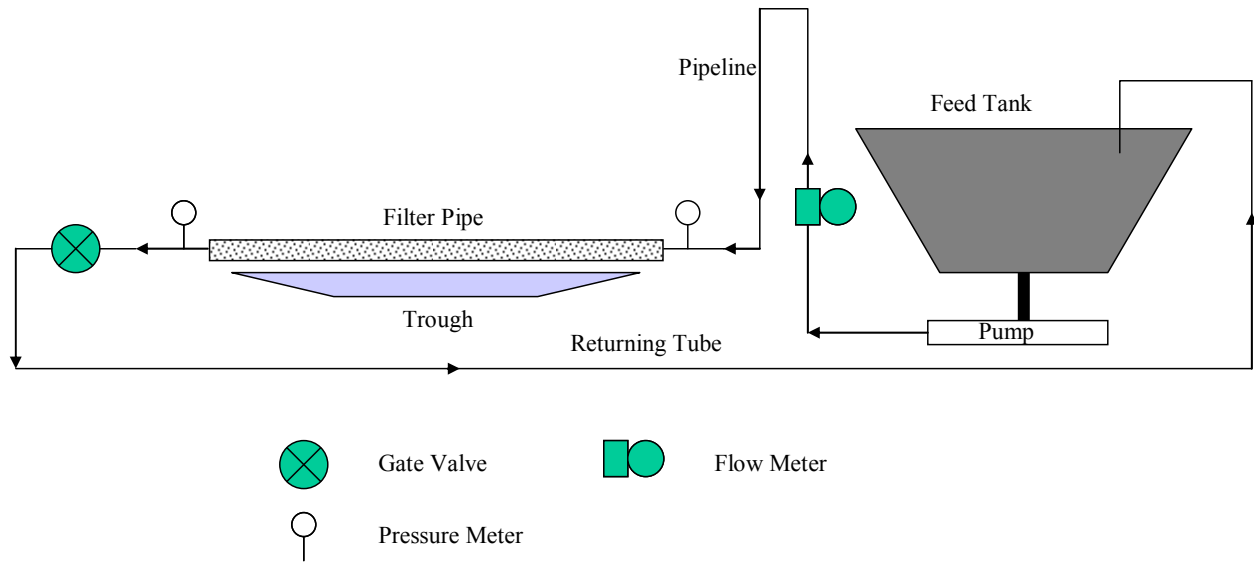


Figure 6. Cross Flow Filtration Operation Loop Setup

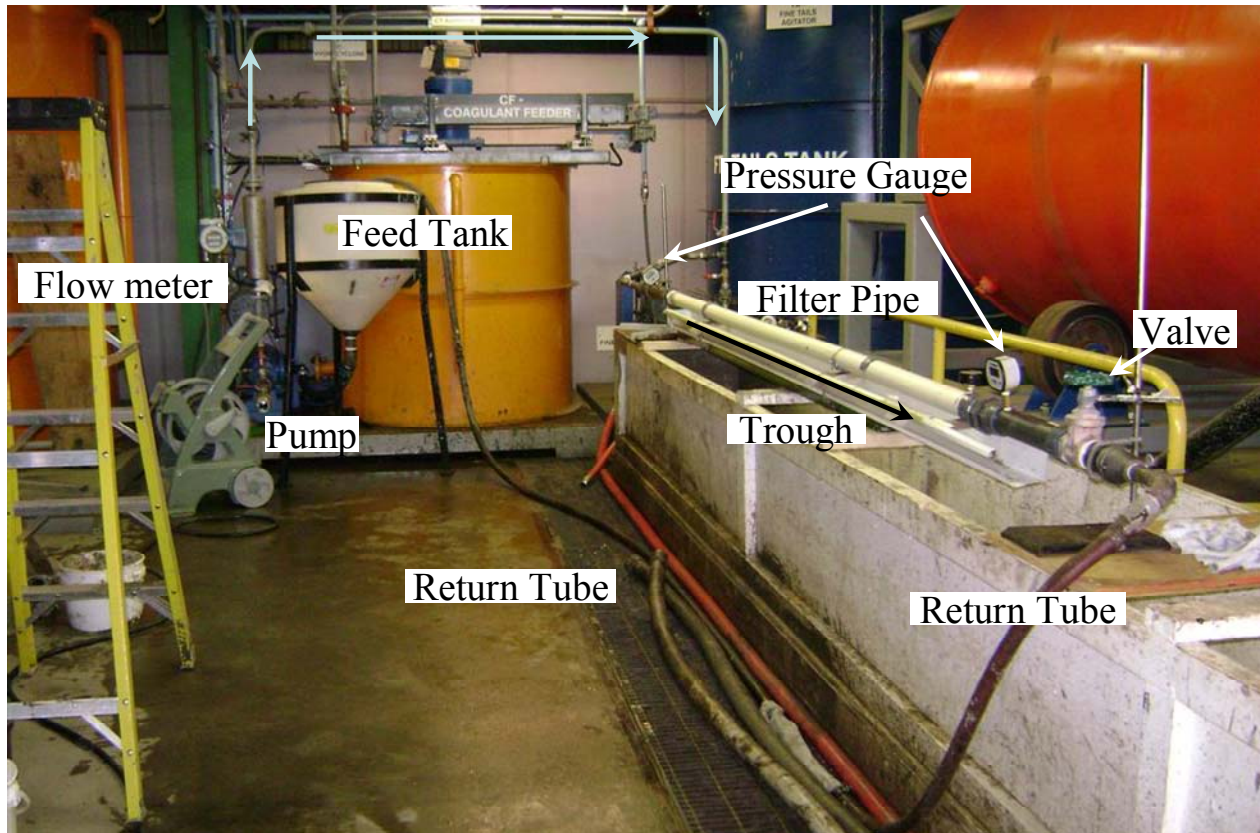


Figure 7. Photo of Cross Flow Filtration Operation Loop Setup

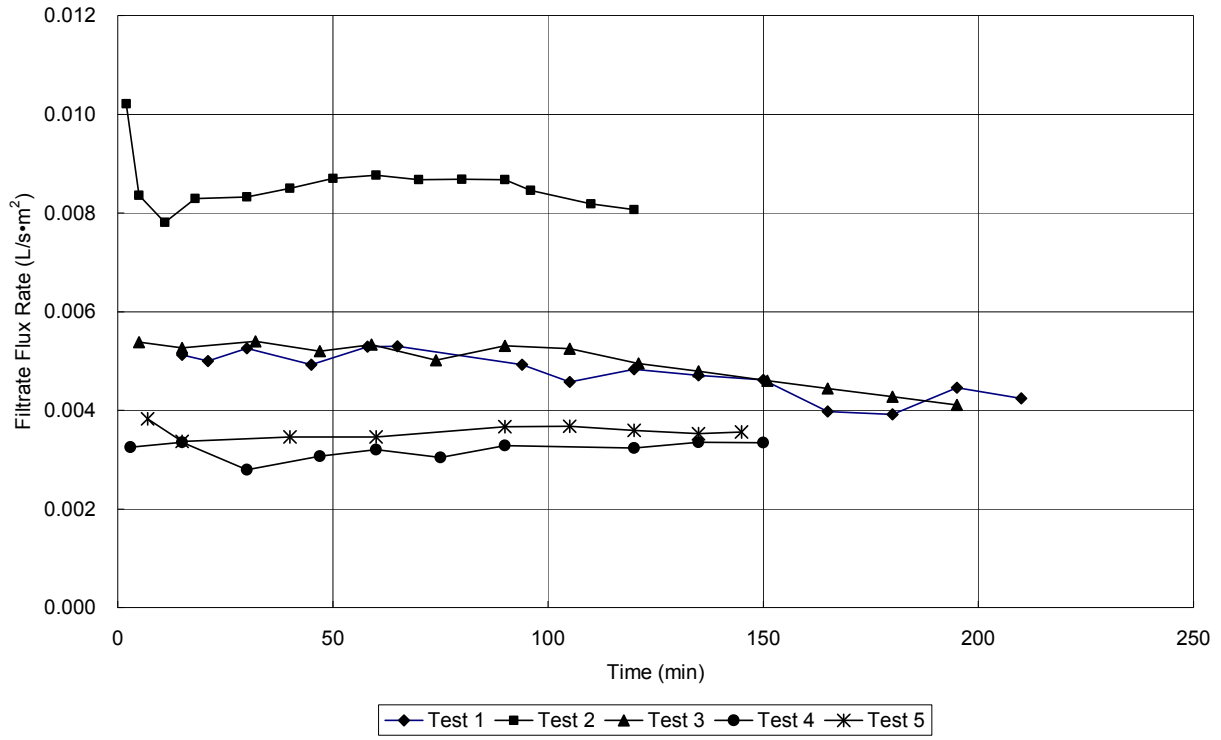


Figure 8. Change in Filtrate Water Quantity (Filtrate Flux Rate) with Time

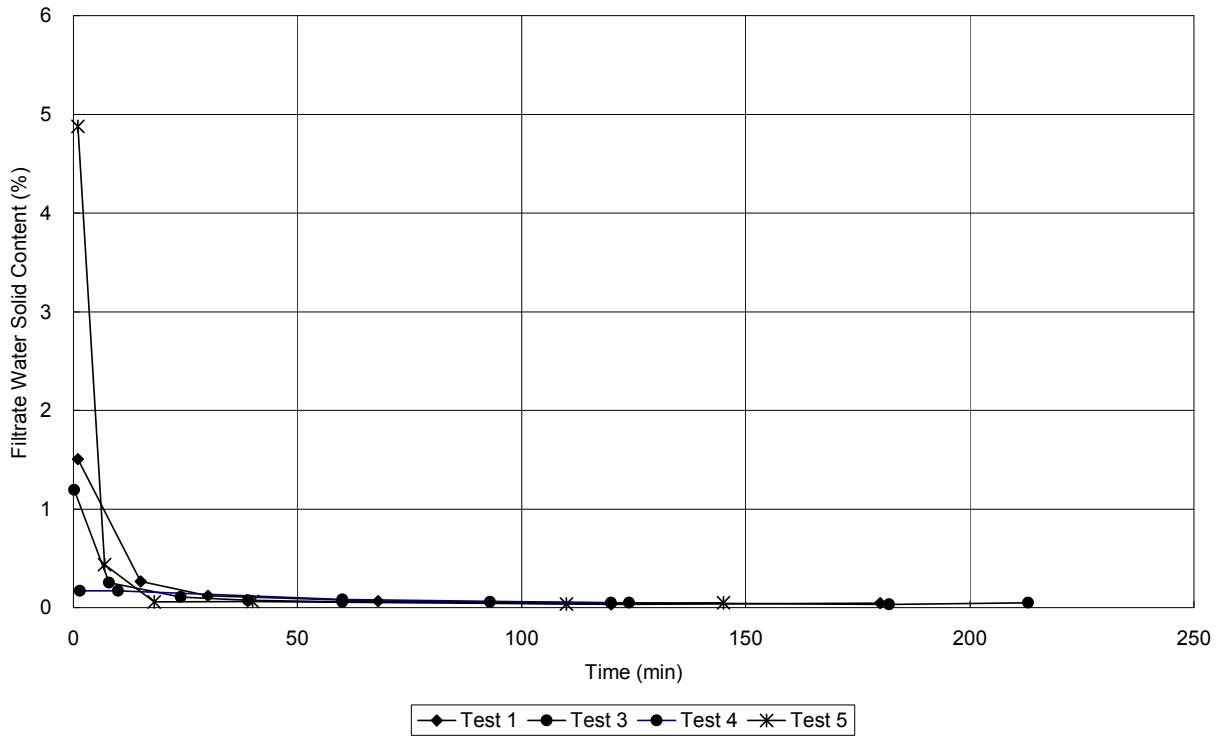


Figure 9. Change of Filtrate Water Quality (Solid Content) with Time

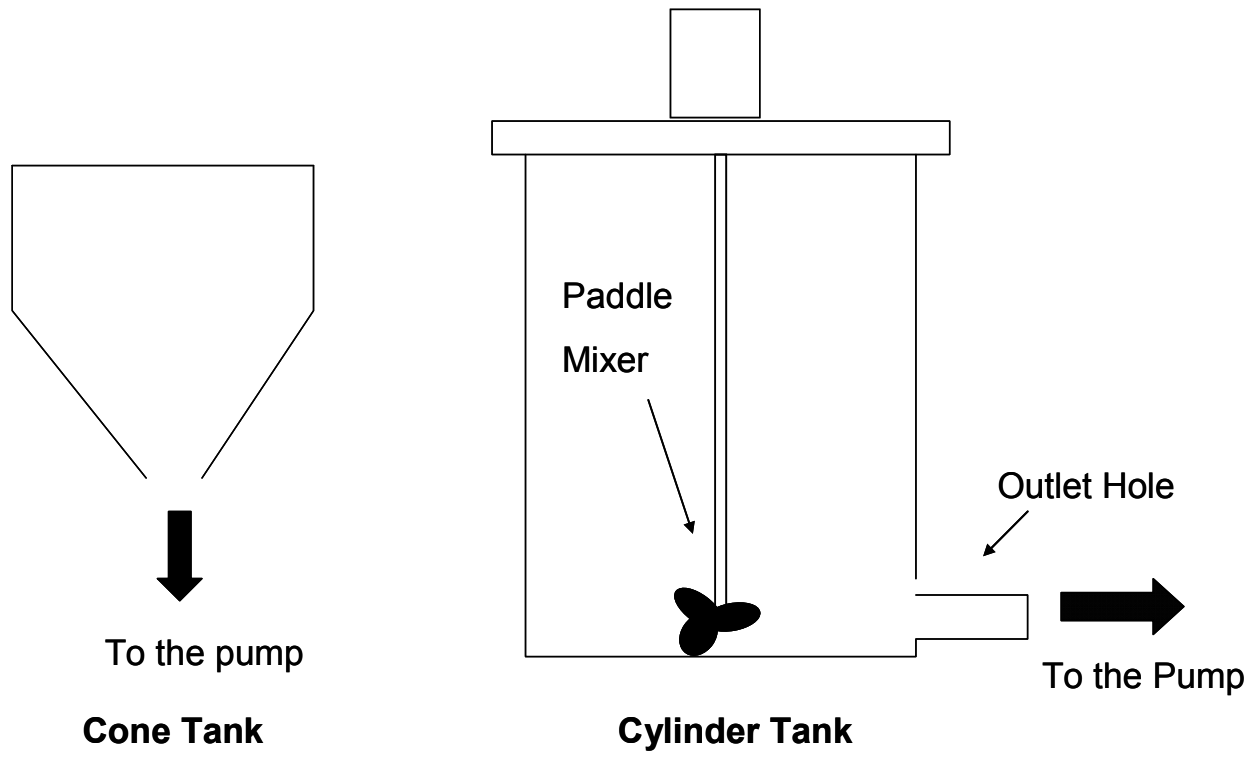


Figure 10. Cone Tank and Cylinder Tank with Pedal Mixer

GEOTECHNICAL CHARACTERISTICS OF LABORATORY IN-LINE THICKENED OIL SANDS TAILINGS

S. Jeeravipoolvarn, J. D. Scott and R.J. Chalaturnyk

Dept. of Civil and Environmental Engineering – University of Alberta, Edmonton, AB, Canada

ABSTRACT: This paper presents a laboratory study of the oil sands in-line thickened fine tailings geotechnical behavior. The in-line thickened tailings were prepared by mixing cyclone overflow tailings with chemical flocculent and coagulant in three consecutive stages. Hindered sedimentation tests, compressibility standpipe tests and large strain consolidation tests with vane shear strength measurements were then performed on both cyclone overflow and laboratory in-line thickened tailings to obtain a full range of sedimentation, consolidation and shear strength characteristics for these materials. Combined test results from the three tests indicate that at void ratios between 80 and 20, the in-line thickened tailings is over three magnitudes more permeable compared to the cyclone overflow. This significant improvement of hydraulic conductivity decreases as the solids content increases and disappears as the material is compressed to a void ratio of about 2. The experimental results also showed that the in-line thickened tailings has higher vane shear strengths compared to the cyclone overflow and requires a higher effective stress to compress to the same void ratio as the cyclone overflow. The laboratory results are compared to field measurements from a full scale field pilot project on in-line thickened tailings performed by Syncrude Canada Ltd. Good agreement between field and laboratory behavior was obtained.

INTRODUCTION

The oil sands mining operations in Northern Alberta produce large volumes of tailings composed of sand, silt, clay and a small amount of bitumen. Upon deposition, the tailings stream segregates with the sand and about one-half of the fines (defined as < 45 μ m in the oil sands industry) dropping out forming dykes and beaches. The remaining water, bitumen and fines flow into the tailings pond as thin fine tailings (TFT) which have about 8% solids and 90% fines. In the pond, sedimentation occurs and in about two years the tailings settle to

approximately 30% solids (void ratio of about 5). At this solids content, the material does not appear to be compressing further in the tailing ponds and the fine tailings at this point is called mature fine tailings (MFT). The MFT's slow compression behavior causes major problems for oil sand companies to manage containment ponds and to obtain recycle water for bitumen production.

To develop an alternative to MFT formation, a new type of tailings called in-line thickened tailings (ILTT) is being investigated. This process is aimed to

improve settling and strength characteristics of TFT. To achieve these new tailings, flocculants and coagulant are mixed with cyclone overflow tailings by an in-line multi stage fashion which is also known as tapered flocculation (Yuan and Shaw 2007). Conceptually, by binding fine particles at low solids content into flocs, the hydraulic conductivity is increased, tortuosity is decreased and the mass of the falling flocs is increased. The improvements of the ILTT over the TFT will result in a reduction of tailings storage by rapidly dewatering the cyclone overflow tailings stream which is a high fines stream with a small amount of sand and a source of new MFT. The higher shear strength characteristics of ILTT will create an opportunity to cap a tailings pond with a layer of sand or coke with a higher success rate. Sand layering with vertical drains is also foreseen as a possibility to be implemented on an ILTT deposit.

In order to evaluate ILTT behavior, a pilot scale in-line thickened tailings program was demonstrated by Syncrude in 2005. Field results indicated that the in-line thickening process produces tailings that undergo rapid hindered sedimentation from void ratios of 66 to 5 followed by fairly rapid consolidation at lower void ratios (Jeeravipoolvarn et al. 2008(a)). Shearing during deposition is believed to cause some segregation of the sand particles. The field pilot ponds were history matched by utilizing a conventional finite strain consolidation theory (Gibson et al. 1967) and by searching compressibility and hydraulic conductivity functions. Field measurements of interface height and average solids content with time were satisfactorily matched. Compressibility and hydraulic conductivity functions of the field ILTT obtained from this analysis showed that ILTT requires a higher applied stress to compress when compared to cyclone overflow and the field ILTT was more

permeable than cyclone overflow at the same void ratio. These characteristics of ILTT are believed to be caused by the stronger and more porous floc structure made by the in-line thickening process (Jeeravipoolvarn et al. 2008(a)).

In order to fully understand the sedimentation and consolidation behavior and to determine a full range of geotechnical parameters in a laboratory environment, a test program to determine a wide range of compressibility and hydraulic conductivity functions (Scott et al. 2008) was performed on both cyclone overflow and in-line thickened tailings. Sedimentation and consolidation characteristics of in-line thickened tailings were then compared to those of cyclone overflow to evaluate this new tailings treatment process. The sedimentation and consolidation characteristics of the ILTT determined in the laboratory were also compared to those measured in the field pilot project to determine whether the small scale laboratory tests could accurately forecast large scale field performance.

CYCLONE OVERFLOW TAILINGS

Typical oil sands tailings deposition to make nonsegregating or CT tailings is shown in Figure 1. After extraction, the oil sands tailings stream is passed through a cyclone to separate coarse particles and fines particles. The cyclone overflow tailings, a fine tailings stream, are discharged into a tailings pond and with time MFT is formed. Cyclone underflow, a coarse tailings stream, is mixed with MFT and a chemical additive to create the nonsegregating tailings (NST) which is deposited in a designated NST tailings disposal area for reclamation.

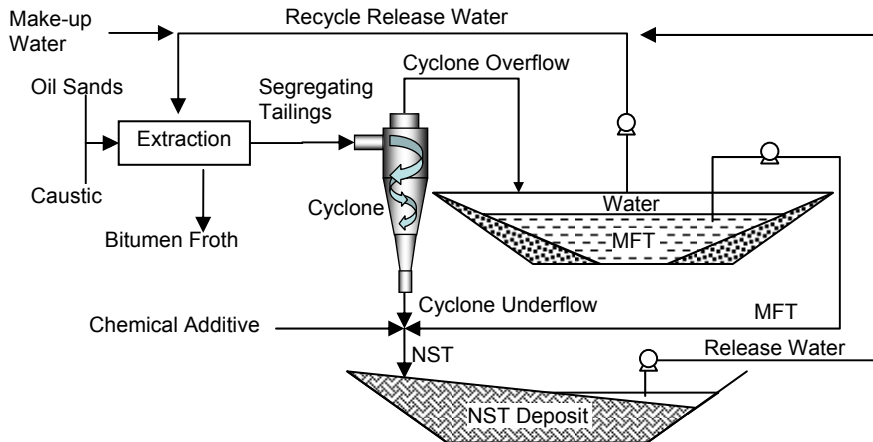


Figure 1. Typical oil sands tailings deposition

Cyclone overflow tailings for this test program were delivered from Syncrude’s composite tailings plant to the University of Alberta in April 2008. A total of 2 m³ of cyclone overflow were shipped. Dispersed and nondispersed particle size analyses were performed on the cyclone overflow sample and the results are shown in Figure 2. Nondispersed particle size distribution of cyclone overflow indicates that the material has approximately 94% fines and 30% clay size particles (< 2 μm) while the dispersed test indicates 94% fines and 50% clay size particles. These results contradict the previous findings that the fine tailings are completely dispersed by the bitumen extraction process and there is no difference between dispersed and nondispersed tests for the oil sand fine tailings (Jeeravipoolvarn et al. 2008(b)). The lower amount of clay size material in the nondispersed test might suggest a change in water chemistry possibly an increase in electrolyte concentration in the pore water.

The specific gravity of the solids (minerals + bitumen) was measured to be 2.46 and the calculated bitumen content was about 5% of the dry mass. A plasticity chart for cyclone overflow is plotted together with other oil

sands tailings materials in Figure 3 indicating that the cyclone overflow clay is of low to medium plasticity. The Activity of the cyclone overflow was calculated to be 0.49 which is classified as inactive clay. This confirms the dominant kaolinite clay mineral in these fine tailings materials (FTFC 1995).

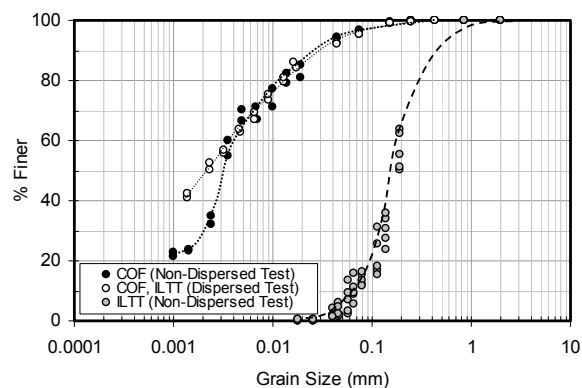


Figure 2. Comparison of particle size distributions of COF and Laboratory ILTT

Cyclone Overflow Sedimentation-Consolidation Characteristics

Testing procedures

In order to capture the wide range of compressibility and hydraulic conductivity of

the cyclone overflow and in-line thickened tailings from a void ratio of 80 to less than 1, a test procedure that combines three types of tests (Scott et al. 2008) was utilized in this test program. These tests include a large strain consolidation test, a compressibility standpipe test and a number of hindered sedimentation tests.

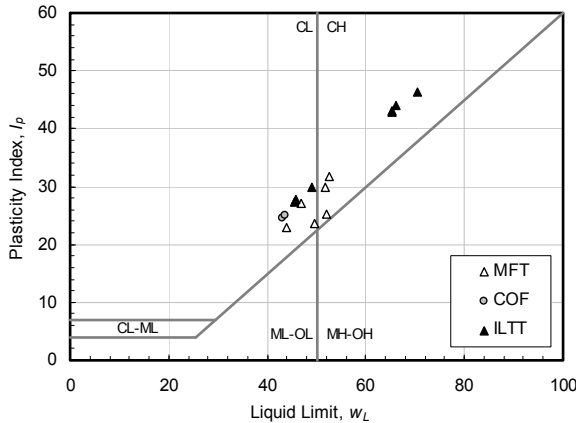


Figure 3. Plasticity chart of oil sands tailings

A large strain consolidation test is performed at moderate to low void ratios where application of stresses is possible. The compressibility standpipe is performed to obtain an effective stress-void ratio relationship at high void ratios and the hindered sedimentation test is utilized for determining hydraulic conductivity at high void ratios. The results from all the tests are combined to determine the effective stress-void ratio and the void ratio-hydraulic conductivity relationships from very low effective stresses to high effective stresses for finite strain consolidation modeling.

In this paper, the same testing procedure given by Scott et al. (2008) was strictly followed with one modification that two large strain consolidation tests were run in parallel for a single material. One consolidation test is performed with a vane shear strength test at the end of each loading increment while another test was done without a shear strength test to evaluate whether the vane

tests were influencing the compressibility and hydraulic conductivity characteristics.

Cyclone overflow test results

A total of five hindered sedimentation tests were performed for cyclone overflow tailings. Initial solids contents of 3.2, 4.9, 9.7, 14.7 and 23.5% (void ratios of 74.4, 47.7, 22.9, 14.3 and 8.0 respectively) were selected for the hindered sedimentation tests to cover large void ratios up to 80 (solids content of 3%) and to overlap results from the large strain consolidation tests at lower void ratios and higher effective stresses. Interface settlement measurements for the hindered sedimentation tests are shown in Figure 4.

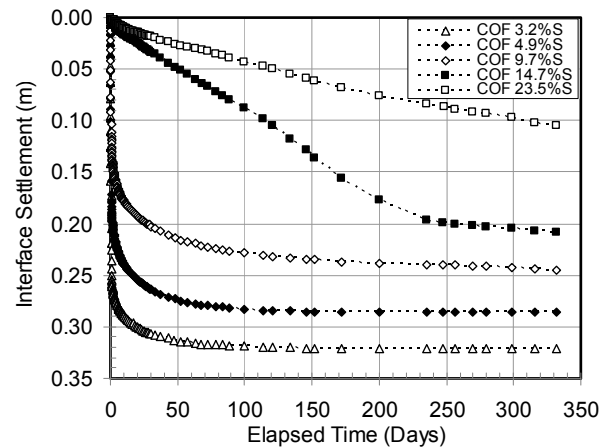


Figure 4. Hindered sedimentation tests for cyclone overflow

The slope of the initial linear portion of the interface settlement from each test is used to calculate hydraulic conductivity corresponding to the initial void ratio via Equation 1 (Been 1980, Pane and Schiffman 1997).

$$v_s = -\left(\frac{\gamma_s}{\gamma_w} - 1\right) \frac{k}{1 + e} \quad [1]$$

Where v_s is initial settling velocity, γ_s is unit weight of solids, γ_w is unit weight of water, k

is hydraulic conductivity and e is the initial void ratio.

Similarly to Equation 1, a non linear part of the settlement curve may also be used to obtain hydraulic conductivity via Kynch theory (Tan et al. 1990). In order to perform this analysis the surface solids concentration must be determined. Based on Kynch theory, Tan et al. (1990) proposed an expression to calculate solids concentration as Equation 2.

$$\left(x + t \frac{dx}{dt}\right)_p = \frac{M}{\eta} \quad [2]$$

Where x is height, t is time, M is total mass of solids, η is concentration and subscript p indicates a point on a settlement curve. Equation 2 is similar to an equation proposed by Renko (1998) which is derived in terms of solids concentration. In this paper, settling characteristics are expressed in terms of void ratio therefore Equation 2 is reformulated in terms of height and void ratio as shown in Equation 3.

$$e = \frac{(1 + e_0)(h + v_{sp}t)}{H} - 1 \quad [3]$$

Where e is void ratio, e_0 is initial void ratio, h is height at an interest point, v_{sp} is a tangential velocity at an interest point and H is initial height.

It is noted that the use of Equation 1 is widely accepted when slurry is undergoing hindered sedimentation but it is generally believed that during consolidation this method can not be used. Pane and Schiffman (1997) stated that this equation is valid only when there is a suspension at the initial void ratio at the sediment water interface or as long as the settling velocity is constant. Toorman (1999) indicated that the initial settling rate of self-weight consolidation can also be used to estimate hydraulic conductivity where

diffusive effects are negligible. Due to the fact that the influence of consolidation is not included in Equation 1 and diffusion can not be monitored by the current laboratory set up, this technique was applied only on the early portion of the nonlinear settling curve in this study.

Two 36 cm high compressibility standpipes were performed at initial solids contents of 3.2 and 4.9% (void ratio of 74.4 and 47.7 respectively). Compressibility results are shown in Figure 5. It can be seen that with this particular experimental procedure, compressibility can be measured from void ratios of 16 to 5 which covers effective stresses from 6 to 100 Pa.

The compressibility determined from a large strain consolidation test which employs effective stresses of 100 Pa and higher is also shown in Figure 5. Continuous compressibility data from the compressibility standpipe test and the large strain consolidation test is obtained. From the test results, the compressibility of cyclone overflow abruptly changes at void ratio of about 5 (solids content of about 33%). This result shows that as the fine tailings reaches a void ratio of 5, its compressibility is dramatically decreased which will result in a significantly smaller settlement as consolidation proceeds. Field measurements in oil sands tailings ponds also show this behaviour as fine tailings settle to about 30% solids in about two years and further consolidation is very small (Jeeravipoolvarn et al. 2009(a)).

The hydraulic conductivity of cyclone overflow from hindered sedimentation tests and large strain consolidation tests is shown in Figure 6. Similar to the compressibility, combined test data provides continuous hydraulic conductivity measurements from void ratios of 80 to 0.5 (solids content of 3 to 83%).

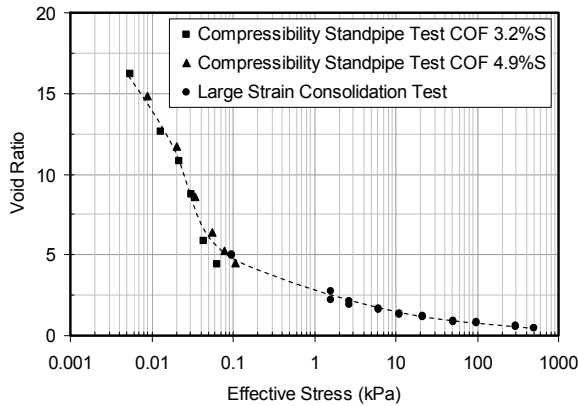


Figure 5. Compressibility of cyclone overflow

Figure 7 shows vane shear strength measurements for cyclone overflow tailings. According to Directive 074: Tailings Performance Criteria and Requirements for Oil Sands Mining Schemes (ERCB 2009), it is required that oil sands tailings deposits have a minimum shear strength of 5 kPa for successful reclamation. By interpolating the cyclone overflow test results in Figure 7, a void ratio corresponding to a shear strength of 5 kPa will be about 1.1 (solids content of about 69%). This would require an applied effective stress of about 25 kPa on a MFT deposit according to the measured compressibility data (Figure 5).

The test procedure given by Scott et al. (2008) was successfully performed and the compressibility of cyclone overflow was measured from a void ratio as high as 16 or an effective stress as low as 6 Pa while the hydraulic conductivity was measured from a void ratio as high as 80 and lower.

IN-LINE THICKENED TAILINGS

In-line Thickened Tailings Sedimentation-Consolidation Characteristics

The in-line thickening process refers to a process that injects chemical flocculent and

coagulant in three consecutive stages into cyclone overflow to maximize the floc formation during pipe line transportation to a designated deposition pond. This process is illustrated in Figure 8. During the first stage (Figure 8(a)), a flocculent solution is added and distributed into the cyclone overflow tailings.

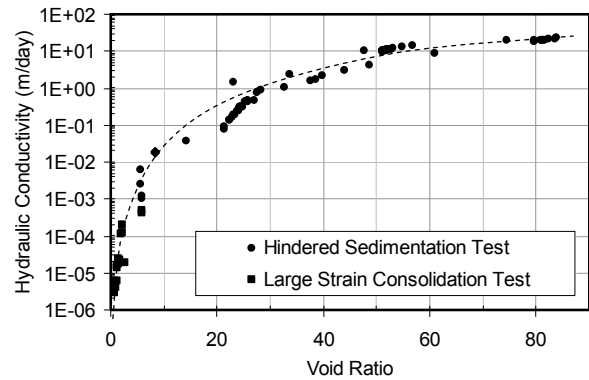


Figure 6. Hydraulic conductivity of cyclone overflow

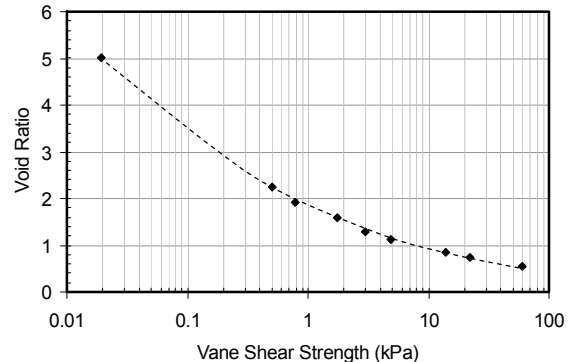


Figure 7. Vane shear strength of cyclone overflow

The long chain molecules of the flocculent, which has various charges along the chain, attach to coarse and fine particles and brings these particles together to form a floc. Some clay particles are not captured during this stage. In the second stage (Figure 8(b)) the coagulant solution is added into the tailings from the first stage. The coagulant alters surface charges on the clay particles and results in coagulation of the particles. The final stage (Figure 8(c)) is to add a flocculent solution into the product of the second stage

to bind the coagulated clay with the flocs to form large aggregates.

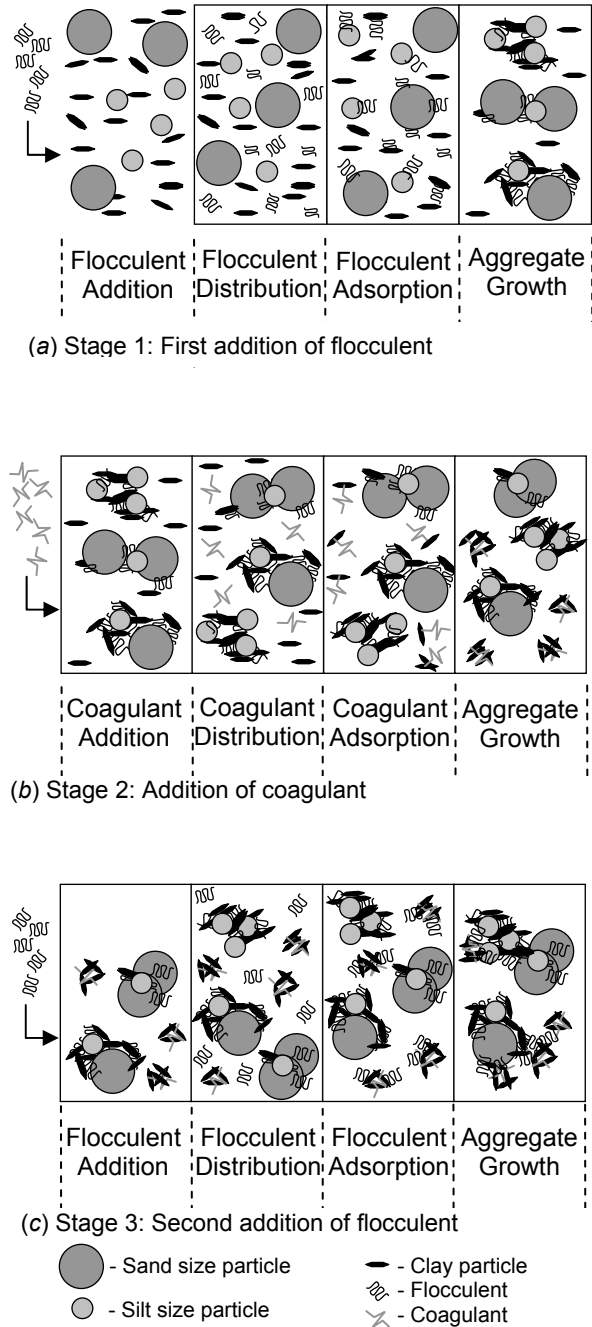


Figure 8. ILTT Process

By following the above process, the hydraulic conductivity of the mixtures is significantly increased because the aggregates are far apart, tortuosity is decreased and the mass of the falling aggregates is increased. This results in tailings that can undergo sedimentation very quickly and as some consolidation occurs, suitable shear strength is obtained which allows a wide variety of reclamation methods.

The schematic implementation of ILTT into the conventional oil sands operation is shown in Figure 9. After extraction, the oil sands tailings are passed through cyclones which produce coarse and fine tailing streams. Cyclone overflow tailings are thickened via the in-line thickening process. Rapid water release results in a smaller required tailings containment pond and hot water which can be returned to the extraction plant.

A reclamation option is also shown in Figure 9. The field pilot project showed that after deposition in a containment pond the ILTT consolidates to 50% solids in a few months. The higher solids ILTT can then be pumped out and mixed with the cyclone underflow to form NST. The higher solids ILTT may require little or no coagulant to form robust NST.

ILTT laboratory simulation

In order to produce ILTT for laboratory experiments, the cyclone overflow shipped from the Syncrude composite tailings plant was characterized to obtain initial solids content, specific gravity and grain size distribution. Anionic flocculent was prepared by mixing powder flocculent with demineralized water to a concentration of 0.5 g/L. Cationic coagulant was similarly

prepared by mixing powder coagulant with demineralized water to a concentration of 1g/L

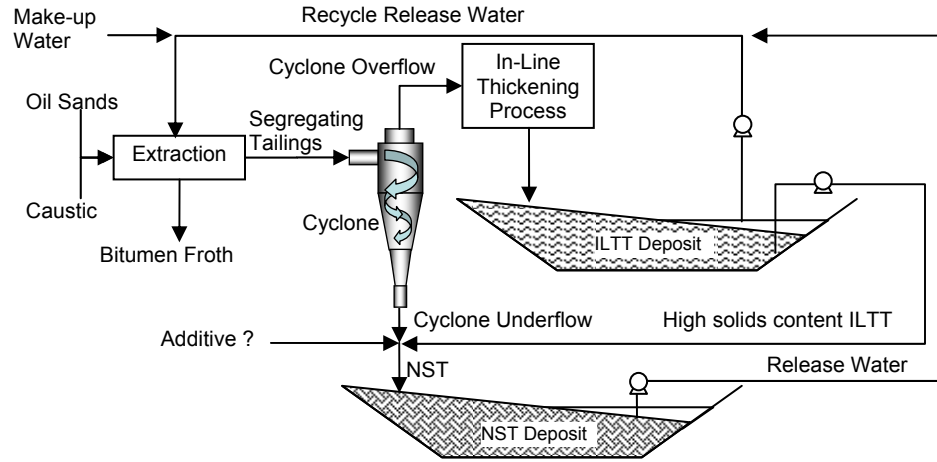


Figure 9. Syncrude ILTT production with NST reclamation.

In order to prepare ILTT to a design solids content and volume, total mass and solids mass of cyclone overflow is calculated by Equations 4 and 5. Total mass of a design mix is calculated by Equation 6.

$$M_{COF} = \frac{SV}{S_{COF}} \left(\frac{Gs}{Gs + S(1 - Gs)} \right) \quad [4]$$

$$M_s = SV \left(\frac{Gs}{Gs + S(1 - Gs)} \right) \quad [5]$$

$$M = V \left(\frac{Gs}{Gs + S(1 - Gs)} \right) \quad [6]$$

Where M is total mass of design ILTT, M_{COF} is total mass of cyclone overflow, S is design solids content, V is design volume and G_s is specific gravity of the solids.

With a known mass of solids from Equation 5, the amount of chemicals used for the three mixing steps is calculated by Equation 7 and the amount of water required for the mix is subsequently calculated by Equation 8.

$$V_i = \frac{d_i M_s}{c_i} \quad [7]$$

$$M_{wa} = M - M_{COF} - \sum_{i=1}^3 \rho_i V_i \quad [8]$$

Where V is the volume of solution required, d is the dosage of the prepared chemical solutions, c is the concentration of the prepared chemical solutions, M_{wa} is the additional recycled water required and ρ is the density of the solution. The subscript i defines mixing steps which run from 1 to 3.

To prepare ILTT at a solids content of S and a volume of V , cyclone overflow with a total mass of M_{COF} is mixed with recycled water with a mass of M_{wa} . Flocculent for step 1, coagulant for step 2 and flocculent for step 3 are prepared at volumes of V_1 , V_2 and V_3 respectively.

To start the mixing process, cyclone overflow and the recycled water are mixed for 1 minute with a controlled propeller tip speed of about 0.8 m/s. Then a timer is started and the first flocculent is added slowly through a syringe into the middle of a mixing container. Within 30 seconds all of the first flocculent is mixed at a dosage of 200 g/T of dry solids. Then the second coagulant and third flocculent are added

continuously with the same time and discharging technique at dosages of 800 g/T and 60 g/T respectively. After 1.5 minutes the mixing is completed, the mixer is stopped and ILTT tailings is ready for laboratory geotechnical testing.

ILTT test results

Apparent grain size distribution of ILTT was measured by a nondispersed hydrometer test and the results are shown in Figure 2. The ILTT apparent grain size distribution indicates that the material has an individual fines content ($< 45 \mu\text{m}$) of less than 5%. All other fines are tied up in larger flocs. The large apparent grain size of the material indicates the strong influence of the in-line thickening process that brings small particles together forming large aggregates that should settle in a very rapid manner.

Atterberg limits for ILTT are shown in Figure 3. The average liquid limit and the plasticity index of ILTT are found to be 66 and 43 indicating that ILTT may behave as clay of high plasticity. The Activity of ILTT is calculated to be 0.87 which is classified as normal activity.

A total of 17 hindered sedimentation tests were performed for ILTT at solids contents of 3, 5, 7.5, 10 and 18.5% (void ratios of 79.5, 46.7, 30.3, 22.1 and 10.8 respectively). It is noted that for higher solids contents than 5%, ILTT was prepared at 5% and was allowed to release water to the design solids content before the hindered sedimentation test was commenced.

Interface settlement results for ILTT are shown in Figure 10. It can be seen that the material settles very rapidly at all solids contents and completes most of the settlement in less than 20 minutes.

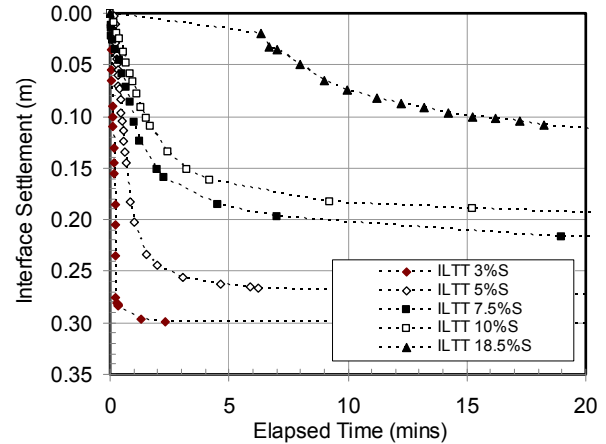


Figure 10. Hindered sedimentation tests on ILTT

Two compressibility standpipe tests for ILTT were performed at an initial solids content of 5% in 36 cm and 120 cm high standpipes. Data from both standpipes are shown in Figure 11. The 120 cm high standpipe test was performed to reach an effective stress of about 350 Pa. This height was chosen to provide an ample overlap of effective stress measurements with a large strain consolidation test which can measure effective stress as low as 100 Pa.

Compressibility measurements from large strain consolidation tests are also shown in Figure 11. Continuous compressibility for ILTT is obtained and with these measuring techniques, the compressibility of ILTT was measured between void ratios of about 17 to 0.6 or effective stresses of about 9 Pa to 500 kPa respectively.

Hydraulic conductivity measurements from hindered sedimentation and large strain consolidation tests are shown in Figure 12. The combination of hindered sedimentation tests and large strain consolidation tests provide a continuous hydraulic conductivity measurement for ILTT from void ratios of about 80 to 0.6 and the results suggest that .

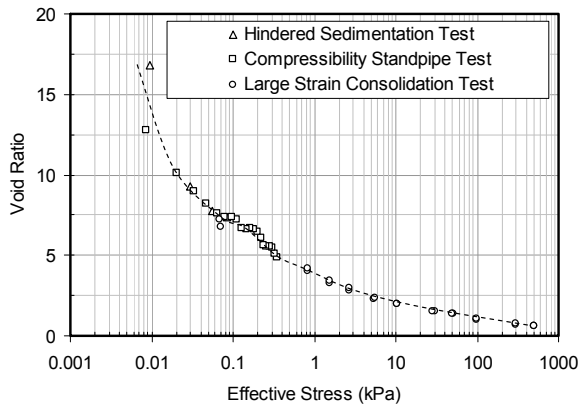


Figure 11. Compressibility of ILTT

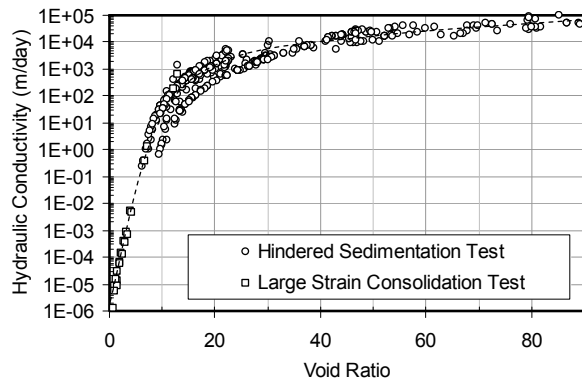


Figure 12. Hydraulic conductivity of ILTT

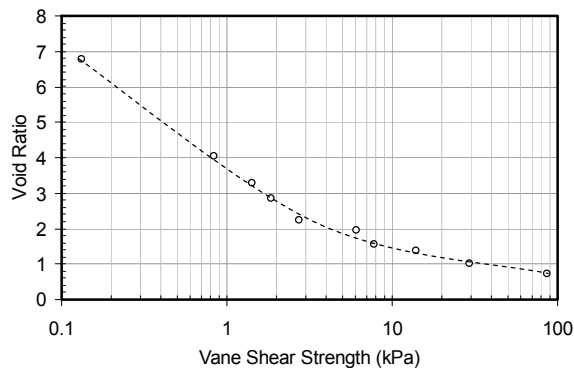


Figure 13. Vane shear strength of ILTT

The hydraulic conductivity of ILTT starts to drop dramatically at a void ratio of about 15. It is noted that the maximum void ratio that effective stress can be measured with the present techniques is at about the same void ratio of 15. This void ratio may be regarded as a maximum suspension void ratio (e_m)

that corresponds to the initial development of a distinct slurry microstructure (Azam et al. 2007). As the material is compressed further this physiochemical effect is overcome at a lower void ratio of e_s or a structural void ratio where effective stress is the major control on the compressibility, that is, the physics dominates the chemistry (Azam et al. 2009, Jeeravipoolvarn et al. 2009(b)).

Vane shear strength of ILTT is shown in Figure 13. Instead of the 25 kPa effective stress requirement to reach a vane shear strength of 5 kPa for cyclone overflow, ILTT requires an effective stress of about 10 kPa which is only 40% of that for the cyclone overflow.

COMPARISON OF LABORATORY RESULTS AND FIELD MEASUREMENTS

In this section, the laboratory determined properties of the cyclone overflow and the ILTT are compared and discussed. The field performance of ILTT which was determined through history matching (Jeeravipoolvarn et al. 2008(a)) is also compared with ILTT made in the laboratory.

Comparison of COF and ILTT

In Figure 14, the compressibility of cyclone overflow and laboratory ILTT are compared. The laboratory data suggests that the compressibility of cyclone overflow and ILTT are similar from void ratios of about 16 to 8. The compressibility of both materials, however, follows different paths at lower void ratios. The cyclone overflow below a void ratio of about 5 becomes much less compressible. For ILTT, the change in its compressibility appears to occur at a higher void ratio and is more gradual than that of cyclone overflow. ILTT

compressibility starts to change as it reaches a void ratio of around 8. ILTT compressibility behavior appears to withstand higher effective stresses at void ratios of 8 and below. The compressibility of both materials converges as the effective stress gets higher.

The hydraulic conductivity comparison between cyclone overflow and ILTT is shown in Figure 15. ILTT hydraulic conductivity is more than three magnitudes greater than that of the cyclone overflow at a void ratio of 80. This significant increase in the hydraulic conductivity also persists throughout void ratios larger than 20. The increase of hydraulic conductivity due to the in-line thickening process is decreased as the void ratio is decreased below 20 and when the void ratio is reduced to about 2 there appear to be little difference between the two materials.

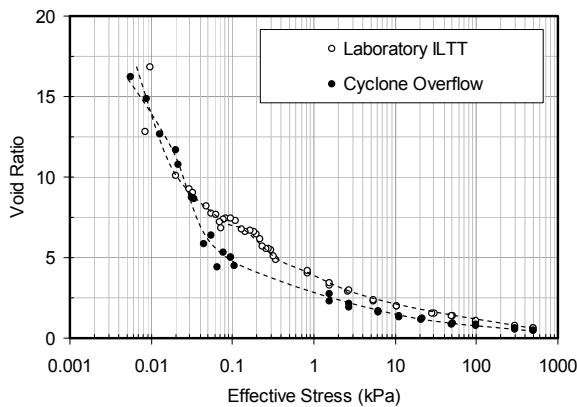


Figure 14. Compressibility of COF and Laboratory ILTT

Comparison of laboratory ILTT and ILTT field performance

ILTT pilot ponds were started in late 2005 to demonstrate the pilot scale behavior of tailings produced from the in-line thickening process (Jeeravipoolvarn et al. 2008(a)).

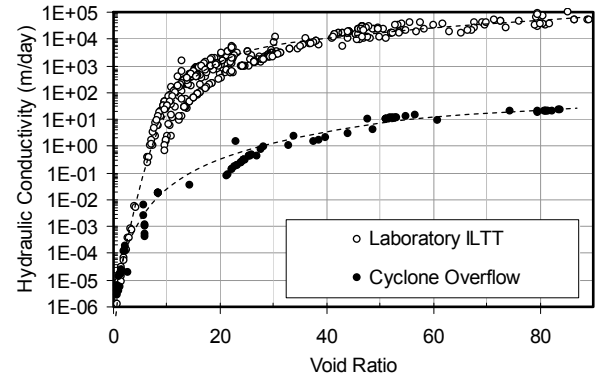


Figure 15. Hydraulic conductivity of COF and Laboratory ILTT

Geotechnical field investigations including pore pressure measurements, solids and fines content measurements and vane shear strength measurements were performed to monitor the consolidation behavior of the deposits. Field history matching for consolidation performance was also performed by using a conventional finite strain consolidation theory to determine the field compressibility and hydraulic conductivity relationships. Both relationships are expressed as Equations 9 and 10.

$$e = \begin{cases} 4.000\sigma'^{-0.375_1} & \text{for } \sigma' < 10\text{kPa} \\ 2.676\sigma'^{-0.201} & \text{for } \sigma' \geq 10\text{kPa} \end{cases} \quad [9]$$

$$k = 2.0 \times 10^{-5} e^{5.0} \quad [10]$$

Where e is void ratio, σ' is effective stress in kPa and k is hydraulic conductivity in m/day. These two relationships are compared with the ILTT laboratory data in Figures 16 and 17 for compressibility and hydraulic conductivity respectively.

In Figure 16, it can be seen that the field history matching function is generally similar to the laboratory measurement. It can also be observed that the field deposit is less compressible at a void ratio of about 7 and higher. This may be a function of thixotropy

as deposition in the field deposit took much longer than deposition in the laboratory.

From the final solids content profile and knowing the initial solids content of 3.7%, it was calculated that the pond would have an initial fill height of about 20.4 m if the pond were filled instantaneously. With this information, large strain consolidation analysis shows that the error of the history matching compressibility function will be less than 4% of the final height when compared with the laboratory results. This error is small considering that the average interface measurement from the field data used in the analysis has readings fluctuating as much as 10% within each measuring station. This small 4% difference is because only a small percentage of the material in the pond has a void ratio larger than 7. Compressibility of the material at this void ratio and higher is very high, therefore the error in the history matching function at this range of void ratios does not contribute to a large difference in the interface settlement calculation.

The good comparison below a void ratio of 7 in Figure 16 suggests that the history matching approximation of using the average interface settlement measured in the field deposit provides a good approximation of the compressibility behavior of the field ILTT.

In Figure 17, a good agreement between field history matching hydraulic conductivity and laboratory measurements is obtained. It can be observed that between void ratios of 0.6 to 10 and 50 to 80, the laboratory hydraulic conductivity behavior of the ILTT well models the field history

matching analysis. Between void ratios of 10 and 50 it appears that the field hydraulic conductivity is lower than the laboratory measurements. The reason for the lower hydraulic conductivity behavior in the field is postulated to be caused by pumping and pipelining shearing during the ILTT deposition. As floc aggregates are closer at higher solids content, the possibility of aggregates to collide and break is higher. This influence is significantly lower in a controlled laboratory environment.

The vane shear strength comparison is shown in Figure 18 for laboratory ILTT, field samples of ILTT, field vane shear measurements and laboratory cyclone overflow. The laboratory ILTT has the highest vane shear strength at void ratios of 3 and higher. At void ratios lower than 3, the field samples and laboratory ILTT show similar shear strength response. The field vane shear strength measurements also agree well with the laboratory and field samples at lower void ratios. Cyclone overflow vane shear strength is the lowest throughout the full range of void ratios.

The ILTT field and laboratory undrained shear strength to effective stress ratio, τ_u/σ'_{vo} , is plotted against void ratio in Figure 19. The results show that τ_u/σ'_{vo} is not constant at all void ratios but increases linearly with void ratios at void ratios above 1.5. Below a void ratio of 1.5 where the slurry is becoming a typical soil deposit, the τ_u/σ'_{vo} ratio appears to be quite constant at 0.29. The large values at high void ratios are indicative of the strong bonds in the flocs. As the flocs are compressed during consolidation the flocs break and their high bond strength is lost.

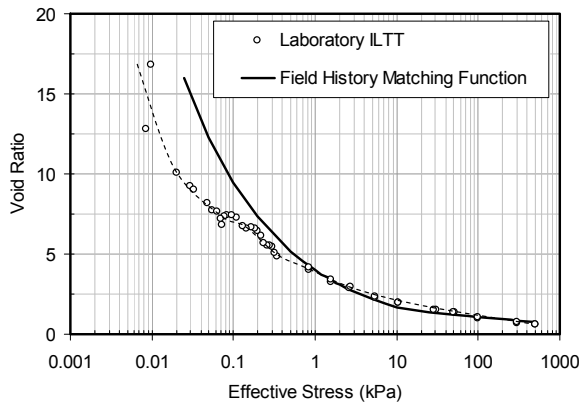


Figure 16. Compressibility comparison of field performance and laboratory measurements

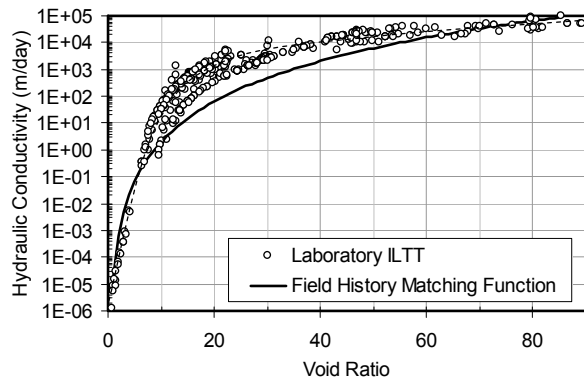


Figure 17. Hydraulic conductivity comparison of field performance and laboratory measurements

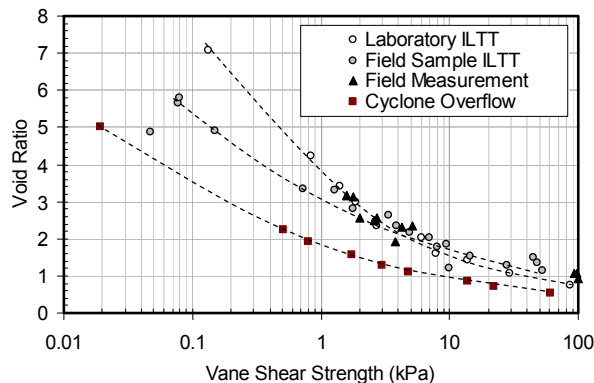


Figure 18. Vane shear strength of COF, Laboratory ILTT and Field sample ILTT

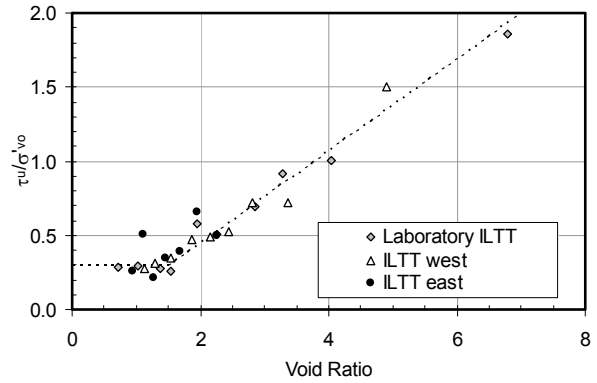


Figure 19. Laboratory determined shear strength-effective stress relationship

SUMMARY AND CONCLUSIONS

A laboratory study of sedimentation and consolidation behavior of cyclone overflow and in-line thickened tailings was conducted to investigate the changes in compressibility, hydraulic conductivity and vane shear strength induced by the in-line thickening process. Cyclone overflow was directly obtained from Syncrude Canada Ltd. and ILTT was prepared by mixing the cyclone overflow tailings, recycle water, flocculent and coagulant to a design solids content under the specified mixing conditions.

The research objective of comparing ILTT and cyclone overflow properties was that the difference in the behavior of the materials would be directly related to the effect of the flocculent and coagulant added during in the in-line thickening process. The role of the additives is to bring soil particles together to form large aggregates that can settle quickly. The hypothesis is that as the additives associate the soil particles, the shear strength of the soil will increase as structural breakage requires additional energy. The soil structure therefore becomes stronger as it is treated through the in-line thickening process. Compared to the cyclone overflow, the ILTT compresses less when subjected to the same applied stress. This appears to be

true based on the laboratory results. The hydraulic conductivity should also be affected by the in-line thickening process because the additives change the structure of the soil reducing the tortuous channels of the soil resulting in greater hydraulic conductivity. This statement is affirmed by the laboratory program presented in this paper.

Three sub tests, a hindered sedimentation test, a compressibility standpipe test and a large strain consolidation test were combined to measure the full range of sedimentation and consolidation characteristics for both materials. With the given testing techniques, the void ratio-hydraulic conductivity relationship can be measured from a void ratio of 80 and lower and the effective stress-void ratio relationship can be measured from a void ratio of 16 and lower. Continuous data for both relationships were obtained for both tailings materials.

The comparison of the cyclone overflow and ILTT compressibility showed that the compressibility of cyclone overflow and ILTT are similar at void ratios between 8 and 16. For void ratios lower than 8, the compressibility of the materials follow different paths. Cyclone overflow below a void ratio of 5 becomes much less compressible. ILTT appears to withstand higher effective stresses and becomes much less compressible below a void ratio of 8. The compressibility of both materials is converging at high effective stresses.

The hydraulic conductivity comparison of cyclone overflow and ILTT indicates that the ILTT hydraulic conductivity is more than a thousand times greater than that of the cyclone overflow from a void ratio of 20 to 80. The increase of hydraulic conductivity

due to the in-line thickening process is decreased as void ratio is decreased and as the void ratio reaches to about 2 there appears to be little difference between the two materials.

At void ratios of 3 and higher, the vane shear strength comparison indicates that the laboratory ILTT has the highest vane shear strengths followed by field ILTT samples and then laboratory cyclone overflow. At void ratios lower than 3, field samples, field measurements and laboratory ILTT show a similar shear strength response. Amongst all the materials, the cyclone overflow tailings provide the lowest vane shear strength throughout all measured void ratios.

The τ_u/σ'_{vo} ratio for ILTT is found to increase linearly with void ratio but as the ILTT is compressed below a void ratio of about 1.5, τ_u/σ'_{vo} appears to be quite constant at 0.29. The large values at high void ratios are an indication of the strong bonds in the flocs. As the flocs are compressed during consolidation the flocs break and their high bond strength is lost.

The comparison of the field history matching and the laboratory measured compressibility and hydraulic conductivity data of ILTT resulted in good agreement. Small discrepancies were observed. A dissimilarity in the compressibility occurred at a void ratio of 7 and higher and appeared to be due to the fact that the history matching analysis, which uses the field interface measurements, is not sensitive in the very high compressible region. For the hydraulic conductivity comparison, a small difference is believed to be caused by the shearing during the material deposition in the field which does not occur in a laboratory controlled environment.

ACKNOWLEDGEMENTS

The authors are grateful for the financial support from the University of Alberta and Syncrude Canada Ltd. The continued support of Warren Zubot, Geoff Halferdahl and Ron Lewko of Syncrude Canada Ltd. is greatly appreciated especially for procuring large amounts of field cyclone overflow which enabled the laboratory research program to be performed. The authors also appreciate the field supervision, the opportunity to assist with the field ILTT pilot test and continued advice on the research program from Bill Shaw of WHS Engineering and Nan Wang of Syncrude Canada Ltd. The technical support from Gerry Cyre, Geoforte Services Ltd. and Steve Gamble, Department of Civil and Environmental Engineering, University of Alberta was of great aid.

REFERENCES

- Azam, S., Jeeravipoolvarn, S., and Scott, J.D., 2009. "Numerical modeling of tailings thickening for improved mine waste management", *Journal of Environmental Informatics*, 13(2):111-118.
- Azam, S., Scott, J.D., and Jeeravipoolvarn, S. 2007. When does a slurry become a soil? *Geotechnical News. BiTech, BC*, 25(3), 44-46.
- Been, K. 1980. Stress strain behaviour of cohesive soil deposited under water. *Ph.D. Thesis*, Oxford University.
- Gibson, R.E., England, G.L. and Hussey M.J.L. 1967. The Theory of One-dimensional Consolidation of Saturated Clays. I. Finite Non-linear Consolidation of Thin Homogeneous Layers. *Géotechnique*, 17(3): 261-273.
- ERCB 2009. Directive 074 Tailings Performance Criteria and Requirements for Oil Sands Mining Schemes. The Energy Resources Conservation Board of Alberta (ERCB), Calgary, Alberta, pp. 5-10.
- FTFC 1995. Clark hot water extraction fine tailings. *In* Advance in oil sands tailings research. Fine Tailings Fundamental Consortium (FTFC, Oil Sands and Research Division, Alberta Department of Energy, Edmonton, Alberta. Vol I. pp.79-84.
- Jeeravipoolvarn, S., Scott, J.D., and Chalaturnyk, R.J., 2009 (a). "10 m standpipe tests on oil sands tailings: long term experimental results and prediction". *Canadian Geotechnical Journal*, 46:875-888.
- Jeeravipoolvarn, S., Chalaturnyk, R.J., and Scott, J.D., 2009 (b). "Sedimentation-consolidation modeling with an interaction coefficient", *Computer and Geotechnics*, 36(5):751-761.
- Jeeravipoolvarn, S., Chalaturnyk, R.J. and Scott, J.D., 2008 (a). Consolidation Modeling of Oil Sands Fine Tailings: History Matching, *Proceedings of 61st Canadian Geotechnical Conference*, Edmonton, AB, September 22-24, 190-197.
- Jeeravipoolvarn, S., Scott, J.D., Donahue, R., and Ozum, B., 2008 (b). "Characterization of Oil Sands Thickened Tailings", *Proceedings of International Oil Sands Tailings Conference*, December 7-10, Edmonton, AB, pp.132-142.
- Pane, V. and Schiffman, R.L. 1997. Permeability of clay suspensions, *Géotechnique*, 47:273-288.

Renko, E.K. 1998. "Modeling hindered batch settling Part II: A model for modeling solids profile of calcium carbonate slurry", *Water SA*, 24(4): 331-336.

Scott, J.D., Jeeravipoolvarn, S. and Chalaturnyk, R.J., 2008, "Tests for Wide Range of Compressibility and Hydraulic Conductivity of Flocculated Tailings", *Proceedings of the 61st Canadian Geotechnical Conference*, September 22-24, Edmonton, AB: 738-745.

Tan, T.S., Yong, K.Y., Leong, E.C. and Lee, S.L., 1990. Sedimentation of clayey slurry. *Journal of Geotechnical Engineering*, 116(6): 885-898

Toorman, E.A. 1999. Sedimentation and self-weight consolidation: constitutive equations and numerical modeling. *Géotechnique*, 49(6):709–726

Yuan, S. and Shaw, W. 2007. Novel Processes for Treatment of Syncrude Fine Transition and Marine Ore Tailings. *Canadian Metallurgical Quarterly*, 46(3): 265-272.

THICKENED TAILINGS (PASTE) TECHNOLOGY AND ITS APPLICABILITY IN OIL SAND TAILINGS MANAGEMENT

Simon Yuan and Rick Lahaie

Research & Development Center, Syncrude Canada Ltd., Edmonton, Alberta

ABSTRACT : Management of fine tailings is a common challenge faced by many mining companies. In some cases, this can become the potential bottleneck problem determining the fate of a company, either surviving or closing down for not meeting environmental regulations. Thickened tailings (paste) technology is an integrated engineering system. It generally includes the thickener feed preparation process, thickener type selection and thickening process, flocculant selection and flocculation technology development, thickened tailings (TT) transport, TT deposition and consolidation, strategy of reuse of thickener overflow water, and impacts on environment and existing plant operation, etc. Specific to the oil sand industry, several unique situations present themselves. The first is heat recovery; with large amounts of heat required in the oil sand extraction process, thickeners offer the opportunity to recover significant heat from tailings. Secondly, the tonnage and volume of materials handled along with the varying clay content demand a thickener that can handle significant variability in feed characteristics (flow rate, slurry SG, sand to fines ratios, and mineralogy, etc) and thirdly, minor amounts of bitumen in the oil sand tailings reporting to the thickener feed demand special engineering control. This paper will give an overview of the development of thickened tailings technology worldwide in mineral industry and highlight what Syncrude Research & Development has done in developing this technology to tackle the specific circumstances of fine oil sand tailings. With consideration of the new Oil Sand Tailings Directive released in February 2009, the applicability of thickened tailings (paste) technology in the oil sand tailings management framework is assessed.

INTRODUCTION

Although the thickened tailings disposal concept was conceived in 1965 by Robinsky and first commercially implemented in Kidd Creek Mine of Timmins, Ontario in 1973 (Robinsky, 1978), its importance and benefits to fine tailings management in the mineral industry had not been realized until the 1990s. The thickened tailings and thin-lift dry stacking technology, pioneered by the aluminum industry, has found more and

more applications in base metal, precious metal, mineral sands and coal industries since 1995. Syncrude Canada Ltd independently and in collaboration with other research institutes and oil sand developers has conducted many years of research and development work to evaluate the applicability of various flocculation and thickening technologies to treat its tailings from bench, pilot to field scales (Xu and Cymerman 1999; Cymerman et al. 1999; Sworska et al. 2000a and 2000b; Shaw et al.

2003, 2004; Kwong et al. 2005; Yuan and Shaw 2006; Lee and Yuan 2007; Yuan, 2007; Yuan and Shaw 2007; Yuan and Shaw 2008). In the circumstance of oil sand tailings disposal, there are more challenges in application of the TT (paste) technology than in the mineral industry. The full picture of TT (paste) technology in oil sand tailings application is proposed in Figure 1. As shown in Figure 1, this technology is an integrated complex engineering system, which can be simply classified into five blocks, i.e., Thickening Process, Transport, Deposit, Water Recycle and Environment. Specific to the oil sand industry, several unique situations present themselves. The

first is heat recovery; with large amounts of heat required in the oil sand extraction process, thickeners offer the opportunity to recover significant heat from tailings. Secondly, the tonnage and volume of materials handled along with the varying clay content demand a thickener that can handle significant variability in feed characteristics (flow rate, slurry SG, mineralogy, sand to fines ratios, and mineralogy, etc) and thirdly, minor amounts of residual bitumen in the oil sand tailings reporting to the thickener feed and the recycle water demand special engineering control.

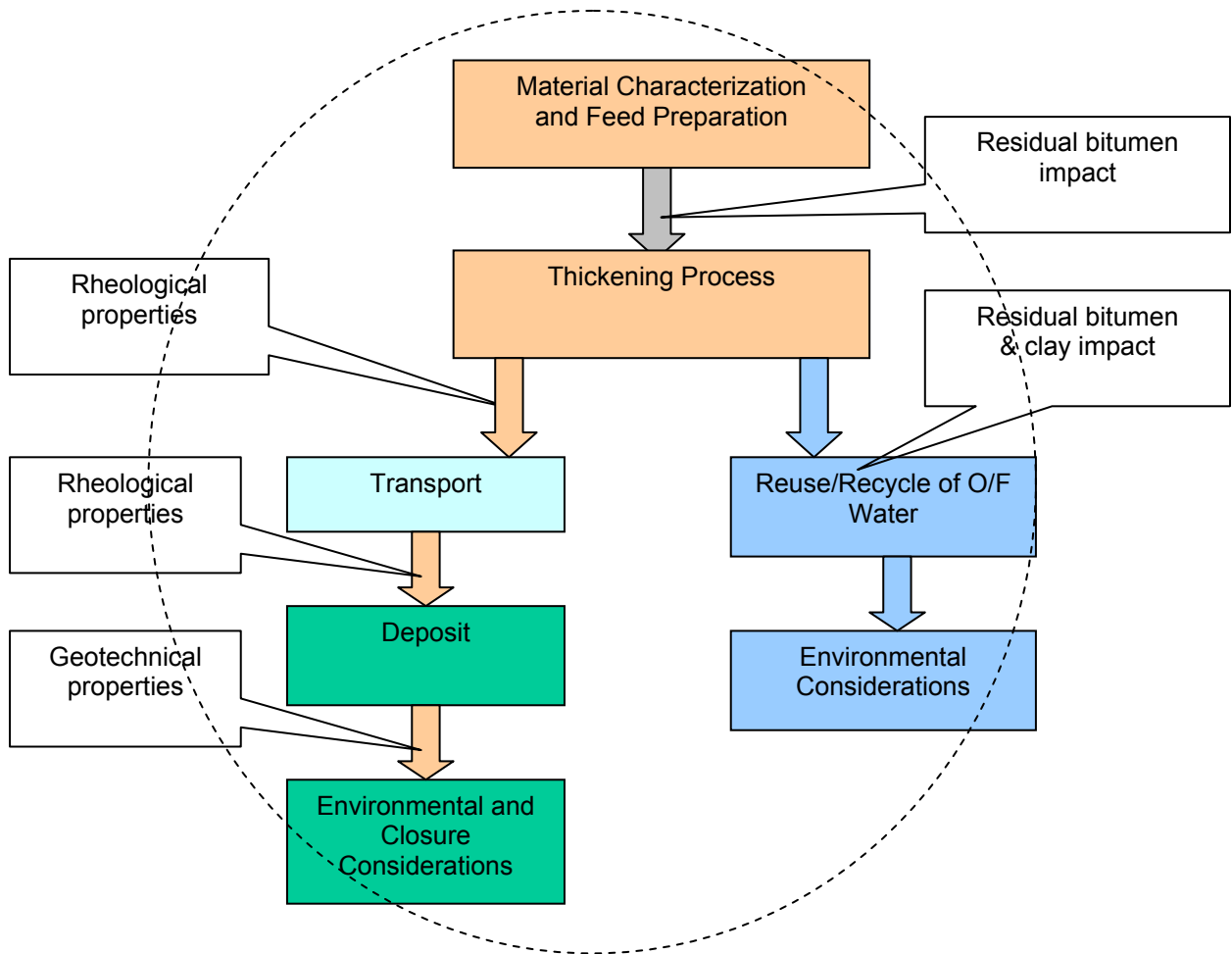


Figure 1 Full picture of thickened tailings (paste) technology in fine oil sand tailings management

In this paper, all the issues listed in Figure 1 will be briefly addressed based on the practical applications of thickened tailings (paste) technology in the mineral industry and the research and development work completed by Syncrude. After completely evaluating the applicability of thickened tailings (paste) technology in fine oil sand tailings management, the benefits and the gaps or opportunities for improvements will be identified.

AWARENESS OF THE THICKENED TAILINGS (PASTE) TECHNOLOGY

Although more and more successful applications of the thickened tailings (paste) technology in the mineral industry have taken advantage of savings through water recovery and dry stacking of thickened tailings since 2000, it is still new to many people who have been used to the wet tailings disposal method using dams for containment. Therefore, there is a process to educate and promote this technology, and get more and more people aware of the benefits of application of the thickened tailings (paste) technology. The take-home message is that companies should evaluate the thickened tailings technology in terms of full life-cycle costs, permitting time, and business objectives, including management of environmental and societal risks. As pointed by Regensburg and Tacey (2002), conventional “cheap” wet disposal of tailings may well be very expensive in the long term.

The benefits of implementation of TT (Paste) technology include the reduced costs and financial risks based on full life-cycle costs; improved environmental benefits; improved public perception and safety; and other spin-off technology benefits.

Capital costs and financial risks could be reduced through capital costs reductions in tailings containment – less with thickening

and TT dry surface stacking, pumping and piping costs. Operational costs can potentially be offset by improved water conservation, energy conservation, reagent conservation, operator safety, and process/plant safety. The benefits at tailings closure include the reduced costs and increased certainty, reduced financial provision and insurance costs, and time value of money, etc. (Regensburg and Tacey, 2002).

Figure 2 shows the cost comparisons of wet and dry bauxite tailings disposal (Cooling 1997). In the beginning of the implementation of the dry tailings disposal technologies, the costs were higher than wet disposal methods due to capital investments. However, the costs of dry disposal methods trended lower than the wet disposal methods after about 5 years of operation.

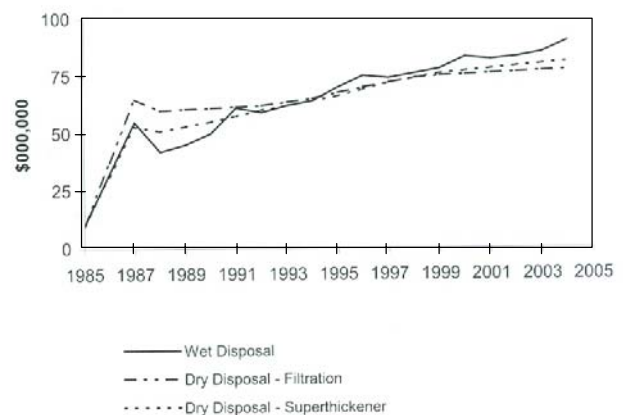


Figure 2 Cost comparisons of wet and dry bauxite tailings disposal (Cooling, 1997)

With regards to social and environment benefits, they may be hard to estimate in dollar value. These include reduced risk of tailings failures, public safety, reductions in future liability, reductions in greenhouse gas emissions, reduced regulatory risk, public perception and the “license to operate” (Regensburg and Tacey, 2002).

THICKENED TAILINGS (PASTE) TECHNOLOGY

As mentioned earlier, the thickened tailings (paste) technology includes five individual blocks of technology development. In this section, they are briefly reviewed together with the research and development work completed at Syncrude.

After many years of research work and implementation practices, people (Boger et al. 2002; Crozier et al. 2005) have realized that to design a new thickened tailings (paste) disposal system, it would be better to follow the systematic deposit-transport-thickening process approach. Their relationship is depicted in Figure 3 as a triangular diagram. It starts from the disposal method selection (surface disposal or underground backfill) and depositional requirements such as the slope prediction, spreading and drying characteristics and stability. To answer these questions the material and rheological properties of thickened tailings such as yield stress and viscosity for various solids concentrations and particle size distributions are required. In addition, the geotechnical properties such as the permeability and compressibility of the thickened tailings should be measured. In TT transport, the effect of the material and rheological properties (e.g., shear-thinning behavior) on pump selection and pipeline friction loss (pressure drop) should be studied. When designing the thickening process, we need to produce a thickener product that will meet the depositional requirements such as the slope and permeability. The thickener feed characterization and impact of the feed properties on flocculation and the thickener products (both overflow and underflow), internal dilution of the feed, thickener type, size, hydraulic and solids loading rates, effect of rake and pickets on thickened tailings density and rheology, and the sediment rheology within the thickener on thickener

rake and drive head torque design, etc., should be tested in bench and continuous pilot scale. At this point, it is wise to check if all the requirements are met. If not, an iterative procedure should be followed until the requirements and cost estimates are satisfied.

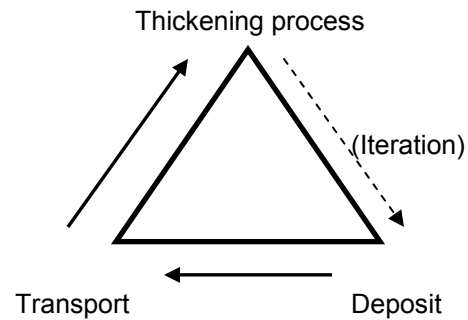


Figure 3. The triangle relationships between the deposit, transport and thickening process.

Thickening Process

The sedimentation based thickening process usually falls into two categories: clarification in water treatment or thickening in tailings or concentrate dewatering. The difference in emphasis on a clarified overflow or a highly concentrated underflow has resulted in significant differences in testing methods, equipment design and operation. In the past 100 years, the thickening technology has evolved and undergone a lot of innovations in harmony with the advances in flocculant chemistry from conventional, high rate, high compression to paste thickeners (different vendors may have their own names of the four generic types of thickeners). The main innovation areas in the thickening process include high efficient flocculants, new feedwell and feed dilution systems such as Eimco E-Duc feed system and Supaflo Autodil feed dilution system, low profile rake arms, high torque thickener drives, new underflow shear-thin systems, (Bedell et al.

2002; Arbuthnot and Triglavcanin 2005; Easton et al. 2007; Gupta and Johnson 2007; Courtenay and Triglavcanin 2007; Harper et al. 2007), and the latest shear enhanced thickening technology developed by Outotec (Cook, 2009). As they claimed, the patented shear enhanced thickening technology, in which a gentle shear is applied in the hindered settling zone to help water release, could increase the underflow density by 5-15% solids by weight and enhance the solids loading rate 300-400% higher than the same type of thickener.

In developing this technology for treating the fine tailings, Syncrude has conducted many years of research and development work. They are summarized as follows.

(1) Flocculant screening

An initial flocculant screening test procedure (beaker test) was used to evaluate various flocculants and coagulants with different molecular structures, molecular weights (MW) and charge densities. It was found that for the anionic polyacrylamide based flocculants, a charge density of about 25-30% and a MW of 10-24 millions were most effective for flocculation of fine oil sand tailings.

(2) Lab flocculation and sedimentation tests

The lab flocculation and sedimentation tests were performed in a 2-L graduated cylinder to investigate the effect of feed solids contents, particle size distributions (fines content), mineralogy, water chemistry, and the effect of mixing hydrodynamics of flocculant and slurry on supernatant clarity, settling rates and sediment density, and sheared and unsheared rheology. In the past, the graduated cylinder tests were also used to size the conventional thickener by using the Kynch, Talmage and Fitch models to predict the underflow density and thickener unit area, where in most cases, a correction factor must be applied to the predicted unit area and

thickener sidewall height based on actual similar full-scale thickener experience (Bedell et al. 2002). Numerous flocculation tests have been done at Syncrude and institutions to study different flocculation technologies and the flocculant mixing hydrodynamics (Xu and Cymerman 1999; Cymerman et al. 1999; Sworska et al. 2000a and 2000b; Yuan and Shaw 2006; Lee and Yuan 2007; Yuan, 2007; Yuan and Shaw 2007, 2008). It was found that the way or sequence the flocculants and coagulants were added, and the hydrodynamic conditions under which the flocculant solution and the oil sand tailings slurry were mixed had a profound impact on the flocculation performance (Yuan and Shaw 2007, 2008).

(3) Continuous pilot thickener test

Today the thickener hydraulic and solids loading rates are more accurately determined by a lab continuous pilot test thickener for thickener sizing. In the pilot tests, the effects of feed fines content, density and dilution, the flocculant dosages and concentration, the water chemistry (e.g., pH, Ca^{2+} and Mg^{2+} and conductivity), the maximum hydraulic and solids loading rates, water rising rate, and the sediment bed heights on the overflow clarity and the underflow density and sheared and unsheared rheology can be investigated.

Figure 4 shows the schematic flowsheet of the Outotec 190 mm x 4.5 m pilot thickener test conducted in 2005 on Syncrude Aurora oil sand tailings. Table 1 is a summary of the average pilot thickener feed conditions. The average pilot thickener test results are presented in Table 2. For feed with 12-13% solids content by weight and 48-52% -44 um fines content, an average solids loading rate of 0.62 to 0.72 t/hr/m² and an average hydraulic loading rate of 5.1 to 6.0 m³/hr/m² were obtained (Yuan 2007).

Flocculant dosages of 84 to 90 g/t were used, resulting in an overflow of less than 0.51%

total solids and a thickener underflow of 59% to 60% solids by weight. As shown in Table 2, the yield stress for the unsheared thickened tailings was 317-409 Pa. The yield stress was significantly reduced to 100-115 Pa after double shearing with the vane of the VT-550

viscometer (Yuan 2007). Therefore, the shear-thinning characteristic of the thickened oil sand tailings is evident, which will help the pipeline transport of the thickened tailings if the pump system is properly designed.

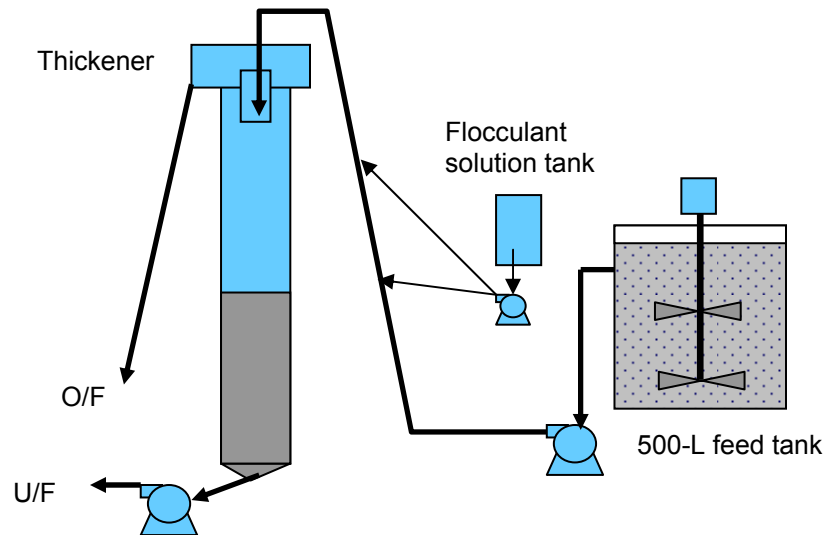


Figure 4. Schematic flowsheet of the Outotec 190 mm x 4.5 m pilot thickener test

Table 1 Summary of the average pilot thickener feed conditions

Test date	Feed				Thickener load			Flocculant	Bed
	Slurry	Solids	SFR	Fines	Hydraulic	Solids	Unit area	Dosage	Level
	L/min	%		%					
Sep. 22 2005	2.15	12.56	0.91	52.42	5.10	0.62	0.067	90	1
Sep. 23 2005	2.45	12.76	1.05	48.84	5.79	0.72	0.058	84	2
Sep. 24 2005	2.56	11.98	1.00	50.03	6.02	0.70	0.059	84	3

Table 2 Summary of the average pilot thickener test results

Test date	Thickener overflow		Thickener underflow				U/F yield stress	
	Solids	Rise rate	Solids	SFR	Fines	F/(F+W)	Unsheared	2x sheared
	%	m/hr	%		%	%		
Sep. 22 2005	0.41	4.53	58.95	0.88	53.33	43.38	409	114
Sep. 23 2005	0.49	5.12	59.94	0.94	51.68	43.61	404	113
Sep. 24 2005	0.51	5.32	58.42	0.79	55.79	43.94	317	104

The thickener underflows generated from the pilot tests were collected in buckets and pumped with a Moyno and centrifuge pump separately into a flume. It was found that the Moyno pump could only shear and reduce the thickened tailings yield stress from about 400 Pa to 250 Pa, while the centrifuge pump

could significantly reduce the yield stress from 400 Pa to about 120 Pa. It was found that the TT yield stresses after double shearing with the vane probe of the VT-550 viscometer were quite in line with the TT yield stresses after centrifugal pumping. This means that it is appropriate to use double

shearing with a vane probe to simulate the rheological performance of a centrifugal pump (Yuan 2007).

In addition to the lab scale pilot thickener tests, Syncrude independently and in collaboration with other oil sand developers completed a series of field tests with a 10-m conventional thickener (high rate) from 2001 to 2003, a 1.5-m deep cone paste thickener and a 4-m high compression thickener in 2003 and 2004. In 2006, a 4-m high compression Aurora Thickener Prototype (ATP) was designed, built and operated until 2008. With the prototype, the sensitivity of feed sources, the winter operation challenges, bitumen removal from the thickener feed, the thickener overflow impact on utilities, the thickened tailings rheology and pumping characteristics and the TT deposit consolidation were comprehensively evaluated (Wang, 2009). From the thickening process point of view, the thickened tailings (paste) technology is ready to implement in the oil sand industry.

TT (Paste) Transport

The thickened tailings (paste) produced from fine oil sand tailings is non-Newtonian with Bingham viscosity characteristics, which means a yield stress exists and shearing of the thickened tailings results in a significant reduction of the yield stress (i.e., the shear-thinning characteristics). The pumping and pipeline system to transport TT (paste) should be designed based on the rheological properties and the thickened tailings (paste) density. In addition to the yield stress and viscosity measurements of the lab test materials, a pilot pipeline loop test typically with pipes of 2" or 4" in diameter should be conducted to determine the pressure drops and friction loss as a function of pipeline velocity and the unsheared and sheared rheological properties. These parameters form the foundation for engineering design of the pumping and pipeline system. The

technologies available to transport the thickened tailings (paste) include centrifugal pump for low yield stress TT, positive displacement (PD) pump for high yield stress TT (paste) and conveyor belt for extremely high yield stress cakes. In general, the centrifugal pump is relatively inexpensive, while the PD pump and conveyor belt are considered more expensive in terms of capital costs. That is why it is suggested to select the TT (paste) transport technology based on the minimum deposition requirements following the procedure in Figure 3. For example, if a TT (paste) with 55% solids and yield stress of 100 Pa would produce a deposit slope of 1-2% while another TT (paste) with 60% solids and yield stress of 400 Pa would produce a deposit slope of 3-4%, which TT (paste) density and yield stress should be chosen for designing the TT (paste) transportation system to meet the minimum deposit slope requirement? The geotechnical engineer should have a rationale for the minimum deposit slope design based on the actual site topography and other site constraints. If the minimum deposit slope is 1-2%, the TT with 55% solids and 100 Pa yield stress could be selected as the basis to design the transportation system. In this case, a relatively inexpensive centrifugal pump and pipeline system could be selected. If the geotechnical engineer rationalized that the minimum deposit slope must be 3-4%, the TT (paste) with 60% solids and 400 Pa yield stress could be selected as the basis to design the transportation system. In this case, a more expensive PD pumping and pipeline system could be selected. For a long distance transportation of thickened tailings (paste), a multi-stage of pump stations would be used in series. The TT transportation distance, the site topography and elevations should be considered in calculating the hydraulic grade line and energy line in pump and pipeline design. Syncrude completed some preliminary test work with a Moyno pump and a centrifugal pump respectively. The

results from the test pipeline loop will be available soon (Wang, 2009).

TT (Paste) Deposit

There are two deposition technologies to handle the thickened tailings (paste), i.e., the thin-lift dry stacking technology and the conventional containment method. Selection of a deposition method depends on the actual site conditions such as the local climate conditions and the available site areas and topography etc. The modern TT (paste) technology seems largely to lean on the thin-lift dry stacking technology because only minimum berms to collect the run-off are needed.

Thin-lift dry stacking technology:

The benefits of TT (paste) thin-lift dry stacking technology when designed and operated properly are summarized as follows:

- Minimal start-up and ongoing earthworks costs.
 - Generally only low rain runoff bunds are required.
- Higher stacked heights and consequent lower footprint areas by “dry stacking” concept.
- More efficient volumetric storage.
 - Higher density can be achieved by progressive thin layer deposition.
- Improved water management.
- More rapid drying and self-weighting consolidation.
- Improved deposit stability and reduced safety risk.
 - Well-mixed non-segregating tailings.
 - No decant pond water.
 - Maximized strength with center thickened discharge (CTD).
 - Reduced liquefaction potential.

- Lower operational cost and risk.
- Accelerated rehabilitation.
- Improved closure appearance-gently sloping landform.

The thin-lift dry stacking technology can be illustrated by a case application example in Africa (Lord et al., 2002). Figure 5 shows the thickened tailings (paste) were being deposited with very little water release and no segregation. Therefore, only 1-3 m high berm surrounding the deposits was built to manage the rain run-off water. Usually a thin layer of 20-30 cm deposit was placed depending on the local weather conditions (Shuttleworth et al., 2005; Wells and Riley, 2007).

Depending on the site constraints, multiple discharge towers or stations as shown in Figure 6 can be installed, so that deposition can be switched progressively from one tower to another when the pre-determined thickness of deposit is reached. The distance between the deposition towers is determined based on the deposit slope and the site topography. Some extent of overlap of the deposits between two towers is allowed.

When the thin layer deposit was dried and certain strength of the deposit (e.g., about 15-20 kPa) is gained as shown in Figure 7, the next layer of thickened tailings (paste) could be placed on top of the previous deposits. This deposition procedure is progressively repeated until the designed total height of deposits is reached.

For thickened fine oil sand tailings a flume test was performed to determine the deposit slope and the consolidation rate without under-drain following the 190 mm Outotec pilot thickener test in 2005. The thickened tailings (paste) with 58-60% solids and sand to fine ratio (SFR) of 0.8-1.0 were pumped with a centrifuge pump to the flume. The discharge slurry yield stress was 120 Pa.



Figure 5. Thickened tailings (paste) being deposited (Lord et al., 2002).



Figure 6. Multiple deposition towers installed on site (Lord et al., 2002).



Figure 7. Desiccation and cracking of the deposited TT (paste) after 5 days (Lord et al., 2002).

An initial slope of 4.33% of the deposit was measured. Then the flume was sealed with plastic sheets and no water was allowed to drain to monitor the pure consolidation rate vs. time. During the flume-monitoring period, the slope of the deposit was measured, and the solids content, SFR, and yield stress were determined by taking samples at different depths and horizontal locations of the deposit. After 4.5 months consolidation in the flume, the plastic sheets were removed and the final sample properties were measured. The data is shown in Figure 8. It was found that the final slope of the deposit was slightly changed to 3.59%. The yield stresses and densities increased with the depths at the same sampling location, while they decreased gradually from the discharge point to the toe of the deposit. The strength of the deposit was improved from an initial 120 Pa up to 1910 Pa in the deposit in 4.5 months, however the yield stress of the deposit toe was only 300 Pa. This was because most of the water and condensed moisture flowed toward the toe.

Figure 9 shows the typical yield stresses measured with the VT-550 viscometer compared with the cylinder slump tests. As shown in Figure 10, the average density of 70% of the deposit was recorded at the end of the flume test on March 1, 2006. Then the deposit was subjected to natural desiccation in the lab at 20 °C (without sun shining and wind blowing) until March 29, 2006. The solids contents in the deposit quickly increased to 80% and up to 100% at the toe of the deposit after 29 days exposure to air in the flume. This is because the thickened tailings with flocculant treatment have an order of magnitude higher permeability than gypsum-made composite tailings (CT) at the same void ratio (Mian, 2005).

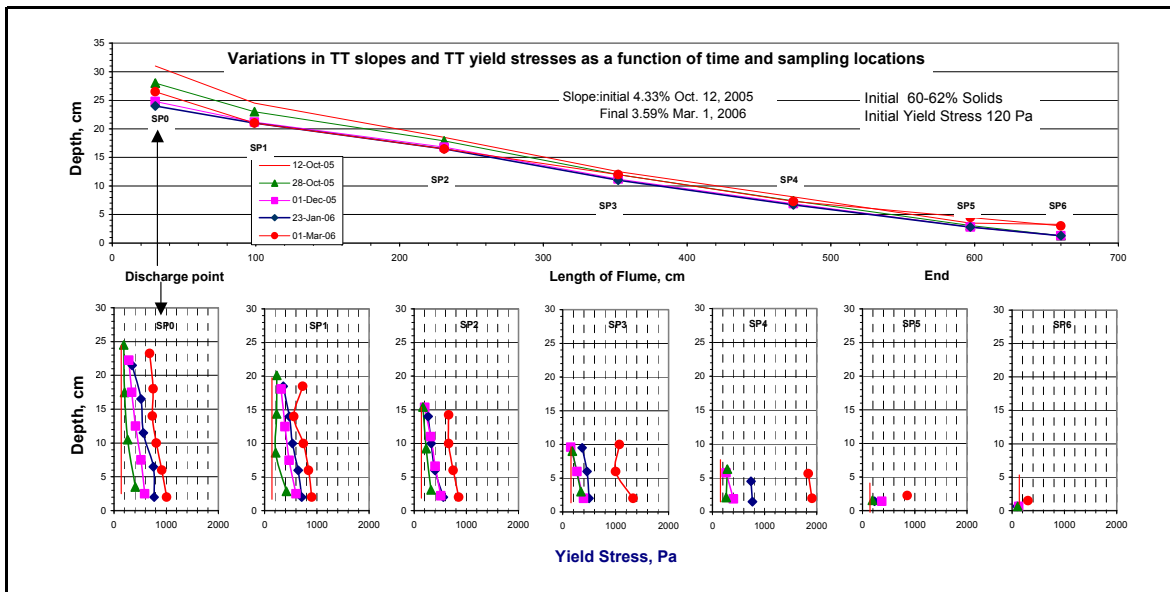


Figure 8. Flume test results- yield stress vs. elevations at different sampling locations.



Figure 9. Yield stresses measured with VT-550 viscometer compared with cylinder slump tests.

Syncrude has not yet done any thin-lift desiccation tests in the field. It is expected that the desiccation rate for thickened tailings would be much faster in the field than in the lab. This is because in the field the deposit is subject to sun shining, wind blowing, and lateral and under drains. This is one gap/opportunity identified to test in the future to determine the optimal deposition thickness and the desiccation rate if the thin-lift dry stacking technology is used.

The Atterberg limits for the thickened tailings from the flume test were also measured (Yuan, 2007) and shown in Table 3. The plastic limit (PL) is the water content where soil starts to exhibit plastic behavior. The liquid limit (LL) is defined as the water content where a soil changes from plastic to liquid behavior.

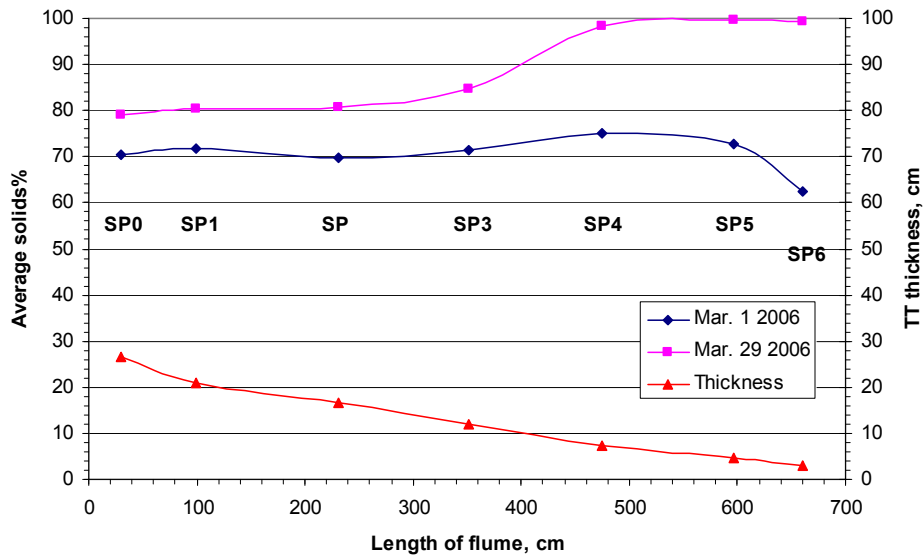


Figure 10. Natural desiccation and evaporation test in the lab

Table 3 TT liquid limit and plastic limit test results (Atterberg Tests).

Date Sampled	Sample ID	Sample Location	Depth From bottom	Liquid Limit	Plastic Limit	Plasticity Index
15-Mar-06	SP-A	SP 0 (Start Point)	0 - 8 cm	25.70	15.95	9.75
15-Mar-06	SP-B	SP 0 (Start Point)	8 - 16 cm	26.00	15.78	10.22
15-Mar-06	SP-B REDO	SP 0 (Start Point)	8 - 16 cm	25.50	15.78	10.22
15-Mar-06	SP-C	SP 0 (Start Point)	16 - 26.5 cm	26.85	16.19	10.66
15-Mar-06	SP1-A	SP 1	0 - 12 cm	24.85	15.16	9.69
15-Mar-06	SP1-B	SP 1	12 - 21 cm	25.30	15.33	9.97
15-Mar-06	SP2-A	SP 2	0 - 8 cm	26.80	16.47	10.33
15-Mar-06	SP2-B	SP 2	8 - 16.5 cm	27.30	16.96	10.34
15-Mar-06	SP3	SP 3	0 - 12 cm	25.95	16.09	9.86
15-Mar-06	SP4	SP 4	0 - 7.3 cm	25.35	16.05	9.30
15-Mar-06	SP5	SP 5	0 - 4.5 cm	25.05	15.44	9.61
15-Mar-06	END	SP 6 (End Point)	0 - 3.0 cm	25.10	16.42	8.68
Average				25.81	15.97	9.89

It should be noted that the water (moisture) content for Atterberg limits calculations is a geotechnical term defined as the mass ratio of water to dry solids in percentage. It is not the same as the water content used in the process technology. The plasticity index (PI) is a measure of the plasticity of a soil. The plasticity index is the size of the range of

water content where the soil exhibits plastic properties. The PI is the difference between the liquid limit and the plastic limit ($PI = LL - PL$). Soils with a high PI tend to be clay, those with a lower PI tend to be silt, and those with a PI of 0 tend to have little or no silt or clay. The liquidity index (LI) is used for scaling the natural water content of a soil

sample to the limits. It can be calculated as a ratio of difference between natural water content, plastic limit, and plasticity index: $LI=(W-PL)/(LL-PL)$ where W is the natural water content.

As shown in Table 3, the average liquid limit of the thickened tailings (paste) is 25.81%, the average plastic limit 15.97% and plasticity index 9.89%.

For example, when the TT consolidates to 70%, 80% and 90% solids by weight, the corresponding geotechnical water (moisture) contents are 42.86%, 25.00% and 11.11% respectively. This means the TT deposit must consolidate to more than 80% solids by weight to ensure the moisture content in the soil is below the TT liquid limit of 25.81%.

Containment disposal:

In addition to the thin-lift dry stacking technology, conventional containment is an alternative method to store the thickened tailings (paste). Figure 11 is a picture of the deposition cell for the thickened tailings placed in October 2003 on top of the 2002 TT deposit (Shaw et al, 2003; 2004).

The thickened tailings were transported with a centrifugal pump to the deposition cell containing about 2m thickness of TT in October 2002. After 8 months of desiccation and freeze-and-thaw in the field, it consolidated to a strength that people could easily walk on it, which was similar to the status in Figure 12. Then in 2003 a second layer of about 1m of thickened tailings was placed on top of the previous TT deposit. The slope was 0.7-1% with the initial solids content 47-53% solids and SFR 0.6-1.5. The geotechnical survey data conducted in June 2004 was shown in Figure 12 after 8 months of desiccation and freeze-and-thaw in the field (Shaw et al, 2004).

The final solids contents were 70 – 75%. The crust vane strengths were in 20 –30 kPa, and the average vane strength was 10 –20 kPa. It was found that there was no change in pore water quality (Shaw et al, 2004).

It is worth noting that the TT deposition cell shown in Figure 12 was successfully capped with 2m coarse tailings sand (pilot cyclone underflow) and trafficable with a light pick-up truck right after the sand was placed in summer of 2004.

Warm water return and heat recovery

It was found from the pilot test runs which integrated a pilot thickener into a pilot extraction plant that the thickener overflow water had no detrimental impact on bitumen recovery in oil sand extraction when it was re-used as slurry prep water, PSV flood and under-wash water if its clarity was controlled less than 0.5% total solids (Kwong et al, 2005). In this way, heat was recovered through recycling the thickener overflow water to the extraction process. However, if the thickener overflow water is intended to pass through heat exchangers to heat it up, more test work is needed to investigate the potential impact of the residual bitumen and clay on heat exchanger scaling and fouling.

Closure and environmental consideration

Although it was found that there was no change in deposit pore water chemistry compared with the process water, the life cycle and fate of the flocculant in both thickener overflow and TT deposit as well as its effect on environment need further studies. Some of the environmental test work is ongoing.

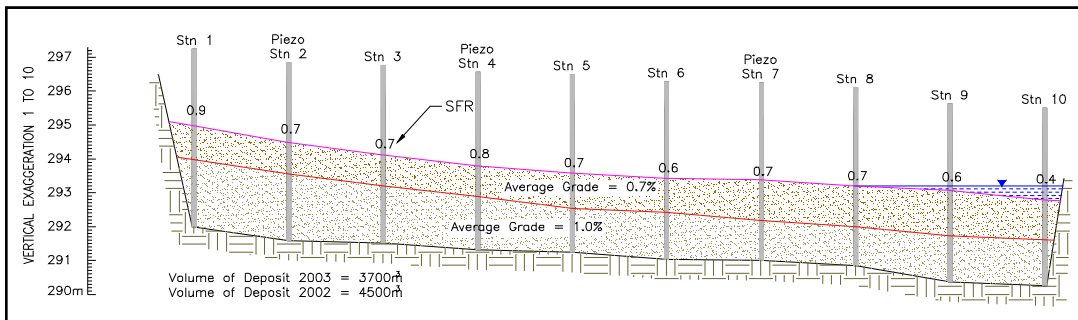


Figure 11. The deposition cell of thickened tailings in 2002 and 2003 field thickener tests.

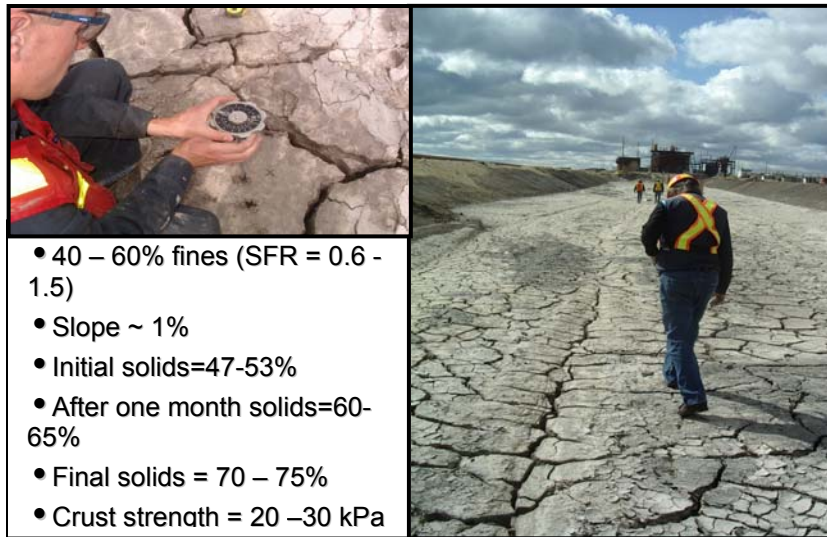


Figure 12. The geotechnical survey of the thickened tailings deposit after 8 months desiccation and freeze-and-thaw from October 2003 to June 2004 in the field.

In closure and reclamation of TT (paste) deposit, the safety, the deposit stability, the aesthetic acceptability, the landforms and the

environmental effect should also be addressed.

Residual bitumen and other challenges

It was found that bitumen accumulation in the thickener feedwell impaired the flocculation efficiency. This issue should be well addressed before engineering design. The valuable residual bitumen can be recovered with flotation cells or other units from the thickener feed before it enters into the thickener feedwell. The other method to deal with the residual bitumen is to design a special flocculation system and a bitumen skimmer for the thickener. In addition, the challenges of integration of the thickened tailings system into an existing oil sand extraction plant and the sensitivity of process variations on thickener operation should be evaluated.

Tailings Directive 74

According to Tailings Directive 74 released by ERCB in February 2009, the following criteria must be achieved annually:

- Minimum undrained shear strength of 5 kilopascals (kPa) for the material deposited in the previous year.
- Removal or remediation of material deposited in the previous year that does not meet the 5 kPa requirement; and
- Ready for reclamation within five years after active deposition has ceased. The deposit will have the strength, stability, and structure necessary to establish a trafficable surface. The trafficable surface layer must have a minimum undrained shear strength of 10 kPa.

Based on the data shown in Figure 12, if using the thickened tailings (paste) technology for fine tailings management the minimum strength of 5 kPa of deposit per year and the minimum strength of 10 kPa of a trafficable surface layer in five years could be achievable.

CONCLUSIONS

Companies should evaluate the thickened tailings technology in terms of full life-cycle costs, permitting time, and business objectives, including management of environmental and social risks. Conventional “cheap” wet disposal of tailings may well be more expensive in the long term.

Thickened tailings (paste) technology is applicable in fine oil sand tailings management. TT (paste) technology could be an effective alternative to manage fine tailings. Before applying this technology, the identified gaps/ concerns such as the optimal thin-lift thickness, the residual bitumen accumulation in the feedwell, the life cycle and fate of flocculant polymer in thickener overflow and the TT deposit etc., also need to be addressed. The choice to commercially implement TT (paste) technology to manage oil sand fine tailings is ultimately dependent upon the ability to achieve the necessary tailings deposition requirements using a thickening process that is suited to the oil sands extraction process. It must also be cost competitive relative to other tailings management options.

ACKNOWLEDGEMENT

Syncrude approved the public release of the testing results. The authors would like to thank our Syncrude colleagues, our consultants and contractors who contributed to the tailings test programs in the past decade.

REFERENCES

Arbuthnot I.M. and Triglavcanin R.A., 2005. Designing for paste thickening-testwork and sizing for paste thickeners. Past 2005, proceedings of the 8th International Seminar

- on Paste and Thickened Tailings, Jewell R. and Barrera S. (Editors), Santiago Chile, p99-116.
- Bedell D., Slottee S., Parker K. and Henderson L., 2002. Section 5: Thickening process. Paste and Thickened Tailings-A Guide, Jewell R.J., Fourie A.B. and Lord E.R. (Editors), p49-79.
- Boger D., Scales P.J. and Sofra F., 2002. Section 3: Rheological concepts. Paste and Thickened Tailings-A Guide, Jewell R.J., Fourie A.B. and Lord E.R. (Editors), p23-34.
- Cook M., 2009. Outotec Thickener Technology –Shear Thickening. Private communication.
- Cooling, D.J., 1997. Dry stacking of bauxite tailings. AIC Tailings Disposal Management Summit, November 1997.
- Courtenay S. and Triglavcanin R., 2007. Paste thickeners – design and engineering options to meet today’s project needs. Past 2007, proceedings of the 10th International Seminar on Paste and Thickened Tailings, Fourie A. and Jewell R. (Editors), Perth, Australia, p41-50.
- Crozier M., Johnson J. and Slottee J.S., 2005. A systematic approach to designing paste thickener project. Past 2005, proceedings of the 8th International Seminar on Paste and Thickened Tailings, Jewell R. and Barrera S. (Editors), Santiago Chile, p139-146.
- Cymerman G., Kwong T., Lord E., Hamza H. and Xu Y., 1999. “Thickening and Disposal of Fine Tails from Oil Sand Processing”. Polymers in Mineral Processing, J.S. Laskowski (Editor), Proc. 3rd UBC-McGill Int. Symp. Fund. Miner. Process., Met. Soc. of CIM, Aug. 22-26, 1999, Quebec City, Que., Canada, pp605-619.
- Easton J.H., Slottee J.S. and de Oliveira E.M., 2007. Design of a WestTech HiDensity™ paste thickener for bauxite tailings. Past 2007, proceedings of the 10th International Seminar on Paste and Thickened Tailings, Fourie A. and Jewell R. (Editors), Perth, Australia, p17-24.
- Gupta B.K. and Johnson J.L., 2007. Arch coal paste thickener case study. Past 2007, proceedings of the 10th International Seminar on Paste and Thickened Tailings, Fourie A. and Jewell R. (Editors), Perth, Australia, p33-40.
- Harper H., Wyatt D., Konigsmann E. and Kujawa C., 2007. Pogo plant paste thickener design. Past 2007, proceedings of the 10th International Seminar on Paste and Thickened Tailings, Fourie A. and Jewell R. (Editors), Perth, Australia, p57-64.
- Kwong T., Cymerman G., Lord E., MacKinnon M., Matthews J., Yeung A. and Yuan S., 2005. “EXP 2000 Thickener Research Module-2004 Pilot Test Programs”, Edmonton, Alberta, Canada, May 2005.
- Lee A. and Yuan S., 2007. “Effect of Hydrodynamic Conditions on Flocculation of Aurora Flotation Tailings March to April 2004”. Fort McMurray, Alberta, Canada, May 2007.
- Lord E.R., Robinsky E.I., Cooling D.J., Williams P., and Landriault D., 2002. Section 10: Case Studies. Paste and Thickened Tailings-A Guide, Jewell R.J., Fourie A.B. and Lord E.R. (Editors), p143-158.
- Mian H., 2005. Consolidation study on case 8, 9 and 10. Internal communication of AMEC for Syncrude project, December 12, 2005.
- Robinski, E.I., 1978. Tailings disposal by the thickened discharge method for improved

economy and environmental control. Tailings Disposal Today, vol. 2, Proceedings of the Second International Tailings Symposium, G.O. Argall Jr. (Editor), Denver, Colorado, May 1978.

Regensburg B. and Tacey W., 2002. Section 2: Key business issues. Paste and Thickened Tailings-A Guide, Jewell R.J., Fourie A.B. and Lord E.R. (Editors), p9-22.

Shaw W., Dawson R. and Boese C., 2003. "2002 Thickened Tailings Field Trial Project Report", Fort McMurray, Alberta, Canada, June 2003.

Shaw W., Yuan S., Wang N., Wallwork V., Hlady M., Dawson R., Boese C., Ennis S., and Mikula R., 2004. "2003 Thickened Tailings Field Pilot Project Report", Fort McMurray, Alberta, Canada, July 2004.

Shuttleworth J.A., Thomson B.J. and Wates J.A., 2005. Surface paste disposal at Bulyanhulu - practical lessons learned. Past 2005, proceedings of the 8th International Seminar on Paste and Thickened Tailings, Jewell R. and Barrera S. (Editors), Santiago Chile, p207-218.

Sworska A., Laskowski J.S. and Cymerman G., 2000a. "Flocculation of the Syncrude Fine Tailings Part I. Effect of pH, Polymer Dosage and Mg²⁺ and Ca²⁺ Cations". Int. J. Miner. Process., 2000, vol. 60, pp143-152.

Sworska A., Laskowski J.S. and Cymerman G., 2000b. "Flocculation of the Syncrude Fine Tailings Part II. Effect of Hydrodynamic Conditions". Int. J. Miner. Process., 2000, vol. 60, pp153-161.

Wang N., 2009. Aurora Thickener Prototype Project Report in progress. Internal communication.

Wells P.S. and Riley D.A., 2007. MFT drying-Case study in the use of rheological modification and dewatering of fine tailings through thin lift deposition in the oil sands of Alberta. Past 2007, proceedings of the 10th International Seminar on Paste and Thickened Tailings, Fourie A. and Jewell R. (Editors), Perth, Australia, p271-284.

Xu Y. and Cymerman G., 1999. "Flocculation of Fine Oil Sand Tails". Polymers in Mineral Processing, J.S. Laskowski (Editor), Proc. 3rd UBC-McGill Int. Symp. Fund. Miner. Process., Met. Soc. of CIM, Aug. 22-26, 1999, Quebec City, Que., Canada, pp591-604.

Yuan S. and Shaw W., 2006 "Laboratory Flocculation and Dynamic Thickening Tests on Aurora Oil Sand Tailings". Fort McMurray, Alberta, Canada, November 2006.

Yuan S., 2007. OK 190 mm x 4.5 m Pilot Thickener Test and Thickened Tails Pumping and Flume Tests, Syncrude Research and Development Internal Report, pp1-71.

Yuan X.S. and Shaw W., 2007. "Novel Processes for Treatment of Syncrude Fine Transition and Marine Ore Tailings". CMQ, Vol. 46, No. 3, 2007, pp265-272.

Yuan X.S. and Shaw W., 2008. "Effect of hydrodynamic conditions on flocculation of Syncrude oil sand tailings". Proceedings of XXIV International Mineral Processing Congress, D. Wang, C. Sun, L. Zhang and L. Han (Editors), Beijing China, pp4033-4041.

NATURAL DEWATERING STRATEGIES FOR OIL SANDS FINE TAILINGS

N. Beier, M. Alostaz, & D. Segó

University of Alberta, Edmonton, Alberta, Canada

ABSTRACT: The Athabasca region of northern Alberta, Canada, is home to massive deposits of oil sands, estimated to contain approximately 300 billion barrels of recoverable bitumen. There are currently three oil sands mining and extraction operations; Suncor Energy, Syncrude Canada Ltd. and Albian Sands, with CNRL in commissioning and several more mines under development. Production of the bitumen is based on open pit mining and oil sands processing using different extraction processes. Tailings management practices at the three operating plants over the last four decades have resulted in massive inventories of fine tailings (750 million m³) requiring long term storage within fluid containment structures (Houlihan and Mian, 2008). In lieu of a recent tailings management directive issued by the Energy Resource Conservation Board (oil sands regulatory agency in Alberta) and public awareness, there is renewed interest by the industry in natural dewatering strategies for the fine tailings. The objectives of the paper are to outline historic and current tailings management strategies at the oil sands mine sites and discuss alternatives including managing the coarse and fine fractions separately. Alternative management strategies will focus on potential natural dewatering strategies for the fine tailings (both the massive inventory of legacy tailings and future tailings). A critical review of various “drying” and freeze-thaw dewatering methods will be presented.

BACKGROUND

The Athabasca region of northern Alberta, Canada, is home to massive deposits of oil sands, estimated to contain approximately 300 billion barrels of recoverable bitumen. These oil sands are composed of bitumen (~12 wt%), sand, silts, clays (mineral content ~85 wt%) and water (3 - 6 wt%). The clay component is comprised of mainly kaolinite (50-60 %) and illite (30-50%) with some montmorillonite (Chalaturnyk et al. 2002; FTFC, 1995). At Suncor the clays in the parent ore body are typically less than 1%, however they make up to 50 % of shale bed lenses within the deposit (Wells and Riley,

2007). Due to their proximity, these shale beds are excavated and processed with the ore.

In the Fort McMurray area, there are currently three oil sands mining and extraction operations; Suncor Energy (Suncor), Syncrude Canada Ltd. (Syncrude) and Albian Sands (Albian), with Canadian Natural Resources Ltd. (CNRL) in commissioning and several more mines under development. Production of the bitumen is based on open pit mining and oil sands processing using a hot water extraction process (Chu et al., 2008; FTFC 1995; Masliyah et al. 2004; Wells and Riley, 2007).

Processing begins with crushing of the excavated ore. The crushed ore is then conditioned with warm to hot water, steam, and process aides such as caustic (NaOH) or citrate (Albian only) and hydrotransported via pipeline to the extraction plant. Bitumen is separated from the coarse fraction as a floating froth in large gravity separation vessels. The bitumen froth is further processed to remove fine solids. Typical bitumen recoveries range from 88 to 95% depending on oil sands grade and origin. Tailings include a mixture of water, sand, silt, clay and residual bitumen. This tailings slurry is approximately 55 wt% solids (82 wt% sand and 17 wt% fines < 44 µm). Upon deposition, the tailings stream segregates with the coarse fraction forming beaches and the fines flowing with the water stream. Significant portions of the fines remain in suspension after deposition resulting in a significant management challenge for the industry.

OBJECTIVE

The objectives of this review are to outline historic and current tailings management strategies at the oil sands mine sites and discuss alternatives including managing the coarse and fine fractions separately. Alternative management strategies will focus on potential natural dewatering strategies for the fine tailings (both the massive inventory of legacy tailings and future tailings). A critical review of various “drying” and freeze-thaw dewatering methods will be presented.

TAILINGS MANAGMENT

Historical Tailings Management

Historically at Suncor and Syncrude, tailings were pumped into large settling basins

(external tailings facilities [ETF]) where the sand fraction settled out rapidly to form beaches. Some fines were trapped within the sand matrix of the beaches. However, the remaining thin slurry of fines and water (8 wt%) flowed into the settling basin where the solids settled gradually to form a densified zone of fine tailings at depth. Released water was recycled back to the extraction plant. After a few years, the fines settle to 30 to 35 wt % and are referred to as mature fine tailings (MFT). Further consolidation of the MFT is expected to take centuries (Chalaturnyk et al. 2002; FTFC, 1995). Figure 1 shows schematically a conventional oil sand extraction and tailings disposal system (Beier and Sego, 2007).

At Albian’s Muskeg River Mine site operating since 2002, tailings from the primary separation and floatation cells are not directly deposited into the (ETF) (Matthews, 2008). The total tailings first pass through a hydrocyclone to separate the coarse and fine fractions. The cyclcone overflow (mainly fines, water and residual bitumen) is pumped to a thickener for dewatering prior to deposition in the ETF. Dewatered fines from the thickener underflow are referred to as thickened fine tailings (TFT). Coarse cyclcone underflow is typically used to construct the ETF embankments via upstream cell construction methods or beached within the impoundment. Runoff (fines and water) from cell construction and direct beaching then drains into the settling basin to form MFT. Tailings originating from the froth treatment and solvent recovery process (TSRU) are directly deposited into the ETF. The TSRU tailings consist of high fines content (12%), high asphaltene content (8%), and residual solvent (Yasuda, 2006).

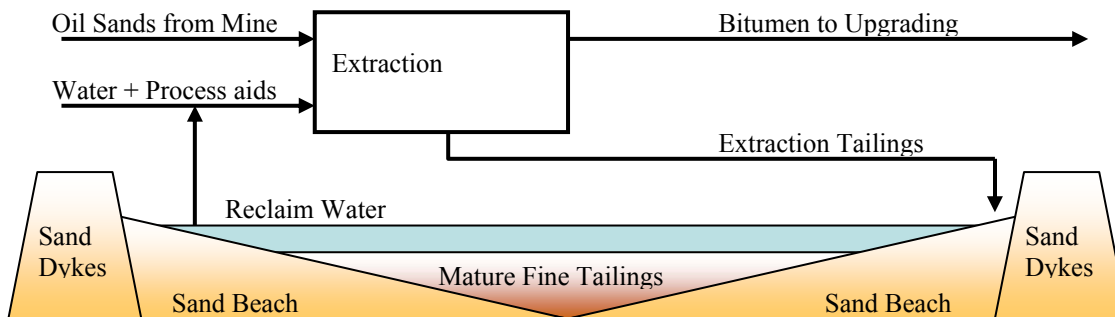


Figure 1. Schematic of historical oil sands tailings management (modified from Beier and Seg0, 2007).

On average, for every barrel of crude oil produced, approximately 1 m³ of sand and 0.25 m³ of MFT are produced (FTFC 1995; Mikula et al. 1996). An average 200,000 barrel per day operation can produce up to 800,000 m³ of total tailings (Mikula and Omotoso, 2006). Tailings management practices at the three operating plants over the last four decades have resulted in massive inventories of MFT (750 million m³) requiring long term storage within fluid containment structures (Houlihan and Mian, 2008). This massive inventory will be further referred to as “Legacy tailings”. Water management is also an issue for these mine sites in addition to managing large volumes of fluid fine tailings. The mines are currently operating under a zero-effluent discharge policy preventing release of accumulated water on site. Continual recycle of process water (tailings release water) to the extraction plant has led to a build up of dissolved ions within the recycle water. Elevated ion concentrations can lead to various operational issues including poor extraction recovery and scaling/fouling of piping and equipment.

CURRENT TAILINGS MANAGEMENT

In an effort to deal with the Legacy tailings and provide a stable landscape in a timely

manner, the industry has moved towards the use of non segregating tailings (NST) by implementing NST or CT technology (NST – Albion/CNRL; Composite tailings or CT – Syncrude, Consolidated tailings or CT– Suncor). NST tailings are a mixture of coarse sand, coagulant (gypsum at Syncrude/Suncor/Albion or carbon dioxide at CNRL) and MFT at sand to fines ratios of approximately 4:1. To produce NST, total tailings from the extraction plant are passed through a hydrocyclone with the overflow (mainly fines) pumped to a settling basin to form MFT. In some cases (i.e. Albion/CNRL) the cyclone overflow or floatation tailings may be sent to a thickener to further dewater the fines prior to deposition in the settling basin or use in NST. The coarse cyclone underflow is then combined with dredged MFT or TFT and coagulant to form the NST. The resulting mixture is pumped to the disposal area and should not segregate during transport, discharge, or deposition. Production of NST provides an opportunity to consume the Legacy tailings and also releases water rapidly for reuse (Matthews et al. 2002). A typical NST process is shown schematically in Figure 2.

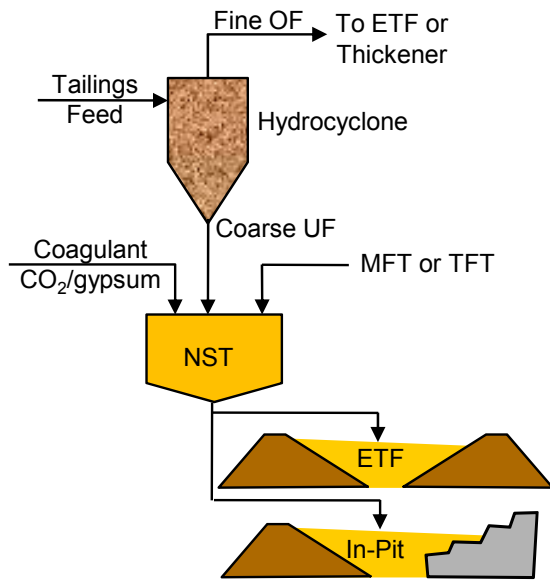


Figure 2. Schematic of a typical NST process.

Disposal areas for NST mixtures include constructed cells within the mined out pit or an ETF. As the in-pit mine face progresses, additional deposition cells may be constructed with available coarse cyclone underflow, overburden materials or lean oil sands. The NST deposits may then be capped with sand and overburden prior to final reclamation. Under the current operating approvals, all runoff water from the NST deposits and remaining fine tailings not consumed by NST production will be transferred and stored within end pit lakes (EPL).

CHALLENGES OF CURRENT TAILINGS MANAGEMENT

When NST was initially implemented, it was anticipated that the deposits would reach a geotechnically stable state in a timely manner so reclamation activities could proceed. However, reduced dewatering rates are preventing the deposit from reaching the strength required to support reclamation. Also segregation of the NST was occurring upon deposition allowing fines to re-suspend

in the pond. Variable clay content in the tailings stream due to heterogeneous oil sands and/or difficult to control tailings management and deposition techniques are factors that contribute to segregation of NST. Production of NST and consumption of fines also relies on a continuous supply of coarse sand from the extraction plant. When coarse tailings are needed for dyke construction or upsets in the extraction process reduce sand production, fine tailings will continue to accumulate.

Over the past 10 years, only Syncrude and Suncor have produced NST(CT) at the commercial scale. To date, the technology has not performed as expected and no NST(CT) or fine tailings ponds have been reclaimed. Additionally, plans to place fluid tailings remaining at the end of project life in end-pits capped with water have yet to be demonstrated on a commercial scale (Houlihan and Mian, 2008). The Energy Resource Conservation Board (ERCB) has expressed concerns over the past years regarding the current tailings management practices, continual accumulation of fine tailings and associated risk to reclamation activities. As such, they have recently decided to regulate fluid fine tailings through performance criterion. In February 2009, the ERCB issued Directive 074: *Tailings Performance Criteria and Requirements for Oil Sands Mining Schemes*. The aim of the directive is to reduce fluid tailings accumulation and create trafficable surfaces for progressive reclamation (Houlihan and Mian, 2008). Based on the challenges of implementing NST experienced at Suncor and Syncrude, the recent ERCB Directive 074, and increasing public awareness, the industry is looking at alternative tailings management options to reduce their inventory of fluid fine tailings and expedite the reclamation process.

ALTERNATIVE MANAGEMENT STRATEGIES

There are several options available to the mine operator for management of the various oil sand tailings streams that may lead to a reclaimable (“trafficable”) deposit as illustrated in Figure 3. There are generally

four typical streams that may be encountered at an oil sands operation including segregating total tailings, non-segregating tailings (combined coarse and fine streams), fine tailings, and coarse tailings.

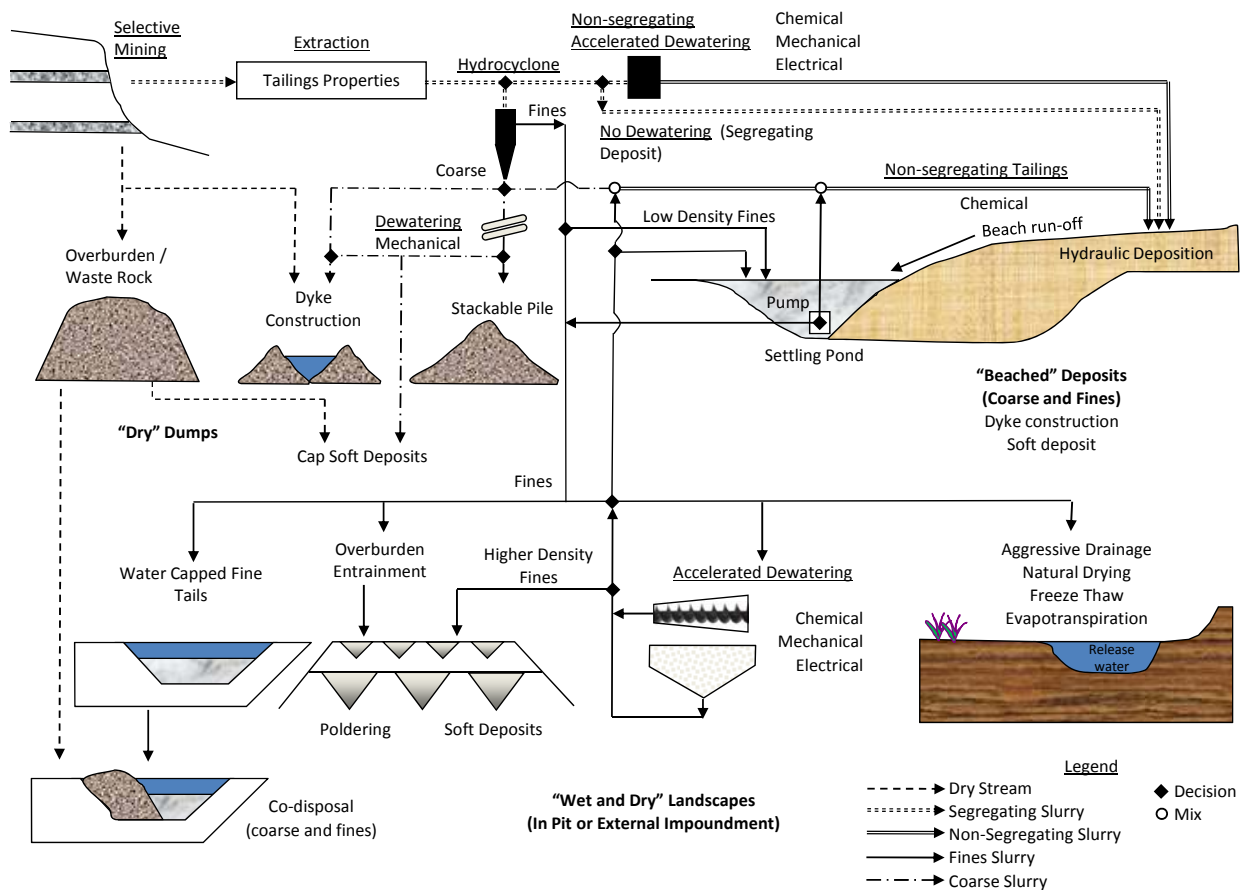


Figure 3. Tailings Management Options (modified from Sheeran, 1993).

Historically, the total tailings were deposited as a segregating deposit forming a coarse beach and fluid fine tailings within the pond. This stream may be rendered non-segregating through accelerated dewatering via mechanical (i.e. high pressure filters), electrical methods and/or chemical additives to decrease the segregating potential of the

tailings slurries resulting in a homogeneous deposit.

If sufficient dry waste is not available for the external impoundment dyke, the coarse fraction from the tailings stream may be used. The coarse fraction may be obtained through either natural segregation during beaching or

by classification with hydrocyclones. (Morgenstern and Scott, 1995).

As discussed previously, managing the fines stream is a significant challenge to the mine operator. Fine tailings inevitably will have high moisture content and low permeability thereby decreasing the consolidation rates (volume reduction) and strength gain (Morgenstern and Scott, 1995).

Management and reclamation of the segregated fine and coarse fractions may be accomplished separately or in combination. Recombination of the fines and coarse fraction with the use of a chemical binder (coagulant) can provide an opportunity to consume the inventory of fines and develop a stable landscape in a timely manner (Matthews et al., 2002). This is the current state of practice for oil sands operations.

Coarse tailings or cyclone underflow not utilized for beaches, dyke construction, or NST production may be mechanically dewatered with high pressure filters and dumped into stackable piles (Davies and Rice, 2001). The filtered tailings must be transported via truck or conveyor and form an unsaturated, dense, stable stacks (“dry stack”). Compaction may be required to enhance the stack stability and prevent liquefaction.

To achieve a “dry” final landscape as mandated by Directive 074, aggressive fines dewatering techniques, beyond natural self weight consolidation in water capped deposits, is required. Fine tailings from cyclone overflow or dredged from settling basins may be dewatered through several natural or mechanical methods. Mixing of the fine tailings with sufficient dry, clay-shale overburden may result in a soft clay deposit. This new deposit could be strong enough to support a reclamation layer directly or

incorporated into geotechnically stable land masses (Lord et al., 1993; Morgenstern and Scott, 1995). Accelerated mechanical/chemical dewatering of fines may be achieved with high density/high rate thickeners or paste thickeners (Bussiere, 2007; Lord and Liu, 1998), high pressure/vacuum filters such as drums, stacked plates, or belt filter presses (Bussiere, 2007; Xu et al., 2008); or centrifuges including the horizontal solid bowl scroll or filtering basket types (Lahaie, 2008; Mikula et al., 2007; Nik et al., 2008). Fines from accelerated dewatering could be incorporated into geotechnically stable land mass, poldered within overburden or coarse sand deposits, or deposited in-pit. These deposits may be strong enough to support a reclamation layer directly within a short time frame.

Natural, aggressive dewatering of fines, the focus of this review, can be accomplished through actively managing release water from an existing deposit or careful deposition and management of stock fine tailings. The degree of dewatering is highly dependent on the climatic conditions at the mine. Aggressive drainage can be invoked in fine tailing deposits by removing free water with perimeter ditching and decant structures. Once exposed to the atmosphere, the fine tailings may desiccate forming an over-consolidated crust that may be able to support reclamation materials (Carrier et al., 1987; Lahaie, 2008). Removal of surface water also exposes the fine tailings to freezing conditions. Yearly freezing/thawing and wetting/drying has been shown to cause moisture reduction and potential shear strength increases in the surface of fine grained coal wash tailings. The increase in strength and solids content has the potential to provide a surface layer capable of supporting re-vegetation and reclamation efforts (Beier and Segó, 2009; Stahl and Segó, 1995). Dewatering and strength gain

of these fine tailings deposits may also be enhanced by promoting evapotranspiration via suitable plant species (Carrier et al., 1987; Silva, 1995).

Optimal sub-aerial deposition of fine tailings into an impoundment or in-pit may also lead to an increase in density and strength through desiccation and freeze/thaw consolidation. Deposition in summer months will allow the tailings to desiccate during depositional cycles reducing the total volume of tailings and increasing the shear strength (Burns et al., 1993; Qiu and Segó, 2006). Thin layer deposition of fine tailings under freezing conditions will also result in significant dewatering and strength gain (Dawson and Segó, 1993; Dawson et al., 1999; Proskin et al., 1996; Wells and Riley, 2007). Benefits of volume reduction due to freeze/thaw may only be realized if the released water is managed and stored separately from the fines deposit. Both methods may result in higher tailings placement densities capable of supporting re-vegetation and reclamation efforts.

REVIEW OF NATURAL DEWATERING STRATEGIES

Desiccation of Fine Tailings

With proper management, optimal sub-aerial deposition or aggressive drainage techniques within existing deposits have been shown to over-consolidate various fine tailings leading to a potentially reclaimable deposit. Since these disposal options rely on evaporation/desiccation it is important to understand the factors that influence these processes.

Desiccation of tailings depends upon material properties, as well as the top and bottom boundary conditions (Newson and Fahey,

2003; Simms and Grabinsky, 2004). These various factors are illustrated in Figure 4.

As evident in Figure 4, the upper boundary condition, evaporation, controls the rate of water transfer from the tailings surface to the atmosphere. The evaporation rate at the surface depends on the available energy (radiation), the distribution of energy within the system (albedo effects), and the local meteorological conditions which impact the ability of the air to transfer water vapour away from the surface (Newson and Fahey, 2003; Qiu and Segó, 2006).

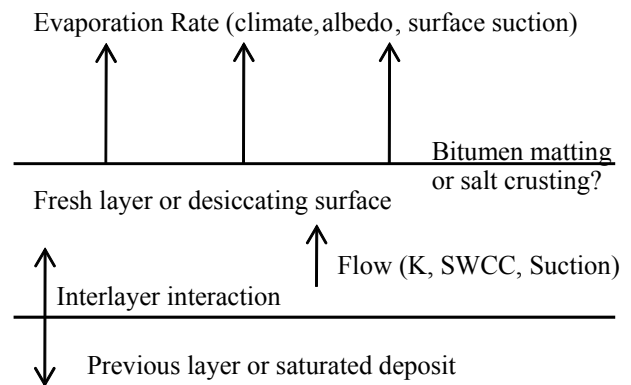


Figure 4. Factors influencing desiccation of tailings (modified from Simms and Grabinsky, 2004).

Material properties such as particle size distribution, saturated/unsaturated hydraulic conductivity and soil-water characteristic curve influence the availability and flow of water to the evaporation surface.

In fine tailings where bitumen content is relatively high, the bitumen may form a surface coating that thickens as the tailings dewater. This layer may impede moisture transfer from the tailings to the atmosphere essentially reducing or halting evaporation. The presence of salts within the fine tailings leading to salt crusting may also lead to a reduction in the evaporation rate. This may be due to an increase in the tailings surface albedo, resistance to moisture transfer at the

surface and decrease in the saturation vapour pressure (Newson and Fahey, 2003). A detailed description on the impacts of salts on the evaporation rate can be found in Newson and Fahey (2003).

Conditions below the evaporating layer may also impact the amount of desiccation occurring. Suction from a dry underlying layer may contribute to desiccation of a fresh layer of fine tailings. In deep deposits of fine tailings, underlying saturated tailings may provide moisture to recharge the desiccating surface. These interlayer interactions will depend upon the moisture conditions and hydraulic conductivity of the underlying layer.

Evaporation from saturated tailings occurs in three stages (Newson and Fahey, 2003). In stage 1, evaporation from the saturated tailings is governed by the climatic and environmental conditions. As the tailings layer dries, its moisture content will reduce from well above the liquid limit down to the plastic limit. The rate of evaporation in stage 1 is near the potential evaporation rate (E_p).

Common methods of for estimating E_p include using the pan evaporation rate or calculating E_p from detailed weather data using one of several available models (Simms and Grabinsky, 2004; Qiu, 2000). In Fort McMurray, Alberta, the average annual precipitation (rain and snow) from 1971-2000 was 455 mm (EC, 2009). Of which 334 mm were measured between April 1 and September 30 (days with average daily temperature above 0°C). Yearly evaporative conditions from 1972- 1994 were 572 mm (Abraham, 1999) leading to a rainfall deficit of 238 mm. Assuming all precipitation was drained away from the surface of a tailings deposit, the potential evaporation may be

3.13 mm/day. Qiu (2000) calculated E_p for Fort McMurray, Alberta to be 5-8 mm/day.

Stage 2 begins when tailings can no longer satisfy the evaporation demand, and they begin to desaturate. Moisture content continues to drop below the plastic limit approaching the shrinkage limit. In stage 2, a rapid decrease in the evaporation rate occurs and is dependent on both the climatic conditions and soil properties (permeability). Once the moisture content drops to residual (below the shrinkage limit), evaporation has reached stage 3 and is effectively zero.

Models are available for estimating the degree of drying that may occur in fine tailings. However, they require material properties such as SWCC, saturated and unsaturated conductivity and the maximum or potential evaporation rate (Simms and Grabinsky, 2004; Qiu, 2000). Given the particle size distribution it is very difficult to obtain the SWCC for MFT.

To achieve maximum evaporation, excess surface water from precipitation or consolidation must be adequately drained from surface of drying tailings. If adequate drainage is not provided, desiccation of the tailings will not occur until the evaporation rate exceeds the rate of water release from consolidation and precipitation.

Other factors such as climatic conditions may also impact the effectiveness of the desiccation process. In field trials of atmospheric drying of oil sands fine tails, Burns et al. (1993), found wind and rain lead to shifting islands of dry, crusted tailings surrounded by ponded water. Fresh fine tailings would then well up through the surface crustal cracks preventing the formation of a uniform stable crust.

Freeze-Thaw dewatering of Oil Sands MFT

Considerable effort has been spent in developing feasible methods to rapidly increase the solids content of MFT. Freeze-thaw is believed to be an effective natural way for dewatering the MFT. Freeze-thaw alters the macro and micro-fabric to enhance the water release and allow the MFT to consolidate rapidly under self-weight conditions and then under the effective stress induced during freezing. It creates a three dimensional reticulate ice network surrounding peds of overconsolidated MFT. During thaw the remnant ice fissures provide channels for fluid flow and account for the increased hydraulic conductivity at low stresses. The MFT micro-fabric also changes from an edge to face flocculated, disaggregated card house fabric to a compact, aggregated fabric. The latter micro-fabric retains less water which accounts for the increase in solids content (Proskin 1998).

MFT Freeze-Thaw Dewatering

Sego (1992) reported the results of a laboratory study of freeze-thaw dewatering of 150 mm thin layers of as-received (no chemical amendment) and chemically amended Suncor MFT frozen with a top and bottom cold plate temperatures of -8 °C and -15 °C, respectively. The solids content of the test specimens increased from an initial value of 30% to 40%, 44% and 50% for first, second and third cycles of freeze-thaw. Johnson et al. (1993) conducted research over a six year period examine the dewatering of Syncrude MFT via freeze-thaw and evapotranspiration. Small scale specimens were frozen at -24°C or outside during the winter and subjected to 1 to 3 cycles of freeze-thaw. The test data indicated that small specimens with initial solids contents between 29 and 35% increased to 52 to 54% when frozen and thawed with no drainage

was allowed. Similarly, larger scale specimens with 35% solids increased to 56% in the settled MFT due to freeze-thaw treatment. An exponential relationship was observed between initial solids content and the increase in solids content upon thaw suggesting that the benefits of freeze-thaw were very sensitive to the initial solids content. A multi-cycle freeze-thaw test was performed by Dawson et al. (1999) using MFT to examine the effect of freeze-thaw dewatering and indicated that during the first cycle the initial solid content increased from 28 to 34%. After a second cycle the settled solids content increased to 43%. The solids content increased to 45% after the third cycle. These results show that freeze-thaw becomes less effective in dewatering as the initial frozen solids content increases.

Dawson et al. (1999) also examined the effect of layer thickness and temperature boundary conditions on the solids content increase of Syncrude MFT associated with freeze-thaw. The experiments were conducted under three temperature boundary conditions: (a) 0°C at top, -8°C at bottom, (b) 0°C at top, -15°C at bottom, and (c) -8°C at top, -15°C at bottom. The results indicated that as the layer thickness increased, the thawed settled solids increased under different boundary conditions. The -8°C at top and -15°C at bottom data were used to simulate deposition on a previously frozen layer and the quickest freezing. This boundary resulted in thawed settled solids contents of 35 to 38% as compared to 38 to 44% for the other two boundary conditions. Similar results were observed in multi-layer freeze-thaw tests: the lower freezing rates, the higher thawed settled solids contents. Both the single layer and multi-layer tests suggest that layer thickness, temperature gradient and boundary temperature affect freeze-thaw dewatering.

Johnson et al. (1993) performed multi-layer freeze tests using Syncrude MFT to evaluate the effect of multi-layer freezing on subsequent dewatering and volume change in the fine tailings. The multi-layer test exhibited an increase in solids content from 25% to 46%. When comparing the single layer tests with the multi-layer test, the multi-layer test underwent greater volume change (49% versus 44%) and greater increase in solids content. Proskin (1998) performed similar multi-layer laboratory freeze-thaw test using Suncor acid and quicklime amended MFT and found that freeze-thaw treatment can decrease the MFT volume by 55% and the increase its solids content from 33% to 59% immediately after complete thaw. In a two years field study, he observed that freeze-thaw can reduce the volume of acid and quicklime amended Suncor MFT by 61% and increase its average solids content from 35% to 68% over one cycle of freeze-thaw. MFT experienced volume reductions ranging from 48 to 56% during the 2nd year field test, with less change than the first cycle of freeze-thaw due to the previously frozen-thawed MFT.

Johnson et al. (1993) reported that evaporation can further increase the solids content of large scale freeze-thaw treated MFT specimens from 56% to 75%. Proskin (1998) found that Suncor MFT settled an additional 21% and the solids content increased to 68% due to additional post-thaw seepage consolidation and desiccation. Water balance measurements showed that 77% of the MFT initial water content was removed during the experiment, with 58% of this amount removed as surface decant, 16% removed as bottom drainage, and 26% removed by surface evaporation. Additional post-thaw surface desiccation and seepage consolidation were found to raise the matric suction in the upper MFT, which increases the solids content profile. He found in his

field studies that a surface crust up to 0.3 m thick in better drained areas of the ponds was created due to post-thaw drying processes of seepage consolidation and surface desiccation combined to lower the groundwater table. The crust consisted of high solids content (>80%) MFT and soil suctions as high as 66 kPa existed in this MFT at 100 mm depth.

Proskin (1998) observed a significant effect of freeze-thaw on hydraulic conductivity. For as-received and amended MFT specimens, the hydraulic conductivity results indicated an increase of 100 times at low void ratios. Field falling head tests provided values of in situ hydraulic conductivity for the saturated MFT at depth that ranged between 4 and 90×10^{-8} cm/s w. The hydraulic conductivity data obtained by Dawson et al (1999) for never-frozen MFT and the frozen and thawed MFT also indicated that the frozen and thawed material has a higher hydraulic conductivity at a given void ratio than the never-frozen material. However, this difference diminishes as the effective stress is increased to 100 kPa and the void ratio approaches one.

Laboratory tests by Proskin (1998) indicated that the compressibility of sulfuric acid and quicklime amended and as-received (not amended) Suncor MFT was dependent on the initial solid. The study reported that freeze-thaw was able to reduce the initial void ratio and the compressibility of amended and not amended MFT. Based on the observed thaw parameters and coefficient of consolidation obtained during tests, the thaw consolidation ratio was calculated to be 0.1 inferring that the degree of consolidation at the end of thaw was 98%. By the end of the 1st year of this field study, field vane shear strength of the MFT increased to 2 and 3 kPa. The compressibility tests by Dawson et al. (1999) suggested that effective stress of 2 to 4 kPa represents the strength limit of the soil

peds (masses of compressed soil about 2 mm in diameter) created during the freezing process. At higher stresses the peds break down and the thawed MFT responds as if it was never-frozen.

The effect of freeze thaw dewatering can be enhanced via chemical amendment and altering drainage conditions. Sego (1992) investigated the effect of chemical amendment of the MFT by adding sulfuric acid (H_2SO_4) and replacing monovalent sodium cations with divalent calcium cations (from quicklime CaO) prior to freezing. He found that chemical amendment causes an additional 18% increase in solids content associated with freeze-thaw. Chemical amendment of the MFT yielded decant water with no measurable solids as compared to the 2.5% solids contents measured in decant water in freeze-thaw tests conducted on as-received MFT. A thaw settlement analysis performed by Proskin (1998) indicated that given adequate time, the MFT would settle under self-weight conditions by 30% and the solids content would increase to 44%. The acid and quicklime amendment and freeze-thaw increase the settlement to 45% and the solids content increases to 52%. Johnson et al. (1993) Additional small scale model tests employed different drainage configurations (one with a single vertical sand channel down the middle of the specimen and the second with a sand liner along the bottom and sides) to enhance the freeze-thaw dewatering process. The results indicated that MFT experienced increases in solids contents from 35% to 52% and even up to 63%.

DISCUSSION

In a recent study by Wells and Riley (2007) to evaluate evaporation dewatering of Suncor MFT through thin lift deposition, they suggested that dewatering by freeze-thaw can

be an important mechanism to treat thin lifts of MFT, in addition to evaporation. They reported an increase in the MFT solid content from 30% to 50% with a single cycle of freeze-thaw dewatering treatment in successive lifts up to a total frozen thickness of one and 2 meters. It was suggested freeze-thaw dewatering can be used to increase the volume of treated MFT/unit surface area from the $2m^3$ MFT/ $1m^2$ surface (based on anticipated efficiency of evaporation dewatering only) to 3 to $4.5 m^3$. This is consistent with the freeze-thaw dewatering rate estimated by Dawson et al. (1999) of $3.5-5 m^3/m^2$ based on a thaw constrained environment. Compared to evaporation drying, freeze-thaw dewatering is expected to maximize the total volume of water returned to the system.

Regardless of the method used, adequate drainage is required to remove water from the dewatering tailings surface. Wells et al. (2007) utilized chemical amendments to change the rheology of fine tailings prior to deposition and subsequent evaporation and freeze-thaw dewatering. The enhanced fine tailings attained a steeper slope on deposition allowing release water to drain away from the surface.

CONCLUSION

Historic tailings management strategies in the Oil Sands industry has lead to the accumulation of significant volumes of fluid fine tailings. In lieu of a recent tailings management directive issued by the ERCB and public awareness, there is renewed interest by the industry in natural dewatering strategies for the fine tailings. Tailings management options are available to meet the directive include managing the coarse and fine fractions separately. Alternative management strategies using natural

dewatering strategies can be utilized for fine tailings (both the massive inventory of legacy tailings and future tailings).

It was suggested that freeze-thaw dewatering can be used to increase the volume of treated MFT/unit surface area from the 2m³ MFT/1m² surface (based on anticipated efficiency of evaporation dewatering only) to 3 to 4.5 m³. Compared to evaporation drying, freeze-thaw dewatering is expected to maximize the total volume of water returned to the system.

To achieve the goal of a trafficable deposit of fine tailings utilizing natural dewatering, management of surface water (excess precipitation, consolidation and thaw release water) is required. Adequate drainage measures and collection are required as well as a separate storage area for this water.

ACKNOWLEDGEMENTS

The authors are thankful for the financial assistance from National Sciences and Engineering Research Council of Canada and the Oil Sands Tailings Research Facility. Thanks also to Alberta Research Council and Prairie Mines and Royalty Ltd. for the financial support of Mr. Beier.

REFERENCES

- Abraham, C. 1999. Evaporation and Evapotranspiration in Alberta. Report 1912-1985, Data 1912-1996. Water Sciences Branch, Water Management Division, Alberta Environmental Protection. January, 1999.
- Allen, E. 2008. Process water treatment in Canada's oil sands industry: I. Target pollutants and treatment objectives. *Journal of Environmental Science*, 7: 123-138.
- Beier, N. and Segó, D. (2007). The Oil Sands Tailings Research Facility. 60th Canadian Geotechnical Conference and 8th joint IAHCNC Groundwater Specialty Conference, Ottawa, Ontario, October 22-24, 2007. 8 pp
- Bussiere, B. 2007. Colloquium 2004: Hydrogeotechnical properties of hard rock tailings from metal mines and emerging geoenvironmental disposal approaches, *Canadian Geotechnical Journal*, 44:9 1019-1052.
- Burns, R., Cuddy, G., and Lahaie, R. 1993. Dewatering of fine tailings by natural evaporation. *Fine Tailings Symposium*, Environment Canada, Edmonton, Alberta, April 4-7, 1993, 36 pp
- Carrier, W.D. III, Scott, J.D., Shaw, W.H., and Dusseault, M.B. 1987. Reclamation of Athabasca oil sand sludge. *Proceedings of Geotechnical Practice for Waste Disposal*, June 15-17, 1987, Ann Arbor, MI. pp. 377-391.
- Chalaturnyk, R.J., Scott, D., and Ozum, B. 2002 Management of oil sands tailings. *Petroleum Science and Technology*, 20(9&10):1025-1046.
- Chu, A., Paradis, T., Wallwork, V., and Hurdal, J. 2008. Non segregating tailings at the Horizon oil sands project. *First International Oil Sands Tailings Conference*, Edmonton, Alberta, December 7-10, 2008. 10 pp
- Davies, M.P., and Rice, S. 2001. An alternative to conventional tailings management - "dry stack" filtered tailings. *Proceedings of the International Conference on Tailings and Mine Waste '01*, Vail, Colorado, pp 411-419

Dawson, R.F., Sego, D.C., Pollock, G.W., 1999. Freeze-thaw dewatering of oil sands fine tails. *Canadian Geotechnical Journal* 36 (4), 587-598.

Environment Canada (EC). 2009. National Climate Data and Information Archive. Accessed May 11, 2009, www.climate.weatheroffice.ec.gc.ca

FTFC (Fine Tailings Fundamentals Consortium), 1995. *Advances in oil sands tailings research*, Alberta Department of Energy, Oil Sands and Research Division, Edmonton, Alberta, Canada.

Houlihan, R. and Mian, H. 2008. Past, Present, Future Tailings – Regulatory Perspectives. *First International Oil Sands Tailings Conference*, Edmonton, Alberta, December 7-10, 2008. 8 pp.

Johnson, R.L., Bork, P., Allen, E.A.D., James, W.H., and Koverny, L. 1993. Oil sands sludge dewatering by freeze-thaw and evapotranspiration. *Alberta Conservation and Reclamation Council Report No. RRTAC 93-8*, 247p.

Lahaie, R. 2008. Syncrude Canada Ltd. - New Tailings Concepts. *First International Oil Sands Tailings Conference*, December 7 to 10, 2008, Edmonton, AB, Canada, pp. 17

Lord, E.R., Maciejewski, W. Cymerman, G., and Lahaie, R. 1993. Co-disposal of fine tails and overburden utilizing pipeline techniques. *Oil Sands – Our Petroleum Future Conference*, Edmonton, Alberta, April 4-7, 1993.

Lord, E.R. and Liu, Y. 1998. Depositional and geotechnical characteristics of paste produced from oil sands tailings. *Tailings and Mine Waste 1998*. Balkema, Rotterdam. pp. 147-157

Matthews, J.G., Shaw, W.H., MacKinnon, M.D., and Cuddy, R.G. 2002. Development of composite tailings technology at Syncrude. *International Journal of Surface Mining, Reclamation, and Environment*, 16(1): 24-39.

Masliyah, J., Zhou, Z., Xu, Z., Czarnecki, J. and Hamza, H. 2004. Understanding water-based bitumen extraction from Athabasca oil sands. *The Canadian Journal of Chemical Engineering*, 82: 628-654.

Matthews, J. 2008. Past, Present, and Future Tailings – Tailings Experience at Albion Sands Energy. *First International Oil Sands Tailings Conference*, Edmonton, AB, December 7-10, 2008. Presentation only.

Mikula R.J., Kasperski, K.L., Burns, R.D., and MacKinnon, M.D. 1996. Nature and fate of oil sands fine tailings. *Suspensions: Fundamentals and Applications in the Petroleum Industry*. Edited by Laurier L. Schramm. *Advances in Chemistry Series 251*. American Chemical Society, Washington, DC, USA.

Mikula, R.J., Munoz, V.A., and Omotoso, O. 2008. Centrifuge options for production of "dry stackable tailings" in surface mined oil sands tailings management. In *Canadian International Petroleum Conference / Petroleum Society's 59th Annual Technical Meeting*, Calgary, AB, Canada, pp. 7.

Morgenstern, N.R. and Scott, J.D. 1995. *Geotechnics of fine tailings management; geoenvironment 2000; characterization, containment, remediation, and performance in environmental geotechnics*, *Geotechnical Special Publication*, 46: 1663-1683.

- Newson, T.A. and Fahey, M. 2003. Measurement of evaporation from saline tailings storages. *Engineering Geology*, **70**(2003): 217-233. doi:10.1016/S0013-7952(03)00091-7
- Nik, R. M., Sego, D.C. and Morgenstern, 2008. Possibility of Using Centrifugal Filtration for Production of Non-Segregating Tailings. First International Oil Sands Tailings Conference, December 7 to 10, 2008, Edmonton, AB, Canada, pp. 200-208.
- Proskin, S. 1998. A Geotechnical Investigation of Freeze-Thaw Dewatering of Oil Sands Fine Tailings. PhD thesis, University of Alberta.
- Qiu, Y. and Sego, D. C. 2006. Optimum deposition for sub-aerial tailings disposal: concepts and theories. *International Journal of Mining, Reclamation and Environment*, **20**:4, 272 — 285
- Sego, D. 1992. Influence of pore fluid chemistry on freeze-thaw behaviour of Suncor Oil Sand Fine Tails (Phase I). Submitted to Reclamation Research Technical Advisory Committee, Alberta Environment, 35p.
- Sheeran, D. 1993. An improved understanding of fine tailings structure and behavior. Fine Tailings Symposium, Environment Canada, Edmonton, Alberta, April 4-7, 1993, 11 pp.
- Simms. P. and Grabinsky, M. 2004. A simple method for estimating rates of drying and desaturation of paste tailings during surface deposition. *Tailings and Mine 2004*, October 11-13, 2004, pp 287-292.
- Wells, P.S. and Riley, D.A. 2007. MFT drying – case study in the use of rheology modification and dewatering of fine tailings through thin lift deposition in the oil sands of Alberta. *Paste 2007*, Tenth International Seminar on Paste and Thickened Tailings, Perth, Australia, March 13-15, 2007. Pp. 271-284.
- Xu, Y., Dabros, T., and Kan, J. 2008. Filterability of oil sands tailings, *Process Safety and Environmental Protection*, **86**(4): 268-276.
- Yasuda, N. 2006. Hydraulic performance of the seepage collection ditches at the Albian Sands Muskeg River Mine. MSc Thesis Department of Civil Engineering, University of Waterloo, Waterloo, Ontario, Canada.

APPLICATIONS IN THE OIL SANDS INDUSTRY FOR PARTICLEAR® SILICA MICROGEL

Robert H. Moffett,

E. I. DuPont de Nemours and Company, Wilmington, DE, USA

ABSTRACT: DuPont™ Particlear® silica microgel solution is used in a number of industrial processes to coagulate and clarify water streams. Particlear® is made at the intended point of use, from commodity chemicals using DuPont proprietary technology. This paper will review how Particlear® is made, some select industrial applications and how Particlear® can be used in various applications in the oil sands industry.

Particlear® is a proprietary, ultrahigh surface area silica microgel solution. Particlear® can add unique properties to flocculation and coagulation treatment schemes, including the removal of select dissolved solids and organics, as well as enhanced coagulations of fine solids such as clays. Particlear® has been demonstrated to increase dewatering of flocculated oil sand tailings. Additionally, silica microgel solutions have been historically used to enhance the warm lime softening process and could help improve SAGD water treatment.

INTRODUCTION

Numerous flocculants and coagulants are used by the mining industry to effect liquid/solids separation. Unit operations utilizing these chemicals include, settling, clarification, filtration, dissolved air flotation and centrifugation. The principal organic flocculant used by the mining industry is polyacrylamide, which may carry an anionic or cationic charge, or it may be non-ionic. Coagulants used by the mining industry usually carry a cationic charge, and include polyamine, polydadmac, as well as various metal salts. Silica microgel solution is an anionic, inorganic coagulant prepared from sodium silicate solution. A number of silica based microgels that have been disclosed in the patent literature including polyaluminosilicates, polysilicic acid and polysilicate microgels. Silica based

microgels have been used for over 70 years in industrial liquid/solids separation and have often been referred to as “active or activated” silica. Particlear® is the DuPont trade name for its silica microgel solution.

As shown in Figure 1, silica microgel solutions are composed of primary silica particles, which are linked together to form a three-dimensional microgel network¹. Typically the primary silica particles are 1-2 nm in diameter yielding microgels with a surface area of about 1000-1400 m²/gm. The surface of the silica particles is covered with hydroxyl groups. Calculations show there are about 8 hydroxyl groups per square nm of surface area on a silica microgel. These hydroxyl groups can ionize in water and impart an anionic charge to the microgel (Figure 2) at pH >2. The extent of the ionization is pH dependent. Due to the high

reactivity and high surface area, silica microgel solutions are stable only as very dilute solutions. This precludes their economical shipment from a fixed manufacturing location to the intended point of use. To overcome this obstacle, Particlear® is produced at the point of use.

PARTICLEAR® PREPARATION

Particlear® is prepared from readily available commodity chemicals using a proprietary patented process^{2,3}. Sodium silicate is diluted with water and then reacted with carbon dioxide to initiate silica polymerization of the silica. After a few minute aging period, the microgels grow to the desired size and the solution is diluted to retard further polymerization as shown in Figure 3. If the Particlear® solution is to be stored for later use, the solution is further acidified or re-alkalinized to improve its stability. The Particlear® generator as shown in Figure 4 is a fully automated process. Microgels of varying size and molecular weight can be produced with the generator and tailored to meet the requirements of the liquid/solids separation.

PARTICLEAR® USE

Particlear® is usually employed to improve the performance of other flocculation chemistries. Particlear® can be utilized to enhance the performance of various synthetic and natural flocculants such as polyacrylamide and guar gum. Particlear® can also be used to boost the performance of coagulants such as aluminum sulphate and polyamine.

In most applications, Particlear® functions through network formation via charge neutralization as shown in Figure 5. In some applications, however, hydrogen bonding

between the silica microgel and the material to be flocculated is believed to be the dominate mechanism. Experience has shown that the microgel size is key to generating good performance when using silica microgel solution⁴. The microgel size must be large enough to extend or bridge between particles to be flocculated.

GENERAL INDUSTRIAL APPLICATION OF PARTICLEAR®

Particlear® and activated silica have been used in many diverse applications over a number of years. A few of the noteworthy applications and the benefits from the use of the silica microgel are listed below.

- Potable water clarification. Activated silica was originally used in this application in 1937 by Baylis⁵. Typically, activated silica has been used in conjunction with aluminum or iron salts. Addition of activated silica has been found to create stronger, denser flocs, which exhibited faster settling rates. Activated silica has been found to expand the water clarification operational pH window. Solids separation is normally achieved through sand bed filtration. The use of activated silica has been shown to improve filtration rates and extend filter runs before backwashing of the sand bed was necessary.
- Paper manufacture. Paper manufacture can be viewed as a large-scale filtration process. Silica microgel solution is utilized in this industry as a retention and drainage aid. Use of silica microgels was shown to dramatically improve water drainage rate through the paper web while retaining filler and fiber fines

within the forming paper sheet³. In paper manufacture, silica microgels are used with cationic starch, polyacrylamides (both cationic and anionic) as well as with various coagulants including aluminum salts and polyamines.

- Animal processing wastewater treatment. Particlear® is used in conjunction with cationic polyacrylamides to remove both soluble and suspended animal fats and proteins from wastewater⁶. Dissolved air flotation is the conventional water treatment process. Particlear® has been shown to improve removal of the protein and fats, while reducing the required polymer dose and expanding the operational pH window.
- Sugar juice clarification. Particlear® has been demonstrated to reduce undesirable compounds in clarified raw sugar cane juice⁷. In this application, Particlear® is employed along with a low dose of anionic polyacrylamide. Solids separation is conducted in a settler/clarifier.

GENERAL MINING APPLICATIONS

Particlear® and activated silica have been applied in numerous mining related liquid/solids separations.

- A coal mine was using a combination of cationic and anionic polyacrylamide to thicken their wash water sludge. In this application, Particlear® was shown to be able to replace the anionic polyacrylamide and reduce the cationic

polyacrylamide dose while improving solids consolidation (Figure 6).

- An Australian ilmenite dredge mine was using polyamine along with anionic polyacrylamide to settle and clarify a clay slime stream. The mine was investigating the alternative use of a sulfonated acrylamide terpolymer to improve settling of the clay fines. Particlear® used in conjunction with a non-ionic high molecular weight polymer was shown to give equivalent settling to the best alternative treatment, but with much improved turbidity (Figure 7).
- A Florida dredge mine was investigating the potential to eliminate the use of settling ponds for consolidation of humates released from the soil during the mining operation. Because of their small particle size and high anionic charge, the humates create a colloidal dispersion, which does not settle even after years of storage in the settling ponds. Laboratory testing of traditional synthetic polymer treatment programs determined that a dose of 23 kg/MT of polyamine and 4.9 kg/MT of polyacrylamide were required to flocculate the humate. An alternative flocculation scheme was demonstrated which utilized 10 kg of ferric chloride, 0.7 kg of cationic polyacrylamide and 0.7 kg of anionic polyacrylamide. This provided good flocculation of the humate, but the pH of the treated stream was too low to allow discharge of the water into the water table. Increasing the stream pH caused formation of non-settling metal hydroxides. Alkaline stabilized Particlear® was used to adjust the pH of the stream and precipitate the metal

hydroxides along with the flocculated humate. The flocculated humate and metal hydroxides were then pumped onto the mined sand to dewater and dry. Figure 8 shows the humate dispersion before and after flocculation. Figure 9 demonstrates the water clarity after the flocculated humate is deposited onto a column of sand.

OIL SANDS APPLICATIONS

Particlear® has multiple potential applications within the oil sands industry, both in traditional liquid/solids separation as well as a processing aid. The following describes some applications.

- Oil sand tailings from a TSRU (Tailings Solvent Recover Unit) having a very fine particle size distribution (Figure 10) were found to have very limited response to flocculation with a high molecular weight, medium charge, anionic polyacrylamide (APAM). TSRU tailings samples containing 2 wt. % solids were treated with varying amounts of APAM and then vacuum filtered through Whatman 41 filter paper as a relative indication of dewatering ability. The amount of water passing the filter cake was recorded with time. Filter cake solids were then calculated from this data (Figure 11). Addition of calcium (as gypsum) along with the APAM was shown to provide only limited improvement in dewatering (Figure 12). As shown in Figure 13, addition of Particlear® silica microgel solution was found to significantly boost the dewatering rate and ultimate dryness of the TSRU tailings.
- MFT (mature fine tailings) drying has been proposed as a means to remediate the fine tailings from oil sands mining. Blending of the MFT with gypsum has been documented as a method to achieve a minimum acceptable yield stress and to accelerate drying. In laboratory experiments, MFT treated with silica microgels have been shown to dry at a faster rate than MFT treated with gypsum or gypsum + lime (Figure 14)
- Bitumen production using the SAGD (steam assisted gravity drainage) process produces large quantities of water, which must be treated before it can be recycled. Warm lime softening is a preferred method of treating the recovered water to reduce the dissolved mineral content. Addition of activated silica has been shown to improve sedimentation rates with increased color removal when used in conjunction with lime softening⁸.
- Sodium silicate is a well-known clay dispersant used in the mining industry⁹. Li¹⁰ discloses the use of partially neutralized sodium silicate solution as being superior to sodium hydroxide as a bitumen processing aid. Li shows the use of partially neutralized sodium silicate produces bitumen froth having reduced mineral and water content compared to froth prepared using sodium hydroxide as the processing aid. Gong¹¹ et. al. indicates polymeric silica is superior to the silicate ion as a processing aid. Particlear® is prepared by fully neutralizing sodium silicate solution alkalinity resulting in highly polymerized silica particles (microgels). This is an area that

requires further investigation to determine if silica microgels may offer an advantage as a bitumen extraction aid.

Although sodium silicate can be used to enhance bitumen extraction it has a negative impact on the ability to chemically flocculate fine tailings. Particlear® can however be used to enhance fine tailings flocculation. To demonstrate this principle, TSRU tailings were treated with aluminum chlorohydrate, APAM and SiO₂ as either sodium silicate or Particlear® silica microgel solution. As can be seen in Figure 15 the tailings treated with sodium silicate did not dewater as fast or to the same extent as those treated with Particlear®.

CONCLUSIONS

Particlear® and activated silica have been used in numerous industrial liquid/solids separation processes. Oil sands processing, and mining in general, have many liquid/solids separation processes that may benefit from the use of silica microgel solution. The benefits that could be realized by the use of silica microgel solution in the oil sands and mining industries include:

- Potential reductions of polyacrylamide and/or other organic flocculants.
- Increased floc strength and settling rates.
- The ability to remove select dissolved solids and organics.
- Increased solids dewatering rate.
- More environmentally sustainable materials.

REFERENCES

Iler, R., *The Chemistry of Silica*, John Wiley and Sons, New York, 1979

Moffett, Robert H., Simmons, Walter J., Jones, Roy C., U.S. Patent 6,060,523 (July 20, 1998)

Moffett, Robert H., Simmons, Walter J., U.S. Patent 6,274,112 (December 8, 1999)

Rushmere, John D., U.S. Patent 4,954,220 (September 4, 1990)

Baylis, John R., U.S. Patent 2,217,466 (September 17, 1937)

Moffett, Robert H., U.S. Patent 6,132,625 (October 17, 2000)

Dionisi, Fabio A.R., and Calabrese, Rafael J. U.S. Patent Application 2009/1026720 A1 (May 21, 2009)

Activated Silica A New Chemical Engineering Tool, Merrill, Reynold C., *Chemical Engineering Progress*, Vol. 1, No. 1, 1947, pg. 27-32

Sodium Silicates, Bulletin 17-103, The PQ Corporation, pg. 5

Li, H., Shou, Z.A., Xu, Z. and Masliyah, J.H., Role of Acidified Sodium Silicate in Low Temperature Bitumen Extraction from Poor-Processing Oil Sand Ores, *Ind. Eng. Chem. Res.*, 2005, 44, 4753-4761.

Gong, Q., Klauber, C., Warren, L.J., Mechanism of Action of Sodium Silicate in the Flotation of Apatite from Hematite, *Int. J. Miner. Process.* 993, 39, 251

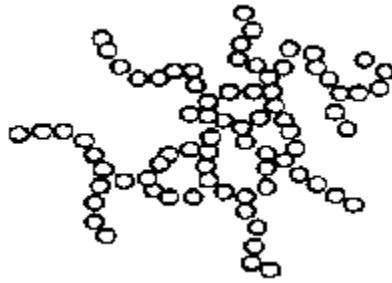


Figure 1. Silica Microgel Diagram

Silica Particle Surface

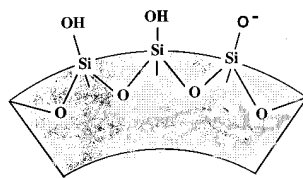


Figure 2. Silica Microgel Surface Diagram

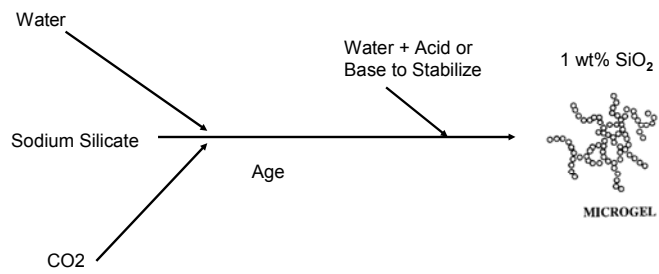


Figure 3. Particlear® Process Flow Diagram



Figure 4. Particlear® Generator

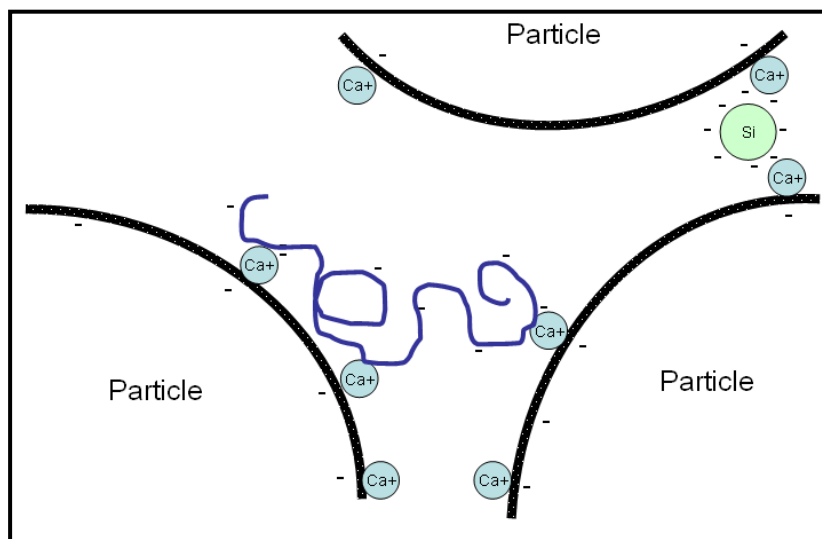


Figure 5. Network Formation Through Charge Neutralization

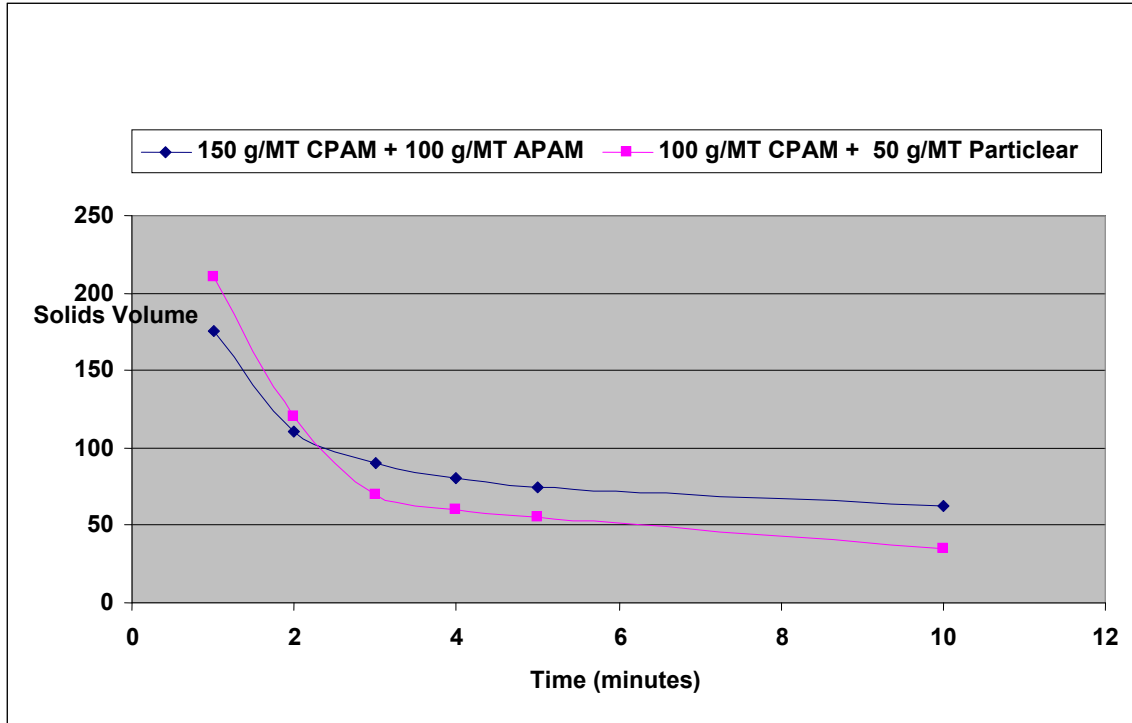


Figure 6. 500 ml Cylinder Settling Test

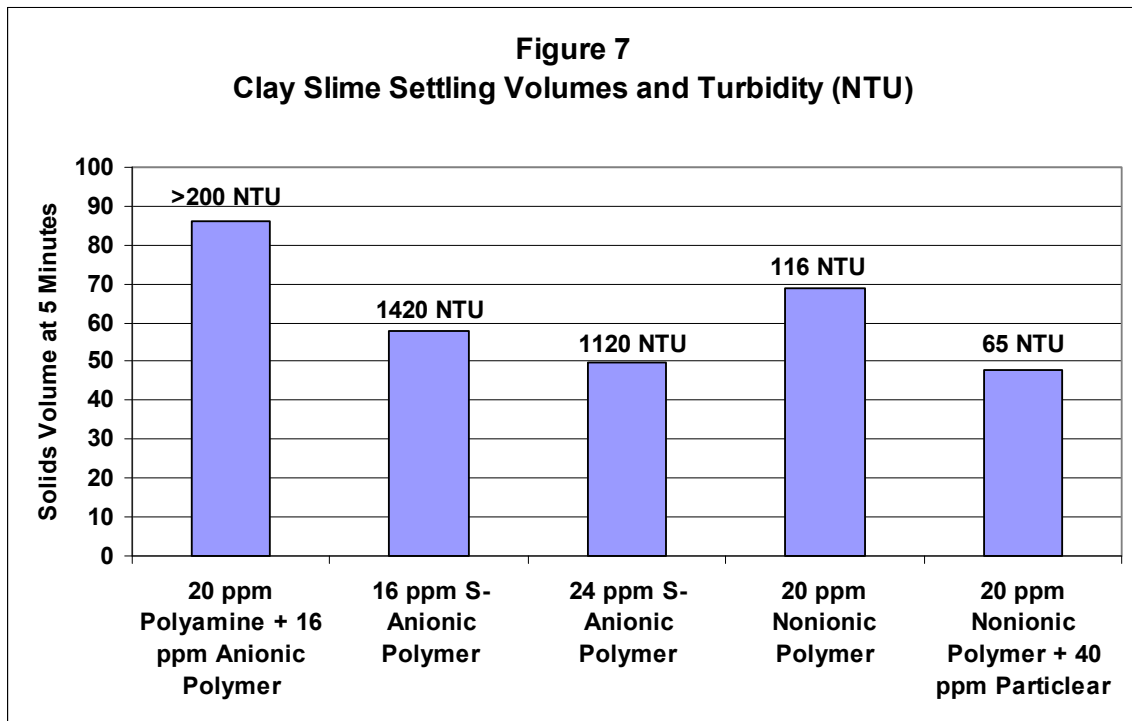


Figure 7. Clay Slime Settling Volumes and Turbidity (NTU)



Figure 8. Humate Settling Test



Figure 9. Humate Sand Filtration

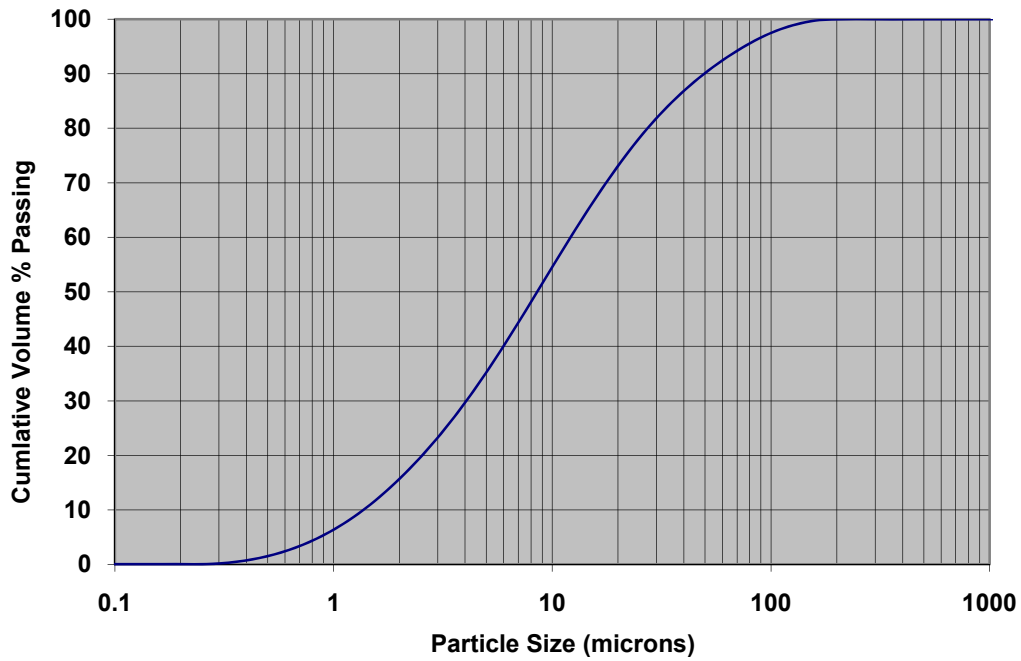


Figure 10. TSRU Tailings Particle Size

Figure 11
APAM Dose Effect

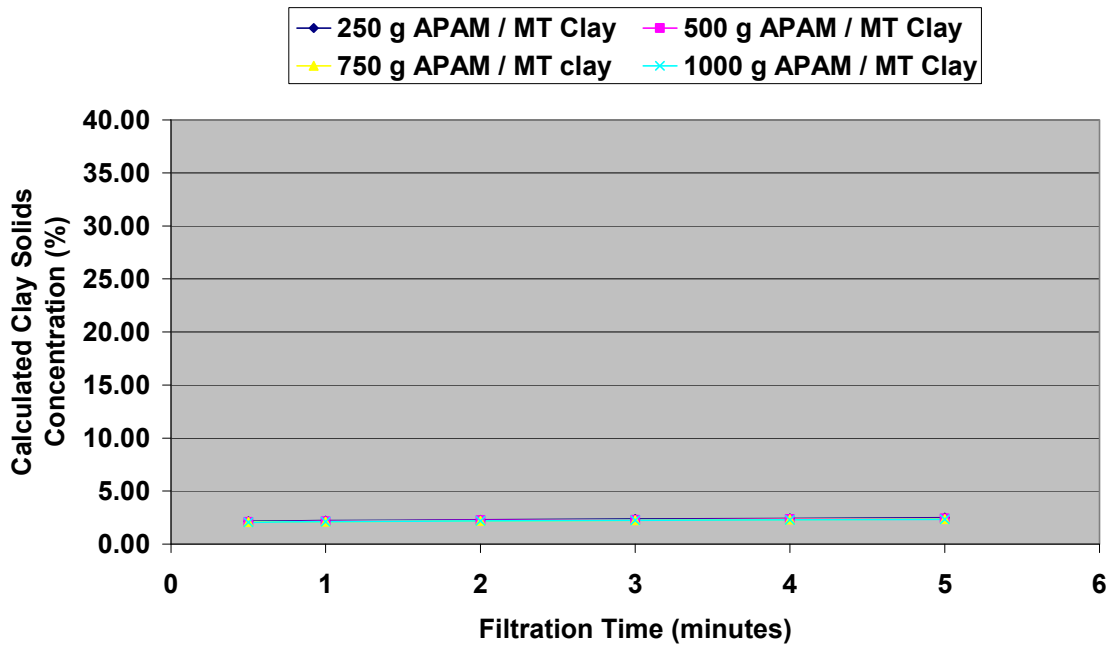


Figure 11. APAM Dose Effect

Figure 12
Calcium Effect; 17 Kg Gypsum / MT Clay

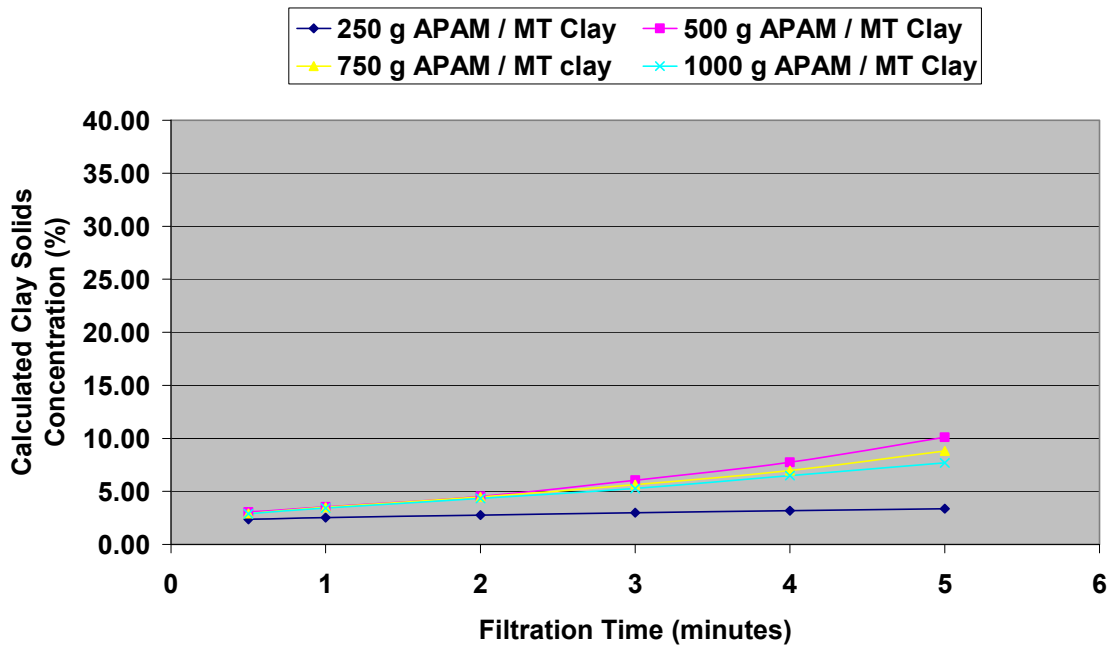


Figure 12. Calcium Effect: 17Kg Gypsum/MT Clay

Figure 13
Particlear® Dose Effect
(7.5 g APAM + 17 Kg Gypsum / MT Clay)

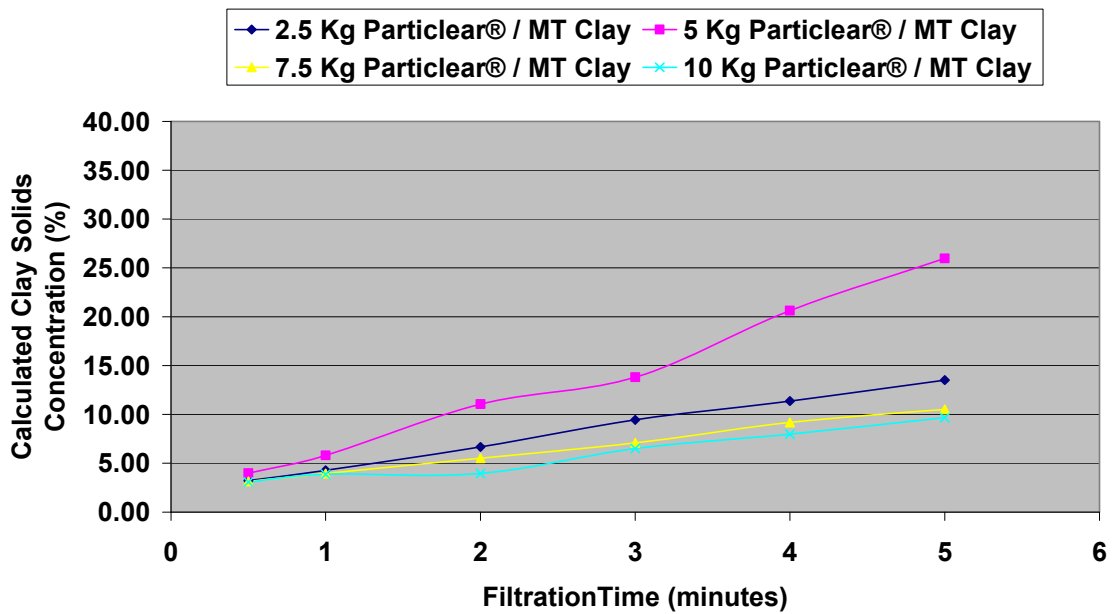


Figure 13. Particlear ® Dose Effect

Figure 14
5 cm Thick MFT Drying

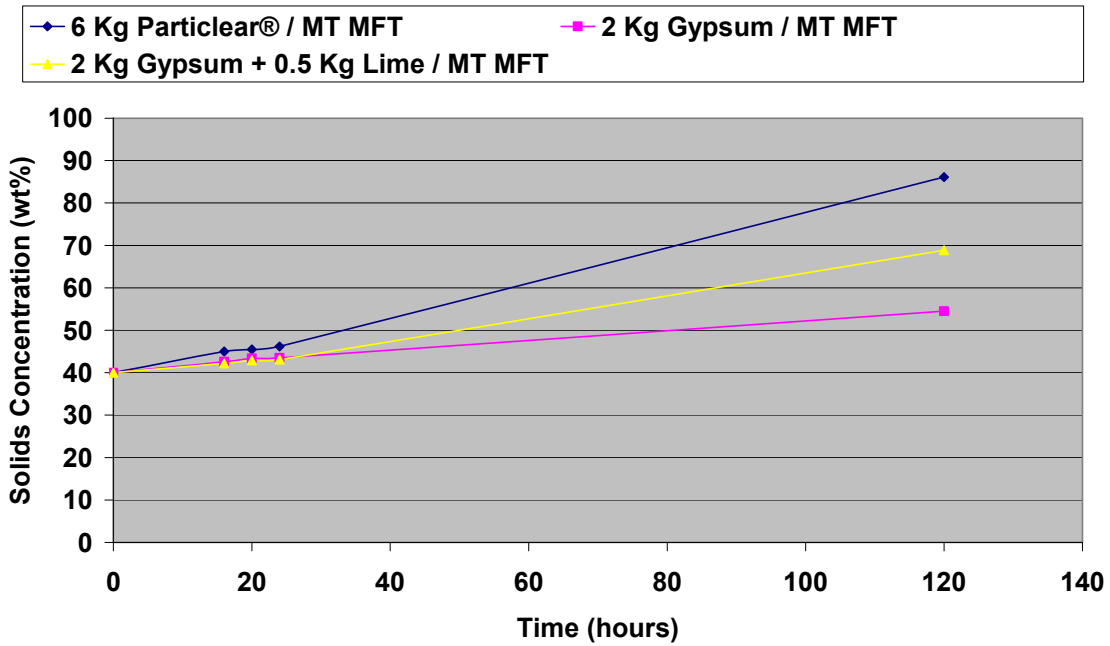


Figure 14. 5 cm Thick MFT Drying

Figure 15
TSRU Tailings Flocculation with Sodium Silicate and Silica Microgel

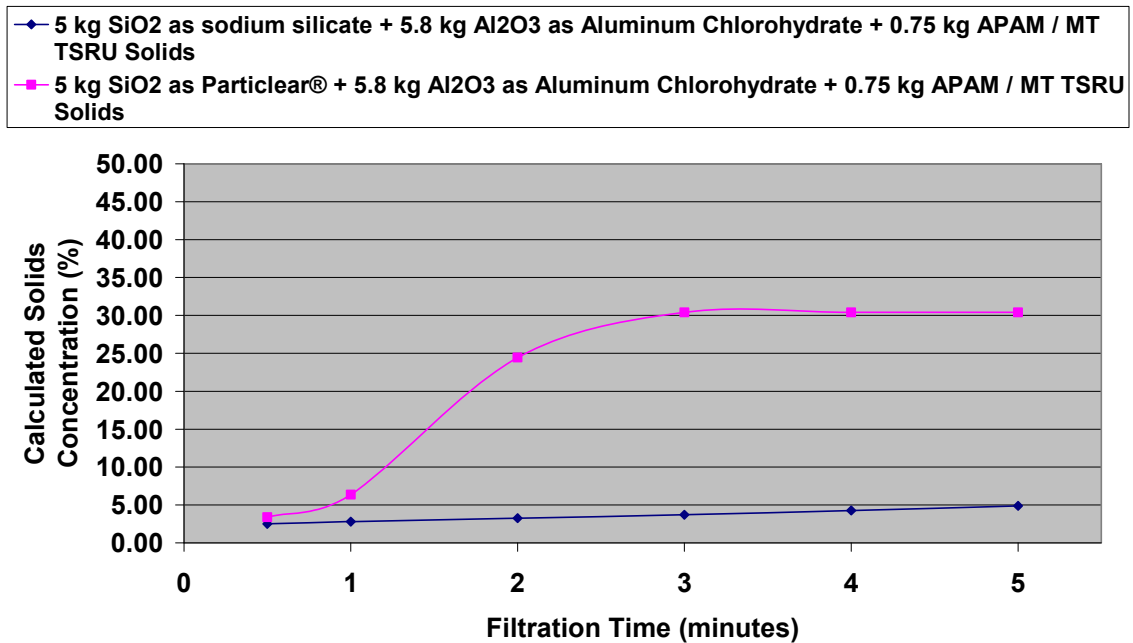


Figure 15. TSRU Tailings Flocculation with Sodium Silicate and Silica Microgel

SCREENING STUDY OF OIL SAND TAILINGS TECHNOLOGIES AND PRACTICES

Richard Nelson Program Director

Alberta Energy Research Institute, Edmonton, Alberta

Dr. David Devenny P. Eng., P. Geol.

The Rock Doctor, Calgary, Alberta

ABSTRACT: A screening study appraised different tailings technologies for mineable oil sands. Technologies included conventional tailings, treatment using thickeners, cyclones, centrifuges and finally CT treatment.

Goals assumed for closure: create solid waste and qualify for a timely reclamation certificate.

Each technology was studied by developing a material balance, an integrated plant to use the technology and full life cycle plans. Technologies were studied in sufficient detail to identify differences and the related costs.

Conclusions: Conventional tailings technology is not leading to closure. Thickeners and cyclones save heat and support other processes such as CT. CT has the potential to create solid waste, requires containment and is limited by sand availability. Centrifuge treatment is very promising and has favourable economics.

The centrifuge option warrants further study and pilot verification.

INTRODUCTION

This paper documents results of a scoping study that was undertaken to provide insight on the potential of alternative tailings technologies to:

- Reduce fresh water make-up needs in oil sand extraction and processing.
- Facilitate projects qualifying for a timely reclamation certificate.

Components of the study involved:

1. An overview of oil sands practice to identify current practice. Information was obtained from the literature and project applications. Over 25 practitioners were interviewed to obtain their views on oil sand practice.
2. Background topics such as requirements for closure and when to invest in reclamation activities, were explored and documented.
3. An overview of soil properties was prepared and novel data was derived.

4. Key technologies were studied in sufficient detail that process flow sheets and material balances could be prepared and appraised.
5. A generic platform was developed to provide a common basis for comparing the technologies. The common basis overcomes differences between each project that complicate comparisons.
6. Each technology was studied in sufficient detail that cost differences could be identified and compared. Environmental liabilities were booked by assuming that funds equal to the liability were deposited in an environmental Trust at the time the liability was created. Liabilities managed in this way included reclaiming disturbed land, reclaiming fluid tailings, establishing a fund to process water for discharge and establishing a fund to pay for closure activities.
7. Technologies were evaluated against
 - a. Ability to progress projects to closure,
 - b. Water demand and potential to save energy,
 - c. Economic evaluation using two approaches:
 - i. A simple NPV of capital and operating costs,
 - ii. Evaluation in a project economic model that reflects the project financial environment encompassing capital, operating costs, income, royalty and income tax. This evaluation is

necessary to capture fiscal offsets.

HIGHLIGHTS OF INDUSTRY PRACTICE

Overview

Today there are four operating mineable oil sand plants. Mineable oil sand projects are large and are getting larger.

Table 1 compares key attributes of the first three projects: Suncor, Syncrude and Albion Sands. The CNRL plant was not included because it is just starting.

Each project is different – a reflection of different site geology, project design, and management philosophy. The differences make comparison difficult.

Fluid tailings have been accumulating since commercial production of the oil sands started. Syncrude, the largest commercial operator, has produced 470 million cubic metres of fluid tailings. 20 million cubic metres of that inventory has been solidified through CT treatment. (Fair 2008).

The total fluid tailings inventory for the region is 750 million (Houlihan et. al). Extrapolation based on current applications, suggests that the volume of fluid tailings will triple in the next 20 years.

Table 1. Characteristics of three mineable oil sands projects.

Project/Component	Suncor	Syncrude	Albian Sands
Start-up date	1967	1978	2002
Years in operation	41	30	6
Configuration	Integrated facility Mine Mine Waste disposal Extraction Upgrading Upgrader Tank farm Utilities Tailings ponds	Integrated facility Mine Mine Waste disposal Extraction Upgrading Upgrader Tank farm Utilities Tailings ponds	Separate facilities At site Mine Extraction Waste disposal 455 km 24" diluted bitumen and 12" diluent return line. Upgrader at Scotford (near Edmonton)
Satellite	Mine and extraction satellites nearby Remote In situ	Large satellite contains mine, extraction, tailings	Expanding on site
Start-up production	45,000 bbl SCO/day	105,000 bbl SCO/day	150,000 bbl SCO/day
Current production	260,000 bbl SCO/day	300,000 bbl SCO/day	150,000 bbl SCO/day
Planned production	500,000 bbl SCO/day in 2010-2012	500,000 bbl/day	500,000 bbl/day
Extraction process	Hot water Use NaOH dispersant	Hot water Use NaOH dispersant	Hot water Originally no dispersant. Now use Na Citrate. Thickener for heat recovery.
Extraction efficiency %	92%	90.7%	80% (after asphaltene loss)
Upgrading yield	84%	87.5%	100%
Coke production	2 million tonnes/year	2.5 million tones/year	Asphaltenes rejected and added to tailings
Tailings	Conventional MFT followed by CT	Conventional MFT followed by CT	Produce thickened tails. Less MFT because not using dispersant.
Green house Gas Tonnes / m3 SCO	0.6	0.85	NA
VOC emission (kg/m3)	1.73	NA	NA
Naphtha loss	NA	.0043 bbl/bbl	NA
Energy use GJ/m3 SCO	7.4	8.1	NA
Water import m3/m3	2.4	2.03	NA
Water recycle %	N/A	88%	NA
Cumulative disturbance hectares	13,093	21,282	NA
Cumulative area reclaimed	949	4,668	NA
Reclamation certificate ha	0	104	0

Table 2. Land use at the Syncrude Mildred Lake Facility (Base Plant)

Land use/area	Ha	%
Plant site related	550	3%
Mining		
Open pit space	4,250	25%
Overburden waste dumps	1,100	6%
Tailings ponds and related	6,400	38%
Miscellaneous	4,700	28%
Total disturbed area	17,000	100%

TAILINGS

Overview

Tailings are the waste products from processing oil sand ore. On the path from ore to waste the ore is crushed, and then slurried in warm water, and pumped to extraction. On the way, transport conditions the slurry. It breaks it into individual components so they can be separated in extraction.

In the extraction plant, the first vessel contains still water. In that environment, sand settles out and is sent to tailings. Air bubbles attach themselves to bitumen droplets and float them to the top of the vessel. There the bitumen is skimmed off as froth. The remaining slurry is processed to extract bitumen. The froth is cleaned to remove solid and water.

Eventually, all waste components are blended and pumped to the tailings disposal site. The slurry is about two parts water to one part sand. Effluent from a 100,000 barrel per day plant is about 200 cubic metres of slurry per minute.

At the disposal site, the slurry is discharged onto the ground surface. Sand accumulates.

The rest fills voids in the sand or flows to the pond. Three sand deposits form:

1. Broad construction cells are used to trap sand for construction of dykes. The deposit is compacted by dozers to give it stability.
2. Sand that is surplus to construction is discharged onto a beach above water. The slurry flows over the beach depositing, eroding and re depositing sand with captured material in the voids.
3. Sand slurry that reaches the pond deposits on a beach below water. Conditions are quiet there so a loose deposit forms.

Almost one third of the sand deposit is void space. It is filled with water and suspended material. The rest flows into the pond. Material that reaches the pond is water, silt, clay, unrecovered bitumen, and process aids.

In the pond, the suspended fines slowly settle until they reach a density of about 30% solids. Repulsive forces between clay particles halt further settling. The weak deposit at that stage is called mature fine tails or MFT.

Clear water collects on the surface of the pond and is available for recycle to the plant. In that sense the tailings pond acts as a water clarification vessel. It is an extension of the extraction plant.

It takes a few years for the water to clarify and for MFT to form.

Historic records from Syncrude suggest that, on average, 0.266 cubic metres of MFT are created for every cubic metre of ore processed.

Processes To Densify MFT

Figure 6.8 shows the relative volumes of mineral solids and water in fluid tailings of different densities. The range varies from 24 parts water to one part solid at the top of the chart to 1:1 at the bottom. The Figure also shows the dominant behaviour. At the top of the chart, the material behaves as a fluid. At the bottom, it behaves as a solid. There is a transition zone in the middle. That is where MFT is shown.

Mechanical Processes to Densify Fines

The right side of Figure 6.8 shows manufactured processes that can be used to

densify tailings. They encompass settling, filter belts, thickeners, centrifuges and filter presses. Centrifuges apply the most energy (a few thousand times the force of gravity) so achieve the highest densities – between 50 and 60% clay. Filter presses are capable of higher densities but their production capacity is small.

Natural Processes to Densify Fines

The left side of Figure 6.8 shows natural processes. They start with sedimentation and then progress to suction based processes that are very powerful.

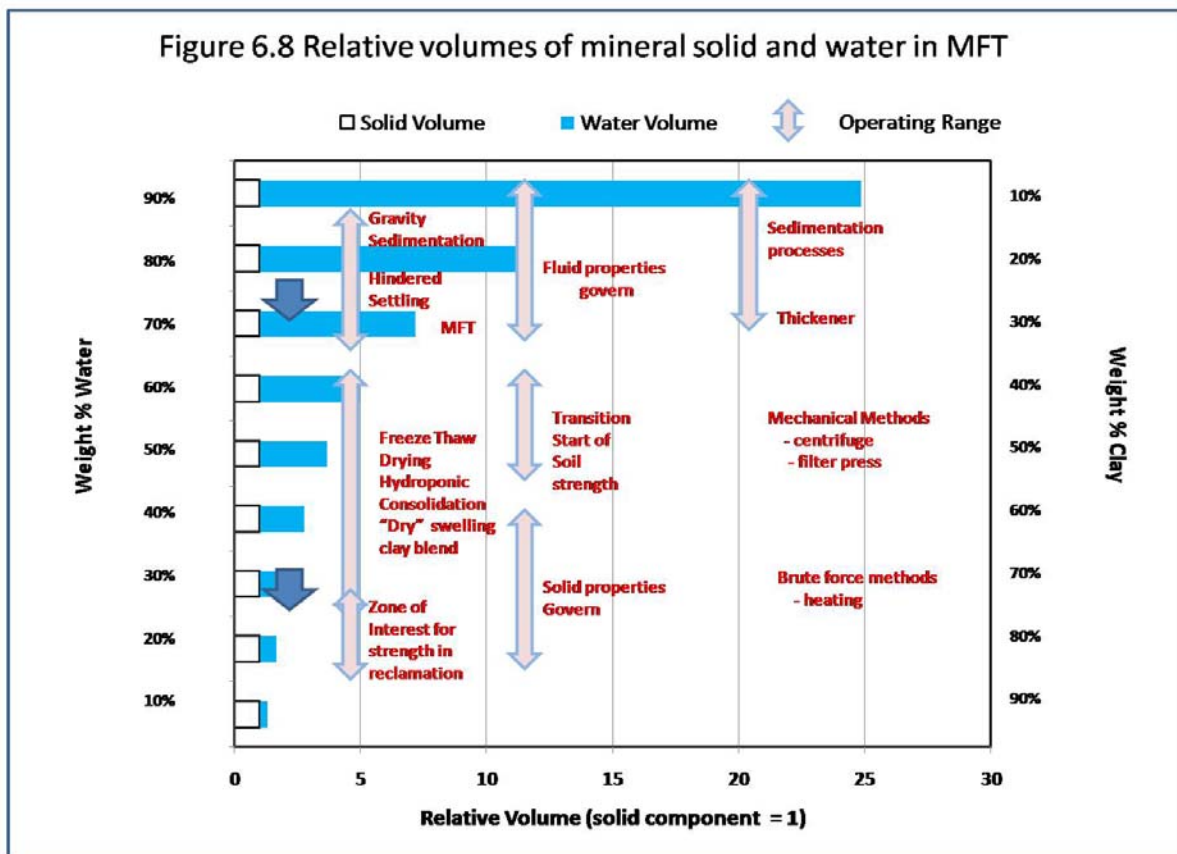


Figure 1. Densification Measures

The suction based processes: drying, hydroponics and freeze/thaw, and adding “dry” swelling clay are able to exert suction as high as 10 atmospheres. That is enough to collapse the soil to very high density. The first three suction based processes are limited to surface activity so can only process a thin layer at a time. The exception is the bending with swelling clay. It can act in thick layers and continues working if buried.

Natural Consolidation

Natural consolidation densifies all natural material below the water table. It is not likely to help tailings because the deposits are placed with a geometry that will take a long, long time to respond. Processes that can accelerate consolidation by shortening the drainage path include drainage wicks and bubble paths noted in the next paragraph.

Bacterial Action

Bacterial action consumes solvent in the MFT and releases gas bubbles that shorten the drainage path from 10's of metres to centimetres. That is speeding up consolidation in some areas.

Devices to De-Water Sand

If clay and sand will be blended, it is important that the sand be well drained. Processes that dewater sand include hydrocyclones – capable of yielding a sand density of 72% solids.

NON-SEGREGATING TAILINGS NST

Another approach to densify fines involves mixing it with sand to form non-segregating tailings or NST.

A great place to store fines is in the void space in sand. However, too much fines can alter the behaviour of sand. If too much is hidden in the voids, the fines will dominate sand strength.

Processes in Use

CT technology

Composite Tailings or CT is an ingenious approach to solidifying fluid tailings. Blending mature fine tails with a coagulant (gypsum) and three to six parts sand creates a non-segregating mix. The mix can be pumped to the disposal site and deposited. In place, the mix consolidates and develops strength from touching sand grains. The time required to gain strength depends on the mix. CT made with four parts sand to one of MFT will take 10 years to develop strength. If the mix is five parts sand to one of MFT, consolidation might be accomplished in 5 years.

The CT process replaces one volume of unstable material with two, and must be contained like fluid tailings until it consolidates and develops strength. CT shrinks more than 40% as it consolidates.

CT processing is only a partial solution because there is insufficient sand to treat all fluid tailings. That is especially true in areas where stranded stockpiles of fluid tailings exist (Syncrude and Suncor base plants.)

Cyclones and Thickener Technology

Cyclones are excellent devices for separating particles according to their size. They work well on sand but are not very effective on fines. Cyclones can achieve an underflow density of about 70% - a product that is too dense to pump.

Thickeners are large circular vessels that concentrate and dewater silt and clay. The fine-grained stream is diluted, one or more flocculating agents added and the mix allowed to settle. Stirring rakes often provide drainage pathways that speed drainage. Thickeners can achieve an underflow density of 25% to 30% by weight solid. The same density is achieved naturally in a tailings pond. Some manufacturers claim a density of 50%. They may have discovered a super flocculating agent but we suspect that the higher density is due to sand. At low sand to fines ratios, sand adds to volume and density, but has no effect on strength (Devenny 2009)...

A main advantage of thickeners is they recover process water and the heat contained in it. Otherwise, hot process water is discharged to the tailings pond.

The logical place to use a thickener is in a stand-alone plant that must make its own heat. Plants that have a nearby upgrader often have access to an abundant source of low cost heat.

Thickener/Cyclone/Centrifuge technology

Centrifuges can increase the density of fine-grained material to 50 and possibly 60 weight percent solids. They were reviewed in depth in the current study.

Centrifuges are not high capacity machines so production volumes are met by adding more units.

It is difficult to scale up from pilot work that employs small centrifuges. Small units are able to generate higher “G” forces, so may achieve higher densities than the large units can.

Sand accelerates wear on centrifuges. Consequently, planners should seek allocations where sand is less likely to

contaminate feed. Most plant locations will experience sand surges at some time. MFT extracted from the centre of a tailings pond is most likely to be sand free. That suggests the ideal use of centrifuges may be in stand-alone facilities near a tailings pond.

The current study gathered public domain information on tailings technologies from many sources. The focus was as follows:

- Base case project making MFT – Syncrude,
- Converting to CT – Syncrude,
- Cyclone thickener to make paste – Joslyn North Mine Project,
- Thickener Centrifuge technology to make solid cake – the RTR Gulf pilot.

A generic base was developed so new projects could be developed for each technology. That was undertaken to facilitate comparison. Then differences in behaviour would be due to the process, not quirks of site differences such as the grade of ore, fines content, or the overburden thickness.

Six technology cases developed were as follows:

1. Base case – similar to the start of Syncrude,
2. Thickener without cyclone,
3. Thickener with cyclones,
4. CT option processing MFT from external sources,
5. CT option processing thickened fine tails from within the plant,
6. Centrifuge option yielding “solid waste”. The plant also used cyclones to dewater sand and a thickener to prepare feed for the centrifuge.

Detailed work sheets were developed for each technology. The data assembled vs. time includes:

- Capital equipment required for the particular technology,
- Ore and waste handling,
- Earthwork associated with starter tailings ponds and in-pit dykes,
- Environmental liabilities incurred such as land disturbed, fluid tailings etc.
- The operating cost of each of the above,
- NPV of costs for each technology and for each major activity.

A tailings forecast model was developed and then used to illustrate the effect of process or handling conditions on the behaviour of tailings. The model allows user input so is an excellent learning tool. Highlights of trends noted from the model study include:

- Solid sand forms 75% of the tailings deposits. It has relatively predictable volumetrics.
- Void space in the sand is quite large. The void volume is similar to the volume of fluid tailings.
- When the sand deposit forms, water and fine grained material is captured in the sand voids.
- Fluid and suspended fines surplus to those needs, overboard to the pond.
- The model assumed the volume of MFT formed in the pond would be equal to the Syncrude historic average of 0.266 cubic metres per cubic metre of ore.
- Water that is surplus to making MFT is available for recycle to the plant.

An economic model was developed that would allow a realistic evaluation of the performance of the different technologies. Oil sand projects are highly taxed. Between 45% and 55% of profits flow to governments. However, in a reverse fashion 45% to 55% of expenditures are borne by governments. The model was built to generate this type of fiscal sharing.

Traditional economic models when applied to long periods of time discount future obligations. That is a major problem for oil sand projects that can operate for 100 years. That aspect was overcome by recognizing and booking liabilities as they are created. The vehicle for booking environmental liabilities was to assume that funds equal in value to the environmental liability were deposited to a Qualifying Environmental Trust at the time the liability was created. (Devenny and Nelson 2009).

CONCLUSIONS

The study methodology provided a credible appraisal of tailings technologies.

The simple Base Case technology, of stockpiling fluid tailings, prevents reclamation and preparation for closure. Other technology must be introduced to prepare the project for closure.

Thickener based technology is similar to the Base Case technology. The waste product is still fluid tailings that accumulates and prevents reclamation.

CT Technology offers promise for reclamation and closure. CT treatment creates slurry that can be pumped to the waste disposal site. There the slurry consolidates to

a solid reclaimable material. However, CT technology has limitations that should be recognized:

- The success of CT technology is still being evaluated.
- There is not enough sand to treat all MFT deposits with the CT process. Another approach is needed to deal with the rest of the MFT.
- The CT slurry is a fluid that requires containment. Construction of fluid retaining structures is expensive – especially when compared to technologies that do not need them.
- Steps to maximize sand for CT treatment cause projects to use other materials to build fluid retaining structures. There is a cost associated with that substitution.
- CT processing is not the system to treat stranded deposits of MFT, where mining operations with associated sand streams, are winding down or are concluded.

The appraisal concludes that centrifuge treatment looks promising. It creates a fine-grained cake that is approaching a solid consistency. It also produces a separate sand stream that should be able to contain the cake. Both the Bitmin and RTR/Gulf pilot projects produced wet but stackable waste.

The centrifuge option involves more equipment, and has high capital and operating costs. However, it used the least amount of water. It also had the lowest unit cost of the tailings technologies studied. Savings come from the fact that water-retaining structures are not needed, and less heat is lost to tailings.

Centrifuge based technology has not been demonstrated at a large scale on MFT materials. Large scale tests, using the largest centrifuges available are needed because scale-up from smaller machines is problematic.

The Dry Tailings option also looks promising. It was designed to operate as an independent operation to convert MFT to cake strong enough for reclamation. If the water content of the centrifuge cake is not low enough it can be lowered further by adding “dry” swelling clay.

Figure 2 provides a generalized cost comparison of the different tailings technologies examined in this study.

Full life cycle evaluations need to include environmental obligations in the analysis. This study assumed that funds are placed in an environmental trust as soon as reclamation obligations were incurred. That offsets the trend of traditional economic analysis that applies discounts over long periods of time to discount the value of future obligations. It also helps to recognize technologies that facilitate reclamation.

RECOMMENDATIONS

- 1 Undertake an independent review to verify the procedures and conclusions of this report. Confirm:
 - a. That the approach followed was reasonable and effective.
 - b. That the closure plans and indicated costs are directionally correct.
 - c. The potential of the centrifuge option.
- 2 Undertake research to build confidence in the centrifuge solid waste option including confirmation that:

Figure 8 Cost comparison of Different Tailings Technologies

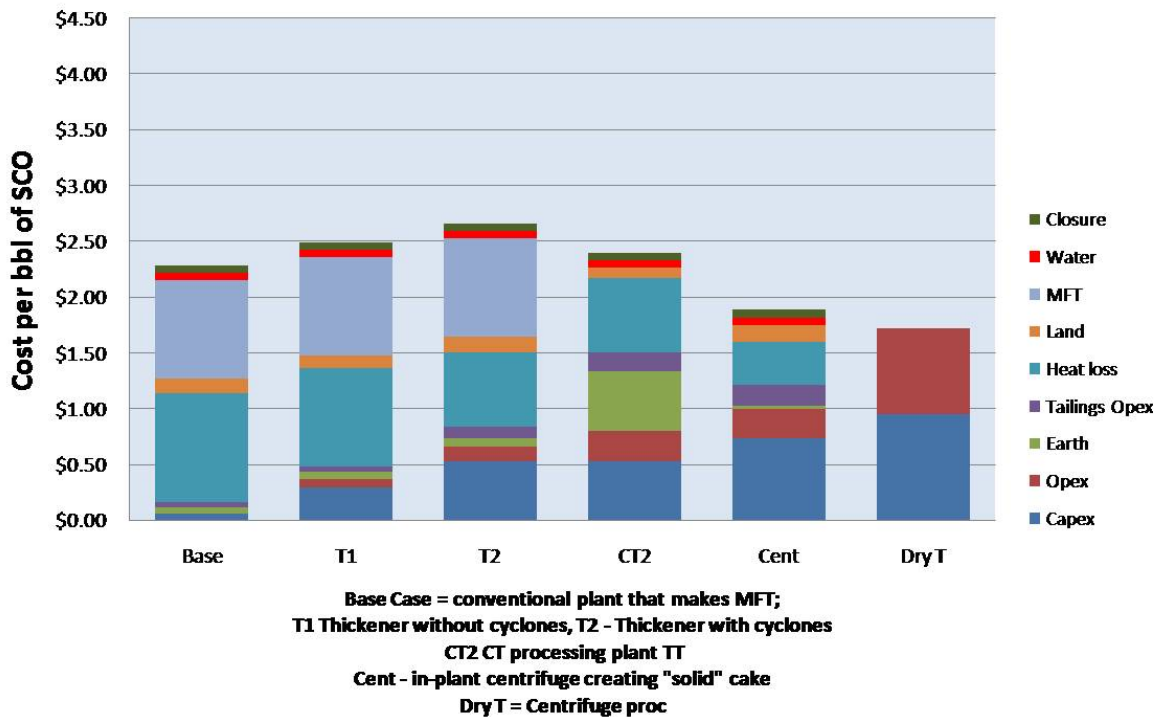


Figure 2. Cost Comparison of Different Tailings Technologies

- the target strength for soil in the closure landscape is 10 kPa or more.
- That large centrifuges can dewater MFT to a consistency suitable for reclamation – especially if deposited with the abundant sand that centrifuging makes available.
- That cyclone sand will drain in a reasonably short period of time.
- That centrifuge cake can be permanently stored in the cyclone sand as proposed.
- If a method cannot be found to reclaim centrifuge cake with all that sand, confirm that it is feasible to blend it with swelling clay to achieve the desired solid content.

REFERENCES

Devenny, D. 2009. A Screening Study of Oil Sand Tailings Technologies and P – a report prepared for the Alberta Energy Research Institute.

Fair, A. 2008. The Past, Present and Future of Tailings at Syncrude. A presentation at *International Oil Sands Tailings Conference, Edmonton, Alberta.*

Houlihan R., Haneef, M. 2008. Oil Sands Tailings: Regulatory Perspective. In *Oil Sands Tailings Conference, Edmonton, Alberta.*

ECONOMIC SCREENING OF TAILINGS OPTIONS FOR OIL SANDS PLANTS

David Devenny P Eng P Geol

The Rock Doctor, Calgary, AB

Richard Nelson

Program Director, Alberta Energy Research Institute, Edmonton, AB

ABSTRACT: This paper explores options for economic screening of reclamation options for a mineable oil sand project. The topic is important because incorrect economic screening methods lead to poor decisions about reclamation.

Traditional economic evaluations apply discounts to the project cash flow. Discounting over the long periods of time involved in oil sand projects distorts future values. Long term discounting significantly diminishes the value of reclamation obligations. This favours deferring reclamation and diminishes the incentive to prove the viability of reclamation plans.

An alternative approach recognizes reclamation obligations as they are created and places funds to pay for them in a qualifying environmental trust. This approach is preferred because it overcomes the negative effects of long term discounting.

Examples illustrate the effect of each approach.

INTRODUCTION

This paper is about economic analysis used to screen tailings options for a mineable oil sand plant.

The paper reviews characteristics of oil sands projects, economic screening tools, and how they interact. Then it shows, through examples, how the outcome is affected by the economic screening tools.

The recommended approach yields conclusions that are very different from current approaches to tailings technology.

HOW WE SCREEN OPTIONS

Steps in screening tailings technologies are outlined in Table 1.

Table 1 Typical steps to screen technology options.

1. Establish goals for the project.
2. Identify candidate options that will achieve those goals.
3. For each option:
 - a. Identify plans to use the option through development, operations and closure.
 - b. Identify full life-cycle capital and operating costs associated with the above.
 - c. Conduct an economic assessment.
 - d. Appraise the probability of success.
4. Choose the option that will most economically meet project goals.

Projects spend considerable effort exploring the viability of different technologies and the probable cost vs. time. Equivalent effort should consider the economic evaluation process because it can have a major effect on the outcome of screening studies.

CHARACTERISTICS OF OIL SAND PROJECTS

Mineable oil sand projects have unique characteristics that affect the appropriate approach to economic screening. Table 2 summarizes some important characteristics of oil sand projects. Table 3 shows the timeline for site use

Information in Figure 1 was derived from Fair, 2008, Syncrude 2006 and Syncrude 2007. It shows that reclamation of tailings and disturbed lands can be delayed by 20 or 30 years. It also shows why closure activities can be delayed by up to 100 years.

Table 2 Characteristics of mineable Oil Sand Projects

- Large size,
- Long project life (up to 100 years),
- Large reclamation liabilities linked to production:
 - Land disturbance,
 - Fluid tailings,
 - Closure costs.
- Long time between when a reclamation liability is created and when it is dealt with:
 - Fluid tailings – currently 25 to 40+ years,
 - Land reclamation – currently 30 to 40+ years,
 - Closure activities - 50 to 100 years.
- After pay-out, between 45% and 55% of profits is directed to fiscal terms,
- A high project rate of return is needed to justify investment.

Table 3 Typical time line for site use

<u>Year</u>	<u>Land use</u>
0 – 2	Site preparation
2-20	Open pit mine
20-30	Site occupied by tailings pond
30-40	Solidify tailings
40-50	Reclaim surface
100	Site closure

RESULTS OF SCREENING STUDY OF TAILINGS OPTIONS

A recent study of oil sand tailings technologies provides a database that can be used to illustrate the effect of economic evaluations. (Devenny 2009, Nelson and Devenny 2009)

Table 4 lists the tailings options studied. Table 5 lists steps followed in the study.

Table 4. Tailings options studied

1. Conventional tailings that produces fluid tailings.
2. As above but with a thickener added to indicate the advantage of recovering process water from the fines waste stream.
3. As above but with cyclones to recover water from the sand waste stream.
4. Use of CT technology to convert some of the fluid tailings to “solid” waste.
5. A centrifuge case that creates “solid” waste

Table 5 Steps involved in the study of tailings options

1. Project goal :
 - a. Reclaim tailings as a solid landscape.
 - b. Qualify for a reclamation certificate within a few decades after operations cease.
2. A generic oil sand project was developed to provide a base for comparison studies.
3. A project was developed for each tailings option.
4. Development plans were prepared to identify activities over the full life cycle of each project – from development, through operations, and closure.
5. Differences between the cases were identified along with associated costs.
6. Identified cost vs. time for the differences between tailings options.
7. Economic evaluation of the cost differences vs. time.

The goal of qualifying for a reclamation certificate is not new. The timing could be new.

Developers have proposed to store fluid tailings remaining at the end of their project below an end -pit -lake. That technology is unproven and has not been formally accepted by the regulators. Regulators have favoured reclamation as a solid landscape for the past decade or more. Last year that preference became a directive that requires part of the fine-grained tailings be solidified to a specified strength each year. (Houlihan and Haneef, 2008).

CHARACTERISTICS OF ECONOMIC EVALUATIONS

Economic evaluations appraise the cash flow over the life of a project. They convert future expenditures to today by applying discounts. All economic evaluations apply some form of discounting to future income or expenditures to convert them to present value.

Figure 1 shows the effect of discounting to determine the present value of future obligations. The plot shows a rapid drop in value with time. The rate of loss is greatest when high discount rates such as 20% or 30% are used. They reduce the value to near zero in 20 to 30 years.

Traditional economic evaluation of tailings options would combine the trends of Figure 1 (effect of high discount rates) with the trends of Table 3 (long time spans). The combination significantly reduces or eliminates future expenditure obligations. That means that decisions about the suitability of tailings options will be made without consideration of future expenditure obligations.

Table 6 lists three methods used to appraise cost vs. time data from the tailings screening study.

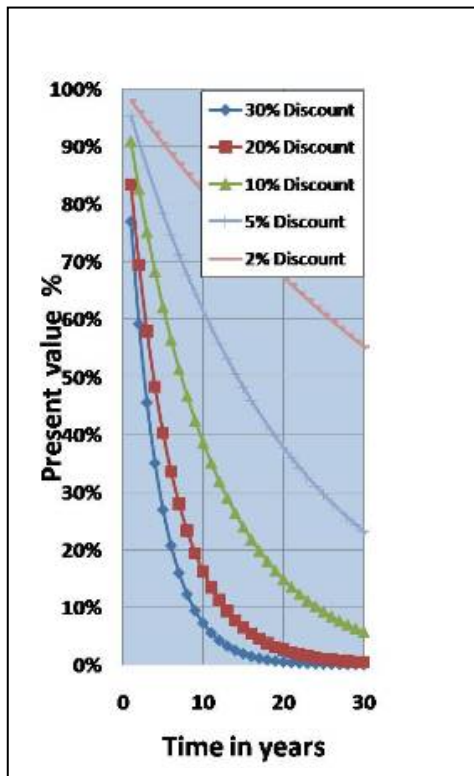


Figure 1 Effect of time and discount rate on the value of future obligations

Table 6 Three economic screening methods used to evaluate oil sand tailings options.

1. Compare the net present value of cost differences vs. time for each option.
2. Compare the net present value of cost differences vs. time considering:
 - a. Cost vs. time as in Case 1 above.
 - b. Recognize the value of reclamation obligations as they are created.
 - c. Deposit an amount equivalent to the reclamation liability as it is created to a Qualifying Environmental Trust.
 - d. Treat deposits to the Trust as operating expenses.
 - e. Funds are deposited in the Trust as reclamation liabilities are created and withdrawn as the liabilities are reclaimed.
3. Finally, leading contenders are compared in a project economic model that duplicates the

project financial environment. The model considers all applicable fiscal terms such as Alberta royalty, capital cost allowances and income tax.

Cost differences are entered in the model while other project parameters are held constant. The preferred tailings option is the one that yields the best rate of return to the developer.

RESULTS

Figure 2 shows the NPV₁₀ of differences in component costs spent over the life of each tailings option. Projects to the left are simple facilities. Projects to the right are more complex and involve higher capital and operating costs. Figure 2 favours the base case on the extreme left. Unfortunately, it is an incomplete process. Other technology will have to be added to solidify fluid tailings.

Figure 3 is Figure 2 with the NPV₁₀ of funds donated to a Trust to recognize reclamation liabilities as they were created. The reclamation obligations were linked to production. Reclamation costs per barrel of production included \$0.06 for land disturbance, \$1.25 to solidify fluid tailings and \$0.20 to fund closure.

Figure 3 favours the high capital, high operating cost technologies – the opposite of what Figure 2 favoured.

Explanations for cost components for earthwork and heat loss are in order.

Earthwork relates to higher costs associated with building tailings retention facilities using mine waste instead of sand. The sand is being saved for CT treatment of fines.

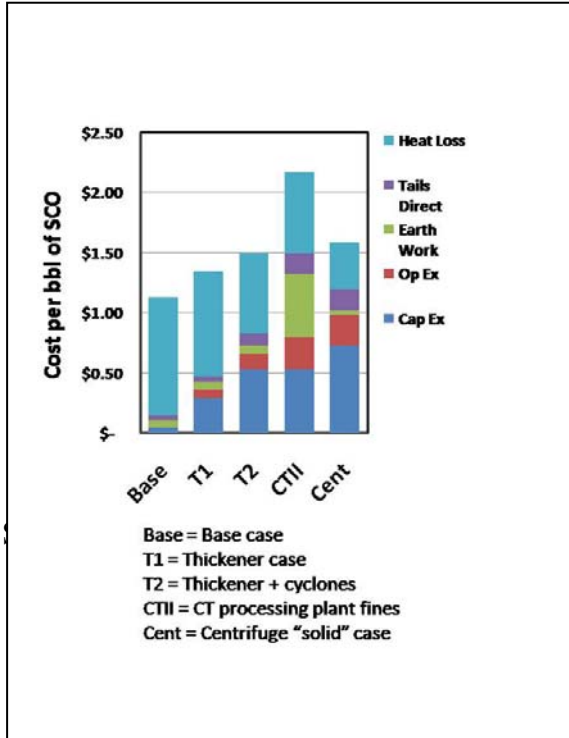


Figure 2. Traditional analysis of tailings options based on cash flow analysis.

Heat loss identifies the heat discharged to the tailings pond. The base case wastes the most heat because it discharges the most hot water to the tailings pond. Some developers claim that heat is not important to them because they have surplus heat from the on-site upgrader. The heat component was left in the figure because it is a significant cost component, it varies widely from technology to technology, it is a measure of project efficiency, and it relates to CO₂ emissions.

Figure 2 represents the traditional approach to economic evaluation of tailings options. Results are skewed by discounting that removes future liabilities from the evaluation. Reclamation obligations removed by discounting are not trivial. For a 100,000 barrel per day plant, they represent over one billion dollars that must be restored at a future date.

Figure 3 shows the effect of recognizing environmental liabilities as they are created. Favoured technologies are the opposite of those favoured by traditional screening methods.

Table 7 compares performance of the centrifuge option with the CT tailings option when evaluated in the project economic model. The result favours the centrifuge case. The small impact on the rate of return indicates that tailings costs only represent a small portion of project economics.

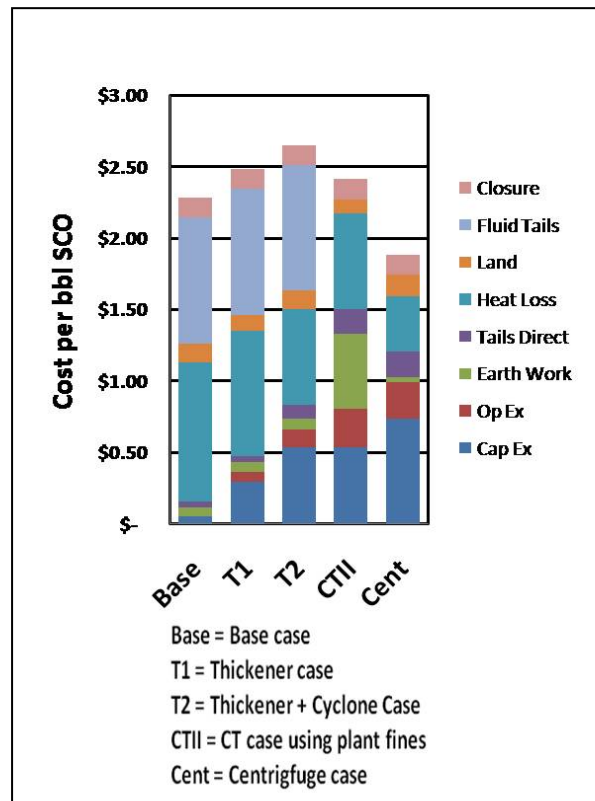


Figure 3. Evaluation of tailings options recognizing liabilities as they are created.

Table 6 Three economic screening methods applied to evaluate oil sand tailings options.

1. Compare the net present value of the cost vs. time for each option.
2. Compare the net present value of cost vs. time considering;
 - a. Cost vs. time as in case 1.
 - b. Recognize the value of reclamation obligations as they are created.
 - c. Deposit an amount equivalent to the reclamation liability as it is created to a Qualifying Environmental Trust.
 - d. Recognize deposits made to the Trust as operating expenses.
 - e. Funds are placed in the Trust as reclamation liabilities are created and withdrawn as the liabilities are reclaimed.
3. Finally leading contenders are compared in a project economic model duplicates the project financial environment. The project model considers all applicable fiscal terms such as Alberta Royalty, capital cost allowances, and income tax. Cost differences vs. time are entered in the economic model while other project parameters are held constant. The preferred tailings option is the one that yields the best project rate of return.

Table 7. Results of economic analysis using the integrated project economic model

Technology	Developer's Return
Centrifuge case	11.03%
CT case	10.89%

DISCUSSION

Relevance of cash flow models

In oil sand practice, many years can separate the time when a reclamation liability is created and the time when reclamation occurs. As a result cash flow vs. time representing expenditures on reclamation activities will have gaps in it that may be decades long.

Representing a project by actual expenditures vs. time can be misleading because it does not recognize reclamation liabilities that adversely affect the project asset value as soon as they are created. If the project is sold, the new buyer will reduce the asset value by the extent of outstanding reclamation liabilities.

Evaluating future reclamation costs

The suggested approach to identifying future reclamation costs is:

- The cost of undertaking reclamation now,
- Using existing proven technology,
- At today's costs.

If the technology is unproven, or if there are uncertainties about the technology or reclamation cost, a risk premium should be added to the cost.

Economic Evaluation

Economic evaluation involves putting today's value on a series of future expenditures or incomes. All models involve some form of discounting. The appraisals are skewed when applied to long periods of time because discounting reduces or removes the future obligations.

What discount factor is appropriate?

The final economic screening tool is the project economic model that duplicates the financial environment that the project must live with. It is run to determine the return to the developer considering all fiscal terms. However, to finance the fiscal terms, the project must make a superior return before fiscal terms are considered. That superior rate of return (probably a minimum of 20%) is the factor that the project economic model uses.

Compounding evaluation problems

The combination of discounting and long times characteristic of oil sand reclamation, removes future reclamation liabilities from the evaluation. That removes the very factors that the screening study is intended to address.

Figure 2 illustrates the effect of traditional economic analysis. It favours tailings options that will not qualify for closure unless fluid tailings are an acceptable end product. The risk of the outcome is not appraised because discounting minimizes the value of events in the distant future.

The impact of traditional economic appraisal of oil sand tailings options

Traditional economic analyses applied to cash flow vs. time on oil sand projects:

- Reduce or eliminate the value of future reclamation obligations.
- Set a low value for future reclamation obligations.
- Set a low value on the risk that current plans may not work.
- Favour deferral of reclamation activities.
- Favour technology options that defer reclamation activities.

- Discourage progressive reclamation.
- Discourage improving technology.
- Discourage research to prove/improve technology.
- Transfers reclamation cost to future generations.
- Favours action that is contrary to public and regulatory expectations.

Recognizing reclamation liabilities as they occur

The current study recognizes reclamation liabilities as they are created by depositing equivalent funds in an environmental trust. That process duplicates the reality that the reclamation liability affects asset values as soon as the liability is created.

Figure 3 shows the merits of the different tailings options. It favours the solid waste case that appeared to be too expensive in Figure 2.

The impact of economic appraisal that recognizes reclamation liabilities as incurred

- Retains the value of future obligations.
- Favour :
 - Options that lead to acceptable and timely closure.
 - Proving the viability of closure plans.
 - Improving technology.
 - Research to verify and improve closure plans.
 - Progressive reclamation.
- Actions that regulators expect a responsible developer to undertake.

CONCLUSIONS

Long time spans between the time reclamation obligations are created and corrected are a characteristic of oil sand projects. Long periods coupled with high discount factors cause future liabilities to disappear. The economic analysis removes the feature that the screening study of tailings options was undertaken to address.

Traditional economic analyses provide misleading results when used to screen tailings options for an oil sand project. They also suppress initiatives that address closure.

Economic analysis that recognize reclamation liabilities as they are created:

- overcome the adverse effects of discounting over long periods of time.
- Yield results that are more credible.
- Provides a business outlook that is more in line with expectations of the public and of the regulators.

Tailings options favoured by the recommended approach differ from traditional favourites. The appraisal showed merits for a solid waste centrifuge case that is ranked poorly by traditional evaluations.

RECOMMENDATIONS

Screening studies of tailings options should use economic evaluation techniques that recognize reclamation liabilities as they are created.

REFERENCES

Devenny D. 2009. A Screening Study of Oil Sand Tailings Technologies and Practice – a report prepared for the Alberta Energy Research Institute

Fair A. 2008. The Past, Present and Future of Tailings at Syncrude. A presentation at *International Oil Sands Tailings Conference, Edmonton, Alberta, Canada.*

Houlihan R., Haneef M, 2008. Oil Sands Tailings: Regulatory Perspective. In *International Oil Sands Tailings Conference, Edmonton, Alberta, Canada.*

Nelson, R., Devenny, D. 2009. Screening Study of Oil Sand Tailings Technologies and Practices, in *Tailings and Mine Waste 09 Conference, Banff, Alberta.*

Syncrude 2007. Syncrude Sustainability Report, 2007

Syncrude 2006. Syncrude C&R Plan 2006, Submitted to Alberta Environment as part of Syncrude's Renewal Application for their operating licenses

A ROBOTIC SYSTEM TO CHARACTERIZE SOFT TAILINGS DEPOSITS

M.G. Lipsett & S.C. Dwyer

Department of Mechanical Engineering, University of Alberta, Edmonton AB Canada

ABSTRACT: Soft soil conditions are challenging for vehicles, including earthmoving machinery. Tailings from mining operations are often difficult to cover with reclamation material such as sand and topsoil. Reclaiming soft tailings is a priority for oil sands operations, to reduce the environmental footprint associated with large impoundments. The deposits have variable soil strength, which is a challenge for navigation and may present a hazard to workers. This paper describes the development of a small-scale demonstration prototype system for navigation in very soft terrain to characterize surface soil strength, with error recovery for slippage and sinking.

INTRODUCTION

The Need for Soft Tailings Characterization

Oil sands processes produce a significant amount of tailings, and much of it is fine silt and clay that densifies very slowly. Although there has been progress on densifying soft tailings through chemical amendments (Caughill, Morgenstern & Scott 1993), there is as yet no demonstrated method to cap the tailings with reclamation material. The tailings deposit can have uneven strength, and so conventional equipment often gets stuck or even sinks, which puts operators at risk.

Some types of mobile equipment has been designed to have low ground contact pressures for driving over soft ground. This equipment may offer insights into how to design equipment for capping soft material, such as hydrocyclone sand stackers fed by flexible slurry lines; however, this equipment

requires a certain minimum bearing strength, which must be assessed prior to deploying equipment onto a deposit. This work proposes autonomous robotic equipment for characterizing soft tails capping where there is insufficient shear strength for conventional trucking of capping material, and describes a laboratory-scale demonstration prototype with on-board sensing and a payload to test subsurface shear strength and to take samples for analysis.

Current State of Technology

Tailings from oil sands extraction plants are hydraulically deposited into impoundments, which are sand dykes containing water and fine solids (clays and fine sand) in a loose sediment typically of not more than 30 wt% solids (Morgenstern & Scott 1983). After the sand settles on the tailings beach and the fines are carried into the pond, the dykes are constructed from the sand beaches using bulldozers to flatten the sand. Navigation is

problematic because the pore pressure and strength of the sand is highly variable and prone to liquefaction in some situations. Sinkholes can suddenly appear. Equipment is prone to getting stuck. This presents a risk to workers, and also potential loss of equipment.

The fine tailings do not readily densify, although in some locations natural consolidation may occur to up to 70 wt % solids, which has considerable strength. Generally, however, engineered tailings are formed of fine material mixed with gypsum (or another coagulant) and then mixed with sand to form a self-dewatering composite tailings (CT) deposit. Tailings with flocculants added form thickened tailings (TT).

Although CT and TT will densify over time, the depositional characteristics are variable and the amount of shear strength is often too low to support earthmoving equipment to cap the deposit with sand and topsoil. Dynamic loading conditions can produce positive pore pressure and liquefaction failure of the soil. On conventional tailings beaches, such failures can occur even in winter, when all the ground surface should be frozen.

Hydraulic transport has potential to deliver capping material onto soft tailings. There are three challenges. 1) The capping material must be laid down in such a manner as to maintain the integrity of the existing soil: kinetic energy must be dissipated to prevent erosion. 2) Capping material must deliver a predictable level of post-depositional strength: material must not be so watery that it remains liquefied. 3) The equipment delivering the material must be designed to move over the entire soft tailings deposit: low-ground-pressure equipment and gentle piping moves are necessary (and the material must be transported without bogging pipelines if there is a process upset).

Sand stacking has been demonstrated as a method for depositing material hydraulically for dyke construction. Stacking entails pumping a sand slurry to a hydrocyclone on an elevated portable boom; most of the water is recycled and wet sand drops out of the hydrocyclone onto the ground. Thus stacking may be a method for placing reclamation material with sufficient shear strength to be trafficable for earthmoving and hauling equipment to lay down successive lifts of other materials, such as topsoil, provided that there is a sufficient liquid fraction to maintain negative pore pressure. Stacking equipment will have to meet low ground pressure specifications.

Field robotic systems have been developed for excavation and other earthmoving activities, and have been demonstrated in mining operations (Singh 1997). Navigation on very soft terrain remains a challenge.

All of these technologies have a common theme: they depend on a good understanding of soft tailings properties and post-deposition soil properties. At present, surveys of densification and consolidation of soft tailings deposits (such as composite tailings or thickened tailings) are done by manual sampling and geotechnical instruments such as penetrometers. These methods are labour-intensive, slow, expensive, and can be hazardous to workers; and the characteristics of samples can be affected by handling transportation after collection.

Ideally, classification of soft soil would occur at a distance, so that surveyors can avoid trouble spots. Non-contact methods would allow for fast mapping of surface properties, although direct estimation of soil shear strength has not been demonstrated on soft tailings using non-contact techniques. A number of methods have been proposed for soil characterization and strength estimation

with a focus on key parameters (Viscarra & McBratney 1998), as enumerated in Table 1.

Non-contact sensors are likely to be more practical to implement on a mobile platform. Near infra-red (NIR) sensors appear to have both the sensitivity and flexibility to measure a variety of characteristics, and warrants continued investigation. The sensors with limited practicality are also invasive, and thus do not provide effective pre-emptive hazard warning for vehicles taking surveys. Contact-based sensors such as penetrometers will likely be required for soil strength measurements, both at the surface and subsurface (as there is currently no validated noncontact method for soil strength estimation); and these measurements will be

useful to provide a method of updating system soil map with accurate information at a limited number of locations.

A promising recent technique is hyperspectral image analysis for classifying different soil types and particle size (Rivard, Feng, Lyder, Gallie & Cloutis 2007). This method is an extension of conventional NIR reflectometry. Additional work is required to evaluate different soil characterization and classification techniques for real-time control applications on equipment in tailings service, starting with building soil surface maps for characterizing the variability of deposits and for navigation.

Table 1. Potential Soil Characterization Methods.

Soil Property	Sensor Type	Practicality
Water Content	Near Infra-red (NIR)	Good
	Ground Penetrating Radar	Good
	Microwave Reflectance	Good
	Electrical Resistance	Limited
	Capacitance	Limited
Clay Content	NIR	Good
Organic Matter	NIR	Good
	660nm Single Wavelength	Good
Strength	Penetrometer	Limited

This work presents a system concept for characterizing and mapping a soft tailings

deposit, and a proof-of-concept prototype to demonstrate the feasibility of robotic control of such a system.

SYSTEM DESCRIPTION

Overview

A small microprocessor-controlled vehicle has been modified to navigate on soft terrain and execute imaging and sampling tasks. Wireless links to a ground control station enable system monitoring and control. A hierarchical control system is used, with microcontrollers executing low-level sensing and actuation, and an on-board 2.13 GHz Intel-based microcomputer (MacMini) handling most path planning and sensor processing. The block diagram in Figure 1 illustrates the sensing, actuation, and control system. Image-based sensors have not been implemented to date, other than simple webcams to acquire images for display on the remote operator ground station.

Vehicle

There are several options for navigating on very soft and wet flat ground. Options include:

- Low-ground-pressure, crawler-tracked vehicle
- Airboat
- Amphiroller
- Hovercraft.

For proof-of-concept, a wheeled vehicle was chosen, because preliminary demonstrations do not require specialized propulsion systems. The mobile platform is a gasoline-engine powered, hydraulic-drive, skid-steer Parallax QuadRover (Parallax 2008) shown in Figure 2.

Extensive customization has been done to measure velocity and torque at the wheels, to carry the control computer (in a protective ventilated case), and to integrate sensor payloads. The mass of the machine is

approximately 45 kg without the sensor payload, and the wheel load is approximately 30 kPa, and so modifications would be required to be able to use this machine on an actual soft tailings deposit.

Soil Classifier

The ability to discriminate between soft and hard soil is mission-critical, specifically within some neighbourhood of the vehicle. This is true even though the first commercial deployment of a robotic characterization system will likely be teleoperated, with a combination of video and range sensing for environmental telepresence, rather than autonomous operation.

Methods of measuring key soil characteristics have been the subject of many investigations, for example (Viscerra & McBratney 1998; Gardner, Dean, & Cooper 1998). Soil classifications will be made based on fusion of data obtained from the imaging system on the vehicle and other sensor data. A simple static penetrometer design is being developed for installation on the payload package, as illustrated conceptually in Figure 4. A robotic sampling payload package is also under development. A rotary viscometer will be used for initial contact measurements of soft tailings viscosity. This type of viscometer has no moving parts and can measure viscosity to 40×10^4 cP (which is roughly the thickness of peanut butter).

A separate study is in progress to field test hyperspectral image acquisition, and extraction of image features related to fines fraction less than $9 \mu\text{m}$ and residual bitumen fraction, as well as features that correlate well to areas of low and high soil strength. Image regions that have been identified as soft can then be combined with range sensing information are then combined to identify and geolocate different soil features.

Navigation System

System mission planning and navigation relies on a map relating the vehicle to its environment. The map holds information pertaining to vehicle position, soil types, mission objectives, identified hazards, and other mission-critical information. Onboard sensors include a GPS receiver, a compass module and a five-degree of freedom inertial measurement unit to allow the vehicle to determine current location, orientation, and attitude, as well as velocity.

The soil classification also helps the system infer hazardous regions (poor trafficability) and locations that require reclamation work. These regions of hazards and objectives can be preloaded by an operator into the map. Information from the system map is used in a trajectory generation algorithm to plan the vehicle movements and monitor mission progress. The algorithm balances route trafficability and route length to create efficient paths between objective regions and around hazard regions within the operational environment. These planned paths comprise the desired trajectory used by the navigation controller to allow the vehicle to navigate along the planned path, with dynamic control of traction when required.

Figure 5 shows a screenshot of the graphical display of the ground station program, which was developed using Cocoa and Composer software packages. The current version of the navigation software has the following capability:

- receives and parses data sent from the on-board sensors
- displays a map, with a editable picture and coordinate system
- receives input from the user to create and update waypoints, by clicking on the map or inserting GPS coordinates

- flags to tell the robot where to sample or use any other equipment
- animates a horizon and display video from a connected webcam
- generates trajectories and error-handling functions to direct the robot from waypoint to waypoint
- has features to control turning radius at waypoints
- sends NMEA strings to the control board for kinematic control of the robot.

Traction Controller

A suite of sensors measures shaft speed, torque and normal force of each wheel riding on the ground, to characterize ground pressure and traction force during locomotion on soft ground. This data will be used to tune a traction control algorithm for detecting sinking and slippage, and to modify wheel speed to drive out of a soft location.

There are a number of wheel-soil interaction models for different scenarios (Wong 1993). An implementation based on that described by (Yoshida & Hamano 2002) is used to model wheel dynamics in the traction control algorithm. The slip ratio of each wheel is the key state indicator for the vehicle; the slip ratio is related to the difference between intended wheel velocity (tire circumferential velocity) and actual wheel velocity (travelling velocity), and is defined by the following equation,

$$S = \begin{cases} \frac{(r\dot{\theta}_w - v_w)}{r\dot{\theta}_w} & (r\dot{\theta}_w > v_w : \text{accelerating, } S \text{ is positive}) \\ \frac{(r\dot{\theta}_w - v_w)}{v_w} & (r\dot{\theta}_w < v_w : \text{braking, } S \text{ is negative}) \end{cases} \quad (1)$$

where r is the radius of the wheel, $\dot{\theta}_w$ is the rotation angle of the wheel ($\dot{\theta}_w = \omega$), $r\dot{\theta}_w$ is the tire circumferential speed, and v_w is the linear traveling speed of the wheel.

These two values are relatively simple to measure accurately in real-time onboard the vehicle. Figure 6 shows a simplified interaction between a wheel and soft media. W is the load on the wheel, while σ is soil normal stress and τ is soil shear stress. The shear stress and normal stress imparted in the material below the wheel is related by:

$$\tau(\theta) = (c + \sigma(\theta) \tan \varphi)(1 - e^{-\alpha(\theta)}) \quad (2)$$

$$e^{-\alpha(\theta)} = -\frac{r}{k} \{ \theta_1 - \theta - (1 - S)(\sin \theta_1 - \sin \theta) \} \quad (3)$$

and

$$\tau_{\text{max}} = c + \sigma \tan \varphi \quad (4)$$

where c is cohesive stress of the soil, φ is internal friction angle of the soil, b is wheel width, h is depth of vertical sinking, and n, k, k_1, k_2 are empirically determined constants.

The normal stress is related to vertical wheel sinkage by:

$$\sigma(h) = (k_1 + k_2 b) \left(\frac{h}{b} \right)^n \quad (5)$$

The soil exerts both normal force f_n and tangential force f_t on the wheel, which are balanced by the load W and the drawbar pull of the vehicle, respectively, and calculated by

$$f_n = rb \left\{ \int_{\theta_2}^{\theta_1} \sigma(\theta) \cos \theta d\theta + \int_{\theta_2}^{\theta_1} \tau(\theta) \sin \theta d\theta \right\} \quad (6)$$

and

$$f_t = rb \left\{ \int_{\theta_2}^{\theta_1} \tau(\theta) \cos \theta d\theta - \int_{\theta_2}^{\theta_1} \sigma(\theta) \sin \theta d\theta \right\} \quad (7)$$

To ensure continued vehicle traction, the load-traction factor is examined. This is the ratio between the tangential (traction) force, or drawbar pull, and normal force acting on the wheel. This ratio aids in estimating the state of the robot and is related to the slip ratio. This relationship is complex, and is estimated numerically.

Different schemes have been proposed for traction measurement (Ojeda, Cruz, Reina & Borenstein 2006). A wireless strain gauge measurement package has been developed and implemented to measure torque at each wheel set, and communicate the torque back to the control computer. Normal loads are measured with strain gauges on the vehicle frame. Both sets of gages are calibrated using known static loads.

Difficulty arises in using any wheel-soil interaction model in the control loop, as they contain constants describing soil properties that are difficult to measure in real-time (*i.e.*, soil cohesion stress and internal friction angle). As the tailings environment is highly variable, a constant set of properties will not give a good estimation of soil behavior. A recursive parameter estimation method such as Kalman filtering will be used to update the parameter set.

If a machine does begin to bog down, a fault recovery strategy is needed to adjust wheel speeds for traction control to maintain continued progress or remove itself from soft ground and retreat to trafficable ground. This is not expected to be a significant challenge for a survey and mapping vehicle; but for a machine depositing reclamation material, traction control would have to work for a machine dragging a thick heavy tether (e.g., a flexible pipe full of slurry for hydraulic deposition of sand).

Fault detection and identification is necessary for sinking of the whole vehicle, excessive

tipping, or bogging down (accumulating excessive error from the desired trajectory). There are also activities that may be initiated when a particular objective is met, whether it is a waypoint or a fueling stop or a location to conduct a reclamation activity. The control scheme allows for a number of faults to be identified and specific actions to be taken to recover from each fault.

Alternative propulsion methods will have their own dynamics, and force and velocity constitutive relationships that can be used for system identification and control, for example, vehicles with crawler tracks (Hutangabodee, Zweiri, Seneviratne & Althoefer 2007).

CONCLUSIONS AND FUTURE WORK

Preliminary trials of machine navigation and traction control were conducted in August 2009. Sensors for measuring ground forces and an image analysis method for classifying soft and hard ground are being developed. System integration and full commissioning testing is planned for Spring 2010, with the image acquisition and classification system on the platform tested simultaneously with the navigation and control systems.

The initial prototype is employing a very straightforward, idealized approach for determining these key characteristics to demonstrate the concept. Soil bin test media will be artificially coloured to provide distinction between media type. A visible spectrum imaging system will then be used to characterize the terrain around the vehicle. A stereo vision system, or more likely a single camera supplemented with a laser ranging sensor, will help create a soil trafficability map around the vehicle. Image processing and soil region classification will be accomplished on the on-board computer.

Navigation and traction control systems will be tested on various terrain types, starting with sand and dirt bins, with both simulated and real media, in laboratory conditions to test simplified image classification, mapping, trajectory generation, and traction control. Results obtained during these trials will be used to optimize the system prior to field trials in more realistic outdoor conditions.

Future modifications to the system will include switching out the balloon tires for a tracked drive system, and testing the traction controller with tracked equipment in comparison to wheeled equipment. The sampling and soil strength measurement packages will be commissioned and tested.

The vision system will be upgraded with cameras capable of hyperspectral imaging, with refinement of the classification algorithm for a new feature set, including field trials at a tailings facility. A learning algorithm will be assessed for improving accuracy of soil trafficability estimates during operation of the vehicle.

Once technical feasibility has been demonstrated on a small scale, a new platform will be developed on a low-ground-pressure vehicle, which will be modified to demonstrate the technical feasibility of mapping soft tailings features on soft ground.

ACKNOWLEDGMENTS

Nicolas Olmedo contributed to the system architecture, developed the navigation software, and produced the CAD sketches of the sensor payload package. Financial support is gratefully acknowledged from the Natural Sciences and Engineering Research Council of Canada (NSERC) and the University of Alberta.

REFERENCES

Angelova, A; Matthies, L; Helmick, D; Perona, P, 2007. "Learning and Prediction of Slip from Visual Information." *Journal of Field Robotics* 24(3), pp. 205-231.

Caughill, DL; Morgenstern, NR; Scott, JD, 1993. "Geotechnics of nonsegregating oil sand tailings." *Canadian Geotechnical Journal*.

Gardner, CMK; Dean, TJ; Cooper, JD 1998. "Soil Water Content Measurement with a High-Frequency Capacitance Sensor." *J. Agric. Engng Res.* 71, 395-403.

Hutangkabodee, S; Zweiri, YH; Seneviratne, LD; Althoefer, K, 2007. "Validation of Soil Parameter Identification for Track-Terrain Interaction Dynamics." *Proc IEEE/RSJ Int'l Conf on Intelligent Robots and Systems*, San Diego, CA, USA, Oct 29 - Nov 2, 2007.

Morgenstern, NR; Scott, JD, 1983. "Geotechnics of Fine Tailings Management." *Geotechnical Special Publication*, pp. 1663-1683.

Ojeda, L; Cruz, D; Reina, G; Borenstein, J 2006. "Current-Based Slippage Detection and Odometry Correction for Mobile Robots and Planetary Rover." *IEEE Transactions of Robotics*, Vol. 22, No. 2, APRIL 2006

Parallax, Inc. Propeller Quadrover Robot. Retrieved July 2009 from <http://www.parallax.com>

Rivard, B; Feng, J; Lyder, D; Gallie, A; Cloutis, E, 2007. "Rapid characterization of oil sand properties using near infrared and thermal infrared reflectance spectroscopy." *57th Canadian Chemical Engineering Conf.*, Sept. 2007.

Singh, S, 1997 "The State of the Art in Automation of Earthmoving." *Journal of Aerospace Engineering*.

Viscarra, RA; McBratney, AB, 1998. "Laboratory evaluation of a proximal sensing technique for simultaneous measurement of soil clay and water content." *Geoderma* 85, pp. 19-39.

Wong, JY 1993. "Theory of Ground Vehicles, 2nd Ed." John Wiley and Sons, Inc., New York.

Yoshida, K; Hamano, H 2002. "Motion Dynamics of a Rover With Slip-Based Traction Model." *Proc. IEEE Int'l Conf on Robotics & Automation* Washington, DC.

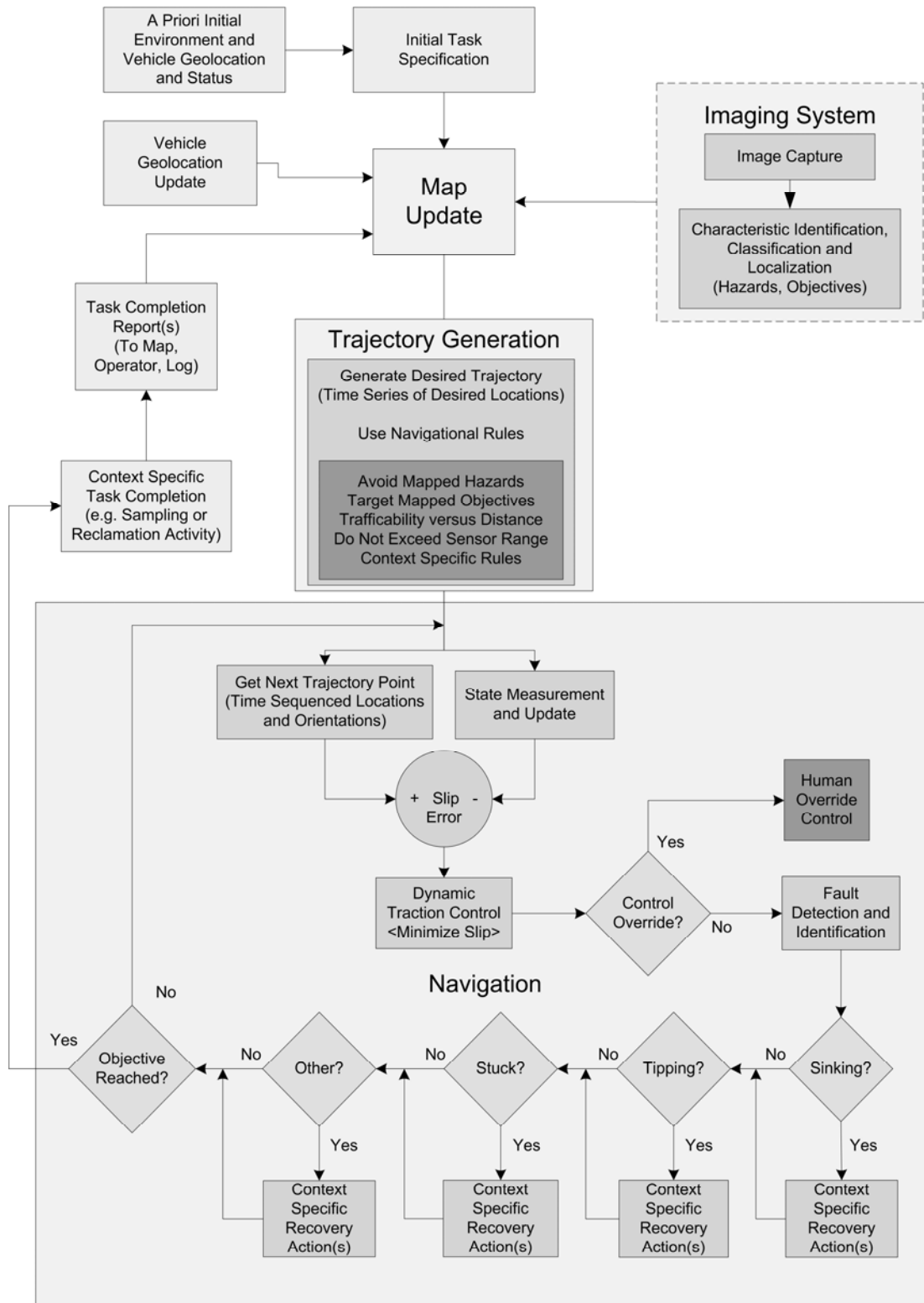


Figure 1. System Block Diagram



Figure 2: Mobile Vehicle Platform

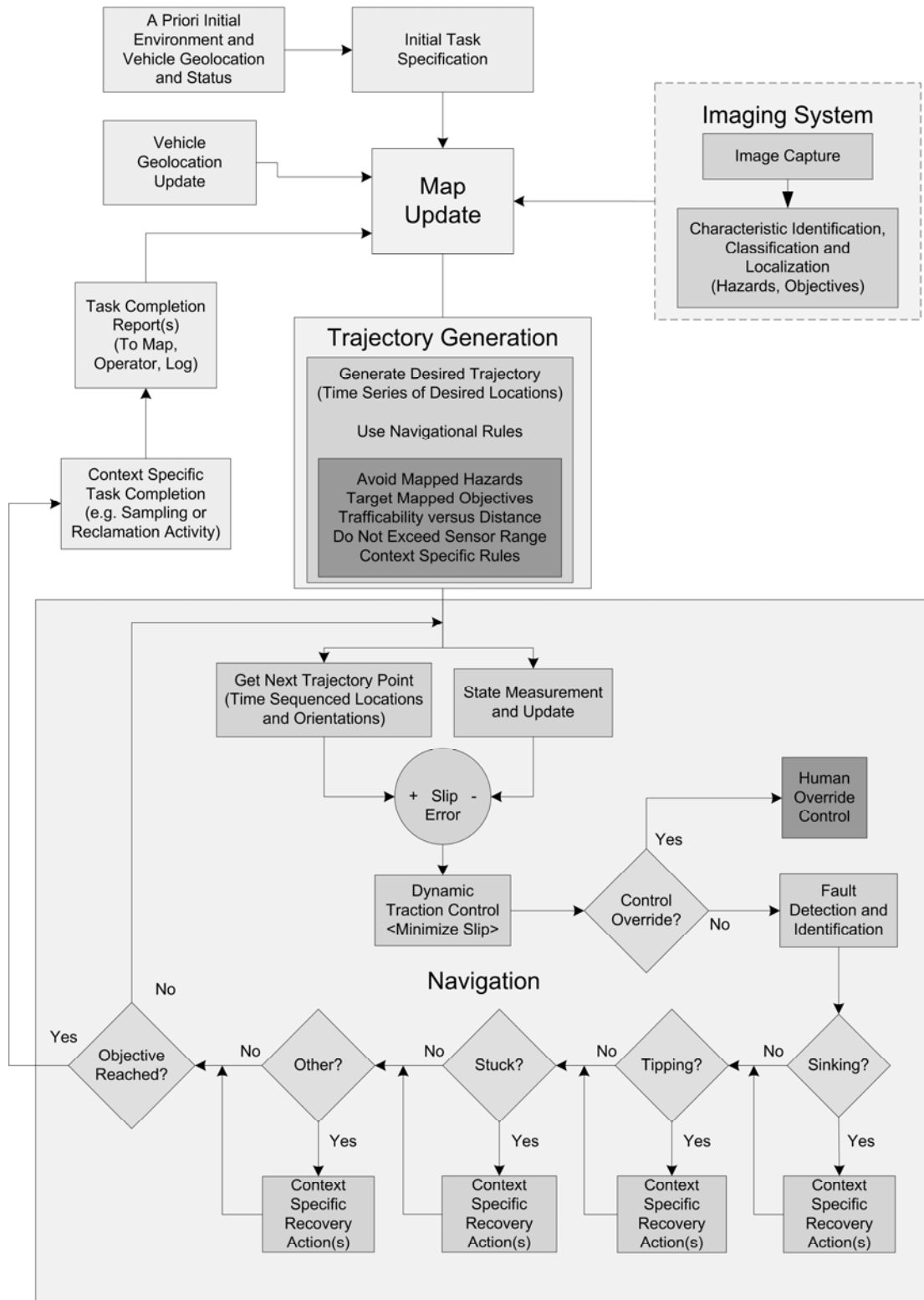


Figure 3: Vehicle Control Scheme Block Diagram

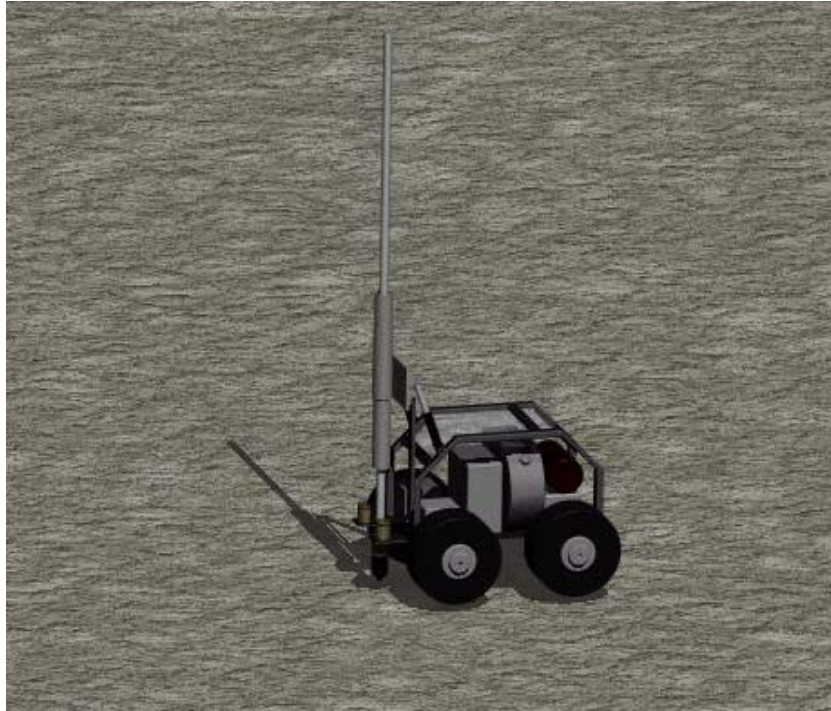


Figure 4: Conceptual Sketch of Contact Sensor Payload

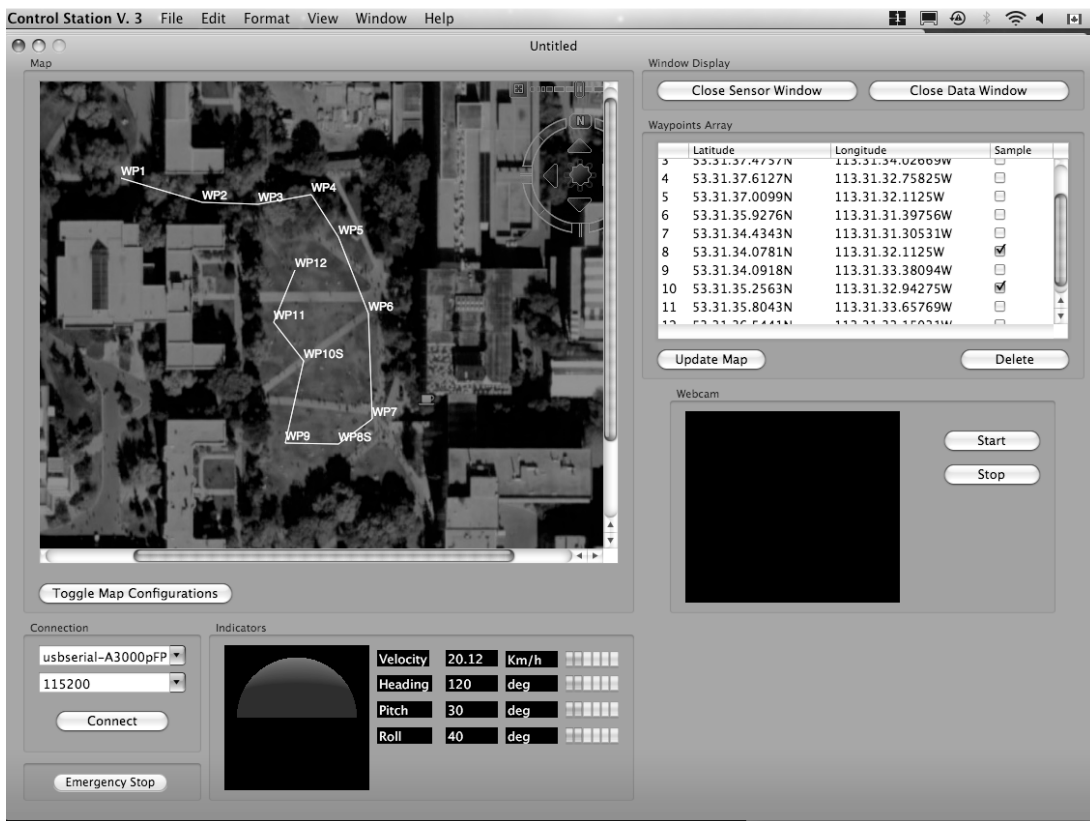


Figure 5: Graphical Display of Navigation

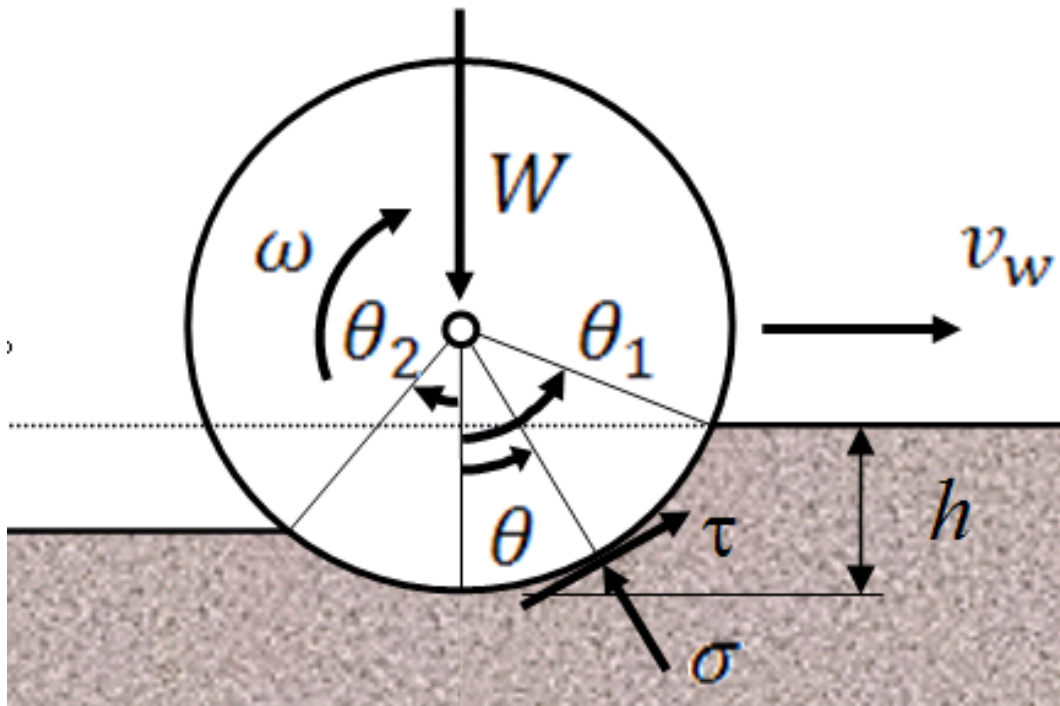


Figure 6: Soft Soil Wheel Traction Model

